IAHS Publication 308
ISSN 0144-7815

friend 2006

IAHS AISH

Climate Variability and Change – *Hydrological Impacts*

Edited by

Siegfried Demuth
Alan Gustard
Eduardo Planos
Fred Scatena
Eric Servat

Co-editors: Arthur Askew, Christel Prudhomme, Denis Hughes, Lena Tallaksen, Lorena Menéndez Fernández-Cuesto, Mike Bonell, Trevor Daniell & Wolfgang Grabs

IAHS AISH

www.iahs.info

INTERNATIONAL ASSOCIATION OF HYDROLOGICAL SCIENCES

IAHS, established in 1922, is a nonprofit-making nongovernmental scientific organization committed to serving the science of hydrology and the worldwide community of hydrologists

IAHS is concerned with all components of the hydrological cycle and related processes, as well as the application of hydrology and its implications for society and the environment. Currently nine International Commissions deal with the hydrological cycle, water for society and the environment, and specific techniques:

- Surface Water
- Groundwater
- Continental Erosion
- Snow and Ice Hydrology
- Water Quality
- Water Resources Systems
- Coupled Land–Atmosphere Systems
- Remote Sensing
- Tracers

The Prediction in Ungauged Basins initiative (PUB, 2003–2012) involves all the Commissions.

Information about IAHS, the Commissions, PUB, and their activities is available at *www.iahs.info*, or from the IAHS Secretary General:

Dr Pierre Hubert, Secretary General IAHS,
L'Ecole des Mines de Paris, 35 Rue Saint-Honoré, F-77305 Fontainebleau, France
e-mail: *iahs@ensmp.fr*

Membership of IAHS is *free of charge* and open to anyone wishing to participate in IAHS activities, such as IAHS symposia and workshops. The worldwide membership is now more than 4000. The registration form can be downloaded from the IAHS website or obtained from:

Mrs Jill Gash, Membership Secretary,
IAHS Press, Centre for Ecology and Hydrology, Wallingford, Oxfordshire OX10 8BB, UK
e-mail: *jilly@iahs.demon.co.uk*

Members receive the Newsletter and information about IAHS activities, and can obtain discounts on *Hydrological Sciences Journal* and most other IAHS publications; at least 25% discount to all members, and 80% discount for members in financially disadvantaged countries.

IAHS Publications IAHS has a long tradition of publishing titles on topics in hydrology and related themes. This series, the IAHS Red Books (ISSN 0144-7815), provides a means for international dissemination of research results and discussion from authors worldwide. Many of the publications are collections of peer-reviewed papers and discussions selected from the proceedings of IAHS-convened and other international meetings. Others are reports on specific topics. IAHS also publishes *Hydrological Sciences Journal* (ISSN 0262-6667; available on-line) and produces a *Series of Special Publications* (ISSN 1024-4891), and the *Benchmark Papers in Hydrology Series*. More information at *www.iahs.info*, or ask *jilly@iahs.demon.co.uk* (address as above) for catalogues and flyers.

Distribution of IAHS Publications to "Countries in Need" is funded by the IAHS Task Force for Developing Countries (TFDC). *Hydrological Sciences Journal* and other IAHS publications are distributed free to more than 70 organizations worldwide, to help scientists there to acquire pioneering results of hydrological sciences and their application. The publications are provided on the understanding that they are made available to specialists both inside and outside the recipient organizations. All correspondence concerning the distribution of IAHS publications to "countries in need" should be sent to:

Prof. Xia Jun, Department of Hydrology and Water Resources, College of Water Resources and Hydropower Engineering, Wuhan University, East Lake Road no. 8, Wuhan 430073, China
e-mail: *xiaj@igsnrr.ac.cn*

Cover illustration: Flooding in Havana, Cuba, October 2005, associated with Hurricane Wilma, the most intense hurricane ever recorded in the Atlantic basin.
Photograph courtesy Alejandro Planos; cover design by Claudine Dieulin.



Climate Variability and Change – *Hydrological Impacts*

Edited by:

SIEGFRIED DEMUTH
IHP/HWRP Secretariat, Federal Institute of Hydrology, Koblenz, Germany

ALAN GUSTARD
Centre for Ecology and Hydrology, Wallingford, Oxfordshire, UK

EDUARDO PLANOS
Centre for Climate, Institute of Meteorology of Cuba, Havana, Cuba

FRED SCATENA
University of Pennsylvania, Philadelphia, PA, USA

ERIC SERVAT
Institut de Recherche pour le Développement, Montpellier, France

Co-editors:

Arthur Askew, Christel Prudhomme, Denis Hughes,
Lena Tallaksen, Lorena Menéndez Fernández-Cuesto,
Mike Bonell, Trevor Daniell, Wolfgang Grabs

IAHS Publication 308
in the IAHS Series of Proceedings and Reports

Published by the International Association of Hydrological Sciences 2006

IAHS Publication 308

ISBN 978-1-901502-78-7

British Library Cataloguing-in-Publication Data.
A catalogue record for this book is available from the British Library.

© IAHS Press 2006
This publication may be reproduced as hard copy, in whole or in part, for educational or nonprofit use, without special permission from the copyright holder, provided acknowledgement of the source is made. No part of this publication may be electronically reproduced, transmitted or stored in a retrieval system, and no use of this publication may be made for electronic publishing, resale or other commercial purposes without specific written permission from IAHS Press.

The papers included in this volume have been peer-reviewed and some were extensively revised by the Editors, in collaboration with the authors, prior to publication.

IAHS is indebted to the employers of the Editors for the invaluable support and services provided that enabled them to carry out their task effectively and efficiently.

The information, data and formulae provided in this volume are reproduced by IAHS Press in good faith and as finally checked by the author(s); IAHS Press does not guarantee their accuracy, completeness, or fitness for a given purpose. The reader is responsible for taking appropriate professional advice on any hydrological project and IAHS Press does not accept responsibility for the reader's use of the content of this volume. To the fullest extent permitted by the applicable law, IAHS Press shall not be liable for any damages arising out of the use of, or inability to use, the content.

The designations employed and the presentation of material throughout the publication do not imply the expression of any opinion whatsoever on the part of IAHS concerning the legal status of any country, territory, city or area or of its authorities, or concerning the delimitation of its frontiers or boundaries.

The use of trade, firm, or corporate names in the publication is for the information and convenience of the reader. Such use does not constitute an official endorsement or approval by IAHS of any product or service to the exclusion of others that may be suitable.

Publications in the series of Proceedings and Reports are available from:
IAHS Press, Centre for Ecology and Hydrology, Wallingford, Oxfordshire OX10 8BB, UK
tel.: +44 1491 692442; fax: +44 1491 692448; e-mail: jilly@iahs.demon.co.uk

Printed in The Netherlands by Krips BV, Meppel.

Preface

Over more then two decades the international FRIEND (Flow Regimes from International Experimental and Network Data) research programme of UNESCO has developed to become a global network of researchers from universities, research organizations, operational hydrological agencies and policy makers to exchange and share scientific knowledge and data.

Eight regional FRIEND groups have been established to investigate global change, impacts on the hydrological cycle, statistical analyses of hydrological extremes, flow forecasting, hydrological modelling at different scales, variability of hydrological regimes, uncertainties in applying hydrological and water resources models and region-wide surface water assessment, and to enhance capacity building in developing countries.

The research results of the regional groups are reported every four years to a wider scientific community at an international FRIEND conference. These proceedings publish the key research developments which were presented at the fifth International FRIEND conference which took place for the first time in the Caribbean region, in Havana, Cuba. This was a unique opportunity to exchange research results among the regional FRIEND groups and the international research community. The previous conferences were held in Bolkesjo (Norway, 1989), Braunschweig (Germany, 1993), Postojna (Slovenia, 1997) and Cape Town (South Africa, 2002).

A focus of the Havana conference was to discuss how advances in analytical techniques and process hydrology are improving our assessment of water resources variability and the impacts of environmental change. The conference gave a high priority to establishing links with related WMO and IAHS international programmes and the related disciplines of ecohydrology and climatology. The conference topics were:

- Data
  databases; networks; GIS
- Hydrological extremes
  low flow prediction and forecasting; flood prediction and forecasting; rainfall runoff modelling
- Hydro-climatology
  precipitation spatial and temporal variability and prediction; large scale variability and tele-connections; climate change and impacts of climate change; trends
- Ecosystems
  in-stream ecology; flood plains; water quality; sediments; groundwater; water balance, soils, land cover; human influences

This volume contains 117 reviewed papers from over 30 countries, published in English, French and Spanish, which reflect both the international dimension of FRIEND and the key challenges facing hydrologists in the 21st Century.

Siegfried Demuth

Contents

Preface *by Siegfried Demuth* iii

1 INTRODUCTION

FRIEND: key achievements and opportunities in international co-operation *Alan Gustard & Mike Bonell* 3

Human impacts, complexity, variability and non-homogeneity: four dilemmas for the water resources modeller *Trevor M. Daniell & Katherine A. Daniell* 10

2 DATA

Databases

SIEREM: an environmental information system for water resources *J. F. Boyer, C. Dieulin, N. Rouche, A. Cres, E. Servat, J. E. Paturel & G. Mahé* 19

Operational management of hydrological extremes using global-scale atmospheric models *Arnold H. Lobbrecht, Schalk Jan Van Andel & Frans Van Kruiningen* 26

Real-time monitoring and management of point and areal hydrometeorological data in the Athens metropolitan area *Maria Mimikou & Andreas Grammatikogiannis* 31

Hydrological assessment of Makanya catchment in South Pare Mountains, semiarid northern Tanzania *Marloes L. Mul, Hubert H. G. Savenije, Stefan Uhlenbrook & Maurits P. Voogt* 37

L'Observatoire de Recherche en Environnement, ORE HYBAM sur les grands fleuves amazoniens / The Environmental Observation and Research project, ORE HYBAM, and the rivers of the Amazon basin 44
Gérard Cochonneau, Francis Sondag, Jean-Loup Guyot, Boaventura Geraldo, Naziano Filizola, Pascal Fraizy, Alain Laraque, Philippe Magat, Jean-Michel Martinez, Luis Noriega, Eurides Oliveira, Julio Ordonez, Rodrigo Pombosa, Frédérique Seyler, Jonathan Sidgwick & Philippe Vauchel

Networks

The decline of hydrological data collection for development of integrated water resource management tools in Southern Africa *Helen Houghton-Carr & Matt Fry* 51

The use of spatial information to improve hydrometric network design and evaluation *Cedric Laize & Terry Marsh* 56

Modelación hidrológica empleando isoyetas de relieve, una aproximación geoestadística / Hydrological modelling using relief-isohyets: a geostatistical approximation 62
Raúl Becerra-Soriano & Alfonso Gutiérrez-López

GIS

The contribution of GIS to hydrological modelling *C. Dieulin, J. F. Boyer, S. Ardoin-Bardin & A. Dezetter* 68

An evaluation of the potential use of satellite rainfall data for input to water 75

Impact assessment of measures in the upstream part of Dutch basins to reduce flooding *Erik Querner & Menno Rakhorst* 180

Propuesta para minimizar el impacto de las inundaciones en una cuenca costera de la costa de Chiapas, Mexico / Proposals for minimizing flooding in the Chiapas coastal river basin, Mexico *Martín D. Mundo Molina* 186

Numerical estimation of flood zones in the Vistula River valley, Warsaw, Poland *Małgorzata Gutry-Korycka, Artur Magnuszewski, Jarosław Suchożebrski, Witold Jaworski, Michał Marcinkowski & Michał Szydłowski* 191

Sistema de alerta temprana por inundaciones experiencia en El Salvador / Experience of the Flood Early Warning System in Salvador *Ana Deisy Lopez Ramos* 196

Pronóstico de lluvia sobre territorio cubano al paso de los huracanes Charley e Iván, usando MM5V3 / Rainfall forecasting in Cuba for hurricanes Charley and Iván using MM5V3 *Ida Mitrani Arenal, Israel Borrajero Montejo & Arnoldo Bezanilla Morlot* 201

Índices y grados de riesgo de inundación comunales en sistemas de alerta: uso de lógica difusa / Indices and grades of regional flood risk in a flood alert system: use of fuzzy logic *Arnaldo Santander & Ximena Vargas* 207

AIGA: un dispositif d'alerte des crues. Application à la région méditerranéenne française / AIGA: a flood forecasting tool. Application to the French Mediterranean region *Jacques Lavabre & Yves Gregoris* 214

Impact of the Amazon tributaries on major floods at Óbidos *Josyane Ronchail, Jean-Loup Guyot, Jhan Carlo Espinoza Villar, Pascal Fraizy, Gérard Cochonneau, Eurides De Oliveira, Naziano Filizola & Juan Julio Ordenez* 220

Bayesian priors based on regional information: application to regional flood frequency analysis *Mathieu Ribatet, Eric Sauquet, Jean-Michel Gresillon & Taha B. M. J. Ouarda* 226

Flash floods in mountain areas *Manfred Spreafico* 232

Rainfall–runoff modelling

Rainfall–runoff modelling of Bua River basin, Malawi *S. H. Mkhandi & P. G. Kumambala* 239

Modelación distribuida de la cobertura nival para el pronóstico de volúmenes de deshielo / Estimating snowmelt volume using snow cover distribution modelling *Patricio Valck C., Ximena Vargas M. & Mauricio Cartes* 244

Essais de modélisation avec peu de données en Afrique de l'Ouest / Trying to model with little data in West Africa *Jean Emmanuel Paturel, Christophe Laroche, Lawani Mounirou, Lamine Mar, Sandra Ardoin-Bardin, Alain Dezetter, Gil Mahe & Eric Servat* 250

Precipitation elasticity of streamflow in catchments across the world *Francis H. S. Chiew, Murray C. Peel, Thomas A. McMahon & Lionel W. Siriwardena* 256

Quel scénario de changement climatique retenir pour une analyse d'impacts? / Which climate change scenario to keep for analysing impacts? *Claude Bocquillon, Wajdi Najem & Antoine Hreiche* 442

Relation entre hydrologie et climat dans le bassin versant de l'Oued Inaouène (pré-Rif marocain) / Relationship between hydrology and climate in the Inaouene River basin, pre-Rifian Morocco *Abdelkader El Garouani & Abdellatif Tribak* 447

Regionalization of a distributed catchment model for highly glacierized Nepalese headwater catchments *Markus Konz, Ludwig N. Braun, Stefan Uhlenbrook, Siegfried Demuth & Arun Shrestha* 454

Climate change impacts on glacial lakes and glacierized basins in Nepal and implications for water resources *Suresh Raj Chalise, Madan Lall Shrestha, Om Ratna Bajracharya & Arun Bhakta Shrestha* 460

Variability of runoff from Alpine basins *David N. Collins* 466

An assessment of the potential impacts of climatic warming on glacier-fed river flow in the Himalaya *H. Gwyn Rees & David N. Collins* 473

El glaciar 15 del Antisana investigaciones glaciológicas y su relación con el recurso hídrico / Glacier 15, Antisana, Ecuador: its glaciology and relations to water resources *Bolivar Caceres, Bernard Francou, Vincent Favier, Guillaume Bontron, Pierre Tachker, Rodolphe Bucher, Jean Denis Taupin, Mathias Vuille, Luis Maisincho, Fanny Delachaux, Jean Philippe Chazarin, Eric Cadier & Marcos Villacis* 479

Trends

An historical analysis of drought in England and Wales *Gwyneth A. Cole & Terry J. Marsh* 483

The effect of record length on the analysis of river flow trends in Wales and central England *Harry Dixon, Damian M. Lawler, Asaad Y. Shamseldin & Paul Webster* 490

High and low flow trends in a national network of undisturbed indicator catchments in the UK *Jamie Hannaford & Terry J Marsh* 496

Past and future changes in flood and drought in the Nordic countries *Hege Hisdal, Lars A. Roald & Stein Beldring* 502

Changes in runoff regimes in small catchments in Central Europe: Are there any? *Ladislav Holko, Andreas Herrmann & Alena Kulasová* 508

A national study on trends and variations of French floods and droughts *M. Lang, B. Renard, E. Sauquet, P. Bois, A. Dupeyrat, C. Laurent, O. Mestre, H. Niel, L. Neppel & J. Gailhard* 514

Long-term trends and runoff fluctuations of European rivers *Pavla Pekarova, Pavol Miklanek & Jan Pekar* 520

Influence of the North Atlantic Oscillation on spatial and temporal patterns in Eurasian river flows *Raimund Rödel* 526

Análisis del Comportamiento Hídrico en El Salvador: posibles causas e implicaciones / Analysis of river flow trends in El Salvador: possible causes and consequences *Adriana Maria Erazo Chica, Tomas Rivas Pacheco & Oscar Hernández* 533

Methodologies for trend detection *Zbigniew W. Kundzewicz & Maciej Radziejewski* 538

5 ECOSYSTEMS

In stream ecology

Water demand in the Zhalong Wetland ecosystem *Wang Jian-qun, Han Li & Ma Tie-min* 553

Estimation of minimum acceptable (compensatory) flow for the rivers of Costa Rica *Sadí Laporte, Alexia Pacheco & Carlos R. Rodriguez* 558

Hidrología de laguna albúfera Reserva El Yali, humedal RAMSAR, Chile / Hydrology of the El Yali coastal marsh reserve, a RAMSAR site in Chile *Pablo Galdames, Chi Sun & Alejandro Dussaillant J.* 563

Environmental demands for sustainable regulation schemes in the humid tropics *Anny Chaves, Irina Krasovskaia & Lars Gottschalk* 569

Flood plains

Interaction between surface and groundwater in the flooding of riparian wetlands: Biebrza wetlands case study *Tomasz Okruszko, Jarosław Chormański & Dorota Świątek* 573

Modelling of inundation patterns on the Pilica River flood plain, Poland *Mustafa Altinakar, Edyta Kiedrzyńska & Artur Magnuszewski* 579

Water quality

A global assessment of chemical effluent dilution capacities from a macro-scale hydrological model *Virginie D. J. Keller, Mick J. Whelan & H. Gwyn Rees* 586

Wet and dry deposition of atmospheric nitrogen in three hydrographic basins in Cuba *Osvaldo Cuesta-Santos, Arnaldo Collazo, Maria Gonzalez & Antonio Wallo* 591

Application of hydrogeochemical modelling to the characterization and water quality control of coastal karst aquifers *J. R. Fagundo Castillo, P. González Hernández, J. Fagundo Sierra, M. Suárez Muñoz, C. Melián Rodríguez & E. Alvarez Varela* 596

Studying waste load dispersion in Songkhla Lake using a simulation model *Winai Sae-Chew* 601

Risques d'eutrophisation et de comblement des retenues d'eau au Burkina Faso / Risk of eutrophication and filling-up of small reservoirs in Burkina Faso *Amadou Hama Maiga, Yacouba Konate, Kokou Denyigba, Harouna Karambiri & Joseph Wethe* 606

Sediments

Characteristics of sediment and nutrient flows in the lower reach of the Yellow River *Jianyao Chen, Dong Ke, Xinfeng Zhao, Yoshihiro Fukushima & Makoto Taniguchi* 612

Groundwater

Factors affecting the groundwater regime in the High Tatra Mountains *Miriam Fendekova & Marian Fendek* 617

A new, physically-based, numerical runoff generation model system for study of surface–shallow groundwater relationships and system reactions to environmental changes *Andreas Herrmann, Matthias Schöniger & Sybille Schumann* 623

Isotopic evidence of the overexploitation of karst aquifers *L. F. Molerio León* 629

Contaminación del acuífero yucateco por lixiviado de residuos municipales / Contamination of the Yucatan aquifer by leachate from municipal waste 635
Roger González Herrera & Ramiro Rodríguez Castillo

Water balance, soils, land cover

Interpolation of water balance components for Costa Rica *Federico Gómez, Irina Krasovskaia, Lars Gottschalk & Etienne Leblois* 641

Physical insights into soil water storage in the soil–plant–atmosphere system 646
Urszula Somorowska

Determination of the soil hydrophysical characteristics and vegetation parameters of a river basin in a permafrost region *Yeugeniy Gusev & Olga Nasonova* 651

Minor changes of water conservation capacity in 50 years of forest growth: analysis with data from the Ananomiya Experimental Forest, Japan *Michio Hashino & Huaxia Yao* 656

Respuesta de los caudales máximos al manejo de bosques de plantaciones en cuencas experimentales en el sur de Chile / Peak flow changes in a managed-forest experimental basin in southern Chile 662
Andrés Iroumé, Claudia Castillo, Helen Primrose, Anton Huber & James Bathurst

UNESCO Working Group on the impacts of climate variability and land cover change on flooding and low flows as a function of scale *Günter Blöschl, Sandra Ardoin-Bardin, Mike Bonell, Manfred Dorninger, David Goodrich, Dieter Gutknecht, David Matamoros, Bruno Merz, Paul Shand & Jan Szolgay* 667

Overview of land cover change in tropical regions *Rudi Drigo* 672

The impacts of land use/land cover change and climate variability on the hydrology of the Sahel *Gil Mahe* 679

Human influences

Impact des modifications d'habitats (déforestation, aménagements hydro-agricoles, extension des cultures) sur la santé des populations rurales: cas de l'ulcère de Buruli en Côte d'Ivoire / Environment change (deforestation, agricultural-water management, increased cultivation) impact on rural population health: Buruli ulcer prevalence in Ivory Coast 685
Telesphore Brou, Helene Broutin, Mireille Dosso & Jean-Francois Guegan

Methodologie et application d'une demarche de modelisation hydrologique prenant en compte l'evolution des etats de surface en milieu sahelien d'Afrique de l'ouest / A hydrological modelling approach that allows for evolution of the land surface in African Sahel basins 691
Pierre Diello, Jean-Emmanuel Paturel, Gil Mahe, Bruno Barbier, Harouna Karambiri & Eric Servat

Efecto de las plantaciones de *Pinus radiata* sobre el recurso agua en Chile / The effect of *Pinus radiata* plantations on water resources in Chile 698
Anton Huber & Andrés Iroumé

Key word index 703

1 Introduction

Climate Variability and Change—Hydrological Impacts (Proceedings of the Fifth FRIEND World Conference held at Havana, Cuba, November 2006), IAHS Publ. 308, 2006.

FRIEND: key achievements and opportunities in international co-operation

ALAN GUSTARD[1] **& MIKE BONELL**[2]

1 *Centre for Ecology and Hydrology, Wallingford, Oxfordshire OX10 8BB, UK*
agu@ceh.ac.uk

2 *Former Chief of Section UNESCO Division of Water Sciences, 1 rue Miollis, F-75732 Paris, France*

Abstract This paper introduces the key objectives of the FRIEND (Flow Regimes from International Experimental and Network Data) 2006 Conference (Demuth *et al*., 2006). These are to review progress, to establish new research priorities and to identify opportunities to increase co-operation with related international initiatives. Understanding natural and human induced impacts on hydrological regimes and predicting both floods and low flows at gauged and ungauged sites continue to be the key FRIEND objectives. FRIEND initially focussed on research, however, capacity building including software and data base development, training courses, the publication of operational guidance and text books and support to MSc and PhD students have now become a major component of FRIEND activities. The paper reviews key FRIEND achievements since its inception in 1985 and advances proposals of how co-operation with allied international programmes may be improved.

Key words international co-operation; FRIEND; HELP; PUB; capacity building; networks; hydrological processes; extremes; prediction; forecasting

INTRODUCTION

This paper summarizes some of the key achievements of FRIEND and identifies opportunities for improving co-operation between FRIEND (Flow Regimes from International Experimental and Network Data) and related international hydrology initiatives, specifically HELP (Hydrology Environment Life and Policy), the PUB (Predictions in Ungauged Basins) programme of IAHS, and related WMO initiatives. The paper is presented from a FRIEND perspective and in the context of the current level of activity of FRIEND research and capacity building. A summary of each programme is presented below and a detailed review of FRIEND is presented in Servat & Demuth (2006). The paper concludes with proposals for advancing co-operation between FRIEND and related programmes.

FRIEND, HELP AND PUB

FRIEND was initiated in 1985 as a key part of IHP–III (third phase of the International Hydrological Programme, UNESCO) by a small team of European hydrologists who sought to realise the operational benefits of the extensive databases gathered from representative and experimental basins during the International Hydrological Decade (1965–1974) of UNESCO. A generic scientific objective was to improve the understanding of the spatial and temporal variability of hydrological regimes across different regions of the world and to advance the estimation of hydrological extremes at ungauged sites. More recently a high priority has been given to bridging the gap between research and operational water management (Gustard & Cole, 2002) and in capacity building in developing countries (Meigh & Fry, 2004; Rees, 2004). The FRIEND project has always had a “bottom up approach” with the project being implemented on a regional basis. Research proposals are developed by hydrologists in the region with a steering committee establishing a research and capacity building strategy. Each regional group has elected a co-ordinator who is responsible for maintaining co-operation, motivating participants and identifying funding opportunities. A high priority has always been given to the secondment of staff between countries and organizations and the sharing of data, models and research tools (van Lanen & Demuth, 2002). Most regional groups have scientific sub-projects, for example low flows, floods and large-scale variations and have established a FRIEND database bringing together hydrological data in a region onto a common database platform.

HELP (Hydrology for the Environment, Life and Policy) was established in 1999 (Anderson & Moody, 2004; Bonell, 2004) to improve integrated catchment management through the creation

Copyright © 2006 IAHS Press

of a framework for water law and policy experts, water resource managers and scientists to work together on water-related problems. The broad objectives of HELP are to strengthen field-oriented, experimental hydrology using the drainage basin (up to scales 10^4 to 10^6 km^2) as the framework. The desire for this programme to be truly "user-driven" requires the active involvement of both policy and facilitating (water and land resource managers) groups to set the policy agenda and ensure the scientific results will benefit societal needs through the revision of policy and management practices. Unlike most FRIEND groups (the exception is Nile FRIEND) implementtation is at the basin level. HELP is also a cross cutting theme of IHP-VI.

PUB (Predictions in Ungauged Basins) is an initiative of the IAHS Decade on Prediction in Ungauged Basins and was launched in 2002. PUB is geared towards developing methodologies for assessing and reducing the uncertainty in hydrological predictions (Sivaplan *et al.*, 2003). PUB is implemented through the following six thematic working groups based on a detailed science plan: Basin inter-comparison and classification, Conceptualization of process heterogeneity, Uncertainty analyses and model diagnostics, Data collection approaches, Hydrological theory, and Hydrological models.

FRIEND: KEY ACHIEVEMENTS AND FUTURE DIRECTIONS

The growth of FRIEND

FRIEND has been a major programme of the IHP since its inception in 1985. FRIEND is a cross cutting theme of IHP VI and a major achievement is the development over a 21 year period to include active participation from over 140 countries in eight regional groups (Fig. 1). The number of papers published in the five FRIEND conference proceedings illustrate the growth of and development of FRIEND research (Table 1). Papers are allocated to the region which is the subject of the paper, excluding papers with a generic content. The Northern European FRIEND has been most active since the inception of FRIEND. This is due to the longer period for project development, easier access to national and EU research funding and, most importantly, a larger number of research hydrologists in the region. The Table also illustrates the development of other FRIEND groups, notably AMHY from 1993, activities in Africa from 1997, HKH from 2002 and the considerable contribution to the FRIEND 2006 conference from the AMIGO region. Over this period there has been a change in emphasis between research topics. For example, early Northern European contributions were dominated by papers on hydrological process and detailed water balance studies. These are now fewer in number, as a result of the establishment of a series of parallel conferences by the European Research Basin Network. Compared with earlier conferences, FRIEND 2006 has a reduction of papers on low flow estimation at the ungauged site but an increase in papers on regional regime analysis, teleconnections, trends and climate change. Research on groundwater, water quality and ecology has also seen an increase at FRIEND 2006.

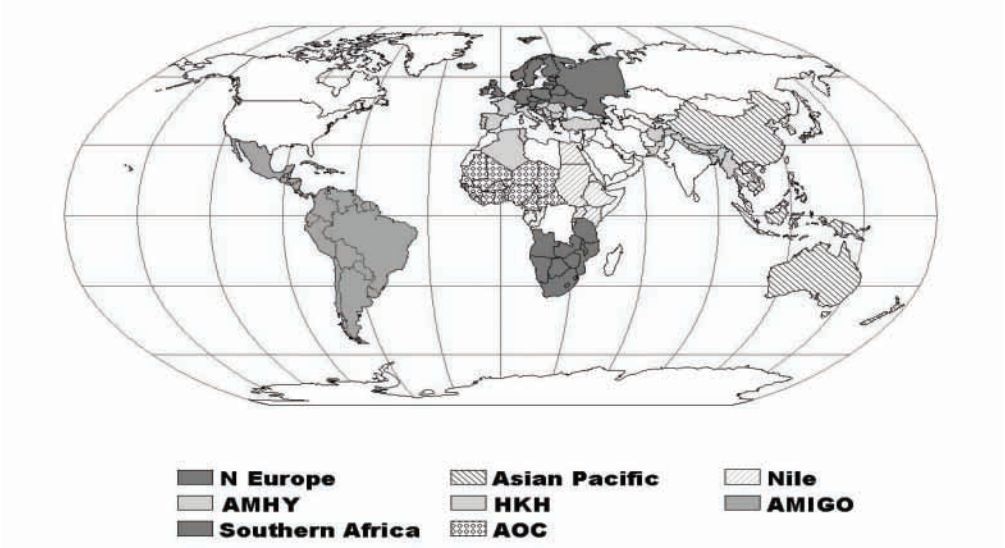


Fig. 1 FRIEND Regional groups.

Table 1 Distribution by region and topic of papers published in FRIEND conference proceedings in the year shown for the period 1989–2006.

Year	Topic	Number of Papers from each FRIEND region						
		AMHY	AOC	AMIGO	NE	SA	AP	HKH
1989	Data networks and GIS				2		1	
	Water Balance, processes	1	1		10		2	
	Low Flows				8			
	Floods		1		6			
	Precipitation		1		1			
	Trends, telecon, climate variability							
	Groundwater, water quality, ecology							
1993	Data networks and GIS	2			3			
	Water Balance, processes	3			13		1	
	Low Flows				8			
	Floods	2			7	1	1	
	Precipitation	1			1			
	Trends, telecon, climate variability				4			
	Groundwater, water quality, ecology				11			
1997	Data networks and GIS	1				1		
	Water Balance, processes	1			2			
	Low Flows	1			8	1		
	Floods	4			1			
	Precipitation	5	3		1	1		
	Trends, telecon, climate variability	1			4			
	Groundwater, water quality, ecology		2		2			1
2002	Data networks and GIS							1
	Water Balance, processes	1	3		1			
	Low Flows		1		2	3	1	2
	Floods	2	2		4	3	2	
	Precipitation	1	4			1	1	
	Trends, telecon, climate variability	1			5			2
	Groundwater, water quality, ecology		2		4	1		4
2006	Data networks and GIS	3		4	3	1		
	Water Balance, processes		2	7	2			1
	Low Flows	2		2	10			1
	Floods	3		4	3	1		
	Precipitation		3	10		2	1	
	Trends, telecon, climate variability	2		6	12		1	3
	Groundwater, water quality, ecology			9	5		4	1

Data for 2006 is provisional.
Information from Nile FRIEND which held a regional conference in 2005 is excluded.

The current status of FRIEND

FRIEND research covers a diverse range of topics, including low flows, floods, variability of regimes, rainfall/runoff modelling, processes of streamflow generation, sediment transport, snow and glacier melt, climate change and land-use impacts. The level of activity varies significantly between research groups and over time. These conference proceedings describe FRIEND research covering a wide spectrum of research topics from a diverse range of hydrological regimes. This diversity is illustrated by some examples of FRIEND activities which are summarized below.

In Northern European FRIEND a major activity of the Low Flow group has been the publication of a text textbook on *Hydrological Drought* (Tallaksen & van Lanen, 2004) based on nearly 20 years of cooperative research. The “Large Scale Variation” project is very active in researching hydrological regimes at the continental scale and establishing links between hydrological response and climate (Bower *et al*., 2004). The main AMHY FRIEND activity was the organization of two international conferences one on the “Hydrology of the Mediterranean and Semiarid regions” and the other on “Climatic and anthropogenic impacts on water resources variability”. These conferences brought together participants from all eight regional FRIEND groups and provided a good model of how co-operation across FRIEND can be enhanced in order to develop capacity for research in developing countries.

Western and Central Africa (AOC) FRIEND now have several projects including low flows and groundwater, the variability of water resources, estimation at ungauged sites and database and website development. Southern Africa FRIEND published a major report on the regions research and capacity building activities (Meigh & Fry, 2004) primarily in the area of water resource modelling and low flow estimation. The Nile FRIEND has been very active, holding four training workshops in Tanzania, Ethiopia, Kenya and Egypt, including low flow and drought analysis and a major international conference in Egypt in November 2005.

In Asia, HKH-FRIEND is working on water resources, floods, deglaciation, and water quality and there is a growing interest in environmental flows and ecosystem health. A new HKH-FRIEND website has been established providing information about the group's activities and is also the Internet platform for the Regional Hydrological Data Centre (Rees, 2004). Asia Pacific FRIEND is planning the publication of a fourth volume of a Catalogue of Rivers in Southeast Asia and the Pacific. The AMIGO group has been active in research on floods, droughts, climate change and eco-hydrology and in extending the project from the Caribbean to the whole of Latin America. Activities across FRIEND groups include developing a common database platform and websites for FRIEND AMIGO, AMHY and AOC regions. Table 2 illustrates the high priority given by FRIEND to capacity building and the transfer of research to the user community with over 28 technical courses being presented in the period 1995–2005, involving 400 participants from over 50 countries.

Table 2 Technical courses organized by regional FRIEND groups 1995–2005.

Region	Number of courses	Number of countries involved	Total number of participants	Topics
NE	3	10	60	Low flows
AMHY	1	7	25	Low Flows
SA	6	8	90	Data, GIS, extremes, modelling
Nile	3	10	30	Floods, droughts, modelling
HKH	11	10	177	Low Flows, sediments, water quality, glaciers, database
AP	3	20	45	Floods, water resources, low flows
AMIGO	1	12	20	Low Flows

Future FRIEND research

One of the key objectives of this conference (FRIEND 2006) is to develop a strategy for research for the next five year period. Proposals from each region are presented in Servat & Demuth (2006) and some typical examples of proposed research drawn from the Northern European group are summarized below. The Low Flow group will continue to be active in EU funded research and development programmes including the WATCH (Water and Global Change) project. The objective of the project is to analyse, quantify, predict and evaluate the uncertainties of the components of the current and future global water cycles. The impact of changes in drought frequency on water resources including the energy, industry, agriculture and water supply sectors will be evaluated. The group will also seek to develop the European Drought Centre to improve the coordination and dissemination of drought related research and operational experience in Europe.

The Large-Scale Variations group is developing a programme that includes seasonal river flow forecasting, understanding the impact of climate and land-use change on river basin functioning and publishing a textbook on hydrostochastics—presenting new approaches for interpolation and regionalization. The Extreme Rainfall and Flood Runoff Estimation group will focus on estimating the uncertainty of modelling extreme events. Topics will include estimating design hydrographs of long return periods from flood frequency simulation, using saturated area mapping to improve the performance of the TOPMODEL and using data on snow extent for improved modelling of snowmelt floods.

The Catchment Hydrological and Biogeochemical Processes group will maintain cooperation with the European Research Basin (ERB) group and participate in biannual ERB conferences. Specific research proposals include investigating the relationships between runoff generation

(including water chemistry) and catchment geology, geomorphology, climate, soils, land use and land management.

Although the current phase of the IHP has seen a growth in FRIEND both scientifically and geographically, future proposals for cooperation should be based on a realistic appraisal of the level of activity in the next biennium. In Europe there is continued success in obtaining EU research funds with a change of priority towards coupling hydrological and climate models at the pan-European scale. In contrast, the outlook in the HKH and Southern Africa region is much less encouraging following a reduction in funding from some development agencies. Although UNESCO funding can act as a catalyst for attracting research funds it will not alone be able to support FRIEND. In all regions FRIEND will continue to depend on active support by operational agencies, universities and research institutes. Except for the Nile region, a useful guide to the current geographic and thematic strength of FRIEND is provided by the papers accepted for FRIEND 2006 (Table 1). This indicates those regions where additional resources are needed to develop FRIEND and the more active regions where cooperation with associated international initiatives can be more easily developed, but perhaps is less essential.

CO-OPERATION BETWEEN FRIEND AND RELATED INTERNATIONAL PROGRAMMES

HELP

It is anticipated that any HELP led proposals for joint activities would be welcomed by the FRIEND community, although in many regions the FRIEND and HELP programmes are not active in the same area. There are clear opportunities to integrate current HELP activities in South America in specific basins, e.g. Panama Canal (Panama), Tacuarembo (Uruguay), Jequetepeque (Peru), Sao Francisco Verdadeiro (Brazil) and Chaguana (Ecuador), with proposed FRIEND research in the AMIGO region. The next HELP International Symposium will be held in South Africa and enable the benefits of focusing FRIEND activities on HELP Basins in the region, e.g. Greater Ruaha (Tanzania), Olifants (South Africa/Mozambique) and Thukela (South Africa) to be discussed. Consideration could be given to a full merger of the two cross-cutting themes in the region in order to optimize the limited financial and staff resources. The conference also provides an opportunity to identify opportunities for pan-African cooperation on HELP basins, e.g. Blue Nile (Sudan-Ethiopia-Egypt), Gash (Sudan-Eritrea-Ethiopia), Nakambé (Burkina Faso) and Upper Ouémé (Benin).

Operational applications of low flow research are most frequently carried out within the framework of national and international law and policy Directives. In Europe the most important of these is the Water Framework Directive (WFD), which has established a strategic framework for the sustainable management of both surface and groundwater resources. Many FRIEND participants are playing an important role in implementing the Directive through the development of national design techniques. In addition, FRIEND has contributed to a consultation document for developing a European drought Policy. These pan-European initiatives provide an opportunity for cooperation with the HELP community and the newly established UNESCO HELP Centre for Water Law, Policy and Sciences.

WMO

A major new WMO initiative is to produce three manuals on: low flows, water resource assessment and flood estimation. This provides an excellent opportunity to establish cooperation between these WMO working groups and FRIEND participants, following earlier examples of co-operation with WMO, including the publication on trend analysis (Kundzewicz, 2004).

PUB

The IAHS programme which has most in common with both FRIEND and HELP is PUB. Following the emergence of the PUB Science Plan in 2003 (Sivapalan *et al.*, 2003), a joint IHP-IAHS (PUB) Technical Liaison Group was established in Koblenz in May 2004 to identify potential synergies between these programmes. Bonell (2006) identified overlaps between these

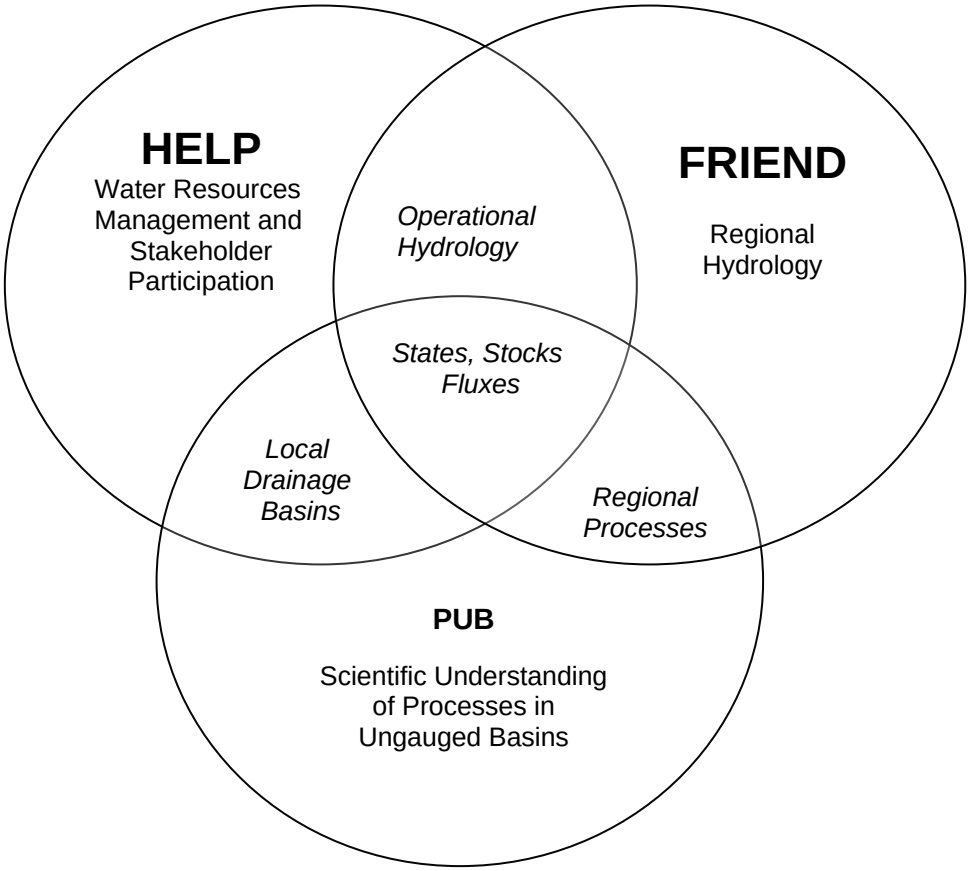


Fig. 2 The common intersections of PUB, HELP and FRIEND, (Bonell, 2006).

three global initiatives, summarized potential linkages and highlighted areas where programmes complement each other. All three initiatives have common interests but they each have a unique focus and user community (Fig. 2). Areas for co-operation between FRIEND, HELP and PUB include understanding of processes in pristine basins, watershed classification, comparative model evaluation, prediction of extreme events in ungauged basins under changing circumstances, and new technologies for measuring and monitoring of groundwater.

CONCLUSIONS

The success of both FRIEND and HELP is indicated by the decision of the Seventeenth Session of the Intergovernmental Council of the IHP held in July 2006 to continue both initiatives as cross-cutting themes in IHP-VII until 2013. This paper has summarized the key achievements of FRIEND, provided some examples of proposed future research and identified opportunities for improved cooperation with the HELP, PUB and WMO programmes. One issue which is common to all programmes and the links between them is the lack of financial resources and experienced man-power to deliver their objectives in most developing countries. The result is that all these initiatives are less well established in these regions and the potential for essential research and capacity building is often not realised. There continues to be a degree of duplication in the objectives of these programmes and it is of concern that new programmes are initiated but the total budget to support them is constant or declining. If the programmes described in this paper are to continue for a further decade then consideration should be given to rationalizing the content of each and holding a major joint conference every four years to improve communication and avoid duplication.

REFERENCES

Andersson, L. & Moody, D. W. (eds) 2004 Special Thematic Issue: Hydrology for the Environment, Life and Policy (HELP) Programme. *Int. J. Water Resources Development* **20**(3), 267–429.

Bonell, M. (2004) How do we move from ideas to action? The role of the HELP Programme. *Int. J. Water Resources Development* **20**(3), 283–296.

Bonell, M. (2006) HELPing FRIENDs in PUBs: Charting a course for synergies within international water research programs in gauged and ungauged basins. Invited commentary, HP*Today* in *Hydrol. Processes* **20**(4).

Bower, D., Hannah, M. & McGregor, G. R. (2004) Techniques for assessing the climatic sensitivity of river flow regimes. *Hydrol. Proces*ses **18** (13), 2515–2543.

Demuth, S., Gustard, A., Planos, E., Scatena, F. & Servat, E. (eds) (2006) *Climate Variability and Change – Hydrological Impacts* (Proceedings of the Fifth FRIEND World Conference). IAHS Publ. 308. IAHS Press, Wallingford, UK.

Gustard, A. & Cole, G. A. (eds.) (2002) *FRIEND—A Global Perspective 1998–2002*. Centre for Ecology and Hydrology, Wallingford, UK.

Lanen, H. A. J. van & Demuth, S. (eds) (2002) *FRIEND2002—Regional Hydrology: Bridging the Gap between Research and Practice*. IAHS Publ. 274. IAHS Press, Wallingford, UK.

Kundzewicz, Z. W. (ed.) (2004) Detecting change in hydrological data—Editorial. Special issue *Hydrol. Sci. J.* **49**, 3–12.

Meigh, J. & Fry, M (ed.) (2004) Southern Africa FRIEND Phase II 2000–2003, UNESCO Technical Documents in Hydrology no. 69.

Rees, H. G. (ed) (2004) HKH FRIEND 2000–2003 UNESCO Technical Documents in Hydrology no. 68.

Servat, E. & Demuth, S. (eds) 2006 *FRIEND - A Global Perspective* 2002–2006. Koblenz, Germany

Sivapalan, M., Takeuchi, K., Franks, S. W., Gupta, V. K., Karambiri, H., Lakshmi, V., Liang, X., McDonnell, J. J., Mendiondo, E. M., O'Connell, P. E., Oki, T., Pomeroy, J. W., Schertzer, D., Uhlenbrook, S. & Zehe, E. (2003) IAHS Decade on Predictions in Ungauged Basins (PUB), 2003–2012: Shaping an exciting future for the hydrological sciences. *Hydrol Sci. J.* **48**(6), 857–880.

Tallaksen, L. M. & van Lanen, H. A. J. (eds) (2004) *Hydrological Drought. Processes and Estimation Methods for Streamflow and Groundwater*. Developments in Water Science 48. Elsevier Science, The Netherlands.

Climate Variability and Change—Hydrological Impacts (Proceedings of the Fifth FRIEND World Conference held at Havana, Cuba, November 2006), IAHS Publ. 308, 2006.

Human impacts, complexity, variability and non-homogeneity: four dilemmas for the water resources modeller

TREVOR M. DANIELL[1] **& KATHERINE A. DANIELL**[2]

1 *School of Civil and Environmental Engineering, University of Adelaide, Cooperative Research Centre e-Water, North Terrace, Adelaide 5005, Australia*
trevord@civeng.adelaide.edu.au

2 *CEMAGREF/ENGREF, UMR G-EAU, France* and *Centre for Resource and Environmental Studies (CRES), Australian National University / CSIRO (CMIT), Australia*

Abstract Water modellers are commonly faced with a range of dilemmas due to the complex, uncertain and conflicting nature of the problems currently studied. The limitations of present techniques to deal with the variability and non-homogeneity of future data sets in complex water systems are examined. The main limitations are in part due to changing human behaviour and linked anthropogenic land- and water-use impacts, as well as the uncertainty of climatic variability. Suggestions and questions for future practice are raised, as are technical based methods which are more likely to provide successful outcomes for integrated river basin management.

Key words water resources; variability; complexity; resilience; non-homogeneity; human impacts; modelling; ANN; Australia

INTRODUCTION

The construction and use of models to support understanding and decision making for water resources management and planning questions have been commonplace in a number of forms for many decades. Water engineering and management training is predominately based on learning a range of modelling techniques (mainly quantitative), which allows series of data to be analysed and used for a variety of purposes including optimization, forecasting and short- and long-term predictions. This paper aims to investigate whether such techniques are sufficient for dealing with the water management and planning problems faced by today's (and tomorrow's) practitioners, especially when the issues of complexity, variability, non-homogeneity and human impacts linked to water resources are taken into account.

COMPLEXITY

In the last 40 years, there have been major changes in the work requirements for a water engineer or manager. Doubling of populations in cities, environmental degradation and resource depletion all pose challenges to resolving water management problems, fuelled by the complexity, uncertainty, and conflict surrounding these problems. On the other hand, the rapid advances in computing power, new technologies and availability of information have assisted in the resolution of these problems, although one could now argue that they are just adding to the complexity of problem resolution. There is a current push for "sustainable" water management and development that "meets the needs of the present without compromising the ability of future generations to meet their own needs" (WCED, 1987). This means that physical system attributes, economic constraints and environmental impacts need to be considered when trying to manage water resources sustainably, as well as recognition of people's beliefs, values and practices. Due to such needs, use of "systems approaches" (Forrester, 1961; Checkland, 1981) has been heralded as the way forward to sustainable water management.

Defining system sustainability and measures of system performance

Loucks (1997) defined system sustainability in terms of reliability, resilience and vulnerability. Various criteria in terms of economic, environmental and social measures also need to be determined. In water resources problems, a specification of performance levels for a particular system needs to be established. The system is then considered to be in a satisfactory or unsatisfactory state relative to the threshold performance value for a particular criterion. A more in-depth discussion of system sustainability thresholds can be found in Foley *et al*. (2003) and Daniell *et al*. (2005).

Copyright © 2006 IAHS Press

Reliability can be defined by the probability that a system will achieve satisfactory performance for a certain period of time. For example, if there is a system that only fails to achieve the threshold performance for 36 days in a year, then: Reliability = number of satisfactory performance days/total number of days, i.e. 329/365 = 90%.

Resilience measures how quickly the system recovers from failure. In the example above, if the system recovered the next day to a satisfactory performance in 30 days out of the 36 days, then the resilience of the system would be the number of satisfactory days following unsatisfactory performance/total number of unsatisfactory performance days, i.e. 30/36 = 83%.

Vulnerability of a system aggregates both duration of failure and the severity of the failure. What are the implications of having a data set with more variability? If measures of reliability, resilience and vulnerability are used for measurement of system performance, then a simple appraisal of modelling will show that changes of state need to be measured.

What state was the system in at the start of modelling? If a particular change in a model forces other systems to adapt, then those systems also should be measured in terms of reliability, resilience and vulnerability. This should be paramount for man-made systems, but what about natural systems that man has altered by changing flows and then tries to manipulate by reversing some of the flows? Can ecosystems be modelled against the same criteria as the man-made systems?

Even if it is possible to determine a number of criteria (or indicators) which the system can be measured against, another factor, the system scale under analysis, must also be decided upon. Systems occur within a seemingly infinite nested hierarchy of other systems, the behaviours of which are likely to have some impact on "the system" under examination. Considering the complexity of the majority of water resources problems, many system elements on a large scale may have a small effect on the problem being studied. It is suggested that unless these effects are considered to be significant, the minimum necessary system size to deal with the problem "adequately" should be sought. It is noted that this "minimum" system size may not be an explicit spatial scale, but could also be a "problem scale" (Loucks, 1998).

Problem formulation, politics and human values

Another question related to the complexity of water resources problems, which is more commonly avoided by modellers or managers, is how these problems are formulated. What the problem may be (or even if there is a problem) is relative to the point of view of the beholder. Whether this is the modeller who is attempting to inform or solve his/her problem, a manager or politician, or another "stakeholder" who sees the problem from an entirely different point of view, it is necessary to be aware from which point, or points, of view the problem has been investigated. This issue is closely related to the "system scale" choice previously mentioned, as both factors will significantly impact upon the solutions proposed and whether the model produced is of use for decision makers if it is not "their model", and what final mitigation strategies can perhaps be implemented or alternatively blocked by stakeholders.

Increasing conflict over problems such as the sharing of water resources has driven many management projects to a halt around the world. There are many examples of dam construction and grey-water recycling projects, amongst others, that have found themselves in this position. In the majority of these cases, the points of view and values of many important stakeholders were not sufficiently taken into account by the water management authorities at the earliest stages of these projects. Acceptance and use of models for aiding water resources management decisions are largely based on similar requirements for complex problems. If those stakeholders, who are to use or be affected by the decisions stemming from the use of a particular model, are not closely involved in the process of formulating the problem that the model is based upon, then there is a high chance of rejection of the model, its proposed solutions, and the final implementation. It is perhaps with this reasoning in mind that adding more "social stuff" (Nancarrow, 2005) to water models seems to be a current pre-occupation for those embracing the "sustainable and integrated" water management paradigms. However, exactly how these so-called "integrated" models are finally going to be used commonly appears less well thought through. It is suggested, therefore, that water modellers and managers decide prior to investing in these models: (a) Who will decide what the problem is to be studied in the model? (b) For whom and for what purpose is the model to be produced? (c) Will these

peoples' needs be met by the model? (d) Should these people be involved, and in which capacities, throughout the modelling process, from problem formulation to model use?

VARIABILITY

Rainfall and streamflow variability is generally measured by the coefficient of variation which is the standard deviation divided by the mean value of a record. Australia and South African rivers have the world's greatest variability (McMahon, 1988; Finlayson & McMahon, 1988). Many form into a series of water holes for some part of the year and sometimes for many years. This variability is shown in Fig. 1 by the coefficient of variation of annual flows (Cv) for rivers with catchments greater than 1000 km^2 with a Cv of 0.9 for Australia and a Cv of 0.73 for South Africa rivers. Australian rivers also have larger peak and annual floods (relative to mean annual runoff and catchment size) than rivers elsewhere in the world (Finlayson & McMahon, 1988). This characteristic of variability, when harnessing water, results in larger storages being constructed relative to the streamflow mean. The size of the storage as a multiple of the mean annual flow to achieve 80% use of the mean annual flow, at 95% reliability, is also shown in Fig. 1. This characteristic means that if climate change increases variability in rivers, much more storage will be needed relative to the present state; or expressed another way, the reliability will drop significantly as variability increases.

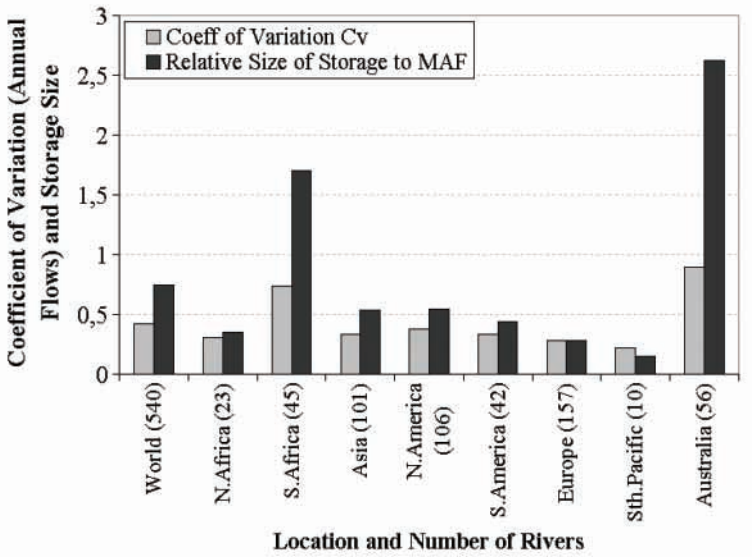


Fig. 1 Coefficient of Variation and Size of storage relative to Mean Annual Flow to achieve 80% draft of MAF at 95% reliability with catchments >1000 km^2 (adapted from data in Finlayson & McMahon, 1988).

Coping with changing variability

There are many contributing factors to increased variability. The way watersheds are cleared and managed, as well as climate change, already contribute to the variability of streamflow. Stream-flow from pristine catchments can be dramatically changed by bushfires, not just in quantity terms but also in quality terms. The variability of quality and quantity of flows is not only very dependent on anthropogenic activities, but also on seasons and climate. The design and modelling of systems to cope with this increased variability has not generally been considered by water resources managers.

Recently, there has been a push to manage rivers so that environmental and ecological systems are not destroyed by the resulting change in variability of flows due to water supply and hydro-electric schemes. This is an attempt to improve degraded ecosystems and get them to adapt to a different variability. This allocation of water for the environment is in turn forcing water supply authorities to change demands on the system by various strategies to match the reduced supply. A changing boundary of variability around both these systems is that due to climate change, where increased overall variability of rainfall, and hence runoff, will impinge on how water systems are managed. Most water supply authorities now look at demand management with

a focus on improving water use efficiency. Such methods of dealing with variability are therefore often linked to changing human behaviour, or at least encouraging the uptake of new technologies. It is human values and beliefs which largely govern whether such changes will be acceptable and whether conflicts over competing water uses and management strategies can be resolved. Exactly how to initiate change and incorporate competing human values into water related decision making practices should be a question that modellers reflect upon if their models are to be of practical use under variable and uncertain conditions.

HOMOGENEITY AND STATIONARITY

Where does homogeneity exist in a catchment? Certainly not in soil moisture, nor in soil types, nor in rainfall distribution for any event, nor in river flow, nor in evaporation, nor in land use as there is always a different distribution of vegetation dependent on non-homogenous factors such as moisture, radiation, fauna, temperature and soil types. Perhaps the only valid assumption of homogeneity is in time (but maybe not for a quantum physicist!). So our catchment is non-homogeneous; but what of the flow records emanating from it? Statistical tests on streamflow information to test homogeneity are commonly performed, but how valid are these? Vogel *et al.* (1998), in a major study of 1500 rivers for persistence, concluded that it only confirmed their "inability to discern the complex long-term persistence structure of natural flow records due to the fact that only short records are available. Assessment of the long-term persistence structure of actual flow records is further confounded by non-stationarity and non-homogeneity of those flow records".

Data are considered to be non-stationary if trends are present over time. It could be said that the assumption of *stationarity* has persisted because generally historical records of data are too short to accurately detect *non-stationarity*. For flood frequency analysis, data are examined for the statistical criteria of independence, stationarity and homogeneity. Anyone who has been involved in frequency analysis knows that removing outliers is necessary to develop a seemingly correct distribution. However, in reality, the "correct" probability distribution of extreme events has changed over time as frequency analysis models have developed that can cope with the non-stationarity aspects of trends, jumps and different causal mechanisms. Many researchers are working on frequency analysis methods and regionalization, and Kuczera & Franks (2004) highlight the non-homogeneous nature of flood peaks related to Interdecadal Pacific Oscillation events. Short-length data sets can meet homogeneity and stationarity considerations but in longer timeframes the climate causal mechanisms can relate to two or more populations of floods. Are the outliers the most important data points in a small data set? When confronted by an "outlier" flood event due to a landslip or a bushfire on a catchment, can it be justified that it was an unusual event and does not fit the homogeneous assumption for analysis? How often will this type of an event occur in 1000 years? Alternatively, if in a data set of 1000 years there were floods due to snow melt and there have been no significant snow falls for 200 years, is it reasonable to use the full data set for developing a frequency distribution? The issues of homogeneity and stationarity are ever present.

MODEL DILEMMAS AND EXAMPLES

We believe that there is no panacea for dealing with complexity, human impacts, variability and non-homogeneity in water resources problems, related data and their modelling processes. However, increasing general awareness of the importance of such issues is vital to improve water management and planning practices.

Modelling requirements and techniques—questions for reflection

Is it possible that if complexity, uncertainty and variability are too great, traditionally employed quantitative techniques may not be useful, or even possible, to use? In this case, would it be better to use qualitative techniques (such as cognitive mapping, causal diagrams or qualitative physics) or deliberation to find and debate management strategies or problem solutions (followed by cycles of monitoring and evaluation, continuous improvement and adaptive management)? One problem

decision makers encounter when using most models is not knowing the range of uncertainty and potential errors related to outputs (or even inputs, in the case of varying qualities of data sets), and the assumptions employed in the model design. This often means that decision makers discard models and base their decisions on other information. If this is the case, should the model have been made in the first place, should another technique have been used, or should the decision maker have been more involved in the modelling process (i.e. “participatory modelling”)?

Considering that the defined problem requires a model for a defined purpose, the next question is to determine what data is available and its quality. Depending on the type and quality of this data, as well as the final purpose of the model (optimization, prediction, forecasting, increasing understanding through scenario analyses), a relevant modelling technique may be chosen. For example, conventional deterministic or probabilistic models could be used with good quality quantitative data, as could data mining techniques such as Artificial Neural Networks (ANNs). Results for an ANN rainfall–runoff model developed for the Scott Creek catchment, an APFRIEND River (RSC, 2000), are shown in Fig 2. The results show how reasonably well behaved these models can be with suitable validation data. These models are not good at predicting outside the data regime that they were trained and tested on, but research is being carried out with Bayesian approaches to enhance their forecasting ability. The dilemma of the modeller here is to decide whether predictions can be made from current data, and which data are relevant to include.

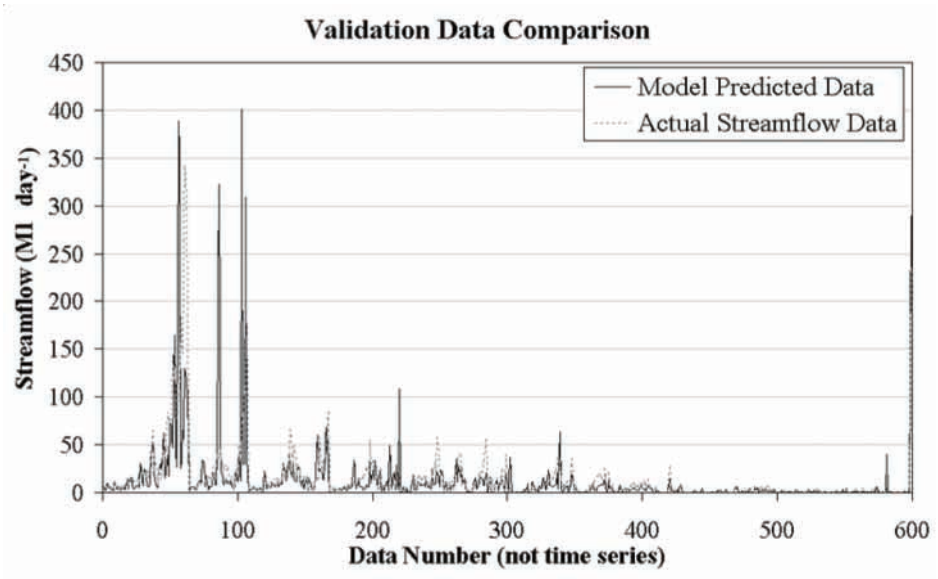


Fig. 2 ANN modelling results for Scott Creek in South Australia.

With lower quality quantitative data (or simply less data), techniques more capable of incorporating uncertainty or error bounds, such at Bayesian Networks or Markov Chains, may be more applicable. If qualitative and quantitative data need to be incorporated into a model, such as human behaviour, opinions, beliefs, goals and expert information, then modelling methods such as multi-agent systems could be used. A good example of such multi-agent systems modelling applied to water management in the Pacific island of Tarawa is given in Dray *et al.* (2006).

FINAL REMARKS

Although we can offer no definitive answers to water modellers who are (or will be) attempting to cope with the issues of variability, complexity, non-homogeneity and human impacts, we believe that it could be beneficial to reflect more deeply on a range of issues including:

(a) How, for whom, and for what purpose the models are being produced;

(b) How measures of resiliency, reliability and vulnerability can be used to monitor and more effectively manage water systems;

(c) What possible changes in current or future conditions (i.e. sudden climatic shifts or behavioural changes) could render data-driven models irrelevant;
(d) What methods (modelling or otherwise) are needed to cope with today and tomorrow's complex, uncertain and variable conditions; and
(e) Whether more data collection (i.e. streamflow, spatial climatic data) is needed so that changes can be identified.

REFERENCES

Checkland, P. B. (1981) *Systems Thinking, Systems Practice*. J. Wiley & Sons Ltd., Chichester, UK.

Daniell, K. A., Foley, B. A., Kingsborough, A. B., Maier, H. R., Malovka, D. J. & Sommerville, H. C. (2006) The AUSTIME methodology: quantifiable sustainability assessment coupled with multi-agent simulation. In: *Sustainable Urban Development: the Environmental Assessment Methods* (ed. by M. Deakin, P. Nijkamp, G. Mitchell & R. Vrekeer). Routledge, London, UK, (in press).

Dray, A., Perez, P., Jones, N., Le Page, C., D'Aquino, P., White, I. & Auatabu, T. (2006) The Atoll Game Experience: from knowledge engineering to a computer-assisted role playing game. *JASSS* **9**(1) http://jasss.soc.surrey.ac.uk/9/1/6.html.

Finlayson, B. L & McMahon, T. A. (1988) Australia *vs* the World: a comparative analysis of streamflow characteristics. In *Fluvial Geomorphology of Australia* (ed. by R. F. Werner), 17–40. Academic Press, Sydney, Australia.

Foley, B. A., Daniell, T. M. & Warner, R. F. (2003) What is sustainability and can it be measured? *Aust. J. Multidisciplinary Engng* **1**(1), 1–8.

Forrester, J. (1961) *Industrial Dynamics*. Productivity Press, Cambridge, Massachusetts, USA.

Kuczera, G. & Franks, S. (2004) At site flood frequency analysis. In: *Australian Rainfall and Runoff*, book 4, chapter 2. Engineers Australia (draft).

Loucks, D. P. (1997) Quantifying trends in system sustainability. *Hydrol. Sci. J.* **42**(4), 513–530.

Loucks, D. P. (1998) Watershed planning: changing issues, processes and expectations. In: *Water Resources Update 111*, 38–45. Universities' Council on Water Research, Illinois, USA.

McMahon, T. A. (1988) Droughts and arid zone hydrology. *Civil Engineering Trans.* (*Inst. Engrs Australia*) **CE30**(4), 175–186.

Nancarrow, B. E. (2005) When the modeller meets the social scientist or vice-versa. In: *MODSIM2005 International Congress on Modelling and Simulation* (ed. by A. Zerger & R. M. Argent), 38–44.

RSC. (2000) Catalogue of Rivers for Southeast Asia and the Pacific, vol. 3. (ed. by P. Hidayat, A. W. Jayawardena, K. Takeuchi S. & Lee). UNESCO-IHP Regional Steering Committee (RSC) for Southeast Asia and the Pacific.

Vogel, R. M., Tsai, Y. & Limbrunner, J. F. (1998) The regional persistence and variability of annual streamflow in the United States. *Water Resour. Res.* **34**(12), 3445–3459.

WCED (1987) *Our Common Future*. Oxford University Press, Oxford, UK.

2 Data

Databases *19–50*

Networks *51–67*

GIS *68–96*

Climate Variability and Change—Hydrological Impacts (Proceedings of the Fifth FRIEND World Conference held at Havana, Cuba, November 2006), IAHS Publ. 308, 2006.

SIEREM: an environmental information system for water resources

J. F. BOYER, C. DIEULIN, N. ROUCHE, A. CRES, E. SERVAT, J. E. PATUREL & G. MAHÉ

UMR HydroSciences Montpellier, IRD, BP 64501, F-34394 Montpellier cedex 5, France
boyer@msem.univ-montp2.fr

Abstract The joint research unit "HydroSciences Montpellier" (HSM) aims to study hydrological variability on the African continent. SIEREM, an environmental information system for water resources, has been developed at HSM. The POLLEN method was used to design and achieve this successful system. This method is adapted from the OMT (Object Modelling Technique) method, which is specific to the design of environmental information systems. The main part of the analysis technique consists of modelling the data, i.e. identifying the objects of the system, defining their structure and describing their relationships. The information system is then described according to the different services it has to fulfil. This permits one to define the processes asked for by the users and to provide a description of the functions and algorithms. The system is thus divided into sub-systems. Each one is described according to its interface, the piece of software implemented, the managed object classes and the services provided, and the relationships with the other sub-systems. The final result of this information system is a package of different software products. Depending on their rights and needs, the users get specific accesses to information. Each information type, such as a GIS layer or a rainfall chronicle, is managed in every different product of the system. The public can get metadata through the web site, a researcher in the laboratory can work with the data using the Orion software, etc.

Key words GIS application; DBMS; web interface; environmental base of knowledge; water resources; hydrological modelling; West and Central Africa

INTRODUCTION

SIEREM was developed as a tool to help rainfall–runoff models. The area on which these models are used is West and Central Africa. It was required to also be useful for explaining, *a posteriori*, possible variations in this area of the world. And finally, another objective of SIEREM is to provide data inventory and software tools to help the end users to manage, select and handle the information.

The development of SIEREM started in 1999 with two simultaneous phases: data collection and the system analysis and design. The challenge was to build a system with both chronological data and spatialized information (such as soil, vegetation and DEM layers). HydroSciences Montpellier formed a team of engineers to start three tasks: collection of hydro-meteorological data and metadata, collection and building-up of geographical information, and the required data homogenization and integration into an environmental system built using a specific method of system analysis and design.

THE SYSTEM ANALYSIS AND DESIGN METHOD

The method used is POLLEN (Gayte *et al.*, 1997) adapted from the OMT method (Rumbaugh *et al.*, 1991). This method is based on two simple principles: graphical representation and respect of the logical steps in the software life cycle such as: the conceptual modelling of data (object diagram, dictionary), process modelling (functional model, function dictionary) and system, sub-system and reservoir identification (system diagram, dictionaries, etc.).

CHRONOLOGICAL DATA CONCEPTUAL MODELLING

The chronological data are measurements done at one time in one place. All the object modelling which describes such type of data is described and the description of the place, the date of the measurement, the person who measured out, and the owner of the data. Figure 1 shows how the modelling of the chronological series in SIEREM operates.

Copyright © 2006 IAHS Press

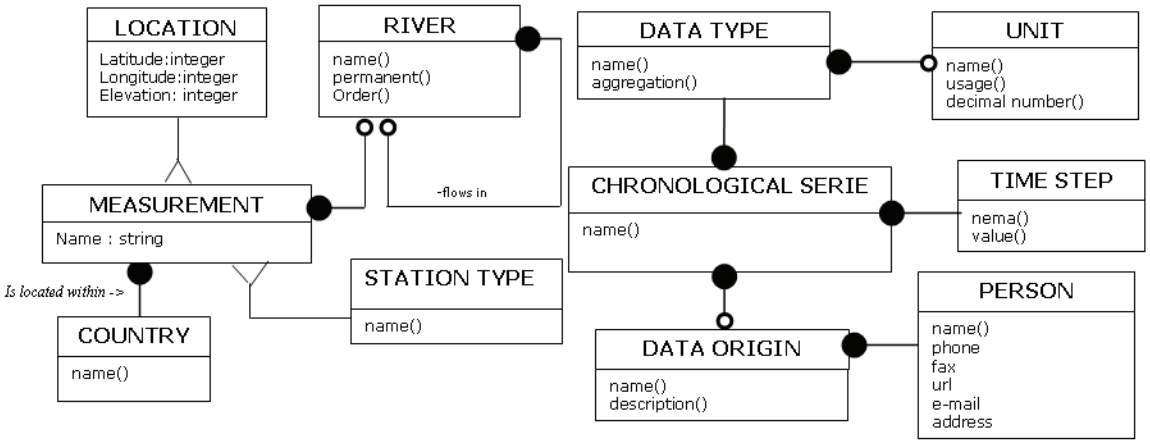


Fig. 1 The conceptual modelling of chronological data.

SPATIAL DATA MODELLING

POLLEN provides special classes called “abstract classes”, for designing the basic spatial objects. There are three abstract classes: **point**, **line** and **polygon**. Using these classes, it is easy to build derived classes with point, line and polygon geometric structures. Those derived classes will design surface areas with geometric and topological properties. Figure 2 displays an example of the use of the abstract classes to build a conceptual model of a basin and a river.

Another type of class provided by the method is the opaque class. This type permits modelling free of the GIS internal structure and consideration of only the function provided by the class. The DEM object is a good example of an opaque class and, with this facility, can be integrated into the design diagram.

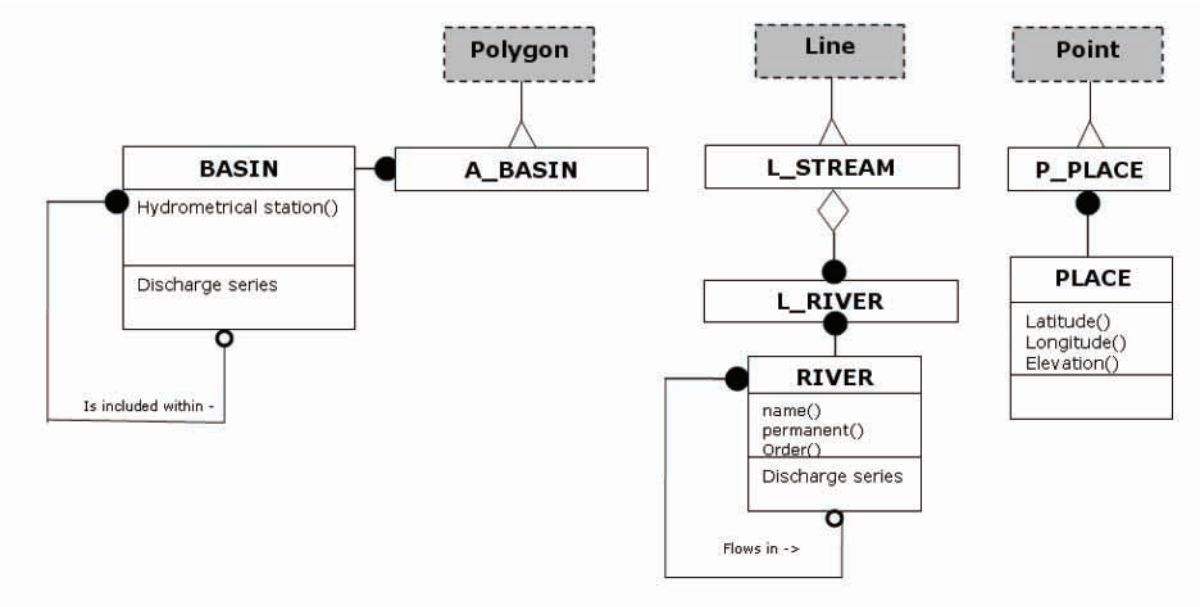


Fig. 2 Part of the conceptual modelling of spatial data.

FUNCTION MODELLING

The function model is another part of the POLLEN method. The aim is to identify the different functions provided by the system, such as the chronological series management which allows one to create and to exploit personal sets of series, and the website, which displays GIS layers and station metadata to the public.

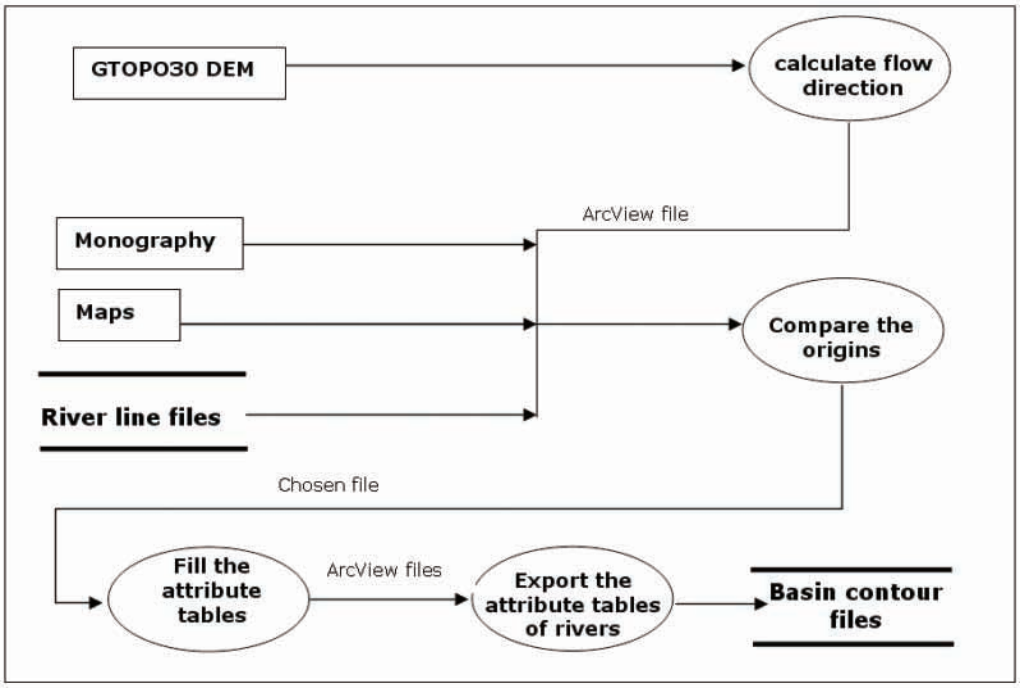


Fig. 3 Example of a functional model. Data flow diagram for the processing of basin contours.

The answer is the accurate identification of data used by the functions and the flow of information that the system has to manage. Figure 3 displays the data flow diagram for the processing of basin contours. At this step of the analysis, there is a good knowledge of what are the devices and the information needed to create the information set called “basin contour”.

SYSTEM CONCEPTION DIAGRAM

The system conception step is the description of the system in an architecture closer to the final system. Figure 4 displays the system diagram with the nodes representing sub-systems and lines representing the links between them. Two principal tasks are required at this step of the achievement of the system design: the sub-system identification, which allows separation into sub-systems corresponding more or less to the future pieces of software of the system, and the reservoir identification which points out the sub-system dedicated exclusively or not, to the data storage.

SUB-SYSTEM INDENTIFICATION

The data warehouse sub-systems are drawn with a bold frame on Fig. 4. The users of the different sub-systems are represented with the two different levels. The first level is the technician who is the information system builder, updating data with appropriate criteria and scale. The second level is either the hydrologist or the researcher. This type of user is considered as a final user of the system using the information as an entry for another piece of software such as a GIS application or hydrological modelling software.

For example, the sub system *Chronological data management* operates the data entry, update, extraction and inventory for the hydrometeorological data. The sub-system *DBMS*, provides data and metadata management, etc.

DATA RESERVOIR IDENTIFICATION

This task is quite simple but it is very important to identify it properly in order to be sure that the data reservoir structure fits with the data classes stored. In the SIEREM case, there are three

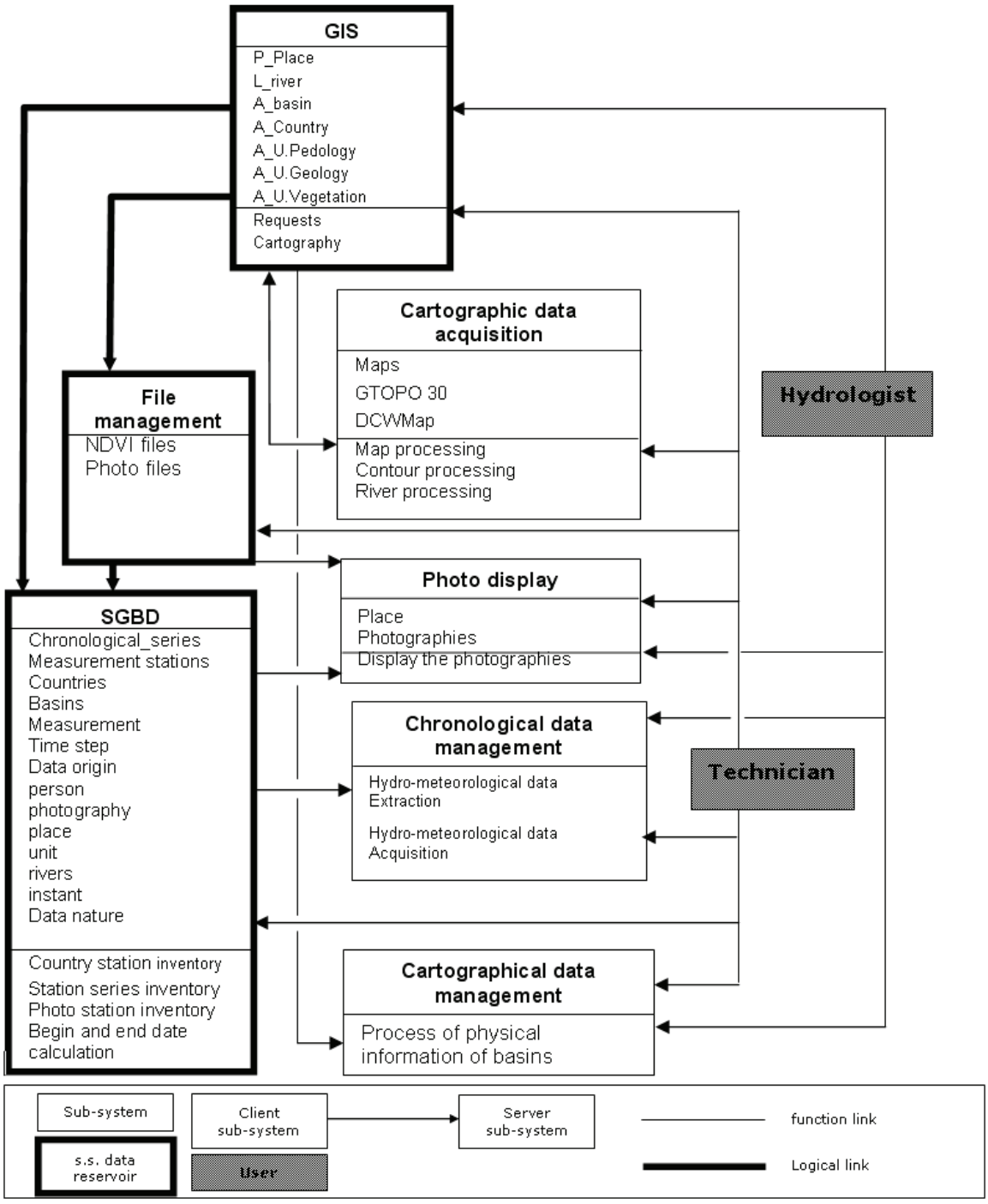


Fig. 4 SIEREM system diagram.

reservoirs: the *DBMS* to store the chronological data and metadata, the *files system management* to store logically picture files, NDVI files, and photography files and the *GIS* to store spatial information.

Integrity links exist between these three systems because all information refers to the metadata managed by the DBMS. The implementation and the checking of these integrity links are assumed to be conducted by the technician.

THE DEVELOPED PROCESSES

There are mainly five client applications using the SIEREM resources. First of all HydroSciences Montpellier implemented a stand-alone piece of software called “ORION” which is the main tool

for researchers to build most of the hydrometeorological data set for their modelling session. The second part is the web site that allows the publication of the systems content and result products. The third client of SIEREM is made of some pieces of software implemented by HydroSciences Montpellier and called “Plateform”. This set brings together model algorithms and puts the results interpretation procedures at the researchers’ disposal. The fourth client is the software ArcGIS which provides all GIS functions for using and working with the spatial data layers and linking them with the chronological data sets. The fifth client is the set of all applications which came with the DBMS MS SQL Server for the administration of the database. Database administration mainly means all the tasks linked to the security management of the system and all the automatic backup functions. The first two clients are detailed below.

THE ORION SOFTWARE

This stand-alone piece of software is the toolbox used by the researchers on their own computers to choose, select and extract their data set to use either for statistical calculation or for running models. Of course, the data access criteria are targeted at hydrological parameters, i.e. basin, type of measurement station, origin of data, data consistency, etc. Therefore, Orion also provides a large format of extracted data and some tools to present and publish inventory or data yearbooks.

SIEREM WEB SITE http://www.hydrosciences.fr/sierem

The aim of the SIEREM web site is to provide to the scientific community with the metadata of all the environmental information managed in the project and the major scientific results produced. First of all, the web site displays through various ways of selection, the metadata on the hydro-meteorological set used by HydroSciences Montpellier to carry out their research. In this way, the web site tries to list the contacts of all national departments in Africa in order to permit everyone to ask for data. Figure 5 displays the sequence of screens in order to obtain information about chronological data.

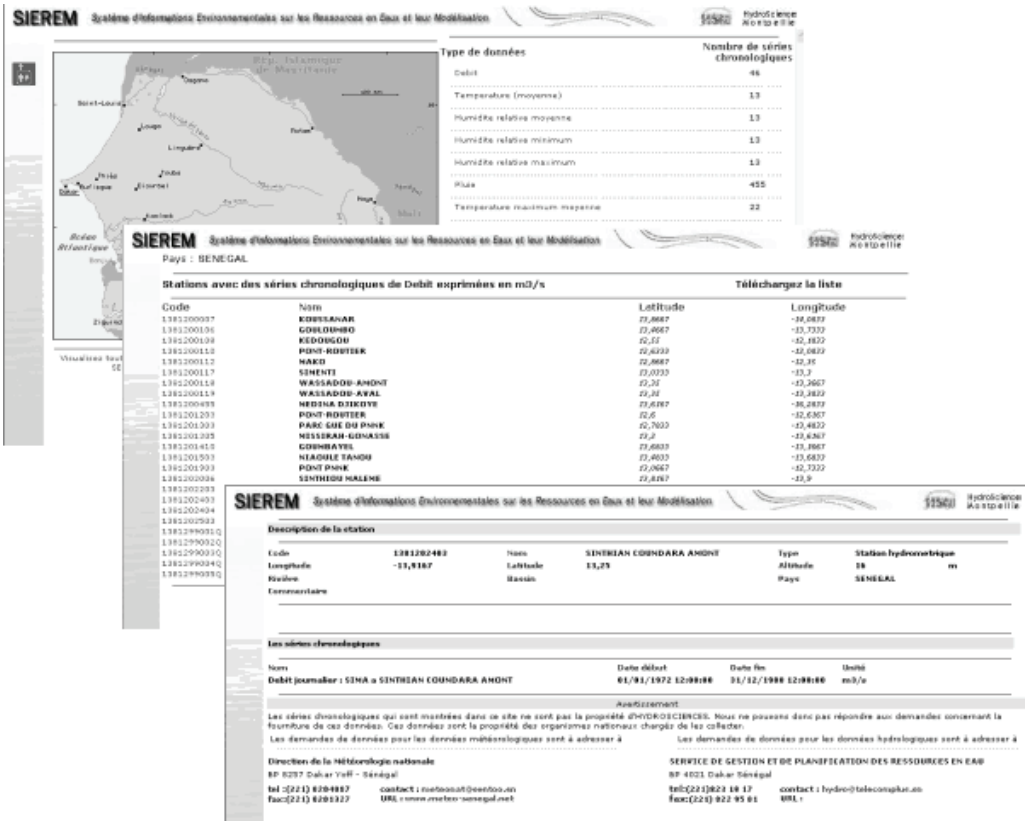


Fig. 5 Series of web site windows concerning the metadata on hydrometeorological chronological series.

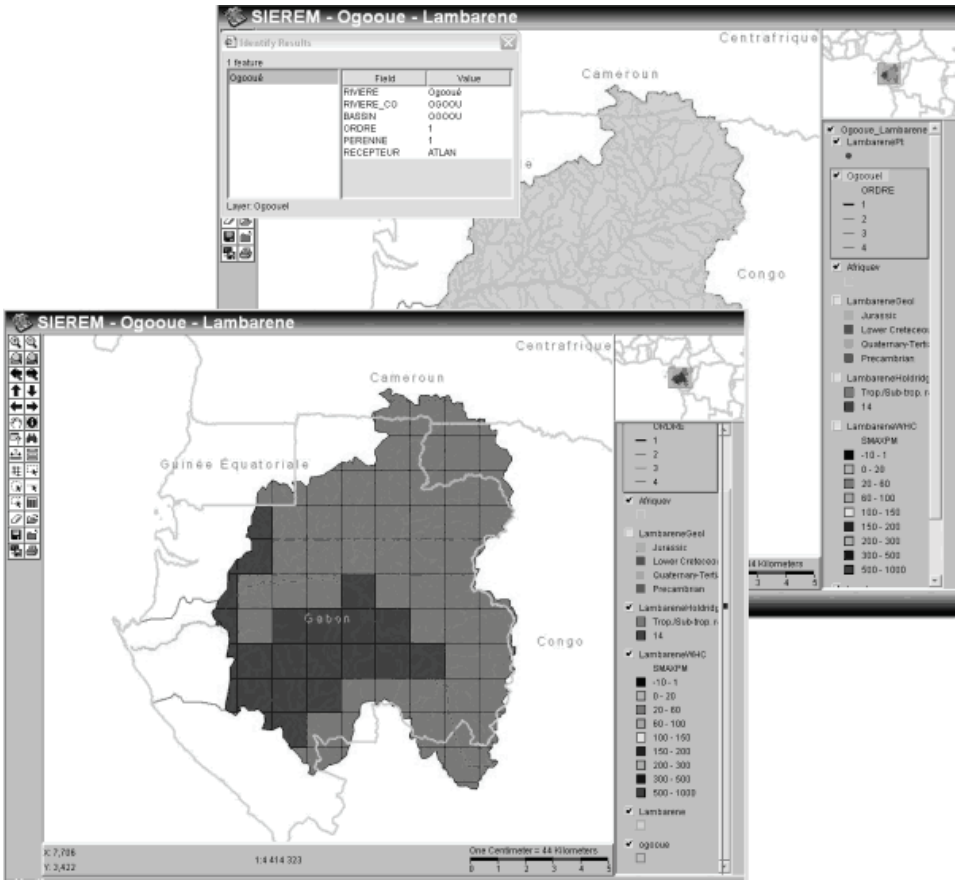


Fig. 6 SIEREM Web GIS application: the Ogoowe basin example.

Another important part of the website is the GIS application. This function runs under an ARCIMS software and provides GIS layers implemented by HydroSciences Montpellier. This application gives users several GIS tools to work with the SIEREM spatial information. It also provides the possibility of creating personal work sessions by adding and processing one's own GIS layers into the application. Figure 6 shows the web GIS application for the Ogoowe basin.

There are two other important sections in the web site. First, the landscape pictures section which is an attempt to build a significant base of African landscapes in terms of soil and vegetation cover information as well as a (not exhaustive) catalogue of the principal hydraulic installations. The second part is the product section. This allows HydroSciences Montpellier to provide for download several hydrological and research products, e.g. the entire data grid used by the team for their modelling session.

There is also free access to download the metadata of the hydrometeorological series, all basin boundaries and all basin hydrographic network data. This part of the website is specially built in order to enhance the knowledge of the scientific community in Africa and to assist the African national services in their efforts to provide good environmental data.

Therefore, SIEREM provides a large set of tools with which to access the information. The system was built in order to distinguish between some classes of users and this is carried out by the piece of software every user is allowed to use.

For example, everybody can check the runoff series metadata for the Ogoowe basin through the web site. Also, everybody can also download the GIS layers for the Ogoowe basin, such as the hydrographic network or the Water Holding capacity grid, and so on. Using Orion, all researchers and students working on the HydroSciences Montpellier network can choose a set of runoff series on the basin. Orion provides functions to extract the time series in several formats, to copy and aggregate them to other time steps. With other SIEREM tools the researchers can calculate their own mean rainfall grid from a chronological series data set built with Orion. And at last, they can run their modelling session with this information package.

CONCLUSION

Computer science has an important role in the management of the very heterogeneous sets of data involved in the development of environmental information systems. The problems posed to computer scientists are of many kinds: information must be located, information must be dated, information are heterogeneous and metadata must be linked to the information.

Given the importance of such systems, which are now used systematically in every large-scale project, the analysis methods must be homogenized too. In this context, POLLEN brings an attempt to define the design and the analysis. A big effort must be made by the project managers of such systems to carry and to adapt old systems to the ISO 19115 metadata norm. SIEREM is totally compatible with this norm.

REFERENCES

Rumbaugh *et al.* (1991) *Object-Oriented Modeling and Design*. Prentice Hall, Englewood Cliffs, New Jersey, USA.

Gayte, O., Libourel, T. *et al.* (1997) Conception des systèmes d'informations sur l'environnement—HERMES. Collection Géomatique.

Climate Variability and Change—Hydrological Impacts (Proceedings of the Fifth FRIEND World Conference held at Havana, Cuba, November 2006), IAHS Publ. 308, 2006.

Operational management of hydrological extremes using global-scale atmospheric models

ARNOLD H. LOBBRECHT[1,2], **SCHALK JAN VAN ANDEL**[1] **& FRANS VAN KRUININGEN**[3]

1 *Department of Hydroinformatics and Knowledge Management, UNESCO-IHE Institute for Water Education, PO Box 3015, 2601 DA Delft, The Netherlands*
s.vanandel@unesco-ihe.org

2 *HydroLogic BV, PO Box 2177, 3800 CD Amersfoort, The Netherlands*

3 *Hoogheemraadschap van Rijnland, PO Box 156, 2300 AD Leiden, The Netherlands*

Abstract Many places on Earth face both droughts and floods. There is no argument about the desirability of preventing droughts and floods or at least mitigating the negative consequences of these hydrological extremes. Operational management of controlled water systems enables efficient use of water resources by considering system states and system requirements throughout the entire water system. Developments in meteorological products can be used more effectively in operational water management as is shown for a regional water system in The Netherlands. The case study applies early control actions to manage extreme precipitation events. It is shown that global-scale ensemble weather forecasts from the ECMWF can be used to decide on early control actions in medium-scale regional water systems. Economic pressure and scarcity of water, land, and time, demands that we use all available information to optimize operational water-system control.

Key words The Netherlands; water-system control; floods; weather forecast; EPS; precipitation; event analysis; storage basin; pumping strategy

INTRODUCTION

Up to now, most research, management and policy efforts have been focused towards solving the two problems of droughts and floods separately. With the growing insights into the hydrological cycle and the interdependence of the different components of natural and anthropogenic systems, the need for integrated water resources management becomes more and more accepted. The ability to analyse the water system at larger spatial (catchments) and temporal (seasons, years) scales has improved considerably over the past years. It enables the water community to look for management practices that benefit both drought and flood management on the local and catchment scales.

One such practise is real-time control (RTC) of water systems. Real-time control is meant here following Schilling's (1990) definition of controlling the system while the process or disturbance is evolving. Since real-time control of water systems has developed from local control to central control (Lobbrecht, 1997), it enables efficient use of water resources by considering system states and system requirements throughout the entire water system. In central control, several structures, controlling different sections of the water system, are operated in such a way that the water is optimally distributed within and discharged from the system. In the context of flooding, this prevents failure of one section of the system while other sections still have storage capacity left. Another development is that not only measurements of target variables, such as water levels, but also measurements of disturbances, such as precipitation, determine the control strategy (feed-forward control). To predict the effects of these disturbances on the target variable, water-system response models, often embedded in decision support systems, are being used.

There are currently many reasons to put effort in further development of water-system control:

(a) Many controlled water systems still face problems during extreme events.
(b) Apart from long-term (structural) prevention and mitigation strategies, there is a need to do what we can with the water systems we have now.
(c) Climate change effects the hydrological cycle posing the need for more flexible water management practices.
(d) New meteorological observations and forecasts have been (further) developed such as radar, satellite and ensemble forecasts (Lobbrecht & Loos, 2004).

These developments in meteorological products can be used more effectively in operational water management. Meteorologists incorporate the needs of water managers in the development of their products and water managers are becoming more aware of the potential of present-day meteorological data.

Copyright © 2006 IAHS Press

Precipitation, while being the main disturbance, is still the most difficult variable to measure. Ground-based and satellite radar provide means to capture the spatial variability of precipitation more accurately, thus allowing us to make improved estimates of the initial system state and extreme events. Satellite-derived precipitation estimates and output from global weather forecasting systems become globally available. These data can be used not only for operational management of large-scale sea defence systems and river systems, but also for medium-scale regional systems (dams, irrigation schemes, and polders). The meteorological products provide high potential for water management in areas with few ground measurement stations and an absence of communication infrastructure (ungauged catchments).

This paper describes a way to improve the operational management of a controlled, regional water system, using a global weather forecast model to decide on anticipatory control actions.

ANALYSIS SETUP

Precipitation forecasts from the Ensemble Prediction System (EPS) of the European Centre for Medium-Range Weather Forecasts (ECMWF, 2006) were used to enhance the water-system control of a low-lying regional water system in The Netherlands. The excessive precipitation event of September 1998 that resulted in high water levels and extensive flooding in The Netherlands was selected. The accuracy of the global ECMWF EPS precipitation forecast for this event was assessed. The historic effects of the precipitation event on the water level in the channelled storage basin of the water system were analysed together with the pumping strategy. A water-system control model was applied to see whether the weather forecast could have been used to reduce the water levels.

CASE STUDY AREA

Rijnland is a polder area in the western part of The Netherlands, bordering the North Sea. The total area is about 100 000 ha of which 72% is occupied by low-lying polders, 15% by free draining areas (high-land) and 8% by dunes. A storage basin, consisting of inner connected channels and lakes, occupies 4500 ha. The storage basin serves to collect all the excess water of the Rijnland area, before it is discharged to the main water system of The Netherlands and finally to the North Sea. The low-lying polders would be subject to flooding if they were not protected by dykes and the excess water would not be pumped to the storage basin. The water level in the storage basin is kept between pre-defined bounds by daily operation of four pumping stations with a combined capacity of ~150 $m^3 s^{-1}$. Hoogheemraadschap Rijnland waterboard is the responsible water authority.

The Rijnland area has recently faced both extreme precipitation events (1998, 2000) and droughts (2003). Next to structural measures, the waterboard seeks to enhance the daily operational management. The ensemble prediction system (EPS) precipitation forecasts of the ECMWF, which are globally available, are tested for their applicability in setting the pumping strategy. The ECMWF EPS has been chosen, because of the long forecast horizon, up to 10 days ahead, and because it gives an estimate on the full range of possible events together with an estimate of the probability of these events to occur.

DATA

The ECMWF EPS prepares 50 different initial conditions for the global circulation model. The assumption is that the disturbances of deterministic (best guess) initial fields are determined in such a way that the 50 new ensemble members are uniformly distributed with equal probabilities (P = 0.02). Research has shown that for The Netherlands, in reality, the higher and lower ensemble members have higher probability of occurrence than the middle ensemble members (Bokhorst & Lobbrecht, 2004). Since the year 2000, the ECMWF has also included variations of parameterizations. The model is run twice a day to produce output for the entire world and the output consists of 50 atmospheric states (expressed in a number of variables, e.g. precipitation, humidity, wind, etc.). The variables are provided for a 6-hour time step, up to 10 days ahead, expressed in grid-averaged values of approx. 80 × 80 km grid-cells (Reduced Gaussian Grid). The ECMWF supplies time series of the 50 runs of selected variables, such as precipitation and evaporation,

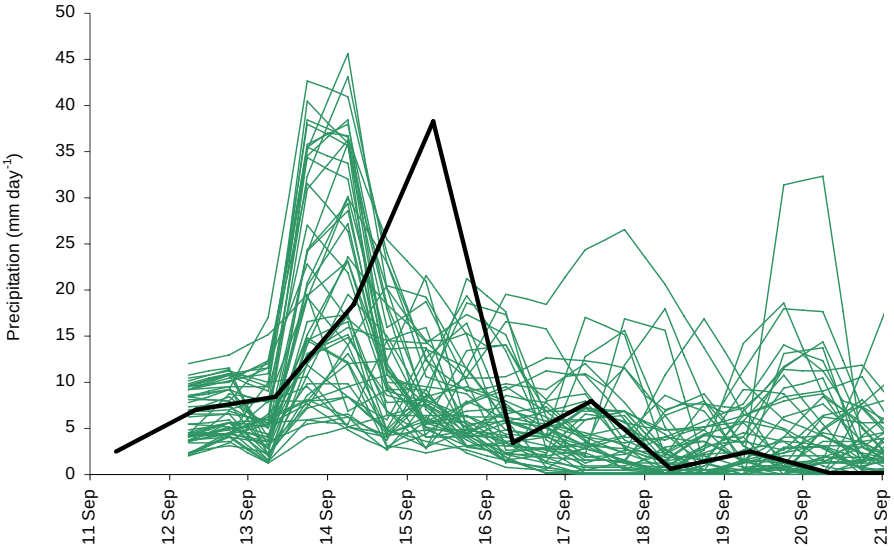


Fig. 1 Area-average measured precipitation in the Rijnland area (thick line) and ECMWF EPS precipitation forecast for the central part of The Netherlands (thin lines). The first day does not display a forecast, because the forecast precipitation volume is accumulated over a day. Forecast time: 12:00, 11 September 1998.

interpolated to requested locations, to national weather institutes. The Royal Dutch Meteorological Institute (KNMI) provides the 50 perturbed time series to water management authorities. The precipitation forecasts of the selected event in September 1998 are presented (Fig. 1).

Daily precipitation data for 16 measurement stations from the KNMI have been used to estimate area-average rainfall in the Rijnland area.

The waterboard operates a telemetry system that contains six water-level stations recording at a 10-min interval. These data were used to analyse the water-level development during the extreme event of September 1998. The operation of the pumping stations is also available. The pumping strategy before and during the precipitation event is analysed.

RESULTS AND DISCUSSION

The area-average rainfall in the Rijnland area on 15 September 1998 was 38 mm (Fig. 1). A forecast precipitation rate of greater than 15 mm day^{-1} is presently used by the waterboard as a warning threshold to consider starting pumping. The ECMWF EPS ensemble interpolated to the station nearest to the Rijnland area shows a very good signal already three days ahead. Half of the 50 members give a forecast for 14 September of 15 mm or more (Fig. 1). However, the precipitation was forecast too early. The precipitation event occurred on 15 September. For anticipatory control actions this does not have to be a problem. Note that this very good result is taken from the ECMWF EPS output directly, showing the applicability of this global model for regional to local extreme precipitation events in The Netherlands.

During normal conditions the four pumping stations are operated such that the area average water level is maintained within a narrow range of 0.15 m. The lower boundary is –0.65 m + NAP (Dutch reference level ≈ mean sea level). Below this level, the risk of (economic) damage increases, due to reduced bank stability of peat dykes, hindrance to navigation or obstruction of houseboats. The upper boundary is –0.50 m + NAP. Above this level the waterboard starts taking emergency measures, like stopping the pumping from the polders to the channelled storage basin. These measures are taken to prevent breaching of the embankments of the storage basin, but may lead to flooding problems in the polder areas.

The event of 15 September did not result in flooding problems in this water system, fortunately. Water levels at the centre of the water system show, however, a rise up to a water level of –0.52 m + NAP (Fig. 2). This shows that the pumping capacity on that day was not sufficient to discharge the hydrological load caused by the heavy precipitation event. High water levels can then only be prevented by lowering the water levels in the storage basin before the start of the precipitation event.

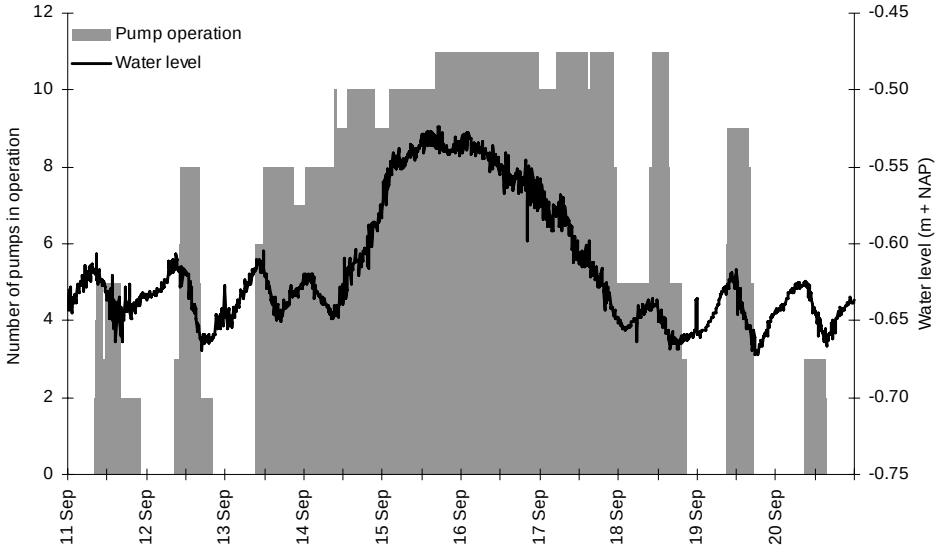


Fig. 2 Pump station operation and water levels (above mean sea level) in the channelled storage basin at the central measurement station of the Rijnland water system, September 1998.

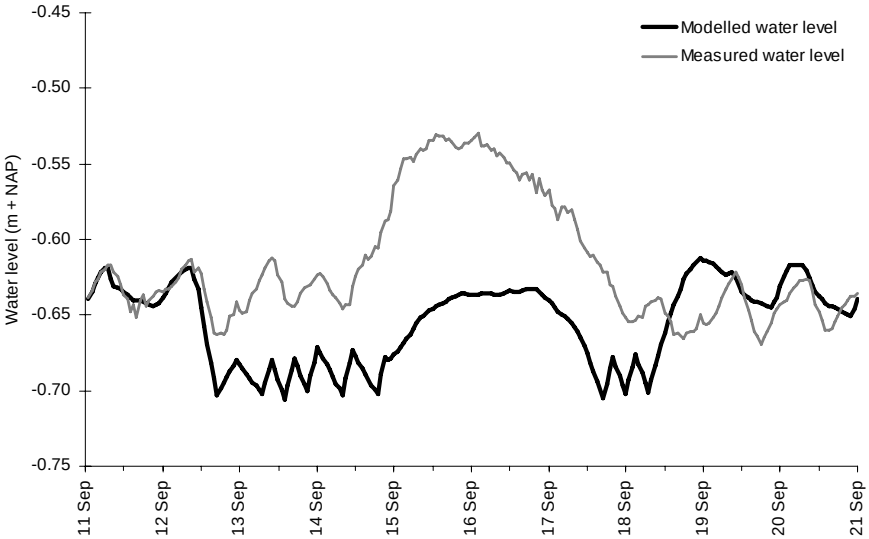


Fig. 3 Modelled prevention of high water levels by starting pumping at 12 September 1998. Aquarius Modelling System.

Historic pumping station data show that not until 15 September were all the pumps put into operation (Fig. 2). If the ECMWF EPS rainfall forecast had been considered as a warning for the high precipitation event, the pumping could have been started earlier to prevent the high water levels. This pumping strategy was simulated using the Aquarius water-system model of the Rijnland water system (Yufeng, 2003; HydroLogic, 2006). In the simulation the pumping stations were put into operation on 12 September. The water level is lowered temporarily from –0.65 to –0.70 m + NAP to accommodate more water in the storage basin (Fig. 3). This creates extra storage capacity at the beginning of the precipitation event. The results show that the water levels are now kept at normal levels and no critical high water levels occur.

This analysis shows the potential of using ECMWF EPS for operational management of extreme events in medium-scale regional water systems in The Netherlands. On the basis of similar events, general decision rules for control strategies with ECMWF EPS can be determined. These strategies have to balance the risks of exceeding the upper water-level threshold and the risk of levels falling below the lower water-level threshold. For this purpose long-term dedicated analysis of ECMWF EPS forecasts is performed (Van Andel & Lobbrecht, 2006). Ongoing research focuses on developing optimum control strategies for regional water systems.

CONCLUSION

Economic pressure and scarcity of water, land, and time, demands that we use all available information to optimize operational water-system controls.

Today's various sources of advanced meteorological data and forecasts are not only valuable for early warning and management of large-scale water systems, but also can enhance the management of medium-scale regional water systems. The globally available ECMWF EPS forecasts can be used to decide on early control actions to manage extreme precipitation events in regional water systems.

Acknowledgements The data for this research was kindly provided by the Royal Dutch Meteorological Institute (KNMI) and Rijnland waterboard. The research is partially funded by the Delft Cluster programme, The Netherlands.

REFERENCES

Andel, S. J. van & Lobbrecht, A. H. (2006) Ensemble weather forecasts and operational management of regional water systems. In: *Seventh International Conference on Hydroinformatics* (ed. by P. Gourbesville, J. Cunge, V. Guinot & S. Y. Liong), 1351–1358. Research Publishing Services, Nice, France.

Bokhorst, J. & Lobbrecht, A. H. (2005) Neerslag-kansverwachting voor het waterbeheer (Probabilistic precipitation forecast for water management). *H2O: Tijdschrift voor watervoorziening en waterbeheer* **13**, 26–29 (in Dutch).

ECMWF (2006) http://www.ecmwf.int.

HydroLogic (2006) http://www.hydrologic.nl/aquarius (in Dutch).

Lobbrecht, A. H. (1997) *Dynamic Water-System Control: Design and Operation of Regional Water-Resources Systems*. A. A. Balkema Publishers, Rotterdam, The Netherlands.

Lobbrecht, A. H. & Loos, S. (2004) From precipitation data to flood forecasting. In: *Sixth International Conference on Hydroinformatics* (ed. by S. Y. Liong, K. K. Phoon & V. Babovic), 1311–1318. World Scientific Publishing Company, Singapore.

Schilling, W. (1990) Applications of operations research to real-time control of water resources systems. Foreword in: *Proceedings of the First European Junior Scientist Workshop* (ed. by T. Einfalt, M. Grottker & W. Schilling), (Kastanienbaum/Luzern, Switzerland, 15–18 March). Schriftenreihe der EAWAG, CH-8600, Dübendorf, Switzerland.

Yufeng, G. (2003) Flood modelling and forecasting for Rijnland area, using physically based and data-driven methods. MSc Thesis, HH 470. UNESCO-IHE, Delft, The Netherlands.

Climate Variability and Change—Hydrological Impacts (Proceedings of the Fifth FRIEND World Conference held at Havana, Cuba, November 2006), IAHS Publ. 308, 2006.

Real-time monitoring and management of point and areal hydrometeorological data in the Athens metropolitan area

MARIA MIMIKOU & ANDREAS GRAMMATIKOGIANNIS

Department of Water Resources, Hydraulics and Maritime Engineering, School of Civil Engineering, National Technical University of Athens, 5 Heroon Polytechniou, 15780 Zographou, Athens, Greece
mimikou@chi.civil.ntua.gr

Abstract This paper focuses on the implementation of a fully automated telemetric network (METEONET) of 11 hydrometeorological stations which was installed for the integrated analysis and management of the meteorological information concerning the Athens metropolitan area in the Attica district of Greece. Various dynamic software applications are linked to the central database of the project supporting the analysis and synthesis of the data, the inspection of the temporal and spatial evolution of meteorological events, as well as the elaboration and dissemination of derivative information through the Internet for public awareness. The entire procedure has been standardized for easy implementation in other similar networks.

Key words METEONET; telemetry; hydrometeorological network; Athens; Greece; database; Internet; public awareness

INTRODUCTION

A well-organized hydrometeorological station network is a basic requirement for the monitoring and processing of the relevant hydrological and climate data, especially in urban areas with high growth rates where all activities are related and mutually influenced by the alterations of the natural environment. Such systems are mainly used for the monitoring of extreme rainfall events and consequently for flood-related events, and this is so in metropolitan Athens, capital of Greece, where intense flood-producing rainstorms often occur, resulting in the loss of human lives and property (Mimikou *et al*., 2000). The importance of such networks is also enforced by the European Union Water Framework Directive's provisions that require the installation of representative monitoring networks of all the parameters of the hydrological cycle (Grammatikogiannis *et al.*, 2005).

Recently, there is a strong tendency of using data from hydrometeorological networks not only for conventional climatic or hydrological studies, but also for bioclimatic or energy studies (Matzarakis & Balafoutis, 2004; Unger, 1999; etc.). It is clear that the ability of these networks to provide reliable data for further processing in various fields depends on the quality and kind of instruments installed and also their correct placement, which is based on specific criteria.

Unfortunately, in Greece, there is still no hydrometeorological station network organized under a main administration that works through a unified scientific and technical medium (Baltas *et al.*, 2005). Various state services have established sectional networks of specific coverage, but the standardization of the equipment used or the procedures followed for all services has not yet been achieved. For example, the network is very variable, with dense networks covering only the lowlands; the majority of stations are not equipped with automatic recording and telemetry systems, there is no unified method of data recording and the specifications of international organizations (e.g. the World Meteorological Organization) are not always fulfilled.

The operational utilization of the networks has serious disadvantages, such as low reliability and accuracy; delay in the availability and the detection of instrument malfunctions; and a lack of compatibility in data measurement and processing between different agencies. Thus, the existing conventional measuring systems cannot efficiently support the need for the development of modern management plans in the relevant fields of interest (Mamassis *et al.*, 2002).

PROJECT OVERVIEW

From the above, it can be appreciated why the absence of a modern fully-automated hydro-meteorological network, which could provide processed hydrometeorological information in real-time, led to the development of the METEONET project in Greece. In the project, emphasis was put on the collection and exploitation of all available knowledge together with the latest technological achievements in each of the contributing scientific fields (measuring sensors, software applications, GIS techniques, etc.).

Copyright © 2006 IAHS Press

The project is a pilot implementation of what will become a complete monitoring hydro-meteorological network. Based on the experience gained from this project, a proposal is under preparation for the formation of a National Network of Gauging Stations, an operational extension of the Greek National Data Bank of Hydrological and Meteorological Information (NDBHMI). This aims at providing a basic infrastructure in Greece for the pilot implementation of the European Union's Water Framework Directive for the protection, rational management and exploitation of the water resources. The NDBHMI was a technological infrastructure project which comprised, among others; a database necessary for the exploitation of the water resources of the country; the planning of important technical works; the estimation and mitigation of natural hazards; and the protection and management of the aquatic environment in general (Mimikou, 2000).

Within this scope, the METEONET project is intended to summarize and standardize all the necessary procedures for the implementation of a reliable network and it is considered as one of the first attempts in Greece at the integrated management of hydrometeorological data, that is: the collection, storage, elaboration and dissemination of climatic conditions in real-time.

As shown in Fig. 1, the network consists of 11 automated telemetric hydrometeorological stations, installed so as to provide the optimum recording of the weather conditions in the Athens Metropolitan area (687 km^2). The siting of the stations was based on the following criteria:

(a) meteorological, because the low barometric systems arrive from the west, southwest or northwest (Mimikou, 1999);
(b) elevation, so as to record the increased amounts of precipitation in upland areas;
(c) security, accessibility and infrastructure facilities;
(d) topographical, according to the World Meteorological Organization (WMO) regulations (WMO, 1983, 1996).

Each of the stations is equipped with sensors that monitor weather conditions (precipitation, temperature, relative humidity, wind and radiation); a data logger for recording data; a transmission system; and finally an energy supply unit.

The design of the system addressed three main issues: the selection of the appropriate technologies for data measurement, transmission and storage; the location of the stations at appropriate sites; and software applications that were suited for different categories of users, from

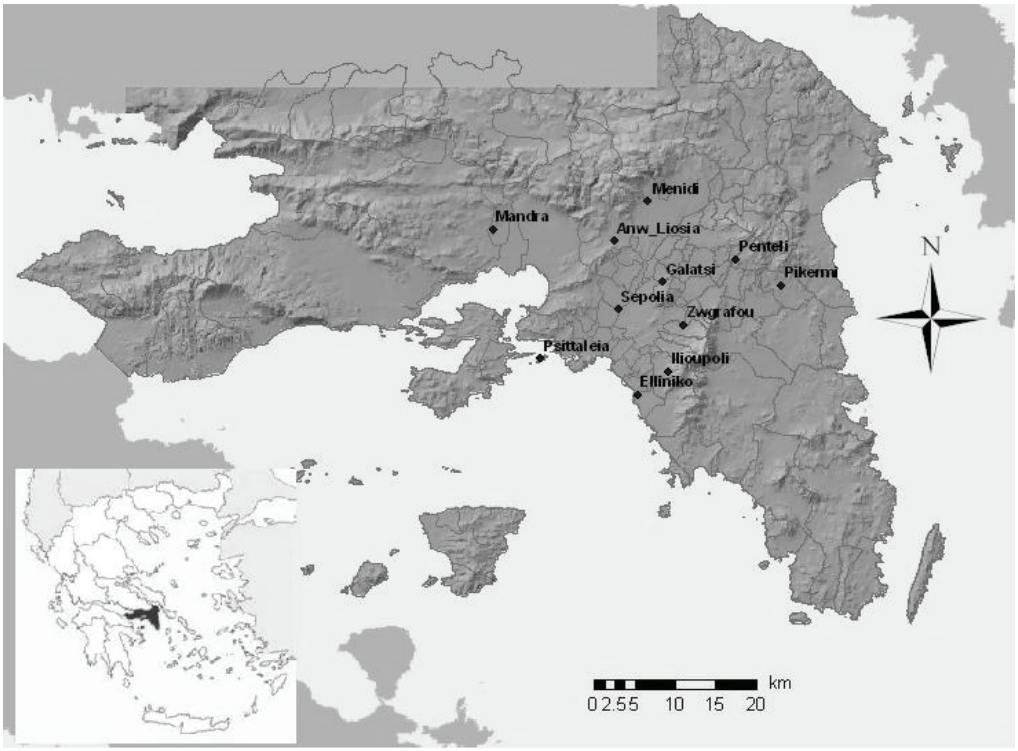


Fig. 1 The METEONET network.

researchers and scientists to the general public who are not familiar with the terminology. For all issues, international and local experience proved to be very important for the effective system design. Experience with a pilot telemetric station, located on the campus of the National Technical University of Athens and operated for seven years, provided the basis for decisions regarding the network design: types of sensor and energy supply; as well as data acquisition, logging and transmission techniques.

PROCESSING AND MANAGEMENT OF POINT DATA

According to the system's general architecture (Fig. 2) the ASCII files from the stations data loggers are transmitted to and stored in the main server, via a mobile telephone network. A subprogram transfers and allocates the data from the ASCII files to the relational database, by taking into account the correspondence between the ASCII files columns and the time series identification numbers. The main aspects considered in the design of the data base were the following:

(a) data reliability, integrity and availability;
(b) data security and database performance;
(c) friendly user interface.

The processing of point measurements includes the following procedures in three consecutive stages (Fig. 3):

(a) range and time consistency checks;
(b) conversion of irregular to a strictly regular time step;
(c) detection of missing or false values;
(d) aggregation and generation of derived time series (Fig. 4).

In order for the dynamic system to manipulate successfully more than 15 million records per year, several triggers, functions, rules, constraints and sequences were implemented, resulting in an easing of the load on the network and server, reducing the necessary disk space (20 times less than storing times series with conventional methods) and speeding up the frequently needed operations (e.g. retrieving the first and last records).

GIS APPLICATIONS

As well as point measurements, the system is equipped with a GIS platform so as to provide standardized maps, depicting the spatial evolution of the measured variables within the research

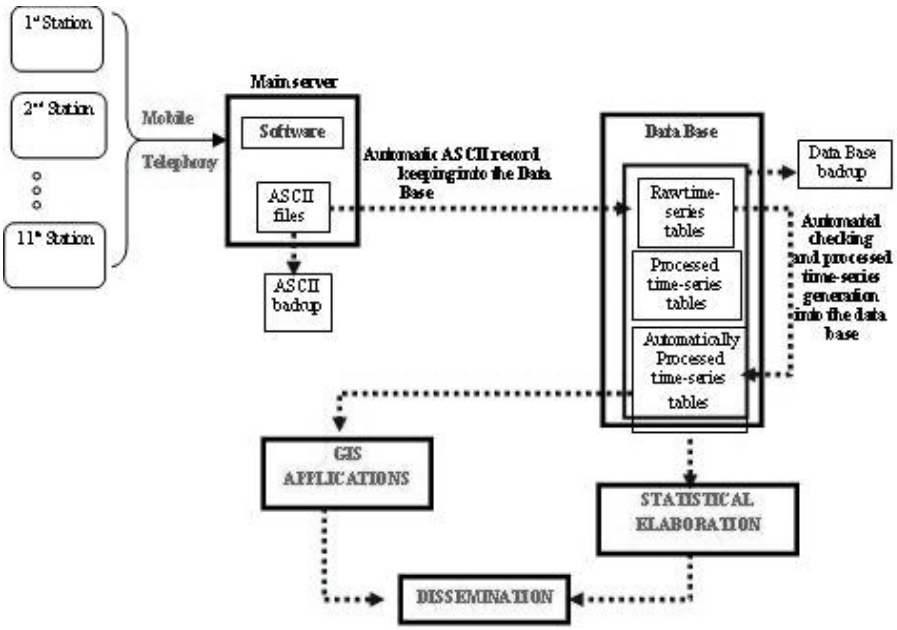


Fig. 2 METEONET architecture.

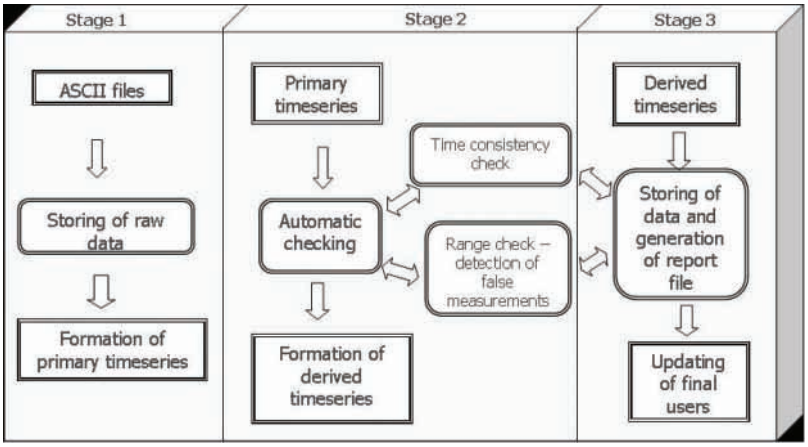


Fig. 3 Data manipulation and processing.

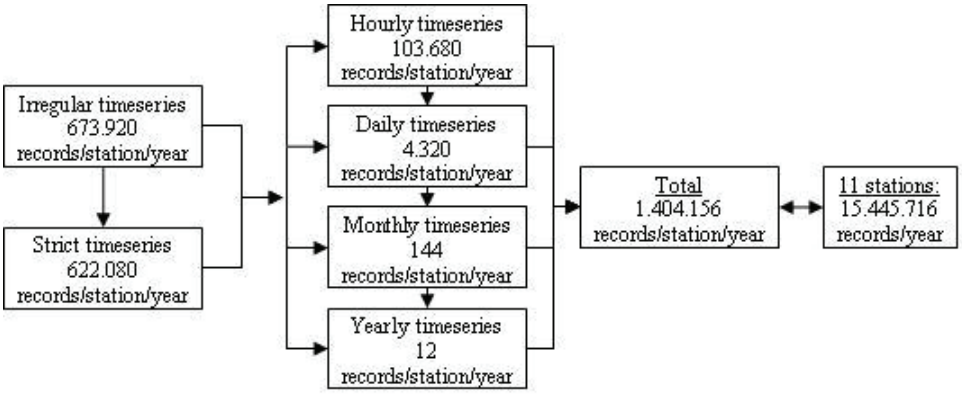


Fig. 4 Time series generation.

area. The developed application collects data measurements for all monitored meteorological variables in various time periods and generates the corresponding maps. The program is executed after every data entry and the completion of all data checks. Three basic steps are included within this function:

(a) automated generation of Thiessen polygons. It must be stressed that Thiessen polygons are dynamically generated to take account of all possible combinations between the stations (in case a number of stations are deactivated);
(b) automated areal integration of the stations' measurements using the Inverse Distance Weighted method and the Kriging method;
(c) production of the corresponding maps for the area of interest.

The entire function has been developed independently from the rest of the functions so that the area of application will not be limited to the particular geographical region, thus allowing it to be adapted according to different needs.

During data entry, the following checks are carried out:

(a) incoming data are ignored if they are not followed by the station's coordinates;
(b) station files with no data are ignored, as well as files with multiple data entries for the same station;
(c) if the total number of stations with valid data entries is less than a predefined limit (e.g. three stations), the program's execution is terminated.

The resulting maps depict the spatial distribution of various meteorological parameters and can be used to assess quantitatively the impact of different regional characteristics of the area's climatic regime (distance to the coast, elevation, etc.) and thus they can become very useful tools for urban planning and management. A typical output of the procedure is presented in Fig. 5.

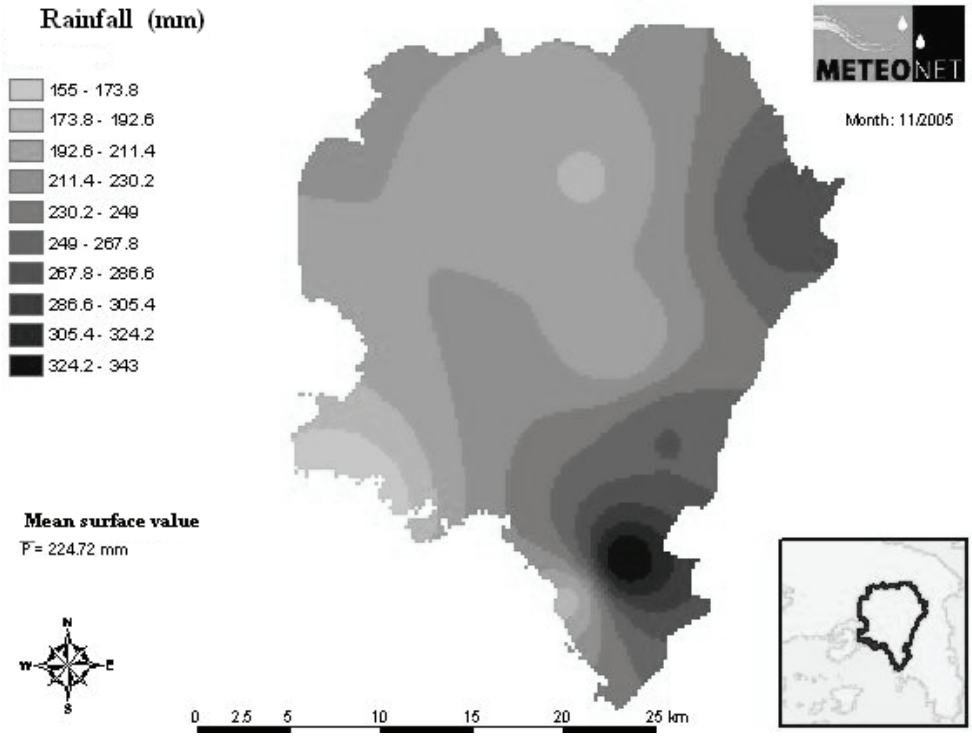


Fig. 5 Automated generation of a rainfall map with the IDW method.

PUBLIC AWARENESS – INTERNET TOOLS

The need for readily available hydrometeorological information, combined with the overall nature of the METEONET project as providing very important infrastructure for the monitoring of the climate conditions of the Athens metropolitan area, led to the design and the implementation of an Internet suite of applications to support researchers, scientists and in general all end-users who are interested in the relevant issues. This platform is the first integrated real-time Internet support system of such extent and with such a volume of data in Greece. The available tools cover a wide range of statistical applications, GIS-based visualizations, and other derivative information in the form of graphs, tables and maps, automatically updated as new data become available.

There can be no doubt as to the importance of the information provided and of making this contribution to public awareness regarding the weather conditions in Athens. During the first year of operational exploitation, the METEONET site was visited by more than 18 000 different users, not only from Greece, but also from more than 40 countries worldwide (Italy, Canada, Denmark, USA, Vietnam, etc). At the time of writing this paper, visiting rates were increasing by approximately 100% per month, indicating that the METEONET web site has become a very useful tool, not only for specialists, but also for the general public.

DISCUSSION

The retrieval of reliable processed hydrometeorological data is considered to be one of the most difficult tasks in integrated hydrological, climatic or urban planning. Experience has shown that problems that arise, not only with the quantity and quality of the available data, but also with the ease of acquisition. New technologies can provide powerful new ways for recording, processing and managing hydrometeorological data.

Nonetheless, automated telemetric networks, support systems and software applications require extensive collaboration between different areas of expertise as well as continuous updating concerning new technologies. The METEONET network is the first attempt at the collection, storage, elaboration and dissemination of hydrometeorological information in real-time on the Internet, thus contributing to the public awareness.

With this system in operation, the definition and the mapping of areas that are most likely to be subjected to extreme events, in relation to a better understanding in general of the evolution of meteorological events over Athens, can lead to the specification of measures that need to be implemented for sustainable management, reliable decision making and the prevention of human suffering and property damage.

REFERENCES

Baltas, E., Eleftheriadis, A. & Mimikou, M. A. (2005) Optimization of the hydrological stations network. In: *Integrated Management of Water Resources, Based on the River Basin* (Fifth National Congress of the Greek Committee for Water Resources Management (EEDYP), organized by the Democritus University of Thrace, Xanthi, Greece).

Grammatikogiannis A., Mamassis, N., Baltas, E. & Mimikou M. (2005) A meteorological telemetric network for monitoring of the Athens wider area (METEONET). A real time approach from point to areal measurements, In: *Proc. Ninth International Conference on Environmental Science and Technology, Rhodes Island, Greece.*

Mamassis, N. & Koutsoyiannis, D. (2002) A hydrometeorological telemetric network for the water resources monitoring of the Athens water resource system. In: *Water Resources Management in the Era of Transition* (Proc. Fifth International Conference of European Water Resources Association), 157–163, European Water Resources Association, Athens, Greece.

Matzarakis, A. & Balafoutis, C. (2004) Heating degree-days over Greece as an index of energy consumption. *Int. J. Climatology* **24**, 1817–1828.

Mimikou, M. (1999) Floods and flood protection: modern techniques – non constructive measures for urban and non-urban areas. Workshop in the Municipality of Rio, Rio, Greece.

Mimikou, M. (2000) National data bank of hydrological and meteorological information, Final Report. Sponsored by the Cohesion Fund and the Ministry of Public Works, 1997–2000, Athens, Greece.

Mimikou, M., Baltas, E. & Varanou, E. (2000) A study of extreme events in the Athens greater area. Int. IAHS Symposium on Extraordinary Floods, Reykjavic, Iceland.

Unger, J. (1999) Comparisons of urban and rural bioclimatic conditions in the case of a central European city. *Int. J. Biometeorology* **43**, 139–144.

WMO (1983) *Guide to Meteorological Instruments and Methods of Observation* (fifth edn), Chapter 7. WMO, Geneva, Switzerland.

WMO (1996) *Guide to Meteorological Instruments and Methods of Observation* (sixth edn), Chapter 7. WMO, Geneva, Switzerland.

Climate Variability and Change—Hydrological Impacts (Proceedings of the Fifth FRIEND World Conference held at Havana, Cuba, November 2006), IAHS Publ. 308, 2006.

Hydrological assessment of Makanya catchment in South Pare Mountains, semiarid northern Tanzania

MARLOES L. MUL[1,2], HUBERT H. G. SAVENIJE[1,3], STEFAN UHLENBROOK[1] & MAURITS P. VOOGT[3]

1 *UNESCO-IHE, Institute for Water Education, PO Box 3015, 2601 DA Delft, The Netherlands*
m.mul@unesco-ihe.org

2 *Department of Civil Engineering, University of Zimbabwe, PO Box MP600, Mt. Pleasant, Harare, Zimbabwe*

3 *Faculty of Civil Engineering and Geosciences, Delft University of Technology, PO Box 5048, 2600 GA Delft, The Netherlands*

Abstract This paper focuses on a catchment in northern Tanzania, the Makanya catchment in the South Pare Mountains, where people have only recently started monitoring rainfall and runoff. The main interest of this research is to assess the hydrological situation in this widely ungauged catchment, both in the past and the present, and special attention is given to different scales. The largest scale is the Makanya catchment with an area of 320 km^2, and the smallest scale the Vudee sub-catchment with an area of 24 km^2. The ungauged history of the hydrology has been assessed through interviews and transect walks with local elders. Subsequently a timeline has been established of the hydrology and related driving forces. This has been compared to the meteorological data observed in a nearby catchment. A multiple linear regression (MLR) model for the Vudee sub-catchment based on the 2004–2005 data set was used to assess the current state of the hydrology.

Key words PUB; ungauged basin; conceptual model; historical runoff; rainfall trends

INTRODUCTION

Many river basins worldwide are not or poorly gauged. This is even more the case in Sub-Saharan Africa where countries lack the financial, human and technical resources for developing and maintaining monitoring networks (Mazvimavi, 2003). In poorly gauged catchments, conceptual hydrological models, requiring a limited amount of data, can be useful for a better understanding of the hydrology by quantifying the basic components of runoff generation including: net runoff coefficient, evaporation, catchment response, etc. Limitations and uncertainties associated with this approach are discussed extensively in the literature (e.g. Beven, 2001). Database approaches, as in this case multiple linear regressions between rainfall and runoff, can provide further insights into the thresholds above which storm flow is generated. Additionally the net runoff coefficient and response time of the catchment can be determined.

Indigenous knowledge has often been neglected in establishing the runoff characteristics of an ungauged catchment. In a rapidly changing environment indigenous knowledge is sometimes the only source of information about the runoff characteristics of a catchment under pristine conditions. The objective of this study is to gather information about the changes relevant for hydrology that have taken place under population pressure in a predominantly ungauged catchment, both through interviews and through the use of a conceptual model.

STUDY AREA

The study area is located in the South Pare Mountains in northern Tanzania and is a tributary to the River Pangani. The Makanya catchment, as it is called, covers an area of approximately 320 km^2 (Fig. 1). The altitude ranges between 500 and 2000 m. Four tributaries, Mwembe, Vudee, Chome and Tae, join the main stream in the Makanya catchment, which drains into the River Pangani only during exceptional flooding events (Vyagusa *et al.*, 2006).

The soils on the forested summit area and the scarp slopes of the Pare Mountains are red loamy clays; surface limestones occur sporadically. A series of northwest trending faults cuts the South Pare Mountains, but the nature and age of these faults is unknown. The general structure of the area has a foliation dipping east–north–east, at moderate angles up to 40% (Geological Survey of Tanzania, 1965).

Copyright © 2006 IAHS Press

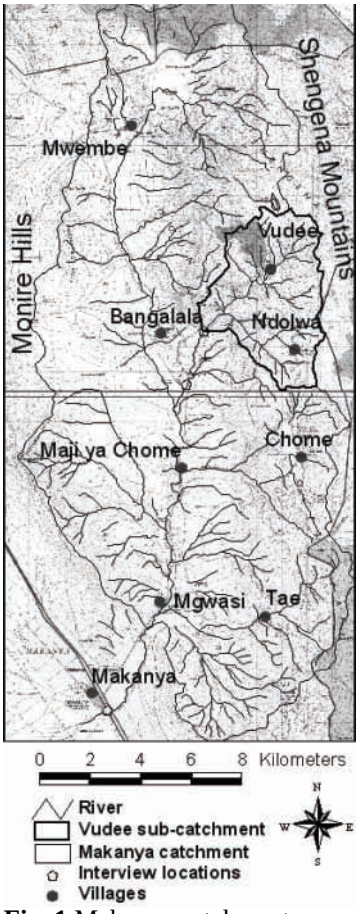


Fig. 1 Makanya catchment.

The Makanya catchment is practically ungauged, except for three rainfall stations located in the catchment and operated by individuals with records from the early 1990s. The nearest meteorological station with a long record (from 1957 onwards) is located in Same in a neighbouring catchment, approximately 10 km west of the catchment. In 2004, several raingauges were installed in the catchment, complemented by a compound weir installed on the River Vudee, one of the sub-catchments.

The hydrological year spans the period from 1 October to 30 September of the next year. The rainfall distribution in the catchment is bimodal with the short rainy season occurring in November–January (locally called "Vuli") and the long rainy season in March–May (locally called "Masika"). The average annual rainfall is between 570 and 660 mm year^{-1} (Same and Tae, respectively). The potential evaporation in general exceeds 2000 mm year^{-1}.

HISTORICAL HYDROLOGICAL ASSESSMENT

Historical runoff in the catchment was assessed by using structured interviews with local elders; emphasis was put on establishing when the river used to be perennial (if at all), the current flow patterns and extreme events, both droughts and floods. These interviews were done at two locations in the catchment, Makanya and Bangalala (see Fig. 1). This was cross-checked with historical rainfall data (station in Same). This data set was used for trend analysis, using the Spearman rank test.

Vudee

The first catchment, the Vudee sub-catchment (24 km^2), was investigated at two locations. The first is where the River Vudee arrives at the main river valley, at Bangalala, while the second site is some 2 km downstream, just before the confluence with the main Makanya stream, downstream of two diversions for supplementary irrigation of 500 ha (Fig. 1). At the upstream site, flows are

permanent, both in the past and present, with the exception of a few extremely dry events, which occurred in 1948, 1974, 1997 (before the El Niño rains) and early 2006. People observed that base flow has steadily decreased over the years since the 1950s. At the downstream site, the flow in the past reportedly resembled the flow of the upstream site. However, in the present situation flows only occur during the rainy season and then quickly recedes. This is mainly due to the increasing abstractions between these sites. Flood flows at both sites are not very different, indicating that the influence of the abstractions is mainly recognizable during the base flows. Flood flows have reportedly increased over the years, with the most extreme event during the El Niño year 1997, although in 1951 a heavy flood was also observed.

Makanya

In Makanya the flows at the outlet of the catchment have also been analysed through interviews. In Makanya, flows from the mountains are diverted in a spate irrigation scheme, established in the 1960s. From there they flow into a so-called seasonal wetland, occasionally linking the Makanya catchment with the River Pangani, 50 km downstream. The historical flow regime, both upstream and downstream of the spate irrigation, has been analysed. Upstream of the spate irrigation system, continuous flow was observed during the 1960s. At present the river bed is dry except after heavy rainfall events in the catchment, occurring on average five times a year, and flowing for at most a week at a time. During the El Niño season (1997–1998) a continuous flow reached Makanya from March until May. Downstream of the spate irrigation system, in the 1960s water regularly reached the River Pangani after heavy rains in the catchment, nowadays only extreme floods reach the River Pangani.

Most people in the two villages indicated that they feel that the rainfall has decreased over the years and that this is the main cause for the changes in the flow regime. Other causes mentioned by the locals were increased population and deforestation.

Rainfall trend analysis

The Same meteorological station is located near the western fringe of the Makanya catchment at the foot of the South Pare Mountains. A correlation analysis with the Tae station (1990–2000) within the Makanya catchment shows a good correlation (0.69 on a monthly basis), although the absolute values differ substantially (1990–2000), Tae (655 ± 250 mm year^{-1}), Same (500 ± 260 mm year^{-1}). Daily data from Same were used for trend analysis to represent the hydroclimatic situation in the Makanya catchment.

The meteorological data suggest that the rainfall in the area decreased during the period of observation (1957–2004) from an average of nearly 630 mm year^{-1} (1960s) to 500 mm year^{-1} (1990s) (Table 1). Enfors (personal communication) also indicated that changes in the rainfall pattern are mainly apparent in the larger occurrence of long dry spells (>21 days). Long dry spells have increased in occurrence significantly from 20% before the 1980s to 80% after the 1980s.

Spearman rank tests were performed on annual totals, Vuli and Masika seasons and for the dry season. The test for annual totals showed a visible but not significant trend (test statistic $t = -1.48$ within the interval –2 and 2; Voogt, 2005), although Fig. 2 shows that since 1990 a period with clearly below average rainfall predominates, with the exception of the 1997–1998 El Niño season.

The tests for Vuli and Masika also showed no significant trend ($t = -0.46$ and –0.96 respectively; Voogt, 2005), although in Fig. 2 it can be seen that the Masika season has a clear visible trend, whereas Vuli rainfall shows no visible trend. The variations in Vuli are higher, with an average rainfall of 220 mm season^{-1} and standard deviation of 150 mm season^{-1}, than in Masika, with an average rainfall of 320 mm season^{-1} and a standard deviation of 130 mm season^{-1}.

Table 1 Average rainfall and standard deviation of the rainfall, Same station.

	Annual (mm season^{-1})		Vuli (mm season^{-1})		Masika (mm season^{-1})	
	Average	Stdev	Average	Stdev	Average	Stdev
1960s	627	193	263	185	330	175
1970s	615	250	241	162	339	135
1980s	587	140	216	90	343	105
1990s	499	276	213	240	264	66

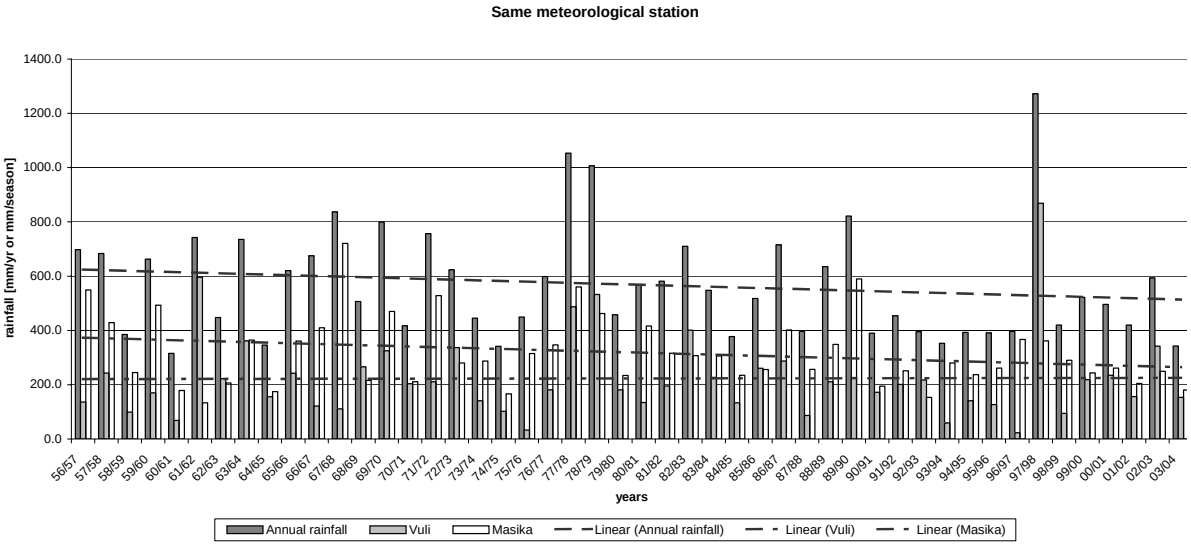


Fig. 2 Annual, Masika and Vuli rainfall Same station with trend lines (mm year^{-1}or mm season^{-1}).

The previous analysis is consistent with the study performed by Valimba (2004) indicating that in northern Tanzania changes in rainfall patterns cannot be found in annual totals, however occurrences of low intensity rainfall (<10 mm day^{-1}) have significantly decreased, whereas high intensity rainfall has increased. This trend is particularly apparent during the Masika season.

CURRENT STATE OF THE HYDROLOGY IN VUDEE SUB-CATCHMENT

Multiple linear regression model

The assessment of the current state of the hydrology has been done with the data gathered from the Makanya catchment during the rainy season of 2004/2005. Data was collected from one operating rainfall station in the upper catchment, which was used for the rainfall input and a gauging station where the River Vudee enters the valley. A multiple linear regression (MLR) model for rainfall–runoff (RAINRU) was developed by Savenije (1997), where rainfall in the previous time steps is linked with the runoff in the present time step. A threshold value is used in the model before runoff is generated. On a monthly time step this threshold value converges to the interception value. Since runoff in a particular month depends not only on the rainfall for that month, but through storage also on the rainfall in the preceding months, a linear transfer function is used (Savenije, 1997):

$$Q(t) = \sum_{i=1}^{n} b_i * \mathrm{Max}\left(P(t-i) - D, 0\right)$$

where $i \in [0, 1, 2, \ldots n]$ is the counter backward time step from the start of the rainfall at time step t. The parameters Q, P and D are expressed in mm (time step)$^{-1}$. The coefficients b_i are determined through multiple linear stepwise regression. The coefficients generated by the regression model give information on runoff response to rainfall, and how long a rainfall event impacts on the runoff. Finally it gives a quantification of the percentage of the net rainfall that comes to runoff (net runoff coefficient). This study uses the concept of RAINRU and applies it to daily and weekly rainfall and runoff data as done by Woltering (2005) for a catchment in Zimbabwe.

Daily linear regression

Initially the threshold value was set to 3 mm day^{-1} corresponding to a realistic daily interception value. The net runoff coefficient (percentage of net rainfall ($P - D$) coming to runoff) is 6.3%. The results for the Vuli 2004 season are shown in Fig. 3. Basically 80% of the runoff is generated in the first three days, with subsequent days generating less than 5% of the total runoff. Increasing the number of days beyond 5 days did not enhance the simulation regarding the peaks; in general the model also could not simulate the base flow. The model accuracy, r^2 is 0.62, when considering

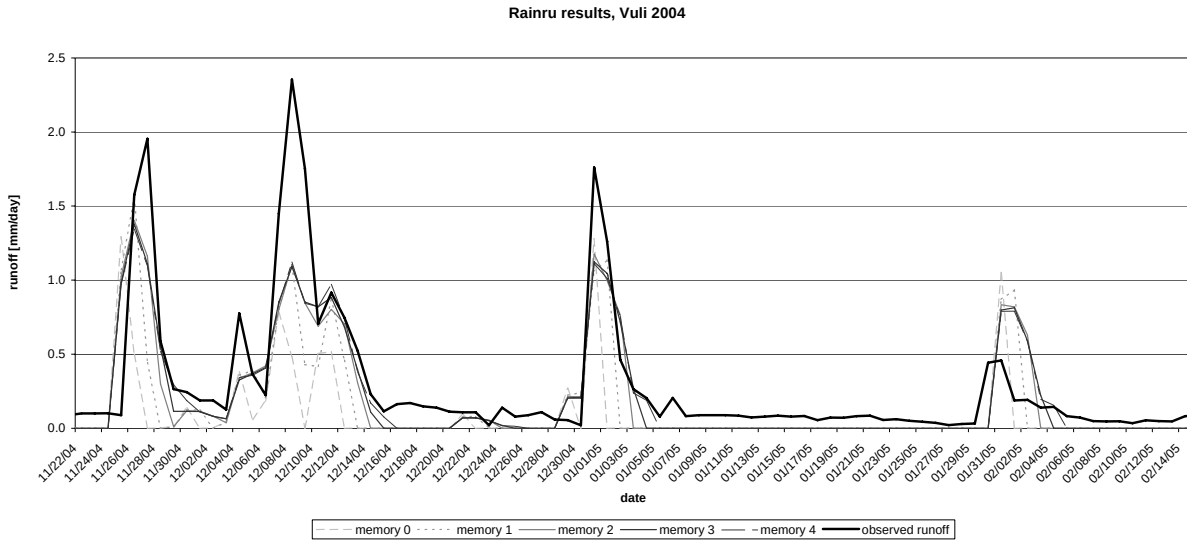


Fig. 3 Results for Rainru on a daily basis with threshold of 3 mm day^{-1}, Vuli season 2004.

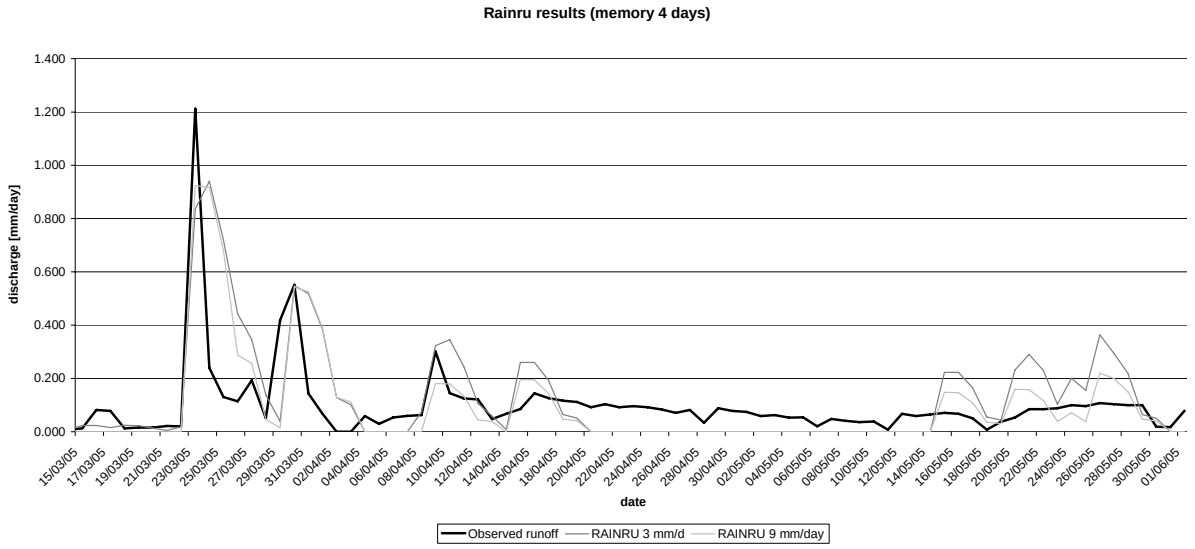


Fig. 4 Results for RAINRU on a daily basis with threshold of 3 and 9 mm day^{-1} memory of 4 days, Masika season 2005.

more than 2 days in the computation. The MLR model could not account for the base flow that is observed almost continuously. Currently the base flow rises to a steady 25 L s^{-1} during the rainy season and decreases to 5 l s^{-1} during the dry season. The failure of the model to predict this base flow indicates that a different system is responsible for the generation of this flow.

In the model run (Fig. 4) it shows that during the Masika rains in May hardly any increase in flow was observed. This indicated that the threshold value of 3 mm day^{-1} did not adequately address the threshold behaviour of the system. Rainfall in this period ranged from 11–17 mm day^{-1} and did not generate a substantial increase in runoff. A threshold value of 9 mm day^{-1} was then used, reducing the overshoot of the runoff simulation (Fig. 4). The net runoff coefficient also increased because of the increasing threshold value (net precipitation decreases) to 5.9%. The performance of the model remained the same (r^2 = 0.62), whereas increasing the threshold value to a higher value affected the performance negatively. The need for a threshold value higher than 3 mm day^{-1} to increase overall performance indicates that the threshold on a daily basis is more then interception.

Weekly linear regression

The daily MLR model clearly had a deficiency in predicting base flow. An attempt was made to model this by increasing the time step of the model to a week. The threshold value was tested. An

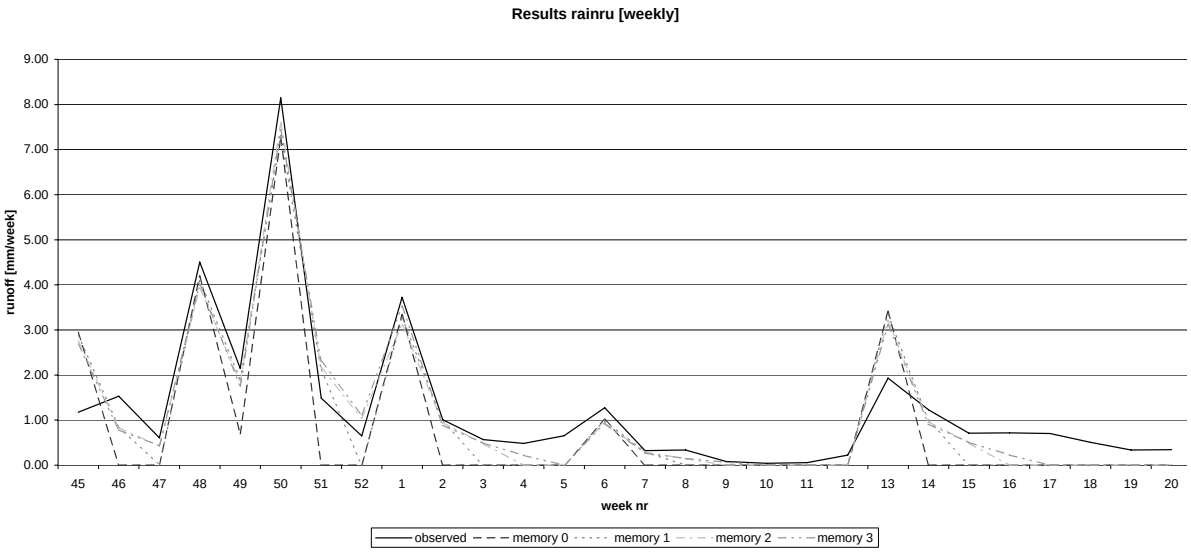


Fig. 5 Results for Rainru on a weekly basis with threshold of 35 mm week^{-1} Vuli 2004 and Masika 2005 season.

optimum of the model performance was obtained with a threshold value of 35 mm week^{-1}. The model performance is better on a weekly basis than on a daily basis (r^2 amounts to 0.90 compared to 0.62), with a better prediction of base flow. As the previous model indicated, most runoff is generated in the first three days. This model shows similar response, with 90% of the total runoff generated in the first week (Fig. 5).

CONCLUSIONS

The interviews suggest that the River Makanya at the railroad bridge (320 km^2) changed from a perennial river in the 1950s to an intermittent river in the 1990s. The flow from the River Makanya into the River Pangani ceased and the seasonal wetland turned into a steppe terrain. On the sub-catchment scale, flows from the mountains have reportedly dried up and the base flow decreased significantly. Decreasing rainfall amounts were predominantly mentioned as the main causes of the changes, although this could not be substantiated with a rainfall trend analysis with data from a nearby station.

The rainfall–runoff data collected for the Vudee sub-catchment (24 km^2) suggest that no more than 6% of the net rainfall forms runoff. It also shows that there are two flow paths, one very slow, contributing to long-lasting base flow from the mountains to the villages at the foot of the mountains (between 5 and 25 L s^{-1}, at the end of the dry season and during the wet season, respectively). The other flow path is fast runoff, with the peak reaching the foot of the mountain within one day with 80% of the runoff generated in the first 3 days after the rainfall.

Even with a limited amount of data, a good initial hydrological picture could be established for a widely ungauged catchment through the MLR model. Interviews with locals and a comparison with a nearby meteorological station established an historical overview of the runoff regime and its variability.

Acknowledgements The work reported here was undertaken as part of the Smallholder System Innovations (SSI) in Integrated Watershed Management Programme funded by the Netherlands Foundation for the Advancement of Tropical Research (WOTRO), the Swedish International Development Cooperation Agency (Sida), the Netherlands Directorate-General of Development Cooperation (DGIS), the International Water Management Institute (IWMI) and UNESCO-IHE Institute for Water Education. Implementation on site was assisted by the Soil-Water Management Research Group (SWMRG), Sokoine University of Agriculture, Tanzania.

REFERENCES

Beven, K. (2001) How far can we go in distributed hydrological modeling? *Hydrol. Earth System Sci.* **5**(1), 1–12.

Geological Survey Tanzania (1965) Quarter Degree Sheet 89. Published by Geological Survey Division, Dodoma, Tanzania.

Mazvimavi, D. (2003) Estimation of flow characteristic of ungauged catchments, case study in Zimbabwe. PhD Dissertation, Wageningen University, The Netherlands.

Savenije, H. H. G. (1997) Determination of evaporation from a catchment water balance at a monthly timescale. *Hydrol. Earth System Sci.* **1**, 93–100.

Valimba, P. (2004) Rainfall variability in southern Africa, its influences on streamflow variations and its relationships with climatic variations. PhD Thesis, Rhodes University, South Africa.

Voogt, M. P. (2005) Hydrological history of the Makanya River, changes in stream profile examined. MSc Thesis, Delft University of Technology, Delft, The Netherlands.

Vyagusa, F. N., Mul, M. L. & Makurira, H. (2006) Water allocation practices for smallholder farmers in South Pare Mountains, Tanzania, A case study of Manoo microdam (ndiva). *Physics and Chemistry of the Earth* (submitted).

Woltering, L. (2005) Estimating the influence of on-farm conservation practices on the water balance, case of the Mzinyathini catchment in Zimbabwe. MSc Thesis, Delft University of Technology, Delft, The Netherlands.

L'Observatoire de Recherche en Environnement, ORE HYBAM sur les grands fleuves amazoniens

GÉRARD COCHONNEAU[1], FRANCIS SONDAG[1], JEAN-LOUP GUYOT[2], BOAVENTURA GERALDO[3], NAZIANO FILIZOLA[4], PASCAL FRAIZY[2], ALAIN LARAQUE[5], PHILIPPE MAGAT[6], JEAN-MICHEL MARTINEZ[1], LUIS NORIEGA[7], EURIDES OLIVEIRA[8], JULIO ORDONEZ[9], RODRIGO POMBOSA[10], FRÉDÉRIQUE SEYLER[1], JONATHAN SIDGWICK[1] & PHILIPPE VAUCHEL[11]

1 *IRD/LMTG 14 Av. Edouard Belin, F-31400 Toulouse France*
gerard.cochonneau@mpl.ird.fr

2 *IRD/LMTG Casilla 18 1209, Lima 18, Peru*

3 *UnB/LAGEQ Campus Darcy Ribeiro, Asa Norte, CEP 70919-970 Brasília, DF, Brasil*

4 *UFAM Av. Gal. Rodrigo Otávio Jordão Ramos, 3000/Bl. T, 69077000 Manaus, AM, Brasil*

5 *IRD/OBHI Martinique. BP 8006, F-97259 Fort de France cedex, France*

6 *IRD/LMTG AP 17 12 857, Quito, Ecuador*

7 *SENAMHI Calle Reyes Ortiz no. 41 2do Piso, La Paz, Bolivia*

8 *ANA Setor Policial - Área 5 - Quadra 3 Bloco L, CEP 70610-200 Brasília, DF, Brasil*

9 *SENAMHI Jr. Cahuide 805, Casilla Postal 1308 Lima 11, Perú*

10 *INAMHI Iñaquito N36-14 y Corea, Código Postal 16-310, Quito, Ecuador*

11 *IRD/LMTG CP 9214 00095 La Paz, Bolivia*

Résumé L'ORE HYBAM permet d'acquérir, à un pas de temps journalier, décadaire ou mensuel, des données hydrologiques, sédimentaires, géochimiques et physico-chimiques à une quinzaine de stations, réparties sur les grands fleuves amazoniens, afin de contrôler les zones de piedmont, les affluents de plaine, ceux originaires des Andes et ceux drainant les boucliers brésilien et guyanais. Maintenu par des institutions de recherche et des organismes gestionnaires de réseaux hydrométriques nationaux, l'ORE HYBAM s'intéresse aux transferts de matières à l'intérieur du bassin et vers l'Atlantique, à leur sensibilité à la variabilité climatique actuelle et aux activités anthropiques, au rôle des zones humides dans la transformation des éléments transportés. Importantes également pour la connaissance des bilans globaux, ces informations obtenues avec des méthodes de collecte homogènes, sont disponibles librement sur Internet (http://www.ore-hybam.org/), sous forme de graphiques et peuvent être extraites sous forme de fichiers.

Mots clefs Amazone; géochimie; hydrologie; observatoire; ORE HYBAM; sédiments

The Environmental Observation and Research project, ORE HYBAM, and the rivers of the Amazon basin

Abstract Thanks to the ORE HYBAM project, hydrological, suspended sediment, geochemical and physico-chemical data can be acquired at daily, ten-day and monthly time steps at about fifteen gauging stations, mainly on the larger rivers of the Amazon basin. The aim of this network is to investigate the piedmont areas, the flood plain tributaries, the tributaries that originate in the Andes and those that are draining the Brazilian and Guiana shields. The ORE HYBAM network, operated by research institutions and national agencies, is interested in the mass transfer within the Amazon basin and towards the Atlantic Ocean, in its sensitivity to climatic variability and anthropogenic activities, and in the key role of wetlands for mass transfer. These data, acquired with standardized collection and analysis methods, are also important for determining the global balance. They are freely available via the Internet (http://www.ore-hybam.org) in the form of graphics, and can be downloaded in ASCII files.

Key words Amazon; geochemistry; hydrology; observatory; ORE HYBAM; sediments

INTRODUCTION

Les grands fleuves tropicaux, par les volumes d'eau et de matières qu'ils transportent à l'océan et par l'étendue des surfaces qu'ils drainent, contribuent largement au fonctionnement global de la planète. Exprimée en pourcentage du flux total provenant des continents, leur contribution est estimée à 57% de l'eau douce, 50% des apports solides, 38% des apports en solution et 45% du carbone organique (Baumgartner & Reichel, 1975; Stallard, 1988; Degens *et al.*, 1991). Du fait de l'étendue géographique de leur bassin de drainage, ces grands fleuves tropicaux sont sensibles à la variabilité climatique. La plupart de ces grands bassins sont aujourd'hui soumis à une forte

Copyright © 2006 IAHS Press

pression anthropique (déforestation, activités agricoles et minières, urbanisation), qui se traduit par une altération de l'état de la couverture pédologique et forestière, qui induit une modification hydrologique et géochimique, mais qui peut aussi induire en retour une altération du régime climatique. Les effets conjugués de la variabilité climatique et de l'altération de la couverture influent sur les processus de transfert dans les bassins versants. Malgré leur importance pour les bilans globaux, et plus généralement pour l'étude de l'environnement, il n'existait pas de réseau pérenne permettant un suivi à long terme des transferts de matières dans ces grands bassins fluviaux tropicaux.

En 2002, le Ministère de la Recherche français a lancé un appel d'offres pour des Observatoires de Recherche en Environnement (ORE) pour fournir aux chercheurs, sur de longues périodes, des données scientifiques de qualité pour comprendre et modéliser le fonctionnement des systèmes et leur dynamique à long terme.

Labellisé dans ce cadre en 2003, l'ORE HYBAM (*Contrôles géodynamique, hydrologique et biogéochimique de l'érosion/altération et des transferts de matière dans le bassin de l'Amazone*) a pour objectifs de répondre aux questions scientifiques suivantes: (a) Quels sont les apports à l'océan Atlantique, leur variabilité saisonnière et interannuelle? (b) Quel est l'impact de la variabilité climatique actuelle sur l'érosion/altération et les transferts de matière dans le réseau hydrographique? (c) Quel est l'impact de l'activité anthropique (déboisement, activité minière) sur l'érosion/altération et les transferts d'éléments dans le bassin? (d) Quel est le rôle des zones humides (processus biogéochimiques, rôle de la végétation) sur les transferts d'éléments et leur transformation à l'intérieur du bassin amazonien?

Il est à la charge d'un consortium associant: (a) deux Unités Mixtes de Recherche françaises (LMTG-Laboratoire des Mécanismes et Transferts en Géologie et LEGOS-Laboratoire d'Etudes en Géophysique et Océanographie Spatiales); (b) deux unités de service de l'IRD (ESPACE et OBHI-Observatoires Hydrologiques et Ingénierie); (c) les organismes gestionnaires des réseaux nationaux: ANA (Agence Nationale de l'Eau) pour le Brésil, DIREN (Direction régionale de l'environnement) et IRD pour la Guyane Française, SENAMHI (Service National de Météorologie et Hydrologie) pour la Bolivie, SENAMHI pour le Pérou, INAMHI (Institut National de Météorologie et Hydrologie) pour l'Equateur, IDEAM (Institut d'Hydrologie, Météorologie et Etudes Environnementales pour la Colombie, MARN (Ministère de l'Environnement et des Ressources Naturelles) pour le Venezuela, SCEVN (Service Commun d'Entretien des Voies Navigables) pour le Congo; (d) des centres de recherche universitaires: Universités de Brasilia (UnB), Niteroi (UFF), Rio de Janeiro (UFRJ), Manaus (UFAM), La Paz (UMSA), Lima (UNALM), Bogota (UNC), Caracas (UCV), Brazzaville (UMN).

DESCRIPTION DE L'ORE HYBAM

Sites de mesure retenus

Actuellement, l'observatoire est présent dans quatre pays amazoniens (Brésil, Bolivie, Pérou, Equateur) ainsi qu'en Guyane Française, au Venezuela (bassin de l'Orénoque) et au Congo (bassin du Congo). La Colombie intègrera ce dispositif en 2006. Plusieurs critères ont été retenus pour orienter le choix des stations (Fig. 1): (1) l'existence de longues séries journalières de hauteurs d'eau et de débits; (2) leur appartenance au réseau de référence de suivi des flux sédimentaires du projet HYBAM (Guyot, 2005) en place depuis 1994; (3) leur représentativité d'une entité (bassin hydrographique) qui contribue aux cycles hydrologique et géochimique. La répartition des stations est la suivante: (a) quatre stations de piedmont pour contrôler l'érosion de la chaîne andine (Rurrenabaque, Atalaya, Borja, F. de Orellana); (b) quatre stations sur les affluents de l'Amazone originaires des Andes, dont deux sur le Rio Solimões (Tabatinga, Manacapuru) et deux sur le Rio Madeira (Porto Velho, Fz. Vista Alegre), afin d'appréhender l'évolution amont-aval des flux de matières (érosion/transport/sédimentation) lors de la traversée de la plaine amazonienne au Brésil; (c) deux autres stations dans la plaine amazonienne (Lábrea, Serrinha); (d) deux stations sur les fleuves drainant le bouclier guyanais (Caracaraí) et le bouclier brésilien (Itaituba); (e) la station d'Obidos, dernière station de contrôle des débits du fleuve Amazone où l'influence de la marée océanique est négligeable à 900 km de l'embouchure; (f) deux stations sur les deux principaux fleuves de Guyane (Langa Tabiki, Saut Maripa) ; (g) deux stations sur le Congo et l'Orénoque

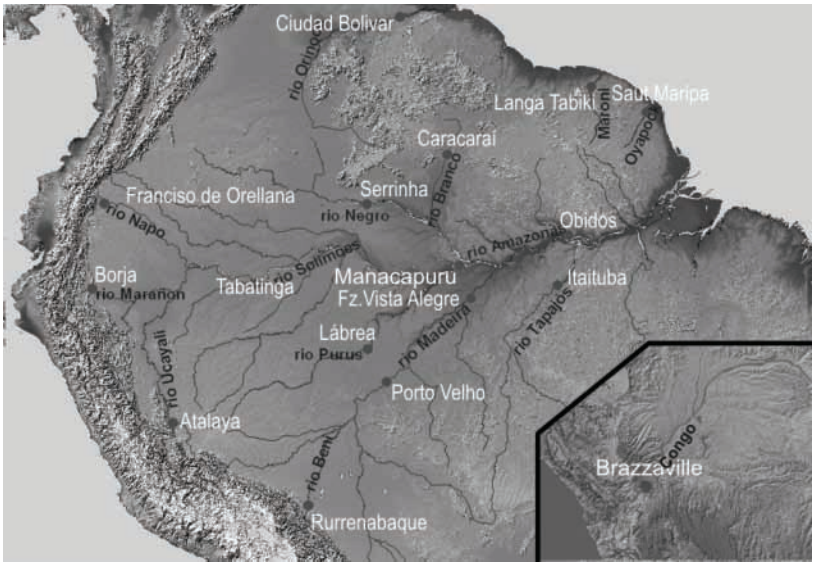


Fig. 1 Carte de situation des stations de l'ORE HYBAM.

(2ème et 3ème fleuves mondiaux en débits liquides) afin d'évaluer plus précisément les apports continentaux à l'Océan Atlantique.

Les paramètres mesurés

Les variables hydrologiques Les niveaux d'eau sont obtenus, avec la précision du centimètre, sur des échelles limnimétriques par une lecture journalière ou bi-journalière ou, pour certaines stations seulement, à l'aide d'un limnigraphe enregistreur. La collecte de l'information est assurée par les services hydrologiques nationaux, parfois en collaboration avec les hydrologues de terrain de l'IRD, notamment dans les pays andins. Les débits moyens journaliers sont obtenus par calcul à partir de la cote moyenne journalière et de la courbe d'étalonnage de la station, construite à partir des jaugeages réalisés à différentes époques du cycle hydrologique, par les organismes gestionnaires de réseau. Dans le bassin de l'Amazone, toutes les stations sont maintenant jaugées avec des courantomètres à effet Doppler (ADCP), associant facilité de mise en oeuvre et précision de la mesure, afin de contrôler la qualité (précision, dérive dans le temps) des courbes d'étalonnage. Le couplage en routine de ces ADCP avec un échosondeur et une antenne GPS permet d'affiner la précision des résultats, notamment dans le cas fréquent de fond mobile lors des crues à certaines stations (Filizola & Guyot, 2004; Laraque *et al.*, 2005). Pour certaines stations de la plaine amazonienne soumises à une influence aval, le calcul des débits, fonction de la pente de la ligne d'eau, fait intervenir les cotes d'autres stations des réseaux hydrométriques nationaux non comprises dans l'ORE. A la plupart des stations de l'ORE la durée des séries journalières des paramètres hydrologiques atteint/dépasse 20 années consécutives.

Les paramètres physico-chimiques Les paramètres physico-chimiques tels que température de l'eau, conductivité électrique et pH sont mesurés lors de chaque échantillonnage de 1000 ml, réalisé par des observateurs spécialement recrutés et formés à cet effet, et destiné à la détermination des matières en suspension (MES). Cet échantillonnage est décadaire sur la plupart des stations de l'observatoire mais mensuel pour le Maroni, l'Oyapock, et le Congo, fleuves à faible teneur en MES. Ces échantillons sont ensuite expédiés aux laboratoires des partenaires nationaux et la détermination des MES est effectuée, selon un protocole identique pour tous les sites, par filtration frontale sur filtre en acétate de cellulose de 0.45 µm, puis pesée des filtres sur balance de précision après séchage en étuve. Les flux sédimentaires totaux sont calculés à partir des débits et des concentrations décadaires de MES, en utilisant une relation entre les concentrations moyennes et de surface obtenues par des campagnes de mesures du flux particulaire total par un échantillonnage sur l'ensemble de la section.

Les variables géochimiques A chaque station, un échantillon mensuel est prélevé en surface par les observateurs du réseau, filtré sur place le jour même et conditionné en divers flacons selon

Tableau 1 Variables hydrologiques, géochimiques et physico-chimiques.

Paramètre	Fréquence	Instrument/méthode
Niveau d'eau	journalier	Echelles/limnigraphes
Débit	journalier	Etalonnage/jaug. ADCP
Température de l'eau	décadaire/mensuel	Thermo-conductivimètre
Conductivité	décadaire/mensuel	Thermo-conductivimètre
pH	décadaire/mensuel	pHmètre
MES de surface	décadaire/mensuel	Echantillonnage de surface
Majeurs (Ca,Mg,K,Na,HCO3,Cl,SO4,Fe,AL,Si,Sr,NO3,F,PO4)	mensuel	HPLC, ICP-AES
Traces, terres rares (Ti,V,Cr,Mn,Co,Ni,Cu,Zn,As,Rb,Zr, Mo,Cd,Ba,U,La,Ce,Pr,Nd,Sm,Eu,Gd,Tb,Dy,Ho,Er,Yb,Lu,Tm	mensuel	ICPMS
Silice	mensuel	ICP-AES
Carbone (COD, COP)	mensuel	Spectro IR
Isotopes	trimestriel	TIMS, MS

le type d'analyse (cations et anions majeurs, silice, éléments en traces, terres rares). La collecte des échantillons est réalisée par les services nationaux, et les flacons et filtres sont envoyés à l'un des laboratoires de l'ORE HYBAM : celui du LMTG Toulouse ou le LAGEQ (Laboratoire de géochimie de l'UnB) à Brasilia selon le type d'analyse (Tableau 1). Des analyses isotopiques sont aussi réalisées au pas de temps trimestriel en quelques stations. L'exactitude des résultats est contrôlée dans ces deux laboratoires par l'analyse répétée de matériaux de référence. Ont été retenus les échantillons SLRS4, du National Research Council of Canada, 1640 et 1643d du National Institute of Standards and Technology, ION 915 et BMOOS du National Water Research Institute situés dans des gammes de concentration proches de celles rencontrées dans les fleuves amazoniens.

RÉSULTATS

Le système d'information associé à l'ORE

Les séries chronologiques La base de données hydrologiques de l'ORE est gérée par le logiciel multilingue gratuit HYDRACCESS (Vauchel, 2004) dans tous les pays associés à l'observatoire, à l'exception du Brésil où les données sont d'abord saisies dans la base de données HIDRO, utilisée au niveau national par l'ANA, puis converties au format HYDRACCESS. Tous les paramètres physico-chimiques sont également saisis localement à l'aide du logiciel HYDRACCESS qui contient de nombreuses procédures d'étalonnage et de contrôle de qualité des données, notamment par corrélation multiple avec les données d'autres stations sur le même cours d'eau, et permet de calculer les séries temporelles des flux de matières selon plusieurs méthodes. Les résultats issus des analyses en laboratoire sont numérisés et font l'objet d'une validation dans les laboratoires d'analyses (LMTG et LAGEQ). Deux fois par an les données consolidées sont intégrées à la base en ligne de l'ORE.

Les caractéristiques des bassins drainés Les informations thématiques de sols, d'occupation du sol, de lithologie et de relief des bassins drainés à chaque station sont disponibles sous forme de cartes en format raster (Fig. 2) ou de graphiques. Il en est de même de la courbe hypsométrique. Ces informations ont été obtenues à partir d'un modèle numérique de terrain de résolution 90m (USGS 2004), d'une carte de types et d'occupation du sol au 1:5 000 000 (Eva *et al.*, 2002; FAO *et al.*, 2000).

La structure de la base de données Les informations collectées par l'observatoire sont organisées dans une base de données relationnelle dont l'entrée principale est le bassin hydrographique drainé aux sites de mesure. La Fig. 3 présente une version de la structure ne montrant que les tables principales. La base est installée sur un serveur MySql et proposée sur Internet via un serveur Web, les pages dynamiques étant générées sur le serveur par une application développée en PHP. Une "applet" permet d'obtenir des graphiques plus élaborés (Fig. 4) et d'extraire les données sous forme de séries chronologiques dans un format exploitable par les applications du commerce ou spécialisées.

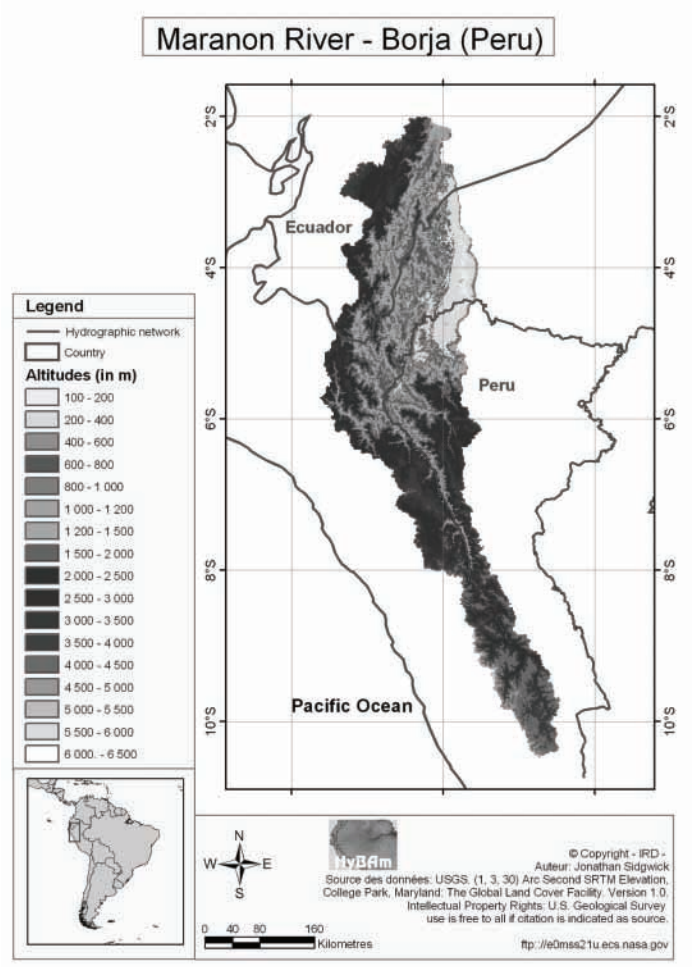


Fig. 2 Un exemple de carte thématique.

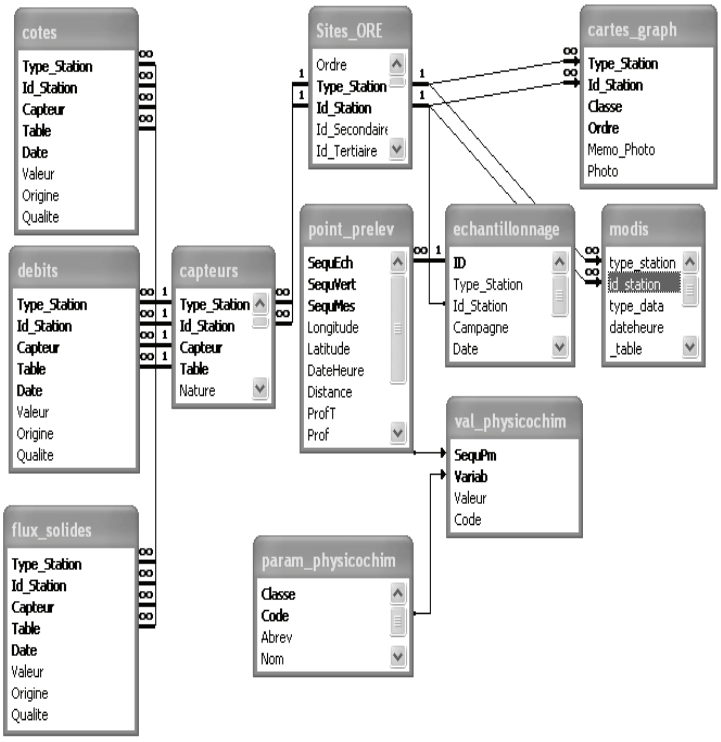


Fig. 3 Structure de la base de données.

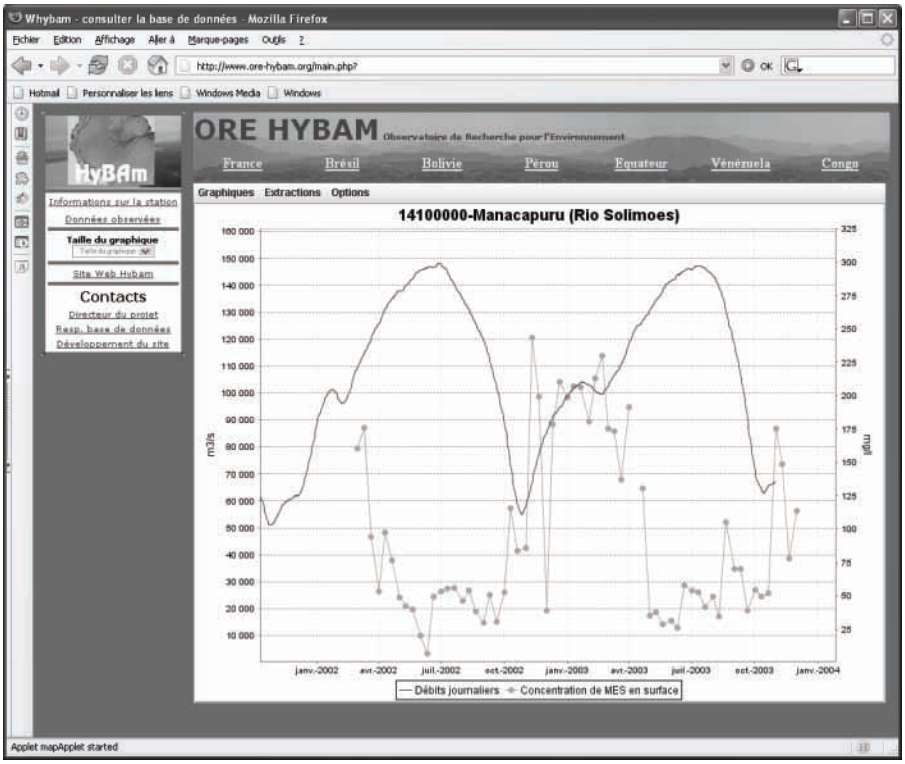


Fig. 4 Un exemple de graphique de données obtenu sur le site.

Utilisation des données de l'ORE HYBAM

Conformément à la politique des Observatoires de Recherche en Environnement, les informations fournies par l'ORE HYBAM sont librement accessibles sur le site (http://www.ore-hybam.org/), à l'aide d'une carte réactive, moyennant une référence à l'origine des données. Ceci concerne aussi bien les données statiques (généralités, photos, cartes, graphiques) que les séries de paramètres observés. En dehors des partenaires directs de l'ORE, les données sont déjà utilisées par de nombreuses équipes de recherche, essentiellement sud-américaines mais aussi européennes ou installées aux Etats-Unis. Une amélioration de la mesure de l'audience du site et du téléchargement des données permettra de mieux appréhender l'utilisation qui en est faite.

Une plate-forme de modélisation déterministe du transfert hydrique (hydrologie de versant et transfert dans les fleuves), sédimentaire et géochimique du bassin de l'Amazone est en cours de développement et regroupera un ensemble de modèles numériques dont les formulations sont adaptées aux données disponibles dans les différents sous-bassins. Cette plate-forme, interfacée avec un SIG et la base de données de l'ORE HYBAM constituera un exemple d'utilisation directe de la base de données.

Apport des données satellitaires

L'ORE HYBAM participe au développement de l'hydrologie spatiale en contribuant à la validation des mesures des radars altimètres (TOPEX/POSEIDON, ERS 1 et 2, JASON, RA2 ENVISAT, GFO) et des lasers altimètres (ICESat). L'existence d'une base de données de terrain pérenne unique en zone tropicale, permettra la poursuite des expérimentations dans le cadre des capteurs futurs (CRYOSAT, WATER). Les résultats du projet CASH (CASH Team, 2006), qui cherche à définir les variables hydrologiques pouvant être dérivées des données d'altimétrie spatiale, pourront compléter les informations fournies par l'ORE (nivellement de stations, pente de ligne d'eau, lacunes).

Par ailleurs, des travaux sont en cours pour calibrer, à partir des données de MES de surface fournies par le réseau ORE, des données d'imagerie spatiale (radiomètres spatiaux à moyenne résolution de la série MODIS et MERIS) au voisinage des stations où le plan d'eau est suffisamment large (Martinez *et al.*, 2004). Les images journalières fournies par MODIS depuis 2000,

devraient permettre de compléter les lacunes qui existent dans les mesures de MES de surface et éventuellement de corriger les données collectées dans le cas d'une hétérogénéité des MES de surface d'une rive à l'autre.

CONCLUSION

Le dispositif mis en place dans le cadre de l'ORE HYBAM répond aux attentes de la communauté scientifique intéressée par l'étude de l'évolution des flux dans le bassin amazonien et leur comparaison avec les deux autres grands bassins tropicaux de l'Atlantique. Reconnu comme un projet régional associant tous les pays du bassin, l'ORE HYBAM est l'une des bases sur lesquelles s'appuiera le Programme Régional pour le Gestion Intégrée des Ressources Hydriques Trans-frontalières dans le Bassin Amazonien. Ce projet, exécuté par l'OTCA (Organisation du Traité de Coopération Amazonien) et les pays du bassin, est financé par le GEF (Global Environment Facility) et a pour objectif la mise en place d'un outil d'aide à la décision, sur tout le bassin amazonien, incluant les composantes socio-économiques, la gestion des risques, les changements climatiques.

REFERENCES

Baumgartner, A. & Reichel, E. (1975) *The World Water Balance*. Elsevier, The Netherlands.

CASH Team (2006) Online altimetry service for hydrology: the CASH project. In: Fifteen Years of Progress in Radar Altimetry (Venice, 13–18 mars 2006).

Degens, E. T, Kempe, S. & Richey, J. E. (1991) Biogeochemistry of major world rivers. In: *Biogeochemistry of Major World River*s (ed. by E. T. Degens, S. Kempe & J. E Richey), 323–347. SCOPE 42. Wiley, Chichester, UK.

Eva, H. D., Belward, A. S., de Miranda, E. E., Di Bella, C. M., Gond, V., Huber, O., Jones, S., Sgrenzaroli, M. & Fritz, S. (2004) A land cover map of South America. *Global Change Biology* **10**(5), 732–745.

FAO, ISRIC, UNEP, CIP (1998) Soil and terrain digital database for Latin America and the Carribean at 1:5 million scale. *Land and Water Digital Media Series 5*. FAO, Rome, Italy.

Filizola, N. & Guyot, J. L. (2004) The use of Doppler technology for suspended sediment discharge determinations in the River Amazon. *Hydrol. Sci. J*. **49**(1), 143–153.

Guyot, J. L. (2005a) HYBAM: contrôles géodynamique, hydrologique et biogéochimique de l'érosion/altération et des transferts de matière dans le bassin de l'Amazone. *La Lettre du Changement global*, PIBC-PMRC France **18**, 21–22.

Laraque, A., Filizola, N. & Guyot, J. L. (2005) Sediment budget in the Brazilian Amazon basin, based on a 10 days sampling procedure. IAHS, Foz de Iguaçu April 2005.

Martinez, J. M., Maurice-Bourgoin, L., Moreira-Turcq, P. & Guyot, J. L. (2004) Use of MODIS and MERIS data for the monitoring of the water quality of the Amazonian rivers and floodplain lakes. Third LBA Scientific Conference, Brasilia, Brésil.

Stallard, R. F. (1988) Weathering and erosion in the humid tropics. In: *Physical and Chemical Weathering in Geochemical Cycles*. (ed. by M. Meybeck & A. Lerman)), 225–246. Kluwer, The Netherlands.

USGS (2004) (1, 3, 30) Arc Second SRTM Elevation, version 1.0. The Global Land Cover Facility, College Park, Maryland, USA.

Vauchel, P. (2004) http://www.mpl.ird.fr/hybam/outils/hydraccess_en.htm.

Climate Variability and Change—Hydrological Impacts (Proceedings of the Fifth FRIEND World Conference held at Havana, Cuba, November 2006), IAHS Publ. 308, 2006.

The decline of hydrological data collection for development of integrated water resource management tools in Southern Africa

HELEN HOUGHTON-CARR & MATT FRY
Centre for Ecology and Hydrology (CEH), Wallingford, Oxfordshire OX10 8BB, UK
hahc@ceh.ac.uk

Abstract The Commission for Africa report (2005) recommends a doubling of arable land under irrigation by 2015, and the World Bank water resources strategy (2004) calls for increased investment in water infrastructure in Africa. The NEPAD environment initiative (2003) states that addressing environmental issues is necessary for achieving goals of sustainable growth and development and a lasting solution to the eradication of poverty. Water resource management is clearly recognized as critical to economic development in Africa, but the value of the data on which decisions are based is less well appreciated, with a decline in data collection and management in recent years. The paper reviews the achievements of two regional initiatives to address the "data problem" and discusses how to use the experience gained for the benefit of future projects.

Key words Southern Africa; data collection; integrated water resource management; FRIEND; SADC-HYCOS

INTRODUCTION

The Southern Africa region experiences great spatial and temporal variations in climate. Lack of storage means water availability is determined primarily by precipitation, which varies annually between about 25 and 2000 mm. The rains are seasonal in nature, extremely variable and uncertain, and evaporation losses are generally high. Drought is a frequent event, as the regional droughts in 1991–1992, and 1994–1995 demonstrate. Flooding can have just as devastating an effect, as shown by the February/March 2000 disaster in Mozambique. There are few areas where there is water of assured quantity and quality throughout the year and, as populations increase, demands for water for irrigation, hydropower, and domestic and industrial supply are growing rapidly. At the same time, there is increasing emphasis on the maintenance of aquatic ecosystems and habitats through environmental flows. Water resource planning is further complicated by the large number of international river basins (e.g. the Okavango, the Zambezi).

The challenge for sustained economic growth and poverty alleviation to meet the Millenium Development Goals (MDGs) in the Southern Africa region is closely associated with sustainable use of natural resources and better management of the environment. Forecasts of the predicted impacts of climate change, in particular the more frequent occurrences of droughts, emphasize the need for a cooperative approach to water resource management across the region. Countries need to develop and implement long-term national programmes based on a multi-sectoral approach to water resources management to improve human welfare, ensure more efficient use of scarce water resources, maintain water quality, and provide options for future use.

THE STATUS OF HYDROMETRIC SERVICES

Within the Southern Africa region, there is a recognized lack of institutional capacity to monitor, plan and manage water resources effectively and sustainably. Many governments have only a limited ability to collect the data needed for long-term water resources management, particularly good quality hydrometeorological time series, such as rainfall and river flow. Long flow records are necessary to obtain reasonable estimates of flow statistics and their variability. In general, the higher the inter-annual variability in rainfall and river flow, the more important long record lengths become (Sene & Farquharson, 1998). At best, short periods of observation of water levels and flows provide only a glimpse of the true, long-term behaviour of a river and, at worst, can be misleading. Furthermore, there are several factors, both natural (e.g. climatic variability) and artificial (e.g. land-use change), that influence flow regimes over time.

However, in sub-Saharan Africa, and elsewhere, there has also been a marked decline in hydrometeorological data collection and management in recent years (e.g. World Bank, 1993;

Copyright © 2006 IAHS Press

WMO, 1996; Giles, 2005). This has been seen in the neglect and abandonment of stations, reductions in budgets for field maintenance and inspection, and insufficient discharge measurements being made to adequately define rating curves. Consequences include a lack of real-time data for monitoring the progress of droughts and floods, and insufficient long-term data for the design of water-related schemes and for the integrated management of large multinational river basins.

In addition, many governments have few skilled people and a high turnover of qualified staff, and lack the funds, equipment and facilities to do the planning and analysis necessary to guide water resource management decisions. The number of technical specialists remains small because of unattractive salaries and poor career prospects. The development of in-house expertise has been further compromised by previous over-reliance on external technical assistance that has not given sufficient attention to developing indigenous capabilities or adapting to the constraints of local circumstances. Furthermore, since water management issues are constantly changing, there is a need for continual training to ensure that organizations have sufficient human resources and technical expertise to meet their operational responsibilities.

THE SOUTHERN AFRICA FRIEND PROJECT

Since 1991, the Southern Africa FRIEND project (SA FRIEND) has aimed to improve the assessment and management of regional water resources through applied research (UNESCO, 1997, 2004). SA FRIEND is coordinated by the University of Dar es Salaam, and implemented by the national hydrological agencies (NHAs) of 12 Southern African countries. The objectives of SA FRIEND include developing improved operational hydrological methods and tools, based on knowledge of flow regimes, and establishing them within the NHAs in the region. Effective tools assist NHAs and water resource managers to more fully appreciate the variability and complexity of the water resource situation, to make improved surface water assessments, and to study the impacts of changes in water demand and climate.

Improved tools for water resource assessment and management developed under the SA FRIEND Phase II (UNESCO, 2004) include the ARIDA (Assessment of Regional Impact of Drought in Africa) software which enhances the abilities of NHAs to analyse historic river flow droughts and to monitor ongoing droughts, and the LF2000-SA (LowFlows-2000-Southern Africa) software which enables water resource managers to estimate flow characteristics and account for artificial influences at ungauged locations. The development of the analytical methods underlying these tools relies on the ready availability of the necessary data. Between 1992 and 1997, SA FRIEND Phase I (UNESCO, 1997) developed the first regional database of flow data from 676 stations across the region (Table 1). The period of record ranges from 1940 to 1992, and from 1 to 51 years per station, with an average of 23 years per station.

Table 1 Number of gauging stations and station years of flow data contributed to the SA FRIEND river flow database in 1997 by partner countries.

Country	No. of gauging stations	No. of station years
Angola	19	107
Botswana	24	371
Lesotho	23	222
Malawi	37	783
Mauritius	not a member in Phase I	
Mozambique	16	384
Namibia	46	847
South Africa	287	7828
Swaziland	35	632
Tanzania	79	1447
Zambia	25	600
Zimbabwe	85	1696
Total	676	15190

The intention was that future research projects could utilize these data, but both the ARIDA and LF2000-SA projects subsequently experienced some difficulties in this regard. The ARIDA project considered just 15 of the stations suitable for development of the drought analysis methods, and the LF2000-SA project obtained data instead directly from the NHAs. Problems with the database included: insufficient coverage of the range of basin areas, geomorphological conditions, climates and flow regimes; poor geographical spread, especially in the more arid areas; lack of information about artificial influences affecting flow regimes; and lack of long, validated records of good quality. Furthermore, the database was by then at least 10 years out of date and there was no provision for updates and maintenance during Phase II and beyond.

THE SADC-HYCOS PROJECT

During the period from 1998 to 2001, a network of 48 data collection platforms (DCPs) was established at key locations on the major rivers in the region (excluding South Africa which already had 46 established sites) under Southern African Development Community–Hydrological Cycle Observation System (SADC-HYCOS; Table 2). This EU-funded project was the second regional component of the World Hydrological Cycle Observation System (WHYCOS) of WMO, and the first attempt to implement a project of such technical complexity and magnitude in the Southern Africa region. Rodda *et al.* (1993) give a more detailed introduction to WHYCOS, and Houghton-Carr *et al.* (2000) provide further information on the aims and activities of SADC-HYCOS. Data are transmitted from each DCP on a 3-hourly basis using the METEOSAT satellite system, and stored in a regional database in the Department of Water Affairs in Pretoria.

Early in 2006, a review was undertaken to assess the current operational status of the 48 installed DCPs. Although a rather crude indicator of the long-term success, or otherwise, of the project, this is a readily available and quantifiable measure. Contact with eight out of the ten NHAs revealed that only seven out of the 38 DCPs installed in those countries were still operational (Table 2). Five of these are in Tanzania; Namibia also has five working DCPs, but has actually replaced and reinstalled all the original DCPs at its own expense. However, it was not possible to access data for the operational stations through the SADC-HYCOS website (http://sadchycos.dwaf.gov.za). Problems reported by the NHAs, some of which should have been foreseen, include: broken water level sensors, vandalism, wildlife damage (chewing cables), theft of solar panels, batteries and cables, electrical faults, transmission faults, flood damage, breakdown, and need for general maintenance and lack of resources to carry it out.

Table 2 Number of SADC-HYCOS DCPS, originally installed (1998-2001) and operational in February 2006.

Country	No. of DCPs installed	No. of DCPs operational
Angola	5	N/A
Botswana	4	1
Lesotho	5	N/A
Malawi	6	0
Mozambique	3	1
Namibia	5	0*
Swaziland	4	0
Tanzania	5	5
Zambia	6	0
Zimbabwe	5	0
Total	48	7

* Namibia has five operational DCPs which are replacements of their HYCOS DCPs.

DISCUSSION

The particular problems of data collection, and investment in data collection, in Southern Africa, and other developing countries, have been addressed to some extent by regional initiatives such as SA FRIEND and SADC-HYCOS. Through regular opportunities for communication and face-to-face interaction with counterparts from other countries in the region, both projects were successful

in promoting cooperation between water resources managers and researchers, and the free exchange of data, information, expertise and ideas. All the countries regarded this as highly beneficial, and several of these contacts, usually between neighbouring countries, have continued.

However, a recent review of the SA FRIEND countries revealed disappointingly little use of the tools produced in Phase II, given that these were identified as priorities by the NHAs on the project steering committee. Furthermore, there has been little, if indeed any, communication between the coordination centre and the NHAs since Phase II finished and the last steering committee meeting in February 2004: regional communications have not been maintained. SA FRIEND was very much driven by funding from the UK Department for International Development (DFID), and when DFID-funding ceased, SA FRIEND activities ceased. There appears to be little drive within the Southern Africa region itself to sustain SA FRIEND and take it forwards, not because the project is of little relevance, but for reasons of personnel and resources.

Similarly, SADC-HYCOS was seen by several of the NHAs as yet another donor-driven activity using inappropriate equipment, tools and software and requiring inputs from already over-stretched hydrometric staff. The failure of some DCPs is not unexpected, but the failure of the majority is a cause of concern; many NHAs did not budget for maintenance as they had committed to do. Comments from the NHAs have referred to: poor project planning and implementation, lack of input from the NHAs, poor design and installation of the DCPs, inappropriate sensors for the climate and environment, no direct contact with the DCP supplier, inadequate training of local staff, and late implementation of the website which has experienced repeated malfunctioning.

Looking to the future, the extension of the WR90 water resources modelling system, started in SA FRIEND Phase II, provides an opportunity for assessing water resources availability at ungauged locations across the whole of Southern Africa using an approach based on the Pitman rainfall–runoff model (UNESCO, 2004). The Netherlands government has recently finalized an agreement with SADC for financial support to SADC-HYCOS Phase 2, a first step of which would involve re-establishing contact with the NHAs and rehabilitating the existing DCPs. If initiatives like SA FRIEND and SADC-HYCOS are to be successful in subsequent phases, it is imperative that the issues relating to their long-term lack of achievement to date are resolved.

THE WAY FORWARD

It is important that water resources are developed in an equitable, integrated and sustainable manner, and in such a way as to support enhanced socio-economic development. However, hydrological systems are complex with many uncertainties. It is essential that methods and tools such as those developed in SA FRIEND are based on consistent, good quality, and readily available data from sites of key importance throughout the region and representing the full range of probable flow conditions. The Commission for Africa (2005) recommends improved capture and storage of existing data, new monitoring stations in low coverage areas, and the uptake and use of data by African institutions. A regularly updated regional database of such records, whether sourced from existing manually-read gauges or new automatic DCPs, or from a combination of the two, would be an invaluable data set for many hydrologists wishing to solve practical water resource problems. Whilst the data might not be ideal for every application, they would at least provide a starting point for initial assessments, particularly to support investments into major water resource projects e.g. irrigation schemes, and a foundation from which to respond to new challenges.

In recognition of the need for African researchers to become more involved in the design and planning of projects, African Water is a current EU initiative to increase the involvement of Africans in the water-related research programmes of the EU (http://www.africanwater.net). There is no lack of research ideas within SADC NHAs; identified topics include: sedimentation issues, water balances of lakes, impacts of climate change, water use efficiency in irrigation, flood prediction and warning, transmission losses, environmental flows, transboundary water issues, and future data collection strategies. African Water will give African hydrologists, water resource managers and researchers, including those in SA FRIEND NHAs, the capability and opportunity to actively participate in EU-funded research, either through collaboration with European researchers, or through their own proposals.

There is also a need for better communication and coordination of the water-related research activities of donor development agencies, and recognition by the donors that sustaining an established and successful programme (which covers many data-related projects) can be as beneficial as, and possibly more valuable than, support to a comparatively exciting, but untested, new initiative. Donors also need to envisage a longer time horizon (10–15 years) for project funding than the 3–5 years typical now. The EUWI-ERA-NET is an EU scheme to provide a framework through which member states can work together more effectively (http://www.euwi-era.net). The ERA-NET aims to work with developing country partners to develop a strategy and work plan to identify their priorities for water-related research and potential collaboration, and to establish tools for more efficient sharing of information on member state research programmes.

Finally, whilst both the SA FRIEND and SADC-HYCOS projects did involve significant capacity building components, they perhaps relied too heavily on key individuals trained in regional workshops who did not necessarily pass on their knowledge to their colleagues, with the result that when some of these staff left the NHAs (often for better paid jobs in the private sector), the capacity was lost. Therefore, capacity building requirements will feed into the design of future systems and tools, and future capacity building activities will place greater emphasis on the dissemination of training to ensure maximum potential impact in terms of numbers of people reached.

CONCLUDING REMARKS

Water resource management is clearly recognized as critical to economic development, unlike the value of the data on which crucial decisions are made. Institutional reform is needed to acknowledge the importance of hydrometry and data management within, and by, the NHAs. A more coherent approach to data collection requires local capacity, appropriate technology, and long-term donor and institutional commitment, combined with the more intimate involvement of pro-active African water engineers and researchers from the initial concept stage of new projects. The implementation of SA FRIEND and SADC-HYCOS was costly in terms of both effort expended and resources used, and it is essential that the valuable experience gained and lessons learned are not forgotten, and are used to inform future proposals and investments into water resource schemes.

Acknowledgements The views expressed in the paper are those of the authors, and not necessarily of the coordinating or funding bodies of any of the projects mentioned, or of the NHAs in the partner countries. The authors pay tribute to the contribution of Jeremy Meigh (1954–2006) who lead the CEH component of the SA FRIEND project.

REFERENCES

Commission for Africa (2005) Our common interest. http://www.commissionforafrica.org.

Giles, J. (2005) Solving Africa's climate data problem. *Nature* **435**, 863.

Houghton-Carr, H. A., Sene, K. J., Fry, M. J., Boyer, J. F. & Booysen, G. (2000) Towards development of a regional hydrometric database system for Southern Africa. In: *Proc. BHS Seventh National Hydrology Symp*. (Newcastle, UK), 4.53–4.58.

New Partnership for Africa's Development (NEPAD) (2003) Action plan for the environment initiative. NEPAD, Midrand, South Africa.

Rodda, J. C., Pieyns, S. A., Sehmi, N. S. & Matthews, G. (1993) Towards a world hydrological cycle observing system. *Hydrol. Sci. J.* **38**(5), 373–385.

Sene, K. J. & Farquharson, F. A. K. (1998) Sampling errors for water resources design: the need for improved hydrometry in developing countries. *Water Resour. Manage.* **12**, 121–138.

UNESCO (1997) Southern Africa FRIEND. *IHP-V Tech. Documents in Hydrology no. 15.* UNESCO, Paris, France.

UNESCO (2004) Southern Africa FRIEND Phase II 2000–2003. *IHP-VI Tech. Documents in Hydrology no. 69.* UNESCO, Paris, France.

WMO (1996) The adequacy of hydrological networks: a global assessment. *Tech. Document no. 740*. WMO, Geneva, Switzerland.

World Bank (1993) Sub-Saharan Africa hydrological assessment: project summary document. World Bank, Washington DC, USA.

World Bank (2004) Water resources sector strategy: strategic directions for World Bank engagement. World Bank, Washington DC, USA.

Climate Variability and Change—Hydrological Impacts (Proceedings of the Fifth FRIEND World Conference held at Havana, Cuba, November 2006), IAHS Publ. 308, 2006.

The use of spatial information to improve hydrometric network design and evaluation

CEDRIC LAIZE & TERRY MARSH

Centre for Ecology and Hydrology, Wallingford, Oxfordshire OX10 8BB, UK
clai@ceh.ac.uk

Abstract Operational needs commonly dictate the evolution of hydrometric networks. Such an approach can fail to meet strategic water management information objectives (e.g. to estimate flows at ungauged sites, to detect hydrological change). This paper examines the role of digital spatial information to inform network evolution. Capitalising on a range of catchment physical descriptors and spatial characteristics commonly used in hydrological studies, the UK National River Flow Archive (NRFA) developed two indices that assess the strategic value of individual gauged catchments, independently from the performance of the associated gauging station. The Representative Catchment Index (RCI) quantifies how representative a catchment is of a specified area, in relation to a selection of spatial characteristics. The Catchment Utility Index (CUI) examines the influence of individual catchments in the context of a regionalization methodology used for flood estimation. A large UK catchment is used as a case study to demonstrate how these indices can support network reviews.

Key words hydrometric network; hydrometry; network management; network rationalization; regionalization; representative catchment; spatial information

INTRODUCTION

Hydrometric data are the foundation of water management and gauging station networks throughout the world and service a rapidly growing need for river flow data. However, many networks are in decline due to funding, technical and institutional constraints triggering reductions in flow measurement capabilities and gauging station densities in many parts of the world (Vörösmarty, 2002).

Conceptually, hydrometric networks should evolve to address both operational and, increasingly, more strategic needs, e.g. to estimate flows at ungauged sites (Thomas, 1994) and to detect hydrological change (Kundzewicz & Robson, 2004). Yet, in practice, most reviews of networks focus principally, if not exclusively, on assessing how well individual stations meet operational requirements (e.g. flood warning, resource assessment, river regulation), and do not take into account their strategic value.

Significant research effort has been devoted to optimizing hydrometric networks and maximizing their information delivery. Network appraisal mechanisms have evolved from simple gauging station density guidelines based on physiographic regions (World Meteorological Organization, 1994) to more sophisticated statistical analyses, e.g. using both catchment physiography and flow characteristics, or focusing on the information content of the flow record (see Markus *et al.*, 2003). This paper examines the approach taken by the UK National River Flow Archive (NRFA) that, unlike the aforementioned techniques, relies specifically on spatial characteristics to assess the strategic value of individual gauged catchments, independently from their associated gauging station.

Despite the increasing availability of digital geodatasets, which is widely capitalized on in regionalization procedures, there have only been a few studies (e.g. Black *et al.*, 1994) exploring the potential of spatial information to inform network evolution. Capitalizing on a wide range of catchment physical descriptors (e.g. size, average rainfall) and spatial data sets (e.g. elevation, land use), the NRFA developed two indices: the Representative Catchment Index (RCI) and the Catchment Utility Index (CUI). Both are used by the NRFA to review the UK gauging station network.

In the UK, hydrometric data from the various measuring authorities are collected by the NRFA, which maintains a comprehensive database of river flows totaling approximately 45 000 years of records. In this paper, the UK gauged network comprises 1236 gauging sites, for which catchment boundaries and spatial information have been derived. After a brief presentation of both indices, the assessment procedures used by the NRFA are demonstrated in a case study focusing on a single gauged catchment.

Copyright © 2006 IAHS Press

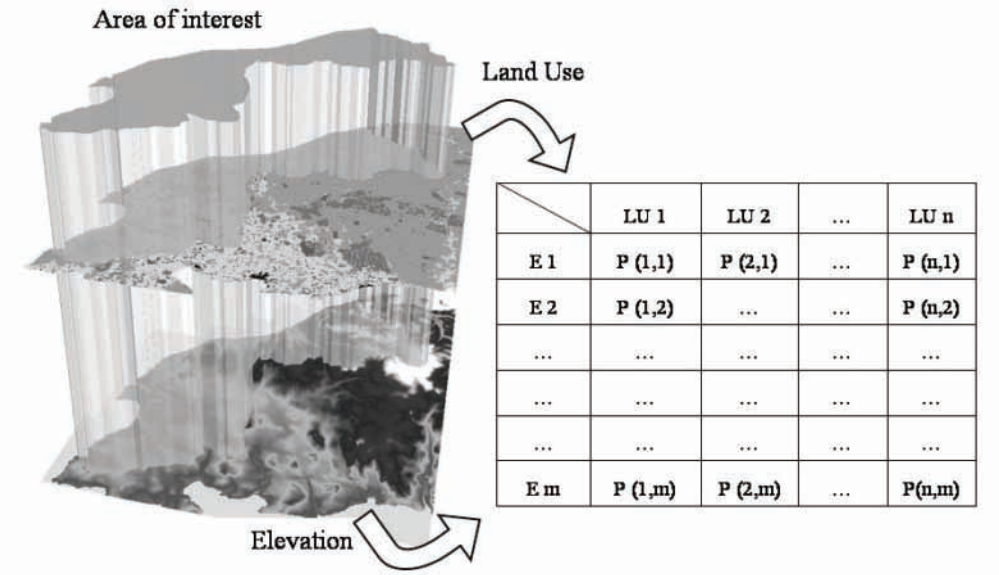


Fig. 1 Example of the integration of two spatial data sets to characterize an area of interest (e.g. catchment) as a bi-dimensional matrix storing the proportion of any combination of datasets occurring within the analysis mask.

REPRESENTATIVE CATCHMENT INDEX

The WMO recommends that hydrometric networks should include at least one gauged catchment that is representative of each region where hydrological similarity is presumed (Toebes & Ouryvaev, 1970). The RCI (Laizé, 2004) quantifies how representative a catchment is of a reference area, in relation to a selection of spatial characteristics. First, using a Geographical Information System (GIS), raster data sets are integrated in order to characterize the relationship between spatial data sets within the catchments and reference areas. The boundary of an area of interest is used as an analysis mask, i.e. all operations are constrained to the points located within this area. For each location within the mask, the corresponding raster values are extracted. Each area is described by a matrix storing the proportion of any combination of characteristics occurring within the area. This is illustrated in Fig. 1 using two characteristics. Once a selection of catchments and a reference area have been processed, the catchment matrices are compared to the reference matrix on a cell-by-cell basis in order to calculate the catchments' RCI, ranging from 0 (no match) to 100 (identical matrices). The resultant score allows for the ranking of the catchments relative to each other. For this study, the RCI implementation used three characteristics: elevation, land use, and soil type.

CATCHMENT UTILITY INDEX

The CUI is based on procedures developed for the UK *Flood Estimation Handbook* (FEH; Institute of Hydrology, 1999). The FEH capitalizes on a digital terrain model (DTM) of the UK (Morris & Flavin, 1990), which was designed to be consistent with the drainage network and allows the boundaries of around four million catchments to be derived. Catchment descriptors have been automatically generated for those catchments whose area exceeds 0.5 km^2.

To estimate flood peaks at an ungauged site, the FEH combines data from a number of stations—usually 20 for a 100-year return period—whose catchments are similar to that of the target site in terms of size, wetness, and responsiveness. These characteristics are expressed as three catchment descriptors: Area, Standard-period Average Annual Rainfall (SAAR), and Base Flow Index (BFI). Catchment similarity is expressed as the geometric distance in a three-dimensional Area–SAAR–BFI (ASB) space from the gauged catchment to the target catchment. The selected stations constitute a pooling-group (PG).

Figure 2 shows the geographical distribution and order of selection of the PG stations for a target ungauged catchment in the Pennines. The PG exercise is replicated for each of the four million ungauged catchments derived from the DTM, using an automated implementation of the FEH procedure; each PG includes 20 catchments selected from the gauged network.



Fig. 2 Geographical distribution of the 19 gauging stations (white dots) from the pooling-group (100-year return period) of an ungauged site (solid black).

From the four million pooling-groups thus constituted, two sets of statistics are derived for each of the gauged catchments: number of inclusions (NI), i.e. the number of times a catchment is included in a PG; average score (AS) based on a catchment's average ranking position in the pooling-groups, ranging from 1 (always included last) to 20 (always first). The CUI synthesizes both into a single index, which ranges from 0 (lowest) to 100 (highest). Due to its construction, the CUI is not suitable for application across catchments of all sizes (Laizé *et al*., 2006), and it is recommended that catchment appraisals are undertaken within a designated size range (see Case Study).

CATCHMENT SPATIAL ASSESSMENT

Typically, a comprehensive spatial assessment would begin by analysing individually the catchment descriptors and spatial data sets, then applying the RCI and CUI. The initial analysis identifies broad catchment types (e.g. lowland permeable, afforested upland), and gives an insight into how individual catchments relate to the gauged network and the country as a whole (e.g. to identify over- or under-gauged catchment types). This information is also necessary to guide the application of the RCI (e.g. selecting the reference area) and CUI (e.g. selecting the size range). In order to describe the reviewing procedure, this paper presents the assessment of a single gauged catchment associated with the Royal Windsor Park gauging station (39072) on the River Thames (Fig. 3).

Analysis of the catchment descriptors

Catchment 39072 has an area of 7125 km^2, an average annual rainfall of 690 mm, and a BFI of 0.66. According to the catchment size typology used in the European Water Framework Directive (WFD; European Commission, 2000), it is a large catchment (>1000 km^2). There are 101 gauged catchments of this type in the UK but only nine with an area >5000 km^2. Table 1 gives an indication of the density of the UK gauging network relative to the area descriptor. Catchment 39072 belongs to a type that is slightly less well gauged (higher ratio ungauged to gauged) in comparison to medium-sized catchments (100–1000 km^2). A similar picture emerges from the SAAR and BFI descriptors. It is therefore likely that 39072 belongs to an under-gauged catchment type. Indeed, within a distance of 0.5 point in ASB space (i.e. similar catchments), 39072 has only five neighbours; as a comparison, 80% of the gauged catchments have at least 12 other similar catchments, and the most well represented type has 71.

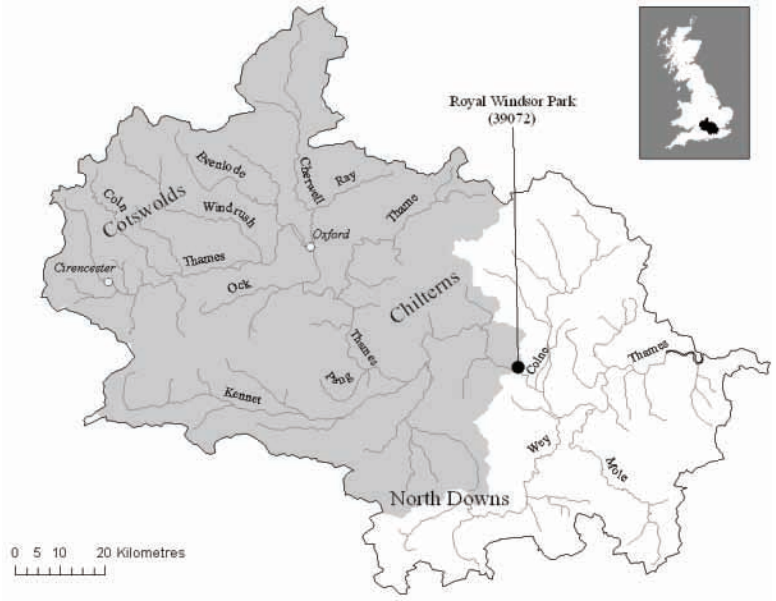


Fig. 3 Thames at Royal Windsor Park (39072); gauging station (black dot), catchment (grey area).

Table 1 Comparison of the number of UK gauged catchments with mainland Britain ungauged catchments relatively to their area; catchments larger than 0.5 km^2 only.

	Area (km^2) 0.5–10	10–100	100–1000	1000–10 000
Number of ungauged catchments	2 749 855	646 899	218 479	43 414
Number of gauged catchments	43	501	591	101
Ratio ungauged to gauged	63 950	1 291	370	430

Table 2 Land-use breakdown for catchment 39072 and England.

Land use category	Proportion (%) Catchment 39072	England
Sea/Unclassified	0.0	0.3
Woodland	13.2	11.0
Arable & horticulture	40.6	34.8
Grassland	34.0	38.1
Mountain, heath, bog	1.3	3.6
Built-up areas	10.4	11.2
Water (inland)	0.6	0.5
Coastal	0.0	0.5

Analysis of the spatial data sets

Elevation With more than 90% of its area below an elevation of 200 m, 39072 is a lowland catchment according to the WFD altitude typology; around a third of the gauged catchments in the UK are of that type.

Land use Catchment 39072 is very typical of England (Table 2). Considering the two main categories (Arable and Grassland), there are only around 35 lowland catchments with a similar mix of land use.

Hydrogeology The catchment hydrogeology comprises a mix of high permeability and very low permeability bedrock (about 40% each), which is typical of lowland England.

Application of the RCI

The initial assessments suggest that 39072 may be representative of UK lowlands, especially lowland England. This information guides the choice of reference areas to use in the RCI analysis. Following the procedure described earlier, the RCI for all UK gauged catchments were calculated using both England and lowland England (below 200 m) as reference areas. With an RCI of 48.3,

39072 is the 23rd most representative catchment for England in the entire gauged network. For lowland England, it is the 11th most representative catchment considering only the 101 gauged catchments with a size greater than 1000 km^2 (RCI = 51.8).

Application of the CUI

In this case study, catchment 39072 is included in nearly 4000 pooling-groups (Table 3), and has a high average rank within each PG. Correspondingly, 39072 has the second highest CUI for large catchments (>1000 km^2) across the UK. This confirms how influential this catchment is in relation to FEH applications, and, generally, to regionalization techniques.

Table 3 Ranked CUI for large catchments (>1000 km^2); first ten only (out of 101).

Station number	River	Area (km^2)	SAAR[a] (mm)	BFI[b]	NI[c]	AS[d]	CUI
15006	Tay	4586.8	1424	0.47	848	17.74	84.55
39072	Thames	7125.0	696	0.66	3862	16.49	79.18
15003	Tay	3211.0	1609	0.44	1486	16.70	77.27
28074	Soar	1300.9	641	0.41	5887	14.68	65.44
39002	Thames	3480.8	690	0.65	5452	14.47	63.28
39046	Thames	3425.7	691	0.65	5547	14.27	61.69
39130	Thames	4627.8	680	0.64	4894	14.32	61.52
43003	Avon	1455.1	807	0.89	2236	14.72	61.50
28093	Soar	1110.7	640	0.40	6016	13.48	55.41
43001	Avon	1616.5	809	0.88	2260	14.00	55.29

[a] Standard-period Average Annual Rainfall
[b] Base Flow Index
[c] Number of inclusions
[d] Average Score

DISCUSSION

The procedures presented in this paper are based solely on the physical characteristics of the gauged catchments. The procedures can be potentially applied to any of the four million catchments derived from the DTM, and to other countries where there is a GIS of key catchment descriptors. Although computationally demanding, the methodology could allow hydrometric network managers to identify the most influential ungauged catchments, and to explore the impact of adding stations to, or removing stations from the existing network.

In practice, it is expected that the catchment spatial indices will be used in combination with an appraisal of the time series (e.g. length of record), station hydrometric performance, artificial influences, and operational issues (e.g. logistics, maintenance costs) in order to provide measuring authorities with an objective assessment of the gauging station long-term strategic value. Using the indices, gauged catchments are assessed independently from their associated gauging station, so that network managers can particularly focus on sites where there are discrepancies between hydrometric capability and regional value (e.g. an unreliable station monitoring a very valuable catchment may be worth upgrading). The application of these indices to improve the overall cost-effectiveness of gauged network management is also investigated. Combined with information on flow regime characteristics and the hydrometric performance of gauging stations, catchment spatial indices constitute a powerful decision support mechanism to guide network evolution.

Acknowledgement This paper benefited from helpful discussion with colleagues. Some of the features in the figures are © NERC, and based upon © Crown Copyright 100017897 2005.

REFERENCES

Black, A. R., Lees, M. L., Marsh, T. J. & Dixon, J. M. (1994) A review of the Northern Ireland hydrometric network. Report to the Department of the Environment (NI). Institute of Hydrology, Wallingford, UK.

European Commission (2000) Directive 2000/60/EC, Establishing a framework for Community action in the field of water policy. *Official Journal of the European Communities* **L327**, 1–72.

Institute of Hydrology (1999) *Flood Estimation Handbook*. Five volumes and associated software. ISBN 0 9485540 94X.

Kundewicz, Z. W. & Robson, A. J. (2004) Change detection in hydrological records – a review of the methodology. *Hydrol. Sci. J.* **49**(1), 7–19.

Laizé, C. L. R. (2004) Integration of spatial datasets to support the review of hydrometric networks and the identification of representative catchments. *Hydrol. Earth System Sci.* **8**(6), 1103–1117.

Laizé, C. L. R., Marsh, T. J. & Morris, D. G. (2006) Capitalising on regionalisation methodologies to support the appraisal and evolution of hydrometric networks. *Proc. ICE Water Management.* (submitted).

Markus, M., Knapp, H. V. & Tasker, G. D. (2003) Entropy and generalized least square methods in assessment of the regional value of streamgages. *J. Hydrol.* **283**, 107–121.

Morris, D. G. & Flavin, R. W. (1990) A digital terrain model for hydrology. In: *Proc. 4th International Symposium on Spatial Data Handling* (University of Zurich, Switzerland), **1**, 250–262.

Thomas, W. O. Jr (1994) An overview of selected techniques for analysing surface-water data networks. *Operational Hydrology Report no. 41, WMO-no. 806.* WMO, Geneva, Switzerland.

Toebes, C. & Ouryvaev, V. (eds) (1970) Representative and experimental basins. *Studies and Reports in Hydrology 4*, UNESCO.

Vörösmarty, C. J. (2002) Global water assessment and potential contributions from Earth systems science. *Aquat. Sci*. **64**(4), 328–351.

World Meteorological Organization (1994) *Guide to Hydrological Practices*, fifth edn. WMO-no. 168. WMO, Geneva, Switzerland.

Climate Variability and Change—Hydrological Impacts (Proceedings of the Fifth FRIEND World Conference held at Havana, Cuba, November 2006), IAHS Publ. 308, 2006.

Modelación hidrológica empleando isoyetas de relieve, una aproximación geoestadística

RAÚL BECERRA-SORIANO & ALFONSO GUTIÉRREZ-LÓPEZ

Instituto Mexicano de Tecnología del Agua, IMTA, Subcoordinación de Hidrología y Mecánica de Ríos, Paseo Cuauhnáhuac 8532, CP 62780, Jiutepec, Morelos, México

rabs_@hotmail.com, agutierrez@tlaloc.imta.mx

Resumen En el marco del cálculo de la disponibilidad hídrica, este trabajo plantea un esquema geoestadístico para describir la distribución espacial de la precipitación, considerando el relieve topográfico como el principal generador de su variabilidad espacial. Se utiliza un variograma direccional ajustado a los datos de la topografía, como una ecuación de transferencia para generar campos de lluvia con relieve. Los resultados muestran que la disponibilidad hídrica de una región, varían cuando se estima el volumen anual precipitado, empleando isoyetas tradicionales, respecto al calculado con isoyetas de relieve.

Palabras clave geoestadística; kriging; precipitación media; isoyetas; relieve

Hydrological modelling using relief-isohyets: a geostatistical approximation

Abstract This paper describes the spatial structure of precipitation by a geostatistical approach, using topography as a main component in the rain field variability. A directional semi-variogram fixed to the topography data was used for rain field construction. When the mean annual precipitation is calculated using traditional isohyets, the results show important variations of hydrological availability in the region, with respect to the relief-isohyets.

Key words geostatistics; kriging; mean precipitation; isohyets; relief

INTRODUCCIÓN

Con el incremento en la capacidad de procesamiento de información durante la década de los 1980s, se establecieron metodologías que parametrizan y describen la distribución espacial de la precipitación (Gyasi-Agyei, 1999). Con el aumento de la parametrización y la reciente aplicación de los métodos estocásticos y multivariados en el análisis de las series hidrológicas, los errores cometidos en las interpolaciones son cada vez menores debido a que los modelos empleados son cada vez mas complejos (Goovaerts, 2000; Herr & Krzysztofowicz, 2004; Young, 2005). El concepto de regionalización hidrológica se inició con (Matheron, 1969; Delhomme, 1978), Para el caso de la hidrología y específicamente en la interpolación espacial de la precipitación tradicionalmente se realiza la interpolación óptima con kriging (Ahrens, 2005), en estos análisis se obtiene el modelo que mejor ajustó al variograma experimental. Otros trabajos realizan un análisis exhaustivo del variograma, analizando la anisotropía de los datos (Desbarats *et al*, 2002; Lloyd, 2004). Con el objetivo de estudiar adecuadamente la regionalización hidrológica se presentan los siguientes conceptos.

INTERPOLACIÓN ESPACIAL

La interpolación espacial es un procedimiento matemático utilizado para predecir el valor de un atributo en una localidad precisa a partir de valores obtenidos de puntos vecinos, ubicados al interior de la misma área de estudio. La interpolación se utiliza para transformar un número finito de observaciones, por ejemplo cotas de terreno, en un espacio continuo de manera que su patrón espacial sea comparable con aquel presentado por las observaciones puntuales de base (Burrough & McDonnell, 1998). La literatura describe diferentes métodos de interpolación. Estos se clasifican en globales y locales, de acuerdo a la cantidad de información que utilizan, y en exactos e inexactos, de acuerdo al valor de las estimaciones respecto a los datos de origen (Tabla 1).

VARIABLES REGIONALES

Las variables regionales designan un fenómeno ocurrido en una cierta área y en un lapso de tiempo formando una estructura espacio-temporal definida. Generalmente en los modelos regionales la lluvia aparece como una función aleatoria $Z(x_i,y_i)$ conocida por sus magnitudes históricas medidas

Copyright © 2006 IAHS Press

Tabla 1 Métodos de interpolación especial.

Método	Global/Local	Tipo de interpolación
Clasificación	Global	Inexacta
Superficies de tendencia	Global	Inexacta
Modelos de regresión	Global refinamiento local	Inexacta
Polígonos de Thiessen	Local	Exacta
Interpolación lineal	Local	Exacta
Inverso de la distancia y medias móviles	Local	Inexacta cuando se aplica un suavizado de la superficie interpolada
Kriging	Local, pero con un variograma global	Exacta

en diversos puntos experimentales $Z(t_i)$. El principio de estos métodos de transferencia se resume en la búsqueda de un estimador lineal:

$\hat{Z}(x, y) = \sum w_i(x, y)\, Z(x_i, y_i)$; en donde los coeficientes verifiquen la condición de sesgo nulo:

$$\sum w_i(x, y)\, E\left[Z(x_i, y_i)\right] - E\left[Z(x, y)\right] = 0 \tag{1}$$

Un criterio de minimización del error cuadrático medio de estimación puede expresarse como:

$$w_i E\left[Z_i Z_j\right] - E\left[Z_t Z_i\right] = 0 \tag{2}$$

donde: $E[Z(t)]$ es la media de $Z(x,y)$ sobre el espacio de eventos $E[Z_t, Z_t]$. De esta forma, el objetivo principal de esta transferencia es calcular los coeficientes $w_i(x,y)$ del estimador $Z(x, y)$. El cálculo de los coeficientes w_i , se obtiene de solucionar el sistema de ecuaciones formado por las ecuaciones 1 y 2; sin embargo, no es posible resolverlo en tanto no se disponga de una función de covarianza $E[Z_t, Z_t]$ que permita calcular los términos $E[Z_t, Z_i]$. El principio de la interpolación espacial se basa en una *hipótesis de homogeneidad* llamada "hipótesis intrínseca" menos restrictiva que la tradicional hipótesis de estacionariedad conocida como hipótesis de orden 2. La hipótesis de homogeneidad supone ante todo que la derivada del valor medio de las mediciones es localmente constante; esto implica que los dos primeros momentos de las variables estudiadas se correlacionan en forma espacial con una función aleatoria invariante dentro de la región hidrológicamente homogénea, esto es:

$$E\left[Z_{t+h} - Z_t\right] = 0 \tag{3}$$

$$E\left[\left(Z_{t+h} - Z_t\right)^2\right] = 2\gamma(h) \tag{4}$$

Con las funciones de covarianza:

$$\gamma(h) = \left[C(0) - C(h)\right];\ C(h) = E\left[Z_t - m(h)\, Z_{t+h} - m(h)\right]$$

De esta forma, cualquier función aleatoria $Z(x, y)$ será llamada *Función Aleatoria Intrínseca de orden 1*, en donde la función γ *variograma* permite exprimir así los términos de la covarianza, independientemente de la derivada de la media de las mediciones locales. Esta formulación es también la base del procedimiento del kriging ordinario. Con una función de covarianza, podríamos decir *generalizada*, se tienen las herramientas necesarias para realizar una transferencia de información hidrológica (Creutin, 1979).

INTERPOLACIÓN POR KRIGING

En el caso de la hipótesis de estacionaridad de segundo orden, la media m se considera constante (Obled, 1996). La condición insesgada es: $\sum w_i(x, y)\, E\left[Z(x_i, y_i)\right] - E\left[Z(x, y)\right] = 0$ con: $E\left[Z(x_i, y_i)\right] = E\left[Z(x, y)\right] = m$; se escribe: $w_i = 1$.

La condición óptima $E\left[\left(\hat{Z} - Z\right)^2\right]$ mínima se escribe:

$$\frac{\partial}{\partial w_i}E\left[\left(Z-\hat{Z}\right)^2\right]=\frac{\partial}{\partial w_i}\left\{E\left[\left(Z-\sum_i w_i Z_i\right)^2\right]\right\}-0$$
$$=\frac{\partial}{\partial w_i}\left\{E\left[Z^2\right]-2\sum_i w_i E(Z_i Z_0)+\sum_i\sum_j w_i w_j E\left[Z_i Z_j\right]\right\} \quad (5)$$
$$=\frac{\partial}{\partial w_i}\left\{C(0)-2\sum_i w_i C(t^i-t)+\sum_i\sum_j w_i w_j C(t^i-t)\right\}$$

Si se tiene en cuenta la condición insesgada con μ multiplicador de Lagrange:

$$\frac{\partial}{\partial w_i}E\left[\left(Z-\hat{Z}\right)^2+\mu\right]=\frac{\partial}{\partial w_i}\left\{C(0)-2\sum_i w_i C(t^i-t)+\sum_i\sum_j w_i w_j C(t^i-t)+\mu\sum_i w_i\right\}=0$$

sea: $\sum_i C(t^i-t^j)+\mu'=C(t^i-t)$; $\mu'=\mu/2$; En el caso de la hipótesis intrínseca en donde se introduce el variograma como una función de la covarianza, le sistema de Krigeage simple será:

$$\sum_{i=1}^{n} w_i=1;\ \sum_{i=1}^{n} w_i\gamma(t^i+t^j)+\mu'=\gamma(t^i-t)$$

$$\begin{bmatrix}\gamma(t^1,t^1) & \cdots & \gamma(t^1,t^n) & 1\\ \vdots & & \vdots & \vdots\\ \gamma(t^n,t^1) & \cdots & \gamma(t^n,t^n) & 1\\ 1 & \cdots & 1 & 0\end{bmatrix}\begin{bmatrix}w_1\\ \vdots\\ w_n\\ \mu\end{bmatrix}=\begin{bmatrix}\gamma(t^1,t)\\ \vdots\\ \gamma(t^n,t)\\ 1\end{bmatrix} \quad (6)$$

De esta forma se puede representar el variograma sobre un diagrama $[h,\gamma(h)]$.

DESCRIPCIÓN DE LA ZONA EN ESTUDIO Y DE LA RED PLUVIOMÉTRICA

La cuenca del río Amacuzac, en el centro de la república mexicana, tiene una superficie de 7821 km^2, pertenece a la cuenca del río Balsas, y tiene una red pluviométrica que consta de 84 estaciones, con un periodo de registro de 1950–1999 (Fig. 1). Se analizó la precipitación media anual histórica con un mínimo de 5 años, los valores que varían entre 566 y 1554 mm.

Como primer análisis se define el comportamiento del relieve en la zona de estudio, utilizando el MDE (Fig. 2), se aprecia una buena distribución de las estaciones climatológicas para las diferentes elevaciones de la cuenca. También se pueden identificar dos regiones: la montañosa (norte, oeste y sur) y la de planicie (centro y este); debido a que la precipitación se registra de manera diferente en ellas, se buscará preservar el comportamiento del régimen de precipitación en las isoyetas de relieve.

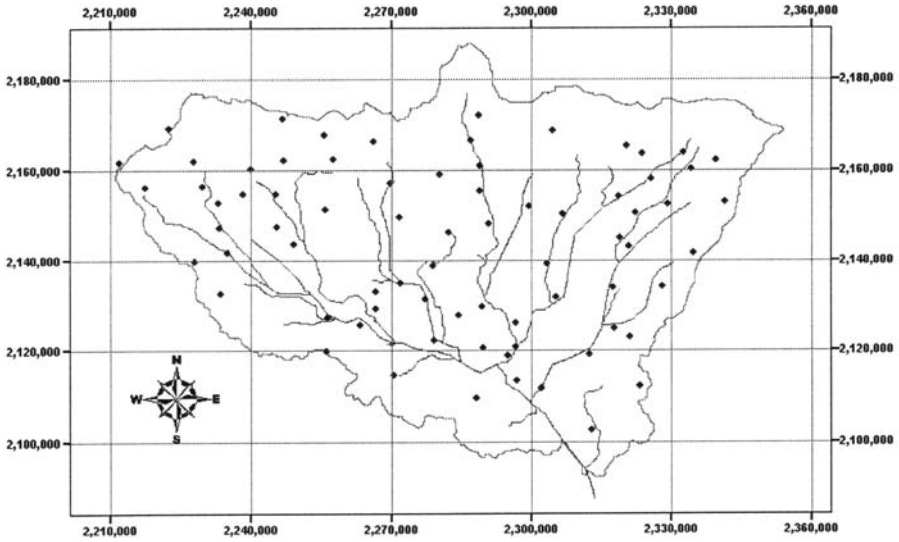


Fig. 1 Distribución espacial de las estaciones climatológicas.

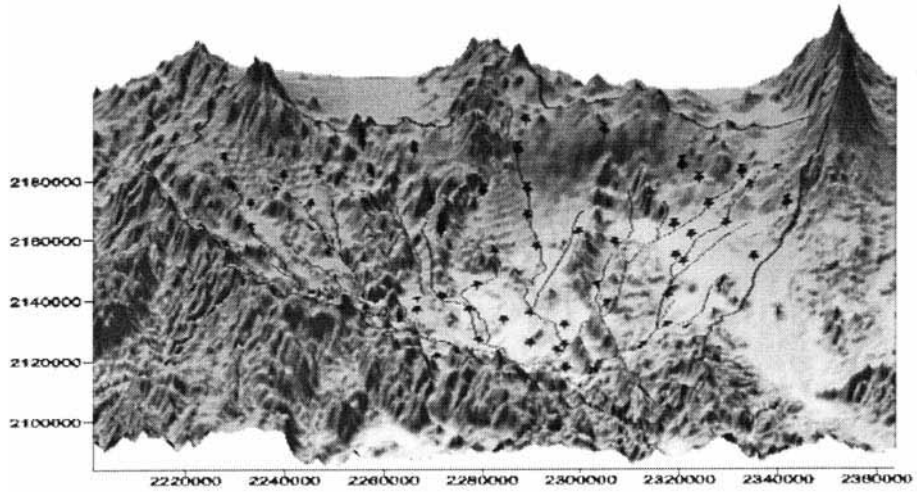


Fig. 2 Representación tridimensional (MDE) de la zona de estudio.

METODOLOGÍA

Para el ajuste del variograma se utilizaron dos criterios: mínimos cuadrados y mínimos cuadrados absolutos (Cressie, 1991), además se realizó una comparación entre estos dos criterios (Zimmerman & Zimmerman, 1991). A continuación se realizaron los ajustes de los modelos: exponencial, gaussiano, potencial, cuadrático, esférico y el cúbico. Se analizaron primero los datos de precipitación, para los cuales se ajustaron los seis modelos, además para cada modelo se revisó, utilizando la anisotropía de los datos, qué dirección presentaba mejor ajuste al modelo, teniendo cuatro direcciones principales (N–S, NE–SW, E–O y SE–NW), para la precipitación, el modelo cúbico presentó el mejor ajuste, es decir, es el modelo que mejor acota a la precipitación. En donde, el factor de escala es C = 36 100, el de rango es de 0.332, y una anisotropía de radio 2 y un ángulo 89.64° (Fig. 3(a)).

Ecuación del modelo cúbico: $\gamma(h) = 7h^2 - 8.75h^3 + 3.5h^5 - 0.75h^7)$ (7)

De manera análoga se ajusta el modelo a los datos de topografía. Donde, el modelo potencial fue el de mejor ajuste, con un factor de escala es 1.29, un rango 1, una potencia de 1.16 y la anisotropía tiene un radio de 2 y un ángulo 179° (Fig. 3(b)).

Ecuación del modelo potencial: $\gamma(h) = C\left|h^n\right|$ donde: $0 < n < 2$ (8)

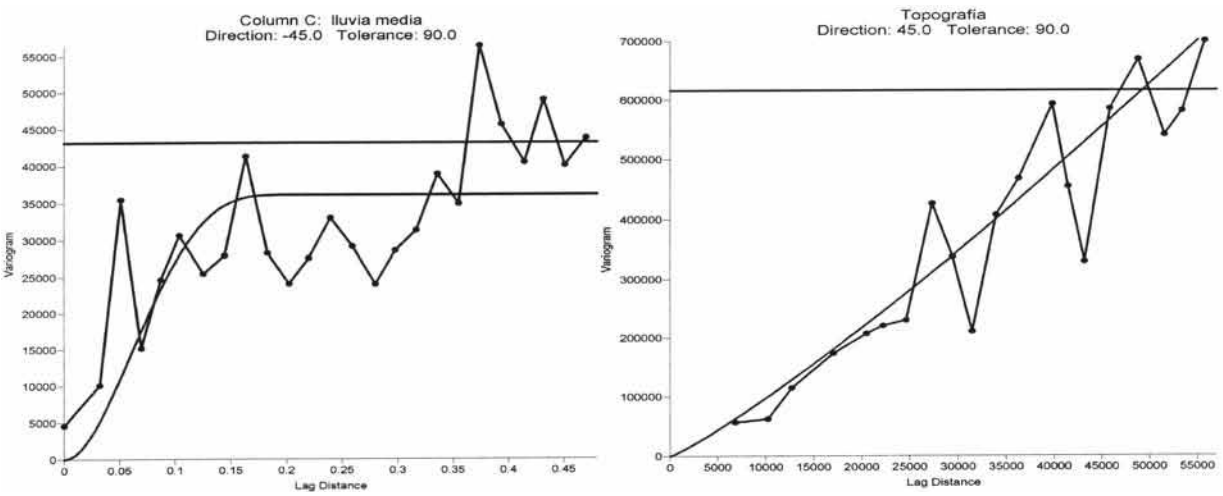


Fig. 3 (a) Variograma cúbico ajustado a los datos de precipitación. (b) Variograma potencial ajustado a los datos de topografía.

Aplicación con la interpolación con kriging

Terminados los ajustes de los modelos, se procede realizar la distribución espacial de la precipitación. Se toman los 84 registros de las estaciones climatológicas y se realizó la interpolación utilizando el modelo cúbico, dando como resultado; un plano de isoyetas tradicional (Fig. 4). Como se puede ver en la Fig. 4, no existe una tendencia para la cual se puedan identificar las dos regiones mencionadas; lo que representa una desventaja al utilizar isoyetas tradicionales. Análogamente, se realiza la distribución espacial de la precipitación, utilizando el variograma direccional (número de pares aproximado igual a un millón y medio) obtenido del modelo topográfico; en la Fig. 5 se aprecia el resultado de este procedimiento. Se puede observar una marcada tendencia en la isoyeta 1,000 mm, la cual sigue la frontera de la zona montañosa; lo cual representa una gran ventaja si se considera que el principal factor generador de lluvia es el relieve. A manera de comparación se obtuvo la precipitación media de la región, de esta forma se obtiene que: el promedio aritmético es de 965 mm, utilizando polígonos de Thiessen de 975 mm, con isoyetas tradicionales 980.6 mm y con las isoyetas con relieve se obtuvieron 994.6 mm. La diferencia de 14 mm entre los métodos de isoyetas, se considera importante, ya que esta diferencia representa un volumen anual de 109 Hm^3 adicionales; cuando se calcula con isoyetas con relieve.

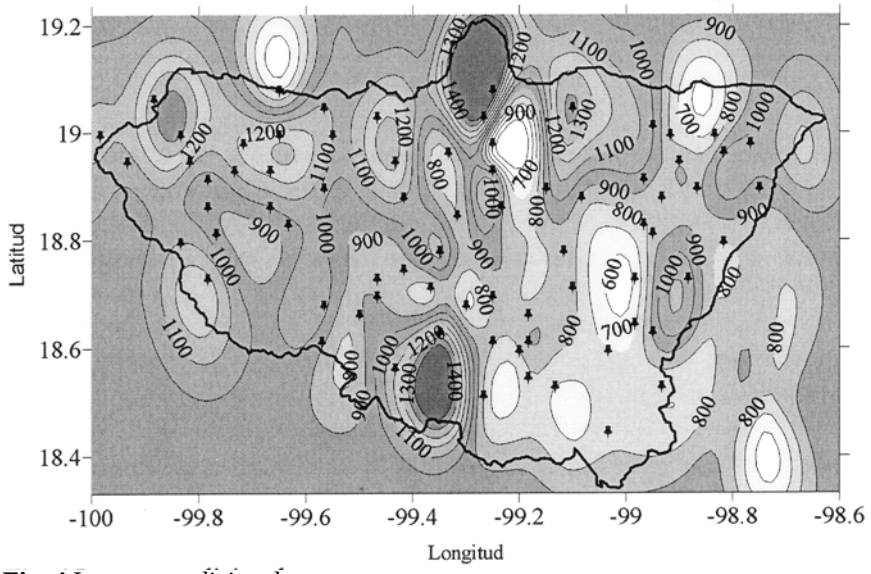


Fig. 4 Isoyetas tradicionales, en mm

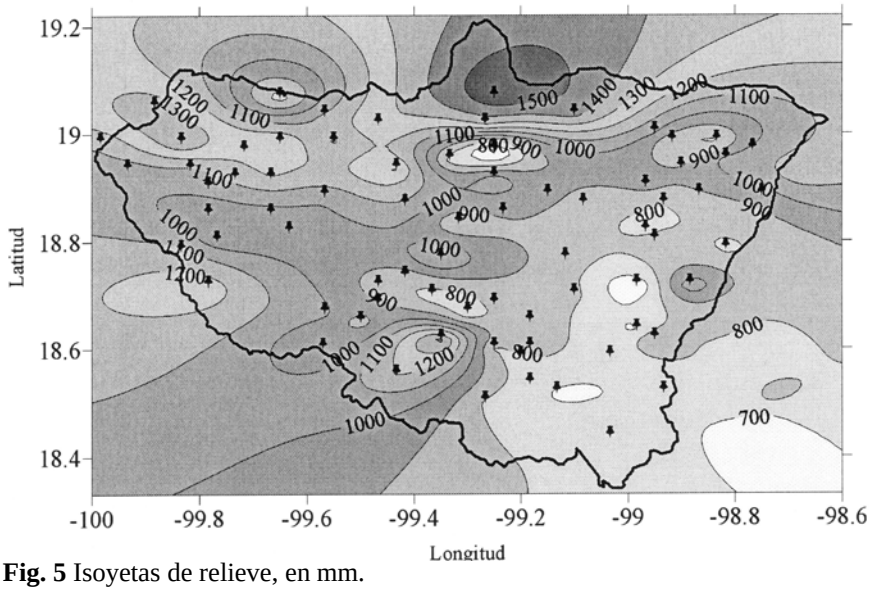


Fig. 5 Isoyetas de relieve, en mm.

CONCLUSIONES

Haciendo un análisis de las Figs 4 y 5 podemos decir que los resultados obtenidos cumplen con lo esperado, es decir; la ecuación del variograma direccional de topografía afecta la distribución de la precipitación, haciendo que la correlación entre estas dos variables (lluvia-relieve) aumente. Además; reforzando la hipótesis de que la topografía es el principal generador de precipitación en una cuenca. La calibración, validación y análisis de sensibilidad de este procedimiento hidro-geoestadístico, se llevaron a cabo en cuencas aforadas, en donde el control hidrométrico permite validar los resultados. Finalmente se espera que este esquema pueda aplicarse para estimar la precipitación en sitios sin registros, considerando las características fisiográficas y topográficas de la región.

REFERENCIAS

Ahrens, B. (2005) Distance in spatial interpolation of daily rain gauge data. *Hydrol. Earth System Sci.* **2**, 1893–1923.

Burrough, P. & McDonnel, R. (1998) *Principles of Geographical Information Systems*. Oxford University Press, New York, USA.

Chica-Olmo, M. (1987) Análisis Geoestadístico en el Estudio de la Explotación de Recursos Minerales. Tesis Doctoral, Universidad de Granada, España.

Clark & Isobel, (1977) *Practical Geostatistics*. Geostokos Limited, United Kingdom. Versión digital descargada http://uk.geocities.com/drisobelclark/PG1979.

Cressie, N. (1991) *Statistics for Spatial Data*. John Wiley and Sons, New York, USA.

Creutin, J. (1979) Méthodes d'interpolation optimale de champs hydrométéorologiques. Comparaisons et applications à une série d'épisodes pluvieux cévenols. Thesis Doctoral USMG, INP Grenoble, France.

David, M. (1977) *Geostatistical Ore Reserve Estimation*. Elsevier Scientific Publishing Company, New York, USA.

Desbarats, A. J., Logan, C. E., Hinton, M. J. & Sharpe, D. R., (2002) On the kriging or water using collateral information from a digital elevation model. *J. Hydrol.* **255**, 25–38.

Delhomme, J. P. (1978) Applications de la théorie des variables régionalisées dans les sciences de l'eau. *Bull B.R.G.M.* **III**(4), 341–375.

Goovaerts, P. (2000) Geoestadistical approaches for incorporating elevation into the spatial interpolation in rainfall. *J. Hydrol.* **228**, 113–129.

Gyasi-Agyei, Y. (1999) Identification of regional parameters of stochastic model for rainfall disaggregation. *J. Hydrol.* **223**, 148–163.

Henry, D. Y. & Krzysztofowicz, R. (2004) Generic probability distribution of rainfall in space:the bivariate model. *J. Hydrol.* **306**, 234–263.

Journel, A. G. & Huijbregts, C. J. (1978) *Mining Geostatistics*. Academic Press, New York, USA.

Lehucher, P. M. (1986) Etude des episodes pluvieux intenses sur la région Provence-Côte d'Azur-Riviera Italienne. Thesis Doctorat, INP Grenoble, France.

Lloyd, C. D. (2005) Assessing the effect of integrating elevation data into the estimation of monthly precipitation in Great Britain. *J. Hydrol.* **308**,128–150.

Matheron, G. (1969) *Le krigeage universel*. Les Cahiers du C.M.M., fasc.1.

Krajewski, S. A. & Gibbs, B. L. (1993) *A Variogram Primer*. Gibbs Associates.

Samper, C. & Carrera, R. (1996) *Geoestadística, Aplicaciones a la hidrogeología subterránea* (2e édn). Centro Internacional de Métodos Numéricos en Ingeniería, Universitat Politècnica de Catalunya, Barcelona, España.

Young, A. R. (2005) Stream flow simulation within UK ungauged catchments using a daily rainfall-runoff model. *J. Hydrol.* **320**, 155–172.

Zimmerman, D. & Zimmerman, M. (1991) A comparison of spatial semivariogram estimators and corresponding ordinary kriging predictors. *Technometrics* **33**(1), 77–91.

Climate Variability and Change—Hydrological Impacts (Proceedings of the Fifth FRIEND World Conference held at Havana, Cuba, November 2006), IAHS Publ. 308, 2006.

The contribution of GIS to hydrological modelling

C. DIEULIN, J. F. BOYER, S. ARDOIN-BARDIN & A. DEZETTER
UMR HydroSciences Montpellier, IRD, BP 64501, F-34394 Montpellier cedex 5, France
claudine.dieulin@msem.univ-montp2.fr

Abstract In this communication, we aim to show our contribution towards the building of a grid containing the water holding capacity (WHC) parameter of the soils. This parameter is used as input data in a hydrological balance type model running at the scale of half a square degree for estimating the soil water reservoir. The Digital Soil Map of the World drawn and edited by FAO is the soil map we used to determine the WHC parameter.

Key words hydrological balance model; water holding capacity; grid; FAO; soil classes; West and Central Africa

OBJECTIVES

A key objective of the research lead by the Vahyne group of the Joint Research Unit HydroSciences Montpellier is to determine the impact of a climatic variability on water resources in West and Central Africa in an arid and semiarid context. This research is being achieved through the application of semi-distributed modelling to determine the water balance. The studied area being over 6 million km^2, the scale for studying this impact is using the half-degree grid. The time step for the data of discharge, rainfall and evapotranspiration is monthly.

The chronological data base managed in the Environmental Information System for Water Resources and Modelling (SIEREM) enabled the selection of 356 measurement sites observed on a period long enough to calibrate the model. For all these sites we delineated the drained basin. Before this delineation, we had to build GIS entities of the hydrological network (one file per major river). The basins on which this modelling process was carried out exceed 5000 km^2.

To delineate the drainage basins, we used GTOPO30 DEM provided by USGS. This choice was made mainly because of the size of our study area. No other DEM existed over such a surface area. (SRTM and SRTM30 were not available at that time.) From this DEM, we ran ArcInfo programs that calculate the flow direction and the flow accumulation and then the program delineates the basins. This was the automated procedure, but on our study area, the nature of the topography is such that additional human interpretation is required based on existing published studies of IRD hydrologists for the region.

The next step was to determine the WHC for every delineated basin, within each of the cells within the model.

To calculate the soil reservoir of the model, we needed a soil cover information data base mapped for the whole modelled region. We found only one map fitting this need: the Digital Soil Map of the World distributed by the FAO (1995) in a numeric format. This digitized version is of particular interest in that it covers most of the globe and makes our operating method more applicable everywhere.

THE SOIL UNITS DEFINED BY FAO

On the worldwide map cover, FAO defined 4930 soil units. A unit does not correspond to a homogeneous soil type and the symbol used to identify a soil unit is made of:

- the symbol of the dominant soil type;
- a numeric digit that qualifies the soil associations (dominant soil unit, associated soil units and inclusions);
- a numeric digit that qualifies the texture of the dominant soil of the unit (1 stands for rough, 2 for mean and 3 for thin);
- a lower case letter that qualifies the slope of the soil unit (*a* for flat to wavy, *b* for undulating to uneven, *c* for hilly to mountainous).

Copyright © 2006 IAHS Press

Here are two examples of soil units of the map:

(1) *Ag1-3a*: gleyic acrisoils t(*Ag*), with thin texture (*3*) and plinthic acrisoil, flat to wavy (*a*).
(2) *Lc6-3b*: chromic luvisoils (*Lc*), thin (*3*), chromic litho soils and vertisoils with orthic solonetz, hilly to mountainous (*b*).

This description can only be found at the back of the paper maps published by FAO in 1973.

THE INFILTRATION DEPTH VALUES DETERMINED BY FAO

Within the corresponding CD of the FAO soil map (one ArcInfo cover per continent), a file called SMAX.ASC is provided. In this file are stored the pieces of information that permitted us to calculate the WHC parameter. FAO defined seven classes, each one corresponding to a depth of infiltration of water in the soil, depth that is calculated according to granulometric values, characteristic of the soil types which make up each soil unit. In the SMAX.ASC file, in front of every soil unit symbol, are listed seven values corresponding to the percentage of occupation of the current soil unit in the class. A program called image.exe located on the CD permits one to view this map by continent.

The seven classes Every class corresponds to a range of depth of water storage in the soil unit. At every soil unit are associated seven values in percentage, one for each class. The total for every soil unit must be 100%.

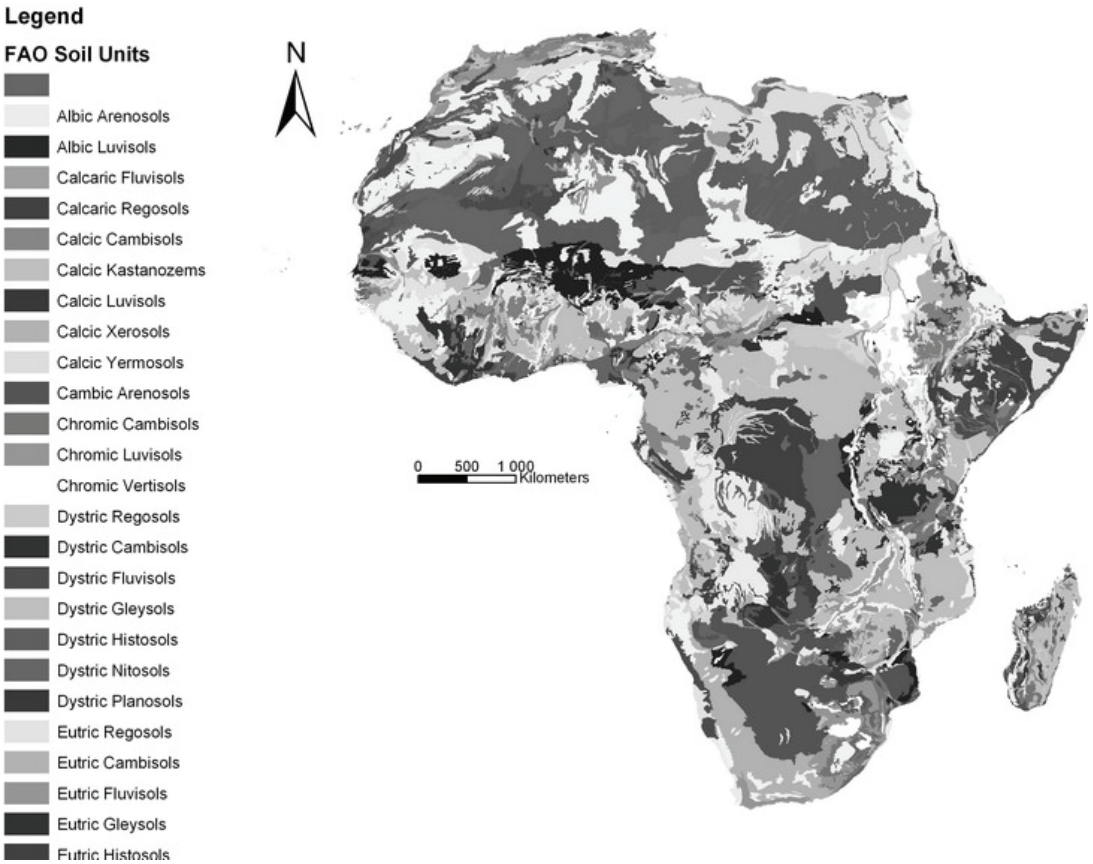


Fig. 1 Map of the soils of Africa: FAO classifications.

Table 1 FAO classes defined in the SMAX.ASC FAO file.

Wetlands	A	B	C	D	E	F
NC (mm)	200/300	150/200	100/150	60/100	20/60	0/20

For instance, lets take the Albic Arenosoil soil unit whose FAO symbol is Qa5-1a, the values stored in the SMAX.ASC file are: 860, Qa5-1a, 10, 0, 0, 40, 25, 25, 0.

860 is the "unit code" given for that soil unit; Qa5-1a is the FAO soil codification, and the seven values, 10, 0, 0, 40, 25, 25, 0, are the percentage of occupation of this soil unit in the classes wetlands (10%), A (0%), B (0%), C (0%), D (25%), E (25%) and F (0%), respectively.

THE GIS PROCESSES TO OBTAIN THE WHC PARAMETER

For every class in the FAO files, the depth of infiltration is given for a range of values (except for the wetland class which is not quantified). For instance, class F stands for a depth going from 0 to 20 mm. The first tests done with the WHC parameter in modelling were carried out by Mahaman Ouedraogo (2001) who used the mean value of the FAO range, i.e. taking again the example of class F, he gave it the value 10 mm.

We decided to improve this model input and chose to calculate the WHC parameter for the limit and mean values, so we calculated three values for every class which we expressed as SMIN (for the F class, it was 0), SMOY (for the F class, it took the value 10) and SMAX (20 for F class). The class called wetlands had no digital value in the FAO classification, it is affected by swampy soils and we gave it a single very high value: 1000 mm.

We then calculated three absolute depth values for every soil unit, using the following operating procedure. Every soil unit had seven percentage values, ranging from 0 to 100 in every class, we calculated a depth for every class of each soil unit, for instance, 10% in class A (ranging from 200 to 300 mm in SMAX.ASC FAO file) was calculated as 20 mm for SMIN (10% of 200 mm), 25 mm for SMOY (10% of 250 mm) and 30 mm for SMAX (10% of 300 mm). This was done for every class of every soil unit and we then summed the seven minimum values to get one SMIN value, then the seven mean values to obtain SMOY and the seven highest values to get SMAX. Such a procedure was done for the 4930 soil units of the FAO file. We give in the following table the example of the calculation for the soil unit called *Qa5-1a*.

Table 2 WHC parameter calculation from percentages to absolute values: SMIN in roman characters, SMOY in italic and SMAX in bold.

Qa5-1a	Wetlands	A	B	C	D	E	F	Total
	1000	200–300	150–200	100–150	60–100	20–60	0–20	
SMAX.ASC (%)	10	0	0	40	25	25	0	100
Abs. Min	100	0	0	40	15	5	0	160
Moy	*100*	*0*	*0*	*50*	*20*	*10*	*0*	*180*
Max	**100**	**0**	**0**	**60**	**25**	**15**	**0**	**200**

This calculation was repeated on the 4930 soil units, for the respective seven classes for every soil unit and for the three limit values of every class, i.e. a total of 103 530 values.

Reynolds (1999) recalculated the SMAX.ASC file from the FAO taking account other pedo-transfer of the soil functions (Saxton model, 1986). We added the results of this recalculation as a fourth value we called Saxton in the attribute table of the GIS cover of the soil unit map of Africa. With the specific GIS commands we added the four SMIN, SMOY, SMAX and SAXTON values to every polygon of the African soil cover (Fig. 2). Once this new cover was built, we intersected it with a half a square degree grid layer to obtain a map at the step of the model (Fig. 3).

The soil map of FAO over Africa was made up of 4985 polygons, and after the intersection with the grid, we got 36 849 polygons, that is an average of 7.3921 soil units per cell of the grid. In fact, there are from 1 to 23 units per cell, and the most frequent case is 3 units per cell, 1981 cells are in this case on the African continent (see distribution in Fig. 4).

Every cell contains several polygons of soil units; these have the SMIN, SMOY, SMAX and SAXTON values of the soil unit. We then decided to weigh these WHC values at the surface area of each polygon within the cell. We then obtained SMINP, SMOYP, SMAXP and SAXTONP

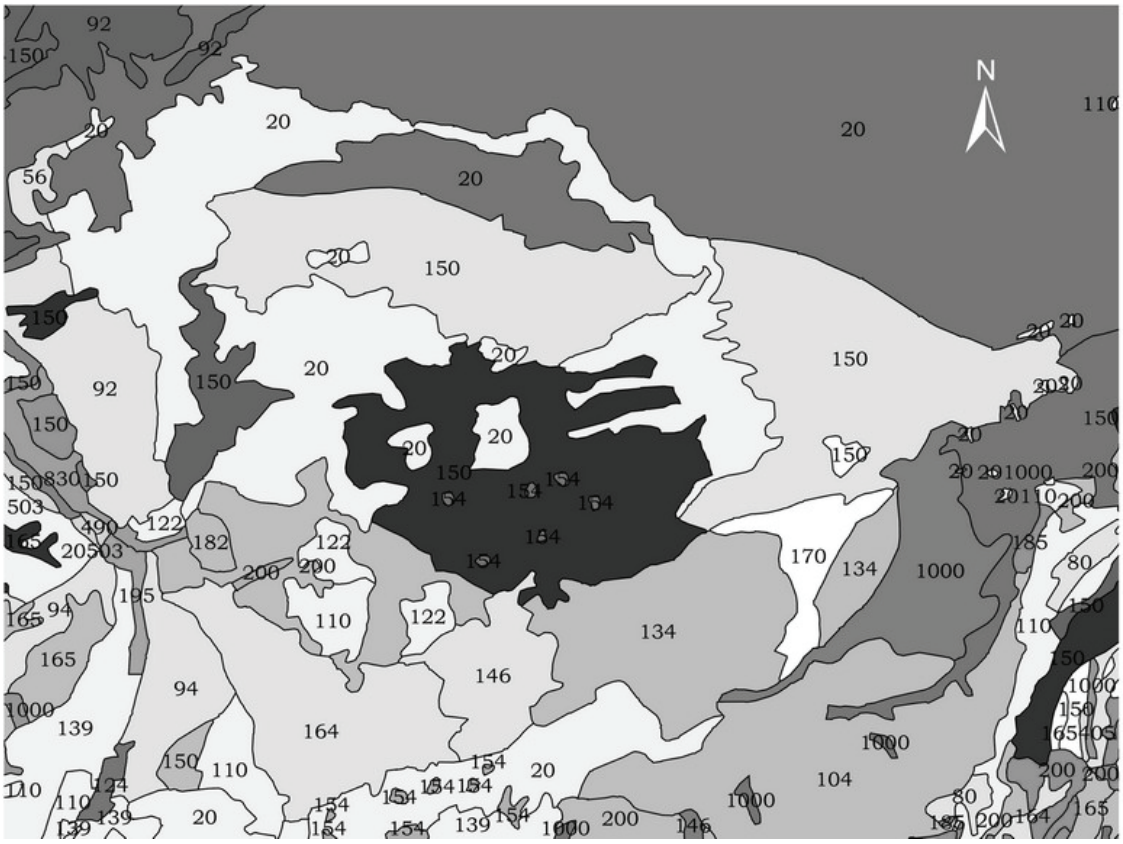


Fig. 2 Smax value for every soil unit, before being weighted.

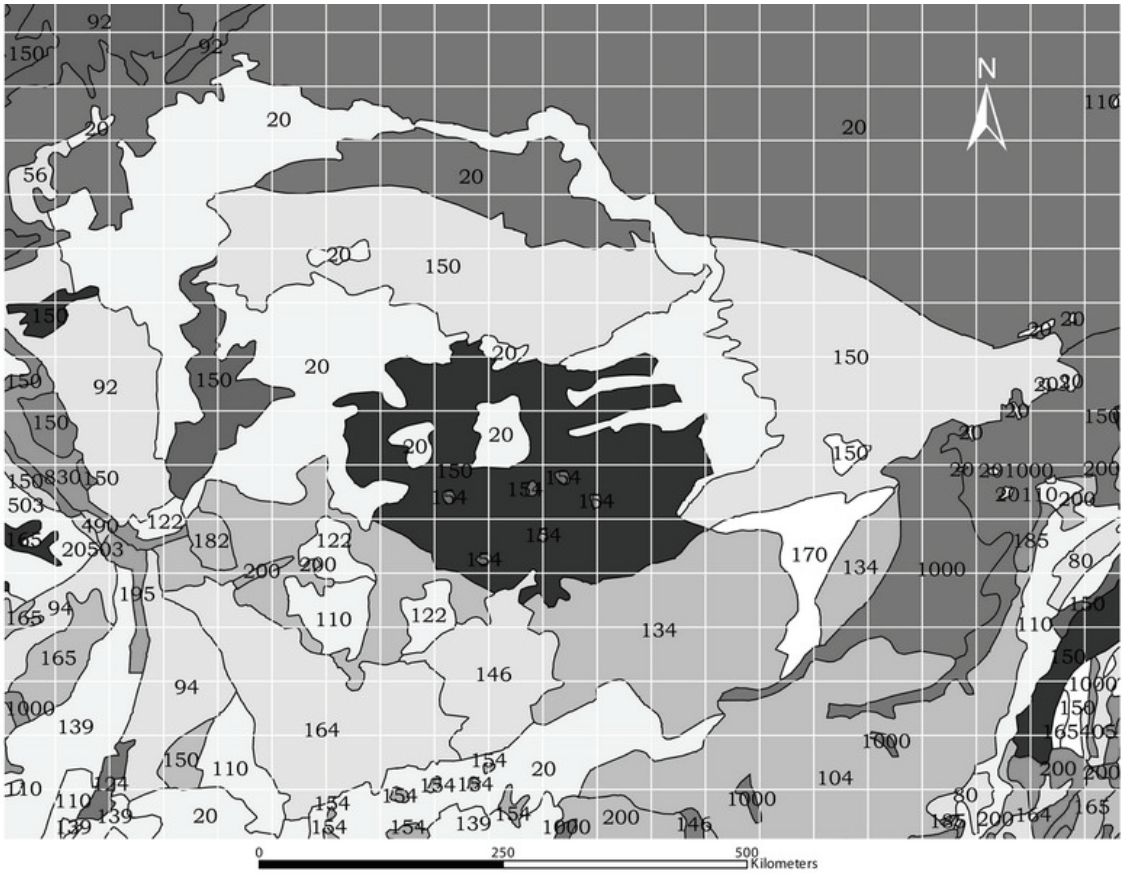


Fig. 3 The cover of the soil map intersected with a half of a square degree grid.

values. Once this calculation ran, we summed these values to get only one value per cell. In a first series of tests, we used these values and "cut" the map of Africa with the polygons of each basin that was to be modelled.

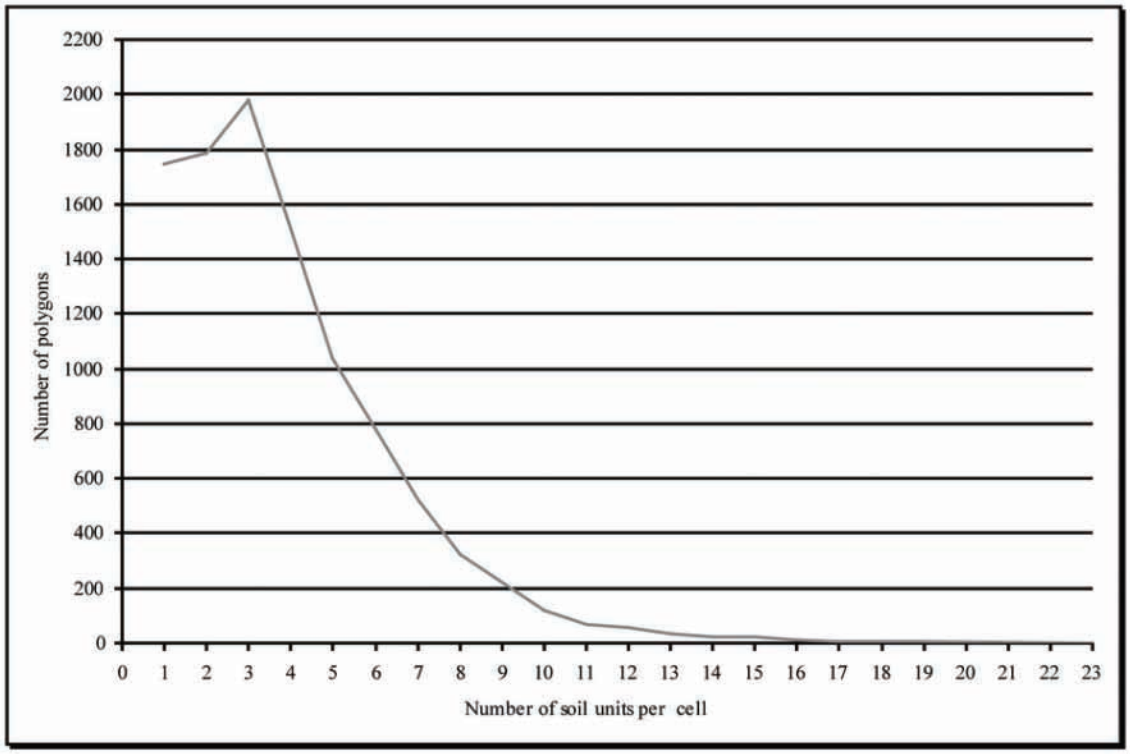


Fig. 4 Distribution of the number of soil units per cell over the whole map of Africa.

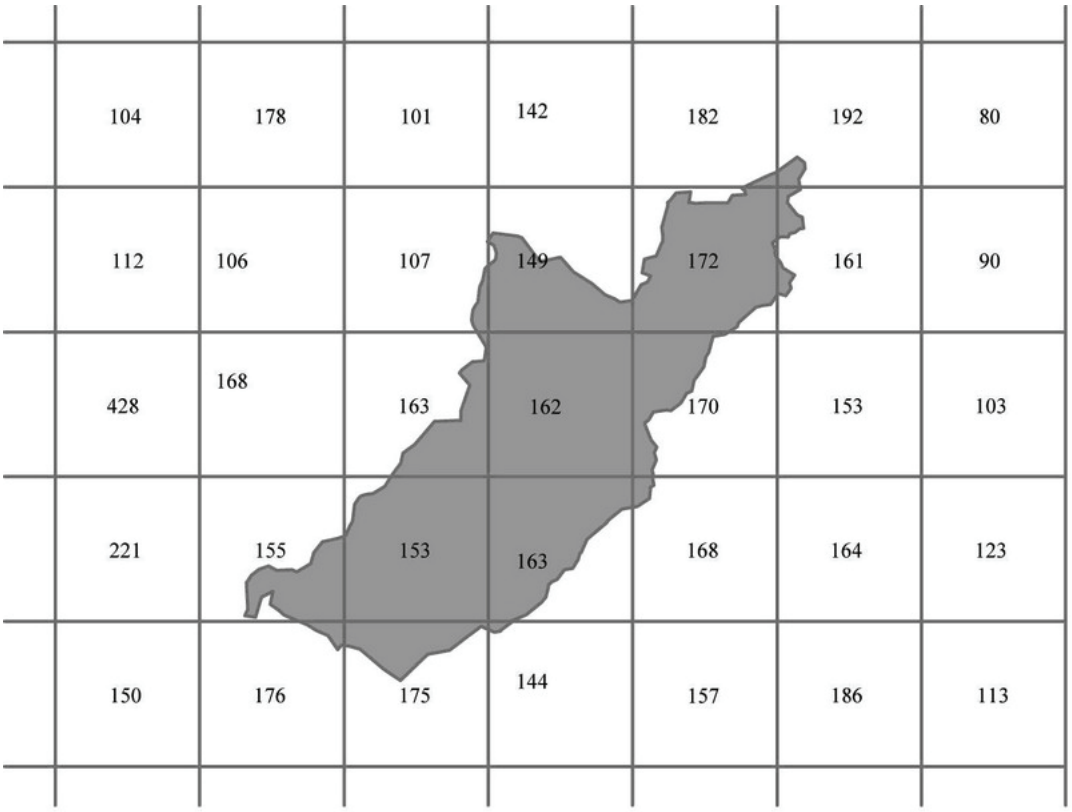


Fig. 5 WHC values of the first tests.

FINAL CALCULATIONS TO ENHANCE THE WHC PARAMETER

But, we noticed that the cells at the edge of the basins were not complete cells and even some were very small parts of a cell and thus, the calculated WHC were not representative of the "real" ones. We then decided to "cut" the grid at the limits of the basins before weighting the WHC values to obtain the most accurate possible value. The final procedure we adopted is the following one:

– intersect the FAO soil map with the 0.5 square grid
– "cut" this grid with the basin polygons
– calculate the SMINP, SMOYP, SMAXP and SAXTONP values for every soil unit in every cell by multiplying the SMIN, SMOY, SMAX and SAXTON values by the surface area of the polygon in the cell
– calculate a SMINPM, SMOYPM, SMAXPM and SAXTONPM values by adding the different values of the n polygons in the cell. Figure 6 shows the differences in the results obtained with the two calculations we tried.

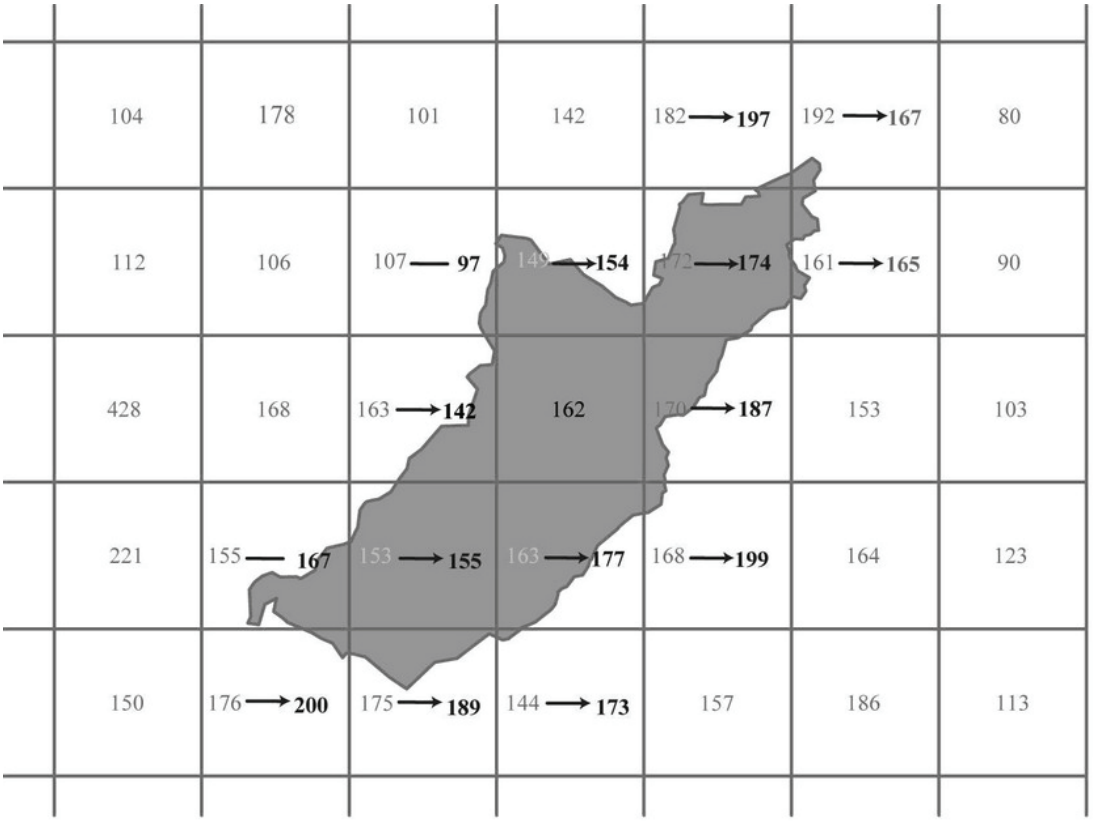


Fig. 6 Final WHC values (here SMAXPM) recalculated after having been "cut" with the basin delineation. Previous value, arrow and then new value in bold.

PROSPECTIVE

The first tests we carried out were done on the occasion of the thesis of Sandra Ardoin-Bardin (2004) and were positive in the improvement provided by this parameter. We took as a postulate that the WHC value was steady over the 20-year period of calibration of the model. But, in fact, depending on the intensity of human pressure such as agriculture practices, erosion; this parameter varies. Our future investigations will be to estimate the variation of this value based on human activity in the basins and the modification of the basins behaviour depending on the anthropogenic pressure.

REFERENCES

Ardoin-Bardin, S. (2004) Variabilité hydroclimatique et impacts sur les ressources en eau de grands bassins hydrographiques en zone soudano-sahélienne. Thèse de Doctorat en Sciences de l'Eau. Université Montpellier II, France.

FAO (1995) *Digital Soil Map of the World and Derived Soil Properties* (CD-ROM). FAO Land and Water Digital Media Series. FAO, Rome, Italy.

Ouedraogo, M. (2001) Contribution à l'étude de l'impact de la variabilité climatique sur les ressources en eau en Afrique de l'Ouest. Analyse des conséquences d'une sécheresse persistante : normes hydrologiques et modélisation régionale. Thèse de Doctorat. Université Montpellier II, France.

Reynolds, C. A., Jackson, T. J. & Rawls, W. J. (1999) Estimating available water content by linking the FAO soil map of the world with global soil profile databases and pedo-transfer functions. In: *Proc. AGU 1999 Spring Conference* (31 May–4 June, Boston, USA).

Climate Variability and Change—Hydrological Impacts (Proceedings of the Fifth FRIEND World Conference held at Havana, Cuba, November 2006), IAHS Publ. 308, 2006.

An evaluation of the potential use of satellite rainfall data for input to water resource estimation models in southern Africa

DENIS A. HUGHES
Institute for Water Research, Rhodes University, Grahamstown 6140, South Africa
denis@iwr.ru.ac.za

Abstract Global or near global satellite rainfall data are becoming readily available and have the potential to provide the rainfall data inputs required for water resource availability modelling in the face of shrinking ground-based networks. However, the difficulties of using both sets of rainfall data in models with existing calibrations based on raingauge data are not well understood. An assessment using three basins in southern Africa yielded mixed results. There is clearly a need for some "corrections" to be applied to the satellite data to achieve consistency with the gauged rainfall information, but it is not usually clear what form these "corrections" should take. It is important to note that in some areas there are very few gauges currently available and the satellite data represent a viable substitute.

Key words satellite data; rainfall data; hydrological models; developing countries; water resources; southern Africa

INTRODUCTION

The quality of rainfall data input to hydrological models is of primary importance (Brath *et al.*, 2004). Without adequate rainfall data, other issues such as model choice, number of parameters and parameter estimation procedures become somewhat superfluous. However, the ground-based recording networks of many countries are shrinking and in parts of southern Africa, notably those that have experienced recent political and social upheaval, gauging networks have either almost ceased to exist or have large spatial and temporal discontinuities. These are also the regions where the availability of water resource information is important for managing the future sustainable use of water resources for social and economic development. Issues such as which spatial interpolation approach to use (Tabios & Sala, 1985) become irrelevant as there are too few gauges to represent the spatial variations of rainfall.

Where observed river flow data are not available, hydrological models offer a viable alternative for generating water resource availability information. However, their successful application relies on, *inter alia*, an accurate representation of basin precipitation inputs. Given the lack of ground-based observations in many areas of southern Africa, alternative sources need to be identified and assessed. Near-global datasets of a wide range of terrestrial information derived from satellite imagery are becoming increasingly accessible. While their use in a southern Africa context is not new (Thorne *et al.*, 2001; Grimes & Diop, 2002), they have not been applied extensively and there have been few assessments of using satellite data in conjunction with gauge data. Hughes (2006) reports on some comparisons of rainfall information available from near-global datasets (GPCP; Huffman *et al.*, 1997, 2001 and PERSIANN; Hsu *et al.*, 1999; Sorooshian *et al.*, 2000) with ground-based observations. This earlier paper was limited to comparisons based on four study areas representing different climate regimes. The results were encouraging enough to justify further investigations, although indications are that the satellite data cannot be used without modification and further processing. The current objective is to assess whether the satellite data can be used in conjunction with gauge data as inputs to a hydrological model, based on the premise that existing model calibrations using available historical gauge data already exist and that satellite data records are still relatively short and unable (on their own) to adequately represent long-term variability. The main questions to be answered by this phase of the investigation are:

(a) Is it possible to identify relatively simple scaling factors that can be applied to the satellite data so that they can be successfully used in a rainfall–runoff model calibrated using historical rainfall data?
(b) Can comparisons with gauged rainfall data or the model results be used to suggest more complex transformations of the satellite rainfall data which are still straightforward to apply?

Copyright © 2006 IAHS Press

THE SATELLITE PRECIPITATION PRODUCTS

The full details of the two satellite precipitation products can be found in Hughes (2006), as well as the original sources. They have been selected primarily on the basis of their ease of access, in recognition of the limited resources normally available in developing regions. The GPCP (Global Precipitation Climatology Project) 1DD estimates have a time resolution of one day and a spatial resolution of one degree. The period of record is currently October 1996 to January 2005. The PERSIANN (Precipitation Estimation from Remotely Sensed Information using Artificial Neural Networks) datasets have a temporal resolution of six hours, a spatial resolution of 0.25^o and start in March 2000.

THE MODEL AND TEST BASINS

The rainfall–runoff model used is the Pitman monthly model with additional surface–groundwater interaction routines as discussed in Hughes (2004). Three basins are included: the Kafue basin (156 995 km^2) in Zambia, the Thukela River basin (29 046 km^2) in Kwa-Zulu Natal and the Kat River basin (1715 km^2) in the Eastern Cape province of South Africa. Further details (including maps indicating the location of raingauges and the one degree grid squares) of these basins can be found in Hughes (2006). The model tests are based on smaller sub-basins due to the availability of suitable observed flow data. The comparisons between observed and simulated data are based on visual assessments of time series graphs, as well as six standard goodness-of-fit statistics; percentage deviation of the simulated mean from the equivalent observed values (% Error MMQ and % Error MMlnQ), R^2 (Q and lnQ) and coefficient of efficiency: CE(Q) and CE(lnQ) from Nash & Sutcliffe (1970), based on both untransformed (Q) and natural logarithmic transformed (lnQ) monthly flows.

RESULTS

Kafue River, Zambia

Two streamflow gauging stations (4050, Kafue at Raglan Farm, 5000 km^2; 4560, Lunga at Chifumpa, 21 445 km^2) on the Kafue River (Mwelwa, 2005) have been selected. The historical rainfall data consist of some 12 gauges located in the northern part of the Kafue basin, all having varying length records and months of missing data. An inverse distance squared weighting procedure has been used to determine basin average rainfall, but after 1990 the average rainfall is largely based on a single gauge. Table 1 lists the goodness-of-fit statistics for the calibration period (October 1961 to September 1990), as well as for the extended period (October 1990 to September 2000). It is evident that the simulations for the extended period are very poor and this is largely due to very high rainfalls and over-simulations in 1998 and 1999. The calibration for sub-basin 4560 is also not very good and it was found to be extremely difficult to reproduce the very rapid seasonal recession curve.

The GPCP rainfall input to sub-basin 4050 uses a single 1^o grid. The larger basin (4560) was further sub-divided into three sub-basins during the calibration process and their rainfall inputs based on single 1^o grids. Table 1 indicates that the un-scaled GPCP data is very low, but that even after scaling to ensure that the observed and simulated mean monthly flows are similar, the fit is not very good. The poor fit is also largely due to years 1998 and 1999, but in this case caused by under-simulations.

The PERSIANN rainfall inputs to 4050 are based on averages of seven 0.25^o grids, while the three sub-basins of 4560 used averages of between 3 and 15 grids. As indicated in Hughes (2004), and in contrast to the GPCP data, the PERSIANN rainfalls are much higher than the historical data and led to large over-simulations. When scaled to reproduce the observed mean monthly flow, the results for 4050 were encouraging (Table 1), although based on only 31 months of data. The results for 4560 were not very good and could be a reflection of an inadequate model calibration (a problem of over-simulating the late wet season recession flows). However, for both examples (4050 and 4560), the results using the PERSIANN data are better than when using the available

Table 1 Simulation results for the Kafue River (4050 and 4650 sub-basins).

Statistic	Calibration	Historical rainfall data	GPCP No scaling	Scaling	Persiann No scaling	Scaling
Record period	1961–1990	1990–2000	1996–2002		2000–2004	
Sub-basin 5040, Kafue River at Raglan Farm						
% error MMQ	2.0	78.5	–59.3	–0.2	47.4	–0.4
% error MMlnQ	0.0	16.8	–26.5	2.8	10.7	3.8
R^2(Q)	0.804	0.624	0.368	0.427	0.664	0.811
CE(Q)	0.803	–0.648	0.174	0.213	0.249	0.797
R^2(lnQ)	0.860	0.816	0.660	0.707	0.718	0.862
CE(lnQ)	0.37	0.664	0.335	0.694	0.617	0.850
Scaling factor	N/A	N/A	1.0	1.307	1.0	0.830
Sub-basin 4560, Lunga River at Chifumpa						
% error MMQ	0.4	22.0	–63.3	–1.8	126.0	1.0
% error MMlnQ	0.7	1.0	–32.9	–11.5	6.5	–1.6
R^2(Q)	0.498	0.668	0.460	0.534	0.779	0.657
CE(Q)	0.454	0.246	–0.083	–1.312	–7.978	0.635
R^2(lnQ)	0.614	0.654	0.465	0.462	0.595	0.524
CE(lnQ)	0.545	0.383	–8.728	–2.070	–1.080	–0.024
Scaling factor	N/A	N/A	1.0	1.188	1.0	0.840

Notes: Applicable to Tables 1 to 3.
The period is given as hydrological years starting in October. See text for the key to the statistics

recent raingauge data. While simple linear scaling of the satellite data is unlikely to be the best approach, there is insufficient evidence within the available data, or in the model results, to suggest a straightforward alternative.

Thukela River basin, South Africa

The assessments within the Thukela River basin are based on a gauged tributary (Mooi River at V2H004, 1546 km^2 in area). There are two active rainfall measuring stations with reasonably complete recent records, one in the headwaters and one near the gauge. The basin is covered by three 0.25º Persiann grids and falls across the boundary of two 1º GPCP grids and the total area has been divided into five sub-basins for modelling purposes. The rainfall–runoff model was calibrated satisfactorily (Table 2) using existing spatially averaged rainfall data (Midgley *et al.*, 1994). Four additional model runs were made using the calibration parameters. The first used the nearest point gauge rainfall as input, the second used weighted averages of the two gauges, while the third and fourth used appropriate grid data from the GPCP and PERSIANN data, respectively, based on the locations of the sub-basins. The results of the simulations are provided in Table 2 and some are illustrated in Fig. 1.

Table 2 Simulation results for the Thukela basin (Mooi River gauging station).

Statistic	Calibration (WR90 rainfall)	Gauges 2 gauges	Average	GPCP	Persiann
Record period	1950–1990	1996–2004			2000–2004
% error MMQ	1.6	12.7	–5.6	–4.0	44.1
% error MMlnQ	8.4	8.7	1.3	16.6	28.9
R^2(Q)	0.737	0.519	0.472	0.640	0.287
CE(Q)	0.736	0.076	0.196	0.621	–0.408
R^2(lnQ)	0.785	0.723	0.721	0.832	0.455
CE(lnQ)	0.754	0.700	0.720	0.667	0.237

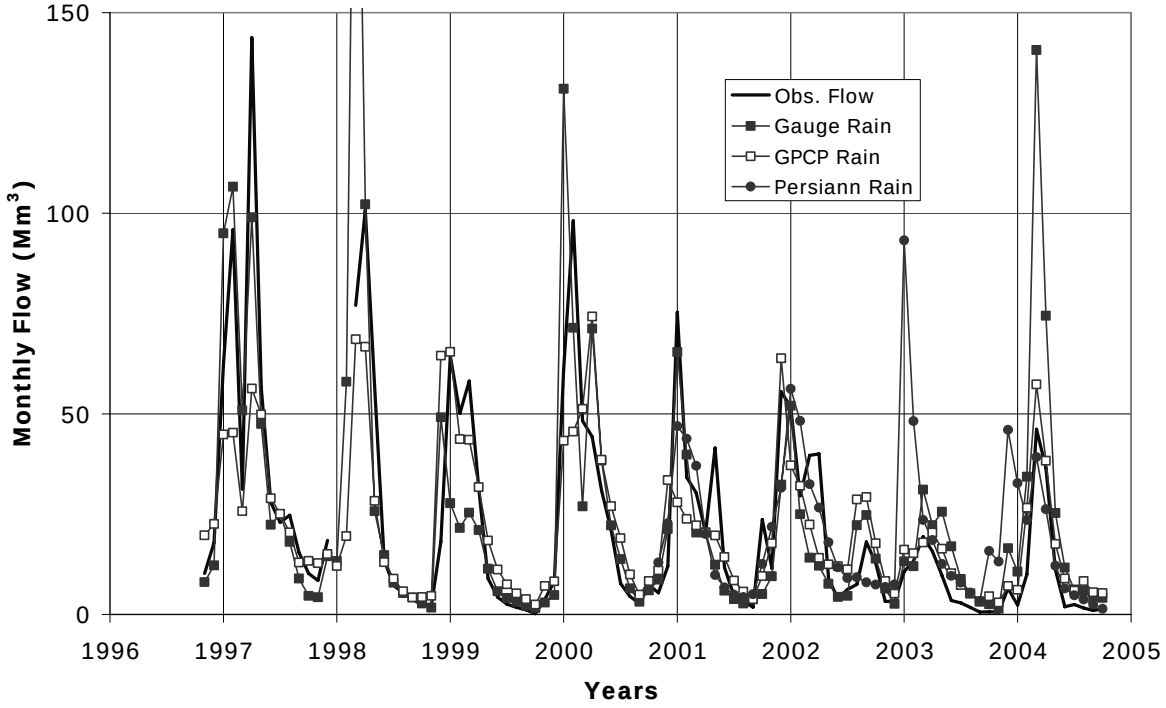


Fig. 1 Time series comparisons of observed and simulated monthly flows for the Mooi River, Thukela basin, South Africa (horizontal axis marks at December of the indicated years).

The main problem with the ground based rainfall inputs is that extreme monthly values generate excessive peak flows in some years (Fig. 1, early 1999, 2001 and 2005). A similar problem occurs with the PERSIANN data (December 2003 and 2005) as already noted by Hughes (2006). The GPCP data provide the most satisfactory rainfall inputs to the previously calibrated model. There are no indications that simple adjustments, such as linear scaling, will improve either of the satellite data sets.

Kat River basin, South Africa

Within the Kat River basin there is only one flow gauging station that has recent data and that is relatively unaffected by anthropogenic modifications to the flow regime. The sub-basin has an area of 79.6 km^2, which is less than 20% of a 0.25º grid square, experiences substantial topographic influences on precipitation and has only one active rainfall gauge (100 329) within its boundary. A further rainfall gauge (Q9E001) exists some 10 km to the east in a lower rainfall region. The rainfall–runoff model was calibrated using existing spatially averaged historical rainfall data (Midgley *et al.*, 1994).

The calibration parameters were used with the un-scaled rainfall available from the satellite sources, as well as a relatively arbitrary combination of the two available gauge records (0.6*100329 + 0.4*Q9E001). All the rainfall records were then linearly scaled to reduce the % errors in simulated mean monthly runoff. The results are presented in Table 3 and Fig. 2 where it is apparent that none of the currently available rainfall sources are particularly suitable for input to the model and that most of the errors are associated with both over- and under-estimations of the rainfall signals during individual months. However, all of the scaled rainfall inputs generate flow duration curve characteristics that are close to the observed data, with the GPCP data being slightly better. There are no systematic patterns in the results that can be used as a basis for more complex transformations of the original rainfall data sources. There appears to be insufficient information contained within the original sources to adequately represent the spatio-temporal rainfall inputs to the sub-basin.

Table 3 Simulation results for the Kat River sub-basin.

Statistic	Calibration	GPCP		Persiann		Gauges	
		No scaling	Scaling	No scaling	Scaling	No scaling	Scaling
Record period	1920–1989	1996–2003		2000–2003		1990–1999	
% error MMQ	–13.7	–54.4	–0.6	–65.6	–0.4	–16.1	–0.5
% error MMlnQ	0.2	–116.3	1.06	–232.5	–29.2	–29.1	13.2
R^2(Q)	0.807	0.691	0.674	0.721	0.659	0.551	0.566
CE(Q)	0.801	0.384	0.662	0.312	0.592	0.502	0.465
R^2(lnQ)	0.651	0.367	0.469	0.335	0.346	0.582	0.590
CE(lnQ)	0.647	–0.394	0.395	–2.120	–0.009	0.423	0.490
Scaling factor	N/A	1.0	1.259	1.0	1.378	1.0	1.051

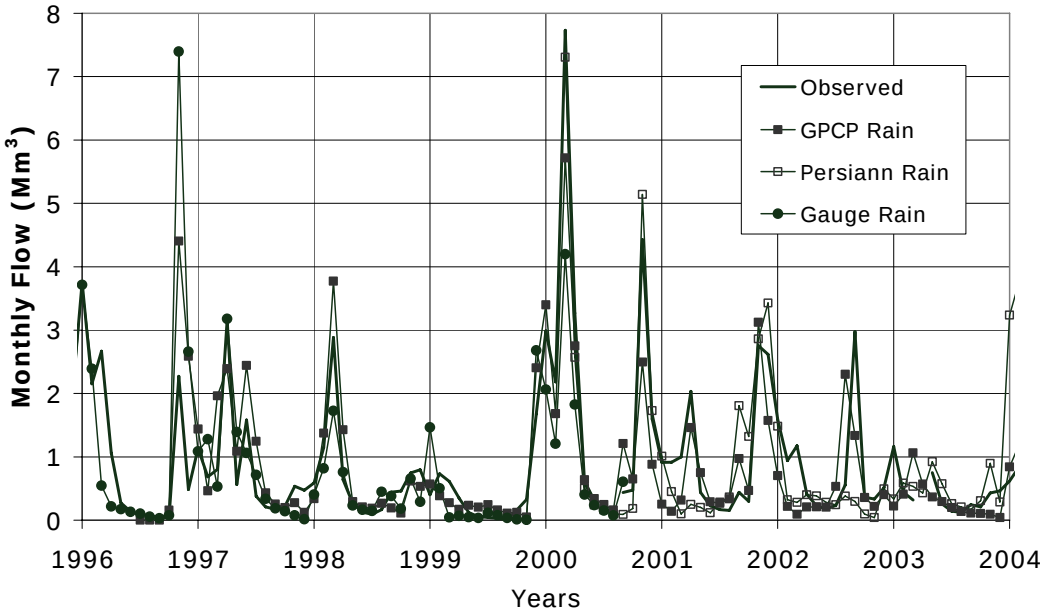


Fig. 2 Time series comparisons of the simulation results for the sub-basin of the Kat River basin based on scaled rainfall (horizontal axis marks at December of the indicated years).

DISCUSSION AND CONCLUSIONS

The model calibrations will reflect any inadequacies in the ground-based rainfall gauge data, including a lack of spatial representation, and it should be recognized that no data source is likely to provide "true" rainfall inputs. The calibrated parameters are therefore not independent of the rainfall inputs to the model. When using two different sources of rainfall data, as in this study, a choice has to be made between adjusting the rainfall data to be consistent, or using different parameter sets. For a model where the parameters are expected to reflect physical basin properties, the former option is the logical choice. As the overlap between the observed flow and the gauge rainfall data is typically longer in the southern Africa situation, it also seems logical to adjust the satellite data to be consistent with the gauge data. Further justification for this approach is that while gauge data are commonly not adequate to completely quantify spatial variations due to topographic influences, the satellite data appear to ignore these completely.

The three study areas represent very different climate regimes within southern Africa and some of the results are encouraging enough to warrant the use of satellite data. The corrections applied to the satellite data are very simple, but there are no clear indications that more complex, non-linear or seasonal corrections will be more successful. One issue that has been highlighted is that the currently available ground-based rainfall data are frequently inadequate. This introduces a great deal of uncertainty in the results of extending water resource simulation models, based on historical rainfall data, into the present and future.

Acknowledgements David Bolvin of the Mesoscale Atmospheric Processes Branch, NASA and Dan Braithwaite of the Center for Hydrometeorology and Remote Sensing, University of California, Irvine provided help with the GPCP and PERSIANN data, respectively. Elenestina Mwelwa provided the Zambian data and the South African data are derived from the databases of the South African Weather Service and the Department of Water Affairs and Forestry.

REFERENCES

Brath, A., Montanari, A. & Toth, E. (2004) Analysis of the effects of different scenarios of historical data availability on the calibration of a spatially-distributed hydrological model. *J. Hydrol.* **291,** 232–253.

Grimes, D. I. F. & Diop, M. (2003) Satellite-based rainfall estimation for river flow forecasting in Africa. Part 1. Rainfall estimates and hydrological forecasts. *Hydrol. Sci. J.* **48**(4), 567–584.

Huffman, G. J., Adler, R. F., Arkin, P. A., Chang, A., Ferraro. R., Gruber, A. Janowiak, J. J., Joyce, R. J., McNab, A., Rudolf, B., Schneider, U. & Xie, P. (1997) The Global Precipitation Climatology Project (GPCP) combined precipitation data set. *Bull. Am. Met. Soc*. **78**, 5–20.

Huffamn, G. J., Adler, R. F., Morrissey, M. M., Curtis, S., Joyce, R. J., McGavock, B. & Susskind, J. (2001) Global precipitation at one-degree daily resolution from multi-satellite observations. *J. Hydromet.* **2**, 36–50.

Hughes, D. A. (2004) Incorporating ground water recharge and discharge functions into an existing monthly rainfall–runoff model. *Hydrol. Sci. J.* **49**(2), 297–311.

Hughes, D. A. (2006) Comparison of satellite rainfall data with observations from gauging station networks. *J. Hydrol*. **327**, 399–410.

Hsu, K., Gupta, H. V., Gao, X. & Sorooshian, S. (1999) Estimation of physical variables from multi-channel remotely sensed imagery using a neural network: Application to rainfall estimation. *Water Resour. Res.* **35**(5), 1605–1618.

Midgley, D. C., Pitman, W. V. & Middleton, B. J. (1994) Surface Water Resources of South Africa 1990, volumes I to VI. *Water Research Commission Reports nos 298/1.1/94 to 298/6.1/94.* Pretoria, South Africa.

Mwelwa, E. M. (2005) The application of the monthly time step Pitman rainfall-runoff model to the Kafue River basin of Zambia. MSc Thesis, Rhodes University, Grahamstown, South Africa.

Nash, J. E. & Sutcliffe, J. V. (1970) River flow forecasting through conceptual models. Part I—a discussion of principles. *J. Hydrol*. **10**, 282–290.

Sorooshian, S., Hsu, K., Gao, X., Gupta, H. V., Imam, B. & Braithwaite, D. (2000) Evaluation of PERSIANN system satellite-based estimates of tropical rainfall. *Bull. Am. Met. Soc*. **81**, 2035–2046.

Tabios, G. Q. & Salas, J. D. (1985) A comparative analysis of techniques for spatial interpolation of precipitation. *Water Resour. Res.* **21**, 365–380.

Thorne, V., Coakley, P., Grimes, D. & Dugdale, G. (2001) Comparison of TAMSAT and CPC rainfall estimates with rainfall, for southern Africa. *Int. J. Remote Sens.* **22**(10), 1951–1974.

Climate Variability and Change—Hydrological Impacts (Proceedings of the Fifth FRIEND World Conference held at Havana, Cuba, November 2006), IAHS Publ. 308, 2006.

Application of digital terrain analysis to estimate hydrological variables in the Luquillo Mountains of Puerto Rico

ANDREW S. PIKE

Department of Earth and Environmental Science, University of Pennsylvania, 240 South 33rd Street, Philadelphia, Pennsylvania 19104, USA

apike@sas.upenn.edu

Abstract Techniques of digital terrain analysis were applied to estimate hydrological variables in basins draining the Luquillo Mountains of northeastern Puerto Rico. A 10-m resolution Digital Elevation Model (DEM) was interpolated from 10 m elevation contour lines and used as the template for hydrological analysis. A high density stream network representing all perennial streams, including previously unmapped 1st order streams, was defined using the DEM. Similarly, for each 10 m grid cell within the stream network, mean annual rainfall, runoff, and discharge were estimated using regression equations derived from long-term rainfall and streamflow gauges. The result is a simple spatial framework to estimate hydrological variables in the region.

Key words GIS; Puerto Rico; surface water; stream network; spatial interpolation

INTRODUCTION

Estimating hydrological variables in ungauged drainage basins is challenging in montane environments. Fortunately, digital terrain analysis can be used to derive a wealth of information about the morphology and hydrodynamics of a land surface. When coupled with the spatial distribution of basic hydrological variables, such as rainfall and runoff, digital terrain analysis is a powerful tool for estimating river network variables and generating spatially explicit water budgets (Montgomery *et al.*, 1998). However, digital terrain analysis is often underutilized in tropical drainage basins due to a scarcity of appropriate data. This paper details how digital terrain analysis is used to estimate hydrological variables in the region draining the Luquillo Experimental Forest (LEF), a montane subtropical rainforest in northeastern Puerto Rico.

In the steep landscape of the LEF, estimates of elevation, slope, and drainage areas from topographic maps may not always be accurate. Moreover, the stream network portrayed on US Geological Survey (USGS) maps does not include many 1st order streams in the region. However, the LEF is an ideal landscape to estimate surface water variables using topography because most of the streamflow is derived from surface water and no major groundwater sources contribute to the stream system (Schellekens *et al.*, 2004).

This paper develops a simple framework to estimate hydrological variables for all 10 m × 10 m cells within a stream network that acts as a template for hydrological analysis of the streams draining the LEF. The process involves (1) creation of a hydrologically correct Digital Elevation Model (DEM), (2) definition of the stream network using a drainage area threshold and (3) estimation of mean annual rainfall, runoff, and discharge from topographic factors.

STUDY AREA

The Luquillo Mountains in northeastern Puerto Rico are characterized by rugged terrain and steep gradients in elevation and climate. Over a distance of 10 to 20 km, the mountain range rises from sea level to an elevation of 1075 m. Mean annual rainfall increases with elevation from approximately 2000 mm at the coast to >4500 mm at the highest elevations (García-Martinó *et al.*, 1996).

The climate is characterized as humid tropical maritime, and is influenced by both north-easterly trade winds and local orographic effects. The principal weather systems affecting climate are convective storms, easterly waves, cold fronts, and tropical storms (van der Molen, 2002). Rainfall events at mid-elevations are generally small (median daily rainfall 3 mm day^{-1}) but numerous (267 rain days per year) and of relatively low intensity (<5 mm h^{-1}) (Schellekens *et al.*, 1999). At mid to upper elevations (>100 m), most streamflow results from direct surface runoff in the form of saturated overland flow or through shallow (>30 cm depth) soil macropores. There are no significant groundwater sources or sinks in this montane landscape (Schellekens *et al.* 2004).

Copyright © 2006 IAHS Press

The Rio Mameyes is the principal drainage basin highlighted in this study, but the techniques can be applied to other basins draining the LEF. Streams draining the mid to upper elevations are relatively pristine, surrounded by protected forest, and are laterally confined by steep valley walls. In contrast, streams flowing across the broad alluvial coastal plain readily migrate laterally, although many are physically altered to attend to local needs. The main channels of all major rivers in the region have either a dam or water intake device for local municipal use (March *et al.*, 2003).

DEM CONSTRUCTION

The main principle of digital terrain analysis is that a continuous landscape surface can be generated from the abundance of topographic information contained within elevation contour lines (elevation, geomorphic position, slope, etc.). Surface water flow can then be routed across this surface under the assumption that water flows downslope according to principles of least energy, i.e. water follows the path of steepest descent (Jenson & Domingue, 1988). Using this simple rule, the drainage network of a landscape can be extracted.

A high-resolution Digital Elevation Model (DEM) is critical for terrain and hydrological analysis. While a 30 m DEM exists for the entire island of Puerto Rico, this is not sufficient resolution to model the complex topographic structure of the Luquillo Mountains. In particular 1st order streams that typically have an active channel width of <10 m are not defined in the 30 m DEM. Therefore a 10 m × 10 m grid cell resolution DEM was constructed for northeastern Puerto Rico.

Many Geographical Information Systems (GIS) packages are available that provide the necessary tools and algorithms to generate a hydrologically correct DEM from contour data, e.g. the ArcGIS Spatial Analyst and ArcHydro (Maidment, 2002). The 10 m elevation contours from the US Geological Survey (Seiders, 1971) were used for the basis of the DEM (Fig. 1). Contours were first converted to a Triangulated Irregular Network (TIN) surface, which is constructed by

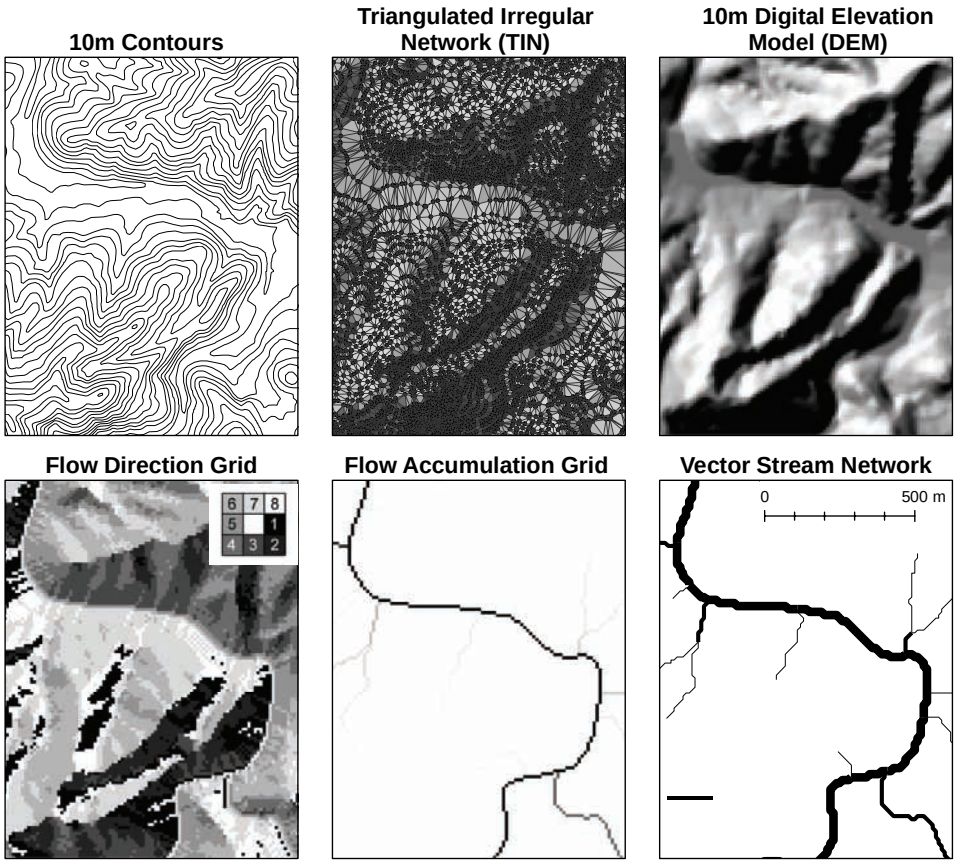


Fig. 1 The process of extracting a stream network from contour data. Contour → TIN → DEM → Flow Direction → Flow Accumulation → Vector Stream Network. The area illustrated is known locally as "Puente Roto", on the Rio Mameyes.

triangulating a set of vertices to form a network of triangles. For the purpose of flow routing, the TIN was interpolated to a raster DEM at 10 m × 10 m grid cell resolution using ArcGIS Spatial Analyst. The resolution of the raster determines how well the raster represents the features of the TIN surface. In the Luquillo Mountains, 10 m resolution is sufficient to capture many elements of the TIN.

The resulting DEM generated from contour lines contains topographic errors that create problems in hydrological models, such as pits and depressions, but are easily corrected to ensure continuous hydrological flow (Tarboton *et al.*, 1991). Similarly, in flat terrain, fine-scale features such as river meanders and river courses may not be well constrained by the contour lines. For better accordance with known river paths, the river can be forced into a DEM by lowering the cells of the river several metres to ensure that they are topographically lower than surrounding cells (Maidment, 2002).

Flow direction was calculated according to the simple D8 algorithm, whereby flow is routed to the adjacent cell with the greatest elevation drop (Jenson & Domingue, 1988). With this algorithm, a flow direction matrix is computed where each grid cell is assigned a value (1–8), corresponding to the eight cardinal directions, routing the flow to the appropriate adjacent cell. The flow accumulation grid was computed using this flow direction grid. First, the total number of upslope cells contributing to a given cell was calculated. Cells were then weighted so that the accumulated surface represents the sum of upslope weights. For example, if the weight is a constant 100 m^2 area for each 10 m cell, then the accumulation represents the drainage area. Similarly, if the weight for each cell is the yearly runoff, then the accumulated surface will represent mean annual discharge.

STREAM NETWORK EXTRACTION

To extract a stream network from a DEM, a drainage area threshold can be applied to the flow accumulation surface (Tarboton *et al.*, 1991). The threshold represents the critical drainage area that distinguishes perennial from ephemeral streams; grid cells that exceed this threshold represent streams with year-round flow. The threshold for perennial streams in the mid-elevations of the LEF has been determined to be approximately 6 ha (Scatena, 1989). While this threshold may vary across the landscape due to rainfall differences, a 6 ha threshold is an appropriate mean estimate for the catchment.

The resulting map of the perennial stream network has a higher drainage density than the USGS stream network (Fig. 2). For the Rio Mameyes, the resulting total length of the stream network at 6 ha drainage area is 133 km, compared to a total length of 70 km for the USGS stream network. This increased length is due to the inclusion of a large number of previously unmapped 1st order streams that do not appear at the scale of the 1:24 000 USGS map but are known to exist. Several of these small streams have community water intakes, and thus the extraction of these streams from the DEM is critical for estimating the available water.

The resulting stream network accurately represents the path of major stream channels. However, some of the smaller streams may not be accurately represented. This problem is most apparent in flat terrain, where flow can follow artefacts of the surface interpolation procedures rather than real topographic features. Similarly, small streams have been diverted in the lowland agricultural fields and urbanizations. In these areas, the digital estimation and reality may not agree. Therefore, for the purpose of mapping small 1st order streams, the digitally defined stream network should be used with caution when outside of natural, valley confined upland streams.

RAINFALL, RUNOFF AND DISCHARGE

The spatial distribution of rainfall and runoff the in LEF is strongly influenced by elevation. Small drainages in the uplands have distinctly more runoff than comparably sized lowland drainages. To estimate the spatial distribution of mean annual rainfall, runoff and discharge, the following elevation-based regression equations, estimated from long-term rain and streamgauges throughout the LEF, were used (García-Martinó *et al.* 1996):

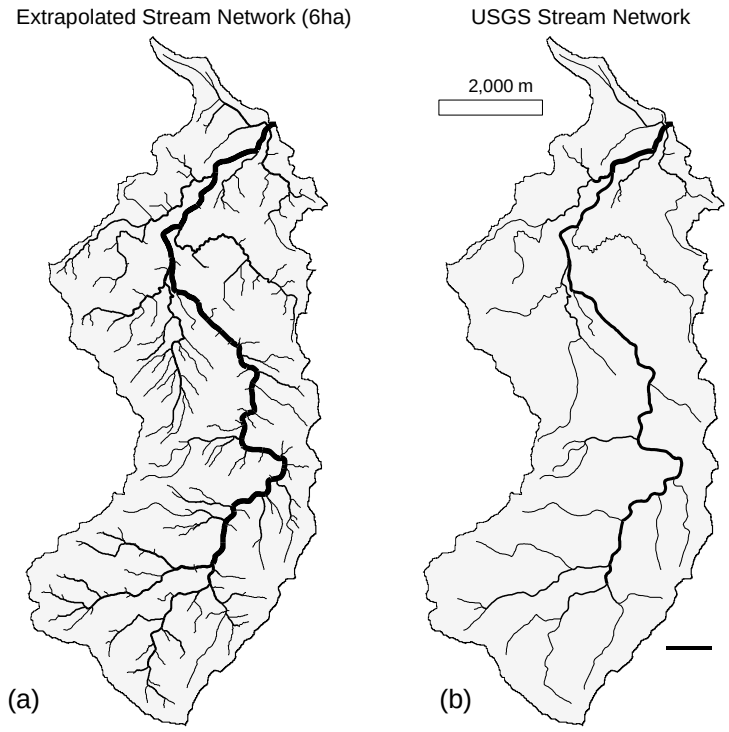


Fig. 2 Comparison of the USGS stream network (a) to the DEM generated stream network at 6 ha drainage area threshold (b) for the Rio Mameyes. Lines widths are scaled according to stream order. While only the Rio Mameyes is illustrated (to show fine scale features), other drainage basins show a similar comparison between USGS and DEM generated stream networks.

$$P = 2300 + 3.8h - 0.0016h^2 \qquad n = 17,\ r^2 = 0.91,\ p < 0.001 \tag{1}$$

$$R = 4.26WAE + 360 \qquad n = 9,\ r^2 = 0.77,\ p = 0.002 \tag{2}$$

Discharge is estimated from runoff by multiplying by the drainage area:

$$Q = 3.17 \times 10^{-5} A(4.26WAE + 360) \qquad n = 9,\ r^2 = 0.97,\ p < 0.001 \tag{3}$$

P = mean annual rainfall (mm), R = mean annual runoff (mm), Q = mean annual discharge ($m^3\ s^{-1}$), h = elevation (m a.s.l.), WAE = weighted average elevation (m), A = drainage area (km^2), n = number of gauges used, p = significance level.

Using these equations, maps of mean annual rainfall, runoff, and discharge for the Rio Mameyes are shown (Fig. 3). Rainfall and runoff very closely resemble the elevation structure, while discharge pattern is similar to flow accumulation grid. This is due to the fact that both rainfall and runoff are based on elevation, while discharge is a largely a function of drainage area.

The weighted upstream elevation variable, used in calculating runoff, is an accumulated function. That is, it is the sum the elevation of all upslope cells, divided by the number of accumulated cells. This accounts for the fact that basins at higher elevations have greater mean annual runoff than corresponding basins of equal area at lower elevations.

A simple water budget was constructed for the Rio Mameyes drainage basin, using equations (1) and (2): mean annual rainfall is 3320 mm, runoff is 2090 mm, and by difference, evapotranspiration is 1230 mm (García-Martinó *et al.*, 1996). This budget is comparable to a recently estimated evapotranspiration rate, averaged for the entire LEF, of 3.08 mm day^{-1}, or 1120 mm $year^{-1}$ (Wu *et al.*, 2006). According to this budget, 63% of rainfall becomes runoff, and estimates of discharge derived from runoff (equation (3)) agree with the water budget. Similarly, the discharge equation derived from runoff is superior to a simple drainage area–discharge relation because it takes the upstream elevation and rainfall into account. Thus, the simple regression-based approach mentioned here is sufficient to make accurate predictions of rainfall, runoff, and discharge in these drainages.

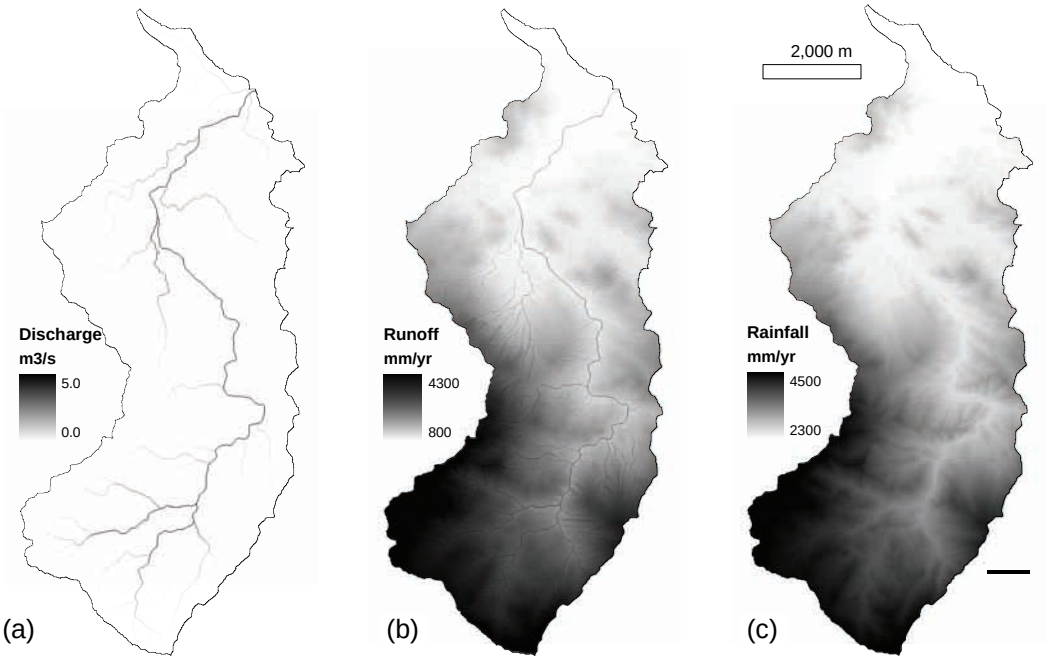


Fig. 3 Spatial distribution of mean annual (a) rainfall, (b) runoff, and (c) discharge within the Rio Mameyes drainage basin according to elevation-based regression equations.

CONCLUSIONS

The stream network and mean annual rainfall, runoff, and discharge can be accurately estimated at 10 m spatial resolution according to a simple DEM-based process for basins draining the LEF. The estimates are better applied to streams in the forested upland regions than flat and anthropogenic disturbed areas. However, the simplicity of this DEM-based approach allows any researcher with limited rainfall and runoff data to estimate key hydrological variables in ungauged areas.

Acknowledgements The author thanks Dr Fred Scatena for advice on the manuscript, and Dr Lena Tallaksen for strengthening comments. Funding for this study was provided by the National Science Foundation Biocomplexity Grant (NSF #030414)—Rivers, Roads, and People: Complex Interactions of Overlapping Networks in Watersheds.

REFERENCES

García-Martinó, A.R ., Warner, G. S., Scatena, F. N. & Civco, D. L. (1996) Rainfall, runoff, and elevation relationships in the Luquillo Mountains of Puerto Rico. *Caribbean J. Sci.* **32**(4), 413–424.

Jenson, S. K. & Domingue, J. O. (1988) Extracting topographic structure from digital elevation data for geographic information system analysis. *Photogrammetric Engineering and Remote Sensing*. **54**(11), 1593–1600.

Maidment, D.R. (2002) ArcHydro: GIS for water resources. ESRI Press, USA.

March, J. G., Benstead, J. P., Pringle, C. M. & Scatena, F. N. (2003) Damming tropical island streams: problems, solutions, and alternatives. *BioScience* **53**(11), 1069–1078.

Montgomery, D. R., Dietrich, W. E. & Sullivan, K. (1998) The role of GIS in watershed analysis. In: *Landform Monitoring, Modelling and Analysis*. (ed. by S. N. Lane, K. S Richards & J. H. Chandler), 241–261. John Wiley & Sons Ltd, West Sussex, UK.

Scatena, F.N. (1989) An introduction to the physiography and history of the Bisley Experimental Watersheds in the Luquillo Mountains of Puerto Rico. *US Dept. Agriculture Forest Service General Tech. Report SO-72.*

Schellekens, J., Scatena, F. N., Bruijnzeel, L. A. & Wickel, A. J. (1999) Modelling rainfall interception by a lowland tropical rain forest in northeastern Puerto Rico. *J. Hydrol.* **225**, 168–184.

Schellekens, J., Scatena, F. N., Bruijnzee, L. A., van Dijk, A. I. J. M., Groen, M. M. A. & van Hoogezand, R. J. P. (2004) Stormflow generation in a small rain-forest catchment in the Luquillo Experimental Forest, Puerto Rico. *Hydrol. Processes* **18**(53), 503–530.

Seiders, V. M. (1971) Geologic map of the El Yunque quadrangle, Puerto Rico. *US Geological Survey Miscellaneous Geologic Investigations Map I-658*, 1:20 000 scale.

Tarboton, D. G., Bras, R. L. & Rodriguez-Iturbe, I. (1991) On the extraction of channel networks from digital elevation data. *Hydrol. Processes* **5**, 81–100.

van der Molen, M. K. (2002) Meteorological impacts and land use change in the maritime tropics. PhD Thesis, Vrije Universiteit, Amsterdam, The Netherlands.

Wu, W., Hall, C. A. S., Scatena, F. N. & Quackenbush, L. J. (2006) Spatial modeling of evapotranspiration in the Luquillo Experimental Forest of Puerto Rico using remotely-sensed data. *J. Hydrol.*(in press).

Climate Variability and Change—Hydrological Impacts (Proceedings of the Fifth FRIEND World Conference held at Havana, Cuba, November 2006), IAHS Publ. 308, 2006.

Submodelo de erosión en laderas para modelo precipitación–escorrentía en SIG

ALEJANDRO DUSSAILLANT J.

Departamento de Ingeniería Hidráulica y Ambiental, Pontificia Universidad Católica de Chile, Vicuña Mackenna 4860, Santiago, Chile

adussa@ing.puc.cl

Resumen La erosión hídrica en laderas produce pérdidas de suelo y fertilidad, así como contribuir al transporte de contaminantes—el mismo sedimento más compuestos adsorbidos a él (agroquímicos). Además, la erosión contribuye al embancamiento de ríos y lagos, canales de regadío y embalses. Es un problema particularmente serio en el secano central de Chile. Se presenta un modelo de erosión en laderas de base física que considera erosión por impacto de lluvia, erosión por flujo laminar y erosión por canalículos. Se basa en el concepto de capacidad de transporte, potencia de flujo disponible y en la presencia de una capa de sedimento depositado. Los resultados del modelo se comparan con resultados de parcelas experimentales, sin calibración previa, entregando buenos resultados para los eventos de lluvia más importantes del año 2002 para parcelas en el secano interior de Ninhue, VIII Región, Chile. Se propone que el actual modelo puede resultar útil para la estimación de la erosión en base a modelos hidrológicos distribuidos en SIG.

Palabras claves erosión, erodibilidad, potencia de flujo, Chile, zona árida

A hillslope erosion submodel for use with rainfall–runoff models in GIS

Abstract Hillslope erosion causes important soil and fertility loss, as well as contributing to contaminant transport (sediment and adsorbed chemicals). Also, erosion contributes to stream and lake sedimentation. Recent studies estimate that, worldwide, the 45 000 dams over 15 m high, trap more than 25% of global sediment and that these are losing between 0.5 and 1% of their capacity annually. The increase in soil erosion due to human mismanagement causes advancing desertification of the landscape. The aim of this work is to provide tools for decision making regarding erosion management decisions in the semiarid Secano area of Chile. A physically-based numerical erosion model has been developed so that it can be incorporated into distributed hydrological models; it considers rainfall erosion, sheet erosion, and rill erosion on a hillslope. The model will be applied to field plots where soil loss has been monitored. The numerical model (Hillslope Erosion Model, HES) is an event model and considers the hillslope length as divided into 1 m elements. Water and sediment can enter each element from upslope, and the Manning equation is used to estimate mean velocities. HES estimated total soil loss during the events rather well, obtaining good approximations for the different plot treatments, without using calibration of parameters. Sensitivity analysis showed that for sheet flow, the most sensitive parameters are percent cover and cohesion, and for rill flow, these are cohesion and slope. For both, the rill network has little effect.

Key words erosion; erodibility; stream power; Chile; arid zone

INTRODUCCIÓN

La erosión hídrica en laderas produce pérdidas de suelo y fertilidad, así como contribuir al transporte de contaminantes—el mismo sedimento más compuestos adsorbidos a él (agroquímicos). Además, la erosión contribuye al embancamiento de ríos y lagos, canales de regadío y embalses. Estudios recientes estiman que a nivel mundial, 45 000 represas de 15 m o más de muro, atrapan más del 25% del sedimento global (Vorosmarty *et al.*, 2003), y la Comisión Mundial de Represas estima que éstas estarían perdiendo entre 0.5 a 1% de su capacidad anualmente.

El aumento de la erosión hídrica de suelos debido al mal manejo de estos por la humanidad, inserto en una progresiva desertificación del territorio (Batchelor, 1995), requiere de información que permita priorizar las áreas que requieren protección, así como seleccionar las opciones de manejo más apropiadas para el contexto particular.

En particular, la motivación de este trabajo es proveer herramientas para la toma de decisiones para contribuir a la reducción de la erosión del secano central chileno, con potenciales beneficios para agricultores de subsistencia así como para la industria exportadora de altos ingresos (plantaciones forestales, frutales, viñedos, paltos).

Interesa desarrollar un modelo de erosión numérico con base física, para ser incorporado en modelos hidrológicos, que considere la erosión por impacto de lluvia, erosión laminar, y erosión por canalículos en una ladera. Se cuenta con datos de erosión para algunas localidades, así como un modelo de precipitación-escorrentía (Calle & Varas, 1998), al cual se pretende añadir el submodelo de erosión que concentra nuestra atención en este trabajo. El modelo será aplicado a parcelas donde se ha medido pérdida de suelo para evaluar su desempeño.

Copyright © 2006 IAHS Press



Fig. 1 Parcelas de erosión en Ninhue, secano interior, VIII Región, Chile.

METODOLOGÍA

Datos y modelo

Los datos provienen de 9 parcelas de 10 × 3 m (3 repeticiones de tratamiento: rotación, mínima labranza y pradera natural) del INIA-Chillán (Fig. 1). Se cuenta con datos para 2001–2003 de precipitación cada 15 minutos y totales de sedimentos por evento.

El modelo numérico es por evento, y considera dividir la ladera en elementos de 1 m de longitud o menos. Se prevé el ingreso de agua y sedimento desde la celda pendiente arriba, y se utiliza la ecuación de Manning para la estimación de la velocidad.

Erosión por impacto de agua de lluvia

Para estimar la erosión por impacto de lluvia, el modelo utiliza algoritmos del modelo EUROSEM (Morgan *et al.*, 1998). Para la erosión por flujo, la base física sigue al modelo propuesto por Hairsine & Rose (1992) y Siepel *et al.* (2002). Se asume una red y sección dada, y se utiliza el concepto de capacidad de transporte.

Para la erosión por lluvia (Morgan *et al.*, 1998), la energía cinética por mm de lluvia caída e_k (J m^{-2} mm^{-1}) se estima de la intensidad de lluvia R, despreciando efectos del viento (van Dijk *et al.*, 2002) y con una correlación con la altitud z (m) para $z > 100$ m:

$$e_k = 28.3\left[1 - 0.52\exp(-0.042R)\right]\left[0.0101z\right] \quad (1)$$

Para la pérdida de suelo por impacto de gotas KED (g m^{-2}), se usa (Morgan *et al.*, 1998):

$$KED = k \cdot E_k \exp(-bh) \quad (2)$$

donde k (g J^{-1}) es la erodibilidad, determinada experimentalmente (valor entre 1 y 6). E_k es la energía cinética total de la lluvia (J m^{-2}), h es la profundidad del agua (mm), y el valor de b varía entre 1 y 3 según textura del suelo.

Erosión por escurrimiento de agua superficial

Para la erosión por flujo, se modela según Fig. 2 (Hairsine & Rose, 1992), que asume $i = 1...I$ clases de partículas, una tasa de depositación d_i, una tasa de resuspensión no selectiva r_{ri} y un equilibrio dinámico para la masa M de partículas, es decir:

$$\frac{\partial M_i}{\partial t} = d_i - r_{ri} = 0 \quad (3)$$

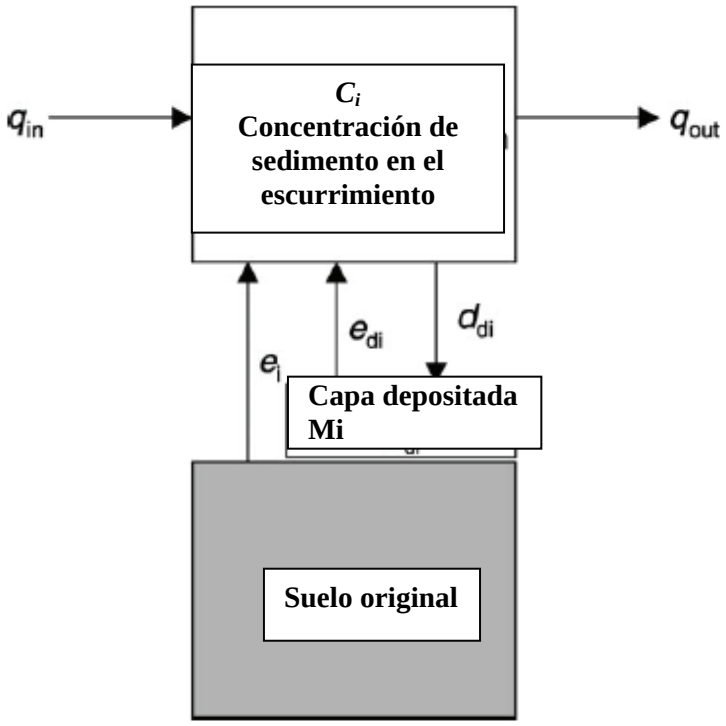


Fig. 2 Esquema del modelo de Rose de erosión por escurrimiento.

La capacidad de transporte es proporcional a la potencia del flujo ω (= $\rho g S R_h V$, con ρ masa específica del agua, *g* aceleración de gravedad, *S* pendiente del terreno, R_h radio hidráulico y *V* velocidad). La fracción disponible se estima como $F(\omega - \omega_0)$ – donde ω_0 es la potencia del flujo mínima para el movimiento – dado que la fracción 1 – *F* es disipada. Si la condición es limitada por transporte (i.e. todo el suelo está cubierto por capa depositada, Hairsine & Rose, 1992), la concentración de sedimento *C* es:

$$C_t = \left(\frac{\rho_s}{\rho_s - \rho}\right) \frac{F}{gh \sum_{i=1}^{I} v_i / I} \left[(\omega - \omega_0) + KED\right] \tag{4}$$

La vegetación reduce la potencia del flujo efectiva, reduciendo la velocidad por la rugosidad, y al proteger la capa depositada; reduciendo la suspensión y resuspensión.

Siepel *et al*. (2002) modificaron el modelo, suponiendo una partición de la tensión de corte debida al suelo, τ_s, y a la cubierta vegetal C_{veg} (% de cobertura), τ_{ss}:

$$\frac{\tau_{ss}}{\tau_s} = (1 - C_{veg})^p \tag{5}$$

donde *p* es un parámetro.

Con ello, la potencia efectiva queda definida como:

$$\omega = \tau_{ss} V = \rho g S R_h V (1 - C_{veg})^p \tag{6}$$

Por tanto, el modelo de erosión por flujo laminar queda:

$$C_t = \left(\frac{\rho_s}{\rho_s - \rho}\right) \frac{F}{\phi g h} \left[(\omega - \omega_0) + KED\right] \cdot \left(1 - C_{veg}\right) \tag{7}$$

con φ velocidad de sedimentación promedio entre clases de partículas.

Para los elementos con canalículos (surcos en el suelo), se siguen los supuestos de Hairsine & Rose (1992), que son: flujo hidráulicamente suave; canalículos trapezoidales y sin cubierta vegetal; erosión por gotas despreciable; potencia del flujo uniformeme en el perímetro mojado (P_{wr}); capa depositada restringida al fondo (ancho W_r); resuspensión no selectiva; equilibrio dinámico.

Así, el modelo de erosión por canalículos queda:

$$C_t = \left(\frac{\rho_s}{\rho_s - \rho}\right)\frac{F}{\phi g h}(\omega - \omega_0)\left(\frac{W_r}{P_{wr}}\right) \quad (8)$$

Finalmente, la solución de la erosión en cada elemento de ladera sigue los pasos: (1) asumir erosión neta en el elemento bajo cálculo; (2) calcular la concentración usando $C = C_t^{\beta}$, con (Morgan *et al.*, 1998): $\beta = 0.79 \cdot \exp(-0.85 \cdot J)$, con β coeficiente de eficiencia de pérdida por flujo y J (kPa) cohesión de la superficie; (3) realizar balance de masa para verificar que el supuesto de (1) fue correcto—si el sedimento entrante es mayor que el que sale, asumir depositación neta y recalcular C con $\beta = 1$ (i.e. $C = C_t$).

Para probar el modelo, se utilizaron los eventos del año 2002 con mayor transporte de sedimentos (julio 24, junio 3 y julio 22, Tabla 1). Los parámetros de erosión fueron los mismos utilizados por Siepel *et al.* (2002) (Tabla 2). Los parámetros de manejo para los 3 tratamientos se presentan en la Tabla 3. El exceso de lluvia fue diferente para cada tratamiento, y se utilizó el entregado por los datos de terreno sobre captura de escurrimiento.

Tabla 1 Eventos de lluvia para comparación con resultados del modelo de erosión.

Evento	Duración (h)	$I_{\max 15\ min}$ (mm h^{-1})	I_{15min} (>4 mm h^{-1}) (frecuencia)	Precipitación total (mm)
3 junio 2002	66	14.8	24	60.6
22 julio 2002	87	6.4	14	52.1
24 julio 2002	50	10.4	25	64.5

Tabla 2 Parámetros de erosión utilizados (según Siepel *et al.* 2002).

Parámetro	Unidad	Valor usado
Potencia unitaria de flujo crítica, ω_0	W m^{-1}	0.2
Velocidad de sedimentación promedio, φ	m s^{-1}	0.1
Fracción efectiva de potencia de flujo, F	–	0.1
Parámetro de efecto de vegetación, p	–	3
Concentración mínima inicial, C_{min}	mg L^{-1}	1

Tabla 3 Parámetros para tratamientos de barbecho, mínima labranza y pradera natural.

Parámetro	Barbecho	MinLab	Pradera
Cohesión (kPa)	10	14.5	20
Cubierta vegetacional, C_{veg}	0.1	0.7	0.7

RESULTADOS Y DISCUSIÓN

Los resultados se resumen en la Tabla 4. Se puede observar que salvo 2 casos a pendiente 12% y 18.5%, el modelo aproximó la producción de sedimentos relativamente bien, obteniendo buenos resultados cualitativos para los diferentes tratamientos de cubierta vegetal.

Se puede hipotetizar que las sobreestimaciones al inicio de la temporada pueden deberse a la compactación durante la siembra, y las sobreestimaciones hacia el final de la temporada de crecimiento vegetal pueden deberse a que se utilizó un porcentaje de cobertura fijo para toda al temporada. Estos son elementos a abordar en una profundización futura del presente ejercicio.

Se realizaron estudios sobre la sensibilidad de parámetros del modelo, de los cuales se concluyó que para flujo laminar, los parámetros más sensibles son la cubierta y la cohesión; para flujo en canalículos, éstos son la cohesión y la pendiente; para ambos, la red de canalículos no afecta mayormente.

En resumen, pareciera que una buena estimación del escurrimiento de agua, acoplada con estimaciones apropiadas de la cohesión y la cobertura, producen una estimación adecuada para la erosión, al menos para estos sitios y eventos. Debemos hacer notar que no se realizó calibración alguna, lo que es auspicioso. Esperamos en un futuro cercano complementar este análisis con más datos de forma de profundizarlo.

Tabla 4 Resultados del modelo (HES) *versus* resultados experiencias de terreno.

Tratamiento	*S* = 12% Sedimento (g)	Modelo HES (g)	HES/medición	*S* = 18.5% Sedimento (g)	Modelo HES (g)	HES/medición
Tradicional	2889	2547	88%	3504	9205	263%
Mínima labranza	1451	1800	124%	2831	1854	65%
Pradera	411	1682	409%	3268	1712	52%
Tradicional	2583	2230	86%	2169	5393	249%
Mínima labranza	845	937	111%	1728	1432	83%
Pradera	168	174	104%	759	706	93%
Tradicional	5425	5863	108%	10122	9390	93%
Mínima labranza	2264	1717	76%	8136	2862	35%
Pradera	395	910	230%	3521	2269	64%

Dado que este es un trabajo limitado y preliminar, resta aún mucho por hacer. Nuestro trabajo futuro incluye mayor análisis de datos: determinar la infiltrabilidad, cohesión y cubierta durante la temporada en las parcelas; y consideraremos un experimento de laboratorio bajo condiciones más controladas. En cuanto al modelo, se planifica: calibrar y validar con más datos (2004 a 2006); incorporar el algoritmo en nuestro modelo en GIS; y comparar los resultados con datos de pequeñas cuencas con monitoreo de sedimentos en la misma zona de estudio.

Agradecimientos El autor agradece el financiamiento entregado por la beca Coimbra para jóvenes investigadores latinoamericanos, la cual financió al autor en su estadía en Padova, Italia, entre Noviembre 2004 y enero 2005, período donde se realizó el estudio teórico, así como la gentil acogida del Departamento IMAGE de Ingeniería de la U. de Padova (profesores Di Silvio, Rinaldo, Gaion). Sinceros agradecimientos al INIA-Chillán, y particularmente Octavio Lagos, por la gentil entrega de los datos de terreno.

REFERENCIAS

Abrahams, A. D., Li, G., Krishnan, C. & Atkinson, J. F. (2001) A sediment transport equation for interrill overland flow on rough surfaces. *Earth Surf. Process. Landf.* **26**, 1443–1459.

Agassi, M. & Bradford, J. M. (1999) Methodologies for interrill soil erosion studies. *Soil Tillage Res.* **49**, 277–287.

Barthes, B & Roose, E (2002)Aggregate stability as indicator of soil susceptibility to runoff and erosion: validation at several levels. *Catena* **47**,133–149.

Bryan, R. B. (2000) Soil erodibility and processes of water erosion on hillslope. *Geomorph.* **32**, 385–415.

Calle, G. & Varas, E. (2003) Hydrodynamic and geomorphologic processes in the hydrologic response of a watershed. *Revista Ingeniería Hidráulica en México* (in Spanish).

Dussaillant, A. R. (2002) Stormwater infiltration and focused groundwater recharge in a rain garden: numerical modeling and field experiment. PhD Thesis, Civil & Environmental Engineering, University of Wisconsin, Madison, USA.

Gao, B., Walker, M. T., Steenhuis, T. S., Parlange, J.-Y., Nakano, K., Rose, C. W. & Hogarth, W. L. (2003) Investigating ponding depth and soil detachability for a mechanistic erosion model using a simple experiment. *J. Hydrol.* **277**, 116–124.

Hairsine, P. B. & Rose, C. W. (1992) Modeling water erosion due to overland flow using physical principles. 1. Sheet flow. *Water Resour. Res.* **28**(1), 237–243.

Hairsine, P. B. & Rose, C. W. (1992) Modeling water erosion due to overland flow using physical principles. 2. Rill flow. *Water Resour. Res.* **28**(1), 245–250.

Hogarth, W. L., Parlange, J.-Y., Rose, C. W., Sander, G. C., Steenhuis. T. S. & Barry, A. (2004) Soil erosion due to rainfall impact with inflow: an analytical solution with spatial and temporal effects. *J. Hydrol.* **295**, 140–148.

Jetten, V., de Roo, A. & Favis-Mortlock, D. (1999) Evaluation of field-scale and catchment-scale soil erosion models. *Catena* **37**, 521–541.

Léonard, J. & Richard, G. (2004) Estimation of runoff critical shear stress for soil erosion from soil shear strength. *Catena* **57**, 233–249.

Liu, Q. Q. & Singh, V. P. (2004) Effect of microtopography, slope length and gradient, and vegetative cover on overland flow through simulation. *J. Hydrol Engng* **9**(5), 375–382.

Morgan, R. P. C, Quinton, J. N., Smith, R. E., Govers, G., Poesen, J. W. A., Auerswald, K., Chisci, G., Torri, D.,Styczen, M. E. & Folly, A. J. V. (1998) The European soil erosion model (EUROSEM): documentation and user guide. Version 3.6 July 1998. Silsoe College, Cranfield University, UK.

Nearing, M. A., Norton, L. D., Bulgakov, D. A., Larionov, G. A., West, L. T. & Dontsvova, K. M. (1997) Hydraulics and erosion in eroding rills. *Water Resour. Res.* **33**(4), 865–876.

Raff, D.A., Ramírez, J. A. & Smith,. J. L. (2004) Hillslope drainage development with time: a physical experiment. *Geomorph.* **62**, 169–180.

Siepel, A. C., Steenhuis, T. S., Rose, C. W., Parlange, J.-Y. & McIsaac, G. F. (2002) A simplified hillslope erosion model with vegetation elements for practical applications. *J. Hydrol.* **258**, 111–121.

Climate Variability and Change—Hydrological Impacts (Proceedings of the Fifth FRIEND World Conference held at Havana, Cuba, November 2006), IAHS Publ. 308, 2006.

A European case-based reasoning tool to inter-compare hydrological information on water stress among drainage sub-basins

JASPER GRIFFIOEN, SOPHIE VERMOOTEN, NENO KUKURIC & SLAVEK VASAK

TNO Geological Survey of the Netherlands, PO Box 80015, 3508 TA Utrecht, The Netherlands
jasper.griffioen@tno.nl

Abstract To deal with water stress, there is a need to compare the water management issues of hydrological regions in order to inter-compare them and transfer knowledge from one area to another. An approach is presented using case-based reasoning (CBR) to inter-compare European drainage sub-basins. The CBR uses indicators for the natural hydrological potential of drainage sub-basins, the types of water stresses and the mitigation measures to cope with this stress. A prerequisite for the success of this tool is that the indicators are publicly and digitally available for the whole of Europe and contain insight to the appropriate information scale. This sets strong limits to the indicators used. In some cases, a proxy indicator may be more appropriate than a primary indicator, when these are not publicly available at the appropriate information scale. The set-up of the CBR is illustrated using some examples of indicators.

Key words indicators; natural conditions; water stress; proxy; water management; drainage sub-basin

INTRODUCTION

Water stress results when water resources are not able to satisfy, temporarily or continuously, a demand and is frequently encountered in many regions across the world. Various types of water stress occur and they may refer to surface water and groundwater, and to quantity and quality. If a type of water stress is a problem than mitigation measures could be a solution to the problem. A water situation is fully described only if the natural conditions are included in addition to types of water stress and potential mitigation measures. Accordingly, a water-related case consists of information/knowledge on these three main aspects.

Information on these three aspects is lacking in many regions where water management measures are necessary, due to lack of monitoring, insufficient resources for characterization and lack of awareness. Optimization of the re-use of knowledge/information on how to mitigate water stress from studied/monitored regions to unmonitored regions, is therefore of major importance (Franks *et al.*, 2005). Various regions encounter similar kinds of water stress, due to comparable physiographic conditions and land use functions. Similar mitigation measures may therefore be used as solution to water stress. One way to re-use knowledge is to compare unmonitored regions with monitored regions based on a description of the expected natural conditions and water stress.

The objective of this study is to develop a tool that allows inter-comparison between different European regions in relation to aspects of water management. The tool should assist in finding the most similar situation and retrieval of the required information. Case-based reasoning (CBR) was chosen to meet this objective.

A CASE-BASED REASONING TOOL FOR WATER MANAGEMENT IN EUROPE

The concept of case-based reasoning

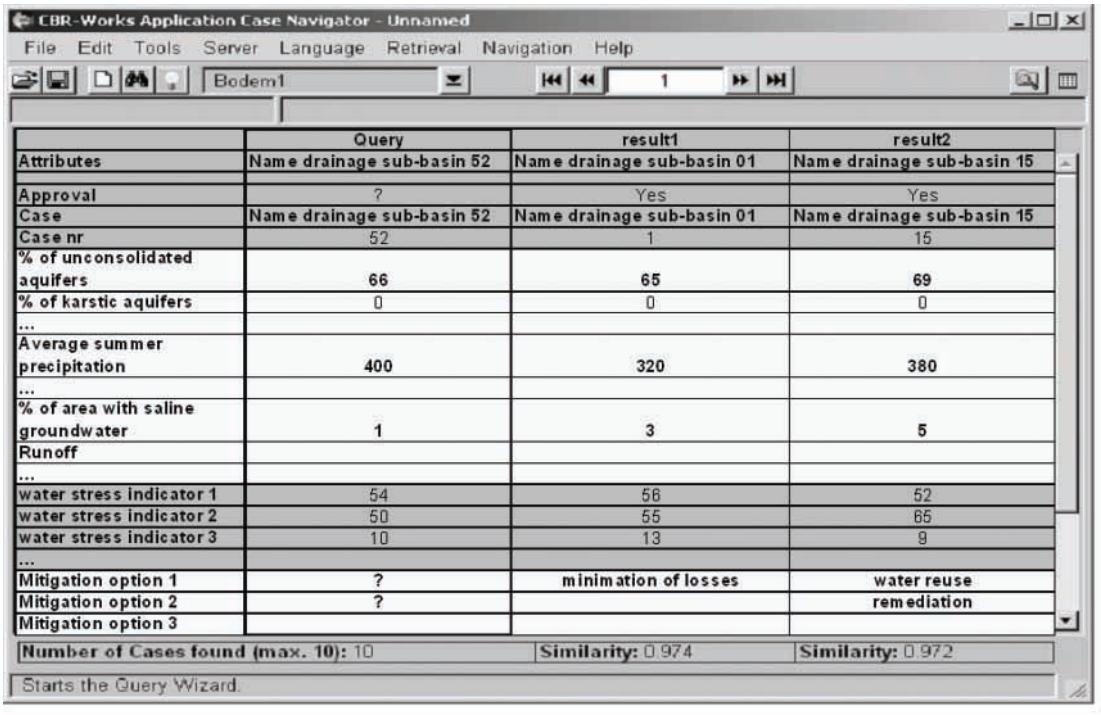
Initially, CBR was developed to re-use encapsulated knowledge: to identify the current problem situation, to find a past case similar to the new one, to use that case to suggest a solution to the current problem, to evaluate the new solution and to re-use the knowledge gained (Aamodt & Plaza, 1994). More recently, CBR has been as a "help desk system", where case-based indexing and retrieval methods are used to retrieve cases, offering to the user large amounts of filtered information. The application presented in this paper has this purpose.

A region-related water situation can be considered as a "case", being always "case-specific". In each case, the water situation is described by: (a) its natural water conditions (potential), (b) its

Copyright © 2006 IAHS Press

present water stress (problem), and eventually (c) the mitigation measures used to combat the water stress (solution). Case-based reasoning (CBR) is a technique that can be used for this purpose. In the case of water management, resemblances among cases are used to search for the regions with the most similar natural water conditions and water stress, in order to re-use information/knowledge available there or apply similar water management measures.

Regardless of the software tool selected, the CBR application consists of a few main steps, namely: (a) structuring and formalization of the cases, (b) building the reasoner, (c) selection of retrieval preferences, (d) retrieval procedure, and (e) updating the retrieval preferences and the knowledge base. In step (a), cases need to be described by a number of indicators making up a conceptual model of the case. The indicators could be of different type, such as symbol, taxonomy, real, integer, free text or comment, but are restricted to alpha-numeric information. Thus, spatial characteristics and its variability within a case cannot be dealt with in terms of spatial coordinates. This sets limits to the way in which information is used, as illustrated later. Step (b) encompasses encapsulation of the conceptual model into a software tool and development of the knowledge bases. Step (c) addresses the estimation of weights, similarities and definition of match rules. Since not all the indices are equally important for the retrieval, the relative weights (usually with the range 0.1–1 or 1–10) are assigned to each index. Where appropriate, similarity matrixes for index values are determined with the purpose of retrieving the most similar information in the absence of exact matching. Step (d) yields an ordered subset of the higher resembling cases. Figure 1 shows an example of the result of a retrieval procedure. It illustrates the match between one "query" case, drainage sub-basin 52, and two "result" cases, drainage sub-basins 01 and 15, with the calculated degree of similarity below each case. Since CBR is an iterative process based on user inference of retrieved results, knowledge of both the retrieval procedure and the content (e.g. natural water conditions, water stress and mitigation measures) is necessary to achieve optimal matching in undertaking the final step (e).



	Query	result1	result2
Attributes	Name drainage sub-basin 52	Name drainage sub-basin 01	Name drainage sub-basin 15
Approval	?	Yes	Yes
Case	Name drainage sub-basin 52	Name drainage sub-basin 01	Name drainage sub-basin 15
Case nr	52	1	15
% of unconsolidated aquifers	66	65	69
% of karstic aquifers	0	0	0
...			
Average summer precipitation	400	320	380
...			
% of area with saline groundwater	1	3	5
Runoff			
...			
water stress indicator 1	54	56	52
water stress indicator 2	50	55	66
water stress indicator 3	10	13	9
...			
Mitigation option 1	?	minimation of losses	water reuse
Mitigation option 2	?		remediation
Mitigation option 3			
Number of Cases found (max. 10): 10		Similarity: 0.974	Similarity: 0.972

Fig. 1 Example of the result of a retrieval procedure.

The European drainage sub-basins as a CBR unit

In implementing CBR, a challenge was to select the area to be represented by a "case". In CBR, this is called the representative elementary volume (REV). For this specific purpose, it is a natural case-specific unit, with a water situation defined by specific natural conditions, present water stresses (and eventually mitigation measures). The choice for the REV scale was carried out by

taking into account various factors, including public availability of data, their sub-regional spatial variability and the framework within which the research was performed. A case should represent water conditions in a single drainage sub-basin. Drainage sub-basins are typically discrete regions, the water resources of which can be assessed, developed and managed in a near independent manner from the rest of the basin. Even within the implementation of the EU Water Framework Directive, that explicitly asks for river basin management planning, drainage sub-basins are used as regional entities. Inter-comparison at this level is hypothesized to be most worthwhile because different kinds of supra-regional patterns are combined in drainage sub-regions: climate, hydrogeology, water economics and land use.

Comparison of the cases will be carried out across Europe or at least the EU member states. This reduces the importance of spatial variability within the case (a sub-basin area) for most of the indices. Nevertheless, some spatial variability within the drainage sub-basin remains important and needs to be "converted" into alpha-numerical information recognizable by a CBR tool. This is especially true in situations where a joint appearance of certain values of various indices creates new conditions, as in the example that a dominant local water function may be spatially coupled to a local hydrological feature. In CBR, this problem is addressed by creating additional, joined indices.

INDICATORS AND PROXIES FOR A CASED-BASED REASONING TOOL

Every case representing the water conditions in a drainage sub-basin, must be described by a set of indicators describing its specific natural conditions and water stress. Table 1 shows a set of possible indicators to describe the natural conditions related to water in a drainage sub-basin. The indicators used will most likely consider quantity and quality of water, and need to be combined with indicators on: (a) water use in agricultural, industrial, domestic, and tourist sectors; (b) technical water stress mitigation options (water saving, water re-use, remediation); (c) socio-economic aspects of water management (water pricing, institutional organisation, planning methodologies); and (d) environmental issues (in particular conservation of freshwater ecosystems).

Table 1 Examples of indicators to describe the natural conditions for a case in relation to water stress.

Information topic	Indicators
Aquifer typology	areal % of unconsolidated aquifers
Climate	average summer precipitation
Hydrology	river runoff
Groundwater quality	areal % of saline groundwater
Soil	areal % of area with impervious soils
Land use	areal % of forest

The focus of this article lies on the first step of the CBR application: the "structuring and formalization of the cases". In this conceptual CBR, all possible cases, equivalent to all European drainage sub-basins, are integrated in the CBR, which implies that all indicators describing the natural conditions and/or the water stress in these drainage sub-basins should be available and retrievable for the whole of Europe. This is not always the case as for some of the indicators considered, pan-European digital information is not available or not delivered.

To circumvent this problem, a method is used to create proxy maps for indicators for which pan-European data is not yet available or delivered. It is based on the simple theory that information abstracted from available thematic maps can be combined and used as a proxy to generate new maps providing regional information on natural conditions of groundwater quality and quantity. Figure 2 shows how new hydrogeological and hydrodynamical maps are generated from available European maps by combining data on soil, geology, and other factors. (FAO, 1993; CGMW & UNESCO, 2000). Below, two examples of indicators and their relation to drainage sub-basins (cases) are presented.

Example of a proxy indicator for aquifer typology

In the case of groundwater, the publicly available hydrogeological data are not suitable to generate information on both groundwater quantity and quality. For example, the digital geological map of

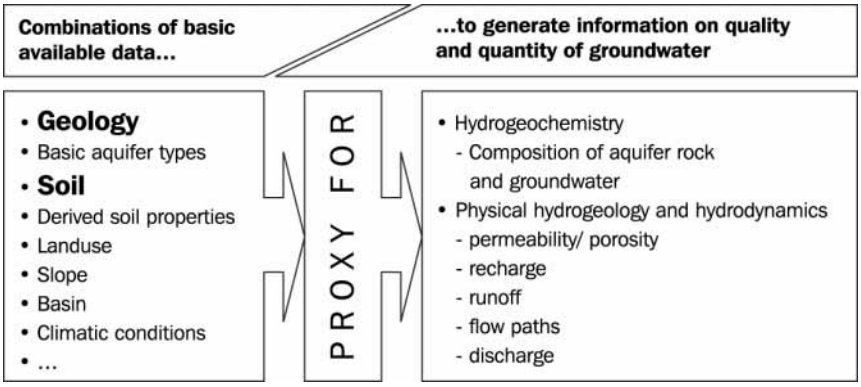


Fig. 2 Schematization of the proxy methodology for groundwater related data.

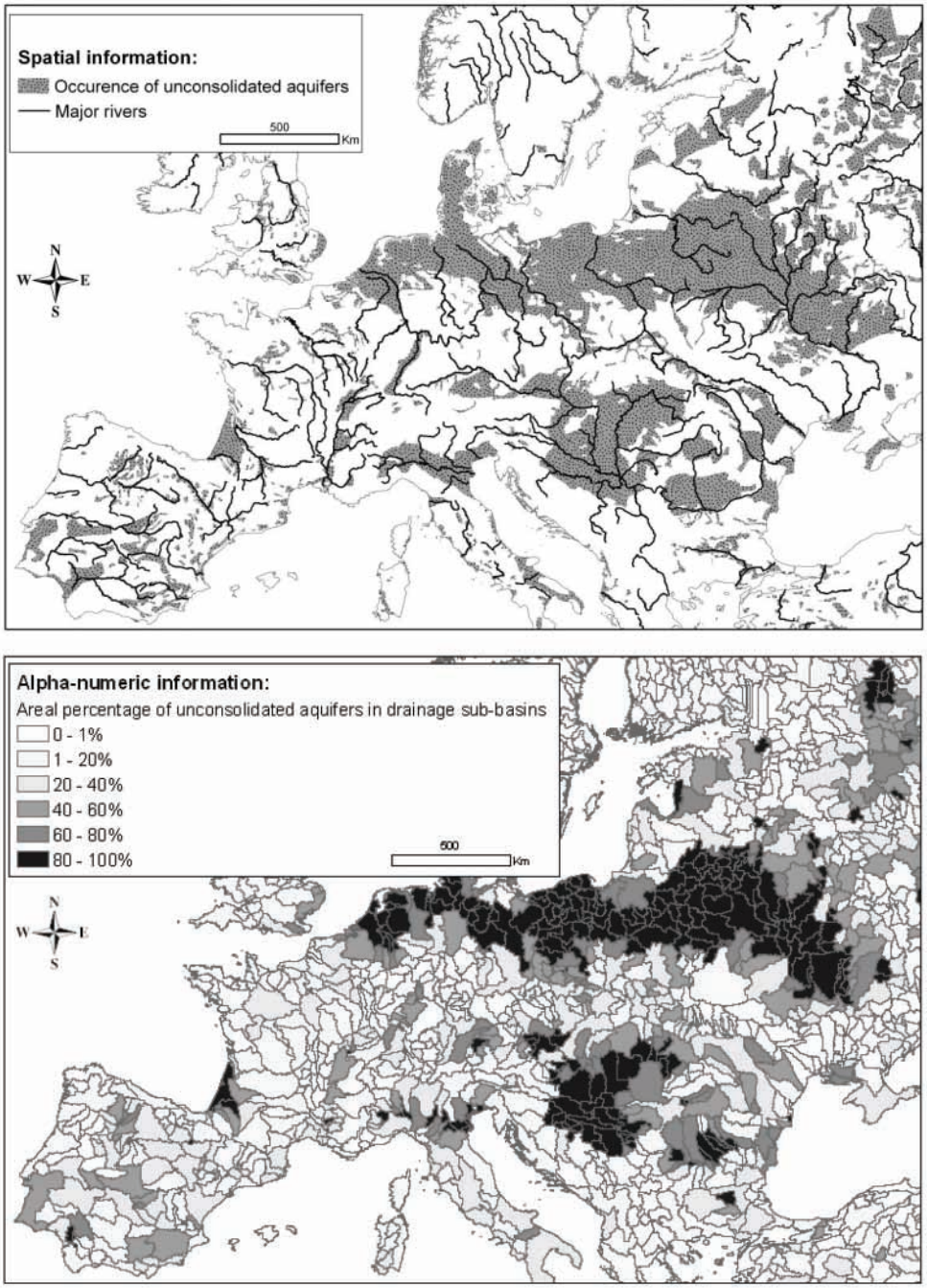


Fig. 3 Example of transforming spatial information on the extent of unconsolidated aquifers across Europe (above) to alpha-numeric information per drainage sub-basin (below).

Europe (CGMW & UNESCO, 2000) focuses on chronostratigraphy and provides only limited information on the aquifer lithology required. Moreover, a large part of the hydrogeological information is directed to physical hydrogeology and not available in digital form (RIVM, 1995). By combining different available thematic maps, an aquifer typology for Germany (Kunkel *et al*., 2004) is reproduced that addresses both hydrodynamics and groundwater quality. Figure 3 shows the result of the proxy map for the unit "unconsolidated aquifers", which are highly productive aquifers in drainage sub-basins. To integrate this data towards alpha-numeric information in the CBR, the proxy map is then combined with the drainage sub-basin map (USGS, 2006) and areal percentages of unconsolidated aquifers within each drainage sub-basin are calculated. This creates new insight into the occurrence of easily accessible groundwater resources in drainage sub-basins in Europe.

Example of an indicator for water availability

An important indicator for surface water is the runoff in a drainage sub-basin. At present, these data were not yet digitally available. Climate data (CRU, 2000) are thus used as an example to give an idea of the possible water availability related to precipitation in the hydrological summer season (April to September). Figure 4 presents the average precipitation in the summer season in each drainage sub-basin. The data used corresponds to an average of all monthly precipitation averages for the months April to September for the years 1961 to 1990. Combination of precipitation data with evapotranspiration data would yield a proxy for run-off and recharge.

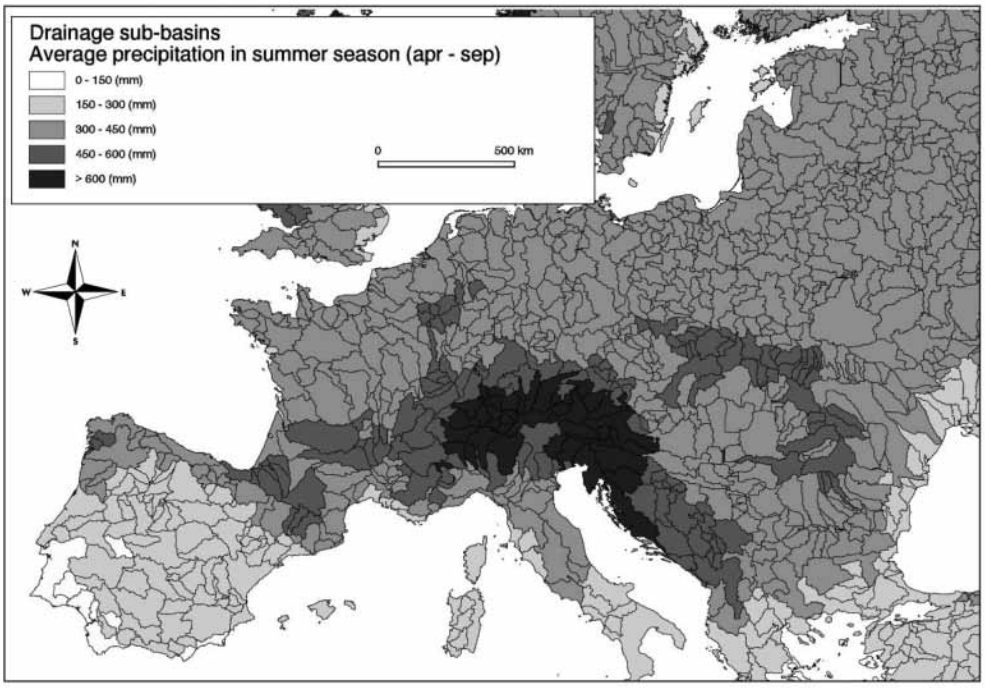


Fig. 4 Alpha-numeric information on average precipitation in summer season (Apr–Sept) in drainage sub-basins.

CONCLUSIONS

Case-based reasoning is a promising approach for inter-comparing drainage sub-basins when mitigating water stress. Indicators for three categories of water-related topics need to be considered when dealing with water stress, i.e. natural potential, type of water stress and technical or socio-economic mitigation options. A major practical problem is the availability of public data on indicators at regional level. Proxy indicators may, therefore, be more useful than the prime indicators on water-related topics.

Acknowledgement The research described was co-financed by the European Commission within the framework of the Framework Program 6 project AquaStress. Josef Reckman is gratefully acknowledged for his contribution to the data handling.

REFERENCES

Aamodt, A. & Plaza, E. (1994) Case-based reasoning: foundational issues, methodological variations and system approaches. *AICom* **7(**1), 39–59.

CGMW & UNESCO (2000) Geological map of the world at 1:25 000 000.

CRU (2000) Datasets Global Land Precipitation (1961–1990) Climatic Research Unit, Univ. of East Anglia, United Kingdom.

FAO (1993) *Digital soil map of Europe and West of the Urals*. FAO, Rome, Italy.

Franks, S. W., Kuylenstierna, J. & Sivapalan, M. (2005) PUB: Assessing the need for the integration of hydrological techniques. In: *Predictions in Ungauged Basins: International Perspectives on the State of the Art and Pathways Forward* (ed. by S. Franks, M. Sivapalan, K. Takeuchi & Y. Tachikawa), 323–340. IAHS Publ. 301. IAHS Press, Wallingford, UK.

Kunkel, R., Voigt, H. J-J., Wendland, F. & Hannappel, S. (2004) Die natürliche, ubiquitär überprägte Grundwasserbeschaffenheit in Deutschland. Schriften des Forschungszentrums Jülich, Reihe Umwelt/Environment, Band/volume 47.

Le Grand, H. E. (1983) *A Standardized System for Evaluating Waste Disposal Sites*. NWWA, Worthington, Ohio, USA.

RIVM (1995) *Digital hydrogeological map of Europe based on IAH/UNESCO UN Water Series 24/2*. RIVM, Bilthoven, The Netherlands.

USGS (2006). Hydro1k. http://edcdaac.usgs.gov/gtopo30/hydro/.

3 Hydrological Extremes

Low flow prediction and forecasting 99–174
Flood prediction and forecasting 175–238
Rainfall–runoff modelling 239–262

Climate Variability and Change—Hydrological Impacts (Proceedings of the Fifth FRIEND World Conference held at Havana, Cuba, November 2006), IAHS Publ. 308, 2006.

Stochastic model of flow duration curves for selected rivers in Bangladesh

M. F. BARI[1] **& KH. MD. SHAFIUL ISLAM**[2]

1 *Department of Water Resources Engineering, Bangladesh University of Engineering & Technology, Dhaka 1000, Bangladesh*
bari@wre.buet.ac.bd

2 *Department of Civil Engineering, Khulna University of Engineering & Technology, Khulna 920300, Bangladesh*

Abstract To overcome the difficulty of a traditional flow duration curve (FDC) in which the chronological sequence of occurrence of flows is masked, a stochastic approach has been applied to obtain a calendar year FDC. Estimates of mean flows by rank based on order statistics enable the construction of such a FDC once the underlying frequency characteristics and distribution of the population is known. This paper discusses the theoretical development of a stochastic FDC and the choice of a suitable probability distribution for mean daily discharges. The flow duration curve model is then applied to records from four selected rivers in north-western Bangladesh. Based on visual as well as χ^2 and Kolmogorov-Smirnov goodness-of-fit tests, the mixture lognormal distribution exhibited a better fit. Expected flow duration curves were generated for each gauging station using the chosen distribution and visually compared with observed curves. These flow duration curves represent, respectively, the computed and observed mean discharges by rank and showed a close agreement. Reliability of the FDC was investigated by comparison of computed standard deviations for the chosen distribution with those observed for all ranks, and the mixture lognormal was found to be a flexible distribution for the highly seasonal regimes of the selected rivers.

Key words flow duration curve; goodness-of-fit; mean daily discharge; mixed lognormal distribution; northwest Bangladesh; stochastic model

INTRODUCTION

Knowledge of the frequency of various flow rates in a river is essential for assessment of water available for consumptive uses, such as municipal and industrial supply, irrigation as well in-stream needs for navigation, hydropower, dilution of wastes, fish and aquatic ecology. Traditionally, the entire flow frequency regime has been summarized by a flow duration curve, which describes the average characteristics of all flow quantiles in a year by representing the proportion of time that a particular discharge in a river is equalled or exceeded during the period of observation. One drawback of this type of flow duration curve is that the chronological sequence of occurrence of the flows is masked. To overcome this difficulty, LeBoutillier & Waylen (1993) used a stochastic approach and obtained a calendar year flow duration curve. In this approach, observations of discharge in each year are ranked and averages by rank over all years of record are calculated. Then the flow duration curve represents the average ranked flow and preserves such flow frequency measures as the mean annual flood. In calculating the calendar year flow duration curve, both the mean discharge of each rank and an associated distribution about the mean may be retained. The nature of this distribution reflects the physical processes within the basin. The estimation of this curve has a strong theoretical parallel to order statistics that permit estimation of the mean discharge at any rank and its variance. LeBoutillier & Waylen (*1993*) discussed the theoretical development of a stochastic flow duration curve and applied the model to records from several rivers in British Columbia, Canada. The objective of this paper is to apply this methodology to discharge records from selected rivers in Bangladesh and obtain stochastic flow duration curves.

STOCHASTIC MODEL OF FLOW DURATION

Stochastic model of flow duration curve is based on the principle of order statistics. An order statistic is a ranked observation from a sample (Galambos, 1984). Let X_1, X_2, X_3, … X_n denote a random sample from a parent population with continuous cumulative distribution function F_x. Arranged in decreasing order, $X_{(1)}$, > $X_{(2)}$, > $X_{(3)}$, >…,…> $X_{(n)}$ are collectively termed the order statistics of the random sample, such that $X_{(r)}$, for $1 < r \leq n$, is the rth order statistic (Gibbons, 1985). Then annual maximum flow in a year will be denoted by $X_{(1)}$, the annual minimum value by $X_{(365)}$, and the annual

Copyright © 2006 IAHS Press

median by $X_{(183)}$ in a non-leap year. Estimates of $\mu_{(r)}$, the mean by rank, from the order statistics theory should enable the construction of a flow duration curve, once the underlying frequency distribution of the population is known. Gibbons (1985) presents the general results of the large sample approximation to the mean and variance of the *r*th order statistic $X_{(r)}$ of a sample of size *n* from the continuous distribution F_x.The approximation to the mean by rank, $\mu_{(r)}$, is:

$$\mu_{(r)} = F_x^{-1}[h(r)] \tag{1}$$

The approximation to the variance, by rank is:

$$\sigma^2_{(r)} = g(r)\{f_x[F_x^{-1}(h(r))]\}^{-2} \tag{2}$$

where $h(r) = 1 - [\frac{r}{n+1}]$, and $g(r) = \frac{r(n-r+1)}{(n+1)^2(n+2)}$

F_x and F_x^{-1} are the cumulative distribution function of the parent population and its inverse, f_x is the density function. Generally the distribution of daily discharge is similar to those of many seasonal series and is both highly skewed and peaked. This shape is suggestive of a lognormal, gamma or a generalized extreme value distribution (LeBoutillier & Waylen, 1993).

DATA

Mean daily discharge from four gauging stations on four rivers, the Baral, Dharla, Punarbhaba, and Teesta in the northwest region of Bangladesh, were selected for this study. The available daily discharge record lengths used were 29 years for the Baral River at Malanchi railway crossing (Station 16.1), 18 years for the Dharla at Kurigram (Station 76), 29 years for the Punarbhaba at Phulhat (Station 236), and 34 years for the Teesta at Kaunia (Station 294). The rivers in this region are dominated by two main seasons, the monsoon and dry season. The monsoon lasts from June to September and is characterized by heavy rainfall, high humidity and high flows in rivers. In the dry season river discharges reduce significantly, exhibiting skewness and peakedness over the annual cycle. The steps involved in application of the stochastic flow duration curve model are: (a) rank each year's data from largest to smallest, (b) calculate means by rank across all years, (c) pool all observations and fit probability distributions to the aggregate of all daily discharge observations, (d) select a suitable distribution on the basis of goodness-of-fit, (e) generate the means by rank, and (f) assess the performance of the chosen distribution's ability to reproduce the flow duration curve.

ANALYSIS AND RESULTS

Analysis began by ranking the daily discharge data of each year in descending order for each station. The mean and variance of rank across all years of data were calculated. Then the 365 values of calculated means by rank were used to determine a suitable probability distribution to model the stochastic flow duration curve. The model stochastic flow duration curve was then obtained and reliability assessed.

Estimation of parameters of selected distributions

Four probability distributions: lognormal, gamma, GEV, and mixture lognormal, possessing the ability to match the combination of skewness and peakedness were chosen. The parameters of the lognormal, gamma, and mixture lognormal distributions were estimated by the maximum likelihood method and that of the GEV distribution by the probability weighted method (Greenwood *et al*., 1979). Parameter estimates are summarized in Table 1.

Goodness-of-fit tests

For visual goodness-of-fit tests, theoretical distributions were superimposed on empirical distributions. For deriving empirical distributions, observations of mean daily discharge for each of the four selected rivers were assembled into 20 equal groups, relative frequencies computed and plotted

Table 1 Parameter estimates and goodness-of-fit test statistics for selected distributions.

Distribution	Parameter	River Baral	River Dharla	River Punarbhaba	River Teesta
Two-parameter Lognormal	μ_y	2.300	5.412	3.073	6.230
	σ_y	2.182	0.992	1.495	1.083
	K-S	0.0812	0.0988	0.0374	0.0398
	χ^2	48.6	70.3	25.8	19.5
Three-parameter Lognormal	μ_y	2.190	4.801	2.672	5.664
	σ_y	2.284	1.583	1.900	1.617
	a	0.251	55.16	2.671	102.9
	K-S	0.0788	0.0877	0.0358	0.0366
	χ^2	42.1	52.3	24.1	18.7
Two-parameter Gamma	η	0.341	1.108	0.501	1.005
	λ	212.6	338.3	152.8	874.0
	K-S	0.1533	0.2064	0.1126	0.1088
	χ^2	77.3	142.5	251.9	35.5
Three-parameter Gamma	α	1.284	1.284	1.284	1.284
	β	84.78	309.8	87.4	750.1
	γ	–36.5	–23.0	–35.7	–85.5
	K-S	0.1677	0.1729	0.2662	0.1125
	χ^2	81.9	137.3	373.0	38.9
Generalized extreme value	K	–0.51	–0.40	–0.66	–0.34
	α	35.95	170.1	25.90	448.8
	ξ	16.09	170.4	16.74	398.7
	K-S	0.2066	0.2009	0.0596	0.1443
	χ^2	93.7	155.6	39.1	42.7
Mixture Lognormal	μ_{y1}	0.830	4.649	2.006	5.345
	σ_{y1}	0.857	0.355	0.560	0.420
	ρ	0.652	0.570	0.586	0.562
	μ_{y2}	5.054	6.422	4.585	7.302
	σ_{y2}	0.505	0.568	1.026	0.540
	K-S	0.0536	0.0766	0.0290	0.0299
	χ^2	29.9	42.2	23.6	15.5

against class intervals. Four candidate distributions were then superimposed on the empirical distributions. As expected, the mixture lognormal distribution exhibited a better fit because the daily discharge data series at hand were skewed and peaked with accentuated upper tails. Two quantitative tests, the χ^2 and K-S tests, were also applied to further ascertain the goodness-of-fit. The values of the χ^2 and K-S statistics are included in Table 1 and these also suggest that the mixture lognormal distribution exhibit a better fit.

Stochastic flow duration curve

The mean daily flow values by rank for each of four selected rivers were computed using the mixture lognormal distribution with the aid of equation (1). Model stochastic flow duration curves based on the mixture lognormal distribution were then obtained for each river plotting the computed rank flow values against respective ranks. Similarly, observed stochastic flow duration curves were obtained by plotting measured mean flows by rank, which were computed earlier, against corresponding ranks. Figure 1 shows a visual comparison of the model stochastic and observed stochastic flow duration curves for the Baral River at Malanchi railway crossing. Figure 1 and similar comparisons for other rivers showed that the mixture lognormal distribution is suitable for deriving stochastic flow duration curves for the four selected rivers.

To assess the structure and reliability of the flow duration curve, rank variances computed by the mixture lognormal distribution were compared with the rank variances obtained from observed discharges. In Fig. 2 the computed and observed standard deviations are compared for the Baral River. It is seen that the shapes are similar but the magnitudes are different and similar differences were found for other rivers. The consistent underestimation of the variance for all rivers is probably due to the inflation of the total variance in the time series resulting from seasonality. The year to year consistency of the seasonality function controls variance in the intermediate ranks.

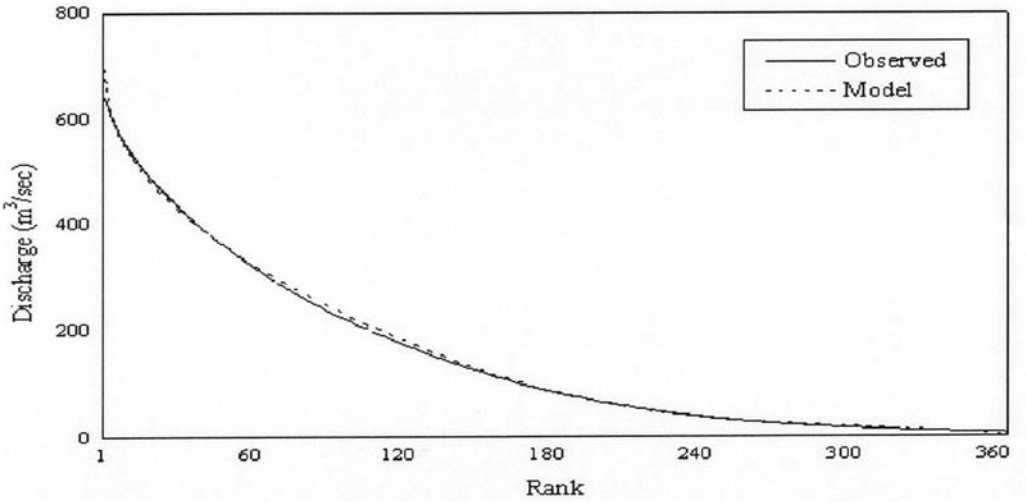


Fig. 1 Observed and model stochastic flow duration curve based on mixture lognormal distribution for Baral river at Malanchi railway crossing.

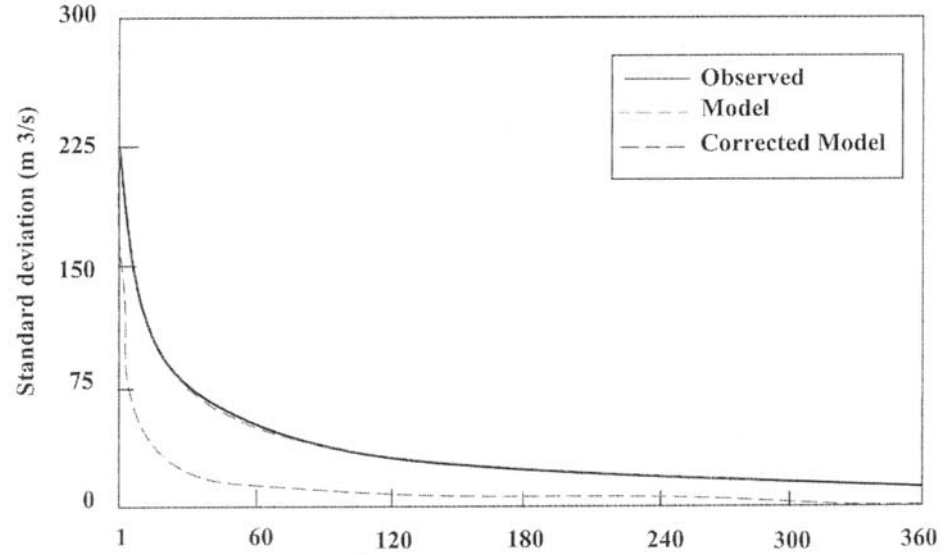


Fig. 2 Observed, model and corrected standard deviation by rank for Baral River at Malanchi railway crossing.

The more consistent the seasonality function, the higher would be the variance across all ranks that may be expected. The Baral River appeared to possess greater seasonal consistency in both the daily discharge and its variability, whereas the Dhrala, Punarbhaba and Teesta rivers were found to be the less consistent. Application of the following nonlinear regression correction (LeBoutillier & Waylen, 1993; Islam, 2000) may improve fit:

$$\hat{\sigma}^2_{(r)} = a(\sigma^2_{(r)})^b r^c \tag{3}$$

The correction contains a simple arithmetic scaling factor, *a* to inflate the variances and applies a proportional scaling by rank, *c*, and an inverse scaling for the model variances, *b*, such that the greater scaling is placed at higher ranks where the large sample approximations perform the poorest. Selection of the form of the nonlinear regression correction equation was made because of its intrinsic linearity, ease of estimation and its ability to reproduce the lack-of-fit characteristics of the variance model (LeBoutillier & Waylen, 1993). As shown in Fig. 2, the corrected model standard deviation by rank are superimposed on the observed and the model standard deviation for the Baral River and this was done for each river. Finally, the envelope of stochastic flow duration curves about ±1 standard deviation, corrected by nonlinear regression equation by rank, was generated and Fig. 3 shows one such curve for Baral River.

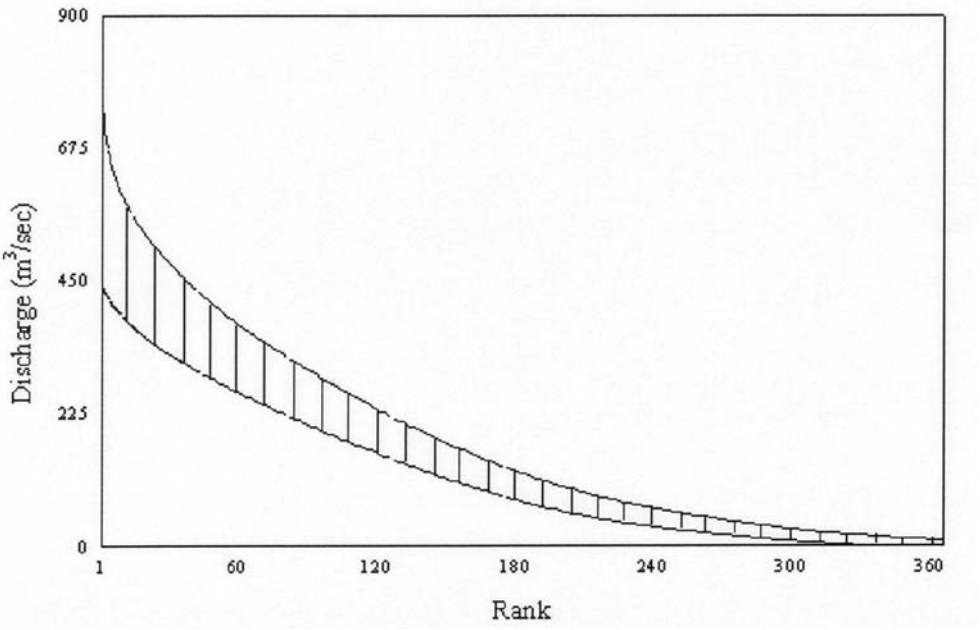


Fig. 3 Envelope of flow duration curves by ranks about ±1 standard deviation for the Baral River at Malanchi railway crossing.

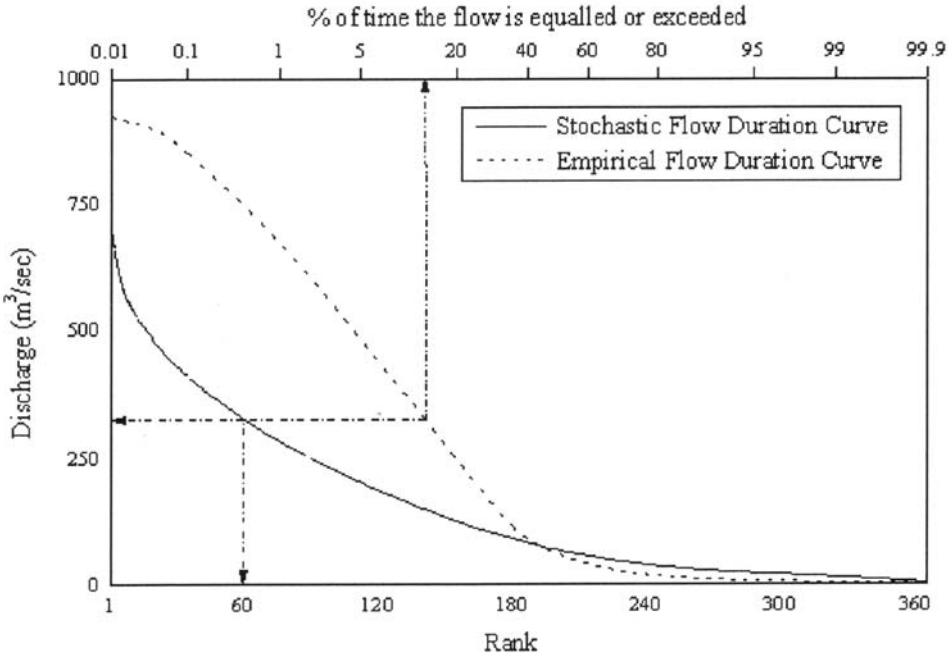


Fig. 4 Comparison of stochastic and empirical flow duration curve for Baral River at Malanchi railway crossing.

Comparison of stochastic and empirical flow duration curve

Empirical flow duration curves for each of four rivers at selected stations were calculated, using available daily discharge data, for comparison with respective stochastic flow duration curves. For this purpose, the available discharge record of each station was divided into equal class intervals and the exceedence probabilities for each class interval were calculated. The empirical flow duration curve for the Baral River is presented in Fig. 4 together with the stochastic flow duration curve. An inspection shows that the flow obtained from the stochastic flow duration curve for a given rank compares reasonably well with the value obtained from the empirical flow duration curve at the corresponding exceedence probability.

CONCLUSIONS

Identification of a parent distribution of daily discharges allows the estimation of rank means and variances for flow duration curves. The inclusion of the estimation of variances by rank adds information about the structure and reliability of the flow duration curve. Both mean and variance by rank may be derived using the form and parameters of the parent distribution instead of by calculating these from the ranked observations of the daily discharges. Performance on the variance can be improved through the use of nonlinear regression.

It can be concluded from this study that the mixture lognormal distribution can be used for deriving stochastic flow duration curves for the four selected rivers. The stochastic model, which is numerically based on large sample approximations of order statistics, duplicates the otherwise empirical construction technique of the calendar year flow duration curve. Moreover, the use of a mixed lognormal distribution permits the representation of a variety of flow regimes. It requires the estimation of parameters of the distribution for obtaining the 365 calculated means for construction of the stochastic flow duration curve. The basic modelling procedure may be used in any hydrological environment, and it can be expected that the parameters of the parent distribution will vary along physiographic and hydrometeorological variations which corresponds to climate and topography.

REFERENCES

Galambos, J. (1984) Order statistics. In: *Handbook of Statistics, Nonparametric Methods* (ed. by P. R. Krishnaiah & P. K. Sen), vol. 4, 359–382. Elsevier, New York, USA.

Gibbons, J. D. (1985) *Non Parametric Statistical Inference.* Marcel Decker, New York, USA.

Greenwood, J. A., Lendwher, J. M., Matalas, N. C. & Wallis, J. R. (1979) Probability weighted moments: definition and relation to parameters of several distributions expressible in inverse form. *Water Resour. Res.* **15**(5), 1049–1054.

Islam, K. M. H. (2000) A stochastic model of flow duration curves for selected rivers in northwestern Bangladesh. MSc Engineering Thesis, Department of Water Resources Engineering, Bangladesh University of Engineering and Technology, Dhaka, Bangladesh.

LeBoutillier, D. W. & Waylen, P. R. (1993) A stochastic model of flow duration curves. *Water Resour Res.* **29**(10), 3535–3541.

Climate Variability and Change—Hydrological Impacts (Proceedings of the Fifth FRIEND World Conference held at Havana, Cuba, November 2006), IAHS Publ. 308, 2006.

Regionalization of flow duration curves

IRINA KRASOVSKAIA[1], LARS GOTTSCHALK[1], ETIENNE LEBLOIS[2] & ALEXIA PACHECO[3]

1 *Department of Geosciences, University of Oslo, PO Box 1047 Blindern, N-0316 Oslo, Norway*
irina.gottschalk@geo.uio.no

2 *Cemagref, 3 bis quai Chauveau, CP 220, F-69336 Lyon Cedex 09, France*

3 *Instituto Costarricense de Electricidad, PO Box 10032-1000, San José, Costa Rica*

Abstract A method for estimating the flow duration curve (FDC) in an ungauged basin (i.e. regionalization of FDCs) is developed. An FDC can be described by the mean value and the coefficient of variation either in terms of empirically determined regional FDCs or as fitted theoretical regional curves. The development of these two first order moments of the FDC along the river network and with the spatial scale, i.e. the basin area, is analysed and a scheme for their interpolation along the river network is elaborated. Daily runoff data records from Costa Rica are used to demonstrate the findings. The estimation errors are highest in relative terms (~30%) for the durations longer than 85%, somewhat smaller for durations less than 20% (~10%) and small for central parts of the FDC (~8%). Differences between the empirical and theoretical curves are minor, although the latter give systematically better results especially in central parts of the FDC.

Key words flow duration curve; regionalization; Costa Rica

INTRODUCTION

The Flow Duration Curve (FDC) represents the relationship between the magnitude and frequency of daily, weekly, monthly (or other time interval) streamflow for a particular river basin, providing an estimate of the percentage of time a given streamflow was equalled or exceeded over a historical period (Vogel & Fennessey, 1994). Foster distinguished (1933) two uses of the FDC: (i) as a probability curve to determine the probability of occurrence of future events; and (ii) as a conventional tool to study the data. The FDC, however, gives a static and incomplete description of a dynamic phenomenon. For a complete description a multivariate distribution, which defines the parent distribution of the data, must be considered, the FDC being its marginal distribution. The FDC is a natural start when analysing streamflow data, as evident from its wide practical application (Vogel & Fenessey, 1995; Holmes *et al.*, 2002b).

Usually the FDC is founded on daily records (e.g. Holmes *et al.*, 2002b) although exceptions exist when monthly and 10-day data have been used (e.g. Singh *et al.*, 2001). Foster (1933) compared daily, monthly and annual FDCs noting that the differences between the curves for different duration (time scale) change with the type of river basin. He handled the problem by constructing a dimensionless flow duration curve (DFDC), dividing all observations by the mean annual flow and assuming that this curve is transferable to an ungauged site, although with caution.

The DFDC is often a starting point for the regionalization of FDCs, i.e. when predicting the FDC within ungauged basins. While some authors mainly concentrate on the properties of empirical FDCs (quantiles) and map these (e.g. Holmes *et al.*, 2002a) other studies assume a theoretical distribution (e.g. LeBoutillier & Waylen, 1993; Singh *et al.*, 2001). The lognormal, or the more general Box-Cox transformation, are those used most. For regionalization, two approaches are utilised, *viz.* the delineation of homogenous regions (e.g. by means of cluster analysis) and the use of multiple regression. A DFDC is selected for a homogeneous region, defined by, e.g. physical, climatic and streamflow characteristics of basins. Multiple regression is used to explain the geographic variation of each statistic of the FDC (quantiles, distribution parameters). Size of drainage area and the length of the main river course from the divide of the basin to the site of interest are most often used in regression equations. They implicitly indicate a spatial scale dependence of the FDC, an aspect that will be further developed herein.

In a given river basin with its river network the statistical characteristics are related through contextual rules (Gottschalk *et al.*, 2006). Such rules are commonly not defined in regional hydrology, where river basins are rather seen as independent not interacting objects. Neither multiple regression nor cluster analysis, widely used in hydrology for regionalization, considers

Copyright © 2006 IAHS Press

different parts of the basin as interacting objects. An approach for regionalization of FDCs presented here, acknowledges that statistical characteristics of runoff develop along the river system in a basin from the headwaters to the outlet. By this the regionalization problem is turned to interpolation of runoff characteristics along this network. The approach for regionalization of FDCs is tested on daily runoff data records from Costa Rica.

EMPIRICAL FLOW DURATION CURVES

Daily runoff series for 74 runoff stations in Costa Rica with record lengths over 40 years have been used. The deviations between the empirical FDC proved to be significant, which contradicts Foster's assumption about transferability. Thus it is necessary to go at least one step further considering not only the mean value (the first order moment) but also the second order moment.

The second order moment in terms of the coefficient of variation (*V*) shows a big variation with a range 0.5–2.2 for the analysed daily data. This can be considered by standardizing DFDC, i.e. a subtraction of 1.0 and division by *V*. These standardized FDC (SFDC) might then be used as "regional" duration curves (cf. Fig. 1). It is seen that the average curve (thick line) represents the series well for the majority of durations. Discrepancies shown by a few stations could be explained by specific geology and climate. Figure 2 shows the DFDC-quantiles as a function of the coefficient of variation, *V*. In general a strong dependence noted allows establishing linear regression relationships for all the quantiles used. The dependence on *V*, for example, is high at the duration level 50%, i.e. the median (*Me*), while at Q25% it is almost constant and independent of *V*.

These two ways of considering the role of *V* are quite similar: both assume a linear dependence on *V*, but in the first case the zero intercept is 1. In both cases there might be a risk that for very high values of *V* the linear relations cross the zero line for values with duration near 100%.

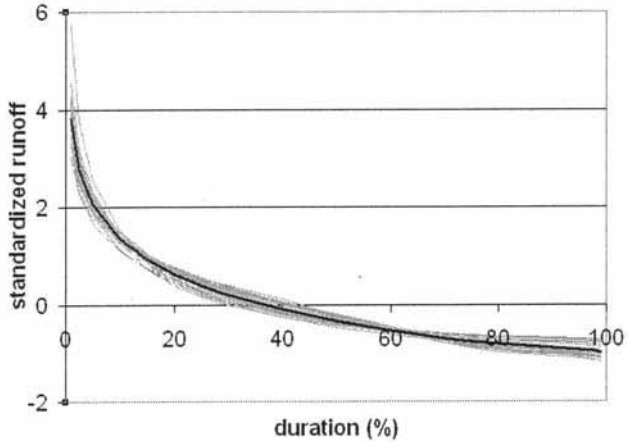


Fig. 1 Regional SFDC (thick line) for the rivers of the Caribbean slope of Costa Rica. DFDCs for individual rivers are given as a background.

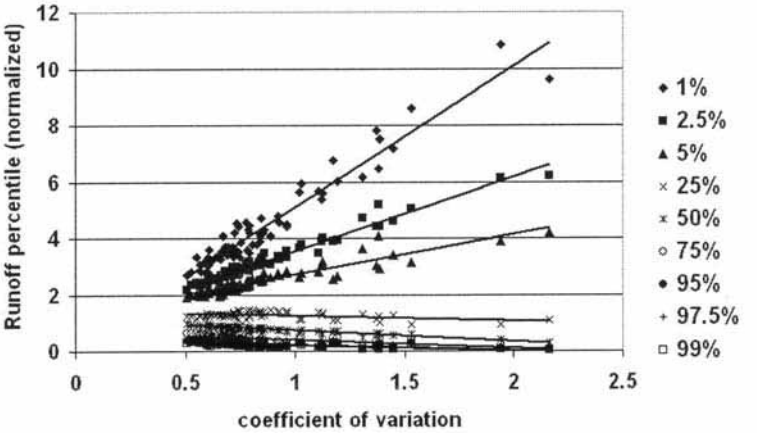


Fig. 2 Relationship between the coefficient of variation (*V*) and normalized runoff (daily values) for Costa Rica.

THEORETICAL FLOW DURATION CURVES

Following Foster (1933), an FDC is a plot of the empirical quantile function Q_p i.e. the pth quantile or percentile of streamflow for a certain duration versus exceedance probability p, where p is defined by:

$$p = 1 - P\{Q \le q\} = 1 - F_Q(q) \tag{1}$$

As noted earlier, many regionalization studies rely on the assumption of a theoretical distribution of FDC. The two most widely used distributions are the 2-parameter gamma and the lognormal. For normalized data both these distributions can be expressed in terms of the coefficient of variation only. For the lognormal we thus have:

$$F_Y(y) = \int_0^y \frac{1}{y\sqrt{2\pi \ln\left(1+V^2\right)}} \exp\left\{ -\frac{1}{2} \frac{\left(\ln y + \frac{1}{2}\ln\left(1+V^2\right)\right)^2}{\ln\left(1+V^2\right)} \right\} dy \tag{2}$$

The quantile y_p is determined from $y_p = m_Y + k_p \sigma_Y$ where k_p is the quantile (frequency factor) of the normal distribution. For normalized data (i.e. DFDC) quantile function is:

$$y_p = \exp\left(z_p \sqrt{\ln\left(1+V_Y^2\right)} - \left(\ln\left(1+V_Y^2\right)\right)/2 \right) \tag{3}$$

where z_p is the Gaussian variate of the probability p. For the special case of the median ($Me=y_{0.5}$) for which $z_{0.5}=0$ we find:

$$Me = y_{0.5} = \left(1+V_Y^2\right)^{-1/2} \tag{4}$$

The corresponding cdf of the two parameter gamma distribution for normalized data is:

$$F_X(x) = \int_0^x \frac{1}{V^{2V^{-2}}\Gamma\left(V^{-2}\right)} x^{V^{-2}-1} e^{-xV^{-2}} dx \tag{5}$$

The calculation of quantiles x_p must in this case be performed by numerical inversion of the cumulative distribution.

For both distributions the quantiles are thus functions of the coefficient of variation only, as illustrated in Fig 3. The diagrams look very similar in the linear scale with a small difference in the curvature for high values, the gamma having an almost linear growth of the 1% quantile. In a logarithmic scale the difference is more drastic: the gamma distribution declines very quickly towards zero, while the lognormal declines smoothly along concave curves for increasing values of the coefficient of variation.

There is a strong resemblance between the empirical plot in Fig. 2 and the theoretical curves in Fig. 3. For the high flow values (<Q25) the resemblance is highest with the gamma curves while for low flow values (>Q75) the similarity is strongest with the lognormal distribution.

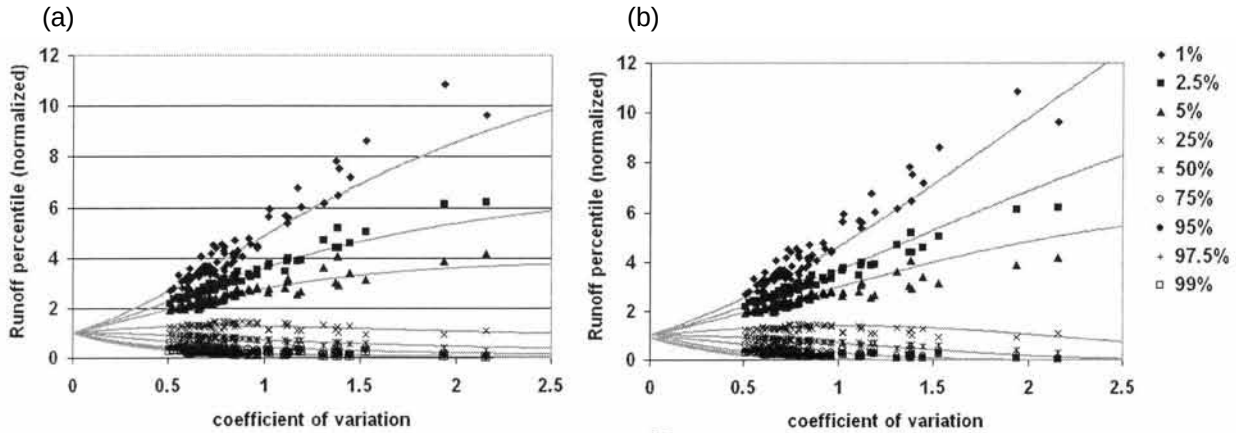


Fig. 3 Quantiles (grey lines) of the lognormal distribution (a) and the gamma distribution (b) as a function of the coefficient of variation.

REGIONALIZATION OF DURATION CURVES

The regionalization problem is here divided into two. The first step is the establishment of an empirical DFDC and/or the parameterization of the DFDC. The analyses referred to earlier indicate a possibility of describing the DFDC through two parameters, namely the long-term annual mean (*MAR*) and the coefficient of variation for daily data (*V*). The second step is to map *MAR* and *V* along rivers. The patterns of spatial variability of the mean and variance of runoff that can be identified from observations are influenced by the fact that observations represent averaged values over drainage basins. To map these quantities, the existence of an instantaneous point runoff (IPR) process is assumed, turning the task into the inverse problem of identifying this process from the observations representing averages in time and space. Then this IPR process is averaged along rivers yielding the desired map.

Mapping the *MAR* value is a rather straightforward task and is basically a problem of stochastic interpolation with local support (or in another vocabulary, block kriging) with a possibility of including a water balance constraint (Gottschalk, 1993b). In the case of Costa Rica, the values at the outlet of the rivers to the ocean are not known and therefore constraints on the water balance were not possible to apply. However, stochastic interpolation with local support is an appropriate method. A complexity in the structure of the covariance/semivariogram for runoff data, representing a mixture of nested and non-nested basins was handled according to the approach by Gottschalk (1993a). The resulting *MAR* map needs to be scrutinized carefully for errors and inconsistencies. Gomez *et al.* (2006) develop this topic further presenting the *MAR* map for Costa Rica.

The variability pattern of the variance identified from observations is still more complex than that for the mean. There are two sources of variability, *viz.* natural variability of the IPR process and variability induced by the variance reduction dependent on the support (i.e. the basin area). This latter part may constitute a significant part of the total variability and it also introduces a dependence on the basin area. The regionalization procedure herein is based on the developments by mainly Gottschalk *et al.* (2006). First, we benefit from the fact that the variation pattern of *MAR* is also reflected in the variance by introducing a new variable, namely the normalized instantaneous point runoff, i.e. IPR divided by the point mean. The covariance function between normalized values $Z(A_1)$ and $Z(A_2)$ over two (basin) averages with areas A_1 and A_2, respectively, is calculated from:

$$\mathrm{Cov}\left[\mathrm{Z}(\mathrm{A}_1)Z(A_2)\right] = \frac{1}{A_1 A_2}\int_{A_1}\int_{A_1}\sigma(\mathbf{u}')\sigma(\mathbf{u}'')\rho(\mathbf{u}',\mathbf{u}'')d\mathbf{u}'d\mathbf{u}'' \tag{6}$$

where $\rho(\mathbf{u}',\mathbf{u}'')$ is the point correlation function, $\sigma(\mathrm{u})$ the point standard deviation and with u' representing a point within the basin area A_1 and u'' within the basin area A_2. As we deal with normalized values $Z(A)$ the standard deviation equals the coefficient of variation of the original variable *V*. The variance is accordingly:

$$\mathrm{V}ar\left[Z(A)\right] = \frac{1}{A^2}\int_{A}\int_{A}\sigma(\mathbf{u}')\sigma(\mathbf{u}'')\rho(\mathbf{u}',\mathbf{u}'')d\mathbf{u}'d\mathbf{u}'' \tag{7}$$

Second, a power relation between *V* and *MAR* of the IPR process is established. Finally, the *MAR* map and the theoretical expression for variance reduction due to local averaging over the basin support (equation 7) is used to produce a map of *V*. The system HydroDem for structuring hydrographical networks (Leblois & Sauquet, 2000) has been used as a background for interpolation. The resulting *V* map (Fig. 4) is consistent with the statistical law for variance reduction and also considers the spatial variability through the dependence of *V* on *MAR*.

APPLICATION

Estimation of the FDC at an ungauged site starts with estimation of the coefficient of variation *V* for this site from the map Fig. 4. Using the dependences illustrated in Figs 2 and 3, either an

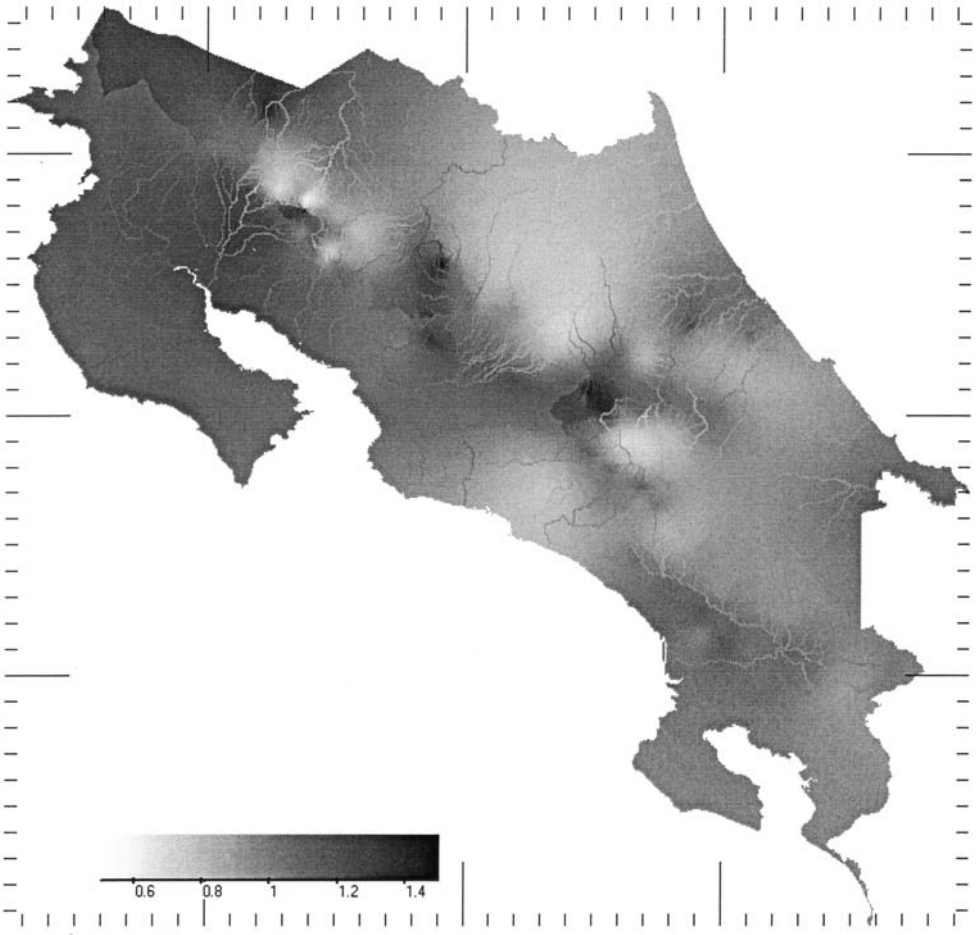


Fig. 4 Map of the coefficient of variation *V* of daily runoff for Costa Rica. The map shows basin integrated values along rivers.

empirical or a theoretical normalized FDC can be estimated. *MAR* is estimated from the corresponding map. Finally, multiplying the normalized FDC by the estimated *MAR* yields FDC at the ungauged site.

Table 1 offers some information about the results. The multiplication by MAR in m^3 or mm $year^{-1}$ yields high correlations between observed and estimated quantiles due to differences in the size of the river basins. Therefore the table shows the normalized values that are more informative with respect to the FDC. As the estimates of SFDC and the theoretical gamma both proved to be inferior, for briefness only estimates of the empirical regional FDC obtained by regression and the theoretical FDC based on the lognormal distribution are compared. The estimation errors are highest in relative terms (~30%) for the percentage points higher than 85%, somewhat smaller for percentage points less than 20% (~10%) and small for the central parts of the FDC (~8%). Differences between the empirical FDC and the lognormal FDC are minor, although the latter gives systematically better results especially in the central parts of the FDC.

Table 1 Estimates of regionalized FDC (normalized values).

Quantile parameter		Q05	Q10	Q25	Q50	Q75	Q90	Q95
Mean		2.53	1.94	1.27	0.77	0.44	0.31	0.28
Standard deviation		0.46	0.25	0.12	0.12	0.12	0.11	0.10
Regional Lognormal FDC	Correlation	0.84	0.59	0.53	0.87	0.68	0.63	0.61
	Abs.std.error	0.25	0.20	0.10	0.06	0.09	0.08	0.08
	Rel.std.error (%)	9.9	10.4	7.9	7.7	20.2	26.0	27.6
Regional emp.FDC, regression	Correlation	0.83	0.53	0.47	0.86	0.64	0.58	0.56
	Abs.std.error	0.26	0.21	0.10	0.06	0.09	0.09	0.08
	Rel.std.error (%)	10.2	10.9	8.4	7.8	21.3	27.3	28.8

CONCLUSIONS

Empirical regional FDC, as well as theoretical FDC based on the lognormal distribution applied here, are standard tools in the regionalization of FDC. A first contribution of this study is the use of not individual but a whole ensemble of FDCs in a basin/region, as shown in Figs 2 and 3. This illustrated that this regional FDC is well described through the two first order moments—the mean annual runoff (*MAR)* and the coefficient of variation (*V*) of daily runoff.

The second contribution of this study is the innovative approach for interpolation of the mean annual runoff (*MAR)* and the coefficient of variation (*V*) of daily runoff that were mapped for all major rivers of Costa Rica. This approach considers the fact that patterns of spatial variability of the mean and variance of runoff reflect observations representing averaged values over drainage basins and furthermore are subordinated through the hierarchical structure of the river network

REFERENCES

Foster, H. A. (1933) Duration curves. *Trans. ASCE* **99**, 1213–1267

Gómez, F., Krasovskaia, I., Gottschalk, L. & Leblois, E. (2006) Interpolation of water balance components for Costa Rica. In: *Climate Variability and Change—Hydrological Impacts* (Proc. Fifth FRIEND World Conf., Havana, Cuba, November 2006). IAHS Publ. 308. IAHS Press, Wallingford, UK (this volume).

Gottschalk, L., Krasovskaia, I., Leblois, E. & Sauquet, E. (2006) Mapping mean and variance of runoff in a river basin. *HESS Discuss*. **3**, 1–35.

Gottschalk, L. (1993a) Correlation and covariance of runoff. *Stochastic Hydrol. Hydraul.* **7**, 85–101.

Gottschalk, L. (1993b) Interpolation of runoff applying objective methods. *Stochastic Hydrol. Hydraul.* **7**, 269–281.

Holmes, M. G. R, Young, A. R., Gustard, A. & Grew, R. (2002a) A new approach to estimate mean flow in the UK. *Hydrol. Earth System Sci*. **6**(4), 709–720.

Holmes, M. G. R, Young, A. R., Gustard, A. & Grew, R. (2002b) A region of influence approach to predicting flow duration curves within ungauged catchments. *Hydrol. Earth System Sci* **6**(4), 721–731.

Leblois, E. & Sauquet, E. (2000) *Grid elevation Models in Hydrology*, Parts 1 & 2. Technical Notes, Cemagref, Lyon, France.

LeBoutellier, D. W. & Waylen, P. R. (1993) A stochastic model of flow duration curves. *Water Resour. Res.* **29**(10), 3535–3541.

Sauquet, E., Gottschalk, L. & Leblois, E. (2000) Mapping average annual runoff: a hierarchical approach applying a stochastic interpolation scheme. *Hydrol. Sci. J.* **45**(6), 799–815.

Singh, R. D., Mishra, S. K. & Chowdary, H. (2001) Regional flow-duration models for large number of ungauged Himalayan catchments for planning microhydro projects. *J. Hydrol. Eng.* **6**(4), 310–316.

Vogel, R. M. & Fenessey, N. M. (1994) Flow duration curves. I: New interpretation and confidence intervals. *J. Water Resour. Plan. Manage.* **120**(4), 485–504.

Vogel, R. M. & Fenessey, N. M. (1995) Flow duration curves. II: A review of application in water resources planning. *Water Resour. Bull.* **31**(6), 1029–1039.

Climate Variability and Change—Hydrological Impacts (Proceedings of the Fifth FRIEND World Conference held at Havana, Cuba, November 2006), IAHS Publ. 308, 2006.

Regionalization of low flow in Costa Rica

ALEXIA PACHECO[1], LARS GOTTSCHALK[2] & IRINA KRASOVSKAIA[2]

1 *C.S. Estudios Básicos de Ingeniería, Instituto Costarricense de Electricidad, PO Box 10032-1000, San José, Costa Rica*
apacheco@ice.go.cr

2 *Department of Geosciences, University of Oslo, PO Box 1047 Blindern, N-0316 Oslo, Norway*

Abstract The starting point of this study is the so-called derived distribution function approach for low flows. This approach is extended to apply to PUT (Pit Under Threshold) data from humid tropical conditions. A general theoretical distribution is derived that applies to exponentially distribute dry spells with a nonlinear low flow recession below a threshold level. Regionalization of PUTs is based on a fixed threshold level—the median, which is mapped for the whole country. The low flow data are normalized with respect to the median. The normalized sample distributions are grouped with respect to characteristic features (form of sample distribution, average length of dry spells and intensity of events) and a theoretical regional distribution is estimated for each grouped sample. The methodology has been applied to a set of low flow data from 63 gauging stations in Costa Rica. Important issues are the definition of the common threshold, the relation between dry spells defined from precipitation and runoff records, respectively, characteristic features for grouping of sample distributions as well as principles for parameter estimation of the regional curves of the grouped samples.

Key words regionalization; low flow; dry spells; Costa Rica

INTRODUCTION

The frequency analysis of low flow data in hydrology has by tradition not differed from such analysis of other types of hydrological data. The task has been to find any theoretical distribution function that best fits to a set of observed low flow data. The so-called derived distribution function approach for low flow (Gottschalk & Perzyna, 1989; Gottschalk *et al*., 1997) offers an alternative. In this case, the choice of theoretical distributions is limited to a family of distributions derived by combining the theory of extreme minimum values with, and basic understanding of, the generating hydrological processes of low flow. Two theoretical principles are exploited in the study of extremes, namely the block method (BM) (Annual Maximum, AMax; Annual Minimum, AMin) and the threshold method (TM) (Embrecht *et al*., 1999). For maxima, in hydrology the latter method is called "the Peak Over Threshold" (POT). Minimum values are treated less in the literature than maxima. Here the name "Pit Under Threshold" (PUT) is suggested for this type of hydrological data.

The family of derived distributions for low flow referred to earlier are based on the BM principle. Here this approach is extended to PUT data for humid tropics. A general theoretical distribution is derived that applies to exponentially distributed dry spells τ with a nonlinear low flow recession $q_c = f(q_0, \tau)$, where q_0 is a threshold level. The PUT method has the same advantage compared to the BM method for minimum, as the FPOT method has compared to the BM method for maxima, namely it guarantees that the selected events will always be extreme, provided the threshold is well defined. The parallels between PUTs and POTs can, however, not be brought too far, at least for application in hydrology. While maxima above a threshold might be well described as sudden outbursts above this threshold, minima below a threshold is produced by the emptying of a reservoir during a dry spell.

Regionalization of POT data is done by firstly normalizing the individual series by a so-called index flood (mean or median annual flood) and secondly joining all the normalized series into one sample and fitting a regional theoretical curve to this sample. The selection of the critical threshold is usually done individually for each series with the criteria of having equal intensity of events per year λ for all series (say λ = 2–3). Technically this may be an advantage, but at the same time fundamental information is lost about the process compared to the situation of using a common threshold and allowing λ to vary.

Regionalization of PUTs may be carried out in exactly the same manner as for POTs, viz. defining a normalizing "index low flow" and constructing a regional low flow curve. This approach has also been attempted here but yielded a poor result, as it was very difficult to find a

Copyright © 2006 IAHS Press

regional pattern in the variation index low flow. The alternative developed herein takes advantage of the fact that the derived theoretical distribution gives a direct indication of which processes influence the parameters. The following basic steps are followed:

– a fixed threshold level q_0 is used, determined from the flow duration curve and this threshold also defines the upper bound of the low flow distribution;
– the low flow data are normalized with respect to q_0;
– the normalized sample distributions are grouped with respect to characteristic features (form of sample distribution, average length of dry spells m_τ, intensity of events λ);
– a theoretical regional distribution is estimated for each grouped sample.

This methodology has been applied to a low flow data for 63 gauging stations in Costa Rica, with an average record length over 40 years. The variation patterns of the distribution of dry spells from a sample of 204 precipitation stations for the same observation periods have been jointly analysed. The presentation starts with the derivation of the theoretical PUT distribution. This distribution is then used as a tool to analyse the variation in the pattern of sample low flow distributions across Costa Rica. The key issues in the study are the definition of the common threshold, the relation between dry spells defined from precipitation and runoff records, respectively, characteristic features for grouping sample distributions, as well as principles for parameter estimation of the regional curves of the grouped samples.

A DERIVED DISTRIBUTION FOR LOW FLOW PUTS

A power law distribution for low flow appears when combining an exponential distribution $F_T(\tau) = 1 - \exp(\tau/m_T)$ for the length of dry spells τ with a simple exponential recession curve for low flow $q_c = q_0 \exp(-\tau/K)$ of the form:

$$F_Q(q) = (q/q_0)^{K/m_T} \; ; \; 0 \le q \le q_0 \tag{1}$$

This distribution will be accepted as a possible basic model for PUTs, although it is limited to the situation of a relatively quick decay towards zero. In situations with a recession with a long tail, i.e. rivers with a large contribution of deep groundwater during dry spells, a nonlinear recession might be more appropriate. The point of departure in this latter case is the discharge q from a non-linear storage S: $q = K^{-1}S^c$ where K and c are parameters. The outflow function in a decay situation (with no inflow) can in this case be calculated as: $q_t = q_0(1 + t/ba)^{-a}$ where $b = K^{\frac{1}{a}-1} q_o^{\,-1/a}$ and $a = c/(c - 1)$. The expression for a linear reservoir with an exponentially decaying recession $q_t = q_0 \exp(-t/K)$ is derived as a limiting form for $c \to 1$ and $a \to \infty$, respectively. Assuming an exponential distribution of the length of dry spells as above and introducing the inverse $t = b\,a\left((q_\tau/q_0)^{-1/a} - 1\right)$ in its expression results in the following theoretical distribution for PUT low flow values:

$$F_Q(q) = \exp\left(-\frac{ba}{m_T}\left((q/q_0)^{-1/a} - 1\right)\right); \; 0 \le q \le q_0; \, a < \infty \tag{2}$$

It is important to note that both equations (1) and (2) are truncated distributions. If the number of events observed over a time interval follows the Poisson distribution and the intensity of PUTs per time interval (year) is λ, the general expression for the distribution of annual minima (AMin) Ξ under a threshold is $F_\Xi(\xi) = \exp\{-\lambda F_Q(\xi)\}$. Insertion of $F_Q(q)$ in the latter expression leads to the distribution:

$$F_\Xi(\xi) = \nu^{-1}\left(1 - \exp\left\{-\lambda\left(\frac{\xi}{q_0}\right)^{K/m_T}\right\}\right); 0 \le \xi < q_0 \tag{3}$$

This distribution is identified as a truncated Weibull distribution for minima where

$\nu = \left(1 - \exp\{-\lambda\}\right)$ is the level of truncation. It was first introduced by Bernier (1964). It is important to note that the power in the parent distribution is brought forward in the extreme value distribution to determine the behaviour of the tail for the Weibull type of distributions for minima. For the nonlinear case we can proceed accordingly to derive an AMin-distribution:

$$F_{\Xi}(\xi) = \nu^{-1}\left(1 - \exp\left\{-\lambda \exp\left(-\frac{ba}{m_T}\left(\left(\xi/q_0\right)^{-1/a} - 1\right)\right)\right\}\right); 0 \le \xi < q_0 \quad (4)$$

The distribution equation (3) can be compared to the truncated Weibull AMin-distribution proposed by Gottschalk *et al*. (1997) for low flow with origin in Gumbel distributed maximum dry spells with parameters u and α and a linear recession with the recession coefficient K:

$$F_{\Xi}(\xi) = \nu^{-1}\left[1 - \exp\left\{-\left(\frac{\xi \exp(u/K)}{q_0}\right)^{K/\alpha}\right\}\right]; 0 \le \xi < q_0 \quad (5)$$

where $\nu = P\{Q > q_0\} = 1 - \exp(-\exp(u/\alpha))$, is the level of truncation. Both are truncated Weibull distribution with effectively two parameters but with different interpretations. The difference is in the fact that the latter one is directly formulated for AMin data.

APPLICATION—REGIONAL CURVES OF LOW FOR COSTA RICA

When applying the distribution derived in the previous paragraph with the aim of analysing the patterns of low flow formation across Costa Rica, the four steps indicated in the introduction were followed.

The choice of the threshold level is a very important issue for the selection of extremes. To be in accordance with the developed theory the threshold must be defined so that it not only allows identification of extreme low flow but also the sample of extreme dry spells (duration of recession). Dry spells were also identified from the rainfall records and for each drainage basin an average "rainfall dry spell" was estimated and compared with the dry spell from a corresponding runoff record. Furthermore the sensitivity of the statistical properties (mean and variance) of dry spells, low flow, and recession coefficients to the choice of the threshold level was analysed with a hope that they would stabilize at some level. This was not the case in general. The first criterion became decisive and indicated a rather high level of the duration curve, so the median $q50$ of the daily records was finally accepted as the proper threshold level for the study. The median was mapped for all Costa Rica in accordance with the methodology presented by Krasovskaia *et al*. (2006). The values develop along the river system and are consistent with the statistical laws for how the mean value and the variance change with the increasing support (basin area) when moving downstream.

PUTs for the dry period ("verano"—December to May) were extracted from each of the original daily records including low flow and length of dry spell (recession duration) in accordance with the illustration in Fig. 1. The low flow values were normalized with respect to the median of each daily record. The PUT normalized sample distributions for each station were plotted using the Gringorten plotting position in log–log diagrams. If data follow the theoretical distribution originating from a linear recession curve equation (1) they should plot as a straight line with maximum at zero ($\ln(q/q_0) = 0$ for $q/q_0 = 1$) with the slope (K/m_T). Figure 2 shows examples of sample distributions. It is seen that straight lines are exceptions. The rule is rather a nonlinear recession giving rise to a long tail of the distribution. This indicates a significant contribution of base flow. Even for very long dry spells the majority of rivers do not dry out but are fed by a considerable groundwater discharge. Only seven (Fig. 2, left shows one such station) of the total of 63 showed an approximately linear behaviour with a quick diminishing of low flow into the dry spell. All must be considered as outliers in otherwise quite regular behaviour. Besides these outliers, five record samples showed erroneous behaviour as seen in Fig. 2 (left) for three stations where 1 to 3 of the smallest observations are very close to zero.

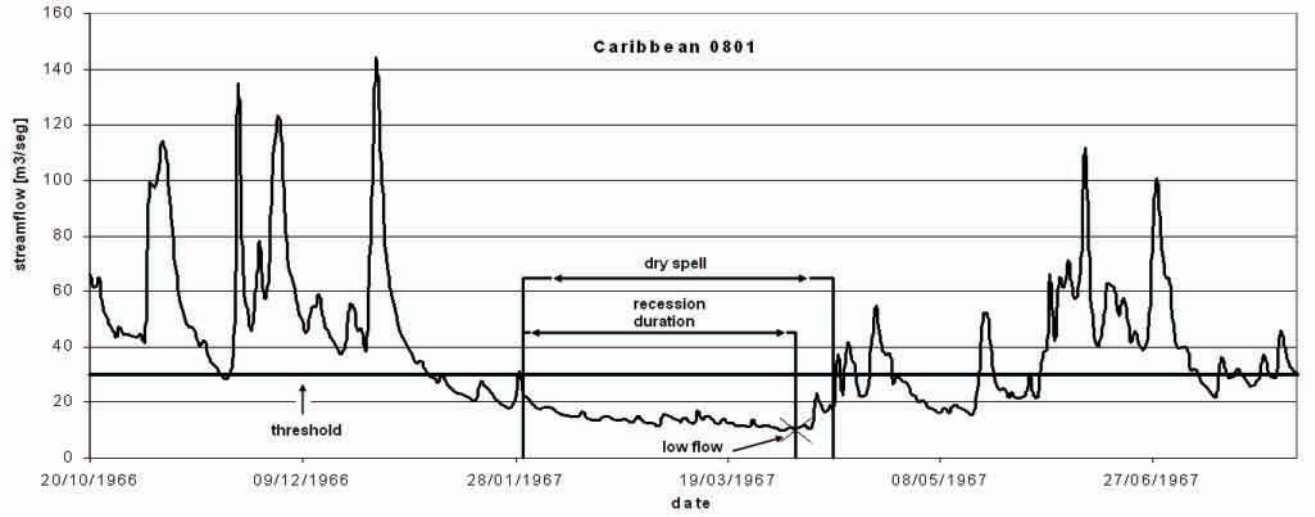


Fig. 1 PUT characteristics extracted from the daily flow record, example for a gauging station in the Pacuare River on the Caribbean slope.

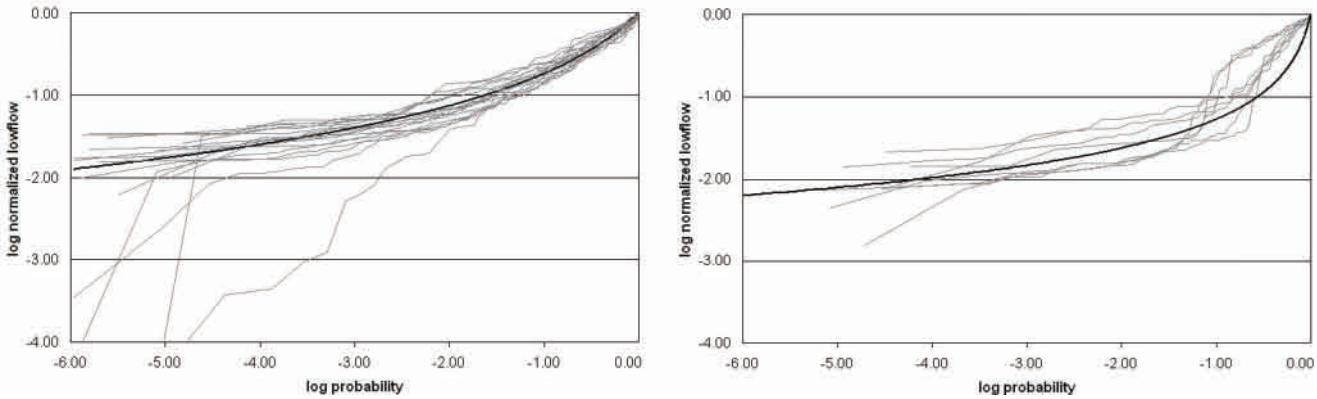


Fig. 2 Sample distributions of PUT low flow for the North Caribbean (left) and the Central Pacific (right). Estimated regional curves are shown by a bold line.

Table 1 Characteristics of regional low flow curves for Costa Rica.

Region	No. stations	No. events	λ	σ_λ	m_T	σ_T	a	$\frac{ba}{m_T}$
S. Caribbean	5	851	6.13	0.89	19.4	6.4	0.713	0.704
N. Caribbean	13	1950	5.51	0.89	26.7	6.5	0.855	0.850
Central Valley	13	1555	3.60	0.72	32.5	13.3	0.813	1.140
N. Pacific A	9	860	3.50	0.95	50.2	16.2	1.349	1.184
N. Pacific B	5	219	2.90	0.87	60.8	14.9	1.269	0.502
Central Pacific	8	529	2.44	0.47	67.3	12.8	0.542	0.195
S. Pacific	10	865	2.77	0.27	57.1	6.3	0.573	0.164
Total	63	6829						

The examples of sample distributions shown in Fig. 2 have already been grouped. Visual inspection of the form of the sample distributions allowed easy manual grouping of stations with similar forms. The statistics of λ and τ were also used as controls. Seven groups were identified in this manner and their characteristics are given in Table 1. The groups are coherent in geographical space and first of all reflect the different character of the dry seasons in Costa Rica, especially between the Caribbean and Pacific slopes. On the Caribbean side short rain episodes are frequent, also during the dry season. This gives rise to several low flow events and relatively short dry spells. The distribution of dry spells fits perfectly with the exponential distribution, which also

explains the very smoothly decaying form of the sample distributions shown in Fig. 2 (left) for the North Caribbean region. On the Pacific side, on the other hand, it is typical, with long dry spells up to several months. Figure 2 (right) shows sample distributions from the Central Pacific region with a very sharp bend indicating two populations of dry spells, the shorter ones being of minor interest.

There is a very clear tendency among the identified regions: starting with a high λ and a low m_T for the South Pacific region, then with a gradual decrease in λ and a corresponding increase in m_T when first going north along the Caribbean coast, turning west to the Pacific slope and finally south along the Pacific coast. The regions thus coincide with the climatic regions of Costa Rica. It should be noted that the outlying stations with a linear recessions do have the same dry spell characteristics as the region they are placed in. The, in general, very high baseflow component of runoff far into a dry spell gives evidence of a large contribution from groundwater flow for the majority of stations, while the outlying stations are exceptions in this respect with low baseflow. The outliers are mainly found in the South Caribbean and North Pacific regions, respectively. Consulting a hydrogeological map (SENARA, 2000) of Costa Rica these two regions are partly covered by hydrogeological formation classified as "without potential" while the rest of the country is classified as "high or moderate potential". The outlying behaviour is interpreted as an effect of the local hydrogeological conditions, but more detailed studies are necessary to confirm this. For the time being the regional curve must be used carefully with the awareness that local factors can have a significant influence.

In the introduction it was mentioned that the PUT (and POT) method guarantees that the selected events always will be extreme provided the threshold is well defined. The threshold used is quite high and this was motivated by the fact that the identified dry spells from runoff records should agree with corresponding dry spells identified from rainfall records. The population of low flow events identified thus includes a wide range of periods of runoff recession, all not really extremes. For the samples from the Caribbean slope the assumption of an exponential distribution of dry spells was very well satisfied. This also results with the fact that the whole population of events, also the not very extreme ones, agrees very well with the theoretical distribution. For the samples from the Pacific slopes this is not the case, especially for those from the Central and South Pacific regions. Here the assumption of exponentially distributed dry spells is not satisfied and it was already commented on the existence of two populations of dry spells, long and short. It is not possible to include both populations in one theoretical model. The problem is solved by using censored samples for parameter estimation for these two regions.

We note that the theoretical distribution equation (3) effectively contains two parameters: q_0, (K/m_T); and the distribution equation (4)–three: q_0, a, ba/m_T. The theoretical moments of the distributions in terms of these parameters have been derived but are not shown here. Expressions for the l-moments, on the other hand, still wait to be investigated. For the time being, we have chosen to apply a least square method to fit the theoretical curves to that of the sample distributions. The same method has been used to fit samples for individual stations and for the regionalized samples. For two regions (CPa and Spa) censored samples were used below an event probability of 0.368 (= exp(–1)), as has already been commented on. The regional parameter values are shown in Table 1.

It is important to note that the graphs in Fig. 2 show event probabilities and not annual probabilities. They thus do not illustrate the variation pattern of the frequency of low flow across Costa Rica, as the number of events for each regional sample is so different. As a final step, the regional curves can be transferred to annual frequencies by applying equation (4). Figure 3 illustrates the seven AMin regional curves confirming that the Northern Pacific is the driest region and that the rivers on the Caribbean slopes have relative high low flow also during the dry period. It is worth mentioning that attempts were made to perform a regionalization directly based on the AMin distribution equation (5) with less successful results.

CONCLUSIONS

Regionalization of low flow has been approached in an innovative way by a joint analysis of information about frequency of low flow and dry spells and the recession. The derived distribution

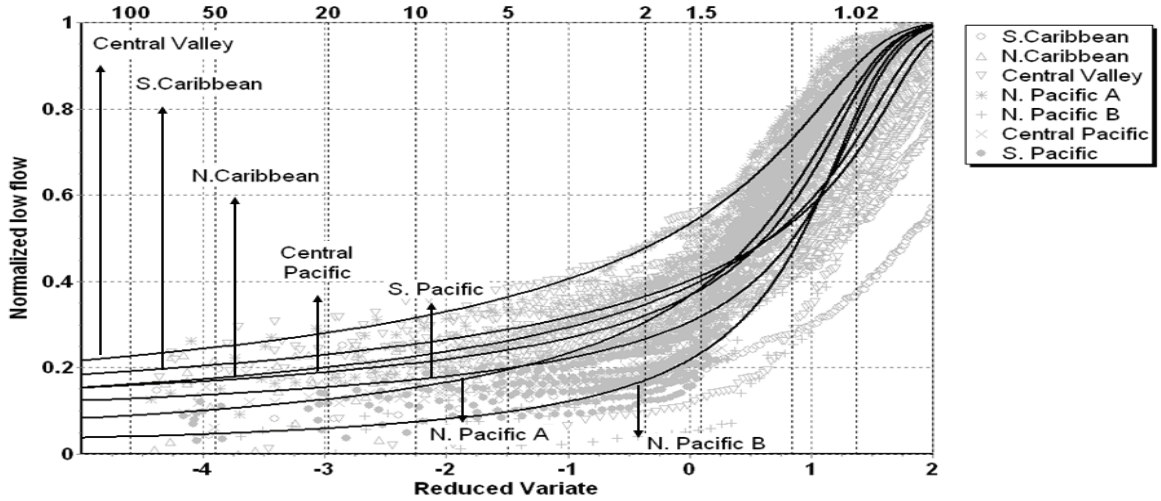


Fig. 3 Regional AMin curves for Costa Rica.

function approach used limits the choice of theoretical distributions to a family of distributions derived by combining the theory of extreme minimum values with a basic understanding of the generating hydrological processes of low flow. The derived theoretical distribution gives a direct indication of which processes influence the parameters.

Unlike many other studies on regionalization, a fixed threshold level determined from the flow duration curve was used, which offered a unique possibility to discern the differences in the processes behind the differences in frequencies of dry spells, called here "PUTs", i.e. "Pits Under Threshold". The median $q50$ was adopted as a threshold to be able to match dry spells identified from runoff data and rainfall.

It was possible to group the normalized sample distributions with respect to the form, the average length of dry spells m_τ, and the intensity of events λ. On the Caribbean side, frequent short rain episodes also during the dry season gave rise to many low flow events and relatively short dry spells, perfectly following the exponential distribution. On the Pacific side with several months-long dry spells, two populations of dry spells could be discerned. The obtained regional curves can be transferred to annual frequencies of low flow AMin.

The strength of the suggested approach is in its coherence with the theory of extreme events and possibility to discern the processes behind the occurrence of low flow extremes as well a possibility of consistent mapping of low flow values in a river basin.

REFERENCES

Embrechts, E., Klüppelberg, C. & Mikosch, T. (1999) *Modelling Extremal Events, For Insurance and Finance*, second edn. Springer Verlag, Germany.

Gottschalk, L. & Perzyna, G. (1989) A physically based distribution function for low flow. *Hydrol. Sci. J.* **34**, 559–573.

Gottschalk, L., Tallaksen, L. & Perzyna, G. (1997) Derivation of low flow distribution function using recession curves. *J. Hydrol.* **194**, 239–262.

Krasovskaia, I., Gottschalk, L, Leblois, E., Pacheco, A. (2006) Regionalization of flow duration curves. In: *Climate Variability and Change—Hydrological Impacts* (ed. by S. Demuth *et al.*) (Proc. Fifth FRIEND World Conference, Havana, Cuba, November 2006). IAHS Publ. 308. IAHS Press, Wallingford, UK (this volume).

SENARA (2000) *Hydrogeological Map of Costa Rica*. SENARA, Costa Rica.

Climate Variability and Change—Hydrological Impacts (Proceedings of the Fifth FRIEND World Conference held at Havana, Cuba, November 2006), IAHS Publ. 308, 2006.

Low flow estimation in Austria

GREGOR LAAHA[1] **& GÜNTER BLÖSCHL**[2]

1 *Institute of Applied Statistics and Computing, University of Natural Resources and Applied Life Sciences, BOKU Vienna, Gregor Mendel Str. 33, A-1180 Vienna, Austria*
gregor.laaha@boku.ac.at

2 *Institute for Hydraulic and Water Resources Engineering, Vienna University of Technology, Karlsplatz 13, A-1040 Vienna, Austria*

Abstract This paper gives an overview of river low flow processes and low flow estimation methods in Austria. Streamflow data from 325 sub-catchments in Austria, ranging in catchment area from 7 to 963 km^2, are used for the analyses. The performance of a number of regionalization methods for q95 low flows is assessed by leave-one-out cross-validation which emulates the case of ungauged catchments. A regional regression model based on a catchment grouping according to low flow seasonality performs best, but low flow estimates from short (one year) streamflow records outperform the best regionalization method when using an appropriate climate adjustment method. A q95 low flow map for all of Austria is compiled that combines local stream flow data with the regionalization estimates. It is argued that a combination of different sources of information—various types of regionalization models and streamflow records of various lengths—provides a wealth of information that should be exploited for low flow estimation.

Key words catchment grouping; cross validation; low flow; prediction at ungauged sites; PUB; regionalization; regional regression; seasonality

INTRODUCTION

Estimation of environmental flows generally requires long streamflow records that represent natural flow regimes. In a practical context, for instance when specifying minimum flows for hydropower operation or other water uses, estimates are usually required for sites where the natural river flow regime has been altered in recent years and/or no streamflow records are available. Regionalization techniques can be used to infer environmental flows from neighbouring, undisturbed catchments where streamflow data have been collected. These regionalization methods should take into account the main processes driving low flows as this will likely improve the estimates over purely statistical methods.

This paper gives a synopsis of several low flow studies in Austria which have been carried out in the general context of developing a national low flow regionalization procedure. Runoff data in a standard period, 1977–1996, from 325 sub-catchments in Austria ranging in catchment area from 7 to 963 km^2 are used. The low flow measure chosen is the q95 flow quantile (P[Q > q95] = 95%) which is used for numerous purposes in water resources management, including the specification of residual flows in water abstraction licenses. The analyses in this paper focus on specific low flows, q95 (L s^{-1} km^{-2}), i.e. q95 divided by the catchment area.

SEASONALITY OF LOW FLOWS

Summer and winter low flows are subject to important differences in the underlying hydrological processes. Thus one would expect that summer and winter low flows exhibit different spatial patterns caused by the variability of physical catchment properties and climate forcing. The seasonality of low flows was investigated by using the circular seasonality index (Laaha, 2002). The index consists of two parameters, the mean day of occurrence and the strength of seasonality. A vector map of the seasonality index is presented in Fig. 1. The clear patterns of low flow seasonality indicate that river low flows in the different parts of Austria are produced by vastly different processes. In the lowland east of Austria, river low flows mainly occur in the summer and are a result of evaporation exceeding precipitation, which depletes the soil moisture stores of the catchments. In the Alpine areas of the west of Austria, in contrast, river low flows mainly occur in the winter and are a result of snow storage and frost processes. The link between seasonality patterns and dominant processes suggests that regionalization of low flows should take seasonality patterns into account as they reflect the main processes driving low flows.

Copyright © 2006 IAHS Press

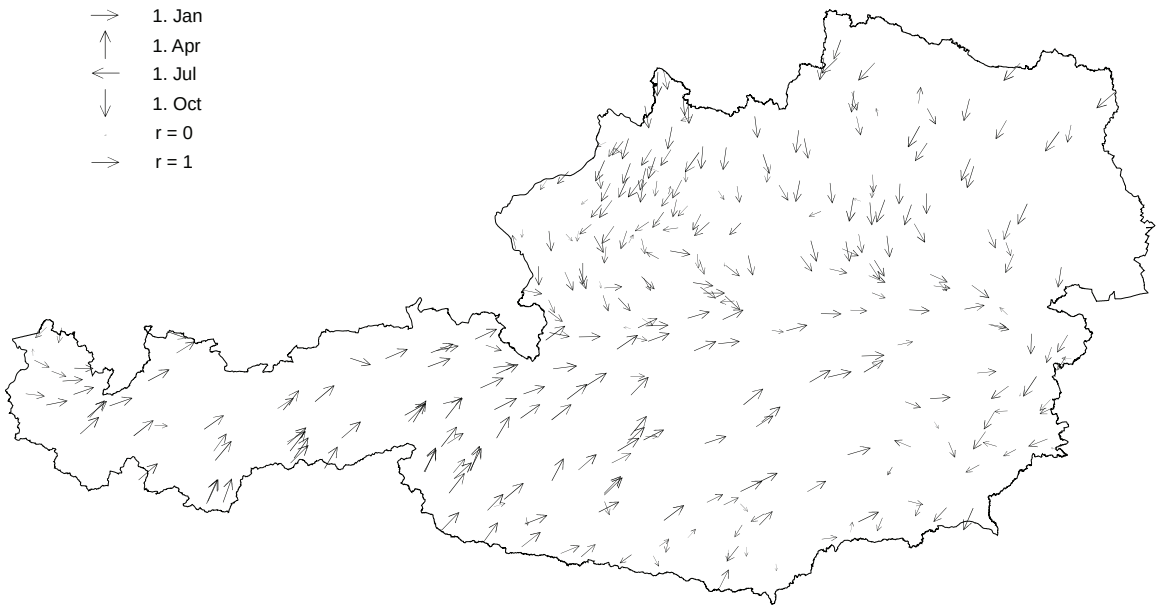


Fig. 1 Low flow seasonality index of 325 sub-catchments in Austria. Long arrows indicate strong seasonality and their direction represents the mean day of occurrence of specific low flow discharges less than q95.

REGIONALIZATION

To put the predictive power of the seasonality indices into context and to find the best grouping method for low flow regionalization, four catchment grouping methods were compared in terms of their performance in predicting specific low flows q95 for ungauged catchments (Laaha & Blöschl, 2006a). These grouping methods are the residual pattern approach (e.g. Hayes, 1992; Aschwanden & Kan, 1999), weighted cluster analysis (Nathan & McMahon, 1990), regression trees (Breiman *et al*., 1984; Laaha, 2002), and regions of similar low flow seasonality (Laaha & Blöschl, 2003). All of these methods use low flow data and most of them use catchment characteristics as well. For each group, a regression model between q95 and catchment characteristics, representing catchment topography, precipitation, geology, land cover and stream network density, has been fitted independently, using a stepwise regression approach. For the purpose of regionalization of low flows to ungauged sites, each site of interest needs to be allocated to one of the regions. For groupings that form contiguous regions, the ungauged site has been allocated by its geographical location. For groupings that are not contiguous in space, a classification tree fitted between group membership and catchment characteristics was used.

The performance of the methods was assessed by leave-one-out cross-validation of the regression estimates, which emulates the case of ungauged catchments. The allocation rules were integrated in the procedure, in order to give a full emulation of the prediction at ungauged sites. The results (Fig. 2) indicate that the grouping based on seasonality regions performs best. It explains 70% of the spatial variance of q95. The favourable performance of this grouping method is likely related to the striking differences in seasonal low flow processes in the study domain. Winter low flows are associated with the retention of solid precipitation in the seasonal snow pack while summer low flows are related to the relatively large moisture deficits in the lowland catchments during summer. The regression tree grouping performs second best (explained variance of 64%) and the performance of the residual pattern approach is similar (explained variance of 63%). The weighted cluster analysis only explains 59% of the spatial variance of q95 which is only a minor improvement over the global regression model, i.e. without using any grouping (explained variance of 57%).

An analysis of the sample characteristics of all methods suggests that, again, the grouping method based on the seasonality regions has the most favourable characteristics although all methods tend to underestimate specific low flow discharges in the very wet catchments. It appears that the seasonality characteristics as illustrated in Fig. 1 contain a lot of information highly relevant to low flow regionalization.

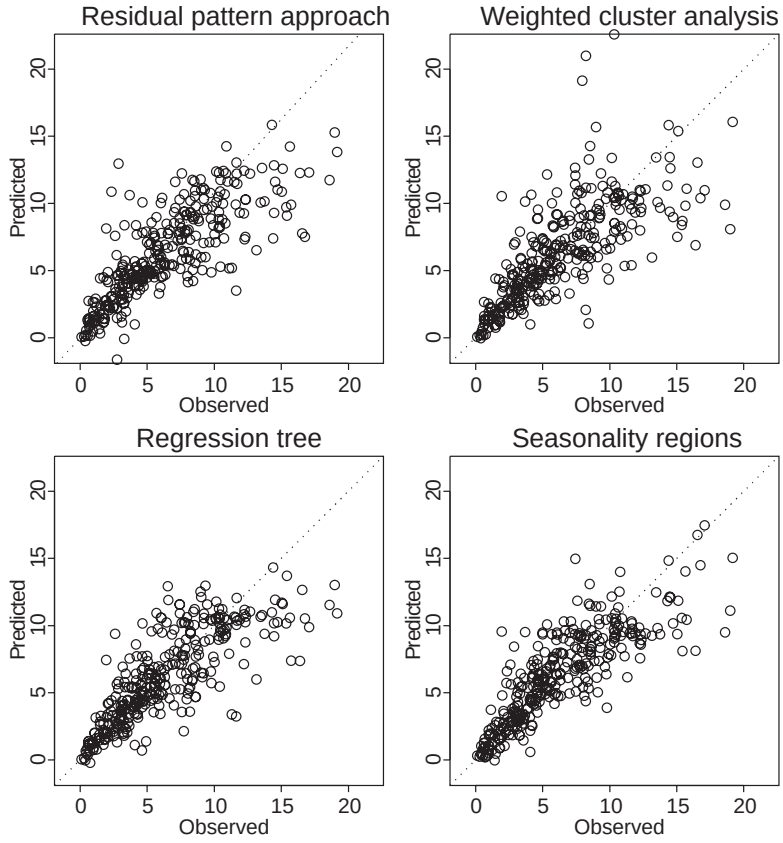


Fig. 2 Scatter plots of predicted *vs* observed specific low flow discharges q95 (L s^{-1} km^{-2}) for ungauged sites in the cross-validation mode. Each panel corresponds to one regional regression model and each point corresponds to one catchment.

SHORT RECORDS

Runoff data from the standard period are available in 325 catchments but short records and spot gaugings are available in a much larger number of catchments. It is, however, not obvious how they can be best used for low flow estimation. Due to climatic variability and other sources of variability that occur over short time scales, low flow characteristics estimated from a few years of streamflow data may deviate from the long-term average. Hence, some adjustment is necessary to make low flow estimates from short records consistent with low flow characteristics of the 20-year standard period. A number of methods of adjusting q95 specific low flow estimates from short streamflow records for climate variability were compared for the study area (Laaha & Blöschl, 2005). The climate adjustment methods consist of two steps, donor site selection and record augmentation using information from nearby sites with longer stream flow records. The accuracy of the methods is assessed here by comparing the adjusted estimates from hypothetically shortened records with estimates from the full 20-year record at the same site. The results (Fig. 3) indicate that the downstream donor selection method, which uses an adjacent gauge on the same river as donor, performs best on all scores. Alternative methods, which are based on catchment similarity and correlation of annual minimum flows, do not perform as well. The coefficient of determination of q95 specific low flows increases from 63 to 89% for one-year records, and from 86 to 93% for three-year records when adjusting the estimates by the downstream site method. For five years or more, the value of the climate adjustment methods is much lower, and low flow estimates from records longer than five years are less sensitive to the availability of suitable donors. A method that uses spot gaugings of streamflow during a low flow period only performs slightly better than a simple regionalization procedure in terms of predicting q95 at an otherwise ungauged site. Comparisons with more sophisticated regionalization procedures suggest that, on average over the study region, one year of continuous stream flow data clearly outperforms the more sophisticated regionalization method while the spot gauging method provides less accurate low flow estimates than the sophisticated regionalization method.

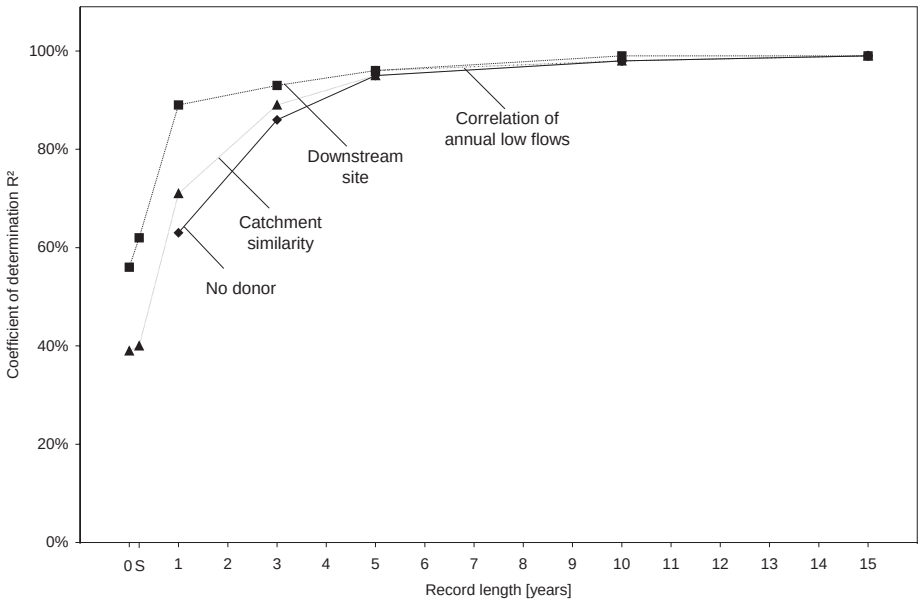


Fig. 3 Coefficient of determination R^2 (%) of specific low flow discharge q95 estimated from records of less than 20 years as compared to 20-year records. Various climate adjustment techniques are used. 0, no local streamflow data; S, spot gaugings.

LOW FLOW MAPPING

Estimates of low flows for all streams in Austria will be most accurate if regionalization methods and local information from both long- and short-record sites are combined. The mapping procedure for Austria combines these sources of information. As a starting point, the regional regression model is applied to small sub-areas of catchments. To this end, catchment characteristics of sub-areas need to be calculated, and each of them needs to be allocated to one region by geographic location or based on catchment characteristics. The regression model assigned to the region is then used to predict the specific low flow value.

Regression models are always associated with residual errors, so the observations will not be exactly reproduced by the predictions. To match the observed low flows, for consistency, the initial low flow estimates for river sub-basins are therefore calibrated to the observed low flows using water balance constraints for the low flow situation (Laaha & Blöschl, 2006b). Gauges with at least five years of continuous streamflow data are used for local calibration. The low flow characteristics calculated from the short records are adjusted for climatic variability using the downstream site method in order to make them compatible with low flow characteristics of the standard observation period.

Although the proposed mapping procedure makes maximum use of the available data, significant uncertainty due to the regional variability of low flow processes remains. This uncertainty can be quantified by error propagation methods. This is the subject of ongoing research that will be presented in the near future.

CONCLUSIONS

A seasonality analysis of low flows has been presented which suggests that river low flows in different parts of Austria are produced by vastly different processes. In the lowland east of Austria river low flows mainly occur in the summer and are a result of evaporation exceeding precipitation, which depletes the soil moisture stores of the catchments. In the Alpine areas of Austria, river low flows mainly occur in the winter and are a result of snow storage and frost processes. The relative accuracy of different approaches to catchment grouping for low flow regionalization has been examined by cross-validation. A regional regression model that is based on a catchment grouping according to the seasonality of low flows explains 70% of the total

variance of specific low flows and performs better than regional regressions based on alternative grouping techniques. The information from short streamflow records for estimating Q95 has been examined by an analysis of hypothetically shortened records to evaluate the performance of different climate adjustment methods. A method that uses the adjacent downstream gauge on the same river as the donor site performs best. One year of continuous streamflow data outperforms the best regionalization method, although estimates from less then five years of streamflow data are sensitive to the presence of an adequate donor site. A mapping procedure is proposed which combines regionalization estimates and low flow measurements. The initial estimates of the regional regression model are adjusted to observed specific low flows of the sub-catchment of all available gauges that exhibit at least five years of continuous streamflow records. It appears that a combination of different sources of information—various types of regionalization models and stream flow records of various lengths—provides a wealth of information that should be exploited for low flow estimation. The analyses of the regional low flow processes and the comparisons of the regionalization methods suggest that process understanding can indeed assist in regionalizing low flow characteristics to provide more accurate estimates than existing standard methods.

Acknowledgements Analyses are based on data provided by the Geological Survey of Austria, by the Austrian Federal Ministry of Agriculture, Forestry, Environment and Water Management, and by the Austrian Hydrographic Service.

REFERENCES

Aschwanden, H. & Kan, C. (1999) *Le débit d'étiage Q347—Etat de la question*. Communications hydrologiques 27. Service Hydrol. et Géol. National, Berne, Switzerland.

Breiman, L., Friedman, J. H., Olshen, R. & Stone, C. J. (1984) *Classification and Regression Trees*. Wadsworth International Group, Belmont, California, USA.

Hayes, D. C. (1992) Low flow characteristics of streams in Virginia. *US Geological Survey, Water Supply Paper 2374.*

Laaha, G. (2002) Modelling summer and winter droughts as a basis for estimating river low flows. In: *FRIEND 2002 - Regional Hydrology: Bridging the Gap between Research and Practice* (ed. by H. A. J. van Laanen & S. Demuth), 289–295. IAHS Publ. 274. IAHS press, Wallingford, UK.

Laaha, G. & Blöschl, G. (2003) Saisonalität von Niederwasserspenden in Österreich. *Mitteilungsblatt des Hydrographischen Dienstes in Österreich* **82**, 59–68. Bundesministerium für Land- und Forstwirtschaft, Wien, Austria.

Laaha, G. & Blöschl, G. (2005) Low flow estimates from short stream flow records—a comparison of methods. *J. Hydrol.* **306**, 264–286.

Laaha, G. & Blöschl, G. (2006a) A comparison of low flow regionalization methods—catchment grouping. *J. Hydrol.* **323**(1–4), 193–214.

Laaha, G. & Blöschl, G. (2006b) Niederwasserspende (Specific low flow). In: *Hydrologischer Atlas Österreichs*, Karte 5.8. Österreichischer Kunst- und Kulturverlag, Bundesministerium für Land- und Forstwirtschaft, Umwelt und Wasserwirtschaft (BMLFUW), Wien, Austria.

Nathan, R. J. & McMahon, T. A. (1990) Identification of homogeneous regions for the purpose of regionalization. *J. Hydrol.* **121**, 217–238.

Climate Variability and Change—Hydrological Impacts (Proceedings of the Fifth FRIEND World Conference held at Havana, Cuba, November 2006), IAHS Publ. 308, 2006.

Drought propagation through the hydrological cycle

HENNY A. J. VAN LANEN

Hydrology and Quantitative Water Management Group, Wageningen University, Nieuwe Kanaal 11, 6709 PA Wageningen, The Netherlands

henny.vanlanen@wur.nl

Abstract Time series of simulated recharge, groundwater heads and streamflow were obtained for temperate humid and semiarid climate regions and for quickly and slowly-responding catchments. These were analysed to investigate the propagation of drought through the subsurface, i.e. the change in characteristics (onset, duration and severity) from a meteorological drought to a hydrological drought. In two selected contrasting climate regions (Spain and The Netherlands) the propagation of recharge droughts generally leads to smaller hydrological droughts, except for severe recharge droughts, which might generate very severe hydrological droughts. In quickly-responding catchments more minor droughts will occur, whereas the probability of a very severe drought is higher in slowly-responding catchments. It is anticipated that quantitative knowledge on drought propagation will advance if recharge droughts derived from real instead of synthetic recharge can be better defined, i.e. by use of recharge anomalies.

Key words drought; propagation; subsurface; modelling; threshold approach; humid temperate; semiarid

INTRODUCTION

Drought is a sustained and regionally extensive occurrence of below average natural water availability, and can thus be characterized as a deviation from normal conditions (Tallaksen & van Lanen, 2004). It occurs in all hydroclimatological regions, although frequency and severity vary. A drought starts with a lack of precipitation over a large area and for an extensive period of time (meteorological drought). This water deficit propagates through the subsurface part of the hydrological cycle and gives rise to different types of droughts (Wilhite, 2000). The low precipitation might cause a soil moisture drought to develop. Subsequently, groundwater recharge will be reduced and a hydrological drought (low groundwater heads, groundwater discharge and streamflow) may start.

It is well-known that not all meteorological droughts develop in a hydrological drought and conversely a series of minor meteorological droughts can turn into a severe hydrological drought. Although it is obvious that the characteristics of droughts (e.g. onset, duration) change on its way through the subsurface, it is hard to show the propagation of droughts in reality, i.e. to derive it from simultaneous time series of observed precipitation, soil moisture, groundwater levels and streamflow (Peters, 2003). As a first, explorative step, often simplified hydrological models with generalized input (synthetic recharge: sinusoid function) have been developed to study the propagation of drought. Based upon this very simplified input, it was demonstrated that catchment characteristics, especially the stores (e.g. soil moisture, aquifer storage, glaciers, bogs) determine if and to what extent a meteorological drought turns into a hydrological drought. So far, however, understanding of the propagation of a drought through the subsurface and the role of catchment characteristics is rather limited (e.g. Calow *et al.*, 1999; Peters *et al.*, 2003). Nevertheless, thorough understanding of drought propagation is urgently required for adequate long-term drought forecasting.

This paper explores the propagation of a meteorological drought through the subsurface part of the hydrological cycle. The effect of different catchment characteristics on the propagation is illustrated for contrasting climates.

APPROACH

Different type of droughts was derived from long time series of hydrometeorological variables (e.g. precipitation, soil moisture, groundwater heads, streamflow). Usually not all these data have been monitored over long periods of time. In this study different hydrological models (simple to comprehensive) were applied to generate time series of non-monitored data for temperate humid and semiarid climatic regions, i.e. The Netherlands and Spain. Next the threshold method was used to identify droughts.

Copyright © 2006 IAHS Press

Catchments

Data from the Poelsbeek and the Bolscherbeek catchments in the eastern part of The Netherlands (e.g. Tallaksen & van Lanen, 2004) and the Noor catchment (van Lanen & Dijksma, 1999; van Lanen & Dijksma, 2004) on the Dutch–Belgian border were used to characterize catchments with a temperate humid climate. Additionally data were obtained from a catchment in south-central Spain (Upper-Guadiana) with a semiarid climate (Peters, 2003). The average precipitation in the humid temperate catchments varies from 748 to 775 mm year^{-1} and the average potential evapotranspiration is about 450 mm year^{-1}. In the Upper-Guadiana the average precipitation varies from 350 mm year^{-1} in the central part to 580 mm year^{-1} at higher elevations. The potential evapotranspiration is about 960 mm year^{-1}. In the Upper-Guadiana the inter-annual variability in precipitation is higher than in the temperate humid catchments. Time series of precipitation and potential evaporation were used to calculate groundwater recharge with soil water balance models.

Simple hydrological model

Linear reservoir theory (Tallaksen & van Lanen, 2004) has been applied to calculate time series of groundwater discharge for hypothetical catchments with a temperate humid climate (i.e. Noor catchment) or a semiarid climate (Upper-Guadiana catchment). The following equation was used:

$$q_{gr,t} = q_{gr,t-1} \exp(\frac{-m_t}{j}) + \frac{I_t}{m_t}(1 - \exp(\frac{-m_t}{j})) \quad (1)$$

where $q_{gr,t}$ is groundwater discharge at month t [L T^{-1}], $q_{gr,t-1}$ is groundwater discharge at month $t-1$ [L T^{-1}], m_t is number of days in month t [–], I_t is groundwater recharge at month t [L T^{-1}] and j is reservoir coefficient [T].

The characteristics of the catchment are represented by the reservoir coefficient j (day):

$$j = \frac{S_y L^2}{\pi^2 kD} \quad (2)$$

where L is the distance between streams [L], kD is the aquifer transmissivity [L^2 T^{-1}] and S_y is the storage coefficient [–].

The groundwater discharge is not specifically calculated for the Upper-Guadiana or Noor catchments, but for a range of hypothetical groundwater catchments with a range of reservoir coefficients. Thus, the hypothetical groundwater catchments have either the recharge of the temperate, humid climate (Noor) as input or the recharge of the semiarid climate (Upper-Guadiana). A catchment with a small j represents a quickly-responding groundwater system, whereas a catchment with a large j has the opposite response (Peters, 2003; Peters *et al.*, 2003; Tallaksen & van Lanen, 2004).

Comprehensive hydrological model: SIMGRO

SIMGRO is a spatially-distributed physically-based model that simulates regional transient saturated groundwater flow, unsaturated flow, actual evapotranspiration, sprinkler irrigation, streamflow, hydraulic heads and surface water levels as a response to, for example, rainfall, reference evapotranspiration, and groundwater abstraction (Querner, 1997). SIMGRO has been applied to the Poelsbeek and Bolscherbeek catchments to obtain daily time series over the years 1951–1999 (Tallaksen & van Lanen, 2004). The model allows input of spatially-variable catchment properties (e.g. land use, soil type, transmissivity, stream network). SIMGRO simulates for each node and day the actual evapotranspiration, recharge, $I(x,y,t)$, the groundwater hydraulic head, $H(x,y,t)$, and soil moisture storages in the root zone and in the unsaturated subsoil. Additionally, SIMGRO simulates transient streamflow in the longitudinal profile as a response to drainage of the aquifer by ditches and streams, overland flow and water from a sewage treatment plant.

Threshold level approach: NIZOWKA

Drought characteristics (i.e. onset, duration, severity) have been derived from the simulated time series by using the software package NIZOWKA (Tallaksen & van Lanen, 2004). The software is

based upon the threshold level approach (Yevjevich, 1967). Time series of daily recharge, groundwater hydraulic heads and streamflow were used in the Poelsbeek and Bolscherbeek catchments with threshold levels of I_{90}, Q_{90} and H_{90} (recharge, streamflow or head that is equalled or exceeded in 90% of the time). The threshold levels apply to the whole year and not to a specific period (e.g. a day or a month). For the recharge a moving average of 30 days was applied to reduce the peaky nature. In the Upper-Guadiana and Noor catchments time series of monthly recharge and groundwater discharge were used with I_{70} and Q_{70} as threshold levels, which hold for the whole year. The monthly recharge was first aggregated to annual values, because otherwise droughts would have occurred in almost all dry seasons.

RESULTS

First, the propagation of droughts was analyzed in detail by using simulated data with SIMGRO for a catchment with in a humid temperate climate (Poelsbeek and Bolscherbeek catchments; Verwij, 2005). Table 1 gives some drought characteristics for the three major droughts in the second part of the twentieth century. Obviously, droughts in recharge start first. Droughts in the groundwater heads and streamflow are observed later, 10–61 and 10–38 days, respectively. In this catchment, streamflow usually responds earlier than the groundwater head (except 1996). Verwij (2005) illustrates that, of course, the onset and duration depend on the selected threshold level. The duration of all three major droughts is substantially smaller for the recharge drought than for the hydrological droughts (heads and streamflow). The 1996 drought clearly reflects this. A minor drought in the recharge has been observed, whereas droughts over 100 days occur in the groundwater heads and the streamflow. This clearly reflects the antecedent conditions, i.e. low aquifer storage at the start of 1996 due to dry conditions before.

The detailed study above shows that propagation of droughts is complex and dependent on catchment characteristics and a specific year. Subsequently, a more simple approach was adopted using soil water balance models to compute groundwater recharge and linear reservoir models to simulate groundwater discharge to explore the propagation in a more general way. Compared to Peters *et al.* (2003) the simplified approach in this study uses more realistic estimates for the recharge for two contrasting climate regions, i.e. Noor and Upper-Guadiana catchments.

Table 1 Onset and duration of the different types of drought for three major droughts in the Poelsbeek and Bolscherbeek catchments.

Year	Drought in	Onset	Duration (days)
1959	recharge	1 May	62
	groundwater heads	1 July	174
	streamflow	8 June	154
1976	recharge	10 April	50
	groundwater heads	30 May	189
	streamflow	15 May	162
1996	recharge	27 April	5
	groundwater heads	7 May	181
	streamflow[(1)]	7 May	19
	streamflow	2 June	123

[(1)] Two separate droughts occurred in the streamflow.

The maximum annual recharge in temperate humid climate (Noor catchment, 1945–2001) and the semiarid climate (Upper-Guadiana catchment, 1940–1996) was 481 and 192 mm year^{-1}. In 30% of the years the recharge is smaller than 202 and 19 mm year^{-1}, respectively. Figure 1 gives a flow duration curve of the simulated monthly groundwater discharge using the simple hydrological model. Clearly the discharge is high for the temperate humid climate and the discharge varies more for the quickly-responding catchment (j = 100 day). In extremely dry years the stream runs dry in flashy catchments, irrespective of the climate region.

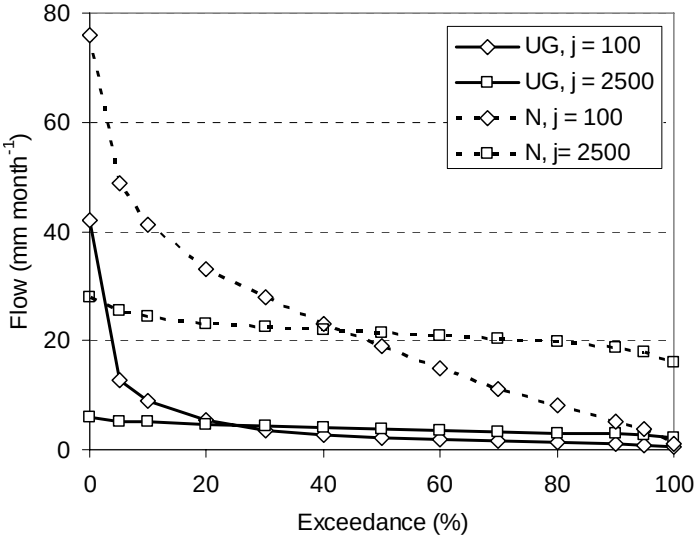


Fig. 1 Flow duration curves for quickly (j = 100 days) and slowly (j = 2500 days) responding catchments with a semiarid (UG) and a temperate humid climate (N).

The drought duration (month) and the severity, which is expressed as deficit (in mm water depth), are plotted in Fig. 2 for the two contrasting climate regions and quickly and slowly responding catchments. Six multiple-year droughts in the recharge came about in the semiarid climate region (Upper-Guadiana, Fig. 2(a)), whereas not more than four of such droughts occurred in the temperate humid climate (Noor, Fig. 2(c)). Note that the number of recharge droughts is affected by the chosen time resolution (aggregation of monthly recharge to annual values). The duration and severity graphs show that in both climate regions the quickly-responding catchments have a larger number of discharge droughts than the slowly responding ones. For instance, in the semiarid region, 42 discharge droughts were identified in the quickly-responding catchment (Fig. 2(a)), whereas in the slowly-responding catchment the number equals 13 events (Fig. 2(b)). In general the (minor) discharge droughts last longer and are more severe in the quickly-responding catchments as opposed to slowly-responding catchments (Fig. 2, compare left and right columns). A rather small number of very severe discharge droughts would have occurred in the second part of the 20th century. In the semiarid climate one such drought would have been happened in the quickly-responding catchment (early 1990s, Fig. 2(a) and 2(e)) and two in slowly-responding (early 1950s and early 1990s, Fig. 2(b) and 2(f)). In the temperate humid climate no very severe drought would have taken place in the quickly-responding catchment (Fig. 2(c) and 2(g)) and one in the slowly-responding catchment (1950s, Fig. 2(d) and 2(h)).

The graphs for the quickly-responding catchment (Fig. 2, left column) show that substantial droughts in the recharge do not lead to severe discharge droughts, except for the early 1990s drought in the semiarid climate. This effect, i.e. decrease of duration and severity of droughts through subsurface processes, is even stronger in the slowly-responding catchments (Fig. 2, right column). The discharge droughts in the quickly-responding catchments are hard to link to the recharge droughts (propagation) probably due to the aggregation of monthly recharge to annual values. The graphs for the slowly-responding catchments suggest that there might be a better link between the severity of the recharge and discharge droughts (Fig. 2(f) and 2(h)) than with the duration (Fig. 2(b) and 2(d)).

CONCLUSIONS AND DISCUSSION

The analysis shows that there is more clustering of droughts in the recharge in dryer climate regions (higher persistence). Both the complex and the more simple hydrological modelling approach demonstrate that in contrasting climate regions the propagation of recharge droughts through the subsurface generally leads to smaller hydrological droughts (less severe in terms of deficit). However, severe droughts in the recharge (long duration and/or high deficit) may result in

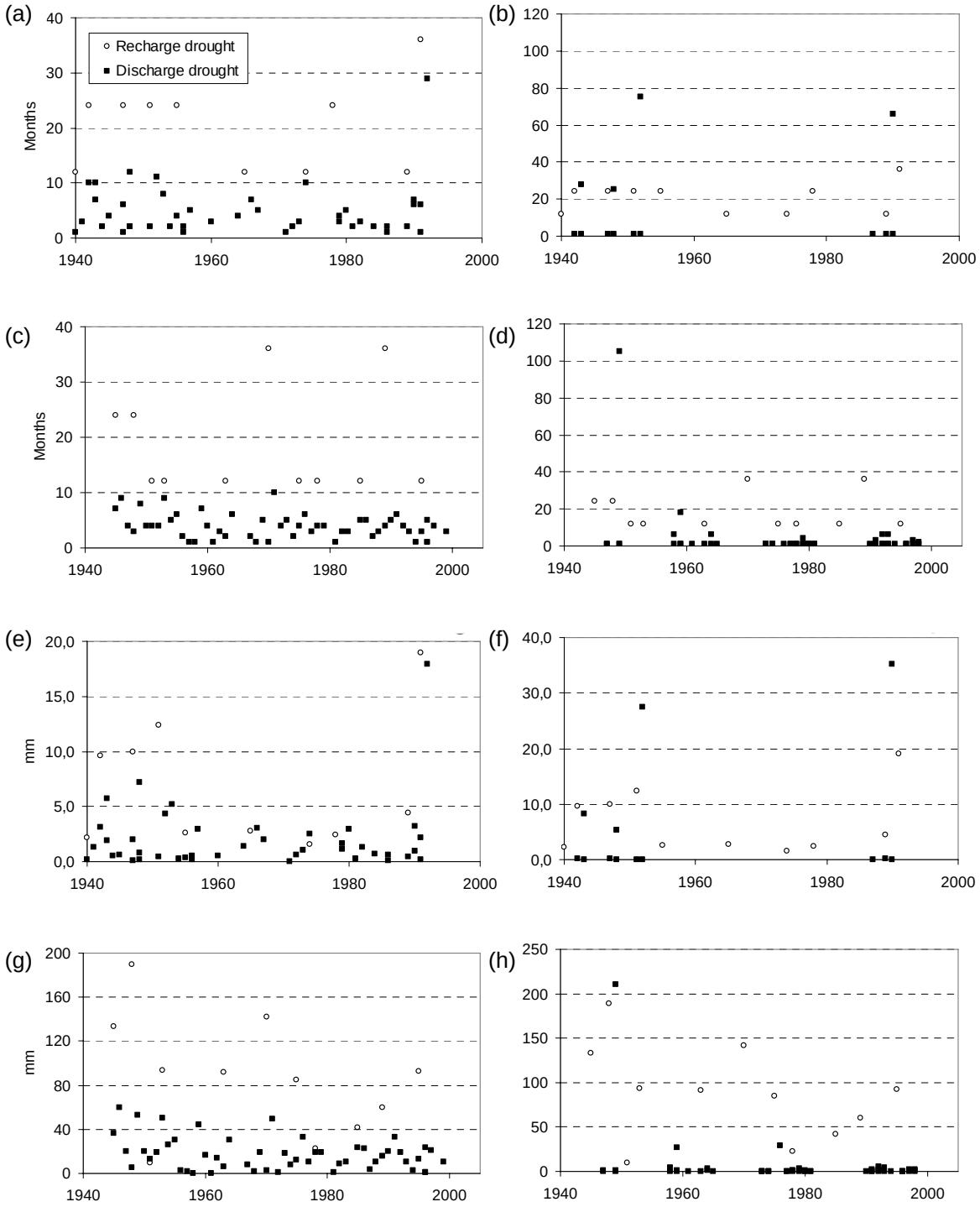


Fig. 2 Duration (month) and severity (deficit in mm) of drought in the recharge and the discharge for different catchment characteristics for a semiarid climate region (UG) and a temperate humid climate region (N): (a) duration, UG and j = 100, (b) duration, UG and j = 2500, (c) duration, N and j = 100, (d) duration, N and j = 2500, (e) deficit, UG and j = 100, (f) deficit, UG and j = 2500, (g) deficit, N and j = 100, (h) deficit, N and j = 2500. In case of multiple year droughts the duration and deficit are plotted at the onset year.

very severe hydrological droughts. Catchment characteristics, such as storage properties (soils, aquifers), aquifer transmissivity and river network determine the propagation of a drought in the subsurface. In quickly-responding catchments more minor droughts will occur, whereas the probability on a very severe drought is higher in slowly-responding catchments.

Peters *et al.* (2003) give quantitative relationships for the propagation of droughts in the subsurface using synthetic recharge as input. The current study shows that it is still hard to give

these relationships if more realistic recharge estimates are used. Clearly, a higher time resolution is required to define recharge droughts, especially for the quickly-responding catchments. However, it should be avoided to have a recharge drought every summer due to seasonality because by definition a drought cannot occur every summer. The use of threshold levels for the recharge for specific periods (varying thresholds, e.g. per month) instead of for the whole year to define recharge anomalies might help to advance understanding of propagation of droughts through the subsurface.

Acknowledgements The research was carried out under the programme of the Wageningen Institute for Environment and Climate Research (WIMEK-SENSE) and contributed to the FRIEND project (UNESCO-IHP-VI). The author thanks the members of the Low Flow Group of the FRIEND (Northwest Europe) for the valuable discussions and contributions, especially Dr Wojciech Jakubowski (Agricultural University, Wroclaw, Poland) for developing the NIZOWKA software. This research was partly supported by the ASTHyDA project, EC Energy, Environment and Sustainable Development programme, contract EVK1-2001-00166.

REFERENCES

Calow, R., Robins, N., MacDonald, A. & Nicol, A. (1999) Planning for groundwater drought in Africa. In: Proc. Int. Conf. on *Integrated Drought Management: Lessons for Sub-Saharan Africa*. UNESCO Technical Documents in Hydrology, no. 35, 255–270.

Lanen, H. A. J. van & Dijksma, R. (1999) Water flow and nitrate transport to a groundwater-fed stream in the Belgian–Dutch chalk region. *Hydrol. Processes* **13**, 295–307.

Lanen, H. A. J. van & Dijksma, R. (2004) Impact of groundwater on surface water quality: role of the riparian area in nitrate transformation in a slowly responding chalk catchment (Noor, The Netherlands). *Ecohydrology and Hydrobiology* **4**(3), 315–325.

Peters, E. (2003) Propagation of drought through groundwater systems – illustrated in the Pang (UK) and Upper-Guadiana (ES) catchments. PhD Thesis, Wageningen University, The Netherlands.

Peters, E., Torfs, P. J. J. F., Lanen, H. A. J. van & Bier, G. (2003) Propagation of drought through groundwater – a new approach using linear reservoir theory. *Hydrol. Processes* **17**(15), 3023–3040.

Querner, E. P. (1997) Description and application of the combined surface and groundwater model MOGROW. *J. Hydrol.* **192**, 158–188.

Tallaksen, L. M. & van Lanen, H. A. J. (eds) (2004) *Hydrological Drought. Processes and Estimation Methods for Streamflow and Groundwater*. Developments in Water Science, 48, Elsevier Science BV, The Nethlerlands.

Verwij, L. (2005) Drought definitions for groundwater recharge, groundwater depth and streamflow: Poelsbeek and Bolscherbeek catchments (The Netherlands). MSc Thesis, Wageningen University, The Netherlands.

Wilhite, D. A. (ed.) (2000) *Drought, A Global Assessment*, vols I & II. Routledge Hazards and Disasters Series, Routledge, London, UK.

Yevjevich, V. (1967) An objective approach to definition and investigation of continental hydrologic droughts. *Hydrology Paper 23. Colarado State University, Fort Collins, USA.*

Climate Variability and Change—Hydrological Impacts (Proceedings of the Fifth FRIEND World Conference held at Havana, Cuba, November 2006), IAHS Publ. 308, 2006.

Propagation of drought in a groundwater fed catchment, the Pang in the UK

LENA M. TALLAKSEN[1], **HEGE HISDAL**[1] **& HENNY A. J. VAN LANEN**[2]

1 *Department of Geosciences, University of Oslo, PO Box 1047 Blindern, NO-0316 Oslo, Norway*
lena.tallaksen@geo.uio.no

2 *Hydrology and Quantitative Water Management Group, Wageningen University, Nieuwe Kanaal 11, 6709 PA Wageningen, The Netherlands*

Abstract Regional drought characteristics, such as the area covered by drought and the total deficit over that area, are important measures of the severity of a drought event. Gridded, monthly data from the Pang catchment, UK, are analysed here to study the spatial aspects of the drought as it propagates from a meteorological drought, through a drought in the groundwater system and finally appears as a drought in discharge at the catchment outlet. Drought events are derived separately for each grid cell and variable (rainfall, recharge and hydraulic head) using the threshold level method, and combined to yield regional or catchment-specific drought characteristics. The results demonstrate the catchment control in modifying the drought signal from a series of short duration droughts in rainfall covering large parts of the catchment, through fewer and longer droughts in groundwater recharge, head and discharge. The most severe hydrological droughts in the period 1961–1997 occurred in 1975–1977 and 1991–1992. The average area covered by drought is smaller for groundwater recharge than hydraulic head. Hydraulic head and discharge exhibit similar drought behaviour, which can be expected in a groundwater fed catchment.

Key words regional drought characteristics; hydrological drought; groundwater; rainfall; spatial aspects; Pang catchment, UK

INTRODUCTION

Drought is regional in nature and unlike flood its impacts are not limited to the river network and its direct neighbourhood. Drought affects all components of the water cycle as it develops from its origin as a meteorological drought through a deficit in soil moisture, reduced groundwater recharge and levels, and finally shows up as a low streamflow or dried-up river. Regional characteristics, such as the area covered by the drought and the total deficit over that area, are thus important measures of the severity of the event. An early warning system for drought is seen as an important measure for mitigation or adaptation to the impact of drought. Our ability to forecast seasonal drought depends on the potential to link large-scale climate drivers to the frequency and occurrence of drought in the river basin. This requires knowledge about the temporal and spatial development of drought causing processes both in the climate and the hydrological system. In this study focus is on the hydrological system, namely how the spatial aspects, i.e. regional drought characteristics, of a meteorological drought (deficit in rainfall) is propagated in the hydrological cycle to appear as a drought in groundwater recharge, hydraulic head and discharge. The detailed analysis is done using data from the Pang catchment in the UK.

A general approach for estimating regional drought characteristics is through stochastic modelling of monthly precipitation as reviewed by Rossi *et al.* (1992). An application, adapted to precipitation as well as streamflow, was presented in Hisdal & Tallaksen (2003) in a regional study of drought in Denmark. In their work, a procedure based on the severity-area-frequency (SAF) approach was introduced, which allows the probability of a specific area to be affected by a drought of a given severity to be estimated by the derivation of SAF curves. Subsequently, return periods can be assigned to historical events. Regional drought characteristics were calculated based on drought events selected using the threshold level method with time series of gridded monthly data. The threshold level method, which captures both the duration and the severity of a drought event, has proved to be a flexible approach for characterizing various types of drought (Tallaksen & van Lanen, 2004). Gridded data were obtained from interpolated and simulated long time series derived using a combination of Empirical Orthogonal Functions (EOF), kriging and Monte Carlo simulations.

In this study, gridded time series are obtained using interpolated rainfall and simulated groundwater recharge, head and discharge derived from physically-based soil water and groundwater models. SAF curves are not generated due to the limited number of events in the historical

Copyright © 2006 IAHS Press

time series. Instead observed frequencies of the area covered by drought and the drought duration and deficit over the area are derived. The approach further differs in terms of the spatial scale of the region of interest and variables analysed. Whereas the whole of Denmark was the basis for the development of the methodology, emphasis is here on the propagation of drought in the hydrological system at the catchment scale. Accordingly, one might refer to these as catchment specific, rather than regional drought characteristics. Finally, the results are compared with the spatial distribution of drought in groundwater as presented by Peters *et al.* (2006) in a similar study of the Pang.

CATCHMENT DATA AND METHODOLOGY

The Pang catchment is situated about 25 km south of Oxford and the topographic catchment area is approx. 170 km^2 (Fig. 1). It covers an altitude range from 40 (catchment outlet) to about 230 m a.m.s.l. (surface water divide). The main aquifer supplying water to the Pang is the Chalk aquifer and around two thirds of the discharge is estimated to come from groundwater storage (Peters & van Lanen, 2005). In the south the Chalk is covered by a thick layer of almost impermeable Tertiary deposits with low conductivity, which generates fast shallow subsurface flow. The hydrology of the catchment is simulated using the SWAP model for recharge (Peters, 2003) and the transient MODFLOW model for hydraulic head and groundwater discharge (Peters *et al.*, 2006). The model area is divided into cells with a spatial resolution of 500 m, and the total area (475 km^2) exceeds that of the Pang catchment to allow proper conditions at the boundary of the variable groundwater catchment. In total there are about 1900 cells of which 1089 constitute the Pang catchment. In cells with a low conductivity Tertiary cover, the aquifer recharge is set to a constant low value (~23% of the catchment area). The catchment is separated into five rainfall zones (Peters, 2003), and the models are run for the period 1961–1997 (37 years). The average annual rainfall over the period is about 690 mm and varies little throughout the year. Rainfall is highest in the west (740 mm), where there are slightly higher elevations, and lowest in the northeast (650 mm). Average annual potential evapotranspiration is 520 mm (grassland), and average annual streamflow 120 mm. This rather low streamflow is influenced by groundwater

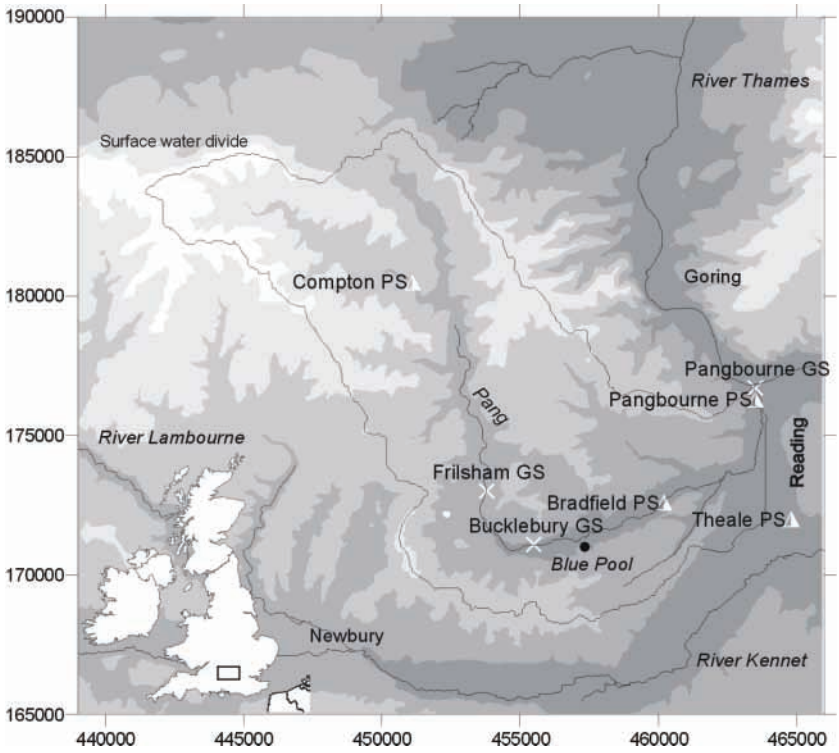


Fig. 1 The Pang catchment (coordinates of the British National grid (m); PS: Pumping station, GS: Gauging station) (from Peters, 2003).

abstractions and water flow to the River Thames during periods of low flow. Simulated groundwater discharge for the Pangbourne gauging station (Fig. 1) is therefore used instead of observed streamflow in the analysis of drought.

Interpolated gridded rainfall is used as input to the SWAP model for simulation of daily recharge. On the basis of catchment characteristics such as soil, land use and rainfall, each cell is assigned to so-called physiographic units. In total 45 combinations are distinguished within the Pang catchment. Daily recharge is calculated for the set of physiographic units (and thus for each cell) for the period 1961–1997 and then aggregated to monthly values. Negative values, representing capillary rise, occur in 119 of the cells. The recharge for each cell is fed into the MODFLOW model (with a time step of three days) to simulate groundwater heads and discharge. These are subsequently aggregated to monthly values.

Drought events are selected from time series of interpolated rainfall and simulated recharge, hydraulic head and groundwater discharge using the threshold level method, which defines drought as periods during which the variable is below a certain threshold level. All events below the threshold are included, i.e. a partial duration series (PDS). Whereas rainfall, recharge and groundwater discharge are fluxes with units [LT^{-1}], hydraulic head is a state variable with unit [L], here mm $month^{-1}$ and metres are used, respectively. The 80 percentile from the duration curve (P80, R80 and H80), is calculated separately for each grid cell and variable (rainfall, recharge and hydraulic head), and then used as a threshold to identify whether a cell is experiencing drought or not. Accordingly, the total area with deficit and the total deficit over that area can be estimated for each variable and month. In this study, the total duration of a drought event (the number of consecutive months where any grid cell is in a drought) and the average area covered by the drought (average over the total duration) are derived for rainfall, recharge and hydraulic head. The (total) deficit volume of a drought event in rainfall and recharge is derived as the sum of the average deficit volume (average deficit over all affected cells) for each month in a drought. The deficit volume in each cell (mm) is standardized with its threshold level (mm $month^{-1}$) to allow a comparison over the area and between different variables.

Drought in discharge is derived for the time series at the catchment outlet (using Q80 as a threshold level) and standardized similar to rainfall and recharge. This implies that the deficit volumes are given in months for rainfall, recharge and discharge. As hydraulic head is a measure of storage, rather than summing up the deficit in each time step, the average deficit over the grid cells and months (defined as the average deviation from the threshold over the affected area and over the drought period) is calculated. This can also be referred to as the intensity of the drought, which has the unit [L] similar to deficit volume for fluxes. Deficit in hydraulic head is given in metres.

DROUGHT IN THE PANG CATCHMENT

The distribution of *drought duration* is shown in Fig. 2 for rainfall ($\overline{P}_{dur}$ = 1.5 month, N = 77), recharge ($\overline{R}_{dur}$ = 13.8 month, N = 26), hydraulic head ($\overline{H}_{dur}$ = 5.8 month, N = 36) and discharge ($\overline{Q}_{dur}$ = 3.6 month, N = 25). Average values are given in brackets along with the total number of droughts, N. The number of events decreases and the duration correspondingly increases as the drought transforms from a meteorological to a hydrological drought.

For rainfall there are on average two events each year and these are, due to the delay in catchment response, clustered into fewer and longer hydrological droughts. The use of a percentile from the duration curves as a threshold ensures that the same number of days is below the threshold level for all grid cells and variables, but the distribution will be different. The longest duration is found for recharge due to the presence of multi-year events, caused by its cyclic nature. The high seasonality in recharge will normally result in a drought each summer, but during a dry winter it may happen that the recharge does not exceed the threshold and multi-year droughts result. This is clearly seen in the clustering of events for recharge. On the other hand, only the most extreme years show up as multi-year events in hydraulic head (three events) and discharge (one event). For all variables the distribution is skewed to the left with a high number of short duration droughts.

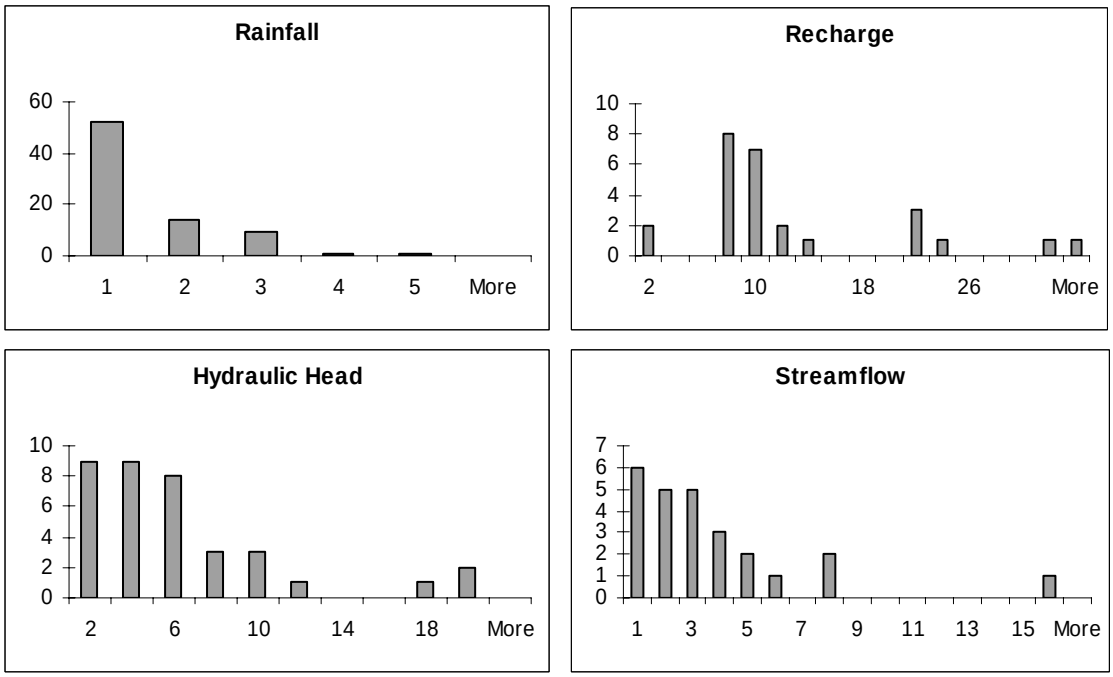


Fig. 2 Drought duration (in *month*) for rainfall, recharge, hydraulic head and discharge (*number of events* is given on the *y*-axis).

The longest drought lasts from December 1975 to April 1976 for rainfall (5 month, followed by a second drought in the summer of 1976 of 3 months), from May 1988 to April 1994 for recharge (72 month), from June 1991 to December 1992 for hydraulic head (19 month) and from July 1991 to October 1992 for discharge (16 month). The 1975–1976 drought is the second longest drought in discharge (8 month) and recharge (31 month, extending into 1977), whereas for hydraulic head it is less extreme, but a clustering of dry years is found between 1973 and 1977. The severe hydrological drought experienced in 1991–1992 results from a series of smaller rainfall droughts between 1990 and 1991, followed by a major event lasting three months during the winter of 1991–1992. Multiyear events in recharge and head were also reported by Peters *et al.* (2006) for the 1991–1992 drought, although shorter durations in recharge were found, resembling more those of groundwater discharge. The study, which focussed on the spatial distribution of drought duration, did not derive regional or catchment aggregated drought characteristic values.

In Fig. 3 the *average area* covered by drought for rainfall, recharge and hydraulic head is given. Rainfall drought covers, in 43% of the cases, the whole catchment (average area 76%), whereas a maximum coverage of 30 and 75% is observed for recharge and hydraulic head, respectively. The corresponding average values are 16 and 25%. It should be noted that this rather low areal coverage partly stems from the definition of drought duration. As long as one cell is in a drought, the drought continues and consequently, the resultant average area covered can be low, particularly for long duration droughts. For recharge it is further influenced by the proportion of the area (~23%) defined in the model to have a constant low recharge. This area will never experience drought and if left out, an area corrected coverage of 39% (maximum) and 21% (average) results as compared to the original 30 and 16%.

Deficit volume (not shown) has for rainfall a more even distribution over the range of values experienced, but also here a higher frequency of smaller volumes is observed. Recharge, hydraulic head and discharge depict similar patterns in the distribution of deficit volume as compared to duration. Deficit volume averaged over the affected area is for rainfall, $\overline{P}_{vol}$ = 0.43 month (N = 77), recharge, $\overline{R}_{vol}$ = 1.1 month (N = 26) and discharge, $\overline{Q}_{vol}$ = 0.52 month (N = 25). It should be noted that the discharge at the outlet integrates the response over the whole catchment and this value is therefore not directly comparable to the average in recharge deficit (average over the drought affected cells).

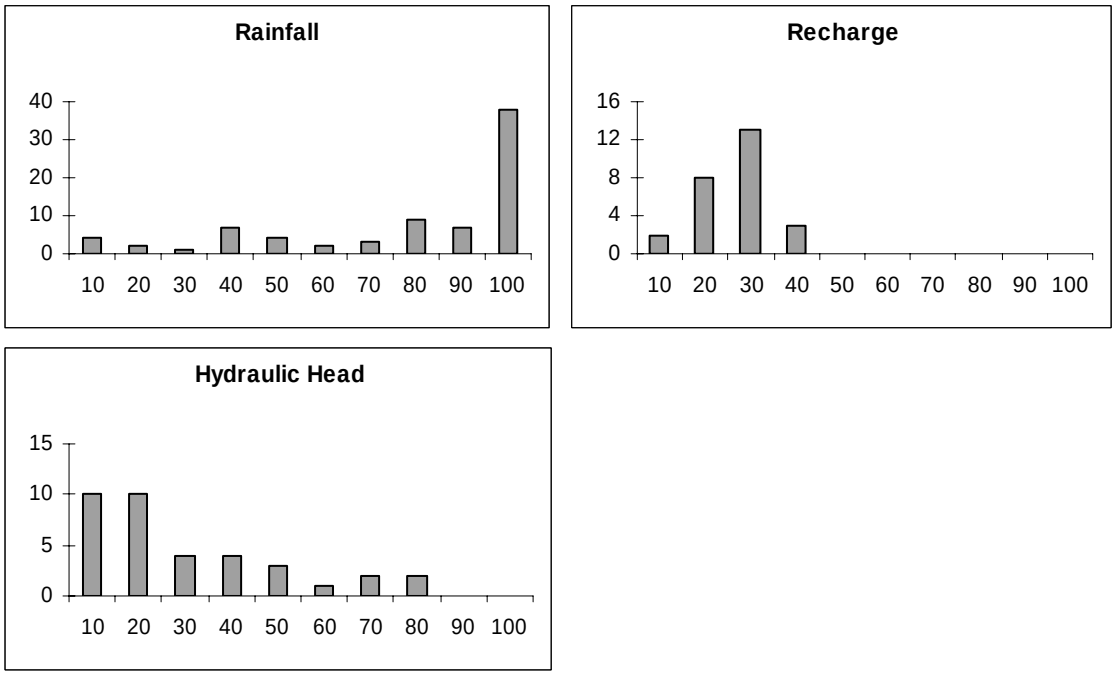


Fig. 3 Average area covered by drought (in *percent*) for rainfall, recharge (area corrected) and hydraulic head (*number of events* is given on the *y*-axis).

DISCUSSION AND CONCLUSIONS

The impact of drought on natural water resources, whether groundwater or streamflow, depends on the climate input as well as the properties of the catchment, as demonstrated in this study. The rather large differences found in drought behaviour (temporal and spatial patterns) as it propagates in the hydrological cycle, stresses the importance of including not only one variable in a study of drought at the regional or catchment scale. Rather the purpose of the study should guide the choice of variables and methods adopted.

This study illustrates the added value of applying regional drought characteristics in analysing the propagation of drought in the hydrological system at the catchment scale. The results clearly demonstrate the catchment's control in modifying the drought signal, from a series of short duration droughts in rainfall covering large parts of the catchment, through fewer and longer droughts in groundwater recharge, head and discharge. The average area covered by drought in groundwater is smaller than for rainfall, and larger in hydraulic head as compared to recharge. The areal coverage is influenced by the way drought duration is defined and, for recharge, also by the size of the area experiencing constant recharge. It is recommended that introducing an additional criterion to the threshold level, namely a critical area, is considered when defining drought events based on a high resolution spatial model (i.e. a drought exists only if a certain percentage of the region or catchment area is in a deficit).

The two most severe historical droughts considering all variables occur in 1975–1977 and 1991–1992, and are most noticeable for hydrological droughts. Multi-year droughts occur more frequently for recharge due to its marked seasonal pattern, but are also observed in hydraulic head and discharge. For recharge, durations of up to six years are observed, and as a result recharge has a markedly longer average duration.

Hydraulic head and groundwater discharge exhibit similar drought behaviour, which can be expected in a groundwater fed catchment like the Pang. Slightly longer durations are obtained for hydraulic head as compared to discharge despite the fact that fewer droughts result for discharge, which partly reflects the higher number of multi-year events for head. Shorter duration droughts in groundwater discharge as compared to hydraulic head were also observed by Peters *et al.* (2006), which used a slightly different approach to the threshold level method, They further found that drought in discharge resembled drought in recharge more than in head and argued that this was a

result of the delay and attenuation in the groundwater system. The latter is not confirmed in this study and care should be taken in concluding that the longer durations derived in head is due to the longer response time of the groundwater system as there is an important difference in the type of variables being studied. Hydraulic head represents, similar to reservoir level, a measure of storage. Analogous to the sequent peak method, SPA, which relates the flow below a threshold to the required storage in a period with storage depletion and subsequent filling up (Tallaksen *et al*., 1997), the drought event can be defined to last until the time of maximum depletion, in which case the maximum depletion equals the deficit volume of the event. The SPA method might, however, overlook drought events occurring shortly after a major event, and is therefore not recommended for analysis of PDS (Fleig *et al*., 2006). Definition of drought in a comparative study involving variables of different units will be the topic of a further study, where also long time series will be simulated to derive severity-area-frequency curves. This will allow return periods of historical droughts to be estimated for regional or catchment specific drought characteristics.

Acknowledgement The authors thank Dr Elisabeth Peters (TNO Geosciences, Utrecht) for providing the observed and simulated monthly data for the Pang catchment.

REFERENCES

Fleig, A. K., Tallaksen, L. M., Hisdal, H. & Demuth, S. (2006) A global evaluation of streamflow drought characteristics. *Hydrol. Earth Syst. Sci.,* **10**, 535–552.

Hisdal, H. & Tallaksen, L. M. (2003) Estimation of regional meteorological and hydrological drought characteristics. *J. Hydrol*. **281**(3), 230–247.

Peters, E. (2003) Propagation of drought through the groundwater systems – illustrated in the Pang (UK) and Upper-Guadiana (ES) catchments. PhD Thesis, Wageningen University, The Netherlands.

Peters, E. & van Lanen, H. A. J. (2005) Separation of base flow from streamflow using groundwater levels – illustrated for the Pang catchment (UK). *Hydrol. Processes* **19**, 921–936.

Peters, E., Bier, G., van Lanen, H. A. J. & Torfs, P. J. J. F. (2006) Propagation and spatial distribution of drought in a groundwater catchment. *J. Hydrol.* **321**, 257–275.

Rossi, G., Benedini, M., Tsakiris, G. & Giakoumakis, S. (1992) On regional drought estimation and analysis. *Water Resour. Manage*. **6**, 249–277.

Tallaksen, L. M., Madsen, H. & Clausen, B. (1997) On the definition and modelling of streamflow drought duration and deficit volume. *Hydrol. Sci. J.* **42**(1), 15–33.

Tallaksen, L. M. & van Lanen, H. A. J. (2004) (eds) *Hydrological Drought—Processes and Estimation Methods for Streamflow and Groundwater.* Developments in Water Sciences 48. Elsevier BV, The Netherlands.

Climate Variability and Change—Hydrological Impacts (Proceedings of the Fifth FRIEND World Conference held at Havana, Cuba, November 2006), IAHS Publ. 308, 2006.

Predicting low flows in ungauged basins: a hydrological response unit approach to continuous simulation

ANDREW R. YOUNG, VIRGINIE KELLER & JIM GRIFFITHS
Centre for Ecology and Hydrology, Wallingford, Oxfordshire OX10 8BB, UK
ary@ceh.ac.uk

Abstract An alternative approach to the problem of the regionalization of a rainfall–runoff model is explored in which the concepts of Hydrological Response Units (HRU) are used to define a flexible model structure where catchment descriptors are used to define relatively complex, specific model structures within each catchment from one generic structure. This model structure has been simultaneously calibrated, and hence regionalized across a large set of catchments within the UK. The simulation results obtained with this approach have been compared with those from a simple lumped model regionalized by relating prior calibrated model parameters to catchment descriptors. The paper concludes by suggesting that model structure and regionalization strategy may not be significant in limiting the performance of regionalized models and that they can be improved by incorporating sparse, at-site measurements.

Key words rainfall–runoff models; continuous simulation; hydrological response units; regionalization; water resources

INTRODUCTION

Access to daily streamflow data at the river reach scale is a central component of many aspects of water resource and water quality management. The requirement for these data within ungauged catchments has been one of the many drivers behind research into the regionalization of conceptual rainfall–runoff models. The theory behind the regionalization objective is that if the structural description of the rainfall–runoff model is correct, the parameters of the model are more likely to be related to physical descriptors of the catchment that can be measured. However, as a consequence of scaling issues and the many unknowns and sources of error there are significant problems in retaining the physical basis of model parameters as models are scaled from the plot to the catchment scale.

The problems in regionalizing rainfall–runoff models are manifold; some key issues are summarized here. The body of literature on model structure, calibration, effect of forcing data errors (including observed streamflow) on calibration, parameter identifiability and whether any model structure has truly identifiable parameters is immense (see, for example Beven, 1993) and is not the subject of this paper. Broadly speaking, identifiability can be increased by reducing the complexity, and hence the number of parameters within a model (if streamflow data are to be the sole source of calibration data), minimizing uncertainty within the input data and by the selection of appropriate objective functions for measuring model simulation performance. If parameters are non identifiable then the likelihood of expressing them as a function of catchment descriptors is reduced. It has been commonly proposed that parameter parsimonious, generally lumped model structures are best suited to regionalization (Seibert, 1999). The consequence of all of these factors is that model parameters may have little physical relevance. Additionally, the catchment descriptors that can be used as predictors are nearly always extrapolated from point measurements, which are inherently erroneous and may not be independent from one another. Furthermore, dependencies are rarely amenable to quantification through the use of classical statistics.

The published approaches to regionalizing the relationships between model parameters and catchment characteristics are varied; the most common approach is to calibrate a model structure, usually lumped, within a set of gauged catchments that are representative of the region in which the model is to be utilized and to subsequently develop relationships (normally statistical) between parameters and descriptors describing the physical and climatological structure of a catchment. The commonest examples of these are regression based relationships (e.g. Abdulla & Lettenmaier, 1997); other approaches have been based on nearest neighbour approaches based on spatial proximity (e.g. Merz & Blöschl, 2004). Young (2006) considered both the multivariate regression approach to the regionalization problem and a nearest neighbour approach based on similarity in catchment descriptors. The study was based on a data set of 260 United Kingdom catchments. The

Copyright © 2006 IAHS Press

approaches were explored using a simple, four parameter rainfall–runoff model based on the PDM model of Moore (1985), the study concluded that the regression based approach gave the best regionalized model performance.

The study presented in this paper builds on this previous work to explore whether the approach of *a priori* calibration of lumped catchment models with the subsequent regionalization of model parameters is the optimal approach to regionalizing the rainfall–runoff process. The approach proposes a flexible hydrological response unit (HRU) based model structure in which catchment descriptors of vegetation and soil type are used to define more complex, specific model structures within each catchment than can be identified from streamflow data from a single catchment. To enable subsequent parameter identification from streamflow data, the model parameters are simultaneously optimized against streamflow data across all catchments to combine model calibration and regionalization in a single step process. The scheme was developed using a data set of 501 UK catchments. This paper compares the simulation results obtained using this new class of regionalized model with those obtained earlier by Young (2006) (using 260 catchments) over the common 163 catchments within the data set. The comparison focuses on predictive uncertainty and concludes with some comments about the importance of hydrological structure and the way forward for the reduction of predictive uncertainty within ungauged catchments.

CATCHMENT DATA SETS

The catchment data set used was an expansion of that used for the previous study which was restricted to the selection of natural, high hydrometric quality catchments. Daily time series of 648 catchment average precipitation and potential evaporation were derived for all catchments using the methods described by Young (2006). The catchment data set was reduced to 501 by excluding those catchments in which a water balance assumption, explicit within the model, was obviously violated. This data set was subdivided into 217 catchments used for model calibration and regionalization, and 284 catchments retained for evaluation.

The catchment descriptors used within the model structure are: a hydrologically referenced 50 m resolution, Digital Terrain Model (DTM) (Morris & Heerdegen, 1988); the Hydrology of Soil Types (HOST) 29 class hydrological response classification of soils across the United Kingdom (Boorman *et al*., 1995) and a classification of land cover based on five broad vegetation classes: Deciduous, Coniferous, Arable, Grassland, and Upland, derived from the CEH Land-cover Map 2000 classification system mapped at a resolution of 50 m (Smith *et al*., 2001).

MODEL STRUCTURE

The model structure is based around two sub model components; the loss module that generates hydrologically Effective Precipitation (EP) and the routing module that subsequently routes the EP to the catchment outlet. The basic model structure for the loss module is a hydrological response unit consisting of an interception sub-module and a treatment of transpiration losses based on the *FAO 56* soil moisture accounting procedures for determining crop water requirements (Allen *et al*., 1998). The interception model was regionalized for inclusion within a rainfall–runoff model by Young (2006). The model has one parameter; the maximum depth of water that can be held by the vegetation, γ. The conceptual structure of the FAO transpiration module is presented within Fig. 1. The module describes vegetation as a function of maximum root depth, Z_r, and "moisture depletion fraction", p, for a range of vegetation and soil types. The Total Available Water (*TAW*), the amount of water available to plants after a soil has drained to its field capacity is defined as the product of the difference between field capacity (*FC*) and wilting point (*WP*) (properties of the soil class) and Z_r. Plants freely transpire until Soil Moisture Deficits (*SMD*) exceed the threshold defined by pZ_r; beyond this threshold the plants become increasingly stressed and evaporation reduces below the potential rate in proportion to the depth of threshold exceedence. EP is generated by the module when the *SMD* within the module is zero.

HRUs were defined by combining the HOST classes and reduced land-cover classes to yield a potential 140 combinations of HOST and land cover classes plus an open water class. In practice

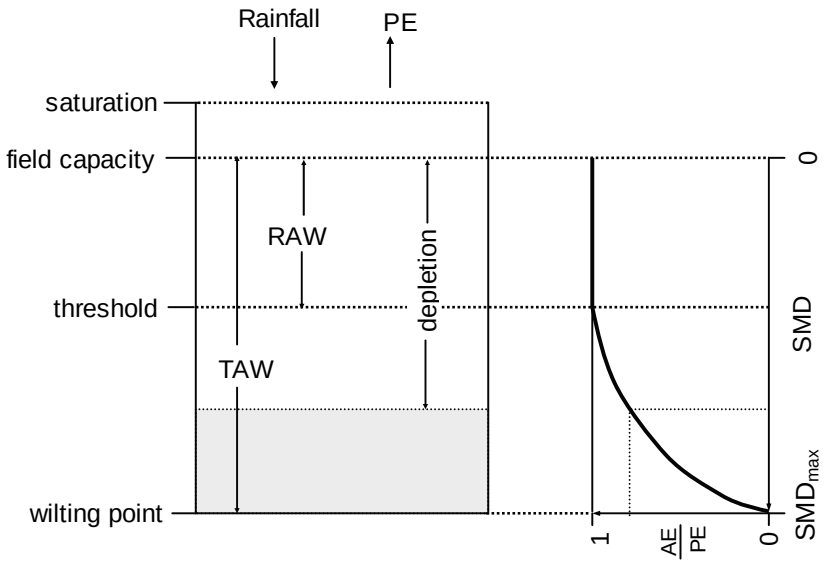


Fig. 1 Conceptual structure of the soil moisture accounting within the loss module.

the number of actual combinations was significantly less as some land-cover/soil class combinations do not occur in practice. At the catchment level the individual cells within the HRUs represented within the catchment are amalgamated to form HRUs with a fractional extent that is not necessarily contiguous within the catchment. The response of each HRU is controlled by the vegetation parameters of γ, Z_r and p and the *FC* and *WP* parameters for the soil class. *FC* and *WP* parameters were defined for each soil class based on extracting the average percentages of sand, silts and clays within each HOST class from the UK National Soil Resource Institute's SEISMIC data set. This process leaves Z_r and p, for each vegetation class as the free parameters for the HRUs within the loss module which equates to 10 parameters in total.

The output from the loss module within a catchment is an EP time-series for each 1 km cell within the catchment. The routing module routes these effective precipitation time series to the catchment outlet via a semi-distributed routing scheme. Within the UK, the dominant influences on the routing of water through the land surface are soils, hydrogeology and topography. In the absence of an appropriate resolution digital hydrogeological classification of the UK, the 29 HOST classes were amalgamated into 11 hydrogeological routing HRUs based on substrate geology. The EP time series for each cell enters the routing HRU corresponding to the HOST class of the cell. A probability distributed storage model is used to represent the free water in the soil column for the routing HRU. This storage model is assumed to be uniformly distributed with a maximum storage depth of 75 mm (determined by preliminary individual catchment model applications), drainage takes place from the base of the store and is proportional to the depth of water held in storage. The constant of proportionality, *Kg*, is a free parameter. The runoff from the store is routed though a topographically defined routing path whilst the drainage is routed through a linear reservoir, with a time constant *Kb*, representing the baseflow for the routing class.

The previous regionalization work on lumped models, in which quick flow routing was via a linear reservoir, demonstrated a strong dependency of the reservoir time constant on both catchment size and soil storage. For this study the quick flow routing within the routing HRUs was subdivided into a topographic component and a component representing transient soil storage along the routing path. The topographic routing of the quick flow from the individual cells within a routing HRU to the catchment outlet was based upon the flow path defined from the DTM and the cell level topographic gradients along the path, β. Total travel time to the catchment outlet, T, is calculated for each cell as:

$$T = \sum_{i=1}^{N} \frac{x_i}{\beta_i v} \tag{1}$$

where x_i is the distance between the centroids of adjacent cells within the flowpath and v is a

routing HRU dependent velocity which conceptually is linked to bulk, lateral hydraulic conductivity. The total topographically routed quick flow for the routing HRU is calculated as the sum of the EP time series for the constituent cells lagged by the corresponding cell travel times. The resultant summed time series is then passed through a linear reservoir of time constant, *Kq*, to represent the transient storage along the flow path lengths. For each routing HRU the model has four free parameters: *Kg*, *V*, *Kb* and *K*1, and with 11 routing class this gives a total of 44 routing parameters within the model which combined with the 10 free loss module HRU parameters yields a total of 54 model parameters for calibration.

MODEL CALIBRATION

The parameters were simultaneously optimized across all catchments within the calibration sets using data from the 15 year period from 1987–2001. This process combines both model calibration and regionalization into a one-step process as the model parameters are a function of the HRUs and hence the descriptors of the catchments. The loss module HRUs were initially calibrated to make the process of simultaneous calibration computationally tractable. The mean and variance of the distribution of the bias between simulated mean EP and the corresponding observed mean runoff, expressed as a percentage of the observed mean runoff (BIAS) over the calibration period was minimized as the objective function. The routing module parameters were subsequently optimized based on the trade off between maximising the Nash-Sutcliffe Efficiency Criterion (NSE) and minimizing the sum of squared deviations between observed and simulated streamflow over the lowest third of the flow distribution (LF_OBJ) and the bias error at the Q95 flow (BEQ95) across all catchments within the calibration data set. The NSE was used as a general measure of fit whilst the latter functions are a measure of fit at low flows. The earlier periods of flow data within the calibration catchments and the evaluation catchments were used to ensure the model was not over fitted within the calibration catchments.

EXAMPLE RESULTS

To facilitate comparison with Young (2006) the common catchments between the studies were grouped into the following classes: R1-catchments that were used in the regionalization of both models; R2-catchments that were not used in the regionalization of either model; R3-catchments that were used in the regionalization of the current model but not used in the development of the regionalization of the previous study and, finally, R4-catchments that were used in the regionalization work within the previous study but not used for the regionalization of the model in the current study. Example simulation results are presented for each catchment class in Table 1

Table 1 Summary of simulation results across catchment classes.

Class	c.i. limits	Bias		NSE		BE_Q95		lf_obj	
R1	68% u.l.	**6**	*4*	**0.80**	*0.81*	**69**	*152*	**78**	*104*
n = 85	median	**–1**	*–2*	**0.73**	*0.73*	**–11**	*26*	**54**	*51*
	68% l.l.	**–10**	*–8*	**0.59**	*0.59*	**–52**	*–26*	**34**	*35*
R2	68% u.l.	**8**	*8*	**0.79**	*0.75*	**17**	*58*	**63**	*69*
n = 31	median	**–7**	*–6*	**0.67**	*0.67*	**–16**	*5*	**49**	*50*
	68% l.l.	**–13**	*–12*	**0.45**	*0.49*	**–41**	*–32*	**36**	*39*
R3	68% u.l.	**5**	*6*	**0.81**	*0.74*	**82**	*133*	**95**	*102*
n = 37	median	**–6**	*–5*	**0.74**	*0.69*	**–8**	*4*	**55**	*56*
	68% l.l.	**–10**	*–9*	**0.58**	*0.51*	**–43**	*–42*	**41**	*42*
R4	68% u.l.	**9**	*13*	**0.75**	*0.80*	**27**	*60*	**61**	*66*
n = 73	median	**–2**	*0*	**0.64**	*0.70*	**–33**	*9*	**47**	*44*
	68% l.l.	**–8**	*–8*	**0.46**	*0.55*	**–51**	*–30*	**34**	*33*
All	68% u.l.	**8**	*8*	**0.80**	*0.79*	**55**	*100*	**76**	*80*
n = 226	median	**–2**	*–2*	**0.69**	*0.70*	**–17**	*13*	**48**	*49*
	68% l.l.	**–10**	*–9*	**0.54**	*0.55*	**–45**	*–32*	**33**	*35*

together with the results over all catchments. The variation of each of the objective functions across the catchments within a class is summarized as the limits defining the 68% confidence interval for the simulation results and the median value within the class. The class membership is also presented in Table 1. The results for the current semi-distributed model are highlighted in bold whilst the results for the lumped model are presented in italics. The stability of both models is similar for the overall model BIAS and NSE. across all catchment classes. This indicates very similar model performances, in terms of water balance closure and general time-series fit, irrespective of model type, whether the catchments were used within the regionalization scheme or whether they are fully independent. The NSE. 68% c.i. for the semi-distributed model tends to be marginally wider than that for the lumped model, but the median values are very comparable. Considering the fit at low flows, the semi-distributed form tends to perform better than the lumped model, particularly with respect to the 68% u.l. for the BEQ95 statistic (representing an over-prediction at Q95). This is also reflected in the LF_OBJ with the values for the semi-distributed model generally being lower for all limits, thus indicating a better fit.

CONCLUSIONS

The approach of using catchment descriptors to define the model structure and the combination of model calibration and regionalization within a one-step process has many conceptual advantages over the traditional approach of seeking statistical relationships between *a priori* calibrated parameters for a lumped model and catchment descriptors. The comparison with the results of a previous study has demonstrated that the approach yields a better fit to low flows but marginal benefits in terms of the simulation of mean flow (BIAS) and overall time-series fit, as measured using NSE. In a UK context, the model structure and regionalization approach may not therefore be the limiting factors within this type of study. This suggest that other factors are limiting; these may include: input data errors, subtle violation of the assumption of a closed water balance at the catchment scale and the limitation of current catchment descriptors in aiding the differentiation of the hydrological regimes between river catchments. It is stressed that the results are preliminary, and research is ongoing to separate the aspects of model performance into those related to these factors and those attributable to model and parameterization error. Given the intractable nature of improving catchment descriptors, a fruitful future research direction is to investigate how sparse measurements, for example a short period of continuous measurement or a set of discrete measurements covering a range of flows, may be used to constrain model uncertainty within ungauged catchments.

REFERENCES

Abdulla, F. A. & Lettenmaier, D. P. (1997) Development of regional parameter estimation equations for a macroscale hydrologic model. *J. Hydrol.* **197**, 230–257.

Allen, R. G., Pereira, L. S., Raes, R. & Smith, M. (1998) Crop evapotranspiration – Guidelines for computing crop water requirements. *FAO Irrigation and Drainage Paper 56*, Food and Agriculture Organization of the United Nations, Rome, Italy.

Beven, K. (1993) Prophecy, reality and uncertainty in distributed hydrological modelling. *Adv. Water Resour.* **16**, 41–51.

Boorman, D. B., Hollis, J. M. & Lilly, A. (1995) *Hydrology of Soil types: A Hydrologically-based Classification of the Soils of the United Kingdom.* Institute of Hydrology Report no. 126. Wallingford, UK.

Merz, R. & Blöschl, G. (2004) Regionalisation of catchment model parameters. *J. Hydrol.* **287**, 95–123.

Moore, R. J. (1985) The probability-distributed principle and runoff production at point and basin scales. *Hydrol. Sci. J.* **30**, 273–297.

Morris, D. & Heerdegen, R. (1988) Automatically derived catchment boundaries and channel networks and their hydrological applications. *Geomorphology* **1**, 131–141.

Seibert, J. (1999) Regionalisation of parameters for a conceptual rainfall-runoff model. *Agric. Forest Met.* **98–99**, 279–293

Smith, G. M., Fuller, R. M., Sanderson, J. M., Hill, R. A. & Thompson, A. G. (2001) Land Cover Map 2000: a parcel-based approach from satellite images. In: *Proceedings of the RSPS meeting in Uncertainty and Remote Sensing and GIS*, 689–702.

Young A. R. (2006) Stream flow simulation within UK ungauged catchments using a daily rainfall-runoff model. *J. Hydrol.* **320**, 155–172.

Climate Variability and Change—Hydrological Impacts (Proceedings of the Fifth FRIEND World Conference held at Havana, Cuba, November 2006), IAHS Publ. 308, 2006.

Temporal and spatial variability of drought in mountain catchments of the Nysa Klodzka basin

TAMARA TOKARCZYK[1] **& WOJCIECH JAKUBOWSKI**[2]

1 *Institute of Meteorology and Water Management, Parkowa 30, 51-616 Wroclaw, Poland*
tamara.tokarczyk@imgw.pl

2 *Agricultural University of Wrocław, CK Norwida 25/27, 50-375 Wroclaw, Poland*

Abstract This paper presents drought assessments on the basis of a climatic water balance and with the application of a three-parameter model of hydrological drought. Analysis of the spatial range and temporal variability of drought phenomena was carried out for the Nysa Klodzka River basin for 1951–2003. The crucial information for hydrological drought assessment delivers the probability of low flow extreme. The low flow extreme characterizes the maximum deficit volume and duration. The two dimensional Bivariate Generalized Pareto Distribution (BGPD) was applied to estimate the extreme values of the low flow deficit volumes and duration probabilities.

Key words Nysa Klodzka River, Poland; drought; climatic water balance; low flow extreme; Bivariate Generalized Pareto Distribution

INTRODUCTION

Drought assessment is a complex problem for which many influencing factors should be taken into consideration, as well as the areal extent and duration aspects of drought. The droughts that have occurred in Poland in recent years have increased the interest in the issues of mitigation of drought consequences in agriculture, economic activities, as well as in the community. Studies including extreme phenomena such as a drought, with spatial and temporal variable scales, constitute the basis for creating state-of-the-art decision support tools that can be used for effective reduction of droughts. The potential impacts of climatic change and variability, according to the 1996 report of the IPCC (Burn *et al.*, 2002), indicate that the frequency and severity of drought events could increase as a result of changes in both precipitation and evapotranspiration.

In this study an effort has been made to describe the space–time variability of drought in the Nysa Klodzka River basin.

AREA OF STUDY

The Nysa Klodzka River is the left side tributary of the Odra River and therefore it plays an important role in the water management of the Odra River basin. Recognition of water resources during drought conditions, when groundwater yield is the only source of river supply, is very significant given the great diversity of basin geological structures.

The headwater area of the Nysa Klodzka River basin is mountainous and composed of crystalline rocks, and is an important groundwater reservoir, characterized by considerable underground runoff and slow groundwater resources bailing (Tarka, 1997). A significant part of the basin, the middle part of the basin area, is composed of Quaternary sediments with average resources. In the south-western division of the basin, a Cretaceous aquifer with high potential groundwater resources occur (Chudowski, 1976).

Moreover a cascade of four reservoirs, which have a significant influence on the discharge formation of the Nysa Klodzka River, is located in the basin.

METHODOLOGY

Climatic water balance

In this study, drought assessment was made on the basis of the climatic water balance (CWB) and with the application of a three-parameter model of low flow.

The first drought indicator is the atmospheric drought phase. The CWB was applied as an index characterizing the deficiency of water during this phase. It is the difference between

Copyright © 2006 IAHS Press

precipitation and potential evaporation. The Nysa Klodzka River basin is characterized by its diversity of climatic conditions. The CWB includes water relations that appear in selected catchments, taking into consideration both income of water from the atmosphere and losses in the form of evaporation. The CWB was calculated for the time period 1966–2003.

Threshold level method

The extent of the occurrence of a meteorological drought causes in the first step agricultural drought and then hydrological drought. The manifestation of hydrological drought is low flow in the river. The definition of a hydrological drought, criteria for drought event separation, and methods of derivation of drought indices have been used in accordance with the criteria recommended by Tallaksen & van Lanen (2004). The threshold level method was established as percentiles from the recession curve ($Q_{0;25\%}$). Q_0 is the initial discharge and it corresponds with the threshold value where surface runoff is substituted by subsurface runoff.

To obtain the probability distribution of the maximum low flow, the two-dimensional Bivariate Generalized Pareto Distribution (BGPD) (Tajvidi, 1996) was used.

Bivariate Generalized Pareto Distribution

Let $\left\{A_i^{(1)}, A_i^{(2)}\right\}_{i=1,\ldots,n}$ be a sequence of mutually independent identically distributed random variables with distribution function $F(x,t)$. These are defined in the one dimensional case as $(M_n^{(1)}, M_n^{(2)}) = (\max_{i=1,\ldots,n} A_i^{(1)}, \max_{i=1,\ldots,n} A_i^{(2)})$. If for each $a_n^{(1)} > 0, a_n^{(2)} > 0, b_n^{(1)}, b_n^{(2)}$ the limit:

$$\lim_{n\to\infty} \Pr\left(\frac{M_n^{(1)} - b_n^{(1)}}{a_n^{(1)}} \le x, \frac{M_n^{(2)} - b_n^{(2)}}{a_n^{(2)}} \le t \right) = G(x,t) \tag{1}$$

exists and if $G(x,t)$ is a non–degenerate distribution function, then $G(x,t)$ is a Bivariate Generalized Extreme Value Distribution (Resnick, 1987; Coles 2001). According to Tajvidi (1996), $H = H(x,t)$ belongs to the family of BGPD with positive support if:

$$\overline{H}(x,t) = \frac{-\ln G(x + x_0, t + t_0)}{-\ln G(x_0, t_0)}, \quad x,t > 0 \tag{2}$$

$$H(x,t) = \begin{cases} 1 - \overline{H}(x,t), & \text{where} \quad x,t > 0, \\ 0, & \text{otherwise} \end{cases}$$

for some extreme values distribution G with (x_0, t_0) in support of G. It can be also shown that (Tajvidi, 1996):

$$\overline{H}(x,t) = 1 - H(x,t) = \Pr\left((D_M, T_M) \not\le (x,t)\right) = \left(\frac{\overline{F}_d^{\,p}(x) + k\overline{F}_d^{\,p/2}(x)\overline{F}_t^{\,p/2}(t) + \overline{F}_t^{\,p}(t)}{\overline{F}_d^{\,p}(0) + k\overline{F}_d^{\,p/2}(0)\overline{F}_t^{\,p/2}(0) + \overline{F}_t^{\,p}(0)} \right)^{\frac{1}{p}} \tag{3}$$

where:

$$\overline{F}_d(x) = \left(1 - \alpha_d \kappa_d (b_d + x)\right)^{1/\kappa_d}, \quad \overline{F}_t(t) = \left(1 - \alpha_t \kappa_t (b_t + t)\right)^{1/\kappa_t}, \tag{4}$$

$0 \le k \le 2(p-1), \quad p \ge 2, \quad \kappa_d, \kappa_t \in (-1;0), \quad \alpha_d, \alpha_t > 0,$ belongs to the BGPD family. Note that the distribution functions $F_d(x), F_t(t)$ are Univariate Generalized Pareto Distributions (UGPD) and they describe each of the indices separately.

RESULTS

The spatial variability of CWB in the Nysa Klodzka River basin during the period 1966–2003 is shown in Fig. 1. The CBW undergoes variability from the mountainous part of the basin (highest value) to the lowland (negative value), and presents the background for low flow processes.



Fig. 1 The spatial variability of CWB in the Nysa Klodzka River basin in 1966–2003.

In this study the low flow maximum analysis was carried out down the Nysa Klodzka River. The estimated results for selected gauging station are shown in Fig. 2 and 3. They present the estimated two dimensional probability plots of extreme low flow deficit volumes and durations.

The shift lines in general divide the observed low flow events into two groups. The first one consists of many "low" low flows, while the second one contains a smaller number of higher low flows. Such a difference confirms the earlier assumed non-homogeneity of the observed low flow values. It means that these lower low flows are caused by different hydrological processes than the higher ones. The group of lower low flows exemplifies seasonal phenomenon, whereas the second

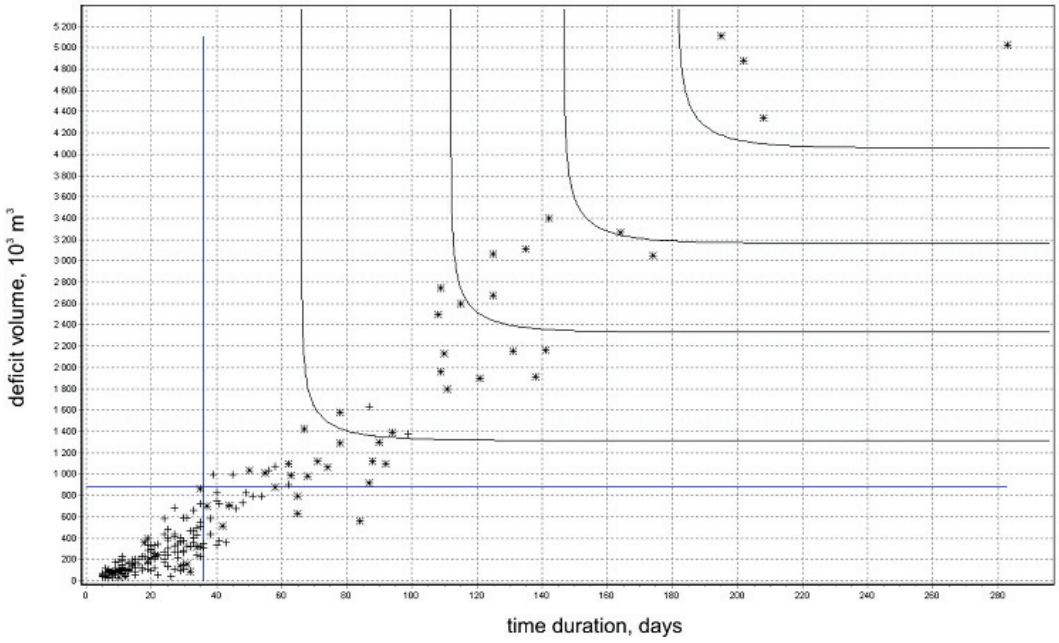


Fig. 2 The Nysa Klodzka River, Miedzylesie gauge, fitting of annual low flows to the Bivariate Generalized Pareto Distribution. (Asterisks denote the observed annual or summer maximums of deficits or durations, crosses refer to other significant observed droughts. Straight lines depict the estimated best shift parameters. The quantile curves constant value probability lines determine the areas laying left or below them which estimated probabilities of non-exceedence are equal to 50, 80, 90 and 95%).

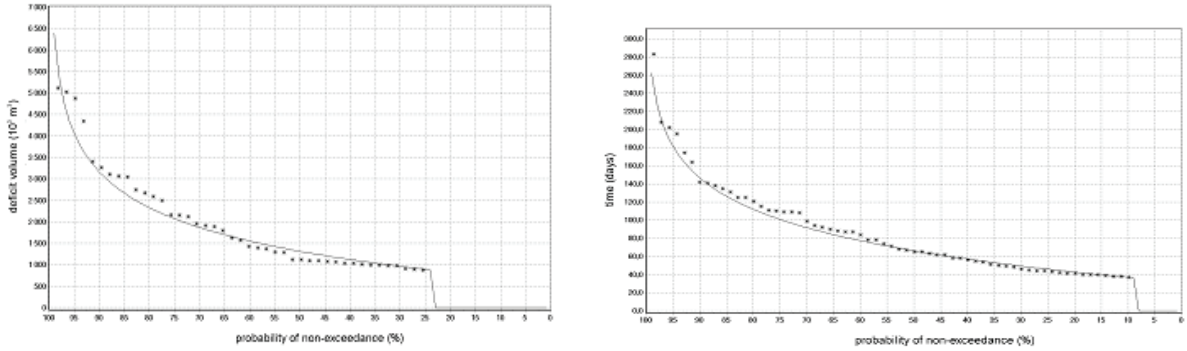


Fig. 3 The Nysa Klodzka River, Miedzylesie gauge, and annual low flows – fitting into marginal distributions of the low flow maximum deficit volume (left side) and duration (right side).

group consists of longer duration linking two or more seasons. Exception are low flows observed at gauging stations located downstream of the cascade of reservoirs. The reservoir's management leads to homogeneity of low flows and there is not a distinct division between the two groups.

Taking the marginal distributions of the estimated BGPD, the probability of each of the examined maximum values of the indices was computed. In Fig. 3 the probabilities of the non-exceedence of the low flow extreme deficit volumes and durations are presented. In the next step, deficit as well as duration, from every gauge upstream of the cascade reservoirs were compared. The deficit volume was depicted in the relative form with reference to the runoff. Such an approach allows a comparison of deficit volumes of consecutive basins. The results are presented in Fig. 4. It turned out that only the Bystrzyca Klodzka profile has a different route indicating dissimilar development and shaping of low flows. The deficit of low flows in the form of relative for the same probability is significantly higher at Bystrzyca Klodzka than the rest of profiles. For example the deficit volume with 50% probability of non-exceedence at BystrzycaKlodzka gauge amounts to 34 whereas at Miedzylesie and Bardo it is about 22. It is concerns both the deficit volume and duration. It may be caused by the specific location of the gauge and the local faulting tectonics and discontinuous fold structures. This location can be characterized by the high bedrock permeability and water support differed from the remaining part of the river.

Furthermore in order to characterize the temporal variation of low flow, the time period 1955–2003 was divided into two sequences: 1955–1984 and 1974–2003. Then the probability distributions for the periods were compared for every sub-basin. In Miedzylesie, the divided periods have a similar pattern (Fig. 5) whereas Bystrzyca Klodzka has a clearly different form in the 1955–1974 period for both deficit and duration (Fig. 6). It means that low flows that occurred in these periods do not have the same characteristics. The deficit volume is much higher and the duration longer. The results of deficit volume with probability 50% and 70% of non-exceedence and for duration for every gauging station on Nysa Klodzka River are presented in Tables 1 and 2.

Table 1 The relative deficit volume with 50% ($D_{v,50\%}$) and 70% probability of non-exceedence ($D_{v,70\%}$) for gauging stations on Nysa Klodzka River.

Gauging station	Period 1955–2003	Period 1974–2003	Period 1955–1984
$D_{v,50\%}$			
Miedzylesie	22.5	16.8	21.1
Bystrzyca Klodzka	34.3	24.2	8.40
Klodzko	00.0	8.27	21.2
Bardo	21.3	8.13	10.0
$D_{v,70\%}$			
Miedzylesie	32.0	25.1	30.7
Bystrzyca Klodzka	46.0	34.7	14.4
Klodzko	29.4	13.6	31.0
Bardo	29.9	13.4	15.8

Table 2 The duration of low flow with 50% ($T_{50\%}$) and 70% probability of non-exceedence ($T_{70\%}$) for gauging stations on Nysa Klodzka River.

Gauging station	Period 1955–2003	Period 1974–2003	Period 1955–1984
$T_{50\%}$			
Miedzylesie	66.1	47.6	61.8
Bystrzyca Klodzka	87.4	60.8	00.0
Klodzko	61.4	00.0	00.0
Bardo	71.5	21.8	31.3
$T_{70\%}$			
Miedzylesie	91.7	69.4	87.8
Bystrzyca Klodzka	115.0	84.8	00.0
Klodzko	82.7	40.4	71.8
Bardo	97.1	35.1	48.3

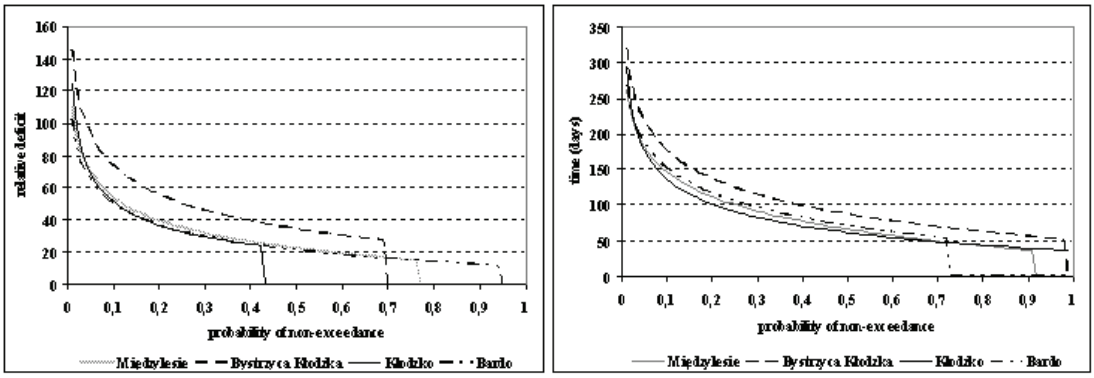


Fig. 4 The Nysa Klodzka River, Miedzylesie, Bystrzyca Klodzka, Klodzko, Bardo gauges down the river; an annual low flows route of the low flow maximum deficit volume and duration marginal distributions.

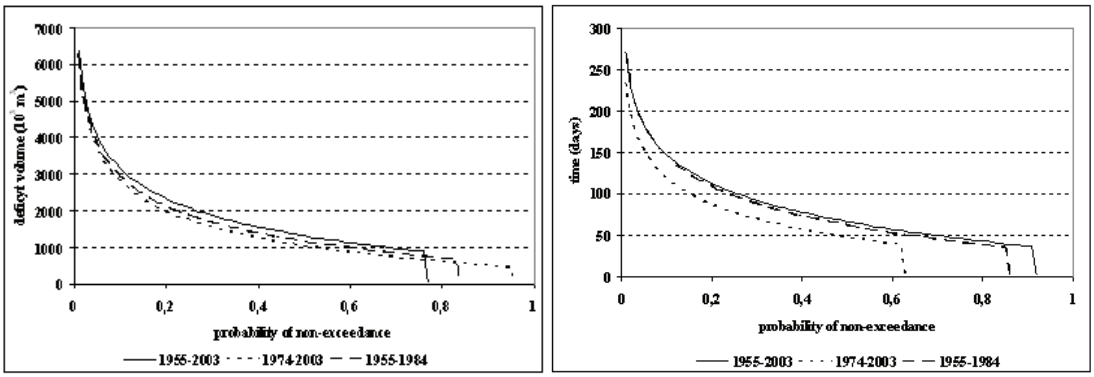


Fig. 5 Route of the low flow maximum deficit volume and duration marginal distributions for the Nysa Klodzka River, Międzylesie gauge for selected periods: 1955–2003, 1955–1984 and 1974–2003.

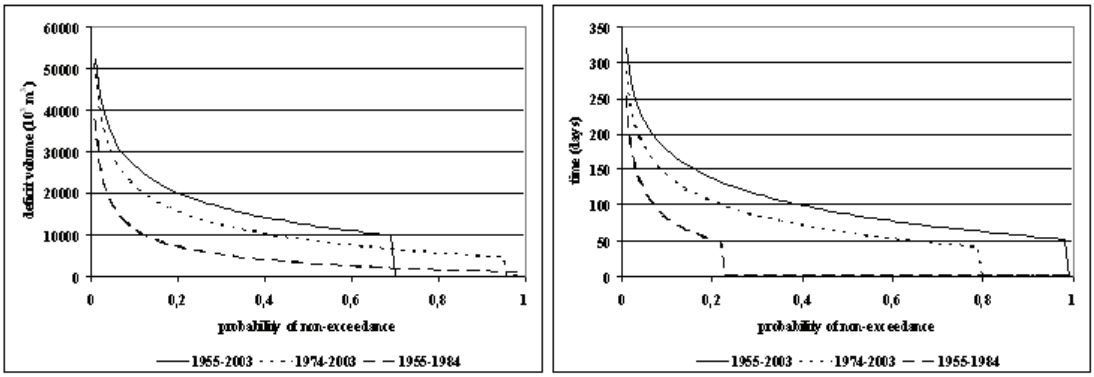


Fig. 6 Route of the low flow maximum deficit volume and duration marginal distributions for the Nysa Klodzka River, Międzylesie gauge for selected periods: 1955–2003, 1955–1984 and 1974–2003.

REFERENCES

Burn, D. H. & Hag Elnur, M. (2002) Detection of hydrologic trends and variability. *J. Hydrol.* **255**, 107–122.

Chudowski, R. (1972) Groundwater of Ziemia Klodzka and its exploitation. *Sesja Naukowa Zasoby Wodne Ziemi Kłodzkiej, Wydawnictwo PAN*, Wrocław, Poland.

Coles S., (2001) *An Introduction to Statistical Modeling of Extreme Values.* Springer-Verlag, London, UK.

Jakubowski, W. (2005) An application of Generalized Pareto Distribution for maximum of the low flows indices distribution determination. *Zesz. Nauk. no. 520*, Agricultural Univ., Wroclaw, Poland.

Dubicki, A., Tokarczyk, T., *et al.* (2002) Water resources in the upper and middle Odra River basin under drought conditions. *Wyd. IMGW*, Warszawa.

Resnick, S. I. (1987) *Extreme Values, Regular Variation and Point Processes*. Springer-Verlag, Berlin, Germany.

Tallaksen, L. M. & Van Lanen, H. A. J. (2004) *Hydrological Drought: Processes and Estimation Methods for Streamflow and Groundwater*. Elsevier, The Netherlands.

Tarka, R. (1997) Groundwater recharge in mountain crystalline massifs on the example of the Śnieżnik Massif in the Sudetes. *Prace geologiczno-mineralogiczne* **L VI**, Wyd. Wroclaw Univ., Wrocław, Poland.

Tajvidi, N. (1996) Characterization and some statistical aspects of univariate and multivariate generalized Pareto distribution. PhD Thesis, Lund Institute of Technology, Sweden.

Tokarczyk, T. & Adynkiewicz-Piragas, M. (2003) Drought in mountain catchments in Sudety region. *Publ. Zeszyty Naukowe, Akademia Techniczno-Humanistyczna*, Bielsko Biała, Poland.

Climate Variability and Change—Hydrological Impacts (Proceedings of the Fifth FRIEND World Conference held at Havana, Cuba, November 2006), IAHS Publ. 308, 2006.

Le dispositif PRESAGES: un ensemble d'outils pour la prévision des étiages

CLAIRE LANG[1], EMMANUEL GILLE[1], DIDIER FRANÇOIS[1] & JEAN-CLAUDE AUER[2]

1 *Centre d'Etudes Géographiques de l'Université de Metz, UFR SHA, Ile du Saulcy, BP 30306, F-57006 Metz cedex 1, France*
clair_lang@yahoo.fr

2 *Agence de l'Eau Rhin-Meuse, Rozérieulles, BP 30019, F-57161 Moulins-les-Metz, France*

Résumé Cet article présente un dispositif de prévision des débits d'étiage à long et moyen terme pour les cours d'eau du bassin Rhin-Meuse. Des modèles conceptuels mensuels et journaliers sont mis en œuvre. Le modèle mensuel permet un suivi de la situation hydrologique et des prévisions à long terme. Le modèle journalier n'est utilisé qu'en cas de risque annoncé d'étiage sévère, et repose sur l'analyse préalable du tarissement des cours d'eau.

Mots clefs étiage; modèle conceptuel; prévision; tarissement

PRESAGES: A collection of tools for predicting low flows

Abstract This article presents a device for long- and medium-term low flow forecasting for the rivers of the Rhine–Meuse basin. Monthly and daily conceptual models are implemented. The monthly model permits monitoring of the hydrological situation and the making of the long-term forecasts. The daily model is used only if a risk of severe low water levels is announced, and is based on the preliminary analysis of the recession periods.

Key words conceptual model; forecasting; low flow; recession

INTRODUCTION

Suite à l'étiage 2003, particulièrement sévère en France, le ministère français de l'Ecologie et du Développement Durable a incité les services de l'état à mieux anticiper les situations d'étiage sévère afin d'assurer une meilleure gestion de la ressource en eaux superficielles. A ce titre, l'Agence de l'Eau Rhin-Meuse a confié au CEGUM (Université Paul Verlaine, Metz) une étude intitulée PRESAGES (PREvisions et Simulations pour l'Annonce et la Gestion des Etiages Sévères) dont l'objectif est d'élaborer des outils de prévision des débits d'étiage.

Le CEGUM développe un dispositif qui évalue à l'échelle mensuelle les risques d'apparition d'un étiage sévère dès la fin de la période de hautes eaux. Dans le cas d'une sécheresse annoncée, des prévisions plus précises sont alors réalisées afin de répondre aux attentes des gestionnaires.

CONTEXTE ET MÉTHODES

Contexte de l'étude

Une soixantaine de stations dispersées sur l'ensemble du bassin Rhin-Meuse (dans sa partie française) sont retenues pour l'étude (Fig. 1). Les bassins versants dont les superficies s'échelonnent de 39 à 10 700 km^2 traversent des milieux variés, avec d'ouest en est une région de plateau, des zones de moyennes montagnes cristallines et gréseuses (Vosges) et la plaine d'Alsace. Cette diversité géographique induit des différences climatiques (les précipitations annuelles varient de 750 à 2200 mm) et physiographiques (bassins aux capacités aquifères plus ou moins importantes). Les cours d'eau de l'étude présentent des régimes analogues de type pluvial océanique, avec des hautes eaux hivernales, liées aux précipitations, et des basses eaux estivales qui s'expliquent par une augmentation des prélèvements évapotranspiratoires.

Si l'accentuation des prélèvements évapotranspiratoires justifie le creux estival observé dans le régime de ces cours d'eau, la sévérité de l'étiage s'explique par l'importance du déficit pluviométrique observé durant la période de recharge. Celle-ci s'étend généralement, pour nos bassins, de novembre à mars, puis, dès le mois d'avril, on passe à la période de vidange des nappes. Ainsi, les débits observés durant l'étiage sont dépendants de l'état des réservoirs au début de la période de vidange et de leur rythme de tarissement. Le régime des cours d'eau en période

Copyright © 2006 IAHS Press



Fig. 1 Localisation des stations de l'étude au sein du bassin Rhine–Meuse.

d'étiage est donc conditionné par les forçages atmosphériques et par les modalités de tarissement de la rivière.

Méthodes et outils

La genèse particulièrement longue des étiages permet un suivi de la situation hydrologique à l'échelle mensuelle. Les épisodes de tarissement font l'objet d'une analyse particulière car ils constituent un indicateur déterminant pour la prévision des débits d'étiage. PRESAGES constitue un enchaînement d'outils qui permettent de réaliser des prévisions à long et moyen terme. Dans ce contexte, nous montrons les difficultés associées à l'emboîtement d'outils utilisant des échelles de travail différentes, ainsi que les problèmes posés par l'échelle mensuelle.

Analyse du tarissement Un travail préalable a montré que la valeur du paramètre gérant le réservoir d'eau gravitaire ne peut être la même pour un modèle journalier et pour un modèle mensuel.

(a) Estimation de la vidange journalière: le tarissement représente "la décroissance des débits correspondant à la vidange des nappes en dehors de toute precipitation" (Roche, 1963). Une procédure automatique extrait, par cours d'eau, les phases de tarissement à partir de critères précis (Lang & Gille, 2005), puis les ajuste à la loi de Maillet. L'importante variabilité des coefficients de tarissement, pour un même cours d'eau, a nécessité la mise en œuvre d'un traitement statistique afin d'obtenir des valeurs fréquentielles des coefficients de tarissement.

(b) Estimation de la vidange mensuelle: l'estimation de la vitesse de vidange mensuelle des nappes est réalisée à partir de l'analyse de la pente des débits moyens mensuels du régime des cours d'eau. Cette démarche est évidemment discutable car les valeurs obtenues ne représentent en aucun cas la vidange des réservoirs car les précipitations et la recharge des aquifères sont intégrées dans le calcul. Néanmoins, les valeurs obtenues sont fortement corrélées aux coefficients d'immodération des cours d'eau, eux-mêmes en rapport avec la géologie des bassins. Pour des rivières soumises à un climat comparable, la pondération du régime est déterminée par des capacités aquifères plus ou moins importantes. Les valeurs obtenues ne correspondent pas uniquement à du tarissement et restent très globales, mais nous montrons plus loin qu'elles s'adaptent bien pour caler la vidange des modèles mensuels.

Contraintes et difficultés liées à la modélisation Le cahier des charges de l'étude impose la mise en œuvre de modèles conceptuels mensuels et journaliers, simples (parcimonieux) et transposables sur un tableur. En terme opérationnel, l'objectif est de produire des outils fonctionnels, modifiables par un utilisateur averti et pouvant s'insérer facilement dans les outils des services gestionnaires. Ces exigences amènent les réflexions et les choix suivants:

(a) Nous proposons d'affecter le coefficient de tarissement médian (voir analyse du tarissement) à la vidange du réservoir d'eau gravitaire. Cette opération a pour but de préserver une certaine représentativité des résultats et de proposer des valeurs fondées sur le fonctionnement hydrologique du bassin versant. Les autres paramètres des modèles sont optimisés.

(b) Difficulté de l'emboîtement des échelles de temps: pour les services gestionnaires, le modèle mensuel fonctionne de manière permanente sur cinq bassins indicateurs représentatifs des principaux aquifères du bassin Rhin-Meuse (alimentation et recalage du modèle chaque mois). L'objectif est d'alléger au maximum la procédure de suivi en temps et en coût des données. Le dispositif PRESAGES prévoit de mettre en œuvre le modèle journalier uniquement pour la période de basses eaux dans le cas d'un étiage sévère annoncé par l'approche mensuelle (sur les bassins indicateurs). La phase d'initialisation du modèle journalier est donc déterminante pour réaliser de bonnes prévisions à moyen terme. Il est donc important que les niveaux des réservoirs d'eau gravitaire des modèles mensuels et journaliers fonctionnent de manière compareable. Une bonne corrélation entre leurs niveaux respectifs facilite l'initialisation du modèle journalier.

(c) Particularité du pas de temps mensuel: si la modélisation mensuelle exige moins de données et permet des prévisions à long terme, elle pose certaines difficultés spécifiques. On constate ainsi que bien souvent, durant la période de basses eaux le modèle ne génère pas de recharge du réservoir d'eau gravitaire. La majeure partie des précipitations est gérée par le bilan hydrique et le reste par le ruissellement. L'absence de recharge durant toute cette période doit être compensée par un rythme de tarissement plus faible. L'estimation de la valeur à attribuer à ce paramètre, par l'observation de la pente du régime des cours d'eau, s'inscrit dans cette même réflexion. Les recharges sont inclues dans le calcul, mais la diminution est observée au pas de temps mensuel et non durant les phases de tarissement pur. Par conséquent les valeurs sont nécessairement plus faibles que celles issues de l'analyse du tarissement (Fig. 2).

Le choix des modèles Dans la bibliographie, on recense un nombre important de modèles à l'échelle journalière et mensuelle (Perrin, 2000). Notre choix s'est porté vers les algorithmes qui utilisent des coefficients de vidange des nappes comparables à ceux estimés préalablement (voir analyse du tarissement).

A l'échelle mensuelle, le modèle ORCHY (Outil de Représentation du Cycle HYdrologique, Gille & Lang, 2003) élaboré au CEGUM d'après Thornthwaite & Mather (in Alley, 1985) répond à cette préoccupation (Fig. 3(a)).

Pour l'échelle journalière, le modèle GR3j (Edijatno & Michel, 1989) est modifié pour respecter notre démarche d'"optimisation assistée". Celui-ci utilise initialement une vidange quadratique paramétrée par la capacité maximale du réservoir d'eau gravitaire. L'introduction d'un coefficient de vidange de nappe a nécessité l'ajout d'un réservoir à ruissellement différé (Fig. 3(b)) car avec un coefficient de vidange des nappes faible, le passage d'une crue à une phase de tarissement est trop brutal. Ces modifications permettent d'obtenir des hydrogrammes plus proches de ceux observés. Le modèle proposé nécessite six paramètres.

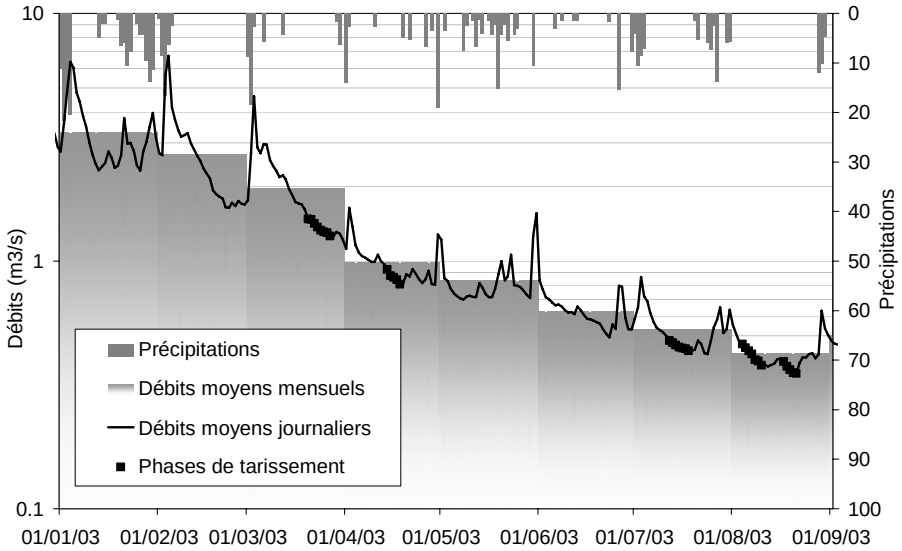


Fig. 2 Phases de tarissement et décroissance mensuelle des débits. L'échelle mensuelle globalise l'alternance des phases de tarissement et de recharge.

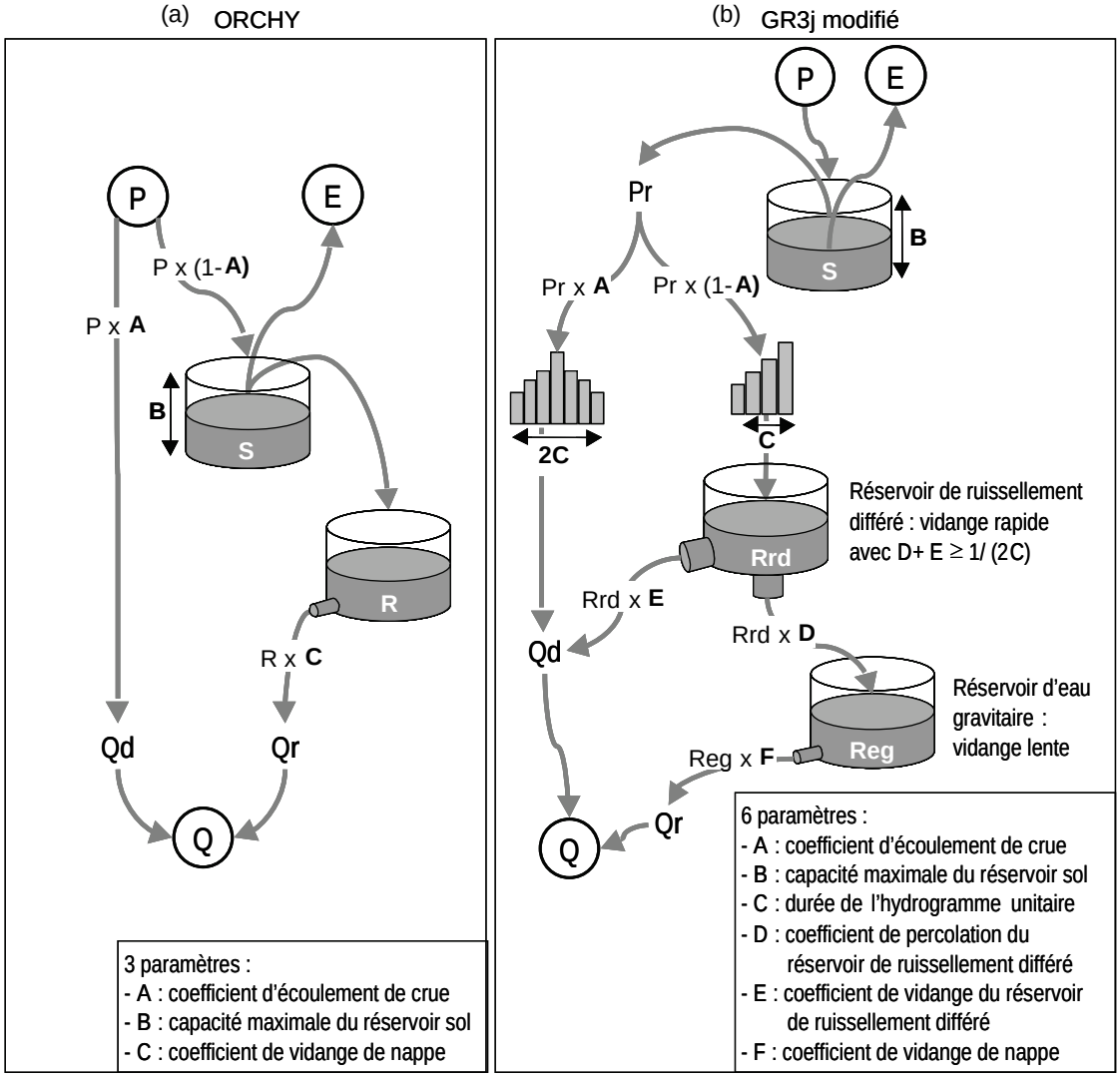


Fig. 3 (a) Architecture du modèle ORCHY (Gille & Lang, 2003). (b) Architecture du modèle GR3j modifié (Edijatno & Michel, 1989).

CALAGE ET APPLICATION DU DISPOSITIF PRESAGES À L'ÉTIAGE 2003

Calage des modèles

La période de calage s'étend de 1971 à 1990 et la période de validation de 1991 à 2000. L'année 2003 permet de tester le dispositif de prévision. Le critère de Nash est calculé à partir du logarithme des valeurs sur la période de validation.

A l'échelle mensuelle Le modèle ORCHY est calé de deux manières:

– seuls les paramètres *A* (coefficient d'écoulement de crue) et *B* (capacité maximale du réservoir sol) sont optimisés de manière itérative, *C* (coefficient de vidange de nappe) est égal à la valeur définie à partir du régime hydrologique du cours d'eau (voir analyse du tarissement);
– les trois paramètres *A*, *B* et *C* sont optimisés.

A l'issue du premier calage, plus des ¾ des stations ont un critère de Nash supérieur à 70%. Après optimisation des trois paramètres, cette proportion passe à 82% et plus d'1/3 présente un critère supérieur à 80% (Fig. 4). Bien qu'ils apparaissent globalement sous-estimés, les coefficients issus directement des régimes sont fortement corrélés avec les valeurs optimisées (Coefficient de détermination, R^2 = 73%). On retrouve une cohérence liée au caractère plus ou moins perméable des bassins versants. ORCHY présente donc des résultats tout à fait acceptables.

A l'échelle journalière A la différence du pas de temps mensuel pour lequel la détermination du coefficient de vidange est entachée d'incertitudes, les coefficients de tarissement journaliers constituent des valeurs fiables. L'optimisation n'a donc concerné que les cinq autres paramètres (Fig. 3(b)). Les performances du modèle proposé sont satisfaisantes car ¾ des stations présentent un critère de Nash supérieur à 70% (Fig. 4).

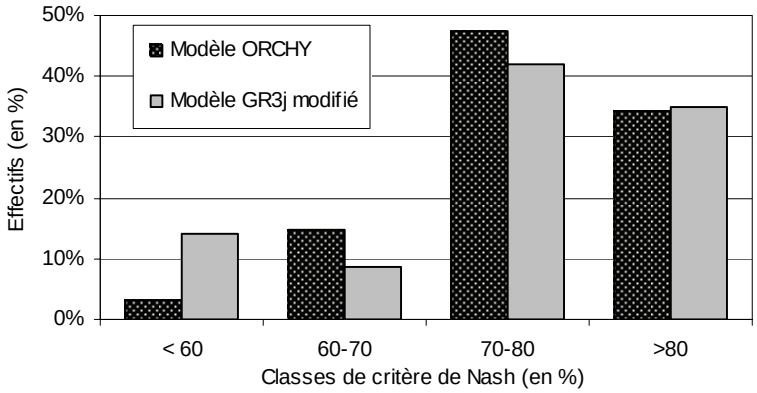


Fig. 4 Distributions des critères de Nash calculés sur le logarithme des débits de la période de validation (1991–2000).

Application à 2003 Le modèle mensuel est normalement recalé jusqu'au début de la période de basses eaux. En 2003, cette opération est inutile car ORCHY simule des valeurs proches des débits observés. A partir du mois de mai, il est alimenté par des pluies fréquentielles et une évapotranspiration potentielle moyenne. La Fig. 5 montre une estimation du débit en août inférieure au débit mensuel d'étiage de fréquence 1/10ème. Pour cet exemple, le modèle, alimenté par des pluies mensuelles biennales, annonce dès le mois d'avril une situation d'étiage sévère. Compte tenu de la fréquence de pluie utilisée, le risque est particulièrement élevé, justifiant la mise en œuvre conjointe du modèle journalier.

A l'échelle journalière, les prévisions s'appuient sur l'hypothèse d'une absence de précipitations, une évapotranspiration potentielle moyenne et sur trois valeurs de coefficients de vidange extraits de l'analyse statistique des tarissements (fréquences au non-dépassement 0.25, 0.5 et 0.75, Lang *et al*., 2006). L'intérêt réside à la fois dans la prise en compte de la situation la plus critique (absence totale de précipitations) et dans la proposition d'un rail de prévision (comparable à l'application du modèle MORDOR sur la Loire; Garçon & Lyaudet, 1999). Les niveaux des réservoirs ont été estimés à partir des données de débits journaliers du mois de mai. Si besoin, il existe une bonne corrélation entre les niveaux des réservoirs d'eau gravitaire des modèles journalier et mensuel (Coefficient de détermination, R^2 = 76%). Les paramètres de calage ne sont

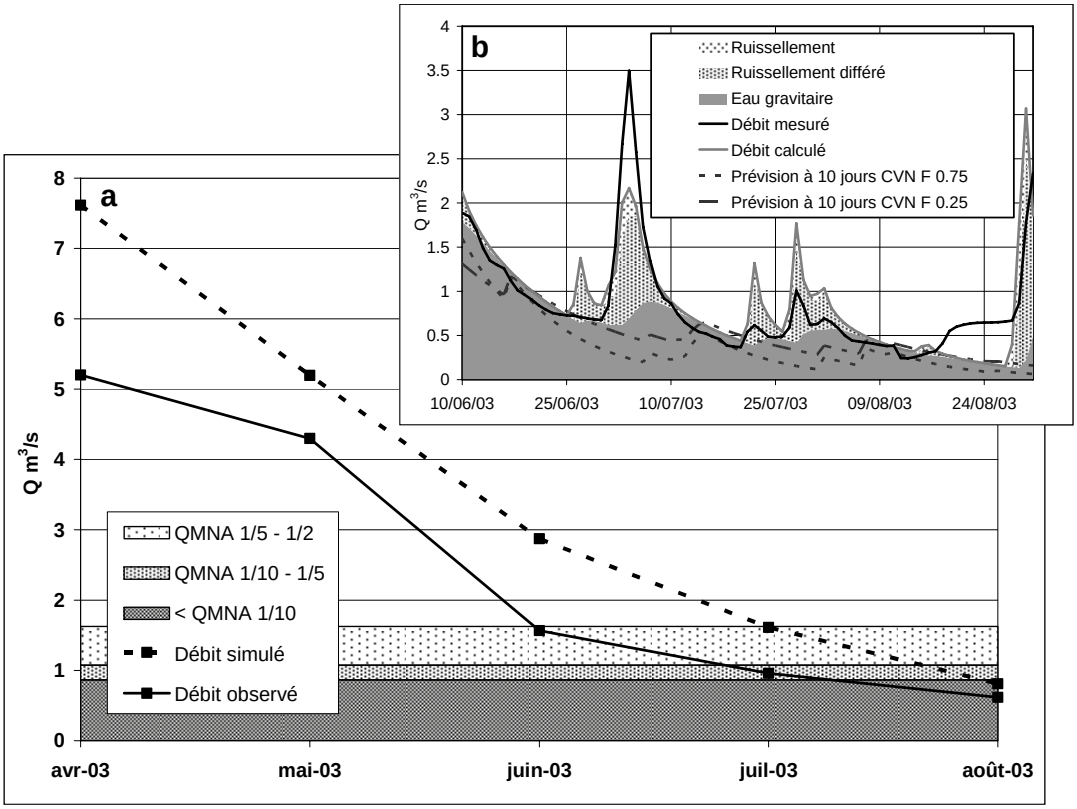


Fig. 5 Validation du dispositif: La Moselotte à Vagney pendant l'étiage 2003. (a) Modèle mensuel ORCHY, QMNA (débit mensuel d'étiage fréquentiels 1971–2000). (b) Modèle journalier GR3j modifié, CVN (coefficient de vidange de nappe de fréquence *F*).

pas modifiés. Sur la période présentée (juin–août 2003), une correction des valeurs de précipitations a été nécessaire pour se recaler après la petite crue du début du mois de juillet.

CONCLUSION

L'analyse des tarissements, peu développée dans cet article, a fait l'objet d'un travail spécifique à chaque station. La connaissance du rythme de vidange des aquifères est déterminante en période d'étiage et permet des prévisions fiables à moyen terme (10 jours maximum). Si la prévision mensuelle à long terme apparaît plus incertaine, elle présente néanmoins l'avantage d'une mise en œuvre moins contraignante qui peut être assumée par les services gestionnaires. Toutefois les outils présentés dans ce travail ne seront véritablement éprouvés que dans une situation de sécheresse hydrologique grave à venir. Il semble que le modèle journalier soit perfectible pour répondre aux conditions hydrométéorologiques particulières à un étiage sévère (type 2003). D'autre part, pour les cours d'eau drainant de grands bassins versants, les influences anthropiques doivent être prises en compte.

REFERENCES

Alley, W. M. (1985) Water balance models one month ahead stream flow forecasting. *Water Resour. Res.*, **21** (4), 597–606.

Edijatno, E. & Michel, C. (1989) Un modèle pluie-débit journalier à trois paramètres. *La Houille Blanche* **2**, 113–121.

Garçon, R. & Lyaudet, P. (1999) Exemple de prévision et de simulation opérationnelle des débits d'étiage pour les besoins d'EDF. *La Houille Blanche* **54**, 37–42.

Gille, E. & Lang, C. (2003) Problématique d'optimisation des paramètres de calage d'un bilan hydrologique: application aux bassins versants de la Sauer. *Mosella* **28**(1–2), 157–172.

Lang, C., Freyermuth, A., Gille, E. & François, D. (2006) PRESAGES: un outil pour évaluer et prévoir les étiages. *Géocarrefour* **81** (à paraître)**.**

Lang, C. & Gille, E. (2005) Une méthode d'analyse du tarissement des cours d'eau pour la prévision des débits d'étiage. Actes du colloque Les rencontres de Géo13: Le risque hydrologique du concept à sa gestion, Villetaneuse, 28 octobre 2005.

Perrin, C. (2000) Vers une amélioration d'un modèle global pluie-débit au travers d'une approche comparative. Thèse de doctorat, Cemagref, Antony, France.

Roche, M. (1963) *Hydrologie de surface*. Gauthier-Villars Editeur, Paris, France.

Climate Variability and Change—Hydrological Impacts (Proceedings of the Fifth FRIEND World Conference held at Havana, Cuba, November 2006), IAHS Publ. 308, 2006.

Multi-model technique for low flow forecasting

MARY-JEANNE ADLER & VALENTINA UNGUREANU

National Administration "Apele Romane" – National Institute of Hydrology and Water Management, 97 Sos Bucuresti-Ploiesti, Sector 2, Bucharest, Romania

adler@hidro.ro

Abstract In forecasting low flows, four models, two determinist-statistic models (the VIDRA Model and a modified Stanford Model), a statistical model based on hydrometeorological analogues and an ARIMA class of model, were used to simulate the non-stationary and seasonal nature of the monthly flows. The result obtained was a large range of forecasted values which required a procedure in order to reach a decision on the most appropriate forecast. A solution was found in the development of a packet of procedures including both forecasting models and a decision procedure. This procedure is weight-based and uses the model errors on the last time step in its computing, so that with the help of model-weighting it is possible to incorporate in the procedure those models which best match the actual data (multi-model results optimization procedure).

Key words low flow forecast; multi-model procedure; forecasting decision support

INTRODUCTION

In hydrological forecasting, some of the problems that can occur in real time are a lack of information necessary to the model (problems of data transmission), errors of measurement or errors of representation of the variables, and a particular situation that cannot be simulated with good results by the model.

So the hydrologist has to perform several operations, each with some hazards, and so he needs good software which should include both forecasting models and a decision procedure. Given these tools, the forecaster will have more time to look for supplementary data and make a better analysis of the existing situation. The reduction of subjectivity and a better understanding of the situation will lead to improved forecasting.

MULTI-MODEL DECISION PROCEDURE

A simple description of the problem is given below.

- There are several forecast models available.
- It is presumed that each model checks a group of hypotheses.
- The forecast quality of each model is only guaranteed if it checks these hypotheses.
- In real time it is not possible to check all the hypotheses.
- The relative quality of the results of various models depends on the situation (operating configuration) of the system at the time.

The simple real-time estimating procedure for the weight given to each model presumes that the errors registered on the last time steps allow construction of an operating configuration available for the given moment and different from the normal operating configuration of the system. This procedure uses the model errors on the last time step in its computing so that, with the help of model-weighting, it is possible to incorporate into the procedure those models which best match the actual data (Roche & Tamin, 1986a,b; Roche & Torterotot, 1987).

The formula to compute the weighting is:

$$W_k = (e_k^2)^{-1} / \Sigma_{j=1}^{m} (e_j^2)^{-1}$$

where m is the number of models used for low flow forecast and e_k is the forecast error of the kth model. The sum of all models' weights is $\Sigma_{k=1}^{m} W_k = 1$.

LOW FLOW FORECASTING

The major objective in modelling the hydrological behaviour of a watershed is to simulate its streamflow hydrograph in response to an input of precipitation. To accomplish this, the hydrological cycle is analysed and expressed as a collection of mathematical formulations based on

Copyright © 2006 IAHS Press

rational parameters that may be adjusted after trial simulations with known input and output. This may be continued until the model is judged to be an adequate representation of the hydrological cycle for a study area – for low flows in our case. The test gauging station was Bals on the Oltet River, in an endemically droughty area of the southeastern part of Romania. The applied models were calibrated using the climatic series of monthly data 1960–1990 and validated on the 1991–2004 period. An excessively droughty period during the vegetation growth period was identified in 1994. Using this critical period, imposing high precision in forecasting low flows, the multi-model methodology was tested.

Deterministic-statistical model

The deterministic-statistical model simulates separately the two main components of the monthly mean discharge: the mean pluvial discharge and the base flow (Q_b).

The base flow is forecast using the recession curve during low flows:

$$Q_b = \frac{1}{T}\int_0^T Q_0 \times \mathrm{e}^{-\alpha \times t}\,dt = \frac{Q_0}{\alpha \times T}\left(1 - \mathrm{e}^{-\alpha \times T}\right)$$

where T is the number of days of the considered month, Q_0 is the initial value at the beginning of each month and α the recession coefficient. The α parameter is a function depending on Q_0:

$$\alpha = \frac{\ln Q_0 - \ln Q(t)}{t}$$

For each basin the $\alpha = f(Q_0)$ relations are calculated for each month or groups of months. In this case, two distinct cases were found, see Table 1.

Table 1 The recession parameters for each characteristic interval.

Q_o ($m^3 s^{-1}$)	a (10^{-2} day^{-1})		Q_o ($m^3 s^{-1}$)	a (10^{-2} day^{-1})	
Month	VI–VIII	IX–XI	Month:	VI–VIII	IX–XI
1	5.6	3.2	6	8.1	5.1
2	6.3	3.9	7	8.3	5.3
3	6.9	4.5	8	8.6	5.4
4	7.3	4.7	9	8.8	-
5	7.8	4.9	10	8.9	-

For a forecasting condition Q_0 is known and the coefficient α is determined from Fig. 1 and using the equation for Q_b, the monthly mean discharge of the base flow is calculated.

In order to determine the contribution of precipitation to the mean discharge (Q_p) a multiple regression was used for each month giving: $Q_P = f(Q_0,P)$; Fig. 1(a) and (b).

A long-term meteorological forecast is usually a qualitative one (excessively droughty period, drought, normal droughty period, and similar for rainy periods. The transformation into numeric values was obtained using the frequency of the mean precipitation in the basin, and associating a probabilistic interval to each forecast indication:

– excessive drought p = 90–95%
– drought p = 80–90%
– normal drought p = 60–80%
– normal rainy p = 20–40%
– rainy p = 10–20%
– normal rainy p = 5–10%

The rainy interval is obtained for each meteorological forecast from the probability curve of each basin; an example is given for Bals - Table 2.

Finally, the forecast discharge (Q_F):

$$Q_F = Q_b + Q_P$$

is calculated taking the superposition of the effects of the mean monthly discharge into consideration. An application of this model is presented in Table 3.

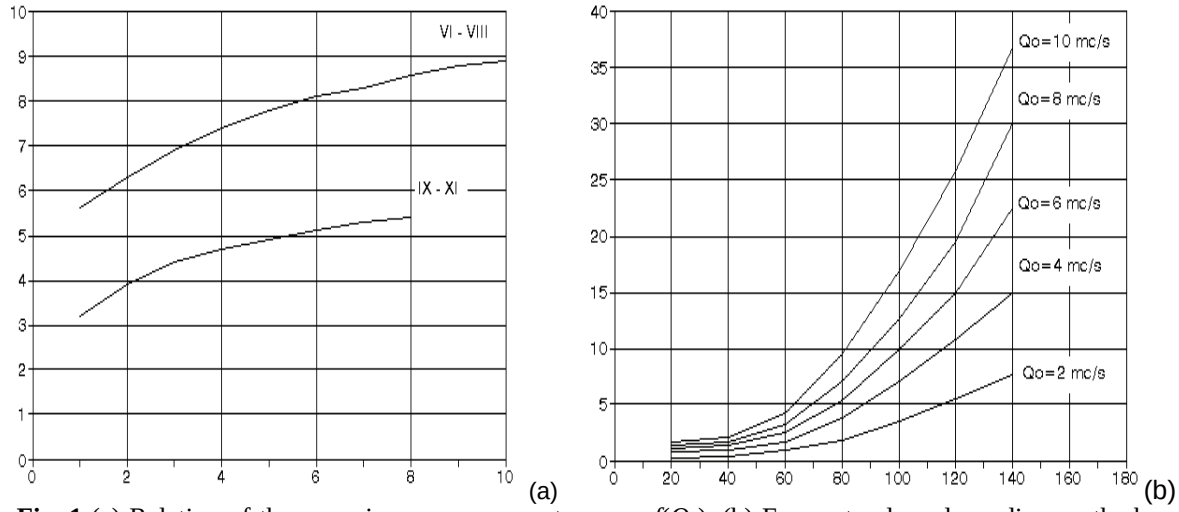


Fig. 1 (a) Relation of the recession curve parameters, $a = f(Q_0)$. (b) Forecast values depending on the base discharge and precipitation $Q_p = f(Q_0,P)$ (Bals application).

Table 2 Monthly precipitation for Bals.

No.	*P* (%)	VI	VII	VIII	IX	X	XI
1	10	155	130	117	100	100	108
2	20	135	104	88	76	63	86.5
3	50	94	65	50	39	42	55
4	80	60	38	27	35	19.5	29
5	90	45	28	17.8	6.4	9	19.5

Table 3 The mean monthly forecasted discharges during the summer-autumn period for the excessively droughty year 1994.

Month	*P* (mm)	Q_o ($m^3 s^{-1}$)	a (10^{-2} zi^{-1})	Q_b ($m^3 s^{-1}$)	Q_P ($m^3 s^{-1}$)	Q_F ($m^3 s^{-1}$)	Q_{obs} ($m^3 s^{-1}$)
VI	20.0	3.36	7.5	1.03	2.0	3.03	3.61
VII	17.1	3.36	6.9	1.86	1.5	3.36	3.18
VIII	59.8	1.86	6.9	0.784	0.25	1.09	1.19
IX	4.00	0.03	3.0	0.020	0.20	0.22	0.474
X	68.4	1.86	6.9	0.784	1.00	1.78	2.98
XI	7.84	1.70	4.5	0.820	0.20	1.02	1.71

Model using hydrometeorological analogues

The forecasting model based on the hydrometeorological analogues presumes the follow stages:

- the definition of the characteristic scale, of the quantitative and/or qualitative variables, determining the analogy with an anterior stage;
- the definition of the position in the space of characteristics in the forecasting moment;
- the search of an analogue position using the theory of shapes.

The forecasting algorithm estimates two tendencies:

- a regime tendency using the hydrological information only,
- a regime tendency using the information from the analogue years from the meteorological point of view furnished by the meteorological prevision (Matreata, 1997).

The first tendency (C_h) is obtained using the percentage from the mean multi-year discharge (Q_{mean}) of the forecasted discharge (Q_F): $C_h = Q_F^j / Q_{mean}^j$.

The mean monthly forecast discharge Q^j_F is obtained from the annual hydrograph of droughty type (dimensioned by the mean annual discharge: Q^j_{mean}) or excessively droughty type for the physico-geographical space of interest and re-dimensioned using the mean annual forecast discharge Q^j_{meanF}, Fig. 2.

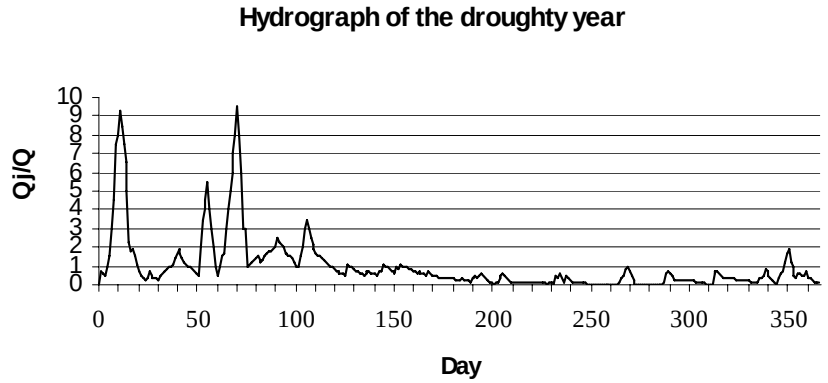


Fig. 2 Hydrograph of the droughty year for the Oltet Basin (regional analysis).

The estimation of the second tendency is based on the evolution of the mean monthly discharges from the meteorological analogue year ($N_{analogs}$), for each month, using the relation:

$$C_m = \frac{\frac{1}{N_{ana\log s}\sum_{i=1}^{N} Q_i^j}}{Q_{mean}^j}$$

where Q^j_i is the monthly mean discharge of the *j*th month from the *i*th analogue year from the meteorological point of view. The droughty analogue characteristic years were determined using the deciles method.

The final forecast is obtained using the equation:

$$Q_F = (0.6C_h + 0.4C_m) \cdot Q_{mean}^j$$

An example of such a calculation is presented below. The mean annual discharge forecast using ARMA (1,1) was 2.86 $m^3 s^{-1}$ and the computed monthly low flows are presented in Table 4.

Table 4 The forecasted low flows using the hydrometeorological analogue model.

Year	Month	Q^j_{analog}	Q^j_{mean}	Cm	Q^j_F	C_h	Q_F	Q_{obs}
1994	VI	5.77	4.53	0.676	4.03	0.473	3.12	3.61
	VII	1.66	4.28	0.200	1.23	0.148	3.80	3.18
	VIII	1.02	3.38	0.302	0.532	0.157	0.727	1.19
	IX	0.922	2.02	0.456	0.406	0.201	0.624	0.474
	X	1.67	2.06	0.811	0.669	0.325	1.50	2.98
	XI	2.30	3.66	0.628	0.947	0.259	1.49	1.71

Stochastic models used for the mean monthly discharges during low flow period

The non-stationary and seasonal nature of the monthly flows is modelled using the ARIMA class of models. A step-by-step procedure was used to obtain valid models through proper model identification, parameter estimation, performance evaluation, model parsimony and validation of the residuals. In building the model it was especially important to obtain the parsimonious models with white residuals. The procedure was applied to the monthly flows of the River Oltet at Bals and a valid model capable of acceptable prediction results was obtained: ARIMA (2,1,1). The forecast monthly mean discharges (Q_F) and the observed ones (Q_{obs}) are presented in Table 5.

Deterministic model for the mean monthly low flows forecast

The model used was VIDRA, a reservoir model similar to the Stanford Watershed Simulation Model (Crawford & Linsley, 1966; Corbus & Adler, 2004), a mathematical model programmed for a PC, synthesizing a continuous hydrograph (watershed outflow *vs* time) of streamflow from climatic data (precipitation and evaporation) and watershed parameters (soil surface moisture and

Table 5 The mean monthly forecasted discharges using the ARMA Model.

Year	Month	Q_F ($m^3 s^{-1}$)	Q_{obs} ($m^3 s^{-1}$)
1994	VI	3.40	3.80
	VII	3.13	3.26
	VIII	1.25	1.26
	IX	0.65	0.550
	X	2.80	3.20
	XI	1.98	2.02

retention properties, interflow storage and flow conditions, groundwater storage and flow conditions, and the physical state and geomorphic properties of the basin).

The computer program was carefully studied, flow diagrammed in detail and an adequate calibration for low flows was obtained, using mainly the facilities of the multiple recession constants: CB, infiltration index; LZSN, soil moisture storage index; UZSN, soil surface moisture index; K24L, parameter indicating groundwater flow leaving the basin; KK24, daily base recession constant; and GWF, base flow, determined for low flow period calibration of the model.

The 1990–1993 period was used for calibration and the low flow period June–November 1994 was forecast (Table 6).

Table 6 The mean monthly forecasted discharges using the Stanford Model.

Year	Month	Q_F ($m^3 s^{-1}$)	Q_{obs} ($m^3 s^{-1}$)
1994	VI	3.80	3.50
	VII	3.26	3.20
	VIII	1.26	1.50
	IX	0.55	0.900
	X	3.20	3.00
	XI	2.02	1.59

RESULTS FOR THE MULTI-MODEL REAL-TIME DECISION PROCEDURE IN THE HYDROLOGICAL FORECAST

The multi-model procedure for low flow forecasts was applied for the four models presented. As the forecast errors of the four models for May are unknown, the value for June, the first month of the forecasted interval, was considered to be the same for all models ($e_k = 1.00$, where $k = 1,2,3,4$). In this case, the weight of each k model was calculated with the weight formula $w_k = (1/(1+1+1+1)) = ¼ = 0.25$ and the forecast mean monthly discharge for June is:

$$Q_F^{VI} = 3.03 \times 0.25 + 3.12 \times 0.25 + 3.80 \times 0.25 + 3.50 \times 0.25 = 3.36$$

In July, the forecast errors of the four models for June was calculated and those values have been used to compute the weight of each model as in the following example: measured discharge in June – 3.61 $m^3 s^{-1}$, deterministic-statistical model – 3.03 $m^3 s^{-1}$, hydrometeorological analogues method – 3.12 $m^3 s^{-1}$, stochastic model ARIMA – 3.80 $m^3 s^{-1}$, Stanford model – 3.50. The forecast errors in June were as follows: –16.066%, –13.573%, 5.263%, –3.047%. The weights of the models computed for July were:

$$w_1 = [(-16.066)^2]^{-1}/\{[(-16.066)^2]^{-1} + [(-13.573)^2]^{-1} + [(5.263)^2]^{-1} + [(-3.047)^2]^{-1}\} = 0.0253$$

and similarly the rest of the weights were obtained, $w_2 = 0.0354$, $w_3 = 0.2358$, $w_4 = 0.7035$. The forecasted value using the multi-model procedure for July, is:

$$Q_F^{VII} = 3.36 \times 0.0253 + 3.80 \times 0.0354 + 3.26 \times 0.2358 + 3.20 \times 0.0253 = 3.24.$$

A similar procedure was applied for August, September, October and November. The results are presented in Table 7 and in Figs 3 and 4.

The results obtained show clearly the usefulness of the application of the multi-model procedure in providing an increase in the precision of forecast values.

Table 7 Observed discharge, calculated discharges (Q_C), forecast values (Q_F) and errors (Er) provided by each of the four models and by the multi-model procedure, for the six month period, June–November 1994.

Month	Observed discharge	Determinist-statistic model (1)		Hydromet. analogues method (2)		Stochastic model ARMA type (3)		Stanford type model (4)		Multi-model procedure (mm) (5)	
	($m^3 s^{-1}$)	Q_{C_3} ($m^3 s^{-1}$)	Er (%)	Q_{C_3} ($m^3 s^{-1}$)	Er (%)	Q_{C_3} ($m^3 s^{-1}$)	Er (%)	Q_C ($m^3 s^{-1}$)	Er (%)	Q_{F_3} ($m^3 s^{-1}$)	Er (%)
VI	3.61	3.03	–16.07	3.12	–13.57	3.80	5.26	3.50	–3.05	3.36	–6.86
VII	3.18	3.36	5.66	3.8	19.50	3.26	2.52	3.20	0.63	3.41	7.08
VIII	1.19	1.09	–8.40	0.727	–38.91	1.26	5.88	1.50	26.05	1.48	24.42
IX	0.474	0.220	–53.59	0.624	31.65	0.550	16.03	0.900	89.87	0.46	–3.14
X	2.98	1.78	–40.27	2.5	–16.11	3.20	7.38	3.00	0.67	2.79	–6.50
XI	1.71	1.02	–40.35	1.49	–12.87	2.02	18.13	1.59	–7.02	1.59	–6.82

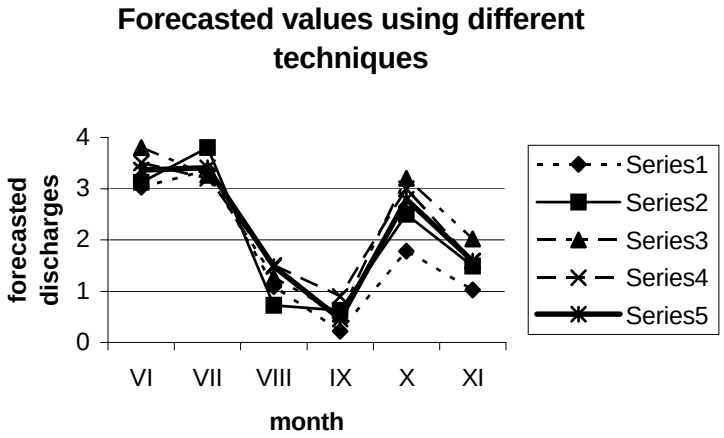


Fig. 3 Forecast of discharges using four mathematical models and the multi-model procedure.

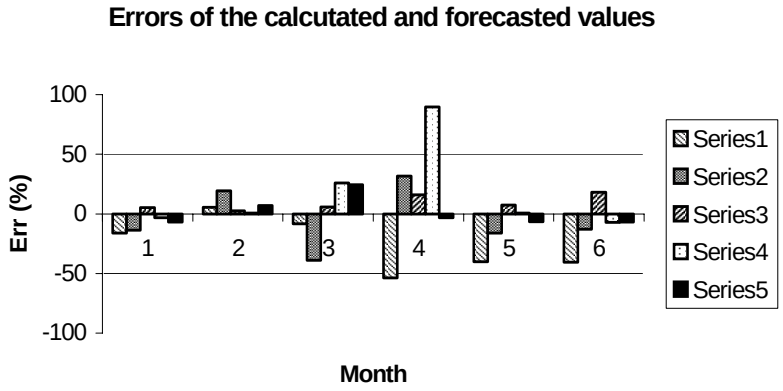


Fig. 4 Representation of the forecasting errors of the four mathematical models and of the multi-model procedure.

CONCLUSIONS

Four models were used for low flow forecasting for the extreme droughty period June–November 1994. The models which best match the data are the stochastical model and the Stanford model. The multi-model approach ameliorates the forecast; in these five months the forecasted errors are less then 10%. The multi-model procedure is very efficient. The weights of the model which had provided the worst result in a given month diminish the influence of that forecasted value on the following month, while for those giving better results, the weights increase their contribution to the forecasted value for the following month. The multi-model procedure increased the

performance of the forecasts and it is for this reason that we recommend it for application in operational activity.

REFERENCES

Crawford, N. H. & Linsley, R. K. (1966) *Digital simulation in hydrology: Stanford Watershed Model IV*. Technical Report 39, Department of Civil Engineering, Stanford University, Palo Alto, California, USA.

Cavadias, G. & Morin, G. (1985) Amélioration des performances des modèles hydrologiques par combinaison des débits simulés. *Revue internationale des sciences de l'eau* **1**(1/4), 12–28.

Makridakis, S. & Wincler, R. L. (1983) Average of forecast: some empirical results. *Manage. Sci*. **29**, 42–46.

Matreata, M. (1997) Dinamico-statistic model for low flows. *Studii de hidrologie*, INMH, 24–37.

Newbold, P. & Granger, C. W. J. (1974) Experience with forecasting univariate time series and the combination of forecasts. *J. Royal Statist. Soc*. A **137**, 57–69.

Roche, P. A. & Tamin, R.(1986) Procédures de décision en temps réel pour la prévision des crues. CERGRENE.

Roche, P.A., Torterotot, J. P. (1987) Prévision des crues sur la Haute-Garonne. Utilisation d'une procédure Multi-Modèles. Méthodologie et critique des données. CERGRENE.

Climate Variability and Change—Hydrological Impacts (Proceedings of the Fifth FRIEND World Conference held at Havana, Cuba, November 2006), IAHS Publ. 308, 2006.

Seasonal forecasting of river flows: a review of the state-of-the-art

JENNIFER EASEY[1], CHRISTEL PRUDHOMME[1] & DAVID M. HANNAH[2]

1 *Centre of Ecology and Hydrology, Wallingford, Oxfordshire OX10 8BB, UK*
chrp@ceh.ac.uk

2 *School of Geography, Earth and Environmental Sciences, University of Birmingham, Edgbaston, Birmingham B15 2TT, UK*

Abstract This paper reviews the state-of-the-art in seasonal forecasting of river flows. Most previous studies have used statistical methods, which been shown to be more reliable than dynamical approaches. However, empirical techniques have limitations; and successful applications of downscaled GCM data show that this approach may also have potential for seasonal forecasting of hydrology.

Key words dynamical models; downscaling; GCMs; river flow; seasonal forecasting; statistical models; UK

INTRODUCTION

The scientific challenge of seasonal forecasting of river flows has clear societal relevance because forecasts have the potential to inform the operational management of water systems as varied as reservoir control for hydro-electric power generation, flood alleviation or agricultural irrigation schemes (Wedgbrow *et al.*, 2002). Moreover, river flow forecasting helps increase human preparedness in anticipating water-related hazards (e.g. floods or droughts).

Associations between river flow and atmospheric/oceanic indicators have been shown in many parts of the world: Costa Rica (Krasovskaia *et al.*, 1999), USA (Dracup & Kahya, 1994; Ely *et al.*, 1994), Australia (Abawi & Dutta, 1998; Kiem & Franks, 2001), Germany (Stahl & Demuth, 1999), and Spain (Trigo *et al.*, 2004). Nonetheless, most seasonal forecasting studies have focused on climatic variables, particularly precipitation (Washington & Downing, 1999; McGregor & Phillips, 2004). Eshel *et al.* (2000) achieved statistically significant forecasts of meteorological droughts in the Eastern Mediterranean at up to 13 months lead time. Yet, Wilby (2001) has suggested better forecasts may be possible for river flow than for precipitation because of the delays and combination effects between precipitation and groundwater discharges. Seasonal forecasting studies have also largely been confined to tropical regions, possibly because of the predictability of the El Niño Southern Oscillation (ENSO) and the impacts of ENSO events (Mason *et al.*, 1999; Goddard *et al.*, 2001). However, growing evidence suggests that seasonal river flows of more northern extratropical regions may be predictable (Trigo *et al.*, 2004; Wilby *et al.*, 2004; Svensson & Prudhomme, 2005).

This paper aims to review the state-of-the-art in seasonal forecasting of river flows and the skills associated with different techniques by investigating their applications to different regions of the world, including the UK.

STATISTICAL METHODS

Empirical models are developed from historical data to find statistically significant relationships between one or more predictors and the target variable of interest (e.g. river flow or precipitation). Linear regression techniques are most commonly used (Table 1). Svensson & Prudhomme (2005) used multivariate regression for two regions of Great Britain (i.e. the Southeast and Northwest) to predict summer river flow anomalies using eight predictors from winter river flow, airflow indices, sea surface temperatures (SSTs) and temperature differences. The models explained 55% (61%) of the variance in river flow in the Northwest (Southwest). Prediction of extreme flows was more skilful than for intermediate flows. Similarly, Wilby (2001) found that the winter North Atlantic Oscillation (NAO) explained 40% of the variance in August river flow of three UK rivers. For the River Thames (UK), Wilby *et al.* (2004) reported the greatest variance explained in flows for August (46%) and summer months (35%) using winter geopotential height, mean sea level pressure (MSLP), SSTs and sea ice concentrations (SIC).

Copyright © 2006 IAHS Press

Table 1 Summary of studies using statistical methods to predict river flow.

Region	Method	Predictand	Most significant predictor(s)	Reference
UK	Stepwise linear regression	Monthly mean river flow	500 hPa Geopotential height, Bering Sea ice concentration and Madeira MSLP	Wilby *et al.* (2004)
UK	Regression	Summer monthly mean river flows	Winter NAOI	Wilby (2001)
UK	Regression	Regional mean summer river flow	SST and temperature differences between different regions of the North Atlantic	Svensson & Prudhomme (2005)
UK	Expert System	Summer river flow	Geopotential heights, SIC, MSLP, SST, Central England Temperature and Arctic Oscillation Index	Wedgbrow *et al.*(2005)
Australia	Categorical composites	December–May river flow	ENSO indices	Kiem & Franks (2001)
Australia	Categorical composites	August–February river flow	Southern Oscillation Index	Abawi & Dutta (1998)

A classification approach was used by Kiem & Franks (2001) whereby annual, December to May average river flows in Australia were grouped according to the ENSO index. Using a *t*-test, the mean flow of each group (defined as El Niño, La Niña or Neutral) was shown to be significantly different. Future river flow forecasts could be made based upon the past mean flow of the group corresponding to the ENSO forecast. Similar results were found by Abawi & Dutta (1998) who also studied the impact of ENSO on spring and summer (August to February) stream-flow in Australia. Forecasts were possible several months in advance based on phases of the Southern Oscillation Index (SOI).

An Expert System (ES) was used by Wedgbrow *et al.* (2005). The aim of ES is to classify the target variable (i.e. predictand) according to predictor value and then to create a set of rules for prediction in the form of a decision tree comprising of "IF…THEN" statements. This method has been applied to summer river flows in the River Thames (UK) using seven variables including geopotential heights, SIC, MSLP and SST. Initial results showed a success rate of 79% and 89% for August and summer river flow, respectively (Wedgbrow *et al.*, 2005).

Many statistical studies for the UK focus upon the forecast of summer river flows from winter indicators because water resources are under greatest demand and stress at this time (Wedgbrow *et al.*, 2002). For example, Wedgbrow *et al.* (2002) explored the relationship between monthly river flows (June to November) with atmospheric and oceanic indices, and found the most significant correlations occurred in the summer months whilst there were few to no correlations in September, October and November. This reveals that river flow forecasting skill may be weaker in winter than summer.

DYNAMICAL MODELLING

Currently the most reliable tools for seasonal forecasting are statistical; but potential for reliable dynamical forecasts is great (Table 2; Zwiers & Von Storch, 2004). Dynamical based forecasts involve the integration of General Circulation Models (GCMs) that represent atmospheric, oceanic, land surface and hydrological interactions and processes as a set of mathematical equations. GCMs are started with a set of initial conditions, which are run through the equations and solved every few minutes at a large number of grid points covering the Earth. Observational data are incorporated into the GCMs using Data Assimilation Systems (DAS). DAS have allowed the development of large climatic data sets, such as the NCEP/NCAR[1] re-analysis and ECMWF[2] ERA-15 and ERA-40. The latest data set (ERA-40) is based on a re-analysis of meteorological observations from 1957 to 2002, providing 45-year records for a large number of meteorological variables (Uppala *et al.*, 2005). The outputs from re-analyses can be used to explore GCM limitations and potential. For example, ERA-15 precipitation data were tested for their ability to represent observed river runoff in the Aral Sea Basin, Central Asia (Schar *et al.*, 2004). The results showed that December–April precipitation was significantly correlated (r = 0.92) with observed

[1] National Centres for Environmental Prediction/National Centre for Atmospheric Research
[2] European Centre for Medium Range Weather Forecasts

Table 2 Summary of studies using dynamical models to predict river flow.

Region	GCM model	Downscaling	Reference
Northeastern Brazil	Hadley Centre LDA model	Linear regression	Galvao *et al.* (1999)
USA	NCEP/NCAR reanalysis	Stepwise, multiple linear regression and RCM (RegCM2)	Wilby *et al.*(2000)
USA	NCEP Medium Range Forecast	Pacific Northwest National Laboratory RCM	Leung *et al.* (1999)
South Africa	Centre for Ocean-Land-Atmosphere Studies T30	Canonical correlation model	Landman *et al.* (2001)
Asia	ERA-15	None	Schar *et al.* (2004)

May to September river discharge; and it was concluded that a reliable river flow forecasting system may be possible using real-time precipitation data from an operational DAS.

The atmospheric–oceanic system is chaotic. As a result, dynamical model runs made with small, random perturbations in input data may produce a different output than without perturbations (Harrison, 2005). To overcome this, multiple (ensemble) runs are made with slightly different initializing conditions to capture the climatic variability from a range of possible outcomes. However, Palmer *et al.* (2004) argued that because of the uncertainty in the GCM equations, runs with a single GCM are not reliable and ensembles should consist of a number of runs from GCMs developed at different research centres, to provide a more representative sampling of possible equation sets. DEMETER[3] is one such project which aims to synthesize data from a multi-model ensemble (Palmer *et al.*, 2004).

Data outputs from GCMs can be used to forecast river flow by driving rainfall–runoff models. Leung *et al.* (1999) simulated streamflow in the Columbia River, USA, using data from the NCEP Medium-Range Forecast (MRF) GCM as input to a rainfall–runoff model. Modelled peak flow in January and February overestimated observations, which was attributed to an overestimation of atmospheric warming driving snowmelt. This weak forecast skill could be due to limitations in physical representation and the coarse spatial resolutions used by GCMs.

DOWNSCALING

GCMs operate at a resolution in the order of 2.5 to 5° latitude and longitude (Barry & Chorley, 1998). To be useful in hydrological forecasting, data need to be of a finer resolution (~0.2° latitude by longitude) to represent regional climate and river flow variations between drainage basins (Wilby *et al.*, 2000). Two techniques were developed to address this issue: Regional Climate Models (RCMs) and Statistical Downscaling (SD).

Regional climate models simulate atmospheric processes similar to GCMs but at a resolution of 20–50 km; thus, they are more accurate than GCMs at representing climate features induced by land surface variations, such as orographic precipitation (Wilby *et al.*, 2000). When Leung *et al.* (1999) used the Pacific Northwest National Laboratory (PNNL) RCM outputs to simulate stream flow in the Columbia River basin (USA), they found the results were consistently better than using the MRF GCM.

Statistical downscaling methods aim to specify the local, river basin-scale predictand (e.g. precipitation) from a synoptic-scale predictor (e.g. MSLP or geopotential height). These methods include: regression analyses, weather-type classifications and artificial neural networks (Wilby & Wigley, 1997; Feddersen & Andersen, 2005).

Wilby *et al.* (2000) compared the use of SD (step-wise multiple linear regression) and an RCM[4] to downscale NCEP/NCAR re-analysis data to simulate discharge in the Animas River Basin, Colorado (USA). The results showed that both SD and RCM outperformed re-analysis data. SD was the best overall technique explaining 78% of the variance in discharge, compared with 69% for RCM. However, SD showed a bias of –22% whilst RCM showed a bias of only –11%. From these results, Wilby *et al.* (2000) concluded that modelled processes are sensitive to the choice of downscaling technique.

[3] Development of a European Multi-model Ensemble system for seasonal to inTERannual prediction
[4] RegCM2 from the Project to Intercompare Climate Simulations in the USA

DISCUSSION

Theoretically, dynamical approaches should be able to outperform statistical approaches to seasonal forecasting of river flows because of their ability to model climate processes and interactions (Van Oldenborgh *et al.*, 2005). However, in practice, errors and uncertainties in models mean that this is not yet the case. Dynamical models are also more complex and computationally intensive than statistical methods (Goddard *et al.*, 2001). In comparison, statistical methods are based on unrealistic assumptions of stationarity (Wedgbrow *et al.*, 2005). Although this problem can be overcome by continually updating data sets in order to monitor and, if necessary, refine model performance (Washington & Downing, 1999, Zwiers & Von Storch, 2004), there are still limitations caused by the co-linearity or dependence of the predictors in multiple regression analyses. For example in their study, Svensson & Prudhomme (2005) noted co-linearity between temperature differences used as predictors of river flow, and they were able to adjust their methods accordingly to avoid instability in the regression equation.

An alternative method would be to combine both statistical and dynamical techniques to improve river flow forecasts. Downscaling techniques applied to GCM outputs could be used to provide information that could in turn be used in a conceptual hydrological model. This is a promising route as experimented by the University of Washington Hydrology Group[5], Galvao *et al.* (1999), Leung *et al.* (1999) and Wilby *et al.* (2000). However, further research into the potential of combined forecasting approaches is required.

REFERENCES

Abawi, G. Y. & Dutta, S. C. (1998) Forecasting of streamflows in NE-Australia based on the Southern Oscillation Index. In: *International Conference on Engineering in Agriculture, 27-30 Sept.* Proc. Univ. of Western Australia, Perth, Western Australia, Australia.

Barry, R. G. & Chorley, R. J. (1998) *Atmosphere, Weather and Climate*. Routledge, London.

Dracup, J. A. & Kahya, E. (1994) The relationships between US streamflow and La Nina events. *Water Resour. Res.* **30**, 2133–2141.

Ely, L. L., Enzel, Y. & Cayan, D. R. (1994) Anomalous North Pacific atmospheric circulation and large winter floods in the Southwestern United States. *J. Climate* **7**, 977–987.

Eshel, G., Cane, M. A. & Farrel, B. F. (2000) Forecasting Eastern Mediterranean Droughts. *Mon. Weath. Rev* **128**, 3618–3630.

Feddersen, H. and Andersen, U. (2005) A method for statistical downscaling of seasonal ensemble predictions. *Tellus A* **57**, 398–408.

Galvao, C. O., Clarke, R. T., Davies, T. D. & Jones, P. D. (1999) Evaluation of seasonal forecasting methods for water resource management in northeastern Brazil. In: *Hydrological Extremes: Understanding, Predicting, Mitigating* (ed. by L. Gottschalk, J.-C. Olivry, D. Reed & D. Rosbjerg), 289–295. IAHS Publ. 255. IAHS Press, Wallingford, UK.

Goddard, L., Mason, S. J., Zebiak, S. E., Ropelewski, C. F., Basher, R. & Cane, M. A. (2001) Current approaches to seasonal-to-interannual climate predictions. *Int. J. Climatol.* **21**, 1111–1152.

Harrison, M. (2005) The development of seasonal and inter-annual climate forecasting. *Climatic Change* **70**, 201–220.

Kiem, A. S. & Franks, S. W. (2001) On the identification of ENSO-induced rainfall and runoff variability: a comparison of methods and indices. *Hydrol. Sci. J.* **46**, 715–727.

Krasovskaia, I., Gottschalk, L., Rodriguez, A. & Laporte, S. (1999) Dependence of the frequency and magnitude of extreme floods in Costa Rica on the Southern Oscillation Index. In: *Hydrological Extremes: Understanding, Predicting, Mitigating* (ed. by L. Gottschalk, J.-C. Olivry, D. Reed & D. Rosbjerg), 81–89. IAHS Publ. 255. IAHS Press, Wallingford, UK.

Landman, W. A., Mason, S. J., Tyson, P. D. & Tennant, W. (2001) Statistical downscaling of GCM simulations to streamflow. *J. Hydrol.* **252**, 221–236.

Leung, L. R., Hamlet, A. F., Lettenmaier, D. P. & Kumar, A. (1999) Simulations of the ENSO hydroclimate signals in the Pacific Northwest Columbia River basin. *Bull. Am. Met. Soc.* **80**, 2313–2329.

Mason, S. J., Goddard, L., Graham, N. E., Yulaeva, E., Sun, L. Q. & Arkin, P. A. (1999) The IRI seasonal climate prediction system and the 1997/98 El Nino event. *Bull. Am. Met. Soc.* **80**, 1853–1873.

McGregor, G. R. & Phillips, I. D. (2004) Specification and prediction of monthly and seasonal rainfall over the south-west peninsula of England. *Quart. J. Roy. Met. Soc.* **130**, 193–210.

Palmer, T. N., Alessandri, A., Andersen, U., Cantelaube, P., Davey, M. & Delecluse, P., *et al.* (2004) Development of a European multimodel ensemble system for seasonal-to-interannual prediction (DEMETER). *Bull. Am. Met. Soc.* **85**, 853–872.

Schar, C., Vasilina, L., Pertziger, F. & Dirren, S. (2004) Seasonal runoff forecasting using precipitation from meteorological data assimilation systems. *J. Hydromet.* **5**, 959–973.

Stahl, K. & Demuth, S. (1999) Investigating the influence of atmospheric circulation patterns on regional streamflow drought in southern Germany. In: *Hydrological Extremes: Understanding, Predicting, Mitigating* (ed. by L. Gottschalk, J.-C. Olivry, D. Reed & D. Rosbjerg), 19–27. IAHS Publ. 255. IAHS Press, Wallingford, UK.

Svensson, C. & Prudhomme, C. (2005) Prediction of British summer river flows using winter predictors. *Theoretical Appl. Climatol.* **82**, 1–15.

[5] See http://www.hydro.washington.edu/ (Accessed 25 January 2006)

Trigo, R. M., Pozo-Vazquez, D., Osborn, T. J., Castro-Diez, Y., Gamiz-Fortis, S. & Esteban-Parra, M. J. (2004) North Atlantic oscillation influence on precipitation, river flow and water resources in the Iberian peninsula. *Int. J. Climatol.* **24**, 925–944.

Uppala, S. M., Kallberg, P. W., Simmons, A. J., Andrae, U., Bechtold, V. D., Fiorino, M. *et al.* (2005) The ERA-40 reanalysis. *Quart. J. Roy. Met. Soc.* **131**, 2961–3012.

Van Oldenborgh, G. J., Balmaseda, M., Ferranti, L., Stockdale, T. N. & Anderson, D. (2005) Did the ECMWF seasonal forecast model outperform a statistical model over the last 15 years? *J. Climate* **18**, 3240–3249.

Washington, R. & Downing, T. E. (1999) Seasonal forecasting of African rainfall: Prediction, responses and household food security. *Geographical J.* **165**, 255–274.

Wedgbrow, C. S., Wilby, R. L., Fox, H. R. & O'Hare, G. (2002) Prospects for seasonal forecasting of summer drought and low river flow anomalies in England and Wales. *Int. J. Climatol.* **22**, 219–236.

Wedgbrow, C. S., Wilby, R. L. & Fox, H. R. (2005) Experimental seasonal forecasts of low summer flows in the River Thames, UK, using Expert Systems. *Climate Res.* **28**, 133–141.

Wilby, R. L. (2001) Seasonal forecasting of river flows in the British Isles using North Atlantic pressure patterns. *J. CIWEM* **15**, 56–63.

Wilby, R. L. & Wigley, T. M. L. (1997) Downscaling general circulation model output: a review of methods and limitations. *Progr. Phys. Geogr.* **21**, 530–548.

Wilby, R. L., Hay, L. E., Gutowski Jr, W. J., Arrit, R. W., Takle, E. S., Pan, Z., *et al.* (2000) Hydrologic responses to dynamically and statistically downscaled climate model output. *Geophys. Res. Lett.* **27**, 1199–1202.

Wilby, R. L., Wedgbrow, C. S. & Fox, H. R. (2004) Seasonal predictability of the summer hydrometeorology of the River Thames, UK. *J. Hydrol.* **295**, 1–16.

Zwiers, F. W. & von Storch, H. (2004) On the role of statistics in climate research. *Int. J. Climatol.* **24**, 665–680.

Climate Variability and Change—Hydrological Impacts (Proceedings of the Fifth FRIEND World Conference held at Havana, Cuba, November 2006), IAHS Publ. 308, 2006.

Predicting low flows in ungauged catchments

KOLBJØRN ENGELAND, HEGE HISDAL & STEIN BELDRING
NVE, Postboks 5091 Majorstua, N-0301 Oslo, Norway
koe@nve.no

Abstract The aim of this study was to compare the regression method and a regional precipitation–runoff model to estimate low flow indices at ungauged sites. Southwestern Norway was chosen as the study region. As the first step in the regression method, two homogeneous sub-regions were established according to the dominant low flow season, winter or summer. Then individual regression equations were established for each sub-region between the low flow index "common low flow" and catchment characteristics using a step-wise procedure. A gridded version of the HBV model was applied as a regional precipitation–runoff model. The model was calibrated to a subset of the catchments and validated on independent catchments. The calibration criterion was selected to fit the low flow part of the streamflow record. Comparison of the predicted low flow index by the regression method and the HBV model showed that the regression method gave the best estimates.

Key words low flow indices; prediction in ungauged basins; regionalization; HBV model

INTRODUCTION

Estimation of low flow indices at ungauged sites is needed for many decisions in water resources management. In Norway an increasing demand for low flow data, especially for small catchments, is related to the increasing request to build small hydropower plants. Also, related to other water management issues such as river pollution and ecological aspects, irrigation, reservoir design and management, drinking water supply and fish farming, there is a need to estimate low flow indices.

Due to the Norwegian Water Resources Act the construction of small hydropower plants requires estimation of the low flow index "common low flow" (clf) in small ungauged catchments. This index is a starting point to set the residual flow when a licence is needed, and is often used as the residual flow if a licence is not needed. Clf is defined as follows (preferably based on at least 15–20 years of data): (a) remove the 15 smallest values every year in a daily streamflow record, (b) calculate the annual minimum series, (c) rank the values in the annual minimum series, and (d) remove 1/3 of the smallest values. The smallest value left is the clf.

A standard procedure for obtaining the best possible estimation of low flow indices in ungauged catchments is needed. In this paper, two methods are studied: multiple regression and precipitation–runoff modelling.

Regression techniques aim to establish regression equations between low flow indices and catchment characteristics. An overview is given in Demuth & Young (2004). Norwegian studies were recently presented in Væringstad & Hisdal (2005). In heterogeneous areas it is necessary to establish individual regression equations for sub-regions that are homogeneous with regard to the low flow generating processes (e.g. Laaha & Blöschl, 2006). In Norway, there is a major difference between catchments with dominant summer and winter low flow (Væringstad & Hisdal, 2005).

A regional precipitation–runoff model can produce streamflow series from which the desired low flow indices can be calculated. This method requires good procedures to transfer model parameters from gauged to ungauged catchments and for interpolation of the meteorological input variables (temperature, precipitation, etc.). The gain is that you can calculate any low flow index from one model. The loss is the increased model complexity that might increase the uncertainties in the estimation.

The aim of this study is to evaluate and compare regression and precipitation–runoff modelling methods for estimation of clf in ungauged catchments in Norway. This was achieved by estimating regression equations between clf and catchments characteristics for 56 catchments in southern Norway. The performance of the regression equations was evaluated by a cross-validation procedure. A gridded version of the HBV-model was calibrated to a subset of the 56 catchments using objective criterions that give good fit to low flows. The calibration results were validated on an independent set of catchments. The two methods were compared using the root mean square error, explained variance (R^2) and bias for the predicted low flow.

Copyright © 2006 IAHS Press

This paper starts with a presentation of the streamflow and geographical data. Then the regression method is described and regional regression equations are derived. It is followed by a presentation of the HBV model and how the two methods were compared before the results are presented and some conclusions are drawn.

DATA

The study region is the southwestern part of Norway (Fig. 1). In the inland and the mountainous areas the low flow period is in the winter due to precipitation being stored as snow, whereas in the coastal lowlands the low flow period is in the summer due to increased evapotranspiration and slightly lower rainfall. The vegetation cover is mainly coniferous and deciduous forests in the lowlands, and grass and bushes in the mountains. The area is covered by several lakes and mires that are very important for the hydrological response. The soils are mainly thin till deposits on bedrock. Fluvial deposits are mostly found in the valley bottoms.

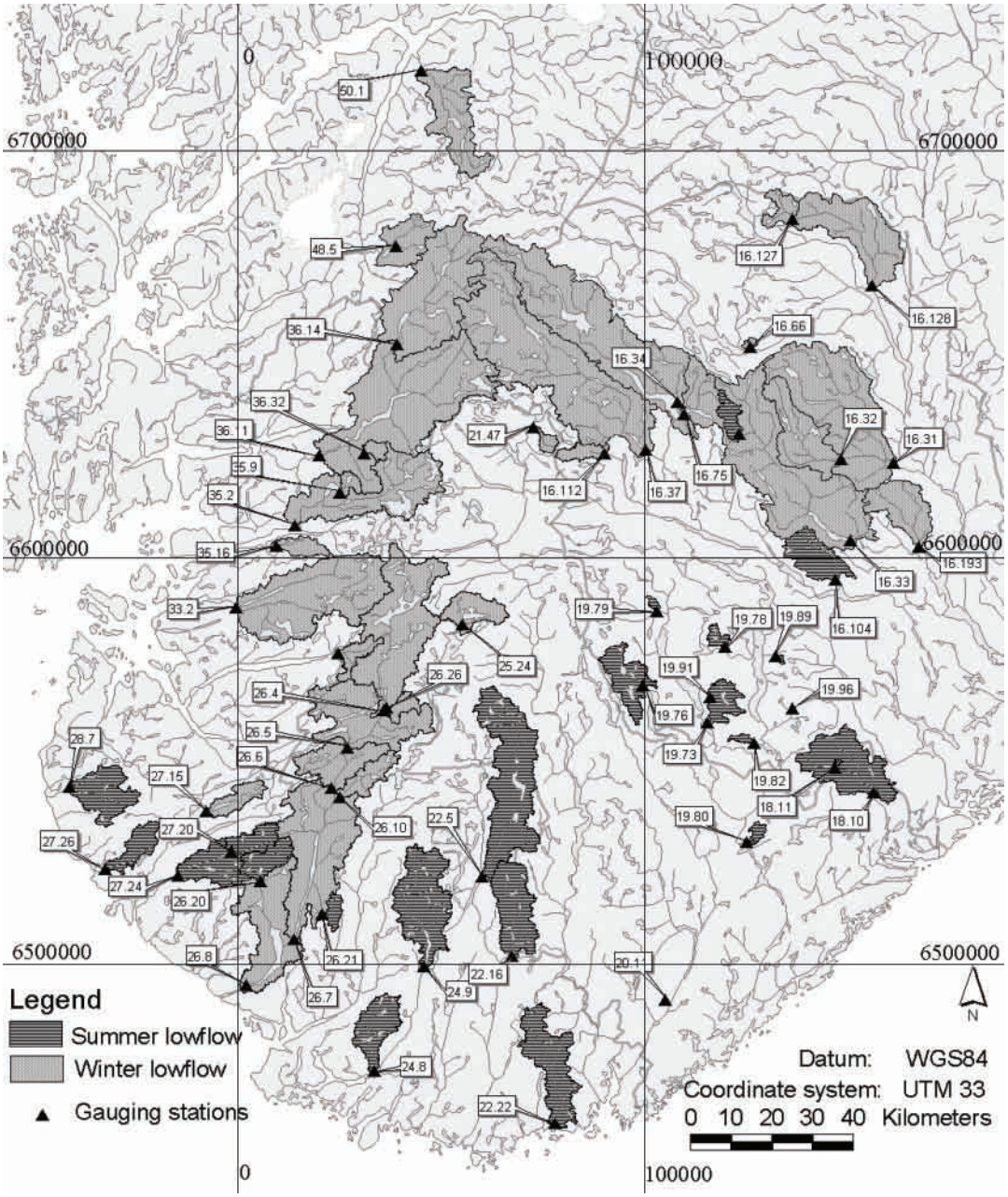


Fig. 1 Catchments and corresponding streamflow stations used in this study.

Table 1 The catchment characteristics included in the regression analysis.

Symb.	Description	Symb.	Description
A	Catchment area (km^2)	C_G	Catchment gradient (m km^{-1})
Q_M	Mean annual runoff (l s^{-1} km^{-2}) obtained from the runoff map of Norway	G_{1085}	River gradient excluding the 10% lowest parts and the 15% highest parts 1085 (m km^{-1})
R_L	Length of main river (km) from the outlet to the most distant river string.	C_L	Catchment length (km) from outlet to the most distant point at the water divide
R_G	River gradient (m km^{-1})	$M_{\%}$	Mountainous areas (%)
$F_{\%}$	Forested areas (%)	$L_{\%}$	Lake percentage (%)
$B_{\%}$	Bogs (%)	L_{eff}	Effective lake percentage (%)
C_W	Catchment width (km)	T_A	Average annual temperature (^oC)
$A_{\%}$	Agricultural areas (%)	Ts	Average summer temperature (^oC)
H_{max}	Maximum elevation (m a.s.l.)	Tw	Average winter temperature (^oC)
H_{min}	Minimum elevation (m a.s.l.)	P_A	Annual precipitation (mm)
D_H	Elevation gradient (m)	Ps	Summer precipitation (mm)
$U_{\%}$	Urbanised areas (%)	Pw	Winter precipitation (mm)

Daily streamflow data was obtained from 56 stations (Fig. 1). The stations were selected according to the record length (a minimum of 20 years) and the quality of the low flow measure ments. The dominant low flow season is indicated in Fig. 1. The summer was defined as May–October and winter as November–April. The average flows for the three winter months and the three summer months with the lowest streamflow were used to find the dominant low flow period.

Table 1 lists the physiographic and climatic catchments descriptors. All the land cover percentages are based on the N50 maps (scale 1:50 000). The gradients are based on a digital elevation model with resolution of 100 × 100 m. A digital river network was used to calculate the river gradients. The average precipitation: P_A, P_S and P_W, and temperature: T_A, T_S and T_W, were provided by the Norwegian meteorological institute. They were given as average values for the period 1961–1990 on a regular grid with a 1 × 1 km resolution and aggregated to catchment averages.

REGIONAL REGRESSION ANALYSIS

The regional regression analysis was performed in two steps: (a) divide the data into groups that can be regarded as homogeneous with respect to their low flow behaviour, (b) establish regression equations for each sub-region.

Classification

The catchments with observations were divided into two groups according to their dominating low flow period, as previously described. In order to decide whether an ungauged catchment has low flow during winter or summer, the average July temperature in combination with the ratio between summer and winter precipitation was found to be the best indicator. If the July temperature is higher than 10.4°C and the winter precipitation is more than 0.7 times the summer precipitation, the catchment has summer low flow (Fig. 2). It should be noted that the latter criterion is based only on one station (16.193 Hørte) and is therefore not very robust.

Regression models

In the second step multiple linear regression was used to obtain relationships between clf and catchment characteristics for the winter and summer regions separately. In total, 24 catchment characteristics (Table 1) were potential candidates for the regression equation. A stepwise procedure based on the Akaikes information criterion was used to select the most important characteristics to explain the clf. In order to evaluate the predictive capability of the model, a cross validation test was carried out. Each observation was successively left out in the estimation of the regression parameters. The clf was then predicted at the independent site. The explained variance R^2_{CV} for the predictions was then calculated.

Different transformations of the dependent variable, clf, were tested in order to obtain homoscedasdic residuals and the log-transformation was found to be the best alternative. Several

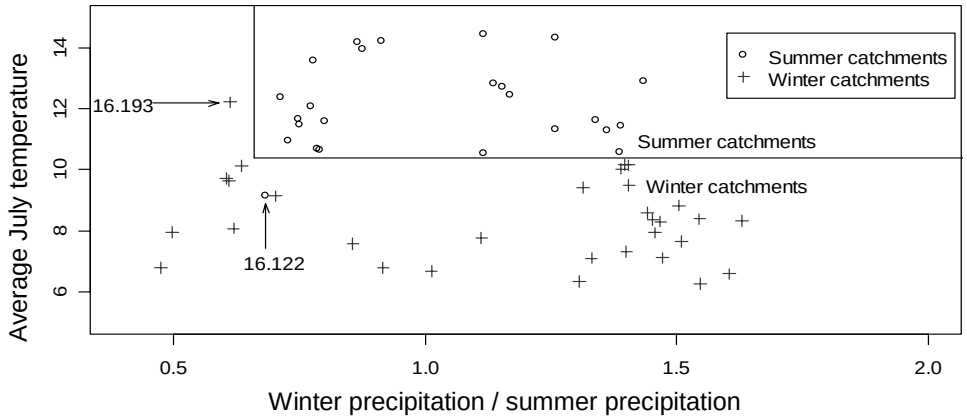


Fig. 2 Classification of summer and winter catchments. The circles and crosses indicate the summer and winter catchments respectively according to the initial classification, whereas the lines indicate the limits according to the classification based on climatic conditions.

alternative models were evaluated. The best model fit was obtained when the independent variables were either log-transformed or kept un-transformed. Equations (1) and (2) show the estimated regression coefficients for the winter and summer region respectively. R^2_{CV} for the winter region was 0.816/0.711 (log-transformed clf/un-transformed clf), and for the summer region 0.820/0.757.

$$\ln(Q_c) = -3.3325 + 0.0102C_L + 0.03298\ln(L_{eff}) + 0.026485Q_M + 1.601\ln(T_S) - 0.215\ln(F_{\%} + 0.1) - 0.0173M_{\%} \quad (1)$$

$$\ln(Q_c) = -4.734 + 1.301\ln(Q_M) - 0.448\ln(B_{\%} + 0.1) + 0.102L_{\%} + 0.0130C_L \quad (2)$$

Figure 3 shows some diagnostics. There are two plots for the summer catchments and two plots for the winter catchments. All four show predicted clf based on equations (1) and (2) *versus* observed clf. For a good model fit the points should be close to the 1:1 line. In the first plots clf is untransformed, whereas the second plots show the results as log-transformed clf.

The bias of the residuals is centred on zero, but the model underestimates the highest values. A better fit is obtained for summer catchments than for winter catchments since the low flow data in the winter are more uncertain than the summer low flow. During winter the instrument might freeze, there are often measurement errors due to ice at the gauging station, or the low flow might actually be an estimated flow based on an ice reduction procedure.

The average runoff, the lake percentage and the catchment length is included for both summer and winter catchments. The clf increases with increasing values for all these three variables. Bogs have the opposite effect of lakes. Increasing bog percentage gives decreasing clf. Bogs seem to act as swamps in the landscape. This variable is included for the summer region. For the winter region also temperature, forest areas and mountainous areas are selected. The clf increases with increasing temperatures since less precipitation is stored as snow.

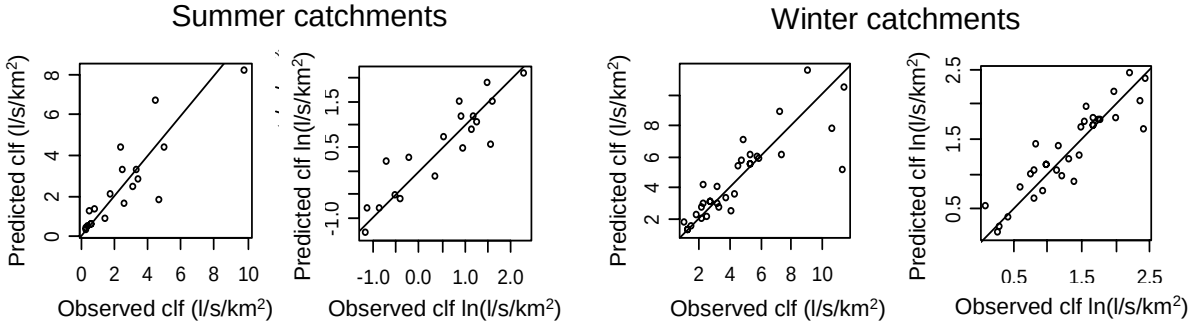


Fig. 3 Cross-validation of regression model. The left plot of each pair of plots show the results as untransformed clf, whereas the right plot shows the results with clf log-transformed.

THE HBV MODEL

A gridded version of the Norwegian HBV model (Beldring *et al*., 2003) was used. The HBV model operates on daily time steps and calculates the water balance for grid cells of 1 × 1 km. For each grid cell the percentage of lake was decided in addition to the proportion of the two dominant (out of five) land-use classes. Some of the model parameters were common for the whole region whereas others were determined for each land-use class. The same process parameterizations were applied to all grid-cells.

Precipitation and temperature observations were interpolated to each grid cell using an inverse distance weighting routine with elevation correction. The precipitation gradients were calibrated according to the procedure described in Beldring *et al*. (2003).

Calculation of common low flow

We chose to let the HBV model give the clf for each grid cell. The clf for the catchment is the average of the clfs in the grid cells within the catchment. This procedure might be difficult to use for large catchments where all parts of the catchment do not simultaneously contribute to the low flow events, e.g. some parts of the catchment have summer low flow and other parts winter low flow. Other alternatives exist, but would be complicated if applied for operational purposes.

Calibration and validation

To evaluate the predictability of clf in ungauged catchments using the HBV model, a split sample test was applied. Daily streamflow observations from 36 stations were used for calibration. A calibration was performed using the average Nash-Sutcliffe coefficient for log-transformed streamflow to give weights on low streamflow values. In order to compare the prediction of clf using the regression method and the HBV model in a proper way, a split sample test was also performed for the regression method using the same 36 catchments to estimate the regression coefficients. The explained variance R^2 and bias for the clf estimated by both methods was calculated both for the calibration and the validation sets.

RESULTS AND DISCUSSION

Figure 4 shows the observed and HBV-estimated clf for the calibration catchments and the validation catchments. The figure also shows the results for the regression method.

The regression method in general gives better prediction of clf in ungauged catchments than the HBV model. The regression method is especially superior to the HBV model for the smallest clf-values. The predictive power for clf-values smaller than 2-3 L s^{-1} km^{-2} for the HBV-model is rather limited.

The use of log-transformation to obtain heteroscedastic residuals indicates that the error is relative for the regression model. This means that the absolute error is small for small predicted values of clf and larger for larger predicted values of clf. For the HBV model, however, the absolute error is independent of the magnitude of the clf. This means that the precision of the lowest clf predictions is rather low.

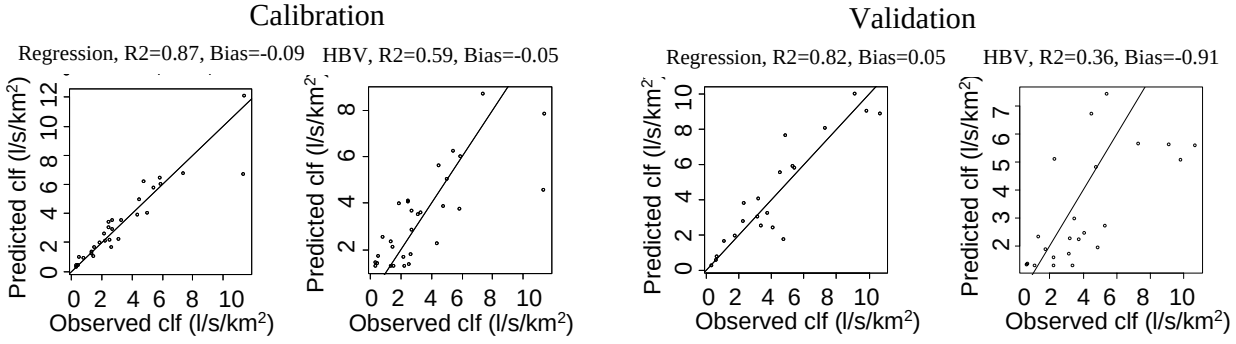


Fig. 4 The observed and simulated clf for the calibration and validation catchments.

The use of the HBV model to calculate clf demands high performance for the simulated recession and low flow periods. Since the estimates are to be used in ungauged catchments, it is necessary to use a regional parameter set where the parameters depend on landscape characteristics. The regression method indicates that, in addition to climatic descriptors, lakes and bogs are important landscape characteristics that control the low flow. Better results might be obtained by using improved interpolation of precipitation, explicit representation of lake and bog elements and introduction of soil and land-use classes important to recession and low flow.

The regression results are limited to the selected region, and the quality of the estimates might decrease if the equations are applied in an extrapolation mode for the catchment characteristics. The regression procedure does not account for strongly correlated clf along the river network, so application of streamflow data further up- or downstream can give better results than the regression equations.

The regression method provides the best prediction of low flow indices, but separate regression equations are needed for each index and region. Also, a routine to automatically estimate the catchment characteristics of ungauged basins need to be at hand. The HBV model allows calculation of any low flow index based on the simulated time series and would be able to provide a static map of clf and other indices.

CONCLUSIONS

A multiple regression procedure to estimate common low flow in ungauged catchments has been compared to the application of the HBV model. The following conclusions can been drawn: (a) the regression method gives better predictions of clf than the HBV model; (b) for the regression method, the best results are obtained when the clf is log-transformed, and the independent variables should be either log-transformed or kept un-transformed; and (c) important catchment characteristics are average runoff, lakes, bogs, catchment length and temperature.

For the development of a low flow map for Norway, several challenges are identified of which the most important are the need for quality control of low flow data, the development of regression equations for several low flow indices for the whole of Norway and the development of automatic procedures to extract the catchment characteristics required.

Acknowledgements The study presented is funded by the “Small hydropower” project at the Norwegian Water Resources and Energy Directorate.

REFERENCES

Beldring, S., Engeland, K., Roald, L. A., Sælthun, N. R. & Voksø, A. (2003) Estimation of parameters in a distributed precipitation-runoff model for Norway. *Hydrol. Earth System Sci.* **7**(3), 304–316.

Demuth, S. & Young, A. R. (2004) Regionalisation procedures. In: *Hydrological Drought – Processes and Estimation Methods for Streamflow and Groundwater* (ed. by L. M. Tallaksen & H. A. J. van Lanen), 307–343. Developments in Water Sciences 48. Elsevier Science Publisher, The Netherlands.

Laaha, G. & Blöschl, G. (2006) A comparison of low flow regionalisation methods—catchment grouping. *J. Hydrol.* (in press).

Væringstad, T. & Hisdal, H. (2005) Estimation of common low flow in ungauged catchments (in Norwegian), Miljøbasert vannføring rapport 06-2005. Norwegian Water Resources and Energy Directorate, Oslo, Norway.

Climate Variability and Change—Hydrological Impacts (Proceedings of the Fifth FRIEND World Conference held at Havana, Cuba, November 2006), IAHS Publ. 308, 2006.

Drought indices suitable to study the linkages to large-scale climate drivers in regions with seasonal frost influence

ANNE K. FLEIG, LENA M. TALLAKSEN & HEGE HISDAL
Department of Geosciences, University of Oslo, PO Box 1047 Blindern, NO-0316 Oslo, Norway
a.k.fleig@geo.uio.no

Abstract Based on a literature study the suitability of several common drought indices is evaluated for application in regional drought forecasting in climates with seasonal frost influence. In these regions hydrological droughts caused by a deficit in precipitation (summer droughts) and frost (winter droughts) have to be distinguished. Suitable drought indices should be objective, spatially and temporally robust, sensitive, interpretable and practical. They also need to enable drought forecasting, which is in this study considered to be based on a statistical model linking the drought indices to large-scale ocean and atmosphere patterns. None of the studied indices were found to be optimal for regional forecasting mainly due to a lack of robustness. It is suggested to use a set of three or four indices, including the Standardized Precipitation Index for meteorological drought, a streamflow drought index based on the threshold level method with a constant seasonal threshold, and a flow anomaly index to detect deviations from normal hydrological conditions.

Key words drought indices; hydrological drought; cold climate; regional forecasting; SPI; PDSI; PDHI; threshold level method; flow anomaly; streamflow

INTRODUCTION

Drought is a slowly developing natural hazard that can persist for a long time and extend over a large region. Water deficits during a drought can be large and in order to mitigate the impact of droughts long-range, forecasts are an important tool. Currently, drought forecasting exists mainly in warm and drier climates, and often in the form of monthly and seasonal precipitation and temperature forecasts based on relations to large-scale climate drivers like the El Niño–Southern Oscillation Index or sea surface temperatures, e.g. seasonal outlooks in Southern Africa (SADC-DMC, 2006) and Australia (Bureau of Meteorology, 2006). An exception is the US Seasonal Drought Outlook (NWS-CPC, 2006), that also considers other variables, e.g. soil moisture. Drought impacts can also be severe in temperate and cold regions and regions receiving water from cold mountainous regions such as large areas in the Mediterranean (Vicente-Serrano & López-Moreno, 2005). This study focuses on regions which experience prolonged frost periods of varying duration in the winter season.

Precipitation forecasts mainly address meteorological drought, which is defined as a deficit in precipitation. Temperature forecasts give an indication about snow accumulation and melting, and loss of water through evapotranspiration. A meteorological drought can develop into a soil moisture drought and a hydrological drought (deficit in surface water and groundwater; Wilhite & Glantz, 1985; Tallaksen & van Lanen, 2004). The different drought types affect different sectors of water usage, e.g. agriculture, water supply, hydropower and other industrial uses. The propagation of drought in the hydrological cycle depends on regional and local climatological and hydrogeological characteristics, and the different types of drought do not necessarily occur simultaneously or with the same severity. Separate forecasts for meteorological, soil moisture and hydrological droughts are therefore favourable. They should preferably be regional as severe droughts are often of large spatial extent. In regions with prolonged frost periods, soil moisture conditions are mainly of interest during the growing season. However, special considerations are needed in case of hydrological drought. When precipitation falls as snow it is temporarily stored on the surface. This implies that water levels in surface waters and groundwater can be low due to temperatures below zero (winter drought) and not because of a deficit in precipitation (summer drought). In regional studies hydrological droughts should be quantified so that consistent information for the whole range of climatological and hydrogeological characteristics in the region is provided. The quantification should also reflect local differences and be relative to "normal" hydrological conditions.

In drought monitoring, droughts are often described and quantified by indices, such as streamflow percentiles or the Palmer Hydrological Drought Severity Index (PHDI). Considering

Copyright © 2006 IAHS Press

only one variable, streamflow percentiles are a single index, whereas the PHDI is a complex index, being based on several meteorological and hydrological variables. Not all drought indices are suitable for all regions and purposes. A general evaluation of some of the most common indices for different drought types is presented by Keyantash & Dracup (2002) and for streamflow drought by Fleig *et al.* (2006). In frost influenced regions a robust hydrological drought index needs to distinguish between summer and winter droughts, and should give consistent results for regions with and without frost influence. For streamflow drought important challenges are to allow a consistent quantification when a summer drought continues into a winter drought, which implies that the end of the summer drought is not clearly defined, and when the duration of the frost-free period varies between years or within the basin due to its large area or altitude range (Fleig *et al.*, 2006). Basins with glaciers have to be treated separately as they can experience above normal flows during a warm and dry summer period due to increased melt-water contribution.

In this study drought indices are evaluated for their suitability to study the linkages between hydrological drought and large-scale ocean and atmosphere patterns for regions with seasonal frost influence. The presence of such linkages could provide the basis for long-range monthly or seasonal drought forecasting with lead times of weeks or months. Considering the aforementioned challenges in frost influenced regions, the advantages and disadvantages of common hydrological drought indices are identified based on a literature study, and the applicability of each index is evaluated. The following requirements, which are mainly in accordance with general requirements listed by other authors (e.g. Keyantash & Dracup, 2002; Steinemann, 2003; Steinemann *et al.*, 2005, Fleig *et al.*, 2006), are considered to be important. Drought indices should be:

- objective, i.e. clearly defined, not requiring subjective choices of e.g. parameter values;
- spatially and temporally robust, i.e. statistically consistent and comparable for all climatological and hydrogeological conditions in the region;
- sensitive enough to show temporal development and within-regional drought patterns;
- interpretable for different user groups;
- practical in terms of calculations and data requirement, implying that sufficient historical data for developing a forecasting model are available.

As consistent groundwater data seldom are available for large regions, groundwater drought is not included in this evaluation. In the following sections four single and two complex indices are presented and evaluated. Conclusions are drawn in the final section.

SINGLE INDICES

Threshold level method

The threshold level method (theory of runs; Yevjevich, 1967) applied to annual, monthly or daily streamflow series identifies droughts as periods during which streamflow is below a predefined threshold. Derived indices include e.g. drought severity, which is expressed in terms of the total deficit volume (total water deficit) during such a period, and drought duration. For short time steps, e.g. daily, subsequent deficit periods separated by short excess periods are recommended to be pooled into larger events (e.g. Fleig *et al.*, 2006). This can be done by introducing a moving average procedure or a duration/volume based criterion for the excess periods (inter event method). A pooling procedure based on the Sequent Peak Algorithm (Vogel & Stedinger, 1987) is less favourable as drought events following major events might not be recognized. The threshold can either be constant or varying over the year (Fig. 1), representing a specific demand or determined relative to the natural flow regime. In comparative studies, percentiles from the flow duration curve (FDC) are often used, which give more consistent regional results than percentages of the mean (Tallaksen *et al.*, 1997). The constant and varying thresholds both have advantages and limitations. The disadvantage of a varying threshold is that it may include periods which are commonly not considered as droughts, e.g. periods with flow lower than normal due to a delayed onset of the snow melt flood. On the other hand, a varying threshold identifies deficit periods independently of seasonal characteristics and is therefore better suited to study the linkage to atmospheric circulation (Stahl, 2001). A constant threshold should only be applied to a predefined summer or winter season as otherwise mixed summer and winter droughts might result (Fleig *et*

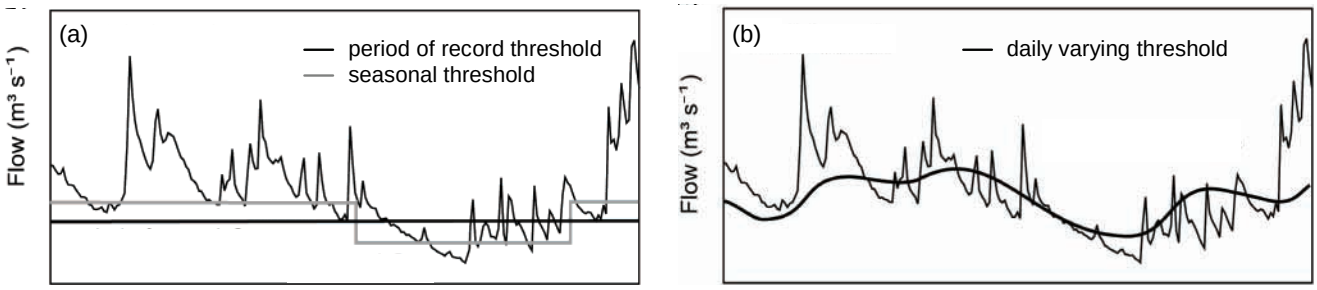


Fig. 1 Illustration of thresholds: (a) constant period of record and seasonal thresholds; (b) daily varying threshold (modified from Stahl, 2001).

al., 2006). Consequently, the threshold should be calculated based on data from this period only. However, FDCs for the summer season can vary considerably for summer seasons, differing only by a few weeks (Fleig, 2004) making a consistent regional threshold selection difficult. Furthermore, the threshold level method is often subjective in terms of choosing seasonal limits, threshold and pooling criteria. The major problem is that of mixed summer and winter droughts. This sets some limitations when using the otherwise well suited threshold level method in frost influenced regions.

Streamflow percentiles

Streamflow percentiles compare the average streamflow of the last *n* days to the FDC of *n*-day averages for that calendar day. Droughts can be classified in terms of daily exceedance frequencies determined from the *n*-day FDCs. The USGS (2006) classifies percentiles in the lower range (<10) as moderate, severe and extreme drought. They have, however, not yet defined duration and overall severity of a drought event, which could be done e.g. by introducing a threshold. Similar to the above-mentioned streamflow drought indices, streamflow percentiles are not capable of distinguishing between summer and winter droughts, but can be derived for a predefined season. This again delimits somewhat the applicability of streamflow percentiles in frost influenced regions.

Flow anomaly index

The flow anomaly index was introduced by Zaidman *et al.* (2002). For each day of the year the historical streamflow series for that day are transformed into a normal distribution by taking the natural logarithm. Subsequently, the daily flow anomaly index is calculated as the standardized departure from the mean daily flow for the considered day of the year. A basin is regarded to be under drought conditions when the index value equals or exceeds a threshold of 2.0, i.e. when the flow is at least two standard deviations lower than the mean flow for that day. An instantaneous deficit is defined as the difference between the flow anomaly and the threshold. These daily values can be summed up to a cumulative deficit over a period of days. Similar to the varying threshold approach, the flow anomaly index identifies atypical flows in both the low-flow and high-flow season, and droughts are defined independently of seasonal characteristics. The index has not yet been thoroughly tested, but the adopted standardization procedure is expected to make it spatially consistent (provided long enough data records) with the exception of the period during which both summer and winter droughts can occur. As the above-mentioned indices, the flow anomaly index is thus suited for frost influenced regions only when applied to a predefined season.

Standardized Precipitation Index

The Standardized Precipitation Index (SPI; McKee *et al.*, 1993) only considers precipitation and is thus a meteorological drought index defined for a single site. It can, however, be calculated for different averaging intervals ranging from one month to several years, and the intermediate and longer time scales can be considered to reflect the slower developing deficits in soil moisture, surface waters and groundwater. The SPI quantifies the current drought situation in terms of its occurrence probability, which is determined by fitting a probability distribution (usually a Gamma

distribution) to at least 30 years of monthly data and transforming it into a standard normal distribution. It is therefore considered spatially consistent (Guttman, 1998). Droughts are indicated by negative SPI-values. Furthermore, the overall duration and magnitude (severity) of a drought event are defined, the latter as the negative sum of monthly SPI-values from the first month of a drought until its end (McKee *et al.*, 1993). A disadvantage is that the SPI might be misleading at short time scales (1–3 months) in regions with low seasonal precipitation. Understanding the climatology improves the interpretation of the SPI in these regions (Hayes *et al.*, 1999). Its spatial and temporal comparability with respect to the identification of hydrological drought is, however, limited since precipitation–runoff processes are variable in space and time. As such the SPI time-scale highest correlated with streamflow varies between basins (Szalai *et al.*, 2000) and seasons (Vicente-Serrano & López-Moreno, 2005). It is concluded that the SPI is well suited for meteorological drought forecasting, in particular as it is spatially robust, capable of quantifying the current deficit as well the deficit of the total drought event, and requires precipitation data only. For regions with a short growing season, a shorter time resolution, e.g. a biweekly SPI or a moving 30-day SPI calculated weekly, could be tested. However, no regionally comparable streamflow drought studies can be based solely on the SPI due to differences in runoff response.

COMPLEX INDICES

Palmer Drought Severity Index and Palmer Hydrological Drought Severity Index

The Palmer Drought Severity Index (PDSI) and the Palmer Hydrological Drought Severity Index (PHDI) were developed by Palmer in the mid 1960s (Heim, 2002) to quantify droughts for relatively homogenous regions. They are based on a water balance model considering two soil layers and the Thornthwaite method to estimate potential evapotranspiration. The two indices differ mainly in defining the end of a drought. The PDSI considers a drought to end as soon as an uninterrupted rise in moisture conditions begins, whereas the PDHI waits until the moisture deficit has vanished. The PDSI is therefore often regarded as a meteorological drought index and the PDHI as a hydrological drought index. Several drawbacks of the Palmer indices have been identified (e.g. Alley, 1984). Among these are: (a) the indices have been developed for semiarid and subhumid climates and are based on several arbitrary assumptions and values for variables and constants; (b) the natural lag between precipitation and runoff response is not considered for the PDSI; (c) snowfall, snow cover and frozen ground are not included; and (d) seasonal and annual changes in vegetation cover and root development are not considered. Consequently, the indices are not fully spatially and temporally comparable and the frequency with which drought events are classified into different severity classes varies between locations for the PDSI (and possibly the PHDI; Heim, 2002). The latter has been addressed by Wells *et al.* (2004), who developed a self-calibrating PDSI to enhance spatial comparability. However, as commented upon by the authors, it is not as spatially comparable as an index using nonlinear methods (e.g. the SPI). In particular the lacks of spatial robustness and consideration of snow make the Palmer drought indices less suited for regional studies in frost influenced regions.

Surface Water Supply Index

The Surface Water Supply Index (SWSI) was developed by Shafer & Dezman (1982) for regions where snow is an important component of the hydrological system. It is a monthly index representing the sum of weighted surface water supplies of a basin, including precipitation, snow-pack, streamflow and reservoir storage. It thus accounts for snow storage and delayed runoff. Each component is expressed in a normalized way through its non-exceedance probability determined from a historical record. As the SWSI monitors the total surface water supplies, including snow-pack, there is no need to distinguish between summer and winter droughts. However, a clear definition of “surface water supplies” is missing, and the weights are determined in different ways and often subjectively (Garen, 1993). According to Heddinghaus & Sabol (1991) the weights have to be redefined after changes in the basin and it is thus difficult to obtain a homogeneous time series of the SWSI. Furthermore, SWSI values are not comparable between basins, as the non-exceedance probabilities of the four components are summed up, resulting in a non-uniform

distribution. It would be preferable to derive a single joint non-exceedance probability from a description of the components by a multivariate probability distribution (Garen, 1993). In its current form, the SWSI is not suitable for regional studies due to its lack of objectivity and robustness.

CONCLUSIONS

In this literature study several drought indices are evaluated for their suitability for regional forecasting of hydrological drought in areas with seasonal frost influence. In these regions two types of streamflow drought caused by different processes can occur, summer and winter droughts. Robust drought indices should be able to distinguish between these two types. However, none of the studied single drought indices are adequately capable of this distinction. A consistent identification of the drought governing processes based on temperature or precipitation data is also complicated as rivers respond differently. The complex drought indices are similarly not suited for regional studies due to a general lack of spatial robustness. Hence, no index is optimally suited for regional hydrological drought forecasting in seasonally frost influenced regions. One solution is to study summer and winter droughts separately by choosing a predefined season. Alternatively, an annual time resolution can be used. However, the obtained information is limited in these cases. It is therefore recommended to consider a set of drought indices addressing:

– meteorological drought based on the SPI of short and medium time scales, i.e. 1, 3 and 6 months;
– streamflow droughts occurring in a predefined season using a constant threshold;
– streamflow deviations, e.g. based on the flow anomaly index.

In addition, improvements in the presented indices could be tested, e.g. a biweekly SPI or the use of a multivariate probability distribution for the SWSI. The fact that streams with different regimes and characteristics, e.g. length of summer season or glaciers, respond differently to climatic conditions should be addressed by defining homogeneous sub-regions/samples with respect to drought behaviour. Still, it is important to study the linkages between drought and large-scale climate drivers at the scale of drought events, which might extend past the boundary of homogenous sub-regions. This requires that the spatial aspects of the drought are considered. For single indices derived at-site this can be done using various interpolation methods or by defining regional drought characteristics based on spatial information on the input variable at the grid or sub-basin scale. In the latter case the area aspect of the drought is included in its definition, which can be based on both single and complex indices. This will be the topic of a further study, where the above recommended indices will be included, addressing drought forecasting in a northern-European region.

REFERENCES

Alley, W. M. (1984) The Palmer Drought Severity Index: Limitations and assumptions. *J. Clim. Appl. Met.* **23**, 1100–1109.

Bureau of Meteorology, Australia (2006) http://www.bom.gov.au/climate/ahead/ (last visited April 2006).

Fleig, A. (2004) Hydrological drought—a comparative study using daily discharge series from around the world. MSc Thesis Albert-Ludwigs-Universität Freiburg, Germany. Available from: http://www.geo.uio.no/edc/ under "Downloads".

Fleig, A. K., Tallaksen, L. M., Hisdal, H. & Demuth, S. (2006) A global evaluation of streamflow drought characteristics. *Hydrol. Earth Syst. Sci.* **10**, 535–552.

Garen, D. C. (1993) Revised Surface-Water Supply Index for Western United States. *J. Water Resour. Plan. Manage.*, **119**(4), 437–454.

Guttman, N. B. (1998) Comparing the Palmer Drought Index and the Standardized Precipitation Index. *J. Am. Water Resour. Assoc.* **34**(1), 113–121.

Hayes, M. J., Svoboda, M. D., Wilhite, D. A. & Vanyarkho, O. V. (1999) Monitoring the 1996 drought using the Standardized Precipitation Index. *Bull. Am. Met. Soc.* **80**(3), 429–438.

Heddinghaus, T. R. & Sabol, P. (1991) A review of the Palmer Drought Severity Index and where do we go from here? In: *Seventh Conf. on Applied Climatology* (Boston, USA), *Am. Met. Soc*. 242–246.

Heim, R. R. Jr. (2002) A review of twentieth-century drought indices used in the United States. *Bull. Am. Met. Soc.*, **83**(8), 1149–1165.

Keyantash, J. & Dracup, J. A. (2002) The quantification of drought: An evaluation of drought indices. *Bull. Am. Met. Soc.*, **83**(8), 1167–1180.

McKee, T. M., Doesken, N. J. & Kleist, J. (1993) The relationship of drought frequency and duration to time scales. In: *Eighth Conf. on Applied Climatology* (Anaheim, USA), *Am. Met. Soc.* 179–184.

NWS-CPC: National Weather Service—Climate Prediction Center (2006) http://www.cpc.ncep.noaa.gov/products/-expert_assessment/seasonal_drought.html (last visited April 2006).

SADC-DMC: Southern African Development Community—Drought Monitoring Centre (2006) http://www.dmc.co.zw/ (last visited April 2006).

Shafer, B. A. & Dezman, L. E. (1982) Development of a Surface Water Supply Index (SWSI) to assess the severity of drought conditions in snowpack runoff areas. In: *Proc. of the Western Snow Conference*, 164–175. Colorado State Univ., Fort Collins, USA.

Stahl, K. (2001) Hydrological drought—a study across Europe. PhD Thesis Albert-Ludwigs-Universität Freiburg, *Freiburger Schriften zur Hydrologie* no. 15, Freiburg, Germany. Also available from: http://www.freidok.uni-freiburg.de/-volltexte/202.

Steinemann, A. (2003) Drought indicators and triggers: a stochastic approach to evaluation. *J. Am. Water Wks Assoc.*, **39**(5), 1217–1233.

Steinemann, A. C., Hayes, M. J. & Cavalcanti, L. F. N. (2005) Drought indicators and triggers. In: *Drought and Water Crises—Science, Technology, and Management Issues* (ed. by D. A. Wilhite), 71–92. Taylor & Francis, Boca Raton, USA.

Szalai, S., Szinell, C. S. & Zoboki, J. (2000) Drought monitoring in Hungary. In: *Early Warning Systems for Drought Preparedness and Drought Management* (ed. by D. A. Wilhite, M. V. K. Sivakumar & D. A. Wood), 182–199. Lisboa, Portugal.

Tallaksen, L.M. & Lanen, H.A.J. van (eds) (2004) *Hydrological Drought—Processes and Estimation Methods for Streamflow and Groundwater*, Developments in Water Sciences 48, Elsevier BV, Amsterdam, The Netherlands.

Tallaksen, L. M., Madsen, H. & Clausen, B. (1997) On the definition and modelling of streamflow drought duration and deficit volume. *Hydrol. Sci. J.* **42**(1), 15–33.

USGS: US Geological Survey (2006) Drought Watch. http://water.usgs.gov/cgi-bin/ dailyMainW?state=us&map_type-=dryw&web_type=map (last visited February 2006).

Vicente-Serrano, S. M. & López-Moreno J. I. (2005) Hydrological response to different time scales of climatological drought: an evaluation of the Standardized Precipitation Index in a mountainous Mediterranean basin. *Hydrol. Earth Syst. Sci.* **9**, 523–533.

Vogel, R. M. & Stedinger, J. R. (1987) Generalized storage-reliability-yield relationships. *J. Hydrol.* **89**, 303–327.

Wells, N., Goddard, S. & Hayes, M. J. (2004) A self-calibrating Palmer Drought Severity Index. *J. Clim.* **17**, 2335–2351.

Wilhite, D. A. & Glantz, M. H. (1985) Understanding the drought phenomenon: the role of definitions. *Water Int.* **10**, 111–120.

Yevjevich, V. (1967) An objective approach to definitions and investigations of continental hydrologic droughts. *Hydrology Papers* 23, Colorado State Univ., Fort Collins, USA.

Zaidman, M. D., Rees, H. G. & Young, A. R. (2002) Spatio-temporal development of streamflow droughts in north-west Europe. *Hydrol. Earth Syst. Sci.* **6**(4), 733–751.

Climate Variability and Change—Hydrological Impacts (Proceedings of the Fifth FRIEND World Conference held at Havana, Cuba, November 2006), IAHS Publ. 308, 2006.

Sistema de alerta hidrológico de la cuenca del Río Salado, provincia de Santa Fe, Argentina: avances en su implementación

GUSTAVO FERREIRA

Ministerio de Asuntos Hídricos de la Provincia de Santa Fe (MAH), Almirante Brown 4751, Santa Fe, Argentina, y *Facultad de Ingeniería y Ciencias Hídricas (FICH), Universidad Nacional del Litoral, Ciudad Universitaria, Paraje El Pozo, Santa Fe, Argentina*

cgf@fich1.unl.edu.ar

Resumen La crecida extraordinaria del Río Salado en los meses de abril y mayo de 2003 ha sido catalogada como la peor catástrofe ambiental de la Argentina en las últimas décadas. Los efectos sobre la ciudad de Santa Fe—con 23 víctimas fatales y más de un centenar de víctimas colaterales—fueron magnificados por la acción antrópica previa, entre otros factores, la falta de medidas de previsión. En este trabajo se analiza el deterioro de la red de medición hidrométrica en los últimos 20 años y los antecedentes de un sistema de alerta hidrológico para esta cuenca. Se presentan las acciones vinculadas con la reactivación de la toma de datos y los avances en la ejecución de una red telemétrica en el marco del recientemente creado Ministerio de Asuntos Hídricos.

Palabras claves crecidas extraordinarias; Río Salado; red hidrométrica; sistema de alerta; Argentina; Santa Fe

The Salado River basin (Santa Fe, Argentina) flood warning system: advances in its implementation

Abstract The extraordinary flood on the Salado River in April and May 2003 has been catalogued as the worst environmental catastrophe in Argentina in recent decades. The effects on the city of Santa Fe—with 23 people killed and more than one hundred people injured—were increased by the previous human actions, and, among other factors, the lack of prevention measures. This work presents an analysis of the hydrometric network and its deterioration over the last 20 years and the precedents of a flood alert system for this basin. Actions linked with the re-activation of the collection of information and the advances in the establishment of an automatic network are presented within the framework of the recently created Ministry of Water Affairs.

Key words catastrophic flood; Salado River; streamgauge network; alert system; Argentina; Santa Fe

DESCRIPCIÓN DE LA CUENCA INFERIOR DEL RÍO SALADO

La cuenca del Río de La Plata se ubica en segundo lugar por su extensión en Sudamérica (3 150 000 km^2). Tiene tres grandes subcuencas: las de los Ríos Paraná, Paraguay y Uruguay (Fig. 1). La subcuenca del río Paraná es compartida por cuatro países: Argentina, Brasil, Bolivia y Paraguay.

El río Salado es uno de los principales afluentes del río Paraná en territorio argentino y su cuenca tiene una superficie de 94 750 km^2. Descarga sus aguas entre las ciudades de Santa Fe (350 000 hab.) y Santo Tomé (60 000 hab.), con un caudal módulo de 144.70 m^3 s^{-1}. Las condiciones naturales de la cuenca varían enormemente a lo largo de los 1500 km de longitud del curso por lo que la cuenca inferior tiene un comportamiento netamente diferenciado del resto. Ésta abarca una superficie de 30 400 km^2 y el régimen hidrológico está fuertemente influenciado por las precipitaciones locales. Este sector se encuentra casi en su totalidad dentro del territorio de la Provincia de Santa Fe. Recibe además el aporte de un área deprimida denominada Bajos Submeridionales cuya superficie es de 27 900 km^2. La cuenca inferior tiene una suave pendiente Noroeste–Sudeste, entre 0.01% y 0.05% y las cotas del terreno varían entre los 90 y 15 m sobre el nivel del mar. Los suelos son predominantemente limosos, de origen eólico, dedicados en su mayoría a la producción agropecuaria.

En cuanto a las precipitaciones medias anuales existe un gradiente en el sentido Este–Oeste, de 1200 mm a 900 mm (1971–2000), originando una transición desde un clima sub-húmedo en las zonas oriental y central a semiárido en el límite occidental (FICH 2006). El régimen de precipitaciones en la Pampa Húmeda manifiesta un cambio (Canziani, 2003; FICH, 2006), demostrado por el aumento de frecuencia e intensidad de las lluvias convectivas y un incremento generalizado de los montos anuales de precipitación, efectos que se verifican en todo el territorio de la provincia de Santa Fe y se expresan en el desplazamiento de las isohietas hacia el oeste, con un aumento del orden del 25% en los montos anuales en los últimos 30 años.

Copyright © 2006 IAHS Press



Fig. 1 Mapa de la Cuenca del Plata. Las letras designan los principales ríos: (A) Paraná, (B) Paraguay, (C) Uruguay, (D) Pilcomayo, (E) Bermejo, (F) Salado (G) Salado del Sur, y (H) de la Plata.

El caudal del Río Salado se compone principalmente por la descarga de los acuíferos superficiales en períodos secos, y por el exceso de precipitaciones en períodos húmedos.

De acuerdo con estudios previos (INCYTH, 1986) las situaciones más críticas en cuanto a crecidas, se originan por la superposición de los derrames de los Bajos Submeridionales (que son prolongados en el tiempo) con los aportes de las subcuencas locales, que provocan picos de considerable magnitud y corta duración según la localización y extensión de las tormentas. A su vez, el sistema fluvial del Río Paraná influye en los niveles del Río Salado en su descarga por efectos de remanso. Los caudales diarios son muy variables. Antes de la crecida de 2003, se registraron dos picos máximos del orden de los 2500 $m^3 s^{-1}$ durante las crecidas de 1973 y 1998. Entre esas fechas, se registró un caudal mínimo diario de 7 $m^3 s^{-1}$ en enero de 1995.

La crecida de abril–mayo de 2003 y sus efectos

Una serie de tormentas con precipitaciones intensas entre los días 23–25 de abril de 2003—con valores puntuales de hasta 388 mm—cayeron sobre suelos totalmente saturados por lluvias antecedentes, en áreas vinculadas directamente al cauce del río, dando origen a esta excepcional crecida (Ferreira, 2005). El caudal máximo generado en la Estación Ruta Provincial no. 70, situada a 25 km aguas arriba de la ciudad de Santa Fe, fue de 4000 $m^3 s^{-1}$ el día 29 de abril de 2003 y superó a los registros históricos de más de 50 años. La recurrencia calculada para esta crecida, según distintos autores se sitúa entre 500 y 800 años (DPOH, 2003; Ferreira, 2005; Bacchiega *et al.*, 2005).

Los efectos sobre la ciudad de Santa Fe—con 23 víctimas fatales y más de un centenar de víctimas colaterales—fueron magnificados por la acción antrópica previa, (Fig. 2) principalmente la ocupación urbana del valle de inundación y la rotura de un tramo de defensa lateral existente con graves falencias en su proyecto y ejecución, que determinó el ingreso abrupto de caudales, a manera de rotura de presa (DPOH, 2003; Ferreira *et al.*, 2004; Vionnet *et al.*, 2005). Según CEPAL (2003), el monto total de los daños y pérdidas en la cuenca del Río Salado asciende a los 1028 millones de dólares. De la cifra anterior, un 35% representa daños directos y el 65% a pérdidas indirectas. La falta de medidas de previsión hídrica fue otro de los factores coadyuvantes del desastre.



Fig. 2 Vista aérea del Oeste de la ciudad de Santa Fe, donde se aprecian barrios afectados por el ingreso masivo y repentino de agua.

EVOLUCIÓN DE LA RED HIDROMÉTRICA PROVINCIAL

De acuerdo con Bertoni *et al.* (1998) la red de drenaje provincial supera los 9450 km, en tanto que —a fines de los 1990s—un 42% de la misma estaba constituida por canales artificiales. Esta infla-estructura ha sido ejecutada en los últimos ochenta años y en escasas ocasiones fue acompañada con inversiones en instalación y operación de redes de observación hidrométrica.

El inicio de los registros comienza en los 1930s, estando a cargo en su mayor parte de la administración provincial. Un antecedente importante del esfuerzo por instalar y operar estaciones; realizar mediciones y estudios (INCYTH, 1986) fue el proyecto "Análisis y Planeamiento del Uso y Control de los Recursos Hídricos de una Cuenca de Llanura (Río Salado)". Por su parte, la provincia impulsó la instalación de estaciones luego de una inundación que sufrió el área centro de la misma en 1981.

A mediados de la década de1990 y como resultado de una política de abandono por parte de los Estados nacional y provincial de las tareas primordiales de evaluación y monitoreo de los recursos hídricos comienza el deterioro y pérdida de calidad de la red hidrométrica. A fines esa década, desde el sector científico-técnico (p. ej.: FLAGS, 1999) se insistía en la necesidad imperiosa de contar con mediciones sistemáticas de precipitaciones; niveles y caudales en los ríos y de niveles de agua subterránea (Fig. 3). La recuperación de estaciones que se evidencia en los últimos años son acciones realizadas a posteriori del evento de abril–mayo de 2003.

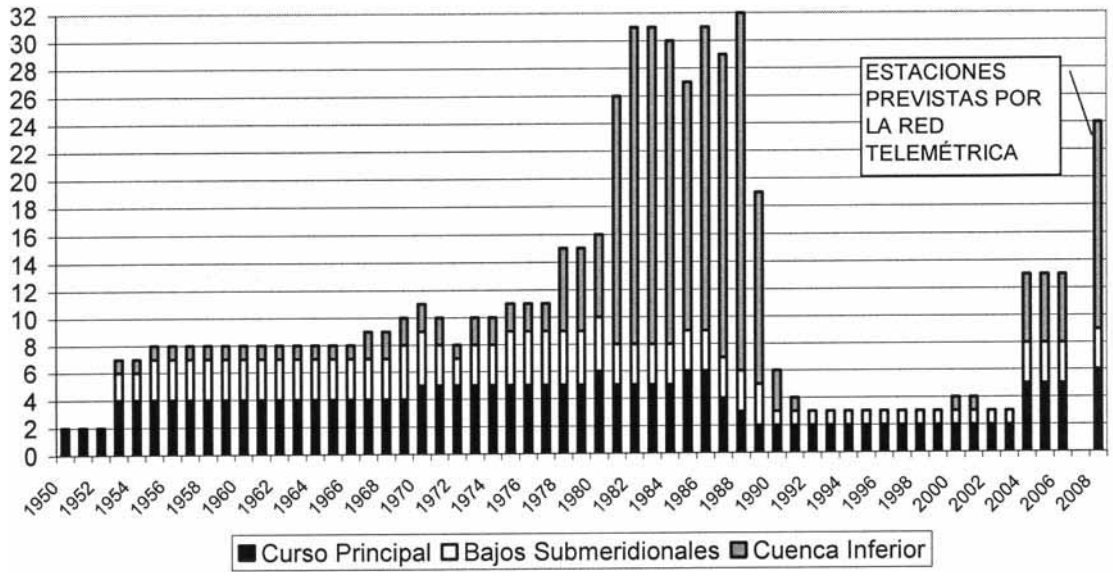


Fig. 3 Evolución del número de estaciones hidrométricas en la Cuenca Inferior del Río Salado. Entre 1992 y 2003, las estaciones correspondientes a los afluentes no operaron.

En coincidencia con Reyna *et al.* (2003) se puede afirmar que la mayoría de las estaciones situadas en el centro de la provincia de Santa Fe poseen insuficiente longitud de años de registro y discontinuidad de datos.

Solicitudes previas de un sistema de alerta hidrológico

Existen -aunque escasos- antecedentes de solicitudes de un sistema de alerta. El primero fue efectuado a posteriori de un conflicto por sequía que desató una crisis interprovincial, se recomendaba: "Planificar un sistema de alerta hidrológico en la cuenca del río Salado que tome en cuenta las situaciones extremas de inundaciones y sequías" (Ferreira, 1997). Más adelante, durante las inundaciones desencadenadas por el Evento El Niño de 1998 se reclamó la automatización de dos estaciones ubicadas en el río Salado, aguas arriba de la ciudad de Santa Fe de las que se consideraba debían integrar la red telemétrica del río Paraná (DPOH, 1998). La zona de confluencia de los ríos Salado y Paraná estaba identificada como una de las principales áreas con riesgo de inundación (Valdés & Fattorelli, 1999). Hacia fines de 2002, en el marco del Proyecto de Protección Contra Inundaciones—Préstamo BIRF 4117-AR, la intención de montar estaciones telemétricas en la cuenca estaba en manos del Estado Nacional (Secretaría de Obras Públicas 2002).

IMPLEMENTACIÓN DE UN SISTEMA DE ALERTA HIDROLÓGICO

La reacción post-desastre del conjunto de la sociedad santafesina dio origen a la introducción de cambios institucionales que derivaron en la creación de un Ministerio de Asuntos Hídricos a nivel provincial, con misiones y funciones específicas relativas, entre otras, a la toma de datos hidrométricos y a la prevención hídrica (Ley Provincial no. 12.257 y Decreto no. 0014/2004).

La experiencia en países desarrollados indica que para lograr un adecuado manejo del riesgo de inundación, los sistemas de alerta y pronóstico hidrológico y los sistemas de respuesta y mitigación contra las inundaciones deben estar fuertemente interrelacionados. Entre los aspectos que hacen al perfeccionamiento de los primeros se encuentran el potenciamiento de las redes hidrométricas y telemétricas de recolección de datos (Fattorelli *et al.*, 1995). La visión es semejante en los países de la Cuenca del Plata y ha sido expresada en diversas reuniones técnicas (p. ej.: OMM-CIC, 2003).

De las acciones encaradas por la Provincia de Santa Fe, hasta el presente merecen mencionarse:

(a) Mejoramiento de la red pluviométrica e hidrométrica: Se instalaron 35 pluviómetros y se inspeccionaron otras 19 estaciones en operación en la cuenca inferior del Río Salado, totalizando 54 estaciones instaladas bajo las normas de la OMM. La información generada está disponible al público a través de la página web del Gobierno Provincial. El seguimiento de niveles del río se informa diariamente a través de medios masivos de difusión, tarea que se realiza en forma ininterrumpida desde el mes de Enero de 2004.

(b) Elaboración de un modelo de pronóstico: En una primera etapa se plantea obtener un modelo hidrológico de tipo estadístico de regresión múltiple. Se pronosticarán los caudales medios (y las alturas hidrométricas correspondientes) del río Salado en la Ruta Prov. no. 70 para 5 plazos de pronóstico, aplicando la siguiente ecuación lineal (FICH 2006):

$$Q_{t+T} = \sum_{i=0}^{n} a_i \, Q_{t-i\Delta t} + \sum_{k=1}^{z} \sum_{j=0}^{m_k} a_j^k \, I_{t-j\Delta t}^k + b \qquad (1)$$

Q: caudal (o altura hidrométrica) en la sección de pronóstico (Ruta Prov. no. 70) en el intervalo de 24 h previo al tiempo indicado por el subíndice (variable dependiente), *t*: tiempo actual, *T*: plazo de pronóstico, variando de 1 Δt a 5Δt (Δt = 24 h), I^k: caudal medio (o altura hidrométrica) en la sección genérica *k* (aguas arriba o aguas abajo), en el intervalo de 24 h previo al tiempo indicado en el subíndice (variable independiente), *z*: cantidad de variables independientes consideradas en la regresión, a_i, a_j^k, y *b*: coeficientes de la ecuación de regresión (*a* ajustar), *n* y m_k: cantidad de términos de las variables dependiente e independiente *k* (correspondientes a tiempos anteriores), respectivamente, considerados en la regresión. Esta etapa está en pleno desarrollo.

(c) Implementación de la red telemétrica: A través de una licitación pública se ha contratado la instalación y la gestión inicial por dos años de una red de monitoreo y transmisión de datos, que constará de una Estación Central y 35 estaciones remotas (las tareas iniciaron en Febrero de 2006). Las estaciones remotas han sido clasificadas de la siguiente manera (entre paréntesis la cantidad): Tipo A1: Medición pluviométrica; pluviográfica y de humedad de suelo (9); Tipo A2: Medición pluviográfica y freatigráfica; temperatura; humedad relativa; presión barométrica; humedad del suelo; evaporación; radiación solar; velocidad y dirección del viento (5), Tipo B1: Medición limnigráfica (14) y Tipo B2: Medición limnigráfica y de calidad de agua superficial–temperatura del agua, oxígeno disuelto; PH y conductividad (10).

Acciones previstas a futuro

Los aspectos organizativos e institucionales están en la etapa de definición y son elementos claves para que se pueda llevar adelante un adecuado servicio de prevención hídrica con la eficiencia requerida para toda la provincia de Santa Fe. Basándose en los requisitos para el manejo de la información hidrológica, que influyen sensiblemente en la forma de organizar el trabajo de operación de las redes (OMM/UNESCO 1998) se deberá disponer a corto plazo de los diferentes tipos de datos, buscando aumentar la resolución espacial y temporal de la información tratando de lograr largas series de datos confiables.

REFERENCIAS

Bacchiega J. D., Bertoni J. C. & Maza J. A. (2005) Pericia hidráulica. Expediente no. 1341/2003. *Poder Judicial de la Provincia de Santa Fe.* Santa Fe. Argentina.

Bertoni, J. C., Zucarelli, G. V., Moréis, M. V. & Rodríguez, D. (1998) Aspectos fisiográficos e hidráulicos asociados a la red de drenaje santafesina. *Anales del XVII Congreso Nacional del Agua. t. 2* (Santa Fe. Argentina), 364–373.

Canziani, O. F. (2003) Extreme precipitation events and floods in the Pampas flatlands, in the Province of Buenos Aires. In: *IPCC-WMO Working Group II 3 UNEP Climate Change Impacts, Adaptation and Vulnerability – IPCC Workshop on the Detection and Attribution of the Effects of Climate Change* (New York, USA. June 2003. http://ensembles-eu.metoffice.com/IPCC/DA.pdf).

CEPAL (2003) Las inundaciones de 2003 en Santa Fe, Argentina. Evaluación del Impacto Socioeconómico y Ambiental. http://www.eclac.cl/argentina/noticias/noticias/0/12620/presentacion.pdf.

Fattorelli, S., Casale, R., Borga, M. & Da Ros, D. (1995) Integrating radar and remote sensing techniques of rainfall estimation in hydrological applications for flood hazard mitigation. The European contribution: perspectives and prospects. European Commission. Directorate General XII Science, Research and Development, Brussels.

Ferreira, G. (1997) Conflicto entre las Provincias de Santiago del Estero y Santa Fe – Argentina – por las aguas del río Salado (Año 1996). *1er. Foro Interamericano de Gestión de los Recursos Hídricos – Encuentro de las Aguas.* Instituto Interamericano de Cooperación para la Agricultura, Fortaleza, Brasil.

Ferreira, G. (2005) La crecida extraordinaria del río Salado en abril-mayo de 2003 (Provincia de Santa Fe – Argentina). Aspectos hidrológicos. *Anales del XX Congreso Nacional del Agua.* Mendoza, Argentina.

FICH (Facultad de Ingeniería y Ciencias Hídricas) (2006) Implementación de un Sistema de Alerta Hidrológico para la Cuenca del río Salado. *Convenio FICH-MAH. Etapa I.* Informe parcial. Enero 2006.

FLAGS (1999) Simulación en gran escala de la interrelación entre el Flujo de AGuas Superficiales y el Flujo de AGuas Subterráneas. Propuesta del Proyecto. PID'99 no. 74. Agencia Nacional de Investigaciones Científicas y Técnicas. Argentina.

INCYTH (1986) *Caracterización Hidrológica de la Cuenca del Río Salado*, vol. 1 y 2. Instituto Nacional de Ciencia y Técnicas Hídricas, Santa Fe, Argentina.

OMM-CIC (2003) Informe sobre reunión técnica de alerta hidrológica con consideración de los aspectos de Calidad de Agua y Anexos. Reunión Técnica en el Marco de la Cooperación OMM – CIC . Buenos Aires, Diciembre de 2003. http://www.oas.org/osde/plata/pdf/anexo-dic03.pdf.

OMM–UNESCO (1998) Evaluación de los recursos hídricos. Manual para la estimación de las capacidades nacionales. UNESCO, París, France.

Reyna J. L., Moréis, M. V., D`Elia, M. P. & Paris, M. C. (2003) Análisis de la información hidrométrica del centro de la provincia de Santa Fe. *Cuadernos del CURIHAM* **9**(1), 43–53. Rosario, Argentina.

Secretaría de Obras Públicas (2002) Proyecto de Protección contra Inundaciones. Préstamo BIRF 4117-AR. En: *OBRAS PÚBLICAS*, Marzo–Diciembre 2002, 6–7. Secretaría de Obras Públicas – Presidencia de la Nación, Argentina.

Valdés, J. B. & Fattorelli, S. (1999) Sistemas operacionales de pronóstico. Revisión y aplicación a las cuencas de los Ríos Paraná, Paraguay y Uruguay. SUCCE Programa de Rehabilitación Contra las Inundaciones, Argentina.

Vionnet C. A., Tassi, P. A., Rodriguez, L. B. & Ferreira, C. G. (2005) Numerical modelling of the catastrophic flooding of Santa Fe city, Argentina. In: *Third International Symposium on Flood Defence. Floods, from Defence to Management* (May 2005, Nijmegen, The Netherlands).

Climate Variability and Change—Hydrological Impacts (Proceedings of the Fifth FRIEND World Conference held at Havana, Cuba, November 2006), IAHS Publ. 308, 2006.

Impact assessment of measures in the upstream part of Dutch basins to reduce flooding

ERIK QUERNER & MENNO RAKHORST
Alterra, PO Box 47, 6700 AA Wageningen, The Netherlands
erik.querner@wur.nl

Abstract Flooding in the northern part of The Netherlands has caused serious economic threats to densely populated areas. Therefore a project has been carried out in a 1200 km^2 area to assess the retention of water in the upper parts of river basins as a way to reduce the downstream flooding. The physically-based groundwater and surface water model SIMGRO was used to model the hydrology of the basins. The model was calibrated using discharges and groundwater levels. Scenarios of measures to assess the possibility of retaining water in the upper parts of the basin were defined and tested. One measure was the retention of higher discharges using culverts or gates, the other was to make the streams shallower and thereby, increase flood plain storage. The analysis indicates that holding water in the upstream parts of the basins proved to be feasible and can result in significant reductions of peak flows.

Key words drainage basin; rainfall; evapotranspiration; groundwater; surface water; modelling; river basin; scenario

INTRODUCTION

Worldwide there has been an increase in the number of floods and droughts that effect large numbers of people and cause enormous economic losses. In the period 1990 to 1998 the number of recorded flood disasters in Europe was higher than in the previous three and a half decades (EEA, 2001). Because of this situation it is clear that measures have to be taken to reduce the impact of these extreme hydrological events. To analyse such extreme events and possible mitigation measures, tools were used to evaluate them in terms of eco-hydrological impact and their effect on agriculture.

The Netherlands was originally a marshy delta formed by the rivers Rhine and Meuse. A rise in sea level, coupled with subsidence of the ground level means that more than half the country is now below sea level (the low-lying part); the remainder is only slightly above sea level. Throughout the country the water table is shallow (between 0.3 and 2.5 m below the soil surface) and a dense network of engineered watercourses is needed to drain the land. Because of these engineered watercourses, water can flow quickly from the upper part of the basins. However, during recent extreme rainfall events in the northern part of The Netherlands the rapid flow from the upper parts of the basin caused by the flooding of polders resulted in a serious threat of flooding of densely populated areas downstream.

After a Dutch national study "Water Management in the 21st Century" a policy was adopted to retain more water in the upper part of river basins in order to avoid flooding in the downstream parts. As part of this national study, measures designed to retain water were analysed in six basins across The Netherlands (Querner, 2002). Understanding the hydrology in these basins provided a proper basis for decision making on feasible measures. Analysis of the complex, and engineered Dutch river systems requires the use of a combined groundwater and surface water model to predict the effect of measures on a regional scale. In this study the SIMGRO model was used (Querner, 1997). This model simulates the flow of water in the saturated zone, the unsaturated zone and the surface water. The model is physically-based and therefore suitable for use in situations with changing hydrological conditions.

In order to make an integrated river basin management plan for the northern part of The Netherlands, one of the problems to solve is how to reduce the peak discharge. The question is: How to retain more storm water in the upper parts of basins? In this paper we report on a project carried out to assess the possible retention of water in the upper part of a river basin. It describes very briefly the SIMGRO model, the schematization of the study area, the input data and then the scenarios and results.

Copyright © 2006 IAHS Press

SIMGRO MODEL

SIMGRO (SIMulation of GROundwater and surface water levels) is a physically-based distributed model that simulates regional transient saturated groundwater flow, unsaturated flow, actual evapotranspiration, sprinkler irrigation, streamflow, groundwater and surface water levels as a response to precipitation, and groundwater abstraction. For a comprehensive description of SIMGRO, including all the model parameters, readers are referred to Querner (1997) or van Walsum *et al.* (2004).

To model regional groundwater flow, as in SIMGRO, the system has to be schematized geographically, both horizontally and vertically. The horizontal schematization allows input of different land uses and soils, in order to model spatial differences in evapotranspiration and moisture content in the unsaturated zone. For the saturated zone, various subsurface layers are considered. The finite element procedure is applied to the flow equation which describes transient groundwater flow in the saturated zone. The unsaturated zone is represented by two reservoirs, one for the root zone and one for the underlying soil. The calculation procedure is based on a pseudo-steady state approach. The height of the phreatic surface is calculated from the water balance of the subsoil below the root zone, using a storage coefficient. Evapotranspiration is a function of the crop and moisture content in the root zone.

In the model the surface water system is considered as a network of reservoirs. The inflow of one reservoir may be the discharge of the various watercourses, ditches and runoff. The outflow from one reservoir is the inflow to the next reservoir. The water level depends on surface water storage and on reservoir inflow and discharge. In the model, four drainage subsystems are used to simulate the interaction between surface water and groundwater. This interaction is calculated for each drainage subsystem using a drainage resistance and the difference in level between groundwater and surface water.

The SIMGRO model is used within the GIS environment Arcview. This allows the possibility of using digital geographical information (soil map, land use, watercourses, etc.) in order to convert these to input data. Further use is the presentation of results and analysis of these together with specific input parameters.

STUDY AREA AND MODEL SCHEMATIZATION

The modelling area covers 1200 km^2 and is located in the northern part of The Netherlands (see Fig. 1). The area of main interest is approximately 750 km^2 and covers the basins of the river Drentsche Aa and Peizerdiep. The ground surface slopes from about 24 m above NAP (reference level in the Netherlands) in the south to about –1 m in the north. The area consists of sandy soils in the upper parts with clay and peat in the stream valleys and the lower part. Land use is predominantly agricultural and forest. About 42% is in pasture, 24% is arable land, 18% is woodland, 11% residential and 5% is other. For the meteorological input data five stations spread over the area were used (Querner *et al.*, 2005).

For the SIMGRO model the groundwater system needs to be schematized by means of a finite element network. The network, comprising 49 050 nodes, is spaced at about 200 m in the interest area, but in the stream valleys it is spaced at 75 m. For the modelling of the surface water the basin is subdivided in 5625 sub-basins. The difference in height of about 25 m means that 570 weirs were constructed in the past to control the water level and flow. Most of the weirs are adjustable, so that the target water level in summer can be raised. The lower part near or below sea level has 58 pumping stations and 41 inverted siphons.

The geology of the area is quite complex, due to influences from the Pleistocene period, permafrost, tectonic movements, and influences from wind and water. A major influence on the groundwater flow patterns is the resistant impermeable layers formed by boulder clay that cause large areas with perched water tables. The groundwater system in the model is build up of four aquifers that are interlaid with three less permeable layers. The second layer consists of the boulder clay. The interaction between groundwater and surface water is characterized by a drainage resistance. This resistance is derived from hydrological parameters and the spacing of the water courses.

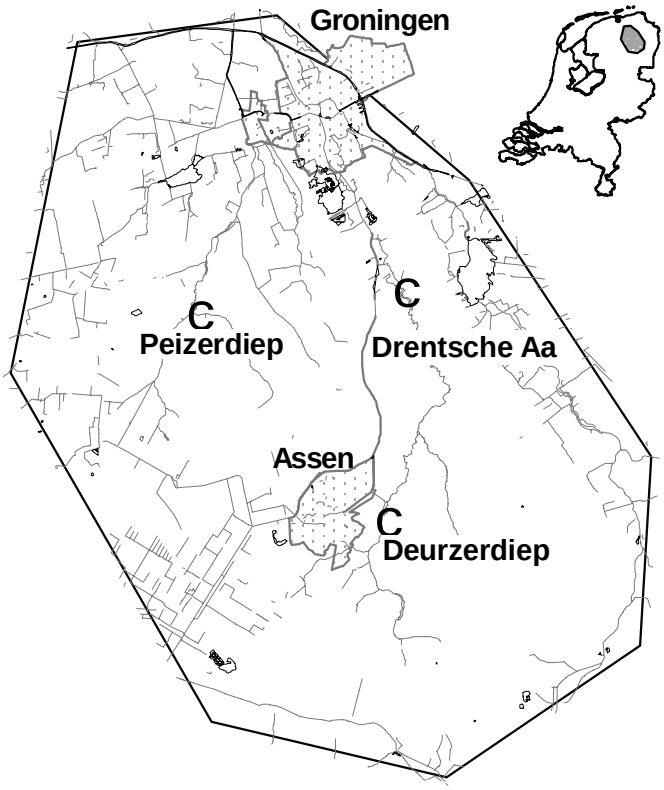


Fig. 1 Location of the modelling area and the main water courses in the northern part of The Netherlands (Rakhorst, 2005).

Perched water tables

The initial Simgro model was not able to simulate the perched water tables caused by the boulder clay (model layer 2). In large areas this resulted in phreatic groundwater levels that were 1–3 m too low. Therefore the model was adjusted so that, on the basis of the hydraulic head below and above the boulder clay, the vertical resistance is corrected to simulate the flux through this clay layer correctly. Also the storage coefficient above and below the clay layer was changed during the calculations depending on the presence of the perched water table. After the model was improved, calculated phreatic levels were close to the measured ones (see next section).

RESULTS OF SIMGRO MODELLING

Present situation

Simulations were carried out for a period of 10 years (1989–1999). The results were compared with measured river discharges (nine locations) and groundwater levels (about 800 piezometers). For three main gauging stations, as shown in Fig. 1, Table 1 gives the measured and calculated discharges. The discharges are given for a recurrence interval of once in five years to a recurrence interval of 15 times per year (denoted as 15× year^{-1}). The last column in Table 1 gives Q95, the flow occurring less than 5% of the time. For the Drentsche Aa the calculated discharge is a bit higher than measured (about 8–20%). For the other two streams the differences are smaller, in the order of 2–14%. When comparing hydraulic heads, for more than half the total number of piezometers, the difference in measured and calculated head is less than 0.25 m. Comparing only the phreatic levels: for the 332 phreatic piezometers there are 239 with a difference less than 0.5 m and 145 with a difference less than 0.25 m. These differences between measured and calculated results were regarded as small, so it was concluded that the final model can be used to analyse possible measures to hold water in the upstream part of the basin.

Table 1 Measured and calculated discharges for three gauging stations ($m^3 s^{-1}$) in the northern part of The Netherlands (for recurrence intervals see text).

Gauging station		Discharge for the given recurrence interval:				
		5 year	1 year	5× year^{-1}	15× year^{-1}	Q95
Drentsche Aa	Measured	11.02	8.91	6.97	5.48	0.57
	Calculated	13.63	11.57	7.58	6.24	0.36
Deurzerdiep	Measured	14.45	11.52	6.34	4.00	0.27
	Calculated	14.05	11.59	6.24	4.31	0.14
Peizerdiep	Measured	13.64	10.45	6.57	5.01	0.08
	Calculated	13.44	10.47	5.97	4.37	0.12

Mitigation measures and the impact

Mitigation measures were defined that would reduce the peak discharges to acceptable volumes. In this research the following measures were analysed:

– **Restrict peak discharges**
  Peak flows can be restricted by installing sluice gates or culverts of such a dimension that only the higher peaks are reduced. In the simulations, the opening of these constructions was such that the flow will be restricted when the flow is higher than occurring one day a year.
– **Make the streams shallower**
  Reducing the depth of the water course will result in water overtopping the side banks and thus increase the amount of water that is stored on the flood plain. The storage of the water on the over banks will reduce the flow propagations and thus reducing the peak flow.

In Fig. 2 the upstream part of the Drentse Aa where measures were considered is shown. At eight locations the flow was restricted and over a length of 29 km the streams were made shallower. In Table 2 the results are shown for the two sub basins; it gives the discharge for the reference situation, the two measures and the change in flow. The impact of the first measure (restrict peaks) is more than the second (shallower streams). Limiting the flow by introducing gates or culverts,

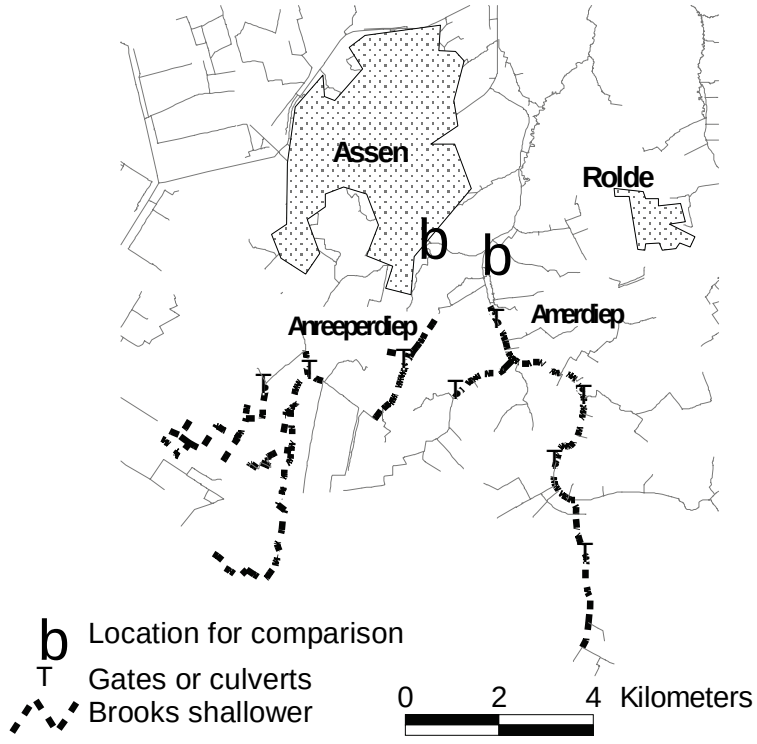


Fig. 2 Location of the mitigation measures carried out in the upstream part of the Drentsche Aa.

Table 2 Change in discharges ($m^3 s^{-1}$) for two sub basins and the two measures as shown in Fig. 2.

Location	Scenario	Discharge for a given recurrence interval				
		10 year	5 year	1 year	5x year^{-1}	15x year^{-1}
Amerdiep	Reference	13.180	9.620	5.418	3.078	2.227
	Gates	5.321	4.980	4.603	3.138	2.245
	Reduction (%)	60	49	15	–2	-1
	Shallower streams	10.078	9.056	4.994	3.071	2.246
	Reduction (%)	24	7	8	0	-1
Anreeperdiep	Reference	9.121	5.807	3.379	1.939	1.472
	Gates	6.973	3.741	3.019	1.972	1.476
	Reduction (%)	24	36	8	–2	0
	Shallower streams	8.475	5.526	3.438	1.929	1.433
	Reduction (%)	7	4	2	1	1

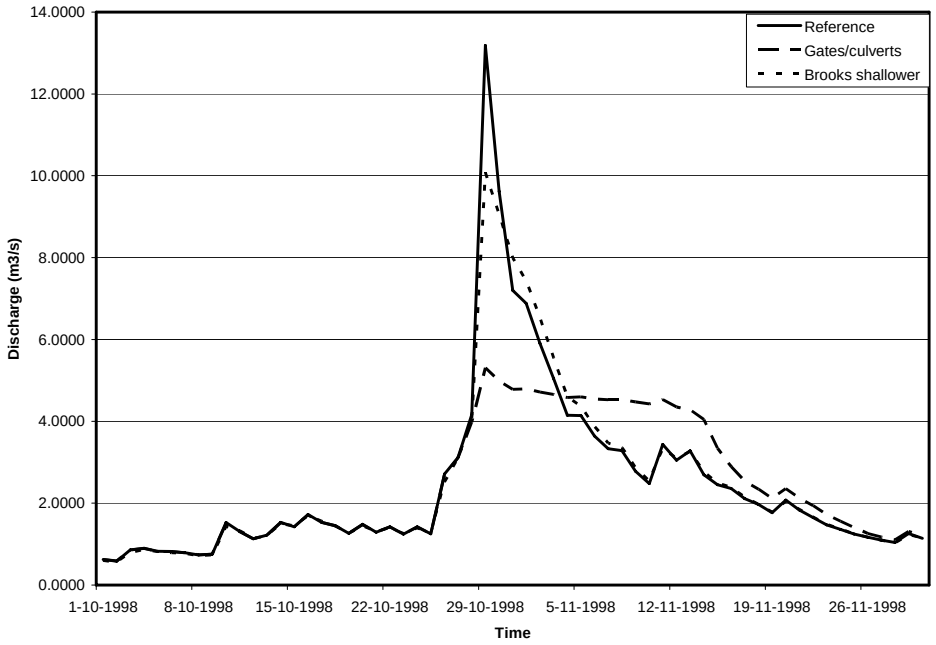


Fig. 3 Discharge for reference situation and the two measures for an extreme wet period in 1998.

means a decrease in peak flow of the order of 25–50%. The large variation depends on local conditions and the number of structures in a stream. Limiting the flow has very little influence on groundwater levels, because the water flow is obstructed only for a number of days or weeks. Local flooding may occur and thus groundwater levels rise. This small and short rise, often in winter time, has no apparent effect on agriculture or nature.

When the stream is made shallower, the reduction of peak discharges is of the order of 5–20% (Table 2). The consequence of this measure is higher water levels in both wet and dry periods. The flow reduction is mainly caused by the water overflowing the river banks and flooding the valley. As a consequence, the groundwater levels adjacent to the stream will be higher. In general the higher levels may have a positive influence on the presence of rare and protected marsh species.

When the above measures are introduced the peak flows will be reduced and discharge is spread over a longer time period. As an example, in Fig. 3 the flow situation is given for October and November 1998, a period with extreme rainfall in the Northern part of The Netherlands. Figure 3 shows the calculated discharge for the present situation and the two measures. In the reference situation the duration of the high flow was about one week, but after flow restriction the maximum flow is much smaller as it is spread over a period of 2.5 weeks (Fig. 3). When the streams are made shallower, the maximum peak reduces, but the flood wave looks very similar to the present situation.

CONCLUSIONS AND DISCUSSION

The physically-based Simgro model was able to simulate streamflow in basins with different land use and climate conditions. The model calibration was limited, but the simulation results show that the model gives satisfactory estimates of the discharges and groundwater levels. The model is therefore an adequate tool to simulate streamflow, and has the potential to assess the impact of measures to reduce flooding.

This study has shown that ecosystems of lowland catchments where the groundwater levels have been lowered by extensive land drainage can be restored by restricting the flow from the upper parts. Holding water in the upstream parts of the basins is feasible. The delay of the peak flow is significant. Limiting the flow by introducing gates or culverts, means a decrease in peak flow in the order of 25–50%. To make the stream shallower results in reduction of peak discharges in the order of 5–20%.

For extreme situations, such as occurred in October 1998, it is also possible to use measures to reduce peak flows that have a recurrence of once in 10 or 50 years. In that way the choice is explicitly to accept local flooding in the upper parts of a catchment where mostly agricultural land is situated, instead of flooding high densely populated areas more downstream.

Acknowledgement The research reported here was part of an MSc Thesis by the second author for Wageningen University. The research was carried out at Alterra, Wageningen, The Netherlands.

REFERENCES

EEA (2001) Sustainable water use in Europe. Part 3: Extreme hydrological events: floods and droughts. *Environmental issue report no. 21*. European Environment Agency, Copenhagen, Denmark.

Querner, E. P. (1997) Description and application of the combined surface and groundwater model MOGROW. *J. Hydrol.* **192**, 158–188.

Rakhorst, M. (2005) Reduction in peak discharges for the Streams in Northwest Drenthe; estimated with the SIMGRO model. MSc Thesis, Wageningen University, Wageningen, The Netherlands (in Dutch).

Querner, E. P. (2002) Analysis of basin response resulting from climate change and mitigation measures. In: *FRIEND 2002–Bridging the Gaps Between Research and Practice* (ed. by H. van Lanen & S. Demuth) (Fourth Int. Conf. on Friend, Cape Town, South Africa, March 2002), 77–84. IAHS Publ. 274. IAHS Press, Wallingford, UK.

Querner E. P., Rakhorst, M., Hermans, A. G. M.& Hoegen, S. (2005) Exploring the possibilities to retain water on the Drents Plateau; Pilot in Northwest Drenthe (in Dutch). *Alterra Report 1240*. Alterra, Wageningen, The Netherlands.

Walsum, P. E. V. van, Veldhuizen, A. A., van Bakel, P. J. T., van der Bolt, F. J. E., Dik, P. E., Groenendijk, P., Querner, E. P.& Smit, M. F. R. (2004) SIMGRO 5.0.1, Theory and model implementation. *Alterra Report 913.1*. Alterra, Wageningen, The Netherlands.

Climate Variability and Change—Hydrological Impacts (Proceedings of the Fifth FRIEND World Conference held at Havana, Cuba, November 2006), IAHS Publ. 308, 2006.

Propuesta para minimizar el impacto de las inundaciones en una cuenca costera de la costa de Chiapas, México

MARTÍN D. MUNDO MOLINA

Centro de Investigación de la Facultad de Ingeniería de la Universidad Autónoma de Chiapas (UNACH), Boulevard Belisario Domínguez km 1081, Tuxtla Gutiérrez, Chiapas, México

ic_ingenieros@yahoo.com.mx

Resumen En la época de grandes avenidas suelen ocurrir inundaciones en las cuencas costeras del estado de Chiapas, debido principalmente al deteriorando del entorno natural de éstas por efectos antropogénicos. Las inundaciones no sólo suelen causar grandes pérdidas económicas sino también la muerte de ciudadanos. Por tal razón el Centro de Investigación de la Facultad de Ingeniería de la UNACH desarrolló un proyecto para estudiar alternativas para minimizar el impacto de las inundaciones en la Costa de Chiapas. Aquí se presentan los principales resultados obtenidos en la cuenca del río Coatán. Se estimaron los caudales (Q) del río Coatán para diferentes períodos de retorno (Tr) y con modelos digitales de elevación del terreno se utilizó un simulador hidráulico para obtener mapas de riesgo. Con dicha información se propuso: (a) La delimitación de la zona federal del río. (b) Desalojar y reubicar a las viviendas de la zona federal a zonas seguras. (c) Sembrar bambú en un tramo que incluye la zona urbana y agrícola del río. (d) Implantar un sistema de alerta temprana para prevenir a la población en situaciones de peligro.

Palabras claves cuenca; eventos hidrometeorológicos extremos; caudal pico; inundación; simulación hidráulica; mapas de riesgo; períodos de retorno; sistema de alerta temprana; manejo de cuencas; deforestación

Proposals for minimizing flooding in the Chiapas coastal river basin, Mexico

Abstract During hurricanes floods occur in the coastal river basins of the state of Chiapas, Mexico. The floods are a result of the deterioration of the natural surroundings of the river basin. The deterioration of the natural surroundings is caused mainly by human activity. The floods cause great economic losses and death of citizens. For this reason, the Research Center of the Faculty of Engineering of the Chiapas State University (Spanish acronym: UNACH) has developed a project to study various alternative measures in order to diminish the impact of the floods on the coast of Chiapas, mainly in the Coatán River. This paper presents the main results obtained for the basin of the Coatán River.

Key words basin; hydrological extremes; peak runoff; flood; hydraulic modelling; risk; return period; hydrological warning; basin management; deforestation

INTRODUCCION

En la época de eventos hidrometeorológicos extremos o de grandes avenidas, como consecuencia de las altas precipitaciones en la cuenca del río "*Coatán*", suelen ocurrir deslaves, procesos de erosión y transporte de material rocoso y de sedimentos de considerable importancia, que junto a los escurrimientos, se transforman en avalanchas que suelen provocar inundaciones en la parte baja de la misma. Lo anterior debido al deterioro, por efectos principalmente antropogénicos, del entorno natural de la parte alta y baja de la cuenca. El arrastre de materiales y el escurrimiento de grandes volúmenes de agua ocasionan el desborde de los ríos. Una vez desbordados los cauces de los ríos, por falta de capacidad hidráulica se amplían en decenas o cientos de metros rellenando las partes bajas con rocas, material granular o azolves finos. Así, ocurren las inundaciones en zonas rurales y urbanas, causando pérdidas económicas importantes, especialmente en la zona urbana de Tapachula como se demuestra en este estudio, correspondiente a un tramo aproximado de 12.5 km de río, simulado mediante Infoworks RS. Es importante destacar que la ciudad de Tapachula es la ciudad con mayor densidad de población de las ciudades costeras, con una población de más de 200, 000 habitantes (INEGI, 2000).

ANTECEDENTES

En septiembre de 1998 y octubre de 2005 ocurrieron en Chiapas dos de los eventos hidrometeorológicos extremos que mayor daño han provocado en las últimas décadas a la zona costera del Estado. En septiembre de 1998 eventos hidrometeorológicos extremos y en octubre de 2005 el huracán Stan (Lawrence *et al*., 2005), dejaron a su paso cuantiosas pérdidas económicas, materiales y además pérdida de vidas humanas (Tabla 1). Las intensas lluvias de ambos eventos

Copyright © 2006 IAHS Press

Tabla 1 Pérdidas materiales y económicas por el paso de eventos hidrometeorológicos extremos (Mundo *et al.*, 2005).

	Eventos extremos, 1998	Huracan Stan, 2005
Damnificados	29 000	92 000
Persona muertas	229	82
Caminos destruidos	712 km	630 km
Puentes dañados	40	253
Sistemas de agua potable y alcantarillados	22	38
Viviendas	16 000	45 166
Escuelas	–	305
Unidades médicas	–	11
Superficie agrícola	51 159 ha	307 000 ha
Costo	63 000 000 US$	1 149 000 000 US$

produjeron deslaves, arrastre de árboles, rocas y sedimentos de la parte alta hacia la parte baja de la cuenca que mezclados con un caudal extraordinario causó severos daños en casi toda la planicie costera, afectando a las principales ciudades y comunidades de la costa, principalmente a Tapachula, la segunda ciudad más importante del Estado, desde el punto de vista económico

PROBLEMÁTICA

Los grandes caudales generado por altas precipitaciones en la cuenca del río Coatán, provocan el arrastre de materiales y el escurrimiento de grandes volúmenes de agua que son potenciados en su movimiento descendente de la parte alta de la cuenca hacia la zona de costa, por las grandes pendientes de la parte alta de la misma, en dirección radial a la franja costera, en la cual ocurre el depósito de los materiales granulares y finos formando abanicos aluviales causando además la reducción de la capacidad hidráulica del cauce principal de la cuenca, que luego ocasiona el desborde de los ríos. Los flujos con alta velocidad proveniente de la montaña pierden energía cinética en su descenso, por lo tanto al encontrar una pendiente menor en la zona baja de la cuenca provocan el incremento del tirante hidráulico y depositación. Una vez desbordados los cauces de los ríos, por falta de capacidad hidráulica, éstos se amplían en decenas o cientos de metros, desviando el sentido del flujo principal en varias direcciones, rellenando en el proceso las partes bajas de la topografía (formándose dunas y acumulación de sedimentos), con rocas, material granular o azolves finos. Así ocurren las inundaciones en zonas urbanas y rurales, provocando pérdidas económicas importantes, de mayor valor en función de la altura del tirante hidráulico de inundación. Desde el punto de vista hidrológico las precipitaciones en exceso se concentra de forma rápida en la parte baja de la cuenca por dos razones: (1) Topográficas: Grandes pendientes de la zona montañosa. La zona montañosa se encuentra muy cerca de la franja costera, 30 km en su parte más ancha y 10 km en su parte más angosta. Esta topografía peculiar provoca altas velocidades del flujo, concentrando los caudales en la parte baja en un tiempo menor, (2) Hidrológicas: Los factores hidrológicos que influyen en la respuesta rápida la cuenca del río Coatán es el número elevado de su densidad de corriente y densidad de drenaje. Así, la respuesta rápida de dicha cuenca significa que el tiempo base del hidrograma es pequeño mientras el caudal es grande (Fig. 1).

MATERIALES Y METODOS

En este trabajo de investigación se planteó simular hidráulicamente el río Coatán, con el objeto de generar manchas hidráulicas de inundación (mapas de riesgo) para diferentes períodos de retorno, asociado a diversos caudales, con el fin de analizar el alcance máximo de las inundaciones. Con los mapas de riesgo obtenido se propusieron varias alternativas para minimizar el impacto de las inundaciones. Para cumplir con el objetivo de esta investigación se utilizaron los siguientes materiales: Planos topográficos de la cuenca a escala 1:250 000; Plano topográfico de la cuenca a escala 1:10 000; Trazo de poligonales y curvas de nivel (topografía); Arc View, para la construcción del TIN (triangulación); Infoworks RS, para la simulación hidráulica del río Coatán.

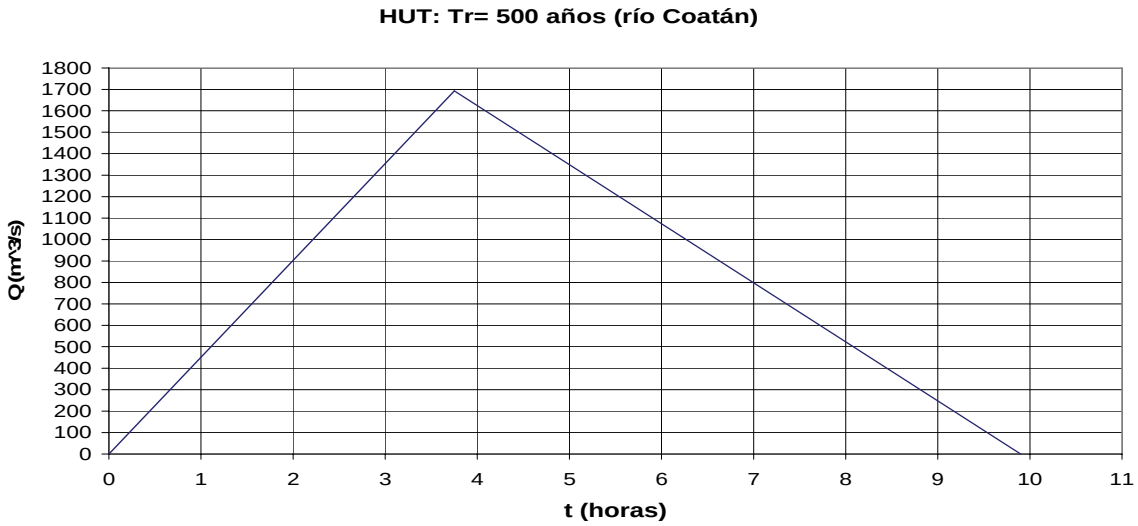


Fig. 1 Hidrograma unitario triangular para un Tr de 100 años (Mundo *et al*., 2005).

Por otro lado, para proponer las alternativas de solución a la problemática planteada en este trabajo, se ejecutó la siguiente metodología: (a) Los datos topográficos escala 1:10 000 en AutoCad [valores (*x*,*y*,*z*)], se transportaron al programa Arc View; (b) Se realizó la triangulación para la obtención de las secciones transversales y longitudinales del río Coatán, en Arc View; (c) Con dicha triangulación se construyó el modelo digital de elevaciones (MDE) del cauce del río; (d) Una vez construido el MDE, se crearon las secciones en el Infoworks RS; (e) Se calibró el Infoworks RS, utilizando n de Manning de 0.030 y la mancha de inundación del río Huixtla del evento hidrometeorológico extremo de septiembre de 1998, (f) Con los datos obtenidos de la escorrentía histórica de la cuenca del río Coatán y del estudio hidrológico realizado para la cuenca, se ejecutó el modelo de simulación hidráulica en flujo permanente; (g) Como producto de la simulación se obtuvieron los mapas de riesgo como el que se muestran en la Fig. 2.

RESULTADOS

Una vez calibrado el Infoworks RS, se realizaron las simulaciones hidráulicas y se obtuvieron los siguientes resultados: Seis mapas de riesgo para los siguientes Tr: 5, 10, 20 50, 100 y 500 años (ver Fig. 2). Con los mapas de riesgo se propusieron las siguientes alternativas para minimizar el impacto de las inundaciones: (a) Sembrar bambú (Bambusa Vulgaris) en doble fila, desde el Puente Malpaso (10 km aproximadamente, aguas arriba del acceso de la ciudad) hasta el Puente de la Planta Trituradora (en las afueras de la ciudad de Tapachula), en una longitud total de 52 km, sobre ambos márgenes, a un costo de 154 000 pesos mexicanos (US$15 400). Los 52 km se deberán sembrar en doble fila, la primera justo a la orilla del cauce, que se constituirá como la primera zona de amortiguación de avenidas y la segunda fila justo en el límite de la mancha hidráulica para un Tr de 5 años (ver Fig. 2), es decir, en el límite de la zona federal que de acuerdo a la Ley de Aguas Nacionales y su Reglamento, se define en el artículo 4º (página 125) y se enuncia de la siguiente manera: "*Por lo que se refiere a la delimitación, demarcación y administración de las riberas o zonas federales contiguas a los cauces de las corrientes y a los vasos o depósito de propiedad nacional, se estará a lo siguiente: Fracción I: El nivel de aguas máximas ordinarias a las que se refiere la fracción VIII, del artículo 3º de la* '*Ley*'*, se entiende como el que resulta de la corriente ocasionada por la creciente máxima ordinaria dentro de un cauce sin que en éste se produzca desbordamiento. La creciente máxima ordinaria estará asociada a un período de retorno de cinco años*" (CNA, 2004). Esta segunda fila, se constituirá como una segunda zona de amortiguación de avenidas. Entre ambas filas quedará un área que podrá usarse con fines de recreo, construyendo áreas verdes y de esparcimiento, (b) Debido a los asentamientos de población localizados en la parte federal del río Coatán (ver Fig. 2), esta superficie es una zona de alto riesgo, que incrementa su exposición ante posibles eventos

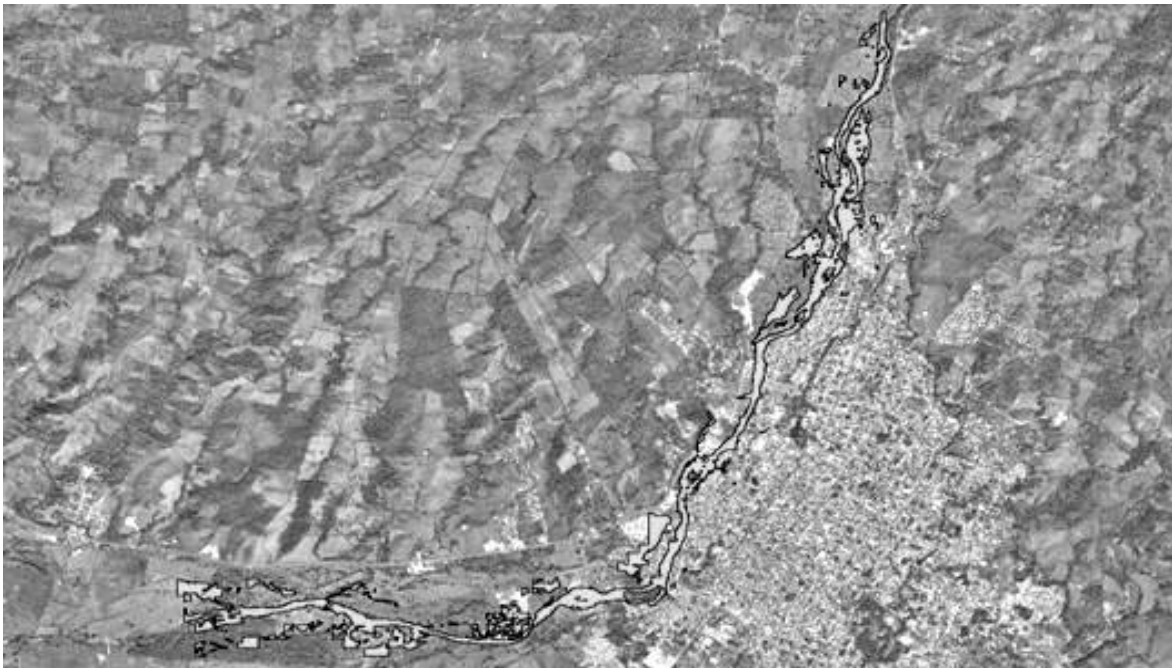


Fig. 2 Mapa de riesgo de la zona federal, para el Tr de 5 años (Mundo *et al*., 2005).

hidrometeorológicos extremos. Por tal razón, deberán reubicarse todas las casas localizadas en dicha zona y deberá además evitarse la construcción de viviendas en la mancha hidráulica para un Tr de 5 años (zona federal), (c) Instaurar un sistema de alertamiento temprano (SAT). El SAT deberá utilizar los mapas de riesgo generados en esta investigación, un hidrograma que permita estimar los caudales de arribo a la sección de medición, así como un sistema de medición de caudales en la salida de la cuenca (estación hidrométrica automatizada o convencional). El SAT aquí expuesto de forma sucinta fue desarrollado en el Centro de Investigación de la Facultad de Ingeniería de la UNACH (Mundo *et al*., 2005).

CONCLUSIONES

A modo de conclusiones se puede enunciar que:

1. El sistema Infoworks RS es una herramienta muy útil para la simulación hidráulica y determinación de áreas de inundación. No obstante la potencialidad del sistema, se recomienda utilizar fotogrametría, productos de vuelos bajos, a escala 1:2000, 1:5000 ó 1:10 000, o también topografía detallada, para obtener buenos resultados. El Infoworks RS calibrado, permite generar "mapas de riesgo de inundaciones" con alta confiabilidad.
2. La reubicación es una acción necesaria y obligada por Ley, sin embargo, es necesario realizar un estudio a detalle para determinar una zona segura para construir nuevas colonias, con el fin de asentar a la comunidad removida y crear la infraestructura necesaria para el buen vivir como: viviendas, escuelas, drenaje, alcantarillado, luz eléctrica, agua potable y pavimentación de calles.
3. Debido a las alteraciones climáticas y al efecto del Enzo, actualmente se está viviendo un período de inestabilidad. Así, el calentamiento del mar en la zona del Caribe está provocando la generación de huracanes que han incrementado no sólo su número sino su intensidad en este período, además con posibles desplazamientos hacia el norte de la Zona de Intertropical de Convergencia. Este escenario suscita el peligro potencial de un evento hidrometeorológico extremo de igual o mayor magnitud que el Mith o el Stan, que no solo supone alto riesgo en las márgenes o zona federal de los ríos, habitado por cientos de miles de personas, sino también en la zonas serranas de la costa de Chiapas, en donde debido a la deforestación de la parte alta de las cuencas pueden ocurrir deslaves, socavones, desgajamientos y corte de caminos que dejarían incomunicados a cientos de pequeños poblados rurales.

4. En las simulaciones hidráulicas realizadas con Infoworks RS para el río Coatán utilizando un período de retorno de 500 años (Q = 1693 m^3 s^{-1}), se estimaron tirantes hidráulicos superior a los 4.5 m (en el Puente Malpaso, 10 km aguas arriba del acceso a la ciudad de Tapachula). Los escurrimiento provocados por el Huracán Stan rebasaron el caudal asociado a un Tr de 500 años, por lo que es necesario simular hidráulicamente los ríos de la zona costera de Chiapas, considerando períodos de retorno superior a 1000 años.
5. No se recomienda construir ninguna obra transversal (muros simples, muros gavión, muros de mampostería, pequeñas presas de machones), para romper el pico de las avenidas o para detener socavones en la zona torrencial, ya que el flujo tiene la energía suficiente como para romper las estructuras y provocar mayores daños aguas abajo. Es más importante en este momento, desde el punto de vista técnico, reforestar o poner barreras naturales (vegetación endémica y árboles nativos de la zona).
6. No se recomienda construir ningún tipo de bordos tanto desde el punto de vista técnico como económico en las márgenes del río Coatán, especialmente en la zona urbana.
7. Es necesario reforestar la parte alta de la cuenca del río Coatán, aproximadamente 9000 ha, así como impulsar un convenio con el gobierno de Guatemala que permita realizar un proyecto conjunto que mejore la situación ambiental de dicha cuenca internacional, en su parte alta.

Agradecimientos Se agradece a la Universidad Autónoma de Chiapas, quien aportó los recursos económicos para financiar este proyecto.

REFERENCIAS

CNA (2004) *Ley Federal de Aguas Nacionales y su Reglamento*. Comisión Nacional del Agua, México, D.F.

INEGI (2000) *Integración territorial del XII censo general de población y vivienda 2000.* Resultados para el estado de Chiapas. Instituto Nacional de Geografía Estadística e Informática, México, D.F.

Lawrence, M. B., Avila., L. A., Beven., J., Franklin., J. L., Pasch, R. J. & Stewart, S. R. (2005) Atlantic Hurricane Season of 2003. *Monthly Weather Review* **133**(6), 1744–1773.

Mundo, M. M., Nájera, B. F., Ballinas, A. R., Altuzar, D. J., Ballinas, L. J., Cano, A. F., Serrano, Z. J. & Sandoval, T. O. (2005) *Cuenca Coatán. Identificación y delimitación de áreas de riesgo por inundación. Propuesta y simulación de alternativas. Análisis de costo beneficio de las alternativas propuestas*, vol. 1. Informe del Centro de Investigación de la Facultad de Ingeniería de la UNACH para la Comisión Nacional del Agua. Tuxtla Gutiérrez, Chiapas, México.

Mundo, M. M., Nájera, B. F., Ballinas, A. R., Altuzar, D. J., Ballinas, L. J., Cano, A. F., Serrano, Z. J. & Sandoval, T. O. (2005) *Sistema de alerta temprana. Cuenca Coatán*, vol. 6. Informe del Centro de Investigación de la Facultad de Ingeniería de la UNACH para la Comisión Nacional del Agua. Tuxtla Gutiérrez, Chiapas, México.

Climate Variability and Change—Hydrological Impacts (Proceedings of the Fifth FRIEND World Conference held at Havana, Cuba, November 2006), IAHS Publ. 308, 2006.

Numerical estimation of flood zones in the Vistula River valley, Warsaw, Poland

MAŁGORZATA GUTRY-KORYCKA[1], ARTUR MAGNUSZEWSKI[1], JAROSŁAW SUCHOŻEBRSKI[1], WITOLD JAWORSKI[1], MICHAŁ MARCINKOWSKI[1] & MICHAŁ SZYDŁOWSKI[2]

1 *University of Warsaw, Hydrology Department, Krakowskie Przedmieście 30, 00-927 Warszawa, Poland* asmagnus@uw.edu.pl

2 *Technical Academy of Gdańsk, Institute of Civil and Environmental Engineering, Narutowicza 11/12, 80-952 Gdańsk, Poland*

Abstract Flood maps (referred to as flood risk maps) are developed for planning purposes and the needs of insurance companies. They usually map the flood with a 100-year recurrence interval ($Q_p1\%$, i.e. discharge of probability of occurrence p = 1%), or flooding during the largest historically recorded flood. Typically these maps identify the zone of highest hazard, the so-called flood path, which is where construction is forbidden, and a zone of high hazard, i.e. the area between the flood path and the edge of the $Q_p1\%$ flood. In this study the assessment of the flood waters between the flood protection dykes of a reach of Vistula River was made using a one-dimensional hydraulic model and a Digital Elevation Model (DEM). The ordinates of water level for the Vistula were determined with the HEC-RAS model, assuming conditions of a steady state flow with a given probability of exceedence. The flood zones obtained from the simulations indicate that a significant part of the town is situated in the potentially dangerous flood hazard zone. The simulations also indicate that under present conditions the elevations of the flood protection dykes are sufficient to convey the $Q_p1\%$ discharge. However, the dykes would not ensure protection of an important part of the city in the case of a $Q_p0.1\%$ discharge.

Key words flood recurrence interval; flood zone mapping; Warsaw, Poland; Vistula River

INTRODUCTION

The creation of flood hazard maps is required by Article 82 of the Polish Water Law. In order to estimate the extent of the flood zones, mathematical models of flood wave propagation and digital models of the river bed and flood plain are usually used. Polish legislation does not specify the models or numerical tools needed to simulate the flood wave propagation for flood hazard mapping. However, some suggestions can be found in the Polish literature (Nachlik *et al*. 2000; Radczuk *et al*. 2001). In general, the flood hazard maps should be prepared for discharges with the probability of occurrence equal to 1%, or for the largest historically recorded flood which is often approximated by the 0.1% probability discharge. These maps are usually made using a one-dimensional mathematical model of open channel flow. For some special cases, for instance levee break analysis, two-dimensional models are suggested. The flood analysis can be done for steady or unsteady water flow depending on the local hydraulic conditions and the availability of hydrological data.

STUDY SITE DESCRIPTION

The geomorphology of the Vistula River valley within the urban area

The valley of the Vistula was developed by fluvial processes throughout the Holocene and during the final stages of the last glaciation. The segment of the Vistula valley studied here (in Warsaw) has a length of 47.05 km (i.e. between 494.76 and 541.81 km of the river course). The width of the lowest over-flood terrace varies between 6 km in the area of Praga, to just several dozen metres on the left bank in the area of the Old Town. The surface of the terrace in the southern parts of the city situated beyond the reach of the flood waters. In the areas of Dolne Łomianki and Kępa Kiełpińska the waters of the most catastrophic floods inundate the surface of the terrace. These floods are typically caused by ice-jams.

The catastrophic flood of July 1884 and the construction of a water uptake for the city water supply were impulses to regulation of the Vistula in Warsaw. In the years 1893–1910, river training work was conducted along both banks of the river. The width of the regulation route of the river was assumed to be 340 m. Between 1923 and 1931, and after the flood of 1924, further stream regulation was carried out to protect the banks and the newly built dykes.

Copyright © 2006 IAHS Press

Immediately after World War II, the river channel of the Vistula in Warsaw became a dumping ground for debris. This caused the high-discharge cross-sections in some areas to be reduced by 50% in comparison with the middle Vistula. This resulted in the so-called Warsaw corset which occurs in the segment of 507–517 km. A little upstream of the Śląsko-Dąbrowski Bridge, the channel of Vistula got narrowed down to approximately 350 m. This is the most significant narrowing of the channel in the entire middle and lower course of the river.

According to the designs of the Central Water Management Bureau from the 1960s, the city should be protected against the flood that has a recurrence of 1000 years (Q_p0.1%) by the protection dykes that are built at distances of 400–600 m from the channel. Upstream and downstream of Warsaw, the protection dykes are located at 1000 to 1700 m and shield agricultural areas against the inundation caused by the Q_p1% flood.

Hydrological conditions

The channel elevation decreased on average by 1.5 cm year^{-1} between 1921 and 1953 and by 9 cm year^{-1} between 1953 and 1959 (Bogdanowicz *et al*., 2000). The narrowing of the high discharge channel has also increased of the height of the flood, increased the water flow velocity and its eroding force. During mean high discharges the bottom of the river can be scoured to a depth of as much as 3 m. The mean annual discharge of the Vistula at the Warsaw Haven cross-section in the years 1951–1995 was 561 m^3 s^{-1}.

In the 19th and 20th centuries, the catastrophic floods in the middle reaches of the Vistula occurred every few or a dozen years (1813, 1838, 1839, 1844, 1845, 1855, 1867, 1884, 1889, 1891, 1903, 1924, 1947, 1960, 1962). The largest flood in the 19th century occurred in 1844. During this flood the lower elevation areas of the city and the suburban areas between Wilanów and Kazuń were inundated. The highest water level in Warsaw noted during this flood was 84.71 m a.s.l. The highest discharge of the March 1924 flood was 5860 m^3 s^{-1} and is the largest discharge measured in the period 1921–1997 (Bogdanowicz *et al*., 2000). The Q_p1% discharge is estimated at to 7210 m^3 s^{-1} (Wierzbicki, 2001). Fal & Dąbrowski (2001) established, on the basis of the 200-year series of maximum water levels and the historical discharge curve, that the Q_p0.1% discharge is 9960 m^3 s^{-1}.

METHOD

The extent of flood waters was determined by jointly using a one-dimensional hydraulic model and a Digital Elevation Model (DEM). While similar approaches have been used in natural river conditions, this study concerns urban area. The ordinates of water level in the Vistula valley were determined with the HEC-RAS one-dimensional model, assuming conditions of a steady-state flow with a given probability of exceedence. The HEC-RAS (River Analysis System) model was developed by the US Army Corps of Engineers Hydrologic Engineering Center. In the study reported here the assessment of flood zone was done assuming steady-state flow conditions by the solution of the one-dimensional energy (Bernoulli) equation. Energy losses are evaluated by friction (Manning's equation). The limitations of 1-D hydrodynamic modelling in the urban area are discussed by Mark *et al*. (2004). Our approach does not take in to consideration the underground pipe system, flow by the street system, areas with stagnant water, and water entry into houses. A useful overview of problems related to urban flood modelling is given by Haider *et al*. (2003).

Data for the model

The data needed for the description of the channel geometry were obtained from the echo-sounder measurements carried out on 24–30 September 1998 on the reach of the Vistula River between 490.760 and 541.800 km (Wierzbicki, 2001). Using these profiles, contour lines were drawn on the map by hand and considering the river bed forms and the more important water engineering structures.

The data on the elevations of the crests of the dykes came from the Hydroprojekt design office in Warsaw. These elevations were originally in the form of a table, in which the elevations of the dykes crests are provided for the consecutive kilometres of the river's course. These values were

transferred to the system of orthogonal cartographic coordinates by interpolation. The calculations result in a set of coordinate values (*x*,*y*,*z*) describing the distribution of the dyke crest elevations on both sides of the river.

The data on the relief of the area between the flood protection dykes and behind them were acquired from photogrammetric processing of the aerial photographs by the District Geodesic and Cartographic Department. The relief of the over-flood terraces and higher terrain were from a digital elevation model obtained from the Office of the Surveyor of the Mazowieckie Voivodship. The spatial resolution of that DEM is in the range of 100 m.

The data describing the course of the dyke crests, the relief of the area between and behind the dykes, and the bottom of the river, were merged to one file which contained around 0.77 million points. On the basis of this data set the digital model of relief (DEM) was interpolated using the procedure of inverse distances and a resolution of 20 m (Fig. 1).

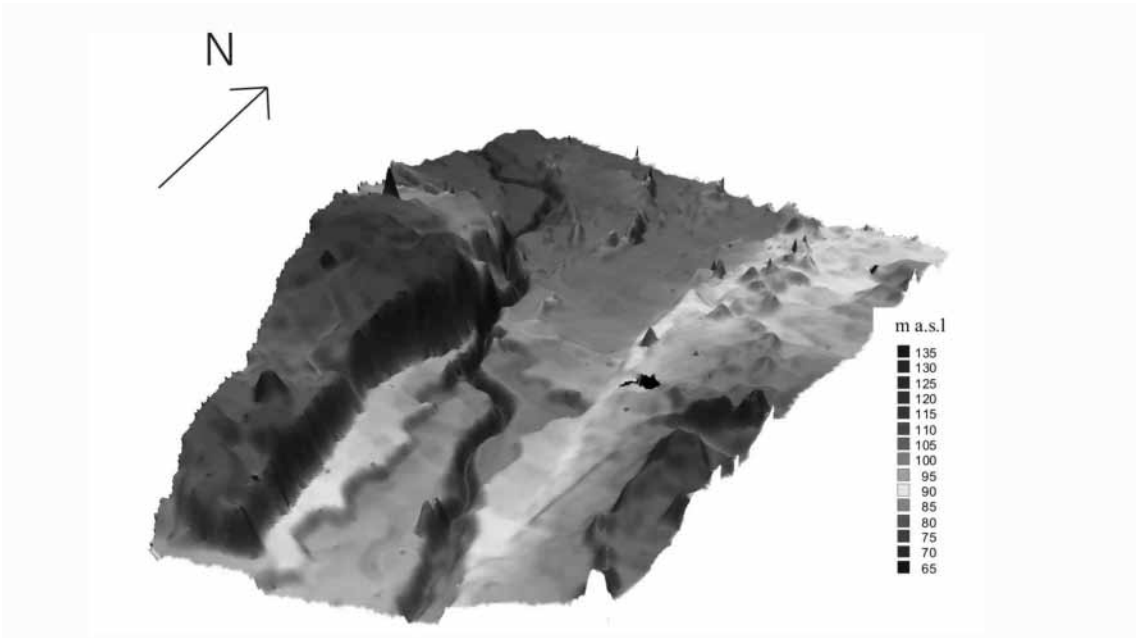


Fig. 1 Digital elevation model of the Vistula valley in Warsaw showing the city "corset" imposed on the river channel (river flows from south to north).

The Manning roughness coefficient values were estimated on the basis of land-use maps and air photographs for the area between the dykes. The following values of the roughness coefficient adopted were: Vistula River channel: 0.03; meadows: 0.04; single trees: 0.045; arable land: 0.05; orchards: 0.055; forests: 0.12; osiers and bushes: 0.15; roads and boulevards: 0.02. Roughness coefficients have been verified during model calibration, to match up to flood level ordinates obtained from HEC-RAS calculations on field measurements from 1998 (Wierzbicki, 2001).

RESULTS

Flood zone ranges for the discharges $Q_p1\%$ and $Q_p0.1\%$ have been obtained by imposing the flood level models on the DEM using the map algebra function of the ILWIS 3.3 software (Figs 2 and 3). Simulations indicate that a significant part of town is situated in the potentially dangerous zone of the flood hazard. Our results are different from previous studies by Jacewicz (1999) and have a closer fit to the morphology of the flood plain. In the present condition, the flood protection dykes are sufficient to convey the $Q_p1\%$ discharge. However, the results indicate that the channel segment between 514 and 515.5 km on the right-hand bank have an inadequate dyke that poses a threat to the Zoological Garden. Likewise, Praga Haven and its hinterland are not properly protected against the $Q_p1\%$ flood. This suggests that the entry to the port should be controlled by a flood gate, if more intensive construction activity in this area is undertaken.

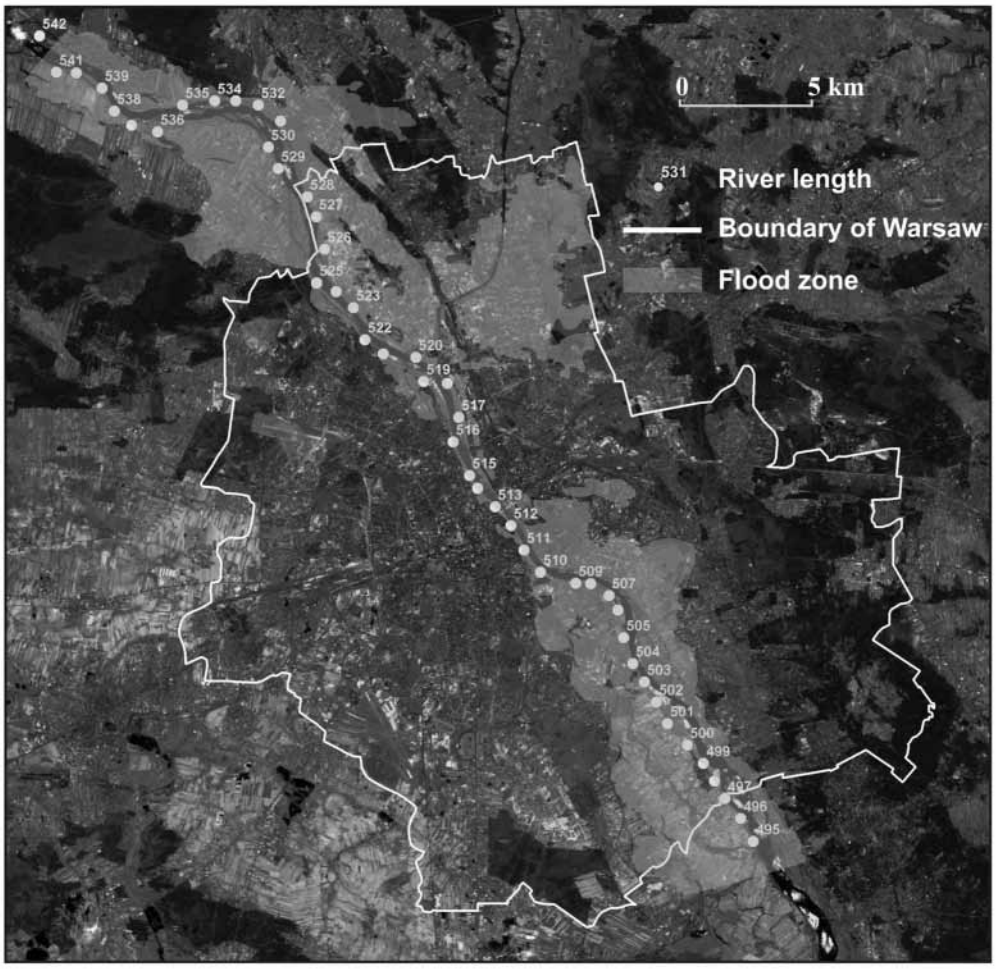


Fig. 2 Range of Qp1% flood zone represented on the background of a Landsat 7 image.

In the case of the occurrence of the Q_p0.1% discharge, the dyes would not ensure protection of important parts of the city. This is especially true on the right bank between 512.5–521 km and 523–535 km, and on the left bank in the segment 525–533.5 km.

The area downstream of 526 km is a not urbanized and so the potential flood losses are lower than in nearby urban areas. Nevertheless, the left bank between 511 and 514 km is not protected by the dykes at all and the elevation of the artificially raised flood terrace does not secure a safe passage of the Q_p0.1% waters. At the same time, this area is attractive for the potential investment projects within Powiśle district, including the extensions to the campus of the University of Warsaw. A similar situation exists over the segment between 517 and 521 km, where the Olympic Centre was established and further developments are planned. A very sensitive area also occurs along the 510–511 km fragment of the left bank, where the flood dykes end, and entry to the area behind the dykes is protected with Czerniaków Head flood gate. Other stretches of the river, where a risk of topping the dikes by the Q_p0.1% flood exists are: 517–521 km on the left bank and 512–523 km on the right bank.

Acknowledgements The authors thank the Global Land Cover Facility, Institute for Advanced Computer Studies, University of Maryland, College Park, USA for making available the Landsat 7 imagery. This research has been financed by the European Commission under the Fifth Framework Programme for Scientific Research: project URBS Pandens, and grant PZB-KBN-086/PO4/2003 – Extreme meteorological and hydrological events in Poland.

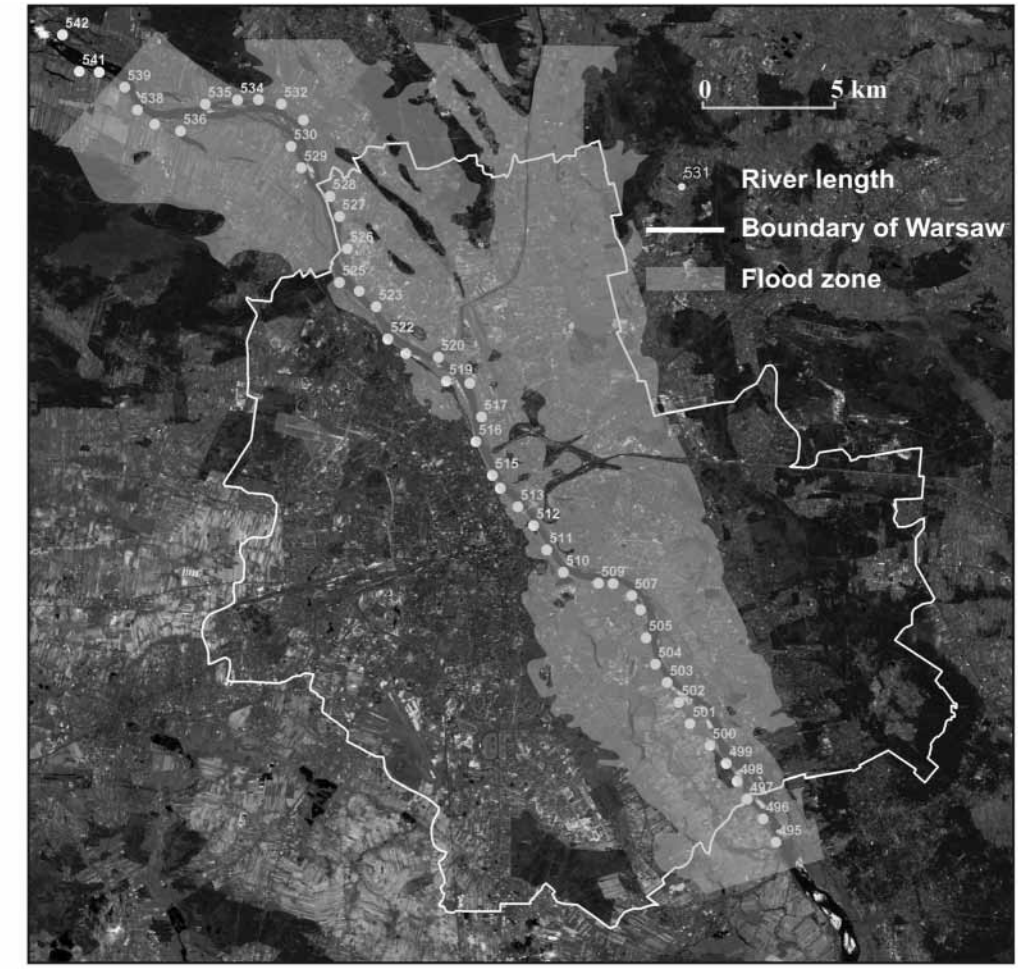


Fig. 3 Range of Qp0.1% flood zone represented on the background of a Landsat 7 image.

REFERENCES

Bogdanowicz, E., Fal, B. & Dobrzyńska, I. (2000) Charakterystyki hydrologiczne (Hydrological characteristics. In: *Wisła w Warszawie*, 9–13. Biuro Zarządu m.st. Warszawy. Wydział Planowania Przestrzennego i Architektury, Warszawa, Poland (in Polish).

Haider, S., Paquier, A., Morel, R. & Champagne, J. Y. (2003) Urban flood modelling using computational fluid dynamics. *Proc. Institution of Civil Engineers: Water and Maritime Engineering* **156**(2), 129–35.

Jacewicz, A. (2000) Ocena i propozycja zabudowy hydrotechnicznej koryta Wisły (The assessment and the proposal of hydro-engineering development of the channel of Vistula River. In: *Wisła w Warszawie,* 154–171. Wydział Planowania Przestrzennego i Architektury, Warszawa, Poland (in Polish).

Fal, B. & Dąbrowski, P. (2001) Dwieście lat obserwacji i pomiarów hydrologicznych Wisły w Warszawie: Obserwacje stanów wody (Two hundred years of hydrological observations and measurements of Vistula in Warsaw. Observations of water levels). *Gospodarka Wodna* **11**, 461–467 (in Polish).

Mark, O., Weesakul, S., Apirumanekul, C., Aroonnet, S. B. & Djordjevic, S. (2004) Potential and limitations of 1D modelling of urban flooding. *J. Hydrol.* **299**(3–4), 284–299.

Nachlik, E., Kostecki, S., Gądek, W. & Stochmal, R. (2000) *Strefy zagrożenia powodziowego* (Flood hazard zones). Wydawnictwo Profil – Biuro Koordynacji Projektu Banku Światowego, Wrocław, Poland (in Polish).

Radczuk, L., Szymkiewicz, R., Jełowicki, J., Żyszkowska, W. & Brun, J. F. (2001) *Wyznaczanie stref zagrożenia powodziowego* (Determination of the zones of flood hazard). Wydawnictwo Safege – Biuro Koordynacji Projektu Banku Światowego, Wrocław, Poland (in Polish).

Wierzbicki, J. (2001) Stałość pionowego układu koryta Wisły oraz położenia zwierciadła wód małych i wielkich na odcinku miejskim w Warszawie (Stability of the vertical setting of the channel of Vistula and the position of the low and high discharges on the urban segment in Warsaw). *Gospodarka Wodna* **4**, 143–149 (in Polish).

Climate Variability and Change—Hydrological Impacts (Proceedings of the Fifth FRIEND World Conference held at Havana, Cuba, November 2006), IAHS Publ. 308, 2006.

Sistema de alerta temprana por inundaciones experiencia en El Salvador

ANA DEISY LOPEZ RAMOS

Servicio Nacional de Estudios Territoriales, Avenida Las Mercedes y kilómetro 5½ carretera a Nueva, frente al Círculo Militar, San Salvador, El Salvador, Centro América

adlopez@snet.gob.sv

Resumen El Salvador es un país con experiencia reciente en Sistemas de Alerta Temprana por Inundaciones. Después del Huracán Mitch en 1998, la población salvadoreña reconoció la vulnerabilidad ante estas amenazas y la carencia de un adecuado monitoreo. Por esta razón, se instaló instrumentación, se elaboraron planes de emergencia y capacitación para las comunidades y se creo el Servicio Nacional de Estudios Territoriales, institución gubernamental para el monitoreo y análisis de amenazas naturales y vulnerabilidades con enfoque de Gestión del Riesgo. Este documento no pretende establecer nuevas teorías acerca de los Sistemas de Alerta Temprana, sino, documentar la experiencia de El Salvador y de cómo estos sistemas puede potenciar capacidades, superando las debilidades de cada uno de los integrantes del sistema. Se demuestra el fortalecimiento de relaciones entre las comunidades y las organizaciones en el ámbito local y nacional, generando una oportunidad de éxito ante situaciones extremas, a veces cotidianas.

Palabras claves red hidrométrica; transmisión telemétrica; red de observadores locales; monitoreo; pronóstico; alerta temprana; tiempo real; inundación; comunicación; crecidas

Experience of the Flood Early Warning System in Salvador

Abstract El Salvador has very recent experience of Flood Early Warning Systems. After Hurricane Mitch in 1998, the population recognized the vulnerability of the country to hydrometeorological hazards and the lack of an adequate monitoring system. Accordingly, a series of instruments were installed, several Emergency Plans were made, and some people were trained, in that order. At the same time, a new governmental institution was created to enhance the monitoring of natural hazards and to work with the risk management. This paper does not intend to describe new theories about the Early Warning Systems, but to present the experience of the Flood Early Warning System Network in El Salvador through the SNET (Servicio Nacional de Estudios Territoriales) experience, and show how a good design can integrate and exploit everyone's capabilities well and overcome individual weakness. Also, through this design and through the System implementation, we have found reasons to break paradigms and expose myths about the FEWS. This way of working, in fact depends on the capacities and "idiosyncrasies" of each country and community that could change from site to site.

Key words hydrometrical network; telemetric transmission; local observers network; monitoring; forecast; early warning; real time; floods; communication

ANTECEDENTES

En los años setenta, la red hidrométrica de El Salvador contaba de 70 estaciones, cuyo objetivo era el manejo del recurso hídrico con fines agrícolas. En los años ochenta, la mayoría de estaciones fueron destruidas o abandonadas debido a la guerra civil, reduciéndose significativamente el sistema de monitoreo hidrológico. Posterior a la firma de acuerdos de Paz en 1992, se realizaron varios esfuerzos con apoyo internacional a fin de rehabilitar la red de estaciones. El Huracán Mitch en octubre de 1998, generó en El Salvador inundaciones que produjeron cuantiosas pérdidas económicas y humanas, por lo que la cooperación internacional, financió la instalación del Sistema de Pronóstico y Alerta Temprana en el Río Lempa, lo cual comprendió la construcción de una red de estaciones hidrometeorológicas en tiempo real, junto con software y modelos hidrológicos que forman parte del Centro de Pronostico Hidrometeorológico. En octubre del año 2001 y después del efecto devastador que tuvieron dos terremotos en El Salvador, se creó el Servicio Nacional de Estudios Territoriales (SNET) entidad adscrita al Ministerio de Medio Ambiente y Recursos Naturales (MARN), que incluye el componente de Estudios Territoriales y Gestión de Riesgos. El Sistema de Pronóstico de Crecidas y Alerta Temprana se instaló junto con sus funciones, en el Servicio Hidrológico Nacional (SHN) del SNET. Durante los años 2002 y 2003, la cooperación internacional financió la construcción de estaciones con transmisión telemétrica en las cuencas de los ríos Grande de San Miguel, Paz, Jiboa y Goascorán, que actualmente forman parte del Sistema de Monitoreo y Alerta Temprana del SNET.

A la fecha se cuenta con una red hidrometeorológica básica de 28 estaciones: 16 con telemetría, 10 automáticas y 2 convencionales (Fig. 1).

Copyright © 2006 IAHS Press

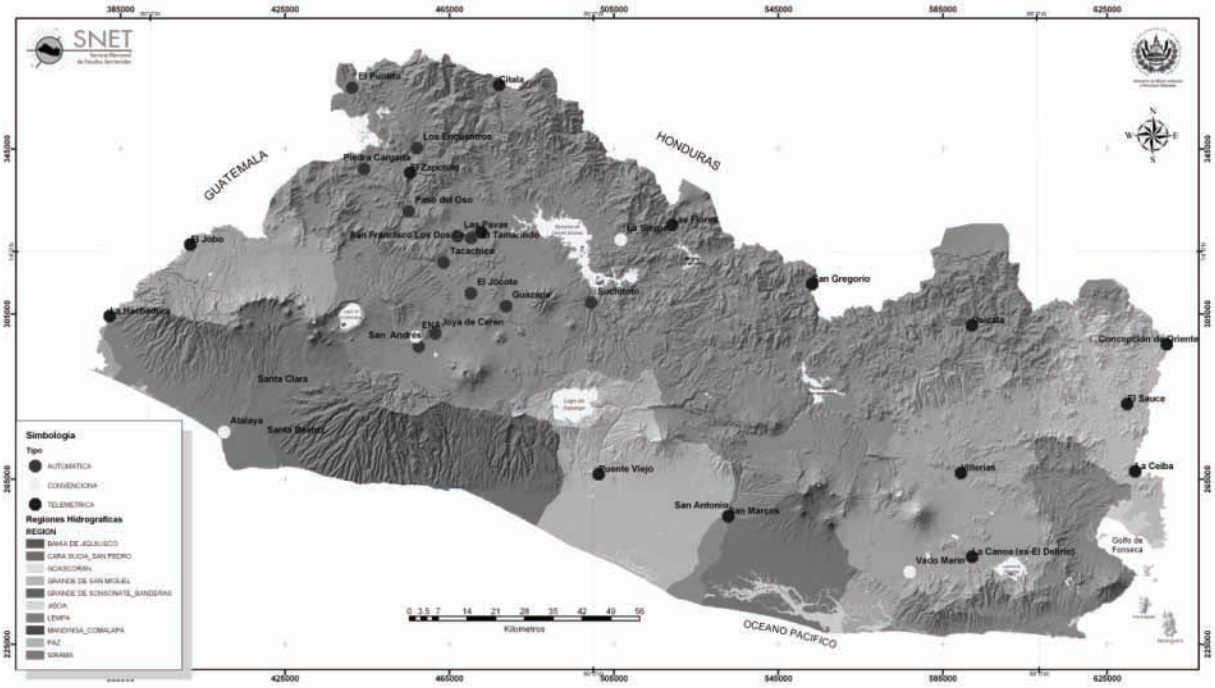


Fig. 1 Red de estaciones Hidrometeorológicas en El Salvador.

DISEÑO CONCEPTUAL DE LOS SISTEMAS DE ALERTA TEMPRANA QUE ACTUALMENTE FUNCIONAN EN SNET

El diseño de los Sistemas de Alerta Temprana, SAT depende básicamente de condiciones como: el tipo de inundación, tipo de pronóstico, características socio-organizativas de los actores locales, experiencia y conocimientos previos de los actores locales en el manejo y gestión de sus riesgos e iniciativa de los gobiernos locales. Es importante destacar que las características e involucramiento de la población y los actores locales, son un factor determinante en el diseño de los sistemas.

Tipos de inundaciones en El Salvador

La problemática de inundaciones ha estado presente en El Salvador desde tiempos remotos. Existen registros históricos de Huracanes, entre los que se destacan el del año 1934, el Huracán Fifí en 1974 y los desastres provocados por Mitch en 1998 y la tormenta tropical Stan en el 2005. En años recientes, las pérdidas por inundaciones se han incrementado debido a diversos factores entre los que se mencionan, incremento de urbanizaciones, cambio de uso de suelo, ubicación de asentamientos humanos sin control en áreas de inundación y cambios en la distribución temporal y espacial de las lluvias.

Se mencionan tres tipos de inundación que normalmente ocurren en El Salvador:

– Inundaciones en cuenca baja de ríos medianos y grandes: Río Lempa, Río Paz, Río Jiboa y Río Goascorán. Ocurren debido a “temporales” o lluvias persistentes durante períodos iguales o mayores a 24 horas, ocasionados la ocurrencia de eventos meteorológicos tales como Huracanes en el Caribe.
– Inundaciones en cuencas de respuestas rápidas: Cuencas provenientes de zonas altas como volcanes y cordilleras. Este tipo de inundaciones es ocasionado por precipitaciones convectivas—lluvias intensas y localizadas—con duración menor de 6 horas.
– Inundaciones en cuencas urbanas, también ocasionadas por precipitaciones convectivas. La problemática es generada por las deficiencias o limitaciones en el sistema de drenaje, obras sin control en cauces de ríos y quebradas y exceso de desechos sólidos en las mismas.

Tipos de pronósticos

En el SNET se desarrollan tres tipos de pronostico (Fig. 2):

– Lluvia Pronosticada – Nivel (caudal) pronosticado: Se realiza por medio de un pronóstico

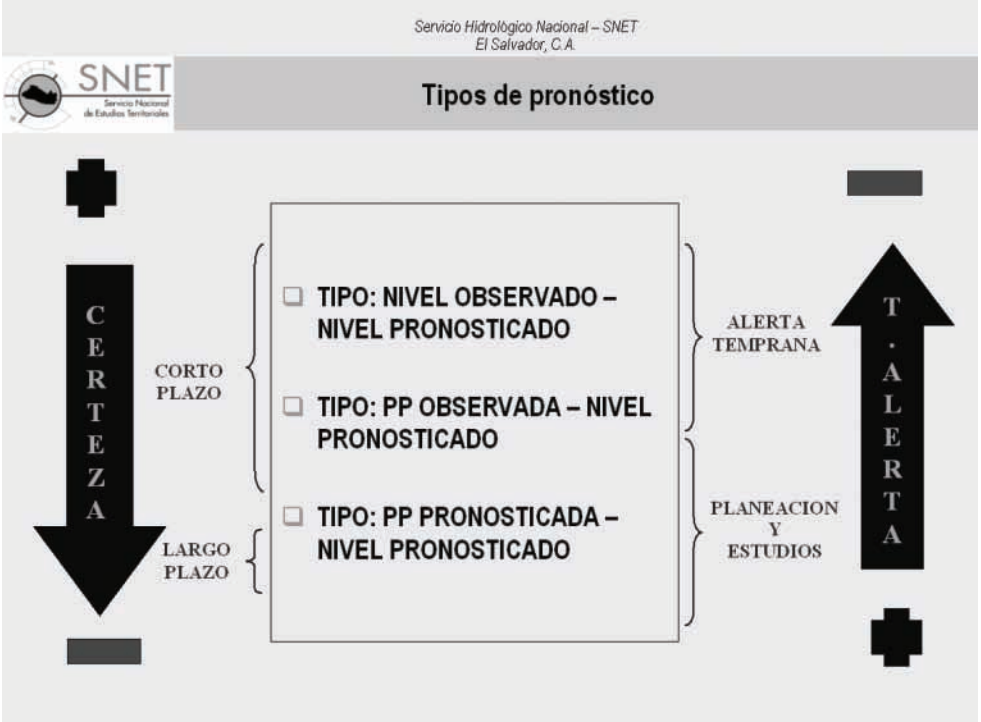


Fig. 2 Tipos de pronóstico que se desarrollan en el SNET.

cuantitativo de lluvia y el uso de un modelo hidrológico. En El Salvador, este tipo de pronóstico se utiliza en cuencas grandes como la del Río Lempa, siendo útil para estimar las entradas a los embalses de generación hidroeléctrica. Proporciona mayor tiempo de alerta, aunque pueden existir más posibilidades de incerteza. Poca aplicación en caso de lluvias convectivas.

– Nivel (caudal) observado – Nivel (Caudal) Pronosticado: Se basa en la utilización de estaciones hidrométricas telemétricas, localizadas en la parte alta y baja de la cuenca. Para este caso se relacionan matemáticamente el nivel observado aguas arriba y el de aguas abajo, estimando el tiempo de llegada y el máximo de crecida por medio de expresiones de regresión. La certeza se incrementa, pero el tiempo de alerta se reduce. En El Salvador se utiliza este tipo de pronóstico para las cuencas del Río Paz, Grande de San Miguel, Goascorán y también tiene aplicabilidad en el Río Lempa, para ello se han determinado los umbrales y las curvas de regresión respectivas. Adicionalmente se ha trabajado en el levantamiento de información en campo sobre las comunidades con problemas de inundación y se ha construido una “red de observadores locales” con las cuales el SNET mantiene comunicación directa.
– Lluvia observada y pronosticada – Nivel (Caudal) Pronosticado: Utilizando modelos se estima el caudal con los datos de precipitación precedente (o de humedad del suelo), observada y pronosticada. Su aplicación es de mucha utilidad en las cuencas de respuesta rápida. Este sistema requiere una mayor atención a las comunicaciones y al trabajo de los observadores locales.

PROCEDIMIENTOS DE OPERACIÓN Y EMERGENCIA DE LOS SAT

En el SNET se tienen 5 etapas o estados de monitoreo que dependen de los niveles de los ríos y de la precipitación pronosticada y observada. Estas etapas condicionan los procedimientos, turnos y operaciones del Centro de Pronóstico, así como los procedimientos de comunicación con la red de observadores locales, a fin de responder de la mejor forma a la emergencia. Estas etapas son de uso interno, al pasar de una a otra por medio de umbrales, implica cambiar de procedimientos de operación.

La comunicación se da directamente del Centro de Pronóstico a la comunidad en riesgo y paralelamente a los Comités de Emergencia Locales y Departamentales. A través de la conformación

de la Red de observadores locales y del levantamiento de información en campo, las comunidades ubicadas en zonas susceptibles a inundación han sido clasificadas de acuerdo a la frecuencia de inundaciones.

EL PAPEL DEL SNET COMO INSTITUCION CIENTIFICA DE MONITOREO

El papel de los servicios técnicos y de monitoreo de hidrología, meteorología y gestión de riesgos en el SNET, es desarrollar y mantener el monitoreo hidrometeorológico de las condiciones hidroclimáticas de las cuencas. Así mismo, desarrollar los análisis que permitan realizar los pronósticos de crecidas y emisión de avisos y alertas a las comunidades y comités de emergencia.

El reto del SNET en servir de soporte científico nacional a estos sistemas es grande, pero existe la disponibilidad local, institucional y comunitaria de poder fortalecer las iniciativas establecidas.

EL PAPEL DE LA RED DE MONITOREO DE OBSERVACIÓN LOCAL

Su construcción debe basarse en el tipo de amenaza de las zonas, en la organización municipal, comunitaria, los organismos locales existentes y en la idiosincrasia y capacidades de las poblaciones.

El Sistema de Gestión de Riesgo como parte de los Sistemas de Alerta Temprana, es un sistema dinámico e integral por medio del cual un grupo humano toma conciencia del riesgo que enfrenta, lo analiza y lo entiende, considera las opciones y prioridades en términos de su reducción.

La Red de observadores locales, es un concepto que abarca un número representativo de ciudadanos, líderes comunales, instituciones descentralizadas de Gobierno, Policía, Fuerza Armada, Municipalidades, Organismos no Gubernamentales, que habitan en zonas susceptibles a inundación asumiendo con responsabilidad la tarea del manejo integral de su riesgo.

EL PAPEL DE LOS MEDIOS DE COMUNICACIÓN

Los comunicadores, como parte de la Red de monitoreo local, pueden ser un aliado muy importante para el desarrollo de la capacitación a distancia de la población sobre los temas de Gestión de Riesgos y Alerta Temprana, por ello, parte de las actividades desarrolladas por el SNET ha sido capacitar a los comunicadores en los temas mencionados y mantener una relación directa en la emisión de boletines, pronósticos y avisos. Si bien para alertas de corto plazo, los medios escritos y la televisión no son los ideales, sí lo han sido para la comunicación de información específica tendiente a orientar y capacitar a la población. En el caso de las alertas de corto plazo, han sido determinantes las radioemisoras locales y nacionales, que pueden llegar a la población en riesgo en poco tiempo.

EL PAPEL DE LA ASISTENCIA INTERNACIONAL Y LOS ORGANISMOS REGIONALES

Es importante que la Cooperación Internacional esté orientada a apoyar el desarrollo y fortalecimiento de las capacidades nacionales y locales que permitan hacer sostenibles los sistemas técnico-científicos de monitoreo, análisis y comunicación.

Así mismo, los entes regionales e instituciones hidrometeorológicas de los países de la región, pueden potenciar sus capacidades a través de un intercambio de conocimientos y experiencias.

FINANCIAMIENTO Y SOSTENIBILIDAD DE LOS SISTEMAS.

Los países en desarrollo afrontan la necesidad de dar sostenibilidad al monitoreo e investigación hidrometeorológica, consumiendo fondos que muchas veces no son sostenibles por los presupuestos de los Gobiernos. Ante necesidades sociales como Salud y Educación, el monitoreo hidrometeorológico, la Gestión de Riesgos y la investigación científica, puede no ser una prioridad en los países.

Posiblemente, una de las opciones de financiamiento de los sistemas de monitoreo y análisis hidrometeorológicos se fundamenta en los servicios paralelos que la información generada y las capacidades instaladas puedan dar para el desarrollo de las actividades económicas y de asegura-

miento de las inversiones que se requieran. El desarrollo de estudios especializados con información adecuada y de calidad, puede contribuir a asegurar las inversiones económicas del país. Por otro lado, la búsqueda de soporte en el ámbito de comunidades y municipalidades, puede disminuir la carga del mantenimiento de redes de observación y comunicación a la institución central.

CONCLUSIONES

(a) Un SAT, en su desarrollo completo, debe ser un Sistema con un soporte técnico científico de conocimiento del comportamiento de ríos y cuencas, de evolución de vulnerabilidades, mapeo de áreas de inundación, soporte nacional y regional en el monitoreo de las amenazas, del desarrollo de una Red de observación local involucrada en el monitoreo de las condiciones locales.
(b) El éxito del diseño de un SAT se fundamenta en la participación compartida de las responsabilidades de monitoreo, investigación, alerta, comunicación y financiamiento de los mismos, en los cuales el involucramiento de todos los componentes de la sociedad en los niveles locales, nacionales, regionales e internacionales juega un papel importante y que potencia las capacidades individuales.
(c) El decidido soporte y apoyo de la Cooperación Internacional, debe ser aprovechado al máximo para construir las capacidades locales y darle continuidad a los sistemas, de tal manera que no se espere un nuevo evento que ocasione desastres, para reiniciar capacidades.
(d) El soporte horizontal, intercambio de experiencias y compartimiento de capacidades de los entes de monitoreo y análisis científico, potencia e incrementa las capacidades individuales.
(e) El financiamiento y sostenibilidad de los Sistemas de Alerta Temprana, pueden estar basados en el desarrollo de productos y actividades paralelas.

REFERENCIAS

Servicio Nacional de Estudios Territoriales (2003) Manual de Operaciones del Centro de Pronóstico Hidrológico. San Salvador, El Salvador.

Servicio Nacional de Estudios Territoriales (2004) Manual de Procedimientos de Comunicación para Alerta del Servicio Hidrológico Nacional y Centro de Pronóstico Hidrológico. San Salvador, El Salvador.

Climate Variability and Change—Hydrological Impacts (Proceedings of the Fifth FRIEND World Conference held at Havana, Cuba, November 2006), IAHS Publ. 308, 2006.

Pronóstico de lluvia sobre territorio cubano al paso de los huracanes Charley e Iván, usando MM5V3

IDA MITRANI ARENAL, ISRAEL BORRAJERO MONTEJO & ARNOLDO BEZANILLA MORLOT

Instituto de Meteorología (INSMET), Apdo. 17032, Loma de Casablanca, Regla, CP. 11700, La Habana, Cuba
imitrani@met.inf.cu

Resumen Se comprueba la habilidad de MM5V3, en el pronóstico de lluvia sobre las provincias habaneras al paso de los huracanes Charley e Iván en el 2004. Para la evaluación de los resultados, se tomaron los registros de lluvia de las estaciones meteorológicas de Batabanó y Casablanca, localizadas en las provincias habaneras. El modelo representa con razonable acierto la ausencia de lluvia, pero cuando hay ocurrencia de precipitación, se sobrevalora la cantidad de lluvia caída; los errores aumentan hacia plazos mayores de 30 horas. La hora de comienzo y la duración, pueden desviarse hasta 12 horas de la realidad. Se concluye que los resultados son aceptables, pero pudieran mejorarse con mallas más finas y representación de los procesos convectivos en forma explícita.

Palabras claves MM5V3, pronóstico de lluvia, trayectoria de huracanes

Rainfall forecasting in Cuba for hurricanes Charley and Iván using MM5V3

Abstract The skill of the MM5V3 model in rainfall forecasting was tested for the Habana provinces (Cuba) during the passing of hurricanes Charley and Iván in 2004. The results were compared with rainfall records from the surface meteorological stations of Batabanó and Casablanca, located in the Habana provinces. The model represents with reasonably success the lack of rain, but when rain occurs, the rainfall amount is overestimated. The bias is greater for forecasting periods of greater than 30 hours. The rainfall event start time and duration may differ by up to 12 hours from reality. The results are concluded to be acceptable, but they can be improved by using a finer mesh and by introducing an explicit representation of convective processes.

Key words MM5V3; rainfall forecasting; hurricane tracks

INTRODUCCIÓN

Al paso de ciclones tropicales por el territorio cubano, ocurren eventos de lluvia intensa que afectan fundamentalmente a la zona occidental del país. Desde la temporada ciclónica del año 2002 se utiliza de forma operativa en el servicio meteorológico cubano el MM5V3 (Mitrani *et al*., 2003, 2005). Es objetivo del presente texto la valoración de los pronósticos de lluvia realizados con este modelo al paso de los huracanes "Charley" e "Iván" sobre y por las cercanías de las provincias habaneras en el 2004, tomando como referencia los registros de dos estaciones meteorológicas.

Charley se originó de una onda procedente de África. Fue reportado como huracán en las proximidades de Jamaica el 11 de agosto. Alcanza la Categoría 2 el día 12, al nordeste de la isla Gran Caimán; con rumbo norte–noroeste se acerca al Golfo de Batabanó, penetra en Cuba por Playa Cajío a las 4:30 UTC del 13 de agosto y sale por el oeste de la ciudad de La Habana a las 06:00 UTC. Se reportaron vientos de más de 54 m s-1 Ya en aguas del Estrecho de la Florida, sobre las 14:00 UTC, alcanza Categoría 4 y tres horas después penetra en tierra de los E.U. (Pasch *et al.*, 2004).

Iván también nace de una onda tropical procedente de África el 31 agosto del 2004. El 2 de septiembre, a las 18:00 UTC ya era depresión tropical y 12 horas después, en una latitud bastante baja (9.7°N), conforma la Tormenta Tropical Iván. Se convierte en huracán alrededor de las 06:00 UTC del 5 septiembre, al Este de Tobago. Alcanza la costa sur de Jamaica con Categoría 4. Continuó un movimiento oeste–noroeste y alcanza la Categoría 5 a las 18:00 UTC del 11 septiembre. Mantiene esta Categoría durante 30 horas; el día 13 atraviesa el Canal de Yucatán, muy cerca del cabo San Antonio, el extremo más occidental de Cuba y sale al sur del Golfo de México en horas tempranas del 14 septiembre.

DATOS

El MM5V3 se alimenta con las salidas del Modelo Global GFS, con los campos de los elementos meteorológicos en superficie y en los niveles 1000, 850, 700, 500, 400, 300, 200, 150 y 100 hPa.

Copyright © 2006 IAHS Press

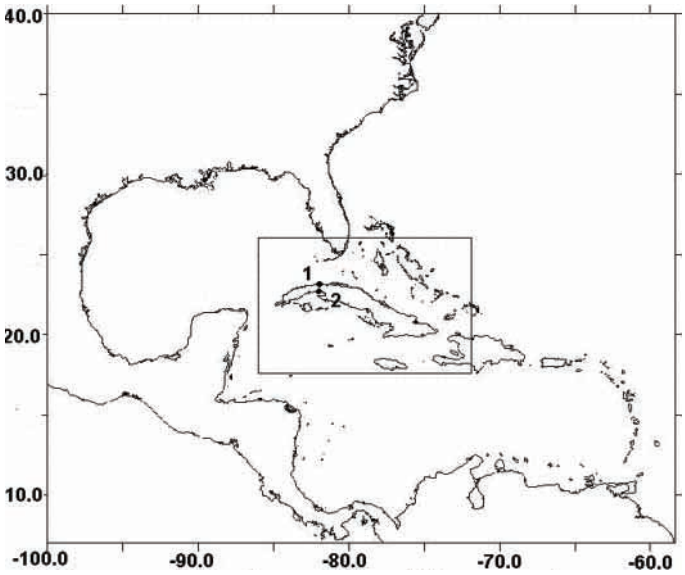


Fig. 1 Dominios anidados de MM5V3 y localización de las estaciones meteorológicas 1. Casablanca, 2. Batabanó.

Para evaluar los pronósticos de lluvia se utilizaron los datos de las estaciones meteorológicas Casablanca, situada en los 23.17°N con 82.35°W, y Batabanó, en los 22.72°N con 82.28°W. (Fig. 1). Las observaciones de lluvia, fueron realizadas cada tres horas con pluviómetros de probeta y regla graduada.

MÉTODOS

Utilización de MM5V3

El Modelo a Mesoescala de Quinta Generación de la Universidad de Pensilvana en su versión 3.7, (MM5V3) ha sido adaptado a las condiciones del territorio cubano y a los recursos de computación disponibles, por especialistas del Centro de Física de la Atmósfera (CFA), del Instituto de Meteorología (INSMET) de Cuba. Se corre la variante no hidrostática sobre LINUX, en una PC Pentium IV a 1.73 GHz con 736 Mb de RAM. Se utilizan dos dominios anidados, en proyección Lambert y coordenadas centrales en los 23°N y 80°W, coincidiendo aproximadamente con el centro de Cuba. El dominio exterior presenta una malla de 30 × 42 puntos, con pasos de 75 km y el interior de 31 × 58 puntos, con pasos de 25 km (Fig. 1). Como la distribución espacial y temporal de las precipitaciones depende de la trayectoria de los huracanes, se aprovechó una experiencia de pronóstico de movimiento del huracán Iván (Mitrani *et al.*, 2005) con distintos esquemas de parametrización de nubes convectivas y de capa límite, recomendados en el manual de PSU/NCAR (2000) en dependencia de la resolución de los dominios. En esta ocasión, los experimentos se realizaron también para el huracán Charley. Se incluyen la parametrización de transferencia radiativa con presencia de nubes, la parametrizacion de convección somera en el dominio interior y el pronóstico de temperatura del suelo Se utiliza una matriz de 25 tipos de uso de suelo, diferenciando invierno y verano. El centro del huracán se localizó por el máximo de vorticidad en el campo de líneas de corriente y se calculó el error de predicción de trayectoria como la distancia en Km entre la posición real y la pronosticada.

Procesamiento de los datos de lluvia

Se estableció una comparación entre las salidas de MM5V3 y los registros de las estaciones de Batabanó y Casablanca. Se analizaron los plazos de pronóstico desde 6 hasta 72 horas. Se calcularon los errores como la diferencia entre la cantidad de lluvia caída registrada en las estaciones, menos la pronosticada. Se determinaron los errores medios de cada caso, en dependencia de las parametrizaciones utilizadas para la capa límite.

RESULTADOS

En las corridas realizadas con MM5V3 para los huracanes Iván y Charley, de las parametrizaciones de la convección a escala de nubes recomendadas para las resoluciones utilizadas, solo la de Grell permitió que el proceso de cálculo fuese estable. Para la capa límite, se pudieron realizar corridas con los esquemas de Blackadar (BL), Burk-Thompson (BT) y ETA Mellor Yamada (MY), notándose diferencias ente las trayectorias pronosticadas. En las Figs 2 y 3 se muestran las trayectorias real y pronosticadas al paso de estos huracanes sobre y por las cercanías del territorio cubano.

En las Figs 4 y 5 aparecen las gráficas de los errores medios para ambas mallas. La parametrización BT da los mejores resultados para el caso de Charley, mientras que al paso de Iván, la mejor fue la MY, seguida por la BT. Este resultado difiere de la experiencia de Romine & Wilhenson (2004); al simular el huracán Opal de 1995 con MM5V3; estos autores utilizaron cuatro mallas, con paso mínimo de 3.3 km para probar las formulaciones BL y BT, en las dos mallas externas combinadas con la parametrización de Betts-Miller para la convección a escala de

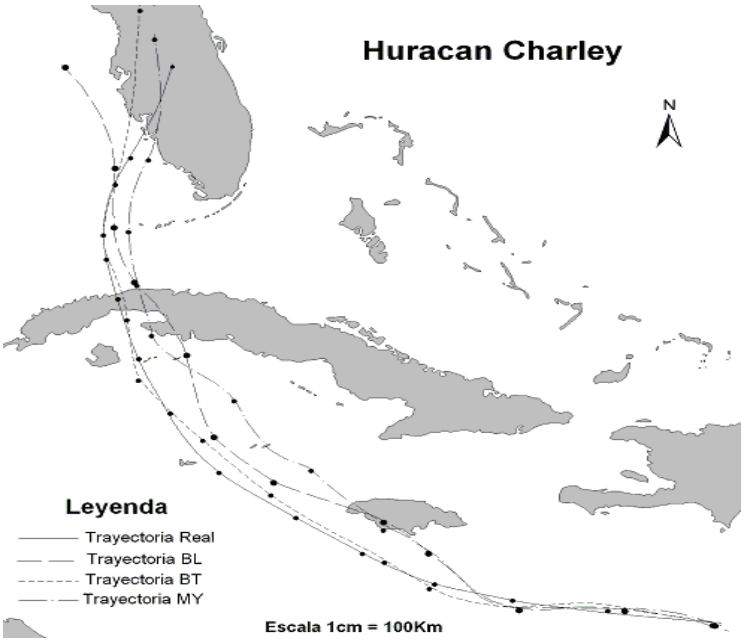


Fig. 2 Trayectorias real y pronosticadas del huracán Charley.



Fig. 3 Trayectorias real y pronosticadas del huracán Iván.

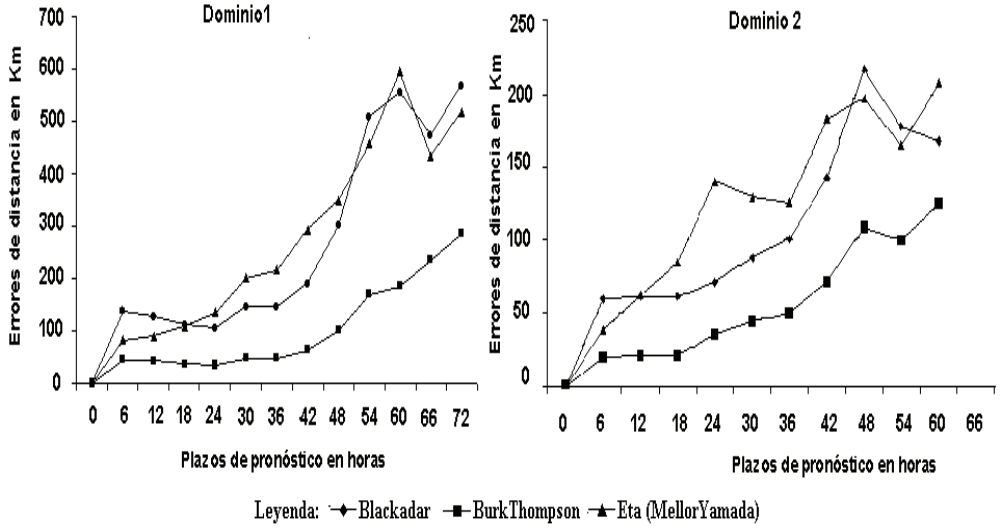


Fig. 4 Errores medios en la predicción de trayectoria del huracán Charley.

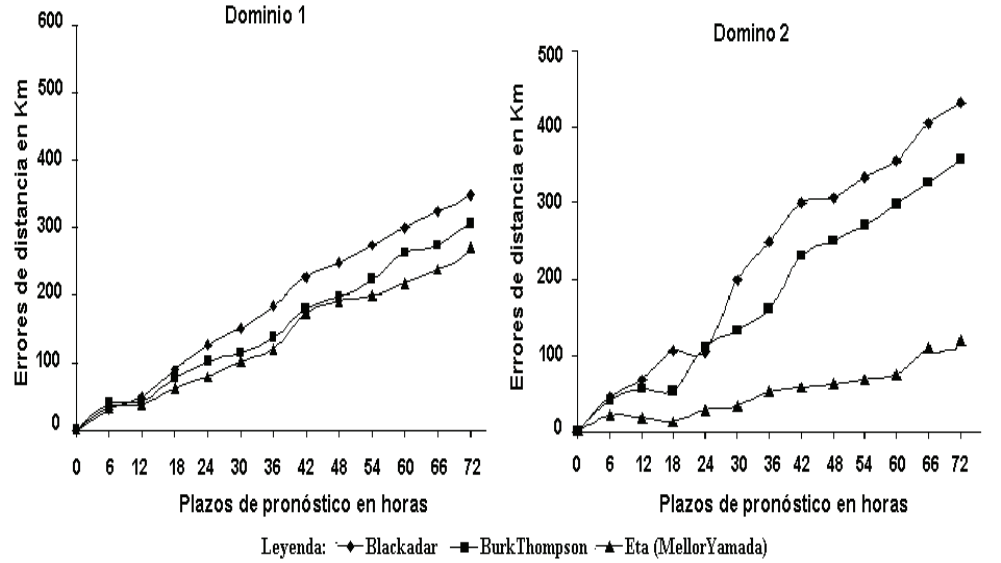


Fig. 5 Errores medios en la predicción de trayectoria del huracán Iván.

nubes y en las internas, con el esquema explícito y microfísica incorporada. La parametrización de capa límite que mejor les funcionó fue la BL en todas las mallas. Por otra parte, Liu *et al.* (1997, 1999), señala que el esquema BL es muy favorable para reflejar la evolución de huracanes de gran intensidad. Sin embargo, en el presente trabajo la BT dio mejores resultados que la BL, incluso para un huracán de gran intensidad como fue Iván, además de ser la más económica en tiempo de máquina. No se encontraron antecedentes de aplicación de MY para representación de huracanes con MM5V3.

En las Figs 6 y 7 se reflejan los errores medios de la lluvia caída para cada plazo de pronóstico y para cada tipo de parametrización de capa límite. Los errores oscilan entre –40 y 20 mm, y del análisis de comienzo y final del evento de lluvia, se observó una desviación de hasta doce horas. En ausencia de lluvia, se notó una alta correspondencia entre el modelo y la realidad, mientras que con ocurrencia de precipitaciones, los pronósticos sobre valoran la cantidad de lluvia caída, sobre todo para plazos mayores de 30 horas en el caso de Charley y para más de 48 horas en el caso de Iván. En esto influyeron la calidad de representación del movimiento del huracán por parte del modelo, que disminuye a medida que aumenta el plazo del pronóstico, y la combinación de parametrizaciones de los procesos diabáticos. Los mejores resultados coinciden con la parametrización

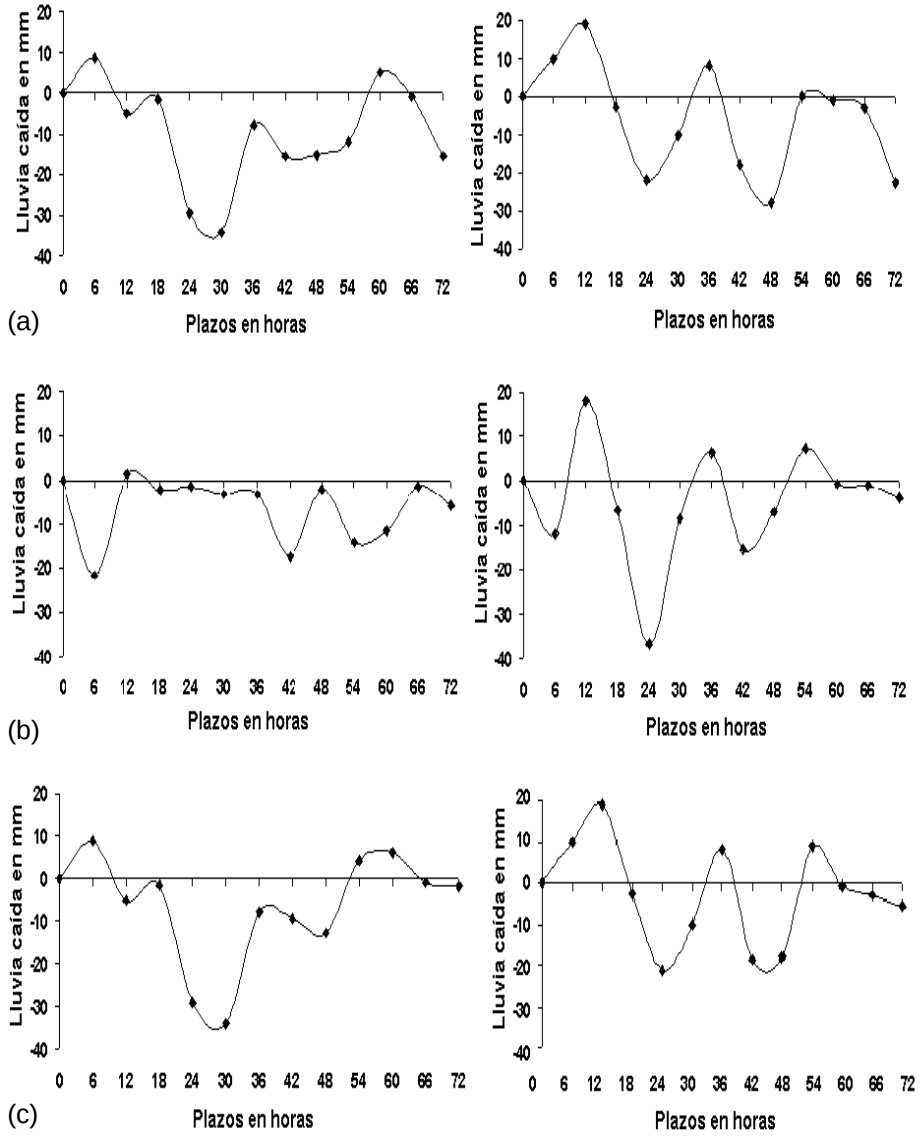


Fig. 6 Errores medios del pronóstico con MM5V3, de lluvia caída al paso de Charley, con las parametrizaciones de capa límite; (a) De Blackadar, (b) de Burk-Tompson, (c) De Eta Mellor-Yamada.

BT para Charley y con la MY para Iván. Al parece, estas diferencias dependen de las particularidades del huracán. Téngase en cuenta que Charley tuvo un movimiento demasiado veloz, mientras que Iván fue un huracán muy intenso, que se profundizó con gran rapidez.

CONCLUSIONES

Los pronósticos de lluvia al paso de los dos huracanes fueron satisfactorios para plazos cortos, tomando en cuenta la baja resolución y los modestos medios de cómputo. Se recomienda el uso de mallas finas, con incorporación explícita de los procesos convectivos. No fue posible definir cual tipo de parametrización de capa límite funciona mejor con los huracanes, puesto que las particularidades de cada evento influyeron en la mejor o peor correspondencia con uno u otro esquema.

Agradecimientos A los Técnicos: Nancy Masó, Alberto Lazo, Lázaro Miguel Sánchez, a la Lic. Rosa Delgado y al Lic. Enrique Pérez por la ayuda en la preparación de datos y documentación y a Microscale and Mesocale Division of the National Center of the Atmospheric Research (NCAR), sustentado por el National Science Foundation, por haber hecho posible el uso de MM5V3.

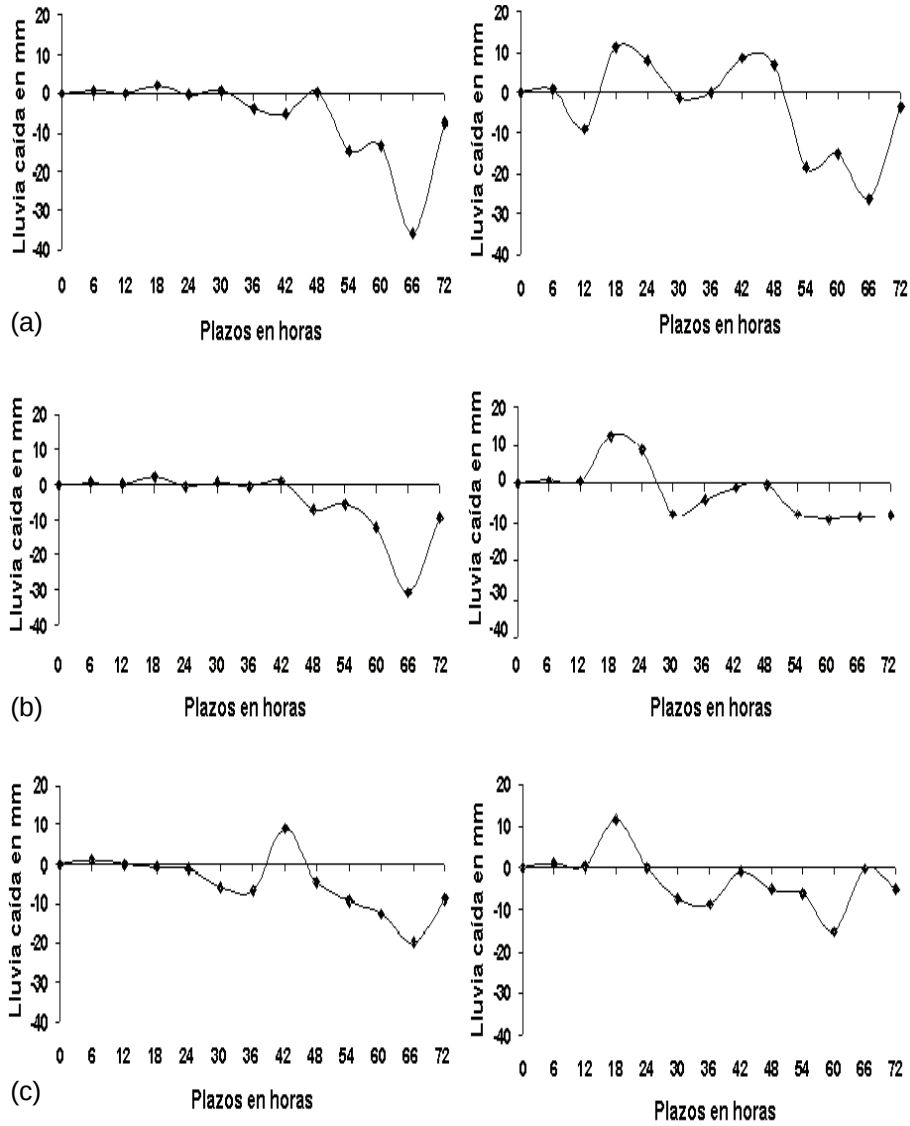


Fig. 7 Errores medios del pronóstico con MM5V3, de la lluvia caída al paso de Iván, con las parametrizaciones de capa límite de (a) Blackadar, (b) Burk-Tompson, (c) Eta Mellor-Yamada. (A la derecha, la Estación Casablanca y a la izquierda la Estación Batabanó).

REFERENCIAS

Liu Yubao, Da Lin Zhang & Yao, M. K. (1997) A multiscale numerical study of Hurricane Andrew (1992). Part I: Explicit simulation and verification. *Monthly Weather Review* **125**(12), 3073–3093.

Liu Yubao, Da Lin Zhang & Yao, M. K. (1999) A multiscale numerical study of Hurricane Andrew (1992). Part II: Kinematic and Inner-core structures. *Monthly Weather Review* **127**(11), 2597–2616.

Mitrani, I. & González, C. (2005) Experiencias con el uso de MM5V3 al paso de los huracanes "Isidore" y "Lili" por territorio cubano. *Revista Brasileira de Meteorología* **20**(2), 227–242.

Mitrani I., Alvarez, L. & Borrajero, I. (2003) Aplicación optimizada del MM5V3 sobre el territorio cubano mediante el uso de computadora personal. *Revista Cubana de Meteorología* **10**(1), 3–7.

Mitrani, I., Forrajero, I., Álvarez, L. & Bezanilla, A. (2005) Influencia de distintos esquemas de parametrización de la capa límite en el pronóstico de trayectoria del huracán "Iván" del 2004, utilizando MM5V3. *Memorias del III Congreso Cubano de Meteorología* (5–9/12/2005), La Habana (en soporte técnico).

PSU/NCAR (2000) Mesoscale Modeling System, MM5 modeling System Version 3. *Tutorial Class Notes and User's Guide.* Mesoscale and Microscale Meteorology Division; National Center for Atmospheric Research.

Pasch, R. J., Brown, D. P. & Blake, E. S. (2004) Hurricane Charley, 9–14 August 2004. *Tropical Cyclone Report*, National Hurricane Center 18/10/2004. www.nhc.gov.

Romine, G. & Wilhelmson, R. (2004) Parameterization impacts on a simulation of Hurricane Opal (1995) Department of Atmospheric Sciences, University of Illinois Champaign-Urbana, www.redrock.ncsa.uiuc.edu/AOS/Opal/index.html.

Stewart, S. R. (2004) Hurricane Iván, 2–26 September 2004. *Tropical Cyclone Report*. National Hurricane Center, 16/12/2004, www.nhc.gov.

Climate Variability and Change—Hydrological Impacts (Proceedings of the Fifth FRIEND World Conference held at Havana, Cuba, November 2006), IAHS Publ. 308, 2006.

Índices y grados de riesgo de inundación comunales en sistemas de alerta: uso de lógica difusa

ARNALDO SANTANDER & XIMENA VARGAS

Departamento de Ingeniería Civil, Universidad de Chile, Casilla 228/3, Santiago, Chile
asantand@ing.uchile.cl

Resumen Se realiza un resumen teórico y discute sobre las propiedades y alcances del uso de Lógica Difusa (FIS) para la formulación de un sistema experto de interpretación del riesgo de inundación geográficamente agregado, que reviste interés en zonas de monitoreo extensas, donde distintos niveles de gestión requieren información jerarquizada conforme a su "criterio" durante la ocurrencia de episodios de inundaciones globales. Usando información recopilada en la zona central de Chile, se concluye que es posible el uso de los FIS tipo Mandami para generar modelos de interpretación del riesgo a distintas escalas espaciales. Así, se define un índice denominado Grado de Riesgo Comunal, G_r^{Comuna}, que traduce el riesgo en valores discretos a partir de valores difusos.

Palabras claves lógica difusa; inundaciones; tiempo real; sistemas de alerta; índices de riesgo; grados comunales de riesgo

Indices and grades of regional flood risk in a flood alert system: use of fuzzy logic

Abstract Theory and practical aspects related to fuzzy logic implementation in a real time flood warning system are provided. Mandami's Fuzzy Inference System (FIS) was used to make a spatial (district) aggregated interpretation model. The proposed model was applied on the Mataquito River basin (Chilean Central Valley). A discrete risk degree from continuous fuzzy risk values was made.

Key words fuzzy logic; flooding; real time; warning systems; risk value; district risk degree

INTRODUCCIÓN

Hoy en día, el estado chileno posee una red nacional de monitoreo de datos hidrométricos en tiempo real con aproximadamente 150 estaciones satelitales a lo largo del país que ha empezado a ser empleada en diversos campos de la gestión del recurso hídrico. En este contexto de modernización, los sistemas de alerta temprana de inundaciones constituyen uno de los potenciales usos de la red, por lo tanto, es razonable prever que la experiencia en este ámbito se acrecentará en los próximos años. Entre las componentes de los Sistemas de Alerta en Tiempo Real (SATR) se distinguen los modelos de pronóstico de caudales y modelos de interpretación del estado del sistema para distintas escalas espaciales (Santander, 2004) en los cuales este último queda determinado por el riesgo, que debe evaluarse a través de algún índice. La motivación del estudio de técnicas que permiten una tolerancia en el pronóstico de caudales e interpretación de los sistemas de alerta viene dada principalmente porque, por una parte, el valor cualitativo del riesgo no es excluyente; es decir, si bien es posible establecer intervalos (conjuntos) en los cuales el riesgo es "bajo", "medio", etc., por lo general los valores frontera de estos intervalos son "difusos" (los elementos de la intersección pueden pertenecer tanto a uno u otro intervalo). Por otra parte, las singularidades de cada evento hacen prácticamente imposible la modelación de la incertidumbre inherente a la ocurrencia de desastres por inundaciones.

Lógica Difusa nace como una técnica perteneciente al área de la llamada inteligencia artificial y ha dado origen a sistemas expertos y sistemas de control automático, área en que se ha utilizado ampliamente. En particular, permite traducir o interpretar un sistema mediante un conjunto de reglas o hipótesis multivaluadas, a diferencia de la lógica binaria, puesto que no impone en las proposiciones o hipótesis valores discretos de las variables de decisión y consecuencia (falso o verdadero). En consecuencia, lo difuso puede entenderse como la posibilidad de asignar valores de verdad intermedios entre "falso" y "verdadero". Además, este tipo de esquema es "tolerante" debido a que las causas (variables de entrada) que producen cierto efecto (variable de salida) pueden variar dentro de cierto rango sin que el resultado se altere mayormente.

En este artículo se realiza un resumen teórico y se discute sobre las propiedades y alcances del uso de Lógica Difusa para la interpretación del riesgo de inundación en zonas pertenecientes a la Hoya del Río Mataquito (Provincia de Curicó, VII Región del Maule) mediante la generación de índices de riesgo agregados a escala espacial.

Copyright © 2006 IAHS Press

MARCO TEÓRICO

Lógica difusa

Los modelos difusos o FIS (Fuzzy Inference System) se basan conceptualmente en agrupar en subconjuntos las variables de entrada de respuesta similar (salida del modelo), quedando la magnitud de la respuesta determinada por el grado de cumplimiento de las variables de entrada a ciertas sentencias o reglas.

Un conjunto difuso es una función que a cada elemento del universo le asocia su grado de pertenencia, función cuyo dominio es el universo y cuyo recorrido, como se muestra en la Fig. 1, es el intervalo [0.1]. Mediante notación matemática, se define un Conjunto Difuso MF (función de pertenencia), para la variable de entrada *x* que pertenece al universo *X*:

$$MF(x) = \{(x, \mu A(x)) / x \varepsilon X\}. \mu A: X [0,1] \quad (1)$$

donde la función de pertenencia "μ_A" se establece de manera arbitraria.

Las funciones de pertenencia de los conjuntos difusos se pueden operar entre sí del mismo modo que los conjuntos clásicos; así, las operaciones de intersección, unión y complemento se pueden definir como:

Operador *Y*: $\mu_{A\cap B}(x) = \mu_A(x) * \mu_B(x)$ (2)

Operador *O*: $\mu_{A\cup B}(x) = \max\{\mu_A(x), \mu_B(x)\}$ (3)

La estructura de las proposiciones lógicas del sistema se pueden expresar considerando que para todas las variables de entrada V_K se dispone de un número de funciones de membresía *m*, donde las *n* reglas del modelo R_i se expresan como:

R_i: Si V_1es $MF(1,i)$ Y/O….Y/O V_k es $MF(k,i)$ Y/O ….Y/O V_p es $MF(p,i)$

Entonces: Implicancia $i = A_i (V_1,\ldots,V_k,\ldots,V_p)$"

Donde: $i = \{1,\ldots\ldots,n\}$, $k = \{1,\ldots\ldots,p\}$ Vk es $MF(k,i) = MF(k,i)(Vk)$

Las funciones de implicancia, o consecuencia, A_i constituyen lo que se denomina "fusificado" del FIS, y son definidas de modo arbitrario.

Un criterio para la caracterización de los conjuntos difusos es el de inclusión difusa "S" (Kosko, 1992) que representa el grado en el que un conjunto difuso está incluido en otro. Así, la inclusión difusa de μ_A en μ_B se obtiene como:

$$S(\mu_A, \mu_B) = \frac{1}{Card(\mu_A)}\left[Card(\mu_A) - \int_{zeZ} \max(0, \mu_A(z) - \mu_B(z))dz \right] \quad (4)$$

siendo Card(*A*) la cardinalidad del conjunto *A*, definida como:

$$Card(A) = \int_{xeX} A(x)dx \quad (5)$$

Luego, sea z una variable para la cual se determinan n conjuntos difusos "μ^i", entonces la matriz de inclusión difusa "*S*(*z*)" se expresa como:

$$S(z) = \begin{bmatrix} 1 & \cdots & \cdots & S(\mu^1, \mu^n) \\ \vdots & \ddots & \ddots & \vdots \\ \vdots & \ddots & \ddots & \vdots \\ S(\mu^n, \mu^1) & \cdots & \cdots & 1 \end{bmatrix}_{n\times n} \quad (6)$$

La salida o respuesta del FIS se obtiene finalmente mediante el proceso de "desfusificado", que consiste en la conjunción de las implicancias A_i individuales de cada regla, entregando un valor único de salida del FIS. La metodología de desfusificado depende del esquema tipo de FIS adoptado (Santander, 2004); así, si se utiliza el esquema tipo Mandami (Mandami *et al*., 1975) cada función de implicancia A_i será un conjunto difuso, siendo el fusificado de cada regla (regla *i*-ésima) el área bajo el truncado de la función de implicancia respectiva. Esta área, tal como se muestra en la Fig. 1, queda definida por el valor de la intersección o unión de las funciones de pertenencia, las cuales están evaluadas en sus respectivas variables de entrada. Luego de calcular las implicancias de todas las reglas se realiza la conjunción los conjuntos obtenidos. En el esquema de la Fig. 2, el conjunto *A* (salida difusa) representa esta operación como:

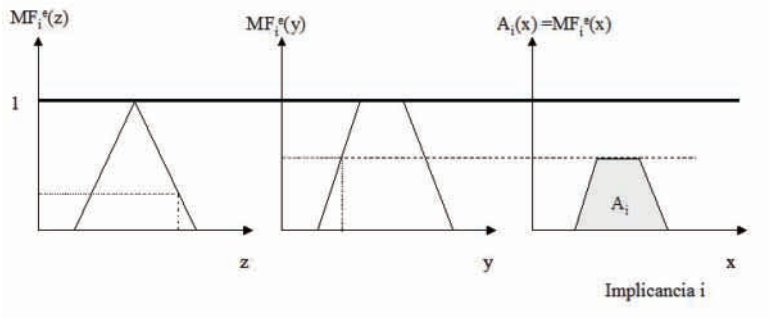


Fig. 1 Esquema de implicancia FIS tipo "Mandami" con funciones de pertenencia triangulares y trapezoidales.

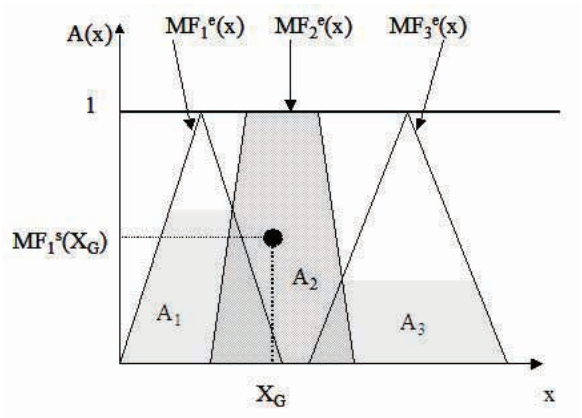


Fig. 2 Esquema "desfusificado" FIS tipo "Mandami" considerando tres reglas y la operación unión de las implicancias A_i.

$$A = \bigcup_{i=1}^{n} Ai \tag{7}$$

Para obtener el valor de las variables "desfusificadas", se emplea el centroide "X_G", tal como se aprecia en el ejemplo de la Fig. 2, que corresponde a la proyección del valor esperado de *A* en el universo *X*:

$$x_G = \frac{\int a(x)xdx}{Card(a)} \quad xeX \tag{8}$$

Índice de Riesgo I_R

El Índice de Riesgo es un instrumento abstracto de evaluación y toma de decisión en tiempo real, por lo que debe ser fácilmente interpretable en términos cualitativos. Además, dicho indicador tiene la propiedad de evaluar en términos jerárquicos el nivel de riesgo de los elementos afectados, según la importancia y vulnerabilidad de los mismos. Se define el índice como una función *f* monótonamente creciente con respecto a las variables *E* (Elemento), *A* (Amenaza) y *V* (Vulnerabilidad):

$$I_R = f(E, A, V) \tag{9}$$

Los Elementos bajo riesgo *E* están agrupados de manera de establecer jerarquías y analogías entre los sectores amagados. La amenaza *A* se define como la razón entre el valor del caudal observado y un caudal umbral de falla "Qfalla" en el cauce asociado a la inundación. La vulnerabilidad *V* representa la propensión de un elemento a dañarse e incluye de forma implícita las dificultades para la recuperación del mismo. No se considera explícitamente la duración de la falla en la formulación del Índice de Riesgo, puesto que en general en cauces como los estudiados, donde dominan los efectos inerciales sobre los gravitacionales (torrentes), la duración de la inundación tiene menor importancia que la magnitud de la misma.

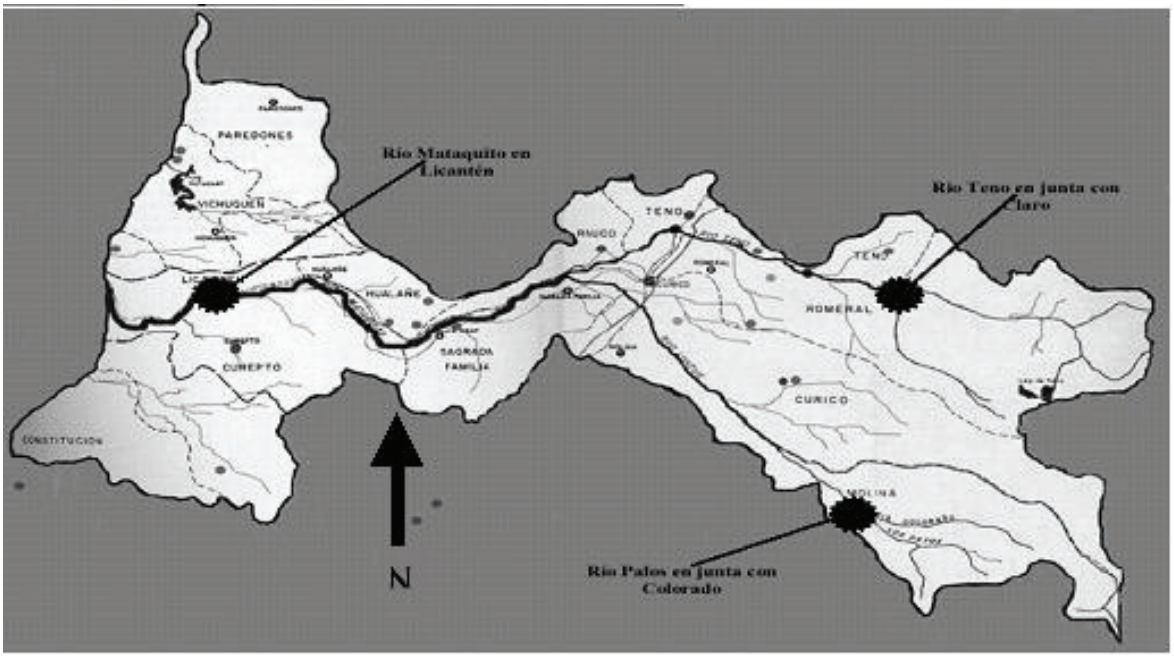


Fig. 3 Zona de estudio perteneciente a la Provincia de Curicó, Chile.

APLICACIÓN Y RESULTADOS

Zona de estudio

La investigación se desarrolló en la Provincia de Curicó, en particular en la hoya del río Mataquito (ver Fig. 3) en la cual se encuentran las estaciones limnigráficas Mataquito en Licantén, Palos en junta con Colorado y Teno en junta con Claro que definen cuencas de superficies de 5923, 514 y 1198 km^2, respectivamente. El régimen del río Mataquito es de tipo nivo pluvial, aunque las crecidas de mayor envergadura, e históricamente más destructivas, se producen en el período pluvial.

Uso de FIS Mandami para la generación de I_R comunales

La estructura y parámetros de la ecuación (9) se determina a partir de un catastro de los elementos amagados en la zona de estudio, en el cual se identificaron el tipo de falla, obras afectadas y eventos para los cuales se registraron las inundaciones (Santander, 2004). Así, los índices de riesgo individuales de los puntos o elementos bajo riesgo se evalúan como:

$$I_T^k(t) = 48.6 \times A(t^2) \times V^{0.122} \times E^{0.139} \tag{10}$$

donde los parámetros: "Q_{falla}", V y E dependen del sector amagado (ver Tabla 1).

En la obtención de los índices comunales $I_R^{Comuna}(t)$ = $FIS_{Mandami}$ ($I_R^1(t)$,….,$I_R^p(t)$) se ocupa un FIS Mandami de cuatro reglas (i = 1,..,4), aplicando la operación Unión de las funciones de pertenencia MF_k^i. Se emplean conjuntos difusos trapezoidales tanto para las funciones de implicancia A_i como para las funciones de pertenencia $MF_k^i = MF_i$ siendo estas últimas iguales todas las variables de entrada. Las variables de entrada corresponden a los índices de riesgo individuales de los elementos pertenecientes a la comuna ($I_R^k(t)$ donde k = (1,…,p) y p = no. de zonas amagadas dentro de la comuna). Los parámetros de los conjuntos difusos se indican en la Tabla 3. Para generar un Índice de Riesgo comunal $I_R^{Comuna}(t)$ escalado se considera que: $X_G(A_1)$ = 30 , $X_G(A_4)$ = 157 definiendo como valor máximo I_R^{max} = 100 y $V_k = I_R^k(t)$.

$$I_R^{Communa}(t) = 100\left[\frac{FIS_{Mandami}(V_1,...,V_P) - 30}{127}\right] \tag{11}$$

Se incorpora el concepto de Grado de Riesgo Comunal $G_r^{Comuna}(t)$ como un valor discreto, de tal forma que: G_r^{Comuna}(t) = {1,2,3,4}, evaluado como:

$$Sea: \quad \underset{i=\{1,2,3,4\}}{Soporte}\ (A_i) = [\alpha_i, \beta_i]$$

$$Si \quad \alpha_1 \le I_r^{Comuna}(t) \le \alpha_2 \Rightarrow G_r^{Comuna}(t) = 1$$
$$Si \quad \beta_3 \le I_r^{Comuna}(t) \Rightarrow G_r^{Comuna}(t) = 4$$
$$Si \quad \alpha_4 \le I_r^{Comuna}(t) < B_3 \Rightarrow G_r^{Comuna}(t) = 3$$
$$\forall i \in \{2,3\}:$$
$$Si \quad \beta_{i-1} \le I_r^{Comuna}(t) \le \alpha_{i+1} \Rightarrow G_r^{Comuna}(t) = i$$
$$Si \quad \alpha_i \le I_r^{Comuna}(t) < \beta_{i-1} \Rightarrow G_r^{Comuna}(t) = \begin{cases} i-1 & Si\ S(A_{i-1}, A_i) \ge S(A_i, A_{i-1}) \\ i & en\ otro\ caso \end{cases} \tag{12}$$

donde Soporte(A_i) es el intervalo en el cual la implicancia i-ésima es distinta de cero y $S(A)$ corresponde a la matriz de inclusión difusa:

$$S(A) = \begin{bmatrix} & A_1 & A_2 & A_3 & A_4 \\ A_1 & 1 & 1/12 & 0 & 0 \\ A_2 & 1/2 & 1 & 1/8 & 0 \\ A_3 & 0 & 1/20 & 1 & 1/8 \\ A_4 & 0 & 0 & 1/72 & 1 \end{bmatrix} \tag{13}$$

El cálculo de los índices se basó en los parámetros indicados en la Tabla 1. En las comunas de Licantén y Hualañé se obtuvo un único índice de riesgo agregado que representa a ambas, ya que por su cercanía a la desembocadura del río Mataquito las amenazas de inundación en éstas están directamente ligadas a crecidas en dicho cauce.

Tabla 1 Parámetros del índice de riesgo I_R.

Comuna	Punto amagado	Caudal de falla ($m^3 s^{-1}$)	Vulnerabilidad	Elemento	Estación Fluviométrica
Curepto	28	800	1	50	Mataquito en Licantén
Curicó	15	210	3	50	Teno en Claro
	13	64	2	100	Palos en Colorado
	14	64	2	100	Palos en Colorado
Hualañé	35	2700	1	50	Mataquito en Licantén
Molina	2	240	3	50	Palos en Colorado
	3	240	3	50	Palos en Colorado
	4	240	3	40	Palos en Colorado
	5	240	2	50	Palos en Colorado
	6	240	3	40	Palos en Colorado
	7	160	3	40	Palos en Colorado
	8	160	3	40	Palos en Colorado
Licantén	141	1700	3	40	Mataquito en Licantén
Rauco	46	210	2	60	Teno en Claro
	47	1500	2	50	Mataquito en Licantén
Romeral	40	370	3	40	Teno en Claro
	41	370	3	40	Teno en Claro

Tabla 2 Antecedentes periodísticos en evento del 28 a 30 de mayo de 1991.

Fecha	Descripción	Comuna afectada
29-05	Aislamiento de la localidad de Los Queñes	Romeral
29-05	Desborde del río Teno provoca corte de camino	Rauco
30-05	Corte de camino ruta J-60	Licantén
30-05	Anegamiento en la comuna de Curepto por desborde del río Mataquito	Curepto
30-05	Río Lontué amenaza con desbordarse	Molina

Tabla 3 Parámetros conjuntos difusos.

Funciones de pertenencia "$MF^i(V_k)$"	Funciones de implicancia $A_i(I_R^{Comuna}{}_{(t)})$
MF1 = Trapezoidal [0,0,60,80]	A1 = Trapezoidal [0,0,60,60]
MF2 = Triangular [60,80,100]	A2 = Triangular [50,60,70]
MF3 = Triangular [80,100,120]	A3 = Triangular [60,90,110]
MF4 =Trapezoidal [100,120,Ω,Ω] (Donde: $\Omega \to \infty$)	A4 = Trapezoidal [100,120,200,200]

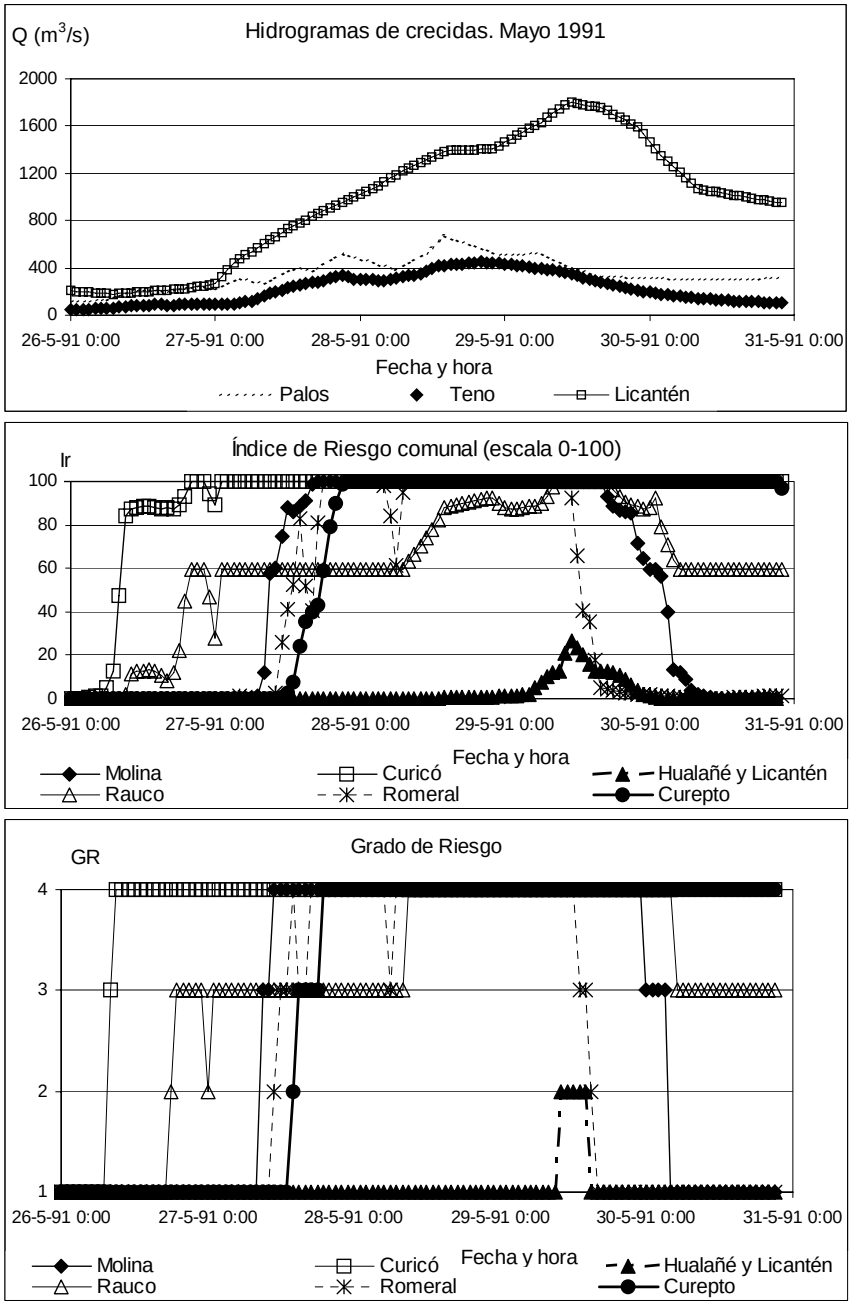


Fig. 4 Evento del 28 a 30 de Mayo de 1991. (a) hidrogramas de crecida; (b) índices de riesgo de inundación comunales y (c) grados de riesgo de inundación comunales.

El resultado de la aplicación tanto de los índices de riesgo comunales "I_r^{Comuna}", como de los grados de riesgo "G_r^{Comuna}", para la crecida ocurrida entre los días 28 a 30 de Mayo de 1991, se presenta en la Fig. 4. Se aprecia que tanto los I_r^{Comuna} como los G_r^{Comuna} son consistentes con respecto a los hidrogramas registrados, mostrados también en dicha figura. Igualmente, estos resultados están en conformidad con el catastro de inundaciones y zonas amagadas en este evento, resumido en la Tabla 2.

Se observa que los índices agregados de las comunas de Licantén y Hualañé son siempre relativamente bajos, puesto que éstas presentan elementos con umbrales de falla muy disímiles (Tabla 1), lo que queda de manifiesto en la Tabla 2 pues se registran problemas en la comuna de Licantén y no en Hualañé. En la comuna de Curicó hay sectores que presentan inundaciones frecuentes, por consiguiente tienen bajos valores del umbral de falla, esto incide en que ésta sea la comuna más susceptible a presentar índices de riesgo altos; luego siguen las comunas de Curepto, Molina, Rauco y Romeral.

CONCLUSIONES

Los resultados obtenidos permiten destacar los siguientes aspectos:

– Los FIS Mandami permiten generar modelos de interpretación del riesgo a distintas escalas espaciales.
– El índice G_r^{Comuna}, basado en las propiedades de la inclusión difusa, traduce el riesgo en valores discretos a partir de valores difusos.
– De la definición del G_r^{Comuna} se concluye, que este índice se fundamenta en el siguiente criterio: "Los elementos pertenecientes a la intersección de dos conjuntos difusos pertenecen en mayor medida al conjunto de menor tamaño de ambos".

REFERENCIAS

Kosko, B. (1992) *Neural Networks and Fuzzy Systems: A Dynamical Systems Approach to Machine Intelligence*. Prentice Hall, Englewood Cliffs, New Jersey, USA.

Mandami, E. H. & Assilian S. (1975) An experiment in linguistic synthesis with a fuzzy logic controller. *Int. J. Man-Machine Studies* **7**(1), 1–13.

Santander, A. (2004) Uso de Lógica Difusa para la estimación de Índices de Riesgo y Falla de Obras Hidráulicas en Tiempo Real. Tesis para optar al título de ingeniero civil y al grado de Magíster en Ciencias de la Ingeniería, Universidad de Chile.

Vargas, X. & Santander, A. (2002) Uso de Lógica Difusa para la estimación de Índices de Riesgo de Inundación y falla de Obras Hidráulicas en Tiempo Real. In: *XX Congreso Latinoamericano de Hidráulica*, La Habana, Cuba.

Climate Variability and Change—Hydrological Impacts (Proceedings of the Fifth FRIEND World Conference held at Havana, Cuba, November 2006), IAHS Publ. 308, 2006.

AIGA: un dispositif d'alerte des crues. Application à la région méditerranéenne française

JACQUES LAVABRE[1] **& YVES GREGORIS**[2]

1 *Cemagref, 3275 Route Cézanne, CS 40061, F-13182 Aix en Provence cedex 5, France*
jacques.lavabre@cemagref.fr
2 *Météo-France, Direction Interrégionale Sud-est, Avenue du Château Double, F-13100 Aix en Provence, France*

Résumé La majorité des outils mis en œuvre pour la prévision des crues utilise en temps réel une information sur les pluies au sol et sur les débits. En absence d'information spécifique sur les cours d'eau, les méthodes classiques sont inopérantes. C'est pour combler ce manque que le Cemagref et Météo-France ont associé leurs compétences, afin de mettre au point un outil permettant de connaître la pluviométrie et les débits des cours d'eau en temps réel sur l'ensemble du réseau hydrographique français. Ainsi a été développée la méthode AIGA qui produit toutes les heures une carte du risque pluvial à l'échelle du km^2 et du risque hydrologique, et ceci, même sur les zones géographiques et les cours d'eau sans aucune instrumentation spécifique.

Mots clefs risque hydrologique; prévision des crues; radar climatologique; modélisation pluie–débit

AIGA: a flood forecasting tool. Application to the French Mediterranean region

Abstract Currently, new flood forecasting schemes are being developed. On the one hand, there are watercourses for which real-time information on ground-level rainfall and flow rates are available, and on the other hand, there are the watercourses for which real-time information on the flow rates is either not useable or unavailable. Cemagref and Météo-France have combined their skills to fill this gap and develop a tool to determine the amount of rain and the streamflow rate in real time on the entire French hydrographical network. Thus AIGA has been developed, which produces a map of rain-related risks on a grid of 1 km^2 and of the hydrological risk, every hour. This is produced even over geographical areas and watercourses with no specific instrumentation.

Key words hydrological risk; flood forecasting; climatological radar; rainfall–runoff model

INTRODUCTION

En ce qui concerne la prévision des crues, la plupart des outils hydrologiques ou hydrauliques utilisent une information, connue en temps réel, du débit des cours d'eau. Ces outils hydrauliques et hydrologiques spécifiques à chaque cours d'eau ne sont pas exploitables pour les cours d'eau en absence de données télétransmises. Ce constat a conduit la Direction Interrégionale Sud-Est de Météo-France (DIRSE) et le Cemagref d'Aix-en-Provence à développer et proposer un outil pour combler cette défaillance d'information. Ainsi, à l'origine AIGA avait essentiellement pour but d'apporter une réponse sur les cours d'eau pour lesquels aucune instrumentation spécifique n'avait été mise en place. L'idée a été d'utiliser une information en temps réel fournie par les radars météorologiques et d'exploiter les mesures pluviométriques temps réel du réseau de base de Météo-France. La zone préférentielle d'application de AIGA est celle des bassins versants de superficie réduite (quelques dizaines à quelques centaines de km^2), qui présentent des crues à cinétique rapide – cas ou il y a intérêt de transformer une information pluviométrique en une information hydrologique – et pour lesquels on ne dispose pas spécifiquement de données hydro-météorologiques télétransmises.

PRESENTATION DE LA METHODE

La méthode AIGA se limite à n'utiliser que des informations disponibles en tout point de l'espace, fournies par les dispositifs métrologiques de base gérés par Météo-France. Elle associe: des estimations, en temps réel, de lame d'eau obtenues à partir des radars météorologiques et des pluviomètres; des estimations du déficit hydrique du sol, calculées en temps réel à partir des modèles de Météo-France et des observations météorologiques; une évaluation de l'aléa dû à l'écoulement hydrologique induit par cette lame d'eau; et des informations statistiques de différentes bases de données hydro-climatiques spatialisées.

Copyright © 2006 IAHS Press

AIGA exploite donc une information temps réel et une information statistique contenue dans des bases de référence. Le croisement de ces deux types d'information permet d'afficher une échelle de gravité de l'événement hydrométéorologique.

LES BASES DE DONNEES HYDROMETEOROLOGIQUES DE REFERENCE

Les bases qui vont être décrites n'ont pas été développées spécifiquement pour AIGA. Elles sont utilisées pour la détermination des quantiles de pluie et de débit dans le cadre d'application des Plans de Prévention des Risques inondation (PPRi). L'élaboration des bases de référence des pluies et des débits repose sur la méthode SHYPRE mise au point par le Cemagref (Arnaud & Lavabre, 1999, 2002) et sur sa version régionalisée SHYREG (Lavabre *et al.*, 2002, 2003).

SHYPRE associe un générateur de pluie horaire et une modélisation de la pluie en débit. Le générateur de pluie horaire simule de longues chroniques de pluie horaire. Outre leur insertion dans une modélisation de la pluie en débit, ces longues chroniques de pluie fournissent directement les estimations des quantiles de pluie de différentes durées et différentes fréquences.

Le générateur de pluie repose sur une description géométrique du signal pluie au pas de temps horaire. Le modèle a été calé et contrôlé sur environ deux cent chroniques de pluies horaires représentatives de climatologies diverses (tempéré, méditerranéen, tropical). *A posteriori*, des tests de sensibilité ont permis de réduire le nombre de variables du modèle. Une analyse multi variables a été ensuite mise en œuvre afin d'établir des liaisons entre les variables caractéristiques du modèle horaire et des caractéristiques synthétiques des chroniques de pluies journalières (pour d'évidentes raisons de plus grande disponibilité de cette information).

Après une phase de régionalisation des caractéristiques pluviométriques synthétiques, le générateur de pluie peut être activé en tout point de l'espace. Des grilles de quantiles de pluie, à la maille de 1 km^2, sont ainsi élaborées pour différentes durées de pluie (entre 1 et 72 h) et différentes fréquences d'apparition (période de retour entre 2 et 100 ans). Ces informations ont été intégrées dans une base de données.

La Fig. 1 présente deux exemples de cartographies ainsi disponibles pour les pluies de durée 1 h et pour les pluies journalières (les zones de faibles hauteurs de pluie apparaissent en clair et les zones de pluies intenses en foncé).

Une technique semblable est utilisée pour l'élaboration de la base de données des débits spécifiques. Chaque pixel de 1 km^2 de l'espace, est considéré comme un bassin versant virtuel. Un modèle de transformation de la pluie en débit, à un seul paramètre, transforme le signal pluie en hydrogrammes de crue. Le paramètre du modèle est déduit d'une table de référence qui a été construite sur des considérations d'occupation de l'espace et des caractéristiques des sols.

Il est ainsi possible d'activer, pour tout pixel de l'espace, le modèle de génération des pluies horaires et la modélisation de ces chroniques en débit.

Les quantiles de débit de différentes durées et de différentes fréquences sont directement issus des scénarios de crue générés par la méthode. Ce qui permet de proposer une grille, à la maille de

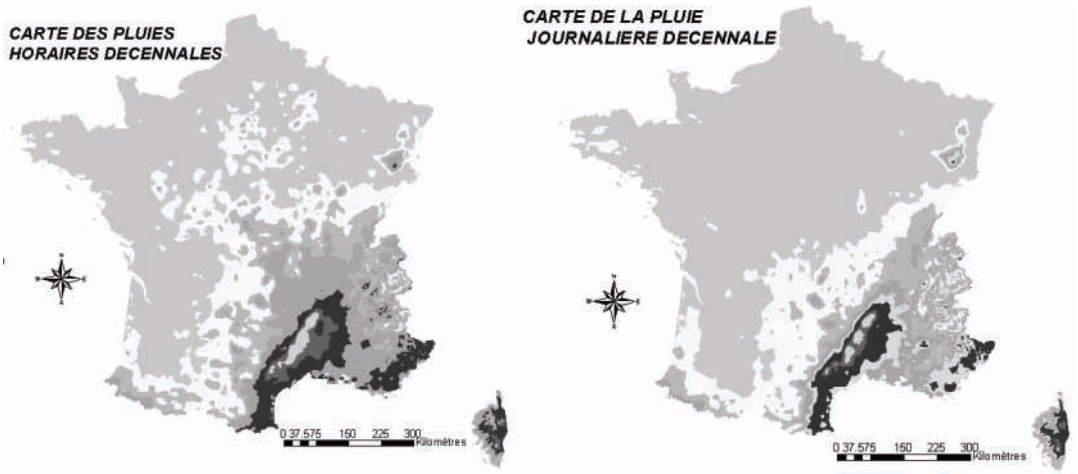


Fig. 1 Exemples de cartographies de quantiles de pluie obtenues par la méthode SHYPRE régionalisée.

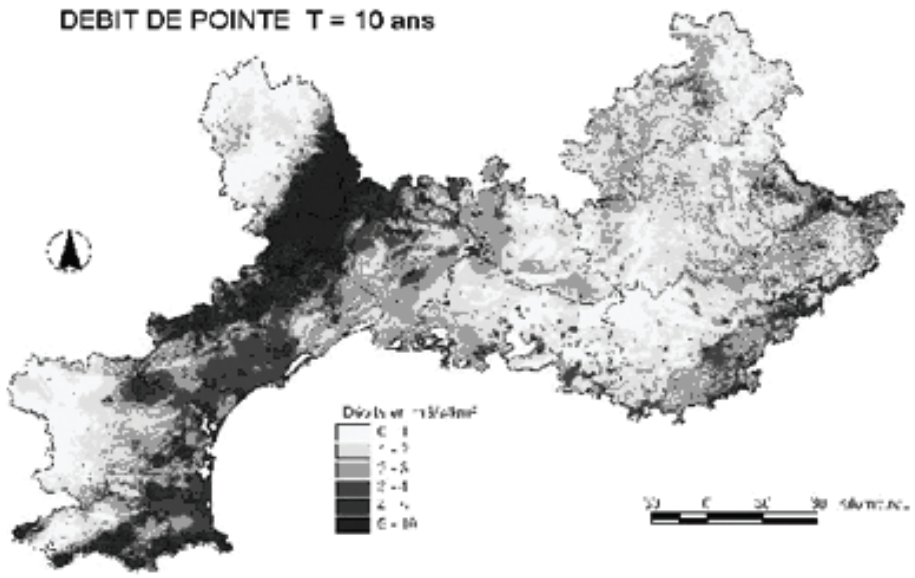


Fig. 2 Cartographie du quantile décennal du débit de pointe obtenue par la méthode SHYPRE régionalisée.

1 km^2, des débits spécifiques, de différentes durées et de différentes fréquences. Cette information pixélisée constitue les bases statistiques de données de référence de débit. La Fig. 2 présente un exemple de cartographie, sur la zone méditerranéenne française, du débit de pointe de crue de période de retour de 10 ans, issue de la base de données qui a été élaborée. On note, en couleur foncée les forts débits spécifiques de la zone cévenole (de l'ordre de 8–10 m^3 s^{-1} km^{-2}) et en clair les débits spécifiques les plus faibles (de l'ordre de 1–2 m^3 s^{-1} km^{-2}) pour les zones à pluviométrie océanique et les zones calcaires de la Provence.

La méthode propose une règle d'agglomération de cette information pixélisée pour estimer les débits de référence de crue pour tout bassin versant de la zone.

LE RISQUE PLUVIOMETRIQUE ET LE RISQUE HYDROLOGIQUE

Météo-France gère le parc des radars météorologiques du réseau ARAMIS. La majorité du territoire national est couverte par ce réseau, à l'exception des zones d'altitude. Des champs de réflectivité des ondes radar sont disponibles à une maille de 1 km^2, à un pas de temps de 15 minutes. Une relation statistique, connue sous le nom de loi de Marshall-Palmer, lie la réflectivité des ondes à l'intensité des précipitations. Cette loi est empirique et les coefficients de calage varient selon le type de précipitation. Des observations des pluies au sol permettent de vérifier la pertinence des taux précipitants restitués grâce à l'imagerie radar, voire de procéder à des corrections des coefficients.

La comparaison, en temps réel, des champs spatiaux des pluies déduits de l'imagerie radar et des bases de données pluviométriques permet d'apprécier la gravité du risque pluvial. Ceci est traduit en une échelle de gravité en trois couleurs: jaune, orange et rouge pour respectivement les événements jugés courants, rares et exceptionnels.

Les estimations temps réel de pluie fournies par le radar sont injectées dans une modélisation de la pluie en débit, à l'échelle des pixels au km^2. La valeur locale du paramètre unique du modèle est déduite du modèle d'humidité du sol, qu'exploite Météo-France en temps réel et de la base régionale du paramètre de production du modèle. Ainsi, la méthode propose, au pas de temps horaire, une estimation des débits pour chacun des pixels de l'espace. Cette information est agglomérée à l'échelle des bassins versants, afin d'estimer les débits, et ceci avec un délai d'anticipation qui est fonction de la taille des bassins versants affectés par l'événement. Ces débits sont alors comparés, en temps réel, à la base statistique hydrologique des débits de crue.

La méthode est ainsi capable de fournir une estimation du risque hydrologique. Cette information est traduite, comme pour les pluies, en une échelle de gravité en trois couleurs: jaune, orange et rouge pour respectivement les débits de crue jugés courants, rares et exceptionnels.

LA PRODUCTION DE AIGA: DES CARTES DE RISQUES PLUVIOMETRIQUE ET HYDROLOGIQUE

Dans sa version actuelle, AIGA produit chaque heure, avec un délai de production de quelques minutes, des cartographies du risque pluvial et du risque hydrologique. Le risque pluvial est affiché au niveau des pixels, selon le code couleur jaune, orange, rouge en fonction de la fréquence d'apparition des pluies observées. La Fig. 3 présente la carte de risque pluvial, émise en temps réel, lors de l'événement du 8 septembre 2002 qui a principalement frappé les départements du Gard et du Vaucluse. AIGA affiche sur cette carte le risque inhérent aux cumuls de pluie sur les deux dernières heures. On note une zone foncée intense autour d'Avignon et l'étendue de la zone jaune (en clair) qui s'étend sur la région Nîmoise et partiellement sur le département de l'Hérault.

Ce genre d'information est extrêmement précieux pour les services ayant en charge la sécurité des biens et des personnes qui doivent gérer la crise en temps réel. Ces cartes permettent d'appréhender d'un simple coup d'œil la zone géographique affectée et la gravité du risque pluvial.

La modélisation de la pluie en débit est effectuée en temps réel (chaque heure) pour chacun des pixels de l'espace. Ces débits spécifiques sont agglomérés sur un ensemble de bassins versants préalablement défini. Pour l'ensemble des bassins versants, les débits prévus sont comparés à ceux de la base de référence. AIGA peut alors afficher le risque hydrologique prévisible qui est traduit par la couleur d'affichage des tronçons du cours d'eau inclus dans le bassin versant. La carte affichée ne fournit pas une estimation instantanée des débits et ne fait référence à aucune mesure limnimètrique. Elle exprime l'évolution prévisible du débit des cours d'eau dans les heures à venir, en fonction des précipitations observées au moment de la production de la carte.

La Fig. 4 présente la carte d'affichage du risque hydrologique émise à 10 h lors de l'événement du 3 décembre 2003. Elle concerne principalement la région montpelliéraine. AIGA affiche, en orange, un risque rare sur la partie amont du cours d'eau de la Mosson et en couleur foncé un risque exceptionnel sur le Lez, la partie aval de la Mosson et le Vidourle à l'amont de Sommières.

Nous avons, *a posteriori*, examiné les cartes d'alerte émises lors de l'événement de décembre 2003 (Grégoris & Lavabre, 2005). Nous ne pouvons valider l'approche que sur les cours d'eau instrumentés pour lesquels la pertinence des alertes peut être analysée par comparaison aux débits réellement observés.

Le Tableau 1 compare les alertes AIGA et la gravité des débits observés. Les couleurs jaune, orange et rouge sont respectivement mises en correspondance avec les débits biennaux, décennaux

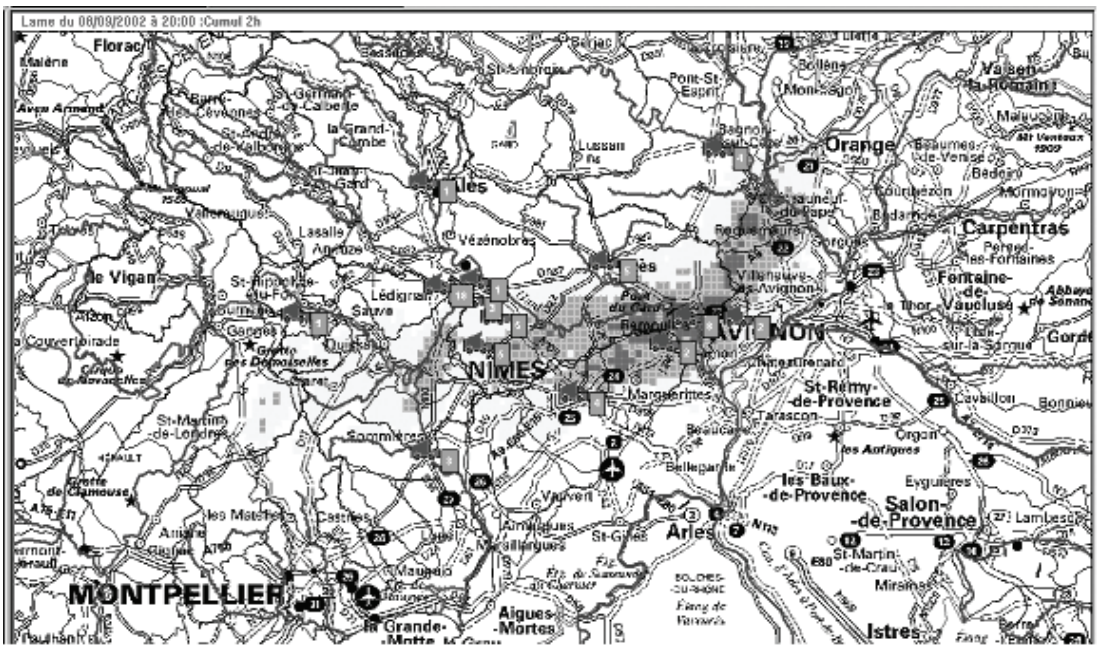


Fig. 3 Affichage du risque pluvial lors de l'événement du 8 septembre 2002 à 20:00 h TU.

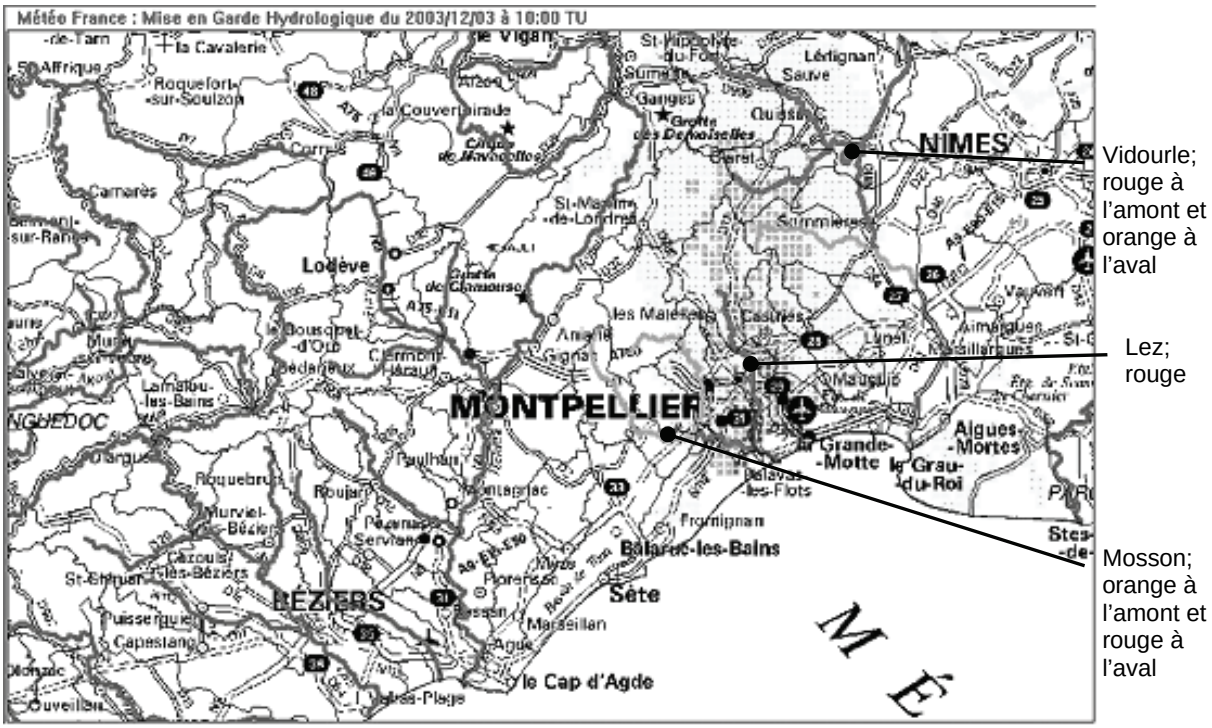


Fig. 4 Affichage du risque hydrologique lors de l'événement du 3 décembre 2003 à 10:00 h TU.

Tableau 1 Evaluation des performances de AIGA sur les alertes relatives au risque hydrologique.

Mise en garde AIGA	Sur-estimées	Pertinentes	Sous-estimées	Totales
Jaune	5 (18%)	23	0	28
Orange	1 (6%)	14 (87%)	1 (6%)	16
Rouge	0	4 (100%)	0	4
total	6 (12.5%)	41 (85.5%)	1 (2%)	48

et cinquantennaux. Sur cet événement, la méthode montre une faible propension à la surestimation du risque (dans 12.5% des cas). Un seul cas de sous estimation est à noter et on remarque que dans 85% des cas les alertes ont été pertinentes (correspondance du code couleur et de la fréquence du débit)

CONCLUSIONS ET PERSPECTIVES.

Au regard des difficultés que rencontrent les hydrologues pour développer des modèles de transformation de la pluie en débit utilisables en prévision des crues, les résultats de la méthode AIGA sont très satisfaisants. Voire inespérés, dans le contexte dégradé d'application de la méthode qui rappelons le, n'utilise pas d'information débit pour se recaler en temps réel. Bien sur la méthode n'affiche qu'une échelle de gravité du risque hydrologique et ne fournit pas des estimations numériques des débits. La méthode n'indique pas non plus l'heure à laquelle le risque hydrologique affiché va apparaître. Elle se limite à anticiper et à quantifier le risque hydrologique. Ce qui est toutefois très précieux en comparaison à une absence totale d'information.

Bien sûr la méthodologie AIGA est encore perfectible: des améliorations dans la modélisation de la pluie en débit peuvent être apportées pour augmenter les délais d'anticipation des alertes; l'intégration de prévisions de pluie permettrait aussi un gain sur les délais d'anticipation; la cadence de production des cartes d'alerte devra être accélérée. La cadence actuelle d'une production horaire peut certainement être réduite à quinze minutes.

Mais le gain de précision et de robustesse de la méthode repose sur la qualité d'estimation des champs spatiaux de pluie. Les efforts consentis par Météo-France pour améliorer les lames d'eau HYDRAM, la prise en compte d'informations volumiques, l'utilisation de radars à bi-polarisation

laissent penser que des progrès significatifs seront effectués à très court terme. Les performances de AIGA n'en seront qu'améliorées.

Remerciements Nous remercions le Ministère de l'Ecologie et du Développement Durable pour son soutien financier qui traduit l'intérêt porté à nos recherches.

REFERENCES

Arnaud, P. & Lavabre, J. (1999) Nouvelle approche de la prédétermination des pluies extrêmes. *C. R. Acad. Sci.*, Sciences de la Terre et des planètes, Géosciences de surface, hydrologie–hydrogéologie **328**, 615–620.

Arnaud, P. & Lavabre, J. (2002) Coupled rainfall model and discharge model for flood frequency estimation. *Water Resour. Res.* **38**(6), doi: 10.1029/2001WR000474.

Grégoris, Y. & Lavabre, J. (2005) Evaluation de la méthode AIGA: étude des situations météorologiques de 2003 et comparaison aux débits de la banque HYDRO. Document interne Météo-France.

Lavabre, J., Folton, N., Fouchier, C. & Faure-Soulet, A. (2002) Prédétermination régionale des débits de crue. Cas de la zone méditerranéenne française. In: *FRIEND 2002 – Regional Hydrololgy: Bridging the Gap between Research and Practice* (4ème Conf. Int. FRIEND, Cape Town) (ed. par H. A. J. van Lanen & S. Demuth), 123-130. IAHS Publ. 274. IAHS Press, Wallingford, UK.

Lavabre, J., Fouchier, C., Folton, N. & Grégoris, Y. (2003) SHYREG: une méthode pour l'estimation régionale des débits de crue. Application aux régions méditerranéennes françaises. Ingénierie EAT, no. spécial *Risque naturel et aménagement du territoire*, 97–111.

Climate Variability and Change—Hydrological Impacts (Proceedings of the Fifth FRIEND World Conference held at Havana, Cuba, November 2006), IAHS Publ. 308, 2006.

Impact of the Amazon tributaries on major floods at Óbidos

JOSYANE RONCHAIL[1], JEAN-LOUP GUYOT[2], JHAN CARLO ESPINOZA VILLAR[2], PASCAL FRAIZY[2], GÉRARD COCHONNEAU[3], EURIDES DE OLIVEIRA[4], NAZIANO FILIZOLA[4] & JUAN JULIO ORDENEZ[5]

1 *Université Paris 7- Denis Diderot and Laboratoire d'Océanographie et du Climat (LOCEAN-IPSL), case 100, 4 Place Jussieu, F-75005 Paris-France*
josyane.ronchail@lodyc.jussieu.fr

2 *Institut de Recherche pour le Développement and Universidad Agraria La Molina, casilla 18 1209, Lima 18, Peru*

3 *Maison de la Télédétection, 500 rue J.F. Breton, F-34093 Montpellier Cedex 05, France*

4 *Agência Nacional de Águas, Setor Policia, CEP 70610-200, Brasília, Brasil*

5 *Servício Nacional de Meteorología y Hidrología, Cahuide 785, Lima 11, Peru*

Abstract Major flooding of the Amazon river (with discharge over 250 000 $m^3 s^{-1}$) is analysed, using daily discharge at (a) Óbidos, the lowest gauged station on the Amazon River, 800 km from the ocean, (b) six gauge stations located on the main tributaries and characterized by different discharge regimes. During the 1984–2001 period major flooding on the main stream was related to the following features: (a) greater than usual high water in the Solimões River, the largest tributary, (b) delayed discharge peaks in the southwestern tributaries and the Amazonas River (Peru) and/or advanced discharge peaks on the Negro-Branco River, (c) unusual February–April discharge peaks in the western and northwestern tributaries, particularly in the Negro River. These two last features contribute to the simultaneous inflow of a great quantity of water from all the tributaries in April–May and may favour major flooding of the Amazon River at Óbidos.

Key words Amazon River; Óbidos; flooding; discharge; Brazil; Peru

INTRODUCTION

The Amazon basin at Óbidos is huge (4 677 000 km^2) and its main tributaries are located in various climatological regions: equatorial, and southern and northern tropics (Fig. 1 and Table 1). This is why different hydrological regimes are observed in the Amazon basin (Pardé, 1936; Molinier *et al.*, 1997). Consequently, flood time differs from one region to another and the peak discharge at Óbidos results from those in the different Amazon tributaries.

Callède *et al.* (2004) pointed out that higher than normal high water and mean discharge were observed around 1920, and 1950, and that they have become very frequent since the early 1970s. Nine events with runoff higher than 250 000 $m^3 s^{-1}$ occurred between 1970 and 2005, while four have been observed since the beginning of the century, in 1909, 1921, 1922 and 1953. Labat *et al.* (2005) also emphasize the Amazon long-term discharge variability using wavelet analysis.

In this paper, particular attention is given to recent major flooding in Óbidos and to the impact of the Amazon tributaries on these events. It is hypothesized that on the one hand, major flooding at Óbidos is associated with positive discharge anomalies in the tributaries. However, we wonder whether an anomalous high water level is observed in some tributaries only, or in all of them. On the other hand, major flooding at Óbidos may depend on the date of the flood in each basin. Is it related to delayed high water coming from the southern tributaries that experience their flood before Óbidos or, on the contrary, to sooner than usual floods in the northern tributaries that experience their peak after Óbidos? Is major flooding in Óbidos due to an anomalous concordance of flooding in the Amazon tributaries?

DATA

This study was realized using daily discharge data for 1984–2001 (Table 1). Water level series were recorded by ANA (Agência Nacional de Águas, Brasília, Brazil, http://www.ana.gov.br/) and SENAMHI (Servicio Nacional de Meteorología y Hydrología, Lima, Peru, http://www.senamhi.gob.pe/). Discharge values are computed within the Hybam project (Hydrogeodynamics of the Amazon basin, http://www.mpl.ird.fr/hybam/). Three virtual stations were created (Fig. 1):

Copyright © 2006 IAHS Press

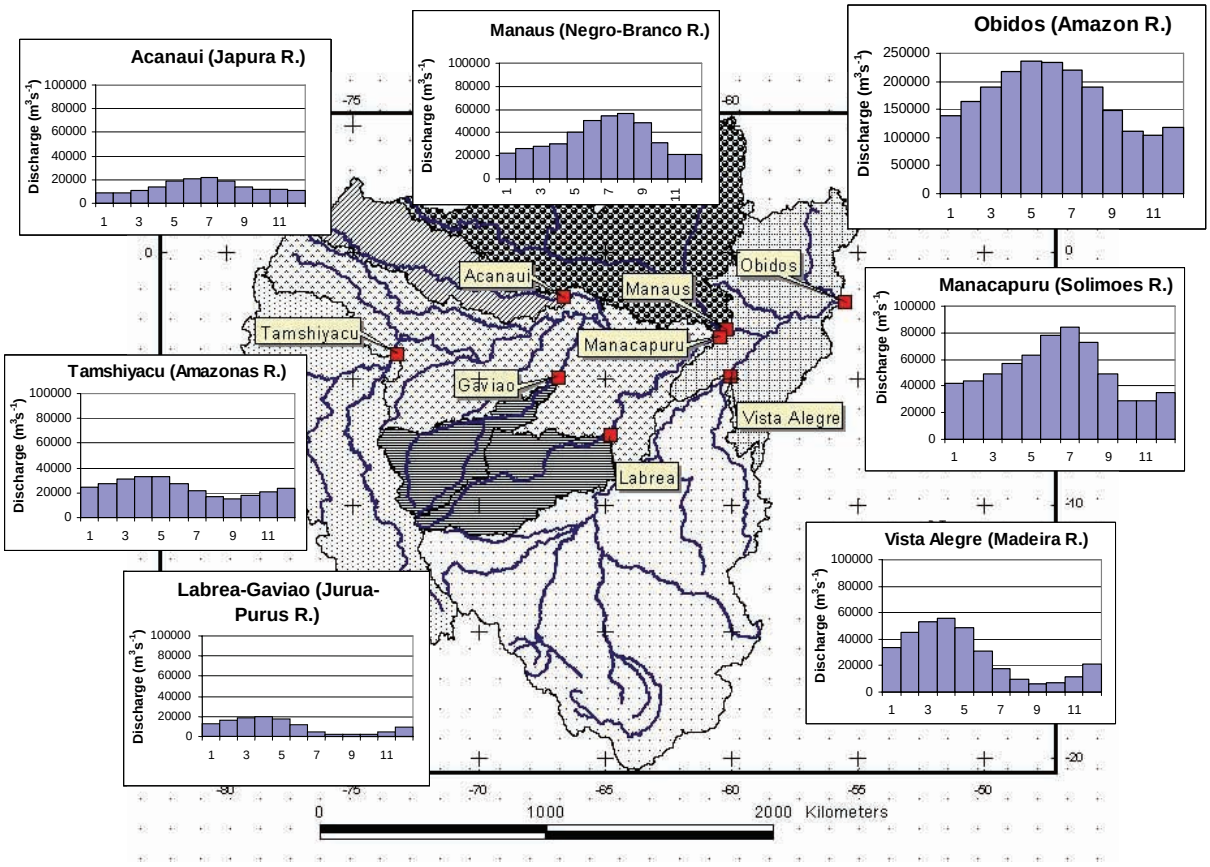


Fig. 1 Location and hydrological regimes of the Amazon River and its tributaries.

Table 1 Main characteristics of the gauging stations. Gavião-Labrea (GL), Solimões-Manacapuru (SM) and Manaus are virtual stations (see text).

	Latitude (°)	Longitude (°)	Surface (km²)	River	Period	Source
Vista Alegre	0.5 S	64.8 W	1 324 000	Madeira	67 / 02	ANA/HYBAM
GL			382 000	Purus-Jurua	72 / 01	ANA/HYBAM
Tamshiyacu	4 S	73.2 W	726 000	Amazonas	83 / 05	SENAMHI/HYBAM
Acanui	1.8 S	66.6 W	242 000	Japura	73 / 01	ANA/HYBAM
SM	3.3 S	62.8 W	797 000	Solimões	83 / 01	ANA/HYBAM
Manaus	3.1 S	60 W	697 000	NegroBranco	77 / 03	ANA/HYBAM
Óbidos	1.95 S	55.5 W	4 677 000	Amazon	68 / 05	ANA/HYBAM

(a) "Gavião-Labrea" values are the sum of the discharge of the Jurua River at Gavião and the Purus River at Labrea.

(b) "Solimões-Manacapuru" values are the difference between the Solimões River discharge at Manacapuru and the sum of its mains tributaries discharge: Amazonas at Tamshiyacu (Espinoza *et al.*, 2006), Japura at Acanui and Jurua-Purus at "Gavião-Labrea". This station represents the main stream of the Solimões River.

(c) "Manaus" values are the sum of the Amazon River discharge at Jatuarana (3.1°S and 59.7°W) and Careiro (3.2°S and 59.8°W), located downstream of the Negro and Solimões rivers confluence, minus the Solimões River discharge at Manacapuru.

The computational package Hydraccess (Vauchel, 2005) was used for data processing.

MAIN CHARACTERISTICS OF FLOODS ON THE AMAZON RIVER AND ITS TRIBUTARIES

The average 1984–2001 Amazon flood discharge at Óbidos is 238 000 m^3 s^{-1} (Table 2) with extreme values varying from 274 400 m^3 s^{-1} in 1989 to 194 600 m^3 s^{-1} in 1992. The average flood

Table 2 Main characteristics of flooding at Óbidos and in the Amazon tributaries (1984–2001). Gavião-Labrea (GL), Solimões-Manacapuru (SM) and Manaus are virtual stations (see text).

	Qm ($m^3 s^{-1}$)	*Qf* ($m^3 s^{-1}$)	*Qfmax* ($m^3 s^{-1}$)	*Qmin* ($m^3 s^{-1}$)	*Df*	*Dfs*	*Dfl*
Vista Alegre	28 000	57 200	71 460 (1997)	50 470 (1987)	14/4	13/3	14/5
GL	10 000	20 000	23 400 (1997)	18 340 (1985)	12/4	10/3	19/5
Tamshiyacu	24 300	34 000	40 720 (1984)	29 460 (1995)	01/5*	22/3	21/5
Acanui	14 200	21 700	27 800 (1989)	18 460 (1992)	30/6	14/5	4/8
SM	53 000	85 000	108 810 (2000)	65 660 (1985)	13/7	6/6	10/8
Manaus	36 000	57 600	75 000 (1990)	48 000 (1992)	2/8	12/6	17/9
Óbidos	173 000	238 000	274 400 (1989)	194 600 (1992)	27/5	1/7	10/5

*A first flooding, equivalent to the May flooding, is sometimes recorded in January or February.

Qm: mean annual discharge; *Qf*: Mean annual flood; *Qfmax*: Maximum flood; *Qmin*: Minimum flood; *Df*: Mean date of the flood; *Dfs*: Date of the soonest flood; *Dfl*: Date of the latest flood.

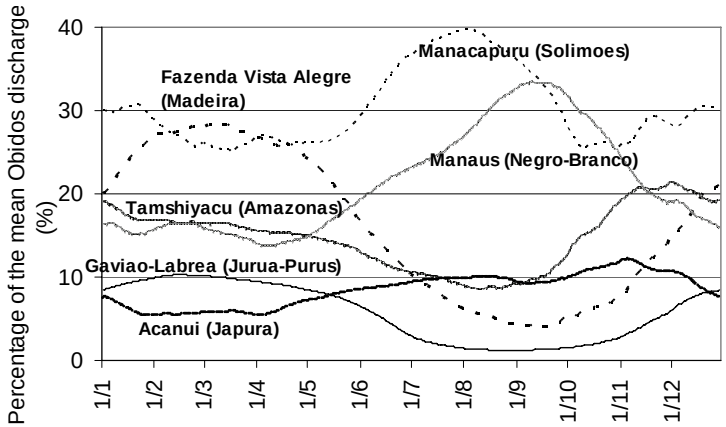


Fig. 2 Daily contribution (%) of the tributaries to the Amazon River discharge at Óbidos.

date is 27 May. However, during 1984–2001, floods occurred as early as 10 May 1992 and as late as 1 July 1994. Low water at Óbidos is observed in November and it represents half the flood value (Fig. 1). The contribution of the different tributaries to the Amazon River runoff varies with time in accordance with their annual cycle (Fig. 2).

The floods on the southwestern Amazon basins (Madeira and Jurua-Purus) occur first, around mid-April (Table 2). The hydrological regime is tropical with high water from March to May and low water in September. The seasons contrast strongly as low water is only a tenth of high water (Fig. 1). As the Madeira watershed is very large (Table 1), its mean discharge accounts for 16% of the Amazon River discharge (Table 2).

The Amazonas River at Tamshiyacu (Peru) drains most of the tropical Peruvian Amazon basin and some equatorial basins (Pastaza, Tigre and Santiago). This is why high water occurs later, 1 May, and discharge seasonality is weak (Table 2). Amazonas discharge at Tamshiyacu represents 14% of the mean Amazon discharge.

Western rivers (Japura, Negro-Branco and Solimões) drain very rainy regions. This explains why the Solimões and the Negro-Branco basins, although half the size of the Madeira basin, account for 30% and 20% respectively of the Amazon River discharge. Runoff seasonality is weak in these near-equatorial basins, with a maximum in July and a minimum in January.

The mean date for high water on the Amazon River at Óbidos is observed on 27 May, after the flood of the Madeira, Purus-Jurua and Amazonas rivers, but before the peaks of the Japura, Solimões and Negro-Branco rivers (Table 2).

THE GENESIS OF SIX MAJOR FLOOD IN ÓBIDOS (1984–2001)

Big floods are characterized by a discharge exceeding 250 000 $m^3 s^{-1}$ (Table 3(a)). During the three greatest floods, in 1989, 1997 and 1999, huge daily discharge values (over 260 000 $m^3 s^{-1}$) were recorded as well as long lasting strong values (2–3 months with over 250 000 $m^3 s^{-1}$ runoff).

Table 3(a) Main characteristics of major floods at Óbidos (1984–2001); Gavião-Labrea (GL), Solimões-Manacapuru (SM) and Manaus are virtual stations (see text).

OBIDOS:	1989	1994	1996	1997	1999	2000
Flood value ($m^3 s^{-1}$)	274 400	259 300	251 200	265 800	268 200	256 200
Date of flood	9/6	1/6	16/5	13/5	2/6	5/6
Days >250 000 $m^3 s^{-1}$	107	69	9	54	67	29
Date beginning > 250 000 $m^3 s^{-1}$	13/4	30/4	15/5	27/4	12/5	18/5
Date end > 250 000 $m^3 s^{-1}$	28/7	7/7	22/05*	19/6	16/7	15/6

* and from the 6/6 to the 10/6

Days >250 000 $m^3 s^{-1}$: number of days with a discharge over 250 000 $m^3 s^{-1}$; Beginning > 250 000 $m^3 s^{-1}$: date of the beginning of discharge over 250 000 $m^3 s^{-1}$; End > 250 000 $m^3 s^{-1}$: date of the end of discharge over 250 000 $m^3 s^{-1}$.

Table 3(b) Flood anomalies (percentage of the 1984–2001 flood average) in the main tributaries.

Percentage of the mean value	1989	1994	1996	1997	1999	2000
Vista Alegre	14	5	-4	25	-3	-7
GL	4	4	7	18	4	-5
Tamshiyacu	4	12	-4	2	14	6
Acanui	28		0	0	17	4
SM	17	23	13	22	28	3
Manaus	7	-5	22	-5	21	5

Table 4 Dates of flooding in the Amazon River tributaries during six major floods and during the 1984–2001 period. Delayed values in the Madeira (Vista Alegre), Jurua-Purus (Gavião-Labrea GL) and Amazonas (Tamshiyacu) rivers and advanced values in the Japura (Acanui), Solimões (Solimões-Manacapuru SM) and Negro (Manaus) rivers are shown in bold when there is a 10-day difference with the average 1984–2001 station value.

	1989	1994	1996	1997	1999	2000	Mean 1984–2001
Vista Alegre	27/3	13/3	**30/4**	9/4	11/4	5/4	14/4
GL	**22/4**	10/3	**13/5**	13/4	21/3	13/4	12/4
Tamshiyacu	9/5	**13/5**	22/4	23/4	**21/5**	**15/5**	1/5
Óbidos	9/6	1/6	16/5	13/5	2/6	5/6	27/5
Acanui	7/7		12/7	27/6	3/7	6/7	30/6
SM	8/8	8/8	14/7	23/7	3/8	10/8	13/7
Manaus	**7/7**	**14/6**	19/8	**12/6**	17/9	**1/7**	2/8

In 1989, strong positive maximum discharge anomalies were registered in the western basins (Solimões and Japura) and in the Madeira river (Table 3(b)). Moreover, the delayed peak of the Jurua-Purus and Amazonas rivers and the advanced flood of the Negro-Branco river (6 July instead of 2 August) led to concomitant high discharge in the different tributaries, during the rising stage on the Amazon River (Table 4). This phenomenon was reinforced by unusually high discharge values in December 1988 and in March–April 1989 in the Negro-Branco and Solimões rivers. The early flood of the Negro-Branco River and the late flood of the Solimões River contributed to the duration of the Amazon river flood (more than 3 months).

The 1994 flood is associated with higher than normal outflow along the Solimões-Tamshiyacu axis, i.e. in rivers flowing from Peru and Ecuador (Table 3(b)). Moreover, two features contributed to a big flood at Óbidos (a) higher than normal discharge values in the Solimões and Negro-Branco rivers from December 1993 to April–May 1994, (b) an advanced peak in the Negro-Branco River (14 June instead of 2 August) (Table 4).

The 1996 flood may be associated with higher than normal maximum discharge in the Solimões and Negro-Branco rivers and with delayed peaks in the southern rivers (Madeira and Jurua-Purus) (Tables 3(b) and 4). Moreover, an unusual discharge peak is notable in March–April in the Negro-Branco and the Japura rivers. This unusual peak, occurring during the southern tributaries' rising stage, may explain a strong and earlier than usual flood in Óbidos (16 May instead of 27 May).

In 1997, unusually high water was observed in southern tributaries, the Madeira and Jurua-Purus rivers, and along the Solimões river (Table 3(b)). Moreover, a February–March peak in the Negro-Branco and Japura rivers, and an earlier than usual flood in Manaus (12 June instead of 2 August) may also have contributed to a big and early flood at Óbidos (Table 4).

In 1999, the maximum discharge was greater than usual in all the tributaries except in the southern ones (Table 3(b)). Flooding was delayed in the River Amazonas (Table 4). Moreover, unusual peaks were observed in the Negro-Branco and Japura rivers in February–March and in the Solimões River in April; they coincide with the rising stage and flood in the southern affluent. On the other hand, a delayed flood in the Solimões and Negro-Branco rivers may have caused a long lasting flood at Óbidos (67 days).

Lastly, in 2000, weak positive maximum discharge anomalies were observed in the western tributaries (Table 3(b)). Moreover, a one-month early Negro-Branco River flood and a delayed flood on the Amazonas River are factors that explain the concomitant high discharge in the southwestern and northwestern affluent (Table 4).

CONCLUSION

The main characteristics of six major Amazon floods in Óbidos, during 1984–2001, are analysed using the daily discharge values of six Amazon tributaries.

In 1989, the biggest flood of the twentieth century was related to positive discharge anomalies across the whole basin. In the other cases, unusually high water is observed in groups of tributaries that are always different. Obviously, as it is the biggest tributary, a positive high water anomaly is generally observed in the Solimões River. The correlation between high water discharge in the Amazon River and in the tributaries is high with the Solimões (r = 0.77), weak with the Jurua-Purus, the Amazonas (Peru) and the Japura and non-significant with the Negro-Branco and the Madeira.

Major flooding at Óbidos is also related to out-of-phase flooding in the tributaries and to concomitant high discharge values in the different rivers. Delayed flooding was observed three times in the Amazonas River, twice in the Jurua-Purus River and once in the Madeira River. Advanced high water occurred four times in the Negro-Branco River. In 2000, as no strong high water anomaly was observed in the main tributaries, the Amazon flood may be directly associated with a delayed peak in the Amazonas River and an advanced one in the Negro-Branco River.

Major flood events are also related to the occurrence of out of phase and secondary peak discharges in the Negro-Branco River (1989, 1994, 1996, 1997, 1999), in the Japura River (1996, 1997, 1999) or in the main stream of the Solimões River (1989, 1994, 1999). In the Negro-Branco River, these discharge anomalies generally occur from February to April, are particularly strong (+20% during the three months) and are associated with an earlier than usual flood in Manaus (Fig. 3). The relationship between high water discharge at Óbidos and February–March–April discharge at Manaus is significant (r = 0.74). In the Japura and Solimões rivers, they are less frequent and the average discharge anomalies are weaker (+10%). The February–March–April discharge anomalies are in phase with the southern tributaries' rising stage and high water and contribute to major floods at Óbidos. The origin of these out-of-phase peaks in the western rivers deserves further investigations.

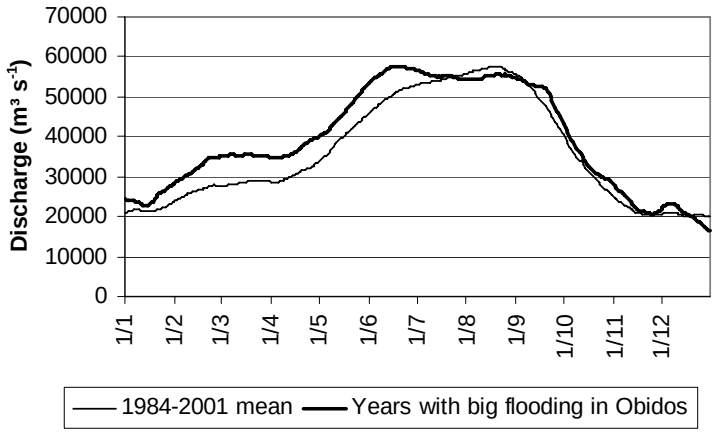


Fig. 3 Mean discharge of the Negro-Branco River during the 1984–2001 period (thin line) and during years with major flooding at Óbidos (1989, 1994, 1996, 1997, 1999 and 2000) (bold line).

In conclusion, each big flood at Óbidos seems to be a special event with its own causes. Nevertheless major floods have some features in common, such as a February–March–April unusual peak in the Negro-Branco River, a delayed flood in the southern basins and in the Amazonas River, and a high water level on the Solimões River, the greatest Amazon tributary. These variables should be accurately monitored in order to predict major floods at Óbidos.

REFERENCES

Callède, J., Guyot, J. L., Ronchail, J., L'Hôte, Y., Niel, H. & de Oliveira, E. (2004) Evolution du débit de l'Amazone à Obidos de 1902 à 1999. *Hydrol. Sci. J.* **49** (1), 85–97.

Espinoza, J. C, Fraizy, P., Guyot, J. L., Ordoñez, J. J., Pombosa, R. & Ronchail, J. (2006) La variabilité des débits du Rio Amazonas au Pérou. In: *Climate Variability and Change—Hydrological Impacts* (ed. by S. Demuth *et al.*) (Proc. Fifth FRIEND World Conference, Havana, Cuba, November 2006). IAHS Publ. 308. IAHS Press, Wallingford, UK (this volume).

Labat, D., Ronchail, J. & Guyot, J. L. (2005) Recent advances in wavelet analysis: Part 2 – Amazone, Parana, Orinoco and Congo: interannual and multidecadal variability. *J. Hydrol.* **314**, 289–311.

Molinier, M., Guyot, J. L., de Oliveira, E. & Guimarães, W. (1997) Les régimes hydrologiques de l'Amazone et de ses affluents. In: *Hydrologie tropicale: geoscience et outil pour le développement* (ed. by P. Chevallier & B. Pouyard), 209–222. IAHS Publ. 238. IAHS Press, Wallingford, UK.

Pardé, M. (1936) Les variations saisonnières de l'Amazone. *Annales de Géographie* **45**, 502–511.

Vauchel, P. (2005) Hydraccess: logiciel de gestion et de traitement de données hydrométéorologiques, version 2.1.4. http://www.mpl.ird.fr/hybam.

Climate Variability and Change—Hydrological Impacts (Proceedings of the Fifth FRIEND World Conference held at Havana, Cuba, November 2006), IAHS Publ. 308, 2006.

Bayesian priors based on regional information: application to regional flood frequency analysis

MATHIEU RIBATET[1,2], ERIC SAUQUET[2], JEAN-MICHEL GRESILLON[2] & TAHA B. M. J. OUARDA[1]

1 *INRS-ETE, University of Quebec, 490 de la Couronne, Quebec G1K 9A9, Canada*
mathieu.ribatet@ete.inrs.ca

2 *Cemagref, 3 bis quai Chauveau CP 220, F-69336 Lyon Cedex 9, France*

Abstract Flood frequency analysis is usually based on the fitting of an extreme value distribution to the series of local streamflow. However, when the at-site time series is short, frequency analysis results become unreliable. In this work, a regional Bayesian model to estimate flood quantile from a few years of stream flow data is proposed. This model is less restrictive than the Index Flood model while preserving the formalism of "homogeneous regions". Performance of the proposed model is assessed on a set of French gauging stations. The accuracy of quantile estimates as a function of homogeneity level of the pooling group is also analysed. Results indicate that the regional Bayesian model outperforms the Index Flood model and local estimators. Furthermore, it seems that working with relatively large and homogeneous regions may lead to more accurate results than working with smaller and highly homogeneous regions.

Key words regional frequency analysis; Bayesian inference; Index Flood; MCMC

INTRODUCTION

Flood frequency analysis is essential in preliminary studies to design flood defence structures. Methods for estimating design flows usually consist of fitting one of the distributions given by the extreme value theory to a sample of flood events. If modelling exceedence over a threshold is of interest, a theoretical justification exists for the use of the Generalized Pareto distribution (GP):

$$F(x) = 1 - \left[1 + \frac{\zeta(x-\mu)}{\sigma}\right]^{-1/\zeta} \text{ where } 1 + \frac{\zeta(x-\mu)}{\sigma} > 0, \sigma > 0 \quad (1)$$

where μ, σ and ζ are the location, scale and shape parameters, respectively. This distribution is defined for $\zeta \neq 0$, and can be derived by continuity in the case $\zeta = 0$, corresponding to the exponential case.

However, frequency analysis can lead to unreliable flood quantiles when few data are available at the site of interest. A convenient way to improve estimates of flood statistics is to incorporate data from other gauged locations in the estimation procedures. This approach is widely applied in hydrology and is known as Regional Flood Frequency Analysis (RFFA).

One of the most popular and simple approaches favoured by engineers is the Index Flood method (Dalrymple, 1960). However, the assumptions of the Index Flood model need often to be relaxed to suit the observations. We suggest here to carry out a Bayesian approach that encompasses the classical Index Flood model and uses the whole data set in a more efficient manner.

The main goal of this paper is to test the efficiency and robustness of the developed regional Bayesian model when dealing with series of short record length. For this purpose, the suggested regional Bayesian approach will be compared to local analysis and traditional RFFA. The next section presents a brief summary of the classical Index Flood model. Next, the data set used to illustrate the method is described, followed by a description of the procedure used to elicit the prior distribution. In the fifth section the weaknesses and strengths of each approach on a typical homogeneous region are outlined. Finally an analysis of the effect of homogeneity level on quantile estimation is presented.

THE INDEX FLOOD MODEL

The Index Flood method states that flood frequency distributions within a particular region are supposed to be identical when divided by a scale factor – namely the Index Flood. Mathematically,

Copyright © 2006 IAHS Press

this assumption is expressed as:

$$Q^{(S)} = C^{(S)} Q^{(R)} \tag{2}$$

where $Q^{(S)}$ is the quantile function at site *S*, $C^{(S)}$ is the Index Flood at site *S* and $Q^{(R)}$ is the regional quantile function.

Equation (2) is supposed to be satisfied if all sites are hydrologically and/or statistically similar. Therefore, one of the main aspects of this approach is to identify a homogeneous region, which includes the target site.

The parameters of the regional distribution are usually derived from weighted average of at-site L-moments. Finally, the target site distribution $Q^{(S)}$ is computed from equation (2). It can be seen that the observations of all samples have the same weight. This is debatable since the most relevant information is certainly the at-site one. Thus, in this approach, the available information is not efficiently used.

DATA DESCRIPTION

The selection of the gauging sites was initially based on the 22 regions into which France is divided for the implementation of the European Water Framework Directive. Therefore it seems reasonable to consider this division as a preliminary guide for pooling stations. The pre-regions were subsequently altered to satisfy the heterogeneity test of Hosking & Wallis (1997). Finally, a set of 14 stations was selected for this study.

The record length of time series ranges from a minimum of 22 years to a maximum of 37 years, with a mean value of 32 years. The drainage areas vary from 32 to 792 km^2. Most of the gauging stations monitored first-order streams. Threshold levels were selected to extract on average around two events per year, while meeting the criteria of independence between floods.

Three stations (U4505010, U4635010 and V3015010) were of particular interest because of their extended record length of 37 years. In this case study, the scale factor was set to correspond to the 1-year return flood quantile. Analysing the influence of Index Flood selection is beyond the scope of this work. The main point is to keep the same Index Flood throughout the case study to compare approaches on the same basis.

ELICITING THE PRIOR DISTRIBUTION

In the proposed regional Bayesian model, the regional information is not used to build a regional distribution but to specify a kind of "suspicion'' about the target site distribution. This is easily achieved in the Bayesian framework through the so-called prior distribution. The prior model is usually a multivariate distribution, which must represent beliefs about the distribution of the parameters, i.e. μ, σ and ζ prior to having any information about the data. Consider all sites of a homogeneous region except the target site – say the *j*th site. A set of "pseudo target site estimates" is computed:

$$\tilde{\mu}^{(i)} = C^{(j)} \mu_*^{(i)} \tag{3}$$

$$\tilde{\sigma}^{(i)} = C^{(j)} \sigma_*^{(i)} \tag{4}$$

$$\tilde{\zeta}^{(i)} = \zeta^{(i)} \tag{5}$$

for all $i \neq j$ where $\mu_*^{(i)}$ and $\sigma_*^{(i)}$ are parameters estimates from rescaled sample. According to the Index Flood model, the set of parameters $(\tilde{\mu}^{(i)}, \tilde{\sigma}^{(i)}, \tilde{\zeta}^{(i)})$for $i \neq j$ is expected to be distributed as ($\mu^{(i)}$, $\sigma^{(i)}$, $\zeta^{(i)}$). Note that, information from the target site sample is not used to elicit the prior distribution. Thus, $C^{(j)}$ in equations (3) and (4) must be estimated without use of the *j*th site sample. In this case study, $\log C^{(j)}$ is estimated through a Generalized Linear Model defined by:

$$\begin{cases} E\left[\log C^{(j)}\right] = \upsilon \\ \mathrm{var}\left[\log C^{(j)}\right] = \phi V(\upsilon) \end{cases} \qquad \eta = \log(\upsilon) = X\beta \tag{6}$$

where X are basin characteristics, ϕ is the dispersion parameter and V the variance function. As $C^{(j)}$ is estimated without the target site sample, it is important to incorporate uncertainties from the elicitation of the prior distribution. Under the independence assumptions between $C^{(j)}$ and $\mu_*^{(i)}$, $\sigma_*^{(i)}$, the following relations hold:

$$\mathrm{var}\left[\log \tilde{\mu}^{(i)}\right] = \mathrm{var}\left[\log\left(C^{(j)}\mu_*^{(i)}\right)\right] = \mathrm{var}\left[\log C^{(j)}\right] + \mathrm{var}\left[\log \mu_*^{(i)}\right] \quad (7)$$

$$\mathrm{var}\left[\log \tilde{\sigma}^{(i)}\right] = \mathrm{var}\left[\log\left(C^{(j)}\sigma_*^{(i)}\right)\right] = \mathrm{var}\left[\log C^{(j)}\right] + \mathrm{var}\left[\log \sigma_*^{(i)}\right] \quad (8)$$

The independence assumptions between $C^{(j)}$ and $\mu_*^{(i)}$, $\sigma_*^{(i)}$ is not too restrictive as the target site Index Flood $C^{(j)}$ is estimated independently from $\mu_*^{(i)}$, $\sigma_*^{(i)}$.

In this case study, the marginal prior distributions were supposed to be independent lognormal for both the location parameter μ and the scale parameter σ and normal for the shape parameter ζ. The lognormal distribution is justified by a physical and theoretical lower bound. Indeed, (a) discharge data are naturally non-negative; so the location parameter should also be non-negative; and (b) the scale parameter is strictly positive by definition of the GP distribution. Furthermore, as the prior distribution is based on the Index Flood model, equation (2) implies that if the scale parameter is lognormally distributed, the location parameter should also be lognormally distributed. This choice is confirmed by the data.

The prior distribution $\pi(\theta)$ is therefore elicited by means of the following equations:

$$E\left[\log \mu^{(j)}\right] \approx \frac{1}{N-1}\sum_{i\neq j} \log \tilde{\mu}^{(i)} \qquad \mathrm{var}\left[\log \mu^{(j)}\right] \approx \frac{1}{N-1}\sum_{i\neq j} \mathrm{var}\left[\log \tilde{\mu}^{(i)}\right]$$

$$E\left[\log \sigma^{(j)}\right] \approx \frac{1}{N-1}\sum_{i\neq j} \log \tilde{\sigma}^{(i)} \qquad \mathrm{var}\left[\log \sigma^{(j)}\right] \approx \frac{1}{N-1}\sum_{i\neq j} \mathrm{var}\left[\log \tilde{\sigma}^{(i)}\right]$$

$$E\left[\zeta^{(j)}\right] \approx \frac{1}{N-1}\sum_{i\neq j} \zeta^{(i)} = \bar{\zeta} \qquad \mathrm{var}\left[\zeta^{(j)}\right] \approx \frac{1}{N-2}\sum_{i\neq j} \left(\zeta^{(i)} - \bar{\zeta}\right)^2$$

where N is the number of stations within the homogeneous region. Thus:

$$\pi(\theta) \propto J \exp\left[-\frac{1}{2}(\theta' - \gamma)^T \Sigma^{-1}(\theta' - \gamma)\right] \quad (9)$$

where γ, Σ are hyper-parameters, $\theta' = (\log\mu, \log\sigma, \zeta)$ and J the Jacobian of the transformation from θ' to θ, namely $J = 1/\mu\sigma$.

Thus, the posterior distribution $\pi(\theta|x)$ is given by the Bayes Theorem:

$$\pi(\theta \mid x) = \frac{\pi(\theta)\pi(\theta; x)}{\int_\Theta \pi(\theta)\pi(\theta; x)\mathrm{d}\theta} \propto \pi(\theta)\pi(\theta; x) \quad (10)$$

where Θ is the space parameter, $\theta = (\mu, \sigma, \zeta)$; $\pi(\theta; x)$ is the likelihood of the GP distribution; and x is the at-site sample. In theory, the posterior distribution is entirely known but is often insolvable. To overcome this problem, the most convenient way is to implement MCMC techniques to sample the posterior distribution.

PERFORMANCE OF THE REGIONAL BAYESIAN POT MODEL ON A HOMOGENEOUS REGION

In this section, three different models are applied. For this purpose, the three stations – U4505010, U4635010 and V3015010 – were selected to assess the robustness and efficiency of the local, regional and Bayesian regional models. These three different approaches correspond to: (a) local: fit the GP distribution to the peaks-over-threshold (POT) data with the maximum likelihood estimator (MLE), unbiased and biased probability weighted moments (PWU, PWB); (b) regional (REG): fit the target site distribution as described in the Index Flood model section; and

Table 1 Benchmark values for 2, 5, 10 and 20 years quantiles and the associated 90% profile likelihood confidence intervals in bracket.

Station	Q_2	Q_5	Q_{10}	Q_{20}
U4505010	10.8 (10.1, 1.7)	15.3 (13.9,17.4)	19.5 (17.2,23.4)	24.4 (20.6,31.5)
U4635010	33.0 (30.0,36.5)	52.2 (45.5,62.5)	72.2 (60.2,95.4)	98.9 (69.2,200.5)
V3015010	7.5 (6.9, 8.3)	11.7 (10.4,13.7)	15.9 (13.6,19.9)	21.3 (17.3,28.8)

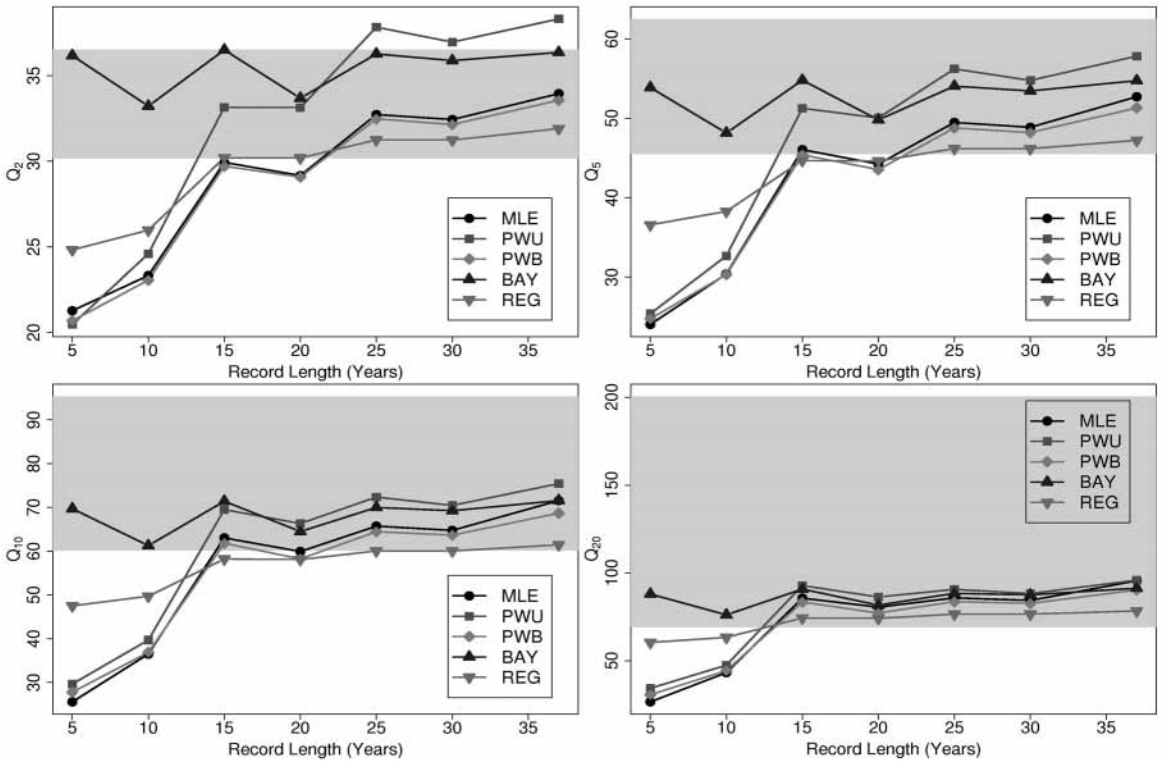


Fig. 1 Evolution of Q_2, Q_5, Q_{10}, Q_{20} estimates as the size increases for the site U4635010 and 90% profile likelihood confidence interval for the benchmark values – grey area.

(c) regional Bayesian (BAY): compute the target site distribution as described in the Eliciting the Prior Distribution section.

As the main goal of this work is to compare models on small samples, efficiency is evaluated on sub-samples from the original data. The MLE on the whole sample is used as a benchmark to assess the performance of each model. For this purpose, the target site sample was truncated to obtain shortened periods of records of m years, $m \in \{5,10,15,20,25,30,37\}$. Quantile estimates corresponding to return period 2, 5, 10 and 20 years are selected – cf. Table 1. Quantiles with return periods greater than 20 years are considered unreliable, as uncertainties on these quantiles are too large with only 37 years of record. The evolution of quantile estimates as a function of the record length period is presented in Fig. 1, considering here only the first m years. Systematic underestimation of benchmark values for local and REG approaches can be noticed. It shows that, on the one hand, for small samples, classical inference models such as MLE, PWB and PWU are too responsive if too many "regular" events occurred. On the other hand, for the REG model, underestimation of quantiles is related to the underestimation of the scale factor $C^{(j)}$ in equation (2) because of these "regular" events. Only the BAY model performs well enough even with record lengths shorter than 15 years. Moreover, it is by far the most robust and accurate model as, on the whole range of record length, and for all benchmark values, estimation lies in the 90% profile likelihood confidence interval. The advantage of incorporating regional information within a Bayesian framework is certainly to define a "restricted space" to which distribution parameters belong. Thus, the impact of a very extreme event – or too many low-level events – should be regarded as an extreme event related to this "restricted space".

EFFECT OF HOMOGENEITY DEGREE ON QUANTILE ESTIMATION

We focus now on the impact of the level of homogeneity of the region. For this purpose, we consider four different regions – denoted He^+, He, Ho and Ho^+ – which correspond to increasingly homogeneous regions according to the test of Hosking & Wallis (1997). The Ho region corresponds to the region analysed in the previous section. All regions have 14 sites, except for the most homogeneous one Ho^+, which contains only eight stations. To evaluate the influence of homogeneity level of a region on quantile estimation, models are assessed using two performance criteria: the Normalized Bias (*NBIAS*) and the Normalized Root Mean Squared Error (*NRMSE*). These indices are defined as follows:

$$NBIAS = \frac{1}{k}\sum_{i=1}^{k}\frac{\hat{Q}_i - Q}{Q} \qquad NRMSE = \sqrt{\frac{1}{k}\sum_{i=1}^{k}\left(\frac{\hat{Q}_i - Q}{Q}\right)^2}$$

where k is the number of estimates of Q, and $\hat{Q}_i$ is the ith estimate of the benchmark value Q. To compute these two indices, we fit all models on all shortened periods of size m years $m \in \{5,10,15,20,25,30\}$. Moreover, the overall performance of each model is evaluated using a rank score $R_S = (pq - R_o)/(pq - q)$, where p is the number of models being considered, q the number of indices and $R_o \in \{1, \ldots, p\}$, 1 corresponding to the best model and p to the worst. A rank score close to 1 – resp. 0 – is associated to a model with a good – resp. poor – performance. Three quantiles are of particular interest: Q_5, Q_{10} and Q_{20}. *NRMSE*, *NBIAS* and the rank score for station U4635010 and a record length of five years are illustrated in Table 2.

From Table 2, it can be seen that the Bayesian model performs quite well independently of the region being considered. However, this model seems to perform even better when applied to a "homogeneous" or "probably heterogeneous" region according to Hosking & Wallis (1997) terminology. In contrast, the overall rank score of the REG model surprisingly decreases with the homogeneity degree of the region. These results may be related to inaccurate estimation of the Index Flood $C^{(j)}$ with only 5 years of recording. Moreover, the overall rank score for the REG model never exceeds the value of 0.6 – reached for the He^+ region. This value remains much lower than the best rank score for the BAY model – i.e. 0.88. These results corroborate the superiority of the Bayesian approach.

From Table 2, two conclusions can be established: on the one hand, for small samples, the Bayesian approach is the most competitive model; on the other, results seem to indicate that there is no need to keep increasing the homogeneity of the region as it increases the risk of being too confident in the "homogeneous region" without increasing significantly the efficiency of the model. These results are in line with similar results obtained for stations U4635010 and V3015010, except for the REG model. Indeed, for the other stations, the REG model score is larger but always lower than the BAY one.

Table 2 Estimation of *NRMSE* and *NBIAS* for station U4505010 with a record length of 5 years.

Model	*NRMSE*:			*NBIAS* :			
	Q_5	Q_{10}	Q_{20}	Q_5	Q_{10}	Q_{20}	Rank Score
MLE	0.35	0.45	0.56	–0.03	–0.10	–0.16	0.17
bHe^+	0.11	0.13	0.17	–0.01	–0.05	–0.09	0.65
rHe^+	0.21	0.20	0.19	0.06	0.03	–0.01	0.59
bHe	0.06	0.08	0.10	–0.03	–0.03	–0.05	0.78
rHe	0.28	0.29	0.29	0.17	0.18	0.19	0.33
bHo	0.06	0.07	0.09	0.02	0.03	0.03	0.88
rHo	0.31	0.33	0.35	0.21	0.24	0.26	0.21
bHo^+	0.10	0.05	0.04	–0.09	–0.04	0.01	0.81
rHo^+	0.34	0.40	0.47	0.24	0.31	0.39	0.07

MLE: maximum likelihood estimator model.
He^+, He, Ho and Ho^+ correspond to increasingly homogeneous regions according to the test of Hosking & Wallis (1997).
b: Bayesian approach.
r: Regional Index Flood.

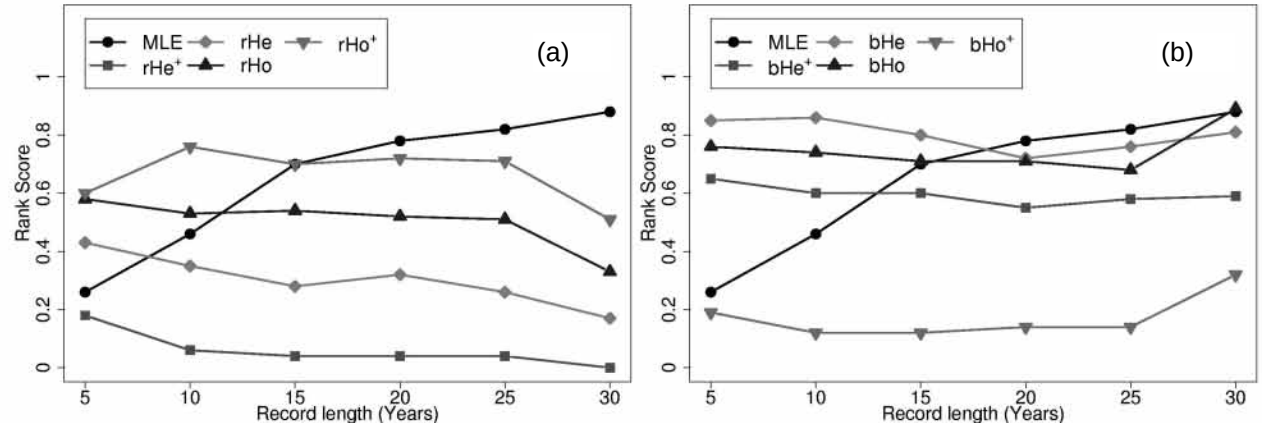


Fig. 2 Score evolution as a function of record length for Station V3015010: (a) REG scores, and (b) BAY scores.

In Fig. 2, the evolution of the overall rank score as a function of the record length is illustrated for station V3015010. The MLE score is also presented. Figure 2 indicates that the evolution of the overall rank score is more stable for regional models – that is REG and BAY models – than for the MLE. Furthermore, the benefit of increasing the homogeneity degree of the region is more relevant for the REG model than for the BAY model. Nevertheless, the worst BAY rank score is always quite close to the best REG rank score. This seems to indicate the superiority of the Bayesian approach. This last point is corroborated with the results corresponding to stations U4505010 and U4635010, except for the bHo^+ model for station U4635010 because of the inaccurate estimation of the scale factor $C^{(j)}$.

As the record length increases, the MLE model becomes more and more efficient. In particular, for record lengths greater than 15 years, it is more effective than rHe^+, rHe and rHo models. For record lengths smaller than 15 years, MLE is always less efficient than Bayesian approaches and even significantly for bHe, bHo and bHo^+ models. This is quite logical as Bayesian estimation can be looked at as a restrictive maximum likelihood estimator – restriction being defined by the prior distribution. So, under the hypothesis that the prior distribution is well defined, the "restrictive estimator" is unbiased and has a smaller variance. On the other hand, for record lengths greater than 15 years, MLE, bHe and bHo seems to be equivalent.

CONCLUSION

A framework to perform a regional Bayesian frequency analysis for partially gauged stations is presented. The proposed model has the advantage of being less restrictive than the most widely used regional model, that is the Index Flood. Several case studies from French sites were analysed to illustrate the superiority of the Bayesian approach in comparison to the traditional Index Flood and to local approaches. The influence of the homogeneity level of the pooling group on quantile estimates was also considered. Results demonstrate that working with quite large and homogeneous regions, rather than small and strongly homogeneous regions, is more efficient. Further work can focus on the regional estimation of other characteristics of the flood hydrograph.

REFERENCES

Dalrymple, T. (1960) Flood frequency analysis. *US Geol. Survey Water Supply Paper 1543A*.

Hosking, J. R. M. & Wallis, J. R. (1997) *Regional Frequency Analysis*. Cambridge University Press, Cambridge, UK.

Climate Variability and Change—Hydrological Impacts (Proceedings of the Fifth FRIEND World Conference held at Havana, Cuba, November 2006), IAHS Publ. 308, 2006.

Flash floods in mountain areas

MANFRED SPREAFICO
Federal Office for the Environment, CH-3003 Berne, Switzerland

Abstract The main causes of flash floods in mountain areas are cloud bursts or stationary rainfall, heavy rainfall and rapid snow melt in high mountain areas, glacial lake outbursts, failure of dams built up by landslides, rock falls or debris flows, and overspill following the failure of water power reservoir dams. The sudden rise and rapid fall of water levels, as well as the high flow velocities combined with large sediment transport, demand special procedures in flood risk management. Some approaches to flood risk management in Switzerland and guiding principles with regard to flash floods, are presented here.

Key words flash floods; extreme precipitation; debris flows; hazard maps; flood risk management; Switzerland

INTRODUCTION

Every year flash floods cause the loss of a great number of lives as well as tremendous damage. The main impact of flash floods is undercutting of check dams, the collapse of river banks, debris flows, debris deposits, river damming by debris, river-bank erosion, channel displacement, clogging of bridges, scour and inundations.

Most of the basins in Switzerland are prone to flash floods, landslides, and debris and mud flows. During the last few centuries, structural protection measures have substantially improved flood prevention and have helped the economic development of the country.

Experience with extreme floods during recent years has shown that structural measures alone cannot guarantee sufficient protection, however, and new approaches are needed. Major efforts in flood prevention are required in future for the following reasons:

– the damage potential has increased considerably in many areas owing to intense land use and increasing economic value in endangered zones;
– in channelized rivers runoff concentration time is affected, often resulting in higher flood peaks;
– a lack of space and retention areas to manage large-scale events;
– poor maintenance of structures and river beds;
– changes in runoff as a result of climate change and variations.

A new flood protection policy has therefore been developed which takes into account not only the safety aspects but also all other aspects of sustainable development. This policy is based on land-use planning, maintenance of the systems and structural measures. Environmental concerns and economic factors must be included in the planning process as early as possible. This comprehensive hazard assessment, with differentiated protection measures, adequate planning of measures and the limitation of the remaining risks are set out in the Federal Flood Control Act of 1993. The modern approach is based on proper risk analysis, risk assessment and risk management (Fig. 1).

ESTIMATING THE HYDROLOGICAL RISK DUE TO FLASH FLOODS

Comprehensive analysis includes the investigation of the hydrometeorological situation, hydraulic conditions, damage potential, the river bed and aquatic and terrestrial issues.

Estimating flood risk is a complex problem. Some selected procedures for obtaining meteorological and hydrological baseline information, as well as the advanced systems for estimating flash floods developed in Switzerland are presented here.

Extreme regional precipitation of varying duration and return period

Precipitation is a phenomenon defined by area and limited in extent and duration. The area covered by a precipitation event, its duration and its depth and spatial distribution are determined by the processes of precipitation generation in the atmosphere and their horizontal movement and evolution.

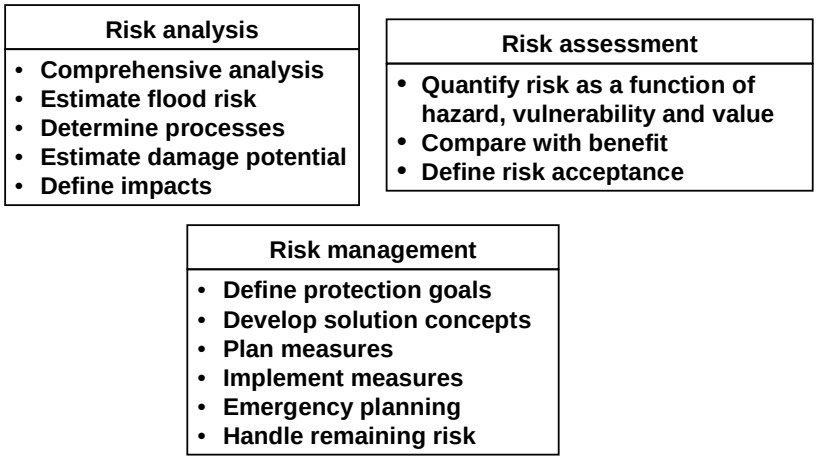


Fig. 1 The pillars of flash flood protection.

A knowledge of regional precipitation is essential for estimating floods. Absolute regional precipitation depths for durations of 3, 12, 24 and 48 hours have therefore been calculated for eight different zones in Switzerland. These precipitation depths have been plotted against the surface area (Fig. 2).

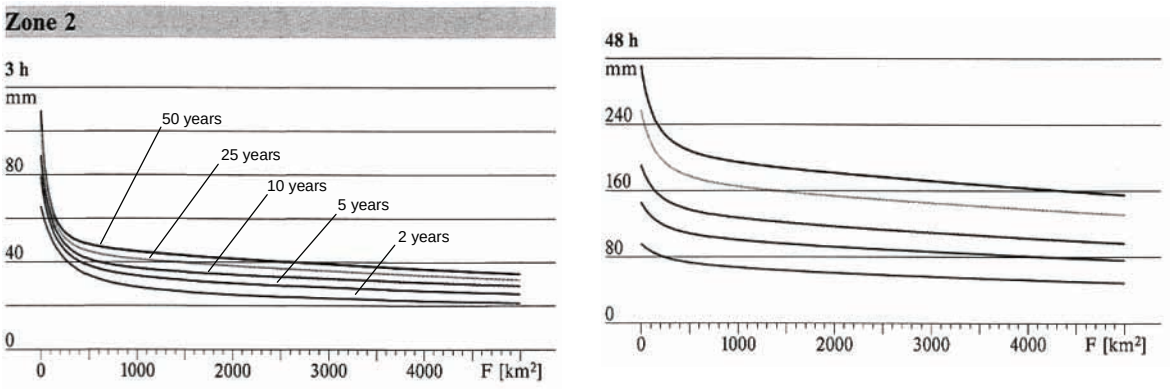


Fig. 2 Extreme regional precipitation of varying duration and return period (HADES, 2000).

Observation of discharge

It is very difficult to measure flood flows in mountain environments owing to high flow velocities and turbulence, floating debris and changes in the profile of the river bed. Floods in small catchments are of short duration, from a few minutes to some hours at the most. A water–solid mixture can be observed in very steep rivers; estimating the percentage of water discharge is fraught with uncertainties. For this reason it is often impractical to use conventional current meters. New technologies for measuring discharge have therefore been developed or implemented by the Swiss National Hydrological Survey (SNHS). Examples are measurement using a light-fibre fluorometer based on the principle of the dilution method or measurement of discharge using various types of acoustic Doppler current profilers.

Documentation and analysis of extreme flood events

Extreme floods during the last three decades have been analysed with regard to meteorological conditions, hydrology, flow generation processes, social, economic and environmental indicators, comparison with historical floods, frequency, etc. This information provides a useful input for drawing up hazard maps (EVED/EDI, 1991; BWG, 2000).

Information about historical floods can be helpful, but it is quite difficult to interpret floods that occurred in previous centuries owing to artificial changes in the water systems and incomplete descriptions of the events.

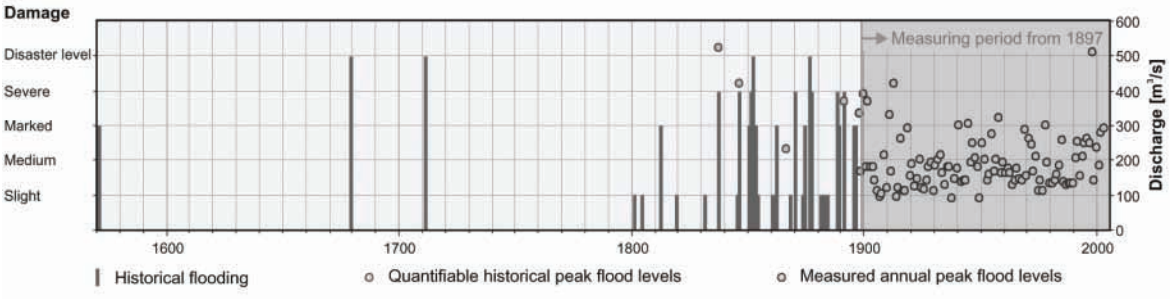


Fig. 3 Flooding of the River Emme: historical flooding with recorded extent of damage within the catchment or known peak discharge rate and peak annual flood maxima measured at the Emmenmatt station by Gees (BWG, 2005a).

Flood generation and concentration processes

To determine the hydrological risk, a knowledge of runoff generation and concentration is very important. Based on experiments involving artificial rainfall on test catchments, as well as geological and pedological maps, it is now possible to define areas in a catchment where the runoff formation process and water retention capacity vary.

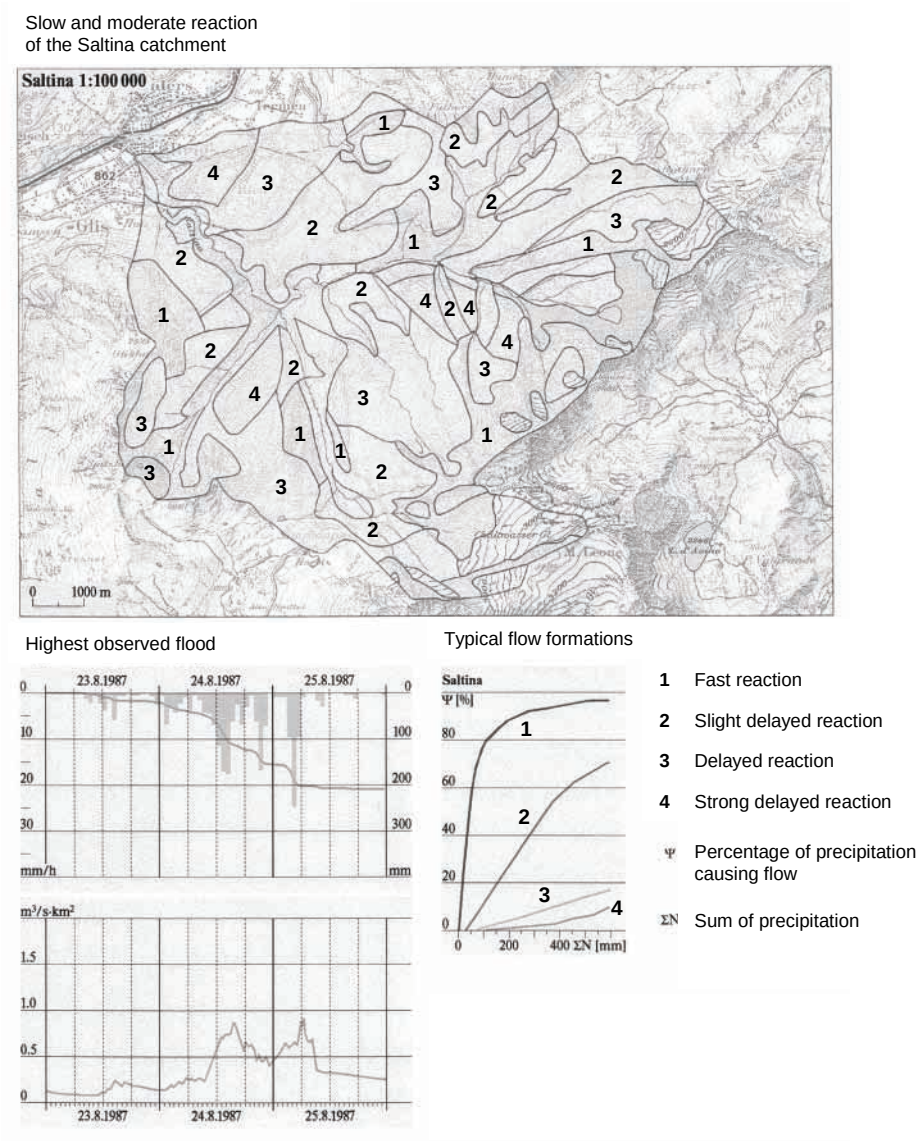


Fig. 4 Reaction of Saltina catchment to rainfall input (HADES, 2000).

Estimation of flood peak discharge in ungauged basins

Owing to the fact that discharge can only be monitored at selected sites, an advanced system for estimating discharge at ungauged sites has been developed in Switzerland. This practical guide is a powerful tool for developing hazard maps (BWG, 2003).

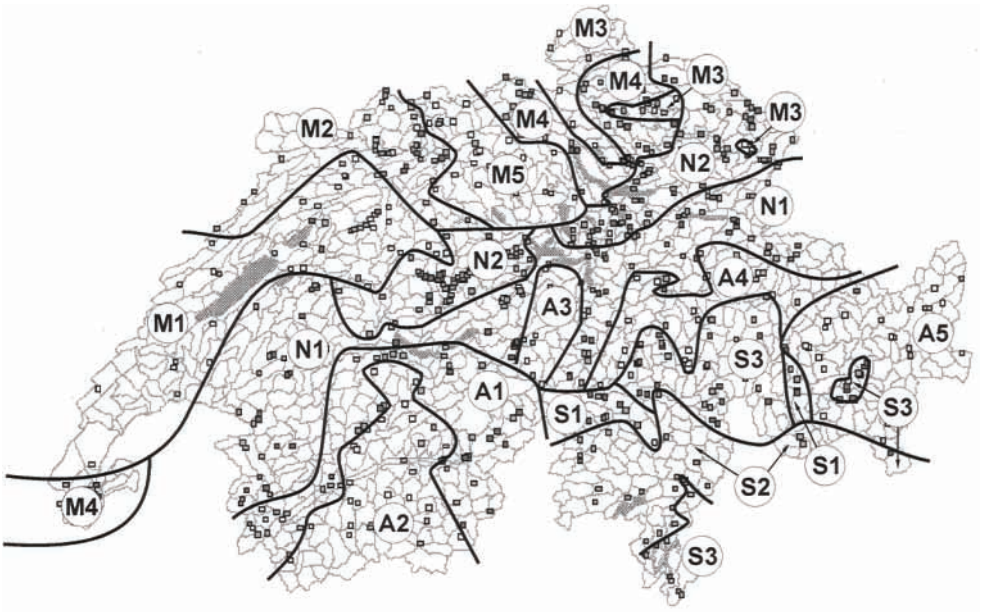


Fig. 5 Different flood flow regions in Switzerland after Kan (BWG, 2003).

Impact of climate change on runoff

This impact was investigated by using different individual climate change scenarios for several basins. Fig. 6 shows the increase of winter peak flows of the Thur catchment. The frequency and height of peak flow vary much less during the summer half year than the winter half year.

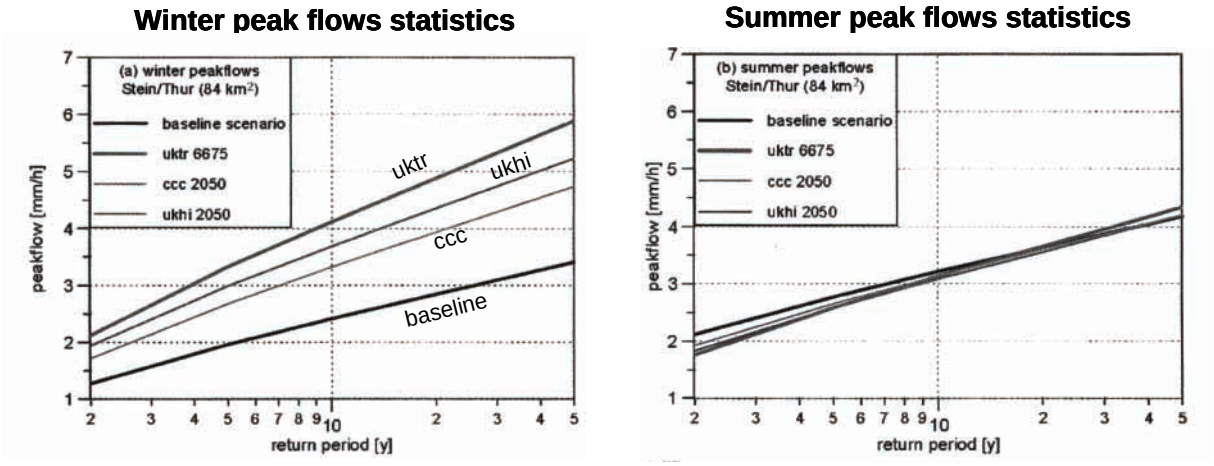


Fig. 6 Changes in winter and summer peak flows in the River Thur with respect to different climate change scenarios (CHR, 1997).

SEDIMENT TRANSPORT

Debris flows cause a huge amount of damage in Switzerland. To gain a better knowledge of the processes involved, research stations with hydrophones are used. The operation of a network of sediment retention basins provides estimates of sediment yield all over Switzerland (Fig. 5). The recommendations for the estimation of sediment potential and sediment transport in catchments are an important aid in drawing up hazard maps (GHO, 1999).

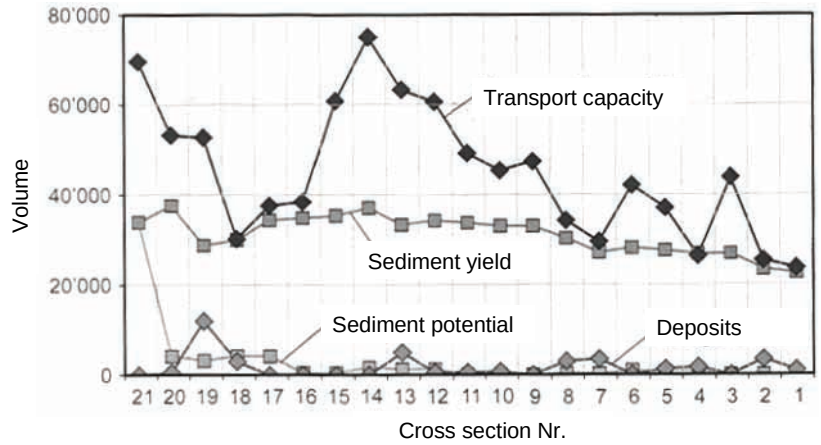


Fig. 7 Sediment transport in the Guppenruns (BWG, 2005b).

HAZARD MAPS

Risk cannot be properly managed without a sound knowledge of what that risk entails. Risk is dependent on the hazard and the potential damage. Since potential damage is a highly dynamic parameter, depending on constantly changing land-use, it was decided that hazard mapping was more important than risk mapping. The risk can be evaluated by each user if the hazard is known. Since different players need different information concerning the hazard, it was decided that hazard maps should be generalized, indicating the type and the degree of the hazard. The types of danger distinguished in the flood risks maps are: inundation (dynamic, static), bank erosion and debris flow (BWG, 2001).

DIFFERENTIATED SAFETY CONCEPT

Different protection levels are used, depending on the damage potential (BWG, 2001). Expensive infrastructure requires more advanced flood protection than cheap infrastructure. Based on this principle, agricultural land and isolated buildings need less protection than dense residential and industrial areas, but detailed investigations are still necessary for decision making.

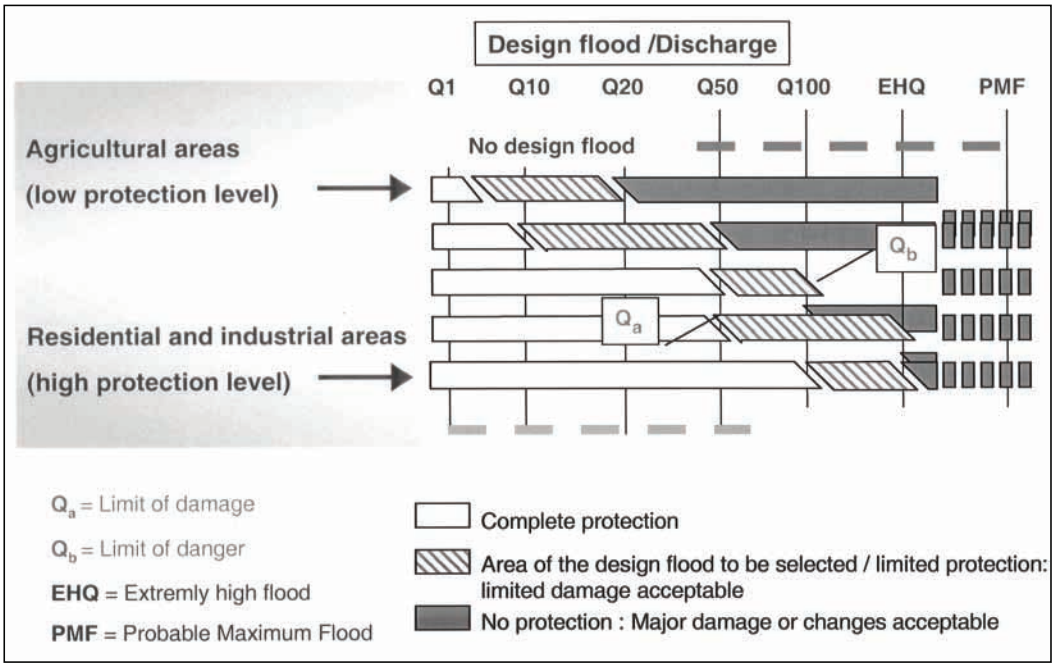


Fig. 8 Differentiated safety concept.

ALTERNATIVE FLOOD PROTECTION MEASURES

Maintenance of the water courses

Means:

– removal of vegetation in the river,
– excavation of sediment retention structures,
– repair of damage to protective structures,
– maintenance of river beds and banks.

A periodic check of the functioning and effectiveness of protective structures serves to identify weak points and to prevent total collapse during a flood event.

Land-use planning

Hazard maps have to be incorporated into regional and local development plans. Within a hazard zone an increase in vulnerability can be limited or even prevented if a few planning principles are respected:

– avoid hazard zones (construction ban),
– reinforce existing structures,
– establish appropriate building codes.

Structural protection measures

Structural protection measures include check dams, block ramps, dam construction, opening of river beds, spurs, debris flow breakers, etc. Structural measures should be kept as close to nature as possible and should avoid interfering with the landscape.

EMERGENCY PLANNING

Even if all measures have been properly carried out there is still a "residual risk". Emergency planning and its implementation therefore becomes an integral component of every flood policy. Flood forecasting, the operation of warning systems, the preparation of evacuation schemes as well as setting up and training rescue units are important parts of the emergency planning in Switzerland.

CONCLUSIONS

After centuries of "fighting floods" the new philosophy of flood risk management is based on "living with floods". The purely engineering approach has changed into a more integrated flood management one. This approach demands integrated problem analysis, sophisticated planning, assessment of measures and decision making and implementation on a river basin level. Hazard maps must be taken into account by development planning, warning and action planning as well as by creating awareness among the people affected.

It is possible that the magnitude and frequency of flash floods in mountain areas will increase in the future as a result of projected climate variability and change.

There is a need to improve our understanding of flash floods, their causes, development and impact.

There is also a great need for better forecasting and warning and communication systems for flash floods in mountain regions.

Dialogue between different sectors and different governance levels regarding management of flash floods and other disasters must be improved.

The general public's lack of awareness and knowledge of the nature of flash floods and the threat they pose to communities needs to be addressed.

The main guiding principles of flash flood management are:

– divert water and sediment to locations where it will cause least harm. Differentiated safety concept!
– distribute the water over larger areas to attenuate the high energy impact;

– maintain enough space on both sides of a torrent, because the destructive forces are too strong to be managed;
– construct houses with strong foundations and entrances sufficiently high above the ground;
– provide or design safe places to which the population can escape.

Preventive measures are a MUST!

REFERENCES

BWW (1995) Procedure for the planning of flood protection measures. Flyer, Bundesamt für Wasserwirtschaft. Biel, Switzerland.

BWG (2000) Hochwasser 1999, Analyse der Ereignisse. *Studienbericht nr. 10, Bundesamt für Wasser und Geologie*. Biel, Switzerland.

BWG (2001) Hochwasserschutz an Fliessgewässern. *Wegleitung des BWG, Bundesamt für Wasser und Geologie*. Biel, Switzerland.

BWG (2003) Hochwasserabschätzung in schweizerischen Einzugsgebieten, Praxishilfe. *Berichte des BWG, Serie Wasser, no. 4*. Bern, Switzerland.

BWG (2004) Sachseln: Drei Bäche neu gebettet. Flyer, Bundesamt für Wasser und Geologie. Biel, Switzerland.

BWG (2005a) The hydrology of Switzerland. *Berichte des BWG, Serie Wasser, no.7*. Bern, Switzerland.

BWG (2005b) Feststoffbeobachtung in der Schweiz. *Berichte des BWG, Serie Wasser, no 8*. Bern, Switzerland.

CHR (1997) Impact of climate change on hydrological regimes and water resources management in the Rhine basin. *CHR-Report no. 1-16*. Lelystad, The Netherlands.

GHO (1999) Recommandations concernant l'estimation de la charge sédimentaire dans les torrents. Groupe de travail pour l'hydrologie opérationnelle. *Communication nr. 4a, BWG*. Bern - Ittigen, Switzerland.

EVED/EDI (1991) Ursachenanalyse der Hochwasser 1987. *Ergebnisse der Untersuchungen, Mitteilung der Landeshydrologie und -geologie no. 14*. Bern – Ittigen, Switzerland.

HADES (2000) *Hydrologischer Atlas der Schweiz*. Karte, Bundesamt für Wasser und Geologie. Bern – Ittigen, Switzerland.

Climate Variability and Change—Hydrological Impacts (Proceedings of the Fifth FRIEND World Conference held at Havana, Cuba, November 2006), IAHS Publ. 308, 2006.

Rainfall–runoff modelling of Bua River basin, Malawi

S. H. MKHANDI[1] **& P. G. KUMAMBALA**[2]

1 *University of Dar es Salaam, PO Box 35131, Tanzania*
s_mkhandi@yahoo.com

2 *M & G Consulting Engineers, PO 219, Mzuzu, Malawi*

Abstract This paper investigates the applicability of three systems-types of models: a Simple Linear Model (SLM), a Seasonally Varying Runoff Coefficient Model (SVRC) and a Linear Perturbation Model (LPM), and two conceptual models: NAM and SMAR, in six sub-catchments of the Bua catchment located in the central region of Malawi. The results of the study indicate that the LPM performed better in simulating streamflow series in the study area than the other system-type models and the two conceptual models. Comparison of the performance of the two conceptual models indicated that the NAM model performed better than the SMAR model.

Key words Bua River; rainfall–runoff modelling; system type of model; lumped conceptual models

INTRODUCTION

Rainfall–runoff models can be classified into three categories depending on the degree of their physical abstraction from the real world system (Dawdy & O'Donnell, 1965; Clarke, 1994):

(a) Systems-based (black or grey box) models which make little or no attempt to simulate the individual constituent hydrological processes and which rely heavily on systems theory developed in other branches of engineering science.
(b) Distributed physically-based models which are based on the complex law of physics generally expressed as systems of nonlinear partial differential equations.
(c) Quasi-physical conceptual models which occupy an intermediate position between the other two types of models in terms of complexity, disaggregation and data requirements.

The physically-based distributed models are well suited to solving problems such as predicting the effects of land-use changes and studying the hazards of pollution (Beven, 1989, 1997; Beven *et al*., 1995). The other two more conventional types of model are often too primitive to present scientifically sound solutions to such problems. Nevertheless, these last two types of models have often proved to be effective in the solution of a wide spectrum of important hydrological problems, such as river flow forecasting and the extension of hydrological records.

In this study, a comparison was carried out to investigate the adequacy of the application of lumped systems and conceptual models in Bua River basin in Malawi.

CANDIDATE SYSTEM AND LUMPED CONCEPTUAL MODELS

Three systems-types of models: the Simple Linear Model (SLM), Seasonally Varying Runoff Coefficient Model (SVRC) and Linear Perturbation Model (LPM), and two conceptual models: NAM and SMAR, were used in the study. Brief descriptions of these models are given below.

Systems Models

Simple Linear Model (SLM) The SLM postulates a linear time invariant relationship between the rainfall x and the discharge y. In discrete form, embodying a model fit error term e_i, it may be expressed as (Kachroo & Liang, 1992):

$$y_i = \sum_{j=1}^{m} h_j x_{i-j+1} + e_i \quad (1)$$

where h_j are the ordinates of the pulse response, and m is the memory length. The pulse response ordinates can be estimated by Ordinary Least Squares in a parametric form, using the well known gamma function model which was introduced by Nash (1957) as a general equation for the instantaneous unit hydrograph. The impulse response of the gamma function model $h(t)$ is given by:

Copyright © 2006 IAHS Press

$$h(t) = \frac{1}{K\Gamma(n)} e^{-(t/k)} \left(t/K\right)^{n-1} \quad (2)$$

where $\Gamma(n)$ is the gamma function of n. K is a constant having the dimension of time, n is a "shape" parameter constant. Moreover in this model form, n and the lag product nk are usually considered as parameters of this model rather than n and k (Kachroo & Liang, 1992).

Seasonally Varying Runoff Coefficient (SVRC) Model This model is introduced in the context of long-term variance to show how much can be achieved by a simple empirical tool. The SVRC model is given by (Kachroo & Liang, 1992):

$$y_i = \mathrm{C_d} \sum_{j=1}^{m} h_j x_{i-j+1} + e_i \quad (3)$$

where C_d is a time-varying coefficient of runoff which is allowed to vary throughout the year in a periodic fashion.

The Linear Perturbation Model (LPM) The LPM was originally proposed by Nash & Barsi (1983). Perturbation models are used to account for the seasonality of the observed rainfall and the runoff. The model is based on the following assumptions:

(a) If, in a particular year, each input function, is equal, for each day of the year to its expected value for that date, then the output will also equal to its expectation for that date (Kachroo & Liang, 1992),
(b) Perturbations, or departures from the date of expected input values are linearly related to the corresponding perturbations or departures from the date of the expected output values.

The transformation is introduced in the observed data of rainfall x_i and the runoff y_i. The transformation has the form of;

$$Q'_i = y_i - y_s \quad \text{and} \quad R'_i = x_i - x_s \quad \text{for} \quad i = 1,2,3,.....,n \quad \text{and} \quad s = 1,2,3,.....,365 \quad (4)$$

where x_s and y_s are the seasonal mean rainfall and discharge respectively. The linear relationship between the perturbations of the discharge Q'_i and rainfall R'_i with a gain factor G is given by:

$$Q'_i = G \sum_{j=1}^{m} R'_j \, h_{i-j+1} + e_i \quad (5)$$

Conceptual Models

The Soil Moisture Accounting and Routing (SMAR) model SMAR is a conceptual type of model that assumes that the catchment is analogous to a vertical stack of horizontal soil layers, which can contain various amounts of water. Evaporation from the top layer occurs at the potential rate. Evaporation from the second layer occurs after exhaustion of the first layer at the potential rate multiplied by a factor C. Evaporation from the third layer occurs at the potential rate multiplied by C^2. Thus a constant evaporation applied to the basin reduces the soil moisture in a roughly exponential manner. The capacity of each layer is taken as 25 mm and the total storage Z (mm) is the parameter to be optimized.

The NAM model The NAM model (DHI, 2000) is a deterministic, lumped conceptual rainfall–runoff model, which represents various components of the rainfall–runoff process by continuously accounting for the water content in five different and mutually interrelated storages where by each storage represents different physical elements of the catchment (Madsen, 2000). These storages are: snow storage, surface storage, lower zone storage, upper groundwater storage and lower groundwater storage.

DATA AVAILABLE

Data used in the study was from gauging stations located in six sub-catchments of Bua River basin. The details of the stations used in the study are presented in Table 1. Rainfall and

Table 1 Discharge data used in the study.

No.	Station code	Data length	Area (km^2)	Missing (%)	Mean daily flow ($m^3 s^{-1}$)	Mean annual flow (mm)	Mean areal rainfall (mm)	Runoff coefficient
1	5C1	11	10654	12.39	44.577	137.24	901	0.147
2	5D2	9	6790	1.98	25.550	120.82	917	0.132
3	5D3	10	233	1.45	1.290	172.64	874	0.200
4	5D4	11	1394	5.95	6.731	152.21	879	0.173
5	5F1	11	2580	7.42	10.116	105.85	879	0.140
6	5E6	8	126	2.02	0.605	151.47	1090	0.138

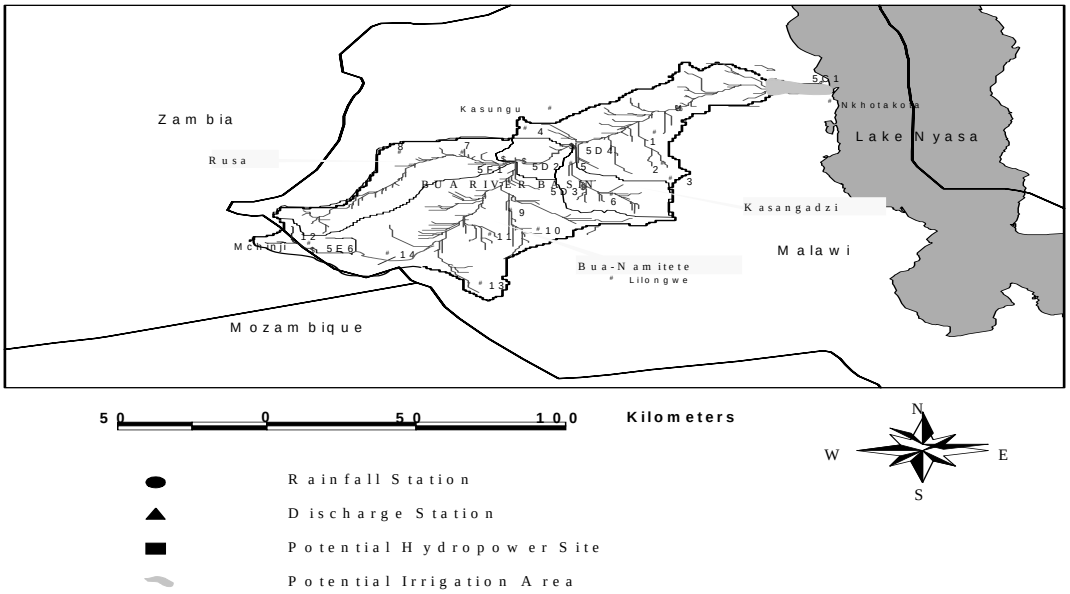


Fig. 1 Map of the Bua River showing the location of rainfall and river gauging stations.

temperature data used in the study were from 14 and 4 stations respectively. Rainfall and temperature data were collected from the Malawi Meteorological Department at Chileka Airport in Blantyre. Temperature data was used to estimate daily potential evaporation since daily climate data for the catchment was not available. Discharge data were obtained from the Ministry of Water (Malawi), Department of Hydrology in Lilongwe. Figure 1 shows the location of river gauging and rainfall stations.

MODEL APPLICATION

Each of the five models used in the study was applied to each of the six sub-catchments of the Bua River basin. The model application involved calibration and verification of the models whereby approximately four-fifths of the available data was used for calibration and one-fifth for verification. In the calibration process, the first portion of the data was used to compute the model parameters for each sub-catchment. During verification, the estimated discharge, sometimes referred to as discharge forecasts, were obtained by using rainfall in the second period as input to the model, which was already calibrated. The model efficiency in the verification period was the measure of the accuracy at which the model can make forecasts in the period different from that on which it was calibrated.

RESULTS AND DISCUSSION

The results of performances of the models used in the study are presented in Table 2 both for the calibration and verification periods. From the results presented, it is observed that the LPM model with its inherent component of seasonal variation performed consistently well in calibration mode

Table 2 Comparison of the results of the five models.

Catchment Area (km^2)	Bua-5C1 10654	Bua-5D2 6970	Bua-5F1 2580	Kasa-5D4 1394	Mtiti-5D3 233	Bua-5E6 126
Calibration efficiency (R^2)						
SLM	38.6	46.74	29.16	46.47	36.61	23.82
SVRC	56.56	67.74	56.78	42.36	42.18	26.19
LPM	65.12	78.93	74.05	38.85	63.84	36.86
SMAR	75.77	69.13	38.02	58.29	33.04	23.44
NAM	71.89	80.95	47.68	65.48	42.00	25.37
Verification efficiency (R^2)						
SLM	63.05	69.20	39.07	33.97	1.90	46.88
SVRC	45.26	53.73	56.37	12.19	–3.76	53.29
LPM	72.15	66.61	77.44	38.84	59.20	38.38
SMAR	56.89	67.45	48.02	58.58	11.05	49.59
NAM	62.14	87.02	57.69	8.41	18.02	50.40

in all cases applied, except for station 5D4, this model out performed all the other models at four (5F1, 5D3, 5E6 and 5D2) out of the six stations with the exception of one station (5D2) where the NAM model performed better. In two stations (5C1 and 5D4) out of six stations, both NAM and SMAR out performed the LPM. On the other hand, the NAM model also performed consistently well, second to the LPM model. Table 2 also shows the performance results of the models in calibration mode. It can be seen from Table 2 that the LPM consistently performed better than all the other models. The NAM and then the SMAR models followed the LPM model in better performance.

Figure 2 shows the observed hydrograph and the hydrograph simulated using the LPM model for one river gauging station (5D2) used in the study for the period 1981–1988. Figure 2 shows that the LPM model has managed to simulate the low flows adequately well. The model has also managed to simulate peak flows fairly well for most of the years. Failure to simulate peak flows is noted for the year 1981. The reason may be due to poor quality of the climatic data. The objective

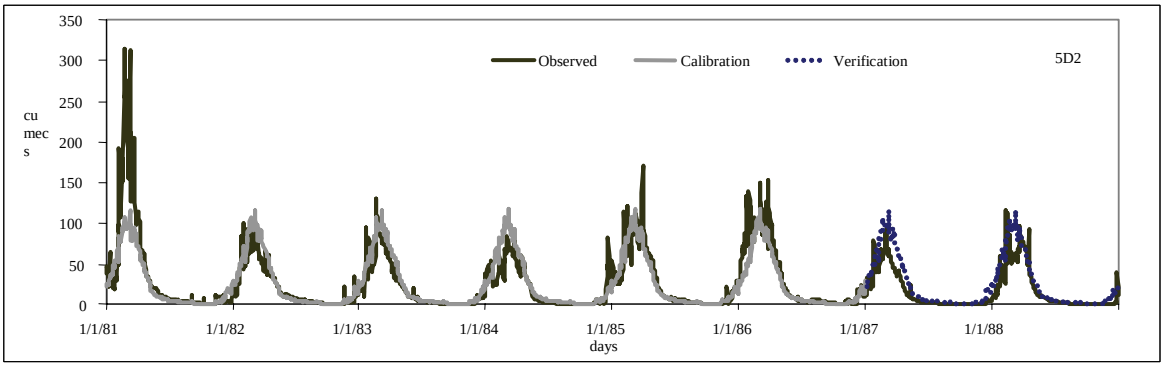


Fig. 2 Hydrographs of observed and estimated discharges by LPM (Station 5D2).

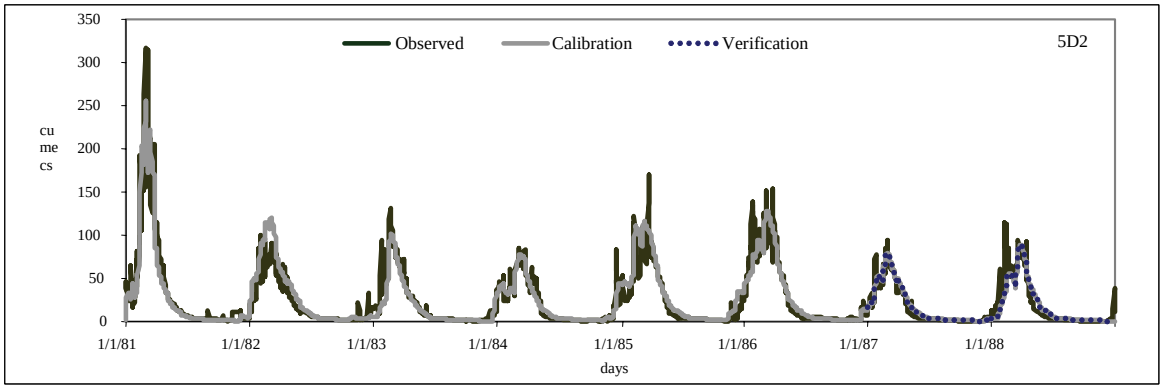


Fig. 3 Hydrographs of observed and estimated discharges by NAM Model (Station 5D2).

criterion of the explained variance gave a value of R^2 = 79% (Table 2). Figure 3 shows the observed hydrograph and the hydrograph simulated using the NAM model for one river gauging station (station 5D2). In Fig. 3, the NAM model has fitted the observed data very well. The model has managed to simulate the low flows adequately well as well as the peak flows. The objective criterion of explained variance gave a value of R^2 = 81% (Table 2).

CONCLUSION AND RECOMMENDATIONS

Conclusion

The results of the performance of the models used in the study indicate that the LPM model is a better model for application to simulate streamflow in the Bua River catchment. The second preferred model is the NAM model.

Recommendations

Based on the analysis of the results from the application of system and lumped conceptual models, further studies on rainfall runoff–runoff modelling in the study area should concentrate on other conceptual models, semi-distributed, and distributed models.

REFERENCES

Beven, K. (1989) Changing ideas in hydrology – the case of physically- based models. *J. Hydrol.* **105**, 157–172.

Beven, K. J., Lamb, R., Quinn, P. F., Romanowicz, R. & Freer, J. (1995) TOPMODEL. In: *Computer Models of Watershed Hydrology* (ed. by V. P. Singh), 627–668. Water Resources Publications, USA.

Beven, K. J. (ed.) 1997. *Distributed Modelling in Hydrology: Applications of TOPMODEL*. Wiley, Chichester, UK.

Clarke, R.T. (1994) *Statistical Modelling in Hydrology.* Wiley, Chichester, UK.

Dawdy, D.R. & O'Donnell, T. (1965) Mathematical models of catchment behavior. *J. Hydraulics Div., ASCE* **91**, 123–137.

DHI (2000) NAM technical reference and model documentation. DHI Water and Environment, Horsholm, Denmark.

Kachroo, R. K. (1992) River flow forecasting. Part 5. Applications of a conceptual model. *J. Hydrol.* **133**, 141–178.

Kachroo, R. K. & Liang, G. C. (1992) River flow forecasting. Part 2. Algebraic development of linear modelling techniques. *J. Hydrol*. **133**, 17–40.

Madsen, H. (2000) Automatic calibration and uncertainty assessment in rainfall–runoff modeling. Paper presented at 2000 Joint conference on Water Resources Engineering and Water Resources Planning and Management, Hyatt Regency Minneapolis, USA.

Nash, J. E. (1958) The form of the instantaneous unit hydrograph. In: *Surface Water, Prevision, Evaporation* Proc. International Association of Scientific Hydrology, Toronto General Assembly), vol. 3. IAHS Publ. 45. http//:www.iahs.info.

Nash, J. E. & Sutcliffe, J. V. (1970) River flow forecasting through conceptual models. Part 1. A discussion of principles. *J. Hydrol.* **10**, 282–290.

Nash, J. E. & Barsi, B. I. (1983) A hybrid model for flow forecasting on large catchments. *J. Hydrol.* **65**, 125–137.

Climate Variability and Change—Hydrological Impacts (Proceedings of the Fifth FRIEND World Conference held at Havana, Cuba, November 2006), IAHS Publ. 308, 2006.

Modelación distribuida de la cobertura nival para el pronóstico de volúmenes de deshielo

PATRICIO VALCK C., XIMENA VARGAS M. & MAURICIO CARTES
Departamento de Ingeniería Civil, Universidad de Chile, Casilla 228/3, Santiago, Chile
pvalck@ing.uchile.cl

Resumen Para la modelación de la cobertura del manto nival y su evolución temporal en el período de acumulación, se plantea un modelo que discretiza la zona en estudio en una grilla regular de 200 m, para resolver en cada elemento las ecuaciones de balance de energía y masa. Las variables meteorológicas de entrada al modelo, son obtenidas de los pronósticos a 24 horas de un modelo meteorológico de meso escala a las que, artificialmente, se aumenta su resolución espacial. La aplicación del modelo a la cuenca alta del río Maipo, Chile, permite validar el procedimiento a través de imágenes satelitales y caudales de deshielo medidos en distintos puntos de control dentro de la cuenca, observándose en promedio errores de estimación del orden del 24% en la cobertura nival y volumen acumulado al final de la temporada de acumulación inferior en 11% con respecto al volumen registrado en el período de deshielo en las subcuencas evaluadas, lo que muestra la potencialidad del modelo de simulación para fines de pronóstico en cuencas pequeñas sin control fluviométrico.

Palabras clave modelación distribuida; nieve; imágenes satelitales; balance de energía; pronóstico meteorológico

Estimating snowmelt volume using snow cover distribution modelling

Abstract The snow cover and its temporal evolution in a region are simulated by solving the energy and mass balance equations on each element of a regular grid of 200 m. The meteorological variables required as inputs for the simulation model are obtained from the 24-hour lead time forecasts of a mesoscale meteorological model, known as MM5/DGF, and artificially increasing its spatial resolution. The procedure is validated for the mountainous Maipo River watershed, Chile. The results obtained are compared with satellite images and snowmelt volumes observed at some gauges in the region. A standard error of 24% is obtained for the snow cover and an error of only 11% is obtained for the total period snowmelt volume, which indicates the potential use of the model for forecasting this variable in ungauged basins.

Key words distributed modelling; snow; satellite images; energy balance; meteorological forecasts

INTRODUCCIÓN

Conocer la cobertura, espesor y calidad del manto nival es de suma importancia para la determinación de la disponibilidad de agua superficial en la temporada de deshielo para riego, hidroelectricidad y otras actividades productivas, especialmente en zonas en que ésta es su principal fuente en los períodos secos.

Los modelos utilizados en la actualidad en Chile para efectuar estos pronósticos son, en general, modelos estadísticos que utilizan como variable registros fluviométricos, precipitación invernal medida en una o más estaciones y/o equivalentes en agua registrados en las escasas rutas de nieve disponibles en el país. Estos modelos, extrapolan una situación puntual hacia todo el manto de nieve estudiado, lo que imposibilita la simulación de subcuencas, y son incapaces de realizar una simulación continua del comportamiento del manto nival siendo válidos sólo en grandes cuencas.

Conocer la evolución del manto de nieve con mayor detalle posibilita hacer pronósticos más acertados de la disponibilidad de agua para temporadas secas. Además, si se obtiene una representación espacial, se pueden implementar políticas de gestión del agua que mejoren el uso de ésta.

En este trabajo, se muestra un modelo espacialmente distribuido para la simulación continua de la evolución del manto de nieve, el que simula el estado del manto aplicando ecuaciones de balance de energía y masa a una representación en grilla regular de la zona de modelación. El modelo utiliza como datos de entrada pronósticos meteorológicos (precipitación, viento, etc.) distribuidos espacialmente que provienen de un modelo meteorológico de meso escala.

En esta oportunidad se expondrán resultados obtenidos en la cuenca alta del río Maipo, Chile, y en dos de sus subcuencas para el período de acumulación del año 2002, los cuales se validan mediante imágenes satelitales y mediciones en terreno.

Copyright © 2006 IAHS Press

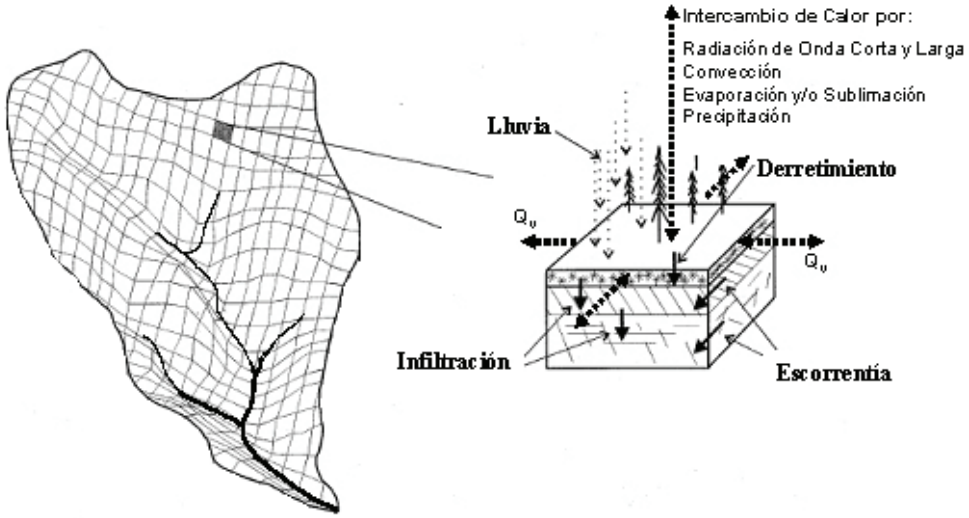


Fig. 1 Esquema de modelación nival general en grilla regular.

DESCRIPCIÓN DEL MODELO

El modelo desarrollado simula el estado del manto discretizando la zona a simular en una grilla regular, tal como se muestra en la Fig. 1, aplicando a cada elemento ecuaciones de balance de energía y masa. La información meteorológica utilizada es la generada por el modelo de pronóstico de meso escala MM5/DGF, operado por el Departamento de Geofísica (DGF) de la Universidad de Chile a una resolución espacial de 15 km y temporal de una hora.

La existencia o no de precipitación sólida distingue el comportamiento del manto. Cuando la nieve no recibe precipitación sólida está expuesto a las acciones del medio caracterizado por precipitación líquida o ausencia de ésta. Producto de esto se produce derretimiento, percolación, evaporación, ablación y densificación que pueden ser cuantificados mediante un balance de energía entre el manto y el medio que lo rodea, y en menor medida un balance de masa. Es así como el US Army Corps of Engineers (1998) y otros autores proponen evaluar el efecto de transferencia de calor en la parte más superficial del manto, la que se designa capa activa (CA), a través de una ecuación de balance de energía.

En cambio, cuando el manto es sometido a precipitación sólida, el efecto de transferencia de calor es mucho menor, predominando el balance de masa sobre el energético. Los efectos de una nevada se resumen en un aumento del contenido de frío, profundidad, equivalente en agua y un cambio en la densidad.

La principal fuente de calor o energía (Q) es el Sol, evaluado por la radiación de onda corta (*roc*) y en una porción menor por la radiación atmosférica o radiación de onda larga (*rol*). Además, se consideran las transferencias de calor por convección (*ss*), por condensación (*lat*), el calor cedido por la lluvia (Q_{pp}), la transferencia de calor entre elementos circundantes (Q_v) y el calor intercambiado con la superficie terrestre (Q_s). En general estas dos últimas componentes son muy poco relevantes en el balance energético, por lo que no afectan mayormente a la metamorfosis del manto. Todas las componentes del balance energético pueden calcularse mediante relaciones termodinámicas que se han descrito en profundidad en la literatura (US Army Corps of Engineers, 1998) y no se detallarán en este trabajo. En síntesis, el balance se expresa como:

$$Q_t = Q_{roc}(1 - Albedo) + Q_{rol} + Q_{ss} + Q_{lat} + Q_s + Q_{pp} + Q_v \quad (1)$$

El modelo MM5/DGF simula la circulación atmosférica a escala regional, mediante leyes no hidrostáticas y ecuaciones de circulación de advección difusión, en un volumen de control de apertura horizontal regular (15 km) y vertical variable. Los resultados de este modelo, son pronósticos meteorológicos a un horizonte máximo de 72 horas (año 2002) y cubren gran parte del territorio Chileno. Se inicializa diariamente a las 0 horas UTC, y genera, cada día, una serie de 72 horas de pronósticos del estado atmosférico para todo su dominio. Utilizando las primeras 24 horas de este pronóstico se puede construir una serie continua de pronósticos meteorológicos de un año,

la que se puede suponer como la secuencia real de variables observadas, las que se utilizan como entrada al modelo de simulación de la cobertura nival planteado. (Otondo *et al.*, 2004). Las variables atmosféricas extraídas del MM5/DGF son: temperatura a 0 y 2 metros sobre la superficie, radiación de onda corta y atmosférica incidente sobre el plano, intercambio de calor sensible y latente con la superficie, precipitación (convectiva y no convectiva) y velocidad del viento.

Lamentablemente, los pronósticos entregados por el modelo meteorológico están a una escala espacial menor a la cuál se requiere hacer la simulación del manto nival, por lo que es necesario aumentar artificialmente la resolución espacial. Para ello se opta por interpolar linealmente en el espacio todas las variables antes citadas.

Para obtener las variables del modelo MM5/DGF representativas de los elementos simulados, se utilizan correcciones de gradientes térmicos típicos de aire seco y húmedo, orientación de los elementos simulados y dirección y magnitud del viento.

ZONA DE APLICACIÓN

La cuenca simulada en este estudio corresponde a la cuenca del río Maipo en El Manzano, cercana a la ciudad de Santiago, capital de Chile (Fig. 2). Las características de la zona de aplicación fueron obtenidas de diversas fuentes, en particular la topografía se obtuvo del programa “Shuttle Radar Topography Mission” a una resolución de 90 m, la que fue suavizada para eliminar anomalías puntuales de la radio – medición topográfica, obteniendo finalmente una grilla de simulación de resolución 200 m, valor adecuado para describir los procesos físicos involucrados (Wigmosta *et al*., 1994). La región simulada, se traduce en una grilla 720 × 360 elementos.

La cuenca del río Maipo en El Manzano, es una cuenca marcadamente nival. Su período de acumulación comprende desde mediados de abril, hasta mediados de septiembre. La cuenca nace de las altas cumbres de la Cordillera del Los Andes, del volcán Maipo, y presenta múltiples glaciares entre los que se puede mencionar el Marmolejo, y Olivares. Sus principales ríos son el río Volcán, El Yeso, Colorado y Olivares. En este trabajo se muestran los resultados obtenidos para las subcuencas de las estaciones pluviométricas Maipo en San Alfonso (1), Colorado antes de Junta con Olivares (2) y Maipo en El Manzano (3) (ver Fig. 2).

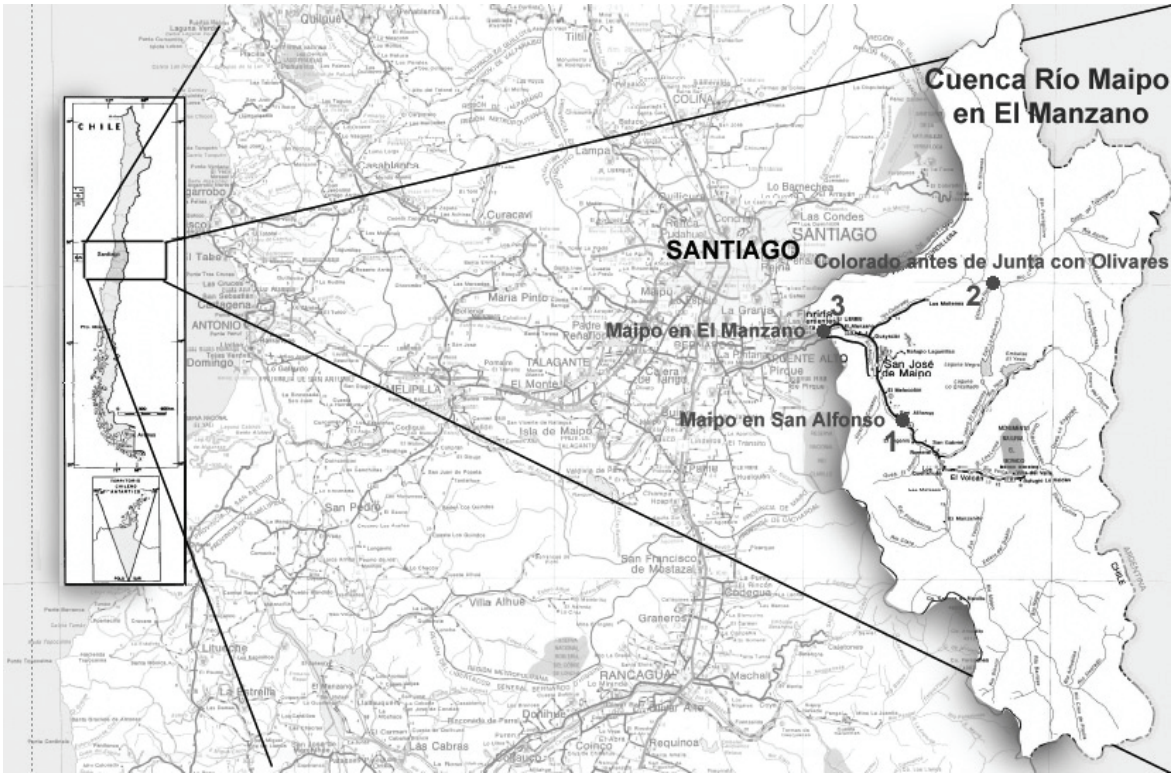


Fig. 2 Ubicación cuenca Maipo en El Manzano.

RESULTADOS

Con los pronósticos realizados por el modelo MM5/DGF para el período abril–septiembre 2002, se simula todo el período de acumulación, desafortunadamente al no contar con pronósticos meteorológicos en el período septiembre – abril no se puede simular el período de derretimiento.

Para analizar los resultados de cobertura se procede a comparar las imágenes de cobertura obtenidas del modelo con imágenes satelitales (NASA/GSFC). Se pueden realizar dos tipos de análisis, comparando el porcentaje de área cubierta por nieve y el acierto o falla del modelo en pronosticar nieve.

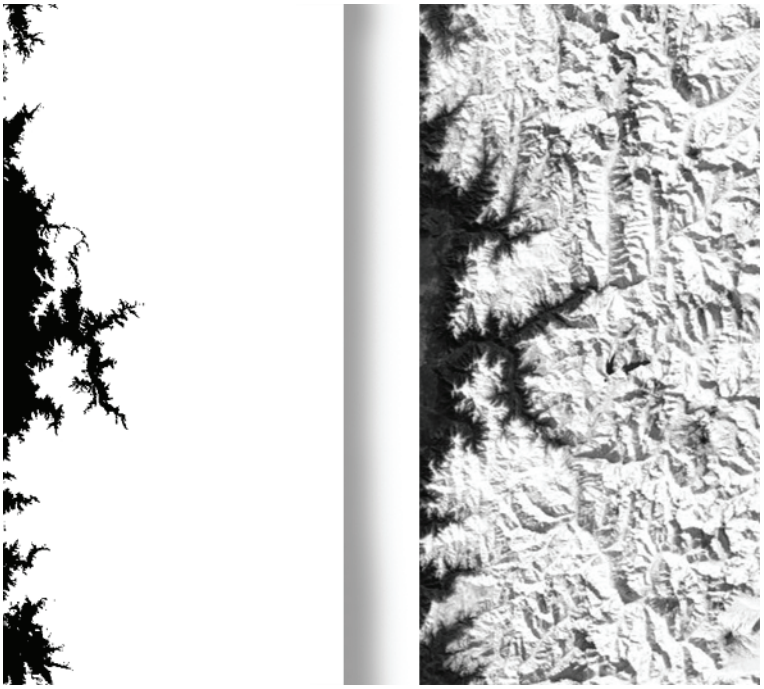


Fig. 3 Cobertura simulada y observada, 18 mayo 2002.

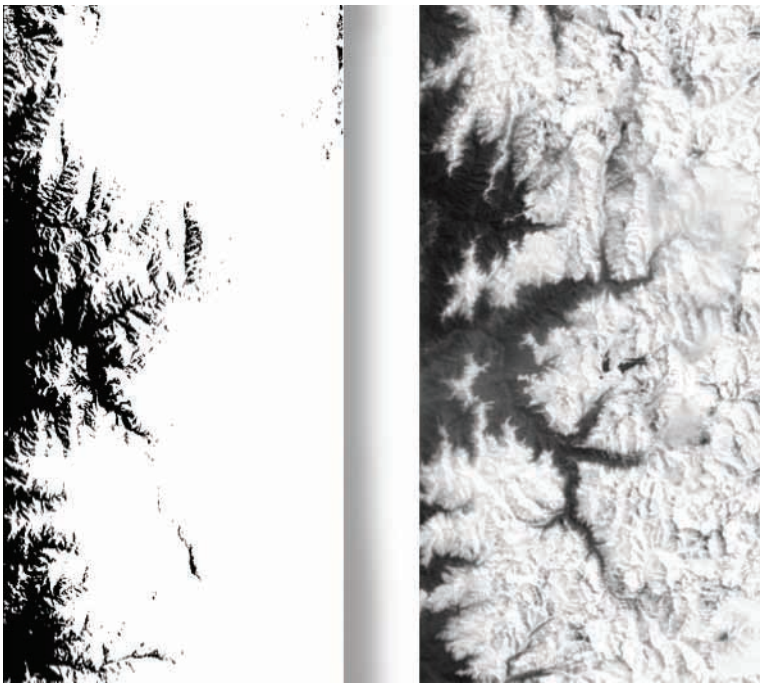


Fig. 4 Cobertura simulada y observada, 20 septiembre 2002.

Tabla 1 Resultados análisis espacial detallado.

Fecha	Subestima	Sobrestima	Porcentaje Área Nevada Simulada	Porcentaje Área Nevada Observada	Diferencia Porcentaje Área Simulada Observada
18-06-2002	20.4%	1.8%	68.1%	86.7%	18.6%
13-07-2002	38.0%	2.2%	43.3%	79.0%	35.7%
08-08-2002	27.1%	2.0%	53.4%	78.5%	25.2%
20-09-2002	12.1%	5.4%	68.6%	75.3%	6.7%
Promedio	23.6%	2.9%	59.1%	79.9%	20.8%

Tabla 2 Volúmenes de deshielo controlados y pronosticados al término del período de acumulación. Subcuencas analizadas.

Nombre Estación	Área (km^2)	Volumen de Deshielo (10^6 m^3)		Error porcentual
		Observado	Pronosticado	
Maipo en San Alfonso	2850	3505	3735	6.6%
Colorado antes de Olivares	834	764	848	11.0%
Maipo en El Manzano	4769	4301	6370	48.1%

En las Figs 3 y 4 se puede apreciar la cobertura observada (satélite), y la simulada. Al comparar píxel a píxel las coberturas observadas y simuladas, se puede contabilizar los elementos sobrestimados y subestimados, el análisis realizado con cuatro imágenes satelitales de resolución equivalente a la de simulación (Tabla 1).

Para la cuenca de Maipo en San Alfonso, que controla un área de 2850 km^2, se tiene que el volumen controlado en el período de deshielo 2002/03 alcanza los 3500 mill m3. En la Fig. 5 se muestra la evolución del volumen almacenado en forma de nieve en dicha subcuenca, llegando a fines de septiembre a valores 3700×10^6 m^3, bastante cercano al valor total de deshielo controlado en dicha cuenca. De igual forma se tiene que la para la subcuenca de Colorado antes de Junta con Olivares (834 km^2) se simula un volumen al final del período de acumulación de 847×10^6 m^3, contra los 760×10^6 m^3 de deshielo controlados en dicha estación. Para Maipo en El Manzano (4769 km^2), se simula un volumen al fin de la temporada de acumulación de 6370×10^6 m^3, en contraposición con los 4300×10^6 m^3 registrados por la estación ahí presente, la que está fuertemente influenciada por los usos del agua que se realizan aguas arriba de ésta. Los resultados de este análisis se muestran en la Tabla 2.

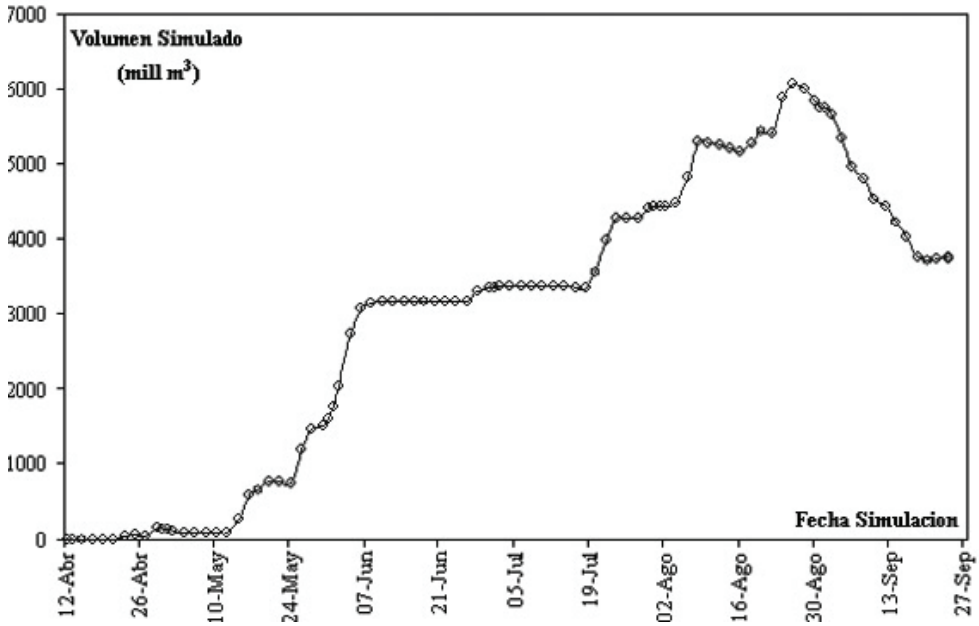


Fig. 5 Evolución del volumen nival simulado, sub-cuenca Maipo en San Alfonso.

CONCLUSIONES

Se tiene que el modelo en general el subestima la espacialidad del manto en un 23%, a diferencia de resultados obtenidos para la cordillera del Maule, Chile, donde se tiene que sobrestima del orden del 17% (Valck *et al.*, 2004).

En términos de volumen, se considera que el modelo mejora su comportamiento con respecto a aplicaciones anteriores, obteniéndose una sobrestimación del orden del 7%.

Al modelar el manto en forma distribuida, se posibilita obtener resultados a cualquier escala requerida, y en particular en subcuencas no controladas. En este trabajo se validó los resultados obtenidos para dos subcuencas de la región simulada contrastando los valores pronosticados con los realmente controlados por las estaciones pluviométricas presentes observándose una sobrestimación leve del volumen total de deshielo. Este análisis a nivel de subcuencas de la región en estudio superan las expectativas, confirmando la gran flexibilidad de simulación del modelo desarrollado.

Si bien, no se cuenta con datos para validar con mayor exactitud el comportamiento del derretimiento del manto en el período de deshielo, se tiene que en forma global se puede pronosticar con un alto grado de confianza el volumen total a escurrir en la temporada de deshielo con 6 meses de antelación.

REFERENCIAS

National Aeronautics and Space Administration (NASA), National Imagery and Mapping Agency (NIMA), German Aerospace Center (DLR), Italian Space Agency (ASI) (2002) *Shuttle Radar Topography Mission* (SRTM) Elevation Dataset. US Geological Survey, Sioux Falls, South Dakota, USA.

NASA/GSFC MODIS Rapid Response Project http://rapidfire.sci.gsfc.nasa.gov.

Orondo, I, Vargas, X. & Garreaud, R. (2004) Validación de campos de precipitación en Chile Central. In: *XXI Congreso Latinoamericano de Hidráulica*. Sao Pedro, Brasil.

US Army Corps of Engineers (1998) *Engineering and Design, Runoff from Snowmelt.* US Army Corps of Engineers, Washington, DC, USA.

Valck, P. & Vargas, M. (2004) Modelo de simulación de la cobertura del manto nival usando pronósticos meteorológicos de meso escala. Aplicación en la cordillera del Maule, Chile. In: *XXI Congreso Latinoamericano de Hidráulica*. Sao Pedro, Brasil, 2004

Wigmosta, M., Vail, L. & Lettenmaier, D. (1994) A distributed hydrology–vegetation model for complex terrain. *Water Res.* **30**(5), 1665–1679.

Climate Variability and Change—Hydrological Impacts (Proceedings of the Fifth FRIEND World Conference held at Havana, Cuba, November 2006), IAHS Publ. 308, 2006.

Essais de modélisation avec peu de données en Afrique de l'Ouest

JEAN EMMANUEL PATUREL[1], CHRISTOPHE LAROCHE[2], LAWANI MOUNIROU[2], LAMINE MAR[2], SANDRA ARDOIN-BARDIN[1], ALAIN DEZETTER[1], GIL MAHE[1] & ERIC SERVAT[1]

1 *UMII, Hydosciences Montpellier, case MSE, Place E. Bataillon, F-34095 Montpellier cedex 5, France*
jean-emmanuel.paturel@msem.univ-montp2.fr

2 *Groupe EIER-ETSHER, 01 BP 594, Ouagadougou 01, Burkina Faso*

Résumé L'idée de trouver une estimation satisfaisante des paramètres d'un modèle sans aucune estimation de débit n'a pour le moment pas abouti. Nous avons exploré une voie différente où l'on exploite à la fois une information régionale qualitative et une information partielle ponctuelle quantitative sur les débits. Les résultats montrent qu'en Afrique de l'Ouest il est possible d'obtenir une estimation fiable des paramètres à partir d'un faible niveau d'information hydrologique.

Mots clefs Afrique de l'Ouest; estimation de paramètres; modèle hydrologique; PUB

Trying to model with little data in West Africa

Abstract It was decided to give up the idea that good estimation of hydrological model parameters can be achieved without runoff data. Another approach has been investigated in which regional information is mixed with local and incomplete runoff information. In western Africa, the results show that using this combination can lead to good parameter estimation even with very little information.

Key words hydrological modelling; parameter estimation; PUB; West Africa

INTRODUCTION

Dans les pays en développement qui sont largement tributaires des ressources en eau, un modèle pluie-débit est particulièrement intéressant puisqu'il peut permettre d'estimer la ressource disponible en vue d'un aménagement mais aussi prévoir l'évolution de cette ressource dans les années ou décennies à venir en le combinant avec des scénarii climatiques.

Cependant, le calage d'un modèle requiert l'existence de séries de débits observés auxquelles on compare les simulations des modèles pour ajuster les valeurs des paramètres et obtenir la meilleure restitution possible du comportement hydrologique du bassin. Il existe cependant de nombreux cas où les données nécessaires pour le calage des modèles peuvent être inexistantes. L'opération devient alors problématique et des méthodes alternatives d'estimation des paramètres ont été recherchées. Cependant, les degrés de succès obtenus dans ces divers travaux ont été souvent trop peu satisfaisants pour pouvoir envisager une application fiable des modèles sur des bassins non jaugés.

RÉGION ET MATERIEL D'ÉTUDE

Région d'étude

Servat *et al.* (1998) ont permis d'identifier les manifestations de la variabilité climatique observée autour des années 1970 en Afrique de l'Ouest. La baisse de la pluviométrie a, bien entendu, des conséquences sur les régimes des cours d'eau et donc sur la disponibilité des ressources en eau. La sécheresse hydrologique est d'ailleurs bien souvent d'une ampleur plus grande. De même, des changements ont affecté la relation pluie-débit (Lubès-Niel *et al.*, 2003). En milieu sahélien, Mahé *et al.* (2005) ont montré que ces changements pouvaient avoir aussi une origine humaine.

Modèle hydrologique

Le modèle retenu est une version mensuelle, adaptée au contexte africain, des modèles de la classe "GR" (http://www.cemagref.fr/webgr/index.htm; Makhlouf, 1994). Le modèle est à 2 paramètres, le premier ($0<X1<1$) est lié au volume annuel total écoulé, le second ($0<X2<1$) est lié à la vidange d'un réservoir de routage.

Copyright © 2006 IAHS Press

Données

Nous avons choisi des bassins versants, disposant de séries hydroclimatiques longues de plusieurs décennies, comportant un nombre de lacunes le plus faible possible. Ainsi, nous avons retenu 29 bassins situés sur 6 pays de l'Afrique de l'Ouest (Bénin, Burkina Faso, Côte d'Ivoire, Mali, Niger, Togo). Le Tableau 1 présente des caractéristiques des stations de mesure et des séries inhérentes.

Les données pluviométriques et d'évapotranspiration potentielle de Penman proviennent des grilles de résolution 0.5° × 0.5° établies par l'unité de recherche climatologique (CRU) de l'Université d'East Anglia à Norwich (New *et al.*, 1999; 2000). Les données hydrométriques des bassins proviennent de la base de données SIEREM gérée par HydroSciences Montpellier (HSM). La capacité maximale du réservoir sol du modèle GR est assimilée à une capacité de rétention en eau du sol qui est issue du CD-Rom, *Digital Soil Map of the World* (FAO/IIASA, 2000).

MÉTHODOLOGIE

On se propose d'abandonner l'idée de trouver une estimation satisfaisante des paramètres du modèle sans aucune estimation de débit et d'explorer alors une voie différente où l'on exploiterait à la fois une information régionale et une information ponctuelle sur les débits.

Information régionale

L'information régionale retenue est la nature du régime d'écoulement du bassin versant tel qu'il a été défini par Rodier (1964) (Tableau 2). Les régimes des cours d'eau d'Afrique Noire présentent un certain nombre de traits communs qui contribuent à leur donner une réelle unité.

Tableau 1 Caractéristiques des stations de mesure de débits pour les bassins de l'étude (en grisé les bassins de régime hydrologique sahélien—les autres bassins sont de régime hydrologique tropical pur).

Pays	Nom du bassin	Nom de la rivière	Superficie (km²)	Chroniques de débit		%age de lacune période avant 1970	%age de lacune période après 1971
				début	fin		
BURKINA FASO	Batie	Poni	5605	1971	1993	–	9
	Boromo	Mouhoun	54499	1955	1995	1	1
	Dapola	Mouhoun	86566	1951	1995	1	0
	Folonzo	Comoé	8366	1969	1992	17	25
	Koriziena	Gorouol	2887	1970	1995	0	40
	Nobere	Nazinon	7851	1965	1995	67	11
	Pont Ouessa	Mouhoun	66653	1969	1995	17	18
	Yendere	Leraba	6288	1955	1992	3	1
	Wayen	Nakambé	20241	1955	1995	51	4
COTE D'IVOIRE	Akakomoekrou	Comoé	58305	1956	1992	0	2
	Aniassue Pont	Comoé	70636	1953	1992	3	3
	Bada	Bandama	23809	1962	1992	0	5
	Fetekro	Nzi	10175	1959	1992	8	3
	Mbahiakro	Nzi	15368	1954	1992	2	0
	Serebou	Comoé	50587	1954	1992	2	3
NIGER	Campement W	Tapoa	5391	1963	1995	0	11
	Diongore	Goroubi	15361	1962	1992	8	13
	Dolbel	Gorouol	7505	1961	1995	0	6
	Garbe Kourou	Sirba	38871	1956	1995	19	9
	Kakassi	Dargol	7460	1957	1994	10	15
	Alcongui	Gourouol	42444	1961	1982	0	1
	Tamou	Diamangou	3839	1962	1995	7	34
	Tera	Dargol	2684	1961	1995	0	5
MALI	Douna	Bani	101225	1950	1995	14	1
TOGO	Amou Oblo	Amou	197	1957	1990	4	1
	Ebeva	Amouchou	408	1957	1990	0	5
	Koloware	Mono	53	1957	1990	0	12
	Kara	Lamakara	1502	1954	1990	1	0
BENIN	Barou	Mékrou	10666	1961	1978	32	26

Tableau 2 Classification des régimes d'écoulement en Afrique Noire (d'après Rodier, 1964).

Régime hydrologique	Limites des isohyètes	Principaux bassins hydrologiques	Principales caractéristiques
SAHELIEN	300 à 750 mm	Sirba, Dargol, Gorouol, Nakambé, Tapoa et une partie du bassin du fleuve Niger	Longue saison sèche, crue sporadique, importantes pertes par évaporation
TROPICAL PUR	750 à 1200 mm	Mouhoun, Nakambé, Comoé supérieure, et une partie du bassin du fleuve Niger	Présente une saison de hautes eaux en juillet à début octobre et une saison de basses eaux de début décembre à début juin.

Information locale

La démarche adoptée est de dégrader la chronique des débits observés sur chaque bassin étudié et d'analyser comment évoluent les paramètres à caler et une fonction critère, le critère de Nash. En fonction du contexte hydroclimatique de la région, les opérations décrites ci-après ont été effectuées 2 fois: sur la période antérieure à 1968 et sur la période postérieure à 1972.

Nous faisons l'hypothèse que l'ordre de grandeur des données de débit a un impact sur le critère de Nash et, donc, sur la détermination des paramètres du modèle. Aussi, avons-nous découpé la série complète des données débimétriques en 5 classes de débits qui sont fonction du module interannuel (voir Fig. 1).

Les opérations à effectuer sont alors:

– un calage avec l'ensemble des données disponibles; le Nash et les valeurs de paramètres obtenus seront appelés "référence" par la suite,
– les différents calages possibles du modèle en ne tenant pas compte des débits d'une classe donnée; soit 5 opérations de calage possible,
– recalculer une valeur de Nash avec les paramètres obtenus lors de l'opération précédente en tenant compte, cette fois, de l'ensemble des classes de débit disponibles; soient 5 "recalculs" de Nash.
– comparer les valeurs de paramètres calés (opération 2) et le Nash correspondant (opération 3) aux valeurs de référence (opération 1). Ces comparaisons doivent permettre d'identifier le poids et l'importance de la classe des débits retirés dans la détermination des valeurs des paramètres du modèle.

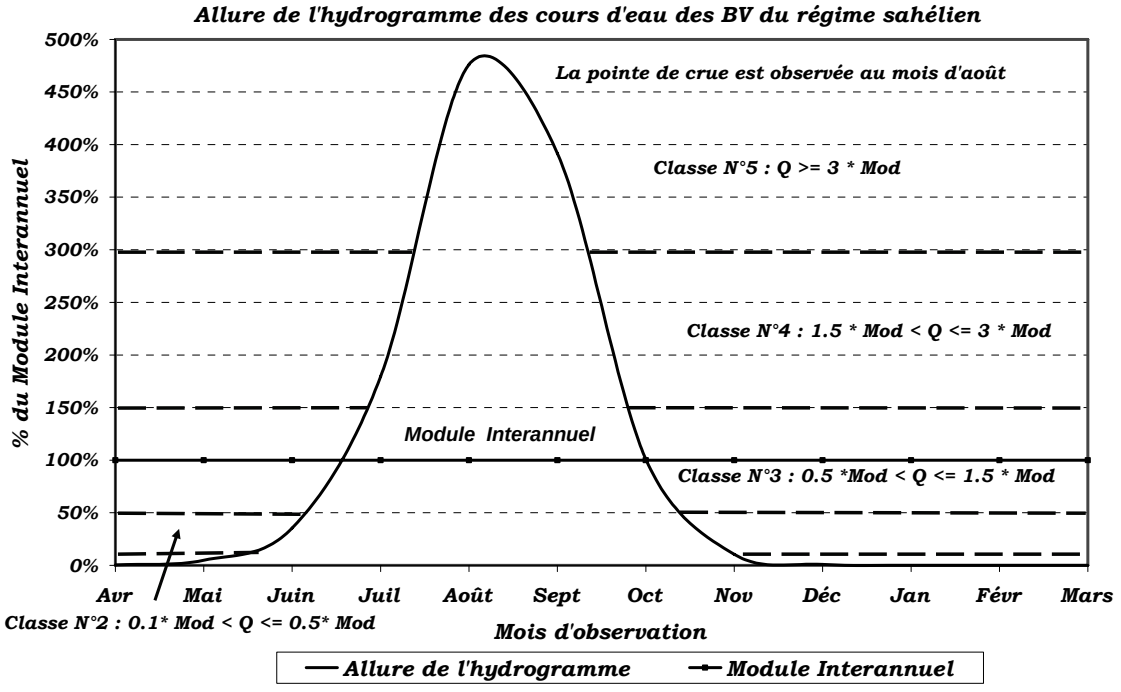


Fig. 1 Hydrogramme-type d'un cours d'eau de régime sahélien.

RESULTATS ET DISCUSSIONS

Nous présentons l'application à quelques bassins en régime sahélien. Les résultats sont de la même nature pour les bassins de régime hydrologique tropical pur.

Application

La Fig. 1 permet de visualiser l'hydrogramme–type d'un cours d'eau en régime sahélien. Les débits de la classe 5 sont bien souvent au nombre de 2 et on dénombre généralement 7 débits au sein de la classe 1 qui sont très proches de la valeur nulle.

Résultats des calages effectués avec 4 classes sur 5 La Fig. 2 montre que, quelle que soit la période de calage du modèle, les valeurs des paramètres et du Nash recalculé changent sensiblement par rapport aux valeurs de référence pour les calages effectués sans la classe 1 et que les changements les plus notables s'observent pour les calages sans la classe 5:

– les écarts entre les Nash peuvent être voisins de 10%, quelle que soit la période de calage considérée,
– le paramètre X1 reste généralement constant sauf lorsque l'on considère le calage en absence des débits de la classe 5; les débits de la classe 5 (les plus forts débits) conditionneraient grandement la valeur du paramètre X1,
– le paramètre X2 varie le plus fortement lors des calages en l'absence des débits de la classe 1.

Il faut savoir que le modèle est bien plus sensible au paramètre X1 que X2. Donc les variations en valeur absolue des paramètres X1 et X2 n'ont pas le même impact sur la variation de Nash.

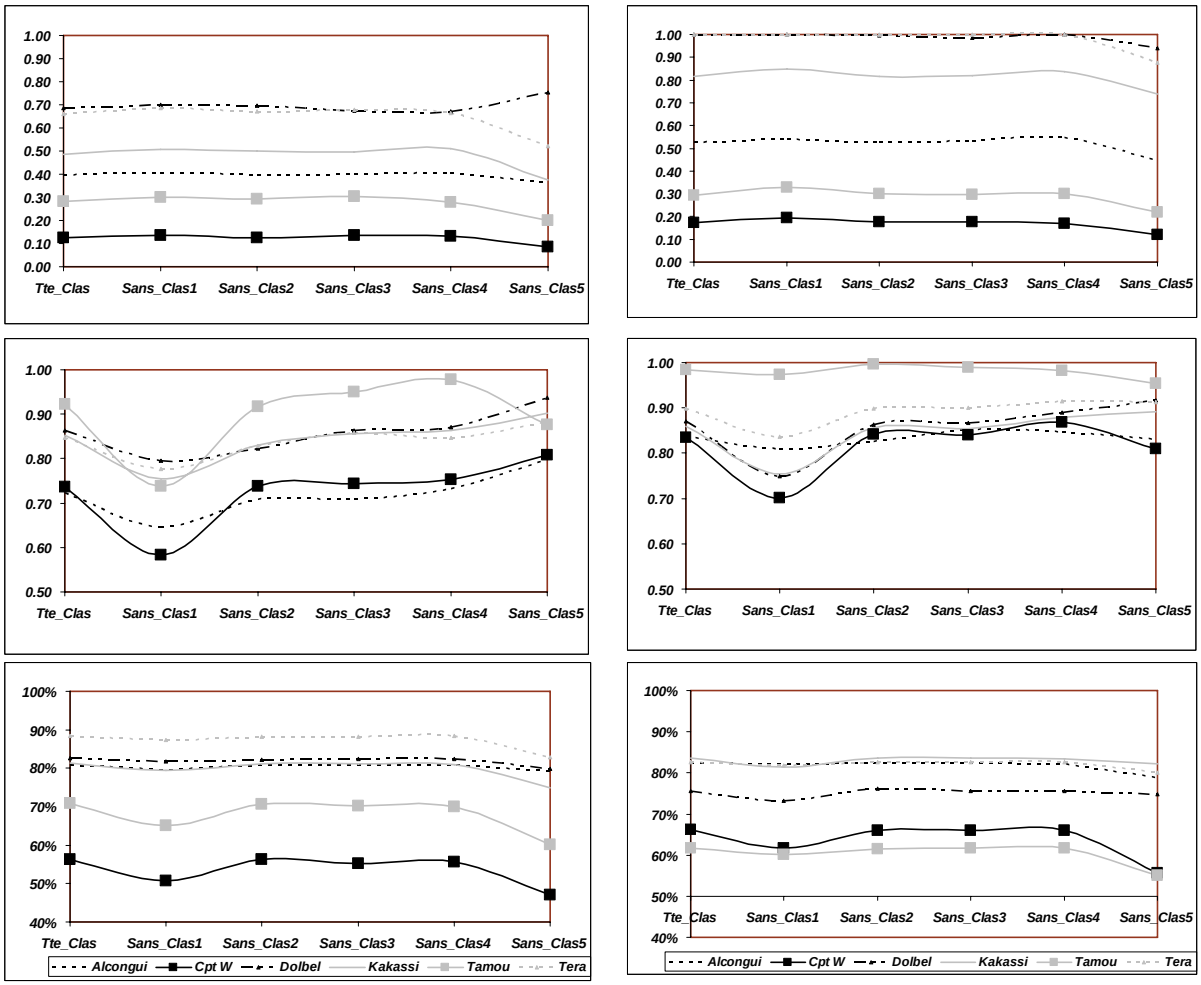


Fig. 2 Bassins sahéliens—évolution des paramètres X1 et X2 et du coefficient de Nash en absence d'une classe de débits (de haut en bas: X1, X2 et Nash; à gauche: avant 1968; à droite: après 1972).

Aux vues des résultats ci-dessus, il convient alors de s'interroger si ces deux classes de débits ne seraient pas suffisantes pour une estimation des paramètres du modèle et une valeur de Nash proches des valeurs de référence. Les débits d'étiage étant très difficilement mesurables, nous avons décidé de fixer toutes les valeurs des débits de la classe 1 à la valeur nulle.

Résultats des calages effectués avec les classes 1 et 5 La Fig. 3 montre que caler le modèle avec les débits des classes 1 et 5 donne des résultats très peu différents de ce que l'on aurait obtenu en utilisant toutes les données disponibles. On peut également noter:

– alors que les calages en absence d'une classe (1 ou 5) aboutissaient à des valeurs de X1 inférieures à X1réf, ici, on obtient l'inverse (X1réf > X1 calé); à l'exception de Dolbel. Même si les débits de la classe 5 conditionnent grandement la valeur du paramètre X1, les autres classes de débit (tout du moins la classe 1) ont également leur importance;
– le comportement particulier de "Campement W", voire de "Tamou", pour la période avant 1968: le fait d'ajouter une information (débits de classe 1) donne un couple de paramètres et un coefficient de Nash qui s'éloigne des valeurs de référence. Est-ce dû:
  – au fait que nous avons considéré comme valeurs nulles les débits de classe 1 ?
  – à la présence d'une crue "exceptionnelle" ?

  Comme pour la période après 1972, les résultats de ces 2 bassins sont proches de ceux de référence, les résultats d'avant 1968 pourraient alors être expliqués par la présence d'une crue "exceptionnelle"; L'analyse de la série chronologique le montre en effet. En enlevant cet valeur "exceptionnelle, le couple de paramètre et la valeur de Nash se rapprochent alors fortement des valeurs de référence.

On peut alors en déduire qu'il est raisonnable de caler le modèle GR2M, en milieu sahélien, avec les seuls débits des classes 1 (considérés comme nuls) et 5.

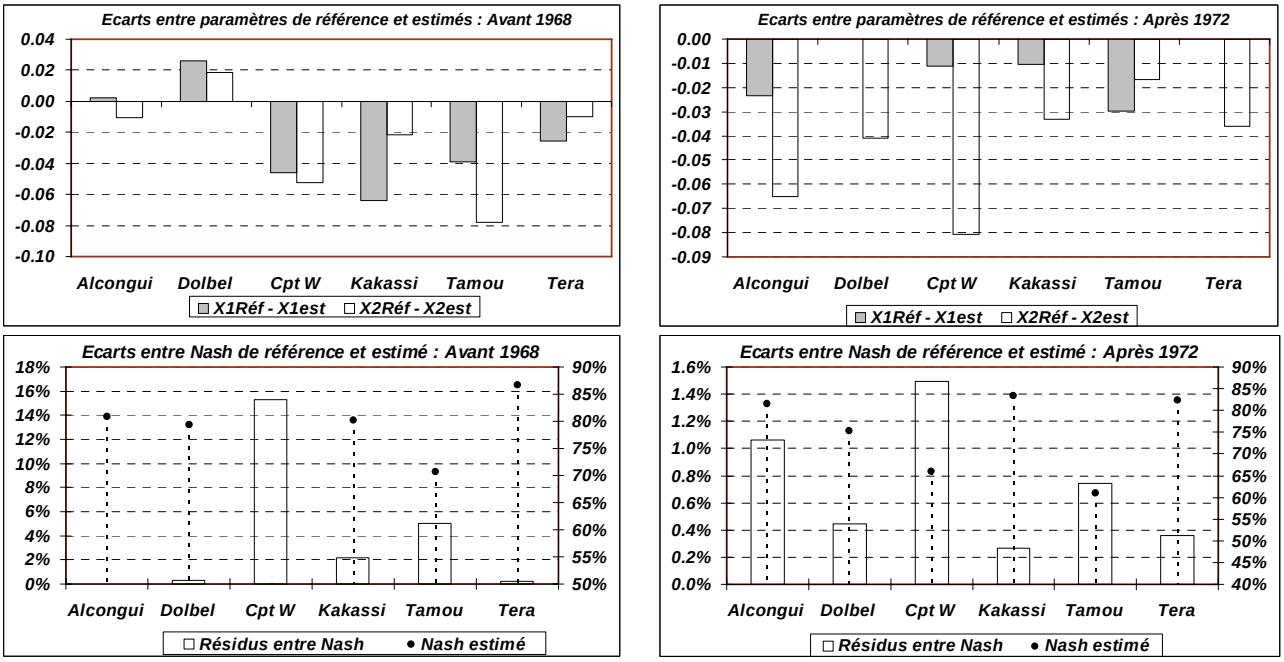


Fig. 3 Bassins sahéliens—résultats comparés des calages avec toutes les données et avec les seules classes 1 (débits nuls) et 5.

CONCLUSIONS

Les résultats ici obtenus montrent que même si l'information est rare, il peut être possible de caler correctement un modèle hydrologique; il suffit qu'il y ait l'information nécessaire et suffisante. Bien sûr, les résultats sont étroitement liés au modèle et aux données disponibles.

Nous avons défini une méthodologie d'approche qui puisse nous permettre de déterminer l'information minimale nécessaire pour caler convenablement le modèle GR2M. Elle nous a

permis de répondre au cas des bassins en régime hydrologique sahélien et tropical pur. Cette information minimale combine une donnée régionale et une donnée locale.

L'information régionale est la nature du régime d'écoulement du bassin versant (Rodier, 1964). Même si cette classification se base sur des études qui datent d'avant les changements climatiques observés en Afrique de l'Ouest et en Afrique Centrale, les résultats obtenus semblent confirmer l'option prise. Il ne serait pas inintéressant d'essayer de mettre à jour cette classification et de mesurer ce que cela apporte.

Pour les hydrogrammes simples des bassins en régime hydrologique sahélien ou tropical pur d'Afrique de l'Ouest et Centrale, l'information à fournir est constituée:

– des écoulements de hautes-eaux qui constituent une bonne approximation des volumes annuels écoulés,
– et d'une partie des écoulements de basses–eaux qui avec les débits de pointe de l'hydrogramme peuvent permettre de caler la décrue.

Pour les bassins en régime équatorial, les hydrogrammes sont généralement bimodaux et les écoulements de basses–eaux sont bien souvent loin d'être négligeables. Nous anticipons sur les résultats à venir mais il est probable que l'information nécessaire sera certainement plus importante pour caler correctement le modèle.

REFERENCES

FAO/IIASA (2000) Global Agro-Ecological Zones. UN Food and Agriculture Organization, Rome, Italy and International Institute for Applied Systems Analysis, Laxenburg, Austria. CD-Rom.

Lubès-Niel, H., Paturel, J. E. & Servat, E. (2003) Study of parameter stability of a lumped hydrologic model in a context of climatic variability. *J. Hydrol*. **278**, 213–230.

Mahé, G., Paturel, J. E., Servat, E., Conway D.& Dezetter, A. (2005) The impact of land use change on soil water holding capacity and river flow modelling in the Nakambe River, Burkina Faso. *J. Hydrol*. **300**, 33–43.

Makhlouf, Z. (1994) Compléments sur le modèle pluie-débit GR4J et essai d'estimation de ses paramètres. Thèse de doctorat, Université Paris-Sud, Paris, France.

New, M., Hulme, M. & Jones P. (1999) Representing twentieth century space-time climate variability. Part I: development of a 1961-1990 mean monthly terrestrial climatology. *J. Clim*. **12**(3), 829–856.

New, M., Hulme, M. & Jones P. (2000) Representing twentieth century space-time climate variability. Part II: development of a 1901-1996 monthly grids of terrestrial surface climate. *J. Clim.* **13**(13), 2217–2238.

Rodier, J. (1964) Régimes hydrologiques de l'Afrique Noire à l'ouest du Congo. ORSTOM, Paris, France.

Servat, E., Paturel, J. E., Kouame, B., Travaglio, M., Ouedraogo, M., Boyer J. F., Lubes-Niel, H., Fristch, J. M., Masson, J. M. & Marieu, B. (1998) Identification, caractérisation et conséquences d'une variabilité hydrologique en Afrique de l'Ouest et Centrale. In: *Water Ressources Variability in Africa during the XXth Century* (ed. by E. Servat, D. Hughes, J. M. Fritsch & M. Hulme) (Proc. Abidjan'98 Conference), 323–337. IAHS Publ. 252. IAHS Press, Wallingford, UK.

Climate Variability and Change—Hydrological Impacts (Proceedings of the Fifth FRIEND World Conference held at Havana, Cuba, November 2006), IAHS Publ. 308, 2006.

Precipitation elasticity of streamflow in catchments across the world

FRANCIS H. S. CHIEW[1,2], MURRAY C. PEEL[2], THOMAS A. MCMAHON[2] & LIONEL W. SIRIWARDENA[2]

1 *CSIRO Land and Water, GPO Box 1666, Canberra, ACT 2601, Australia*

2 *Department of Civil and Environmental Engineering, University of Melbourne, Victoria 3010, Australia*

francis.chiew@csiro.au

Abstract Estimates of the sensitivity of streamflow to climate are required to make informed decisions for managing water resources and environmental systems to cope with hydroclimatic variability and climate change. The precipitation elasticity of streamflow (ε_P), defined as the proportional change in mean annual streamflow divided by the proportional change in mean annual precipitation, is a measure of the sensitivity of streamflow to precipitation. This paper uses a nonparametric estimator to estimate ε_P for over 500 catchments across the world. The nonparametric estimator calculates ε_P directly from concurrent historical annual catchment precipitation and streamflow data, and is particularly useful for global studies such as this because it does not require the selection of a single hydrological model and calibration criteria that are appropriate for catchments across the world. The results indicate that changes in precipitation are amplified in streamflow. The ε_P estimates generally range from 1.0 to 3.0, that is, a 1% change in mean annual precipitation results in a 1–3% change in mean annual streamflow. The higher ε_P values (greater than 2.0) are observed in southeastern Australia and southern and western Africa, while lower ε_P values (lower than 2.0) are observed in southwestern South America and at mid and high latitudes in the Northern Hemisphere. There is a relatively strong inverse relationship between ε_P and runoff coefficient, with higher ε_P values observed in catchments with lower runoff coefficients. The ε_P value is also generally lower than 2.0 in catchments with high mean annual streamflow (greater than 500 mm) or mean annual precipitation (greater than 1500 mm), and in cold climates (mean annual temperature lower than 10°C).

Key words climate change; elasticity; global; hydroclimatic variability; precipitation; streamflow

INTRODUCTION

Climate is a key driver of hydrological processes. Estimates of the sensitivity of streamflow to climate are required to make informed decisions to manage water resources and environmental systems to cope with hydroclimatic variability and climate change. The sensitivity of streamflow to climate is almost always estimated using calibrated hydrological models by comparing estimates of the modelled streamflow for the present climate and the modelled streamflow for a perturbed climate (e.g. Schaake, 1990; Xu, 1999; Chiew & McMahon, 2002). The results from the modelling studies are likely to be dependent on the hydrological model and calibration criteria used in the studies.

The alternative to the hydrological modelling approach is to estimate the sensitivity of streamflow to climate directly from a set of concurrent climate and streamflow data. This paper presents the precipitation elasticity of streamflow for over 500 catchments across the world, estimated using a nonparametric estimator of elasticity which calculates the elasticity directly from a set of concurrent annual catchment precipitation and streamflow data. The precipitation elasticity of streamflow (ε_P) is defined here as the proportional change in mean annual streamflow divided by the proportional change in mean annual precipitation (Schaake, 1990). An elasticity of 2.0 therefore indicates that a 1% change in precipitation results in a 2% change in streamflow. The nonparametric estimator of elasticity is particularly useful for this global study because it is difficult to define a hydrological model structure that is appropriate for large parts of the world, and to obtain the data required to run such models.

This paper first describes the nonparametric estimator of ε_P and its limitations, followed by a description of the compilation of precipitation, temperature and streamflow data sets for catchments across the world. The paper then presents estimates of ε_P for over 500 catchments and discusses the observed relationships between ε_P and hydroclimatic characteristics.

Copyright © 2006 IAHS Press

NONPARAMETRIC ESTIMATOR OF ELASTICITY

The nonparametric estimator of ε_P proposed by Sankarasubramaniam *et al.* (2001) is used here:

$$\varepsilon_P = \text{median}\left(\frac{Q_t - \overline{Q}}{P_t - \overline{P}}\frac{\overline{P}}{\overline{Q}}\right) \quad (1)$$

where $\overline{P}$ and $\overline{Q}$ are the mean annual precipitation and streamflow respectively. To estimate ε_P, a value of $\left(\frac{Q_t - \overline{Q}}{P_t - \overline{P}}\frac{\overline{P}}{\overline{Q}}\right)$ is calculated for each pair of P_t and Q_t in the annual time series, and the median of these values is the nonparametric estimate of ε_P. This nonparametric estimate of ε_P is therefore defined at the mean value of the hydroclimate variable.

Sankarasubramaniam *et al.* (2001) showed, using Monte-Carlo experiments, that this nonparametric estimate of ε_P has low bias and is as robust as ε_P estimated using modelling approaches. Sankarasubramaniam *et al.* (2001) and Chiew (2006) also showed that there is a high correlation between ε_P values estimated using this nonparametric estimator and modelling approaches for catchments in the USA and Australia, respectively, although the hydrological modelling approach gives slightly higher ε_P values.

There are several limitations in the nonparametric estimation approach. As the nonparametric estimator uses annual data, it only provides an estimate of the sensitivity of long-term streamflow to changes in long-term precipitation, and cannot describe the sensitivity of streamflow characteristics, other than the long-term mean, to changes in precipitation characteristics. The estimates, which are derived from historical data, should also be interpreted cautiously in climate change impact studies, because the approach does not consider potential changes in land surface processes and surface-atmosphere feedbacks in an enhanced greenhouse environment.

GLOBAL PRECIPITATION, TEMPERATURE AND STREAMFLOW DATA SETS

To estimate ε_P using the nonparametric estimator, a data set of concurrent (but not necessarily continuous) annual lumped catchment-average precipitation and streamflow data is required. Temperature data are also compiled for catchments with concurrent precipitation and streamflow data.

The streamflow data used in this study are drawn from the global database of monthly streamflow data for over 1200 catchments described in Peel *et al.* (2004). The streamflow data are believed to be unregulated over the period of record in the database. The source of the precipitation and temperature data is the Global Historical Climatology Network (GHCN, Version 2), which contains monthly precipitation and temperature data for over 20 000 and 7000 stations respectively (Peterson & Vose, 1995; Vose *et al.*, 2005).

To compile the catchment-average monthly precipitation data, the catchment boundaries are constructed from the HYDRO1k DEM (1 km × 1 km resolution, USGS, http://edcdaac.usgs.gov/gtopo30/hydro/). The catchment is used only if the area defined by the boundary is within 5% of the published catchment area.

For each catchment, precipitation stations within 200 km of the catchment boundary (with more than 50% of data over the period of streamflow data) that contribute to the Thiessen weighting are used to estimate the lumped catchment-average monthly precipitation time series. Figure 1 shows the number of precipitation stations that account for 70% of the Thiessen weighting plotted against the catchment area. Any missing monthly precipitation data for a station (Station A) are infilled using data from stations within 200 km, each time using data from the station (which has data when data from Station A is missing) with the highest precipitation correlation with Station A. Precipitation data infilled using data from a station with precipitation correlation against Station A that is lower than 0.7 are considered to be poor, and catchments with more than 5% of poor (Thiessen weighted) infilled data are not used.

Like precipitation, temperature stations within 500 km of the catchment boundary that contribute to the Thiessen weighting are used to estimate the lumped catchment-average monthly temperature time series. Missing monthly temperature data for a station are also infilled using data from the station with the highest correlation.

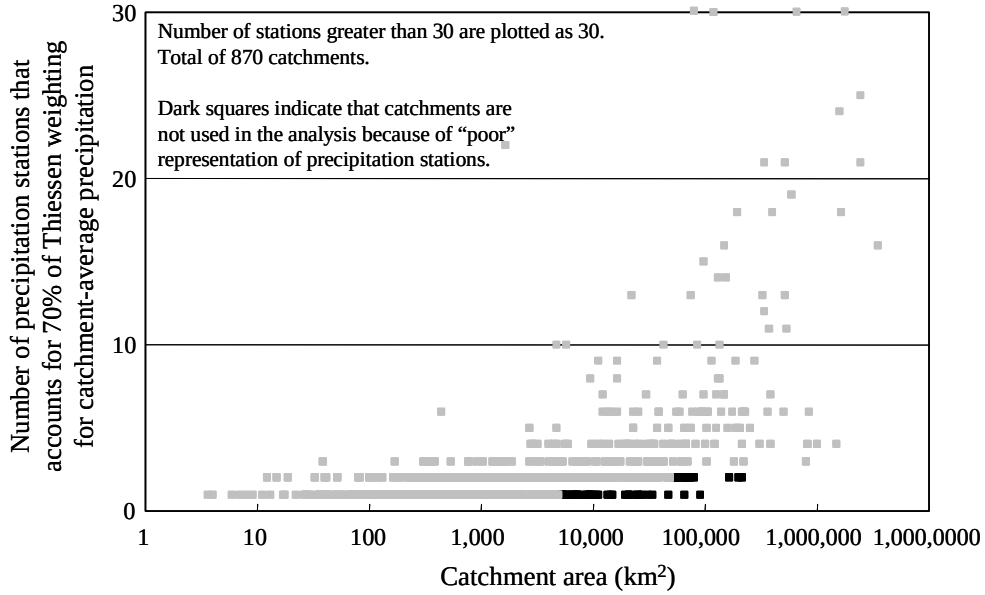


Fig. 1 Number of precipitation stations that accounts for 70% of the Thiessen weighting plotted against the catchment area.

The two biggest sources of error in the data are in the streamflow measurements (particularly the flow-stage rating) and the likelihood of more precipitation stations being located in the lower parts of the catchments where precipitation is usually lower than in the upper parts of the catchments (Milly & Dunne, 2002). The latter problem is highlighted by about 20% of the catchments having runoff coefficients [mean annual runoff (streamflow expressed in mm averaged over the catchment area) divided by mean annual precipitation] greater than one. Other main sources of error include: catchments may not be unregulated as believed and/or may have undergone land-use changes; poor infilling of precipitation data; and insufficient precipitation stations to represent the catchments. The latter two problems are overcome to some degree by removing catchments with more than 5% of "poor infilled data" as described above, and removing catchments larger than 5000 km^2 with only one precipitation station representing 70% of the Thiessen weighting and catchments larger than 50 000 km^2 with only one or two precipitation stations representing 70% of the Thiessen weighting (see Fig. 1).

The monthly precipitation and streamflow data are used to derive concurrent (not necessarily continuous because there can be missing monthly streamflow data) annual precipitation and streamflow data. The annual data are derived for a "water year" (rather than "calendar year"), which starts from the month with the lowest long-term mean monthly streamflow.

This study uses only data from catchments with at least 20 years of concurrent annual precipitation and streamflow data. Catchments with runoff coefficients greater than one and ε_P estimates less than zero are also not used.

Altogether, 521 catchments are used in this study (Fig. 2). They provide a reasonable coverage of different hydroclimatic regions, although they are not evenly distributed across the world. The data length varies from 23 to 64 years (10th to 90th percentile) and the catchment areas range from 100 to 76 000 km^2 (10th to 90th percentile).

RESULTS AND DISCUSSION

The nonparametric estimator is used to estimate ε_P for the 521 catchments across the world. The ε_P values for the 521 catchments are summarized in Fig. 2, and the range of ε_P values and runoff coefficients for the major climatic types (as described by the Koppen climate classification scheme, Henderson-Sellers & Robinson, 1986) are tabulated in Tables 1 and 2 respectively. Figure 3 shows ε_P plotted against various hydroclimatic characteristics. Before discussing the results, it is worth noting that there is no relationship between ε_P and catchment area or data length in the data used here (not shown here).

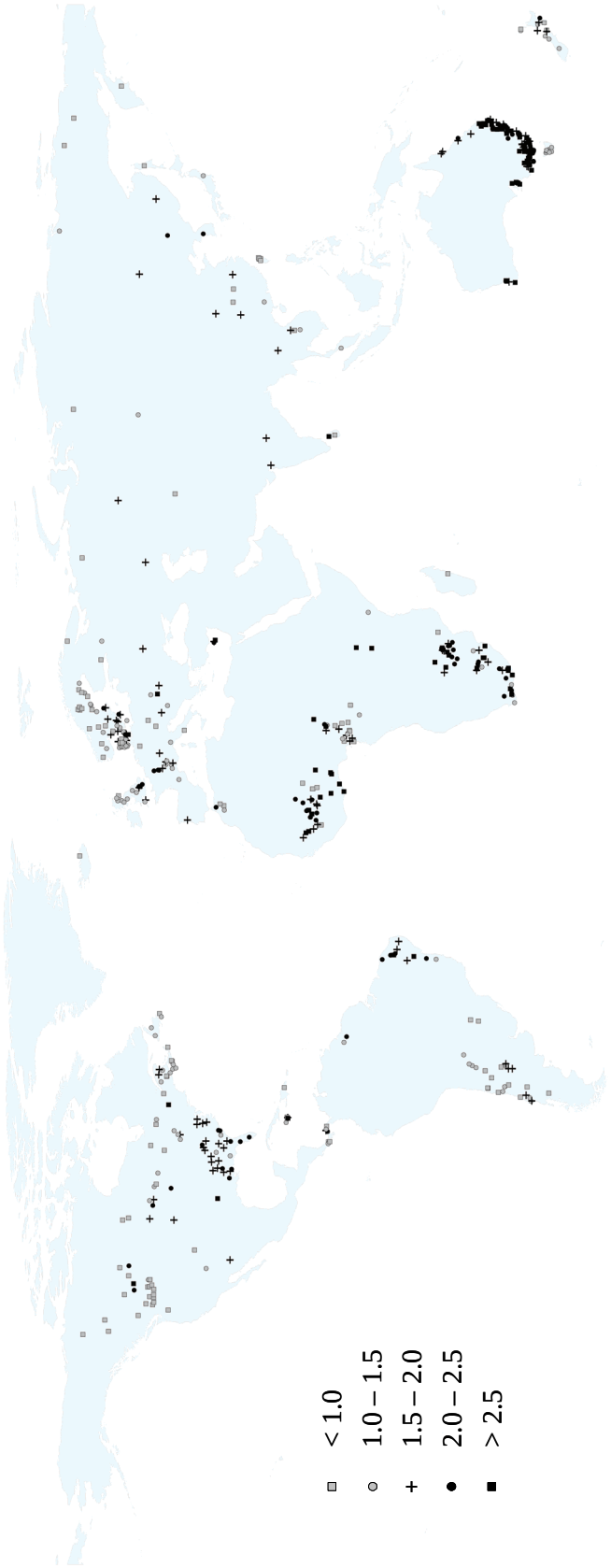


Fig. 2 Estimates of ε_P for 521 catchments across the world.

Table 1 Range of ε_P values for the major climate types.

Climate zone*	Number of catchments	Precipitation elasticity of streamflow: Median	10th and 90th percentiles in brackets
Tropical (A)	**79**	**1.7**	**(0.8 – 3.1)**
Very wet (Af, Am)	20	1.2	(0.8 – 1.9)
Moderately wet (Aw)	59	2.0	(0.9 – 3.3)
Arid (B)	**45**	**1.8**	**(0.4 – 2.9)**
Cold arid (BWk, BSk)	32	1.6	(0.4 – 3.1)
Warm arid (BWh, BSh)	13	2.0	(0.5 – 2.5)
Temperate (C)	**262**	**1.9**	**(0.9 – 3.1)**
Wet winter (Csa, Csb, Csc)	32	2.0	(0.9 – 3.4)
Wet summer (Cwa, Cwb, Cwc)	35	1.8	(0.8 – 2.8)
No seasonality (Cfa, Cfb, Cfc)	195	1.9	(1.0 – 3.1)
Cold (D)	**135**	**1.1**	**(0.5 – 1.9)**

* The climate types are described using the Koppen climate classification scheme (indicated by the letters in brackets).

Table 2 Range of runoff coefficients for the major climate types.

Climate zone	Number of catchments	Runoff coefficient: Median	10th and 90th percentiles
Tropical (A)	**79**	**0.24**	**(0.06 – 0.67)**
Very wet (Af, Am)	20	0.58	(0.34 – 0.83)
Moderately wet (Aw)	59	0.19	(0.05 – 0.40)
Arid (B)	**45**	**0.09**	**(0.02 – 0.45)**
Cold arid (BWk, BSk)	32	0.08	(0.02 – 0.59)
Warm arid (BWh, BSh)	13	0.13	(0.07 – 0.22)
Temperate (C)	**262**	**0.32**	**(0.09 – 0.75)**
Wet winter (Csa, Csb, Csc)	32	0.27	(0.09 – 0.71)
Wet summer (Cwa, Cwb, Cwc)	35	0.14	(0.05 – 0.50)
No seasonality (Cfa, Cfb, Cfc)	195	0.34	(0.12 – 0.77)
Cold (D)	**135**	**0.54**	**(0.21 – 0.82)**

The difficulties in compiling accurate catchment precipitation-streamflow data were discussed in the previous section. Therefore, despite the data used here being the best available global catchment precipitation-streamflow data set, this paper only discusses general trends in the ε_P estimates. For this reason, the upper and lower tenth percentiles of the data points in Fig. 3 are shown as smaller and lighter shaded squares. However, although more accurate estimates of ε_P can be obtained for a particular area using better local data and hydrological models developed and calibrated specifically for a catchment, the results here provide a useful overview of the sensitivity of long-term streamflow to climate in different parts of the world.

The results indicate that 80% of the ε_P estimates are between 0.7 and 3.0. The map in Fig. 2 indicates that the higher ε_P values (greater than 2.0) are in southeastern Australia and southern and western Africa, while the lower ε_P values (lower than 2.0) are in southwestern South America and the mid and high latitudes of the Northern Hemisphere (note that the catchments are not evenly distributed across the world and the catchment elevations are not considered here).

Figure 3(a) shows that there is a reasonably strong inverse relationship between ε_P and runoff coefficient. This is because of the nonlinearity in the precipitation–runoff process, and the same absolute change in streamflow for a given absolute change in precipitation would be reflected as a higher ε_P in a catchment with a lower runoff coefficient. In most cases, the upper limit of ε_P is the inverse of runoff coefficient (when the change in streamflow is the same as the change in precipitation).

The ε_P versus runoff coefficient relationship is also reflected in the ε_P *versus* streamflow relationship (Fig. 3(b)) and to a much lesser extent in the ε_P *versus* precipitation relationship (Fig. 3(c)). Figures 3(b) and 3(c) indicate that ε_P is generally below 2.0 in catchments with high mean annual streamflow (greater than 500 mm) or mean annual precipitation (greater than 1500 mm).

Tables 1 and 2 show that ε_P is generally lower (median ε_P of 1.1 and 90th percentile ε_P of 1.9 in the 135 catchments) and runoff coefficient is generally higher, respectively, in the cold climate

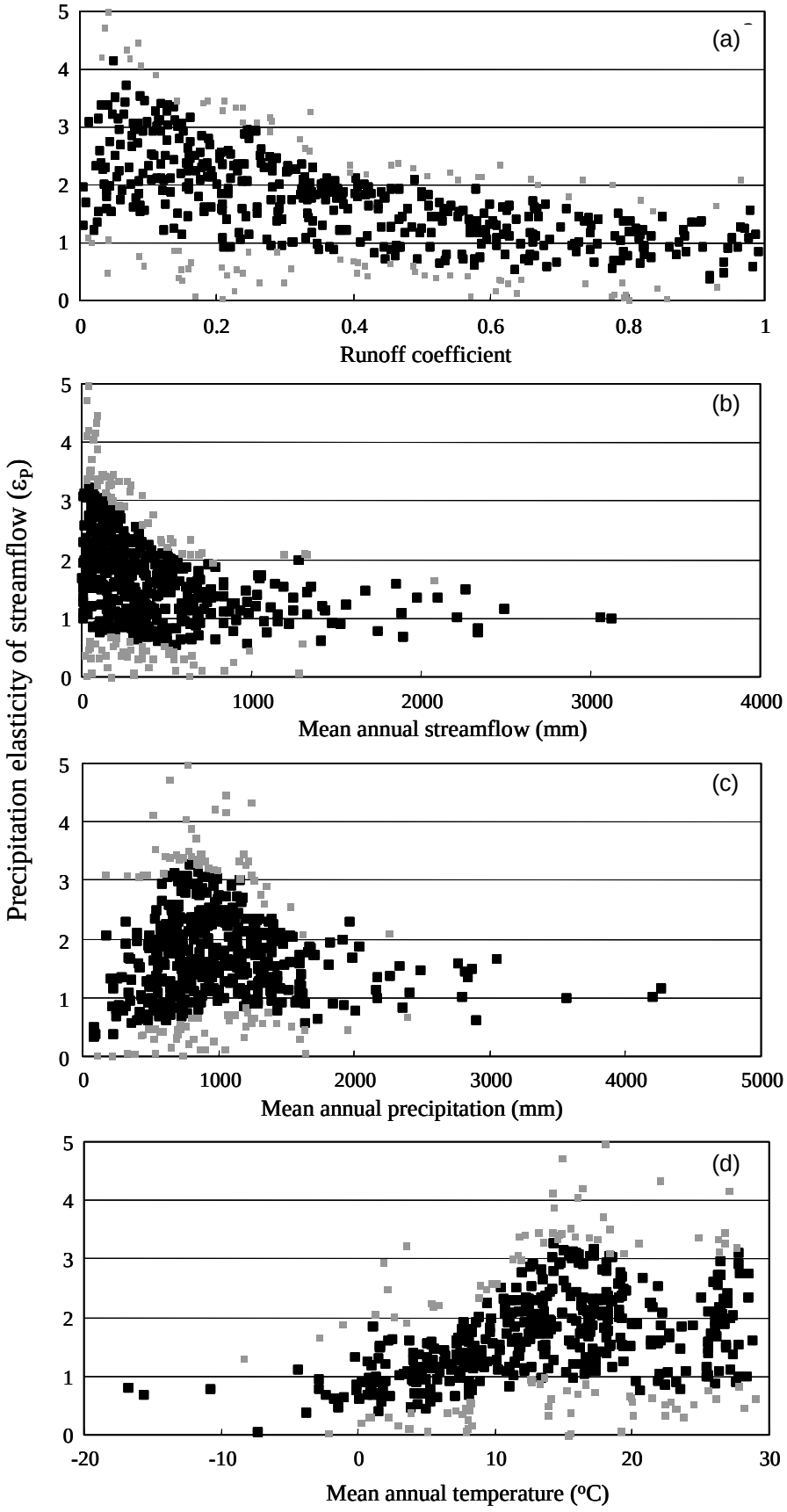


Fig. 3 Relationship between ε_p and various hydroclimatic characteristics.

type compared to the other Koppen climate types. This is also reflected in the ε_P *versus* temperature plot in Fig. 3(d) in which ε_P is generally less than 2.0 where the mean annual temperature is less than 10°C. The runoff coefficient is high in cold climates because of the low amount of energy available for evapotranspiration, and the ε_P value is low in cold climates because of the high runoff coefficient. In addition, where there is significant/permanent snowpack, annual streamflow is also dependent on the temperature which governs the amount of snowmelt and over-year snow storage, which is not considered in the ε_P estimator used here.

Apart from the cold climate type, it is difficult to distinguish the ε_P values in the other three climate types. Nevertheless, the wetter catchments in the tropical climate type generally have lower ε_P and higher runoff coefficient compared to the drier catchments (Tables 1 and 2 respectively). There is also a weak observation that the runoff coefficient in the temperate climate type is higher in catchments dominated by winter rainfall (Table 2), most likely due to lower evapotranspiration losses. It is also interesting to note that although the runoff coefficient is lower in the arid catchments as expected (Table 2), the ε_P values in the arid catchments are similar (and not higher) to the tropical and temperate climate types (although most of the arid catchments in this data set are in colder arid regions).

CONCLUSIONS

The precipitation elasticity of streamflow (ε_P) for 521 catchments across the world, estimated using a nonparametric estimator, is presented in this paper. The nonparametric estimator calculates ε_P directly from concurrent historical annual catchment precipitation and streamflow data, and is particularly useful for global studies such as this because it does not require the selection of a single hydrological model and calibration criteria that are appropriate for catchments across the world.

The results indicate that changes in precipitation are amplified in streamflow. The ε_P estimates generally range from 1.0 to 3.0, that is, a 1% change in mean annual precipitation results in a 1% to 3% change in mean annual streamflow. The higher ε_P values (greater than 2.0) are observed in southeastern Australia and southern and western Africa, while lower ε_P values (lower than 2.0) are observed in southwestern South America and the mid and high latitudes of the Northern Hemisphere. There is a reasonably strong inverse relationship between ε_P and runoff coefficient, with higher ε_P values observed in catchments with lower runoff coefficients. The ε_P value is also generally lower than 2.0 in catchments with high mean annual streamflow (greater than 500 mm) or mean annual precipitation (greater than 1500 mm), and in cold climates (mean annual temperature lower than 10°C).

REFERENCES

Chiew, F. H. S. (2006) Estimation of rainfall elasticity of streamflow in Australia. *Hydrol. Sci. J.* (in press).

Chiew, F. H. S. & McMahon, T. A. (2002) Modelling the impacts of climate change on Australian Streamflow. *Hydrol. Processes* **16**, 1235–1245.

Henderson-Sellers, A. & Robinson, P. J. (1986) *Contemporary Climatology*. Longman Scientific and Technical, London, UK.

Milly, P. C. D. & Dunne, K. A. (2002) Macroscale water fluxes. 1. Quantifying errors in the estimation of basin mean precipitation. *Water Resour. Res.* **38**, 1205, doi:10.1029/2001WR000759.

Peel, M. C., McMahon, T. A. & Finlayson, B. L. (2004) Continental differences in the variability of annual runoff—update and reassessment. *J. Hydrol.* **295**, 185–197.

Peterson, T. C. & Vose, R. S. (1997) An overview of the Global Historical Climatology Network temperature database. *Bull. Am. Met. Soc*. **78**, 2837–2849.

Sankarasubramaniam, A., Vogel, R. M. & Limburner, J. F. (2001) Climate elasticity of streamflow in the United States. *Water Resour. Res.* **37**, 1771–1781.

Schaake, J. C. (1990) From climate to flow. In: *Climate Change and US Water Resources* (ed. by P. E. Waggoner), 177–206. John Wiley, New York, USA.

Vose, R. S., Wuertz, D., Peterson, T. C. & Jones, P. D. (2005) An intercomparison of trends in surface air temperature analyses at the global, hemispheric, and grid-box scale. *Geophys. Res. Lett.* **32**, L18718, doi:10.1029/2005GL023502.

Xu, C. Y. (1999) Climate change and hydrologic models: a review of existing gaps and recent research developments. *Water Resour. Manage.* **13**, 369–382.

4 Hydro-climatology

Precipitation spatial and temporal variability and prediction	*265–337*
Large scale variability and tele-connections	*338–374*
Climate change and impacts of climate change	*375–482*
Trends	*483–550*

Climate Variability and Change—Hydrological Impacts (Proceedings of the Fifth FRIEND World Conference held at Havana, Cuba, November 2006), IAHS Publ. 308, 2006.

An approach to the vulnerability analysis of intensive precipitation in Cuba

EDUARDO O. PLANOS GUTIÉRREZ & MIRIAM E. LIMIA MARTÍNEZ

Centre of Climate, Institute of Meteorology of Cuba, Loma de Casablanca S.N. Ciudad de la Habana, La Habana, Municipio Regla, Cuba

eduardo.planos@insmet.cu

Abstract Hydrological analyses typically use a strict probabilistic approach to predicting extreme hydrological phenomena and analyse the vulnerability of regions to intense precipitation. Although it is well known that probabilistic approaches have weaknesses, when this method is complemented with the physical analysis of precipitation and the analysis of how meteorological systems interact with geomorphology, it can be successfully used to characterize the hydrological vulnerability of regions. This paper presents a methodological approach for the regional analysis of the vulnerability due to intensive precipitation. The methodology uses: (a) probabilistic and stochastic analysis; (b) local geographical scale characterization; (c) regional Intensity-Duration-Frequency graphs; (d) regional relations between the depth of precipitations of different durations; (e) maps of the return periods of maximum precipitation; (e) stochastic maps and (f) graphs of stochastic security. A case study that uses the methodology in Eastern Cuba is presented.

Key words intensive precipitation; probability; frequency; stochastic; vulnerability

INTRODUCTION

In Cuba, an intensive precipitation is considered to be an event that reaches or surpasses 100 mm in 24 hours. One of the most remarkable characteristic of the meteorological systems that produces these precipitations is that in a few hours they can produce rainfall that is close to or even greater than annual precipitation. When these events occur their hydrological impacts often cause lamentable disasters.

The hydrological analysis of this kind of phenomena typically includes a group of deterministic, parametric, probabilistic and stochastic procedures that are used to determine regional generalizations and relations between hydrological variables (OMM, 1994). Extraordinary advances have been made in diagnosing and forecasting dangerous meteorological and hydrological situations. Today, most applied hydrological studies have an integrated vision of the hydrological and meteorological phenomena. Nevertheless, there are limitations in the use of common techniques because certain natural processes are not yet sufficiently described and they are too complex to be defined mathematically. Furthermore, in many cases the analysis is exclusively statistical, the synoptic scale is not well considered, and the geographical conditions are not properly analysed. Therefore, many hydrological characterizations only describe a statistical space and do not include adequate meteorological and geographical analysis. This paper presents a methodology for the regionalization of the intense precipitations and the development of regional vulnerability analysis that is based on a physical-geographical interpretation and probabilistic and stochastic analysis.

DATA

The results presented in this paper are based on two detailed investigations of intense precipitation in Cuba: Planos (2000) and Limia & Planos (2004). This data was based on data collected between 1970 and 1990 in a raingauge network of 835 pluviometers and 135 pluviographs. The density of the raingauge network used in the analysis is consistent with those of the Cuban hydrological network: 8 pluviometers in 1000 km^2, an average of 14 km between pluviometers, and a spatial interpolation error of between 9.5 and 11.5% (Huerta *et al*., 1977). This design insures that the spatial distribution of the precipitation is well represented.

METHODOLOGY

Analysis of the chronological series

The homogeneity and randomness of the series of annual absolute maxima precipitations were examined with the Helmert test of homogeneity and the Autocorrelation Test. Both tests gave

Copyright © 2006 IAHS Press

satisfactory results for most of the stations. The Langbein-Dalrymple test (Stedinger, 1995) was also used to evaluate the regional homogeneity of the probabilistic values that were generated. In this test the series were grouped according to altitude, distance between instruments and the coefficient of variation of the series.

Probabilistic analysis of the intensity of the precipitation

To analyse the intensity of Cuban precipitation a method that is widely used internationally was used. This included: (a) the selection of series of annual absolute maxima values of daily precipitation organized by intervals of time 5, 10, 20, 30, 40, 60, 120, 720 and 1440 minutes; (b) probabilistic distribution analysis; (c) development of local and regional graphs of Intensity-Duration-Frequency; (d) determination of regional values of maximum precipitation, for each interval of time in given probabilities; (e) construction of regional graphs of non-dimensional probabilities of maximum precipitation for different time intervals.

The probabilistic estimations were calculated using the Gumbel distribution function and validated with the Kolmogorov-Smirnov test. The probabilistic analysis itself is an evaluation of the hydrological risk and is expressed in terms of return periods. While this probabilistic technique is widely used, the analysis has many weaknesses, including the short duration of the data series available and the inherent uncertainty in the method. Fortunately, by using the concept of stochastic risk (Díaz Arenas, 1982) that is based on the calculation of the probability that one event will occur after a specific number of years, it is possible to get a more objective evaluation of the danger than can be analysed with the distribution functions alone. In this paper the binomial distribution was used to estimate the probability that a depth of rainfall equal to or bigger than 100 mm would occur in the next 2, 5, 10 and 20 years.

Analysis of the vulnerability

The integrated valuation of Threat, Vulnerability, and Risk should be an integral part of the evaluation of the natural threats in a region. While this is a valuable concept, in practice it is usually simplified when individual maps of hydrological risks are produced. Using the experience of the authors, this paper offers this wider vision for the methodological analysis of the intense precipitation. The methodology used in this paper is based on the integral analysis of: (a) regional IDF graphs; (b) regional graphs representing the relation between the depth of precipitation over different time intervals; (c) maps of return periods; (d) maps of probability that the precipitation of 100 mm be equalled or more in 2, 5, 10 and 20 years; (e) graphs of stochastic security, and (f) an integral map of vulnerability for impact of intense precipitations.

RESULTS

To characterize the behaviour of the precipitation in Eastern Cuba at different time intervals, transfer functions of precipitation over different intervals were developed from statistical relationships between the total event precipitation relative to the precipitation that occurred in 60 minutes (Fig. 1). The linear correlation coefficients of these relationships are good (>0.70). This is partly because the most intense rain is reached in the second and third quartiles of storms that had more that 50 mm of rainfall in one hour (Planos, 2000; Limia & Planos, 2004). The results of similar correlations between precipitations with durations of less than one hour are not as strong. This is apparently because they are caused by a diverse group of meteorological situations. This is especially true of intense precipitations with durations of less than 40 min and rainfalls less than 50 mm (Planos, 2000; Limia & Planos, 2004).

The final transfer functions used in the geographical analysis were based on the pluviographs that had error estimations less than 10%. The average error of the estimation with these equations oscillates between +/– 0.1 and 7%, an excellent value for this type of procedure.

Vulnerability analysis

Using the regression based transfer functions described above, the amount of precipitation over different time intervals was calculated for return periods of 100, 50, 20, 10, 5 and 2 years. As part

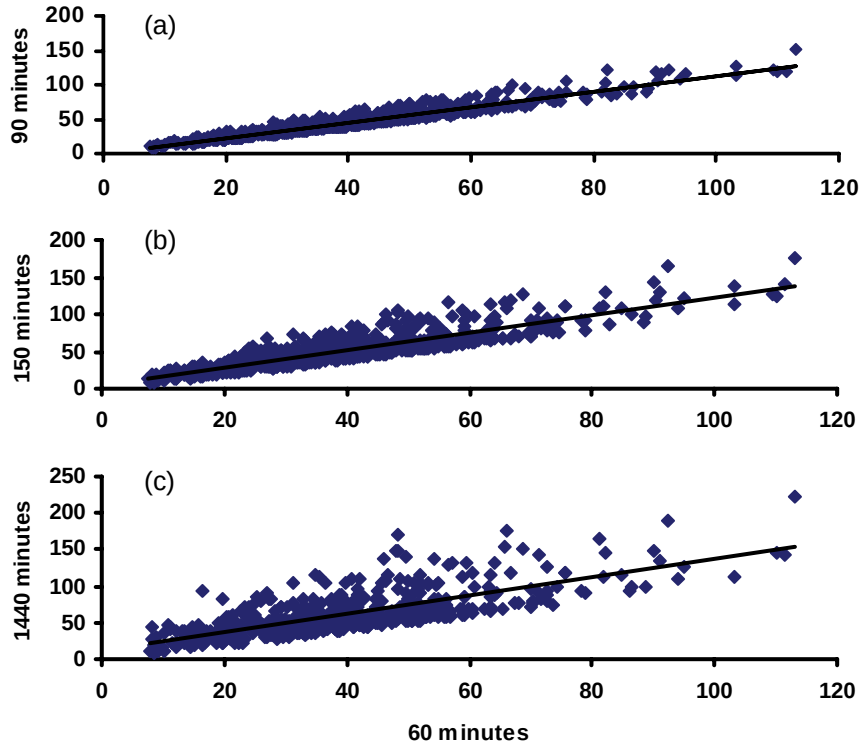


Fig. 1 Relationship between depths of precipitation for different intervals of time: (a) 60 min/90min; (b) 60 min/150 min and (c) 60 min/1440 min.

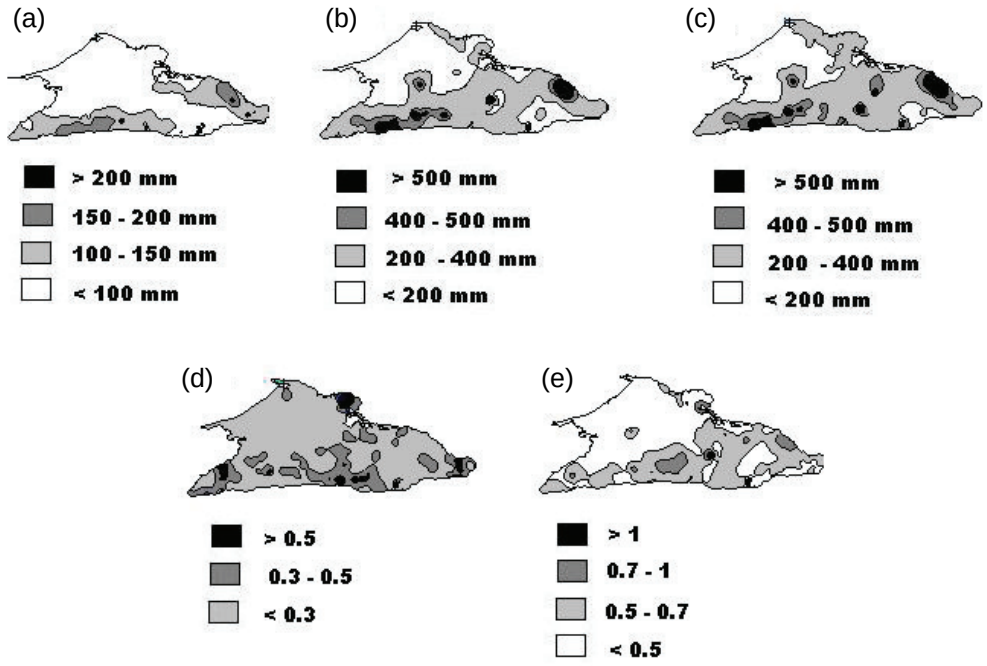


Fig. 2 Cuba Eastern Region. Distribution of statistical parameters associated with intense precipitation: (a) average of annual maximum precipitation in 24 hours; (b) maximum absolute precipitation in 24 hours; (c) 100-year 24-hour maximum precipitation; (d) probability of surpassing the 100 mm depth of precipitation in 2 years; and (e) Coefficient of variation of series of maximum precipitation in 24 hours.

of this analysis the following maps were prepared (Fig. 2): (a) maps of average of maximum precipitation depth; (b) coefficient of variation of the data series, (c) maps of absolute maximum depth of precipitation, (d) maps of 100, 50, 20, 10, 5 and 2 years of return period; (e) maps of 20, 10, 5 and 2 years of probability of surpassing 100 mm of depth of precipitation.

These maps have a structure that clearly reflects major influences on the spatial distribution of the intense precipitation in Cuba (Koshiasvili, 1972; Planos, 2000; Limia & Planos, 2004). In this sense, Planos (2000) and Limia & Planos (2004) determined a strong relationship between the distribution of the maximum values of precipitation, the relief, and the trajectory of the meteorological systems that produce the intense precipitations. Many of which were tropical hurricanes.

Integral map of vulnerability

Independently of the valuable information each of the mentioned maps has for disaster studies, it is more useful to have an integral and mappable valuation of the danger of intense precipitations. To achieve this, maps were developed (Fig, 3) using three levels of danger that were defined using the elements and ranking categories explained in Table 1. These three regions of danger were defined below and their average hydrological and geographic characteristics are presented in Table 2.

Low danger (AI): areas where the average of annual depth of maximum precipitation is less than 100 mm; the frequency of precipitation greater than 100 mm in 24 hours is 0.20%; the probability that a depth of precipitation of 100 mm be surpassed in 5 years is 0.34% and the maximum depth of absolute annual precipitation is less than 200 mm.

Moderate danger (AII): areas where the average of depth of maximum precipitation is less than 200 mm; the frequency of precipitation greater than 100 mm in 24 hours is 0.42%; the probability that a depth of precipitation of 100 mm will be surpassed in 5 years is 0.53% and the maximum depth of absolute annual rain is approximately 250 mm.

Higher and high danger (AIII): areas where the average of depth of maximum precipitation is greater than 200 mm; the frequency of the precipitation greater than 100 mm in 24 hours is 0.46%; the probability that a depth of precipitation of 100 mm be surpassed in 5 years is 0.58% and the maximum depth of absolute annual rain is bigger than 300 mm.

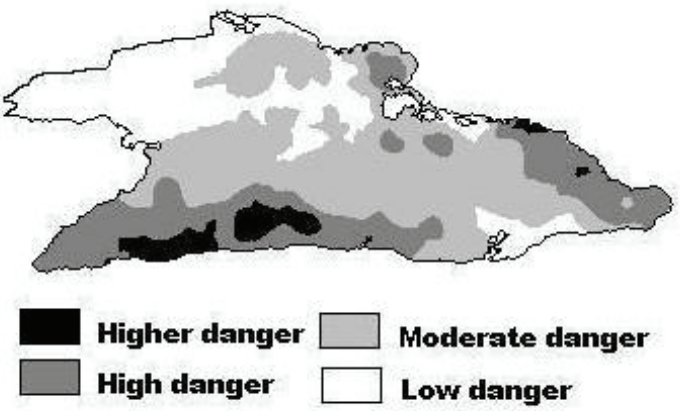


Fig. 3 Map of danger for intense precipitation impact. Cuba Eastern Region.

Table 1 Indicators and category ranking for classification of the vulnerability to intense precipitation impact.

Indicators	Range	Category	Indicators	Range	Category
Average of maxima precipitation	<100	1	Maxima absolute precipitation	<100	1
	101–125	2		100–199	2
	126–150	3		200–299	3
	151–200	4		300–399	4
	>200	5		>399	5
Frequency precipitation =>100 mm	<0.2	1	Probability 100 mm surpassed in 2 years	<0.5	2
	0.2–0.29	2		>0.5	4
	0.3–0.39	3	Danger category according the indicators range	<1	Low
	0.4–0.49	4		2–3.9	Moderate
	>0.49	5		4–4.5	High
				>4.5	Higher

Table 2 Statistical and hydrological characteristic parameters from the areas of danger in the Eastern Region of Cuba.

Average of statistical and geographical attributes	Higher / High danger areas	Moderate danger area	Low danger area
Altitude (m)	220	173	90
Average Annual maximum precipitation (mm)	115	103	80
Frequency of precipitation > 100 mm	0.46	0.42	0.20
Data series coefficient of variation	0.52	0.50	0.42
Annual maximum absolute precipitation (mm)	324	243	172
Precipitation of 100 years of period of return	345	294	225
Probability precipitation = 200 mm	0.58	0.40	0.15
Probability 100 mm precipitation be equalled or surpassed in 5 years	0.58	0.53	0.34

CONCLUSION

The analysis of intense Cuban precipitations was related to the determination of the most severe impacts in the rain by incorporating the analysis of stochastic risk. In the case of Cuba, three levels of danger were defined on the basis of the intensity of the precipitation. Each of these regions had its own identity, expressed through the parameters associated to the intensity of the precipitation and relationships between its statistical parameters, which allows us to define them as homogeneous regions.

REFERENCES

Díaz Arenas, A. (1982) Sobre la seguridad del valor de diseño en la vida útil de la obra. *Actas de la Conferencia Científico-técnica 20 años de desarrollo hidráulico en la Revolución* (noviembre de 1982, La Habana, Cuba).

Huerta, J., Fernández, N. & García, F. (1977) Evaluación de la información hidrológica: diseño de redes. *Revista Voluntad Hidráulica* **42**, 17–19.

Koshiasvili, B. (1972) Características de cálculo de las lluvias torrenciales en la provincia de La Habana. *Revista Voluntad Hidráulica* **22**, 15–23.

Limia, M. & Planos, E. (2004) *Relación espacial de la lluvia con su intensidad máxima. Estudio de casos. Evento Trópico 2004*. Publicación digital, ISBN 959-7167-02-6.

Organización Meteorológica Mundial (1994) *Guía de prácticas hidrológicas. Adquisición y procesos de datos, análisis, predicción y otras aplicaciones* (quinta edición). OMM no. 68, Ginebra, Suiza. WMO no. 68.

Planos, E. (2000) Análisis Hidrológico de las grandes precipitaciones. Informe de investigación. Programa Científico Técnico Nacional "Los cambios globales y la evolución del medio ambiente cubano". Ministerio de Ciencia, Tecnología y Medio Ambiente, La Habana, Cuba.

Stedinger H. J. R. (1995) Homogeneity tests based upon Gumbel distribution and a critical appraisal of Dalrymple's test. *J. Hydrol.* 166, 81–105.

Influencia de los embalses y lagos en las intensidades máximas de precipitación

ROBERTO PIZARRO, CLAUDIA SANGÜESA & DAYANNA ARAVENA

Departamento de Gestión Ambiental, Facultad de Ciencias Forestales, Universidad de Talca, Talca. Chile
rpizarro@utalca.cl

Resumen En el estudio se construyen y analizan las curvas Intensidad–Duración–Frecuencia (IDF) para 31 estaciones pluviográficas, distribuidas en cinco regiones de Chile central, abarcando desde zonas semiáridas por el Norte a zonas subhúmedas por el Sur. Estas curvas se construyen utilizando los registros pluviográficos entre los años 1962 y 2002, de donde se obtienen las intensidades máximas para cada año, las que posteriormente son ajustadas a la función de probabilidad de Gumbel, de donde se obtienen intensidades para duraciones entre 1 y 24 horas, asociadas a distintos periodos de retorno. Posteriormente se analiza el comportamiento gráfico de las intensidades máximas de precipitación para las duraciones de 1 y 24 horas y para el periodo de retorno de 100 años, donde las estaciones fueron ubicadas de Norte a Sur. Según este análisis, el comportamiento de las intensidades máximas de precipitación demuestra un leve incremento de Norte a Sur; asimismo, se encontró que algunas estaciones de la zona semiárida presentaron intensidades de precipitación similares a las que se registraron en zonas subhúmedas. Por otro lado se encontró que las estaciones cercanas a lagos y embalses, denotaron las intensidades más altas de sus zonas.

Palabras clave intensidad-duración-curvas de frecuencia; intensidades maximas de precipitacion; periodos de retorno para intensidades de precipitacion

Influence of reservoirs and lakes on maximum rainfall intensities in Chile

Abstract This study analyses intensity duration frequency curves for 31 raingauge stations located in different climatic zones in Chile, including arid and semiarid zones and humid zones. These curves were built using pluviograph records taken from 1962 to 2002. Maximum intensities for each year were obtained; then, for each duration, Gumbel distribution functions were fit with optimum results, from a statistical point of view. Gumbel functions were used for 1, 2, 6, 12 and 24 hours; then, curves were built using different return periods. With all results, maximum intensities were analysed, mainly for 1 hour and 24 hour, and for a return period of 100 years. The graphical behaviour of maximum intensities showed a slight increase from north to the south; also, some raingauge stations in the semiarid zone showed similar intensity values to southern region stations. On the other hand, raingauge stations located near lakes and dams recorded the highest intensities of their zones.

Key words intensity–duration–frequency curves; maximum rainfall intensities; return period for rainfall intensities

INTRODUCCIÓN

Los fenómenos naturales de intensidad de precipitación extrema en la zona central de Chile, provocan crecidas e inundaciones, principalmente en sectores urbanos, a causa de la evacuación de las aguas lluvias. Por ello, conocer las magnitudes y el comportamiento de las intensidades máximas de precipitación, asociadas a un periodo de retorno y a una duración, junto a una acertada planificación y realización de proyectos de diseño hidrológico, son elementos de vital importancia para el diseño de puentes o sistemas colectores de aguas pluviales (Espíldora, 1971; Mintegui y López, 1990; Llamas, 1993; Osborn, 2002). Por otro lado, se ha observado que en los sectores con presencia de embalses y lagos, las intensidades máximas no presentan el mismo comportamiento que en los sectores sin presencias de dichas masas (Pizarro *et al*. 2001; Cornejo, 2004; Macaya, 2004; Pavez, 2004). En este contexto, el presente estudio construye y analiza el comportamiento de las Curvas Intensidad–Duración–Frecuencia (IDF) para 31 estaciones pluviográficas, distr.-buidas en parte de la zona árida y semiárida de Chile, de las cuales 8 se encuentran ubicadas en la cercanía de embalses y lagos.

DESCRIPCIÓN DEL ÁREA DE ESTUDIO

El área de estudio comprende a 5 regiones de Chile central distribuidas entre los 29°02′ y 39°37′ de Latitud Sur y los 69°49′ de Longitud Oeste y el Océano Pacífico (I.G.M., 1985). Estas regiones corresponden, de Norte a Sur, a Coquimbo, Valparaíso, Metropolitana, Lib. Gral. Bernardo O'Higgins y Maule. Ellas se encuentran inmersas en un sistema climático mediterráneo, semiárido y subhúmedo y se caracteriza por la extrema variabilidad de las precipitaciones entre un año y otro,

Copyright © 2006 IAHS Press

observándose ciclos alternos que se descomponen en períodos muy lluviosos y períodos con precipitaciones por debajo de lo normal. La precitación media en un año normal en la zona central de Chile varía de 312 mm a 900 mm (D.M.C., 2002).

METODOLOGÍA

La metodología contempló en primer lugar, la selección de las estaciones pluviográficas, que en total fueron 31, distribuidas entre las regiones mencionadas anteriormente (Fig. 1). El criterio de selección fue la periodicidad de los datos, donde el registro mínimo fue de 10 años.

Las construcción de las curvas IDF, se basó en el método gráfico propuesto por Témez (1978), el que consistió en la selección de los valores extremos anuales de precitación a partir de las bandas pluviográficas de cada estación, asociadas a distintas duraciones (1; 2; 4; 6; 8; 12 y 24 horas).

Luego se obtuvo la intensidad máxima anual, en mm/h, dividiendo el valor de cada precipitación por su respectiva duración. Posteriormente, estos datos fueron ajustados a la Función de Distribución de Probabilidad de Gumbel, que presenta buenos ajustes para valores máximos de intensidades (Maidment, 1993; Sivapalan & Blöschl , 1998; Mohymont *et al*., 2004), la que se define como:

$$F(x) = P[\varepsilon \leq X] = e^{-e^{-\sigma(x-\mu)}} \qquad -\infty \leq X \leq \infty \tag{1}$$

Donde, X es el valor a asumir por la variable aleatoria *y* σ, μ son parámetros a estimar en función de los valores de la muestra.

De este modo, se obtuvieron las curvas IDF para los periodos de retorno de 5; 10; 20; 30; 40; 50; 60; 75 y 100 años, utilizando como medida de bondad de ajuste el Coeficiente de Determinación (R^2) y el Test de Kolmogorov-Smirnov.

Así, se obtuvieron familias de 9 curvas, asociadas a distintas intensidades, periodos de retorno y duraciones para cada estación, de las cuales se seleccionaron los valores de 1 y 24 horas, las que fueron comparadas gráficamente de norte a sur y para el periodo de retorno de 100 años.

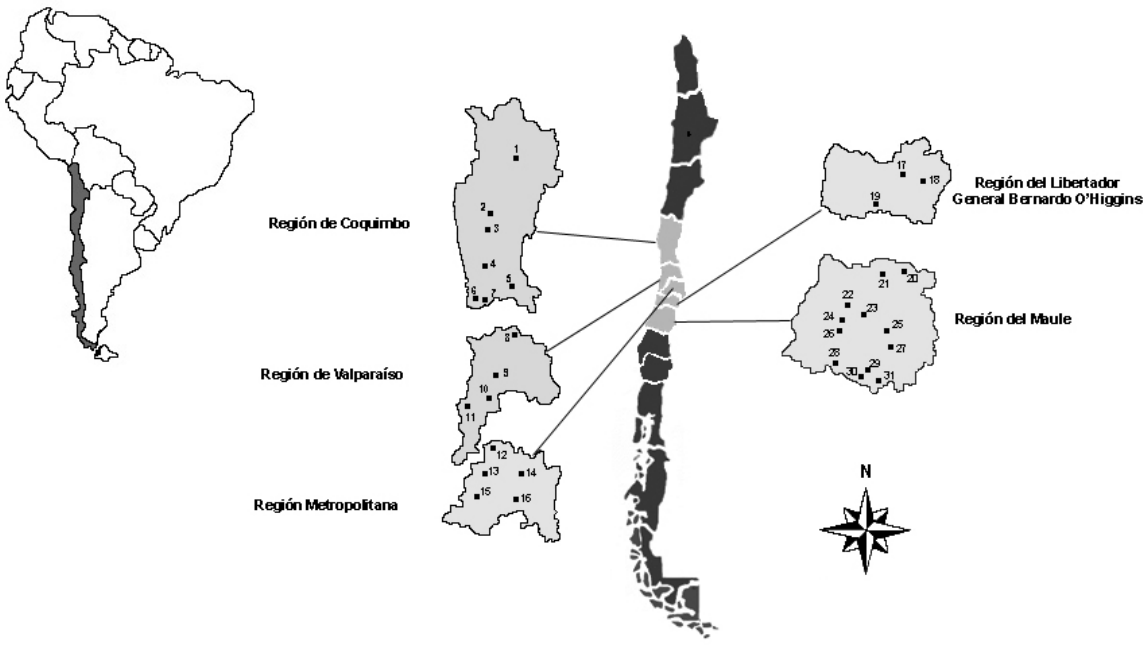


Fig. 1 Mapa de ubicación de las 31 estaciones pluviográficas de Chile Central.
1: Rivadavia, 2: Embalse la Paloma, 3: Embalse Cogote, 4: Illapel, 5: La Tranquilla, 6: Los Cóndores, 7: Quelón, 8: Hacienda Pedernal, 9: Quillota, 10: Embalse Lliu-Lliu, 11: Lago Peñuelas, 12: Embalse Rungue, 13: Los Panguiles, 14: Cerro Calán, 15: Melipilla, 16: Pirque, 17: Rengo, 18: Central las Nieves, 19: Convento Viejo, 20: Potrero Grande, 21: Los Queñes, 22: Pencahue, 23: Talca, 24: San Javier, 25: Colorado, 26: Melozal, 27: Embalse Ancoa, 28: Parral, 29: Embalse Digua, 30: San Manuel,31: Embalse Bullileo.

RESULTADOS Y DISCUSIÓN

La tabla 1 entrega los valores de las intensidades máximas de precipitación para la duración de 1 y 24 horas y para el periodo de retorno de 100 años.

En la tabla anterior, se advierte que no existe mucha diferencia entre algunas estaciones ubicadas al norte, como la estación Rivadavia, con estaciones ubicadas en la región del Maule, entre ellas San Javier y Talca, las que se encuentran a más de 750 km de distancia en línea recta.

Por otra parte, un hecho de gran relevancia que se observó, es que las intensidades más altas, se registraron en estaciones ubicadas cerca de cuerpos de agua, como Embalse la Paloma (23.4 mm h^{-1}) y Embalse Cogotí (20.4 mm h^{-1}), pertenecientes a la Región de Coquimbo (gráfico 6); Embalse Lliu-Lliu (31.8 mm h^{-1}) y Lago Peñuelas (37.4 mm h^{-1}), ubicadas en la Región de Valparaíso (gráfico 7); Embalse Digua (28.2 mm h^{-1}), Colorado (28.2 mm h^{-1}) y Embalse Bullileo (25.6 mm h^{-1}), pertenecientes a la Región del Maule, los que se vieron acrecentados con el periodo de retorno de 100 años.

Para determinar y comprobar el efecto producido por la presencia de cuerpos de agua sobre las intensidades máximas de precipitación, se realizó un análisis gráfico de las intensidades máximas, asociadas a los dos periodos de retorno y las duraciones consideradas (Fig. 2 y 3). Las estaciones se ordenaron de acuerdo a su latitud en forma creciente, es decir, de Norte a Sur. Asimismo, en la Fig. 2 se consideraron todas las estaciones, mientras que en la Fig. 3 fueron eliminadas las estaciones cercanas a cuerpos de agua.

De los gráficos anteriormente expuestos, se desprende que las intensidades máximas de precipitación asociadas a un periodo de retorno de 100 años, se distribuyen de forma creciente conforme se avanza en la latitud. Esta situación se hace más evidente para la duración de 1 hora en relación a la de 24 horas.

Tabla 1 Valores de intensidad de precipitación de 1 y 24 horas, para el periodo de retorno de 100 años.

Región	Estaciones	Intensidad de precipitación (mm h^{-1}) (periodo de retorno 100 años)	
		1 hora	24 horas
Coquimbo	Rivadavia	15.38	4.2
	Embalse La Paloma*	27.5	5.0
	Embalse Cogotí*	20.4	5.8
	Illapel	18.4	4.4
	La Tranquilla	17.1	4.1
	Los Cóndores	18.5	5.9
	Quelón	17.8	3.5
Valparaíso	Hacienda Pedernal	20.2	7.3
	Quillota	22.6	5.7
	Embalse Lliu-Lliu.*	31.8	10.9
	Lago Peñuelas.*	37.4	13.1
Metropolitana	Embalse Rungue*	18.8	6.2
	Cerro Calán	21.5	5.8
	Los Panguiles	19.2	6.9
	Pirque	18.4	6.0
	Melipilla	34.7	5.5
Libertador General	Rengo	21.4	5.4
Bernardo O'Higgins	Central las Nieves	19.4	8.3
	Convento Viejo	23.5	5.8
Maule	Los Queñes	30.1	7.7
	Potrero Grande	30.7	8.7
	Pencahue	19.6	4.5
	Talca	16.3	4.5
	San Javier	18.0	4.3
	Colorado*	28.2	7.5
	Melozal	22.7	6.1
	Embalse Ancoa	23.4	8.3
	Parral	23.7	6.1
	Embalse Digua*	30.9	8.7
	Embalse Bullileo*	25.6	9.0
	San Manuel	28.5	9.1

*****Estaciones cercanas a cuerpos de agua (embalses, lagos).

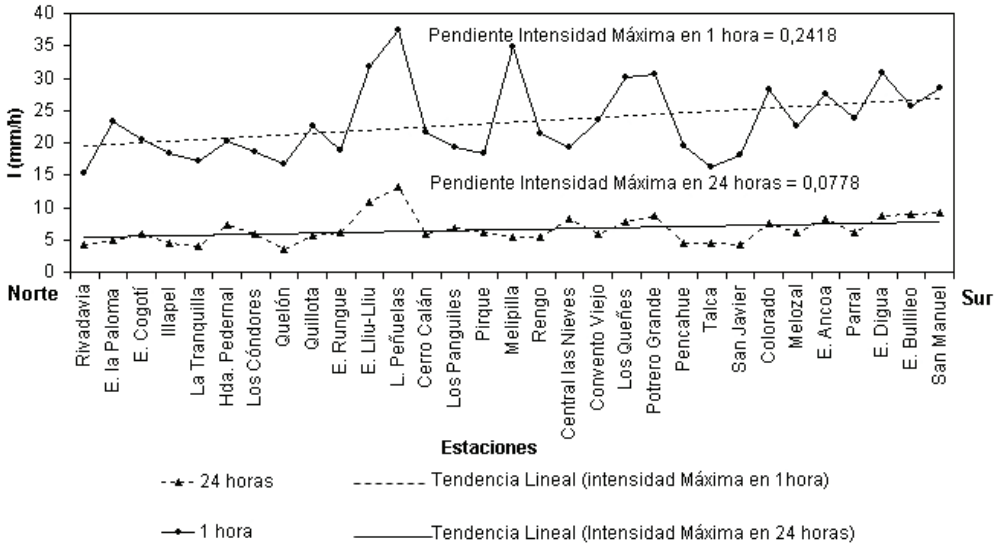


Fig. 2 Gráfico de intensidades de precipitación para un periodo de retorno de 100 años, considerando las estaciones cercanas a cuerpos de agua.

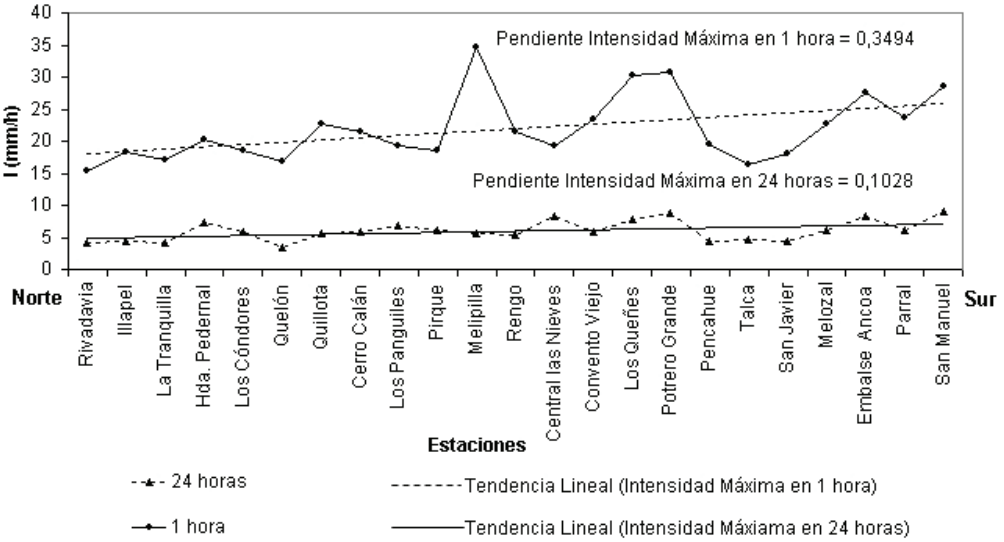


Fig. 3 Gráfico de intensidades de precipitación para un periodo de retorno de 100 años, sin considerar las estaciones cercanas a cuerpos de agua.

Por otro lado, las pendientes de las rectas con presencia de embalses fueron menores a la pendiente de la recta en ausencia de cuerpos de agua. Esta diferencia se hizo más evidente para la duración de 1 hora, que presentó un valor de 0.2418 para el conjunto de todas las estaciones (Fig. 2) y de 0.3494 al ser eliminadas las estaciones cercanas a cuerpos de agua (Fig. 3). Esto lleva a pensar que sí existe una influencia de los cuerpos de agua sobre las intensidades máximas de precipitación, principalmente en regiones ubicadas más al Norte, como la Región de Coquimbo y de Valparaíso, lo que provoca que la pendiente de la línea de tendencia de las intensidades sea menos acusada.

Para ratificar el efecto que los embalses o lagos, ya sean naturales o artificiales, tienen sobre las intensidades máximas, se graficó para cada región el promedio de todas las estaciones; luego, el promedio de todas las estaciones, excluyendo las cercanas a cuerpos de agua y el promedio de las estaciones cercanas a lagos y embalses. Estos fueron determinados para la duración de 1 hora y para 24 horas (Fig. 4(a) y 4(b), ambos para el periodo de retorno de 100 años. En estos gráficos fueron excluidas las regiones que no contaron con la presencia importante de embalses o lagos.

En ambos gráficos se observa claramente que la intensidad promedio de los lagos y embalses, es superior al promedio donde se consideran todas las estaciones y esta diferencia se acrecienta para

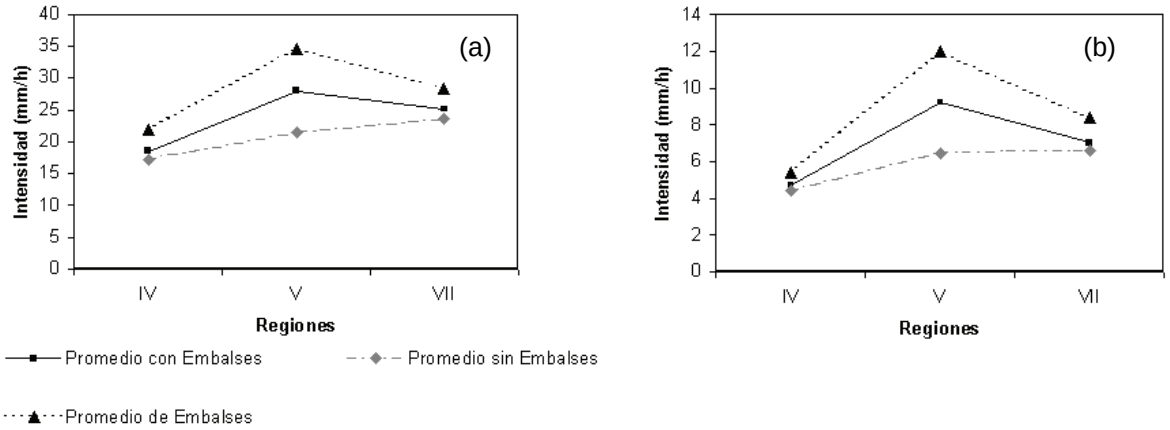


Fig. 4 Promedio regional de las intensidades máximas de precipitación para la duración de: (a) 1 hora y periodo de retorno de 100 años; (b) 24 horas y periodo de retorno de 100 años.

el promedio sin embalses. Además, para ambas duraciones, los promedios más altos están dados para la Región de Valparaíso, la que cuenta con la presencia de 2 embalses, el Lliu-Lliu y el Lago Peñuelas, los que presentaron intensidades de 31.8 y 37.4 mm h^{-1} respectivamente para la duración de 1 hora y 10.9 y 13.1 mm h^{-1} para la duración de 24 horas y el periodo de retorno de 100 años.

CONCLUSIONES

Se observó que algunas de las estaciones ubicadas en el extremo Norte de la zona de estudio, presentaron intensidades similares a las que se obtuvieron en la región del Maule, ubicada al Sur.

El análisis de intensidades máximas arroja un comportamiento de éstas que es levemente ascendente en magnitud de norte a sur.

En general, en casi todas las regiones, las estaciones cercanas a cuerpos de agua, registraron valores de intensidad superior al resto de de sus estaciones, por lo que se concluye que la presencia de cuerpos de agua, aumenta la magnitud de las intensidades, y con ello provoca que el aumento latitudinal de éstas sea más gradual.

REFERENCIAS

Cornejo, M. (2004) Determinación gráfica y matemática de las curvas Intensidad-Duración-Frecuencia en siete estaciones pluviográficas de la región de Coquimbo. Tesis para optar al título de Ingeniero Forestal. Universidad de Talca, Chile.

D.M.C. (Dirección Meteorológica de Chile) (2002) http://www.meteochile.cl.

Espíldora, B. (1971) Estimación de curvas intensidad-duración-frecuencia mediante coeficientes generalizados. *Memorias I Coloquio Nacional Sociedad Chilena de Ingeniería Hidráulica*. Chile.

I.G.M. (Instituto Geográfico Militar) (1985) *Atlas geográfico de Chile*. Talleres gráficos del Instituto Geográfico Militar de Santiago. Chile.

Llamas, J. (1993) *Hidrología general. Principios y aplicaciones.* Editorial Universitaria del País Vasco, Bilbao, España.

Macaya, K. (2004) Construcción de las Curvas Intensidad-Duración-Frecuencia (IDF) para estaciones pluviográficas de las regiones de Valparaíso y de O'Higgins, y análisis comparativo con algunas estaciones de las regiones Metropolitana y del Maule. Tesis para optar al título de Ingeniero Forestal. Universidad de Talca. Talca. Chile.

Maidment, D. (1993) *Handbook of hydrology*. Editorial Mc Graw-Hill. New York, USA.

Mintegui, J. & López, F. (1990) *La ordenación Agrohidrológica en la Planificación*. Servicio Central de Publicaciones del Gobierno Vasco, Vitoria – Gasteiz. Spain.

Mohymont, B., Demarée, G. & Faka, D. (2004) Establishment of IDF-curves for precipitation in the tropical area of Central Africa. Comparison of techniques and results. *Natural Hazards and Earth System Sciences*, **4**, 375–387. EGU.

Osborn, T. (2002) Observed and simulated changes in the distribution and extremes of precipitation over the UK. In: *Proc. EGS XXVII General Assembly, Nice*, vol. 27, 1862.

Pavéz, M. (2004) Determinación gráfica y matemática de las curvas Intensidad-Duración-Frecuencia (IDF), en seis estaciones pluviográficas de la Región del Maule. Tesis para optar al título de Ingeniero Forestal. Universidad de Talca. Talca. Chile.

Pizarro, R., Abarza, A. & Flores, J. (2001) Determinación de las curvas Intensidad-Duración-Frecuencia IDF, para 6 estaciones pluviográficas de la VII Región. Revista Virtual de UNESCO. http://biblioteca.unesco.org.uy.

Sivapalan, M. & Blöschl, G. (1998) Transformation of point rainfall to areal rainfall: Intensity–duration–frequency curves. *J. Hydrol*. **204**, 150–167.

Témez, J. (1978) *Cálculo hidrometeorológico de caudales máximos en pequeñas cuencas naturales*. Dirección General de Carreteras. Madrid. España.

Climate Variability and Change—Hydrological Impacts (Proceedings of the Fifth FRIEND World Conference held at Havana, Cuba, November 2006), IAHS Publ. 308, 2006.

Application of a statistical method for medium-term rainfall prediction

ZHONGMIN LIANG[1], BO LU[2] & XIAOFAN ZENG[3]

1 *State Key Laboratory of Hydrology-Water Resources and Hydraulic Engineering, Hohai University, Nanjing 210098, P.R. China*
zmliang@hhu.edu.cn

2 *Department of Civil & Architectural Engineering, Drexel University, Pennsylvania 19104, USA*

3 *Nanjing Institute of Geography and Limnology, Nanjing 210098, P.R. China*

Abstract This paper presents a statistical approach for prediction of medium-term rainfall class based on the correlation between rainfall and meteorological indicators, including geopotential height, temperature, dew-point deficit, wind direction and wind velocity. Total rainfall of a 10-day period during the rain season (July and August) is classified into two types (dry or wet) using the *K*-mean method. Meteorological indicators that influence rainfall are selected by the *F*-test method for rainfall type and rainfall class, and then used with a bi- or multi-discriminant method to establish prediction models. This procedure is applied to predict rainfall class with a three-day lead time for the Yuecheng basin in China. Results show that it is effective in medium-term rainfall prediction with relatively little data requirement.

Key words medium-term rainfall prediction; antecedent influencing factor (AIF); *K*-mean method; *F*-test method; multi-discriminant method

INTRODUCTION

Medium-term rainfall prediction, normally with a lead time of 3–10 days, plays an important role in flood prevention and drought reduction, and thus has economic benefits for water resources management. Nowadays, medium-term rainfall prediction is still developing and has not yet reached the skills of short-term hydrological forecasting, due to the uncertainty in the driving factors with increased lead time. Even though methods based on numerical weather forecasting have improved, their strict dependence on meteorological and climatic data limits their practical applications in most cases (Zwiers & Van Storch, 2004), thus a method with little data requirement should be of more practical use.

In this region of China (the Yuecheng basin), rainfall types (i.e. wet and dry) are considered to be different representations of different rainfall mechanisms. Therefore, the method suggested here first classifies rainfall into two types, and then, for each of these types, defines distinct models to predict how heavy/light the rainfall is.

The approach used for medium-term rainfall forecasting with a lead time of three days is based on statistical relations between rainfall and meteorological indicators. The procedure includes the following steps: (a) Calculate mean areal rainfall from the historical rainfall data of stations located within the study basin using the Thiessen polygon method (Thiessen, 1911), and calculate rainfall totals for separate 10-day periods of July and August. (b) Classify each 10-day rainfall into dry or wet type using the *K*-mean method. (c) For each 10-day period, select the Antecedent Influencing Factors (AIF) amongst the meteorological indicators showing the highest correlation with rainfall totals by the *F*-test method. (d) Define rainfall type prediction equations using the bi-discriminant method (Hand, 1981) with the AIF. (e) Establish daily rainfall class prediction models for both dry and wet rainfall types for each 10-day period. Four rainfall classes (P) were defined: no rain (i.e. $P < 0.1$mm), little rain ($0.1 \le P < 10$ mm), medium rain ($10 \le P < 25$ mm) and heavy rain ($P > 25$mm). For a given 10-day period, for example the first ten days of July, two groups (wet or dry type) are defined based on measured rainfall totals, and for each dry and wet group the corresponding AIF are selected. Daily rainfall class prediction models are then derived from a multi-discriminant approach (Joachimsthaler & Stam, 1988). This method can be applied for any day in July and August using the rainfall type prediction equation of the 10-day period, including that day to predict rainfall type first, and then using the rainfall class prediction equation in accord with the predicted rainfall type to predict the rainfall class of that day. It was tested on the Yuecheng reservoir basin.

Copyright © 2006 IAHS Press

METHODOLOGY

Mean areal rainfall calculation

Daily mean areal rainfall is computed by the Thiessen method with historical rainfall data from stations within the basin. The whole basin is divided into as many Thiessen polygons as rainfall stations, and areal rainfall for each polygon is considered equal to the rainfall of the station located within this polygon. The mean areal rainfall of the whole basin is given by:

$$\overline{P} = \frac{1}{A}\sum_{i=1}^{n} P_i a_i \tag{1}$$

where P_i and a_i are the mean areal rainfall and area of the polygon i respectively, while A represents the total area of the basin.

Classify rainfall type of historical data

Historical mean areal rainfall for each 10-day period of July and August are calculated, defining six sample series. The *K*-mean method is used to classify the rainfall type (dry or wet type) for each 10-day period. For example, consider the first ten days of July. Suppose there are m historical years, the series of mean areal rainfall samples being denoted as $x_1,x_2,\ldots,x_m$. Define the two samples x_1,x_2, as the two groups (wet and dry) centres; the larger value is attributed to the wet type. Calculate the absolute distance between the group centre and all the samples values, i.e. $|x_i - x_1|$ and $|x_i - x_2|$ ($i = 3,4,...,m$). The smaller distance to x_1 or x_2 determines which type the sample belongs to. If a sample is at the same distance from x_1 and x_2, then it can belong to either group type. Subsequently, the samples can be divided into two groups. Set the mean sample value of each group as a new group centre and repeat the previous steps. This process is iterated until the difference between the last two group centres of the same type can be neglected, e.g. smaller than 0.001. This procedure is repeated for all six 10-day periods.

Antecedent influencing factors

The AIF are selected from meteorological indicators of ten upper-air stations, including geopotential height, temperature, dew-point deficit, wind direction and wind velocity at the 850 hPa, 750 hPa and 500 hPa pressure fields. For a three-day lead forecast, observations three days ahead of each day of the 10-day period of July or August are considered.

For example, to select the AIF for the first 10-day period of July, first, compute the *F*-statistic value for each meteorological factor on each pressure field from each upper-air station, e.g. temperature on 700 hPa pressure field of Nanning station as:

$$F = \frac{\sum_{g=1}^{G} N_g(\overline{x}_g - \overline{x})^2/(N-G)}{\sum_{g=1}^{G}\sum_{k=1}^{N_g}(x_{kg} - \overline{x}_g)^2/(N-2)} \tag{2}$$

where, g represents two classified types and G equals to two; N is the total number of years, while N_1 is dry-type years and N_2 is wet-type years ($N_1 + N_2 = N$); $\overline{x}$ is the mean indicator value of all years, while $\overline{x}_g$ is the mean indicator value of dry or wet type years; x_{kg} is the sample indicator value, i.e. temperature on the 700 hPa pressure field of Nanning upper-air station on 28 June in the kth year of g type group. The larger the *F*-value, the larger the difference between $\overline{x}_g$ and $\overline{x}$, and the better the classification, thus the more effective the factor to determine the rainfall type. A factor is selected as AIF if its *F*-statistic is larger than the criterion value F_α, taken from the *F*-distribution.

Those selected factors could be different meteorological indicators of the same upper-air station, or the same meteorological indicators at a different upper-air station, and they were not classified as dry-type or wet-type factors.

Rainfall type prediction equation

With the selected AIF, the bi-discriminant method (Kim & Moy, 2002) is used to define rainfall type prediction equation for each 10-day period. The basic discriminant function is a linear composition of m factors, $x_1,\ldots,x_m$ with weight coefficient $c_k (k = 1,\ldots m)$ respectively, expressed as:

$$y = \sum_{k=1}^{m} c_k x_k \tag{3}$$

where c_k is determined based on Fisher rule, and y is the forecasted rainfall type.

All the historical years being sorted into two categories dry type (A) and wet type (B) for each 10-day period, the discriminant criterion y_c is computed as:

$$y_c = \frac{N_A \bar{y}^A + N_B \bar{y}^B}{N_A + N_B} \tag{4}$$

where $\bar{y}^A, \bar{y}^B$ are mean discriminant function values y of years of dry and wet type N_A, N_B respectively.

The rainfall type of a given 10-day period can be forecast by comparing the values of y and y_c. Two cases are included:

(a) when $\bar{y}^A > \bar{y}^B$, if $y > y_c$, then y belongs to category A, i.e. dry type; if $y < y_c$, then y belongs to category B, i.e. wet type.

b) when $\bar{y}^A < \bar{y}^B$, if $y < y_c$, then y belongs to category A, i.e. dry type; if $y > y_c$, then y belongs to category B, i.e. wet type.

Daily rainfall class prediction equation

Prediction equations for daily rainfall class are constructed for both dry and wet types. Similarly to the rainfall type prediction equation, select the AIF for predicting the rainfall class of each rainfall type for each 10-day period. Take the dry type of the first ten days in July as an example: from the rainfall totals, determine the daily rainfall class of 1 July to 10 July in dry-type years, select the AIF amongst the rainfall type 3-day lead meteorological indicators (28 June to 7 July) using the F-test method. In equation (2), G represents the number of rainfall classes, equal to four; N is the dry-type years, while N_g is the sample number of g (g = 1,…4) rainfall classes. The final AIF are selected from the F-statistic values. The multi-discriminant method is used to define the daily rainfall class prediction equation from the selected AIF. Similarly to the bi-discriminant method, a linear function is constructed, i.e. a prediction function for rainfall class, as in equation (3), in which the discriminant coefficient c_k is determined by the Fisher rule. For a given day, y is used to determine the rainfall class category as follows:

$$M^{(g)} = \frac{1}{N_g} \frac{\left| y - \bar{y}^{(g)} \right|}{\sigma^{(g)}} \qquad \bar{y}^{(g)} = \sum_{i=1}^{m} c_i \bar{x}_i^{(g)} \qquad \sigma^{(g)} = \sqrt{\frac{1}{N_g - 1} c s^{(g)} c'} \tag{5}$$

where c' is the transposed of matrix (c_1, c_2,…c_m) and s^g is the matrix of correlation coefficient computed in determining c_k. The category of the predicted value is that corresponding to the smallest value of M.

APPLICATION

Basin description

The Yuecheng reservoir is situated on the mainstream of the Zhanghe River, which crosses the boundary between Hebei and He'nan provinces in China (Figs 1 and 2). The controlling area is about 18 100 km^2, which takes up nearly 99.4% of the Zhanghe basin. It is located in the eastern Asian monsoon region of the temperate zone where the climate is influenced by the topography, thus hot and rainy in summer, with storms concentrating in July and August, and dry and cold in winter.

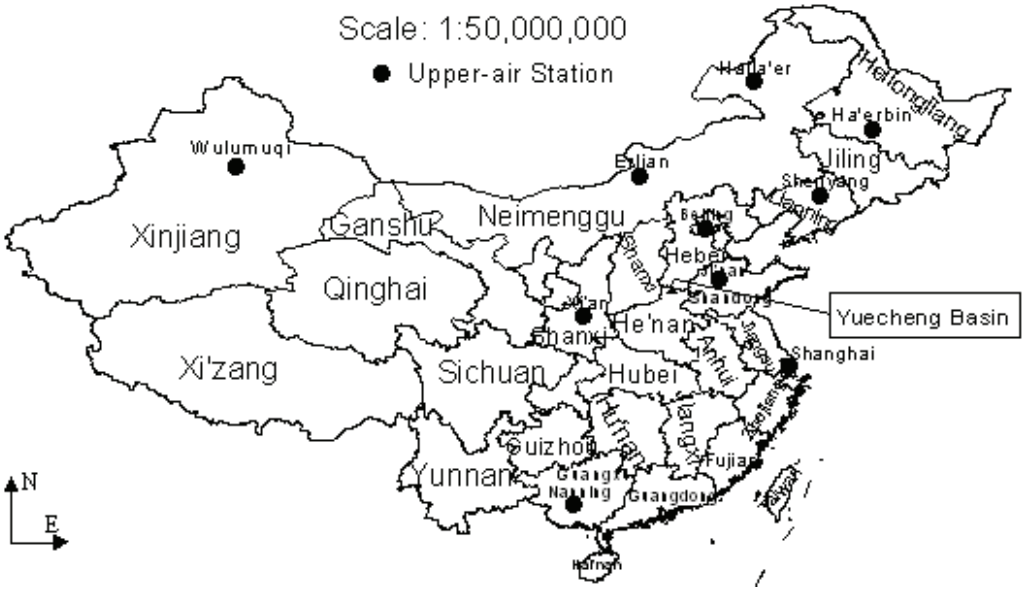


Fig. 1 Distribution of upper-air stations selected for obtaining meteorological data.

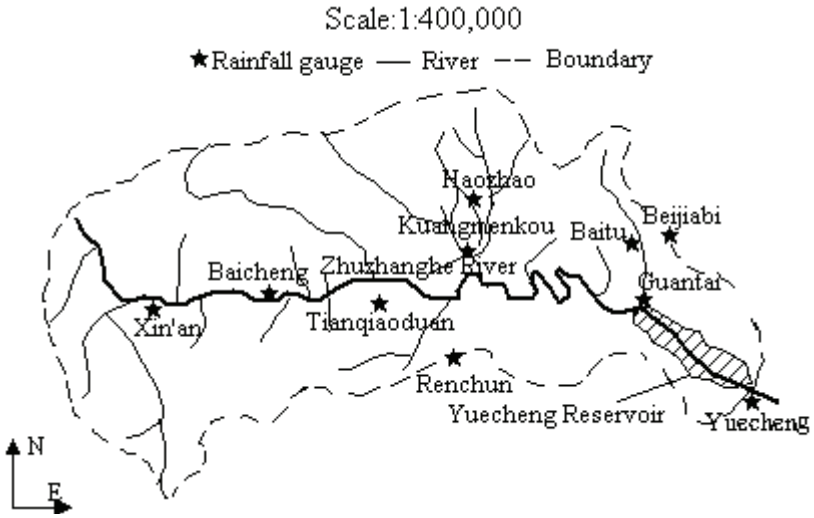


Fig. 2 Distribution of raingauges in the Yuecheng reservoir basin

Meteorological indicators

Meteorological indicators were obtained from ten upper-air stations around China, including Haila'er, Ha'erbin, Wulumuqi, Erlian, Shenyang, Beijing, Ji'nan, Xi'an, Shanghai and Nanning (Fig. 1). Daily upper-air meteorological records of geopotential height (HHHH), temperature (TTTT), dew-point deficit (UUU), wind direction (DDD) and wind velocity (FFF) on 850 hPa, 700 hPa and 500 hPa pressure fields were selected as potential antecedent factors for the prediction models. Meteorological data were collected for the rainfall record period, from 28 June to 29 August in 1980 to 1993. Records of the first twelve years were used for model calibration and that of the last two years (1992–1993) were used for model verification.

RESULTS ANALYSIS

Daily mean areal rainfall series are computed by averaging rainfall from all rainfall gauges using the Thiessen polygon method. Total rainfall of the six 10- (or 11-) day periods of July and August were calculated from 1980 to 1991 and daily rainfall class was identified into four classes. Rainfall data of each 10-day period were partitioned into dry or wet type by the *K*-mean method (Table 1). Meteorological factors discriminating rainfall type were selected by the *F*-test method. *F*-statistic

Table 1 Classification of rainfall type in July and August from 1980 to 1991 in Yuecheng.

Time	Rainfall type	In July	In August
First ten days	Dry type	1980–1982,1984–1986,1988–1991	1980,1982,1984–1986,1988–1991
	Wet type	1983,1987	1981,1983,1987
Second ten days	Dry type	1981–1986,1988–1989	1982–1986,1988–1991
	Wet type	1980,1987,1990–1991	1980–1981,1987
Last eleven days	Dry type	1980,1982–1986,1989–1991	1980–1983,1985–1990
	Wet type	1981,1987–1988	1984,1991

values were computed for all meteorological indicators and compared with the *F*-distribution table. Using the criteria α as 0.05 and 0.1 showed little difference in the number of selected AIF, and 12 indicators were finally selected for each 10-day period. For example, in the first 10-day period of July, the selected AIF are Xi'an_700_FFF (wind velocity on 700 hPa field of Xi'an upper-air station), Shenyang_850_FFF, Haila'er_500_HHHH, Ji'nan_500_FFF, Ji'nan_700_FFF, Beijing_500_UUU, Wulumuqi_850_HHHH, Ha'erbin_850_DDD, Haila'er_850_TTTT, Shanghai_850_TTTT, and Shanghai_500_HHHH. For each rainfall type in each period, the daily rainfall class prediction model is built similarly. Considering the practical application and accuracy requirement, four influencing factors for predicting rainfall classes were selected (Table 2) and the prediction functions were defined (Table 3). Equations for predicting rainfall types are not listed due to the space limitation. The accuracy of the prediction of daily rainfall classes for July and August 1992–1993 is about 86%, which satisfies the requirement for operational rainfall prediction.

Table 2 Factors selected to construct discriminant functions for rainfall class prediction.

Time	Rainfall	X_1	X_2	X_3	X_4
July First ten-day	Dry	Xi'an_700_FFF	Shenyang_850_FFF	Haila'er_500_HHHH	Er'lian_850_HHHH
	Wet	Beijing_500_UUU	Wulumuqi_850_HHHH	Ha'erbin_850_DDD	Haila'er_850_TTTT
July Second ten-day	Dry	Shenyang_500_DDD	Haila'er_500_UUU	Er'lian_850_HHHH	Wulumuqi_850_HHHH
	Wet	Nanning_850_FFF	Nanning_700_FFF	Nanning_500_FFF	Shenyang_850_UUU
July Last eleven-day	Dry	Erlian_700_DDD	Nanning_700_HHHH	Haila'er_700_HHHH	Haila'er_500_HHHH
	Wet	Shenyang_850_DDD	Shanghai_500_HHHH	Shanghai_700_TTTT	Shanghai_700_HHHH
August First ten-day	Dry	Ha'erbin_700_UUU	Haila'er_700_FFF	Shanghai_850_UUU	Nanning_850_HHHH
	Wet	Shanghai_850_FFF	Shenyang_500_DDD	Shanghai_500_FFF	Nanning_850_DDD
August Second ten-day	Dry	Erlian_500_FFF	Haila'er_500_TTTT	Wulumuqi _500_FFF	Wulumuqi_700_HHHH
	Wet	Wulumuqi_700_DDD	Wulumuqi_500_FFF	Wulumuqi_700_UUU	Wulumuqi_700_TTTT
August Last eleven-day	Dry	Xi'an_500_DDD	Nanning_850_UUU	Nanning_500_FFF	Haila'er_700_FFF
	Wet	Beijing_850_UUU	Jinan_700_FFF	Shanghai_850_UUU	Haila'er_500_UUU

Table 3 Discriminant functions for rainfall class prediction of Yuecheng basin.

Time	Rainfall type	Discriminant function (in July)	Discriminant function (in August)
First ten–day	Dry type	$Y = -0.65X_1 + X_2 - 0.12X_3 - 0.08X_4$	$Y = -0.06X_1 + X_2 - 0.21X_3 + 0.28X_4$
	Wet type	$Y = -0.60X_1. + X_2 - 0.31X_3 - 0.54X_4$	$Y = -X_1 + 0.04X_2 - 0.15X_3 + 0.02X_4$
Second ten–day	Dry type	$Y = 0.69X_1 - 0.54X_2 + 0.98X_3 + X_4$	$Y = X_1 + 0.04X_2 - 0.02X_3 + 0.06X_4$
	Wet type	$Y = -X_1 + 0.23X_2 - 0.04X_3 + 0.10X_4$	$Y = -0.20X_1 + X_2 - 0.12X_3 - 0.19X_4$
Last eleven-day	Dry type	$Y = 0.16X_1$-$0.07X_2 - 0.49X_3 + X_4$	$Y = 0.11X_1 - 0.03X_2 + X_3 - 0.76X_4$
	Wet type	$Y = 0.03X_1 + X_2 - 0.08X_3 - 0.05X_4$	$Y = 0.41X_1 + X_2$-$0.27X_3 + 0.11X_4$

Table 4 Number of days that forecasted rainfall class matches with observation

Year	Month	Rainfall type of ten-day period: First	Second	Third	Number of days that forecast matches observation	Relative error (%)
1992	July	Dry	Wet	Wet	27	87.1
	August	Wet	Dry	Dry	28	90.3
1993	July	Wet	Wet	Wet	21	67.7
	August	Wet	Dry	Dry	27	87.1

CONCLUSIONS

In this study, a statistical model was designed for predicting medium-term rainfall classes. Rainfall types for 10-day periods in July and August from 1983 to 1991 were classified by the *K*-mean method, and four rainfall classes defined. The *F*-test method was adopted to select the meteorological indicators significant for predicting rainfall type and rainfall classes independently. With these selected factors, a rainfall-type forecasting model was built using the bi-discriminant method, while the model for rainfall class prediction was derived from a multi-discriminant analysis, thus predictions of both the rainfall type for each 10-day period and rainfall class for each day of the period were obtained.

The procedure was applied to rainfall prediction with a 3-day lead time for Yuecheng reservoir basin. Results show comparatively high forecasting skills with good forecast for about 86% of days. This approach does not require much data, and the required meteorological data could be easily obtained in operational forecast. It is thus a valuable alternative for medium-term rainfall forecast. With better selection of key meteorological factors, the forecasting accuracy of this approach could be improved.

REFERENCES

Hand, D. J. (1981) *Discrimination and Classification*. Wiley, New York, USA.

Joachimsthaler, E. A. & Stam, A. (1988) Four approaches to the classification problem in discriminant analysis: an experimental study. *Decision Sciences* **19**, 322–333.

Kim, F. L. & Moy, J. W. (2002) Combining discriminant methods in solving classification problems in two-group discriminant analysis. *European J. Operational Research* **138**, 294–301.

Thiessen, A. H. (1911) Precipitation for large areas. *Monthly Weather Review* **39**, 1082–1084.

Zwiers F. W. & Von Storch, J. (2004) On the role of statistics in climate research. *Int. J. Climatology* **24**, 665–680

Climate Variability and Change—Hydrological Impacts (Proceedings of the Fifth FRIEND World Conference held at Havana, Cuba, November 2006), IAHS Publ. 308, 2006.

Evaluación de la incertidumbre en la variabilidad espacial de la precipitación usando un modelamiento multiGaussiano

SOLANGE DUSSAUBAT[1], XIMENA VARGAS[1] & JULIAN ORTIZ[2]

1 *Departamento de Ingeniería Civil, Universidad de Chile, Blanco Encalada 2002, Santiago, Chile*
sdussaub@ing.uchile.cl

2 *Departamento de Ingeniería de Minas, Universidad de Chile, Av. Tupper 2069, Santiago, Chile*

Resumen En este trabajo se estudia el modelamiento de la incertidumbre, proponiendo el uso de distribuciones de probabilidad condicional a través del modelo multiGaussiano en una zona cordillerana de la VII Región del Maule, Chile. Para esto se utilizó información extraída del modelo de pronóstico del tiempo MM5-DGF de dos tormentas ocurridas en el año 2002. Los resultados de la media condicional y la varianza condicional en el área de estudio evidencian el carácter heterocedástico de la variable, lo que permite argumentar que la varianza no sólo depende de la configuración geométrica de los datos, sino que varía de acuerdo al valor estimado en cada sitio.

Palabras claves incertidumbre; modelo multiGaussiano; kriging; variabilidad espacial de la precipitación; varianza de estimación; heterocedasticidad; homocedasticidad

Evaluation of the uncertainty of spatial precipitation variability using a multiGaussian model

Abstract. The modelling of the uncertainty of spatial precipitation variability is studied in a mountainous zone at the Maule Region, Chile. Forecast data for two storms that occurred in 2002, which were extracted from the results of the meteorological model MM5-DGF, are used to recommend the use of a conditional probability distribution through the multiGaussian model. The heteroscedasticity of the variable is demonstrated through the results obtained for the conditional mean and the conditional variance in the region, which shows that the variance depends on the geometric configuration of the data and, also, on the estimated value at each site.

Key words uncertainty; multiGaussian model; kriging; precipitation spatial variability; estimation variance; heteroscedasticity; homoscedasticity

INTRODUCCION

En la actualidad, resulta de gran interés contar con valores confiables de la precipitación, puesto que constituyen el cimiento de múltiples propósitos en la gestión misma del recurso hídrico y, por ende, es interesante evaluar la incertidumbre existente en su determinación.

Al realizar un proceso de estimación a través de métodos geoestadísticos se trata de predecir el valor de una variable partiendo de una malla de observaciones. Debido a que la varianza de estimación del kriging depende de la configuración geométrica de los sitios con información y no del valor registrado, muchos autores plantean que ésta es una excelente medida de incertidumbre, y que es una buena herramienta para el mejoramiento, diseño u optimización de una red de estaciones. Sin embargo, en este trabajo se cuestiona su uso como la mejor forma para cuantificar la incertidumbre, esencialmente porque la homocedasticidad es una situación raramente encontrada en la práctica.

El índice de incertidumbre más común es el intervalo de confianza, sin embargo, difícilmente puede ser usado directamente para toma de decisiones, principalmente porque es expresado como un intervalo simétrico y porque, además, proporciona información muy limitada. En este sentido, la función de distribución de probabilidad proporciona considerablemente más información que un simple intervalo de confianza, ya que, entre otras cosas, puede ser usada para describir intervalos de confianza asimétricos o para describir la probabilidad de exceder algún valor umbral (Isaaks & Srivastava, 1989). Como modelo de incertidumbre permite contar con una herramienta de múltiples aplicaciones para la toma de decisión según se requiera en cada caso.

En este trabajo se estudia el modelamiento de la incertidumbre, propiamente tal, proponiendo el uso de distribuciones de probabilidad condicional a través del modelo multiGaussiano en una zona cordillerana de la VII Región del Maule, Chile.

Copyright © 2006 IAHS Press

EL MODELO MULTIGAUSSIANO

Se tienen N+1 variables $Z(x_0)$, $Z(x_1)$, …, $Z(x_N)$, y se transforman a $N + 1$ variables normales estandarizadas $Y(x_0)$, $Y(x_1)$, …, $Y(x_N)$, mediante una transformación adecuada. Sobre las variables estandarizadas, se establece la hipótesis básica del modelo, que consiste en suponer que el vector $(Y(x_0), Y(x_1), \ldots, Y(x_N))'$ tiene una distribución Gaussiana multivariada, y es caracterizado por la matriz de covarianzas σ_{ij}, $(i,j = 0, 1,\ldots, N)$. La distribución condicional de $Y(x_0)$ es, por ende, Gaussiana (Chilès & Delfiner, 1999):

$$Y(x_0) \mid \{Y(x_a) : \alpha = 1,..., N\} = Y_{SK}^{*} + \sigma_{SK} K \quad (1)$$

donde Y_{SK}^* es el estimador del kriging simple de $Y(x_0)$ a partir $\{Y(x_\alpha):\alpha = 1, \ldots N\}$; σ_{SK} es la desviación estándar del kriging asociada; K es una desviación normal estándar independiente (error del kriging estandarizado).

La información condicionante se concentra en el estimador de kriging simple, Y_{SK}^*. El supuesto del modelo multiGaussiano es prácticamente incomprobable, por lo que se verifica que las distribuciones bivariadas sean Gaussianas (Chilès & Delfiner, 1999).

Las etapas para aplicar el kriging multiGaussiano son las siguientes:

1. Distribución representativa: se debe contar con un histograma que sea representativo, vale decir, que no exista un efecto de clusters o grupos de datos.
2. Transformación de los datos originales a una distribución normal estandarizada: la primera condición para que la función aleatoria $Y(x)$ sea normalmente multivariada, es que su función distribución acumulada univariada (histograma) sea normal estandarizada, vale decir, de media cero y varianza uno (Deutsch & Journel, 1998).
3. Verificación de la hipótesis multiGaussiana: la transformación de los datos a una distribución normal estandarizada es una condición necesaria pero no suficiente para que los valores $Y(x)$, distribuidos espacialmente sean normales multivariados. Luego, se debe verificar que la función de distribución acumulada de cualquier par de valores $Y(x)$, $Y(x+h)$, $\forall x$, $\forall h$, sea bivariada normal (Deutsch & Journel, 1998).

   Hay varias maneras de chequear que la distribución de dos puntos (bivariada) de datos sea normal $\{y(x_\alpha),\alpha = 1,\ldots N\}$. Un método consiste en verificar que el valor de la función de distribución bivariada experimental de cualquier conjunto de pares de datos separados por el mismo vector h $\{y(x_\alpha),y(x_\alpha + h),\alpha = 1, \ldots N(h)\}$ sea comparable con el modelo teórico biGaussiano (ver Goovaerts, 1997). Lo anterior se traduce en comparar variogramas de indicadores de los datos con los variogramas de indicadores de una variable multiGaussiana con la misma función de covarianza.

   Otro test consiste en verificar que bajo la hipótesis biGaussiana, el variograma de orden 1 o madograma, $\gamma_Y^{(1)}(h)$, es proporcional a la raíz del variograma usual $\gamma_Y(h)$, vale decir, $\sqrt{\gamma_y(h)} \Big/ \gamma_Y^{(1)}(h) = \sqrt{\pi}$, independiente del valor de h (Emery, 2000).

   Finalmente, se chequea gráficamente que la función de distribución acumulada (bivariada) es biGaussiana. Para esto, se grafican las características de una función de densidad conjunta para dos variables aleatorias, X e Y, y las marginales asociadas.
4. Estimación para determinar las distribuciones condicionales: en el caso multiGaussiano, la distribución es Gaussiana, el estimador de kriging simple se identifica con la media condicional y la varianza de kriging simple con la varianza condicional.
5. Transformación inversa de las distribuciones condicionales: para obtener las distribuciones condicionales de la variable original es necesario realizar numéricamente la transformación inversa de la distribución condicional Gaussiana.

APLICACION

Área de estudio

La zona escogida para evaluar la incertidumbre en la variabilidad espacial de la precipitación, es la zona cordillerana de la Séptima Región de Chile, específicamente entre los paralelos 35.5° y 36.7°

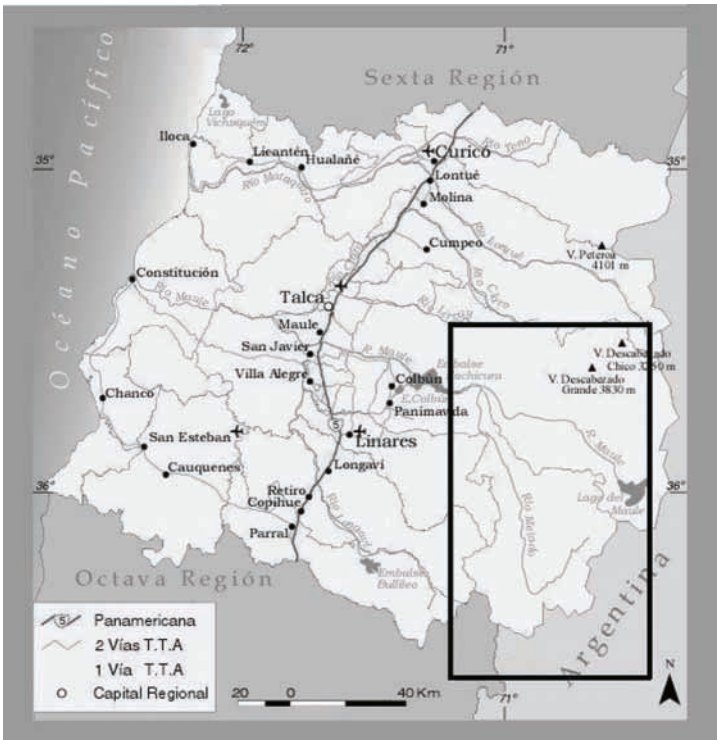


Fig. 1 Mapa de la Séptima Región del Maule, Chile. Se destaca zona de estudio.

Latitud Sur, y los meridianos 70.4° y 71.2° Longitud Oeste. Esta región abarca la mayor parte de la zona cordillerana de la hoya del río Maule, cubriendo un área aproximada de 11 880 km^2 (ver Fig. 1).

Información disponible

Debido a que dentro del área de estudio existen sólo dos estaciones pluviográficas y una de ruta de nieve, lo que resulta insuficiente para caracterizar en forma adecuada la variabilidad espacial de la precipitación, se optó por utilizar datos generados con el modelo regional de pronóstico del tiempo MM5. Este modelo numérico, desarrollado en la Universidad de Pensilvania, ha sido implementado por el departamento de Geofísica de la Universidad de Chile (DGF) en forma operacional desde Abril del 2002 como un apoyo al pronóstico del tiempo en la región central del país. Este modelo, inicializado diariamente, pronostica la circulación atmosférica en Chile central tomando en cuenta un horizonte temporal de tres días. El modelo opera con tres dominios anidados, denominados Dominio 1, 2 y 3, con resoluciones de 135, 45 y 15 [km]. El MM5-DGF permite conocer la distribución temporal y espacial de una serie de variables meteorológicas, de las cuales se obtiene como subproducto la precipitación.

Según la resolución del modelo de pronóstico MM5-DGF en el Dominio 3, el área de estudio corresponde a una grilla de 84 elementos MM5-DGF, siete en dirección Este por doce en dirección Norte.

Para evaluar la incertidumbre en la variabilidad espacial de la precipitación se utilizó información disponible de dos tormentas ocurridas durante el año 2002. Para contemplar sólo la variable espacial se decidió utilizar los datos de precipitación total ocurrida por evento.

Uso de kriging MultiGaussiano: Tormenta del 13 al 18 de Septiembre del año 2002

La transformación de los datos originales a una distribución normal estandarizada se realizó directamente a través del módulo “nscore.exe” del paquete geoestadístico GSLIB (Deutsch & Journel, 1998), que calcula la probabilidad acumulada de los datos usando la fórmula de Hazer (ver Fig. 2). Los resultados gráficos de los tests biGaussianos (Fig. 3) indican que es adecuado aceptar la hipótesis multiGaussiana.

Luego, se procede a aplicar un kriging simple a los datos transformados. Como se mencionó anteriormente, el estimador de kriging simple se identifica con la esperanza condicional y la varianza

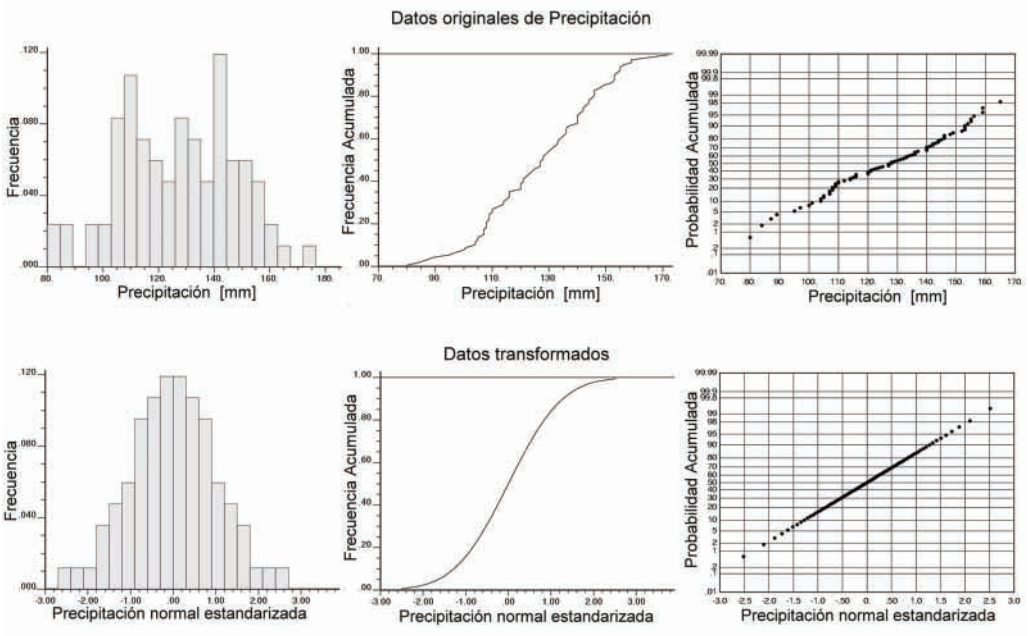


Fig. 2 Transformación de los datos originales a una normal estandarizada. Tormenta del 13 al 18 de Septiembre del 2002.

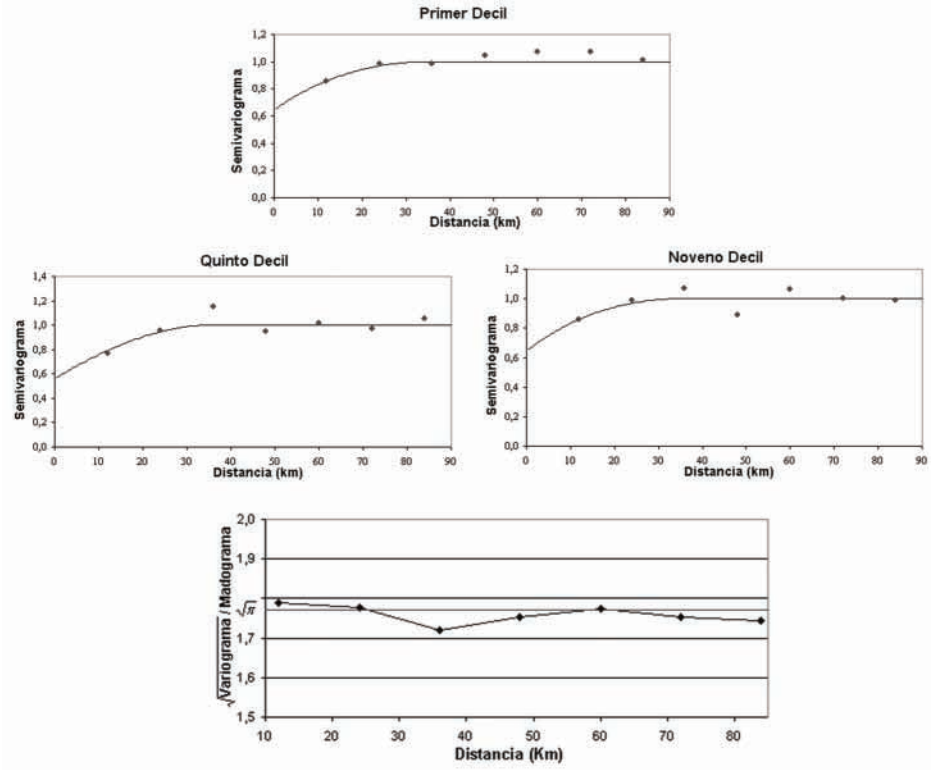


Fig. 3 Tests de binormalidad – Tormenta del 13 al 18 de Septiembre del 2002.

del kriging se identifica con la varianza condicional. Los resultados obtenidos son presentados en la Fig. 4. Aquí se destaca el carácter homocedástico de la varianza condicional, la cual no depende de los valores medidos, sino que exclusivamente de la configuración geométrica de los datos y del modelo de covarianza adoptado.

Para obtener las distribuciones condicionales de la variable original (precipitación), se debe realizar la transformación inversa de la distribución condicional Gaussiana definida en el espacio *Y*. Para esta transformación se utilizó el programa "postMG" (Ortiz *et al.*, 2004), el cual realiza un

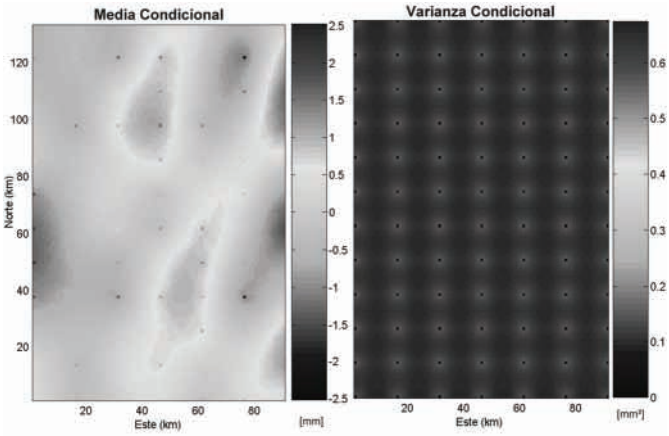


Fig. 4 Media condicional y varianza condicional de la variable transformada. Tormenta del 13 al 18 de Septiembre del 2002.

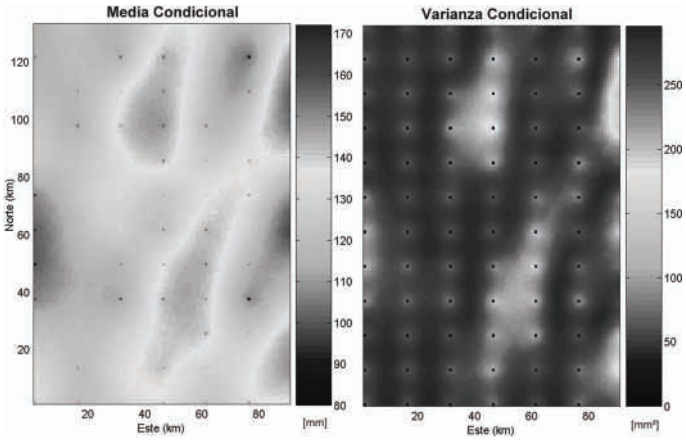


Fig. 5 Media condicional y varianza condicional de la variable original (precipitación).Tormenta del 13 al 18 de Septiembre del 2002.

muestreo regular de los cuantiles con una transformación inversa de cada uno, usando la relación entre las distribuciones globales (a priori).

Finalmente, después de la transformación respectiva se obtiene la media condicional y la varianza condicional de la función de distribución acumulada en el espacio de la variable original (precipitación), siendo ambas presentadas de forma "local" en la Fig. 5. En esta imagen se ve que la varianza condicional es heterocedástica, con una clara variación de acuerdo a los datos registrados por el modelo MM5-DGF. La incertidumbre tiende a ser menor en las zonas extremas, vale decir, donde se registran los valores más altos y más bajos de precipitación. Por el contrario, la incertidumbre aumenta en las zonas en donde los valores estimados son cercanos a la media global de la muestra.

Uso de kriging multiGaussiano: Tormenta del 19 al 24 de Julio del 2002

Procediendo en forma análoga al caso anterior, se verifica la hipótesis multiGaussiana y se aplica el modelamiento respectivo. Los principales resultados se muestran en la Fig. 6 en donde se observa la media condicional y la varianza condicional de la variable original (precipitación).

En la Fig. 7 se presenta la varianza condicional en función de la media en el espacio de la variable original para las dos tormentas analizadas. En esta figura se observa que la varianza condicional en ambas tormentas es mayor para los valores cercanos al promedio.

CONCLUSIONES

Los resultados obtenidos ponen en evidencia el carácter heterocedástico de la variable precipitación. Los lugares que presentan mayor incertidumbre son los sitios intermedios entre zonas homogéneas de mayor o menor precipitación.

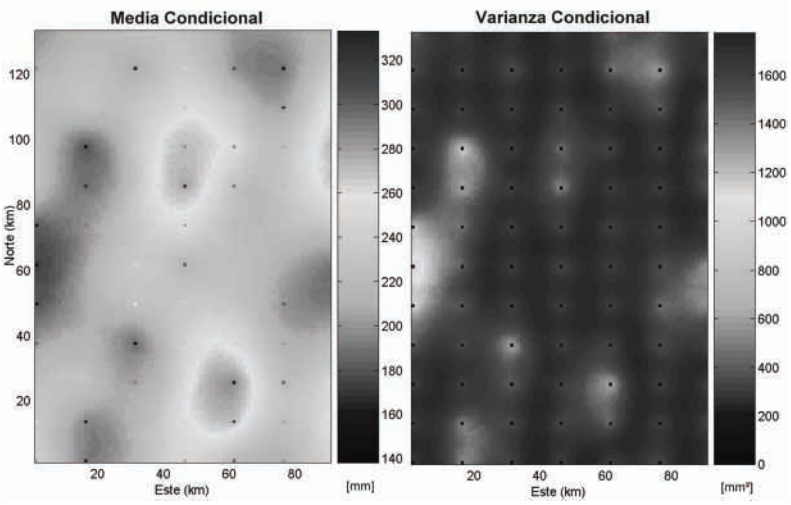


Fig. 6 Media condicional y varianza condicional de la variable original (precipitación). Tormenta del 19 al 24 de Julio del 2002.

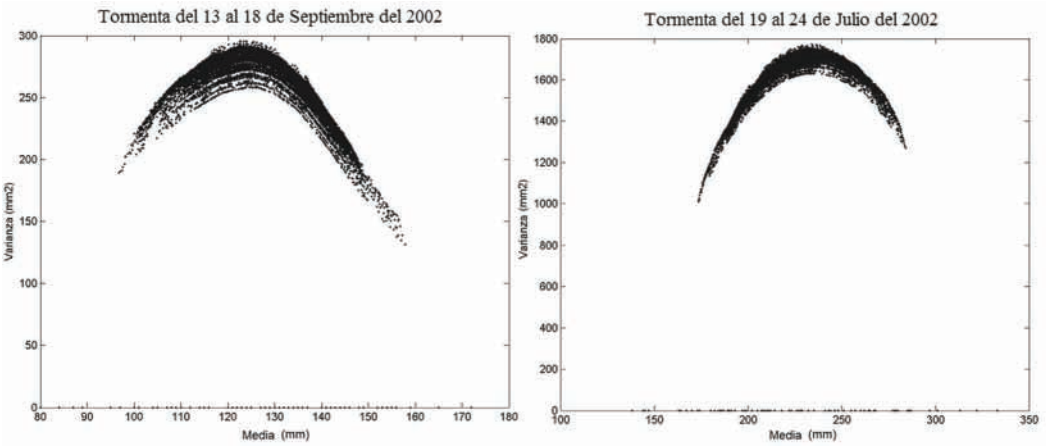


Fig. 7 Media condicional versus varianza condicional. Izquierda: Tormenta del 13 al 18 de Septiembre del 2002. Derecha: Tormenta del 19 al 24 de Julio del 2002.

Todo lo anterior permite argumentar que la incertidumbre no sólo depende de la configuración geométrica de los sitios con información, sino que varía de acuerdo al valor estimado en cada punto.

Es importante destacar, que antes de aplicar el kriging multiGaussiano, es fundamental verificar que los datos transformados cumplan con la hipótesis biGaussiana. Se puede destacar que las dos tormentas analizadas presentan un comportamiento binormal que permite aceptar la hipótesis planteada.

Se concluye finalmente que el uso de funciones de distribución de probabilidad condicional a través de un modelamiento multiGaussiano constituye una poderosa herramienta que permite evaluar la incertidumbre de la precipitación dentro de un área.

REFERENCIAS

Chilès, J. P. & Delfiner, P. (1999) *Geostatistics: Modeling Spatial Uncertainty*. Wiley-Interscience, New York, USA.

Deutsch, C. V. & Journel, A.G. (1998) *GSLIB: Geostatistical Software Library and User's Guide* (second edn). Oxford University Press, New York, USA.

Emery, X. (2000) *Geoestadística Lineal.* Universidad de Chile, Facultad de Ciencias Físicas y Matemáticas, Departamento Ingeniería de Minas.

Goovaerts, P. (1997) *Geostatistics for Natural Resources Evaluation.* Oxford University Press, New-York, USA.

Isaaks, E. H., & Srivastava, R. M. (1989) *An Introduction to Applied Geostatistics*. Oxford University Press, New York, USA

Ortiz, J. M., Leuangthong, O. & Deutsch, C. V. (2004) A multiGaussian approach to assess block grade uncertainty. CIM Conference and Exhibition, Edmonton 2004, May 9 to 12.

Climate Variability and Change—Hydrological Impacts (Proceedings of the Fifth FRIEND World Conference held at Havana, Cuba, November 2006), IAHS Publ. 308, 2006.

Deriving the highest persisting monthly 24-hour dew points in Malaysia for the estimation of PMP

M. N. MOHD DESA & P. R. RAKHECHA
HTC Kuala Lumpur, No 2 Jalan Ledang off Jalan Duta, 50480 Kuala Lumpur, Malaysia
drmohdnor@water.gov.my

Abstract The daily dew point records of 24 meteorological stations in Malaysia, for the 10 years 1994–2003, have been used to provide generalized maps of the highest persisting 24-hour 1000 mb dew points for each month of the year, ranging between 24 and 26ºC. These dew point maps can be used for obtaining the climatologically highest amount of atmospheric moisture that might be expected to occur over any location in Malaysia from tables such as those given in WMO (1986) needed for storm maximization and consequently for estimation of the probable maximum precipitation, PMP.

Key words dew point; probable maximum precipitation; moisture maximization factor, precipitable water

INTRODUCTION

Malaysia (Fig. 1) has an equatorial climate with high temperatures and high humidity of over 80% year round, except in the highlands. The country is greatly influenced by both the southwest (June –September) and the northeast (November–February) monsoons. These monsoons bring heavy rainfall all over the country resulting in severe floods. There are many places in Malaysia which have recorded about 400 to 800 mm of rainfall within a period of 24 hours (Desa *et al*., 2001, 2003; Desa & Rakhecha, 2004). It is of considerable importance in flood hydrology to find out the maximum possible rainfall for a given duration in a given location. Conceptually this value can be seen as the upper bound of rainfall amount, the probable maximum precipitation (PMP) (WMO, 1986, 1994). Estimates of PMP are required for the derivation of probable maximum flood (PMF) for spillways of large dams.

There are two basic methods of PMP estimation, the statistical method and the physical or hydrometeorological method. Most countries often prefer the physical method based on the transposition and moisture maximization of rainfall depths obtained from the major rainstorms. Moisture maximization is the enhancement of storm rainfalls by a numerical factor known as the Moisture Maximization Factor (MMF). The MMF is calculated as the ratio of the highest amount of moisture or precipitable water (W_m) that might be expected in the study area to the amount of moisture estimated in the concerned storm (W_s). The main purpose of moisture maximization is to estimate the upper bound of rainfall. The most important factor in moisture maximization is the estimation of the highest amount of atmospheric moisture in the study area and the amount of moisture in the storm.

The US Weather Bureau (1960) and Reitan (1963) showed that the moisture in an air mass that produces high rainfalls can be estimated from the surface dew point temperatures decreasing with height at the saturated pseudo-adiabatic lapse rate. In such moisture maximization studies, the climatological highest value of atmospheric moisture in the specific area is estimated from the highest persisting 12-h or 24-h dew points ever recorded. On the other hand, the amount of the moisture during the storm is estimated from the highest 12-h or 24-h persisting dew points of the air which produced the rain. Thus, the information on the highest 12-h or 24-h persisting dew points, based on the long period of data for various months of the year at several stations in Malaysia, has potential value in estimating the highest amount of moisture for PMP work. Many countries such as Australia (Bureau of Meteorology, 1994), India (Rakhecha *et al*., 1990), Pakistan (Malik, 1964) and USA (US Weather Bureau, 1960) have published mapped values of the highest 12-h or 24-h persisting dew points, but this information is not published for Malaysia.

This paper presents maps of the highest 24-h persistent dew points generated for Malaysia that can be used to obtain the highest values of moisture that might be expected at any location in Malaysia.

Copyright © 2006 IAHS Press

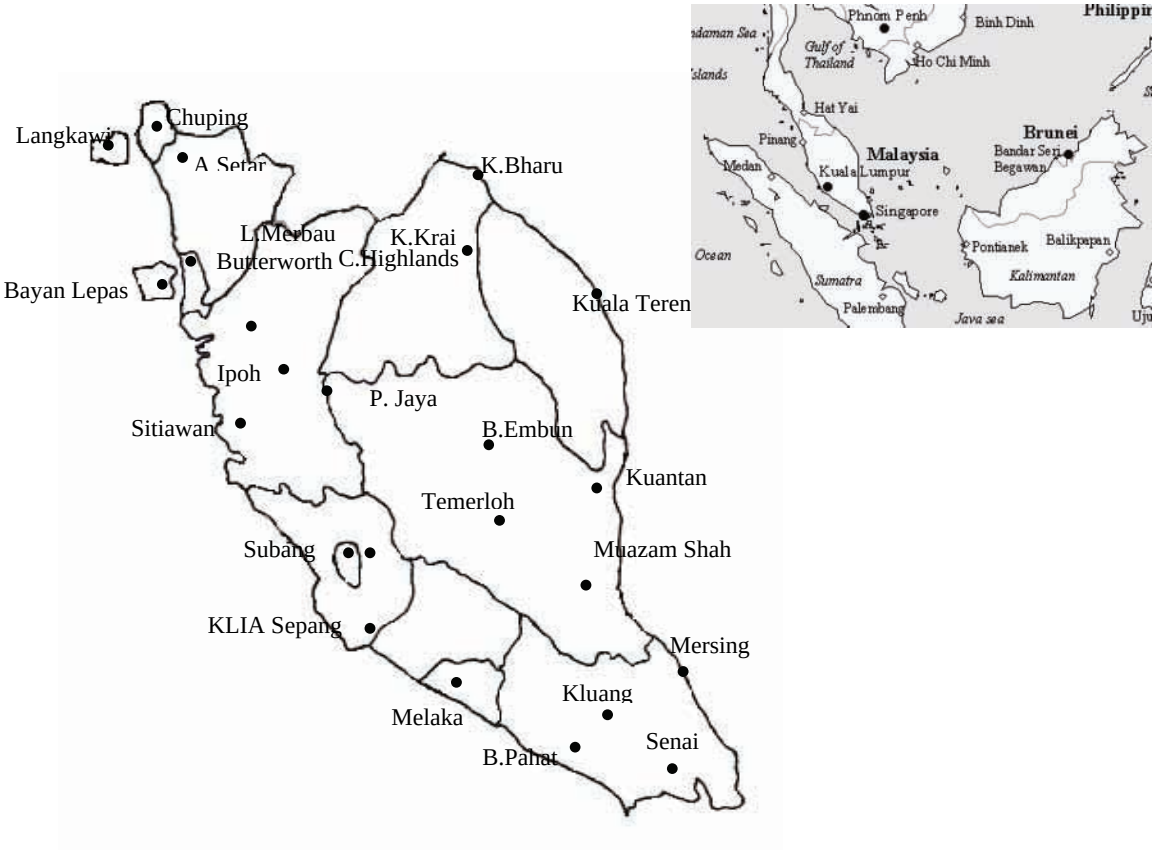


Fig. 1 Locations of meteorological stations in Peninsular Malaysia used for the study (not to scale).

DEFINITIONS OF PERSISTING AND HIGHEST PERSISTING DEW POINTS

The amount of moisture in an air mass can be calculated from the single observation of the highest dew point temperature, but the method has synoptic limitations and such measurements are susceptible to observational error (WMO, 1986). The moisture itself must persist for a period of several hours rather than minutes. The dew point value used to estimate the storm and the highest moisture over an area should be based on all dew point observations during period of 12 or 24 hours. The lowest temperature of all observations during the 12- or 24-h period is called the 12-h or 24-h persisting dew point temperature. For example, Table 1 shows a series of dew points observed at 12 hourly intervals on four days, varying from 20 to 24°C. It shows that the 24-h persisting dew points are 22°C, 23°C, 23°C, 24°C, 20°C and 20°C. Hence, the highest persisting 24-h dew point from the series is 24°C.

Table 1 Dew points observed at 12 hourly intervals.

	Day 1		Day 2		Day 3		Day 4	
Time(GMT)	00	12	00	12	00	12	00	12
Dew point °C	22°	23°	23°	24°	26°	24°	20°	21°
24-hr persisting dew point °C	22		23	23	24	20	20	

DATA USED

The daily dew point temperatures at meteorological stations are continuously observed by the Malaysian Meteorological Service (MMS). For this study, the daily dew point temperatures and the daily minimum temperatures for 24 stations for a period of 10 years, from 1994–2003, and for all 12 months, January to December, were used (Fig. 1 and Table 2).

Table 2 Geographical characteristics of stations used.

Station	Height (m)	(°N)	(°E)	Station	Height (m)	(°N)	(°E)
P. Langkawi	6.4	6° 20′	99° 44′	Batu Embun	59.5	3° 58′	100° 21′
Bayan Lepas	–	5° 18′	100° 16′	Subang	16.5	3° 07′	101° 33′
Butterworth	2.8	5° 28′	100° 23′	Petaling Jaya	45.7	3° 08′	101° 39′
Alor Setar	3.9	6° 12′	100° 24′	Muadzam Shah	33.3	3° 03′	103° 05′
Chuping	21.7	6° 29′	100° 16′	KLIA Sepang	–	2° 43′	100° 42′
Kota Bahru	4.6	6° 10′	102° 19′	Temerloh	39.1	3° 28′	100° 23′
Kuala Krai	68.3	5° 32′	100° 12′	Kuantan	15.3	3° 47′	103° 13′
K. Terengganu	35.1	5° 23′	103° 0′	Melaka	8.5	2° 16′	102° 15′
Setiawan	7	4° 13′	100° 42′	Batu Pahat	–	1° 52′	102° 59′
Lubuk Merbau	–	4° 48′	100° 34′	Kluang	88.1	2° 01′	103° 19′
Ipoh	40.1	4° 34′	101° 08′	Mersing	43.6	2° 17′	103° 50′
Cameron Highlands	1545	4° 28′	101° 22′	Senai	–	1° 30′	103° 40′

DETERMINATION OF THE HIGHEST 24-h PERSISTING DEW POINTS

In determining the 24-h persisting dew point, the daily dew point values of all observation times during the 24-h period were examined for their reliability, and then the lowest of these values was selected as the 24-h persisting dew point. Daily minimum temperatures were also used to ensure that the dew point persisting for any period had not exceeded the minimum temperature observed during the period.

A series of 24-h persisting dew points for each month, January to December, for each of the 10 years were determined for each station. Thus, the maximum persisting dew points for each month and for all years were determined and the highest, out of these was taken as the highest persisting 24-h dew point for that month. The monthly highest persisting dew point values for each station were reduced pseudo-adiabatically to the 1000 mb level so that the estimates at stations at different elevations would be comparable (WMO, 1986).

GENERALIZED MAPS OF THE HIGHEST 24-HR PERSISTING DEW POINTS

The monthly highest persisting 24-h dew point values of 24 stations were plotted on the maps of Malaysia and isotherms were drawn. The resulting generalized maps for January to December are shown in Figs 2 and 3 The spatial pattern of the highest persisting dew points, which is a measure of the climatologically highest moisture over an area, depends upon the direction of moisture flow, topographic barriers and other geographic factors. The isotherms of the highest dew points range from about 24ºC to 25ºC in January–March and in July–December, and from 24ºC to 26ºC in April–June. The coastal areas receive heavy rainfalls from the southwest and northeast monsoons consistent with the high degree of moisture and highest dew points observed around the coasts. The low values of dew points are observed in the interior parts of the country extending from north to south, reflecting the decreasing effect of the inflowing moist currents of the southwest and northeast monsoons.

These dew point maps can be used to determine the highest persisting 24-h dew point for any location during January–December in Malaysia. Moreover, these maps will help in maintaining consistency and uniformity between estimates of dew points in various parts of the country.

MOISTURE AND PRECIPITABLE WATER

The estimation of moisture in the air is extremely useful for storm maximisation. The moisture content of air is the amount of water vapour present in the air. It is highly variable in space and time. The concentration can be as high as about four per cent by volume in hot humid air to more than a hundred times less in very cold air and as such is related to the temperature of the air (WMO, 1986). The temperature at which the unsaturated air becomes saturated when cooled at a constant pressure is the dew point temperature.

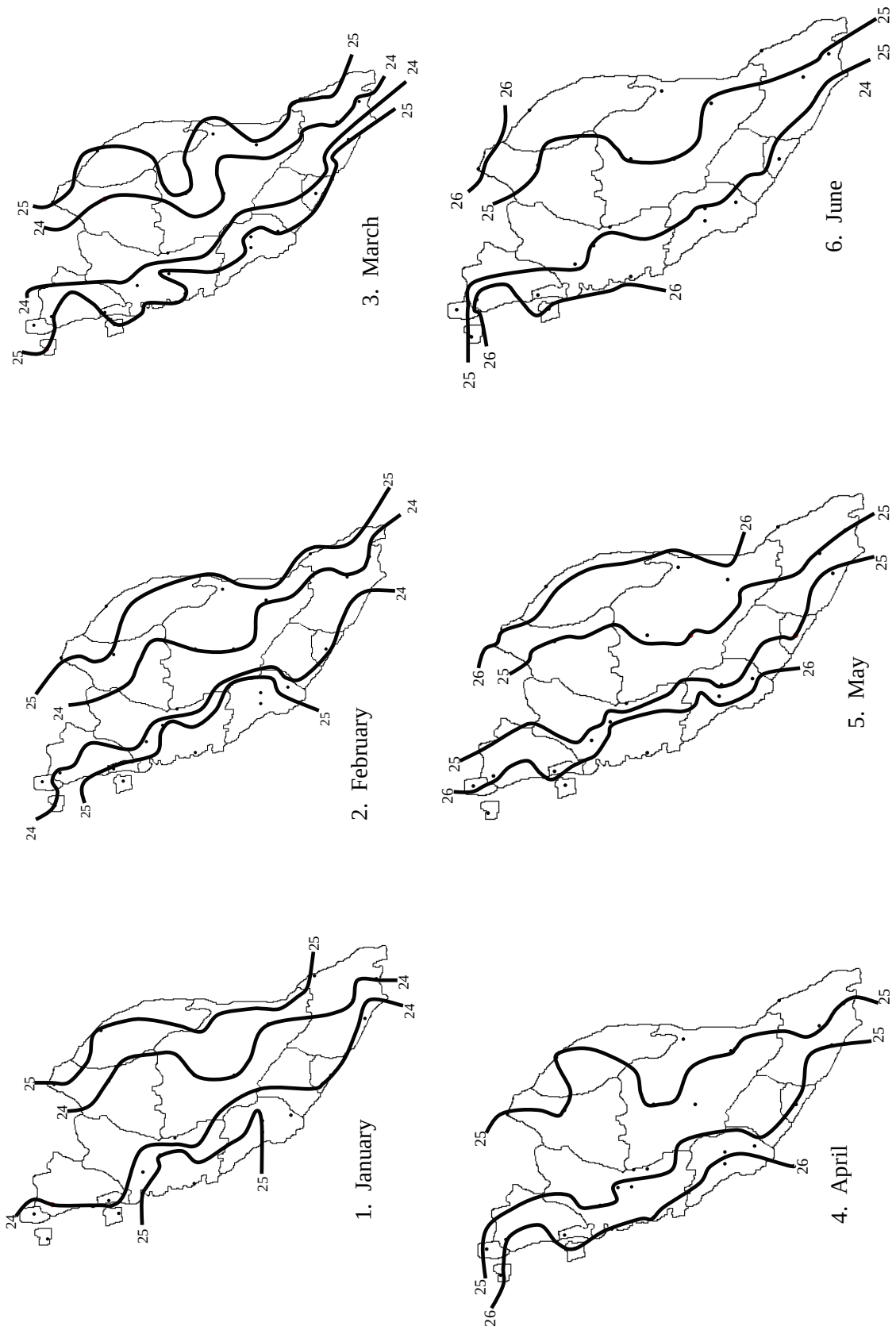


Fig. 2 Highest persisting dew points (°C) for 24-hours 1000 mb for January to June (not to scale).

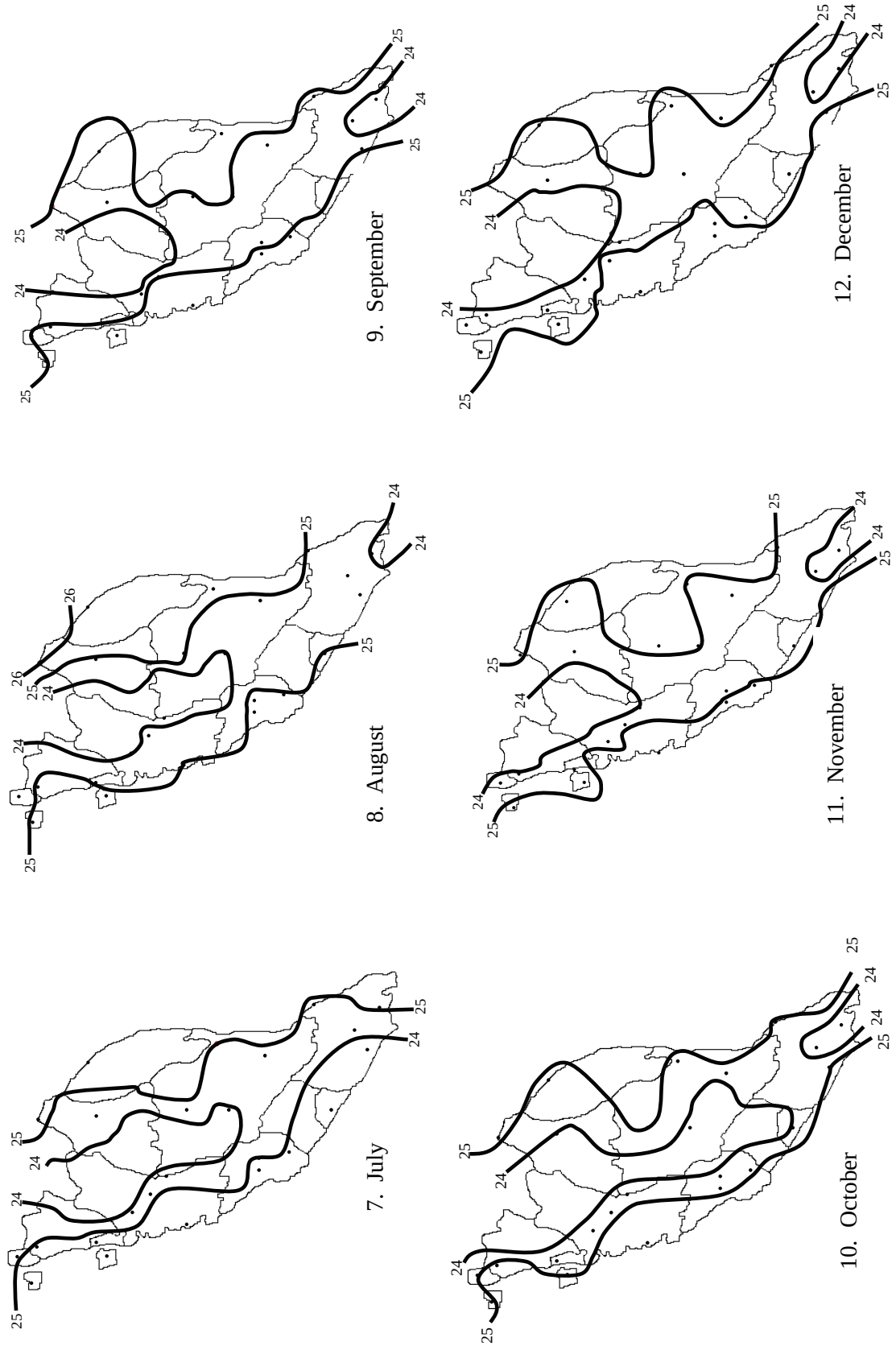


Fig. 3 Highest persisting dew points (°C) for 24-hours 1000 mb for July to December (not to scale).

The moisture content in the air is expressed in terms of the precipitable water, which refers to the amount of liquid water that would form in an air column of unit cross section if all the water vapour in it (extending from the surface to the top of the atmosphere) were condensed. It is expressed in height in millimetres or inches. The largest part of the vapour content of the atmosphere is present in the lower layers, close to the ground. If the dew point and the pressure in a given volume of air are known, the amount of water vapour in the volume can be determined by thermo-dynamic considerations. In the case of the atmosphere, however, the dew point is known only at the surface. So when determining the total precipitable water, the assumption is made that the dew point in the atmosphere varies with altitude according to the pseudo-adiabatic lapse rate. This assumption has been used to compute the precipitable water in a column of the air from different values of dew points.

The depth of precipitable water from the 1000 mb surface to various altitudes or pressure levels as a function of the 1000 mb dew point are given in Eihle *et al*. (1968) and WMO (1986). However, in storm maximization, only the depth of precipitable water from the 1000 mb to the 200 mb level is used. The 200 mb level is generally accepted as the top of the storm (WMO, 1986). Table 3 gives the depth of precipitable water in the column of air from 1000 mb to 200 mb in a saturated pseudo-adiabatic atmosphere as a function of the 1000 mb dew point for use in storm maximization. The precipitable water in a column of air above the 1000 mb level corresponding to a dew point of 25ºC at 1000 mb level is 80.8 mm. If continuous soundings are available, the amount of precipitable water (W) in a column of air of height Z can also be calculated as:

$$W = \int_0^z d_w \, dz \tag{1}$$

$$= \int_0^p \frac{d_w}{d_a * g} dp \tag{2}$$

$$= \int_0^p \frac{q \; dp}{g} \tag{3}$$

where d_a and d_w are the densities of air and water vapour respectively, q is the specific humidity, p is the atmospheric pressure at altitude z, and g is the acceleration due to gravity. The above equations can be used to determine the precipitable water between two levels in an air mass knowing the variation of humidity and pressure with height.

Table 3 The depth of precipitable water (mm) between the 1000 mb surface and 200 mb levels in a saturated pseudo-adiabatic atmosphere as a function of the 1000 mb dew points (ºC).

Dew point (ºC)	Precipitable water (mm)	Dew point (ºC)	Precipitable water (mm)	Dew point (ºC)	Precipitable water (mm)
19.0	48.3	23.0	67.9	27.0	95.9
19.5	50.4	23.5	71.0	27.5	100.1
20.0	52.6	24.0	74.3	28.0	104.5
20.5	54.8	24.5	77.5	28.5	109.1
21.0	57.1	25.0	80.8	29.0	113.9
21.5	59.5	25.5	84.3	29.5	118.9
22.0	62.1	26.0	88.0	30.0	124.2
22.5	64.9	26.5	91.9		

MOISTURE MAXIMIZATION

The moisture maximization of an observed storm rainfall aims to determine the rainfall which would result if the moisture available to the storm was the highest (maximized) over the entire project area. The moisture maximization factor (*MMF*) which is applied to the observed rainfall is defined as the ratio of the climatological highest precipitable water (W_m) to the precipitable water estimated for the storm concerned (W_s). Mathematically:

$$MMF = W_m / W_s \tag{4}$$

Let us assume a rainstorm occurring in November. The representative persisting 24-h, 1000 mb dew point for the storm is 23ºC and the highest persisting 24-h 1000 mb dew point where the storm is transposed is 25ºC, for example near Temerloh. The MMF is computed as follows:

1. Storm dew point = 23ºC
2. Storm precipitable water between 1000 mb and 200 mb (W_s) = 67.9 mm (Table 3)
3. Highest persisting dew point over the area = 25ºC
4. Precipitable water between 1000 mb and 200 mb (W_m) = 80.8 mm (Table 3)
5. Using equation (4), *MMF* = 1.19

The maximized rainfall is given by the product of MMF and the observed rainfall.

CONCLUSIONS

The paper presents a contribution to the knowledge on the highest persisting dew points for Malaysia. The results are presented in mapped form, and should help in calculating the highest moisture content of the atmosphere for any location within the country for any PMP studies.

Acknowledgements The assistance rendered by Mr Lim Boon Seng, Mr Ahmad Zaki Mohamad Saad and Ms Khazainani Salleh from the Malaysian Meterological Services in computing the data are gratefully acknowledged. The authors also express thanks to IRPA (the Ministry of Science and Innovation Malaysia) for kindly providing the financial grant for the study. Last but not least the authors would like to thank Ms Khamsiah Abdul Wahab for helping to plot Figs 2 and 3.

REFERENCES

Bureau of Meteorology (1994) *The Estimation of Probable Maximum Precipitation in Australia: Generalised Short-Duration Method*. Bulletin 53, AGPS, Canberra, Australia.

Desa, M. N. & Rakhecha, P. R. (2004) Characteristics of short duration extreme rainfalls in Selangor, Malaysia. *Weather RmetS* **59**(3), 63–66.

Desa M. N., Sharifuddin, S. & Rakhecha, P. R. (2003) Predicting Malay rain. *International Water Power and Dam Construction* **Nov. 2003**, 37–39.

Desa, M. N., Noriah A. B. & Rakhecha, P. R. (2001) Probable maximum precipitation fo 24-hrs duration over Southeast Asian Monsoon region – Selangor Malaysia. *Atmos. Res.* **58**, 41–54.

Eihle, W. O., Powers, R. J. & Clark, R. A. (1968) Meteorological tables for determination of precipitable water, temperatures, and pressures aloft for a saturated pseudo-adiabatic atmosphere. *Tech. Report no.16, Water Resources Institute*. Texas A and M University, Texas, USA.

Malik, F. M. (1964) Highest persisting dewpoints in the northern region of West Pakistan for June through October. *Sci. Note, vol. 16, 1, Department of Meteorology and Geophysics*, Pakistan.

Rakhecha, P. R., Deshpande, N. R. & Nandargi, S. S. (1990) Maximum persisting dewpoints during the Southwest Monsoon season over India. *Mausam* **41**(1), 140–142.

Reitan, C. H. (1963) Surface dewpoint and water vapour aloft. *J. Appl. Met*. **2**, 776–779.

US Weather Bureau (1960) Sheet of National Atlas of the United States. Maximum Persisting 12-h 1,000 mb Dewpoints – Monthly and of Record. *Tech. Paper No.38.* U.S Weather Bureau.

WMO (1986) Manual for Estimation of PMP. *Operational Hydrology Report no. 1, WMO no. 332*, (second edn).

WMO (1994) *Guide to Hydrological Practices.* WMO – TD no.168.

Climate Variability and Change—Hydrological Impacts (Proceedings of the Fifth FRIEND World Conference held at Havana, Cuba, November 2006), IAHS Publ. 308, 2006.

Multi-decadal variability of rainfall and water resources in Nigeria

OLUSEGUN ADEAGA
Department of Geography, University of Lagos, Nigeria
oadeaga@yahoo.com

Abstract The over-dependence of the economic development process within sub-Saharan Africa on water calls for detailed assessment of the probable impact of climate change on hydrology and water resources within the region. This paper examines the effect of total annual and decadal rainfall fluctuations on the hydrological regime within Ogun-Oshun River Basin Development Authority (Nigeria).

Key words decadal rainfall analysis; rainfall anomalies estimation; hydrological regime; water resources

INTRODUCTION

The hydrology of large parts of sub-Saharan Africa is characterized by temporal and spatial variability of rainfall which has engendered in the region an uneven areal distribution of fresh-water resources over space and time (Ojo, 1987).

Unfortunately, the human activities within the region are highly dependent on water, with little or no resilience to hydrological hazards (flood and droughts) which have major impacts on both the natural and human environments, causing loss of life, damage to infrastructure and socio-economic activities (Gash *et al*., 2001).

Also, it is expected that per capita renewable freshwater supply will drop by 80% in Africa by the year 2025 while the greater part of Sub-Saharan Africa will be experiencing a water scarcity situation (UNEP, 2000). The scarcity situation is due to the stress on the limited available water supply in Africa which can be attributed to both natural and human threats (Gash *et al*., 2001). The natural threats include the present trends in climate change and variability, shrinking of major water bodies (for example, Lake Chad basin) and desertification. The human threats include increased water demand occasioned by the growing population and their socio-economic activities: rapid urbanization, depletion of water quality status, environmental degradation and deforestation, as well as unsustainable management and financing of investments in water supply and sanitation. It should be noted that Nigeria has the eighth largest national population in the world and about a quarter of the total population of all the countries in Sub-Saharan Africa.

Thus, if available water resources within the region are to be wisely managed for the growing population in the 21st century and beyond (Shiklomanov, 1998), assessing the temporal fluctuations of hydroclimatic processes and most especially rainfall, which constitutes the main source of water input, and estimation of the regional water balance is of great importance (Ojo, 1987).

The aim of this study is to examine the probable impact of annual and decadal fluctuations of total rainfall on the hydrological regime and water resources within the Ogun-Oshun River Basin Development Authority (southwestern Nigeria). The basin is a classic example of a basin that is rapidly being modified in its hydrology and morphology by rapid urbanization and increased population growth rate.

STUDY AREA

The Ogun-Osun River Basin Development Authority falls within Nigeria's Hydrological Area VI with an annual runoff of 35.4×10^9 m^3, or depth of runoff of 352 mm per year, with an average annual growth rate of about 1.7% (Federal Dept. of Water Resources, 1986). The basin lies approximately within latitudes 6.25°N and 9.25°N of the equator and longitudes 2.70°E and 5.0°E of the Greenwich Meridian, with a total drainage area of about 56 000km^2 (Fig. 1). It is bounded in the north and east by the Lower Niger and Benin-Owena River Basin Development Authority respectively, in the west by Republic of Benin and in the south by the Atlantic Ocean.

Copyright © 2006 IAHS Press

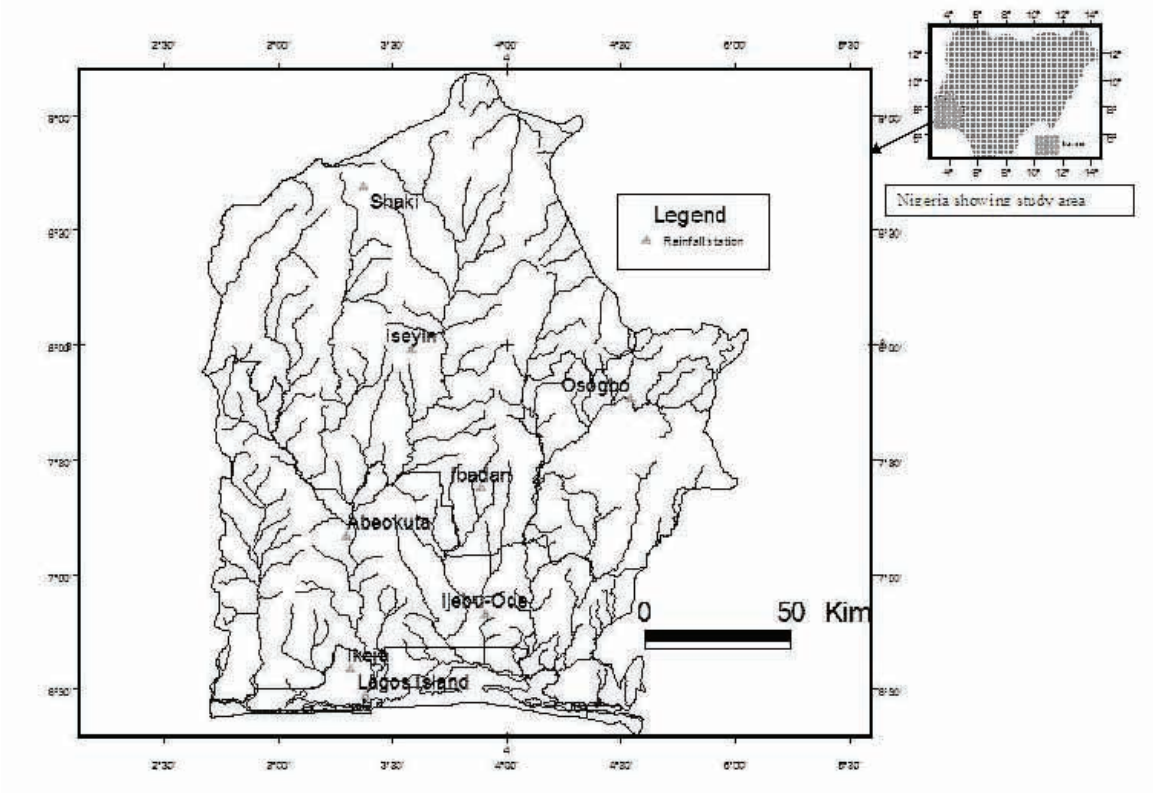


Fig. 1 Ogun-Oshun River Basin Development Authority and major settlement.

Major rivers draining the basin include the Ogun and Osun and their tributaries, Sasa, Ona, Ibu, Ofiki, Omi, Oba and Yewa. The lower portion of the basin is also drained by a network of lagoons, creeks and swamps, as well as rivers.

Climatologically, the drainage basin is located within the tropical rainy climate (Af) zone in accordance to Koppen's climate classification and is under the influence of the tropical continental (cT) and the tropical maritime (mT) air masses. Associated with the tropical maritime air mass are southwesterly winds, while the northeasterly winds are associated with the dry and dusty tropical continental air mass. The narrow zone of convergence of the two air masses is called the Intertropical Convergence Zone (ITCZ) and it usually shifts seasonally with the pressure belts and isotherms. (Iloeje, 1976).

Population density within the drainage basin is about 214 per km^2 with the lower portion of the basin having population density of about 1723 per km^2 in 1991 (Federal Dept. of Water Resources, 1986). Also, the lower portion of the drainage basin which forms Lagos State is the economic and commercial nerve centre of the nation, with over 2000 industries and 65% of the country's commercial activities, in addition to two of the nation's largest seaports, Apapa and Tin-Can (Nigeria Direct, 2006).

Thus, the drainage basin is faced with an increasing per capita water demand, with the estimated water supply requirement for the year 2030 being about 33×10^6 m^3 and 1128.7×10^6 m^3 for Ogun and Lagos areas, respectively (Lagos State Water Corporation, 2000). Also, there is greater pressure on available freshwater resources due to the alarming population growth rate, on the order of about 2.7% average annual growth, in the basin (National Population Commission, 1991). This has often resulted in massive uncoordinated surface and groundwater withdrawals and encroachment on river flood plains.

METHODOLOGY

The methodology entails rainfall data sourcing from the Nigerian Meteorological Agency (formerly Nigerian Meteorological Station, Oshodi) and the decadal analysis was restricted to four

Table 1 Data adopted, their sources and characteristics.

Data	Station	Duration of data	Remark
Rainfall	Ikeja	1944–2003	
	Lagos Island	1941–2000	
	Abeokuta	1981–2000	
	Ijebu-Ode	1974–2003	
	Ibadan	1941–2003	
	Osogbo	1941–2000	Missing years (1948–1956)
	Shaki	1984–2000	
	Isheyin	1982–2000	

Source: Nigerian Meteorological Agency, Oshodi.

`

stations due to the nature of the available rainfall data. Table 1 summarizes the data characteristics and details of the synoptic rainfall stations within the Ogun-Oshun River Basin Authority. The following analyses were carried out, in order to estimate the multi-annual and temporal fluctuations in rainfall totals and its effect on water resources development within the drainage basin.

Normalized distribution analysis was carried-out in order to identify and rank the relationship between the long-term mean annual and the annual total rainfall at the different synoptic stations within Ogun-Oshun River Basin Development Authority (OORBDA).

The normalized distribution (Z) is mathematically expressed as;

$$Z = \left(\overline{X} - \mu\right) \Big/ \delta \tag{1}$$

where, $\overline{X}$ is sample annual rainfall mean for the rainfall station, μ is the long-term mean and σ the standard deviation of long-term annual rainfall in the drainage basin.

The effect of rainfall on the hydrological regime of the Ogun-Osun River Basin Development Authority was validated using the indices of precipitation (rainfall) stability (*RRS*) and instability of the hydrological regime (*IHR*) (Blazejczyk *et al*., 2005).

The *RRS* is defined as;

$$RRS = RRavg / \left(RR\max - RR\min\right) \tag{2}$$

where, *RR*max is the maximum annual total rainfall, *RR*min is the minimum annual total rainfall, and *RR*avg is the average annual total rainfall.

While, the IHR is mathematically expressed as

$$IHR = \left(dRR\max - dRR\min\right) / RRavg \tag{3}$$

where, *dRR*max is the greatest positive year-to-year difference in rainfall, and *dRR*min is greatest negative year-to-year difference in rainfall.

RESULTS

The pattern of rainfall anomalies within Ogun-Oshun River Basin Development Authority of selected stations for the period (1944–2000) shows that the wettest year for the coastal stations (Ikeja and Lagos Island) was 1968 (Fig. 2). Also, fluctuation in annual rainfall totals at selected stations for decadal analysis has similar rainfall amplitude (Fig. 3).

Table 2 shows the various probabilities of the occurrence of wet and dry years. For example at Ikeja station, the probability that the current year will be a wet year given that the previous year was wet is 0.63, and the probability of a wet year being followed by a dry year is 0.18. Similarly, the probability that the current year will be dry year given that the previous year is dry is 0.54 while the probability of a dry year being followed by a wet year is 0.2.

The decadal analysis (Table 3) shows that there were relatively wet conditions in the 1950s and relatively dry conditions in the 1980s, while in the 1960s, phenomenally wet years occurred at all the stations with a slight increase in the mean decadal rainfall in the 1990s. The wet decades were periods of sufficient rainfall, most especially in the 1950s, with surplus water for development. The only exception is at Ibadan station, where the 1950s were relatively drier than

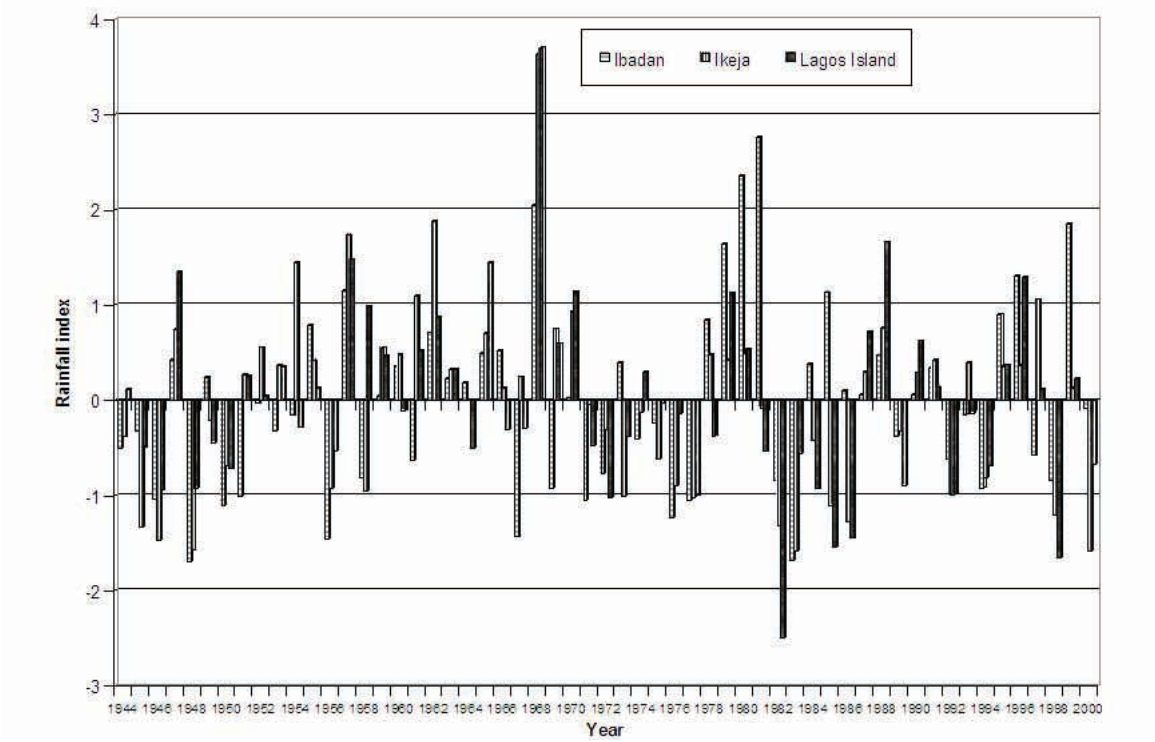


Fig. 2 Annual rainfall variability index in Ikeja and Osogbo Stations (OORBDA).

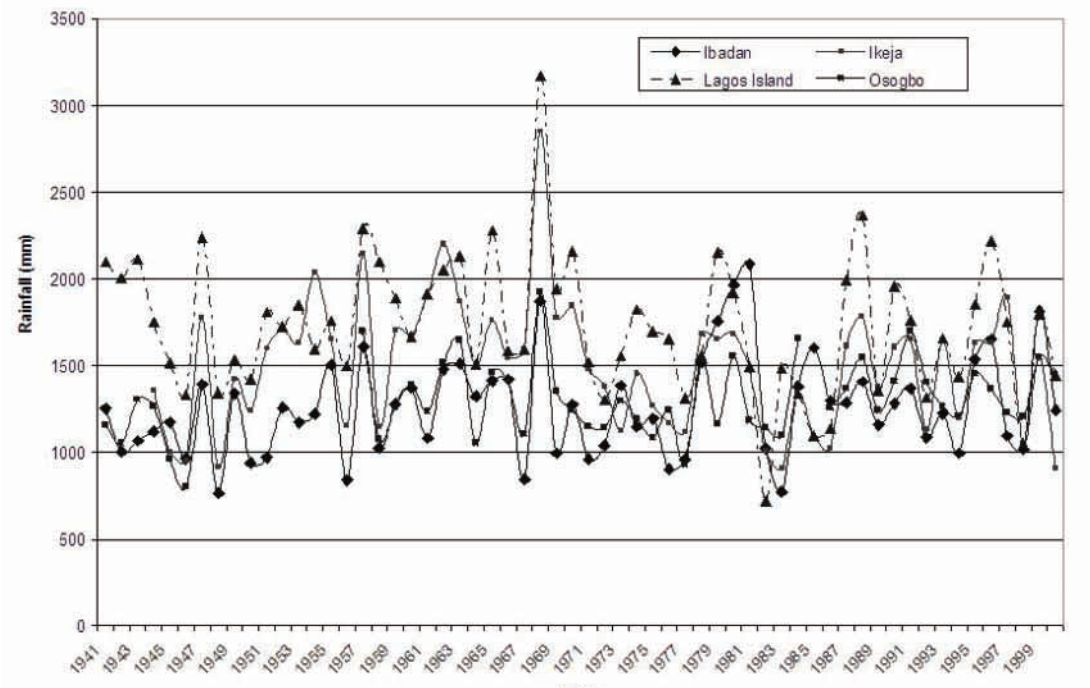


Fig. 3 Fluctuations in annual rainfall totals in several stations in Ogun-Oshun River Basin Development Authority (OORBDA).

other decades and the 1980s were relatively wetter; the station also had an increasing decadal rainfall trend of about +34 mm. Decreasing trends in decadal rainfall of about 95, 70 and 3 mm were recorded, at Lagos Island, Ikeja and Osogbo stations, respectively. The decreasing trend, most especially in the coastal region, calls for a more secured plan in order to match and scale water demand to the natural supply rate average. This is necessary, if the increasing per capita water demand and average annual population growth rate (OORBA, 1990), is to be sustainably managed within a strategic water resources plan.

Table 2 Probability of wet/dry year occurrence within Ogun-Oshun River Basin Development Authority.

	Probability			
Station	Wet/wet	Wet/Dry	Dry/Dry	Dry/wet
Ikeja	0.63	0.18	0.54	0.2
Lagos Island	0.45	0.23	0.48	0.2
Abeokuta	0.36	0.15	0.44	0.1
Ijebu-Ode	0.59	0.17	0.54	0.17
Ibadan	0.55	0.19	0.47	0.21
Osogbo	0.48	0.22	0.55	0.24
Shaki	0.44	0.24	0.5	0.24
Isheyin	0.55	0.14	0.45	0.18

Table 3 Decadal-scale mean rainfall fluctuations in selected station in Ogun-Osun river basin development Authority.

	Decadal scale				
Station	1950s	1960s	1970s	1980s	1990s
Ikeja	1602.68	1868.54	1418.02	1344.93	1514.04
Lagos Island	1834.86	2019.21	1619.54	1443.07	1648.77
Ibadan	1182.3	1331.35	1214.18	1405.19	1316.88
Osogbo		1409.65	1199.02	1320.75	1378.3

Table 4 Characteristics of precipitation at selected stations within Ogun-Oshun River Basin Development Authority, 1944–2000.

Station	*RR*max (mm)	*RR*min (mm)	*RR*avg (mm)	*dRR*max (mm)	*dRR*min (mm)	*RRS*	*IHR*
Ikeja	2850.7	908.8	1519.71	1071.9	–1258.5	0.78	1.53
Lagos Island	3169	721.2	1726.46	1225.4	–1578.1	0.71	1.62
Ibadan	2084.9	766.8	1269.48	1062.6	–1028.6	0.96	1.65
Osogbo	1921.5	803.9	1306.40	618.3	–814.6	1.17	1.10

The relative variability of the decadal rainfall within the drainage basin is low and of the order of about 13% and 7% at the coastal stations (Ikeja and Lagos Island) and northern stations (Ibadan and Osogbo), respectively. The decadal rainfall distribution along the coast varies more than the hinterlands. This is critical to water resources development within the drainage basin, considering the anticipated socio-economic influx and its associated increase in per capita water demand within the coastal area, especially Lagos. The coastal area is also prone to flood-inducing activities, due to its location and nearness to large water bodies like lagoons and the Atlantic Ocean (Oyebande, 1990). This calls for a need to update and review the existing water master plan and storm water drains, through better understanding of the interrelationship between the various components of the drainage basin and development of an appropriate mechanism for hydrological extreme event prediction and forecasting.

The indices of precipitation (rainfall) stability (*RRS*) and instability of the hydrological regime (*IHR*) (Table 4) for selected stations in relation to the year-to-year fluctuation in rainfall shows that the lowest value of rainfall stability was recorded at Lagos Island while lowest instability of hydrological regime was recorded at Osogbo station. The low stability at the coastal stations, calls for a radical reformation and a proper water resources assessment plan and expansion of the existing water resources system. This is necessary in order to improve access to potable water for the populace, which in Nigeria is about 32% (Hanidu, 1990). Such provision will also prevent stretching the available water resources and cope with increasing demand and pressure from competing water uses, most especially in the densely populated region (such as Lagos, Ibadan and, Abeokuta) within the drainage basin.

CONCLUSIONS

Decadal rainfall distribution analysis within the Ogun-Oshun River Basin Development Authority (Nigeria) shows that there were relatively wet conditions in the 1950s and relatively dry conditions in the 1980s and a slight increase in the mean decadal rainfall in the 1990s.

The effect of total annual rainfall fluctuations among the selected stations on the hydrological regime of Ogun-Oshun River Basin Development Authority (Nigeria) shows that Osogbo station had the most stable hydrological regime. The relative decreasing decadal trend, higher variability and instability of the hydrological regime of the coastal rainfall stations (Ikeja and Lagos Island) calls for a robust water resources development within the Ogun-Oshun River Basin Development Authority. This is necessary in consideration of the anticipated socio-economic influx and its associated increase in per capita water demand within the coastal zone.

An easily accessible information network for rainfall forecasting also needs to be put in place for effective dissemination of information and disaster preparedness as well as the protection of available water resources within the basin and its environment.

Finally, an adequate planning policy scheme and its implementation will go a long way toward withstand the pressure that accompanies rapid and often unplanned growth such as that being witnessed in the basin.

REFERENCES

Blazejczyk, K., Kasperska-Wolowicz, W., Labedzki, L., Kunert, A. (2005) Multi-annual fluctuations in precipitation and their hydrological and ecological consequences at regional scale. In: *Regional Hydrological Impacts of Climatic Change-Hydroclimatic Variability* (ed. by S. Franks, T. Wagener, E. Bøgh, H. V. Gupta, L. Bastidas, C. Nobre & Carlos De Oliveira Galvão), 65–70. IAHS Publ. 296. IAHS Press, Wallingford, UK.

Gash, J. H. C., Forsberg, M., Odada E. O., Oyebande, L. & Schulze, R. E. (2001) Freshwater resources research in Africa. In: *Freshwater Resources in Africa* (ed. by J. H. C. Gash, E. O. Odada, L. Oyebande & R. E. Schulze) (Proc. Workshop Nairobi, Kenya, October 1999, Biospheric Aspects of the Hydrological Cycle), 3–8.

Federal Dept. of Water Resources (1986) National Water Resources Masterplan, Draft Preliminary Plan, Nigeria.

Hanidu, J. A. (1990) National growth, water demand and supply strategies in Nigeria in the 1960s. *Nigerian Association of Hydrogeologists (NAH)* **2**(1). Oct. 1990.

Iloeje, N. P. (1976) *A New Geography of Nigeria* (metric edn). Longman, Nigeria

Lagos State Water Corporation (2000) Challenges and issues of privatization of state water institutions in Nigeria; mobilizing finance for water supply in Nigeria. Lagos Water Conference, November, 2000.

National Population Commission (1991) Population Census of Nigeria.

Nigeria Direct (2006) The Official Information Gateway of the Federal Republic of Nigeria. http://www govt_state_lagos_aspx.htm

Ogun-Osun River Basin Authority (OORBA) (1990) Technical Report.

Ojo, O. (1987) Rainfall trends in West Africa. In: *The Influence of Climate Change and Climatic Variability on the Hydrologic Regime and Water Resources* (ed. by S. I. Solomon, M. Beran & W. Hogg), 37–43. IAHS. Publ. 168. IAHS Press, Wallingford, UK.

Oyebande, L. (1990) Aspects of urban hydrology and the challenges for African urban environment. *African Urban Quarterly* **5**(1/2), 39–63.

Shiklomanov, I. A. (1998) *World Water Resources, A New Appraisal and Assessment for the 21st Century*. UNESCO, Paris, France.

United Nations Environment Programme (UNEP) (2000) *Global Environment Outlook – Past, Present and Future Perspectives.* Earthscan, UK, USA.

Climate Variability and Change—Hydrological Impacts (Proceedings of the Fifth FRIEND World Conference held at Havana, Cuba, November 2006), IAHS Publ. 308, 2006.

Relación entre probabilidad de ocurrencia de días con lluvia y tormentas eléctricas en Casablanca y Camagüey

LOURDES ÁLVAREZ ESCUDERO, ISRAEL BORRAJERO MONTEJO, ROSENDO ÁLVAREZ MORALES & LAURA AENLLE FERRO

Centro de Física de la Atmósfera, Instituto de Meteorología, Apartado Postal 17032, CP 11700, Habana 17, Ciudad Habana, Cuba

lourdes.alvarez@insmet.cu

Resumen Se compara la actividad de lluvias y de tormentas eléctricas en Casablanca y Camagüey, dada por la probabilidad de ocurrencia de días con estos fenómenos y se calcula el número promedio de tormentas diarias. Las tormentas en Camagüey explican un 20% más de la variación de la probabilidad de día con lluvia que en Casablanca, aunque en ambas estaciones el número de observaciones con tormentas con lluvia por día con tormenta es de 1.2. La marcha anual de la razón entre la frecuencia de ocurrencia de días con tormenta con lluvias y probabilidad de lluvia diaria para la estación Casablanca presenta una distribución unimodal, con un máximo del 40% de casos de lluvia debidos a tormentas, mientras para Camagüey la distribución es bimodal y el porciento máximo de ocurrencia es de 44. Para Casablanca la cantidad de días con lluvia debido a tormentas ha aumentado con los años.

Palabras claves tormenta eléctrica; día con lluvia; métodos no paramétricos

Relationship between the probability of occurrence of rainfall and thunderstorms at Casablanca and Camiguey, Cuba

Abstract Rainfall and thunderstorm probability of occurrence is compared between the stations of Casablanca and Camagüey (in Cuba) and the average number of daily thunderstorms is calculated. Storms at Camagüey account for up to 20% more of the variation of the probability of days with rain around the mean value than they do at Casablanca, though at both stations the number of observations of storm with rain per day with rain is 1.2. The yearly course of the ratio of the frequency of occurrence of days with storms with rain to the probability of days with rain at Casablanca is unimodal in form, with a maximum of 40% of cases of rain due to storms, while at Camagüey the distribution is bimodal and the number of cases is greater than 44% at the periods of maximum occurrence. For the Casablanca station, the number of days per year with rain due to the occurrence of thunderstorms, has increased over the years.

Key words day with rain; non parametric methods; thunderstorms

INTRODUCCIÓN

Las tormentas eléctricas en Cuba han sido estudiadas desde muchos puntos de vista tales como su climatología dada por la cantidad de días con tormentas, su marcha diaria y anual, el comienzo y final de la temporada de tormentas y las manifestaciones severas de las mismas como tornados y trombas. Sin embargo pocos estudios se han realizado referidos a lo que las tormentas eléctricas representan en los acumulados de lluvia de las diferentes regiones.

Alfonso (1986) realizó un estudio representativo de las tormentas con lluvia en la ocurrencia general de tormentas para la estación Casablanca y encontró que el porcentaje de tormentas que producen precipitación es máximo de diciembre a febrero a pesar de ser los meses donde menos frecuente es el fenómeno. Alfonso & Florido (1993) concluyeron que en la provincia Matanzas las lluvias más intensas son asociadas a tormentas eléctricas con intensidades de hasta 3 mm min^{-1}. Un estudio realizado por Lecha *et al*. (1994) resalta la semejanza entre los mapas de distribución de días con tormentas y los mapas isoyéticos de Cuba, por lo que se plantea que la mayor parte de los días con lluvia se deben a la ocurrencia de tormentas.

El objetivo de este trabajo es la comparación de la actividad de lluvias y de tormentas, dada por la probabilidad de ocurrencia de días con estos fenómenos, para las estaciones de Casablanca y Camaguey donde los autores poseen registros confiables de datos y donde casi no faltan registros y que la metodología aquí aplicada se extienda a otras estaciones del país donde la información pueda ser rescatada y validada con rigor. También se analizará la tendencia de la razón entre frecuencia de ocurrencia de días con tormentas con lluvia y días con lluvias para ambas estaciones en los periodos de estudio.

Copyright © 2006 IAHS Press

MATERIALES Y MÉTODOS

Para la comparación se utilizaron las series de acumulados diarios de lluvia (Álvarez *et al*., 2002a,b) debidamente verificadas y registros de estado del tiempo presente trihorario de las estaciones meteorológicas de Casablanca y Camaguey en los periodos 1972–2000 y 1970–2000 respectivamente.

A partir de los acumulados diarios se determinó la probabilidad de ocurrencia de lluvia diaria para los 365 días del año, suponiendo como día con lluvia aquel cuyo acumulado fue mayor o igual 0.1 mm. Los días 29 de febrero no se tuvieron en cuenta en este análisis para lograr años de igual duración. El otro parámetro derivado de los datos de lluvia fue el acumulado promedio de lluvia diaria para los 365 días del año, aquí el acumulado correspondiente a los 29 de febrero se agregaban a los días 28 del propio mes.

De los registros trihorarios de estado del tiempo presente se derivaron 3 series para cada estación: la de la frecuencia diaria de observaciones con tormenta considerando los códigos 17, 29, 91, 92, 95, 96, 97 y 99, la de día con tormenta y la de día con tormenta con lluvia (solo si ocurrió un código 91, 92, 95, 96, 97 o 99) para cada uno de los 365 días del año tipo. En estos conteos no se tuvo en cuenta los 29 de febrero.

Para el análisis de tendencia se utilizaron las series anual y por meses de la razón entre frecuencia de ocurrencia de días con tormenta con lluvia y días con lluvia, extraídas de las series generales de acumulados de lluvia y registros trihorarios de código de tiempo presente, para las estaciones de Casablanca y Camagüey en los periodos de estudio. La metodología utilizada para este análisis es la propuesta por Sneyers (1990).

RESULTADOS

Las estaciones de Casablanca (325) y Camaguey (355) tienen condiciones físico geográficas diferentes, Casablanca es una estación cercana a la costa norte y Camaguey se encuentra en el centro de la provincia del mismo nombre, que es una de las regiones más anchas de la Isla de Cuba, por lo que se le atribuyen propiedades continentales. Debido a esto es interesante el estudio comparativo de la relación entre sus lluvias y la parte que las tormentas aportan a ellas.

Del ajuste realizado a las series anual y por meses de probabilidad de ocurrencia de día con lluvia y la probabilidad de ocurrencia de día de tormenta con lluvia para la estación Casablanca se constata que la correlación para la serie anual es mala, de hecho se explica solo el 30% de la variación con respecto a la media, conclusión lógica si se tiene en cuenta que las tormentas no son el único fenómeno productor de lluvia. Los meses que presentan mejor correlación son octubre (70%) y abril (60%). En enero, aunque tiene un coeficiente de correlación de 0.65, el número de casos es muy bajo para arribar a conclusiones.

En el caso de Camagüey la variación explicada anual aumenta a un 53%, aproximadamente un 20% mayor que en Casablanca. Aquí los meses que presentan mejor correlación son: mayo con el 70%, julio con el 67% y octubre con el 64%, diferencia esta también con respecto a Casablanca donde el mes de julio presentaba un pésimo ajuste.

Otro elemento interesante para el análisis es la relación entre las observaciones con tormenta y los días con tormenta, tanto en general, como para tormentas con lluvia. Como es lógico si existe al menos una observación con tormenta en el día, el día será catalogado como día con tormenta, pero puede ocurrir más de una observación. La ocurrencia de observaciones con tormenta por día con tormenta promedio para las series usadas, es para Casablanca de 1.21 y para Camaguey de 1.23 y en el caso de observaciones con lluvia es para Casablanca de 1.12 y para Camaguey de 1.13, de lo que puede resumirse que la diferencia no es apreciable. En todos los casos el número máximo de observaciones con tormenta por día es 3, aunque ocurre con muy poca frecuencia. Sin embargo, si se analizan las distribuciones de esta razón para cada uno de los días del año se observa un periodo marcado donde el máximo de ocurrencia es una observación con tormenta por día y otro periodo, aproximadamente coincidente con la temporada más activa de tormentas donde suele haber más de una observación por día. La temporada de observaciones con tormenta por día, para el caso de tormentas con lluvia es más corta en extensión en ambas estaciones y por lo general la fecha de comienzo suele ser más tardía.

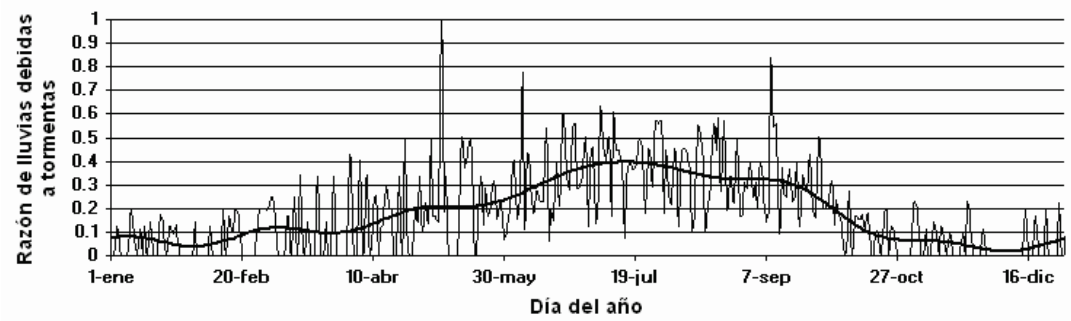


Fig. 1 Estación 325. Marcha anual de la razón entre la frecuencia de ocurrencia de días con tormenta con lluvias y probabilidad de lluvia diaria para la estación Casablanca usando como periodo de cálculo 1972–2000. La línea gruesa representa el ajuste de una función de 7 armónicos.

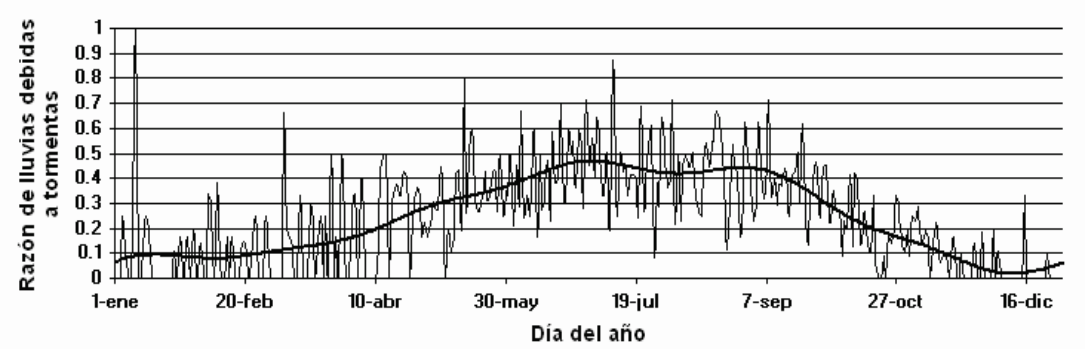


Fig. 2 Estación 355. Marcha anual de la razón entre la frecuencia de ocurrencia de días con tormenta con lluvias y probabilidad de lluvia diaria para la estación Camagüey usando como periodo de cálculo 1970–2000. La línea gruesa representa el ajuste de una función de 7 armónicos.

En las Figs 1 y 2 se representa la razón entre la frecuencia de ocurrencia diaria de días con tormenta con lluvia y la probabilidad de ocurrencia de día con lluvia para las estaciones Casablanca y Camaguey respectivamente. En ambos casos se ajustó una serie de 7 armónicos para suavizar su representación con una correlación superior al 73%. En Casablanca se observa una distribución unimodal con un máximo en torno al 19 de julio y con alrededor del 40% de casos de lluvia debidos a tormentas. La temporada de mayor actividad se extiende de mediados de mayo a principios de octubre, aunque se observan valores de cierto interés entre los meses de febrero y marzo. En Camagüey la distribución es bimodal, con un máximo absoluto en torno al 2 de julio y otro relativo en torno al 2 de septiembre, en ambos casos los valores de la razón están por encima del 44%, la temporada abarca desde principios de abril a finales de octubre (mayor que en Casablanca) y también se observa cierta representatividad en los meses invernales de febrero y marzo un poco más acentuada que en Casablanca.

Si se contabiliza el número casos de días con tormenta en el año por rangos de 0.5 en 0.5 mm de lluvia correspondiente al promedio de acumulado diario de lluvia para las estaciones en estudio, se constata que por lo general, las tormentas no suelen tener la mayor cantidad de número de casos en los rangos de acumulados más bajos ni más altos. En el caso de Casablanca el rango de mayor representación es el de entre 2.6 y 3.0 mm y el 90% de los casos se agrupa entre 0.6 y 7.5 mm. Camagüey por su parte, agrupa la mayor cantidad de casos entre 3.1 y 3.5 mm (un rango mayor que en Casablanca), pero su distribución es más dispersa y los rangos más bajos de acumulado tienen una representatividad significativa, así el 90 % de los casos están entre 0.1 y 8 mm.

El análisis de tendencia anual y por meses para la estación Casablanca está resumido en la Tabla 1. De la misma forma el análisis de tendencia anual y por meses para la estación Camagüey está resumido en la Tabla 2.

De la Tabla 1 se aprecia que la serie anual de razón de frecuencia de ocurrencia entre día con tormenta con lluvia y día con lluvia es creciente altamente significativa con un punto de cambio entre 1986 y 1987. Esto significa que la cantidad de días con lluvia debida a la ocurrencia de tormentas ha aumentado con el paso de los años para la estación Casablanca. No se conocen causas

Tabla 1 Resumen del análisis de tendencia para la estación Casablanca en el periodo 1972–2000.

serie	Conclusión	Posible punto de cambio
Anual	Creciente altamente significativa	1986–1987
enero	Poca representatividad de los datos	---
febrero	Poca representatividad de los datos	---
marzo	Poca representatividad de los datos	---
abril	Poca representatividad de los datos	---
mayo	Poca representatividad de los datos	---
junio	Creciente altamente significativa	1986
julio	Homogénea	---
agosto	Homogénea	---
septiembre	Creciente altamente significativa	1987–1988
octubre	Poca representatividad de los datos	---
noviembre	Poca representatividad de los datos	---
diciembre	Poca representatividad de los datos	---

Tabla 2 Resumen del análisis de tendencia para la estación Camagüey en el periodo 1970–2000.

serie	Conclusión	Posible punto de cambio
Anual	Tendencia global creciente altamente significativa pero no presenta correlación interna.	---
enero	Poca representatividad de los datos	---
febrero	Poca representatividad de los datos	---
marzo	Poca representatividad de los datos	---
abril	Poca representatividad de los datos	---
mayo	Tendencia global creciente altamente significativa pero no presenta correlación interna.	---
junio	Creciente significativa	1985–1986
julio	Homogénea	---
agosto	Creciente significativa	No puede precisarse
septiembre	Homogénea	---
octubre	Homogénea	---
noviembre	Poca representatividad de los datos	---
diciembre	Poca representatividad de los datos	---

antropogénicas para la existencia de un punto de cambio significativo entre los años 1986 y 1987 por lo que habría que buscar causas naturales. De las series mensuales solo 4 de ellas tienen representatividad suficiente para ameritar un análisis; estas series corresponden a los meses de julio y agosto donde las series son homogéneas y a junio y septiembre donde las series son crecientes altamente significativas, al igual que la anual y también presentan puntos de cambios significativos alrededor de 1987.

En Camagüey la situación es diferente ya que aunque la serie anual presenta tendencia global creciente altamente significativa, la persistencia corta no es significativa por lo que no puede arribarse a una conclusión decisiva. Hay 6 series mensuales con representatividad para el análisis de las cuales, las correspondientes a julio, septiembre y octubre son homogéneas, la correspondiente a mayo presenta un comportamiento similar al de la serie anual y las de junio y agosto son crecientes significativas con un punto de cambio entre 1985 y 1986 (punto cercano al encontrado en las series de Casablanca). Estas dos últimas series ven disminuida su significación por tener un nivel más alto para su estadígrafo de correlación interna (Walt-Wolfowitz).

REFERENCIAS

Alfonso, A. P. (1986) Aspectos climatológicos de las turbonadas en la Ciudad de la Habana. *Ciencias de la Tierra y el Espacio* **12**, 85–100.

Alfonso, A. & Florido, A. (1993) *El Clima de Matanzas*. Editorial Academia, La Habana, Cuba.

Álvarez, L., Álvarez, R. & Borrajero, I. (2002a) Caracterización de las precipitaciones en la estación meteorológica de Casablanca y su tendencia. *Revista Cubana de Meteorología* **9**(1), 61–70.

Álvarez, L., Álvarez, R. & Borrajero, I. (2002b) Caracterización de las precipitaciones en la estación meteorológica de Camaguey y su tendencia. *Revista Cubana de Meteorología* **9**(2), 28–37.

Lecha, L. B., Paz, L. R. & Lapinel, B. (eds) (1994) *El Clima de Cuba*. Editorial Academia, La Habana, Cuba.

Sneyers, R. (1990) *On the Statistical Analysis of Series of Observations*. Technical Note no. 143, WMO no. 415. WMO, Geneva, Switzerland.

Climate Variability and Change—Hydrological Impacts (Proceedings of the Fifth FRIEND World Conference held at Havana, Cuba, November 2006), IAHS Publ. 308, 2006.

Causas de la reciente sequía acaecida en la región oriental de Cuba

BRAULIO LAPINEL, ABEL CENTELLA, IDELMIS GONZÁLES, CECILIA FONSECA & VIRGEN CUTIE

Centro del Clima, Instituto de Meteorología, Habana 17, Cuba
braulio. lapinel@.insmet.cu

Resumen Progresivas modificaciones en las características de la circulación atmosférica sobre el Caribe, acentuadas en los últimos años y coincidentes temporalmente con los graduales incrementos globales de la temperatura del aire en superficie y la persistencia de anomalías positivas de la temperatura del mar en la región trópico, han propiciado la incidencia de persistentes eventos de sequía en Cuba, principalmente en su región oriental. Se muestra cómo la mayor influencia simultánea del anticiclón oceánico del Atlántico en los niveles troposféricos bajos y medios y del anticiclón mexicano de verano, en interacción con un desplazamiento al oeste de la vaguada superior atlántica en los niveles altos, ha estado causando una fuerte subsidencia, desfavorable para el proceso de la lluvia. Son obtenidas funciones representativas del perfil Omega en diferentes condiciones relativas a la lluvia. Las tendencias de las magnitudes de Omega, señalan un decremento de las magnitudes negativas e incremento de las positivas, de modo significativo en todos los niveles troposféricos, con puntos de cambios a finales de los años 70.
Palabras claves Caribe; sequía meteorológica; velocidad vertical de presión

Causes of the recent droughts in western Cuba

Abstract Progressive modifications in the characteristics of the atmospheric circulation of the Caribbean, have become accentuated in recent years and coincided, at least temporarily, with the gradual global increase of surface air temperatures and the persistence of positive anomalies of sea surface temperature in the tropical region. These have produced persistent drought events in Cuba, mainly in the western region. The Atlantic anticyclone influence in the low and medium levels of the troposphere, together with the influence of the Mexican anticyclone in summer, in combination with a displacement to the west of the Atlantic superior Tropical Upper Tropospheric Trough at high levels, have caused a strong descending movement, which is very unfavourable for precipitation. Representative functions of the "Omega" vertical distribution were obtained under different relative precipitation conditions. The trends of Omega indicate a decrease of the negative magnitudes and an increase of the positive ones, in a significant manner, at all tropospheric levels, with remarkable trend changes at the end of the seventies.

Key words Caribbean; meteorological drought; vertical speed of pressure

INTRODUCCIÓN

El clima de Cuba en las últimas décadas ha experimentado notables alteraciones, como consecuencia de "un elevado nivel de respuesta de la circulación atmosférica regional a los principales cambios del Sistema Climático ocurridos a escala global" (Centella *et al*., 1997).

Brenes (1994) y Naranjo (1999), detectaron importantes variaciones en las características de la influencia anticiclónica sobre la región durante las últimas décadas, producto de la intensificación de la dorsal anticiclónica del Atlántico, proceso consistente con un paulatino incremento en la intensidad de la corriente zonal del Este vinculada al régimen alisio, el cual sobre Cuba desfavorece los mecanismos productores de precipitación, principalmente en el período estacional lluvioso.

Los principales cambios en las características de la influencia anticiclónica en el área, se han detectado desde mediados de la década de los años 70, fecha plenamente coincidente con las importantes modificaciones de carácter global que se han venido produciendo en las temperaturas del aire en superficie y del mar, observándose una mayor penetración de la cuña anticiclónica oceánica sobre el archipiélago cubano en este último período (Fonseca, 2001).

Dado que las condiciones marcadamente secas o húmedas sobre Cuba, se relacionan estrechamente con la posición, morfología e intensidad del anticiclón oceánico en la troposfera baja y media y el anticiclón mexicano en la troposfera media y alta (Lapinel *et al*., 2001), en interacción con la posición y estructura de la vaguada troposférica superior tropical (TUTT) del Atlántico, los cambios anteriormente señalados resultan del mayor interés respecto al comportamiento de las lluvias y específicamente la sequía.

Copyright © 2006 IAHS Press

DATOS

La información principal empleada procede de las bases de datos de aire superior del NCEP-NCAR Reanalysis Project (CDAS) del Centro de Predicción Climática (CPC) (http://wesley.ncep.noaa.gov/reanalysis.html), y las facilidades de cálculo del Centro de Diagnósticos (CDC), Climate Diagnostics Center de la NOAA-CIRES (http://www.cdc.noaa.gov/cgi-bin/Composites/printpage.pl), ambos de los Estados Unidos de Norteamérica, así como de las bases de datos de lluvia de los Institutos de Recursos Hidráulicos (INRH) y Meteorología (INSTMET) de Cuba. Las variables analizadas fueron los geopotenciales, la velocidad vertical de presión (Vvel) y los acumulados mensuales de las lluvias.

MÉTODOS

La definición detallada Vvel (Omega), se presenta en el RUC13update en el RUC/MAPS del CPC. El signo negativo se interpreta como movimientos ascendentes e inversamente descendentes.

La evaluación de las tendencias de las magnitudes de la velocidad vertical de presión se efectuaron mediante los test estadísticos de Spearman, Kendall - Mann y Pettit**.** que comprueban el nivel de significación y la existencia de puntos de cambio en las series.

El área básica utilizada corresponde a la situada entre 20–25°N y entre 75–80°W y los perfiles verticales principales se computaron en las alturas de 925, 850, 700, 600, 500, 400, 300, 250 y 200 hPa en 22.5°N y 77.5°W. El período de estudio abarcó desde 1948 al 2005. La Norma para la lluvia correspondió al período 1971–2000.

RESULTADOS

Cambios en las alturas geopotenciales y morfología de las superficies de presión en la región geográfica de Cuba. Mes de junio y estación lluviosa (mayo–octubre)

Período 1948–2004

El incremento progresivo y significativo de las alturas geopotenciales de las superficies de presión sobre el área, la mayor intrusión de la cuña anticiclónica oceánica hacia el Oeste, sobre Las Antillas Mayores y en consecuencia un corrimiento en esta misma dirección de la vaguada, se aprecia en la troposfera media (500 hPa) del mes de junio, evaluada por décadas desde 1951–1960 hasta 1991–2000 y el quinquenio 2001–2005 en la superficie de 500 hPa (Fig. 1).

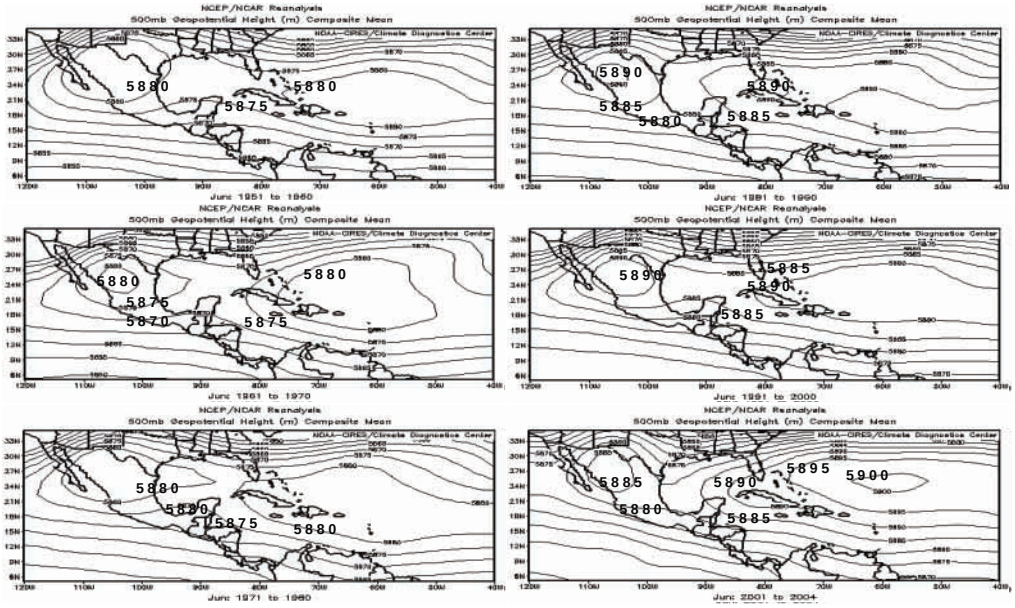


Fig. 1 Alturas de las superficies de presión de 500 hPa durante los meses de junio de las décadas 1951–1960, 1961–1970, 1971–1980, 1981–1990 y 1991–2000, así como en el cuatrienio 2001–2004.

Similar proceso se advierte a este nivel, al evaluar el período lluvioso en su conjunto (mayo–octubre), conjuntamente con la troposfera alta (300 y 200 hPa) durante este mismo período estacional, donde se aprecia la ganancia en altura del anticiclón mexicano y el aumento de la curvatura anticiclónica sobre Cuba, al comparar los períodos 1948–1976, 1977–2005 y 1998–2005 (Lapinel *et al*., 2006) . Por otra parte, al comparar el comportamiento del período 1948–2005 y los años 2003 y 2004 reveló esos mismos procesos fuertemente amplificados (Fig. 2).

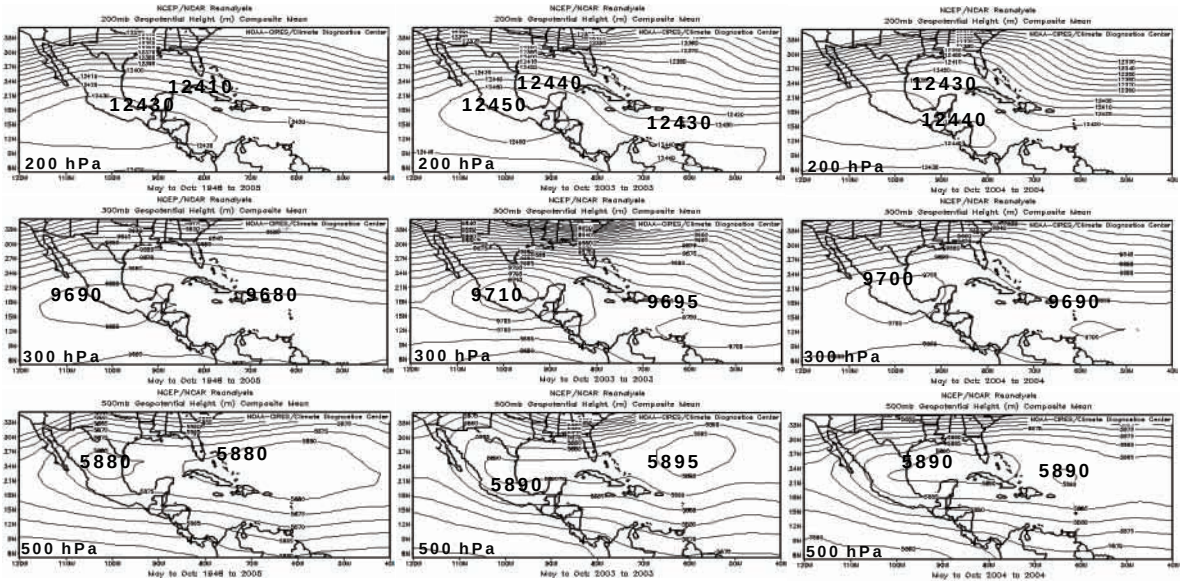


Fig. 2 Alturas de las superficies de presión de 200, 300 y 500 hPa durante los períodos lluviosos (mayo–octubre) de 1948–2005, 2003 y 2004.

Valoración espacial de las modificaciones de Omega sobre Cuba en el curso del período 1948–2005

Consistentemente con lo anteriormente visto, sobre la mitad oriental de Cuba, en la atmósfera alta y media, las magnitudes de Omega negativas en el período estacional lluvioso de 1977 al 2004, han disminuido respecto al anterior período 1948–1976 (Fig. 3), mientras que en la atmósfera baja se han incrementado las positivas.

Estos cambios han propiciado, de manera general, una inhibición progresiva de los movimientos convectivos ascendentes indispensables para el proceso de las lluvias y limitado o modificado las características de influencia de los sistemas organizados productores de las mismas (ondas, hondonadas, frentes, ciclones, etc.) y en consecuencia han estado contribuyendo sustancialmente al incremento de los procesos de sequía, tal y como se ha estado observando sobre esta región.

Omega durante condiciones, secas y húmedas medias, así como secas y húmedas medias extremas durante período estacional lluvioso de la mitad oriental de Cuba

La excelente relación entre las características de Omega y el comportamiento de la lluvia, se revelan en las magnitudes que manifiesta el perfil vertical de la primera, entre 925 y 200 hPa, durante las siguientes condiciones de lluvias: Medias (todo los casos), Secas Medias (deciles 5, 4, 3 y 2), Húmedas Medias (deciles 6, 7, 8 y 9), Extremas Secas Medios (deciles 1) y Extremas Húmedas Medias (deciles 10); véase la Fig. 4.

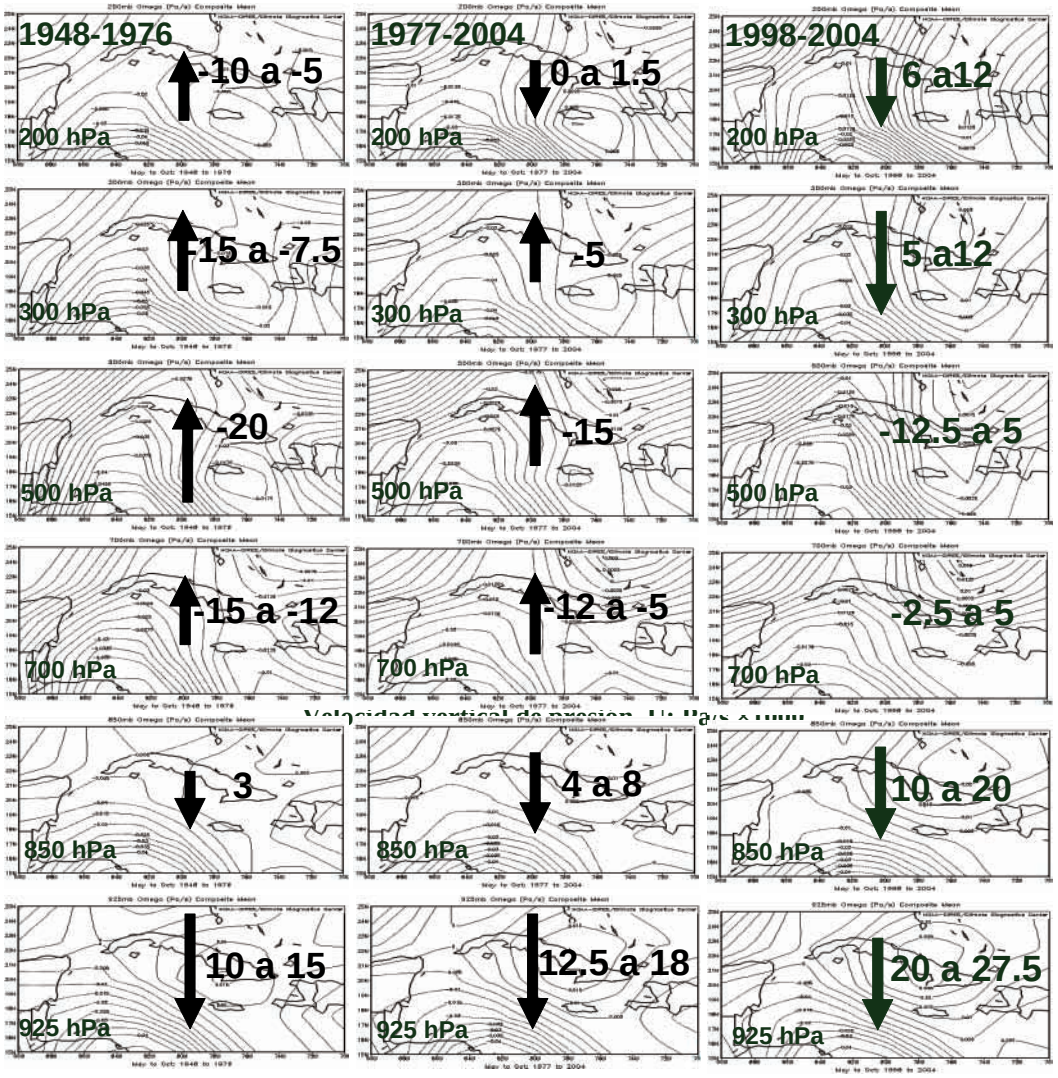


Fig. 3 Omega sobre la región geográfica de Cuba durante los períodos 1948–1976, 1977–2004 y 1998–2004. Superficies de presión de 200, 300, 500, 700, 850 y 925 hPa.

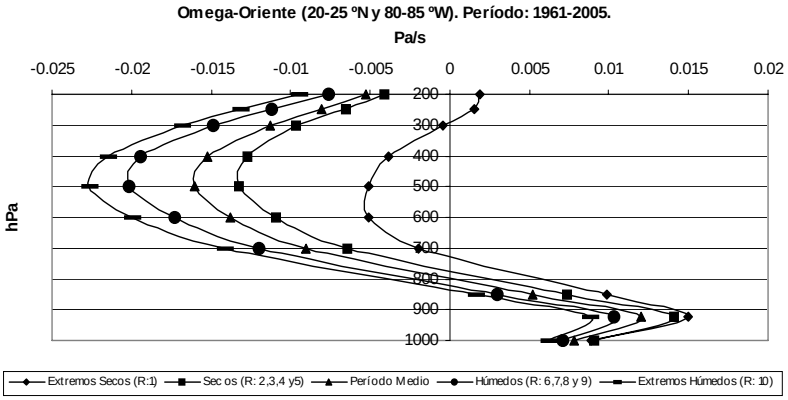


Fig. 4 Perfiles verticales de Omega entre 925 y 200 hPa en diferentes condiciones medias relativas a las lluvias durante el período lluvioso.

Los perfiles de cada una de estas condiciones, pueden ser representados mediante ecuaciones específicas:

Extremos Secos Medios

$y = -0.027939771 + 0.00032532016X - 1.1153376e^{-006}X^2 + 1.4160991e^{-009}X^3 - 5.721018e^{-013}X^4$

$R = 0.99711350$ $S = 0.00083958$

Secos Medios

$y = -0.0087219536 + 9.6400122e^{-005}X - 5.2648229e^{-007}X^2 + 8.17857e^{-010}X^3 - 3.5033344e^{-013}X^4$

$R = 0.99920430$ $S = 0.00063412$

Medias

$y = -0.010356031 + 0.00011183504X - 6.2076325e^{-007}X^2 + 9.653146e^{-010}X^3 - 4.2037162e^{-013}X^4$

$R = 0.99939977$ $S = 0.00055602$

Húmedos Medios

$y = -0.002142397 + 2.2329412e^{-005}X - 4.1848853e^{-007}X^2 + 7.7788152e^{-010}X^3 - 3.5477294e^{-013}X^4$

$R = 0.99953989$ $S = 0.00053805$

Extremos Húmedos Medios

$y = -0.015014751 + 0.00014159127X - 8.0947449e^{-007}X^2 + 1.2890058e^{-009}X^3 - 5.8566543e^{-013}X^4$

$R = 0.99972280$ $S = 0.00041645$

Tendencias y puntos de cambio de las series Omega en el período lluvioso

La visión conjunta de la evolución de Omega desde 1948 al 2004 evaluada para los períodos estacionales lluvioso y poco lluvioso, confirma el progresivo decremento de los valores negativos e incremento de los positivos, hasta llegar al crítico período de 1998 al 2004 donde las magnitudes alcanzan niveles altamente significativos (Fig. 5).

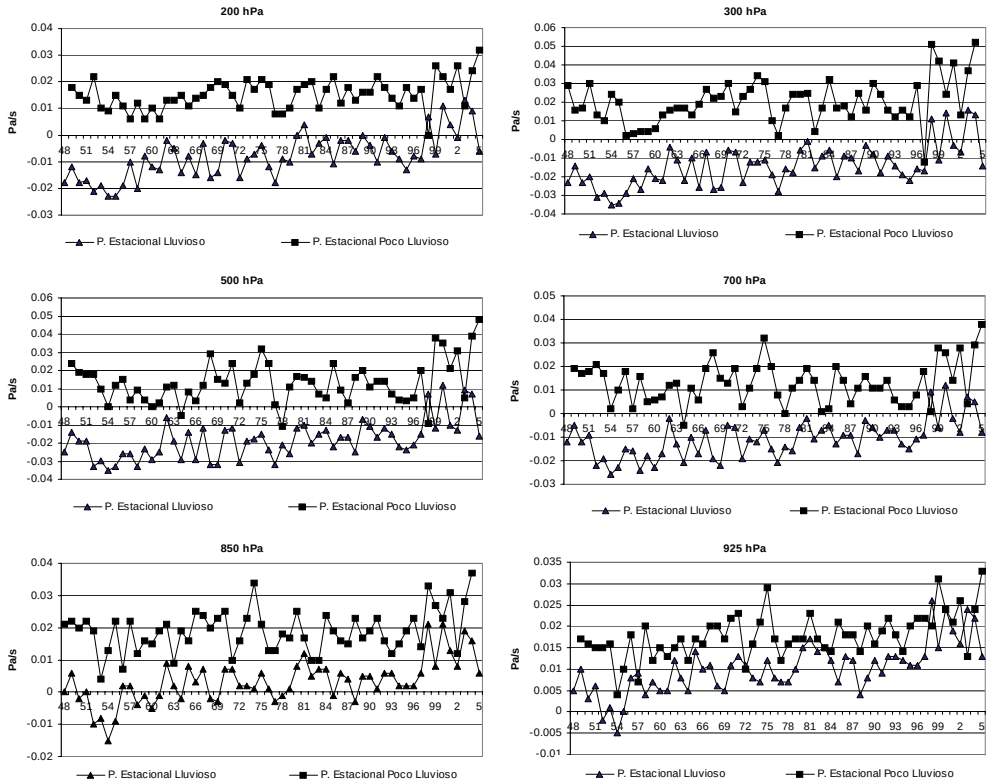


Fig. 5 Tendencias de las magnitudes de Omega en los períodos estacionales lluvioso y poco lluvioso de los años 1948 al 2005 en la tropósfera alta, media y baja sobre la mitad oriental de Cuba (20–25ºN y 75–80ºW).

Tabla 1 I: Estadígrafo de Spearman, II: Nivel de significación calculado para el estadígrafo de Spearman, III: Valor del estadígrafo de Mann Kendall, IV: Nivel de significación calculado para el estadígrafo de Mann Kendall, V: Número de cortes entre las series directa y retrógrada del estadígrafo de Mann Kendall, VI: Valor de la abscisa correspondiente al corte entre las series directa y retrógrada del estadígrafo de Mann Kendall (en caso de ser uno), VII: Valor extremo del estadígrafo de Pettit, VIII: Nivel de significación calculado para el estadígrafo de Pettit, y IX: Valor de la abscisa correspondiente al valor extremo del estadígrafo de Pettit.

	Spearman		Kendall - Mann				Pettit		
Niveles	I	II	III	IV	V	VI	VII	VIII	IX
200	5.178247	0.0000	5.396938	0.0000	3		–592.0	0.0000	1979
300	4.519916	0.0000	4.619063	0.0000	3		–509.0	0.0003	1979
500	4.328080	0.0000	4.467618	0.0000	1	1987	–523.0	0.0002	1979
700	4.118176	0.0000	4.247335	0.0000	3		–523.0	0.0002	1979
850	4.390530	0.0000	4.474502	0.0000	5		–492.0	0.0004	1979
925	5.435686	0.0000	5.851272	0.0000	1	1978	–607.0	0.0000	1979

Los test estadísticos confirman una tendencia creciente altamente significativa en las series de Omega en 925, 850, 700, 500, 300 y 200 hPa. El estadígrafo de Pettit señala un punto de ruptura en el año 1979 en todos los niveles, siendo altamente significativo en 925 hPa (Tabla 1). Estos puntos de cambio, si bien pudieran estar asociados a modificaciones en los sistemas observacionales (Kistler *et al*., 2001), las tendencias evaluadas por períodos independientes (1958–1978, 1979–2005, 1991–2005 y 1998–2005) confirman la existencia real de los progresivos cambios encontrados.

En resumen, durante el período de estudio se ha producido una modificación sostenida de las características de la circulación atmosférica sobre Cuba, que puede ser advertida a través de los cambios en la morfología y alturas geopotenciales de las superficies de presión sobre el área, así como en las magnitudes de los movimientos verticales medios que les están asociados. Tales cambios, muy acrecentados desde finales de los años 90 del pasado siglo hasta el presente, han estado generando condiciones meteorológicas desfavorables para el desarrollo de las lluvias y con ello el establecimiento de la sequía, principalmente en la región oriental del país.

Las tendencias observadas, probablemente relacionadas con variaciones decadales, propias del sistema climático, también son consistentes con las proyecciones de cambio climático regionales más plausibles, los cuales aunque presentan determinados niveles de incertidumbre, proyectan la expansión de los procesos de aridez y sequía, particularmente en su mitad oriental.

REFERENCIAS

Centella, A., Naranjo, L. & Paz, L. R. (1997) *Variaciones y cambios del clima en Cuba*. Centro Nacional del Clima, Instituto de Meteorología, La Habana, Cuba.

Pike, D. (1993) Una revisión del análisis isentrópico con aplicación al PCGRIDS. Western Region Technical Atttachment no. 93-14, de mayo 18, 1993.

Fonseca, C. (2001) Cambios en la posición e intensidad del Anticiclón del Atlántico y modificación del régimen de las lluvias en la región del Caribe. Tesis en opción al título de Master en Ciencias Meteorológicas, Cuba.

IPCC (2001) Cambio climático: La base científica. Resúmenes del Grupo de Trabajo I.

Kistler, R., Kalnay, E., Collins, W., Saha, S., White, G., Woolen, J., Chelliah, M., Ebisuzaki, W., Kanamitsu, M., Kousky, V., Dool, H., Jenne, R. & Fiorino, M. (2001) The NCEP-NCAR 50-year reanalysis: monthly jeans CD-ROM and documentation. *Bull. Am.. Met. Soc*. **82**, 247–268.

Lapinel, B., Centella, A., Fonseca, C., Cutié, V., Rodríguez, C., Pérez, A., Boquet, A., Portelles, R. & Téllez, M. (2006) Sequía, aridez y desertificación en la mitad oriental de Cuba. Un estudio de caso. In: Proceeding of the International Scientific Conference on Desertification and Drylands Research Commemorating 50 Years of Drylands Research

Mellado, E & Borrajero, I. (1997) Software Winstat (Programa para el cálculo de índices de tendencia en series temporales, versión 2.0-beta).Instituto de Meteorología, La Habana (comunicación personal).

Naranjo, L. & Centella, A. (1999) Mecanismos de Circulación de la Atmósfera en la América Tropical. Informe científico. Centro del Clima INSMET, Cuba.

Sneyers, R. (1990) On the statistical analysis of series of observations. Technical Note no.143, WMO no.145. Geneva, Switzerland.

Climate Variability and Change—Hydrological Impacts (Proceedings of the Fifth FRIEND World Conference held at Havana, Cuba, November 2006), IAHS Publ. 308, 2006.

Comportamiento de los días con lluvias intensas en la provincia de Ciego de Ávila en el período lluvioso y su relación con los procesos sinópticos objetivos

ARMANDO MURSULI HERNÁNDEZ & ORLANDO L. CÓRDOVA GARCÍA
Centro Meteorológico Provincial de Ciego de Ávila, Cuba
armando.mursuli@cav.insmet.cu

Resumen En este trabajo se muestra el comportamiento anual, mensual y decenal de los días con lluvias localmente intensas (acumulados de precipitación igual o superior a 100 mm en 24 horas) en la provincia de Ciego de Ávila, en Cuba; y una regionalización geográfica atenida al comportamiento espacial de esta variable hidrometeorológica. Para obtener elementos que ayuden a la mejor predicción de esta variable, se muestra la relación existente entre los días con lluvias intensas y los patrones sinópticos bajo los cuales se desarrollan en los meses del periodo lluvioso en Cuba (mayo-octubre). Este resultado permite conocer las particularidades de los días con lluvias localmente intensas bajo cada uno de los patrones sinópticos en cada zona del territorio estudiado y por tanto permite elevar la calidad y efectividad de los pronósticos de esta variable para la provincia de Ciego de Ávila. Facilitando de esta forma mitigar los daños que puedan producir este fenómeno, tanto a la sociedad, como a la economía.

Palabras claves lluvia diaria; intensidad de la lluvia; patrones sinópticos; predicción de lluvia

Characterization of heavy rainfall days in Ciego de Avilo province (Cuba) and the relationship with objective synoptic processes

Abstract This work shows the annual, monthly and decennial behaviour of the days with local intense rains (accumulated precipitation equal to or greater than 100 mm in 24 hours) in the province of Ciego de Ávila, Cuba, and a special regionalization of this hydrometeorological variable. To identify criteria that help to predict this variable, the relationship between the days with intense rainfall and the synoptic patterns under which they occur during the months of the rainy period (May–October), is determined. This result allows characteristization of the days when there is heavy rainfall due to specific synoptic patterns in the province of Ciego de Ávila. This facilitates the prediction of intense rainfall and so mitigation of the damage produced by this phenomenon.

Key words daily rain; intensity of precipitation; rainfall prediction; synoptic patterns

INTRODUCCIÓN

La lluvia constituye una variable meteorológica difícil de pronosticar por los especialistas que se dedican a esta actividad. A la vez es un elemento importante dentro del clima, que influye directamente sobre el desenvolvimiento económico y social de cualquier país o región en particular. De ahí que desde la antigüedad aún cuando no se contaba con instrumentos de medición el hombre trataba de darle explicación a la ocurrencia de estos fenómenos atmosféricos y otros, con un enfoque mitológico en los inicios y con carácter científico a medida que se fue desarrollando la ciencia gradualmente.

La intensidad de las lluvias esta muy relacionada con el tipo de nube que la origina. Las nubes de deslizamiento ascendente (nimbostratos altostratos) debidas a los frentes dan las lluvias continuas de intensidad media, caen sobre grandes áreas del orden de centenares de miles de kilómetros cuadrados y durante decenas de horas. Los cúmulo-nímbos, debidos a la convección, dan lugar a los aguaceros intensos, pero de corta duración. Después de comenzar pueden alcanzar alta intensidad, pero pueden también cesar bruscamente. En verano cuando los cúmulo-nímbos son muy extensos, los aguaceros pueden durar varias horas.

Las lluvias cuando son intensas pueden dejar de ser un elemento del clima importante para la sociedad y la economía y convertirse en un fenómeno meteorológico peligroso, que entorpece su normal desenvolvimiento y en casos extremos llega a ser la causa de muertes y destrucciones. Por lo que es muy importante la predicción de este fenómeno peligroso con exactitud y efectividad para mitigar los efectos negativos en la sociedad y la economía.

OBJETIVOS

– Conocer el comportamiento de los días con lluvias intensas por zonas en la provincia de Ciego de Ávila.

Copyright © 2006 IAHS Press

– Obtener patrones sinópticos asociados a este fenómeno, con vista a ser empleados en su predicción.

MATERIALES Y MÉTODOS

Para la confección de este trabajo se utilizaron los datos de 20 años (1979–1999), de la red pluviométrica de la provincia, perteneciente a Recursos Hidráulicos, los cuales tienen un número representativo dentro de cada zona. Distribuidos de la forma siguiente: zona norte 23 pluviómetros, zona centro 18 pluviómetros y zona sur 16 pluviómetros. Estas zonas se determinaron con el fin de poder tener una definición más exacta a la hora de pronosticar este fenómeno para cualquier parte o municipio de la provincia. Se tomaron en cuenta las condiciones físico geográficas de cada uno de los municipios.

Posteriormente se relacionaron los días con lluvias intensas con los Patrones Sinópticos Objetivos en el periodo lluvioso del año, bajo los cuales ocurre este fenómeno en cada caso, con vista a poder emplear esta herramienta en el pronóstico del tiempo. Para ello se tomaron los Patrones Sinópticos Objetivos, de Fernández (2003), de los bimestres: mayo–junio, julio–agosto y septiembre–octubre, analizándose la relación de estos con los días con lluvias intensas en cada zona, por meses y decenas, destacándose en cada caso los de mayor persistencia.

RESULTADOS

Comportamiento de los días con lluvias intensas en la provincia de Ciego de Ávila

En el comportamiento anual de los días con lluvias intensas en el período lluvioso (mayo–octubre), indica que los meses con mayor cantidad de estos días son: en primer orden junio con 74 días que representa el 23.0% del total provincial, seguido por mayo con 59 días para un 18.2%, septiembre con 49 días para un 15.1% y octubre con 47 días para un 14.5%. Los meses de menor ocurrencia son: julio con solo 21 días para un 6.5%, seguido de agosto con 39 días para un 12.0% (Fig. 1(a)).

El resultado del análisis decenal de días con lluvias intensas es como sigue: el mes de mayo es el que presenta mayor desbalance entre sus decenas, con 30 días en la tercera decena, 19 días en la segunda y 10 días en la primera, seguido de junio que el mayor número de días ocurre en la primera decena con 30 días, 27 días en la segundad decena y 17 días en la tercera. Aparece también con estas características de desproporción, septiembre con el mayor número de días en la tercera decena con 23 días, 17 días en la primera y solo 9 días en la segunda, seguido de octubre con a mayor cantidad de días en la segunda decena con 20 días, 18 días en la primera y solo 9 días en la tercera. A diferencia de los meses anteriores, agosto presenta una distribución uniforme porque en las tres decenas presentó 13 días con lluvias intensasen cada una y julio con 6 días en la primera decena, 8 en la segunda y 7 días en la tercera, apreciándose la diferencia de solo 2 y 1 día respectivamente (Fig. 1(b)).

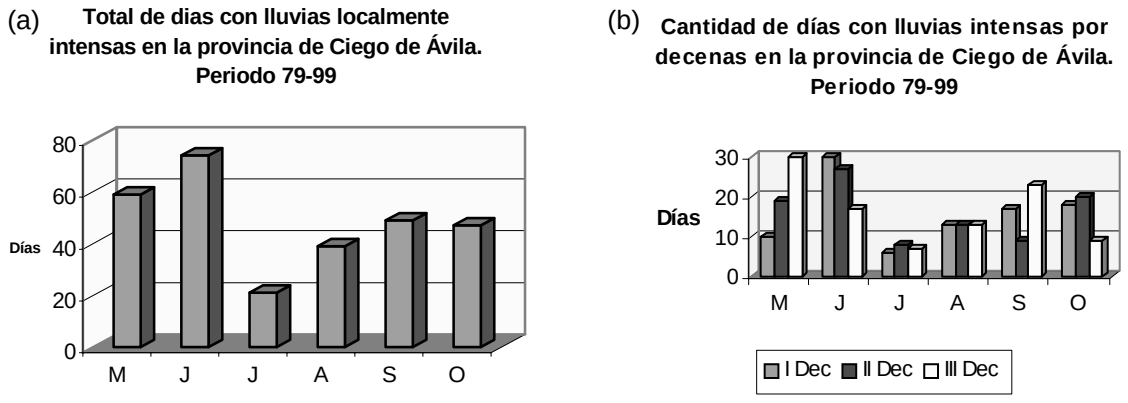


Fig. 1 (a) Comportamiento los días con lluvias localmente intensas; periodo lluvioso. (b) Comportamiento los días con lluvias localmente intensas.

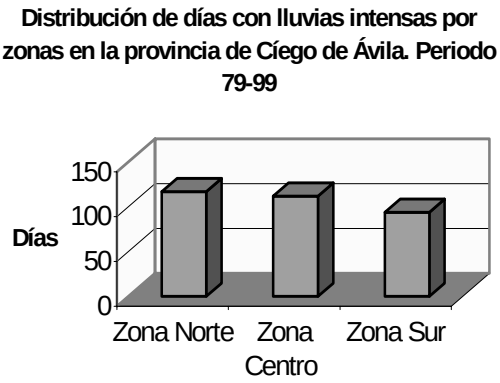


Fig. 2 Distribución por zonas en la provincia de los días con lluvias localmente intensas.

Comportamiento de los días con lluvias intensas por zonas en la provincia de Ciego de Ávila

En la provincia de Ciego de Ávila ocurrieron en el período analizado un total de 323 días con lluvias intensas, distribuidos de la forma siguiente: 117 días en la zona norte para un 36.2%, 112 días en el centro para un 34.6% y la sur con 94 días que representa el 29.1% del total provincial.

Relación de la ocurrencia de lluvias intensas en la provincia de Ciego de Ávila en los meses del período lluvioso con los Patrones Sinópticos Objetivos (PSOs)

Al relacionar los PSOs con los días con lluvias intensas en la provincia de Ciego de Ávila, obtuvimos los resultados siguientes:

El que más se repite durante todo el periodo es el PSO número 11 del bimestre mayo–junio (22 veces):

El mismo representa, un complejo proceso asociado a una profunda hondonada sobre el golfo de México, que interactúa con una profunda vaguada extendida en la circulación de los Oestes sobre el canal de Yucatán, el nordeste del golfo de México y el sureste del continente. Sobre Cuba predomina un marcado flujo de componente Sur, asociado al sector derecho de la onda en los Oestes que inestabiliza el tiempo sobre el archipiélago cubano (Fig. 3).

Seguido del número 1 del propio bimestre con 18 veces. El mismo consiste en la influencia del anticiclón subtropical en superficie, asociado en niveles medios a una potente celda anticiclónica cuyo centro descansa sobre las inmediaciones de La Florida (Fig. 4).

En tercer lugar aparece el número 1 del bimestre septiembre–octubre con 14 veces. El cual consiste en la influencia de las altas presiones oceánicas que interactúan con un centro secundario

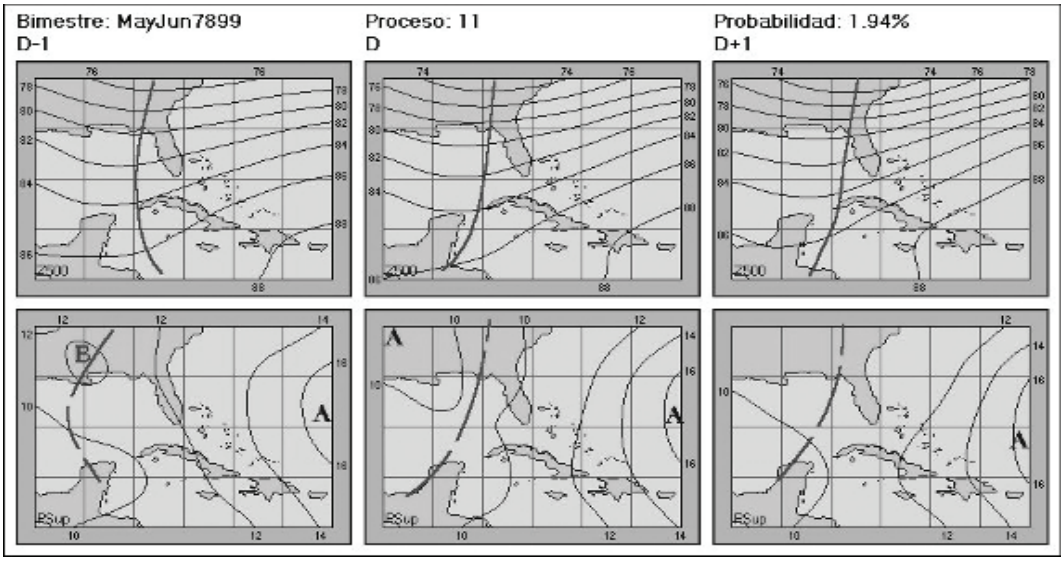


Fig. 3 PSO que más se repite en los días con lluvias localmente intensas.

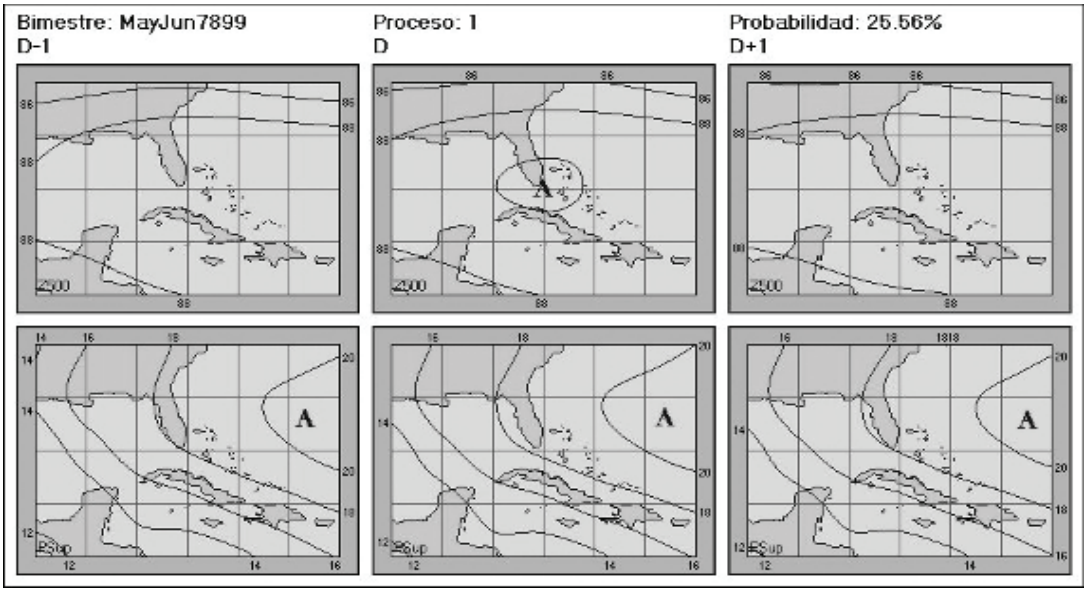


Fig. 4 Segundo PSO que más se repite en los días con lluvias localmente intensas.

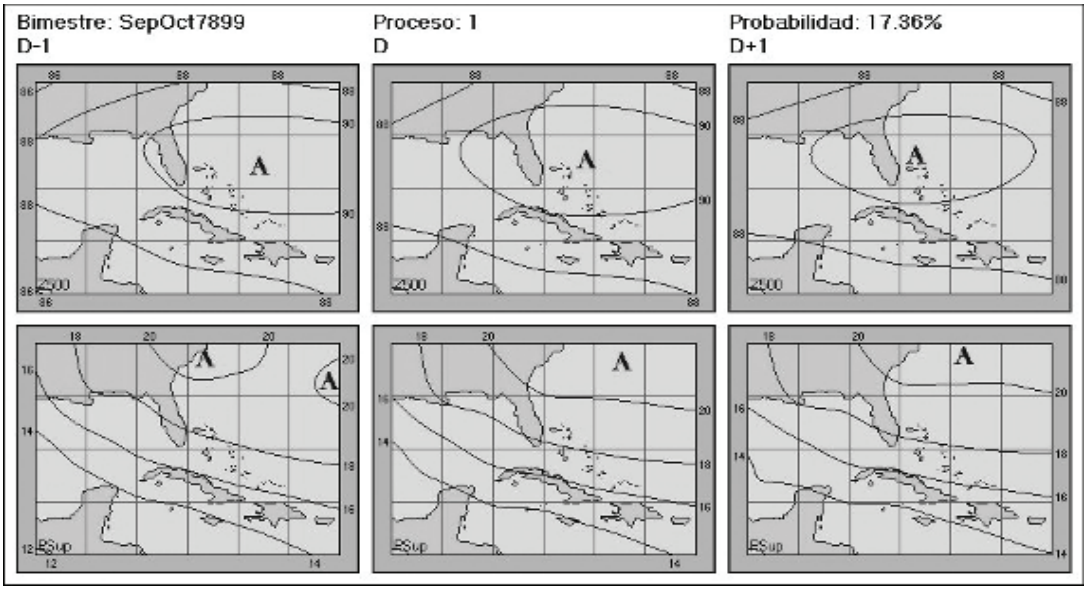


Fig. 5 Tercer PSO que más se da en los días con lluvias localmente intensas.

próximo al continente, típico del mes de septiembre. En niveles medios se aprecia una celda extensa de altas presiones que cubre con su influencia Las Bahamas y La Florida, la cual se expande hacia La Florida y el nordeste del golfo de México (Fig. 5).

APLICACIONES

Desde marzo de 1995, los Centros Meteorológicos Provinciales reciben diariamente una versión del mensaje de pronóstico del ECMWF (Centro Europeo de Pronóstico de Plazo Medio) para el área de trabajo que incluye a Cuba, parte del Golfo de México, las Bahamas, parte del Mar Caribe y la América Central, lo que posibilita que con los nuevos Softwer de la familia “Cuba Forecast” confeccionados por el Centro Meteorológico de Cienfuegos y puestos en práctica de forma operativa en todos los centros provinciales y el Centro Nacional de Pronóstico del INSMET, se obtienen los patrones pronosticados para los plazos de 48, 72, 96, 120 144y 168 horas, los cuales son comparados con los Patrones Sinópticos Objetivos que se ha podido probar en esta investigación que dan lluvias intensas en la provincia de Ciego de Ávila y de esta forma le permite

a los especialistas hacer la predicción de la ocurrencia de este fenómeno meteorológico peligroso en cada una de las zonas del territorio provincial.

CONCLUSIONES

1. En el período lluvioso (mayo–octubre), en los años comprendidos entre 1979–1999 en la provincia de Ciego de Ávila se presentaron 323 días con lluvias intensas.
2. Los meses con mayor cantidad de días con lluvias intensas en la provincia son: en primer lugar junio con 74 días, que representa el 23.0% del total provincial, seguido de mayo con 59 días para un 18.2%, septiembre con 49 días para un 15.1% y octubre con 47 días para un 14.5%.
3. Los meses con menor cantidad de días con lluvias intensas en la provincia son: julio con 21 días para un 6.5% y agosto con 39 días para un 12.0%.
4. En la provincia las decenas con mayor cantidad de días con lluvias intensas son: tercera decena de mayo y primera de junio con 30 días para un 9.3% del total provincial, tercera de septiembre con 23 días para un 7.1%, segunda de octubre con 20 días para un 6.2% y segunda de julio con 8 días para solo un 0.2%.
5. En el mes de agosto las tres decenas se presentaron con 13 días con lluvias intensas.
6. En la zona norte ocurrió la mayor cantidad de días con lluvias intensas, con 117 días que representa el 36.2%, le sigue el centro con 112 días para un 34.6% y por último la zona sur con 94 días que representa el 29.1%.
7. El mes de junio resultó el de mayor cantidad de días con lluvias intensas en todas las zonas de la provincia.
8. El mes de julio esta dentro de los meses con menor cantidad de días con lluvias intensas en todas las zonas de la provincia.
9. La primera decena de junio esta dentro de las de mayor cantidad de días con lluvias intensas en todas las zonas de la provincia.
10. Se logró obtener los Patrones Sinópticos Objetivos asociados a los días con lluvias intensas, en cada una de las zonas en que se dividió la provincia, elemento este de suma importancia para pronosticar la ocurrencia de este fenómeno meteorológico peligroso.

REFERENCIAS

Fernández, A. (2003) Aplicación de los Procesos Sinópticos Objetivos a la Península Ibérica en otoño. *Investigaciones Geográficas* **31**, .31–37.

Fernández, A. & Díaz, Y. (2003) Catálogo de los procesos sinópticos en el Archipiélago cubano. Trabajo presentado en el X Congreso Latinoamericano e Ibérico de Meteorología.

Fernández, A. & Orbe, G. (2003) Distribución mesoescalar de las precipitaciones y su vinculo con los Procesos Sinópticos Objetivos. Trabajo presentado en el X Congreso Latinoamericano e Ibérico de Meteorología.

Climate Variability and Change—Hydrological Impacts (Proceedings of the Fifth FRIEND World Conference held at Havana, Cuba, November 2006), IAHS Publ. 308, 2006.

A study of the spatial extension of agricultural drought in Cuba and its hyper-annual trends

OSCAR SOLANO, RANSÉS VÁZQUEZ & MARÍA E. MARTÍN

Centro de Meteorología Agrícola, Instituto de Meteorología, Apartado postal 17032, CP 11700, Habana 17, Cuba
oscar.solano@insmet.cu

Abstract The average conditions of the spatial extension of agricultural drought in Cuba during a natural year and in the hydrological rainy and semi-rainy seasons were studied. The methods used to diagnose agricultural drought were based upon the water balance results from each element of the soil–plant–atmosphere complex, which made it possible to identify for each period the zones of the country that were most affected by this extreme climatic event and its hyper-annual trend. The results achieved show a trend to a surface increase of severe agricultural drought in Cuba during the study period.

Key words agricultural drought; geographic information systems; agroclimatic zoning; hyper-annual trends; Cuba

INTRODUCTION

The process of adapting to the potential impact of climate change demands adequate interpretation and knowledge about the threat imposed by significant extreme events. Therefore it was deemed appropriate to research those trends, patterns and general behaviour of agricultural drought that has an impact on both food safety and the country's social and economic life.

The general objective of this work was to establish the historical values of the spatial extension of agricultural drought in Cuba during a natural year and in the rainy and semi-rainy seasons as well as its hyper-annual trends on a proper scale, for exploratory purposes.

DATA

Data for the climatic variables used in this research work were taken from 62 meteorological stations and 809 raingauge stations belonging to the Institute of Meteorology and the National Hydraulic Resources Institute networks. This information was processed taking a decade (ten days) as the base temporary period.

A time span from 1951 to 1990 was selected to analyse climate data on the historical values of the spatial extension of agricultural drought in Cuba during a natural year and in the rainy and semi-rainy hydrological periods, and the 1951–2005 period was taken to study hyper-annual trends.

METHODS

For the purposes of this research, agricultural drought was assessed on the basis of the soil moisture deficit resulting from the soil water balance in the rhizosphere. The methods used to this end are based on a temporary and spatial assessment of agricultural drought after analysing the moisture index dry condition described by Solano *et al.* (2005a,b,c).

A summary of the process used to forecast agricultural drought by combining the tools available in computer software packages, such as EXCEL and the Geographic Information Systems (GISs), is shown graphically in Fig. 1.

Due to the exploratory nature of this research work, a 7626-dot grid whose pixel represents a lateral spatial resolution of 4-km was designed for the country.

The term "presence of agricultural drought" in this work corresponds to the dry period that has kept vegetation under moderate or severe water stress for a period of at least four decades following the beginning of soil water depletion.

The scale used to diagnose the spatial extension of agricultural drought, shown in Table 1, comprises seven categories according to the percentage area of the territory being assessed, which

Copyright © 2006 IAHS Press

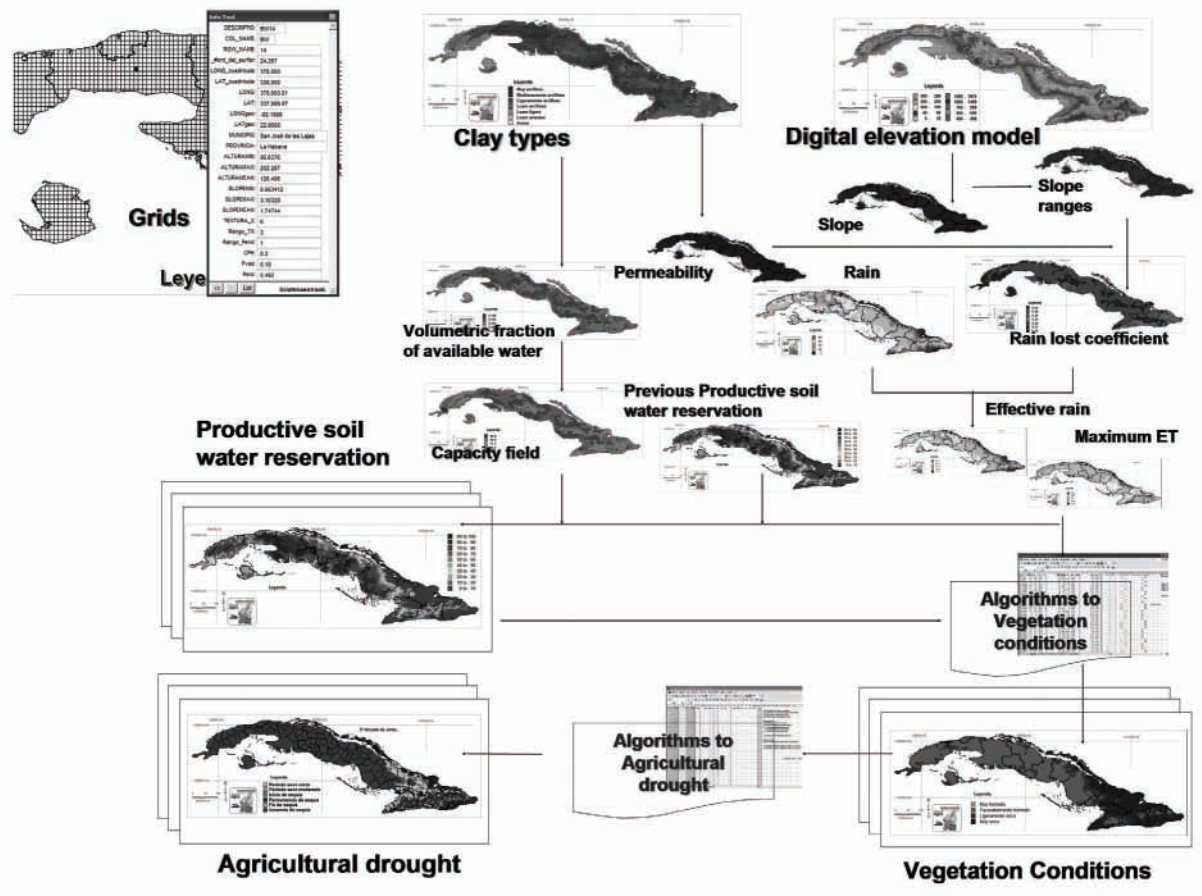


Fig. 1 Flowchart showing the general methodology of the method used to diagnose agricultural drought by using GISs.

Table 1 Diagnose categories for the spatial extension of agricultural drought according to the percentage of the assessed territory.

Minimum threshold (%)		Category		Maximum threshold (%)
0	≤	Absence	<	5
5	≤	Very small	<	20
20	≤	Small	<	40
40	≤	Average	≤	60
60	<	Large	≤	80
80	<	Very large	≤	95
95	<	Total	≤	100

is at different agricultural drought development stages, with respect to the total area including the said territory.

As defined in this study, the severe category indicates the occurrence of at least a 12-decade-long dry period where the total number of very dry or severely dry decades is equal to or greater than 60% of the overall length of that dry period (Solano *et al.*, 2005a).

RESULTS

The Cuban municipalities most affected by the spatial extension of agricultural drought during the rainy period are located in the eastern provinces, and the least affected in the western and central regions (Fig. 2). In the semi-rainy period this surface area increases across the country, the most affected municipalities being those located in the eastern provinces, even if it usually occurs in the central region too (Cienfuegos and Ciego de Avila provinces).

Figure 3 shows 11 episodes of agricultural drought, namely 1951–52, 1956, 1959, 1961–63, 1965, 1967, 1970–71, 1974–76, 1981, 1984–87 and 1989–90.

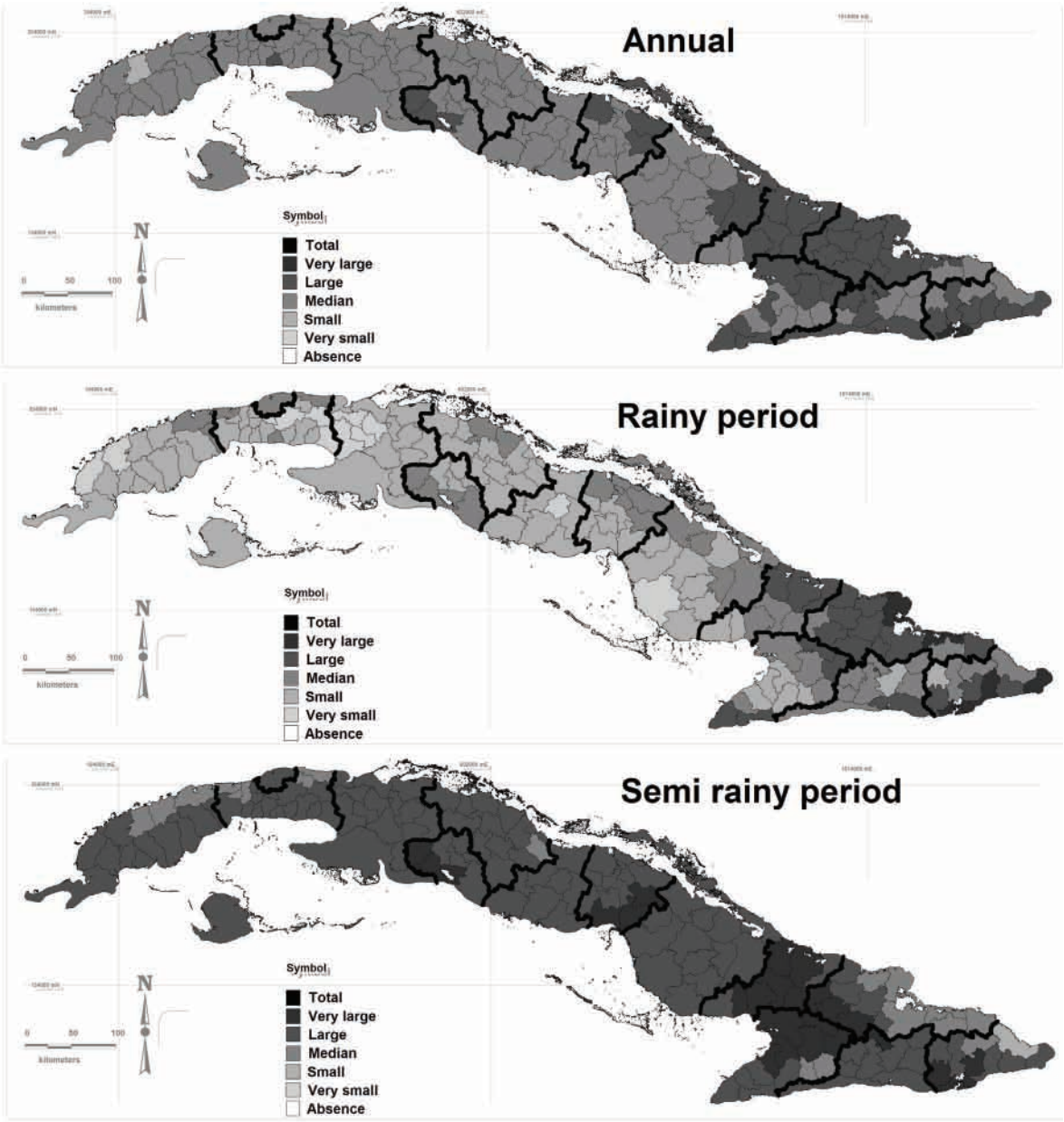


Fig. 2 Diagnose of the average municipal spatial distribution of the spatial extension of agricultural drought in the historical values rainy, semi-rainy and annual periods.

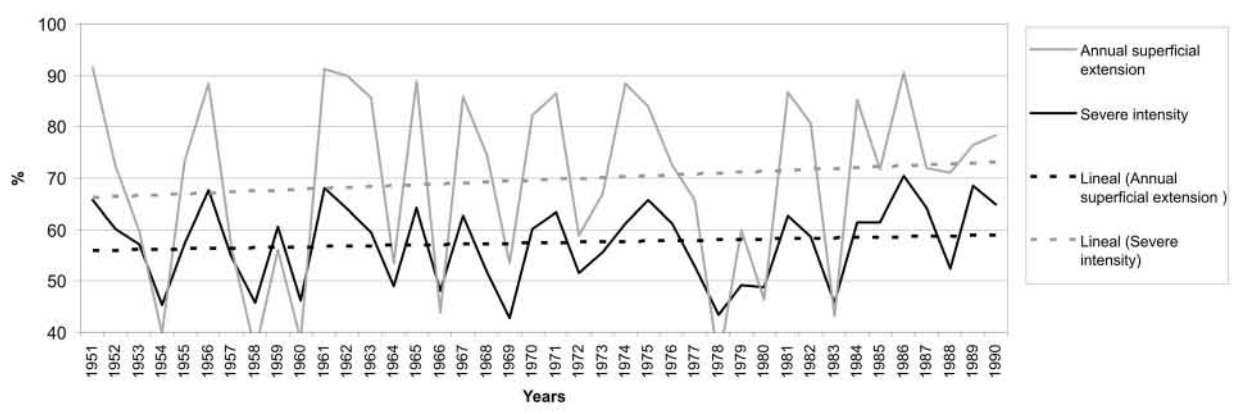


Fig. 3 Hyper-annual behaviour and trends of both spatial extension and (severe) intensity of annual agricultural drought in Cuba, in percent affected area.

The spatial extension of Cuba's annual severe agricultural drought tends to increase in the period under study. As indicated by the equation of this hyper-annual trend ($y = 0.07444x + 55.829$), the area affected by agricultural drought during the said period in Cuba shows an annual increase of about 8000 ha per year.

The results of analysing the spatial extension trends of severe agricultural drought for one natural year in Cuba are in conformity with those from research works made by the Climate Center of the Meteorology Institute of the Republic of Cuba regarding the behaviour of rainfall and meteorological drought in the country (Lapinel *et al.*, 1993; Centella *et al.*, 1997), in the sense that both agricultural and meteorological drought have increased in frequency and intensity, together with a reduction of the overall yearly precipitation from 10 to 20% and a higher year-to-year variability of 5 to 10% and the fact that precipitation has decreased in the rainy period and increased in the semi-rainy period.

When the hyper-annual spatial extension progress was studied as a percent area affected by agricultural drought in Cuba during the more recent 1999–2005 period, an increasing trend in time was also found, which indicates that current trends are in line with those resulting from the 40-year period and those mentioned in the above paragraph.

The diagnosis of the hyper-annual progress and trends in Cuba's agricultural drought surface area and severe intensity corresponding to the natural year indicates that, during the period being studied, this extreme climate event has increased its annual spatial extension and intensity, with an average annual progress in previously unaffected areas of about 8000 ha, an increasing spatial extension and intensity in the rainy period and a reduction of these parameters in agricultural drought in the semi-rainy period, with a smaller value than that achieved in the rainy period increase.

New agroclimatic products developed as a result of this research work provide information both to assess the threat of agricultural drought in our country and to enable handling of climate risk in selecting the best strategic decisions and devising tactics for agricultural operations.

The results stemming from the spatial assessment of agricultural drought in Cuba, generated by and shown in this paper, lay the foundations to undertake new agroclimatic research and study the risk posed by this extreme climate event, since they improve our understanding of agricultural drought and the agrometeorological service's output, and therefore extend scientific knowledge about drought in Cuba.

REFERENCES

Centella, A., Naranjo, L., Paz, L., Cárdenas, P., Lapinel, B., Ballester, M., Pérez, R., Alfonso, A., González, C., Limia, M. & Sosa, M. (1997) Variaciones y cambios del clima en Cuba. Informe Técnico. Instituto de Meteorología, La Habana, Cuba.

Lapinel, B., Rivero, R. E., Cutié, V., Rivero, R. R., Varela, N. & Sardinas, M. (1993) Sistema Nacional de Vigilancia de la Sequía: Análisis del período 1931–1990. Informe Científico Técnico, Centro Meteorológico de Camagüey, Cuba.

Solano, O., Vázquez, R., Menéndez, C. J. & Menéndez, J. A. (2000) Sistema Agrometeorológico Operativo para la Detección y Seguimiento de la Sequía Agrícola en Cuba. In: *Fenómenos Meteorológicos Adversos* (Actas de la Reunión de Expertos de las Asociaciones Regionales III y IV, Caracas, 1999). 45–54.

Solano, O., Vázquez, R., Menéndez, C., Menéndez, J. & Martín, M. E. (2005a) Evaluación de la Sequía Agrícola en Cuba. *Revista Cubana de Meteorología* **12**(2), 3–14.

Solano, O., Vázquez, R., Menéndez, C. & Martín, M. (2005b) Evaluación científica de los riesgos asociados a la ocurrencia de la sequía agrícola en las repúblicas de Cuba y Dominicana. Informe final Proyecto PNUD-CUBA RLA/01/013 Strengthening Links Between Development and Climate Change Adaptation in the Caribbean.

Solano, O., Vázquez, R., Menéndez, C., Menéndez, J. & Martín, M. E. (2005c) Manual de técnicas y procedimientos para el desarrollo de la climatología de la sequía agrícola. Proyecto PNUD-CUBA RLA/01/013 Strengthening Links Between Development and Climate Change Adaptation in the Caribbean.

Climate Variability and Change—Hydrological Impacts (Proceedings of the Fifth FRIEND World Conference held at Havana, Cuba, November 2006), IAHS Publ. 308, 2006.

Critique statistique des séries des pluies annuelles dans le bassin amont du Fleuve Sénégal

SOUSSOU SAMBOU[1] **& EDMOND NICAISE MALANDA NIMY**[2]

1 *Université Cheikh Anta Diop, Faculté des Sciences et Techniques, Département de Physique, BP 5005 Dakar-Fann, Senegal*
sousamb@refer.sn

2 *Université Cheikh Anta Diop, Faculté des Sciences et Techniques, Département de Géologie, BP 5005 Dakar-Fann, Senegal*

Résumé Une étude des propriétés statistiques des séries de hauteurs de pluie annuelles observées dans le bassin amont du fleuve Sénégal situé au Mali et au Sénégal est effectuée à l'aide de tests d'indépendance et d'homogénéité. Les premiers ont fait ressortir une forte irrégularité interannuelle, une tendance au déficit pluviométrique, et dans certains cas une persistance de type markovien. Les seconds ont tous détecté une réduction sensible de la moyenne sur la période étudiée. L'analyse en composantes principales réduites a confirmé l'unité climatique de la zone d'étude. La station de Bakel a cependant un comportement différent face aux tests d'homogénéité et à l'analyse en composantes réduite. Ce comportement singulier de la station de Bakel ne peut pas se justifier par des erreurs systématiques et une analyse plus poussée mériterait d'être menée pour élucider cette singularité.

Mots clefs Fleuve Sénégal; variabilité climatique; tests statistiques; analyse en composantes principales

Statistical analyses of the annual rainfall of the upper Senegal basin

Abstract Classical tests for independence and homogeneity have been applied to annual series of rainfall in the upper part of the Senegal River basin. The first have outlined the different properties of the series, i.e. Markovian persistence for some of them, strong irregularity from one year to the other for all and a long-term trend of decrease of the rainfall except for Bakel; and the second demonstrated a sharp reduction in the mean of the annual rainfall. The statistical tests and principal components analysis show that the raingauge at the Bakel station behaves quite differently. One explanation of this could be the occurrence of systematic errors during the sampling of the observations. But, given the importance of the raingauge station at Bakel for the Senegal River, it is important to explain this singularity.

Key words Senegal River; climatic variability; statistical tests; principal components analyses

INTRODUCTION

La tendance climatique d'une région donnée peut être connue à travers les séries de hauteurs de pluies annuelles, particulièrement lorsque celles-ci sont suffisamment longues. Ces séries constituent en effet les entrées des modèles statistiques et probabilistes. Pour celà, elles doivent être homogènes et représentatives de la population dont est tiré l'échantillon d'une part, et, d'autre part, les observations qu'elles contiennent doivent être indépendantes. La série est représentative lorsque les différentes observations qui la constituent proviennent des mêmes processus physiques; elle est homogène lorsque ces observations sont issues de la même population ou si elles peuvent être représentées par la même loi statistique. En pratique, l'homogénéité est vérifiée à travers l'étude de la stationnarité de la moyenne.

Dans cet article, nous avons utilisé les tests statistiques d'indépendance et d'homogénéité pour étudier la tendance climatique et la structure des hauteurs de pluies annuelles observées dans le bassin amont du fleuve Sénégal, situé au Mali et au Sénégal en amont de Bakel. Ces tests ont pour la plupart été appliqués à l'étude de la variabilité climatique, particulièrement en Afrique Occidentale et Centrale, par des chercheurs provenant d'horizons divers (Aka *et al.*, 1996; Mirza, 1997; Paturel *et al.*, 1998; Ardoin *et al.*, 2003; Sambou, 2005). En comparant les résultats des tests d'indépendance et les graphiques d'évolution interannuelle, nous avons constaté que chaque test d'indépendance illustre une particularité de la pluviométrie annuelle dans la zone d'étude: persistance markovienne ou non, tendance au déficit, forte irrégularité interannuelle. Par contre, les tests d'homogénéité font tous ressortir la non stationnarité de la moyenne des séries annuelles. La série des hauteurs de pluies annuelles à la station de Bakel se singularise par sa stationnarité et son homogénéité, comme l'indiquent tous les tests effectués et les représentations graphiques associées. L'analyse en composantes principales réduites confirme cette opposition entre la station de Bakel et les autres. Ce comportement, que l'hypothèse d'erreurs systématiques dans la collecte

Copyright © 2006 IAHS Press

des observations ne justifie pas, devrait être élucidé par une critique plus approfondie et si nécessaire par recours aux modèles de circulation générale.

MÉTHODOLOGIE

La variabilité climatique en Afrique Occidentale et Centrale est devenue une composante très importante dans la gestion des ressources en eau, et son étude a suscité l'intérêt de la communauté scientifique internationale. L'analyse des propriétés statistiques des séries de cumuls annuels de hauteurs de pluies à partir de tests statistiques a connu un essor. Dans cet article, des tests statistiques éprouvés en Afrique Occidentale et Centrale ont été appliqués: le test de Pettitt (Pettitt, 1979), le test du cumul des résidus (Paturel *et al.*, 1998) et la procédure de segmentation des séries (Hubert, 1989) pour vérifier l'homogénéité des séries, avec comme hypothèse nulle H_0 = "la série est homogène"; le test basé sur l'analyse de l'auto corrélogramme et le test du coefficient d'auto corrélation d'ordre 1 pour déceler une persistance de type markovienne; le test des points de rebroussement (Kottegoda, 1980) pour mesurer le caractère aléatoire de la série et par conséquent l'irrégularité interannuelle; le test de corrélation des rangs de Kendall (Kendall & Stuart, 1961) pour mettre en évidence toute tendance à long terme. L'hypothèse nulle pour ces tests est H_0 = "la série est aléatoire". Nous renvoyons à ces références bibliographiques pour la définition de ces tests.

NATURE ET PROVENANCE DES DONNEES

Les données de base que nous avons utilisées dans cette étude sont constituées des cumuls annuels de hauteurs de pluies journalières que nous avons obtenues, de l'origine à 1965, à partir des publications du CIEH, de l'ORSTOM-Hydrologie et de l'ASECNA (CIEH, 1973–1979), puis de 1966 à 1980 (CIEH, 1989–1990). La période allant de 1981 à 1995 a été obtenue pour certaines stations à partir de la banque ORSTOM. Nous avons critiqué les séries de la zone d'étude et retenu comme stations de référence les stations de Bakel, Kayes, Kidira, Kita, Nioro, Mourdali, Bafoulabé, Toukoto, Faladyé, Kéniéba, Yélimané, Galougo (Fig. 1), et comme période de référence la période 1931-1995. Les calculs ont été faits soit sur tableur Excel (tests du cumul des résidus), à l'aide de programmes écrits en Fortran (test de Pettitt, test de corrélation des rangs de Kendall, coefficients d'autocorrélation) ou à partir d'un éxecutable développé par Hubert *et al.* (1989) pour le test de segmentation des séries. Nous présentons ci-dessous les résultats obtenus.

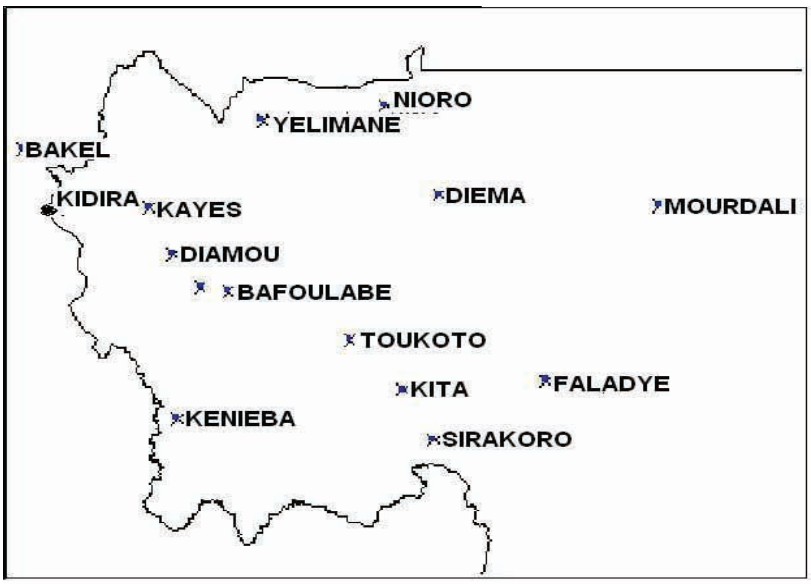


Fig. 1 Emplacement des stations retenues.

SYNTHESE DES TESTS ET RESULTATS

Tests d'indépendance

L'analyse des auto corrélogrammes, au niveau de signification $\alpha = 0.05$, fait ressortir sur l'ensemble des stations, soit des coefficients d'auto corrélation d'ordre 1 trop élevés, soit des points figuratifs hors des limites de confiance, ce qui ne permet pas de conclure (Fig. 2). Le test du coefficient d'autocorrélation d'ordre 1 rejette l'hypothèse nulle pour les stations de Bafoulabé, Faladyé, Galougo, Mourdali, Nioro et Yélimané (Tableau 1). Le test des points de rebroussement accepte l'hypothèse nulle d'une série aléatoire pour toutes les stations (Tableau 1) et le test de corrélation des rangs rejette l'hypothèse nulle d'absence de tendance linéaire pour toutes les stations à l'exception de celle de Bakel (Tableau 1). Les résultats du Tableau 1 peuvent être interprétés à la lumière de l'évolution interannuelle des séries de pluies annuelles (Fig. 3): le test de corrélation des rangs de Kendall traduit la tendance linéaire généralisée à la baisse des précipitations pour toutes les stations à l'exception celle de Bakel; le test des points de rebroussement souligne la forte irrégularité interannuelle des observations contenues commune à toutes les séries de pluies annuelles; le test du coefficient de corrélation d'ordre 1 indique une certaine persistance dans les observations, la tendance de la pluviométrie se maintenant sur quelques années avant de s'inverser pour certaines stations.

Tests d'homogénéité

Le tableau 2 fait la synthèse des résultats des tests d'homogénéité : l'hypothèse nulle est rejetée pour toutes les stations à l'exception de celle de Bakel; la date de rupture se situe entre 1963 et 1971. Les graphes des cumuls des résidus et les ellipses de Bois associées ont été analysées (Fig. 4). Pour la série de Bakel, tous les points figuratifs des cumuls des résidus se trouvent à l'intérieur de l'ellipse alors que pour les séries des autres stations, une bonne partie des points se trouve hors des ellipses associés: l'hypothèse nulle est acceptée pour Bakel, les autres séries présentent une rupture dont l'année de démarrage coïncide avec le maximum du cumul des résidus. Le test de segmentation des séries à l'ordre 2 met en évidence une diminution nette et prolongée de la valeur de la moyenne de toutes les séries à l'exception de celle de Bakel (Tableau 3, Fig. 5).

Liste des abbreviations en les tableaux Bak: Bakel; Baf: Bafoulabé; Fal; Faladyé; Gal: Galougo; Kid: Kidira; Kay: Kayes; Ken: Kéniéba; Kit: Kit; Mou: Mourdali; Nio: Nioro; Tou: Toukoto; Yél: Yélimané.

Tableau 1 Synthèse des tests d'indépendance: H_0= série aléatoire.

Stations	Baf	Bak	Fal	Gal	Kid	Kay	Kéni	Kit	Mou	Nio	Touk	Yél
Test du coeffficient du coefficient d'autocorélation d'ordre 1												
Résultats	Non	Oui	Non	Non	Oui	Oui	Non	Oui	Non	Non	Oui	Non
Test des points de rebroussement.												
Résultats	Oui	Oui	Oui	Oui	Oui	Oui	Oui	Oui	Oui	Oui	Oui	OUi
Tests de corrélation des rangs de Kendall												
Résultats	Oui	Non	Non	Non	Non	Non	Non	Non	Non	Non	Non	Non

Tableau 2 Synthèse des tests d'homogénéité: H_0 = série homogène.

Stations	Baf	Bak	Fal	Gal	Kid	Kay	Kéni	Kit	Mou	Nio	Touk	Yél
Test de Pettitt												
	Non	Oui	Non	Non	Non	Non	Non	Non	Non	Non	Non	Non
Test basé sur l'ellipse de contrôle												
	Non	Oui	Non	Non	Non	Non	Non	Non	Non	Non	Non	Non
Année	1967		1967	1966	1963	1967	1967	1969	1970	1966	1967	1971

Tableau 3 Résultats du test de segmentation des séries. H_0 = série homogène. (D = déficit).

Stations	Baf	Bak	Fal	Gal	Kid	Kay	Kéni	Kit	Mou	Nio	Touk	Yél
Résultats	Non	Oui	Non	Non	Non	Non	Non	Non	Non	Non	Non	Non
Année	1968		1968	1967	1963	1967	1968	1969	1971	1967	1970	1972
	D		D	D	D	D	D	D	D	D	D	D

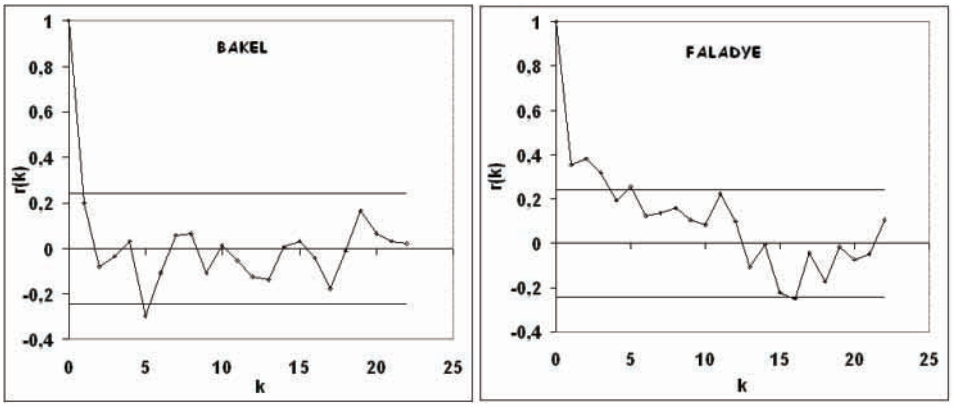


Fig. 2 Auto corrélogramme des séries de hauteurs de pluies annuelles.

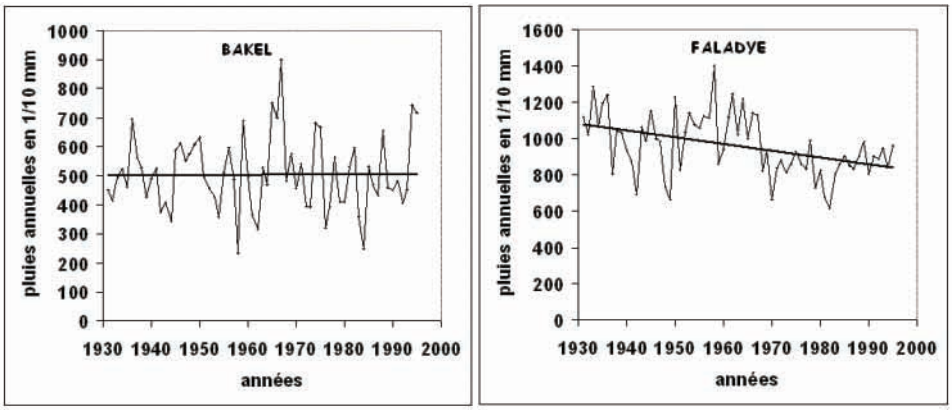


Fig. 3 Evolution inter - annuelle des hauteurs de pluies annuelles.

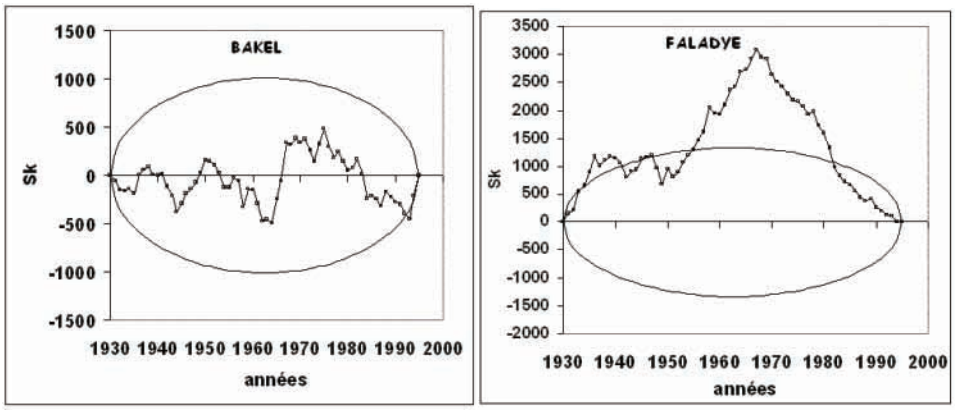


Fig. 4 Tests du cumul des résidus: ellipses de Bois.

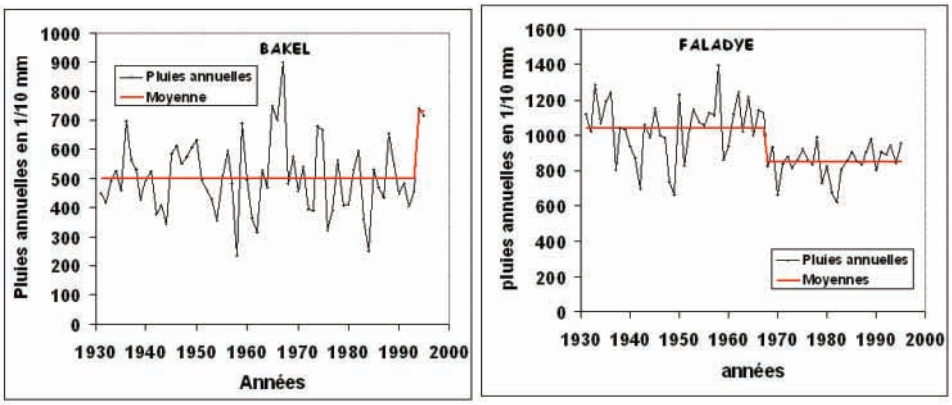


Fig. 5 Tests de segmentation des séries.

REGIONALISATION PAR ANALYSE EN COMPOSANTES REDUITES

Analyse de la matrice de corrélation des variables

La moyenne et l'écart-type des séries de pluies annuelles ainsi que les éléments de la matrice de corrélation ont été calculés (Tableau 4). De l'analyse des éléments de cette matrice, il ressort une faible corrélation entre les stations de Kéniéba et de Bakel et les autres stations (1ère et 10ème colonne). Ce comportement singulier est confirmé par la faible valeur du coefficient de corrélation moyen entre ces stations et les autres.

Tableau 4 Matrice de corrélation des pluies annuelles aux stations retenues.

Stations	Bak	Kay	Kid	Kit	Nio	Mou	Baf	Tou	Fal	Kén	Yél	Gal
Bak	1	0.25	0.22	0.18	0.03	0.20	0.04	0.09	0.00	0.16	0.15	0.07
Kay	0.25	1	0.62	0.49	0.47	0.50	0.38	0.47	0.41	–0.03	0.62	0.55
Kid	0.22	0.62	1	0.37	0.41	0.43	0.30	0.35	0.35	–0.04	0.57	0.33
Ki	0.18	0.49	0.37	1	0.50	0.54	0.31	0.51	0.56	0.02	0.49	0.59
Nio	0.03	0.47	0.41	0.50	1	0.62	0.66	0.52	0.72	–0.00	0.68	0.57
Mou	0.20	0.50	0.43	0.54	0.62	1	0.56	0.49	0.51	–0.10	0.57	0.51
Baf	0.04	0.38	0.30	0.31	0.66	0.56	1	0.31	0.53	0.08	0.53	0.36
Tou	0.09	0.47	0.35	0.51	0.52	0.49	0.31	1	0.52	0.12	0.46	0.45
Fal	0.00	0.41	0.35	0.56	0.72	0.51	0.53	0.52	1	–0.13	0.52	0.51
Kén	0.16	–0.03	–0.04	0.02	0.00	–0.10	0.08	0.12	–0.13	1	0.04	–0.12
Yél	0.15	0.62	0.57	0.49	0.68	0.57	0.53	0.46	0.52	0.04	1	0.62
Gal	0.07	0.55	0.33	0.59	0.57	0.51	0.36	0.45	0.51	–0.12	0.62	1
Moyenne	0.20	0.48	0.401	0.46	0.51	0.49	0.42	0.44	0.42	0.08	0.52	0.45

Analyse du nuage des variables

Les variables sont représentées dans le plan des deux premiers axes factoriels (Fig. 6). Les variables stations de Nioro, Yélimané, Kayes, Kita, Mourdali, Faladyé, Galougo, Kidira, Bafoulabé et Toukoto forment un nuage de points relativement corrélé avec le premier axe (axe horizontal) qui rassemble 46.5% de la variance totale. Les stations de Bakel et de Kéniéba par contre sont très faiblement corrélées avec cet axe: Bakel est fortement corrélée avec le second axe vertical ($\hat{r}$ = 0.76) (10.70 % de la variance totale), et Kéniéba avec le troisième axe factoriel. Les stations se répartissent donc en trois groupes: un premier rassemblant la majeure partie d'entre elles (10 stations), deux autres constituées chacune d'une seule station: Bakel pour le deuxième groupe, Kéniéba pour le troisième.

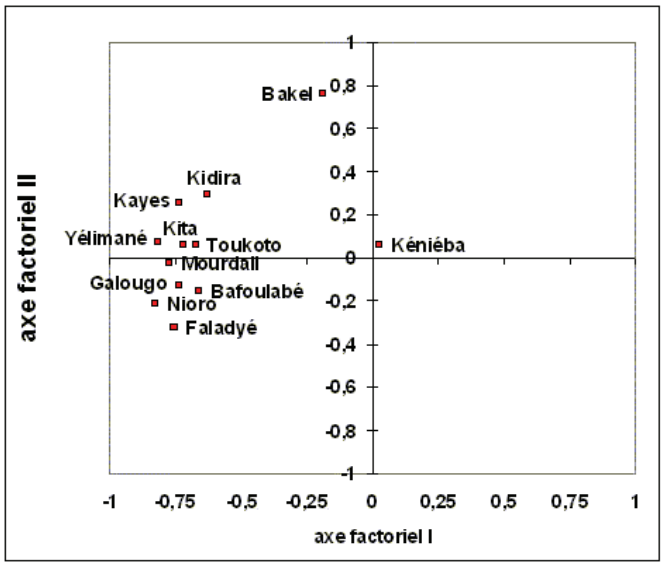


Fig. 6 Analyse en composantes principales réduites : nuage des variables.

Analyse en composantes principales réduites et variabilité climatique

Les résultats des tests d'indépendance et surtout des tests d'homogénéité montrent que le premier groupe rassemble les stations ayant le même comportement climatique sur la série étudiée : tendance linéaire à la baisse des précipitations et une rupture de la moyenne de la série des pluies annuelles dans le sens d'un déficit. Le premier axe factoriel, relativement mieux corrélé avec le nuage, représente donc cette variabilité climatique. La station de Bakel est stationnaire du point de vue climatique ; cette stationnarité est représentée par le second axe factoriel avec laquelle elle est fortement corrélée. La station de Kéniéba est soumise aux mêmes effets de la variabilité climatique tout comme les stations du nuage; par contre sa pluviométrie moyenne annuelle sur la période analysée est la plus élevée, et, surtout, elle se trouve en altitude dans la zone soudanienne. Le troisième axe factoriel avec laquelle elle est fortement corrélée, peut être associée à l'influence soudanienne combinée à l'altitude.

CONCLUSION ET PERSPECTIVES

Les tests d'indépendance que nous avons utilisés ont permis de faire ressortir la forte irrégularité inter annuelle, la tendance à long terme à la décroissance, et dans certains cas la persistance de type markovien dans les séries étudiées. Les tests d'homogénéité quant à eux ont mis en évidence une baisse généralisée et prolongée des précipitations dans la zone d'étude, à l'exception de la station de Bakel. Cette station se distingue par des observations successives indépendantes entre elles et surtout une stationnarité de la moyenne des pluies annuelles. L'analyse en composantes réduites confirme l'effet de la variabilité climatique sur l'ensemble des stations de la zone d'étude et sur la période analysée, et met en relief le comportement singulier des stations de Kéniéba et Bakel. La première est, en plus de la variabilité climatique, soumise à l'influence du relief et à celle de la zone climatique à dominante soudanienne dans laquelle elle se trouve. La seconde est la seule à ne pas subir l'influence de la variabilité climatique. L'hypothèse d'erreurs systématiques survenues au cours de la collecte et de la mise en forme des observations pourrait être avancée, mais ne résiste pas à l'analyse car de telles erreurs se produiraient uniquement pour cette station**.** La station de Bakel est l'une des plus anciennes du bassin du fleuve Sénégal ; elle revêt une grande importance pour la connaissance de l'évolution du climat du bassin versant du fleuve. Les travaux de recherche visant à déterminer l'origine de ce comportement singulier devraient être poursuivis au moyen d'autres techniques (GCM par exemple)

REFERENCES

Aka, A., Lubès, H., Mason, J. M., Servat, E., Paturel, J. E. & Kouamé, B. (1996) Analysis of temporal variability of runoff in Ivory Coast: statistical approach and phenomena characterization. *Hydrol. Sci. J.* **41**, 959–970.

Ardoin, S., Lubès-Niel, H., Servat, E., Dezetter, A., Boyer, F., Mahé, G. & Paturel, E. (2003) Analyse de la persistance de la sécheresse en Afrique de l'Ouest: caractérisation de la situation de la décennie 1990. In: *Hydrology of the Mediterrenean and Semiarid Regions* (ed. by E. Servat, W. Najem, C. Leduc & A. Shakeel), 223–228. IAHS Publ. 278, IAHS Press, Wallingford, UK.

CIEH, Orstom, Hydrologie, Asecna (1973–1979) Services Météorologiques Nationaux. *Précipitations journalières de l'origine à 1965. Républiques du Dahomey, Tchad, Côte d'Ivoire, Mali, Sénégal, Niger, Haute-Volta, Mauritanie, Togo, Gabon, Cameroun* (*début à 1972*), 12 volumes. ORSTOM, Paris, France.

CIEH, Orstom, Hydrologie, Asecna, (1989–1990) Services Météorologiques Nationaux. *Précipitations journalières de 1966 à 1980. Républiques du Dahomey, Tchad, Côte d'Ivoire, Mali, Sénégal, Niger, Haute-Volta, Mauritanie, Togo, Gabon, Cameroun*, 14 volumes. ORSTOM, Paris, France.

Hubert, P., Carbonnel, J. M. & Chaouche, A. (1989) Segmentation des séries hydrométéorologiques – Application à des séries des précipitations et de débits en Afrique de l'Ouest. *J. Hydrol.* **110**, 349–367.

Kottegoda, N. T. (1980) *Stochastic Water Resources Technology*. The MacMillan Press Ltd, Hong Kong.

Kendall, M. G. & Stuart, A. (1961) *The Advanced Theory of Statistics*, vol. 2. Hafner, New York, USA.

Mirza, M. Q. (1997) Hydrological changes in the Ganges system in the Bengla Desh in the post Farakka period. *Hydrol. Sci. J.* **42**, 613–632.

Paturel, J. E., Servat, E., Delattre, M. O. & Lubès-Niel, H. (1998) Analyse des séries pluviométriques de longue durée en Afrique de l'Ouest et Centrale non sahélienne dans un contexte de variabilité climatique. *Hydrol Sci J*. **43**, 937–946.

Pettitt, A. N. (1979)A non parametric approach of the change – point problem. *Appl. Statis.* **28**, 126–135.

Sambou, S. (2005) Modélisation des processus hydrologiques sur l'exemple du bassin amont du fleuve Sénégal. Thèse de Doctorat ès Sciences. Université Cheikh Anta Diop de Dakar, Sénégal.

Climate Variability and Change—Hydrological Impacts (Proceedings of the Fifth FRIEND World Conference held at Havana, Cuba, November 2006), IAHS Publ. 308, 2006.

Impacts of regional land use and land cover on rainfall: an overview

R. A. PIELKE Sr[1,2], A. BELTRÁN-PRZEKURAT[1,2], C. A. HIEMSTRA[2], J. LIN[2], T. E. NOBIS[2], J. ADEGOKE[3], U. S. NAIR[4] & D. NIYOGI[5]

1 *University of Colorado, CIRES, Boulder, Colorado 80309 USA*
pielkesr@cires.colorado.edu

2 *Colorado State University, Department of Atmospheric Science, Fort Collins, Colorado 80523, USA*

3 *Laboratory for Climate Analysis & Modeling (LCAM), Department of Geosciences, 420K Robert H. Flarsheim Hall, 5100 Rockhill Road, University of Missouri-Kansas City, Kansas City, Missouri 64110-2499, USA*

4 *Earth System Science Center, University of Alabama at Huntsville, 320 Sparkman Dr., Huntsville, Alabama 35805, USA*

5 *Purdue University, Department of Agronomy, and Department of Earth and Atmospheric Sciences, Lilly Hall of Life Sciences, 915 W. State Street, Purdue University, West Lafayette, Indiana 47907-2054, USA*

Abstract This paper documents the diverse role of land-use/land-cover change on precipitation. Since land conversion continues at a rapid pace (e.g. see Table 1 in Pielke *et al.* 2006b), this type of human disturbance of the climate system will continue and become even more significant in the coming decades. The regional alteration of landscape also has global climate effects through teleconnections as concluded in NRC (2005); a conclusion which is bolstered by studies such as that of Chase *et al.* (2000) and Fedemma *et al.* (2005).

Key words land–atmosphere interactions; land-use/cover change; numerical modelling; rainfall/runoff; regional climate

INTRODUCTION

The role of landscape change in altering convective rainfall is well documented (e.g. Pielke, 2001; Pitman, 2003; Pielke *et al.* 2006a). This overview paper summarizes this topic by landscape conversion type focusing on how regional change results in changes in rainfall in the same area.

SHORT GRASS CONVERSION TO DRYLAND AGRICULTURE AND IRRIGATED AGRICULTURE

The conversion from native shortgrass grassland to cropland is manifested in biophysical effects that influence energy and water cycling. Seasonality of growing season, albedo, leaf area index, surface roughness, and moisture fluxes were altered with conversion to cropland. Cropland and grassland albedos are similar during the crop growing season (Oke, 1987), but croplands have bare soil for much of the year and native vegetation has a higher albedo than bare soil (Bonan, 2002). Dryland and irrigated crops are taller, and possess more leaf area than native shortgrass steppe (Paruelo *et al*., 2001). Moreover, surface roughness is higher with taller agricultural plants (Chase *et al.*, 1999; Bonan, 2002). Lastly, moisture fluxes are higher in agricultural systems, especially irrigated croplands (Baron *et al*., 1998; Stohlgren *et al*., 1998; Chase *et al*., 1999).

Growing season dynamics change with conversion to agriculture. With shortgrass steppe featuring a mixture of cool- and warm-season grasses, photosynthesis occurs during the entire growing season and peak biomass occurs in early summer (Paruelo *et al.*, 2001). In contrast, croplands have one dominant plant with dramatically different growing seasons and peak biomass, with dryland and irrigated crops peaking earlier and later than shortgrass, respectively (Paruelo *et al*., 2001).

The effect on air temperature and precipitation produced with shortgrass conversion varies with the conversion, spatially and temporally. The magnitude of change from shortgrass steppe to irrigated agriculture is much more dramatic than the shift to dryland agriculture (Baron *et al*., 1998). At relatively fine scales during short periods of the growing season, lower temperatures and higher atmospheric moisture levels are closely tied to irrigated croplands (Chase *et al*., 1999; Segal *et al.*, 1989). At larger scales, given the same brief temporal scale, this difference produces a regional cooling effect and precipitation increase on the adjacent Rocky Mountains (Stohlgren *et al.*, 1998). At a coarse resolution (50-km grid increment) regional modelling comparison of natural and current vegetation change, Eastman *et al.* (2001) showed a 0–1°C increase in maximum temperatures over unconverted shortgrass steppe, while a 2–3°C increase occurred in areas converted to dryland crops. Precipitation changes were heterogeneous.

Copyright © 2006 IAHS Press

TALL GRASS CONVERSION TO DRYLAND AND IRRIGATED AGRICULTURE

The tall grass conversion is similar to the short grass conversion except the loss of aboveground biomass (leaf area index, LAI) is greater when the tall grass prairie was removed, and almost 100% of the original tall grass region is gone. Further studies on the role of grassland conversion include the initial evidence of the role of irrigation in modifying surface climate trends which came from observational studies (Marotz *et al*., 1975; Barnston & Schickendanz, 1984; Alpert & Mandel, 1986; Pielke & Zeng, 1989). Barnston & Schickendanz (1984) found that irrigation increased precipitation in the Texas Panhandle when the synoptic condition provided low-level convergence and uplift such that the additional moisture produced by irrigation was allowed to ascend to cloud base.

Adegoke *et al.* (2006) found that midsummer 2 m temperature over Nebraska might be cooler by as much as 3.4°C under current irrigation (control run) conditions as contrasted with natural landscape conditions. Energy budget differences were identified between current and potential natural vegetation scenarios: the surface latent heat flux was 42% higher, and the water vapour flux (at 500 m) 38% greater in the control run compared to the natural landscape run. Important physical changes between the natural tallgrass prairie of this region and the current land-use patterns include alterations in the surface albedo, roughness length, and soil moisture in the irrigated areas.

These changes are capable of generating complex changes in the lower atmosphere (planetary boundary layer, PBL) energy budget. For example, the simulated increase in the portion of the total available energy partitioned into latent heat rather than sensible heat resulted directly from enhanced transpiration and soil evaporation in the control run. Although not examined in detail in this study, elevated dewpoint temperature and moisture fluxes within the PBL can increase convective available potential energy, promote atmospheric instability, and enhance daytime cloud cover (Alapaty *et al*., 1997; Stohlgren *et al*., 1998; Pielke, 2001; Holt *et al*., 2006).

MID-LATITUDE DECIDUOUS FOREST CONVERSION TO AGRICULTURE

Asner *et al.* (2004) document that agricultural activities associated with grazing operations are an important driver for conversion from deciduous forest to grassland and pastures particularly under poor soil conditions. This conversion is surmised to have hydrological impacts by reducing the rate of spring snowmelt and cloud condensation levels and hence moisture availability, reducing moisture interception due to decreased LAI, increasing runoff and soil evaporation, and decreasing transpiration. This latter effect leads to higher soil moisture fluxes and discharge over the landscape, which causes erosion and poor soil conditions in the region. Typically, the change from forest to grasslands leads to a significant reduction in moisture flux, while a change to cropland can have variable influences on the regional moisture flux (because of crop photosynthetic pathways and transpiration rates, cropping patterns, irrigation, etc.).

Hogg *et al*. (2000) used field measurements over deciduous forest to demonstrate that the distinctive climate of interior western Canada is the feedback associated with the leaf phenology of the aspen forest. Latent heat fluxes are largest under high LAI conditions leading to cooling, but with the resultant higher concentrations of water vapour, moisture availability and precipitation increased. Xue *et al*. (1996) indicate that the LAI changes of deciduous vegetation cause regional changes and propagate high uncertainty into general circulation model (GCM) simulations. Bounoua *et al.* (2000) concluded that for the mid-latitude forest regions, the resulting impact of LAI changes was a decreased albedo, cooling of about 1.8°C during the growing season, and slight warming during winter due to snow albedo masking, decreased effective precipitation, and an increase in the low-frequency variability of weather in the northern latitudes. Baidya Roy *et al*. (2002) simulated a 300-year (1700–1990) time series of USA land use/land cover and found that changing land-use/land-cover patterns can lead to several degrees of warming or cooling at the surface accompanied by significant changes in precipitation patterns. Satellite products can detect this change following techniques similar to those discussed in Shepherd (2005) and Cai & Kalnay (2005) using blended re-analysis data sets.

TROPICAL EVERGREEN FOREST CONVERSION TO AGRICULTURE

Tropical forests, occupying approximately 800 million hectares, are being cleared at the rate of approximately 14 million hectares per year. Observational studies, spanning several decades, and numerical modelling studies both show that tropical deforestation influences cloud formation and rainfall (Sud & Smith, 1985; Meher-Homji, 1991; Cutrim *et al*., 1995; McGuffie *et al*., 1995; Costa & Foley, 2000; Lawton *et al*., 2001; Pielke, 2001; Silva Dias *et al*., 2002; Durieux *et al*., 2003; Sen *et al*., 2004; Fisch *et al*., 2004; Ray *et al*., 2006). Observational studies include Meher-Homji (1991), Pielke (2001), Durieux *et al*. (2003) and Ray *et al.* (2006). These studies report a wide range of changes in rainfall associated with deforestation (1–20% decrease), as well as the alteration of seasonality and frequency of convection. Regional-scale modelling results show that the eastern Asian summer monsoon is sensitive to deforestation in the Indochina region (Sen *et al*., 2004). Heterogeneity-induced mesoscale circulations have the potential to modify cloudiness (Souza, *et al*. 2000; Pielke, 2001; Silva Dias *et al*., 2002; Baidya Roy & Avissar, 2002; Werth & Avissar, 2002). Mesoscale numerical modelling experiments show that lowland deforestation and associated increases (decreases) in the Bowen ratio lead to elevation (lowering) of the orographic clouds forced by terrain downwind (Lawton *et al*., 2001; van der Molen, 2002; Nair *et al*., 2003; Bruijnzeel, 2004; Ray *et al*., 2006), leading to changes in the direct harvesting of cloud water by montane vegetation.

There is some indication that deforestation in a continent surrounded by oceans has more potential to impact tropical circulation compared to deforestation that is further removed from ocean sources of water vapour (van der Molen *et al*., 2006), and this needs to be validated through the use of cloud-resolving and regional modelling experiments.

BOREAL FOREST CONVERSION DUE TO FIRE

Fire in the boreal forest is an integral part of this ecosystem (Stocks, 1991). As shown in Vidale *et al.* (1997), mesoscale circulations develop in response to the spatial variations of surface sensible heat fluxes that occur due to these fires and other landscape pattern disturbances, which also include the lakes that are ubiquitous in the boreal forests. Knowles (1993) reported that cumulus clouds form preferentially downwind of recent burn areas within a boreal forest landscape. These burn areas have a lower albedo than the surrounding landscape. Such a preference also indicates that subsequent lightning strikes from deep cumulus clouds will more likely initiate fires immediately downstream of a recent burn scar, rather then elsewhere in the forest. After a period of time, as the forest regenerates, the burned area may be lighter than the surrounding unburnt landscape, as aspen and other secondary growth forest and shrubs grow.

The environment of the boreal forest, particularly in the spring, is very conducive to fires as the roots are embedded in cold, or even frozen soils, yet the air temperature and solar insolation at this time of year is high. Almost all of the net radiation received at the surface is transferred back into the atmosphere as sensible, rather than latent heat flux (Sellers *et al*., 1995). Pielke & Vidale (1995) show that one consequence of the resultant large heating of the atmosphere by the sensible heating is a particularly deep planetary boundary layer, as well as a preference for the summer polar front to often situate along the boreal–tundra ecotone boundary. The region south of the polar front in the spring (and also in the summer) is a weather location where thunderstorms occur. The spatial variations of the landscape will provide focused regions for thunderstorm development that would otherwise not occur.

URBANIZATION

While the fraction of the Earth's surface currently classified as urban accounts for less than 2% of the available land surface, over 45% of the Earth's population is concentrated there (Arnfield, 2003). Furthermore, future projections indicate this percentage will soon exceed more than 50% (Cohen, 2003). Observational studies over the past three decades have demonstrated that urban areas radically restructure the local energy budget and thus lead to different boundary layer structure (Shepherd, 2005; Arnfield, 2003; Oke, 1988). The anthropogenic influence also includes

altering the aerosol environment. These changes likely lead to alterations in urban precipitation frequency, intensity, and patterns. Shepherd (2005) presents the most recent and complete review of urban precipitation issues.

Observational studies of urban precipitation stretches over three decades (e.g. Huff & Changnon, 1973). Studies in the USA have been mainly concentrated in three urban areas: St Louis, Atlanta, and Houston, and generally demonstrated increases in rainfall over and downwind of urban areas attributed largely to the Urban Heat Island (UHI) initiated convergence zone and to a lesser extent, increased surface roughness (Huff & Changnon, 1973; Huff, 1986; Bornstein & Lin, 2000; Dixon & Mote, 2003; Shepherd & Burian, 2003). Evidence also suggests an increase in heavy rain events (Huff, 1986). In addition, the UHI has been found to decrease the likelihood of freezing rain events in urban areas (Changnon, 2003). Bornstein & Lin (2000) also found urban influence on established thunderstorms approaching an urban area. Model studies have demonstrated significant changes to the convective boundary layer structure (e.g. Hildebrand & Ackerman, 1984; Baik *et al.*, 2001) and even influences on the behaviour of cold fronts (Gaffen & Bornstein, 1988).

A big unknown in the urban-induced precipitation problem is the role of urban aerosols. Studies like that of van den Heever & Cotton (2005) have begun to examine the relative sensitivities involved, but as shown in Shepherd (2005), while evidence strongly points to a link between aerosols and urban precipitation modification, the details of the connection remain highly uncertain.

TROPICAL FOREST FIRES AND RESULTANT BIOMASS BURNING EFFECT ON RAINFALL

Biomass burning produces smoke plumes with large quantities of aerosols (tiny particles) which can potentially affect the regional, and even the global hydrological cycle (Ramanathan *et al.*, 2001). Aerosols serve as cloud condensation nuclei which effect the formation of cloud droplets (Cotton & Anthes, 1992); thus the extensive input of aerosols from fires could significantly affect cloud properties and rainfall. In addition to affecting cloud microphysics, aerosols absorb and scatter radiation. Increased aerosols in the atmosphere from forest fires reduce the radiative energy reaching the Earth's surface (Ramanathan *et al.*, 2001). Because surface radiative input drives evaporation, which is balanced with precipitation on a global scale, aerosol-induced reductions in surface radiation are likely to decrease global rainfall (Lohmann & Feichter, 2005).

Andreae *et al*. (2004) analysed Amazonian aircraft observations and found delays in the onset of precipitation within smoky clouds. Khain *et al.* (2005) show that while elevated aerosol concentrations initially lead to lowered precipitation efficiency due to warm-rain suppression, the delay in raindrop formation decreases the drag on updrafts by falling raindrops and increases the latent heat release by the additional water that reaches higher altitudes where freezing takes place.

Lin *et al*. (2006), based on satellite observations during the entire Amazonian biomass burning season, empirically confirmed the aforementioned results of Andreae *et al.* (2004) and Khain *et al.* (2005). Increased aerosols from fires were correlated with increased observed total (warm + ice-phase) rainfall from the TRMM-TMI sensor, even after accounting for the atmospheric stability environment through the cloud work function. Changes in cloud properties were also correlated with aerosol loading; i.e. higher cloud tops, increased presence of ice, and enhanced cloud cover.

AFFORESTATION AND REFORESTATION

Afforestation and reforestation (A&R) are proposed as possible tools to mitigate desertification (FAO, 1989) and to reduce atmospheric concentrations of CO_2 by sequestering carbon in forest biomass (UNDP, 2003). In southern South America, A&R plans commenced in Chile, Uruguay, and Argentina in the last two decades, supported through government economic incentives or subsidies (World Bank, 2000). In southwestern Australia, A&R are also seen as ways to ameliorate salinity (Walker *et al.* 2002).

Overall, conversion from grasslands or croplands to forest leads to a decrease in albedo and increases of LAI, roughness length, and rooting depth (Sellers, 1992; Pitman, 2003; Jackson *et al*.,

1996). Changes in these parameters can modify the near-surface energy fluxes, which can influence temperature and humidity (Pielke, 2001). In general, observations and modelling studies agree that A&R would decrease near-surface temperature and increase latent heat (e.g. Beltrán, 2005; Fahey & Jackson, 1997; Nosetto *et al*., 2005; Xue & Shukla, 1996). Simulated impacts on precipitation are not so clear, and depend on geographical location, regional atmospheric characteristics, extent of the afforested–reforested area (Pitman & Narisma, 2005; Xue & Shukla, 1996) and biophysical parameters of the land-use/land-cover change (Xue *et al*., 1996).

Observational (Jackson *et al*., 2005) and several modelling studies (Beltrán, 2005; Xue *et al*., 1996) demonstrated that tree plantation establishment may affect the hydrological cycle. Precipitation processes depend on local, regional, and large-scale atmospheric characteristics and therefore regional atmospheric modelling represents an important tool for studying the impacts of realistic patterns of A&R on precipitation. Moreover, model domain size, grid spacing, and parameterizations (e.g. convective schemes) may largely influence simulated precipitation (e.g. Castro *et al.*, 2005). Thus, more comprehensive regional modelling sensitivity studies are needed to assess those impacts.

Acknowledgements The work reported in this article was sponsored by NASA Grant NNG04GL61G, NNG04G184G, and NAG5-11370, USGS Grant 04CRAG0032, and NSF Grants DEB 0217631 and ATM-0233780. Dr John C. Lin was supported by the NOAA Postdoctoral Program in Climate and Global Change, administered by the University Corporation for Atmospheric Research. Dallas Staley completed the editorial work on this paper with her customary outstanding professionalism and efficiency.

REFERENCES

Adegoke, J. O., Pielke, R. A. Sr. & Carleton, A. M. (2006) Observational and modeling studies of the impacts of agriculture-related land use change on climate in the central U.S. *Agric. Forest Met*. Special Issue (accepted).

Alapaty, K, Pleim, J. E., Raman, S., Niyogi, D. S. & Byun, D. W. (1997) Simulation of atmospheric boundary layer processes using local- and nonlocal-closure schemes. *J. Appl. Met.* **36,** 214–233.

Alpert, P. & Mandel, M. (1986) Wind variability – An indicator for mesoclimatic change in Israel. *J. Climate Appl. Met.* **25**, 1568–1576.

Andreae, M. O., Rosenfeld, D., Artaxo, P., Costa, A. A., Frank, G. P., Longo, K. M. & Silva-Dias, M. A. F. (2004) Smoking rain clouds over the Amazon. *Science* **303**, 1337–1342.

Arnfield, A. J. (2003) Two decades of urban climate research: A review of turbulence, exchanges of energy and water, and the Ruban heat island. *Int. J. Climate* **23**, 1–26.

Asner, G. P., Elmore, A. J., Olander, L. P. & Martin, R. E. (2004) Grazing systems, ecosystem responses, and global change. *Ann. Rev. Environ. Resour.* **29**, 261–299.

Baidya Roy, S. & Avissar, R. (2002) Impact of land use/land cover change on regional hydrometeorology in Amazonia. *J. Geophys. Res.* **107**(D20), doi:10.1029/2000JD000266.

Baidya Roy, S., Weaver, C. P., Pacala, S. W. & Hurtt, G. (2002) Impact of historical land-use/landcover change on US summer climate. *Am. Geophys Union*, AGUSM.B41A.12B.

Baik, J. J., Kim, Y. H. & Chun, H. Y. (2001) Dry and moist convection forced by an urban heat island. *J. Appl. Met.* **40,** 1462–1475.

Barnston, A. G. & Schickedanz, P. T. (1984) The effect of irrigation on warm season precipitation in the southern Great Plains. *J. Climate App. Met.* **23**, 865–888.

Baron, J. S., Hartman, M. D., Kittel, T. G. F., Band, L. E., Ojima, D. S. & Lammers, R. B. (1998) Effects of land cover, water redistribution, and temperature on ecosystem processes in the South Platte Basin. *Ecological Applications* **8**, 1037–1051.

Beltrán, A. (2005) Using a coupled atmospheric-biospheric modeling system (GEMRAMS) to model the effects of land-use/land-cover changes on the near-surface atmosphere. PhD Thesis, Department of Atmospheric Science, Colorado State University, Fort Collins, USA.

Bonan, G. B. (2002) *Ecological Climatology: Concepts and Applications*. Cambridge, University Press, Cambridge, UK.

Bornstein, R. & Lin, Q. (2000) Urban heat islands and summertime convective thunderstorms in Atlanta: three case studies. *Atmos. Environ.* **34**, 507–516.

Bounoua, L., Collatz, G. J., Los, S. O., Sellers, P. J., Dazlich, D. A., Tucker, C. J. & Randall, D. A. (2000) Sensitivity of climate to changes in NDVI. *J. Climate* **13**, 2277–2292.

Bruijnzeel, L. A. (2004) Hydrological functions of tropical forests: not seeing the soil for the trees? *Agric. Ecosys. Environ.* **104**, 185–228.

Cai, M. & Kalnay, E. (2005) Can reanalysis have anthropogenic climate trends without model forcing? *J. Climate* **18**, 1844–1849.

Castro, C. L., Pielke, R. A., Sr & Leoncini, G. (2005) Dynamical downscaling: assessment of value retained and added using the Regional Atmospheric Modeling System (RAMS). *J. Geophys. Res.* **110**, D05108, doi:10.1029/2004JDD004721

Changnon, S. A. (2003) Urban modification of freezing-rain events. *J. Appl. Met.***42**, 863–870.

Chase, T. N., Pielke, R. A., Kittel, T. G. F., Baron, J. S. & Stohlgren, T. J. (1999) Potential impacts on Colorado Rocky Mountain weather due to land use changes on the adjacent Great Plains. *J. Geophys. Res.—Atmos.* **104,** 16673–16690.

Chase, T. N., Pielke, R. A., Kittel, T. G. F., Nemani, R. R. & Running, S. W. (2000) Simulated impacts of historical land cover changes on global climate in northern winter. *Climate Dynamics* **16**, 93–105.

Cohen, J. E. (2003) Human population: The next half century. *Science* **302**, 1172–1175.

Costa, M. H. & Foley, J. A. (2000) Combined effects of deforestation and doubled atmospheric CO_2 concentrations on the climate of Amazonia. *J. Climate* **13**, 18–34.

Cotton, W. R. & Anthes, R. A. (1992) *Storm and Cloud Dynamics*. Academic Press, San Diego, USA.

Cutrim, E. D., Martin, W. & Rabin, R. (1995) Enhancement of cumulus clouds over deforested lands in Amazonia. *Bull. Am. Met. Soc.* **76**, 1801–1805.

Dixon, P. G. & Mote, T. L. (2003) Patterns and causes of Atlanta's urban heat island-initiated precipitation. *J. Appl. Met.* **42,** 1273–1284.

Durieux, L., Machado, L. & Laurent, H. (2003) The impact of deforestation on cloud cover over the Amazon arc of deforestation. *Remote Sens. Environ.* **86**, 132–140.

Eastman, J. L., Coughenour, M. B. & Pielke, R. A. (2001) The effects of CO_2 and landscape change using a coupled plant and meteorological model. *Global Change Biology* **7**, 797–815.

Fahey, B. & Jackson, R. B. (1997) Hydrological impacts of converting native forests and grasslands to pine plantations, South Island, New Zealand. *Agric. For Met.* **84**, 69–82.

FAO (Food and Agriculture Organization of the United Nations) (1989) Role of forestry in combating desertification. *FAO Conservation Guide 21*.

Feddema, J. J., Oleson, K. W., Bonan, G. B., Mearns, L. O., Buja, L. E., Meehl, G. A. & Washington, W. M. (2005) The importance of land-cover change in simulating future climates. *Science* **310**, 1674–1678.

Fisch, G., Tota, J., Machado, L. A. T., Silva Dias, M. A. F., da Lyra, R. F., Nobre, C. A., Dolman, A. J. & Gash, J. H. C. (2004) The convective boundary layer over pasture and forest in Amazonia. *Theor. Appl. Climatol.* **78**, 47–59.

Gaffen, D. & Bornstein, R. (1988) Case study of urban interactions with a synoptic scale cold front. *Met. Atmos. Phys.* **38**, 185–194.

Hildebrand, P. H. & Ackerman, B. (1984) Urban effects on the convective boundary layer. *J. Atmos. Sci.* **41**, 76–91.

Hogg, E. H., Price, D. T. & Black, T. A. (2000) Postulated feedbacks of deciduous forest phenology on seasonal climate patterns in the western Canadian interior. *J. Climate* **13**, 4229–4243.

Holt, T., Niyogi, D. S., Chen, F., Manning, K., LeMone, M. & Qureshi, A (2006) Effect of land–atmosphere interactions on the IHOP 24–25 May 2002 convection case. *Mon. Weather Rev.* **134**, 113–133.

Huff. T. E. (1986) Urban hydrometeorology review. *Bull. Am. Met. Soc.* **67**, 703–711.

Huff, F. A. & Changnon, S. A. Jr (1973) Precipitation modification by major urban areas. *Bull. Am. Met. Soc.* **54**, 1220–1232.

Jackson, R. B., Canadell, J., Ehleringer, J. R., Mooney, H. A., Sala, O. E. & Schulze, E. D. (1996) A global analysis of root distributions for terrestrial biomes. *Oecologia* **108**, 389–411.

Jackson, R. B., Jobbágy, E. G., Avissar, R., Baidya Roy, S., Barrett, D. J., Cook, C. W., Farley, K. A., le Maitre, D. C., McCarl, B. A. & Murray, B. C. (2005) Trading water for carbon with biological carbon sequestration. *Science* **310**, 1944–1947.

Khain, A., Rosenfeld, D. & Pokrovsky, A. (2005) Aerosol impact on the dynamics and microphysics of deep convective clouds. *Quart. J. Roy. Met. Soc.* **131**, 1–25.

Knowles, J. B. (1993) The influence of forest fire induced albedo differences on the generation of mesoscale circulations. MS Thesis, Dept Atmos. Sci. Colorado State University, Fort Collins, USA.

Lawton, R. O., Nair, U. S., Pielke, R. A. & Welch, R. M. (2001) Climatic impact of tropical lowland deforestation on nearby montane cloud forests. *Science* **294**, 584–587.

Lin, J. C., Matsui, T., Pielke, R. A. Sr & Kummerow, C. (2006) Effects of biomass burning-derived aerosols on precipitation and clouds in the Amazon Basin: a satellite-based empirical study. *J. Geophys. Res.* (accepted).

Lohmann, U. & Feichter, J (2005) Global indirect aerosol effects: a review. *Atmos. Chem. Phys.* **5**, 715–737.

Marotz, G. A., Clark, J., Henry, J. & Standfast, R. (1975) Cloud fields over irrigated areas in southwestern Kansas—data and speculations. *Prof. Geogr.* **27**, 457–461.

McGuffie, K., Henderson-Sellers, A., Zhang, H., Durbidge, T. B. & Pitman, A. J. (1995) Global climate sensitivity to tropical deforestation. *Global and Planetary Change* **10**, 97–128.

Meher-Homji, V. M. (1991) Probable impact of deforestation on hydrological processes. *Climate Change* **19**, 163–173.

Molders, N. & Olson, M. A. (2004) Impact of urban effects on precipitation in high latitudes. *J. Hydromet.* **5**, 409–429.

Nair, U. S., Lawton, R. O., Welch, R. M. & Pielke, R. A. Sr (2003) Impact of land use on Costa Rican tropical montane cloud forests: sensitivity of cumulus cloud field characteristics to lowland deforestation. *J. Geophys. Res.* **108**(D7), 4206, doi:10.1029/2001JD001135.

NRC (National Research Council) (2005) *Radiative Forcing of Climate Change: Expanding the Concept and Addressing Uncertainties*. National Academies Press, Washington, DC, USA.

Nosetto, M. D., Jobbagy, E. G., Paruelo, J. M. (2005) Land-use change and water losses: the case of grassland afforestation across a soil textural gradient in central Argentina. *Global Change Biology* **11**, 1101–1117.

Oke, T. R. (1987) *Boundary Layer Climates*, 2nd edn. Methuen, London, UK.

Oke, T. R. (1988) The urban energy balance. *Prog. Phys. Geogr.* **12**, 471–508.

Paruelo, J. M., Burke, I. C. & Lauenroth, W. K. (2001) Land-use impact on ecosystem functioning in eastern Colorado, USA. *Global Change Biology* **7**, 631–639.

Pielke, Sr, R. A. (2001) Influence of the spatial distribution of vegetation and soils on the prediction of cumulus convective rainfall. *Rev. Geophys.* **39**, 151–177.

Pielke, Sr, R. A. & Zeng, X. (1989) Influence on severe storm development of irrigated land. *National Weather Digest* **14**, 16–17.

Pielke, R. A. & Vidale, P. L. (1995) The boreal forest and the polar front. *J. Geophys. Res.* **100**, 25755–25758.

Pielke, Sr, R. A., Adegoke, J. O., Beltrán-Przekurat, A., Hiemstra, C. A., Lin, J., Nair, U. S., Niyogi, D. & Nobis, T. E. (2006a) An overview of regional land use and land cover impacts on rainfall. *Tellus B* (submitted).

Pielke, Sr, R. A., Adegoke, J. O., Chase, T. N., Marshall, C. H., Matsui, T. & Niyogi, D. (2006b) A new paradigm for assessing the role of agriculture in the climate system and in climate change. *Agric. Forest Met*, Special Issue (in press).

Pitman, A. J. (2003) The evolution of, and revolution in, land surface schemes designed for climate models. *Int. J. Climatol.* **23**, 479–510.

Pitman, A. J. & Narisma, G. T. (2005) The role of land surface processes in regional climate change: a case study of future land cover change over south western Australia. *Met. Atmos. Phys.* **89**, 235–249.

Ramanathan, V., Crutzen, P. J., Kiehl, J. T. & Rosenfeld, D. (2001) Aerosols, climate, and the hydrological cycle. *Science* **294**, 2119–2124.

Ray, D. K., Nair, U. S., Lawton, R. O., Welch, R. M. & Pielke, R. A. Sr (2006) Impact of land use on Costa Rican tropical montane cloud forests: sensitivity of orographic cloud formation to deforestation in the plains. *J. Geophys. Res.* 111:D02108, doi:10.1029/2005JD006096.

Segal, M., Schreiber, W. E., Kallos, G., Garratt, J. R., Rodi, A., Weaver, J., Pielke, R. A. (1989) The impact of crop areas in northeast Colorado on midsummer mesoscale thermal circulations. *Mon. Weather Rev.* **117**, 809–825.

Sellers, P. J. (1992) Biophysical models of land surface processes. In: *Climate System Modeling* (ed. by K. E. Trenberth), 451–490. Cambridge University Press, Cambridge, UK.

Sellers, P., Hall, F., Ranson, K. J., Margolis, H., Kelly, B., Baldocchi, D., den Hartog, G., Cihlar, J., Ryan, M. G., Goodison, B., Crill, P., Lettenmaier, D. & Wickland, D. E. (1995) The Boreal Ecosystem–Atmosphere Study (BOREAS): An overview and early results from the 1994 field year. *Bull. Am. Met. Soc.* **76**, 1549–1577.

Sen, O. L., Wang, Y. & Wang, B. (2004) Impact of Indochina deforestation on the East Asian summer monsoon. *J. Climate* **17**, 1366–1380.

Shepherd, J. M. (2005) A review of current investigations of urban-induced rainfall and recommendations for the future. *Earth Interactions* **9**: paper 12, 27 pp.

Shepherd, J. M. & Burian, S. J. (2003) Detection of urban-induced rainfall anomalies in a major coastal city. *Earth Interactions* **7**: paper 4, 17 pp.

Silva Dias, M., Rutledge, S., Kabat, P., Silva Dias, P. L., Nobre, C., Fisch, G., Dolman, A. J., Zipser, E., Garstang, M., Manzi, A. O., Fuentes, J., Andreae, M. O., Artaxo, P., Gielow, R. & Gatti, L. (2002) Cloud and rain processes in a biosphere-atmosphere interaction context in the Amazon region. *J. Geophys. Res.* **29**:10.1029/2000JD000335.

Souza, E. P., Rennó, N. O. & Silva Dias, M. A. F. (2000) Convective circulations induced by surface heterogeneities. *J. Atmos. Sci.* **57**, 2915–2922.

Stocks, B. J. (1991) The extent and impact of forest fires in northern circumpolar countries. In: *Global Biomass burning—Atmospheric, Climatic, and Biospheric Implications*, 197–202. MIT Press, Cambridge, USA.

Stohlgren, T. J., Chase, T. N., Pielke, R. A., Kittel, T. G. F. & Baron, J. S. (1998) Evidence that local land use practices influence regional climate, vegetation, and stream flow patterns in adjacent natural areas. *Global Change Biology* **4**, 495–504.

Sud, Y. C. & Smith, W. E. (1985) Influence of local land surface processes on the Indian monsoon: a numerical study. *J. Climate Appl. Met.* **24**(10), 1015–1036.

UNDP (United Nations Development Programme) (2003) The Clean Development Mechanism: A User's Guide. Bureau for Development Policy. UN, New York, USA.

Van den Heever, S. C. & Cotton, W. R. (2005) Modeling the impacts of urban aerosol on convection and precipitation. Presentation, 2nd Urban Symposium, San Diego, California, USA.

Van der Molen, M. K. (2002) Meteorological impacts of land use change in maritime tropics. PhD Thesis, Vrije Universiteit, Amsterdam, The Netherlands.

Van der Molen, M. K., Dolman, A. J., Waterloo, M. J. & Bruijnzeel, L. A. (2006) Climate is affected more by maritime than by continental land use change**: a** multiple scale analysis. *Global and Planetary Change* (in press).

Vidale, P. L., Pielke, R. A., Barr, A. & Steyaert, L. T. (1997) Case study modeling of turbulent and mesoscale fluxes over the BOREAS region. *J. Geophys. Res.* **102**, 29167–29188.

Walker, G. R., Zhang, L., Ellis, T. W., Jatton, T. H. & Petheram, C. (2002) Estimating impacts of changed land use on recharge: review of modeling and other approaches appropriate for management of dryland salinity. *Hydrogeol. J.* **10**, 68–90.

World Bank (2000) *Policy Elements for Sustainable Development in the XXI Century*. Argentina Water Resources Management. February 18, 2000. Latin America and the Caribbean Regional Argentina Country Department and Finance, Private Sector and Infrastructure, and Environment and Socially Sustainable Development.

Xue, Y. & Shukla, J. (1996) The influence of land surface properties on Sahel climate. Part II: Afforestation. *J. Climate* **9**, 3260–3275.

Xue, Y., Fennessy, M. J. & Sellers, P. J. (1996) Impact of vegetation properties on U.S. summer weather prediction. *J. Geophys. Res.* **101**(D3), 7419–7430.

Climate Variability and Change—Hydrological Impacts (Proceedings of the Fifth FRIEND World Conference held at Havana, Cuba, November 2006), IAHS Publ. 308, 2006.

Análisis de la Sequía Agrícola establecida en la Republica Dominicana desde 1971 al 2000

RANSÉS VÁZQUEZ[1], OSCAR SOLANO[1], SOLANGEL YOKASTA GONZÁLES[2], LEONCIO DUARTE[2] & DANIEL CAMACHO[2]

1 *Centro de Meteorología Agrícola, Instituto de Meteorología. Apartado postal 17032, CP 11700, Habana 17, Ciudad de La Habana, Cuba*
ranses.vazquez@insmet.cu

2 *Oficina Nacional de Meteorología de la República Dominicana. Apartado Postal 1153, Los Mameyes, Santo Domingo, DN. República Dominicana*

Resumen Se realizó una investigación científica del comportamiento de la Sequía Agrícola en la República Dominicana basada en la utilización de técnicas avanzadas y actualizadas en el terreno internacional y métodos generados en Cuba. La serie estudiada corresponde a períodos de diez días desde 1971 al 2000 y la resolución espacial empleada corresponde a píxeles de 4 km. de lado. Los tabuladores electrónicos y los Sistemas de Información Geográfica permitieron la ejecución algorítmica y la redacción cartográfica. Los resultados (diagnósticos, tendencias y probabilidades de ocurrencia) aportan una valiosa herramienta para la evaluación y el manejo del riesgo que origina este evento climático extremo, pues permite la prevención y la preparación de las comunidades para atenuar sus efectos negativos y contribuye a la toma de decisiones estratégicas y tácticas de operaciones agrícolas.

Palabras clave sequía agrícola; sistemas de información geográfica; zonificación agroclimática; tendencias; probabilidades; Cuba.

Analysis of agricultural droughts in the Dominican Republic, 1971–2000

Abstract An investigation of the characterization of Agricultural Droughts in the Dominican Republic based on advanced and up to date international techniques and methods generated by Cuban experts was made. The studied series corresponds to ten-day periods from 1971 to 2000 and the spatial resolution used is 4-km grid squares. Use of spreadsheets and Geographical Information Systems allowed the calculations and thematic maps to be obtained. The results (diagnostic, trend and occurrence probabilities) are a valuable tool for the evaluation and handling of the risks associated with this extreme climatic event, because they allow prevention measures and the preparation of communities so as to attenuate the negative effects, and they contribute to the making of strategic and tactical decisions regarding agricultural operations.

Key words agricultural drought; Geographical Information Systems; agroclimatic mapping; trend; probabilities; Cuba

INTRODUCCIÓN

En el contexto de agricultura, la Sequía Agrícola “no comienza cuando cesa la lluvia, sino cuando las raíces de las plantas no pueden obtener más humedad del suelo” y puede ser definida sobre la base de la humedad del suelo más que sobre alguna interpretación indirecta de los registros de precipitación.

Teniendo en cuenta que las tendencias climáticas observadas en la región geográfica del Caribe en los últimos 30 años (Centella *et al.*, 1997) muestran el incremento de la frecuencia e intensidad de este fenómeno, los estudios relacionados con el conocimiento de la Sequía Agrícola deviene en una tarea de prioridad nacional y regional por el aporte que puede poner en manos de los tomadores de decisiones para que éstos puedan gestionar convenientemente el riesgo de sequía en el manejo agrícola.

El proyecto internacional CUB/03/009 “Desarrollo y Adaptación al cambio climático”, determino realizar una investigación científica del comportamiento de la sequía meteorológica y agrícola en el ámbito caribeño. La República Dominicana y Cuba ejecutan esta tarea basada en la utilización de técnicas avanzadas y actualizadas en el terreno internacional y métodos generados en Cuba. El objetivo general de este trabajo fue evaluar y diagnosticar la Sequía Agrícola en la República Dominicana en cuanto a la extensión superficial de su categoría más severa década a década en una serie de 30 años (1971 al 2000), así como el análisis de su tendencia hiperanual y el peligro climático expresado en probabilidades de ocurrencia del mismo.

MATERIALES Y MÉTODOS

Los datos se extrajeron de los archivos del Banco de Datos Climatológicos del Departamento de Climatología – División de Procesamieto de Datos de la Oficina Nacional de Meteorología de la República Dominicana (ONAMET). En la lluvia se utilizaron 76 pluviómetros (30 años de datos).

Copyright © 2006 IAHS Press

Para la evapotranspiración de referencia (ETo) se procesó la información de temperaturas máxima y mínima, humedad relativa, viento e insolación de 12 estaciones meteorológicas (1975–1986). La década (diez días) fue el período temporal base.

La ETo se calculó según Menéndez *et al.* (1999). La formula se modificó a partir de la introducción de los valores empíricos de los coeficientes *a* y *b* en la formula tipo Angström determinados para la estación de Santo Domingo.

Según Solano *et al.* (2005a) fue calculado el Balance Agroclimatológico del Suelo y las Condiciones de Vegetación y de acuerdo a Solano *et al.* (2005a,b,c) se calculó la Sequía Agrícola. De esta última, las seis categorías pueden ser simplificadas a tres: Períodos Secos Cortos (agrupa los estadios iniciales de sequía); Presencia de Sequía Agrícola (agrupa al inicio y permanencia) y Ausencia de Sequía Agrícola (no se presentan períodos secos de ninguna longitud). La escala para la extensión superficial de la Presencia de Sequía Agrícola presenta tres categorías de acuerdo al porcentaje del área del territorio evaluado con Presencia de Sequía Agrícola (X) respecto a la suma total del área: pequeña son valores de $X < 20\%$, moderada son valores $20\% \leq X < 60\%$ y grande si $X \geq 60\%$.

Se generó una rejilla cuya cuadrícula representa una resolución espacial de 4 km de lado. Los límites geográficos del rectángulo: longitud mínima: –72.13, longitud máxima: –68.19, latitud mínima: 17.42, latitud máxima: 20.05, paso 0.04, esto genera una red de 100 columnas y 67 filas. Los valores están referidos a la proyección "Longitude/Latitude (NAD 27 for Carribbean)", expresados en décimas de grado.

Con los Sistemas de Información Geográfica (SIG) se interpolaron los datos de las estaciones para la obtención de los valores por punto de rejilla de los parámetros necesarios para calcular el balance hídrico agroclimático del suelo. El método de interpolación usado fue el kriging con variograma lineal. La filosofía empleada es la de calcular y aplicar los algoritmos a cada cuadrícula mediante la combinación de herramientas disponibles en diversos softwares, tales como: los tabuladores electrónicos (hojas EXCEL), y los SIG, estos permitieron la interpolación a partir de la cual se le asigna a cada cuadrícula un valor temático. La rejilla es exportada como matriz (x,y,z) en formato (ASCII) e importada al EXCEL donde se ejecutan los cálculos para la determinación del balance, las condiciones de vegetación y la Sequía Agrícola, finalmente los resultados se ingresan nuevamente al SIG y se practica la redacción cartográfica y los cálculos áreales. La Fig. 1 nos presenta una síntesis del proceso seguido para diagnosticar la Sequía Agrícola mediante la combinación de herramientas anteriormente dicha.

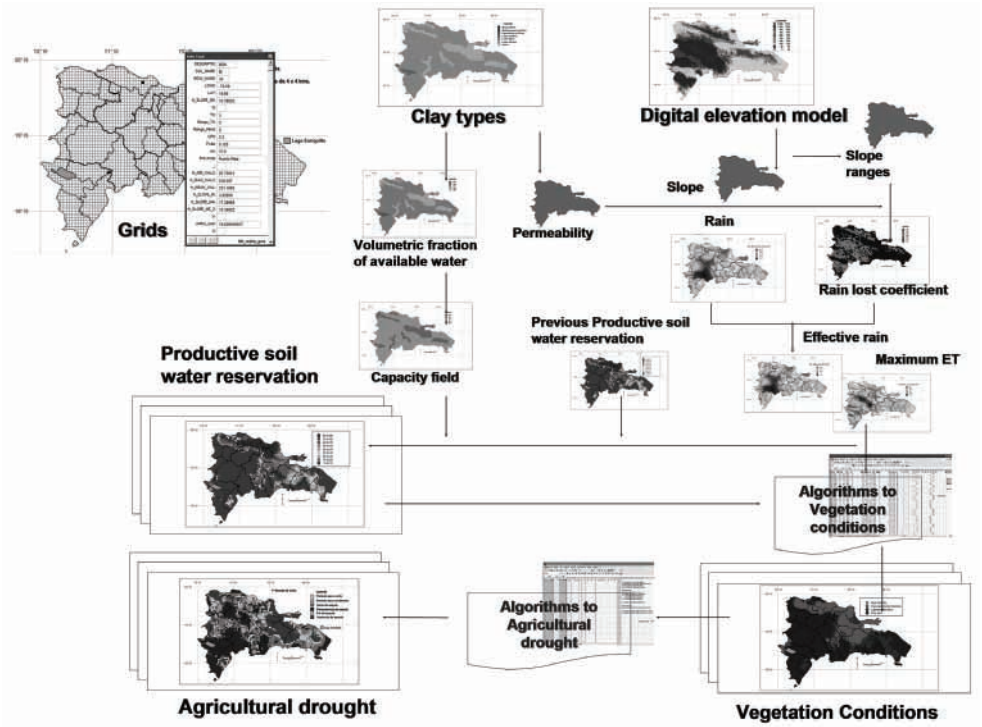


Fig. 1 Diagrama de flujo que muestra las operaciones realizadas y la combinación de herramientas para diagnosticar la Sequía Agrícola en la República Dominicana.

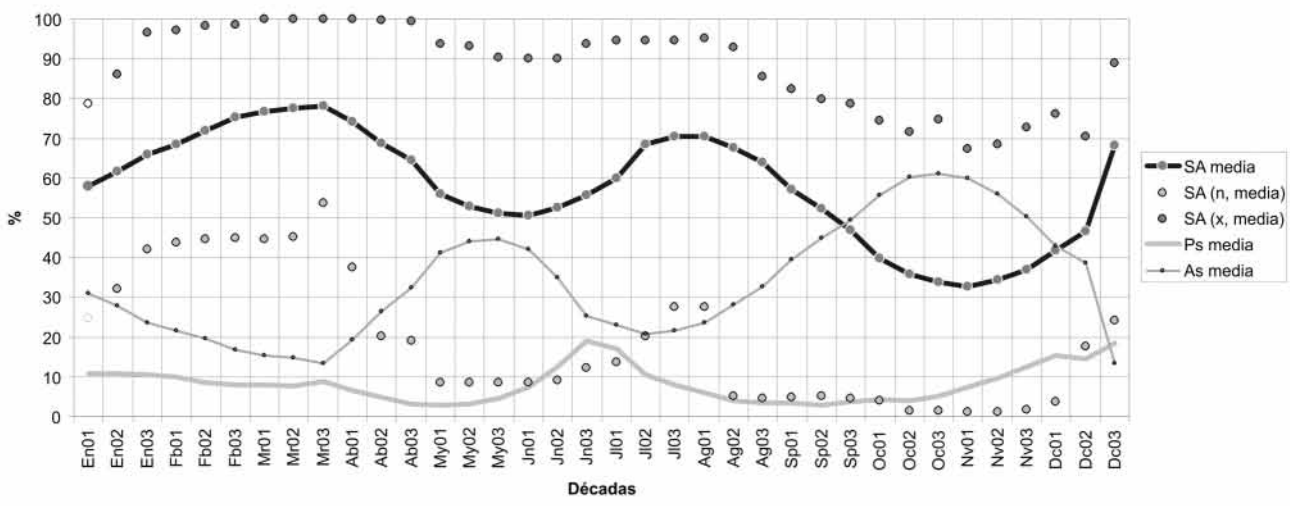


Fig. 2 Marcha anual de distintas categorías de expresión de la extensión superficial de la Sequía Agrícola en la República Dominicana, a escala nacional en el período 1971–2000.

RESULTADOS

La Fig. 2 presenta la marcha media anual nacional de la extensión superficial de las categorías de Sequía Agrícola. El valor representado es el por ciento promedio de casos presentes de la categoría en cuestión para todo el país.

La presencia de Sequía Agrícola en su distribución anual posee tendencias opuestas a la marcha de la ausencia de la Sequía Agrícola. En general la manifestación de la Sequía Agrícola coincide con los períodos estacionales climáticos observándose dos máximos y dos mínimos. El máximo absoluto ocurre en las décadas tercera de marzo y primera de abril (78%), el segundo máximo relativo se registra en la primera década de agosto (71%). El mínimo absoluto se observa en la segunda década de noviembre (33%) y el mínimo relativo se presenta en las primera y segunda décadas de junio (51%). La amplitud entre los puntos rojos y verdes en cada década del año indica el rango de variación de la Sequía Agrícola establecida, para cada una de esas décadas, durante el período 1971–2000. Por ejemplo, la primera década de marzo presenta un máximo de 100%, quiere esto decir que al menos en un año de la serie el país estuvo afectado en su totalidad con Sequía Agrícola; al consultar en detalle los datos se verificó fue en 1975.

Análisis del peligro

La Tabla 1 presenta la probabilidad (%) que el área posee de estar en presencia de Sequía Agrícola para la nación y las 8 regiones climáticas. La misma información fue determinada para cada cuadrícula, donde cada punto del territorio nacional posee una probabilidad para cada década, esta información es indispensable a la hora de valorar el riesgo climatológico de la presencia de la Sequía Agrícola por localidades puntuales o entornos microescalares y los mapas se encuentran disponibles en el SIG.

En la primera década de enero en el territorio nacional predomina una probabilidad de ocurrencia de la Sequía Agrícola entre el 20 y el 60% mientras que las regionales Sur y Suroeste poseen más del 60%. A partir de esta década progresivamente comienza un aumento hacia el Norte y al Este de las áreas con alta probabilidad hasta la primera década de abril cuando el país alcanza el mayor valor (78%). En sentido inverso ahora comienza un decremento de las probabilidades en dirección sur hasta la segunda década de junio, aquí el país alcanza como promedio 51%. Luego aumenta hasta la primera década de agosto momento en que el país alcanza probabilidades promedios del 71% las zonas del centro al oeste y hacia el norte y las provincias del extremo oriental son las mas afectadas con probabilidades mayores al 60%. A partir de esta década y hasta la segunda década de noviembre las probabilidades disminuyen en general para todo el territorio nacional alcanzando su mínimo en este momento con un valor del 33%, aunque la franja centro occidental permanece con probabilidades entre el 20 y el 60%.

Tabla 1 Valores promedios porcentuales areales y decadales de la cobertura espacial de la Sequía Agrícola areales (nación y regiones).

Décadas	Nacional	Regiones Sur	Suroeste	Noroeste	Norte	Norcentral	Central	Nordeste	Este
En01	52	78	80	56	43	54	43	7	46
En02	58	82	88	61	46	63	49	7	57
En03	62	84	91	63	49	67	54	9	63
Fb01	66	86	94	68	52	74	60	14	67
Fb02	69	88	95	69	54	78	63	19	72
Fb03	72	89	94	73	57	82	68	26	76
Mr01	75	91	95	77	62	85	72	33	80
Mr02	77	92	93	78	63	86	75	38	82
Mr03	78	92	92	79	64	84	77	43	82
Ab01	78	93	88	79	65	83	78	48	83
Ab02	74	93	80	76	63	75	75	43	78
Ab03	69	90	73	67	57	69	73	46	66
My01	65	85	67	63	56	62	69	48	59
My02	56	80	60	52	49	54	58	39	47
My03	53	78	57	46	48	50	54	37	44
Jn01	51	76	54	43	49	51	51	35	43
Jn02	51	75	55	41	50	52	48	35	43
Jn03	53	75	58	43	54	55	48	37	46
Jl01	56	77	61	47	60	60	51	36	50
Jl02	60	81	64	51	72	67	52	36	55
Jl03	69	86	75	61	82	75	58	42	67
Ag01	71	87	77	69	87	76	59	41	68
Ag02	70	87	78	71	90	78	55	39	66
Ag03	68	86	75	66	89	75	52	37	62
Sp01	64	81	70	63	86	72	48	36	57
Sp02	57	77	62	55	79	64	43	33	48
Sp03	52	73	57	51	73	61	40	29	41
Oc01	47	69	53	47	64	55	34	23	34
Oc02	40	63	47	36	53	48	28	18	27
Oc03	36	59	45	34	45	41	26	13	23
Nv01	34	58	44	32	40	37	26	10	21
Nv02	33	58	45	33	36	35	26	7	20
Nv03	34	59	49	35	37	37	28	7	21
Dc01	37	63	54	40	38	39	30	7	24
Dc02	42	67	60	44	41	43	35	7	32
Dc03	47	72	71	51	42	49	37	7	39
Media	58	79	69	56	58	62	51	28	53

Tendencia hiperanual de la Sequía Agrícola

La evaluación anual provincial de la extensión superficial de la Sequía Agrícola, para cada año, expresada en porcentaje de área afectada respecto a la superficie total de cada una de ellas se comenta a continuación y la Fig. 3 resalta los años extremos.

Nación: Los años de mayor afectación con más del 63% del área cubierta fueron 2000, 1971, 1982, 1995, 1991, 1973, 1977, 1994, 1975 y 1997 este último con una cobertura espacial de la Sequía Agrícola del 75%. Los años menos afectados con menos del 43% fueron 1988 (43%), 1981 (41%) y 1979 (35%).

Regiones: Las regiones de mayor afectación con más del 80% de su área cubierta con Sequía Agrícola en diferentes años fueron, la Sur (1971, 1972, 1973, 1974, 1975, 1976, 1977, 1978, 1980, 1983, 1984, 1989, 1995, 1996, 1997 y 1998); Suroeste (1975, 1976, 1978, 1995 y 1997); Norcentral (1971, 1973, 1991, 1994 y 1997) y la Este (1997). Las regiones menos afectadas en diferentes años con menos del 30% de su área cubierta con Sequía Agrícola fueron, la Norte(1979) y la Nordeste (1971, 1972, 1973, 1974, 1976, 1978, 1979, 1980, 1981, 1982, 1983, 1984, 1986, 1987, 1988, 1989, 1995, 1996 y 1999).

La tendencia hiperanual (Fig. 4) en la década de los ochenta resultó ser mas húmeda que el resto de la serie, sin embargo al realizar un corte a la serie a partir de 1979 se pone de manifiesto la tendencia al aumento en extensión de área ocupada por la Sequía Agrícola hacia los años más

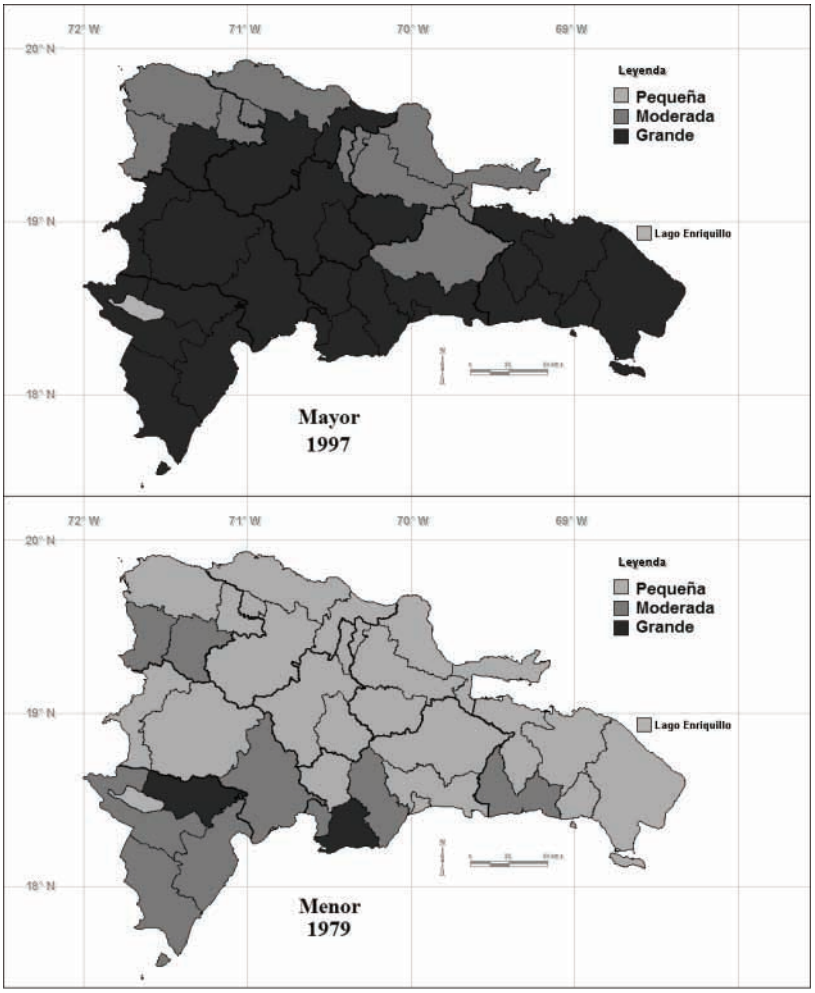


Fig. 3 Rangos de la extensión anual provincial de la Sequía Agrícola (%) de los años extremos.



Fig. 4 Tendencia hiperanual y por períodos estacionales poco lluvioso (P.p.lluvioso) y lluvioso (P. lluvioso) de la afectación nacional de Sequía Agrícola de la serie 1979–2000.

recientes, a excepción del período poco lluvioso cuya tendencia es ligeramente al decremento mientras que en el período lluvioso el incremento si es muy marcado. Como promedio a partir de 1979 anualmente la nación aumentó 30 446 ha para esos últimos 22 años determinados por la ecuación: $y = 0.6587x + 48.079$. Lo anterior corrobora los resultados de las investigaciones del Centro del Clima del Instituto de Meteorología de la República de Cuba, pues Centella *et al.* (1997) concluyen entre otras cosas que en los últimos años se ha elevado la frecuencia e intensidad

de los sures y de las sequías, además Lapinel *et al.* (1993) expresaba que el ascenso general apreciado en las temperaturas ha estado acompañado de una reducción total de precipitaciones anuales de 10–20% y un aumento de la variabilidad interanual de 5–10%, con la característica de que las precipitaciones han estado disminuyendo en el período lluvioso del año y han aumentado en el período poco lluvioso. En general no seria muy aventurado considerar que este comportamiento detectado para la Isla de Cuba ha estado influenciando el Caribe oriental.

REFERENCIAS

Centella, A., Naranjo, L., Paz, L., Cárdenas, P., Lapinel, B., Ballester, M., Pérez, R., Alfonso, A., González, C., Limia, M. & Sosa, M. (1997) Variaciones y cambios del clima en Cuba. Informe Técnico. Instituto de Meteorología, La Habana, Cuba.

Lapinel, B., Rivero, R. E., Cutié, V., Rivero, R. R., Varela, N. & Sardinas, M. (1993) Sistema Nacional de Vigilancia de la Sequía: Análisis del período 1931–1990. Informe Científico Técnico, Centro Meteorológico de Camagüey, Cuba.

Menéndez J. A., Solano, O. & Vázquez, R. (1999) Estimación de la Evapotranspiración de Referencia por el Método de Penman-Monteith. CD Memorias de la Convención Trópico' 99, Ref. MT 001. La Habana, Cuba.

Solano, O., Vázquez, R., Menéndez, C., Menéndez, J. & Martín, M. E. (2005a) Manual de técnicas y procedimientos para el desarrollo de la climatología de la Sequía Agrícola. Proyecto PNUD-CUBA RLA/01/013 Strengthening Links Between Development and Climate Change Adaptation in the Caribbean.

Solano, O., Vázquez, R., Menéndez, C., Menéndez, J. & Martín, M. E. (2005b) Evaluación de la Sequía Agrícola en Cuba. *Revista Cubana de Meteorología* **12**(2), 3–14.

Solano, O., Vázquez, R., Menéndez, C. & Martín, M. (2005c) Evaluación científica de los riesgos asociados a la ocurrencia de la Sequía Agrícola en las repúblicas de Cuba y Dominicana. Informe final Proyecto PNUD-CUBA RLA/01/013 Strengthening Links Between Development and Climate Change Adaptation in the Caribbean.

Climate Variability and Change—Hydrological Impacts (Proceedings of the Fifth FRIEND World Conference held at Havana, Cuba, November 2006), IAHS Publ. 308, 2006.

Drought in Costa Rica: temporal and spatial behaviour, trends and the relationship to atmospheric circulation patterns

CHRISTIAN BIRKEL[1] **& SIEGFRIED DEMUTH**[2]

1 *Escuela de Geografía, Universidad de Costa Rica, Sede Rodrigo Facio San Pedro, San José, Costa Rica*
cbirkel@fcs.ucr.ac.cr

2 *IHP/HWRP Secretariat, Federal Institute of Hydrology, Am Mainzer Tor 1, D-56068 Koblenz, Germany*

Abstract The temporal and spatial behaviour of droughts in Costa Rica has been studied applying the threshold level approach to 17 streamflow stations for the common period 1973–2003. Drought indices such as drought duration, deficit volume (severity) and the number of droughts (frequency) were determined utilizing a constant non-seasonal Q_{90} and seasonal Q_{70} exceedence percentile from a flow duration curve. Temporal drought characteristics were generally of long duration and low deficit volume in the dry season and droughts of short duration and high deficit volume tend to cluster in the wet season. This could be a feature of the threshold, or the standardization procedure or the seasonality of the flow regime. Spatial drought characteristics show distinctive regional patterns in terms of variability indices and drought risk. The non-parametric Mann-Kendall trend test shows just one significant ($\alpha = 0.05$) positive result in terms of historic trends in increased severity and frequency (at the Northern Zone). Although the majority of test results are non-significant, a clear spatial pattern of positive and negative trends can be seen. The link between atmospheric circulation patterns and regional streamflow drought point towards regional patterns of a direct atmospheric-control (Pearson $r > 0.5$).

Key words drought; threshold level method; drought pattern; Mann-Kendall Test; atmospheric circulation; ENSO; El Niño

INTRODUCTION

Drought in the tropics is not a rare or random event, but a normal recurrent feature of the climate. Many studies attempt to regionally associate and quantify dry periods with the warm El Niño phase (Piechota & Dracup, 1996; Waylen *et al.*, 1998, Dettinger *et al.*, 2000), but few efforts have been made to generally analyse temporal and spatial drought behaviour in the region of Costa Rica. However, persisting over months and seasons, drought can affect large areas and cause tremendous social hazard, environmental damage and economic loss.

Recent droughts in Costa Rica have highlighted not only the vulnerability of the Costa Rican economy (agriculture), but also the threat to the local population of shortages in water supply. The unusually dry years of the 1997–1998 El Niño event in Central America led to losses of US$ 32.8 in Costa Rican agriculture alone (CEPAL, 2005). Since the early 1970s, scarcely a decade goes by without at least one region of the country being affected by drought. This study was carried out to improve the understanding of drought characteristics in Costa Rica.

STUDY AREA

The area under investigation, Costa Rica, is located in the south of the Isthmus of Central America with political borders to Nicaragua in the north and Panama in the south. It stretches from 8°00′ south to 11°15′ northern latitude and from 82°30′ east to 86°00′ western longitude with an area of 51 110 km^2 (Fig. 1). With two coastlines, one in the east (Caribbean Sea) and the other in the west (Pacific Ocean) marking its natural borders, the region covers six distinct, but homogeneous land units varying in climate, geology and hydrology (the North Pacific region, the Northern Zone, the Caribbean, the Central Pacific region, the Central Valley and the South Pacific region). Streamflow regimes are, according to Guilcher (1979) and Silva (1991), of a simple pluvial character showing a strong seasonality (low and high flow season) but due to precipitation variability of a regular or irregular type. Comparisons of regimes assigned to geographical land units of comparable climatic properties show similar characteristics and support this regionalization.

The national electricity company (ICE) provided the hydrological data. Seventeen stream gauges all with data from 1973–2003 and with natural flow characteristics were selected (Fig. 1). The size of the basins chosen for this study varies between 200 and 4767 km^2. Drought properties have been calculated for this subset of Costa Rican stations to provide a good regional coverage across Costa Rica in order to derive temporal and spatial drought patterns.

Copyright © 2006 IAHS Press

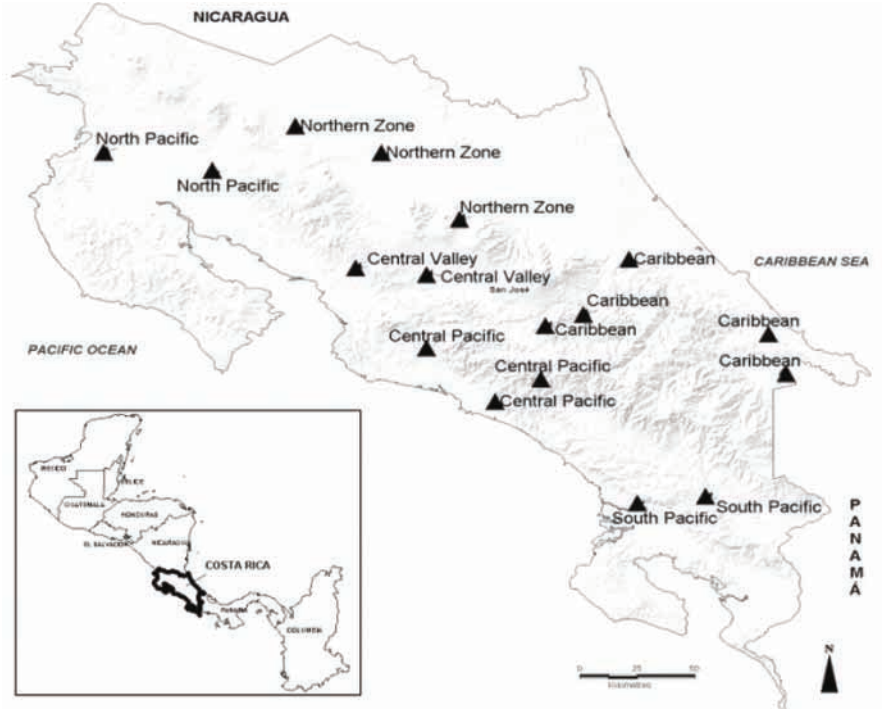


Fig. 1 Streamflow gauges across Costa Rica according to distinct climatic regions.

DROUGHT EVENT DEFINITION

Hydrological drought events can be defined by the threshold level method using a particular discharge value (in this study Q_{90} and Q_{70}), from the flow duration curve. The strong seasonality of tropical flow regimes required the comparison of a constant non-seasonal (hydrological year) with a constant seasonal (low and high flow season) threshold level. Drought events were defined in terms of duration *d* (days), deficit volume s (1000 m^3) and the number of droughts (–) occurring. Annual maximum and accumulated drought indices in terms of duration (AMD, ACD) and severity (AMV, ACV) for the typical low and high flow seasonality were calculated. These indices were derived using a constant non-seasonal (Q_{90}) threshold level and using constant seasonal thresholds (Q_{70}) for high (HF) and low flow (LF) periods respectively.

TEMPORAL BEHAVIOUR OF DROUGHT

Temporal drought behaviour was investigated by comparing averages of distinct drought indices such as the annual maximum duration (AMD in days), the annual maximum deficit volume (AMV in 1000 seconds due to a normalization process by mean flow) and the number of droughts (ND) for the common period 1973–2003. Table 1 shows the results of representative streamgauges for regions with a similar climate. The average annual maximum indices (mean AMD, AMV and ND) indicate that a generalized temporal drought pattern in terms of droughts of long duration and low deficit volume span the dry season, and droughts of short duration and high deficit volume tend to cluster in the wet season, which is e.g. reflected at the North Pacific station "Guardia". Here the mean HF Q_{70} is 17.9 days and the mean LF Q_{70} AMD is 39.2 days. The severity index AMV shows four exceptions out of a total of 17 stations, e. g. the Guardia station has a LF Q_{70} AMV of 220, whereas the HF Q_{70} AMV is 180.6. In terms of the ND index 50% follow the concept of clustering in the high flow season (HF). The clustering of high deficit volumes could also be a feature of the threshold, or the standardization procedure or the strong seasonality of the flow regime.

SPATIAL BEHAVIOUR OF DROUGHT

A variability index was developed to assess how sensitive a basin is to drought, because, the higher the variability, the more sensitive the river flows are to extreme droughts (Demuth & Heinrich, 1997). An increase in deviation from the mean drought index, such as AMD or AMV,

Table 1 Constant drought indices of one representative station according to climatic regions.

Climatic region	Station	Threshold	Mean AMD (days)	Mean AMV (1000 s)	Mean ND
Northern Zone	Guatuso	Q_{90} annual	35.6	127.1	1.2
		Q_{70} LF	40.5	194.1	1.3
		Q_{70} HF	20.1	367.9	2.7
North Pacific	Guardía	Q_{90} annual	32.2	142.3	0.8
		Q_{70} LF	39.2	220.0	0.9
		Q_{70} HF	17.9	180.6	1.7
Central Valley	Tacares	Q_{90} annual	27.5	132.9	1.2
		Q_{70} LF	42.6	252.9	1.3
		Q_{70} HF	23.4	384.0	1.0
Central Pacific	Londres	Q_{90} annual	28.3	94.7	1.4
		Q_{70} LF	28.3	94.7	1.4
		Q_{70} HF	15.3	275.3	1.2
South Pacific	Caracucho	Q_{90} annual	25.9	94.3	1.6
		Q_{70} LF	34.4	138.9	1.7
		Q_{70} HF	28.0	571.8	1.8
Caribbean	Pandora	Q_{90} annual	20.9	104.5	1.9
		Q_{70} LF	34.1	267.8	1.9
		Q_{70} HF	18.3	420.2	2.7

results in higher variability indices, expressed as the ratio of standard deviation to either mean duration or mean deficit volume in percent (%). The calculation was computed for the Q_{90} non-seasonal and Q_{70} seasonal (low and high flow season) AMD and AMV series. Zero drought years were taken into account to obtain the most real spatial data. Results are presented in Fig. 2, which shows the seasonal (HF, LF Q_{70}) variability coefficients for the Annual Maximum Deficit Volumes (AMV). Low variability (<100%) is reflected by a smaller sized clear coloured triangular, while the highest variability (>130%) is assigned by a darker sign.

The seasonal indices vary considerably in magnitude and range from 71 to 179% (Fig. 2). The lowest value was obtained for the low flow (LF) seasonal AMV at the Guatuso station, Northern Zone, and the highest value at station Rancho Rey, North Pacific, for the high flow variability AMV index. The high flow seasonal variability's (HF) principally reveal a higher susceptibility (mean variability: 120% HF AMV – 104% LF AMV) to drought than during the dry season. In general, a clear division between the Pacific and Caribbean drainage basin can be seen for the high flow season AMV. Figure 2 reveals the Central Valley, the North and Central Pacific as the regions most afflicted by extreme droughts, while the western part of the Northern Zone and the Caribbean show the lowest.

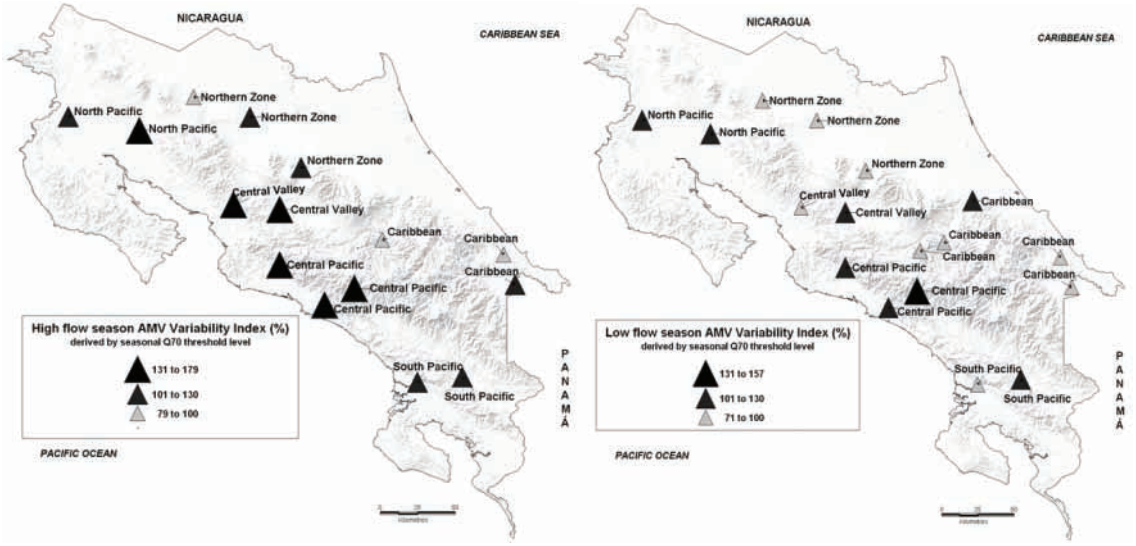


Fig. 2 Regionalized variability indices (%) of seasonal AMVs (HF-left, LF-right) for the period 1973–2003.

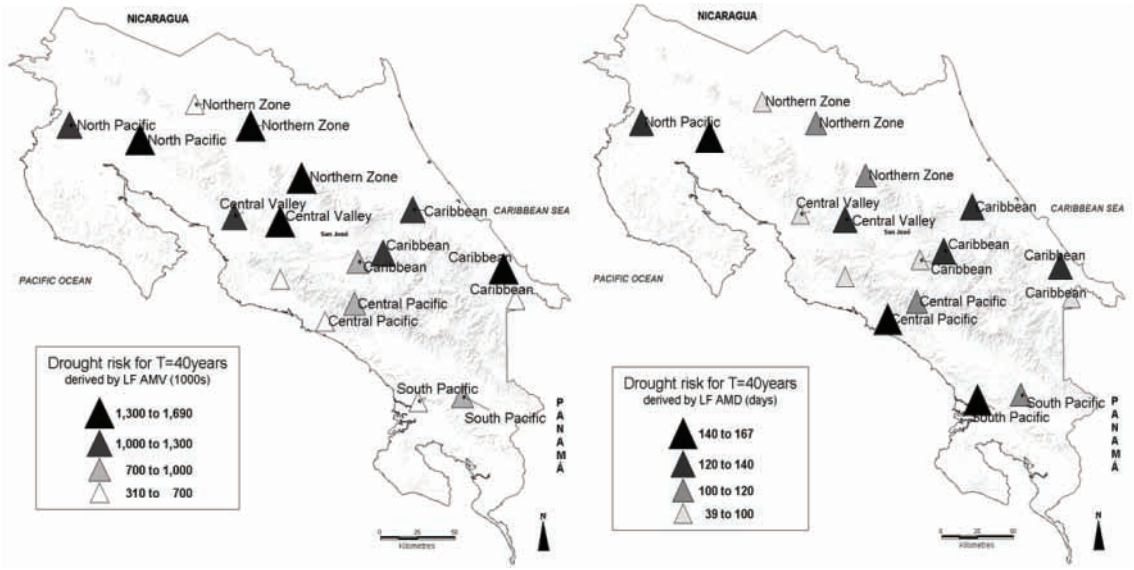


Fig. 3 Estimated 40-year return periods (*T*) for seasonal (LF) AMVs (left) in 1000s and LF AMDs in days (right).

The definition of risk used in this study is that developed by Tallaksen & van Lanen (2004) and is equal to the probability of non-exceedence of a certain minimum level (threshold level) within a certain *T*-year period. The cumulative distribution function (cdf) of the largest event within one year or season from a partial duration series (PDS) of drought events was derived.

The methodology presented by Zelenhasic & Salvai (1987) for describing and analysing the stochastic process of streamflow droughts was adapted using the program NIZOWKA (Jakubowski & Radczuk, 2004) to estimate drought characteristics. The distribution that fitted drought durations and deficit volumes best was the Poisson distribution for the number of droughts and the Lognormal and Pearson distribution for duration. The Poisson distribution was chosen for the number of events and the Generalized Pareto distribution for estimating magnitudes of the deficit volume extreme statistics. The calculated return periods (T – 10, 20 and 40 years) for each gauging station and drought index are regionalized across the study area to gain a general picture of the stations, which run most risk of being affected by severe droughts.

Figure 3 shows the spatial 40-year return periods for the low flow season (LF) Q_{70} AMVs (left panel) and the LF Q_{70} AMDs (right panel). The North Pacific region, the northern Caribbean and several other basins in the Central Valley (Tacares: estimated extreme duration of 169 days), the Central (station Providencia) and South Pacific region (station Palmar) (Fig. 3) are of high drought risk. For drought duration (right panel), the deficit volume characteristics (left panel) indicate a clear north–south division. What is in agreement between the two indices is the high drought risk for the North Pacific and the Caribbean. With one exception (station Guatuso in the Northern Zone) the north of Costa Rica runs more risk of experiencing drought events during the low flow season.

TREND ANALYSIS

Trends in Costa Rican drought series were analysed by conducting the non-parametric rank based Mann-Kendall test (Hisdal *et al.*, 2001). The test was performed on three drought parameters (AMD, AMV and ND) derived with a constant non-seasonal threshold of Q_{90}, applying a two-sided test with a five percent ($\alpha = 0.05$) level of significance. The results were assessed by mapping the spatial variability of the trends. Figure 4 shows the trend statistics for the Mann-Kendall test results on the AMV for each station. The stations exhibiting positive or negative trends tend to show typical spatial patterns. The Central Pacific and Central Valley react identically in their trend characteristics. The most distinctive Costa Rican region, where drought severity significantly increased is the western part of the Northern Zone. There a significant increasing trend towards more severe and more frequent droughts could be seen.

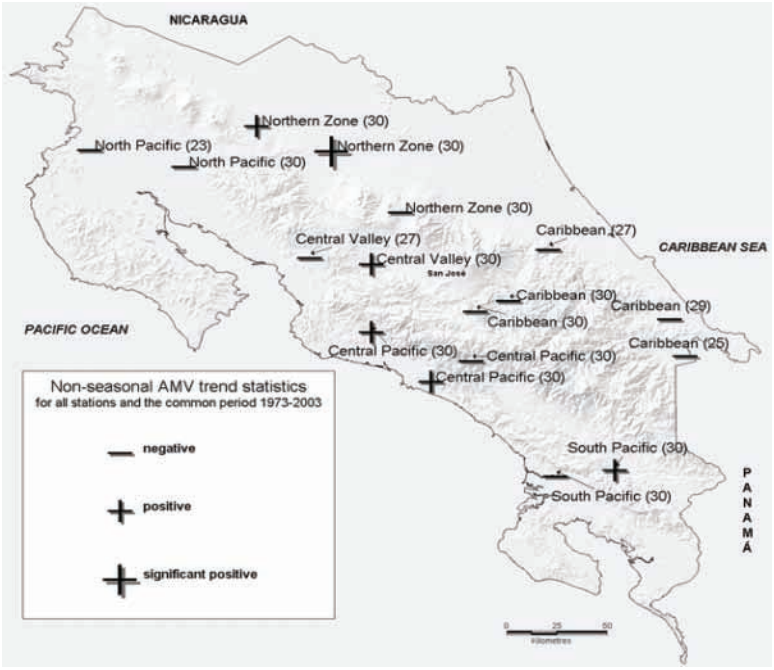


Fig. 4 Trends in AMV drought series of all stations for the period 1973–2003.

Stations with trends towards increased drought severity are clustered in the Central Pacific region, while stations with trends towards decreased drought severity are situated in the Central Valley region. The Caribbean and the North Pacific region exhibit in terms of drought severity a contradictory picture. There, some stations point at a trend towards decreasing severity, despite surrounding stations tending to increase drought severity.

LINKING ATMOSPHERIC CIRCULATION PATTERNS TO REGIONAL STREAMFLOW DROUGHT

To study the influence of atmospheric circulation on regional streamflow drought several aspects were investigated such as a correlation analysis using Pearson correlation coefficients. The statistical pre-processing of the data included the test of autocorrelation, linearity and normal distribution of the indices applied. Drought anomaly indices (ACD, ACV) are according to the pre-defined seasonality (high and low flow season) averaged and adopted for a linear correlation study with ENSO signals (SOI, SST, etc.).

The different seasonal drought anomaly indices (HF, LF ACV and ACD) show a similar relation with the sea surface temperature index (SST). Therefore, it was considered sufficient to concentrate on the spatial interpretation of just one anomaly index (HF ACV). This generally correlates (positively) with the Pacific drainage basin with the SST-ENSO signal.

The main active El Niño phase has more significant correlations for the high flow season. The Northern Zone shows indifference for the SST signal throughout the year and ENSO is considered not to be a major effect on drought behaviour in this region. The South Pacific shows high correlations with the SST index without seasonality and is the region of Costa Rica most directly affected by the El Niño oscillation.

CONCLUSIONS

Seventeen daily discharge series were used to define drought events and obtain a dataset of drought parameters indicating comparable extreme dry periods across Costa Rica's principal climatic regions, physiographic characteristics and flow regimes. Typical temporal and spatial patterns could be found and the seasonality of Costa Rican streamflow droughts described, but

inter- and within-season droughts vary considerably. The spatial behaviour of drought also follows specific patterns and to improve our understanding of drought development and drought processes an improved streamflow data resolution and regionalization methods are required.

Thirty years of data can not be considered as sufficient to fully address the question of whether streamflow drought has become more severe or frequent, due to the narrow time window. Although for Costa Rica as a whole no significant trends could be found, clear spatial patterns can be seen as a result of the trend analysis carried out in this study. Costa Rican streamflow exhibits significant correlations ($\alpha = 0.1$ of $r > 0.5$) between atmospheric circulation patterns (ENSO) and seasonal streamflow anomaly indices (ACD, ACV) with a time lag of a maximum of one year. The Pacific regions significantly interrelate with the Southern Pacific Oscillation, which proves to be an important influence on climate variability affecting regional drought development.

These pronounced, direct effects of climate variability on the hydrological cycle have the potential to form the basis of a regional drought-forecasting model. This statistical approach could provide useful long-range hydrological information for improving the sustainability of water resources in the region.

REFERENCES

Demuth, S. & Heinrich, B. (1997) Temporal and spatial behaviour of drought in south Germany. In: *FRIEND ´97 – Regional Hydrology: Concepts and Models for Sustainable Water Resource Management* (ed. by A. Gustard *et al.*) (Proceedings of the 3rd International conference on FRIEND, October 1997, Postojna, Slovenia), 151–157. IAHS Publ. 246. IAHS Press, Wallingford, UK.

Dettinger, D. M, Cayan, D. R., McCabe, G. J. & Marengo, J. A. (2000) Multiscale streamflow variability associated with El Niño/Southern Oscillation. In: *El Nino and the Southern Oscillation—Multiscale Variability and Global and Regional Impacts* (ed. by H. F. Diaz & V. Markgraf), 113–146. Cambridge University Press, Cambridge, UK.

Economic Commission for Latin America and the Caribbean (CEPAL) http://www.eclac.org/statistics/ (last visited 2005).

Guilcher, A. (1979) *Précis D'hydrologie: Marine et continentale* (second edn). Masson, Paris, France. ISBN 2-225-63680-X.

Hisdal, H., Stahl, K., Tallaksen, L. M. & Demuth, S. (2001) Have streamflow droughts in Europe become more severe or frequent? *Int. J. Climatol.* **21**, 317–333. .

Jakubowski, W. & Radczuk, L. (2004) Estimation of Hydrological Drought Characteristics, software NIZOWKA. Agricultural University of Wroclaw. In: *Hydrological Drought – Processes and Estimation Methods for Groundwater and Streamflow.* (ed. by M. L. Tallaksen & A. J. H. van Lanen), Developments in Water Sciences no. 48, Elsevier, The Netherlands. CD ROM, Software.

Piechota, T. C. & Dracup, J. A. (1996) Drought and regional hydrologic variation in the United States: Associations with the El Niño-Southern Oscillation. *Water Resour. Res.* **32**, 1359–1373.

Silva, E. (1991) *Geografía de Costa Rica* (3rd edn, 2004). EUNED, San José, Costa Rica.

Tallaksen, L. M. & Hisdal, H. (1997) Regional analysis of extreme streamflow drought duration and deficit volume. In: *FRIEND ´97 – Regional Hydrology: Concepts and Models for Sustainable Water Resource Management* (ed. by A. Gustard *et al.*) (Proceedings of the 3rd International conference on FRIEND, 1-4 Oct. 1997, Postojna, Slovenia), 141–50. IAHS Publ. 246. IAHS Press, Wallingford, UK.

Tallaksen, M. L. & van Lanen, A. J. H. (2004) *Hydrological Drought – Processes and Estimation Methods for Groundwater and Streamflow.* Developments in Water Sciences no. 48. Elsevier, The Netherlands.

Waylen, P. R., Quesada, M. E. & Caviedes, C. N. (1998) The effects of El Niño – Southern Oscillation on precipitation in San José, Costa Rica. *Int. J. Climatol.* **14**, 559–568.

Zelenhasic, E. & Salvai, A. (1987) A method of streamflow drought analysis. *Water Resour. Res.* **23**(1), 156–168.

Climate Variability and Change—Hydrological Impacts (Proceedings of the Fifth FRIEND World Conference held at Havana, Cuba, November 2006), IAHS Publ. 308, 2006.

Associations between Western European air-masses and river flow regimes

DAVID M. HANNAH[1], DONNA BOWER[2] & GLENN R. MCGREGOR[3]

1 *School of Geography, Earth and Environmental Sciences, University of Birmingham, Edgbaston, Birmingham B15 2TT, UK*
d.m.hannah@bham.ac.uk

2 *Halcrow Group Ltd, Burderop Park, Swindon SN4 0QD, UK*

3 *Department of Geography, King's College London, Strand, London WC2R 2LS, UK*

Abstract This paper identifies and models statistical associations between monthly air-mass frequencies and annual flow regime shape (seasonality) and magnitude for Western Europe, using 141 river and 48 climate stations (1974–1990). The month of regime peak, or month before the peak, is associated with increased (decreased) frequencies of moister (drier) air-masses. Low (high) magnitude regimes are associated with increased (decreased) frequencies of drier air-masses and decreased (increased) frequencies of moister air-masses. An *a priori*, weighted regional model yields the greatest predictive ability for regime shape; either an *a priori*, weighted global or regional model produces "best" predictions for regime magnitude. Overall model skill is lower for regime magnitude than shape, with model accuracy varying regionally. The development of methods and process knowledge, as herein, is vital to assessing climate–river flow sensitivity and predicting water resource variability in a changing climate.

Key words classification; discriminant function analysis; regionalization; statistical prediction; river flow; regimes; climate; air-masses; hydroclimatology; Western Europe

INTRODUCTION

River flow regimes characterize runoff dynamics over the annual cycle, which are driven by climate and moderated by basin factors (Bower *et al.*, 2004). Commonly, flow regimes are constructed based upon mean monthly flows and regarded as static. Previous studies in Europe have regionalized flows to identify spatial structure and/or estimate flows at ungauged sites (e.g. Krasovskaia *et al.*, 1994). This research concentrates on the timing of flows (regime shape) rather than regime magnitude.

Given heightened concerns about climate change/variability and human impacts upon hydrology, there is a pressing need for research to quantify temporal (inter-annual) variability in flow regimes and to establish hydroclimatological (climate–flow) associations as a basis for predicting future water resources. The few studies of year-to-year fluctuations in European flow regimes focus upon magnitude attributes (e.g. Arnell, 1994); this approach contrasts with regionalization work that emphasizes flow seasonality. Hence, there is a gap for research that investigates consistently spatial and inter-annual variability in both flow regime shape and magnitude at the European-scale.

Many climate diagnostics employed to explore atmosphere–land surface links are of limited utility for locations peripheral to the study region centre. The synoptic climatological approach, which relates large-scale air-mass climatology to the surface environment, provides a means to identify and understand climate–flow associations at the continental-scale. However, most air-mass classifications yield daily sequences of atmospheric circulation types on a station-by-station basis, which does not permit easy comparison of climatologies between locations. The Spatial Synoptic Classification (SSC) and its extension (SSC2) have been developed to overcome this problem (Sheridan, 2002). To date, the SSC2 has been applied only to North America; extension of the SSC2 to Europe offers the prospect of more robust spatio-temporal analysis of large-scale climate, and air-mass influence upon flow regimes across this region.

This paper addresses the above research gaps as it aims: (a) to explore associations between air-mass frequencies (derived using a modified SSC2) and annual flow regime shape (form, seasonality) and magnitude (size) classes at the Western European-scale; (b) to identify the flow regimes and regions exhibiting greatest/least flow sensitivity to air-mass climatology; and (c) to evaluate the utility of statistical models to predict annual flow regimes based upon air-mass frequencies.

Copyright © 2006 IAHS Press

DATA

River flow

Hydrological research at the continental-scale relies upon international data archives, such as the FRIEND European Water Archive (EWA). Long-term (1974–1991) daily flow data were obtained for 141 river gauges: (a) 137 from the FRIEND-EWA, and (b) four from the Global Runoff Data Centre (http://grdc.bafg.de/). This timeframe was chosen as many FRIEND-EWA time-series end in 1992 and European synoptic climate records (below) begin in 1974. Stations were selected that gauge similar basin areas (100–500 km^2) and provide coverage across Western Europe. Only basins with flows approximating natural conditions are included within the FRIEND-EWA. Monthly averages of daily flows (mm $month^{-1}$) were calculated and time-series were divided into hydrological years (commencing in October) to characterise annual regimes.

Climate

Synoptic climate data (1974–2000) were provided by the UK Meteorological Office for 48 Western European stations. At each station, six-hourly observations (0300, 0900, 1500 and 2100 hours GMT) were recorded for air temperature, dew point temperature, mean sea level pressure (MSLP), wind direction, wind speed and cloud cover.

METHODS

The analytical procedure is divided into five linked tasks: (a) regionalization of long-term average flow regimes; (b) classification of annual flow regimes for each station-year; (c) classification of daily air-masses at each station; (d) exploration of associations between monthly air-mass frequencies and annual flow regimes; and (e) statistical prediction of annual flow regimes based upon air-mass frequencies, as detailed below.

River flow regime classification

Since it is important to assess the timing and size of flows over the entire water year, multivariate statistical techniques were employed to separately classify regime shape and magnitude (Bower *et al.*, 2004). The shape classification identifies stations or station-years with similar regime form, regardless of magnitude (i.e. dimensionless, z-scored regimes). The magnitude classification is based upon four indices (i.e. mean, minimum, maximum and standard deviation) derived from long-term mean monthly values or monthly mean values for each station or station-year, regardless of timing.

The flow classification is applied in two modes: (a) to identify regions based upon long-term average regimes at a station; and (b) to assess year-to-year variability in annual regimes using 12-monthly observations for each station-year. It is important to note that: (a) regimes are not interchangeable between long-term and station-year classifications, as analyses are performed upon different data matrices; and (b) magnitude classes for regionalization identify absolute differences between stations, whereas inter-annual magnitude classes identify relative variations at a station.

Air-mass classification

A new weather typing scheme for Western Europe based upon the Spatial Synoptic Classification-2 (SSC2-WE) was developed that classifies daily air-masses into one of six categories based upon nine variables derived from six-hourly synoptic climate observations. SSC2-WE is a modified version of Sheridan's (2002) method. Bower *et al.* (2006) detail analytical procedures for SSC2-WE and evaluate its application.

SSC2-WE identifies temporal air-mass variability on a station-by-station basis but, because the six daily categories are common to all locations, it permits ready spatial comparison of atmospheric conditions. The classes are: (a) Dry Polar (DP): cool or cold, dry and little cloud; (b) Dry Moderate (DM): mild and dry; (c) Dry Tropical (DT): hot, dry and little cloud; (d) Moist Polar (MP): cold, humid and cloudy; (e) Moist Moderate (MM): warm, humid and cloudy; and (f) Warm Tropical (MT): warm, very humid and cloudy in winter or partially cloudy in summer. A

transitional category (TR) is identified for days with changes in MSLP, dew point depression and maximum wind shift that indicate a major switch in air-mass climatology.

Air-mass – river flow regime associations

Associations between monthly air-mass frequencies and annual flow regimes are investigated by matching river gauges with the nearest climate station. Data are pooled by long-term flow regime regions; this is valid as SSC2-WE yields the same air-mass types for each location. Flow regimes associated with anomalous air-mass occurrence (i.e. monthly air-mass frequencies above (+) and below (-) 2.5 times the median for shape and 1.5 times the median for magnitude) are identified to highlight the most climatically sensitive links for months and regions.

Prediction of flow regimes using air-mass frequencies

Multiple discriminant function analysis (MDFA; Klecka, 1980) provides a statistical model of the associations between monthly air-mass frequencies and annual flow regime classes. Air-masses are input as the discriminating variables, with MDFA scores predicting the most probable flow regime. Four MDFA models are developed: (a) global (all 141 river gauges), equal probability (GE), (b) regional, equal probability (RE), (c) global, *a priori* weighted (GW), and (d) regional, *a priori* weighted (RW). Weights are applied based upon frequencies of flow regime classes over the calibration period for the even years (1974, 1976, ...). The "best" models are selected to predict flow regimes from air-mass frequencies for the odd years (1975, 1977, ...). Models are evaluated based upon % correct predictions.

RESULTS AND DISCUSSION

River flow regions and annual regimes

It is beyond this paper's scope to detail results of flow regionalization or spatio-temporal flow regime/air-mass dynamics. Regionalization is used to structure the analyses. Six regime shape regions were identified: (A) January peak with secondary March peak, 17 stations in the western UK; (B) December–March peak, 39 stations across the eastern UK, Denmark and northeast continental Europe; (C) December–April peak, 42 station in the south–east UK and a belt from northern/central France, Germany to Poland; (D) April peak, 16 stations in a more southerly belt than C from Spain to Belarus; (E) April–May peak, 7 stations in southern Norway, Finland, Slovakia and Austria; and (F) May–June peak, 20 stations in Austria and Norway. The regions identify a maritime-continental gradient in the timing of the flow regime peaks (lagged from the Atlantic rim); and summer regime peaks in Region F indicate snow and glacier melt contributions. Five magnitude regime regions were apparent: (1) low mean and seasonality, 77 stations across a wide latitudinal range; (2) low-intermediate mean and seasonality, 33 stations mainly in the western UK, Austria and Switzerland; (3) intermediate mean and high seasonality, 10 stations in Norway, Sweden and Finland; (4) moderately high mean and intermediate seasonality, 16 stations in the western UK, the Alps, southern Norway and northern Spain; and (5) high mean and seasonality, five stations in Austria, Norway and Scotland. These regions map broadly onto patterns of annual average rainfall, although magnitude seasonality is moderated by winter precipitation storage as snow/ ice and summer meltwater release.

Annual classes are used to identify and predict links between flow regimes and monthly air-mass frequencies. Six annual shape regimes were found: (A) November–January peak = 504 station-years; (B) January peak = 321 station-years; (C) February peak = 421 station-years; (D) March peak = 279 station-years; (E) April peak = 463 station-years; and (F) May–June peak = 409 station-years. Five annual magnitude regimes were found: (1) low mean and seasonality = 677 station-years; (2) low-intermediate = 650 station-years; (3) intermediate mean with high seasonality = 414 station-years; (4) intermediate = 457 station years; and (5) high = 199 station-years.

Air-mass – river flow regime associations

In this short paper, it is only possible to outline key generic and region-specific associations. For regime shape (Fig. 1), the main generic finding is increased frequencies of moister air-masses (i.e.

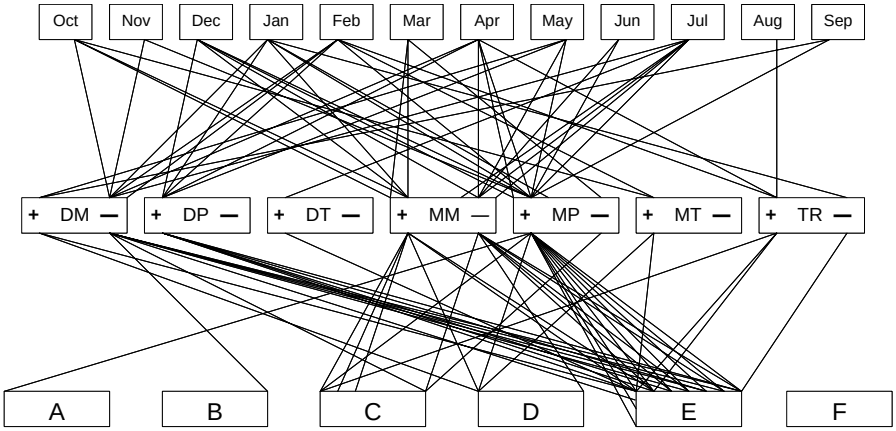


Fig. 1 River flow shape regimes associated with increased or decreased (2.5 ≤ median ≥ 2.5) monthly air-mass frequencies in Region A.

MM, MP and MT) and decreased occurrence of drier air-masses (i.e. DM, DP and DT) during the month of regime peak (month *T*), or the month before peak (month *T* – 1). This suggests advection of moist air causes regimes to peak in the same month, or the following month due to a lag between climatic drivers and runoff response as moderated by basin conditions. Increases (decreases) in drier (moister) air-masses are found to delay timing of regime peaks (i.e. no peak in month *T* or *T* + 1) due to less moisture advection. A second generic finding is that some regimes occur typically in the absence of anomalous air-mass frequencies (i.e. climatological average). Regimes associated with average air-mass occurrence differ between regions, reflecting the climatic situation and secondarily basin characteristics. Notable region-specific associations include: (a) Region A: April peak regimes with an increase in polar air-masses in several months, suggesting increased snow storage and spring melt, (b) Region C: January peak regimes with a decrease in MM in month *T* + 1, which influences recession onset rather than the peak; (c) Region C: April peak regimes with an increase of polar in month *T* – 1 and then hot (DT) in month *T* air-masses, indicating probable snow storage and melt; (d) Region E: April peak regime with increase in DP in January, which may deliver snow for spring melt; and (e) Region E: May–June peak with decrease in MM in month *T* – 1, possibly delaying spring melt onset.

For regime magnitude (Fig. 2), the main generic association is low (high) magnitude regimes with increased (decreased) frequencies of drier air-masses and decreased (increased) frequencies of moister air-masses. Intermediate regimes show least association with anomalous air-mass occurrence, implying these flows occur under average climatologies. There are few region-specific associations that depart from these generic links. However, in Regions 2 to 5, high magnitude regimes are associated with a summer increase (decrease) in dry (moist) air-masses, implying meltwater release.

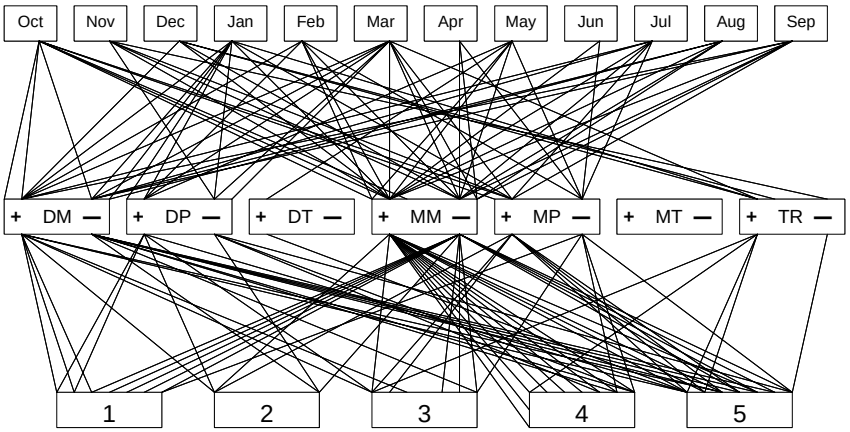


Fig. 2 River flow magnitude regimes associated with increased or decreased (1.5 ≤ median ≥ 1.5) monthly air-mass frequencies in Region 5.

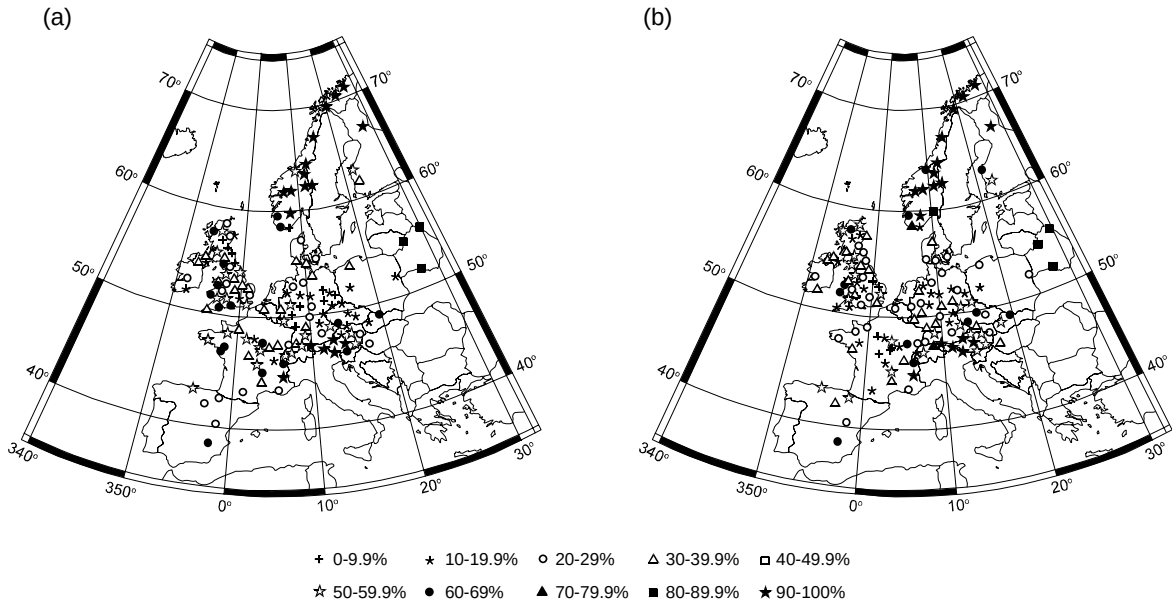


Fig. 3 Spatial pattern in predictive accuracy (% correct) of annual flow regime shape based upon monthly air-mass frequencies: (a) October and (b) April.

Prediction of flow regimes using air-mass frequencies

For regime shape, the *a priori*, weighted regional model yields greatest predictive ability overall; but model accuracy varies regionally (Fig. 3). The most skilful models by far are achieved for Region F (88–96% correct). Regions A, D and E attain similar accuracy levels to one another (27–55% correct). Regions B and C give the least accurate models (14–34% correct). Thus, models show highest predictability for regions characterised by a clear peak in: (a) spring or summer (i.e. snow- and glacier-fed rivers, with limited year-to-year regime variability) and (b) winter (i.e. concurrent rainfall–runoff response). The least predictable regions have broad regime peaks (i.e. December to March (B) or April (C)) and include basins with major aquifers (e.g. the southeast UK), which may weaken direct climate-flow links due to groundwater buffering.

For flow magnitude, either the *a priori*, weighted global or regional model produces the "best" predictions. The global model performs better for the prediction of flow regime magnitude than for

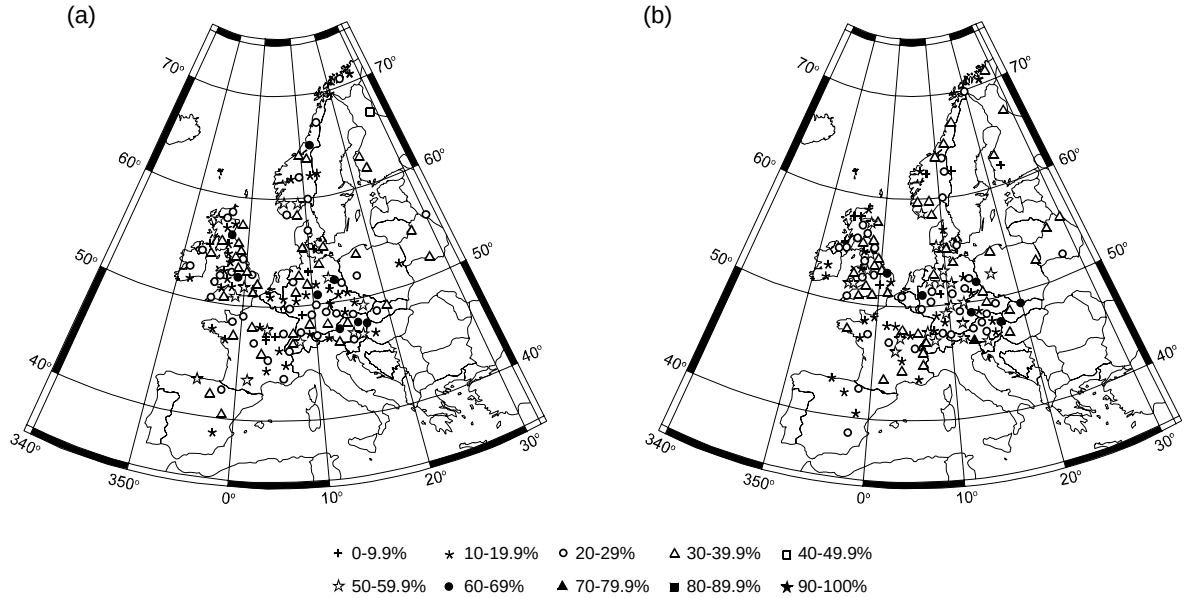


Fig. 4 Spatial pattern in predictive accuracy (% correct) of annual flow regime magnitude based upon monthly air-mass frequencies: (a) January and (b) July.

shape, possibly because annual magnitude classes are relative (not absolute) at a station and/or pooling of data for 141 stations improves regime sampling and statistical robustness. Predictive ability is relatively low across all regions (15–45% correct; Fig. 4); and overall skill is lower than for regime shape. However, some months show greater predictability of specific regimes, with these key months and regimes varying regionally. For example, the following models predict >60% correct: (a) Region 1: November/August = regime 1; (b) Region 3: January–March/May/June/August = 2; (c) Region 4: March = 2; and (d) Region 5: November = 1 and January/February/March = 2. Generally, models are better at predicting lower (i.e. regimes 1 and 2) than higher magnitude regimes, possibly because high magnitude regimes are less frequent and/or due to the complexity of high flow generating mechanisms (e.g. frontal, convective or orographic precipitation, plus snow or glacier melt). Model predictions are high for individual stations (up to 88%), with 12 basins yielding >75% accuracy. These findings indicate further detailed analysis is required of air-mass—flow predictions at a regime-by-regime and station-by-station level for both magnitude and shape regimes.

CONCLUSION

This paper advances methods of wider applicability in the assessment of large-scale hydroclimatological interactions and it provides an insight into climatic drivers of flow regimes at the Western European-scale. The development of such techniques and process knowledge is vital to assessing climate-river flow sensitivity and predicting water resource variability in a changing climate.

Acknowledgements D. Bower was funded by a NERC studentship GTNER/S/A/ 2000/03936 based at the University of Birmingham. G. Rees and I. Akram at the Centre for Ecology and Hydrology, UK, extracted data from the FRIEND-EWA. We are grateful to S. C. Sheridan for collaboration in developing the SSC2-WE.

REFERENCES

Arnell, N. W. (1994) Variations over time in European hydrological behaviour: a spatial perspective. In: *FRIEND: Flow Regimes from International and Experimental network Data* (ed. by P. Seuna, A. Gustard, N. W. Arnell & G. Cole), 179–184. IAHS Publ. 221. IAHS Press, Wallingford, UK.

Bower, D., Hannah, D. M. & McGregor, G. R. (2004) Techniques for assessing the climatic sensitivity of river flow regimes, *Hydrol. Processes* **18**, 2515–2543.

Bower, D., McGregor, G. R., Hannah, D. M. & Sheridan, S. C. (2006) Development of a Spatial Synoptic Classification Scheme for Western Europe. *Int. J. Climatol.* (submitted).

Klecka, W. R. (1980) *Discriminant Analysis.* Sage, London, UK.

Krasovskaia, I., Arnell, N. W. & Gottschalk, L. (1994) Flow regimes in Northern and Western Europe. In: *FRIEND: Flow Regimes from International and Experimental network Data* (ed. by P. Seuna, A. Gustard, N. W. Arnell & G. Cole), 185–192. IAHS Publ. 221. IAHS Press, Wallingford, UK.

Sheridan, S. C. (2002) The redevelopment of a weather-type classification scheme for North America, *Int. J. Climatol.* **22**, 51–68.

Climate Variability and Change—Hydrological Impacts (Proceedings of the Fifth FRIEND World Conference held at Havana, Cuba, November 2006), IAHS Publ. 308, 2006.

Interactions between large-scale climate and river flow across the northern North Atlantic margin

DANIEL G. KINGSTON[1], DAVID M. HANNAH[1], DAMIAN M. LAWLER[1] & GLENN R. MCGREGOR[2]

1 *School of Geography, Earth and Environmental Sciences, University of Birmingham, Edgbaston, Birmingham B15 2TT, UK*
dgk366@bham.ac.uk

2 *Department of Geography, Kings College London, London WC2R 2LS, UK*

Abstract To assess the nature of hydrological sensitivity to climatic change a clear understanding of the cascade of hydroclimatological processes from atmosphere–surface–runoff is necessary, yet this is poorly defined for the northern North Atlantic. This research gap is addressed through a composite analysis of large-scale climatic controls on monthly high and low river flow across this region for 1968–1997. Analyses are structured using hydrological regions defined by cluster analysis, and focus on the month of November. High river flow in all regions is associated with more maritime climatic conditions, driven in northern Europe by a stronger Atlantic pressure gradient and wind-speeds. In eastern North America, high river flow is linked to the opposite conditions. This is suggestive of a positive (negative) relationship between European (North American) river flow and the North Atlantic Oscillation. Additionally, inverse climatic associations between northern European hydrological regions (north *versus* south) appear linked to the Scandinavian pattern.

Key words climate–river flow linkages; composite analysis; hierarchical cluster analysis; North Atlantic Oscillation; northern North Atlantic; Scandinavian pattern

INTRODUCTION

To understand the drivers of hydrological variability, particularly in the context of climate change, fundamental research is required into the process cascade linking the atmosphere and hydrosphere over large spatial domains. The nature of such linkages remains poorly understood, yet such knowledge is crucial for understanding and predicting water resource availability and associated potential stress on society and ecosystems. The ability of atmospheric circulation patterns (such as the North Atlantic Oscillation, NAO) to summarize large-scale climatic variation makes them potentially useful in research on spatial and temporal aspects of climate–environment relationships. To date, the use of such patterns for studying climatic forcing of river flow has been under-utilized (Lawler *et al*., 2003; Kingston *et al*., 2006a). This research gap is addressed through an investigation of the links between large-scale climate and monthly river flow and discussion of possible hydroclimatological mechanisms underlying such associations (i.e. atmospheric circulation patterns). This aim is achieved through a composite analysis of North Atlantic geopotential height and wind vector under monthly high and low river flow conditions for the period 1968–1997. This is conducted on a regional basis, with hydrological regions defined using hierarchical cluster analysis. Analyses are undertaken first for part of the Northern European FRIEND region (Iceland, Scotland, Norway, Sweden, Denmark and Finland), before the study area is extended to the wider northern North Atlantic domain (i.e. northeastern USA and southeastern Canada) to set results in a larger spatial context. In this short paper, results for November are focused upon because previous work (Kingston *et al*., 2006b) has revealed November to be the month with the strongest and most widespread atmospheric links to river flow.

DATA AND METHODOLOGY

Monthly river flow data for Norway, Sweden, Denmark and Finland were primarily sourced from the FRIEND-EWA, supplemented by records from the national hydrometric agencies of these countries. Icelandic data and a small number of Norwegian records were obtained from the Global Runoff Data Centre. Scottish flow data were obtained from the UK National River Flow Archive. The Hydro-Climatic Data Network and Reference Hydrometric Basin Network provided data for the USA and Canada, respectively. A total of 112 river flow records were selected: 69 for northern Europe and 43 for eastern North America. Gauging stations were selected according to the

Copyright © 2006 IAHS Press

following criteria: (a) gauged basin area between 50 and 1000 km^2; (b) a continuous 30-year record; (c) satisfactory record homogeneity, assessed by detailed visual inspection and double mass curve analysis; (d) maximum spatial coverage of the northern North Atlantic margin. These requirements resulted in a study time period of 1968–1997.

Climate data were obtained from the European Centre for Medium Range Weather Forecasting (ECMWF) ERA-40 re-analysis, which provides gridded data at 2.5º resolution (Simmons & Gibson, 2000). Monthly 500 and 1000 hPa geopotential height and wind vector data for 1968–1997 for the North Atlantic region were extracted for this investigation.

Hierarchical cluster analysis (CA) of river flow time series was used to define hydrological regions within the study domain. Regionalization was undertaken to identify spatial structure within the data set and so facilitate interpretation of inter-regional patterns and processes. Ward's clustering algorithm was used, as this was found to provide the most physically meaningful results (in agreement with Bower *et al*., 2004). Whilst CA is an objective method for regionalization, the user has to make a number of decisions at different stages which influence emergent groups (Bower *et al*., 2004). As such, visual inspection and correlation of individual stations with their regional means, and a check of the geographical expression of each region in terms of physical interpretability, were carried out to validate the final cluster solution.

Before regionalization was performed, two steps were taken to ensure that underlying time-series variation was the primary factor determining the definition of river flow regions. Initially, the seasonal cycle was removed. Secondly, river flow time series were standardized (*z*-score transformation) to enable meaningful comparison of time series from basins with different absolute discharge magnitudes. After determination of hydrologically similar regions, monthly data for each region were averaged to produce regional time series, which formed the basis for subsequent composite analysis.

Composites of geopotential height and wind vector across the North Atlantic region were produced based on high and low flow episodes for each monthly regional river flow series. High and low flow are defined as the upper and lower quartiles of river flow for each month over the 1968–1997 study period (equating to eight high flow and eight low flow years). These threshold levels were chosen as the best compromise between sample size and sampling only genuinely high and low flow years. T-tests were used to test for statistical significance of climatic differences between high and low flow composites.

RESULTS

Seven hydrological regions were defined (Fig. 1): four in the Northern European FRIEND area (Regions 1–4) and three in North America (Regions 5–7). Region 1 represents rivers in central Scandinavia, Region 2 northern Scandinavia and Iceland, Region 3 southern Scandinavia and northeast Scotland, and Region 4 southern and central Scotland. For North America, Region 5 includes rivers in central and northern New England, southeastern Quebec, New Brunswick and one in northern Newfoundland. Region 6 covers rivers in Nova Scotia and southern Newfoundland, while Regions 7 represents rivers from southern New England. Although a range of basin sizes has been used herein, no statistically significant (p = 0.05) differences in basin size were found between the regions (using analysis of variance).

Composite analysis

Regions 1–4 (northern Europe) High river flow in Regions 1 and 4 is associated with a stronger and more northwesterly positioned Icelandic Low (IL) and Azores High (AH) (e.g. Fig. 2). The resultant enhanced pressure gradient between the IL and AH causes greater wind speeds and increased advection of moist maritime air masses over Regions 1 and 4 (Fig. 3(a)). Low river flow is associated with decreased wind-speeds over northwest Europe, resulting from weaker pressure gradients in the zone upwind of Regions 1 and 4 (Fig. 3(b)).

For Region 2, geopotential height differences between high and low river flow consist of a positive anomaly over Britain and southwest Scandinavia and a negative anomaly affecting north-east Scandinavia, as part of a circumpolar wave of alternating positive and negative geopotential

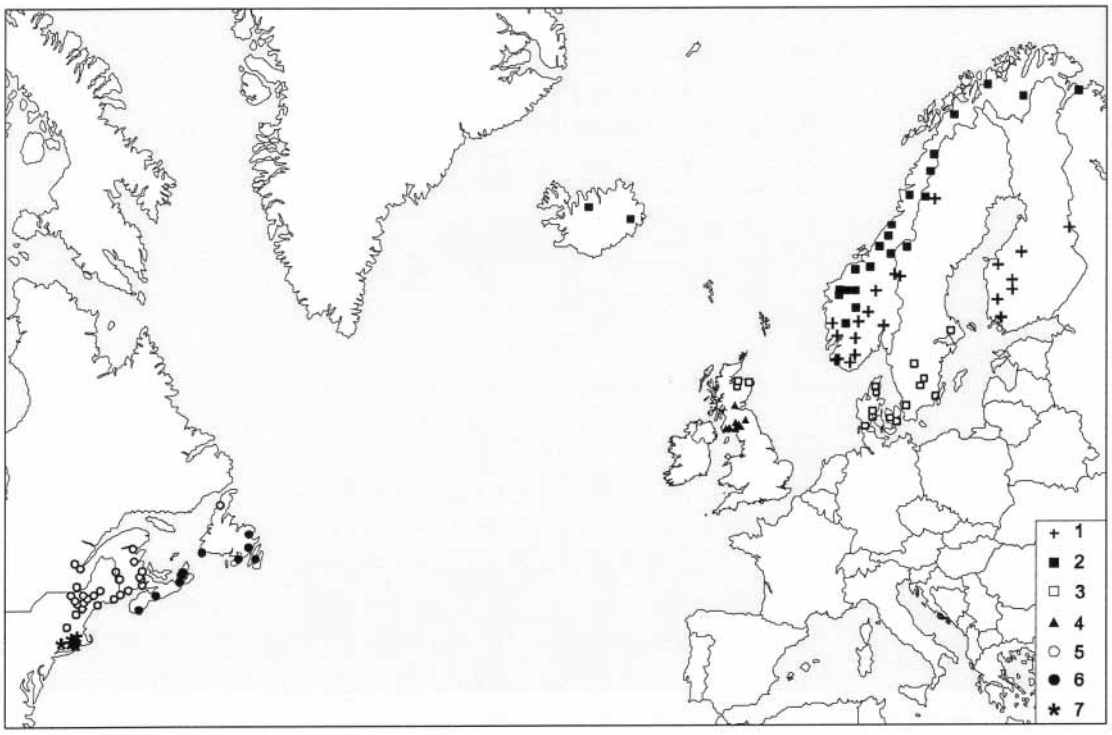


Fig. 1 Locations of river flow gauging stations and hydrological regions.

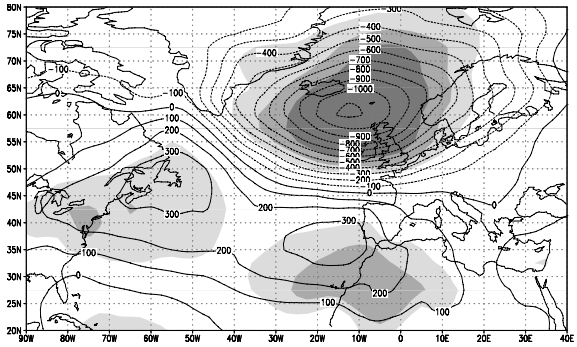


Fig. 2 High minus low flow November 1000 hPa geopotential height for Region 4. (Dotted lines indicate greater geopotential height for low flow; solid lines where greater for high flow. Shading indicates statistical significance at $p = 0.05$, 0.01 and 0.001 from light to dark.)

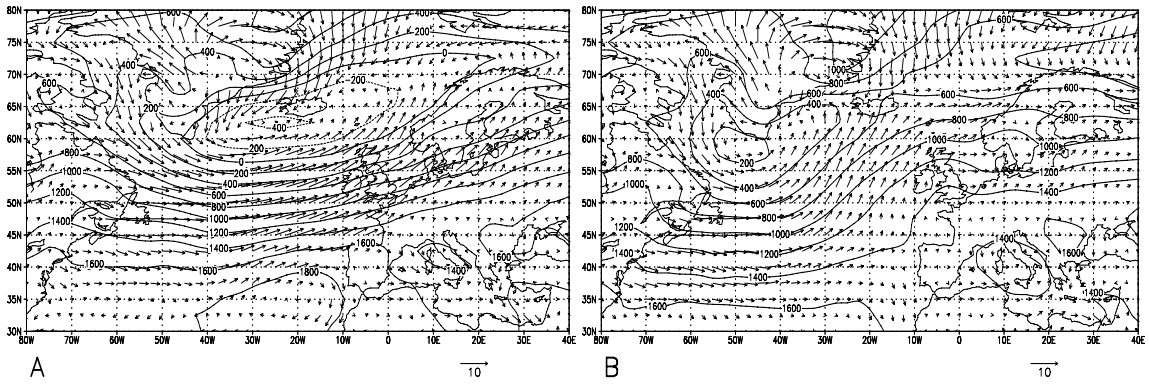


Fig. 3 High (a) and low (b) flow November 1000 hPa geopotential height and wind vector Region 4 composites. (Arrow length indicates wind speed in m s^{-1} – see scale at bottom right.)

height departures (Fig. 4). In high flow situations these pressure differences are associated with an IL displaying two geopotential height minima, a weaker western low and a deeper centre north of

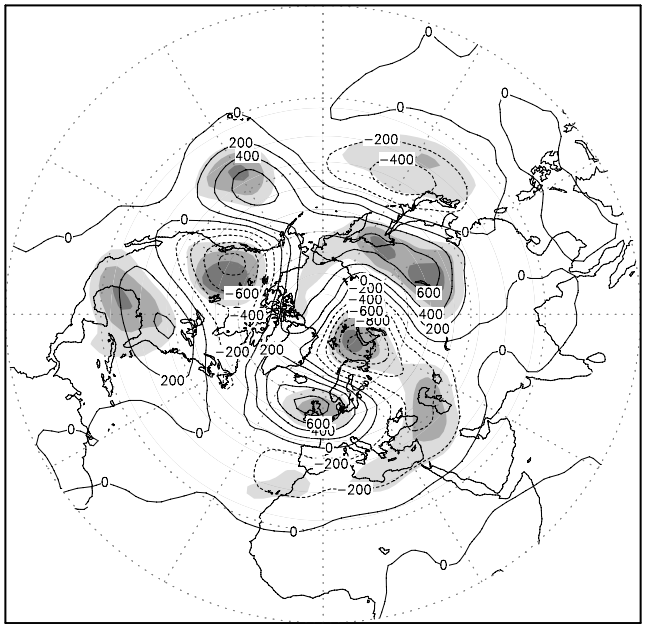


Fig. 4 High minus low flow November 500 hPa geopotential height for Region 2 (lines and shading as Fig. 2)

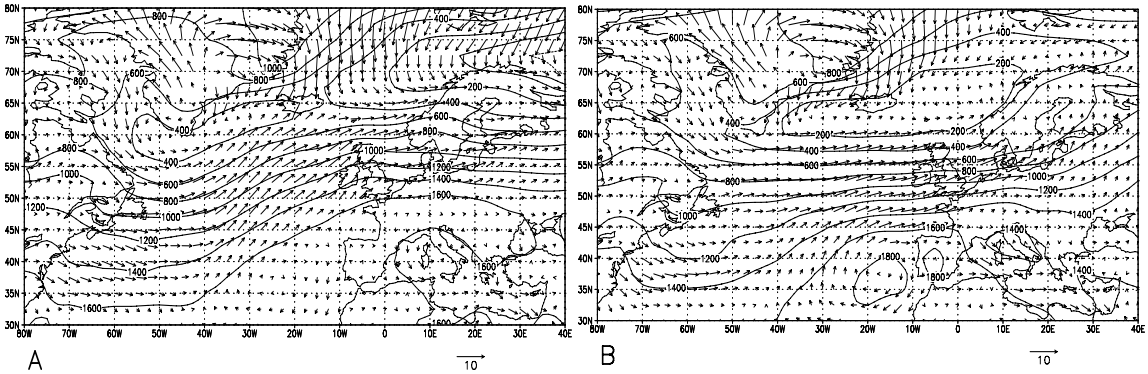


Fig. 5 High (a) and low (b) flow November 1000 hPa geopotential height and wind vector Region 2 composites. (Arrow length indicates wind speed in m s^{-1} – see scale at bottom right.)

Scandinavia. This is associated with strong northerly winds over the north of Region 2 and southwesterly winds in the south of this region (Fig. 5(a)). The low flow composite shows an IL position between Iceland and Scotland, resulting in a relatively strong pressure gradient and wind-speeds south of Region 2, over Britain and southern Scandinavia (Fig. 5(b)). Differences in geopotential height and wind vector between high and low flow for Region 3 (southern Scandinavia and northeast Scotland) are less apparent but in general show the opposite patterns to Region 2.

Regions 5–7 (North America) As for Regions 1 and 4, river flow in Regions 5 and 6 appears closely related to variation in the IL and AH. In contrast to the European regions, high flow in Regions 5 and 6 is linked to a relatively weak IL and AH and consequently a reversal of the meridional pattern of pressure differences shown for Regions 1 and 4. These changes are linked to a stronger pressure gradient in the western Atlantic in low flow composites and associated stronger wind-speeds over Regions 5 and 6.

For Region 7, differences in pressure gradient and wind-speed between high and low river flow are similar to those of Regions 5 and 6. Instead of being primarily related to changes in the IL and AH, however, variation in the East Coast pressure trough appears more influential, with this trough weaker in high flow situations and deeper under low flow conditions. This is shown to be related to a hemispheric wave pattern of alternating positive and negative geopotential height departures (but different to that of Region 2).

DISCUSSION

Interactions between large-scale climate and river flow in November have been revealed for hydrological regions within the Northern European FRIEND region and eastern North America. High river flow for all regions is associated with an increased maritime influence on climate. This is thought to result in greater river flow by directing rain-bearing maritime weather systems (i.e. mid-latitude depressions) over these regions with greater frequency and causing milder temperatures. Milder temperatures are thought to influence river flow primarily through reducing the snow-to-rain ratio, making precipitation more likely to influence river flow concurrently.

The atmospheric mechanisms driving differences in the degree of maritime influence on climate are found to vary between hydrological regions. Regions 5 and 6 show opposing relationships with the IL and AH compared to Regions 1 and 4, yet both experience a more maritime/less continental climate in high flow situations. This apparent discrepancy is linked to the opposite locations of these two groups on the North Atlantic periphery. Thus for Regions 5 and 6 on the lee side of the North American continent a reduction in the prevailing mid-latitude westerly winds results in a reduced continental influence, while the reverse is true for Regions 1 and 4 on the windward side of northern Europe.

Differences in the IL, AH and intervening pressure gradient between high and low river flow for Regions 1 and 4 (Fig. 2), and 5 and 6, are typical of those associated with the NAO (Hurrell, 1995). Region 1 and 4 geopotential height differences are consistent with a positive relationship between river flow and the NAO, while those for Regions 5 and 6 suggest an inverse relationship with the NAO. These findings support previous studies on European NAO-river flow relationships (Kingston *et al.*, 2006a), although are contradictory to suggestions of a positive NAO-river flow association in northeastern USA (Bradbury *et al.*, 2002). This apparent discrepancy may arise because Regions 5 and 6 straddle zones typically believed to be under opposing NAO centres of influence (Hurrell, 1995), although it should be noted that relatively few studies have considered spatial patterns of NAO-climate linkages outside of the December-March winter season.

The contrast in climatic influences on river flow between Regions 2 and 3 is linked to their latitudinal separation causing these regions to be affected in opposite ways by certain weather systems. The consequent geopotential height anomaly dipole between northern and southern Scandinavia in the Region 2 pattern (Fig. 4) (and to a lesser extent in the Region 3 pattern) appears linked to the Scandinavian teleconnection pattern (CPC, 2006), previously referred to as the Eurasia-1 pattern (Barnston & Livezey, 1987). The positive phase of this pattern is associated with a blocking anticyclone over northern Scandinavia and western Russia, and consequent lower temperatures and precipitation over this area (Kauker & Meier, 2003). As such, this apparent connection provides a potential mechanism for river flow variation between Regions 2 and 3, with geopotential height departures consistent with a negative correlation between Region 2 river flow and the Scandinavian pattern and a positive correlation for Region 3.

The association between November high river flow across the northern North Atlantic periphery and a more maritime climate has been shown to be linked to large-scale climatic changes. In a number of cases, these changes appear to be related to atmospheric circulation patterns (the NAO and Scandinavian patterns), with river flow in different hydrological regions associated with opposing phases of these circulation patterns. As such, the relationships defined here represent a promising approach for enhancing understanding of historical discharge behaviour and potential future climate-driven changes.

Acknowledgements Daniel Kingston is funded by a University of Birmingham School of Geography, Earth and Environmental Science PhD scholarship. The authors gratefully acknowledge the help of Gwyn Rees and David Pitson for extracting data from the FRIEND-EWA; Lars Roald for supplying updates and metadata for the FRIEND-EWA; and the national hydrometric agencies of Denmark, Sweden and Finland for additional data. Tom Lüllwitz kindly extracted data from the Global Runoff Data Centre. Kevin Burkhill redrew Fig. 1. The authors would like to thank the reviewer for comments on this paper.

REFERENCES

Barnston, A. G. & Livezey, R. E. (1987) Classification, seasonality and persistence of low-frequency atmospheric circulation patterns. *Mon. Weath. Rev.* **115**(6), 1083–1126.

Bower, D., Hannah, D. M. & McGregor, G. R. (2004) Techniques for assessing the climatic sensitivity of river flow regimes. *Hydrol. Processes* **18**(13), 2515–2543.

Bradbury, J. A., Dingman, S. L. & Keim, B. D. (2002) New England drought and relations with large scale atmospheric circulation patterns. *J. Am. Water Resour. Assoc.* **38**(5), 1287–1299.

CPC (2006) *Northern Hemisphere Teleconnection Patterns*. http://www.cpc.ncep.noaa.gov/data/teledoc/telecontents.shtml (accessed 20/02/06).

Hurrell, J. W. (1995) Decadal trends in the North-Atlantic Oscillation – regional temperatures and precipitation. *Science* **269**(5224), 676–679.

Kauker, F. & Meier, H. E. M. (2003) Modeling decadal variability of the Baltic Sea: 1. Reconstructing atmospheric surface data for the period 1902–1998. *J. Geophys. Res.* **108**(C8), doi:10.1029/2003JC001797.

Kingston, D. G., Lawler, D. M. & McGregor, G. R. (2006a) Linkages between atmospheric circulation, climate and streamflow in the northern North Atlantic: research prospects. *Prog. Phys. Geogr.* **30**(2), 143–174.

Kingston, D. G., McGregor, G. R., Hannah, D. M. & Lawler, D. M. (2006b) River flow teleconnections across the northern North Atlantic region. *Geophys. Res. Lett.* **33**, doi:10.10292006/GL026574.

Lawler, D. M., McGregor, G. R. & Phillips, I. D. (2003) Influence of atmospheric circulation changes and regional climate variability on river flow and suspended sediment fluxes in southern Iceland. *Hydrol. Processes* **17**(16), 3195–3223.

Simmons, A. J. & Gibson, J. K. (2000) The ERA-40 project plan. *ERA-40 project report series no. 1.*

Climate Variability and Change—Hydrological Impacts (Proceedings of the Fifth FRIEND World Conference held at Havana, Cuba, November 2006), IAHS Publ. 308, 2006.

Identification of the distribution of hydroclimatic cycles of field observations in Southeast Asia

MARIA A. SOLERA-GARCIA, NICK A. CHAPPELL & WLODEK TYCH
Lancaster Environment Centre, Lancaster University, Lancaster LA1 4YQ, United Kingdom
a.soleragarcia@lancaster.ac.uk

Abstract The study of hydro-climatic cycles in Southeast Asia is carried out by analysing time series of rainfall, streamflow, evapotranspiration and net radiation from three representative regions: Northern Thailand, Peninsular Malaysia and Borneo. The method used is a data-based mechanistic tool called the Unobserved Component – Dynamic Harmonic Regression (UC-DHR) model, used here to identify both the diurnal and inter-annual variability patterns of existing plot studies data sets.

Key words Southeast Asia; field observations; temporal cycles; DBM modelling

INTRODUCTION

The increasing use of modelling within hydrology and meteorology has highlighted the need to provide an accurate description and quantification of the hydroclimatic processes involved (Bonell, 2004). This is required to improve the definition of model structures and model evaluation that will eventually lead to further improvements in climate change prediction.

General Circulation Models (GCMs), which link hydrological and meteorological phenomena (rainfall, evapotranspiration and rainfall–runoff processes) within land surface schemes (LSSs), are found to be very sensitive to water flux interactions in Southeast Asia. In particular, one of the problems identified relates to the representation of the inter-annual climate cycles and daily patterns of convective rainfall (e.g. Neale & Slingo, 2003).

This study intends to contribute to the understanding of spatial variability in hydroclimatic cycles in Southeast Asia, focusing on three representative geographical areas: Northern Thailand, Peninsular Malaysia and Borneo. These regions have been chosen because they represent the hydroclimatic gradient from the Equator to the Tropic of Capricorn and because of the availability of catchment/plot studies within the area.

METHOD

Data-based mechanistic modelling

Time series data sets of rainfall, riverflow, radiation and evapotranspiration have been analysed using the Data-Based Mechanistic (DBM) methodology (Young, 2001), which uses only the available data to suggest the model structure, through the use of statistical techniques. The DBM methodology follows three steps: (a) Defining the different model structures and parameter estimates obtained using different methods to find models. (b) Application of statistics, R_T^2 (Nash & Sutcliffe, 1970) to data obtained from controlled experiments or passive observations to define a model structure that describes the system behaviour. (c) Finding of a physical explanation of the model results.

By using fewer parameters, there are not as many structure and parameter combinations, which would result in greater parametric uncertainty. DBM techniques explicitly quantify parameter uncertainty (Young, 2001). The DBM methodology includes several different tools, the one used here is the Unobserved Components – Dynamic Harmonic Regression (UC-DHR) model.

Dynamic harmonic regression

UC-DHR is described in detail by Young *et al.* (1999) and is a simpler version of the Unobserved Component (UC) model type, i.e. its components are hypothetical and not readily measured or observed. Its general form is as follows:

$$y_t = T_t + S_t + e_t \quad (1)$$

where y_t refers to the time series, T_t is the trend or less frequent component (i.e. it represents the

Copyright © 2006 IAHS Press

inter-annual variability), S_t is the seasonal component (i.e. it represents the variability within the year) and e_t is the irregular component, which represents noise and uncertainty. S_t is the dominant component and is defined:

$$S_t = \sum_{i=1}^{R_s} \{a_{i,t} \cos(\omega_i t) + b_{i,t} \sin(\omega_i t)\} \quad (2)$$

where $a_{i,t}$ and $b_{i,t}$ are stochastic parameters that vary with time (TVPs) and ω_i, $t = 1,\ldots, R_s$ refer to the seasonal frequencies in the data series.

UC-DHR has been developed to work with the Matlab® software, as part of the Captain Toolbox, developed in Lancaster University for time series analysis and forecasting (see Centre for Research on Environmental Systems (CRES) in http://www.es.lancs.ac.uk/cres/). UC-DHR is used in this study to identify the temporal components included in the time series data sets of rainfall, runoff, radiation and evapotranspiration obtained from field sites in Northern Thailand, Peninsular Malaysia and Northern Borneo.

Evaluation of model performance

The performance of the model is assessed using the simplified Nash & Sutcliffe (1970) efficiency measure, R_T^2 (Young, 2001) or E (Krause *et al.*, 2005):

$$R_T^2 = 1 - \frac{\sigma_r^2}{\sigma_o^2} \quad (3)$$

where σ_r^2 is the variance of the model residuals (i.e. model fit – observations) and σ_o^2 is the variance of the observed time series. R_T^2 varies between $-\infty$ and 1 (perfect fit).

SITE AND DATA SETS

Figure 1 shows a schematic map of Southeast Asia with the three geographical "boxes" chosen for this study as being representative of the Southeast Asia region. Within these boxes, the field sites for the chosen data sets are shown. The size of the box is chosen to roughly match 5 × 5 pixels in HadGAM (The Hadley Centre General Atmospheric Model) mode, where the pixel resolution is 1.25° latitude and 1.875° longitude.



Fig. 1 Map of Southeast Asia showing the location of the data set field sites.

In Northern Thailand, the *Kog-Ma* data set provides four years of hourly rainfall and radiation (1998–2001) and two years of hourly latent heat (1998–1999), where January data is missing for both years. This data was collected from a 50 m tower (18°48.756'N, 98°54.012'E), located within a hill evergreen forest (Ohta *et al.*, 1999; Tanaka *et al.*, 2003; Hashimoto *et al.*, 2004). The *Mae Chaem* dataset provides 47 years of daily rainfall (1952–1999) and 46 years of daily streamflow (1953–1999) from the P14 sub-basin (area 3853 km^2). It belongs to the Royal Irrigation Department (RID) and is fully described elsewhere (Boochabun *et al.*, 2004). *Huai Mai*, a sub-basin of P14, provides three months of 15-min streamflow (Lim *et al.*, 2004).

In Peninsular Malaysia, the *Cameron Highlands* hourly rainfall dataset covers 6 months (April–September 1998). The raingauge is located at 4°28'N, 101°22'E, at an altitude of 1545 m and is part of the routine GAME-T2 observation programme network led by Professor Matsumoto of the Department of Earth and Planetary Science of the University of Tokyo, Japan. The *Bukit Berembun* dataset includes seven years (1981–1987) of daily rainfall and riverflow from a lowland dipterocard forest located at 2°46'N, 102°6'E (Chappell *et al.*, 2005).

In Borneo, the *Bukit Soeharto* data set includes two years (2001–2002) of 30-min rainfall and net radiation, although for net radiation, only the data until August 2002 is used. It also includes hourly latent heat with several data gaps. The data was collected from a 30 m tower (0°51'S, 117°02'E), located in the Bukit Soeharto Education Forest (BSEF). The principal investigator is Minoru Gamo of the National Institute of Advanced Industrial Science and Technology (AIST), Ibaraki, Japan. The *Baru* 5-min riverflow data set (water year 1/7/95–30/6/96) was obtained from a 0.44 km^2 experimental catchment located in Sabah, (Chappell *et al.*, 1999). Finally, the *Tawau* data set, 18 years (1980–1998) of daily rainfall from a raingauge located 83 km to the south-southeast of the Danum Valley Field Centre (4°58'N, 117°48'E), Sabah, (Chappell *et al.*, 2001).

RESULTS AND DISCUSSION

This section describes some of the results obtained from the initial analysis of both the diurnal and annual cycles of the datasets described above.

The diurnal component

Table 1 shows a summary of the diurnal cycle amplitude (*a*) for the relevant time series. The units of rainfall and streamflow are mm h^{-1}, whilst latent heat and net radiation are in hourly means of W m^{-2}.

UC-DHR clearly identifies a 24-h diurnal cycle in the time series of net radiation for both equatorial and northern latitudes. The 24-h diurnal amplitude is shown in Fig. 2, where it can be seen that the northern Thailand amplitude is less variable and of lower magnitude to that nearer the equator. Also it appears to peak in the dry season, just before the wet season starts (May), as described by McGregor & Nieuwolt (1998).

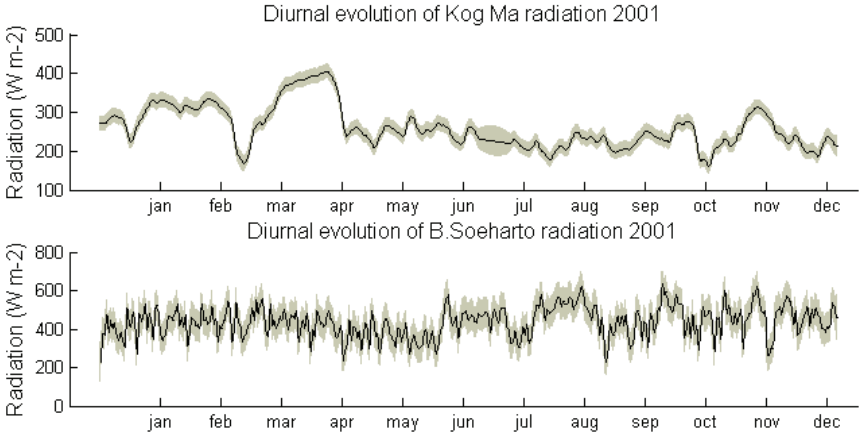


Fig. 2 Diurnal component (24 h) amplitudes of net radiation for the Northern Thailand and Equatorial sites. The greyed area indicates the 95% confidence bands.

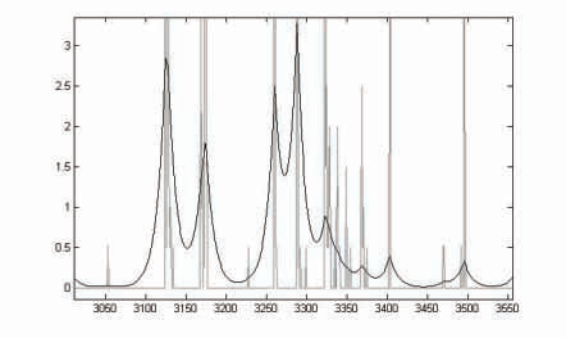


Fig. 3 Example of how filtering transforms data sets. Bars show the raw hourly rainfall, whilst the continuous black line shows the filtered rainfall using RW (random walk).

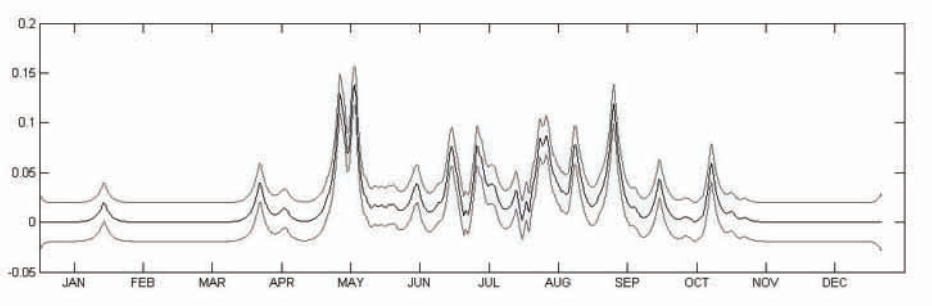


Fig. 4 Diurnal harmonic (24 h) for filtered Kog Ma 1998 rainfall.

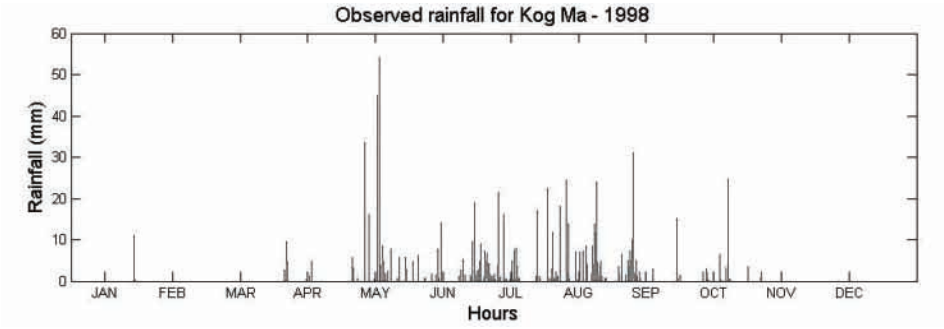


Fig. 5 Hourly time series of rainfall for Kog Ma 1998 (for comparison against Fig. 4).

Regarding rainfall and runoff, the UC-DHR fit may be poorer due to the characteristics of the raw data, which is not normally distributed, with 96% of the rainfall events measuring under 0.5 mm h^{-1} and a mean and median of 0.14 and 0 mm h^{-1} respectively. Because of the way UC-DHR works on the time series averages (W. Tych, personal communication), it is more difficult for UC-DHR to identify the cycles whilst obtaining a good model fit. As a way around this problem, it is thought that data pre-processing may improve the raw data set distribution. This work is currently underway. As an example, rainfall data for Kog-Ma (1998) was filtered using the Captain toolbox mentioned earlier. Fig 3 illustrates how filtering alters the original data set. Applying UC-DHR to the filtered rainfall results in a very good fit (RT^2 = 0.9) for the diurnal harmonic amplitude shown in Fig.4, which can be compared with the original hourly rainfall data set (Fig.5). Interpretation of the results is not as clearly marked though but may be provided in relative terms (e.g. information about the time of the year when the diurnal cycle has a stronger influence on rainfall patterns).

The seasonal component

Table 1(b) shows a summary of the dominant annual cycle amplitude for the time series of all the analysed data sets (see Fig. 1 for location). The units of rainfall and streamflow are mm $fortnight^{-1}$, whilst latent heat and net radiation are in fortnightly means of W m^{-2}. A poorer fit is obtained this time from the equatorial data sets and this coincides with the fact that the annual seasonality for

Table 1 Magnitudes of the diurnal (a) and annual (b) harmonic amplitude.

(a)	Diurnal harmonic				
North Thailand	Range		Mean	Stdev	RT^2
Rainfall[1]	0.0	2.2	0.2	0.3	0.21*
Riverflow[2]	0.00	0.66	0.04	0.08	0.39*
Net radiation[1]	85	406	252	56	0.92
Latent heat[1]	31	206	135	35	0.94
West Malaysia	Range		Mean	Stdev	RT^2
Rainfall[3]	0.0	2.7	0.4	0.4	0.35
Borneo	Range		Mean	Stdev	RT^2
Rainfall[4]	0.0	2.2	0.3	0.3	0.27
	0.0	7.5	0.4	0.6	0.31
Riverflow[5]	0.0	4.1	0.3	0.5	0.43
Net radiation[4]	222	637	436	74	0.89
	283	673	495	79	0.92
Latent heat[4]	0	195	68	38	0.78

* log-transformed data
[+] 4 yrs, one year logged 0.39
[1] Kog Ma
[2] Huai Mai (subcatchment of Mae Chaem)
[3] Cameron Highlands
[4] Bukit Soeharto 2001/2
[5] Baru

(b)	Annual harmonic				
North Thailand	Range		Mean	Stdev	RT^2
Rainfall[1]	14	159	45	20	0.78*
Riverflow[1]	4	21	11	3	0.91*
West Malaysia	Range		Mean	Stdev	RT^2
Rainfall[2]	7	30	19	7	0.6
Riverflow[2]	0	8	5	2	0.64
Borneo	Range		Mean	Stdev	RT^2
Rainfall[3]	12	39	24	7	0.39

* log-transformed data
[1] Mae Chaem
[2] Bukit Berembum
[3] Tawau

Northern Thailand is stronger than that for the equatorial site, which shows virtually no change and is very close to zero. The lack of seasonality of equatorial rainfall and riverflow is translated into very high uncertainty bands (see Fig. 6), which include negative values. The model fit for the Mae Chaem data sets improved after log-transforming the data (see Fig. 7 for the annual component amplitude evolution over 40 years). The *y*-axis units are log(mm fortnight^{-1}).

CONCLUSIONS AND FURTHER WORK

Initial results indicate that UC-DHR is very effective in identifying diurnal cycles of net radiation and latent heat, but obtains poorer RT^2 fits when concentrating on rainfall and riverflow datasets. Regarding the inter-annual variability, it highlights the difference in seasonality between Mae Chaem at 18°N and equatorial Bukit Berembun.

The above mentioned results are not entirely finalised, however they provide an example of the way UC-DHR works on the identification of diurnal and inter-annual cycles from different environmental variables. Once the analysis and interpretation of the results is completed, it will be used to identify the dominant hydro-climatic behaviour to be expected from the analysis of the GCM output, which will take place in the next stage of this project.

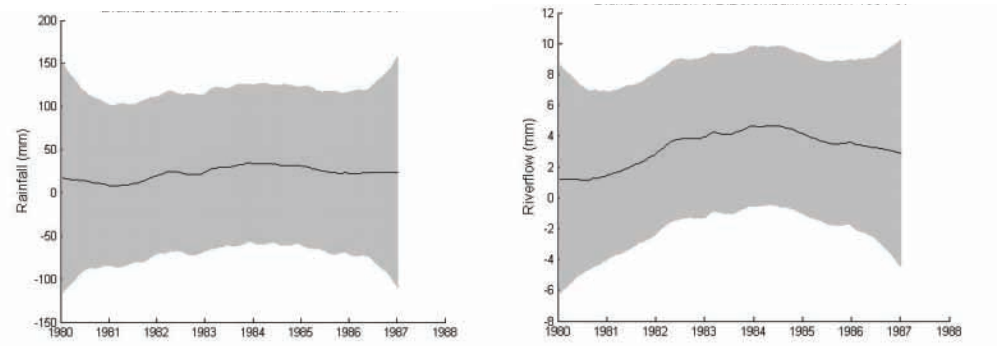


Fig. 6 Bukit Berembun annual evolution of rainfall and riverflow, 1981–1987. The Y axis corresponds to rainfall in mm fortnight^{-1}.

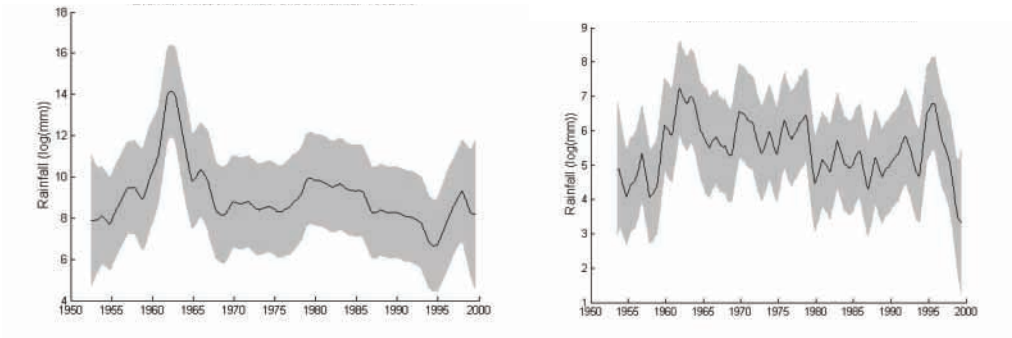


Fig. 7 Mae Chaem, annual component amplitude evolution of rainfall and riverflow. The raw data was log-transformed before applying UC-DHR, therefore the Y axis units are log (mm fortnight^{-1})

Acknowledgements Thank you to all the data owners for allowing public use of their data and to the Natural Environment Research Council (NERC) for funding this project, under studentship NER/S/R/2004/13086.

REFERENCES

Bonell, M. (2004) Runoff generation in tropical forests. In: *Forests, Water and People in the Humid Tropics* (ed. by M. Bonell & L. A. Bruijnzeel), 314–406. Cambridge University Press, Cambridge, UK.

Boochabun, K., Tych, W., Chappell, N. A. & Carling, P. A. (2004) Statistical modelling of rainfall and river flow in Thailand. *J. Geol. Soc. of India* **64**, 503–515.

Chappell, N. A., Bidin, K.& Tych, W. (2001) Modelling rainfall and canopy controls on net-precipitation beneath selectively-logged tropical forest. *Plant Ecology* **153**, 215–229.

Chappell, N. A., McKenna, P., Bidin, K. *et al.* (1999) Parsimonious modelling of water and suspended sediment flux from nested catchments affected by selective tropical forestry. *Phil. Trans. Royal Soc. London B* **354**, 1831–1846.

Chappell, N. A., Tych, W., Yusop, Z. *et al.* (2005) Spatially significant effects of selectively tropical forestry on water, nutrient and sediment flows: a modelling-supported review. In: *Forests, Water and People in the Humid Tropics* (ed. by M. Bonell & L. A. Bruijnzeel), 513–532. Cambridge University Press, UK.

Hashimoto, S., Tanaka, N., Suzuki, M. & Inoue, A. (2004) Soil respiration and soil CO_2 concentration in a tropical forest, Thailand. *J. Forest Research* **9**, 75–79.

Krause, P., Boyle, D. P. & Base, F. (2005) Comparison of different efficiency criteria for hydrological model assessment. *Adv. Geosciences* **5**, 89–97.

Lim, H. S., Richards, K. & Kurji, K. (2004) Runoff response of small forested catchment in the seasonally humid tropics: identification of runoff processes and modelling. In: *Forests and Water in Warm, Humid Asia* (ed. by R. C. Sidle, M. Tani, A. R. Nik & T. A. Tadese), 271–274. Uiji Disaster prevention Research Institute.

McGregor, G. R. & Nieuwolt, S. (1998) *Tropical Climatology*. John Wiley and Sons, Chichester, UK.

Nash, J. E. & Sutcliffe, J. V. (1970) River flow forecasting through conceptual models. Part I - A discussion of principles. *J. Hydrol.* **10**, 282–290.

Neale, R. & Slingo, J. (2003) The Maritime Continent and its role in the Global Climate: a GCM study. *J. Climate* **16**, 834–848.

Ohta, T., Suzuki, K., Kodama, Y. & Kubota, J. (1999) Characteristics of the heat balance above the canopies of evergreen and deciduous forests during the snowy season. *Hydrol. Processes* **13**(14–15), 2382–2394.

Tanaka, K., Takizawa, H., Tanaka, N. & Kosaka, I. (2003) Transpiration peak over a hill evergreen forest in Northern Thailand in the late dry season: assessing the seasonal changes in evapotranspiration using a multilayer model. *J. Geophys. Res.* **108**(D17): 4533.

Young, P. C. (2001) Data-based mechanistic modelling and validation of rainfall-flow processes. In: *Model Validation in Hydrological Science* (ed. by M. G. Anderson), 117–161. Wiley**,** Chichester, UK.

Young, P. C., Pedregal, D. J. & Tych, W. (1999) Dynamic harmonic regression. *J. Forecasting* **18**, 369–394.

Climate Variability and Change—Hydrological Impacts (Proceedings of the Fifth FRIEND World Conference held at Havana, Cuba, November 2006), IAHS Publ. 308, 2006.

Influences of ENSO and SST variations on the interannual variability of rainfall amounts in southern Africa

PATRICK VALIMBA[1], PIERRE CAMBERLIN[2], YVES RICHARD[2], ERIC SERVAT[3] & DENIS HUGHES[4]

1 *Department of Water Resources Engineering, College of Engineering and Technology, University of Dar Es Salaam, PO Box 35131, Dar Es Salaam, Tanzania*
pvalimba@hotmail.com

2 *UMR 5080 CNRS Centre de Recherches de Climatologie, Université de Bourgogne, 6 Bd Gabriel, F-21 000 Dijon, France*

3 *IRD, UMR HydroSciences, Maison de Sciences de l'Eau, Université Montpellier II, BP 64501, F-34394 Montpellier cedex 5, France*

4 *Institute for Water Research, Rhodes University, PO Box 94, Grahamstown 6140, South Africa*

Abstract Relationships between southern Africa rainfall, the El Niño-Southern Oscillation (ENSO) and sea surface temperatures (SSTs) were investigated. Principal Components Analysis (PCA) on rainfall amounts established coherent regions. Results of correlation analysis between rainfall and the Southern Oscillation Index (SOI) and regional SST anomalies indicated strong influences of ENSO and the Tropical Indian Ocean and moderate influences of the Southwest Indian Ocean. The ENSO influence was consistently, moderately negative in equatorial Southern Africa during October–January, strongly positive in the Tropical/Subtropical areas during February–April and highest for light and moderate events in the south and for intense events in the north. SSTs in the Tropical Indian Ocean influence light and moderate events, while SSTs close to the region influence heavy events. Sliding correlations indicated changing rainfall–SOI/SST relationships in the mid-1950s which improved the associations, and since the early-1970s which deteriorated or reversed the relationships.

Key words rainfall variability; ENSO; SST; Principal Components analysis; correlation analysis

INTRODUCTION

There have been significant global-scale changes in oceanic and atmospheric conditions in the 1960s through 1970s. They include warming of the tropical Pacific and Indian Oceans in the late 1970s (Wang, 1995; Trenberth & Hoar, 1996), of the southwest Indian Ocean in the 1970s (Trzaska *et al*., 1996) and of surface air temperatures after 1960. The warming of the tropical troposphere in the 1960s could have contributed to the delayed oceanic warming in low latitudes in the 1970s (Flohn & Kapala, 1989). Some of the consequences are an increase in the frequency and amplitude of warm ENSO events since the mid-1960s (Torrence & Compo, 1998) and changes of rainfall and streamflow characteristics in eastern and southern Africa since the 1960s through to the 1970s (Valimba, 2005). The changes generally led to a declining occurrence of light rainfalls across much of southern Africa, and an increasing occurrence of intense rainfalls particularly in the eastern part of the sub-continent.

To highlight the influence of climate on identified hydrological changes, this study investigates the dynamic nature of relationships between southern African rainfall and climatic variables using seasonal rainfall amounts and the number of raindays in classes of daily amounts (Valimba, 2005). The main questions investigated are:

– In which classes of daily rainfall amounts do ENSO and SST have stronger influences?
– In which parts of southern Africa and in which seasons do ENSO and SST have stronger influences?
– Are lead–lag relationships between rainfall and ENSO/SST stable over time?

DATA AND METHODS

Data

Time series of daily and monthly rainfall at various stations were acquired from various sources: southern African FRIEND database (University of Dar Es Salaam), Department of Water Affairs (Namibia), Computing Centre for Water Research (South Africa) and Tanzania Meteorological Agency. The records were of variable quality and length and selection criteria of period of interest (1950–1990), record length (at least 30 years), continuity (<15% missing) and spatial distribution

Copyright © 2006 IAHS Press

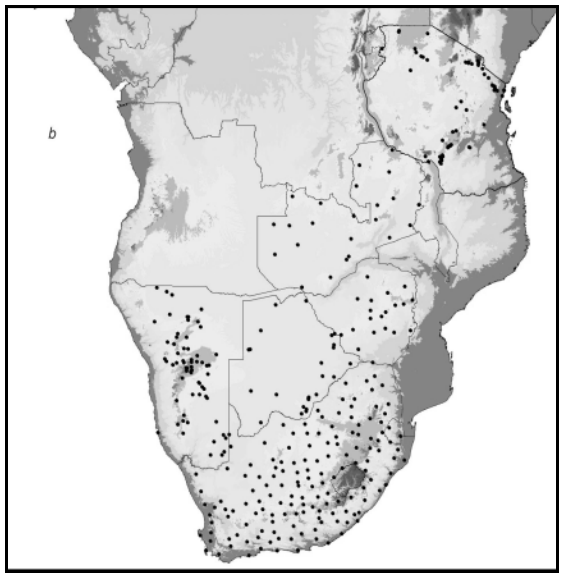


Fig. 1 Spatial distribution of rainfall stations in southern Africa selected for the study.

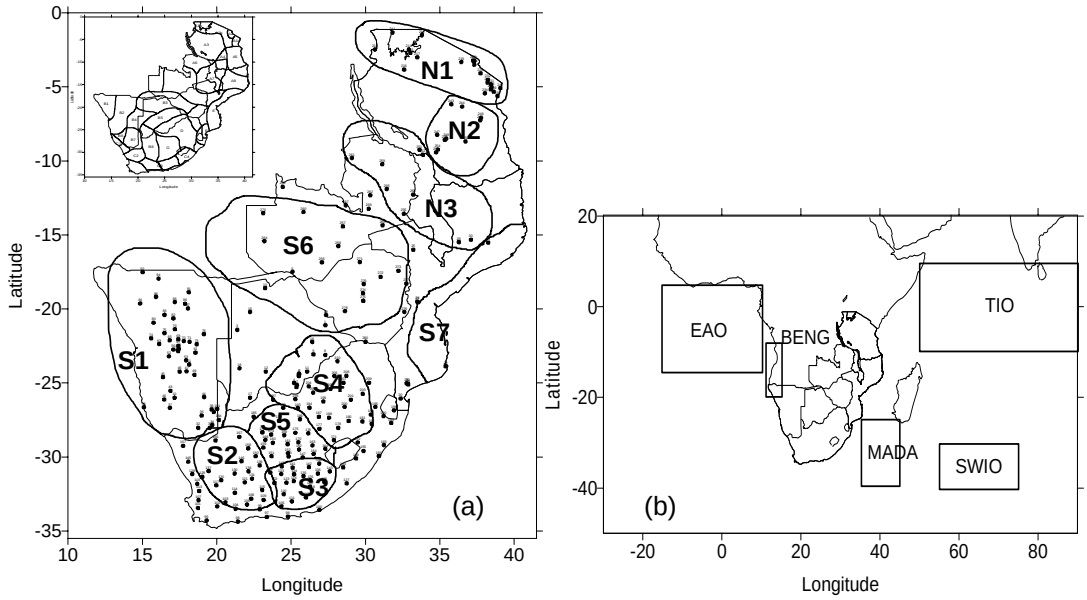


Fig. 2 (a) General coherent clusters from PCA and correlation analysis (Valimba, 2005). (b) Selected oceanic regions in the Atlantic and Indian oceans (Valimba, 2005).

of the stations resulted in 280 stations (Fig. 1) being retained for analysis. Classes of daily rainfall were adopted from Valimba (2005) and include the light rainfall events (class 2; 1–9.9 mm), moderate (class 3; 10–19.9 mm), moderate heavy (class 4; 20–29.9 mm), heavy (class 5; 30–39.9 mm) and extreme heavy (or intense) (class 6; ≥40 mm) events.

ONDJ and FMA seasons were used to define early and late summer seasons. May is omitted from the latter season as atmospheric circulations responsible for rainfall in northern Tanzania at this time resemble those in early summer and differ from March–April (Mutai & Ward, 2000; Camberlin & Okoola, 2003) and May rainfall in the southwestern and southern part of South Africa is predominantly frontal.

Areal average indices of SST anomalies in the key basins of the Atlantic and Indian oceans were used (Valimba, 2005). The regions (Fig. 2(b)) are the Tropical Western Indian Ocean (TWIO), Southwest Indian Ocean (SWIO), Mozambique/Agulhas Currents (MADA), Equatorial Atlantic Ocean (EAO, Phillipon *et al.*, 2002) and Angola/Benguela Front region (BENG), approximately defining the core of extreme warmer SST anomalies during the Benguela Niños (see e.g. Rouault

et al., 2003). ENSO seasons (SON, DJF, MAM and JJA; Trenberth & Caron, 2000) were used to compute seasonal SOI values while seasonal SST anomalies were computed for 3-month rainfall (OND, FMA and JJA) ENSO seasons. In the southern regions, correlations between seasonal rainfall and SOI for ENSO seasons (SON/MAM) were slightly less than for rainfall seasons (OND/FMA). Therefore, only correlations between seasonal rainfall and SOI (defined for ENSO seasons) are presented.

METHODS

Principal components analysis (PCA) and correlation analysis were used to establish coherent rainfall regions from seasonal rainfall. For each season, PCA established a few general coherent regions across southern Africa and a comparison of the regions for all seasons retained only eight main coherent regions (Fig. 2(a); Valimba, 2005). Regional seasonal rainfall amounts were computed as arithmetic averages of standardized anomalies at each station. Pearson's correlation coefficients, computed between regional seasonal rainfall indices and monthly/seasonal SOI and SST anomalies for the 1955–1985 period, were used to assess the ENSO/SST–rainfall lead–lag relationships. Absolute correlations exceeding 0.39 and 0.49 are significant at the 95% and 99% levels, respectively.

The stability of ENSO/SST southern African rainfall associations was investigated for the period 1950–1994, using long Namibian and South African records. Since major changes in oceanic and atmospheric variables had occurred in the late-1970s and only 18 years are available for analysis in the post-1977 period, a 15-year window is used to compute sliding correlations between SOI/SST indices and seasonal rainfall indices. Absolute correlations exceeding 0.5 and 0.43 are significant at the 95% and 90% levels, respectively.

RESULTS

ENSO–southern African rainfall relationships

Results show similar influences of ENSO on seasonal rainfall amounts and number of raindays. In general, the results of the correlation analysis between SOI and seasonal rainfall amounts indicate the seasonality of rainfall responses to an ENSO signal and the spatial variation of the responses. This is summarised according to the strength of the response (Fig. 3(a)) and the nature and seasonality of the relationships (Fig. 3(b)). The results further indicate:

(a) **The consistent influences of ENSO on all classes of daily rainfall** The correlations between SOI and rainfall amounts (Table 1) indicate identical responses of rainfall in the different classes to an ENSO signal with the highest influences on classes III and II.

(b) **The spatial variation of rainfall responses to an ENSO signal** The magnitude and significance of the correlations (e.g. Table 1) indicate the strongest ENSO signals in southern African rainfall in the western parts of southern Africa (Fig. 3(a)) and moderate/weak signals in the northern and eastern parts of the region. These results are consistent with those in the past studies (Nicholson & Kim, 1997; Landman & Mason, 1999; Indeje *et al.*, 2000).

(c) **The seasonality of the influences of ENSO** ENSO signals in early summer rainfall are strong in the eastern regions (*S4* and *N1*) and in late summer in the western (*S1* and *S2*) and southern regions (*S3*). An exception is the central interior of South Africa (*S5*) where the influence is significant in both early and late summer. The influence on late summer rainfall in the northern (*N*) regions is low.

(d) **The lead–lag influences of ENSO** It was found that the SON SOI values produced the highest correlations in both early and late summer. Correlations usually peak in SON (Table 1) and decay thereafter. Correlation peaks are found in October (for early summer rainfall), November (late summer class IV–VI), January (late summer, *S* regions) or April (late summer, N2) for the lower classes.

(e) **Changing influence of ENSO on Southern Africa rainfall** The results of sliding correlation analysis indicate significant changes in the ENSO-southern Africa rainfall relationships. The changes are summarized as:

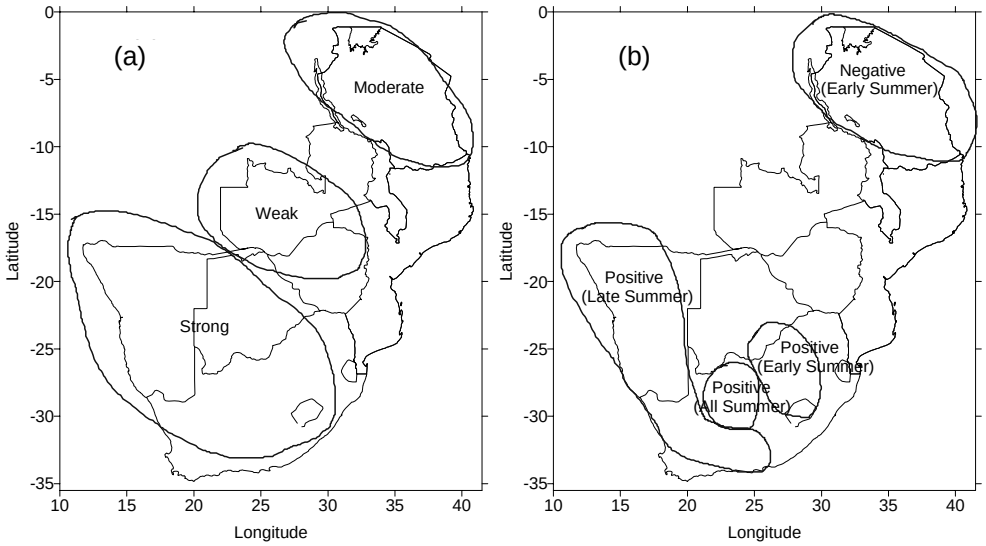


Fig. 3 Generalization of the ENSO-southern African rainfall relationships according to: (a) strength and (b) seasonality and sign of the association with SOI.

Table 1 Correlations between ONDJ and FMA seasonal amounts in southern Africa and seasonal SOI values. Significant correlations at 95% are in bold italics.

Region	Class	ONDJ seasonal amounts against				FMA seasonal amounts against			
		SOI_MAM	SOI_JJA	SOI_SON	SOI_DJF	SOI_MAM	SOI_JJA	SOI_SON	SOI_DJF
S1	II	0.12	0.22	0.25	0.04	0.38	***0.50***	***0.67***	***0.54***
	III	0.12	0.27	0.33	0.03	0.38	***0.45***	***0.68***	***0.65***
	IV	0.11	0.27	0.39	0.00	0.35	***0.43***	***0.62***	***0.61***
	V	0.16	0.28	***0.40***	–0.02	0.31	0.36	***0.54***	***0.54***
	VI	0.13	0.27	0.35	0.03	0.14	0.29	***0.48***	***0.43***
	Overall	0.13	0.27	0.35	0.02	0.36	***0.45***	***0.66***	***0.61***
S5	II	0.07	0.31	0.34	–0.08	***0.41***	0.29	***0.54***	***0.57***
	III	0.30	***0.51***	***0.58***	–0.05	***0.50***	0.36	***0.57***	***0.61***
	IV	0.20	***0.42***	***0.47***	–0.06	***0.43***	***0.42***	***0.46***	***0.53***
	V	0.39	0.29	***0.41***	0.14	***0.40***	***0.52***	***0.58***	***0.55***
	VI	0.20	0.22	***0.43***	–0.04	***0.42***	***0.58***	***0.56***	***0.54***
	Overall	0.29	***0.43***	***0.55***	–0.03	***0.49***	***0.50***	***0.60***	***0.63***
N1	II	–0.18	***–0.40***	***–0.41***	0.11	0.09	–0.07	–0.12	0.08
	III	–0.33	***–0.48***	***–0.53***	0.12	0.18	–0.15	–0.14	–0.08
	IV	–0.34	–0.33	–0.38	–0.09	0.17	–0.17	–0.13	–0.10
	V	–0.27	–0.37	***–0.46***	0.07	0.02	–0.29	–0.19	–0.15
	VI	–0.32	***–0.42***	***–0.52***	0.07	–0.06	–0.38	–0.31	–0.25
	Overall	–0.32	***–0.42***	***–0.49***	0.06	0.06	–0.31	–0.24	–0.16

– *Dates and direction of changes*: Significant changes were mainly observed in the mid-1950s and mid-1970s indicating strong ENSO-summer rainfall association in the period 1956/57–1975/76. The relationships weakened or reversed around 1975/76 (Fig. 4(a)). The two extreme dates correspond to periods of re-occurrence of an active ENSO phase in the late-1950s and warming of the tropical Indian and Pacific Oceans around 1976/77.
– *The changing period of influences of ENSO*: Sliding correlations further indicate weakening or reversing influence of ENSO during September–December on early summer rainfall affecting significantly the three higher classes (class IV–VI) (Fig. 4(a)) and steadily increasing influence of ENSO during June-August (e.g. Fig. 4(b)) on late summer rainfall.
– *Implications of the changes*: The change from positive to negative SOI-early summer rainfall associations suggest that post-1975/76 decaying SOI (warm ENSO) corresponds to enhanced early summer rainfall and reduced late summer rainfall.

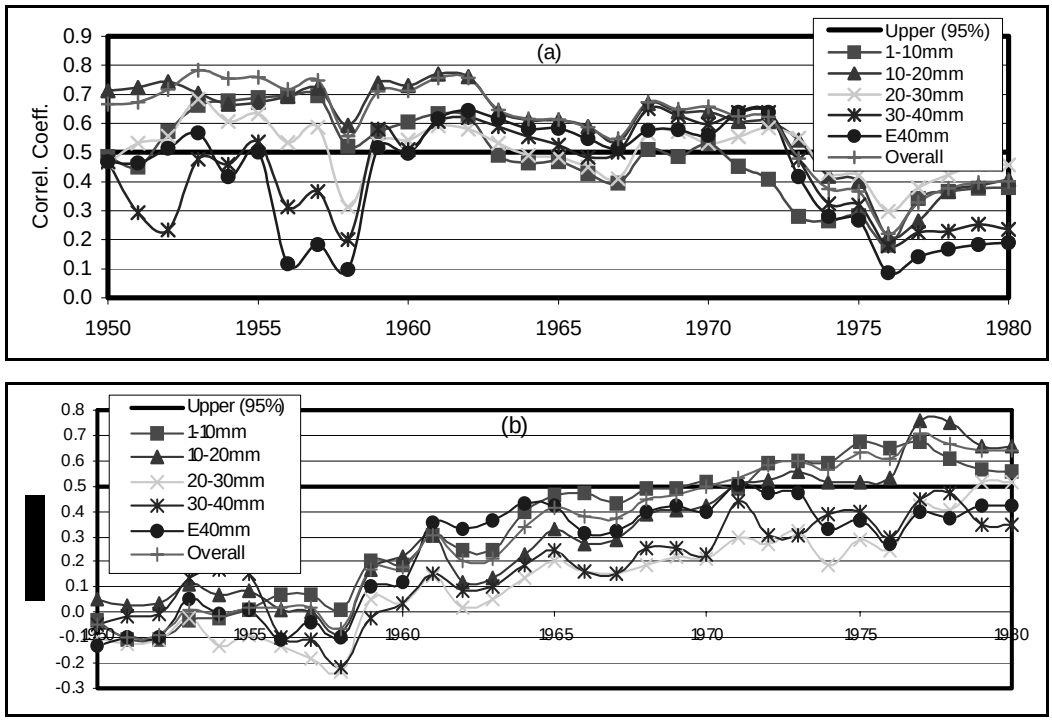


Fig. 4 Temporal evolution of correlations between seasonal rainfall and SOI: (a) FMA seasonal number of events and DJF SOI in S5 and (b) FMA seasonal number of events and MAM SOI in S2. Absolute correlations exceeding 0.50 are significant at 95%.

Table 2 Correlation coefficients between seasonal rainfall amounts in southern Africa and seasonal SST anomalies. Significant correlations at 95% ($r > 0.39$) are bolded. MA = MADA, SW = SWIO, TW = TWIO, EA = EAO and BE = BENG.

Region	Class	ONDJ Seasonal amounts against					FMA Seasonal amounts against				
		MA_OND	SW_OND	TW_OND	EA_OND	BE_OND	MA_FMA	SW_FMA	TW_FMA	EA_FMA	BE_FMA
S1	II	0.21	0.10	–0.18	0.01	0.04	0.34	0.11	***–0.59***	0.05	0.18
	III	0.11	0.05	–0.19	0.00	0.06	0.39	0.20	***–0.57***	–0.04	0.11
	IV	0.09	0.08	–0.22	–0.04	0.04	0.36	0.19	***–0.52***	–0.10	0.04
	V	0.04	0.09	–0.20	–0.03	0.00	0.28	0.18	***–0.40***	–0.29	–0.15
	VI	0.04	0.10	–0.23	–0.03	0.05	0.28	0.04	–0.36	***–0.47***	–0.27
S5	II	0.28	0.04	*–0.36*	–0.02	0.20	0.14	0.13	–0.36	–0.18	–0.06
	III	0.15	0.14	***–0.53***	–0.20	0.12	0.26	0.22	–0.38	–0.02	–0.03
	IV	0.01	0.04	***–0.52***	–0.05	0.11	0.18	0.30	–0.29	0.02	0.00
	V	0.11	0.22	***–0.44***	0.04	–0.05	0.29	0.37	–0.31	–0.24	–0.12
	VI	0.14	0.10	*–0.32*	–0.19	–0.05	0.24	0.19	–0.34	–0.19	–0.08
N1	II	–0.24	–0.05	*0.35*	0.10	–0.04	–0.27	–0.11	0.23	–0.15	–0.08
	III	–0.09	0.02	***0.57***	0.23	0.05	–0.38	–0.29	0.14	–0.21	–0.02
	IV	–0.03	0.06	***0.47***	0.19	0.11	–0.07	–0.08	0.14	–0.24	–0.18
	V	–0.09	0.04	***0.47***	0.16	0.08	–0.06	–0.12	0.25	–0.35	–0.29
	VI	–0.02	–0.04	***0.60***	0.20	0.10	–0.14	–0.24	0.32	–0.13	–0.14

SST–southern African rainfall relationships

Results of correlation analysis between classed seasonal amounts and SST in the Atlantic and Indian Ocean basins (e.g. Table 2) mainly indicate the dominant influence on heavy rainfall events of SST in the Tropical Western Indian Ocean (TWIO) and moderate influence of SST in the south Madagascar (MADA) basin. The influence of TWIO SST are positive in the northern regions and negative in the southern regions while that of MADA is generally the opposite. SST in other oceanic basins show low correlations with southern African rainfall. In the northern regions, the influence of SST is almost consistent for all classes but peaks for the higher classes. In the southern regions, the lower classes of daily intensities are predominantly influenced by the SST in

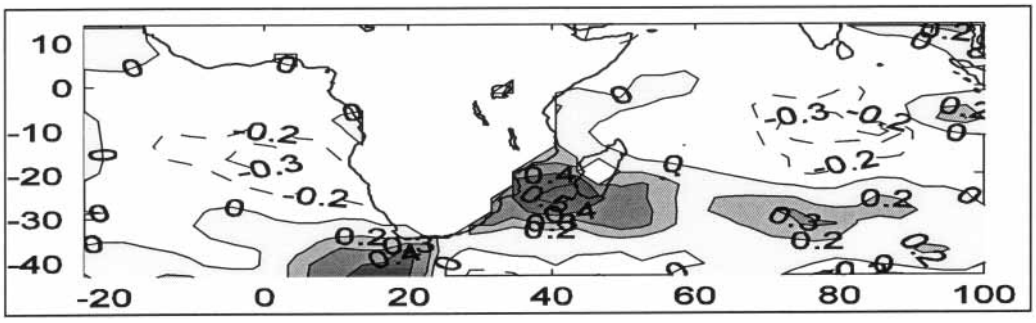


Fig. 5 Correlations between OND SST and S6 (Zambezi) regional ONDJ seasonal amounts. All correlations exceeding 0.39 are significant at 95%.

the tropical Indian Ocean, which are known to modulate regional scale atmospheric dynamics, notably the Walker and Hadley cells. However, the influence generally decreases with increasing intensities suggesting the increasing role of local or regional scale influences on heavy rainfall events (e.g. Fig. 5).

The results of sliding correlation analysis are almost identical to those obtained with SOI which indicate changes in the SST-rainfall associations in the 1956–1966 and 1970–1978 periods. In general, the changes which involve SST in the Indian Ocean basins occurred mainly in the 1970s. The changes in the early-1970s were evident in the relationships involving JJA SST in the TWIO basin and OND SST in the MADA basin. The post-1970 relationships are predominantly positive.

In late summer, the changes involving TWIO SST led to positive associations after the mid-1970s while those involving SST in the two southwest Indian Ocean basins (MADA and SWIO) led to generally negative associations for FMA SST. The influence of SST in the two Atlantic Ocean basins (BENG and EAO) has remained generally insignificant and relatively unaltered.

Increasing influences of the austral winter (JAS) SST and decreasing influences of the austral spring (OND) SST in these three Indian Ocean basins on summer rainfall in southern Africa were observed. This is suggesting a probable shift of the influence from the austral spring to austral winter, increasing the SST lead favourable for forecasting purposes.

CONCLUSIONS

Results show that interannual variability of rainfall in southern Africa is mostly influenced by ENSO and SST in both the tropical Indian Ocean basin and south/southwest Madagascar Ocean basins. The influences of ENSO are consistent in all types of rainfall events and highest in the light (<20 mm) events, and form a dipole-like response of rainfall between the northern and southern part of southern Africa, are moderately negative during the early summer in the north and strongly negative in late summer in the south and have changed since the mid-1970s leading to an increasing influence of the austral winter SOI and decreased or changed associations for austral spring SOI.

The influences of SST in the Indian and Atlantic Oceans indicated the dominance of SST in the tropical Indian Ocean on the interannual variability of rainfall in the region, that the interannual variability of the light/moderate (<20 mm) daily rainfalls is modulated by large-scale influences of the Indo-Pacific signals while regional SST in the south/southwest Madagascar were found to have a considerable influence on heavy daily events. SST in the tropical Indian Ocean have an inverse relationship with rainfall in the southern part and a direct relationship with rainfall in the north, while SST in the south Madagascar basin show the opposite influence

Evolving long-lead SOI/SST–summer rainfall associations in Namibia and South Africa offer the possibility of using SOI and SST as predictors of summer rainfall in these countries. But one should also be cautious when constructing summer seasons as the early and late summers displayed opposing interannual patterns of variability.

Acknowledgements This paper is an extract from the PhD Thesis of Patrick Valimba and the senior author wishes to thank the Institut de Recherche pour le Developpement (IRD, France) for providing financial assistance.

REFERENCES

Camberlin, P. & Okoola, R. E. (2003) The onset and cessation of the long rains in eastern Africa and their interannual variability. *Theor. Appl. Climatol.* **75**, 43–54.

Flohn, H. & Kapala, A. (1989) Changes of tropical sea-air interaction processes over 30-year period. *Nature* **338**, 244–246.

Indeje, M., Semazzi, F. H. M. & Ogallo, L. J. (2000) ENSO signals in east African rainfall seasons. *Int. J. Climatol.* **20**, 19–46.

Landman, W. A. & Mason, S. J. (1999) Change in the association between Indian Ocean sea-surface temperatures and summer rainfall over South Africa and Namibia, *Int. J. Climatol.* **19**, 1477–1492.

Mutai, C. C. & Ward, N. M. (2000) East African rainfall and the tropical circulation/convection on intraseasonal to interannual timescales. *J. Climate* **13**, 3915–3939.

Nicholson, S. E. & Kim, J. (1997) The relationship of the El Niño-southern oscillation to African rainfall. *Int. J. Climatol.* **17**, 117–135.

Phillipon, N., Camberlin, P. & Fauchereau, N. (2002) Empirical predictability study of October–December East African rainfall. *Quart .J. Royal Met. Soc*. **128**, 2239–2256.

Rouault, M., Florenchie, P., Fauchereau, N. & Reason, C. J. C. (2003) Southeast tropical Atlantic warm events and southern African rainfall. *Geophys. Res. Lett*. **30**(5), 8009, doi: 10.1029/2002GL014840.

Torrence, C. & Compo, G. P. (1998) A practical guide to wavelet analysis. *Bull. Am. Met. Soc*. **79**, 61–78.

Trenberth, K. E. & Hoar, T. J. (1996) The 1990–1995 El Niño-Southern Oscillation event: longest on record. *Geophys. Res. Lett.* **23**, 57–60.

Trenberth, K. E. & Caron, J. M. (2000) The Southern Oscillation revisited: sea level pressure, surface temperatures and precipitation. *J. Climate* **13**, 4358–4365.

Trzaska, S., Moron, V. & Fontaine, B. (1996) Global atmospheric response to specific linear combination of the main SST modes. Part I: Numerical experiments and preliminary results. *Ann. Geophys*. **14**, 1066–1077.

Valimba, P. (2005) Rainfall variability in southern Africa, its influences on streamflow variations and its relationships with climatic variations, PhD Thesis, Rhodes University, Grahamstown, South Africa.

Wang, B. (1995) Interdecadal changes in El Niño onset in the last four decades. *J. Climate* **8**, 267–285.

Climate Variability and Change—Hydrological Impacts (Proceedings of the Fifth FRIEND World Conference held at Havana, Cuba, November 2006), IAHS Publ. 308, 2006.

Diagnóstico de probabilidades de lluvias asociados a eventos del ciclo ENOS en la costa de Ecuador

JONATHAN CEDEÑO[1], TELMO DE LA CUADRA[2], KARINA ABATA[1], MA. AUXILIADORA MERIZALDE[1] & M. PILAR CORNEJO-GRUNAUER[1]

1 *Facultad de Ingeniería Marítima y Ciencias del Mar, Escuela Superior Politécnica del Litoral, Campus "Gustavo Galindo V.", Km 30.5 Vía Perimetral, CP 09-01-4382 Guayaquil, Ecuador*
jcedeno@espol.edu.ec

2 *Laboratorio de Oceanografía, División de Investigación de Recursos Bioacuáticos y su Ambiente, Instituto Nacional de Pesca, Letamendi 102 y La Ría. CP 09-01-15131 Guayaquil, Ecuador*

Resumen Datos mensuales de precipitación de cuatro estaciones meteorológicas de la costa ecuatoriana fueron analizados usando el software WFCC y WTC, para diagnosticar probabilidades de lluvia en eventos del ciclo ENOS. En la fase cálida, las probabilidades de lluvia obtenidas fueron consistentes con la realidad, y mostraron altos valores en la FCC y el estadístico G^2; por lo que se deduce que el software trabajaría muy bien en esta fase. En el otro caso, las probabilidades de lluvia en la fase fría no fueron del todo acertadas y estuvieron limitadas a ciertas condiciones como la tendencia de lluvias, que fue cercana al promedio o mayor que este, a pesar de ser años Niña. Esto se debería a que en las series de tiempo de precipitación el menor valor es el cero, existiendo por lo tanto un sesgo hacia valores positivos.

Palabras clave tabla de contingencia; ENOS; probabilidad de lluvias; terciles, Ecuador

Assessing rainfall probabilities using ENSO cycle events on the coast of Ecuador

Abstract Monthly precipitation data from four meteorological stations located on the Ecuadorian coast were analysed, using the WFCC and WTC software, to assess rainfall probabilities during ENSO cycle events. During the warm phase, the rainfall probabilities obtained correlated with the observed data, showing high values on FCC and the statistic G^2. Therefore it is deduced that the software would work very well in this phase. However, rainfall probabilities during the cold phase did not correlate with the observed data and correlations were limited to certain conditions like the rainfall trends, that was close to the average or bigger than this, although the years in the study were Niña. This is probably a response to the fact that the smallest value is the zero, therefore introducing a bias towards positive values.

Key words contingency table; ENSO; rain probability; terciles; Ecuador

INTRODUCCIÓN

Es importante validar la utilidad y aplicabilidad de la metodología de las tabla de contingencia para aplicaciones climáticas, en la cual se basa el software "WFCC & WTC", el mismo que fue desarrollado por Alfaro *et al.* (2003) para lograr unificar la metodología usada en predicciones climáticas en América Latina dentro del proyecto *Una Propuesta Especial para mejorar los Foros de Perspectiva Climática en América Latina*, financiado por la Oficina de Programas Globales de la Administración Nacional para la Atmósfera y el Océano (OGP-NOAA) en conjunto con la Universidad de Costa Rica y el Laboratorio de Meteorología y Oceanografía del Atlántico (AOML) de la NOAA. En este estudio, se propone utilizar el software en modo de diagnóstico para tres eventos El Niño y tres La Niña en cuatro puntos de la costa ecuatoriana.

DATOS

Para el diagnóstico de lluvias se utilizó datos mensuales de precipitación en milímetros, pertenecientes a cuatro estaciones meteorológicas de la costa ecuatoriana manejadas por el Instituto Nacional de Meteorología e Hidrología (INAMHI). (ver Tabla 1 y Fig. 1), datos que corresponden a variables dependientes en el WFCC & WTC. Los índices utilizados como predictores (o variables independientes) fueron: el Índice Multivariado de ENOS (MEI), Niño 3.4, Niño 3 y Niño 1+2 (Fig. 2). Una descripción completa de estos índices puede ser obtenida en Wolter & Timlin (1993) y Glantz (1996).

Copyright © 2006 IAHS Press

Tabla 1 Estaciones empleadas en este estudio y características de las series de tiempo de las mismas. Fuente: INAMHI.

Estación (nombre)	Ubicación	Altura (msnm)	Longitud de la serie	Datos perdidos (%)
Boyacá	00º34′07″S 80º12′20″W	370	1964–1998	22.38
Chone	00º39′26″S 80º02′30″W	40	1962–1998	9.23
Machala	03º16′00″S 79º57′31″W	25	1973–1999	7.72
Milagro	02º06′56″S 79º35′57″W	13	1950–1998	2.04

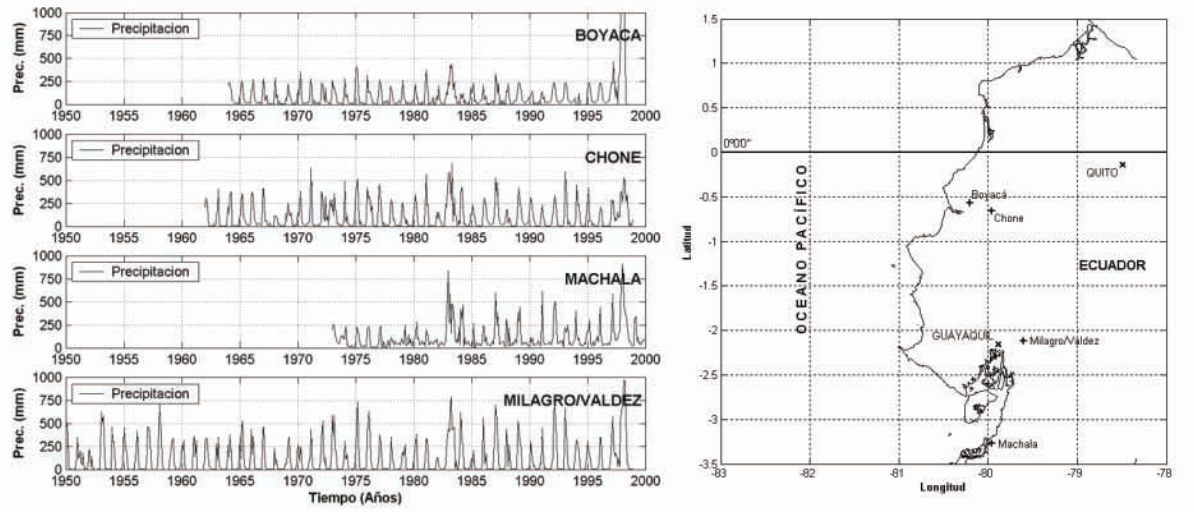


Fig. 1 Series de tiempo para cada una de las estaciones en estudio (izq.) y ubicación geográfica de las estaciones meteorológicas utilizadas en este estudio (der.) Fuente: INAMHI.

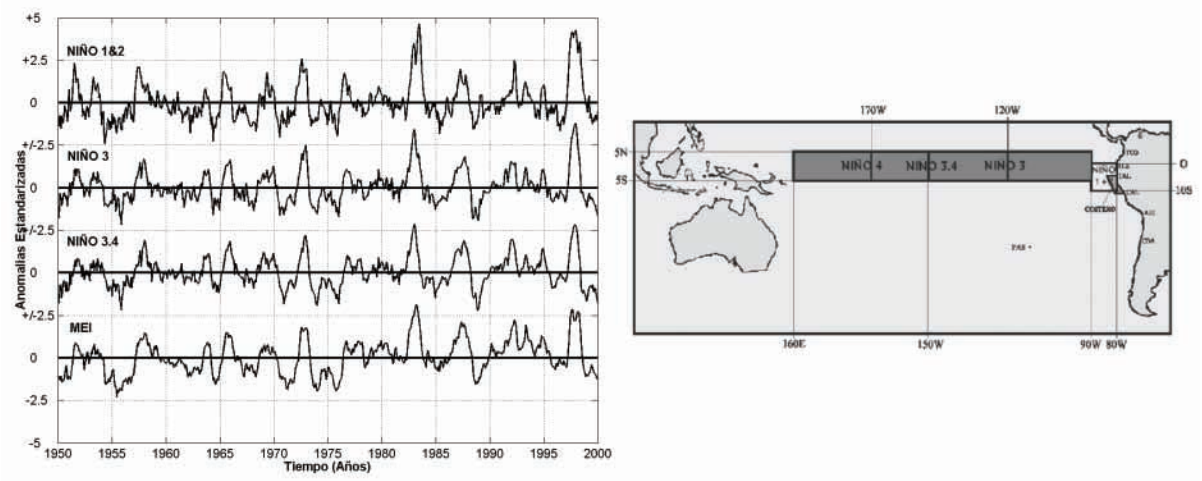


Fig. 2. Índices Climáticos utilizados como variables independientes (izq.) y regiones correspondientes a los índices Niño 3.4, Niño 3 y Niño 1+2 (der.). Fuente: NOAA.

METODOLOGÍA

El software de la Tabla de Contingencia (Alfaro *et al.*, 2003) comprende dos programas cuyo principal objetivo es el análisis cuantitativo y categórico de dos variables usando la teoría de los terciles. El primer programa (WFCC) es el que realiza la correlación cruzada sesgada entre dos variables, además de permitir escoger el predictor apropiado. Para este estudio se resolvió diagnosticar las probabilidades de lluvia en el trimestre diciembre–enero–febrero (DEF) dada las condiciones en el trimestre previo septiembre–octubre–noviembre (SON). El segundo programa (WTC) permite establecer una validación cruzada, que contrasta el comportamiento de los datos, producto de un diagnóstico con respecto a los datos observados; además de realizar el análisis exploratorio entre dos variables que se suponen correlacionadas positiva o negativamente en el tiempo.

Los principales estadísticos que evalúan el grado de asociación entre las parejas de los dos conjuntos de datos son la FCC (Función de Correlación Cruzada), el ensayo de significancia y el G^2. El FCC cuantifica la relación o el comportamiento común entre las variables independiente y dependiente. Si los valores estimados de FCC exceden los niveles de significación, entonces se rechaza la hipótesis nula (esto es, las series no están correlacionadas) y se acepta la hipótesis alternativa (las series están correlacionadas, Alfaro *et al.*, 2003). El WFCC calcula niveles de confianza al 90 y 95%. El G^2 evalúa que tanto se aleja una tabla de contingencia del caso aleatorio. Cuando las variables independientes y dependientes están asociadas positivamente, el G^2 obtiene valores altos y la significación tiende a uno que es el valor máximo posible.

Para comprobar si el total de lluvias en el trimestre seleccionado (DEF) responde a las condiciones de cada uno de los eventos ENSO estudiados, se procedió a calcular el cociente entre la sumatoria tri-mensual de lluvias y la sumatoria de la media inter-anual correspondiente a esos meses. Debido a que existe un sesgo hacia valores de lluvias por sobre el promedio, se resolvió aceptar la "normalidad" de este cociente entre 0.8 y 1.20. Valores por debajo de 0.8 indicarían déficit de lluvias con respecto a la normal y por sobre 1.20, superávit de lluvias. Así mismo, se calculó el cociente entre la sumatoria tri-mensual de lluvias y la sumatoria correspondiente a los meses DEF de una desviación estándar. Generalmente, un máximo sobre una desviación estándar es visto en años El Niño debido probablemente a la respuesta de los regímenes de lluvias durante el verano del hemisferio del sur (Marcos & Cornejo, 2005).

El porcentaje de acierto se obtuvo a través del análisis de los niveles de significancia de la FCC. Si el resultado es estadísticamente significativo, se le asigna un valor de 8.33, resultado de la división entre 100 (porcentaje total) y 12 (número de corridas por fase del ciclo ENOS para cada uno de los índices).

RESULTADOS

Análisis del campo de precipitación

El ciclo anual es el modo dominante de la variabilidad en la costa del Ecuador (Cornejo, 1999; Silva, 1990). La Fig. 3 registra claramente este ciclo anual. En términos generales, la estación lluviosa ocurre entre enero y abril y la seca entre mayo y diciembre (Marcos & Cornejo, 2005). Los rangos del ciclo anual oscilan entre 226 mm (Boyacá), 292 mm (Chone), 214 mm (Machala) y 335 mm (Milagro).

Durante los años El Niño descritos en este estudio, se observa que los regímenes de precipitación comienzan más temprano y terminan más tarde. El caso más extremo se dio en el 1997/1998, en donde las lluvias comenzaron en septiembre y se prolongaron hasta mayo–junio. Durante el trimestre DEF todos los casos de eventos El Niño en las estaciones aquí descritas se ubican por sobre la media y excepto en la estación Boyacá, cuya precipitación fue encontrada sobre una desviación estándar.

Para eventos La Niña, el campo de precipitación es muy cercano al ciclo anual en forma general. Los casos más deficitarios en el trimestre DEF se dieron en Machala y Milagro durante el año 1985. En los años 1975 en Boyacá y Chone, y del 1989 en Milagro, se presentaron valores de precipitación por encima de la media, aún cuando lo esperado son lluvias deficitarias.

Diagnóstico de probabilidades de lluvias en años del ciclo ENSO

Evento El Niño 1982–1983 En las estaciones Boyacá y Machala las probabilidades de lluvias para el período DEF fueron acertadas con todos los índices (50% y 67% por sobre lo normal–SN–, respectivamente), pero no estadísticamente significativas. En Chone, a pesar que la precipitación durante el trimestre DEF fue de 1.62 veces la desviación estándar, las probabilidades más altas estuvieron repartidas en los terciles normal (N) y SN en las corridas con todos los índices, excepto con el MEI, cuya probabilidad más alta se ubica en el tercil N. Milagro obtuvo probabilidades del 50% SN para los índices Niño 3, Niño 3.4 y Niño 1+2, significantes al 95% (excepto con el índice Niño 1+2). Distinto fue el caso al trabajar con el MEI, ya que este no diagnosticó lluvias por SN. El índice que mejor trabajó para el diagnóstico de lluvias de este año fue el Niño 3, ya que tuvo los mayores valores de FCC de todos los índices utilizados.

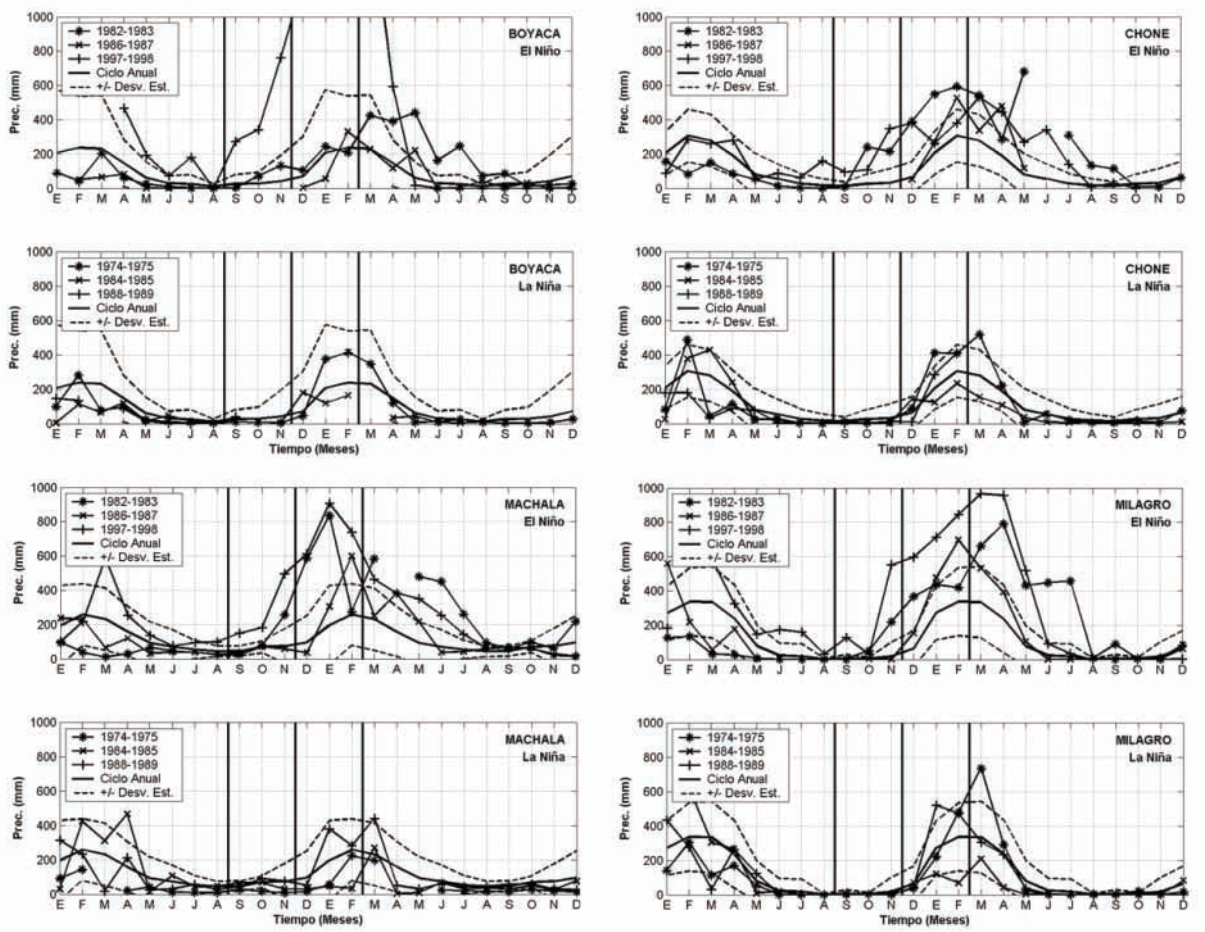


Fig. 3 Régimen de Precipitación durante tres años Niño y tres años Niña para todas las estaciones en estudio. Fuente: INAMHI.

Evento El Niño 1986–1987 Debido a la falta de datos en las series de tiempo de precipitación en el trimestre SON, no es posible diagnosticar probabilidades de lluvia en las estaciones Boyacá y Chone. Para las estaciones Machala y Milagro, el modelo arrojó probabilidades de lluvia SN, significantes al 90% en la mayoría de los casos y al 95% al trabajar con el índice Niño 3 para la estación de Milagro. Para la estación Machala, observamos que consistentemente los valores de G^2 son menores que los de Milagro cuando se ejecutan corridas con todos los índices para estas estaciones, pese a que el diagnóstico si se ajustó a la realidad. Esto se debería a que el registro de datos es menor en comparación con el resto de estaciones. Los mejores predictores para este período de lluvias son los índices Niño 3 y Niño 3.4.

Evento El Niño 1997–1998 En todas las estaciones llovió por sobre una desviación estándar, resultados que se vieron reflejados en las corridas del modelo (superior al 50% SN, significantes al 95%), mostrando coherencia con el régimen de lluvias. Resultados mixtos se obtuvieron con la estación Machala, ya que con los índices Niño 3, Niño 3.4 y Niño 1+2 las lluvias no pudieron ser diagnosticadas ya que la mayor probabilidad de lluvia recayó sobre el tercil N. Con el MEI, la probabilidad de lluvia fue del 50% SN, con una FCC de 0.50, significante al 95%.

Evento La Niña 1975 Pese a que 1975 es considerado como un año Niña, en las estaciones Boyacá, Chone y Milagro llovió ligeramente por sobre el promedio histórico de lluvias (1.62, 1.58 y 1.10 veces, respectivamente para el trimestre DEF). La salida del modelo reflejó estas condiciones para con todos los índices, ya que las probabilidades más altas se encuentran en el tercil N; no obstante los valores de FCC fueron bajos en algunos casos y negativos en otros (no significantes ni al 90%). Para la estación Machala, no se obtuvo un resultado consistente a la realidad. Las salidas contradictorias obtenidas se deben a corta longitud de la serie de tiempo (ver Tabla 1).

Evento La Niña 1985 Las lluvias durante el trimestre DEF del 84/85 se presentaron por debajo de la media histórica para Machala y Milagro (0.20 y 0.38) y muy cercano al promedio en Boyacá y Chone (0.90 y 0.87). Durante las corridas del programa, observamos que las mayores probabilidad de lluvias se encontraron en el tercil N para todas las estaciones, lo cual se ajusta a la realidad únicamente para Boyacá y Chone. El mayor porcentaje de acierto lo obtuvo las corridas con el índice Niño 3, a pesar de que en Machala y Milagro fallara el diagnóstico. En la estación Chone hubo resultados mixtos, ya que en las corridas con los índices MEI y Niño 1+2 la mayor probabilidad de lluvias fue de 50% bajo el tercil BN (bajo lo normal), significante al 90% solo con el Niño 1+2. Con el índice Niño 3.4, la probabilidad más alta en esta estación y en Boyacá se encontró en el tercil N, siendo coherente con la comprobación trimestral.

Evento La Niña 1988–1989 Durante las corridas, los porcentajes de probabilidades de lluvias más altos se encontraron bajo el tercil N; esto fue corroborado para las estaciones Chone, Machala y Milagro, donde los valores de precipitación acumulada en DEF son muy cercanos a una desviación estándar. Los valores de la FCC no lograron ser significantes ni al 90% en gran parte de los casos (solo en Chone con los índices Niño 1+2 y Niño 3; y Milagro con el Niño 3), por lo que se deduce que las series no se encuentran bien correlacionadas. Para el caso de Boyacá, hubo insuficiencia de datos de precipitación en el año utilizado como terminal para el diagnóstico de lluvias (1988).

CONCLUSIÓN Y DISCUSIÓN

Las salidas del modelo mostraron que los resultados del diagnóstico se ajustan a la realidad durante las corridas en años Niño (EN). Los porcentajes de aciertos al 90% y 95% de confianza se ubicaron en 83.33% y 58.33% respectivamente durante las corridas con el índice Niño 3, el cual resultó ser el mejor predictor para las estaciones en estudio. El porcentaje de aciertos más bajo lo obtuvo el índice MEI (Tabla 2).

Tabla 2 Porcentaje de aciertos de las corridas con referencia a las correlaciones existentes entre las series de datos (índices *vs* precipitación) y su significancia al 90% y 95% para los eventos de El Niño estudiados (1983, 1987 y 1998).

Estación	% De aciertos parciales (90%)				% De aciertos parciales (95%)			
	NIÑO 3.4	NIÑO 3	NIÑO 1+2	MEI	NIÑO 3.4	NIÑO 3	NIÑO 1+2	MEI
Boyacá	8.33	8.33	8.33	8.33	8.33	8.33	8.33	0.00
Chone	16.67	25.00	25.00	16.67	8.33	16.67	8.33	8.33
Machala	16.67	25.00	16.67	8.33	8.33	8.33	8.33	8.33
Milagro	25.00	25.00	8.33	8.33	8.33	25.00	8.33	8.33
% Total de aciertos	66.67	**83.33**	58.33	41.67	33.33	**58.33**	33.33	25.00

Tabla 3 Porcentaje de aciertos de las corridas con referencia a las correlaciones existentes entre las series de datos (índices *vs* precipitación) y su significancia al 90% y 95% para los eventos de La Niña estudiados (1975, 1985 y 1989).

Estación	% De aciertos parciales (90%)				% De aciertos parciales (95%)			
	NIÑO 3.4	NIÑO 3	NIÑO 1+2	MEI	NIÑO 3.4	NIÑO 3	NIÑO 1+2	MEI
Boyacá	0.00	0.00	0.00	0.00	0.00	0.00	0.00	0.00
Chone	0.00	16.67	16.67	0.00	0.00	0.00	0.00	0.00
Machala	0.00	8.33	8.33	0.00	0.00	0.00	0.00	0.00
Milagro	8.33	16.67	0.00	0.00	0.00	8.33	0.00	0.00
% Total de aciertos	8.33	**41.67**	25.00	0.00	0.00	**8.33**	0.00	0.00

En la fase fría del ENOS los resultados obtenidos no fueron buenos. El sesgo que existe hacia valores positivos que marcan una tendencia por sobre el promedio en las series de precipitación es

un factor determinante a la hora de diagnosticar y pronosticar probabilidades de lluvias bajo los terciles N y BN. Al 95% de confianza, el porcentaje de aciertos se ubicó en cero para todos los índices trabajados con excepción del Niño 3 (8.33%, ver Tabla 3). Hay que anotar también que no siempre los predictores utilizados explican el régimen de precipitación de manera consistente, en especial cuando se analiza los años "Niña", en donde se espera que hayan lluvias deficitarias en las estaciones en estudio.

Otra posible causa de la diferencia entre los resultados de corridas con el programa WFFC y WTC para las fases extremas de ENSO es la no-linealidad de las relaciones entre los parámetros oceánicos-atmosféricos estudiados, tal como la anota Hoerling *et al.*, 2001; Larkin & Harrison, 2002 y Hoerling *et al,* 1997. A través de un análisis exploratorio de correlaciones entre las variables observadas, pudimos anotar que no necesariamente las variaciones entre ellas son lineales, por lo que la asunción de la no-linealidad inherente nuevamente queda en discusión.

Espacialmente, es probable que la diferencia de resultados entre las estaciones de Machala, Chone y Milagro se deba a condiciones océano-atmosféricas locales, ya que Chone esta afectada más por variaciones en la posición del frente ecuatorial y por diferencias orográficas que Machala y Milagro. En cuanto a la estación de Boyacá, el estado de la serie de tiempo provocó que tuviera el menor porcentaje de aciertos debido a que acumuló el mayor porcentaje de datos perdidos de entre las estaciones estudiadas (ver Tabla 1).

Estos resultados son de particular importancia, ya que demuestra que el programa WFCC & WTC, que es utilizado para predecir probabilidades de lluvia en diversas regiones de Latinoamérica incluido el Ecuador, pronostica escenarios de precipitación SN de manera óptima. En escenarios BN, la probabilidad de aciertos es baja, más aún si se toma en cuenta los estadísticos que la corrida del propio programa genera como medida de confianza del pronóstico previo a su difusión.

Agradecimientos Los autores agradecen a David Enfield y Eric Alfaro por sus comentarios y sugerencias al manuscrito final. La presente investigación fue realizada con el soporte del Proyecto Cuatro del Programa VLIR-ESPOL y de la Fundación de Ciencia y Tecnología del Ecuador FUNDACYT.

REFERENCIAS

Alfaro, E., Soley, F. & Enfield, D. (2002) Guía para el uso de una Tabla de Contingencia para Aplicaciones Climáticas. Ed. por FUNDESPOL-ESPOL, Guayaquil.

Cornejo, M. P. (1999) Variaciones Estacionales e Interanuales de la Climatología en la Zona Costera del Ecuador. *Reporte Técn. FIMCM-ESPOL*. Guayaquil.

Glantz, M. H. (1996) Currents of Change: El Niño's Impact on climate and society. Cambridge University Press, Cambridge, UK.

Hoerling, M. P., Kumar, A., Xu, T. (2001) Robustness of the nonlinear climate response to ENSO's extreme phases. *J. Climate* **14**, 1277–1293.

Hoerling, M. P., Kumar, A., Zhong, M. (1997) El Niño, La Niña and the non-linearity of their teleconnection. *J. Climate* **10**, 1769–1786.

Larkin, N. K. & Harrison, D. E. (2002) ENSO warm (El Nino) and cold (La Nina) event life cycles: Ocean surface anomaly patterns, their symmetries, asymmetries, and implications. *J. Climate* **15**, 1118–1140.

Marcos, J. G. & Cornejo, M. P. (2005) Adaptation Strategies to the Environmental and Socioeconomic Impacts of El Niño for Rural Communities in Ecuador and Peru. *Report of Community Assessments in Ecuador. ESPOL*, Guayaquil.

Silva, G. (1992) Análisis de la variabilidad climática de la zona costera ecuatoriana utilizando Componentes Principales. Tesis de Grado de Oceanografía. FIMCM-ESPOL, Guayaquil

Wolter, K. & Timlin M.S. (1993). Monitoring ENSO in CODAS with a seasonally adjusted principal components index. *Proc. of the 17th Climate Diagnostic Workshop, Norman, OK*. NOAA/ MC/CAC, NSSL, Oklahoma, USA.

Climate Variability and Change—Hydrological Impacts (Proceedings of the Fifth FRIEND World Conference held at Havana, Cuba, November 2006), IAHS Publ. 308, 2006.

GCM and downscaling uncertainty in modelling of current river flow: why is it important for future impacts?

CHRISTEL PRUDHOMME
Centre for Ecology and Hydrology, Wallingford, Oxfordshire OX10 8BB, UK
c.prudhomme@ceh.ac.uk

Abstract This paper compares the uncertainty in flow simulation due to the modelling of precipitation (using three global circulation Models, GCMs, and two downscaling techniques) with the current natural flow variability in three catchments in Scotland. The reference daily flow series, obtained by running a calibrated continuous rainfall–runoff model with observed catchment rainfall and potential evaporation, is compared with simulations from a range of different precipitation scenarios, representative of the climate modelling uncertainty and current natural variability. Results show that the natural variability can be large and differs from one catchment to another. The reproduction of climate variability from different GCMs is not always within this natural variability and there is some regional variation in the GCMs' and downscaling techniques' ability to reproduce the current climate. The uncertainty due to GCMs is consistently larger than that of downscaling techniques.

Key words climate change impact; downscaling; GCM; RCM; SDSM; uncertainty

INTRODUCTION

Climate change impact studies on water resources focus on quantifying changes between current flow and simulations using scenarios of future climate. Climate scenarios are generally provided by global climate models (GCMs), based upon the fundamental laws of physics and are at present the best and most robust tools for assessing the response of the climate system to changes in radiative forcing. However, the ability of the GCMs to reproduce current climate is rarely assessed despite their known deficiencies (e.g. Hulme *et al*., 1999). A number of limitations affect GCMs, including their limited spatial detail, that prevent GCMs from successfully simulating short time scale variability. Techniques that downscale GCM outputs to scales appropriate for climate change impacts assessments, such as dynamical and statistical techniques (e.g. Wilby *et al*., 1998; Trigo & Palutikof, 2001), have been developed to fill this gap. This paper describes a methodology to assess current climate variability from GCMs and downscaling methods and illustrates how to define the significance of potential bias.

METHODOLOGY

Estimation of natural climate variability

Maritime climates such as observed in the British Isles are extremely variable at all scales, with inter-annual climatic variability particularly significant (Wheeler & Mayes, 1997). A simple methodology of block resampling with replacement is used to define natural climate variability in this paper. The resampling procedure randomly selects 3-month blocks from the original series (respecting the annual sequences) to create a new series of equal length. This use of observed data avoids any systematic bias which could otherwise exist (Arnell, 2003). Here, 99 new series were produced, providing a set of 100 scenarios including the observed series. Natural variability is shown in grey in the figures. The same methodology was used to create GCMs and RCMs (Regional Climate Model) scenarios.

Global climate models

The outputs from the following three GCMs were selected for the availability of their simulations at the daily time scale[1]: HadCM3 from the Hadley Centre for Climate Prediction Research (Met. Office, UK), CGCM from the Canadian Centre for Climate Modelling and Analysis (CCCMA, Canada), and CSIRO-mk2 from the Commonwealth Science & Industrial Research Organisation

[1] Data available from the IPCC Data Distribution Centre gateway http://ipcc-ddc.cru.uea.ac.uk/

Copyright © 2006 IAHS Press

(CSIRO, Australia). Here, GCMs ability to simulate current climate variability is only assessed through the analysis of river flows.

Downscaling techniques

Two downscaling methodologies were considered: dynamical downscaling, based on physical/ dynamical links between the climate at the large scale and at smaller scales; and statistical downscaling, that uses empirical relationships between large-scale atmospheric variables and observed daily local weather variables (e.g. rainfall). Sensitivity to downscaling techniques was only considered for rainfall series (Potential Evapotranspiration (PE) series are the resampled observed series).

Statistical downscaling: the model used here, Statistical DownScaling Model (SDSM)[2], is a hybrid between regression-based and stochastic weather generation techniques (Wilby *et al*., 2002). NCEP/NCAR re-analysis data[3] were used to identify the best variables to predict daily rainfall and to calibrate the models. Twenty separate runs were made for each GCM, thus providing some element of climate variability for the current time horizon (1961–1990). A block resampling produced five resampled series for each run, thus totalling 100 resampled series for each GCM.

Dynamical downscaling of data from the Hadley Centre's Regional Climate Model, HadRM3H was used as an example of dynamical downscaling. HadRM3 is driven directly from the HadCM3 simulations and was developed to provide spatially-detailed scenarios over Europe. The daily output series for the 1961–1990 time horizon were block-resampled to produce 100 series representative of the HadRM3 current climate variability. Dynamically downscaled outputs of the two other GCMs were not available to us and thus could not be analysed.

Construction of scenarios

Reference value and calculation of changes Reference values are derived from daily flow series simulated with observed rainfall and PE, to eliminate bias due to hydrological model errors. For each flow series simulated from a different scenario, the mean monthly flow was calculated and the difference with the reference value expressed as a percentage.

Uncertainty For a given month, the uncertainty is represented by the range comprising 90% of the simulated monthly flow (or 90% Confidence Interval CI) using the 5% and the 95% points of the 100-resampled scenarios from the same technique, either the combination of GCM and down-scaling method (whisker boxes in Figures) or 100-resampled observed series (natural variability).

DATA AND HYDROLOGICAL MODEL

Case study and data

The methodology is applied to three catchments in Scotland so that regional characteristics can be explored (Fig. 1). The Feugh and the Eden are located in the eastern part of the Grampian and Fife regions and have a mixed regime with responsive flows but significant baseflows. The White Laggan Burn is a very small catchment in Galloway exposed to high annual rainfall typical of western Scotland. It has a very responsive regime characterized by a low base flow index (BFI) (Table 1). River flow data were obtained from the UK National River Flow Archive maintained by the Centre for Ecology and Hydrology. Catchment average daily precipitation time series were derived using the UK Meteorological Office daily rainfall library and a simplified version of the Triangular Planes interpolation method described by Jones (1983). PE data were obtained from the Meteorological Office Rainfall and Evaporation Calculation System (MORECS) database (Holmes *et al*., 2002).

Hydrological model

The hydrological model used is based on the Probability Distributed Model theory (Moore, 1985) that represents the catchment soil storage capacity as a probability distribution and has two

[2] SDSM can be downloaded at https://co-public.lboro.ac.uk/cocwd/SDSM/IDLogin.html
[3] http://www.cdc.noaa.gov/cdc/reanalysis/reanalysis.shtml

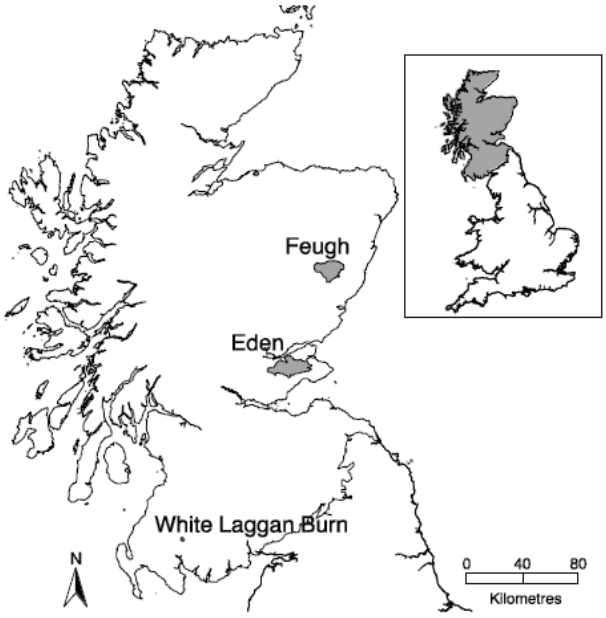


Fig. 1 Location of case study catchments.

Table 1 Case study catchments and their characteristics under current climatic conditions (from Marsh & Lees, 2003).

NWA ID	River	Station	Area (km^2)	Short description	BFI	Mean annual rainfall (mm)
12008	Feugh	Heugh Head	229	Rugged topography, moorland and pasture, granites and metamorphic rocks.	0.45	1151
14001	Eden	Kemback	307	Gently sloping, arable, sandstone, igneous and carboniferous limestone.	0.62	806
80003	White Laggan Burn	Loch Dee	6	Rugged upland with 20% forest. Granite shales and greywackes	0.19	2670

second-order linear routing reservoirs simulating quick and slow flows. The model includes an interception storage term and a soil-moisture related drainage term and has five free parameters for calibration (Young, 2006). Uncertainties due to hydrological modelling are not discussed in this paper.

RESULTS

Reproduction of climate variability by GCMs: GCM uncertainty

Potential bias in reproducing climate variability within a GCM is assessed by comparing the range in river flows simulated from SDSM-derived scenarios with that of natural variability. For the three catchments and three GCMs, the majority of the interannual variability of river flow (as described by the mean monthly flow) is reproduced with a systematic bias (Fig. 2). The box plots, representing the variation captured by the climate variability of the GCM and SDSM combination, are most often on either side of the reference line, showing an overestimation (respectively, underestimation) when boxes are entirely above (resp., below) the reference value (dashed line). However, when considered in context of the natural current climate variability, only a few of these systematic biases are significant, as illustrated by CI within the grey areas.

HadCM3 generates arguably the least biased simulations of the three GCMs with the range of monthly river flow within the expected current natural variability for most of the year. However, this is not true for the Eden in summer (June to August). CSIRO-mk2 and CGCM2 both show deficiencies in reproducing current climate variability. For example, significant biases are observed using CGCM2 in summer months (underestimation) for all three sites and to a lesser extent in winter (overestimation) for the Feugh and Eden. Results using CSIRO-mk2 do not show consistent seasonal bias pattern across the region, winter flows being overestimated in the Feugh and Eden but not in White Laggan Burn, while spring flows are overestimated in the Eden and

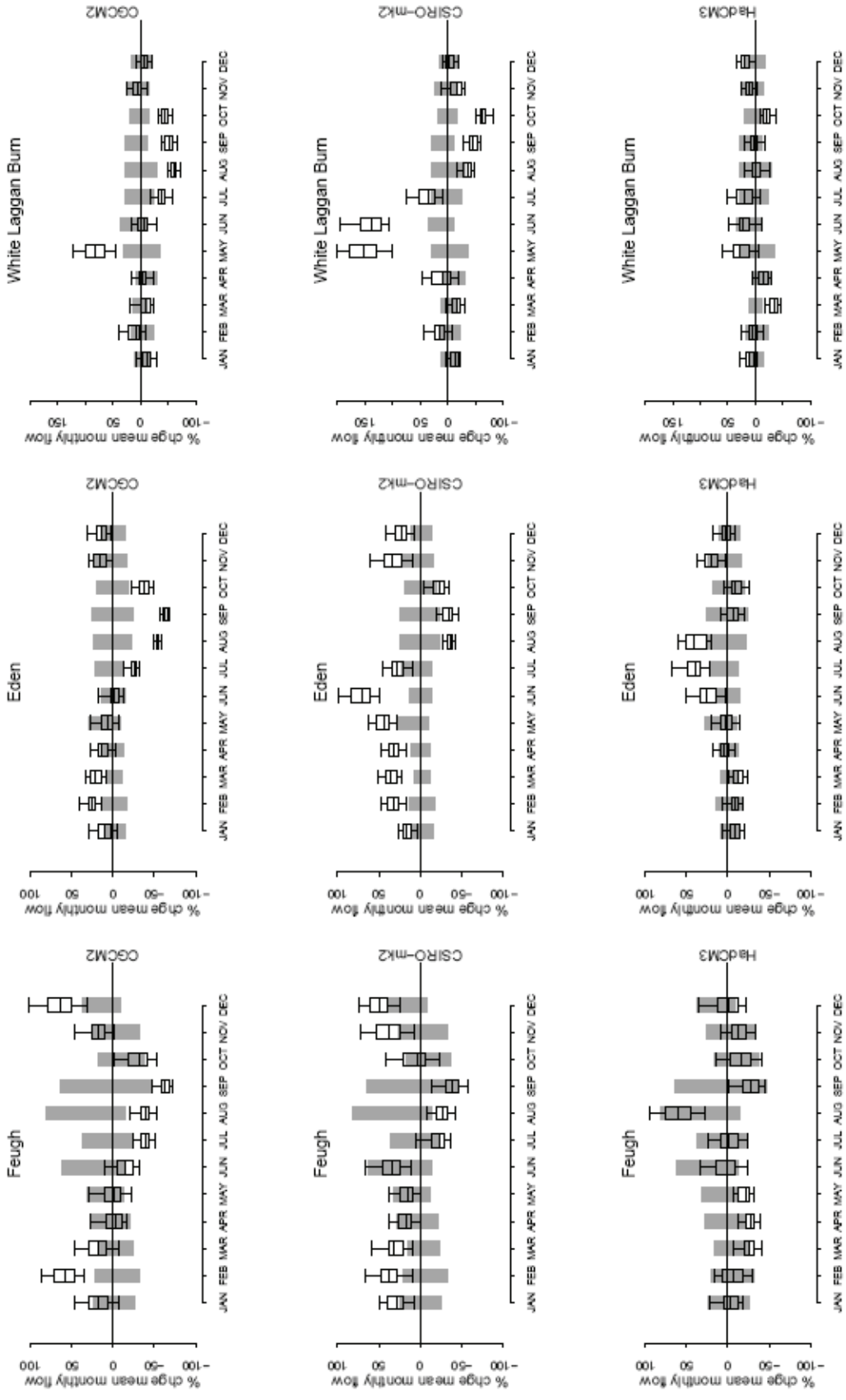


Fig. 2 Reproduction of climate variability by GCMs: monthly river flow confidence intervals from SDSM-downscaled outputs from HadCM3 (top line), CSIRO-mk2 (middle line) and CGCM2 (bottom line) for the Feugh (left), Eden (middle) and White Laggan Burn (right). Grey areas are 90% confidence intervals of current natural variability; Box plots show (from bottom to top) the 5th, 25th, 50th, 75th and 95th percentiles of the 100 simulated series.

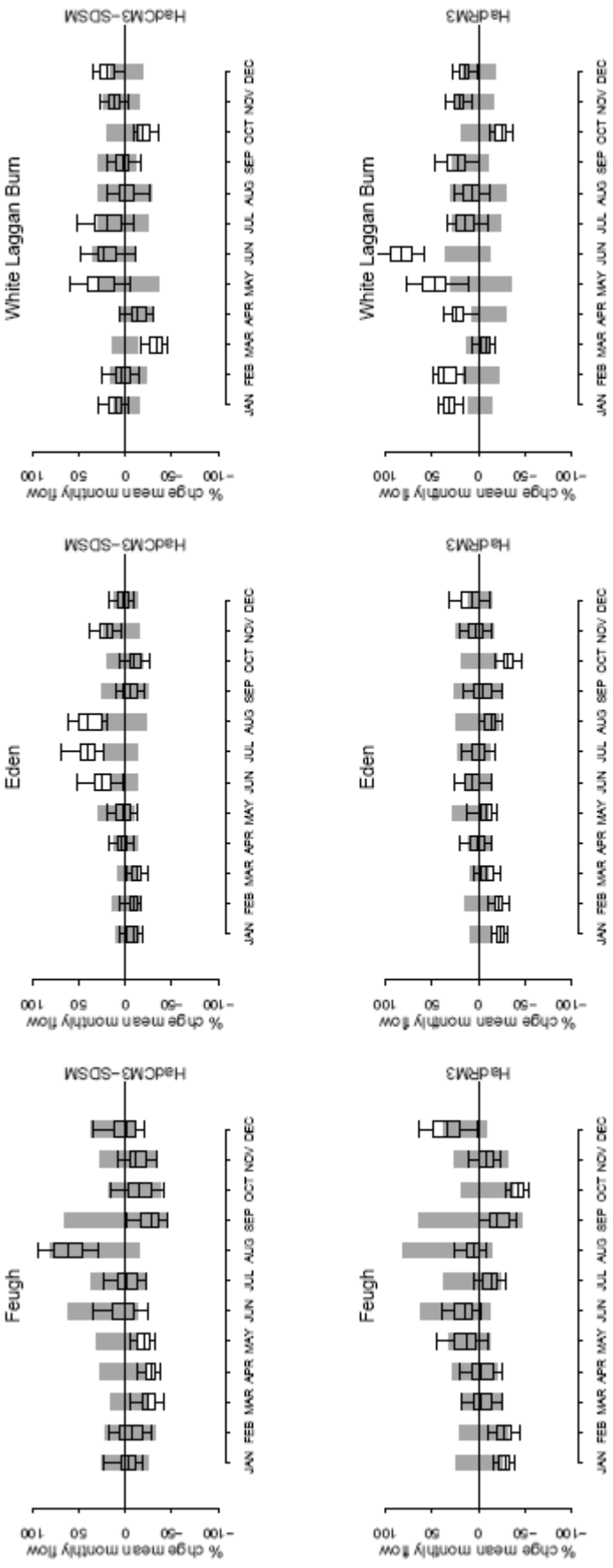


Fig. 3 Sensitivity to downscaling techniques: monthly river flow confidence intervals from HadCM3 outputs downscaled using SDSM (top line) and RCM (bottom line) for the Feugh (left), Eden (middle) and White Laggan Burn (right). Grey areas are 90% confidence intervals of current natural variability; Box plots show (from bottom to top) the 5th, 25th, 50th, 75th and 95th percentiles of the 100 simulated series.

White Laggan Burn, but not the Feugh. Summer flows tend to be underestimated for all sites, but not by the same magnitude in the same months. The ability of GCMs to reproduce correctly current climate variability is not the only factor linked to the results presented in this section. The quality of fit of the SDSM equations and the presence of unusual events in the observed series are elements that could affect the reproduction of the current climate variability and subsequent river flow regime.

Sensitivity to downscaling technique

Sensitivity to downscaling techniques is based on comparing flow series using the 100 resampled scenarios from GCM outputs either downscaled using SDSM, or using the HadRM3 RCM model. The use of two downscaling techniques introduces some uncertainty: the presence or significance of bias is not always similar when the HadCM3 outputs are downscaled with SDSM or through HadRM3 (Fig. 3). For example, SDSM leads to significant overestimation of summer flows (June to August) in the Eden, while river flows remain within the natural variability when using HadRM3. In the White Laggan Burn, winter flows are significantly overestimated when generated using HadRM3 but not when using SDSM-downscaled outputs. Results in the Feugh show similar ranges from both techniques for most of the year (only spring flows are underestimated with SDSM). From the limited sample, no one technique shows better results or any apparent systematic bias for any season. This highlights the difficulty in developing a general methodology that fits all, and uncertainty to downscaling methodology should be considered on a case-by-case basis.

CONCLUSION

The results presented here are from a very limited sample of three catchments in Scotland, three GCMs and two downscaling methodologies, and are not a comprehensive assessment of the skills of GCMs in general or these GCMs in particular. However they illustrate important generic problems arising from the use of GCM outputs in impact assessment. Regional variation in GCM uncertainty is apparent (e.g. Feugh and Eden) and the results are thus only valid for individual catchments and cannot be generalized even at the regional level. Each GCM reproduces the current hydrological regime with variable ability and no GCM was shown to be significantly better nor to have a systematic seasonal bias smaller than the others. Additional uncertainty due to downscaling exists and varies in magnitude from one catchment to another. Despite its flexibility of use, SDSM was found to perform neither better nor worse than HadRM3. Uncertainty due to GCMs, however, is consistently larger than that of downscaling techniques for all three test sites. The existence of a significant bias in reproducing current natural variability and subsequent river flow variations was only assessed from changes in the rainfall series. For a complete sensitivity analysis, biases in modelled PE should be compared with errors introduced by the hydrological modelling.

It is essential that any systematic bias is understood when interpreting the potential impact of climate change as such biases are likely to transfer to the simulations of future flows. Comparing future projections with reference values may result in misleading conclusions if the existing bias in the modelling of the current climate is ignored. While GCMs remain the best tool for providing future water resource scenarios, assessing and allowing for their limitations is a challenge for the hydrology community in particular, and climate change impact researchers in general.

Acknowledgements These results are part of a research study funded by the Environment Agency for England and Wales and the UK Water Industry Research (UKWIR). The SDSM scenarios were produced by Dr T. Osborn and C. McSweeney (Climate Research Unit, University of East Anglia, UK). The HadRM3 data were provided by Dr R. Jones (Hadley Centre, UK Met Office). The hydrological model was developed and calibrated by Dr A. Young, and the map produced by H. Davies. They are gratefully acknowledged.

REFERENCES

Arnell, N. W. (2003) Relative effects of multi-decadal climatic variability and changes in the mean and variability of climate due to global warming: future streamflows in Britain. *J. Hydrol.* **270**, 195–213.

Holmes, M. G. R., Young, A. R. & Sekulin, A. E. (2002) Derivation of climatic data sets. R&D Technical report no. 5 to the Environment Agency. Centre for Ecology and Hydrology, Wallingford, UK.

Hulme, M., Mitchell, J., Ingram, W., Lowe, J., Johns, T., New, M. & Viner, D. (1999) Climate change scenarios for global impacts studies. *Global Environ. Change: Human & Policy Dimensions* **9**, S3–S19.

Jones, S. B. (1983) *The Estimation of Catchment Average Point Rainfall Profiles*. Institute of Hydrology Report 87, Wallingford, UK.

Marsh, T. J. & Lees, M. L. (eds) (2003) *Hydrological Data UK – Hydrometric Register and Statistics 1996–2000.* Centre for Ecology and Hydrology, Wallingford, UK.

Moore, R. J. (1985) The probability-distributed principle and runoff production at point and basin scales. *Hydrol. Sci. J.* **30**, 273–297.

Trigo, R. M. & Palutikof, J. P. (2001) Precipitation scenarios over Iberia: a comparison between direct GCM output and different downscaling techniques. *J. Climate* **14**, 4422–4446.

Wheeler, D. & Mayes, J. (1997) *Regional Climates of the British* Isles. Routledge, London, UK.

Wilby, R. L., Dawson, C. W. & Barrow, E. M. (2002) SDSM – a decision support tool for the assessment of regional climate change impacts. *Environmental Modelling & Software* **17**, 145–157.

Wilby, R. L., Wigley, T. M. L., Conway, D., Jones, P. D., Hewitson, B. C., Main, J. & Wilks, D. S. (1998) Statistical downscaling of general circulation model output: a comparison of methods. *Water Resour. Res.* **34**, 2995–3008.

Young, A. R. (2006) Stream flow simulation within UK ungauged catchments using a daily rainfall-runoff model. *J. Hydrol.* **320**, 155–172.

Climate Variability and Change—Hydrological Impacts (Proceedings of the Fifth FRIEND World Conference held at Havana, Cuba, November 2006), IAHS Publ. 308, 2006.

The impacts of climate change on water resources in the Okavango basin

SONJA FOLWELL & FRANK FARQHUARSON
Centre for Ecology and Hydrology, Crowmarsh Gifford, Wallingford, Oxfordshire OX10 8BB, UK
ssf @ceh.ac.uk

Abstract The need for coherent river basin management plans has become a driving force behind the use of models in understanding how basin hydrology will be affected by change. Of particular interest is how water availability will be affected by climate change and by growing demands for a finite resource. The Okavango basin, located in sub-Saharan Africa is a large, endorheic basin with the river terminating in the vast expanse of the ecologically important Okavango delta. It is also a transboundary basin transecting Angola, Namibia and terminating in Botswana. The end of the Angolan civil war has brought stability and development to the region. With increasing abstractions, due to human development, and possible reductions in available water, due to changing rainfall and evaporation patterns, flows entering the delta will be altered. Considering these possibilities a grid-based model has been used to examine current and future water availability and flows entering the delta system.

Key words water resources; climate change impacts; Okavango basin

INTRODUCTION

The Okavango is a transboundary river basin located in central southern Africa (Fig.1). It has a hydrologically active area of 390 000 km^2 extending from the arid climate of northeast Namibia to the subtropical Angolan highlands which receive an annual rainfall in excess of 1200 mm. The river rises in the Angolan highlands draining south and then eastwards to form the border with Namibia before entering Botswana and terminating in the Okavango delta, a region of great natural and scientific importance. Nearly 95% of the total flow entering the delta system originates in the Angolan highlands. The annual floods peak at Mohembo, just inside Botswana, between February and April but this peak only reaches the end of the delta at Maun between June and August, five months later (McCarthy *et al.*, 2000).



Fig. 1 Map of the Okavango basin

Copyright © 2006 IAHS Press

The permanent and seasonal wetlands of the delta provide habitats for many rare and endangered species of flora and fauna now protected under the RAMSAR convention on wetlands. The delta is economically important generating 4.5% of the GDP in Botswana through tourism (Mbaiwa, 2004). The river is in itself an important resource for Namibia both locally and nationally, forming the main water supply for Rundu and for the commercial irrigation schemes along the river; it could potentially be exploited to augment scarce resources elsewhere in the country. In Angola 30 years of civil conflict have meant the upper basin is largely undeveloped.

The Permanent Okavango River Basin Commission (OKACOM), established in 1994 to increase co-operation between the three countries, recognises that future development is inevitable but must be coordinated to balance the conflicting demands of humans and the ecosystem. Compounding the effects of any development are the possible impacts on the basin water balance due to climate change. Indeed a recent study (Labat *et al*., 2004) of long term continental runoff has detected a link between increasing temperatures and reduced runoff in Africa.

Scenarios can be used in the formulation of river basin development plans and attempt to improve understanding among different users of the pressures within a basin. The use of hydrological models helps to translate the complex and differing pressures in the basin into hydrological outcomes e.g. on low or high flows. Using models it is hoped that scenarios can help to raise awareness of the impacts of various drivers among stakeholders, and strengthen understanding of the basin hydrology; in turn more realistic scenarios may be produced through regional cooperation.

THE GWAVA MODEL

The Global Water AVailability Assessment (GWAVA) model was developed to provide estimates of current and future water resources on a regional or global scale (Meigh *et al*., 1999). The method employs a gridded rainfall-runoff model operating at 0.5 degree resolution (approximately 50 × 50 km) to estimate water supply. Superimposed is the water resource network which estimate water abstractions, returns, transfers and influence of structures such as reservoirs. The approach enables a consistent methodology to be applied across countries at a resolution that can capture the spatial variation in water supply and demands. Key outputs of the model are comparisons of water supply and demands which are made at the grid cell basis, through a set of indices to take account of the annual and inter-annual variability in water supply. Using the GWAVA model both changes in climate and demands can be examined individually or in combination. In terms of water resources as a whole, ground water use is limited to the arid areas of the Namibian Omatako and local schemes across the delta. The results presented here therefore are restricted to the major component of hydrology in the basin: surface water. The main components of the GWAVA model are outlined below, for further details refer to Meigh *et al.* (1999).

Runoff generation

The spatial extent of the model includes the fossil river system of the Omatako and the delta system as far as the delta outlet, at Maun. The basin is modelled on a 0.5 degree grid with 161 cells linked to represent the river network (Fig. 2). Runoff generation is estimated using the probability distributed model (PDM) (Moore, 1985). The PDM parameters *Cmax* and *fc* are derived from soil textures and land surface cover based on the approach by Vorosmarty *et al.* (1989), whilst parameters relating to the shape of the soil moisture distribution and reservoir lag times are derived through calibration. Land cover data are derived from the Global Land Characterization dataset using the IGBP DIS classification. These are reclassified into four classes denoted as bare soil, grass, shrub and tree. At each cell linkage any abstractions from within the cell are removed and return flows added.

Climate data

The model is driven by input of monthly rainfall, temperature and potential evaporation with rainfall disaggregated into daily values using the monthly average rain days and randomly

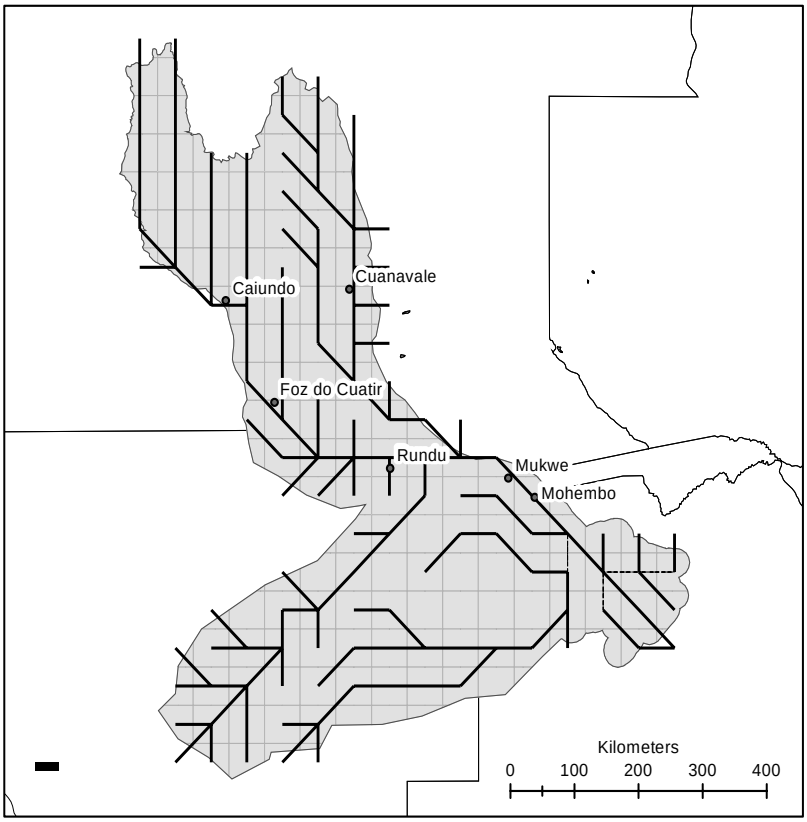


Fig. 2 Gridded river network and stations used for sub-catchment calibration.

assigning rainfall in the each day of the month. Good quality rainfall data are rather scarce within the basin particularly in the upper reaches of the basin where runoff generation is highest. This is partly due to the abandonment of the climate and hydrological monitoring networks within Angola during the civil war. There is a reasonable rainfall network in neighbouring Botswana and Namibia; and the gridded datasets held by Climate Research Unit (CRU) at the University of East Anglia, UK, were used to drive the model (New *et al.*, 2000).

Water demands

Water demands must be defined for each cell. Three broad categories of water demands are considered: Domestic, industrial and agricultural. Domestic demands are estimated for rural and urban water use using the gridded population data (UNEP-GRID) and a per capita water use (25 l h^{-1} day^{-1} for rural and 60 l h^{-1} day^{-1} for urban areas). There were no industrial water users identified with the basin. Agricultural water demand includes livestock water and irrigation. Livestock populations are estimated from the FAO Global Livestock Distributions dataset. Irrigation demands are derived from calculations of crop water demands requiring information on cropping areas, types and cropping calendars.

Calibration

An effect of the civil war in Angola has meant hydrometric stations installed in the early 1960s in the basin were abandoned with records extending for just a few years. This is a particular problem in the Cuito tributary for which there are just 30 months of continuous flow records. The model is calibrated against observed monthly flows at 5 locations for the baseline period 1961 to 1990 against which future scenarios (described below) are compared. Simulated and observed streamflows at two most downstream gauges are shown in Fig. 3. Overall the model captures the flow variability however the model tends to over predict extreme low flows, particularly during the middle period 1967 to 1979.

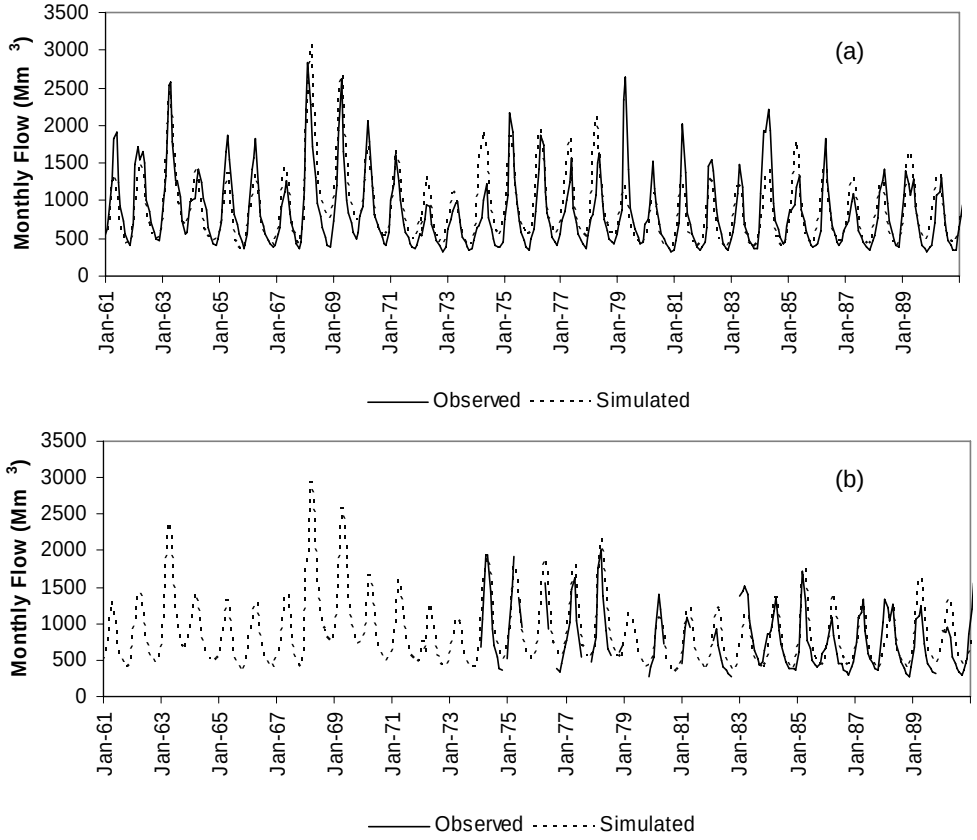


Fig. 3 Calibrated and observed streamflows for: (a) the Okavango at Mukwe; and (b) the Okavango at Mohembo.

Water availability

The amount of water that is 'realistically' available to meet demand is taken as the 90th percentile of monthly flows. This water availability is compared to the total demand in each cell using a suite of indices ranging in complexity from a simple annual ratio of total water demands to supply, to a more complex approach to take account of the varying supply and demand throughout the year. This index (denoted WAI4) expresses the deficit in relation to the demand such that a value of 1 means water supply is in excess of demands, through 0 water supply equals demands, to -1, water supply is insufficient to meet the demand. Indices are calculated and mapped showing the spatial variation of water availability in absolute terms and scaled according to the size of the demand.

CHANGE SCENARIOS

Climate change

Climate change scenarios for the basin are derived from the outputs of General Circulation Models (GCMs) which are available from the IPCC data distribution centre. The scenarios presented here use the UK Hadley centre's HadCM3 GCM under two SRES emissions scenarios, A2 and B2, for which global temperatures rise by between 3.53ºC and 3.69ºC, and 2.60ºC and 2.64ºC by 2080, respectively (Arnell, 2003). The HadCM3 model operates at a coarse spatial scale such that the basin is covered by just six 2.5 × 3.75 degree grids cells, with data downscaled using bilinear interpolation. Results from a Regional Climate Model, PRECIS, whose finer resolution, at 50 km, is commensurate with the hydrological model were also available for the A2 emissions scenario and time horizon 2080 (Tadross *et al.*, 2005). For each scenario, changes in precipitation, temperature and potential evaporation (Table 1), are calculated from the baseline, these changes are then applied to the CRU baseline.

Table 1 Percentage change in rainfall and potential evaporation in the Okavango Basin for time horizons 2050 and 2080 and emissions scenarios A2 and B2.

Year/scenario	Percentage change Precipitation	Potential Evaporation
2050		
HadCMA2	–13.6	18.3
HadCMB2	–15.5	16.3
2080		
HadCM A2	–20.6	30.8
HadCM B2	–27.15	28.4
PRECIS A2	–2.4	15.6

Demand change

Population growth and the corresponding increase in domestic water supply, and increased irrigation are the main drivers for growing water demand. The UNPD World Population Prospects (WWP) Database provides estimates of total and urban national populations up to the year 2050. Whilst the populations in Botswana and Namibia are predicted to plateau by 2050 the Angolan population will continue to rise resulting in a basin population of 5.1 million, assuming a medium variant growth. Increases in population are assumed to be greatest where population centres exist, such that the greatest increase in population would take place in the upper reaches of the Cubango basin. In a study of irrigation potential (Marques, 1998), up to 54 000 ha of land could be utilised in the lower reaches of the Okavango in Angola. A further 8000 ha may be utilised in Namibia.

RESULTS

The results in Table 2 summarize key model output for each scenario in terms of changes to the seasonal flows entering the delta where the dry season extends from February to July. In the final column the total number of cells which have a WAI4 of less than 0, i.e. the water supply does not meet the water demand or experiencing "water stress" is given. Comparing the baseline situation with the scenarios of demand change and climate change demonstrates that the human abstractions will have a moderately small impact on flows both in the dry and wet season.

The predicted changes in precipitation and potential evaporation are summarised in Table 1, and examination of the GCM results shows decreases in precipitation and increases in potential evaporation across the basin for every month. The impacts on both the wet and dry season flows are necessarily dramatic with dry season flows dropping by between 49–54% by 2050, and 68–73% by 2080. In contrast the results from the PRECIS RCM indicate a more modest drop in basin precipitation by 2080 of 2% annually with increasing precipitation in the Angolan highland

Table 2 Relative impacts of change on wet and dry season flows at Rundu and Mohembo.

	Seasonal flow (Mm^3)				
	Rundu		Mohembo		Number of cells
Year/scenario	Dry	Wet	Dry	Wet	WAI4 < 0
Baseline (1961 to 1990)	1552	4108	3010	5677	14
Abstractions					
Increased irrigation	1534	4073	2968	5577	28
Increased population (2050 med. variant)	1529	4087	2989	5657	14
Climate change					
HADCM3_A2 2050	713	1934	1307	2567	26
HADCM3_B2 2050	788	2050	1487	2839	28
HADCM3_A2 2080	495	1470	874	1865	42
HADCM3_B2 2080	418	1243	706	1570	44
PRECIS_A2 2080	1362	4264	2358	5187	14

observed in the winter months contributing to larger wet season flows observed at Rundu. Across the whole basin, annual evaporation increases substantially, however, this is biased by the high increases in the southwest arid regions as such increases in the rest of the basin are more moderate. The impact of increasing evaporation on the water balance in this region is manifest in Fig. 4, comparing the WAI4 for the baseline and 2080, and shows that the majority of cells moving to a more water scarce situation are located within the Omatako sub-basin. These results also indicate the sensitivity of water resources in the basin to the spatial distribution of water supply and patterns of future climate change.

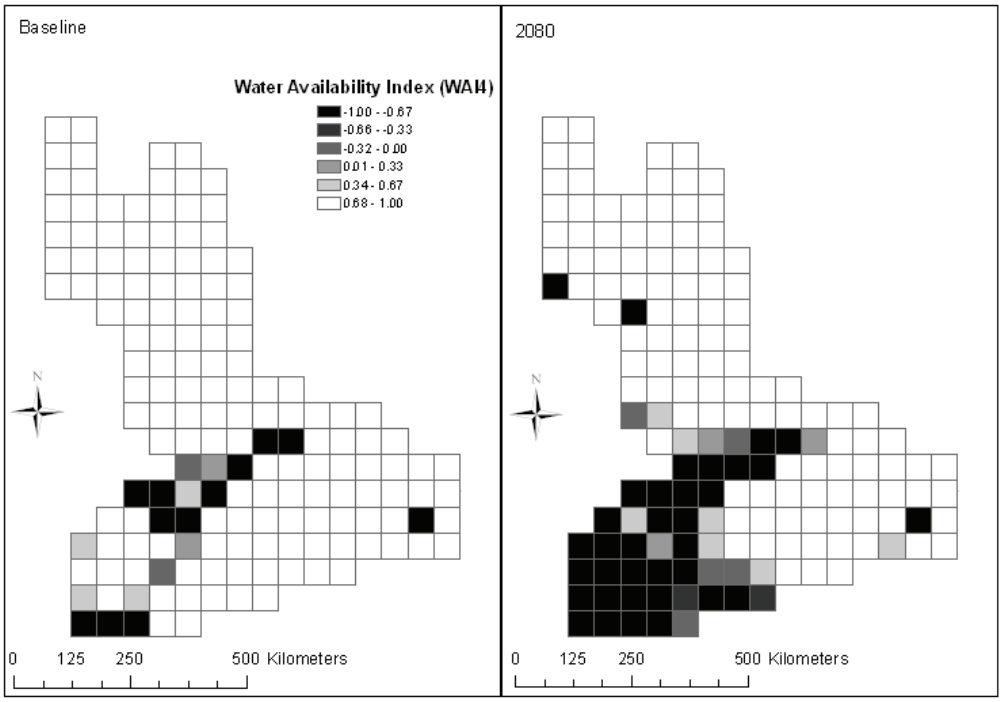


Fig. 4 Water availability indices for the baseline and 2080 (A2 scenarios).

The impacts of increased abstractions whether for irrigation or water supply appear relatively small because the largest population increases will take place in the wettest parts of the catchment, and, although WAI4 falls it remains above zero, indicating water supply is still sufficient to meet increased demand.

CONCLUDING REMARKS

A large-scale gridded model such as GWAVA provides a useful and consistent methodology to model water resources and water availability across large regions. Through the mapping of indices which compare water demand and supply vulnerable areas can be identified. The difference in predicted changes of precipitation and evaporation between the HADCM3-A2 scenarios and the PRECIS model suggest there is considerable uncertainty in the GCMs at present even for the scale of the Okavango basin.

Whilst the basin response to changing aspects of the water budget is useful, ‘realistic’ scenarios using both human development and climate change may be as informative.

Acknowledgements This work has been supported by the EU and NERC through funding of the TWINBAS project. The authors wish to acknowledge the contribution of our former colleague Dr Jeremy Meigh (1954–2006).

REFERENCES

Arnell, N. W. (2003) Effects of IPCC SRES emissions scenarios on river runoff: a global perspective. *Hydrol. Earth System Sci.* **7**(5), 619–641.

Labat, D., Godderis, Y., Probost, J. L. & Guyot, J. L. (2004) Evidence for global runoff increase related to climate warming. *Adv. Water Resour*. **27**, 631–642.

McCarthy, T. S., Cooper, G. R. J., Tyson, P. D. & Ellery, N. W. (2000) Seasonal flooding in the Okavango Delta, Botswana—recent history and future prospects. *South African J. Sci.,* **96**(1), 25–33.

Marques, R. (1998) Climate, Hydrology and Water Resources Angolan Sector. Okavango River Basin Preparatory Assessment Study (Draft translation into English).

Meigh, J. R., McKenzie, A. A. & Sene, K. J. (1999) A grid-based approach to water scarcity estimates for eastern and southern Africa. *Water Resour. Manage.* **13**, 85–115.

Moore, R. J. (1985) The probability-distributed principle and runoff production at point and basin scales. *Hydrol. Sci. J.* **30**(2), 273–297.

Mwaiba, J. (2004) Causes and possible solutions to water resource conflicts in the Okavango River Basin: the case of Angola, Namibia and Botswana. *Phys. Chem. Earth* **29**, 1319–1326.

New, M., Hulme, M. & Jones, P. D. (2000) Representing twentieth century space-time climate variability. Part 2: Development of 1901–96 monthly grids of terrestrial surface climate. *J. Climate* **13**, 2217–2238.

Tadross, M., Jack, C. & Hewitson, B. (2005) On RCM-based projections of change in southern African climate. *Geophys. Res. Lett.* **32**, 23.

Vörösmarty, C. J., Moore, B., Grace, A. L., Gildea, M. P., Melillo, J. L., Peterson, B. J., Rastetter, E. B. & Steudler, P. A. (1989) Continental scale models of water balance and fluvial transport: an application to South America. *Global Biogeochem. Cycles* **3**, 241–265.

Climate Variability and Change—Hydrological Impacts (Proceedings of the Fifth FRIEND World Conference held at Havana, Cuba, November 2006), IAHS Publ. 308, 2006.

Exploring the impacts of climate change on water resources—regional impacts at a regional scale: Bangladesh

CHAK FAI FUNG[1], FRANCIS FARQUHARSON[1] & JAHIR CHOWDHURY[2]

1 *Centre for Ecology and Hydrology, Wallingford, Oxfordshire OX10 8BB, UK*
cffu@ceh.ac.uk

2 *Institute of Water and Flood Management, Bangladesh University of Engineering and Technology, Dhaka, Bangladesh*

Abstract Bangladesh is located at the confluence of three major river basins: the Ganges, Brahmaputra and Meghna (GBM) basins. The GWAVA (Global Water AVailability Assessment) model, a global-scale gridded approach to hydrological modelling, has been applied to all GBM basins to investigate the impacts of climate change on water resources at a regional scale. The entire model set-up is composed of a coarse-scale GBM-wide model at 0.5 degrees resolution and a fine-scale model at 0.1 degrees representing Bangladesh. A suite of climate scenarios have been collated from regional climate data using the Hadley Centre's HadRM2 and that generated by the Indian Institute of Tropical Meteorology using the Hadley Centre's PRECIS. Scenarios for water demands have been developed for the present and future based on socio-economic data from various publicly available sources and local water management plans. The comparison of water demands with supply using spatial-temporal distributed water availability indices enables areas of future scarcity to be identified.

Key words water resources modelling; climate change; impacts study; grid-based models; water demand; water scarcity; regional climate models

INTRODUCTION

Bangladesh is one of the world's most densely populated countries and has a high incidence of poverty. The fact that the country already suffers greatly from flooding and drought, and lacks financial resources, means that Bangladesh has been identified as being highly vulnerable to the effects of climate change. With roughly 80% of the landmass made up of fertile alluvial lowland and the major employer being agriculture, current climate change predictions of wetter wet seasons and possible drier dry seasons, depending on the global climate model used (IPCC, 1998), can only exacerbate an already critical water resources situation. Despite this predicament, climate change has not been considered so far in the National Water Management Plan of Bangladesh. In this paper, a model is presented that is aimed at providing a tool that is both accessible and relevant at a regional scale, which highlights the impacts of climate change on water resources in Bangladesh.

HYDROLOGICAL SITUATION

Bangladesh is located at the confluence of three major river basins: the Ganges, Brahmaputra and Meghna (GBM) basins. In order to understand the future impacts on water resources in Bangladesh, it is necessary to investigate these trans-boundary rivers (only 5% of the Ganges catchment and 7% of the Brahmaputra catchment lie in Bangladesh). The GBM basins are hydrologically complex, ranging from the glaciers of the Himalayas to the deltaic flood-prone Bangladesh. Not only are the river flows glacial but are subject to annual monsoonal rains where more than 80% of the annual rainfall is received during the wet season.

METHODOLOGY

The Global Water AVailability Assessment (GWAVA) model, a global-scale gridded approach to hydrological modelling, has been applied to the basins to investigate the impacts of climate change on water resources in the region. The model was developed to provide a consistent and realistic examination of water resources problems as described in Meigh *et al.* (1999).

Surface flows are estimated using the probability distributed model of Moore (1985), linking climate to runoff and, in the major river basins, the runoff estimates for individual grid cells are accumulated to give estimates for the total flows at all points of interest. GWAVA has been adapted to local conditions in the GBM region in order to stimulate local interest in the impacts of climate change. A new module, specifically developed for the Himalayas, has been included to provide a more sophisticated approach to the modelling of glacial hydrology.

Copyright © 2006 IAHS Press

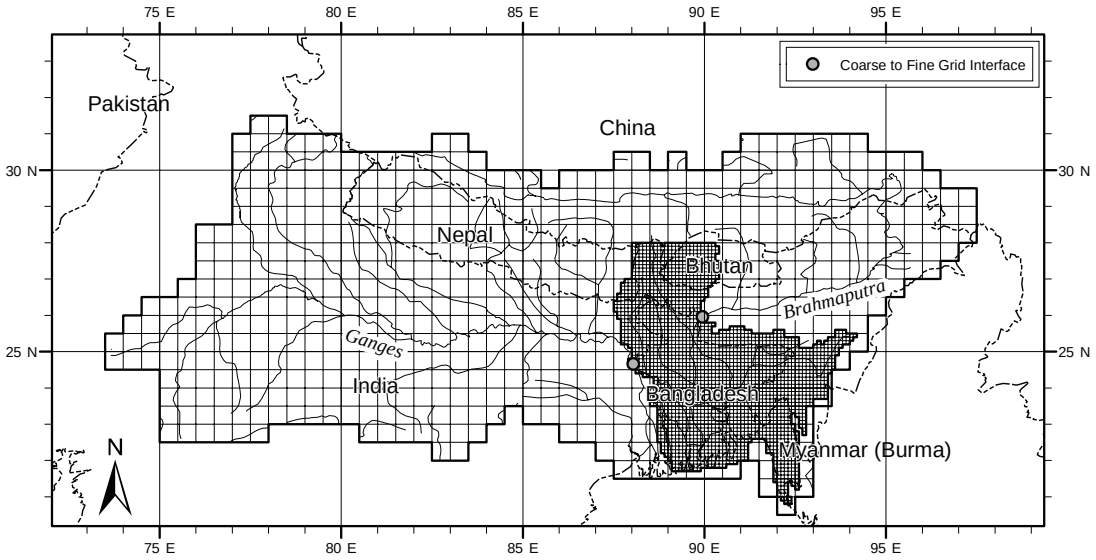


Fig. 1 Map of Ganges-Brahmaputra-Meghna River Basins showing discretization of coarse and fine-scale grids.

The model has been refined such that it is composed of a coarse-scale GBM-wide model at 0.5 degrees resolution and a fine-scale model at 0.1 degrees representing Bangladesh (Fig. 1). The "downscaling" of the model to the fine-scale grid has been necessary not only for scientific interest, but to provide results at a scale that is relevant to water resource managers in Bangladesh (the 0.1 degrees resolution is a balance between the resolution of available data sources and the size of administrative areas).

A finer-scale grid resolves more hydrologically important features, including the complex network of irrigation schemes that exist in Bangladesh. Moreover, the country is low-lying and with its capital city, Dhaka, 225 km from the coast and at about 8 m above the mean sea level, differences in elevation are very small. Therefore the application of digital elevation models to provide automatically-generated drainage networks is very difficult. Using local maps and expertise, a new drainage map of Bangladesh has been produced at the 0.1 degree scale.

As Bangladesh is at the downstream end of all the river basins, the model allows a simple non-dynamic transfer of flow from the coarse grid to the fine grid at two strategically-placed points close to the Bangladesh border, and to flow gauges which are used for calibration purposes. In addition to the explicit modelling of dam operations, lakes, wetlands and water transfers, the water-sharing agreement between India and Bangladesh, which controls river flows into Bangladesh at the Farakka Barrage, have been included in this case study.

CLIMATE SCENARIOS

The advent of regional climate models has made it possible to provide more details of climate characteristics at a scale relevant to nation states. A suite of climate scenarios have been collated from regional climate models (RCM) to drive the hydrological component of GWAVA. These

Table 1 Mean changes in generated daily climate for the whole GBM region relative to the observed climate data set, Mitchell *et al.* (2003). HadRM2 refers to the data generated using RCM results for a perturbed climate where CO_2 doubles during the next century by Hassel & Jones (1999) and PRECISA2 refers to data generated using PRECIS for the SRES scenario A2 with sulphur by IITM (2005).

Season	Climate Variable	2020s		2050s	
		HadRM2	PRECISA2	HadRM2	PRECISA2
Dry	Precipitation (%)	+26	–2	+58	–4
	Temperature (°C)	+0.4	+0.3	+0.7	+0.5
	Potential evaporation (%)	+22	+33	+46	+58
Wet	Precipitation (%)	0	+13	+8	+28
	Temperature (°C)	+0.6	–0.2	+1.0	–0.1
	Potential evaporation (%)	35	21	71	39

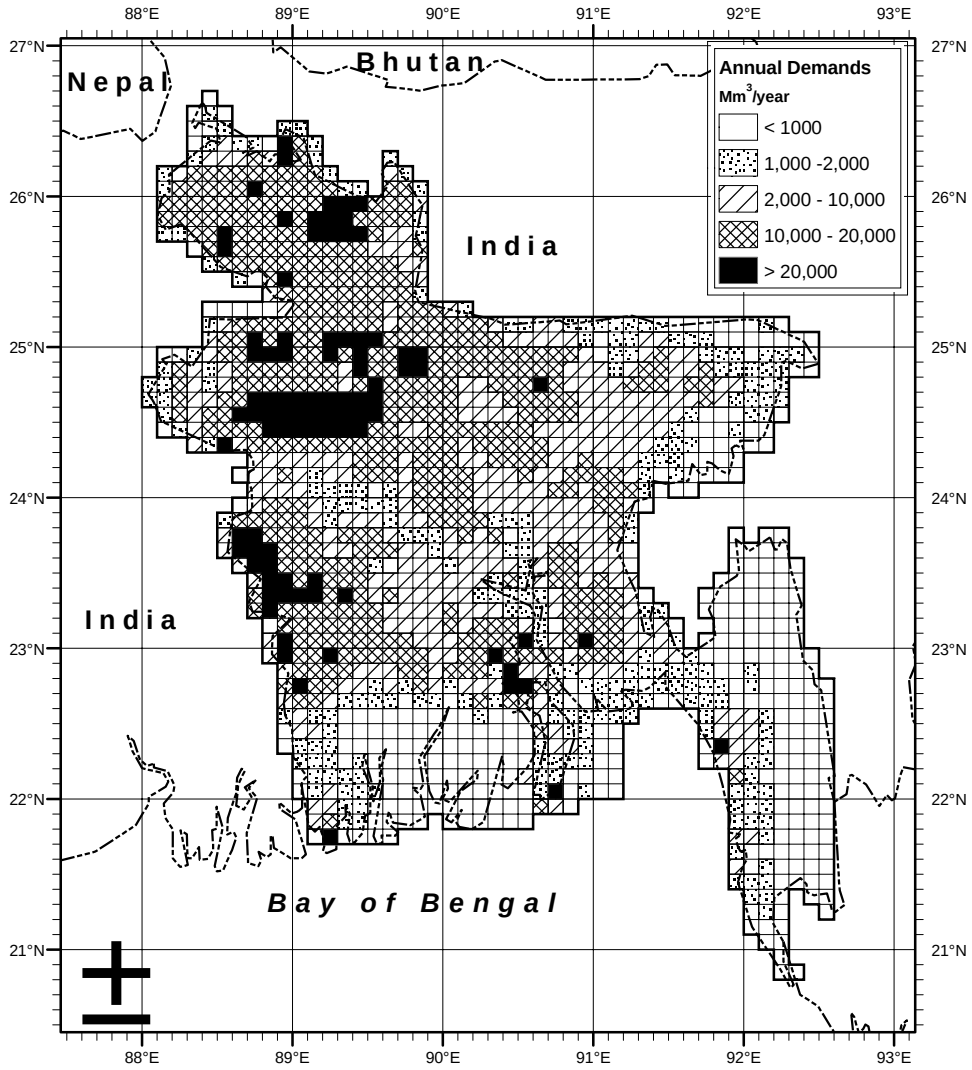


Fig. 2 Baseline annual water demand for Bangladesh based on locally-obtained water use statistics.

have included new data generated using PRECIS at the Indian Institute of Tropical Meteorology (IITM, 2005) and HadRM2 by Hassel & Jones (1999) (at a grid resolution of approximately 50 × 50 km), as well as results of global climate models.

RCM data was provided for baseline (1961–1990) and future horizons (2070–2100 for PRECIS and 2041–2060 for HadRM2). The time horizons available present a problem, as water managers prefer to plan on timescales of a maximum of 25 to 50 years. Moreover, with the inclusion of the more sophisticated glacier model, initial conditions of the glaciers at the start of the future horizon are required. Previous applications of GWAVA where the baseline and future horizons are treated as independent runs are therefore not possible. In order to drive the model for the 2020s and 2050s, climate variables had to be generated during the interim period between the end of the baseline and the start of the future horizon.

Average changes in monthly precipitation, temperature and potential evaporation between the future climate and the baseline (or control climate for HadRM2) were calculated from the daily RCM data. An annual incremental increase in the monthly values of each of the three climate variables was then applied to the baseline climate data set used to calibrate the model. Summary statistics of the driving climate variables for future horizons are presented in Table 1.

WATER DEMANDS DATA

Scenarios for water demands have been developed for baseline and future horizons corresponding to the climate scenarios. Data requirements for their calculation include human and livestock population, domestic, industrial and irrigation water use. Detailed data on water use in countries

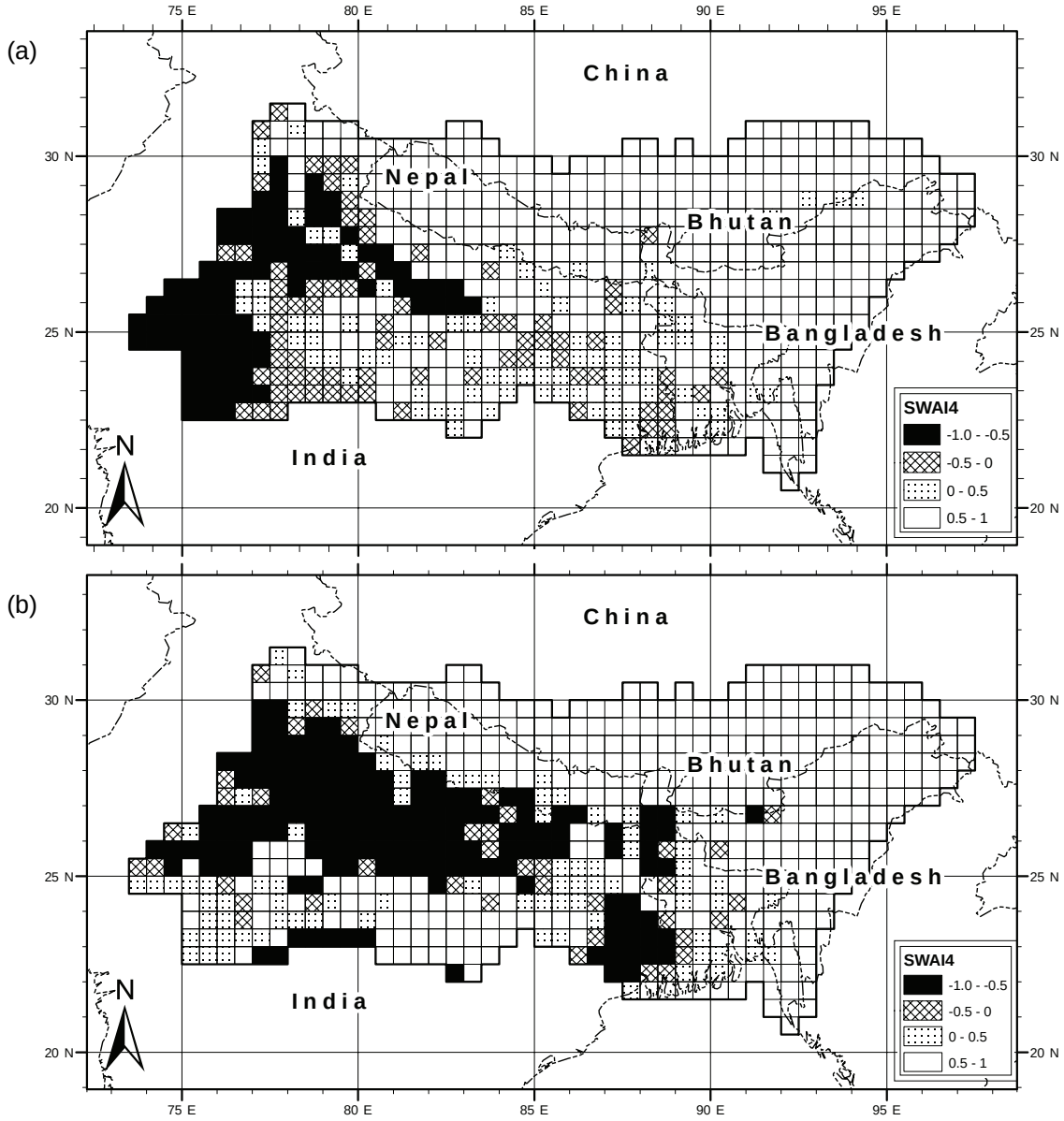


Fig. 3 Annual surface water availability index number 4 (SWAI4) for the whole of the Ganges-Brahmaputra Basin region during: (a) the baseline period 1961–1990, and (b) the 2020s.

upstream of Bangladesh are not available. Hence, for areas outside of Bangladesh, socio-economic data from various publicly available sources were used. Methods to resolve the various formats and resolutions of data were developed similar to that used by Gaffin *et al.* (2004), with an emphasis on providing a set of data that can be represented spatially. For Bangladesh, it was important to use locally sourced data and develop scenarios relevant to local water managers (see Fig. 2). Therefore, for the development of future water demands, the National Water Management Plan for Bangladesh was used.

RESULTS AND DISCUSSION

The socio-economic scenarios were combined with the climate scenarios to provide an ensemble of future scenarios, giving an indication as to the possible impacts of climate change on water resources in Bangladesh. The main outputs of the work are a set of spatial-temporal distributed water availability indices, comparing water demands with supply, enabling areas of future scarcity to be identified. An example of one of these indices is presented in Fig. 3 for the whole of the GBM region. The index presented is the surface water availability index type 4 (SWAI4), which is a ratio comparing the minimum of the 90% reliable monthly runoff during the whole run minus the

water demand for that month, and the overall 90% reliable monthly runoff plus the water demand for that month. Regions of water excess have a positive value and regions of water deficit a negative value. For further details of the different indices see Meigh *et al.* (1999).

Figure 3 shows that despite the large increases in annual precipitation predicted by the RCMs, the dry season is becoming drier for the more recent PRECIS run (see Table 1). With the increases in water demand due mainly to population increases, there is a general increase in the water deficit, especially along the Ganges in India (Fig. 3). The results suggest future changes could have major implications for trans-boundary water management.

The large variation in magnitude of the climate change data from different climate models suggest that ensembles of runs are required to provide a better indication as to the likelihood of the modelled future water availability results. GWAVA provides a useful tool to assess and highlight climate change impacts on water resources and will provide a more reliable picture of future water availability as more climate change data becomes available.

Acknowledgement The authors would like to thank DFID for providing the funds for the CLASIC project from which this paper was derived.

REFERENCES

Gaffin, S. R., Rosenzweig, C., Xing, X. & Yetman G. (2004) Downscaling and geo-spatial gridding of socio-economic projections from the IPCC Special Report on Emissions Scenarios (SRES). *Global Environmental Change* **14**, 105–123.

Hassel, D. & Jones, R. G. (1999) Simulating climatic change of the southern Asian monsoon using a nested regional climate model (HadRM2). HCTN 8. Hadley Centre for Climate Prediction and Research, Bracknell, UK.

Indian Institute of Tropical Meteorology (IITM) (2005) South Asian baseline and future climate data generated using the Hadley Centre's Providing Regional Climates for Impacts Studies (PRECIS) Model. IITM, India.

Intergovernmental Panel on Climate Change (IPCC) (1998) The regional impacts of climate change: an assessment of vulnerability: A special report of the IPCC Working Group II. R. T. Watson, M. C. Zinyowera & R. H. Moss (eds). Cambridge University Press, Cambridge, UK.

Meigh, J. R., McKenzie, A. A. & Sene, K. J. (1999) A grid-based approach to water scarcity estimates for eastern and southern Africa. *Water Resour. Manage.* **13**, 85–115.

Mitchell, T. D., Carter, T. R., Jones, P. D., Hulme, M. & New, M. (2003) A comprehensive set of high-resolution grids of monthly climate for Europe and the globe: the observed record (1901–2000) and 16 scenarios (2001–2100). *J. Climate* (submitted, August 2003).

Moore, R. J. (1985) The probability-distributed principle and runoff production at point and basin scales. *Hydrol. Sci. J.* **30**, 273–297.

Climate Variability and Change—Hydrological Impacts (Proceedings of the Fifth FRIEND World Conference held at Havana, Cuba, November 2006), IAHS Publ. 308, 2006.

Possible impacts of climate variability/change and urbanization on water resources availability and quality in the Benin-Owena River basin

J. N. OKPARA, L. E. AKEH & A. C. ANUFOROM
Nigerian Meteorological Agency, Hydrometeorological Division, PMB 615, Garki, Abuja, Nigeria
juddy_okpara@yahoo.co.uk

Abstract In this study, monthly rainfall and temperature from four Nigerian meteorological stations in the Benin-Owena basin covering the period 1940–2002, and evaporation (1960–2003) and river discharge (1980–2004) data were obtained and analysed to investigate the impact of climatic variability and urbanization on the water resources of the basin and the socio-economic implications. The Benin-Owena basin is heterogeneous in nature and located in the southwest of Nigeria. The study area covers a total land area of 59 787 km^2 and has a human population of over 13 million. Population data, the volume of solid waste generated in the region and water quality data from 32 boreholes distributed across the area were obtained from the UNICEF water and sanitation (WATSAN) project office and also analysed. The analysis showed that climatic variations exist over the region that appear as fluctuations of wet and dry periods every 2–3 years in terms of rainfall and the river flow. Also an increasing temperature trend was observed, rising at the rate of 0.37°C/decade. This, coupled with the high rate of evaporation, will cause increasing water loss in the basin. The borehole results showed that the aquifers are productive with relatively high potential water yields. Their water quality is within the World Health Organization (WHO) acceptable standards in terms of the physico-chemical and bacteriological composition, except for a few boreholes located in the unplanned densely populated areas of the basin; there, abnormal concentrations of chloride (297 mg L^{-1}), turbidity (20FTU), iron (0.43 mg L^{-1}) and faecal coliform counts of 3 per 100 ml of water, occur. Re-assessment of the water quality 10 years after commissioning of the boreholes showed that 18% out of the 96% of boreholes initially with good water quality, now had poor quality due to the high rate of unplanned urbanization.

Key words climatic variability; urbanization; river basin; discharge; borehole; water quality

INTRODUCTION

Human life and socio-economic activities have been subjected to many challenges in the recent time among which climate change/variability is the most important and of great concern. Unfortunately, the rapidly growing population of most cities is the most vulnerable to this climate change. Until recent decades, most water resources projects in Nigeria were planned and designed with the assumption of a stationary climate, whereas climate and hydrology have become both non-stationary stochastic processes. At present, water resources planners in river basins are facing increased uncertainty in evaluating the hydrological condition of the basins under the changing climate. According to the Third IPCC Assessment Report (2001), precipitation will intensify during the 21st century. In some low latitude areas there will be decreases in total quantities (and drought) and increases (and flooding) in others. In addition, many research projects in Nigeria have confirmed that there is a changing climate in Nigeria. For instance, Udoeka (1998) and Udoeka *et al*. (1998a) in their recent work over the six climatic zones of Nigeria showed that there is a steady rise in evaporation and steady decrease in rainfall throughout the country. Okpara *et al*. (2004) also observed that increased "land-use intensity" due to the rapid rate of urbanization and industrialization was a key factor responsible for the unsustainability of groundwater resources in the country, since it leads to imbalance and social malaise in the society. Also urbanization does not only ensue in climatic variations, but leads to inadvertent weather modification of a place as well as creating a micro-climate over the region. Gbuyiro & Aisiokuebo (2003) observed an average temperature increase of 0.4°C across the country in the last 20 years.

According to Obasi (2003), projected temperature increases are likely to lead to increased open water and soil/plant evaporation. As a rough estimate, potential evapotranspiration over Africa is projected to increase by 5 to 10% by 2050. Also, with Africa being the continent with the lowest conversion factor for precipitation to runoff (averaging 15%), the dominant impact of global warming has been postulated to cause reduction of soil moisture in the sub-humid zones, as well as reduction in the runoff. It is against this backdrop that this study tries to investigate the

Copyright © 2006 IAHS Press

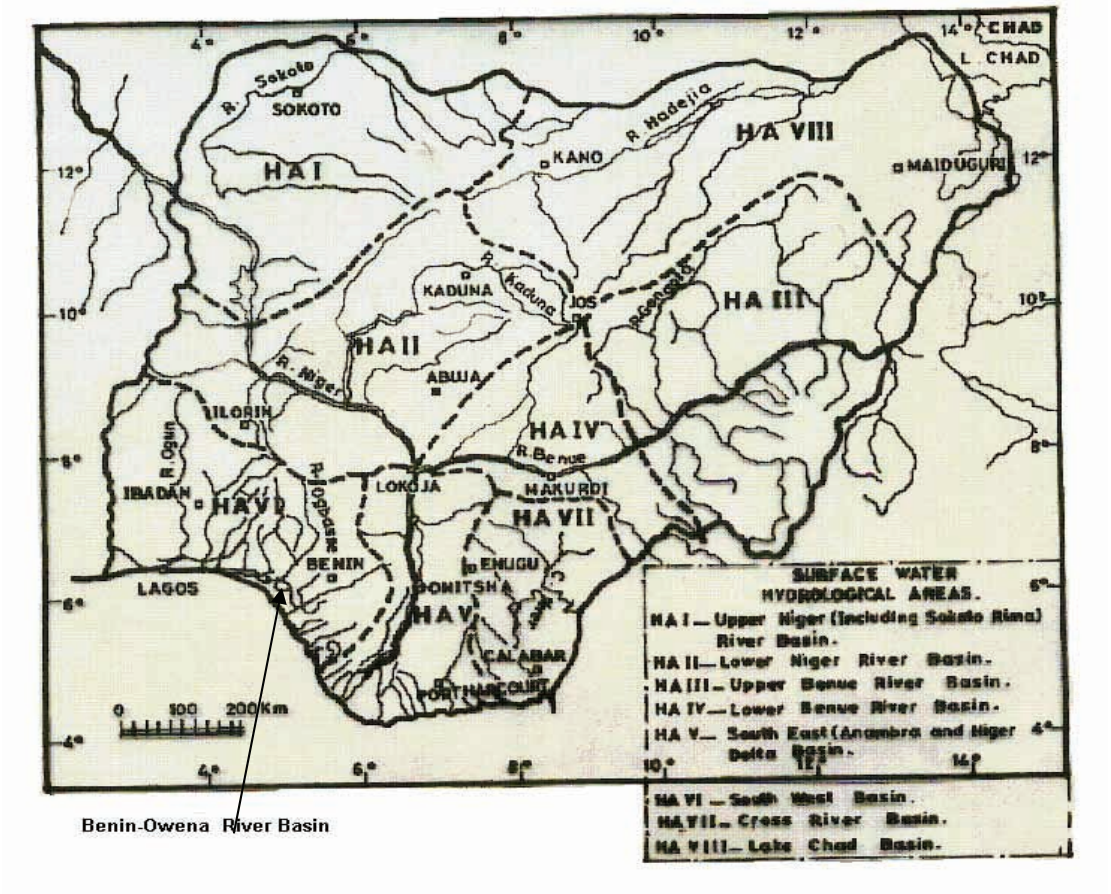


Fig. 1 Location of the Benin-Owena basin in southwest Nigeria.

impacts of climatic variability and urbanization on the available water resources of the Owena River basin, especially as NGOs and State government promote the sinking of shallow boreholes through the UNICEF assisted Water and Sanitation (WATSAN) project.

STUDY AREA

The study area is the Benin-Owena River Basin Area that lies between the west bank of the Niger River in the east and the Oni River in the west, and occupies the territory covered by Ondo, Ekiti, Edo and Delta states (Fig. 1). The basin has a total area of 59 787 km^2, with a human population of over 13 million. The settlement pattern shows compactness in the towns and cities, with the major occupation of the rural population being agriculture; there are a few growing industries scattered across basin. The main north–south flowing rivers/streams of the basin are from west to east namely; Oni, Siluko, Benin, Escravos, Forcados, Ase, Niger and many other streams. Topographically, the basin can be divided into two belts; namely the northern highlands and southern plains or lowlands. It has an undulating land surface that descends gradually from an altitude of over731.52m in Ekiti state to the lowlands. The Ishan plateau of the basin rises steeply from the Niger valley and has such striking characteristics as level topography, easily worked sandy soil and paucity of surface drainage which calls for extensive hydrological study in terms of groundwater occurrences.

Climatologically, the basin area falls into the region of high temperature that ranges from 24.7–33°C on the long-term average and experiences mean annual precipitation of 6604 mm in any normal year and an estimated mean annual evapotranspiration of 4622.8 mm with relatively high humidity (>70%) .

DATA ANALYSIS

Monthly rainfall and temperature data (1940–2002), and evaporation data (1960–2003) from four meteorological stations in the basin, and river flow discharge data (1980–2004) were subjected to a time series and variability analyses. Also, data available for 32 boreholes were obtained from the office records between 1998 and 2002 of the Ondo State-UNICEF assisted water and sanitation (WATSAN) project on the rock formation and water quality of the basin, and subjected to descriptive analysis. Some of the parameters which could be determined immediately, i.e. temperature, pH (measured with a Jenway model 3100 pH meter), and conductivity (measured with a Jenway 4070 conductivity meter) were done. Both meters had automatic temperature compensation. In the laboratory, the total hardness and calcium were determined using EDTA titration, and titration with EDTA using Eriochrome black T as the indicator. Magnesium was estimated as the difference between total hardness and calcium concentration. The coliform counts were determined by the most probable number method, after incubation of Mackonkey Broth-treated samples for 48 hours at 37°C (WHO, 1984). Population data from the Federal Office of Statistics/National Population Commission, and data on the volume of solid wastes generated in the region from the office of Federal Ministry of Housing and Environment, were also obtained and analysed to ascertain the rate of land-use intensity, urbanization and population pressure in the basin. Re-assessment results for the water quality 10 years after the commissioning of the boreholes were also carried out in July 2003.

RESULTS AND DISCUSSIONS

Results in Fig. 2(a) show an increasing temperature trend, with a general increase rate of 0.37°C/decade. The temperature increase of 0.37°C/decade over the basin is still within the increase of 0.5°C/decade projected by the third IPCC Report. This will invariably create a high evaporative demand from the open water and the soil/plants in the basin as we can see from Fig. 2(b). Evaporation has shown an increasing trend since the 1980s, resulting in about 70% of the annual rainfall of the basin being accounted for by natural losses (evapotranspiration). According to Obasi (2003), with Africa being the continent with the lowest conversion factor of precipitation to runoff (averaging 15%), the dominant impact of global warming has been postulated to result in the reduction of soil moisture in the sub-humid zones, as well as reduction in the runoff. Consequently, since the field capacity of the soil has to be attained before recharging the groundwater, the rate of recharge is expected to be affected.

Figure 3 shows that climatic variations exist that appear as oscillations of wet and dry periods every 2–3 years; with increasing rainfall trend pattern. There are also more wet years in this basin than dry years unlike in other river basins of the country with decreasing trends (Fig. 3). However, indications that the trend is tending towards the negative with time is already in evidence. Very long periods of wet years was observed from 1948–1969, with 1949–1965, 1991, 1995, 1999 and 2002 been the wettest years. The only dry periods were 1944–1946, 1950, 1956, 1958, and

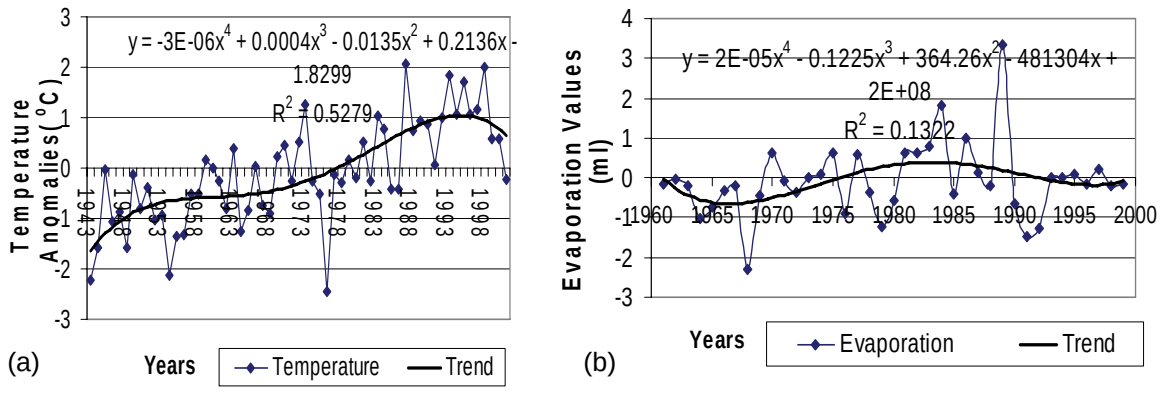


Fig. 2 Benin-Owena basin: (a) temperature variability and trends, (b) evaporation anomalies and trends.

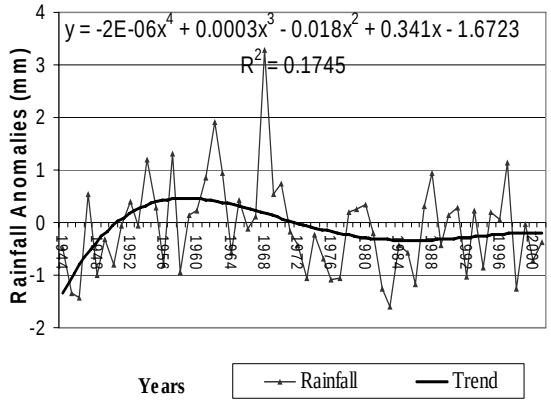


Fig. 3 Rainfall trend over the Ogun-Osum River basin.

1964, 1976–1978 and 1981–1984; most of which coincide with the El-Nino years. Changes in land-use due to urbanization and population pressure also created micro-climatic and inadvertent weather modification of the area; resulting in heat islands developing in the more devegetated and ill-planned urban areas of the basin, Tables 1 and 2. Some descriptive statistical properties of the rainfall for the two reference periods are also given in Table 3, which stresses the large differences in the data between the two periods. All the stations in the basin show statistically significant (95% level) differences in the means of the sub-period rainfall series. This suggests that the recent rainfall patterns of the region are not due to mere chance, but climate variability. This can be linked with intense rainfalls of short duration often experienced in the region causing increased runoff, sediment erosion and destructive flood flows.

Thirty % (1981.2 mm) of the mean annual rainfall (6604 mm) accounts for annual runoff in the basin. Figure 4 describes the Catchment response to the behaviour of the rainfall in terms of the river flow pattern over the basin. Hydroclimatological changes are also visible in the time

Table 1 Comparison of temperature distribution between ill-planned devegetated urban centre and well planned vegetated urban centre.

Time	Devegetated area	Vegetated area
0600Z	24.8	23.2
0900Z	28.0	26.9
1200Z	32.5	30.4
1500Z	31.6	29.9
1800Z	28.6	26.3

Table 2 Comparison of temperature increase in the urban centres of the basin with rural surroundings for both dry and wet season.

Land use	Temperature increase:	
	Wet season	Dry season
Medium class density	2.4	2.6
Low Class Density	3.4	4.6
Commercial areas	2.7	5.3

Table 3 Descriptive statistics for annual rainfall series in the basin.

Station	Reference period	Maximum (mm)	Minimum (mm)	Mean (mm)	Standard deviation (mm)	Reference period as % of long-term mean
Benin	1940–1970	3147.1	1334.3	2143.63	418.88	101
	1971–2002	2668.4	1228.4	2121.98	379.74	99
Warri	1940–1970	3390	2373	2877.53	282.82	101
	1971–2002	3436.8	2072.4	2774.74	318	98
Ondo	1942–1970	368	351	360.80	3.91	99
	1971–2002	385.5	354.1	368.75	6.0	101

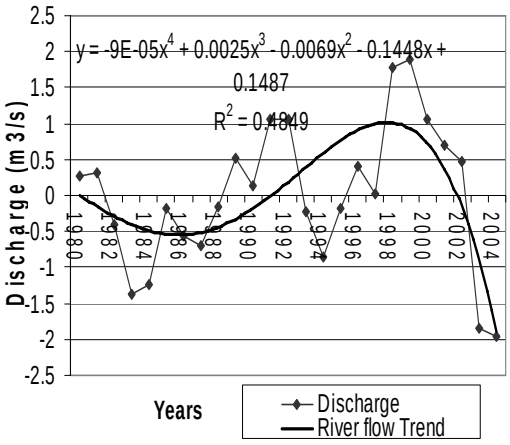


Fig. 4 Time series of Niger River flow over the Niger delta area.

series of the river discharges. The runoff of the Niger River (Fig. 4), the biggest in the basin, shows two climatic periods in the last two decades: a 10-year dry period, from 1980 to 1989, with an average interannual runoff of 51 946 $m^3 s^{-1}$.Then the wet period started, with an average interannual runoff of 62 087 $m^3 s^{-1}$. The driest and wettest years were only 16 years apart (1983 with 34 422 $m^3 s^{-1}$ and 1999 with 90 820 $m^3 s^{-1}$). The trend since 2003 is already tending towards another cycle of dry periods as we can see from the graph. Hence there is need for appropriate water resources management practices to be put in place in the region, so that no excess water is allowed to waste without being harvested. The river basin, unlike other basins in the country, seemed to be rich in water resources, strengthened by the increasing rainfalls; unfortunately, most of the waters are unfit for drinking and domestic uses due to indiscriminate disposal of wastes of all types from the towns and villages, unplanned densely populated settlements and uncoordinated land-use practices.

All these contribute to degradation of the quality of the available water resources. These contaminants are not only washed into the rivers after a heavy downpour but also get into contact with the water table through leaching. Another source of pollution observed is through pronounced sediment erosion and associated pollution. This has silted up and caused eutrophication in most of the reservoirs created for water supply purposes in the basin. The borehole analysis from the WATSAN project confirmed that the aquifers in the region are productive on average with relatively high yield of water potentials: 13 boreholes were categorized as high yield, 15 as medium/relatively high yield, and 4 as low yield. Most of the boreholes are developed within 30–36 m depth with varying water levels. The water quality is within the World Health Organization (WHO), acceptable standard for drinking and domestic use in terms of physical, chemical and bacteriological composition, Table 4.

Table 4 Groundwater quality assessment result of sampled boreholes.

Parameters	WHO prescribed standard (1984)	96% of sampled good bore holes	<5% of sampled bad bore holes
Appearance		Clear	Clear
Colour		Colourless	Colourless
Temperature (°C)		27.8	27.6
Turbidity (FTU)	<1 to 5	7.8	20
pH	6.5–8.5	7.0	7.0
Total Dissolved Solid(TDS) (mg L^{-1})	1000	0.27	0.47
Conductivity		0.56	0.96
Iron (mg L^{-1})	0.3	0.28	0.43
Chloride (mg L^{-1})	250	76.7	297
Nitrate (mg L^{-1})	10	2.1	12.1
Total Hardness (mg L^{-1})	500	95.4	695.4
Calcium (mg L^{-1})		40.7	40.7
Magnesium(mg L^{-1})		61.1	61.1
Copper (mg L^{-1})	1.0	2.2	2.2

On average, 96% of the sample points had good freshwater at the initial time of construction, with average total dissolve solid (TDS) as 0.27 mg L^{-1}, chloride 76.7 mg L^{-1}, nitrate 2.1 g L^{-1}, iron 0.28 mg L^{-1}, pH 7.0 and total hardness 95.4 mg L^{-1}, though the turbidity, 7.8 FTU, was slightly high. Less than 5% had poor water quality, with average turbidity values of 20 FTU, average faecal coliform count of 3 per 100 ml of water, average chloride values of 297 mg L^{-1}, average iron 0.43 mg L^{-1}, all these values are slightly higher than the WHO acceptable safety level. A few samples also have total hardness slightly above the tolerant level, and so is their colour, i.e. slightly brownish or turbid. Such boreholes could have their quality improved by treating and disinfecting them.

Table 6 Relationships between human population and water quality in Benin-Owena River Basin area.

	Urban Area	1991	1992	1998	2002
Population	Delta State	2 590 491		3 149 371	
	Edo State	2 172 005		2 640 600	
	Ondo State	3 785 338		4 601 990	
Water quality	Turbidity		7.8FTU		9.8FTU
	TDS		0.27		100
	Iron (mg L^{-1})		0.28		0.38
	Chloride (mg L^{-1})		76.7		307
	Total hardness (mg L^{-1})		95.4		580
	Faecal coliform		0		3 per 100 ml count

It is pertinent to say that the shallow nature and the location of most of the boreholes in the midst of dense settlements, coupled with the increasing rate of urbanization made some of the boreholes highly susceptible to contamination from septic tanks, pit latrines and solid waste dumping sites. These may have accounted for the abnormal concentration of chloride, faecal coliform counts and iron observed in the unplanned densely populated areas within Akure, Ilu-Oluji, Ilu-Abo and Ondo, Benin, Warri and Asaba. It was also noted that as the population grows, more wastes are generated in those places and the more their dumping sites become potential sources of groundwater pollution in the area (Fig. 5). The graph reflects the rate of solid waste generation growth in the basin. These solid wastes, apart from clogging up the drains and defacing the land area, also harbour all sort of pathogenic micro-organisms. Contaminants from these dumping sites often get into contact with the water table through leaching. Ten years after the construction of the boreholes, signs of serious groundwater contamination appeared in 18% of the supply wells in the region, in terms of chemical and biological (bacteriological) composition. Ironically, these same wells were among the boreholes that were initially of good quality. This result therefore explains the incessant outbreaks of diarrhoea in some of the towns in the basin.

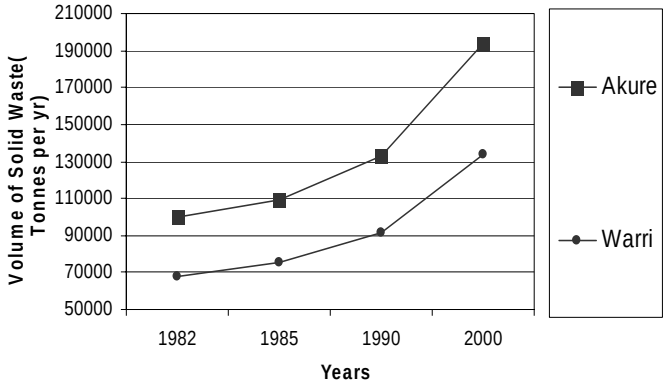


Fig. 5 Growing trend of solid waste generation in the Benin-Owena River basin area.

CONCLUSION AND RECOMMENDATIONS

The high evaporative demand observed over the basin due to rising temperature (0.37°C/decade) caused by changing climate portents danger to the available water resources of the region and a serious threat to the attainment of water security of the region. Also, the increase of intense rainfall of short duration due to observed climatic variations may have been responsible for the perennial ecological problems (flooding and sediment erosion) frequently experienced in the basin. Re-assessment of the quality of the existing borehole after 10 years showed that some have lost their initial good qualities, due to urbanization and increasing population coupled with poor sanitation systems, increasing use of nitrate fertilizers by farmers and change in land-use patterns. Therefore, for groundwater exploitation, determination of an optimum operating policy should be given high priority to take care of the following questions; (a) Where should the wells be located? (b) How many wells are actually needed? (c) How much should be pumped from each well and when? Due to the low travel velocity of groundwater, contamination may not be detected in real time and when detected rehabilitation may either be impossible or very costly. Also adequate sanitation systems should be put in place to meet up with the increasing population growth of the basin, so that domestic sewage and solid wastes can be properly disposed. Proper monitoring is one essential activity in the process of groundwater protection that must also be put in place.

REFERENCES

Gbuyiro, S. O. & Aisiokuebo, N (2003) Climate change in Nigeria—Its reality, expectations and impacts. In: *Proc. International Symposium on Climate Change* (March–April, 2003, China), 238–240. *WMO/TD no. 1172.*

Obasi, G. O. P. (2003) Climate Change and Food Sustainability in Africa. (Keynote address presented at the Regional Conference on Climate Change and Food Sustainability in the 21st Century, Organized by the Nigerian Meteorological Society in collaboration with the Nigerian Meteorological Agency.

Okpara, J. N. *et al*. (2004) Effects of land use intensity and groundwater pollution in the North of Benin–Owena River Basin and its implications for integrated management. Freshwater: Sustainability with Uncertainty Workshop (W7) at VIIth IAHS Scientific Assembly, Foz do Iguacu, Brazil April, 2005.

Udoeka, E. D. (1998) Recent flow regime of Niger: evidence of climate change. In: *Proc. Second International Conference on Climate and Water* (Espoo, Finland, 17–20 August, 1998), vol.1, 410–420.

Udoeka, E. D. *et al.* (1998) Water supply in Nigeria: how sustainable is it in the face of climate change? A paper presented at the Second International Conference on water Resources, Environment and Sustainable Development, organized by Nigerian Association of Hydrogeologists,Abuja, Nigeria, 22–26 November, 1998.

WHO (1984) *Drinking Water Standards*. WHO, Geneva, Switzerland.

Climate Variability and Change—Hydrological Impacts (Proceedings of the Fifth FRIEND World Conference held at Havana, Cuba, November 2006), IAHS Publ. 308, 2006.

Uncertainty in climate change impacts on low flows

MARTIJN J. BOOIJ, MARTIJN HUISJES & ARJEN Y. HOEKSTRA

Water Engineering and Management, Faculty of Engineering Technology, University of Twente, PO Box 217, 7500 AE Enschede, The Netherlands

m.j.booij@utwente.nl

Abstract It is crucial for low flow management that information about the impacts of climate change on low flows and the uncertainties therein becomes available. This has been achieved by using information from different Regional Climate Models for different emission scenarios to assess the uncertainty in climate change for the River Meuse in Northwestern Europe. A hydrological model has been used to simulate low flows for current and changed climate conditions. The uncertainty in the hydrological model is represented by the uncertainty in its parameters. Climate change results in an increase of the average annual discharge deficit (a low flow measure) of about 2.6 10^8 m^3 or 35%. This impact is considerable, resulting in an increase of water shortages in the Meuse basin during low flow periods. The uncertainty in this impact is about 10% as a result of uncertainties in climate change and HBV parameters, and does not disguise the climate change signal.

Key words climate change; discharge deficit; fuzzy objective function; HBV model; low flows; Meuse basin; Monte Carlo analysis; Regional Climate Model; uncertainty

INTRODUCTION

Water management in Western Europe often focuses on water levels and discharges during floods. The reason is obvious, since floods determine maximum water levels and therefore chances of inundation. The focus on floods is partly forced by the fact that, in future, higher and more frequent floods are expected as a result of climate changes (e.g. Arnell, 1999; Middelkoop *et al*., 2001; Booij, 2005). However, climate changes are also expected to lead to drier summers in Western Europe (e.g. Schär *et al.*, 2004). Consequently, low flows in rivers may become more frequent in future, although Hisdal *et al*. (2001) have shown that drought conditions in Europe in general have not become more severe or frequent in the last century. They based their findings on daily stream-flow records of more than 600 stations in Europe. Low flows, occurring during dry periods, may result in several types of problems to society, e.g. lack of water for drinking water supply, irrigation, industrial use and power production, hindrance to navigation and deterioration of water quality. Facing these problems, it is crucial for low flow management that information about the impacts of climate change on low flows and the uncertainties therein becomes available.

Smakhtin (2001) states that despite the obvious importance of the issue of climate change impacts on low flows, the literature specifically investigating such effects is relatively scarce at present. An example of a paper using historical flow records is Arnell (1989). However, Arnell concluded that the approach of using flow records from the past as a reasonable model for the future is unrealistic. A combination of climate change scenarios and hydrological models seems to be more promising, such as Wilby *et al*. (1994) and Querner *et al*. (1997). This enables the assessment of impacts of changing spatial and temporal climate patterns on low flows, where usually impacts of changes in mean temperature and precipitation on hydrological behaviour are determined. Middelkoop *et al*. (2001) found a decrease of summer low flows for the Rhine basin of 5–15% for 2050 using a monthly water balance model and results from two Global Climate Models (GCMs). Other studies, using the conceptual hydrological model HBV (Bergström, 1995) and (downscaled) GCM results, found decreases in summer discharges in Europe as well. For the Mulde basin in Germany, this is caused by an increased simulated evapotranspiration (Menzel & Bürger, 2002) and for six Swedish basins, this is due to both an increased evapotranspiration and a shift of snowmelt from spring to winter (Andréasson *et al.*, 2004). Assessments of climate change impacts on low flows using results from Regional Climate Models (RCMs) are even more scarce than those using GCM results. An example is the climate impact study of Payne *et al.* (2004) on water resources of the Columbia River basin in the USA and Canada.

A cascade of uncertainty sources is present in this climate impact assessment ranging from uncertainties about future greenhouse gas emissions and responses of the global climate models to uncertainties in regional climatic effects, physical catchment characteristics and hydrological models.

Copyright © 2006 IAHS Press

The uncertainty sources in emissions and climate models can be aggregated and represented by scenarios for future radiative forcing for different global climate models (Carter *et al*., 1999). The uncertainty sources in the hydrological model can be grouped into model input uncertainty (including uncertainties from emissions and climate models), model parameter uncertainty and model structure uncertainty. Numerous studies have assessed these different uncertainties, for emissions and climate models (e.g. Visser *et al*., 2000), as well as for hydrological models (e.g. Uhlenbrook *et al*., 1999). However, only a few attempts have been made to evaluate the whole uncertainty cascade associated with the impact of climate change on low flows, a notable one being Wilby (2005) for the River Thames in the UK.

Therefore, the objective of this study is to assess the uncertainty in impacts of climate change on low flows in the River Meuse in Northwestern Europe. This objective is achieved by first assessing climate change and its uncertainty for the study area. Next, an existing hydrological model is calibrated and validated and uncertainty sources in the hydrological model quantified. The different uncertainty sources are propagated through the hydrological model using Monte Carlo simulation. Finally, results are discussed and conclusions are drawn.

METHODOLOGY AND DATA

Climate change and uncertainty

Changes in climate variables relevant for low flow, in particular precipitation and temperature, are assessed using observed station data and results from Regional Climate Models (RCMs) for different greenhouse gas emission scenarios. The RCM results have been obtained from the EU-project PRUDENCE (Christensen *et al*., 2002) in which 10 different RCMs for two different IPCC emission scenarios (A2 and B2), different driving GCMs and different samples have been compared. The uncertainty in the climate change projections of climate variables (input uncertainty of hydrological model) is therefore assumed to be mainly the result of different emission scenarios, sampling errors, different boundary forcing by GCMs and different RCMs. The uncertainty in future emissions is underestimated by using results of only the two scenarios A2 (Medium–High emissions) and B2 (Medium–Low emissions), i.e. the difference in the global mean temperature in 2100 as a result of scenarios A2 and B2 is about 1.1°C compared to 2.6°C for the two most extreme scenarios (IPCC, 2001). The uncertainty in changed climate variables (temperature and precipitation) is captured in Gaussian probability distributions for relevant statistics of these variables based on Déqué (2004) and Christensen (2004). In the uncertainty analysis, statistics are randomly drawn from these probability distributions and used to transform current and changed climate series using the change factor (CF) method. The CF method calculates climate series by adding (temperature) or multiplying (precipitation) climate information from the RCMs to observed time series (see e.g. Middelkoop *et al*., 2001).

Hydrological modelling and uncertainty

The conceptual hydrological model HBV (Bergström, 1995), lumped for each of the 15 sub-basins in the Meuse basin upstream of Borgharen with a daily time step, is used to simulate hydrological behaviour in general and low flows in particular for current and changed climate conditions. This model (HBV-15) has originally been applied to high flow simulation in the Meuse basin by Booij (2005). To improve low flow simulation as well, HBV-15 has been re-calibrated for current climate conditions using a fuzzy measure as an objective function (as in e.g. Seibert, 1997). This fuzzy measure combines several objective functions for low flow simulation (e.g. modelling error in discharge deficit) and simulation of the discharge regime (e.g. Nash-Sutcliffe coefficient). Fuzzy logic allows the handling of the concept of a partial truth value between completely truth and completely false. Validation of the model is done for a different period (1985–1996) to the calibration period (1970–1984).

The uncertainty in the hydrological model is represented by the uncertainty in its parameters. Through consideration of this parametric uncertainty, model structure related uncertainties are not explicitly taken into account. However, these are assumed to be at least partly covered by the parametric uncertainty. In the same manner as for the climate variables, in the uncertainty analysis,

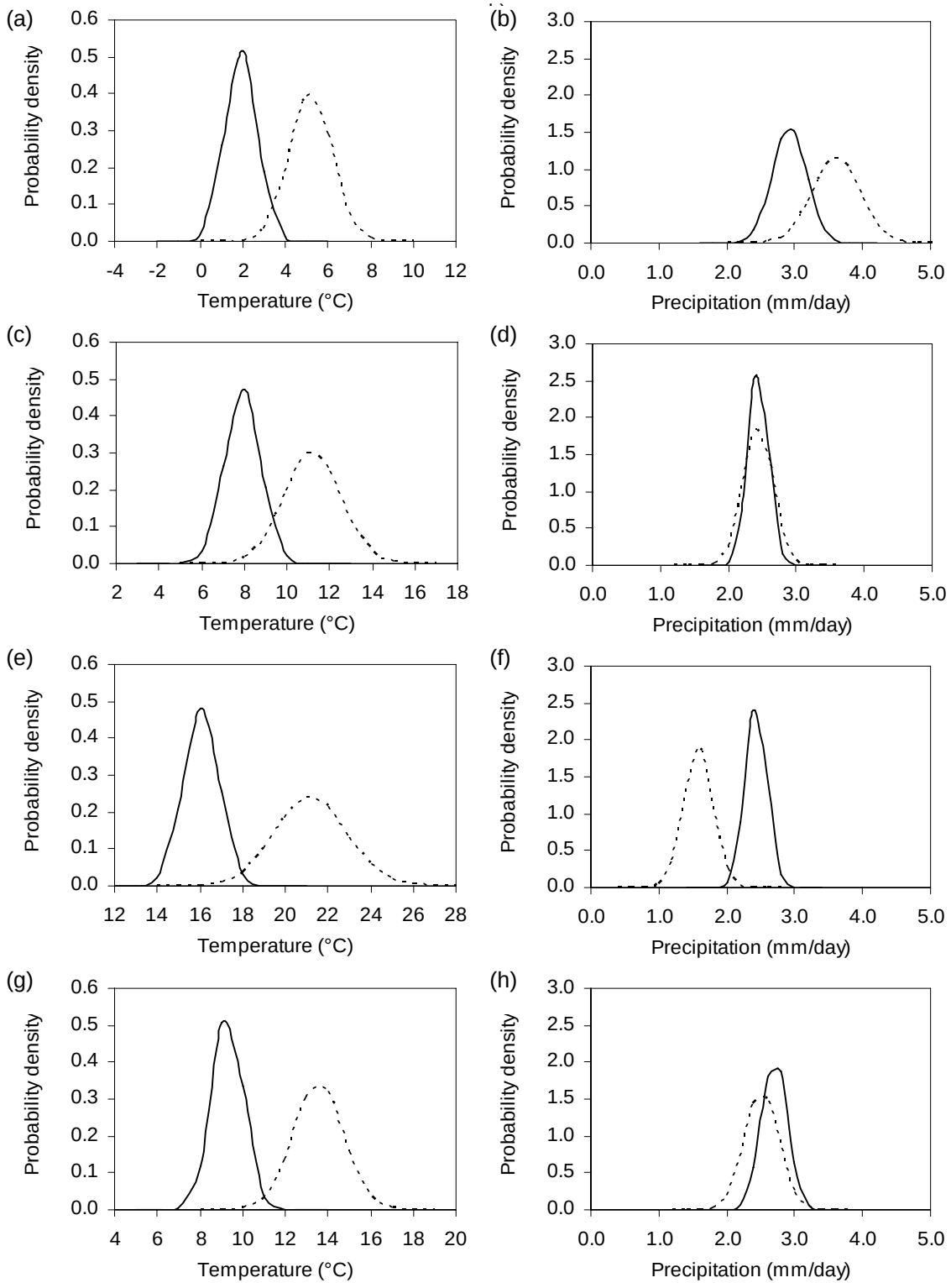


Fig. 1 Probability density functions as a result of different uncertainty sources for current climate (solid) and changed climate (dotted) for DJF (a), MAM (c), JJA (e) and SON (g) temperature (°C), and DJF (b), MAM (d), JJA (f) and SON (h) precipitation (mm day^{-1}).

values for HBV parameters are randomly drawn from uniform probability distributions of these parameters. The HBV parameters are assumed to have the same relative uncertainty range (expressed relative to their means) of 25% (mean value ±12.5%).

Uncertainty analysis

The different uncertainty sources (input uncertainties, HBV parameters) are propagated through the HBV model using Monte Carlo analysis. This finally results in a probability distribution of low flows for current and changed climate conditions. This enables an assessment of the significance of changes in low flow conditions with climate change by comparing changes and uncertainties. Low flows are described by the average annual discharge deficit. The discharge deficit is the cumulative shortage of water with respect to a certain threshold important for river functions like agriculture and drinking water supply. The threshold chosen is 100 $m^3 s^{-1}$ (45% of the mean discharge at Borgharen) corresponding to the starting phase for water allocation measures in the Netherlands and Belgium.

RESULTS AND DISCUSSION

Climate change and uncertainty

Figure 1 shows the probability density functions of basin averaged temperature and precipitation as a result of different uncertainty sources for the current (1970–1996) and changed (2071–2100) climate for DJF (December–January–February), MAM (March–April–May), JJA (June–July–August) and SON (September–October–November). The results show an average increase in annual temperature of 4.0°C for climate change conditions varying between 3.3°C in DJF and 5.1°C in JJA. Precipitation decreases slightly by 2.5% on an annual basis varying between +24% in DJF and –35% in JJA. Uncertainties with climate change (expressed as standard deviation) vary between 1.0°C in DJF and 1.7°C in JJA for temperature and 8.9% in MAM and 13.4% in JJA for precipitation. Uncertainties in these climate variables for current conditions (1971–2000) are somewhat (30–50%) smaller, because emission scenario uncertainties do not apply. In general, changes in temperature seems to be significant for all seasons and changes in precipitation seem to be only significant for winter (DJF) and summer (JJA) taking into account the uncertainty in these variables as a result of different emission scenarios, different RCMs, different boundary forcing by GCMs and sampling.

Hydrological modelling

Results of the HBV model calibration show good performance for low flow as well as for average and high flow simulation using the fuzzy measure. Nash-Sutcliffe coefficients for different sub-basins of the Meuse are between 0.80 and 0.90 and over 0.90 for the complete basin showing a slight improvement with respect to Booij (2005). Differences between observed and simulated discharge deficits are less than 5%. Figure 2 gives an illustration of the calibration results using a fuzzy objective function. It shows dotty plots of values of HBV parameters *FC* (affecting both low and high flow conditions), *ALFA* (primarily affecting high flow conditions) and *PERC* (affecting low flow conditions) against the Nash-Sutcliffe coefficient and the fuzzy measure when varying all other relevant HBV parameters randomly at the same time. For all parameters together, the identifiability has increased using this fuzzy measure with considerable improvements for parameters affecting low flows (e.g. *PERC*, see Fig. 2) and slight deteriorations for parameters primarily affecting high flows (e.g. *ALFA*). Validation results are slightly better than calibration results due to the better data quality for the validation period as has been observed by Booij (2005) as well.

Impacts of climate change on low flows and uncertainty

Combining RCM and HBV results enables an assessment of climate change impacts on low flows and related uncertainties. Figure 3 shows probability density functions of the average annual discharge deficit for the current and changed climate. Climate change results in an increase of the average annual discharge deficit of about 2.6×10^8 m^3 or 35%. This increase is caused by both a decrease of precipitation, in particular in JJA and in SON, and an increase of temperature and related evapotranspiration all year round. The uncertainty in this impact (expressed as standard deviation) is about 0.9×10^8 m^3 as a result of uncertainties in climate change, 0.2×10^8 m^3 as a result of uncertainties in HBV parameters and 1.0×10^8 m^3 as a result of both. For current climate

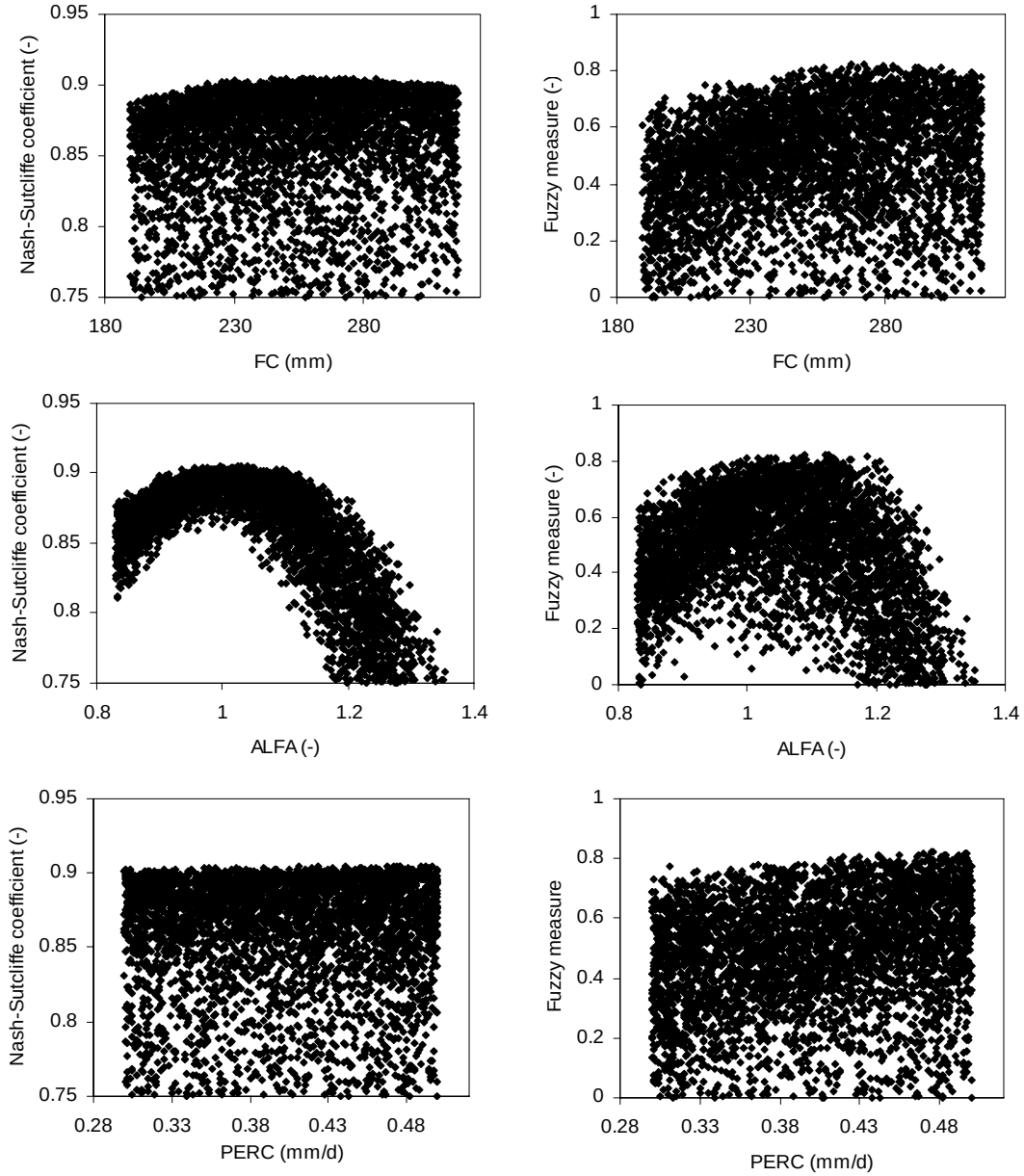


Fig. 2 Dotty plots of the Nash-Sutcliffe coefficient (left) and fuzzy measure (right) for HBV parameters FC (mm), ALFA (–) en PERC (mm).

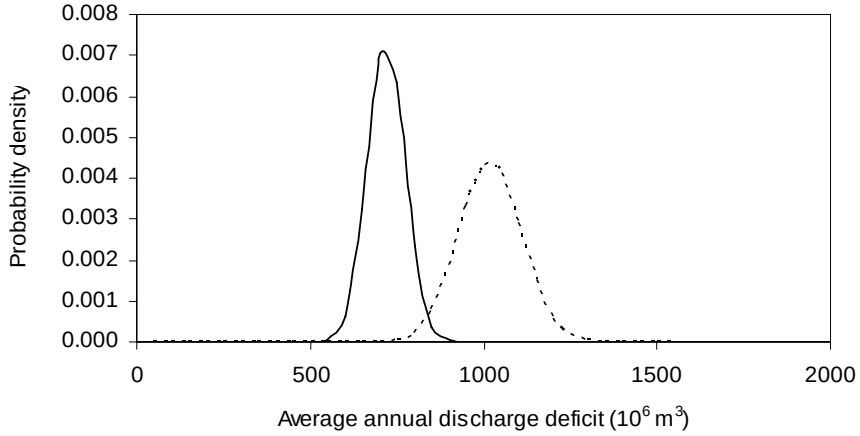


Fig. 3 Probability density functions of the average annual discharge deficit (10^6 m^3) as a result of different uncertainty sources for current climate (solid) and changed climate (dotted).

conditions, these uncertainties are about 0.5×10^8 m^3, 0.2×10^8 m^3 and 0.6×10^8 m^3 respectively. Relative uncertainties of discharge regime variables (with respect to their means) like the standard deviation of daily discharges have a similar magnitude (5–15%).

CONCLUSIONS

It thus can be concluded that the impacts of climate change on low flows are considerable resulting in an increase of water shortages in the Meuse basin during low flow periods. Uncertainties in these impacts are large, although not disguising the climate change signal. These uncertainties are mainly the result of uncertainties in climate variables and to a smaller extent due to uncertainties related to the hydrological model. It is expected that uncertainties in phenomena occurring at low frequencies with climate change will be considerably larger than the uncertainties in relatively frequent-occurring phenomena investigated here (discharge deficit, daily variability).

Acknowledgements The daily station climatological data for Belgium and for France have been provided by respectively Luc Debontridder from the KMI (Belgian Royal Meteorological Institute) and Christophe Dehouck from Météo France. Eric Sprokkereef of RIZA and Joop Gerretsen of Rijkswaterstaat Limburg made the discharge data available.

REFERENCES

Andréasson, J., Bergström, S., Carlsson, B., Graham, L. P. & Lindström, G. (2004) Hydrological change—climate change impact simulations for Sweden. *AMBIO* **33**, 228–234.

Arnell, N. W. (1989) Changing frequency of extreme hydrological events in northern and western Europe. In: *FRIENDS in Hydrology* (ed. by L. Roald, K. Nordseth & K. A. Hassel), 237–249. IAHS Publ. 187. IAHS Press, Wallingford, UK.

Arnell, N. W. (1999) Climate change and global water resources. *Global Environ. Change* **9**, 31–49.

Bergström, S. (1995) The HBV model. In: *Computer Models of Watershed Hydrology* (ed. by V. P. Singh), 443–476. Water Resources Publications, Highlands Ranch, Colorado, USA.

Booij, M. J. (2005) Impact of climate change on river flooding assessed with different spatial model resolutions. *J. Hydrol.* **303**, 176–198.

Carter, T. R., Hulme, M. & Lal, M. (1999) Guidelines on the use of scenario data for climate impact and adaptation assessment. Version 1. IPCC-TGCIA, Norwich, UK. http://ipcc-ddc.cru.uea.ac.uk/guidelines/guidance.pdf.

Christensen, J. H. (2004) Prediction of regional scenarios and uncertainties for defining European climate change risks and effects (PRUDENCE). PRUDENCE Working Document. http://prudence.dmi.dk/public/publications/countries-seasonal.pdf.

Christensen, J. H., Carter, T. & Giorgi, F (2002) PRUDENCE employs new methods to assess European climate change. *EOS, Trans. Am. Geophys. Un.* **83**, 147.

Déqué, M. (2004) Uncertainties in PRUDENCE simulations: Global high resolution models. PRUDENCE deliverable D1A5. http://prudence.dmi.dk/public/publications/D1A5.pdf.

Hisdal, H., Stahl, K., Tallaksen, L. M. & Demuth, S. (2001) Have streamflow droughts in Europe become more severe or frequent? *Int. J. Climatol.* **21**, 317–333.

Menzel, L. & Bürger, G. (2002) Climate change scenarios and runoff response in the Mulde catchment (Southern Elbe, Germany). *J. Hydrol.* **267**, 53–64.

Middelkoop, H., Daamen, K., Gellens, D., Grabs, W., Kwadijk, J. C. J., Lang, H., Parmet, B. W. A. H., Schädler, B., Schulla, J. & Wilke, K. (2001) Impact of climate change on hydrological regimes and water resources management in the Rhine basin. *Climatic Change* **49**, 105–128.

Payne, J. T., Wood, A. W., Hamlet, A. F., Palmer, R. N. & Lettenmaier, D. P. (2004) Mitigating the effects of climatic change on the water resources of the Columbia River basin. *Climatic Change* **62**, 233–256.

Querner, E. P., Tallaksen, L. M., Kasparek, L. & Lanen, H. A. J. van (1997) Impact of land-use, climatic change and groundwater abstractions on streamflow droughts using physically-based models. In: *FRIEND'97 – Regional Hydrology: Concepts and Models for Sustainable Water Resources Management* (ed. by A. Gustard *et al.*), 171–179. IAHS Publ. 246. IAHS Press, Wallingford, UK.

Schär, C., Vidale, P. L., Lüthi, D., Frei, C., Häberli, C., Liniger, M. A. & Appenzeller, C. (2004) The role of increasing temperature variability in European summer heatwaves. *Nature* **427**, 332–336.

Seibert, J. (1997) Estimation of parameter uncertainty in HBV model. *Nordic Hydrol.* **28**, 247–262.

Smakhtin, V. U. (2001) Low flow hydrology: a review. *J. Hydrol.* **240**, 147–186.

Uhlenbrook, S., Seibert, J., Leibundgut, C. & Rodhe, A. (1999) Prediction uncertainty of conceptual rainfall–runoff models caused by problems in identifying model parameters and structure. *Hydrol. Sci. J.* **44**, 779–797.

Visser, H., Folkert, R. J. M., Hoekstra, J. & Wolff, J. J. de (2000) Identifying key sources of uncertainty in climate change projections. *Climatic Change* **45**, 421–457.

Wilby, R. L. (2005) Uncertainty in water resource model parameters used for climate change impact assessment. *Hydrol. Processes* **19**, 3201–3219.

Wilby, R., Greenfield, B. & Glenny, C. (1994) A coupled synoptic-hydrological model for climate change impact assessment. *J. Hydrol.* **153**, 265–290.

Climate Variability and Change—Hydrological Impacts (Proceedings of the Fifth FRIEND World Conference held at Havana, Cuba, November 2006), IAHS Publ. 308, 2006.

Climate change impact on reservoir water supply reliability

DANA HALMOVA & MARIAN MELO

1 *Institute of Hydrology, Slovak Academy of Sciences, Racianska 75, 838 11 Bratislava, Slovakia*
halmova@uh.savba.sk

2 *FMPI Comenius University Bratislava, Mlynska dolina, 842 48 Bratislava, Slovakia*

Abstract Climate is changing gradually as a result of the increased greenhouse effect. Changed climate conditions affect many processes within the landscape and many spheres of our life can thus be influenced. In this contribution, we study the ability of water reservoirs to ensure a required water demand under changed climate conditions. The aim of the first part was to prepare regional scenarios of air temperature and precipitation for some meteorological stations in eastern Slovakia under the assumption of an enhanced greenhouse effect according to two climate models. Reservoir water supply reliability was calculated using the water balance model "WBMOD" that works with a monthly time step. The input data series of precipitation and air temperature and the observed reservoir outflows were used to express the expected changes in the total runoff and the required reservoir capacity. Failures in the required water supply both in volume and in time were evaluated for changed climate conditions.

Key words climate change; climate scenarios; water reservoir; water supply; reliability

CLIMATE SCENARIOS FOR THE LABOREC RIVER BASIN

In this contribution we utilise data from two coupled general circulation models from two World Climate Centres: CCCM2000 (with the IPCC "IS92a" forcing scenario) and GISS1998. CCCM2000 is the second generation coupled global climate model of the Canadian Centre for Climate Modelling and Analysis in Victoria, BC. The atmospheric component is a spectral model with T32 truncation and 10 unequally spaced vertical levels, forced with the 1900 to 2100 greenhouse gases concentrations and aerosol loadings. The ocean component is a grid-point model with 1.875° resolution and 29 vertical levels, based on the GFDL MOM1.1 code (Flato & Boer, 2001). GISS1998 is the coupled atmosphere–ocean model from the Goddard Institute for Space Studies in New York. Model simulations (1990–2099) are compounded by the 1% per year CO_2 increase experiment with tropospheric sulfate aerosol changes. The model contains the monthly and annual values of more than 50 climate variables (Russell & Rind, 1999).

The effect of climate change on hydrological processes varies regionally and between climate scenarios, largely following projected changes in precipitation. Demand for water is generally increasing due to population growth and economic development, but is falling in some countries because of increased efficiency of use. Climate change is unlikely to have a big effect on water demands in general, but may substantially affect irrigation withdrawals, which depend on the extent to which the increase of evaporation is offset or exaggerated by changes in precipitation. Higher temperatures, hence higher crop evaporative demand, mean that the general tendency would be towards an increase in irrigation demands. Water resource management techniques can be applied to adapt to the hydrological effects of climate change, so as to lessen vulnerabilities (IPCC, 2001). Utilization of climate models is the most physically plausible method of deriving regional climate change scenarios (Lapin & Melo, 2004).

Method

We utilize model data from the CCCM2000 model, from the GISS1998 model and data from the Slovak Hydrometeorological Institute in Bratislava (SHMI).

The present horizontal resolution of GCMs does not allow us to identify regional climate features. Therefore, we use a statistical method for downscaling of GCMs outputs. Statistical downscaling consists of developing statistical relationships between locally observed climate variables and outputs of global GCM experiments. In both cases (CCCM and GISS) we take into account model outputs from four grid points near to eastern Slovakia. Interpolation is then used to transfer the information from these grid points to the considered locality, the weights being

Copyright © 2006 IAHS Press

proportional to the distance between the two. These calculations are repeated for the time horizon 1971–1997 and for future time horizons 2030 (2016–2045) and 2075 (2061–2090). We have elaborated the scenarios of air temperature change and precipitation change between these periods in the form of either differences (air temperature) or quotients (precipitation). We use mean monthly values of both climatic elements. Climate scenarios in the case of air temperature have been prepared for three meteorological stations, and in case of precipitation for seven meteorological stations near the Vihorlat reservoir.

Results

The results achieved by both climate models are different, mainly as regards precipitation. According to both climate models (Figs 1 and 2), we can anticipate that air temperature will increase throughout the year during the twenty-first century. The CCCM2000 model projects a greater increase in air temperature for eastern Slovakia in this century. In the first period studied, 2016–2045, this increase is about 0.9°C for the GISS and about 2.0°C for the CCCM. In the next period (2061–2090), and in comparison with the contemporary state (1971–1997), this increase is about 2.3°C for the GISS and about 3.6°C for the CCCM. Selected results of atmospheric precipitation scenarios are presented in Figs 3 and 4. In the case of CCCM2000, an increase of precipitation is projected for the winter period (October–March)—approximately 12% in 2016–2045 and 22% in 2061–2090 in comparison with 1971–1997—and in the summer period (April–September), a decrease in precipitation is projected; approximately 19% in 2016–2045 and about 15% in 2061–2090 in comparison with 1971–1997. In the case of GISS1998, an increase in precipitation during the winter is projected, about 10% in 2016–2045 and 30% in 2061–2090 in comparison with 1971–1997, and in the summer precipitation amounts are approximately without change in both studied periods of the twenty-first century, in comparison with 1971–1997.

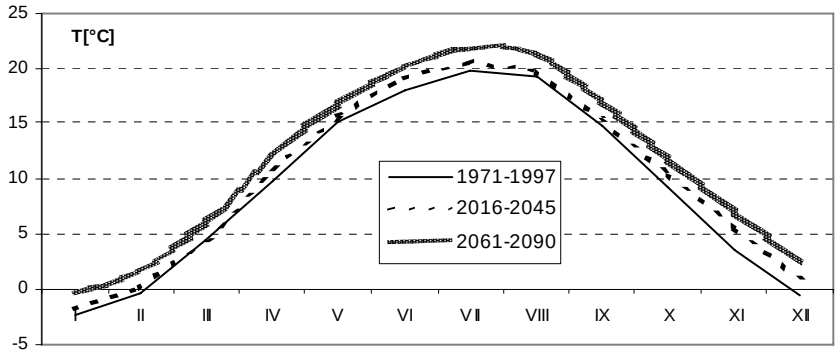


Fig. 1 Annual course of air temperature (°C) at Michalovce station in 1971–1997 and according to the CCCM2000 model for the periods 2016–2045 and 2061–2090.

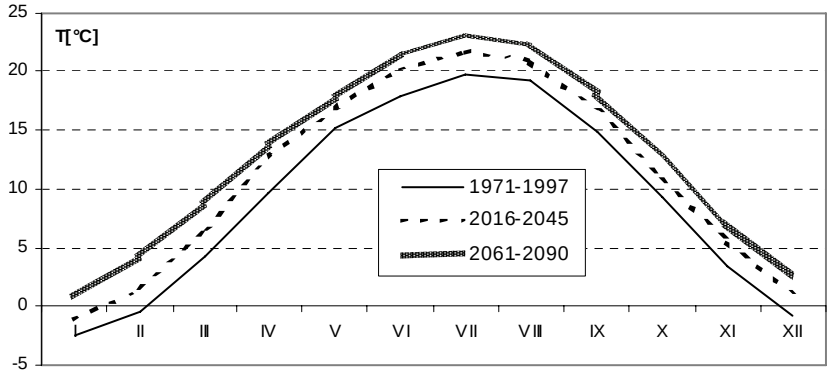


Fig. 2 Annual course of air temperature (°C) at Michalovce station in 1971–1997 and according to the GISS1998 model for the periods 2016–2045 and 2061–2090.

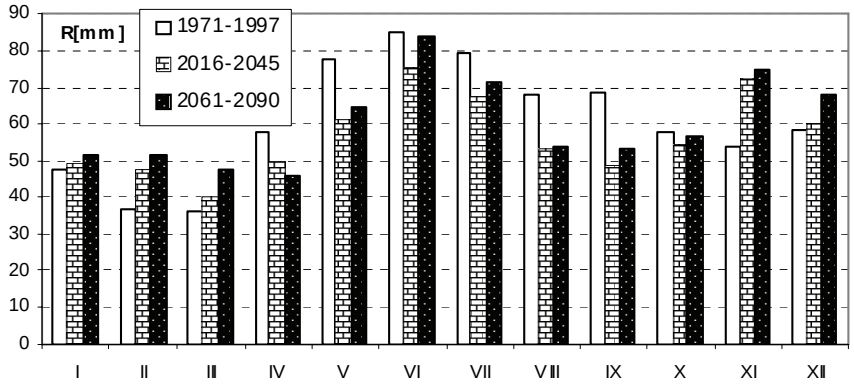


Fig. 3 Annual course of precipitation amount (mm) in Vinne station in 1971–1997 and according to CCCM2000 model in periods 2016–2045 and 2061–2090.

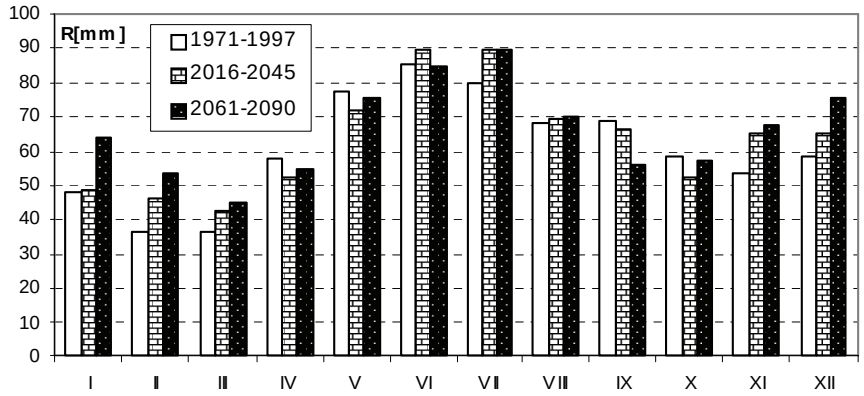


Fig. 4 Annual course of precipitation amount (mm) in Vinne station in 1971–1997 and according to GISS1998 model in periods 2016–2045 and 2061–2090.

UTILIZATION OF HYDROLOGICAL MODELS WITH MONTHLY TIME STEPS

Water balance models with monthly time steps are appropriate tools for the investigation of projects dealing with water supply. The calibration of these models is easier than for models with shorter time steps, as is access to the required input data. Monthly hydrological forecasting would be used for real time operations for irrigation or energy generation.

Xu & Vandewiele (1995) have presented an example of the application of the monthly water balance model. They used this type of model for runoff forecasting and for developing proposals for systems and their operation in water management. Some hydrological models were used for the detection of climate change impact on water resources (Gleick, 1986; Schaake & Liu, 1989; Arnell, 1992). Gleick explored different approaches for determining the impact of climate change on regional hydrology. Schaake & Liu developed and used simple monthly water balance models to determine a relationship between climate change and water reservoirs. Several papers from the Czech Republic as well as from Slovakia demonstrate that the impact of expected climate change on water reservoir management would be fairly negative (Nacházel *et al*., 1995).

Water balance model WBMOD with monthly time step

The WBMOD model uses average monthly data on basic runoff components as well as the models mentioned above. Precipitation is divided into snowfall (in the upper part of the catchment) and rainfall (in the lower part of the catchment). Rainfall is accumulated in soil storage that is reduced by actual evapotranspiration, fast runoff of groundwater and slow runoff of groundwater. The WBMOD model is based on a water balance model that was developed at the Vrije Universiteit Brussel – Hydrologie and its basic equations and structure have been described in several papers (Xu, 1995). The applied calculation technique “RESERVOIR” was developed by Halmova (2005).

Method

The Vihorlat Reservoir is located in the East Slovakia Lowland (ESL), which is a plain within the Bodrog River basin in Slovakia, 2000 km^2 in area. The reservoir was constructed as a part of the water management measures in the ESL and was put into operation in 1965. Its total storage capacity is 334 000 000 m^3, flood control storage is 100 000 000 m^3, useful storage is 177 000 000 m^3 and permanent storage is 57 000 000 m^3.

Input data for the WBMOD model are average monthly discharge at the water level gauging station, monthly precipitation totals for raingauge stations and monthly average temperatures from stations for the period 1971–1997. The operating rules for the reservoir are designed to account for the considerable variability in its outflow, which is why interest in this project focused on the historical outflow for the period 1971–1997 and the impact that changed climate conditions might have had on these flows.

Chronological series of real historical withdrawals from the reservoir were not readily available. Therefore, these were derived from records of continuous water balance and regularly registered time series of water storage at the beginning and end of the each month. Monthly outflow series from the Vihorlat Reservoir during reservoir operation were calculated using these two data sources. Series of changed Laborec River inflows, derived from climate scenarios CCCM2000 and GISS1998 were combined with various minimum operational reservoir water levels and compared with the real chronological series, which represents a historical target. Each individual alternative scenario was compared with the target mentioned above and expressed as a time series of water supply deficits; failures (periods with lower water supply than required), total reliability of the supplied water in terms of volume in mm; and total reliability in terms of the number of days when the demand was met.

Results and conclusions

The reservoir inflow changes are introduced in two runoff scenarios for the Laborec-Humenne gauge and for two time horizons: 2030 and 2075. Outputs from the WBMOD model are denoted as C/G1X and C/G2X (C/G – CCCM2000/GISS1998; 1: time horizon 2030; 2: time horizon 2075; X: alternative model run). Several alternatives model runs (A–E, M) were executed, each with several initial conditions of the reservoir water levels. Water storage was constrained to be between specified minimum and maximum operating water level. Initial and boundary conditions shown in Table 1 are quantified at 10^6 m^3 above minimum operating level and above dead storage capacity. Initial and boundary conditions are STMA – maximal operating storage in water reservoir; STMIL – minimal accepted operating storage during summer months V.–IX.; STMIZ – minimal accepted operating storage during winter months X.–IV.; and SVZPO – initial volume of water stored in the reservoir at the beginning of each model run.

Table 1 Initial and boundary conditions of water reservoir Vihorlat.

Alternative scenarios	Operation water level at STMIL storage (m a.s.l.)	STMA (10^6 m^3)	STMIL (10^6 m^3)	STMIZ (10^6 m^3)	SVZPO (10^6 m^3)
C/G-M1	107.39	177.0	0.0	0.0	0.0
C/G-M2	107.39	177.0	0.0	0.0	0.0
C/G-1A	113.9	177.0	177.0	40.4	40.4
C/G-1B	113.0	177.0	149.1	39.7	39.7
C/G-1C	111.0	177.0	92.7	39.7	39.7
C/G-1D	109.0	177.0	39.7	39.7	39.7
C/G-1E	108.0	177.0	14.6	14.6	14.6
C/G-2A	113.9	177.0	177.0	40.4	40.4
C/G-2B	113.0	177.0	149.1	39.7	39.7
C/G-2C	111.0	177.0	92.7	39.7	39.7
C/G-2D	109.0	177.0	39.7	39.7	39.7
C/G-2E	108.0	177.0	14.6	14.6	14.6

Table 2 Reliability of the given water supply in volume (ZZS) and in duration of non-failure operation (ZZT) for time horizon 2030 and 2075 and scenarios CCCM2000 and GISS1998.

Time horizon 2030			Time horizon 2075		
Alternative scenarios	ZZS	ZZT	Alternative scenarios	ZZS	ZZT
CCCM-1M	0.982	0.963	CCCM-2M	0.975	0.960
CCCM-1A	0.798	0.764	CCCM-2A	0.794	0.761
CCCM-1B	0.879	0.851	CCCM-2B	0.873	0.851
CCCM-1C	0.962	0.966	CCCM-2C	0.957	0.950
CCCM-1D	0.971	0.957	CCCM-2D	0.966	0.957
CCCM-1E	0.978	0.960	CCCM-2E	0.972	0.957
GISS-1M	0.996	0.994	GISS-2M	0.996	0.991
GISS-1A	0.873	0.854	GISS-2A	0.856	0.835
GISS-1B	0.938	0.941	GISS-2B	0.927	0.935
GISS-1C	0.983	0.991	GISS-2C	0.981	0.988
GISS-1D	0.987	0.988	GISS-2D	0.985	0.984
GISS-1E	0.992	0.991	GISS-2E	0.993	0.991

Table 3 Total required water supply volume ZST, total failures in water supply volume ZS (mm), total time period ZTT and time period with non-ensured water supply ZT (day) during 27-years of simulation.

Alternative scenarios	ZST (mm) 1971–1997	ZS (mm) CCCM2000	ZS (mm) GISS1998	ZTT (day) 1971–1997	ZT (day) CCCM2000	ZT (day) GISS1998
C/G-M1	6227.6	115	25.8	9855	366	61
C/G-1A	6227.6	1259.1	789.1	9855	2328	1439
C/G-1B	6227.6	752.7	388.4	9855	1469	579
C/G-1C	6227.6	233.8	104	9855	334	91
C/G-1D	6227.6	182.8	82.8	9855	427	122
C/G-1E	6227.6	136	46.8	9855	396	92
C/G-M2	6227.6	154	25.2	9855	397	92
C/G-2A	6227.6	1284.3	894.9	9855	2357	1622
C/G-2B	6227.6	787.9	452.6	9855	1470	671
C/G-2C	6227.6	266.7	119.5	9855	488	122
C/G-2D	6227.6	211	90.5	9855	427	153
C/G-2E	6227.6	154	46.2	9855	488	92

Listed in Table 2 is the calculated reliability of the reservoir to secure a given water supply, namely the historical water withdrawals from the reservoir during the period 1971–1997. This is expressed in terms of volume of water stored (ZZS) and in terms of the duration of successful operation (ZZT) for each particular alternative. These alternatives (C/G1A–E, C/G2A–E) differ in minimum allowed summer water level (STMIL), which is related to the recreational purpose of the Vihorlat Reservoir. Minimum summer water levels are related to increased risk in supply of a given water volume. From the relationship between reliability of the water supply and minimum summer operating water level, it is obvious that, unless summer water levels rise above the water level 111.0 m a.s.l., the reliability of the water supply from the reservoir will be considerably reduced. Even in the case of the minimum water level limit in summer operating level, 113.94 m a.s.l., the reliability of the water supply over 27 years would be approximately 80%, while during some summer seasons it would be higher.

The total required water supply volume: ZST; total failures in water supply volume: ZS (mm); total time period: ZTT; and the time period with no ensured water supply: ZT (days) during 27-years of simulation for individual alternatives are quantified in Table 3.

The conclusions, which may be drawn from these WBMOD simulations, include the potential of the use of such models for reservoir operations, including those for recreational purposes, and the need for the analysis and development of models for seasonal runoff forecasts. It can also be concluded that, in the particular case of the Vihorlat Reservoir, the possible changes in climate would only have a minor impact on the reliability of the water supply from the reservoir. This

conclusion of course, pertains only for the same level of water supply that was provided during period 1971–1997.

The tool developed can be of use for alternative hypothetical reservoir operation runs with various variants of the water supply regime defined as a time series, and also for case studies for other similar water reservoirs.

Acknowledgement The study was supported by Science and Technology Agency of Slovakia under contract no. APVT-51-017804.

REFERENCES

Alley, W. M. (1992) On the treatment of evapotranspiration, soil moisture accounting, and aquifer recharge in monthly water balance models. *Water Resour. Res.* **20**(8), 1137–1149.

Arnell, N. W. (1992) Factors controlling the effects of climate change on river flow regimes in a humid temperate environment. *J. Hydrol.* **132**, 321–342.

Flato, G. M. & Boer, G. J. (2001) Warming asymmetry in climate change simulations. *Geophys. Res. Lett.* **28**(1), 195–198.

Gleick, P. H. (1986) Methods for evaluating the regional hydrologic impacts of global climatic changes. *J. Hydrol.* **88**, 97–116.

Halmova, D. (2005) Impact of expected climate change on storage volume utilisation of important water reservoirs of the Slovak Republic. PhD Thesis. Slovak Technical University, Bratislava, Slovakia (in Slovak).

IPCC (2001) *Climate Change 2001: Impacts, Adaptation and Vulnerability.* Third Assessment Report of the IPCC. Cambridge University Press, UK.

La`pin, M. & Melo, M. (2004) Methods of climate change scenarios projection in Slovakia and selected results. *J. Hydrol. Hydromech.* **52**(4), 224–238.

Nachazel, K., Prenosilova, E. & Toman, M. (1995) Uncertainty of climate changes and their impact on water resources (in Czech). *J. Hydrol. Hydromech.* **43**(3), 173–196.

Russell, G.L. & Rind, D. (1999) Response to CO_2 transient increase in the GISS Coupled Model: regional coolings in a warming climate. *J. Climate* **12**, 531–539.

Shaake, J. C. & Liu, C. (1989) Development and applications of simple water balance models to understand the relationship between climate and water resources. In: *New Directions for Surface Water Modelling* (ed. by M. L. Kavvas), 343–352. IAHS Publ. 181. IAHS Press, Wallingford, UK.

Xu, C.-Y. & Vandewiele, G. L. (1995) Parsimonious monthly rainfall–runoff models for humid basins with different input requirements. *Adv. Water Resour.* **18**, 39–48.

Xu, C.-Y. (2000) Modelling the effects of climate change on water resources in Central Sweden. *Water Resour. Manage.* **14**, 177–189.

Climate Variability and Change—Hydrological Impacts (Proceedings of the Fifth FRIEND World Conference held at Havana, Cuba, November 2006), IAHS Publ. 308, 2006.

Climate change impacts on water resources in Guyana

KAILAS NARAYAN
Caribbean Institute for Meteorology & Hydrology, Husbands, St. James, Barbados, West Indies
knarayan@cimh.edu.bb

Abstract With climate change and an expected consequent rise in sea level, salt water intrusion into rivers and possible adverse effects on aquifers is a major concern. Guyana is situated on the northeastern coast of South America, has an area of 215 000 square km^2, and a population of about three quarters of a million people more than 90% of whom reside on a narrow coastal strip, less than 10 km from the ocean. The coastal strip is below high tide level of the Atlantic Ocean, is extremely flat, and is protected by a system of dykes that are constructed mainly of concrete and clay. A large number of large rivers flow south to north into the Atlantic Ocean. Water supply for domestic, agricultural and industrial uses is obtained from a combination of ground and surface water sources. In this paper, an attempt is made to analyse situations that could arise as a result of sea level rise. A specific sea level rise of one metre by the end of the century and the impacts of this rise on water resources is investigated. The results indicate that the consequences for the surface water resources could be severe, but not as severe as for the groundwater resources.

Key words contamination; advection; dispersion; stratification; intrusion; aquifer

GENERAL

Guyana lies on the northeastern coast of South America and covers an area of about 215 000 km^2. The vast majority of the 772 755 (1999) people of Guyana live on the narrow coastal strip (approximately 5–15 km wide) between the Pomeroon and Corentyne rivers, where most of the agricultural and industrial activities are concentrated. The climate of Guyana is characterized by high rainfall and humidity, and the narrow range of temperature that is typical of the equatorial region. The annual average rainfall over the country varies between about 3600 mm. and 1600 mm. The seasonal distribution of rainfall is characterized by two rainfall seasons, i.e. May to mid-August and December–January on the coast.

The principal streams (flowing from east to west) which discharge into the Atlantic are the Berbice, Abary, Mahaicony, Mahaica, Demerara, Essequibo, Pomeroon, Waini and Barima rivers.

The coastal artesian basin occupies a total surface area of 20 000 km^2, and is known to contain three main aquifers, the Upper Sands, the "A" Sands and the "B" Sands aquifers, which were described by Gibson (1971).

The Upper Sands is the shallowest of the aquifers. It is found along the coast at a depth varying from 30 to 60 m in an easterly direction, and its thickness correspondingly ranges from about 20 to 150 m. The "A" Sands aquifer underlies the Upper Sands and it is from this aquifer that almost all of the country's domestic water supply is obtained. It varies in thickness from 20 to 60 m and is found at depths ranging from 100 to 300 m. It has a rather high transmissivity of about 2500 m^2 per day. The "B" Sands is the deepest aquifer and extends eastwards from the Demerara River, varying in depth from 400 to 800 m, and in thickness from 20 to 60 m. Its transmissivity is much less than that of the "A" Sands.

Guyana can be divided into the following geomorphologic zones: The Pakaraima Plateau, the Pre-Cambrian Crystallines, the White Sand Series and the Coastal Plain. The sediments of the Coastal Plain together with those of the White Sand Series are referred to as the Coastal sediments. It is their composition and configuration which give rise to the artesian conditions on the coast; such sediments are exploited for the coastal water supply.

SEA WATER INTRUSION INTO RIVERS

The problem

When the freshwater from a river empties into a saline water body (the ocean), the saline water tends to propagate into the river mouth, resulting in contamination of the river in its lower reaches. The density of saline water is higher than that of freshwater; this results in the saline water sliding over the bottom of the river in an upstream direction against the flow of the river. This sea water

Copyright © 2006 IAHS Press

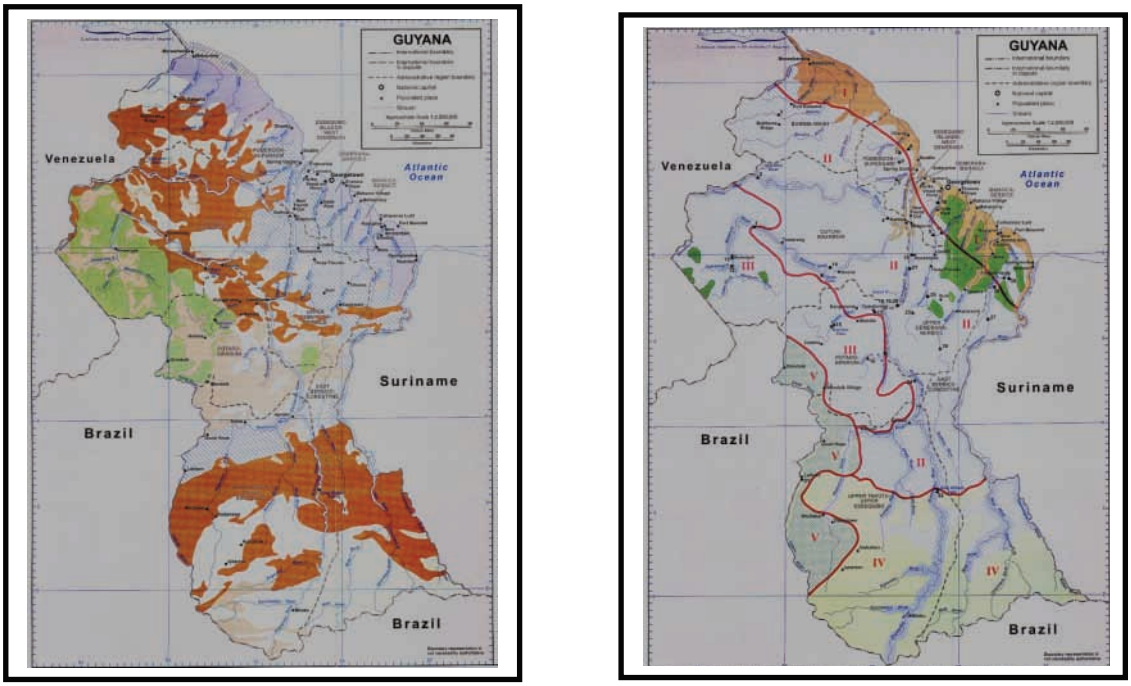


Fig. 1 Left, groundwater resources map of Guyana. Right, surface water resources of Guyana.

LEGEND FOR GROUNDWATER RESOURCES MAP

FRESH WATER GENERALLY PLENTIFUL
Large quantities of fresh groundwater are available from marine sand and clay at depths ranging from 150 to 215 m.

Moderate to large quantities of fresh water are available from unconsolidated sand and sandstone at depths ranging from 3 to 75 m..

FRESH WATER LOCALLY PLENTIFUL
Small to large quantities of fresh groundwater are available from volcanic ash, tuff, sand and conglomerate at depths from 10 to 300 m.

Small to moderate quantities of fresh groundwater are available from fractured granites, cherty mudstones, gravels and sands at depths ranging from 3 to 150 m.

FRESH WATER SCARCE OR LACKING
Meagre to moderate quantities of fresh groundwater are available from igneous and metamorphic rocks at depths from 10 to 300 m.

Meagre to very small quantities of fresh water are available from igneous dikes and andesitic flows at depths ranging from 3 to 150 m.

Large quantities of brackish to saline water are available from unconsolidated sand and clay at depths from 3 to 30 m. Locally fresh water lenses may be present above the brackish to saline groundwater.

Waterfall.

LEGEND FOR SURFACE WATER RESOURCES MAP

FRESHWATER PERENNIALLY PLENTIFUL.
Enormous quantities year-round from perennial rivers and streams, extending throughout the country.

Enormous quantities from April through August and November through January from perennial rivers and streams draining the interior plains, coastal lowlands and western highlands. Large to very large quantities available the rest of the year.

FRESHWATER SEASONALLY PLENTIFUL
Large quantities from April through August and November through January available from perennial and intermittent streams, tributaries, canals and ditches in the coastal lowlands, interior plains and western highlands. Small to moderate quantities available the rest of the year in perennial streams.

Large quantities from April through August generally available from perennial and intermittent streams and tributaries in the southern uplands. Meager to moderate quantities available the rest of the year.

Moderate to large quantities from April through August generally available from perennial and intermittent streams and tributaries in the southwest savannahand tributaries of the Amazon. Meager to small quantities available the rest of the year in perennial streams, while intermittent streams generally have no discharge.

FRESHWATER SCARCE OR LACKING.
Large to enormous quantities of brackish to saline water available throughout the year from tidal influenced rivers and streams, coastal marshes, mangrove swamps and tidal lowlands.

intrusion can be discerned up to several tens of kilometres upstream, and under extreme conditions, the reach of the river affected can extend for more than 200 km.

Mechanisms of sea water intrusion

The salt content of sea water is higher than that of freshwater. Consequently sea water is heavier than freshwater, the density of sea water being higher than that of freshwater. This difference in density has a significant effect on the flow in an estuary, where the sea water is measurably diluted by the freshwater from land drainage (Cameron & Pritchard, 1963).

The differences in density have the major effect of causing stratification in estuaries and also have an effect on pressure.

To overcome this stratification, mixing within the water body is required; this in turn requires energy. This energy is supplied by tidal flow which induces turbulence and effects the mixing. Stratification is therefore most pronounced in estuaries through which a river issues into a non-tidal sea, while it is weaker when tidal action is strong.

On this basis Pritchard (1955) and Cameron & Pritchard (1963) have classified estuaries according to their stratification and salinity distribution. They defined the following types of estuaries: highly stratified salt-wedge type estuaries; partly mixed estuaries; well mixed estuaries. Based on these three types of mixing of sea water and river water, sea water intrusion into rivers can be distinguished as: a well mixed situation; a partly mixed situation; a salt water wedge situation.

The hydrodynamic formulation of well and partially mixed situations are similar and can be carried out on the basis of two concepts : advection and dispersion, and tidal prism. The one dimensional equation of advection and dispersion of salt in the river part of the mouth can be written as:

$$\frac{\delta S}{\delta t} + v\frac{\delta S}{\delta t} = \frac{\delta}{\delta x}\left\{D_x \frac{\delta S}{\delta x}\right\} \tag{1}$$

where: S is water salinity; v is flow velocity; D_x is longitudinal dispersion coefficient. The solution to this equation gives the distance to which brackish water will intrude into the river.

The tidal prism concept allows for the estimation of the length of seawater intrusion into a river at high water slack (HWS). Computations were done based on a deduction by Mikhailov (1971), with the following assumptions:

(i) Water density and salinity are homogeneous over the cross section.
(ii) Freshwater is present at the end of the ebb tide over the whole river part of the mouth.
(iii) The intrusion of salt or brackish water begins through the coastal edge of the river channel just after the reversal of the ebb current into the flood current or at low water slack (LWS).

Applications

The foregoing analyses have been applied to the Mahaica, Demerara and Essequibo rivers of Guyana. Because of the extremely flat nature of the terrain, these rivers are tidal for great distances inland, ranging from in excess of 50 km for the larger creeks to more than 150 km for the bigger rivers. These rivers are therefore very susceptible to salt water intrusion.

The base line conditions used for analysing the extent of salt and brackish water in the rivers are as given in Table 1 (Geer, 1980). The data used in these analyses have been taken from the records of the Hydrometeorological Service of the Ministry of Agriculture (1977). The computations have also been made using long-term mean flows of the rivers. Table 2 summarizes the results obtained.

Table 1 Base line conditions

River	Salt water extent (km)	Brackish water extent (km)
Demerara	4	50
Mahaica	2	20
Essequibo	6	60

Table 2 Extent of salt/brackish water into the Mahaica, Demerara and Essequibo rivers.

	Sea level rise (m)	Salt water intrusion	Brackish water extent (km)
Mahaica River	1.0	2.8	28
Demerara River	1.0	5.6	64
Essequibo River	1.0	8.5	80

DISCUSSION

The results have been obtained using mean flows of the rivers. Rising temperatures will also disrupt the hydrological cycle with the result that rainy seasons may be shorter and more intense, while dry seasons may be longer. This will mean lower flows during the dry season, resulting in greater salt water intrusion into the rivers. Some sensitivity analyses done for a range of low flows indicate that intrusion can be up to four times as great as for the mean conditions analysed above.

Effects of sea level rise

A rise in sea level will inundate wetlands and lowlands, accelerate coastal erosion, exacerbate coastal flooding, threaten or destroy coastal structures, raise water tables and increase the salinity of rivers and aquifers (Barth & Titus, 1984).

Projected impacts on Guyana's coast

Most of the settlements on coastal rivers are located within a few tens of kilometres from the coast and within a few hundreds of metres from the edges of the rivers. Also the vast agricultural areas of the country are adjacent to coastal rivers. From the previous results obtained, these areas are well within the domain expected to be affected by salt/brackish water intrusion. Water for domestic and agricultural requirements are extracted from the rivers. With salt/brackish water penetration getting further inland, the adverse effects expected can be summarized as follows:

(i) The concentration of salt content will be increased. This will be detrimental to agriculture, as there will be further penetration of salt water into the land.
(ii) Water tables will rise and, because of the higher salt content, prime agricultural lands now under cultivation will become useless.
(iii) Population will be displaced because of a reduction of sustainable agriculture and the presence of salt/brackish water in the rivers for extended periods.

Aquifers

Contamination of the aquifer systems in Guyana due to sea level rise can occur from two possible directions.

Assuming hydraulic connection with the ocean, rising sea level will induce saline water penetration from the outlets of the aquifers to the ocean by the amounts in Table 3. The "A" Sands aquifer is the most exploited one of the three aquifers, and even though decline in piezometric levels have not been too significant in general, averaging about 0.03 to 0.06 m per year, (Worts, 1958), in some locations, notably the Georgetown area, the decline has been substantial, about 20 m since extraction started in 1926. However, there has been no problem with saline intrusion into any wells so far.

The other two aquifers, the Upper Sands and the "B" Sands, have not been much used. It is known that private individuals have been extracting freshwater for household uses from the Upper Sands from depths down to about 100 m, on a continuous basis without any detection of increase in salt content.

Table 3 Saline water penetration distance (m) from outlets .

Aquifer	1.0 m. S.L.R.
Upper Sands	150
"A" Sands	180
"B" Sands	380

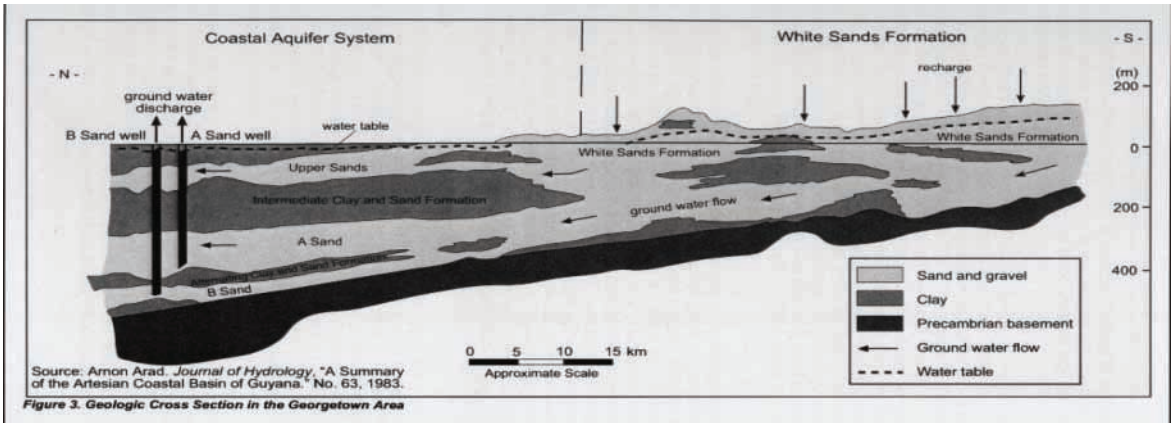


Fig. 2 Geological cross–section in the Georgetown area.

Intrusion from rivers

What will be of greater concern is the possibility of salt water contamination of the aquifers from the rivers and from above land surface. Figure 2 shows a geological cross-section of the coast from the ocean inland. The extremely flat nature of the coastal plains for more than 40 km inland is very evident. This is already in the White Sands formation area, the presumed recharge area for the coastal aquifer systems.

With the estimation of salt/brackish water intrusion into the rivers encroaching on this area, contamination of the aquifers from the rivers will be unavoidable. It is estimated that over the next century salt water will intrude into the recharge zones for a distance of 1–2.5 km. Extraction of water from the aquifers will enhance intrusion.

REFERENCES.

Barth, M. C. & Titus, J. G. (eds) (1984) *Greenhouse Effects and Sea Level Rise: A Challenge for this Generation.* Van Nostrand Reinhold Company, New York, USA.

Cameron, W. M. & Pritchard, D. W. (1963) Estuaries. In: *The Sea* (ed. by M. N. Hill), vol. 2. John Wiley, New York, USA.

Geer, B. (1980) Ground Water Recovery in Guyana – Some Aspects. HYM-No.TP24. Hydrometeorological Service, Guyana.

Gibson, U. (1971) Water Resources Management in Guyana.

Hydrometeorological Service, 1977. Compilation of Surface Water Data to December 31, 1965.

Mikhailov, V. N. (1971) *Dynamics of the Flow and the Channel in Non-Tidal River Mouths*. Hydrometeorological Press, Moscow (in Russian).

Mercado, A. (1997) Management of the Guyana Artesian Coastal Aquifers: Preliminary Assessment of Alternative Approaches. Guyana Water Authority.

Pritchard, D. W. (1955) Estuarine circulation patterns. *Proc. Amer. Soc. Civil Engng* **81**, 717.

Worts, G. F. (1958) A brief appraisal of groundwater conditions and proposed program for water resources investigations in the coastal artesian basin of British Guiana. US Geological Survey.

Climate Variability and Change—Hydrological Impacts (Proceedings of the Fifth FRIEND World Conference held at Havana, Cuba, November 2006), IAHS Publ. 308, 2006.

Climate change impacts and responses in the Czech Republic and Europe

OLDŘICH NOVICKÝ, LADISLAV KAŠPÁREK & MARTINA PELÁKOVÁ

T. G. Masaryk Water Research Institute, Podbabská 30, CZ–160 62, Prague 6, Czech Republic
oldrich_novicky@vuv.cz

Abstract The paper discusses the development of European policies and measures aimed at securing water demands by replenishing, saving and protecting the European water resources. Recent European policies and legislation give preference to soft solutions and measures for water quality protection, rather than hard solutions, such as construction of water storage reservoirs, which were formerly used for meeting water demands. A case study from the Czech Republic describes results showing possible reservoir storage capacities which could be necessary in future for compensation of climate change impacts on flows, and particularly on low flows. The required storage capacities are derived from drought deficit volumes calculated from monthly flow series simulated for natural climate conditions and for the conditions affected by climate change. For the derivation of the deficit volumes, the discharge whose probability of exceedence is 70% ($Q_{70\%}$) was used as the threshold.

Key words deficit volume; BILAN model; climate change; water resources; reservoir storage capacity; EU water legislation; Water Framework Directive

INTRODUCTION

Spatial and temporal variability in the availability of water resources, together with the high increase in the European water demands during the second half of the last century, were reflected in a number of measures that were taken to improve the unfavourable conditions.

In the mid twentieth century (EEA, 2001), the measures were aimed at improving the performance of water distribution systems (hard solutions). Political support for hydraulic structures was reflected in the construction and use of storage reservoirs, which helped to overcome the uneven distribution of water resources and the increasing demands.

Lately, there has been a rapid development of strategies, policies and legislation (soft solutions) in the water sector. The focus has gradually changed from replenishment of water resources to their saving by reducing the demands, and during the last thirty years attention has increasingly been paid to water resource protection.

The development of the European water policy was reflected in adopting a number of water-related EC directives. The most substantial piece of water legislation today is the Water Framework Directive (Directive 2000/60/EC). This Directive establishes a legally binding framework to promote sustainable water consumption based on the long-term protection of available water resources. Rational decision making in water management is predominantly based on a proper permanent water planning and preparation of programmes of measures at a Europe-wide scale.

The new European policy is associated with great investments but the European hard solutions will predominantly focus on the protection of water and mainly its quality (infrastructure is aimed at meeting emission and pollution requirements). Water resource replenishment by using hard solutions (particularly by construction of reservoirs) is not intended or desired.

The feasibility of this European policy is probably conditioned by two assumptions, i.e. a stable water demand and a normal range of climate variability in future. Clear stabilization of the demand in Europe was substantiated in recent assessments (EEA, 2001) but the future climate conditions are much less predictable. It was shown, using historical series (Novický & Kašpárek, 2006), that we could experience a much higher natural climate variability than in past decades, and, in addition, we increasingly live under potential threat of climate change. The drought that affected much of Europe during 2003 (EurAqua, 2004) is one of the warning events.

Future natural climate development is unknown, while the possible climate changes are predicted by running climatic models. The impact of climate change on hydrological conditions can, however, be assessed by using hydrological models with different climate change scenarios. European projects, assessing impacts of the scenarios on hydrological cycle, were focused mainly

Copyright © 2006 IAHS Press

on changes in mean runoff. The results (EEA, 2001; Reynard *et al.*, 1997; Kašpárek *et al.*, 2003) suggest that the general tendency is towards an increase in the annual average runoff in northern Europe and a decrease in southern Europe. In some areas changes of 30% in the mean runoff by 2050 are feasible. It was also demonstrated that the main impact of climate warming is on low flows, which tend to become more extreme across most of Europe.

Few studies that are focused on the implications of climate change on water resources were reviewed in IPPC (2001). The results of the review include the conclusion that different systems respond very differently to climate change but generally in systems with large reservoir capacity, changes in resource reliability may be proportionately smaller than changes in river flows.

Water management in the Czech Republic (CR) is traditionally based on long-term planning, which involves the development of Master Water Management Plans of the CR. Their 1988 version included an updated list of intended water reservoirs (at 210 river sites in the Czech Republic). The need for these additional reservoirs is a controversial issue as part of the preparation of background materials for river basin district planning, which is required by the Water Framework Directive. Another factor was the concern that the existing water resources could be insufficient in future due to the impacts of climate change.

In 2005, the T. G. Masaryk Water Research Institute was commissioned by the Ministry of Agriculture of the Czech Republic to carry out a study, which was aimed at estimating reservoir storage capacities that would be necessary in future to compensate for climate change impacts on flows in the Czech Republic.

The territory of the Czech Republic (Fig. 1) is drained by three main rivers, the Elbe, Odra and Morava, and, accordingly, the country is located on the water divide of three seas, the North Sea, the Baltic and the Black Sea. The paper describes the results of the study (Peláková & Boersema, 2005) for the part of the Czech Republic drained by the Elbe River.

METHOD AND DATA

The basin of the Elbe River on the territory of the Czech Republic is shown in Fig. 1 and Table 1 gives its basic hydrometeorological characteristics. For the purpose of the study, the Elbe basin was divided into 12 upper basins, each represented by data for one water gauging station, and three `intermediate basins between the upper basins and downstream closing river sites on the Elbe and Vltava mainstreams. The required reservoir capacities were calculated from data derived for the water gauging stations in the upper basins and stations representative for the downstream river sites. The results for the intermediate basins were derived from those calculated for the upstream and downstream stations. Basic information and data on the basins are given in Table 2.

Derivation of the storage that is required in a reservoir for ensuring the specific yield (abstraction and outflow) with a given probability is usually based on the yield storage method. Such a detailed solution was not applicable for the purposes of the study, whose intention was to estimate possible impacts of climate change across a number of river sites. It was therefore desirable to develop a rapid method that would be sufficiently accurate compared to other uncertainties, such as those in climate change scenarios.

The method was based on derivation of deficit volumes, which are runoff volumes below a threshold discharge in the time flow series. The threshold can be interpreted as the desired yield from a reservoir, and the drought deficit volume defines the required storage in a given period (e.g. Tallaksen & Lanen, 2004). The idea of the method was that the deficit volumes could be derived from natural flow series and flow series affected by climate change. The greatest difference between the deficit volumes before and after the change indicates the volume that would be necessary in a reservoir to compensate the possible impacts of the change. For the study, the discharge whose probability of exceedence is 70% ($Q_{70\%,}$) was used as the threshold.

In terms of data, the study was based on monthly series of mean air temperature (ºC), relative air humidity (%), basin precipitation (mm month^{-1}) and runoff (mm month^{-1}) from the period 1932–1990. These series were used as input for calibration of the parameters of the BILAN water balance model in the individual basins.

The model, which was developed by the T. G. Masaryk Water Research Institute, simulates time series of monthly potential evapotranspiration, actual evapotranspiration, infiltration across

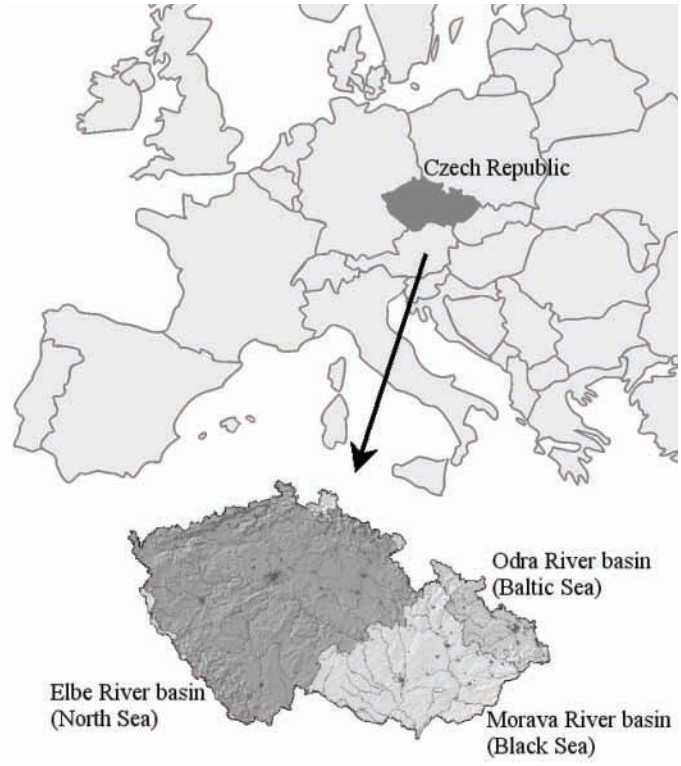


Fig. 1 Three main river basins in the Czech Republic.

Table 1 Basic characteristics of the Elbe River basin in the Czech territory.

Basin area	51394 km^2
Mean altitude	446 m a.m.s.l.
Mean air temperature	7.1ºC
Mean flow	313 m^3 s^{-1}
Specific runoff	6.1 l s^{-1} km^{-2}
Mean annual runoff	192 mm
Mean annual precipitation	653 mm

Table 2 Study basins and representative water gauging stations in the Elbe River basin.

River name	Basin	Basin area (km²)	Basin annual precipitation (mm)	Station name	Station basin area (km²)
Elbe	Above the Úpa tributary	712	947	Království	532
Úpa	Above its discharge into the Elbe	514	939	Česká Skalice	461
Metuje	Above its discharge into the Elbe	539	799	Hronov	248
Orlice	Above confluence of the Divoká and Tichá Orlice River	1 536	863	Týniště n. O.	1 591
Jizera	Above its discharge into the Elbe	2 193	858	Tuřice	2 159
Elbe	Intermediate basin between the upstream river sites and the Jizera tributary	7 520	626	–	–
Elbe	Elbe and Jizera above the confluence	13 014	730	Brandýs n. L.	13 111
Vltava	Above the Malše tributary	1 823	880	Vyšší Brod	999
Lužnice	Above its discharge into the Vltava	3 896	667	Bechyně	4 046
Otava	Above the Lomnice tributary	2 996	733	Písek	2 913
Sázava	Above its discharge into the Vltava	4 348	668	Poříčí n. S.	4 000
Berounka	Above its discharge into the Vltava	8 854	612	Dobřichovice	8 720
Vltava	Intermediate basin between the upstream river sites and the Berounka tributary	4 390	571	–	–
Vltava	Vltava and Berounka above the confluence	26 307	655	Praha-Modřany	26 690
Ohře	Above its discharge into the Elbe	4 820	699	Louny I.	4 983
Ploučnice	Above its discharge into the Elbe	1 195	757	Benešov n. P.	1 156
Elbe	Intermediate basin between the upstream river sites and the Ploučnice tributary	4 523	601	–	–
Elbe	Elbe and Ploučnice above the confluence	49 859	676	Děčín	51 104

the land surface, recharge from the soil to the aquifer, the amount of water that is stored in the snow pack, the soil and aquifer, and three runoff components, i.e. surface runoff, interflow and groundwater flow. Eight free model parameters are obtained by applying an optimization algorithm that compares time series of monthly simulated and observed streamflow. The model is described in Tallaksen & van Lanen (2004).

For the study, the natural conditions were represented by the runoff series that were simulated from the unchanged input series. The calibrated parameters and identical period (1932–1990) but with changed precipitation, air temperature and relative humidity input series were applied for simulation of the monthly flow series affected by climate change.

For the simulation of the affected flow series, the climate conditions were changed by using a climate change scenario that was the most extreme alternative of those that were derived for the Czech Republic (ECHAM4 General Circulation Model, SRESA2 emission scenario and high climate sensitivity). The scenarios (IPCC, 2001), which have the year 2050 as a reference, are implemented by adapting the original time series of air temperature, precipitation and water vapour pressure in the individual months. The largest changes are in the air temperature. For the climate change scenario used, its annual mean value increases by approximately 3ºC.

RESULTS

Figure 2 shows results of the assessment of climate change impacts on flows for the study basins. For conditions before climate change, basin annual precipitation varies between 570 and 950 mm, evaporation is almost constant at a level of 500 mm and consequently the annual runoff is between 80 and 465 mm. After climate change, the annual runoff decreases to values between 35 and 365 mm. The main cause for the runoff decrease by about 50 to 100 mm is an increase in evaporation. Decrease in precipitation does not exceed 12 mm. The evaporation increases with an increase in precipitation (spatial variability between 515 and 595 mm). The most vulnerable areas are lowlands, where even a small increase in evaporation can be responsible for a high relative (40%) decrease in runoff, which was originally already low.

Results of the deficit volume analysis are shown in Figs 3 and 4. Figure 3 compares the deficit volumes before and after climate change in relation to the potential reservoir storage capacities in individual study basins. These results show that the storage capacities (between 0 mm and 344 mm) are at approximately the same level as the deficit volumes (between 19 mm and 292 mm) before climate change. The deficit volumes after the climate change exceed highly the potential reservoir storage capacities. Such capacities would not even be fully sufficient for compensating for an increase in the deficit volumes due to the climate change (difference between the deficit volumes after and before the change).

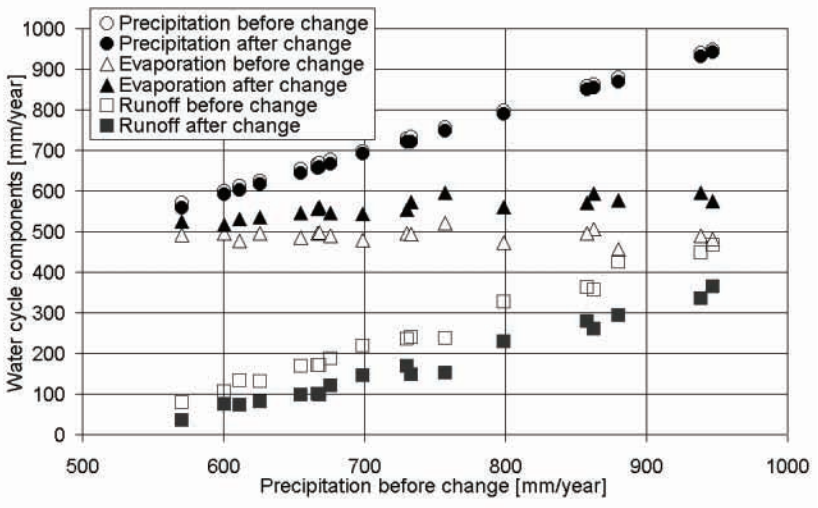


Fig. 2 Water cycle components for natural conditions and conditions affected by climate change in the study basins.

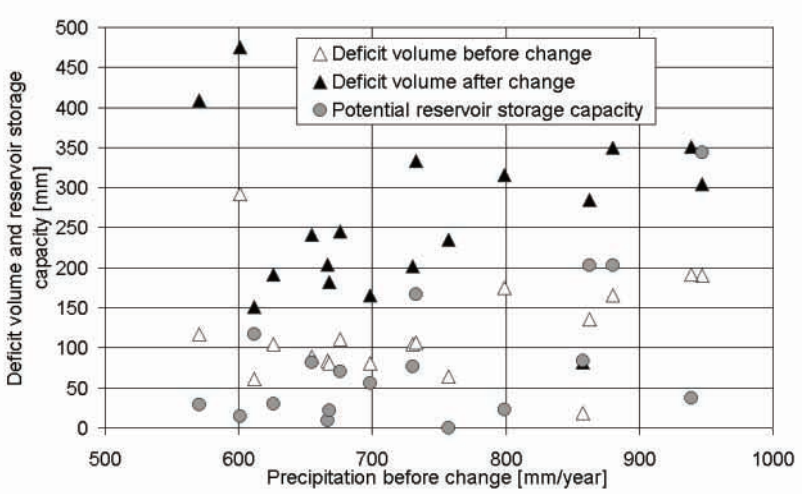


Fig. 3 Maximum deficit volumes for natural conditions and conditions affected by climate change, and potential reservoir storage capacities in the study basins.

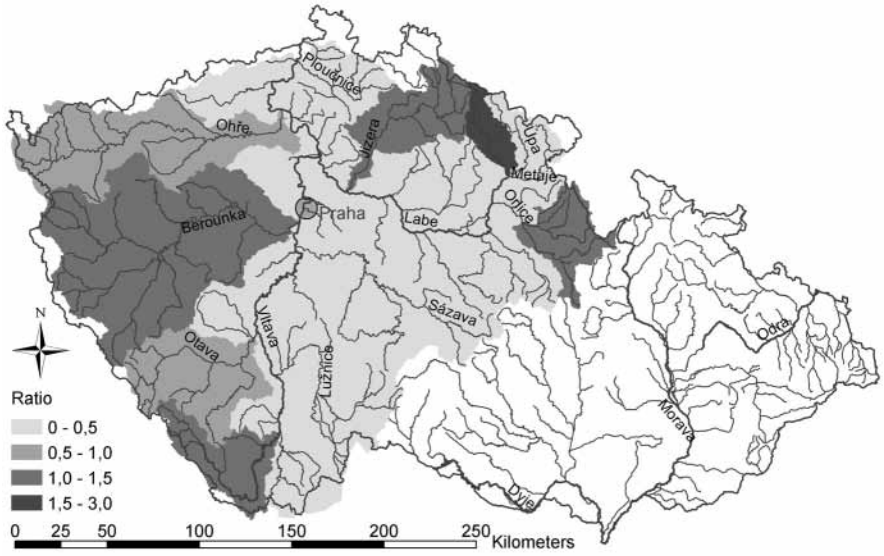


Fig. 4 Map of ratio of the potential reservoir storage capacity to an increase in the deficit volume consequently to the climate change in the study basins.

Figure 4 shows the spatial distribution of a ratio between the potential storage capacity and the increase in the deficit volumes in individual study basins. This ratio for the whole Elbe basin is 70 mm/135 mm = 0.52, which means that the potential storage capacity in the basin could compensate only approximately 50% of the deficit stemming from the climate change. The ratio has high spatial variability (from 0 to 3), which is attributable mainly to the uneven spatial distribution of the potential storage capacities available in some of the highland areas. The ratio category of 0–0.5 covers 54% of the basin area (predominantly lowlands), and is approximately balanced by the conditions where the ratio is 0.5–1.5, that is, over an area covering 45% of the basin. Good conditions occur in the high mountain range in the north (1.4% of the basin area), where the potential storage exceeds the deficit increase by a factor of 3.

CONCLUSION

The climate conditions in Europe, developments in the area of the water infrastructure, particularly in already secured water storage; and current developments in strategies, policies and legislation determined by the EU; all point towards soft solutions which are focused on protecting the quality of water resources.

The results of the study indicate that climate change impacts on future requirements for reservoir storage capacities could be high. They could suggest the need for ensuring a reliable water supply through the construction of new reservoirs to provide additional storage capacity. Such supplementary storage capacities will be needed not only for traditional water supply purposes, but also for the mitigation of climate change, which will impact on flows and particularly on low flows. These needs could also be supported by requirements of the new European water policy, particularly by those stipulations of Water Framework Directive aimed at ensuring minimum acceptable environmental flows. Thus European policies that are focused exclusively on protection of the quality water resources could be insufficient and may well have to be changed towards an adoption of hard solutions focused on water resource replenishment.

REFERENCES

EC (2000) Directive 2000/60/EC of the European Parliament and of the Council of 23 October 2000 establishing a framework for Community action in the field of water policy.

EEA (2001) *Sustainable Water Use in Europe. Part 3: Extreme Hydrological Events: Floods and Droughts* Environmental issue report no 21. European Environment Agency, Copenhagen, Denmark.

EurAqua (2004) Towards a European drought policy. Discussion document prepared by the EurAqua network of Europe leading freshwater research organizations.

IPCC (2001) *The Scientific Basis*. IPCC (Intergovernmental Panel on Climate Change) third assessment report - Climate Change 2001, IPCC, WMO, UNEP. Cambridge University Press, Cambridge, UK.

Kašpárek, L. *et al.* (2003) *Vliv klimatických změn na množství a kvalitu vodních zdrojů a na hydrologické poměry v ČR* (*Impact of climate change on quantity and quality of water resources and hydrological conditions in the Czech Republic*). Final research report of the project VaV/650/3/02. T.G.M. Water Research Institute, Prague, Czech Republic.

Novický, O. & Kašpárek, L. (2006) Grouping of extreme runoff events in Central Europe. In: *Climate Change, Consequences for Water Resources Management* (Wasser Berlin 2006, International DWA symposium on water resources management. Berlin, April 2006).

Peláková, M. & Boersema, M. P. (2005) *Odhad objemu nádrží potřebného pro kompenzaci poklesu odtoku vlivem klimatické změny* (*Derivation of reservoir storage capacities required for compensation of flow decrease consequently to climate change*). T.G.M. Water Research Institute, Prague, Czech Republic.

Reynard, N. S., Hulme, M., Conway, D. & Faulkner, D. (1997) Baseline data and climate change scenarios. In: Impact of climate change on hydrological regimes and water resources in Europe (ed. by N. W. Arnell). Final report to DG XII of the European Commission.

Tallaksen, L. & van Lanen, H. (eds) (2004) *Hydrological Drought – Processes and Estimation Methods for Streamflow and Groundwater*. Developments in Water Science 48, Elsevier, The Netherlands.

Climate Variability and Change—Hydrological Impacts (Proceedings of the Fifth FRIEND World Conference held at Havana, Cuba, November 2006), IAHS Publ. 308, 2006.

La variabilité des débits du Rio Amazonas au Pérou

JHAN CARLO ESPINOZA VILLAR[1], PASCAL FRAIZY[1], JEAN LOUP GUYOT[1], JUAN JULIO ORDOÑEZ GALVEZ[2], RODRIGO POMBOSA[3] & JOSYANE RONCHAIL[4]

1 *IRD/UNALM – FIA, Casilla 18 1209, Lima 18, Perú*
20031189@lamolina.edu.pe

2 *SENAMHI, Casilla 11 1308, Lima 11, Perú*

3 *INAMHI, Iñaquito 700 y Corea, Quito, Ecuador*

4 *IPSL/LOCEAN, Université de Paris 7, Case 100 Place Jussieu, F-75005 Paris, France*

Résumé Le bassin amazonien péruvien (977 920 km^2, 76% de la superficie du Pérou) apporte au Brésil d'importants volumes d'eau. Les débits de l'Amazone au Pérou n'étaient pas connus. A partir des séries de hauteurs d'eau journalières aux stations de Tamshiyacu (1983–2005) et d'Iquitos (1969–2005, 50 km en aval) ainsi que des jaugeages réalisés par ADCP à Tamshiyacu depuis 2001, le débit à Tamshiyacu a été calculé (1969–2005). Le débit moyen de cette station, la seule jaugée sur l'Amazone au Pérou, est 25 000 m^3 s^{-1}. Les données de pluie mensuelles de 234 postes pluviométriques ont été utilisées pour calculer la lame d'eau précipitée (1964–1997). Les précipitations moyennes annuelles sont de 1600 mm. Le relation pluies/débits annuels pour la période commune 1970–1997 est forte (r^2 = 0.77). On observe une tendance globale décroissante, de –0.83% et –0.81% respectivement pour les pluies et les débits sur la période de 28 années étudiées.

Mots clefs hydrologie, Amazone, débit, pluie, Pérou

Variability in discharge of the Peruvian Amazon

Abstract The Peruvian Amazonian basin (977 920 km^2, 76% of the surface of Peru) is supposed to bring to Brazil an important volume of water. However, the discharge of the Peruvian Amazon was not known until now. In this work, the discharge at Tamshiyacu, the only gauging station available in the Peruvian Amazon basin, was calculated (1969–2005) using daily level flow data at Tamshiyacu (1983–2005) and at Iquitos (1969–2005, 50 km downstream), and gauging data measured by ADCP at Tamshiyacu since 2001. The annual average discharge at Tamshiyacu, is 25 000 m^3 s^{-1}. Monthly rainfall data from 234 raingauge stations was used to calculate the depth of runoff (1964–1997). The average precipitation is 1600 mm year^{-1}. The annual rainfall/discharge relationship for the common 1970–1997 period is high (r^2 = 0.77). During this period, decreasing tendencies are observed: –0.83% and –0.81% for rainfall and discharge, respectively.

Key words Amazon basin, Peru, discharge, rainfall

INTRODUCTION

Le bassin amazonien est le plus important bassin hydrographique de la planète (6 10^6 km^2), et le fleuve Amazone présente un débit moyen de 209 000 m^3 s^{-1} (Molinier *et al.*, 1996). Les études récentes réalisées au Brésil sur la variabilité de l'hydrologie de l'Amazone à Óbidos, la dernière station jaugée avant l'Océan Atlantique (1.93ºS et 55.50ºW, à 800 km de l'Océan), ont montré que la série 1945–1998 présentait une évolution sensible des pluies et des débits ces dernières années (Callède *et al.*, 2004). A cette date, les données sur les bassins andins étaient peu nombreuses, et concernaient surtout le haut-bassin du Rio Madeira en Bolivie (Ronchail *et al.*, 2005), alors que le haut-bassin de l'Amazone-Solimões (Equateur et Pérou) restait peu documenté.

Au Pérou, alors que le bassin amazonien représente 76% du territoire et 98% des ressources hydriques du pays (DGAS, 1995), les études hydrologiques se sont essentiellement focalisées sur le versant Pacifique, où sont installées les principales villes du pays. Le programme HYBAM (convention IRD – SENAMHI – UNALM, www.mpl.ird.fr/hybam) réalise depuis 2001 des campagnes de mesure sur les principaux fleuves de l'Amazonie péruvienne (Yerren *et al.*, 2004). La station hydrométrique de Tamshiyacu (Fig. 1) est la première station où sont mesurées les niveaux de l'Amazone, car située à l'aval de la confluence des rios Marañón et Ucayali. A cette station, qui draine un bassin de 726 400 km^2 dont 53% situés dans les Andes, l'Amazone transporte de grandes quantités de sédiments provenant de l'érosion des bassins montagneux d'Equateur et du Pérou.

DONNEES ET METHODES

Le bassin versant de l'Amazone à Tamshiyacu a été délimité à partir du modèle numérique de terrain SRTM, selon une procédure semi-automatique (Mialocq *et al.*, 2005).

Copyright © 2006 IAHS Press

La gestion des séries hydrologiques, la construction de la courbe d'étalonnage, le calcul des débits, la critique des données pluviométriques (MVR), et le calcul des lames d'eau précipitées ont été réalisés avec le logiciel HYDRACCESS (Vauchel, 2005).

RESULTATS ET DISCUSSION

La série des débits mensuels observés à Tamshiyacu (Fig. 4(a)) montre un débit moyen de 25 000 m^3 s^{-1}, pour une valeur maximum de 38 950 m^3 s^{-1} (avril 1971) et un débit minimum de 10 200 m^3 s^{-1} (septembre 1995). La précipitation annuelle moyenne sur le bassin est de 1600 mm pour la période 1964–1997 (Fig. 4(b)), avec une valeur maximum de 258 mm (février 1984) et minimum de 41 mm (juillet 1997). Le cycle hydrologique annuel débute en août pour les pluies et en octobre pour les débits (Fig. 5). Le déphasage de deux mois entre pluies et débits correspond au temps de concentration du bassin versant.

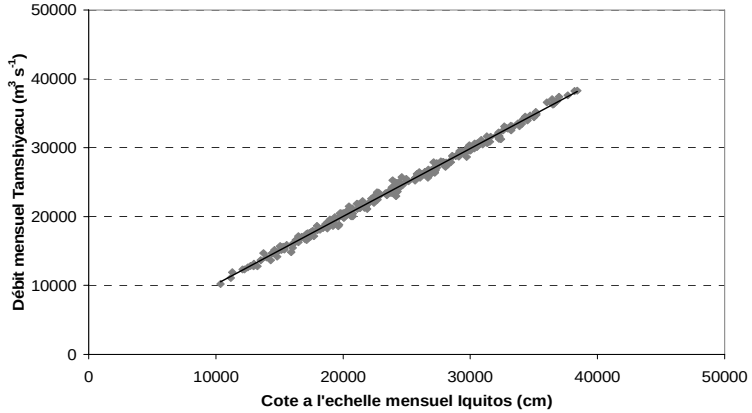


Fig. 3 Corrélation entre hauteurs d'eau mensuelles à Iquitos et débits mensuels à Tamshiyacu (r^2 = 0.996) sur le Rio Amazonas.

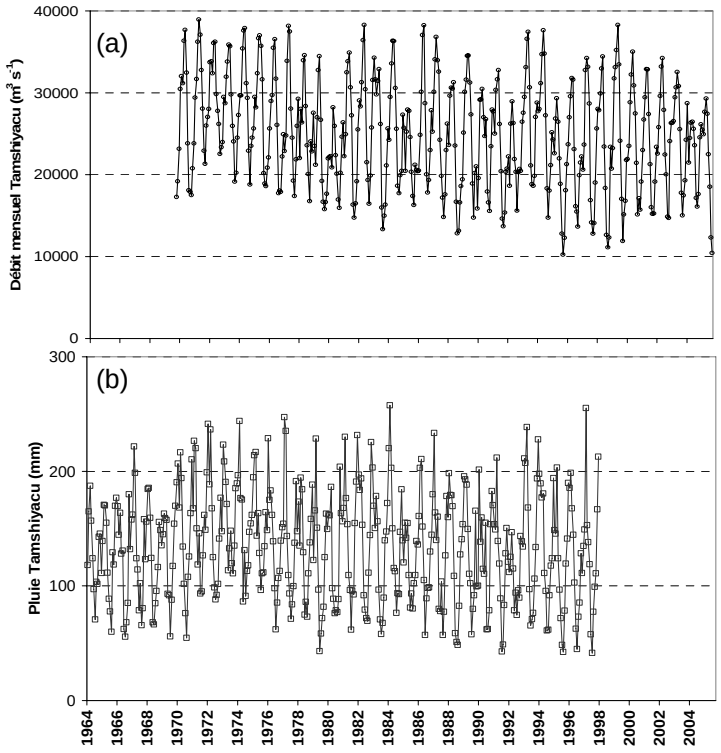


Fig. 4 Rio Amazonas à Tamshiyacu: débits mensuels pour la période 1969–2005 (a), et précipitation moyenne sur le bassin de 1964 à 1997 (b), avec lignes de tendance.

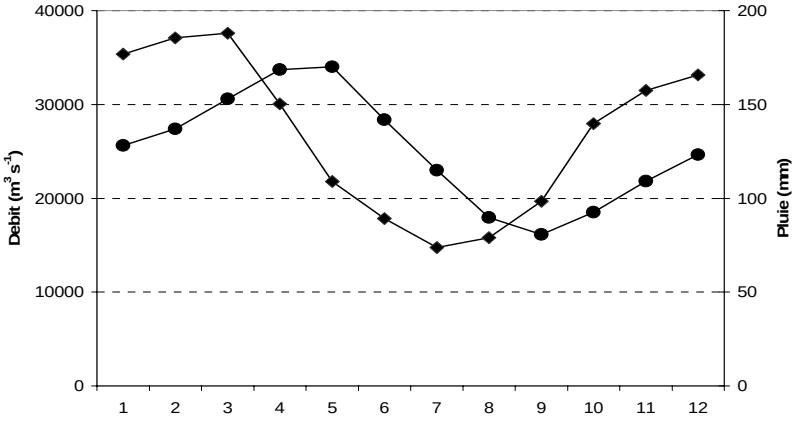


Fig. 5 Cycle annuel moyen des débits (●) et des précipitations (■).

Le cycle annuel des pluies dans le bassin est caractérisé par une grande hétérogénéité de comportements (Fig. 6). Dans la plus grande partie du bassin, le régime des pluies est de type tropical, caractérisé par une saison pluvieuse qui s'accentue vers les basses latitudes et en s'éloignant des Andes. En Equateur, certaines stations pluviométriques appartenant au même sous-bassin, peuvent présenter simultanément des comportements différents voire opposés: régime uni modal ici, bimodal ailleurs, observation d'un maximum de pluie dans certaines stations alors que la saison est sèche dans d'autres. (Laraque *et al.*, 2004).

Le coefficient de variation (CV) saisonnier est de 0.24 pour les débits mensuels et de 0.32 pour les pluies mensuelles. Le rapport des valeurs extrêmes du cycle saisonnier des débits mensuels est de 2.1, traduisant une forte régularité saisonnière des débits. Cette valeur est

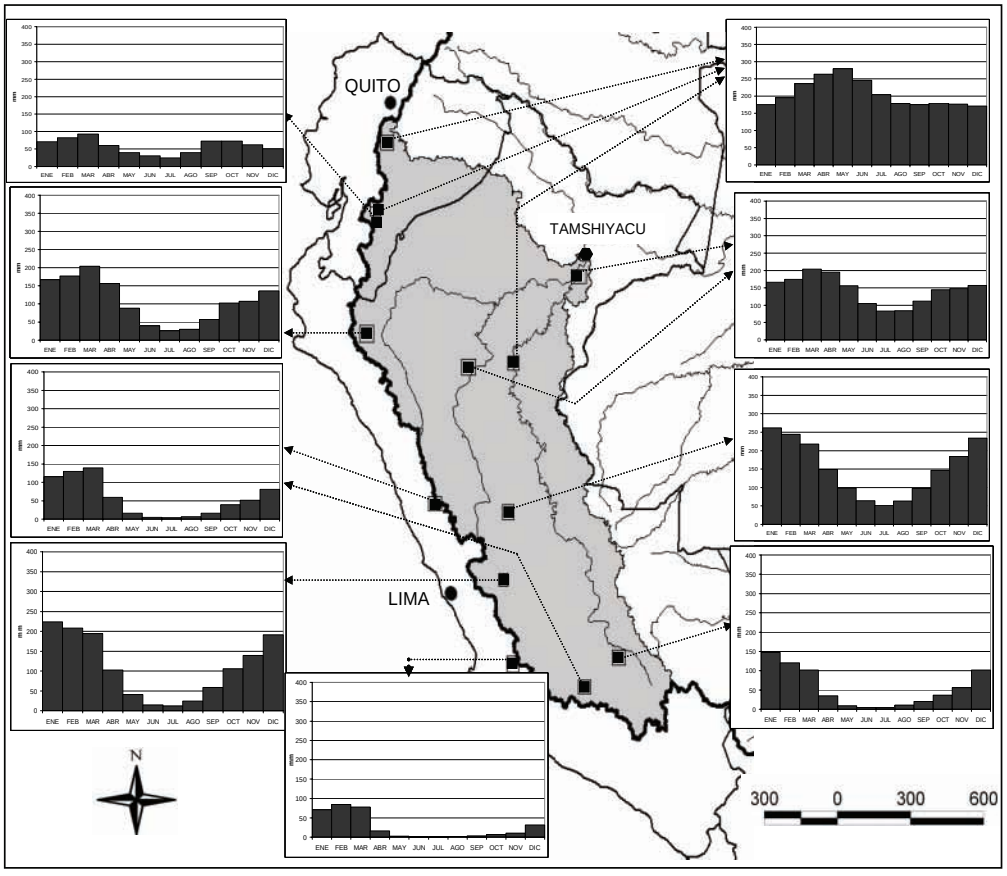


Fig. 6 Régimes pluviométriques (de janvier à décembre) de quelques postes représentatifs du bassin de Tamshiyacu. Pluie mensuelle de 0 à 400 mm (ordonnées).

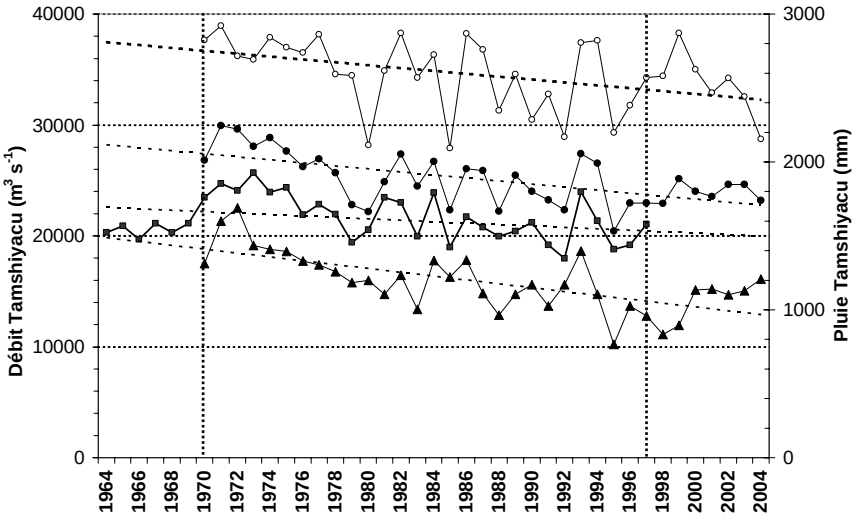


Fig. 7 Rio Amazonas à Tamshiyacu: Variabilité interannuelle des pluies (■) et des débits moyens (●), minimum (▲) et maximum (○) pour la période 1964-2005. Les courbes de tendance correspondent à la période commune 1970-2005.

comparable à celle observée sur les stations du cours principal du Rio Solimões-Amazonas au Brésil (de 1.7 à 2.5), mais elle est inférieure à celles calculées sur les principaux affluents de l'Amazone, tant au Sud, en Bolivie, sur le Rio Beni (de 5 à 15), qu'au Nord, sur le Rio Negro (de 3 à 8) au Brésil (Molinier *et al*, 1996).

Le coefficient de variation interannuel est de 0.09 pour les pluies, mais aussi pour les débits, ce qui traduit là aussi l'extrême régularité multi-annuelle des régimes pluviométriques et hydrologiques de l'Amazone au Pérou, tout comme cela a été observé à Óbidos au Brésil (Callède *et al.*, 2002).

Pour la période commune d'observation des pluies et des débits (28 ans, 1970–1997), les valeurs annuelles (Fig. 7) montrent une diminution nette des précipitations (–0.83% par an), comme des débits (–0.81% par an). Les débits annuels minimum et maximum décroissent également sur la période, avec des valeurs respectives de –0.61% et –1.68%. Il faut cependant signaler que les pluies de 1964 à 1970 présentent une tendance à l'augmentation, montrant que l'année 1970 pourrait ici aussi représenter une rupture dans la série comme cela a déjà été observé sur d'autres fleuves amazoniens (Callède *et al*., 2004; Labat *et al*., 2004). Enfin, le coefficient de corrélation (r^2) entre lame d'eau précipitée et débit annuel est de 0.77.

Les débits observés à Tamshiyacu montrent des valeurs plus élevées durant la décennie des années 1970, du fait de l'augmentation des pluies à cette époque, comme cela a été également confirmé par d'autres études sur le bassin de l'Amazone au Brésil (Cutim *et al*, 2000; Ronchail *et al*, 2002). Aussi la décroissance observée sur la série 1970–1997, peut être le résultat de cette hydraulicité anormalement élevée des années 1970, d'une tendance générale à la diminution des pluies et des débits dans la région, ou bien entendu, d'une combinaison de ces deux facteurs.

CONCLUSION

Les résultats de cette étude, quoique préliminaires, présentent pour la première fois une série historique des débits de l'Amazone au Pérou. Les banques de données seront prochainement complétées, notamment en ce qui concerne les pluies pour la période 1998–2005, et des études plus fines par sous-bassins (Ucayali, Huallaga, Marañón, Napo) seront entreprises, afin de mieux comprendre le régime hydro-climatique du haut bassin de l'Amazone.

REFERENCES

Brunet-Moret Y. (1979) Homogénéisation des précipitations. *Cahiers ORSTOM, Série Hydrologie* **16**, 3–4.

Callède, J., Guyot, J. L., Ronchail, J., L'Hôte, Y., Niel, H. & De Oliveira, E. (2004) Evolution du débit de l'Amazone à Obidos de 1902 à 1999. *Hydrol. Sci. J.* **49**(1), 85–97.

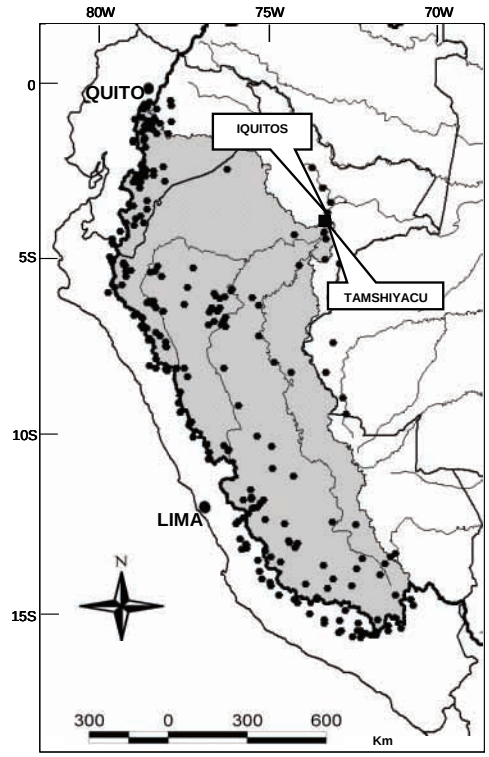


Fig. 1 Carte du bassin du Rio Amazonas à la station de Tamshiyacu (fond gris), et localisation des postes pluviométriques (ronds noirs).

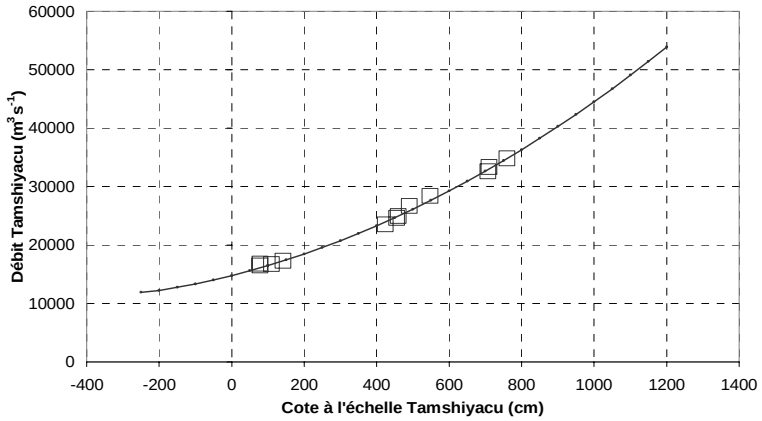


Fig. 2 Jaugeages (carrés) et courbe d'étalonnage de la station de Tamshiyacu.

Les niveaux d'eau journaliers de l'Amazone à la station hydrométrique de Tamshiyacu (4.00ºS et 73.16ºW) sont mesurés par lecture d'une échelle limnimétrique 4 fois par jour, par un observateur du SENAMHI (Service National de Météorologie et d'Hydrologie, www.senamhi.gob.pe) depuis 1983. A cette station, une courbe d'étalonnage fiable a pu être construire par le programme HYBAM (Fig. 2), grâce à 16 jaugeages réalisés de 2001 à 2005 par courantomètre à effet Doppler (ADCP), technique particulièrement bien adaptée aux grands fleuves amazoniens (Filizola & Guyot, 2004).

Les données de hauteurs d'eau de la station d' Iquitos (3.71ºS et 73.25ºW) gérée par ENAPU Pérou (Entreprise Nationale des Ports, www.enapu.com.pe) depuis 1969, ont permis d'étendre la série des débits de Tamshiyacu à la période 1969–2005 (Fig. 3).

Les données mensuelles de 375 postes pluviométriques (Fig. 1) du SENAMHI Pérou et de l'INAMHI Equateur (Institut National de Météorologie et d'Hydrologie, www.inamhi.gov.ec) ont été critiquées par la Méthode du Vecteur Régional, MVR (Brunet Moret, 1979), qui a permis d'éliminer les stations douteuses. La lame d'eau précipitée sur le bassin a été calculée au pas de temps mensuel, selon la méthode du "kriging" à partir des 234 stations validées (62% du total).

Callède, J., Guyot, J. L., Ronchail, J., Molinier, M. & de Oliveira, E. (2002) L'Amazone à Óbidos (Brésil). Etude statistique des débits et bilan hydrologique. *Hydrol. Sci. J.* **47**(2), 321–333.

Cutim, E., Molion, L. & Nechet, D. (2000) Pluies en Amazonie pendant le 20éme siècle (*Chuvas na Amazônia durante o século XX*). In: *XI Congrès brasileiro de Meteorología, Brasilia, Brasil*.

DGAS (Dirección General de Aguas y Suelos) (1995) Vers une gestion intégrée des ressources hydriques au Pérou (*Hacia una gestión integrada de los recursos hídricos en el Perú*). Ministerio de Agricultura, Perú.

Filizola, N. & Guyot, J. L. (2004) The use of Doppler technology for suspended sediment discharge determinations in the River Amazon. *Hydrol. Sci. J.* **49**(1) 143–153.

Labat, D., Ronchail, J., Callède, J., Guyot, J. L., de Oliveira, E. & Guimarães, W. (2004) Wavelet analysis of Amazon hydrological regime variability. *Geophys. Res. Lett.* **31**, L02501.

Laraque, A., Guyot, J. L. & Pombosa, R. (2004) Hydroclimatologie du bassin amazonien en Equateur et son hydro-sédimentologie (Exemple du bassin du Napo). (*Hidroclimatología de la cuenca amazónica del Ecuador y su hidrosedimentología (Ejemplo de la cuenca del Napo)*). *Geología de la cuenca Oriente* (ed. by P. Baby, M. Rivadeneira & R. Barragan). IRD, IFEA, PETROECUADOR. Ecuador.

Mialocq, L., Acuña, M., Seyler, F., Yerren, J. & Guyot, J. L. (2005) Extraction of the topographic limits of the Andean and Amazonian river basins from SRTM. Paper presented at workshop on: Isotope tracers and remote sensing techniques for assessing water cycle variability, IAHS, Foz de Iguaçu, April 2005.

Molinier, M., Guyot, J. L., Oliveira, E. & Guimarães, V. (1996) Les régimes hydrologiques de l'Amazone et de ses affluents. In: *L'hydrologie tropicale: géoscience et outil pour le développement* (ed. by P. Chevallier & B. Pouyaud), 209–222. IAHS Publ. 238. IAHS Press, Wallingford, UK.

Ronchail, J., Bourrel, L., Cochonneau, G., Vauchel, P., Phillips, L., Castro, A., Guyot, J. L. & de Oliveira, E. (2005) Inundations in the Mamoré basin (South-Western Amazon – Bolivia) and sea-surface temperature in the Pacific and Atlantic oceans. *J. Hydrol.* **302**, 223–238.

Ronchail, J., Cochonneau, G., Molinier, M., Guyot, J. L., Goretti de Miranda Chaves, A., Guimarães, V. & de Oliveira, E. (2002) Rainfall variability in the Amazon Basin and SSTs in the tropical Pacific and Atlantic oceans. *Int. J. Climatol.* **22**, 1663–1686.

Vauchel, P. (2005) Hydraccess: Logiciel de gestion et traitement de données hydro-météorologiques, version 2.1.4. Téléchargeable sur www.mpl.ird.fr/hybam.

Yerren, J., Lavado, W., Fraizy, P. & Guyot, J. L. (2004) Les régimes hydrologiques dans le bassin amazonien du Pérou. (*Los regimenes hidrológicos en la Cuenca Amazónica del Perú*). *Surface hydrology and water chemistry*, LBA, Brasilia.

Utilisation optimale de l'information pluviométrique des MCGA aux échelles hydrologiques au Sahel

ABDOU ALI[1], ABOU AMANI[1], THIERRY LEBEL[2] & SIDIBÉ IBRAHIMA[1]

1 *Centre Régional Agrhymet, BP 1101, Niamey, Niger*
a.ali@agrhymet.ne

2 *Institut de Recherche pour le développement(IRD), BP 11416, Niamey, Niger*

Résumé Une méthodologie simple, permettant d'élaborer des scénarios de pluie aux échelles hydrologiques au Sahel, tout en respectant la tendance pluviométrique des décennies futures, que pourrait fournir un MCGA, est proposée. Cette méthodologie est basée sur la caractéristique fondamentale de la climatologie des pluies sahéliennes, à savoir le nombre d'événements comme étant le moteur principal de la variabilité interannuelle et intra-saisonnière. La mise en œuvre d'une Chaîne de Markov d'ordre 1 a permis d'évaluer le modèle et de montrer sa performance à bien restituer la variabilité interannuelle de la pluie, le signal intra-saisonnier, les séquences sèches séparant deux jours pluvieux.

Mots clefs Sahel; pluies des MCGA; scénarios de pluie; échelle hydrologique

Optimal use of GCM rainfall information at the hydrological scale in the Sahel

Abstract A simple methodology that enables the production of rainfall scenarios at the hydrological scale in the Sahel, while taking into account the coming decades' rainfall trends as provided by a Global Circulation Model (GCM), is proposed. This methodology is based on the fundamental characteristic of the Sahelian rainfall climatology, namely the number of events as the major factor in the inter-annual and intra-seasonal variability. The application of a first order Markov Chain made it possible to assess the model and to show its performance in terms of simulating well the interannual and intra-seasonal variability of Sahelian rainfields with respect to the dry spells between two rainy days.

Key words Sahel; GCM rainfall outputs; rainfall scenarios; hydrological scale

INTRODUCTION

Les modèles de circulation générale atmosphérique (MCGA) en mode couplé Atmosphère–Océan sont, actuellement, les seuls outils disponibles pour la prédiction du climat futur. Cette prédiction est faite à de larges résolutions spatiales et temporelles sur la base d'un scénario de production de gaz à effet de serre. La pluie est le paramètre atmosphérique le plus déterminant pour étudier l'impact de la variabilité et du changement climatique sur l'écosystème et les activités socio-économiques au Sahel. La question classique qui vient en tête quand on considère les sorties pluviométriques des MCGA pour des études hydrologiques est le problème d'échelle. La résolution spatiale des MCGA, de l'ordre de 3° × 3°, est trop grossière par rapport aux échelles utilisées en hydrologie, de l'ordre 0.1° × 0.1°. La problématique de l'utilisation des pluies des MCGA en hydrologie, ne porte pas, cependant, sur la seule question de l'échelle spatiale ou temporelle. Un aspect important de cette problématique concerne l'erreur associée aux pluies des MCGA. Nous proposons, dans la présente étude, une méthodologie simple, qui permet de produire des scénarios de pluie aux échelles hydrologiques. Cette méthodologie, utilise de façon optimale la modélisation stochastique à l'échelle de l'événement pluvieux et l'information sur la tendance future de la pluie, susceptible d'être fournie par les MCGA.

PLUIES DES MCGA

Nous rappelons dans cette section quelques caractéristiques des pluies des MCGA couplés. Les MCGA actuels ne restituent pas la sécheresse observée au Sahel. Quand on compare le cycle saisonnier moyen entre pluie observée et pluie simulée par un MCGA, on observe un important biais. Les modèles surestiment fortement la pluie des marges de la saison, mais sous-estiment celle d'août et de septembre. Ce biais dans le cycle saisonnier peut conduire, même en cas de désagrégation, à une très mauvaise évaluation de l'impact du climat sur les ressources en eau. De même quand on compare les distributions statistiques, on observe que la fréquence des pluies journalières nulles des MCGA est plus faible que celle de l'observation. Les pluies comprises entre 1.5 et 8.5 mm sont, cependant, plus fréquentes au niveau des modèles (Hamatan, 2006; Ardoin-Bardin, 2004).

Copyright © 2006 IAHS Press

NOTRE PROPOSITION POUR ELABORER DES SCENARIOS DE PLUIE AUX ECHELLES HYDROLOGIQUES AU SAHEL

Nous avons rappelé à la section qui précède que les sorties pluviométriques des MCGA couplés ne reproduisent ni la variabilité interannuelle de la pluie au Sahel, ni le signal saisonnier, ni la distribution statistique des pluies journalières. Les méthodes de désagrégation utilisant les variables de la circulation à grande échelle (comme le champ de vent, de pression et de température) fournies par un MCGA ne permettent pas d'obtenir les caractéristiques haute résolution de la pluie au Sahel. La méthode que nous proposons consiste à exploiter le fait qu'au Sahel le nombre d'événements est le principal moteur de la variabilité intra-saisonnière et interannuelle de la pluie (Balme, 2004), d'une part, et que la moyenne et la distribution du cumul événementiel paraît stable entre années humides et sèches (Le Barbé & Lebel, 1997), d'autre part. La loi des Fuites et le modèle de Chaîne de Markov, sont deux modèles mixtes qui font explicitement apparaître le nombre et le cumul des événements. Ils sont par conséquent bien adaptés à l'étude des pluies au Sahel. En effet, *toute augmentation ou diminution de la pluie moyenne annuelle pourra se traduire dans les paramètres relatifs au nombre d'événements*: ceci est la base de notre proposition. Ainsi pour générer des scénarios de pluie à partir de ces deux modèles, tout en tenant compte de la tendance pluviométrique des décennies futures fournie par un MCGA, ce sont les paramètres relatifs à l'occurrence des événements qui seront modifiés. On cherche, dans cette approche, que les MCGA soient seulement capables de fournir la tendance de la pluie moyenne interannuelle et, de notre point de vue, c'est le minimum d'information qu'on peut exiger d'eux pour faire des études d'impact. Nous évaluons cette proposition en utilisant l'exemple d'une Chaîne de Markov.

MISE EN ŒUVRE ET EVALUATION DE LA METHODE PROPOSEE

Paramètres des chaînes de Markov au Sahel

Nous considérons une Chaîne de Markov d'ordre 1 pour la modélisation de l'occurrence des jours pluvieux. Une Chaîne de Markov d'ordre 1 est caractérisée par deux paramètres: la probabilité (P_{01}) qu'il pleuve au jour j + 1 sachant qu'il n'a pas plu au jour j et la probabilité (P_{11}) qu'il pleuve au jour j + 1 sachant qu'il a plu au jour j. Ces deux probabilités sont appelées probabilité de transition. Pour estimer ces paramètres au Sahel, 244 stations, bien reparties sur toute la zone CILSS (Comité Inter-états de Lutte contre la Sécheresse au Sahel) et ayant fonctionné sur toute la période (1961–1990), ont été choisies (Fig. 1). Nous allons vérifier que ces deux paramètres (P_{01}, $P1_{11}$) expliquent bien la variabilité interannuelle et intra-saisonnière de la pluie au Sahel, avant de présenter la procédure de simulation.

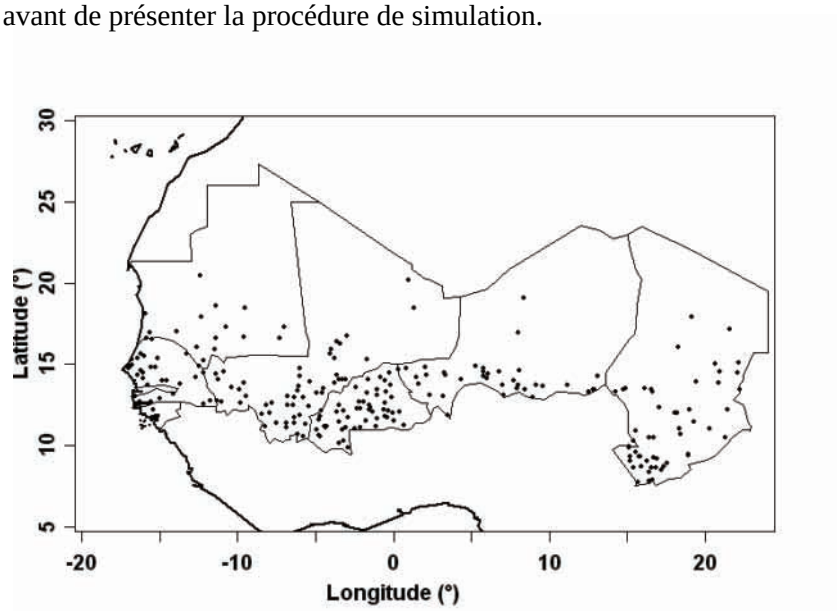


Fig. 1 Le réseau de 244 stations du Centre AGRHYMET utilisé dans le présent travail. Toutes ces stations possèdent des données journalières complètes sur la période 1961–1990.

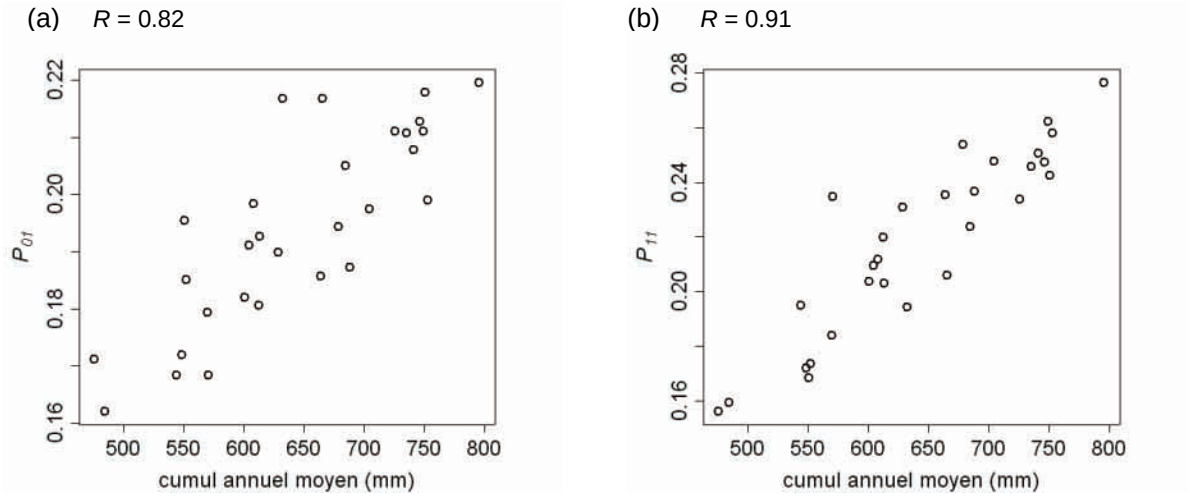


Fig. 2 Corrélation entre les probabilités de transition de la Chaîne de Markov et le cumul annuel. (a) corrélation entre la probabilité de transition de jour sec / jour de pluie (ou P_{01}), et (b) corrélation entre la probabilité de transition jour de pluie/jour de pluie (ou P_{11}).

Variabilité interannuelle En Fig. 2, sont représentées les relations entre la moyenne du cumul annuel de la pluie, d'une part, et la moyenne annuelle des paramètres P_{01} et P_{11}, d'autre part. Les valeurs annuelles de P_{01} et P_{11} sont notées $P_{01}{}^{a}$ et $P_{11}{}^{a}$ et sont calculées de la manière suivante:

$$P_{01}{}^{a} = 1/N_S \left[\sum_{k=1}^{N_S} \left(N_{01}/N_0 \right)_k \right] \quad (1)$$

$$P_{11}{}^{a} = 1/N_S \left[\sum_{k=1}^{N_S} \left(N_{11}/N_1 \right)_k \right] \quad (2)$$

avec N_{01} nombre de couples (jour sec, jour pluvieux) pour une station k sur la saison (la période considérée dans ce travail va du premier mai au 31 octobre); N_{11} nombre de couples (jour pluvieux, jour pluvieux); N_0 nombre de jours sans pluie; N_1 nombre de jours pluvieux; N_S nombre de stations de l'année (N_S = 244 pour toutes les années). Un jour pluvieux est un jour pour lequel le cumul de pluie journalière est supérieure ou égale à 1 mm.

On observe des relations satisfaisantes entre le cumul annuel et ces probabilités de transition de la Chaîne de Markov d'ordre 1. Ces relations entre la pluie moyenne annuelle et les paramètres de la Chaîne de Markov confortent les résultats antérieurs sur la climatologie des pluies au Sahel, à savoir que le nombre d'événements est le moteur principal de la variabilité interannuelle des pluies au Sahel (Le Barbé & Lebel, 1997). L'hypothèse de notre démarche, selon laquelle toute diminution ou augmentation de la pluie moyenne annuelle peut être directement reportée dans les paramètres de la Chaîne de Markov, se trouve renforcée.

Variabilité intra-saisonnière Voyons maintenant si le signal intra-saisonnier de la pluie est aussi expliqué par les paramètres de la Chaîne de Markov. En Fig. 3, nous avons calculé les paramètres P_{01} et P_{11} pour chaque jour de la saison en utilisant les 30 années (1960–1990). On peut remarquer de cette figure que le signal intra-saisonnier de la pluie se retrouve parfaitement expliqué par les probabilités de transition de la Chaîne de Markov (avec le maximum des valeurs pour le mois d'août). Un résultat important à souligner dans ce signal intra-saisonnier est la présence du saut de Mousson (Sultan & Janicot 2000) dans l'évolution intra-saisonnière de la probabilité qu'il pleuve au lendemain d'un jour pluvieux (P_{11}). Il se situe dans les environs du 25 juin. Ce résultat est d'autant plus important car il laisse espérer de retrouver le saut de Mousson dans les simulations de la pluie.

Procédure de la simulation

Nous avons vu dans les sections précédentes que la variabilité interannuelle et le signal intra-saisonnier des pluies au Sahel sont expliqués par les probabilités de transition d'une Chaîne de

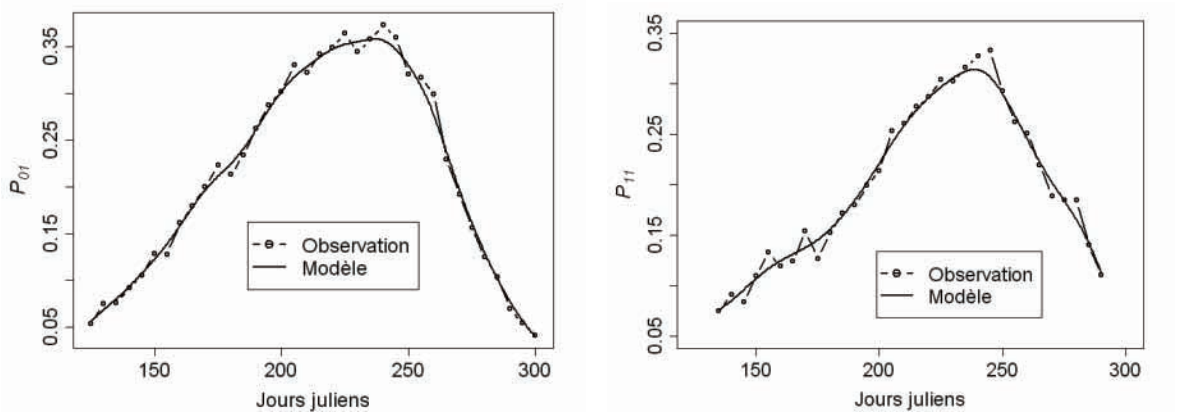


Fig. 3 Signal intra-saisonnier des probabilités de transition de la Chaîne de Markov. Un modèle non paramétrique est calé sur ce signal.

Markov d'ordre 1. Nous allons maintenant élaborer un simulateur de Chaîne de Markov non stationnaire. La Chaîne de Markov est non stationnaire, car les probabilités de transition changent chaque jour au cours de la saison. Cette Chaîne de Markov d'ordre 1 est caractérisée par la matrice P suivante: $P = \begin{bmatrix} 1-P_{01}(t) & P_{01}(t) \\ 1-P_{11}(t) & P_{11}(t) \end{bmatrix}$ où t représente les jours de la saison. Pour utiliser cette matrice non stationnaire, il faut modéliser la variation intra-saisonnière de P_{01} et P_{11}. Vu la forme du signal intra-saisonnier de P_{01} et P_{11}, il a été difficile d'ajuster un modèle paramétrique. Nous avons alors opté pour une solution non paramétrique. La forme du modèle adopté est représentée par l'équation (3) (Bowman & Azzalini,1997):

$$P_{x1}(t) = \frac{1}{N}\sum_{i=1}^{N} K\left[(t - t_j)/\varphi_{x1}\right] \tag{3}$$

où $K(z) = \frac{1}{\sqrt{2\pi}} \exp\left[{(-z^2)}/{2}\right]$ est la fonction de densité normale constituant le noyau du modèle; N est le nombre de jours de la saison, tj les jours de la saison, φ_{x1} la largeur de la bande de lissage du modèle non paramétrique. $\varphi_{01} = 6.80$ et $\varphi_{11} = 5.87$ sont les largeurs des bandes respectivement pour le modèle de P_{01} et de P_{11}. La Fig. 3 montre que le modèle proposé s'ajuste bien aux observations de P_{01} et P_{11}. Le saut de Mousson apparaît plus ou moins bien reproduit par le modèle. La procédure de simulation est la suivante:

(a) on simule en un point les occurrences des pluies (jour pluvieux codé 1 et jour sec codé 0) en utilisant le modèle ainsi proposé pour les probabilités de transition de la Chaîne de Markov;
(b) on tire ensuite le cumul de pluie associé à chaque jour pluvieux suivant une distribution exponentielle obtenue par ajustement aux cumuls observés (la moyenne des pluies journalières supérieures à 1mm est de 16 mm).

RESULTATS

Variabilité intra-saisonnière

Pour savoir si le modèle reproduit bien le cycle saisonnier, nous avons effectué 200 simulations et chaque simulation représente une saison. La Fig. 4 représente la moyenne de ces 200 simulations. On peut ainsi constater que le signal saisonnier de la pluie moyenne journalière est bien reproduit. La courbe de lissage pour les simulations et pour l'observation sont en bon accord. Ces lissages ont été effectués en utilisant l'équation (3) pour les 200 simulations et les trente années d'observation (1961–1990).

Les séquences sèches

La répartition temporelle des jours de pluie est importante en hydrologie, car un cumul de 200 mm tombé en deux jours ou en dix jours n'aura pas le même impact hydrologique. Nous avons calculé

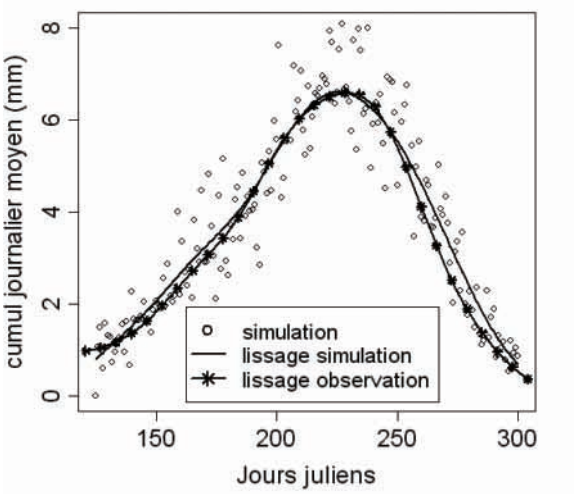


Fig. 4 Simulation, à partir de la Chaîne de Markov et d'une distribution exponentielle des cumuls journaliers, de la variabilité intra-saisonnière de la pluie journalière. On compare le lissage de 200 simulations et celui des 30 années observées (1961–1990).

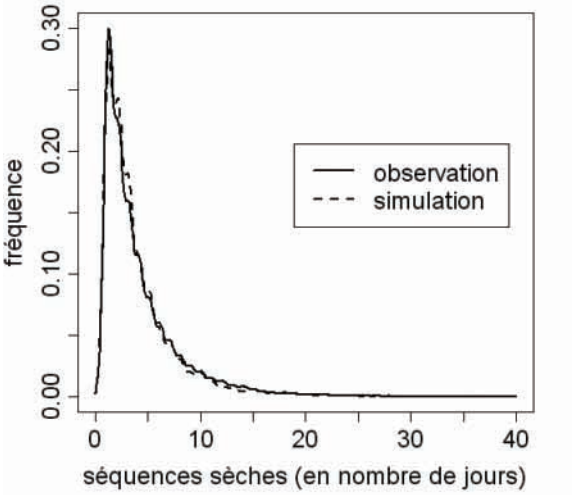


Fig. 5 Comparaison des séquences sèches simulées par l'approche d'une Chaîne de Markov et celles obtenues à partir des pluies observées.

r les séquences sèches séparant deux jours de pluie (nous appelons qu'un jour de pluie est un jour dont le cumul est supérieur ou égal à 1 mm) sur 10 années simulés et 10 années observées et pour la période allant du premier mai au 31 octobre. Les distributions des séquences simulées et observées sont comparées en Fig. 5. Nous notons une forte ressemblance entre l'observation et la simulation.

Variabilité interannuelle

Nous avons noté que, pour le moment, la seule importante information pluviométrique qu'on peut espérer obtenir des MCGA est la tendance générale de la pluviométrie, c'est à dire le pourcentage d'augmentation ou de diminution de la pluie par rapport à une référence donnée. Nous évaluons dans ce paragraphe, la capacité de notre approche à reproduire la variabilité interannuelle des pluies au Sahel sur la base de la seule connaissance de la pluie moyenne interannuelle. Nous considérons pour cela 30 ans de période humide (1941–1970) et 30 ans de période sèche (1971–2000). Une augmentation de 20% par rapport à la moyenne calculée sur (1941–2000) est considérée pour la période humide et une diminution de 20% est considérée pour la période sèche. Ces pourcentages sont reportés dans les probabilités de transition de la Chaîne de Markov pour simuler les soixante ans de la période 1941–2000. On retrouve en Fig. 6, une forme de variabilité

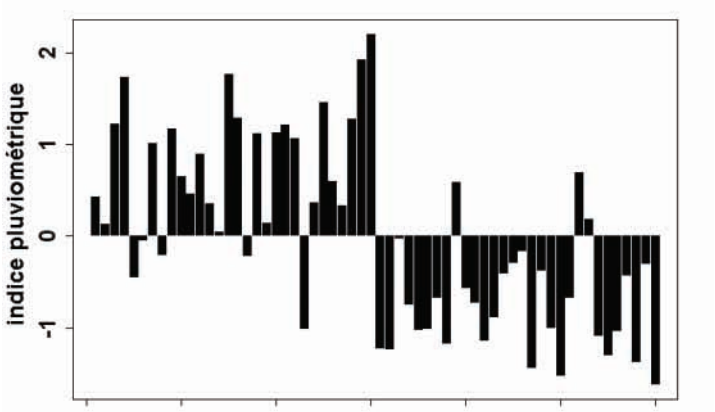


Fig. 6 Simulation de la variabilité interannuelle de la pluie à partir du modèle de Chaîne de Markov et de la distribution exponentielle des cumuls journaliers. Les probabilités de transition de la Chaîne de Markov ont été augmentées de 20% pour la période 1941–1970 et diminuées de 20% pour la période 1971–2000.

interannuelle qui ressemble bien à ce qui est observé. La période 1941–1970 sur laquelle on a opéré l'augmentation, montre une persistance des années humides avec quelques occurrences brutes d'années sèches. De même la période 1971–2000 sur laquelle on a opéré la diminution, montre une persistance des années sèches avec quelques occurrences brutes d'années humides.

CONCLUSION

Les techniques de désagrégation des sorties des MCGA rencontrées dans la littérature ne permettent pas, au Sahel, de passer de manière adéquate de l'information à grande échelle fournie par un MCGA à la pluie à haute résolution aux échelles locales, d'une part. Les méthodes de simulation calées sur les observations prennent difficilement en compte l'information fournie par un MCGA, d'autre part. Partant de ce constat, nous avons, sur la base des propriétés spécifiques de la climatologie des pluies sahéliennes, proposé une approche simple de production des scénarios de pluie au Sahel. L'information sur la tendance générale de la pluviométrie que pourrait fournir par un MCGA est simplement reportée dans les probabilités de transition d'une Chaîne de Markov. La mise en œuvre et l'évaluation de l'approche ont montré que cette procédure permet de reproduire toutes les caractéristiques importantes de la pluie au Sahel: le signal saisonnier, la variabilité interannuelle, la distribution des fréquences sèches. Cette évaluation montre donc, le potentiel que présente une telle approche. Il est envisagé d'utiliser ces scénarios de pluie dans un modèle hydrologique pour tester la pertinence des scénarios hydrologiques qui en résultent. Un aspect important de cette recherche reste, cependant, à poursuivre: il s'agit de la prise en compte de la corrélation spatiale entre les stations lors de la génération des pluies.

REFERENCES

Ardoin-Bardin, S. (2004) Variabilité hydroclimatique et impacts sur les ressources en eau de grands bassins hydrographiques en zone soudano-sahélienne. Thèse de Doctorat, Université Montpellier II, France.

Balme, M. (2004) Analyse du régime pluviométrique sahélien et de son impact sur le rendement mil à l'aide des données de l'Observatoire AMMA-CATCH, Niger. Thèse de Doctorat, Institut National Polytechnique de Grenoble, France.

Bowman, A. W. & Azzalini, A. (1997) *Applied Smoothing Techniques for Data Analysis: The Kernel Approach with S-PLUS Illustrations*. Oxford University Press, Oxford, UK.

Hamatan, M. (2006) Evaluation des Modèles de la circulation générale atmosphérique au Sahel et des modèles hydrologiques. Thèse en cours au Centre Régional AGRHYMET.

Le Barbé, L. & Lebel T. (1997) Rainfall climatology of the HAPEX-Sahel region during the years 1950–1990. *J. Hydrol.* **188**, 43–73.

Sultan, B. & Janicot, S. (2000) Abrupt shift of the ITCZ over West Africa and intra-seasonal variability. *Geophys. Res. Lett.* **27**, 3353–3356.

Climate Variability and Change—Hydrological Impacts (Proceedings of the Fifth FRIEND World Conference held at Havana, Cuba, November 2006), IAHS Publ. 308, 2006.

Application de scénarii climatiques en modélisation hydrologique: utilisation des sorties GCM

SANDRA ARDOIN-BARDIN, ALAIN DEZETTER, ERIC SERVAT, CLAUDINE DIEULIN, LAURENCE CASENAVE, HÉLÈNE NIEL, JEAN-EMMANUEL PATUREL & GIL MAHÉ

UMR HydroSciences Montpellier, IRD, BP 64501, F-34394 Montpellier cedex 5, France
ardoin@msem.univ-montp2.fr

Résumé Cette étude aborde le problème de l'utilisation des données issues des GCM pour évaluer l'impact du changement climatique sur les écoulements, en particulier, pour l'Afrique de l'Ouest. Il s'agit, d'une part, d'évaluer la fiabilité de quatre GCM (HadCM3, ECHAM4, NCAR-PCM, CSIRO-MK2) au regard des précipitations et, d'autre part, d'évaluer les impacts du changement climatique sur les écoulements de quatre grands fleuves (Sénégal, Gambie, Sassandra, Chari). Pour ce faire, les précipitations simulées par les GCM sont comparées à celles observées. Ces données simulées, peu réalistes, ne peuvent être utilisées directement dans les modèles hydrologiques pour les études d'impacts. C'est pourquoi deux scénarii climatiques basés sur les variations prévues par le modèle HadCM3-A2 ont été élaborés et introduits dans le modèle hydrologique GR2M. Les résultats montrent que les variations envisageables des écoulements dans le futur sont très dépendantes des précipitations et donc de la qualité des sorties du GCM utilisé.

Mots clefs impacts; GCM; scénarii climatiques; modélisation hydrologique; ressources en eau; Afrique de l'Ouest et Centrale

Application of climatic scenarios in hydrological modelling: using GCMs outputs

Abstract This study deals with the issue of using GCMs data to assess the impact of climate change on runoff in western Africa. It requires evaluation of the reliability of four GCMs (HadCM3, ECHAM4, NCAR-PCM, CSIRO-MK2) regarding the rainfall they provide, and then assessment of the impacts of climate change on the discharge of four main rivers (Senegal, Gambia, Sassandra, Chari). First, GCM rainfalls were compared to observed ones. It appears that the data generated by the GCMs cannot be used as direct input to hydrological models to evaluate the impacts as they are not realistic enough. For this reason, two climatic scenarios were developed from the results provided by HadCM3-A2. These two scenarios were used as input to the hydrological model GR2M. The results demonstrate that expected runoff variations remain strongly linked to rainfall and so to the quality of the GCMs outputs used.

Key words impacts; GCM; climatic scenarios; hydrological modelling; water resources; West and Central Africa

INTRODUCTION

Le changement climatique annoncé pour le 21ème siècle par les Modèles de Circulation Générale (ou GCM) ne peut être sans conséquence sur les ressources en eau. L'estimation des impacts sur les systèmes hydrologiques est essentielle pour comprendre et prévenir les problèmes potentiels sur les ressources en eau et leur gestion future. Cependant la modélisation du système climatique est complexe et trois problèmes majeurs relatifs à l'utilisation des GCM peuvent être soulevés (IPCC, 2001): leur résolution n'est pas adaptée à celle de la modélisation hydrologique; les différences entre les projections climatiques produites par les GCM sont très marquées; les précipitations sont généralement peu réalistes. Cependant, ces GCM, même imparfaits, sont les seuls outils à notre disposition pour simuler les conditions climatiques futures. Il s'agit ici d'évaluer la fiabilité des données climatiques fournies par divers GCM, et donc, de vérifier que ces modèles climatiques sont suffisamment performants pour reproduire correctement les précipitations en termes de dynamique saisonnière et de variabilité interannuelle. Pour cela, quatre modèles climatiques ont été choisis parmi ceux mentionnés par l'IPCC. Les précipitations simulées par ces GCM sont comparées à celles observées sur la période 1950–1998, lorsque la disponibilité des données le permet. Ensuite, cette étude propose d'évaluer les impacts du changement climatique sur les écoulements de grands fleuves en Afrique de l'Ouest (Sénégal, Gambie, Sassandra et Chari). La méthodologie présentée repose sur l'utilisation de la modélisation pluie-débit comme outil de simulation des écoulements, et les sorties du modèle climatique HadCM3-A2 comme source de prévisions climatiques pour le futur.

Copyright © 2006 IAHS Press

DESCRIPTION DES DONNÉES

Grilles de données climatiques

Les données climatiques utilisées dans cette étude sont spatialisées sous forme de grilles à la résolution du demi-degré carré. Les données observées couvrent la période 1950–1995 et ont été obtenues auprès du Climatic Research Unit (CRU) de l'Université d'East Anglia. Il s'agit de grilles mensuelles, construites par interpolation de séries pluviométriques sélectionnées pour la qualité et la longueur de leurs observations (New *et al.*, 2000), et de données d'évapotranspiration potentielle (ou ETP), calculées à partir de la formule de Penman (1956). Les autres données climatiques utilisées dans cette étude proviennent des simulations produites par les GCM et sont extraites des archives du Data Distribution Centre de l'IPCC (http://ipcc-ddc.uea.ac.uk). Ces archives contiennent les simulations de changement climatique obtenues avec sept modèles climatiques couplés océan-atmosphère et conduites en utilisant divers scénarii d'émissions de gaz à effet de serre. Seuls quatre d'entre eux avec le scénario d'émission A2 ont été retenus pour cette étude (Tableau 1): CSIRO-Mk2, ECHAM4, HadCM3 et NCAR-PCM.

Tableau 1 Caractéristiques principales des quatre GCM retenus.

GCM	Résolution spatiale	Scénario d'émission	Données disponibles
CSIRO–Mk2	3.2°× 5.6°	A1,A2,B1,B2	1961–2100
ECHAM4	2.8°× 2.8°	A2,B2	1990–2100
HadCM3	2.5°× 3.75°	A2,B2	1950–2099
NCAR–PCM	2.8°× 2.8°	A1b,A2	1981–2099

Bassins versants et modèle hydrologique

Cette étude concerne quatre unités hydrographiques situées en Afrique de l'Ouest et Centrale: Sénégal, Gambie, Sassandra et Chari (Tableau 2). Les données hydrologiques mensuelles correspondantes proviennent des données collectées par l'IRD, complétées auprès des Services Hydrologiques Nationaux et rassemblées au sein du système d'informations environnementales SIEREM développé par HydroSciences Montpellier.

Tableau 2 Caractéristiques des unités hydrographiques étudiées.

Rivière	Station	Données disponibles	Surface (km^2)
Sénégal	Bakel	1908–1998	220 818
Gambie	Gouloumbo	1971–1996	42 642
Sassandra	Soubre	1956–1998	62 173
Chari	Ndjamena	1933–1999	601 984

Les écoulements mensuels ont été simulés avec le modèle conceptuel GR2M en utilisant une distribution du bassin versant en un maillage régulier au demi-degré carré. Sur chaque cellule du réseau et à chaque pas de temps, le niveau d'un réservoir sol évolue en fonction de la pluie et de l'ETP. La vidange progressive de ce réservoir produit l'écoulement retardé. L'écoulement à l'exutoire du bassin versant est obtenu par la sommation des contributions des différentes cellules du réseau. Le remplissage maximal du réservoir sol correspond à la capacité en eau du sol, dont les données sont estimées à partir de la carte des sols de la FAO (Dieulin, 2005). Avec la perspective d'utiliser ce modèle hydrologique dans la continuité chronologique des observations pour simuler les écoulements dans le futur, les paramètres du modèle sont calés pour les conditions déficitaires, installées depuis la fin des années 60 et qui perdurent aujourd'hui (L'Hôte *et al.*, 2002). Ainsi pour chaque bassin versant, les deux paramètres du modèle sont estimés à partir d'un calage sur la période 1971–1987 et validés sur la période 1988–1995.

COMPARAISON DES DONNÉES PLUVIOMÉTRIQUES (1990–1998)

Méthodes

Un des problèmes majeurs de l'utilisation des simulations produites par les GCM dans les études d'impacts est leur résolution spatiale "grossière" par rapport aux entités étudiées. Plusieurs méthodes, connues sous le nom de downcsaling, ont donc été développées pour obtenir des projections climatiques à une échelle spatio-temporelle plus fine. Une méthode plus simple consiste à superposer le réseau du GCM à celui du CRU et d'appliquer la valeur d'une cellule de GCM à l'ensemble des cellules observées concernées (désagrégation) et inversement (agrégation). Les formules d'agrégation et de désagrégation utilisées ici peuvent être consultées dans Casenave (2004). Afin de juger de la fiabilité des modèles climatiques à simuler le climat, les précipitations observées sont agrégées à la résolution des GCM puis comparées aux précipitations simulées par les GCM. Les résultats sont donnés soit pour l'ensemble de la zone d'étude, soit pour des cellules représentatives des bassins versants.

Précipitations annuelles

Les quatre GCM retenus pour cette étude reproduisent bien la répartition latitudinale des précipitations moyennes annuelles en Afrique de l'Ouest (Fig. 1). Les trois unités climatiques sahélienne, soudanienne et guinéenne sont bien identifiées sur la fenêtre d'étude, mais leurs limites ne correspondent pas à celles réellement observées et varient selon le modèle climatique étudié. À l'exception du modèle climatique CSIRO-Mk2, les modèles climatiques ECHAM4, HadCM3 et NCAR-PCM surestiment généralement les précipitations moyennes annuelles sur l'Afrique de l'Ouest. Avec ces trois GCM, la limite entre les domaines climatiques sahélien et soudanien, correspondant à l'isohyète 700 mm, se situe au nord de celle observée sur la période 1969-1998. Avec les modèles ECHAM4 et HadCM3, les précipitations sur la Côte d'Ivoire, le Ghana, le Togo et le Bénin sont supérieures à 1400 mm, ce qui ne correspond pas aux observations. Les modèles CSIRO-Mk2 et NCAR-PCM ne restituent pas bien les précipitations annuelles sur les pays de la façade atlantique de l'Afrique de l'Ouest, normalement situés en domaine guinéen, ni d'ailleurs sur la partie septentrionale du Congo.

Concernant la variabilité interannuelle, la Fig. 2 compare les chroniques d'indices pluviométriques annuels observés et simulés par les différents GCM, entre 1950 et 1998. Cet indice traduit un excédent ou un déficit pluviométrique. Durant le 20ème siècle, des périodes sèches et humides ont alterné en Afrique de l'Ouest avec une nette et brutale diminution des précipitations

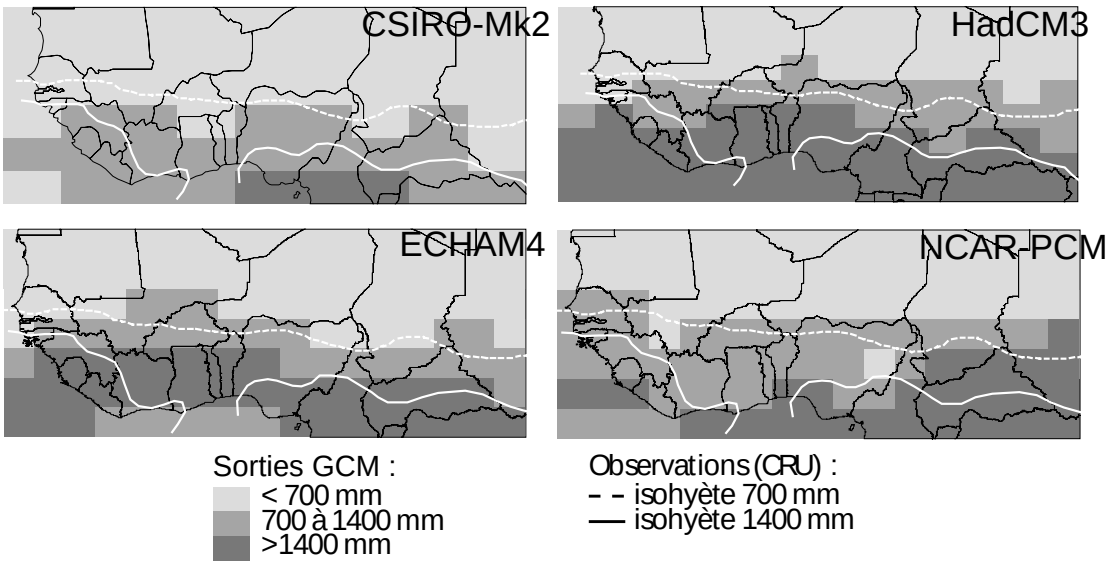


Fig. 1 Position des isohyètes 700 mm et 1400 mm (d'après les données du CRU sur 1969–1998) et précipitations moyennes annuelles simulées par: CSIRO-Mk2 (1961–1998), ECHAM4 (1990–1998), HadCM3 (1950–1998) et NCAR-PCM (1981–1998).

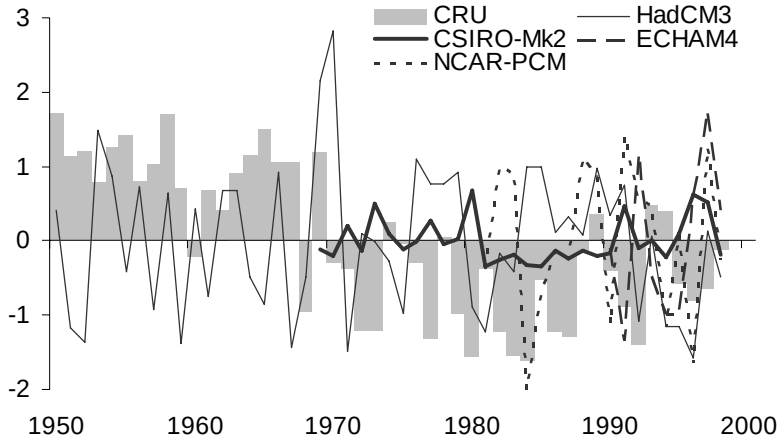


Fig. 2 Anomalies de précipitations observées (CRU, 1950–1998) et simulées par modèles climatiques pour les cellules représentatives des bassins Sénégal et Gambie.

aux alentours de 1969–1970. Cependant, aucun des modèles climatiques étudiés ne reproduit correctement cette alternance. Ainsi le modèle HadCM3 simule une année sur deux comme étant sèche entre 1950 et 1970, période pourtant caractérisée par des précipitations excédentaires (période humide). Sur la période commune aux observations et aux simulations (1990–1998), les quatre modèles climatiques s'accordent en simulant l'année 1994 comme sèche et l'année 1997 comme humide, alors que le contraire a été observé.

Précipitations moyennes mensuelles

Leur aptitude à simuler la saison des pluies a également été étudiée par l'intermédiaire des précipitations moyennes mensuelles calculées sur la période 1990-1998 et comparées aux observations (Fig. 3). Pour le Sénégal et la Gambie, les GCM sous-estiment largement les précipitations mais respectent bien la dynamique saisonnière du domaine soudano-sahélien: la saison des pluies se déroule de mai à octobre avec un maximum centré sur août, à l'exception du modèle NCAR-PCM qui présente un maximum en juillet. Pour le Chari, situé également en domaine soudano-sahélien, seules les précipitations produites par les modèles CSIRO-Mk2, NCAR-PCM et HadCM3 sont corrélées avec les précipitations observées. Le modèle ECHAM4 bien que reproduisant la dynamique saisonnière, surestime largement les précipitations mensuelles, quel que soit le mois de l'année considéré. Le Sassandra est situé en Côte d'Ivoire, en domaine tropical humide où se produisent deux saisons des pluies (avril–juin et août–octobre). Or les modèles climatiques, s'ils sont capables de reproduire cette saisonnalité (excepté HadCM3), montrent de réelles difficultés à simuler correctement les volumes précipités. Aucun des quatre modèles climatiques ne semble vraiment approprié sur cette cellule, et, par extension, probablement sur la zone guinéenne à deux saisons des pluies.

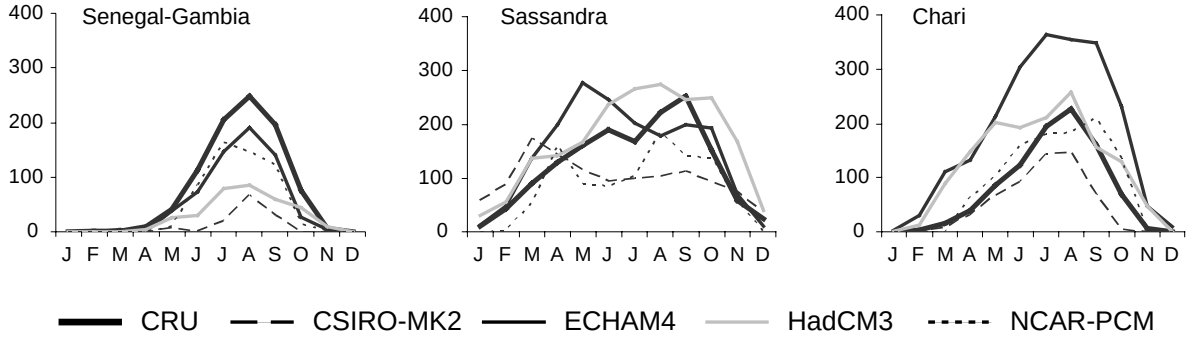


Fig. 3 Précipitations moyennes mensuelles sur la période 1990–1998 observées (CRU) et simulées par les modèles climatiques pour les bassins versants étudiés.

APPLICATION EN MODÉLISATION HYDROLOGIQUE (2006–2095)

Méthodologie

Les précipitations simulées par les GCM ne sont donc pas suffisamment fiables pour être utilisées directement et telles quelles dans les études d'impacts et, *a fortiori*, dans les modèles hydrologiques. L'IPCC recommande, de ce fait, d'établir des scénarii climatiques en utilisant les champs de variations entre le climat futur et une période de référence. Le modèle climatique retenu pour le développement et l'application de ces scénarii climatiques est HadCM3-A2. Les différences entre le climat (précipitations et ETP) de la période de référence et le climat futur sont calculées pour chaque cellule du GCM et à chaque pas de temps. Elles sont alors exprimées en anomalies standardisées (scénario *Anomalies*) ou en taux de variations (scénario *Horizons*) en fonction d'une climatologie moyenne tirée des simulations du GCM sur la même période de référence (Ardoin-Bardin *et al.*, 2005). La méthode employée pour étudier l'impact du changement climatique sur les ressources en eau consiste alors à utiliser les séries mensuelles de précipitations et d'ETP, élaborées à partir des deux scénarii climatiques *Anomalies* et *Horizons*, en entrée du modèle hydrologique GR2M, préalablement calé pour chaque bassin versant, pour simuler les écoulements futurs.

Conséquences hydrologiques du changement climatique

Dans l'ensemble, l'impact du changement climatique sur les écoulements varie en fonction de l'évolution des précipitations projetées par le modèle HadCM3-A2: un excès (déficit) des précipitations selon les scénarii *Anomalies* ou *Horizons* se traduit par une augmentation (diminution) des écoulements. Il semble par contre que l'augmentation continue de l'ETP, liée à celle de la température, affecte peu le bilan hydrologique annuel. Le Tableau 3 illustre l'évolution des écoulements au cours du 21ème siècle selon des taux de variations calculés par rapport à la période 1971–1995. Les variations des écoulements entre le scénario *Anomalies* et le scénario *Horizons* sont de même signe, même si les écarts entre les taux peuvent être importants à l'horizon 2080. Pour les bassins versants du Sénégal et de la Gambie, la tendance est à la diminution des écoulements. Pourtant aux horizons 2020 et 2050, le Sénégal présente des taux de variations positifs alors qu'ils sont négatifs pour la Gambie. Ces différences s'expliquent par la répartition des cellules du modèle HadCM3-A2 au-dessus des bassins versants. Les débits moyens annuels simulés sur les dernières décennies du 21ème siècle seraient alors plus faibles que ceux observés sur la période 1971–1995. Au contraire, les projections climatiques du modèle HadCM3-A2 conduisent à l'augmentation des écoulements pour les bassins du Chari et du Sassandra. Pour le Chari, les débits moyens annuels augmenteraient progressivement tout au long du 21ème siècle. Pour le Sassandra, les taux de variations à l'horizon 2080 sont plus faibles qu'à l'horizon 2050. Malgré cette tendance à l'augmentation, les écoulements ne retrouveraient pas les niveaux observés avant la mise en place de la sécheresse sur l'Afrique de l'Ouest et Centrale.

Tableau 3 Évolution des taux de variations des débits moyens annuels (en %) calculés aux horizons 2020, 2050 et 2080 pour chaque scénario climatique utilisé.

Rivière/Bassin	2020		2050		2080	
	Ano	Horiz	Ano	Horiz	Ano	Horiz
Sénégal	+13.9	+1.9	+12.7	+10.4	–13.9	–44.8
Gambie	–3.6	–17.5	–5.5	–11.6	–29.6	–65.6
Sassandra	+20.3	+17.7	+36.8	+38.3	+5.9	+9.9
Chari	+13.7	+12.3	+20.4	+25.9	+46.7	+53.5

CONCLUSION

Cette étude décrit une approche pour utiliser les sorties des GCM pour évaluer les changements possibles du climat et ses impacts potentiels sur les ressources en eau. Un des objectifs était d'évaluer les limites des modèles climatiques à reproduire le climat observé, du point de vue des

précipitations, dans le but de mieux appréhender les simulations futures. Les comparaisons établies au niveau des précipitations mensuelles (et même annuelles) soulignent bien les différences qui existent: (i) entre les modèles climatiques entre eux et (ii) entre données simulées et observées. Les modèles climatiques semblent atteindre les limites de leurs performances là où les précipitations sont faibles (zone sahélienne) et là où se produisent deux saisons des pluies (zone guinéenne). Par ailleurs, s'ils s'avèrent relativement performants dans la zone soudano-sahélienne en termes de dynamique saisonnière, ils sont en revanche incapables de reproduire les cumuls pluviométriques ainsi que la variabilité interannuelle des précipitations. A l'heure actuelle, ces GCM ne sont pas vraiment en mesure de reproduire les précipitations observées avec un niveau de fiabilité suffisant. Ces résultats ne permettent pas d'utiliser directement les sorties des modèles climatiques mais plutôt de prendre ne compte les tendances qu'ils expriment par l'intermédiaire des scénarii climatiques.

REFERENCES

Ardoin-Bardin, S., Servat, E., Dezetter, A., Mahé, G., Paturel, J. E., Dieulin, C. & Casenave L. (2005) Évaluation des impacts du changement climatique sur les ressources en eau d'Afrique de l'Ouest et Centrale. In: *Regional Hydrological Impacts of Climate Change – Hydroclimatological Variability* (ed by S. Franks, T. Wagener, E. Bøgh, H. V. Gupta, L. Bastidas, C. Nobre & C. De Oliveira Galvão), 194–202. IAHS Publ. 296. IAHS Press, Wallingford, UK.

Casenave, L. (2004) Hydro-climatic variability: comparison of different global circulation model in western Africa. Master Thesis. University of Chalmers. Sweden.

Dieulin, C. (2005) Calcul des capacités en eau des sols à partir de la carte des sols de la FAO. Note interne. UMR HydroSciences Montpellier, France.

IPCC (2001) *Climate Change 2001: Impacts, Adaptation and Vulnerability*. Contribution of Working Group II to the Third Assessment Report of the IPCC (ed. by J. J. McCarthy, O. F. Canziani, N. A. Leary, D. J. Dokken & K. S. White) Cambridge University Press, Cambridge, UK.

L'Hôte, Y., Mahé, G., Somé, B. & Triboulet, J. P. (2002) Analysis of a Sahelian annual rainfall index from 1896 to 2000: the drought continues. *Hydrol. Sci. J.* **47**(4), 563–572.

New, M., Hulme, M. & Jones, P. (2000) Representing twentieth century space-time climate variability. Part II: development of a 1901-1996 monthly grids of terrestrial surface climate. *J. Clim.* **13**(13), 2217–2238.

Penman, H. L. (1956) Evaporation: an introduction survey. *J. Agric. Sci.* **1**, 9–29.

Climate Variability and Change—Hydrological Impacts (Proceedings of the Fifth FRIEND World Conference held at Havana, Cuba, November 2006), IAHS Publ. 308, 2006.

Quel scénario de changement climatique retenir pour une analyse d'impacts?

CLAUDE BOCQUILLON, WAJDI NAJEM & ANTOINE HREICHE
CREEN, Université Saint Joseph, BP 11-0514 Riad-el-Solh, Beyrouth, Liban
claude.bocquillon@fi.usj.edu.lb

Résumé Les horizons de prévision de doublement du CO_2 (2050) avec les conséquences en termes climatiques, sont comparables aux délais de planification et de mise en œuvre des aménagements. Ces risques doivent être pris en compte par les aménageurs. La difficulté réside dans l'évaluation de l'incertitude liée à ce risque dans le cas d'une zone géographique réduite de 10 000 km^2, le Liban. Des problèmes existent à tous les niveaux de la modélisation: les modèles globaux de changement climatique présentent des résultats de validation en conditions actuelles, relativement faibles; les différences d'échelle considérables entre la taille des mailles des GCM et la taille des bassins hydrologiques; l'incertitude sur la signification des paramètres de la modélisation hydrologique; la propagation des incertitudes dans la chaîne des modélisations non linéaires. Cette cascade d'incertitudes, impossible à analyser correctement, rend le diagnostic très subjectif. Il importe de rester réaliste lorsqu'on propose un scénario au décideur.

Mots clefs changement climatique; impacts; Méditerranée

Which climate change scenario to keep for analysing impacts?

Abstract The time horizons of the forecast of doubling CO_2 (2050) and its consequences in climatic terms, are comparable with the times of planning and implementation of installations. It is thus normal that these risks are taken into account by developers. The difficulty lies in the quantification of this risk. A qualitative analysis of uncertainties was made in the case of a specific geographical area, i.e. Lebanon (10 000 km^2). Problems exist at all the levels of modelling: in global models of climatic change and their uncertainties. In particular: their validation in current conditions is relatively weak; the problems of scaling involved in the considerable difference between the size of the meshes of GCM and size of the watersheds; the uncertainty of the significance of hydrological model parameters; and propagation of uncertainties in the chain of modelling. This cascade of uncertainties, which is difficult to analyse correctly, makes the diagnosis subjective. It is important to remain realistic when one proposes a scenario to the decision maker.

Key words climate change; impacts; Mediterranean

INTRODUCTION

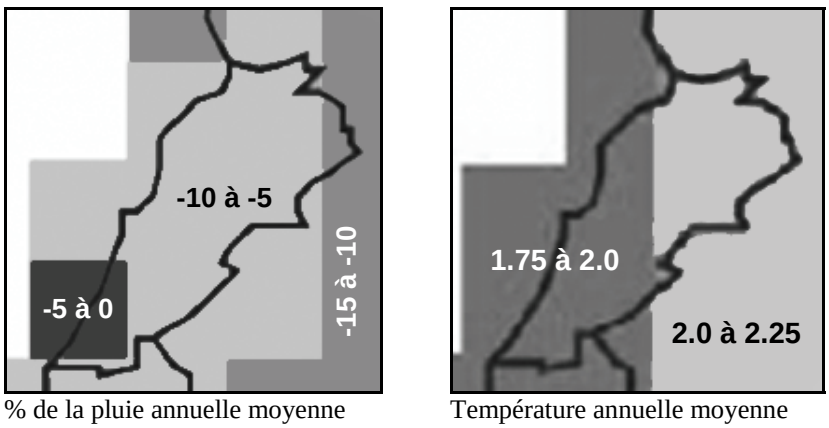
Les caractéristiques du climat, en particulier les précipitations et la température conditionnent le cycle de l'eau qui détermine les conditions de la vie terrestre. Certaines tendances ont déjà été mises en évidence. Le rapport de l'IPCC de 1996 présente l'évolution des données de précipitations et de température durant le 20ème siècle (Karl, 1995) pour 10 régions du globe. Si les tendances de précipitations ne sont pas toujours évidentes pour certaines régions, la température a augmenté régulièrement de l'ordre de 0.01°C an^{-1}. Les outils susceptibles de prévoir les conséquences des perturbations climatiques sur le cycle de l'eau ou "modèles" doivent se baser sur l'analyse de l'ensemble des mécanismes en jeu (physiques, biologiques, et économiques). A chaque étape de l'analyse correspond un type de modèle. Les modèles de climat ou GCM (Global Change Model) peuvent être soit à l'échelle du globe (GCM à basse résolution), soit à une échelle régionale (GCM haute résolution). Les modèles du cycle de l'eau continental, à l'échelle d'un territoire, ou d'un bassin versant peuvent être physiques ou à défaut conceptuels. Les modèles de production agricole peuvent être soit dans le cadre d'un type de production donnée (le blé par exemple), soit dans le cadre du développement agricole en envisageant des évolutions de type culture et de pratiques agricoles. Enfin des modèles économiques, plus ou moins élargis à un ensemble de facteurs économiques avec analyse des coûts génèrent des flux de produits et des flux financiers. Les modèles d'impacts nécessitent le choix d'un scénario climatique. Ce choix se révèle difficile pour les petits territoires.

LES MODELES DE CHANGEMENT CLIMATIQUES

Les modèles de changement globaux ou GCM génèrent l'évolution des variables climatiques à partir des équations de conservation de la quantité de mouvement, de l'énergie et de l'humidité.

Copyright © 2006 IAHS Press

Depuis 1980, plusieurs modèles ont été proposés dont les résultats sont raisonnablement comparables, lorsqu'ils utilisent des hypothèses d'évolution des gaz à effet de serre identiques. Les échéances considérées sont les années 2050 et 2100. Dans le modèle du Hadley Center (à titre d'exemple, les autres modélisations étant très semblables), la surface du globe terrestre est découpée en éléments de 3.75° en longitude et de 2.5 en latitude. La maille de base dans les conditions locales est de 300 × 250 km (longitude × latitude). Cette maille s'étend de Beyrouth au désert syrien, de Haïfa à Lattaquié. La diversité des climats qu'elle est censée représenter est considérable, de sommets toujours enneigés aux déserts totalement arides. La maille représente 75 000 km^2 soit 7.5 fois la taille du Liban. Les résultats obtenus pour la température et la pluviométrie en 2050, sont présentés sur la Fig. 1, extraite des cartes établies par Ragab & Prudhomme (2000). La variabilité saisonnière des écarts est plutôt faible et dans la fourchette des incertitudes. En 2050, il est prévu une augmentation moyenne de 2.5°C (3°C en été et 2°C en hiver). La baisse de pluviométrie est de l'ordre de 5% en hiver, la baisse en été n'est pas significative. Le programme de recherches GICC (Gestion des Impacts du Changement Climatique) a concentré un ensemble de partenaires dans le cadre du bassin du Rhône (dans sa partie française). Une simulation dans les conditions actuelles (300 ppm de CO_2) a été comparée à un état de référence réalisé à partir d'un vaste ensemble de variables hydrologiques rassemblées dans une base de données constituée pour les besoins du programme. Les simulations ont été faites à partir de 6 modèles différents: 4 à basse résolution (mailles de l'ordre de 70 000 km^2) et 2 modèles haute résolution (mailles de 10 000 à 2500 km^2). Les différences entre les basses et hautes résolutions sont faibles. Les températures sont assez bien simulées (surtout en hiver). Les simulations des précipitations sont plus problématiques, avec des pluies hivernales plus dispersées (des écarts allant du simple au double). On peut dire que les GCM représentent assez mal l'état actuel. On peut attribuer cette dispersion aux paramètres des modèles physiques qu'ils contiennent, et tenter de corriger ces erreurs de dérive, par la «méthode des anomalies»: l'état futur est calculé avec l'état actuel, corrigé par la différence entre les simulations de l'état actuel et l'état futur. Malgré cette correction, les divergences restent encore importantes. Stainforth (2005) a mis en place un grand ensemble de calcul parallèle distribué dans le public scientifique, afin de réaliser une analyse de sensibilité des résultats aux estimations des paramètres. Le modèle retenu est le HDM3. Chaque simulation comporte un jeu de deux ou trois valeurs de paramètres et constitue une version possible du modèle. L'analyse des résultats conduit à des conclusions différentes d'une analyse de sensibilité paramètre par paramètre, sans doute en raison de fortes non linéarités, et de la structure chaotique des équations. L'analyse de la courbe de fréquence des élévations thermiques moyennes, montre une accumulation autour de 3°C avec très peu de cas au-dessous de 2°C, et une longue queue avec des cas exceptionnels à plus de 12°C. Cette analyse montre l'incertitude qui règne sur les GCM. Le champ de précipitation obtenu par les divers scénarios est très variable, et des écarts particulièrement importants peuvent être notés dans certaines régions (Murphy *et al.*, 2004). En particulier, certaines versions conduisent à des réductions importantes des précipitations dans l'Est du bassin méditerranéen. Les résultats sont en cours de confirmation.



% de la pluie annuelle moyenne Température annuelle moyenne

Fig. 1 Changement climatique en Méditerranée Orientale (d'après Ragab & Prudhomme, 2000).

LA MODELISATION HYDROLOGIQUE DES BASSINS

Le milieu continental est structuré en bassins hydrologiques dont la taille, la structure et le comportement sous l'action des forçages atmosphériques, sont d'une extrême diversité. Les outils susceptibles de prédire de façon aussi précise que possible le comportement des bassins et les variables qui les caractérisent (débits, niveaux de nappe, états hydriques des sols) existent en grand nombre. Deux conceptions différentes de la modélisation du fonctionnement des bassins s'opposent. Les modèles conceptuels visent à représenter les processus physiques de base des transferts par des algorithmes essentiellement calibrés grâce aux données du passé. Développés depuis les années 60, ils ont fait la preuve de leur efficacité: Stanford Watershed Model (SWM; Crawford et Linsley, 1966), Hydrological Simulation Model (HBV; Bergstrom, 1995). Un modèle spécifique au climat méditerranéen a été développé par Hreiche (2003) et appliqué à plusieurs bassins libanais. La principale critique qui peut être faite à ces modèles tient à la faible consistance physique de leur paramétrage. Ces modèles se trouvent donc très dépendants des mesures passées, et en particulier sont assez peu efficaces sur des bassins non jaugés. Les modèles physiques représentent (dans la mesure du possible) de façon explicite les mécanismes physiques en jeu, par exemple le Système Hydrologique Européen (SHE; Abbot *et al.*, 1986). D'un point de vue prédictif, l'utilisation de paramètres ayant une signification physique claire et théoriquement mesurable est plus satisfaisante. De nombreuses méthodes de détermination des paramètres physiques, leur variabilité spatiale, leurs incertitudes ont été faites. Bathurst (1986) a par exemple défini des procédures de calibration des paramètres. Mais le nombre de mesures à effectuer pour estimer les paramètres physiques fait que cette approche ne peut être appliquée qu'à de petits bassins expérimentaux avec beaucoup d'observations de terrain. Dans l'état actuel des connaissances, aucune des deux approches n'est pleinement satisfaisante.

Le premier impact d'un réchauffement concerne l'évolution du manteau neigeux, par modélisation de la fusion du manteau. Ce terme peut être très important, en particulier au Liban, où le volume stocké par la neige représente près de 50% des précipitations. Le second impact a trait à l'évapotranspiration du sol et de la végétation (ET). La référence de l'évapotranspiration est l'ETmax correspondant à une disponibilité en eau non limitante (potentiel nul dans la plante). Mais l'évapotranspiration ET n'est qu'une fraction de ETmax car les plantes se protègent des pertes en eau afin d'assurer leur survie (Perrier et Tuzet, 2005). Cette adaptation entraîne une certaine régulation du prélèvement sur la ressource. Ces diverses considérations font que la plupart des modélisations de bassin dans l'objectif de tester les impacts hydrologiques de changements climatiques sont des modèles hybrides. La gestion de la neige et l'évaporation sont gérés par des modèles physiques, le transfert étant conceptuel et calé sur les données du passé. Un exemple de cette méthode est fourni par le programme GICC-Rhone: la neige et l'évaporation sont modélisées par le modèle physique ISBA, qui décrit les phénomènes physiques issus des bilans hydrique et énergétique à l'échelle locale.

L'INTERFACE GCM—CONTINENT

Le couplage entre les variables issues des GCM et les modèles hydrologiques pose le problème du changement des échelles spatiales et temporelles. Les modèles de bassins nécessitent des échelles de temps et d'espace adaptées à leur taille. Les bassins libanais ont des tailles allant de quelques centaines à quelques milliers de km^2. Un modèle physique nécessiterait pour une description correcte un pas d'espace de quelques centaines de mètres et de temps de quelques heures. La disponibilité de mesures à de telles échelles étant exclue, la seule alternative est celle de la modélisation conceptuelle. Celle ci nécessite un maillage d'une dizaine de km (ordre de distance des postes pluviométriques disponibles) et un pas de temps journalier (seule donnée climatique disponible). C'est la disponibilité de la donnée qui impose le choix de la modélisation. Mais les GCM sont à des échelles très éloignées de ces exigences. Les GCM à basse résolution comme celui du Hadley Center ont des mailles de 200–300 km, et des pas de temps de calcul journaliers (dont la fiabilité n'est pas considérée comme valable à ce pas). Des GCM à haute résolution ont été élaborés, par exemple pour le modèle Rhône les modèles LMD à pas de 100 km et CNRM à pas de 50 km. Ces échelles sont incompatibles avec la variabilité physique d'un pays comme le

Liban et l'application de scénario GCM à de telles régions apparaît comme hautement problématique. Des procédures de "down scaling" ont été mises au point pour interpoler les résultats issus d'un GCM. Dayan et Kock (1999) ont été utilisé la procédure du Climate Research Unit of East Anglia (IPCC, 1996) pour spatialiser les données d'un GCM sur la région côtière d'Israël. Ces procédures conservent la structure actuelle c'est-à-dire les gradients thermiques et pluviométriques. Ceci implique un changement de température locale identique en tout point de la maille du GCM et un changement de pluviométrie proportionnel en tout point. Ceci ne peut constituer qu'une première approximation, en attendant les résultats de GCM à pas plus fin. Un des résultats les plus nets du programme du GICC-Rhone est que l'incertitude la plus forte réside dans le choix du scénario atmosphérique. Les écarts entre les modèles hydrologiques sont faibles vis-à-vis des écarts issus des divers GCM.

LES MODELES D'IMPACTS

Les impacts principaux à envisager pour le Liban (Hreiche, 2003) concernent la disponibilité de la ressource et l'impact sur la végétation. Bien que la recherche sur le changement climatique date des années 70, peu d'attention a été porté aux impacts potentiels sur la production agricole avant les années 90. L'impact d'un changement climatique sur la production agricole peut être estimé soit par une modélisation structurale qui analyse la réponse d'une plante donnée et les conséquences en termes de productivité, soit par une modélisation par analogie spatiale qui recherche les conditions d'exploitation de régions ayant des climats actuels identiques aux climats locaux modifiés par le changement climatique. Les deux approches se complètent car la seconde exprime la façon dont le milieu agricole va réagir en adaptant ses productions aux nouvelles conditions. Tubiello *et al.* (2000) ont analysé l'impact d'un scénario de changement sur la production de blé sur deux périmètres situés en Italie, à partir d'un modèle de croissance et de productivité: CROPSYST. Ce modèle prend en compte les divers paramètres liés au changement climatique: l'augmentation de CO_2 accroît la photosynthèse et les productivités agricoles (Kimball, 1983). L'augmentation du rayonnement et de la température raccourcit les durées des cycles végétatifs. Ce modèle a été validé sur divers environnements en Italie (Donatelli *et al.*, 1997). Des stratégies d'adaptation ont été retenues, comme des plantations plus précoces des variétés de printemps. Tubiello *et al.* (2000) envisagent un effet négatif sur la production en région méditerranéenne où la limitation de la production est liée au stress hydrique, amplifié par une augmentation de la température. Les travaux récents montrent que les phénomènes sont plus globaux et que les modèles conventionnels d'analyse d'impacts ont des limites. En effet, les producteurs, les circuits de distribution et même les consommateurs sont susceptibles de s'adapter aux changements. Cette adaptation potentielle est reconnue et a déjà été observée dans l'histoire, mais les modèles sous estiment en général son importance et ses conséquences en terme d'économie de marché. L'agriculture est en compétition avec d'autres activités pour l'usage du sol et les investissements en temps et en argent. Les changements de production agricole peuvent amener des extensions de surfaces cultivées au détriment des forets et des écosystèmes naturels avec des rétroactions sur le changement climatique. Enfin les réponses du monde agricole sont affectées par les politiques gouvernementales et les accords mondiaux.

CONCLUSIONS

Dans la perspective d'un changement climatique lié à l'augmentation des gaz à effet de serre, la prise en compte des impacts susceptibles d'affecter les conditions de vie humaine (partage de la ressource en eau, production alimentaire, conflits, etc.) ne peut se faire sans une connaissance quantitative de ces impacts et de leurs aléas. En l'absence de références dans le passé, cette connaissance passe par une représentation du fonctionnement ou "modèle" des divers compartiments physiques du cycle hydrologique: cycle atmosphérique (GCM), cycle continental (modèles de bassins), cycle végétal (ESP) et enfin des modèles macroéconomiques, dont Boussard et Christensen ont fourni un inventaire détaillé en 1997. La mise au point de ces outils, aussi performants que possible pose de nombreux problèmes en liaison avec leur enchaînement, leur

compatibilité, et la propagation de leurs incertitudes. Certaines non-linéarités et des effets de seuil rendent leur comportement parfois chaotique. Ils restent cependant la seule démarche possible et leurs résultats doivent être pris en compte au niveau des décisions, même s'il n'est pas possible de chiffrer leur fiabilité.

Dans un pays de faible dimension comme le Liban, à l'écart des grands programmes multinationaux, le maillon le plus faible dans la chaîne des modélisations est le modèle de climat. Dans ces conditions, il est nécessaire de retenir quelques scénarios de base simples (augmentation uniforme de température allant de 2°C à 4°C; changement de pluviométrie de 0% à 10%) et d'examiner les impacts sur la ressource en eau et la production agricole, afin d'intégrer ces éventualités à la planification du pays. La proximité des échéances, et leur caractère quasi inéluctable exigent leur intégration dans la prospective nationale.

Remerciements Cette étude fait partie du projet "Variabilité climatique en Méditerranée Orientale" ans le cadre du programme CORUS du Ministère des Affaires Étrangères de l'État Français.

REFERENCES

Abbot, M. B., Bathurst, J. C., Cunge, J. A., O'Connel, P. E. & Rasmussen, J. (1986) An introduction to the European Hydrological System—Système Hydrologique "SHE". *J. Hydrol.* **87**, 45–59.

Bathurst, J. C. (1986) Physically-based distributed modelling of an upland catchment using the Systeme Hydrologique European. *J. Hydrol.* **105**, 157–172.

Bergström, S., (1995) The HBV model. In: *Computer Models of Watershed Hydrology* (ed. by V. P. Singh), 443–476. Water Resources Publications, Littleton, Colorado, USA.

Boussard, J. M. & Christensen, A. K. (1997) Modèles Calculables d'Equilibre général, Risque et Place de l'Agriculture dans l'Economie Nationale: Application à la Pologne et à la Hongrie. Economie Rurale, 6.

Crawford, N. H. & Linsley, R. K. (1966) Digital simulation in hydrology, Stanford watershed model IV. *Technical Report* 39. Stanford, University of California, USA.

Dayan, U. & Koch, J. (1999) Implications of Climate Change on the Coastal Region of Israel. Mediterranean Action Plan, United Nations Environment Programme.

Donatelli, M., Stockle, C. O., Ceotto, E. & Rinaldi, M. (1997) Evaluation of CropSyst for cropping systems at two locations of northern and southern Italy. *J. Agron.* **6,** 35-45.

Hreiche, A. (2003) Modélisation-conceptuelle de la transformation pluie-débit dans le contexte méditerranéen. Thèse, Université Montpellier II—Beyrouth, Liban.

IPCC (1996) *The Science of Climate Change* (ed. by J. T. Houghton, L. G. Meira Filho, B. A. Callander, N. Harris, A. Kattenberg & K. Maskell). Cambridge University Press, Cambridge, UK.

Karl, T. R., Bretherton, F., Easterling, W. & Trenberth, K. (1995) Long-term climate monitoring of the Global Climate Observing Systems (GCOS). *Climatic Change* **31**, 135–147.

Kimball, B. A. (1983). Carbon dioxide and agricultural yield: an assemblage and analysis of 430 prior observation. *Agron. J.* **75**, 779–786.

Murphy, J., Sextor, D., Barnett, D., Jones, G., Webb, M., Collins, M. & Stainforth, D. (2004) Quantification of modelling uncertainties in a large ensemble of climate change simulations. *Nature* **430**, 768–772.

Perrier, A. & Tuzet, A. (2005) Le cycle de l'eau et les activités au sein de l'espace rural. *CR Géoscience* **337**, 39–56.

Ragab, R. & Prudhomme, C. (2000) Climate changes and Water Ressources Management in arid and semi arid regions. *S. Agric. Engng Res*. **759**, 1–32.

Stainforth, D. A. (2005). Uncertainty in predictions of the climate response to rising levels of greenhouse gases. *Nature* **433**, 403–413.

Tubiello, F., Donatelli, M., Rosenzweig, C. & Stockle, O. (2000) Effects of climate and elevated CO_2 on cropping systems: model predictions at two Italian locations. *Eur. J. Agron.* **13**, 179–189.

Climate Variability and Change—Hydrological Impacts (Proceedings of the Fifth FRIEND World Conference held at Havana, Cuba, November 2006), IAHS Publ. 308, 2006.

Relation entre hydrologie et climat dans le bassin versant de l'Oued Inaouène (pré-Rif marocain)

ABDELKADER EL GAROUANI[1] **& ABDELLATIF TRIBAK**[2]

1 *Laboratoire de Géosciences et Environnement, Faculté des Sciences et Techniques de Fès, Université Sidi Mohamed Ben Abdellah, Route d'Imouzzer, BP 2202, Fès, Maroc*
abdelkader.elgarouani@fst-usmba.ac.ma

2 *Laboratoire d'Analyse Géo-environnementale et d'Aménagement, Faculté des Lettres et Sciences Humaines, Université Sidi Mohamed Ben Abdellah, Route d'Imouzzer, BP 59, Fès, Maroc*

Résumé La présente étude concerne le bassin versant de l'Oued Inaouène situé entre le Moyen Atlas et le pré-Rif couvrant une superficie de 3320 km^2. Le climat de la zone est marqué par de forts contrastes saisonniers et des irrégularités très nettes des précipitations. Une tendance à la baisse très significative débute en 1980 annonçant une sécheresse exceptionnelle qui s'étend jusqu'à nos jours. La période de sécheresse a accentué les processus de dégradation et, par conséquent, les mouvements migratoires des populations. Afin de mieux gérer une telle situation, la connaissance des facteurs climatiques et la caractérisation de la sécheresse par l'estimation des indicateurs météorologiques et hydrologiques sont indispensables. Au regard des résultats obtenus nous constatons que la variation des écoulements de surface est plus importante que celle des pluviométries, 2.41 pour les apports et 0.92 pour les précipitations.

Mots clefs climat; sécheresse; hydrologie; Oued Inaouène; Maroc

Relationship between hydrology and climate in the Inaouene River basin, pre-Rifian Morocco

Abstract The Inaouene River has a watershed covering an area of 3320 km^2 located between the Lower Atlas and Pre-Rif mountains. In this region, the climate is marked by strong seasonal contrasts and very clear rainfall irregularities. A very significant downward trend begins in 1980 announcing an exceptional drought which extends to the present day. The longer drought period accentuated the degradation processes and, consequently, the migratory movements of the population. In order to manage this situation, it is important to study the climatic and drought factors and to estimate the hydrological indicators. The results indicate that the runoff variation is more significant than that of rainfall (2.41 for the flow contributions and 0.92 for precipitation).

Key words climate; drought; hydrology; Inaouene River; Morocco

INTRODUCTION

Dans une perspective de gestion intégrée des ressources naturelles des bassins versants, les enjeux principaux portent sur: les effets attendus d'un changement climatique sur la ressource en eau et sur le couvert végétal, une meilleure gestion des risques liés aux catastrophes naturelles (inondation, sécheresse), l'analyse spatialisée des effets anthropiques sur le transfert des eaux au niveau des versants et les débits des écoulements des oueds (El Garouani, 2004). Les sécheresses sont plus difficiles à définir que les inondations en termes quantitatifs. En plus, l'état des ressources en eau ne dépend pas uniquement des facteurs météorologiques mais aussi de la manière de gérer cette ressource. Des études sur l'évolution de la fréquence des basses eaux des rivières ont obtenu des résultats assez différents selon l'évolution des précipitations dans le bassin versant (Ducharne *et al.*, 2003; Krasovskaia *et al.*, 2003).

Le travail présenté dans cet article concerne le bassin versant de l'Oued Inaouène qui constitue un affluent principal de l'oued Sebou couvrant une superficie de 3320 km^2. Il est limité à l'est par le bassin versant de la Moulouya, au nord-ouest par les bassins d'Ouargha et Leben et au sud par le bassin du haut Sebou (Fig. 1). Le climat est marqué par de forts contrastes saisonniers et des précipitations très irrégulières. Le total annuel se situe, selon les stations, entre 400 mm (Ain Boukellal) et 1200 mm (Bab Bou Idir). Une tendance à la baisse très significative débute en 1980 annonçant une sécheresse exceptionnelle qui s'étend jusqu'à nos jours (Afkir, 1985; Obda, 2004). Les abats d'eau sont généralement brutaux et l'essentiel des pluies se concentre en quelques semaines de la saison humide (Sibari *et al.*, 2001; Sibari, 2002). Avec la sécheresse des années 1980, la ressource en eau fait défaut dans l'ensemble de la région (plus particulièrement dans le pré-Rif) et constitue un facteur de déstabilisation des populations locales. La période de sécheresse a accentué les processus de dégradation, et par conséquent, les mouvements migratoires des populations (Janati, 2005; Nejjari, 2002; Tribak, 2002).

Copyright © 2006 IAHS Press

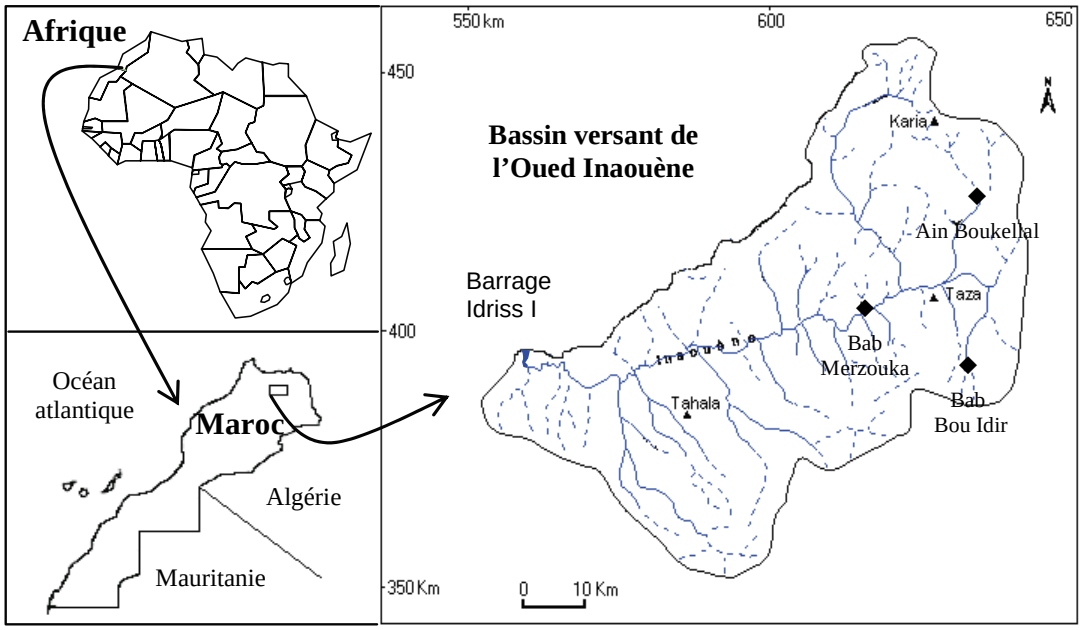


Fig. 1 Situation géographique de la région d'étude.

Afin de mieux gérer une telle situation, la connaissance des facteurs climatiques et la caractérisation de la sécheresse par l'estimation des indicateurs hydrologiques et climatologiques sont indispensables.

L'aspect novateur de cette recherche est la mise au point d'un ensemble d'indicateurs spécifiques pour la description de la sécheresse dans la région d'étude. Cette phase prévoit une première évaluation d'un ensemble d'indices existants dans la littérature, une étude d'adaptation de ces indicateurs à la situation marocaine et enfin la recherche de nouveaux indicateurs capables de la décrire. Dans cette première étape de ce travail, nous proposons de faire l'étude des données pluviométriques et hydrologiques observées sur le bassin d'Inaouène afin de dégager les caractéristiques de la sécheresse météorologique et hydrologique et d'étudier les conséquences de la réduction des précipitations sur l'écoulement.

MATERIEL ET METHODE

Région d'étude

Par sa position géographique, le bassin versant de l'Inaouène présente un climat de type méditerranéen à influence océanique. Les précipitations du bassin d'Inaouène montrent une répartition temporelle qui peut être mise en évidence à partir des données recueillies à la station pluviométrique de Bab Marzouka, située en amont du bassin à une altitude de 365 m. L'analyse des séries pluviométriques montre une succession d'années sèches et d'années humides.

En réponse aux caractéristiques du climat semi-aride, le régime de l'Oued Inaouène montre des variations saisonnières avec une période de crues et une période d'étiage. L'essentiel de l'écoulement correspond à la période d'octobre à avril qui concentre les trois quarts de l'écoulement annuel. Parmi les crues exceptionnelles observées dans le bassin d'Inaouène, on peut citer la crue du 31 janvier 1987 où le débit de pointe enregistré à El Kouchat a atteint 1280 $m^3 s^{-1}$, de même importance que celle enregistrée à la station de Touaba (1120 $m^3 s^{-1}$) le 27 février 1969 (Sibari *et al*., 2001) .

Pendant la période d'étiage les fortes températures atmosphériques peuvent occasionner une évaporation importante et par conséquent un tarissement parfois précoce des lits des affluents de l'Oued Inaouène. Les étiages sont assez sévères; les débits moyens pour les mois les plus secs (juillet et août) sont respectivement de 0.54 et 0.7 $m^3 s^{-1}$. Au cours des périodes très sèches, le débit mensuel minimal peut être de 0.02 $m^3 s^{-1}$ comme celui enregistré en août 1994 (Haida *et al.*, 1999).

Méthodologie

L'analyse des ressources en eau dans la région d'étude a fait l'objet de travaux antérieurs qui ont souvent segmenté la problématique des ressources en eau pour la traiter soit en termes de facteurs géomorphologiques (Heusch, 1970) ou en termes de facteur de risque (Obda, 2004).

Notre approche dans cette étude repose sur l'utilisation des données météorologiques et hydrométriques relatives à une longue série de mesures des paramètres journaliers, mensuels et annuels, aux deux stations hydrométriques (Bab Marzouka et Idriss I) situées respectivement en amont et en aval du bassin versant (Fig. 1). Ces données ont été obtenues principalement à partir des annuaires hydrologiques et des dossiers hydrométriques établis à l'Agence du Bassin Hydraulique de Sebou (ABHS). Les apports mensuels au barrage Idriss I sont calculés à partir des éléments fournis par les bordereaux d'exploitation de ce barrage (ABHS, 2005a,b). Cette démarche est basée sur deux opérations essentielles:

(a) application des méthodes de calcul d'indices existants dans la littérature scientifique (Bergaoui & Alouini, 2001; Beran & Rodier, 1987; McKee *et al.*, 1995) aux séries chronologiques des données hydroclimatiques en se référant en particulier aux périodes historiquement significatives pour la vérification d'épisodes de sécheresse de grande intensité;
(b) mise en place d'une base de données spatiales et non spatiales intégrées, à l'aide des outils de système d'information géographique (SIG) du bassin versant d'Inaouène (occupation du sol, paramètres hydrologiques et climatiques, infrastructures, géographie, etc.) permettant l'élaboration d'indicateurs pertinents pour identifier les conditions de sécheresse et l'étude des conséquences de la réduction des précipitations sur l'écoulement.

CARACTERISATION DES SECHERESSES METEOROLOGIQUE ET HYDROLOGIQUE

La gravité d'une sécheresse est fonction à la fois de l'ampleur du déficit et de la longueur de la période de déficit. Les indicateurs de sécheresse peuvent être multiples, avec en premier lieu des déficits pluviométriques, mais également des débits faibles dans les cours d'eau, des niveaux bas des nappes phréatiques, des situations prolongées de stress hydrique de la végétation, ces différents indicateurs étant généralement liés. Les caractéristiques principales des séries de données pluviométriques et des apports sont récapitulées dans le Tableau 1.

Tableau 1 Caractéristiques des données hydro-pluviométriques.

	Pluviométrie annuelle (mm)		Apports annuel (mm)
Stations	Bab Marzouka	Barrage Idriss I	Barrage Idriss I
Périodes	1970–2001	1974–2003	1973–2002
Effectif (années)	31	29	29
Minimum (mm)	305.3	181.5	37.7
Maximum (mm)	854.1	534.5	370.3
Moyenne (mm)	557.0	382.6	137.9
Médiane (mm)	543.3	385.2	109.2
Ecart type (mm)	143.6	93.8	91.5

Sécheresse météorologique

Le calcul des écarts par rapport à la moyenne, sur les données pluviométriques observées au niveau des deux stations (sur une période de 31 ans pour la station de Bab Marzouka et de 29 ans pour celle du barrage Idriss I) a permis de constater que 45% d'années sont humides et 55% d'années sont sèches au niveau de la station Bab Marzouka et 50% d'années sont humides et 50% d'années sont sèches au niveau de la station Idriss I. Le déficit le plus important enregistré durant toute la période d'observation est respectivement de –251.7 et –201.1 mm à Bab Marzouka et Idriss I (Fig. 2 et Tableau 2). Pour mettre en évidence des épisodes de sécheresse nous avons dégagé les tendances en calculant le cumul des indices d'écart proportionnel à la moyenne

Tableau 2 Caractérisation de la sécheresse météorologique (Barrage Idriss I).

No.	Début	Fin	Durée (an)	Déficit (mm)	Intensité (mm an^{-1})
1	1974	1974	1	64.9	64.9
2	1980	1984	5	104.4	20.9
3	1986	1986	1	62.1	62.1
4	1988	1988	1	5.8	5.8
5	1991	1994	4	453.7	113.4
6	1998	1999	2	314.0	157.0
7	2001	2001	1	96.6	96.6

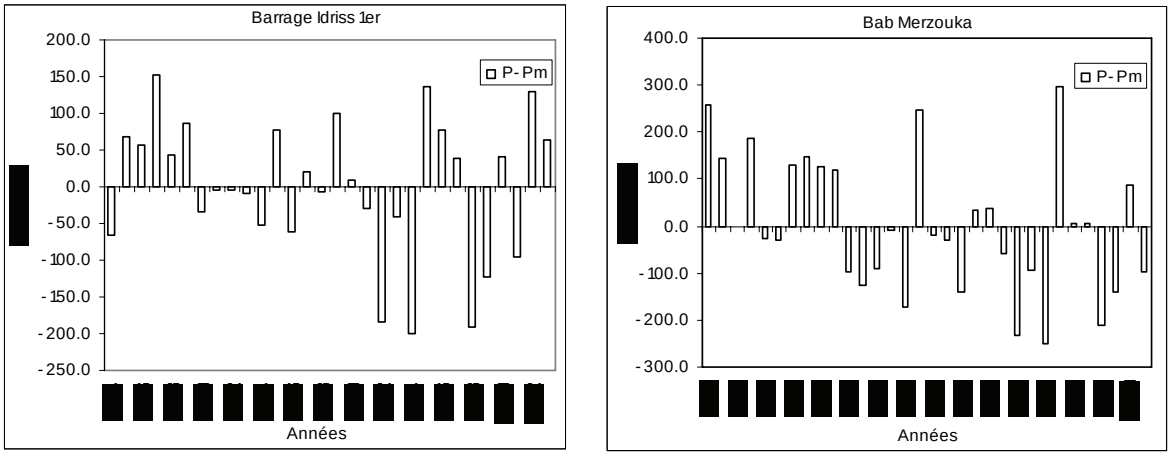


Fig. 2 Ecarts par rapport à la moyenne des précipitations: stations de Bab Marzouka et du Barrage Idriss I.

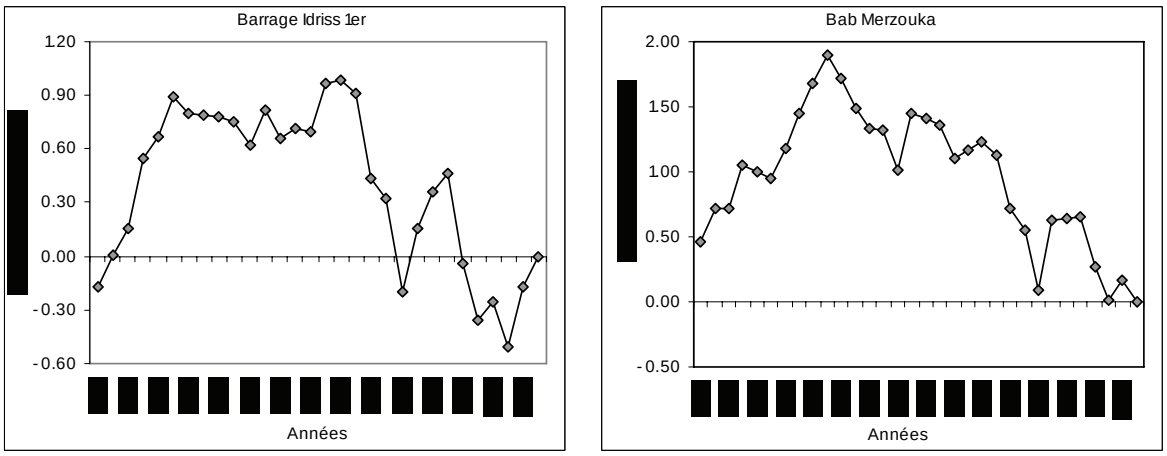


Fig. 3 Indices de pluviosité: stations de Bab Marzouka et du Barrage Idriss I.

(*Pi*/*Pm*) – 1 (indice de pluviosité) d'années successives sur toute la période d'observation au niveau des deux stations (Bab Marzouka et Barrage Idriss I) (Fig. 3). On constate des periodes à tendence sèche et des périodes à tendence humide:

(a) de 1974 à 1979, une tendance humide,
(b) de 1980 à 1984, une tendance à la sécheresse, et
(c) de 1985 jusqu'à 2003, une tendance à la sécheresse entrecoupée de trois courtes périodes à tendance humide.

Sécheresse hydrologique

L'étude de la sécheresse hydrologique en termes d'identification et de caractérisation est effectuée sur les apports d'eau observés au Barrage Idriss I. Les variations des écarts par rapport à la

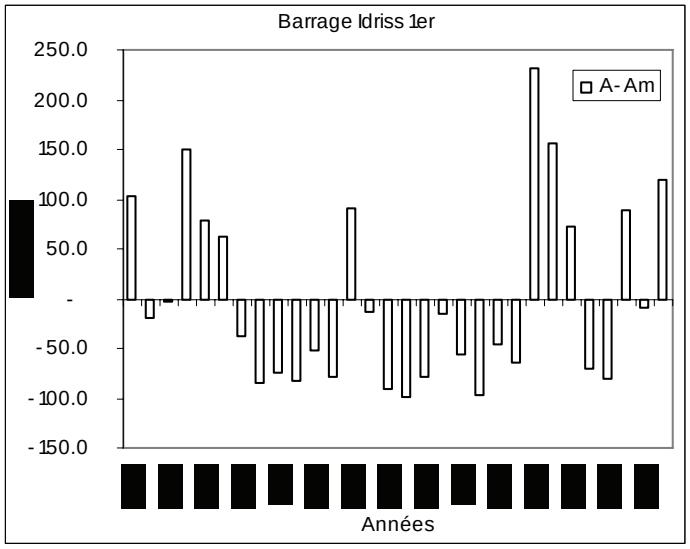


Fig. 4 Ecarts par rapport à la moyenne des apports au Barrage Idriss I (1973–2002).

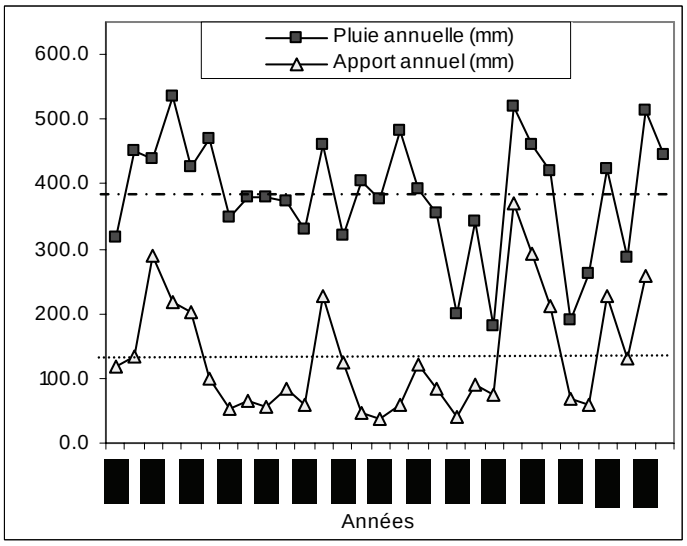


Fig. 5 Variations des précipitations et des apports annuels au Barrage Idriss I.

Tableau 3 Caractérisation de la sécheresse hydrologique (Barrage Idriss I).

No.	Début	Fin	Durée (an)	Déficit (mm)	Intensité (mm an^{-1})
1	1974	1975	2	23.3	11.6
2	1979	1984	6	410.9	68.5
3	1986	1994	9	560.3	62.3
4	1998	1999	2	150.9	75.4
5	2001	2001	1	8.7	8.7

moyenne des apports montre qu'il y a plus d'années sèches que d'années humides (66% d'années sèches) (Fig. 4 et Tableau 3). La durée et l'intensité des sécheresses varient considérablement. La sécheresse peut se produire à l'échelle de l'année comme elle peut durer deux ou plusieurs années consécutives. De même, la Fig. 5 montre la chronologie des pluies et des apports d'eau et permet de faire une comparaison entre les deux séries. Le long de la série chronologique, il apparaît que les fluctuations au cours des années hydrologiques par rapport aux deux variables sont presque les mêmes et ceci peut s'expliquer par:

(a) la forte proportion du ruissellement superficiel lors des crues,
(b) la présence de terrains imperméable (marnes) qui limitent l'infiltration des pluies.

Les périodes sèches du point de vue météorologique sont de courte durée par rapport à aux sécheresses hydrologiques. En effet, pour les années de pluviométrie annuelle inférieure ou égale à 400 mm, les apports sont très faibles (années déficitaires). En se basant sur les données observées au niveau de la station du Barrage Idriss I, on peut dire que les irrégularités des précipitations à l'intérieur du bassin se traduisent ainsi par des fluctuations plus importantes au niveau des écoulements. L'écart relatif (différence entre le maximum et le minimum) rapporté à la moyenne est de 2.41 pour les apports et de 0.92 pour les précipitations. Ces analyses statistiques montrent que la variation dans les écoulements de surface est plus importante que celle des pluviométries.

Pour mettre en évidence la capacité du bassin versant à ruisseler, on a calculé le coefficient de ruissellement pour la période d'observation (Fig. 6). On remarque une tendance à la hausse de ce coefficient. Cela peut s'expliquer par la forte poussée démographique dans la région qui a entraîné un déséquilibre entre les besoins de la population et les ressources naturelles disponibles. Phénomène qui a eu pour corollaire une emprise humaine considérable sur le milieu naturel et une accélération des processus de dégradation de l'environnement (Aghrab, 2006; Fikri Ben Brahim *et al.*, 2004). Le recul des espaces boisés est très spectaculaire; certaines collines pré-Rifaines sont totalement défrichées et les pertes en sols sont, par conséquent énormes.

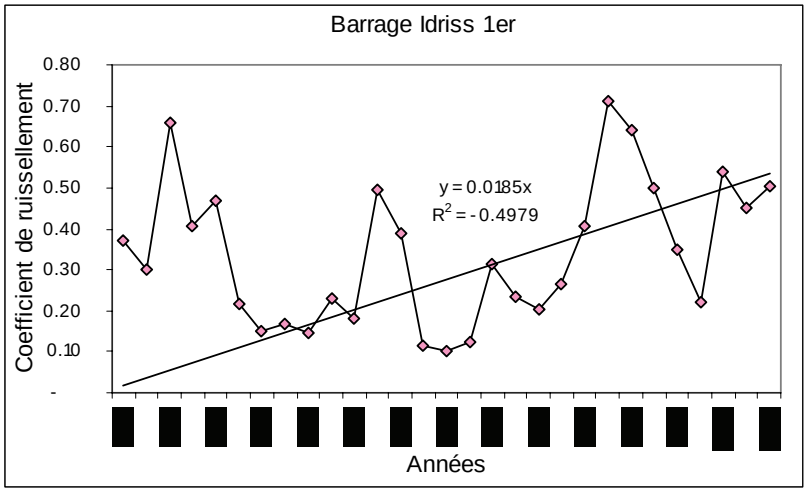


Fig. 6 Coefficient de ruissellement à la station du Barrage Idriss I.

CONCLUSION

Après le dépouillement, la saisie et l'analyse des données nous avons déterminé les caractéristiques statistiques de base des séries pluviométriques et hydrométriques telles que l'effectif, la moyenne, l'écart type, le minimum, le maximum, la médiane, etc. Ensuite, plusieurs indices de sécheresse sont calculés. D'après l'analyse des résultats des deux stations du bassin versant d'Inaouène, nous pouvons retenir que la sécheresse est un phénomène récurrent. L'indice des écarts à la moyenne des apports au niveau du barrage Idriss I donne un pourcentage de 66% d'années sèches. La durée et l'intensité des sécheresses varient considérablement. Les caractéristiques statistiques des séries montrent également que la variation des écoulements de surface est plus importante que celle des pluviométries, montrant ainsi que la sécheresse météorologique se trouve amplifiée dans les écoulements. La sécheresse peut se produire à l'échelle de l'année comme elle peut durer deux ou plusieurs années consécutives. Ces résultats consisteront un support aux décisions en matière de gestion des ressources hydriques, du choix des pratiques agricoles et de la planification de l'environnement pour la réduction de l'impact d'un épisode de sécheresse.

REFERENCES

ABHS (Agence du Bassin Hydraulique de Sebou) (2005a) Annuaire hydrologique du bassin du Sebou (Zone de l'Inaouène): 1973–2003. Rapport, Fès, Maroc.

ABHS (Agence du Bassin Hydraulique de Sebou) (2005b) Bilan hydraulique du barrage Idriss 1er: Situation 1983–2004. Rapport, Fès, Maroc.

Afkir, E. (1985) Le bassin versant de l'Inaouène: caractéristique climatique et comportement hydrologique. Thèse 3éme cycle, Univ. Toulouse, Toulouse, France.

Aghrab, A. (2006) Etude de la sécheresse au Maroc: types, impacts, gestion, caractérisation et alerte précoce. *Collection Savoirs*, Paris, France.

Beran, M. A. & Rodier, J. A. (1987) Aspects hydrologiques des sécheresses. Contribution au programme hydrologique international. *Rapport UNESCO/OMM*.

Bergaoui, M. & Alouini, A. (2001) Caractérisation de la sécheresse météorologique et hydrologique: cas du bassin versant de Siliana en Tunisie. *Sécheresse* **12**(4), 205–213.

Ducharne, A., Théry, S., Viennot, P., Ledoux, E., Gomez, E. & Déqué, M. (2003) Influence du changement climatique sur l'hydrologie du bassin de la seine. *Vertigo* **4**(3), décembre.

El Garouani, A. (2004) Apport de la télédétection et du SIG à la compréhension du fonctionnement hydrologique de bassins versants: évaluation et cartographie de l'évapotranspiration, de l'érosion hydrique et de la pollution des eaux. *Rapport de recherche de l'Habilitation Universitaire*, Fac. Sciences et Techniques, Fès, Maroc.

Fikri Ben Brahim, K., Ismaili, M., Fikri Ben Brahim, S. & Tribak, A. (2004) Problèmes de dégradation de l'environnement par la désertification et la déforestation: impact du phénomène au Maroc. *Sécheresse* **15**(4), 307–320.

Haida, S., Probst, J. L., Ait Fora, A. & Snoussi, M. (1999) Hydrologie et fluctuations hydroclimatiques dans le bassin versant du Sebou entre 1940 et 1994. *Sécheresse* **10**(3), 221–228.

Heusch, B. (1970) L'érosion du pré-Rif, une étude quantitative de l'érosion hydraulique dans les collines marneuses du pré-Rif Occidental. *Annales de la Recherche Forestière du Maroc* **12**, 9–176.

Janati, M. (2005) Le déficit pluviométrique et son impact sur les ressources en eau superficielles dans le basin de Sebou. Thèse d'État, Université Sidi Mohamed Ben Abdellah, Fès, Maroc.

Krasovskaia, I., Gottschalk, L., Leblois, E. & Sauquet, E. (2003) Dynamics of river flow regimes viewed through attractors. *Nord. Hydrol.*, **34**, 461–476.

McKee, T. B., Doesken, N. J. & Kleist, J. (1995) Drought monitoring with multiple time scales. In: *Preprints, 9th Conference on Applied Climatology* (Dallas, Texas, USA, 15–20 January), 233–236. Colorado State University, USA.

Nejjari, A. (2002) La sécheresse, l'eau et l'homme dans le bassin versant du haut Sebou (Moyen Atlas septentrional). Thèse de Doctorat, Université de Metz, Metz, France.

Obda, K. (2004) Indigences extrêmes des écoulements des Oueds méditerranéens cas des oueds Nekor, et du haut Sebou. Thèse d'État, Université Sidi Mohamed Ben Abdellah, Fès, Maroc.

Sibari, H. (2002) Etude hydrologique et hydrochimiques des crues du bassin versant d'Inaouène (Maroc). Thèse de doctorat, Kenitra, Maroc.

Sibari, H., Haida, S. & Ait Fora, A. (2001) Etude du fonctionnement hydrologique d'un bassin versant méditerranéen (exemple du bassin versant de l'Inaouène: Maroc). *Revue Marocaine de Génie Civil* **95**, Septembre–Octobre.

Tribak, A. (2002) Contraintes du milieu et fragilité d'un espace montagnard marocain: les montagnes du pré-Rif oriental. *Annales de Géographie* **625**, 227–245. Armand Colin, France.

Climate Variability and Change—Hydrological Impacts (Proceedings of the Fifth FRIEND World Conference held at Havana, Cuba, November 2006), IAHS Publ. 308, 2006.

Regionalization of a distributed catchment model for highly glacierized Nepalese headwater catchments

MARKUS KONZ, LUDWIG N. BRAUN, STEFAN UHLENBROOK, SIEGFRIED DEMUTH & ARUN SHRESTHA

1 *University of Basel, Department of Environmental Sciences, Applied and Environmental Geology, Bernoullistr. 16, CH-4056 Basel, Switzerland*
markus.konz@stud.unibas.ch

2 *Bavarian Academy of Sciences, Commission of Glaciology, Alfons-Goppel-Str. 11, D-80539 Munich, Germany*

3 *UNESCO-IHE, PO Box 3015, 2601 DA Delft, The Netherlands*

4 *IHP/HWRP Secretariat, Federal Institute of Hydrology, Am Mainzer Tor 1, D-56068 Koblenz, Germany*

5 *Department of Hydrology and Meteorology, Snow and Glacier Hydrology Unit, Babar Mahal, PO Box 406, Kathmandu, Nepal*

Abstract In this study, the distributed catchment model TAC^D was developed further and applied to three highly glacierized Himalayan catchments (141–360 km^2). Snow and ice melt is regionalized using the calculated potential sunshine duration of each 200 × 200 m^2 raster cell. Hydrological response units (glacier covered areas, non-glacier areas, flat glacier parts, valley bottoms) are simulated with different reservoir concepts. The model runs on a daily time step with daily mean air temperature and daily sums of precipitation as input data. It was calibrated successfully for the Langtang Khola catchment, Nepal, and this parameter set formed the starting point for the application of the model to the Modi Khola and Imja Khola catchments. In the case of the Modi Khola catchment the parameter set was left unchanged and used directly for discharge simulation, and only minor modifications of the parameter values of the snow and glacier routine were necessary for the Imja Khola catchment to obtain reasonable runoff simulations. It was demonstrated that this distributed modelling approach enables the assessment of the temporal and spatial distribution of runoff from high mountain areas where data are limited.

Key words TAC^D model; regionalization; Himalayan headwater; Nepal; distributed modelling; process-oriented runoff simulation; Langtang; Annapurna; Khumbu

INTRODUCTION

In 1987, the German Agency for Technical Cooperation (GTZ) initiated a project with the aim to quantify the hydrological conditions of glacierized Himalayan catchments (Grabs & Pokhrel, 1993). Within this project several climate stations were set up in six headwater catchments across the Nepalese Himalaya. Today the measurement programme is maintained by the Snow and Glacier Hydrology Unit (SGHU) of the Department of Hydrology and Meteorology (DHM), Kathmandu, Nepal.

Earlier modelling studies of daily discharge of the Himalayan headwater catchments revealed problems in simulating the hydrograph of the winter and monsoon season (Braun *et al*., 1993, 1998). The winter discharge is relatively high although there is neither liquid precipitation or melt water which contributes to the runoff generation. With our TAC^D model we overcome this problem with storage concepts which enable the storage of water during the monsoon season to maintain winter discharge (Konz *et al*., 2006). In this paper we present the application of the further developed distributed catchment model TAC^D to three remote Himalayan catchments with limited data availability. The model is applied to the Langtang Khola, the Imja Khola and Modi Khola catchments with only minor re-calibration of model parameters. The transfer of rainfall–runoff models to ungauged sites is a topic of wide interest in the scientific community and different approaches to the regionalization of model parameters are suggested (e.g. Gottschalk e*t al*., 2001). Here, we focus on the regionalization of model parameters based on the delineation of hydrological response units; a detailed description of the model can be found in Konz *et al*. (2006).

METHODS AND DATA

The TAC^D model

The conceptual structure of TAC^D consists of separate modules (snow and glacier-, soil- and runoff-generation routines) that are sequentially linked and represent the main parts of the land phase hydrological cycle (for further details see Uhlenbrook *et al*., 2004; Ott & Uhlenbrook, 2004; Johst *et al*., 2006: Konz *et al*., 2006). The meteorological data input requirement is limited to daily

Copyright © 2006 IAHS Press

mean air temperature and daily sums of precipitation. The model is fully distributed with rectangular grid cells of 200 × 200 m^2.

The temperature-index method is used to calculate snow- and ice-melt in a distributed way based on potential sunshine duration expressed by a dimensionless factor (R_{expMap}). In grid cells with high potential sunshine duration melt is increased ($R_{expMap} > 1.0$) and *vice versa*. Temperature is regionalized using a fixed gradient. Water retention in the present snow cover is also considered in the snow and glacier routine. If glaciers are present, ice melt starts as soon as the snow cover is melted. The enhanced melt of ice as compared to snow is a result of reduced surface albedo and considered by a multiplicative factor (R_{ice}) applied to the temperature-index method. The reduced melt rate of ice under thick debris-covered parts of the glaciers is accounted for by another multiplicative factor ($R_{debris} < 1.0$ reduced melt) (Braun *et al*., 1993; Konz *et al*., 2006):

$$Q_{melt} = CFMAX \cdot (Temp - TT)\, R_{expMap}\, R_{ice}\, R_{debris}$$

where Q_{melt}: melt water (mm day^{-1}), *CFMAX*: degree-day factor (mm day^{-1} $°C^{-1}$), *Temp*: daily mean air temperature (°C) and *TT*: threshold value of temperature (°C).

The runoff generation routine is the core of the model which is designed for process-oriented runoff simulation. Units with similar dominating runoff generation behaviour (hydrological response units, HRUs) were delineated using maps of topography and land use, aerial photographs and a digital elevation model (DEM) as well as experiences gained during field visits. Four units were distinguished for which different runoff generation processes are assumed and incorporated into the model as a raster map (200 × 200 m^2):

1. non-glacier area;
2. glacier area;
3. glacier area with an inclination of less than 3° and debris cover;
4. valley bottoms with an inclination of less than 8°.

Sequentially connected or overflowing reservoirs simulate the runoff processes of unit Types 1 and 2. In these units, upper and lower storages exist which are vertically linked via a constant percolation rate. For conceptualization of the runoff generation processes of the third unit type, only a single storage is used. This conceptualization is based on the assumption that the large valley glaciers can store a great amount of water in pools or small sub- and supra-glacial lakes (Jansson *et al.*, 2002). Storage capacity is limited by an upper limit. Runoff of this storage is computed by applying a storage coefficient with additional water if the storage content exceeds the storage capacity. The valley bottom with an inclination of less than 8° is considered to be an aquifer consisting of glacial moraine and gravel beds where water can be stored. The same structure of storage as in Type 3 is used to simulate the hydrological processes but with different parameterization for different flow dynamics.

Catchments and data used in the study

Three highly glacierized Himalayan catchments were investigated: Imja Khola (Khumbu region), Langtang Khola (Langtang region) and Modi Khola (Annapurna region). Catchment characteristics are shown in Table 1. SGHU provided air temperature (T), precipitation (P) and discharge (Q) data sets. There is one climate station in each catchment and gauge height is measured at an undefined cross-section in the river using dilution techniques to derive discharge data. The number of missing data in the observation series varies between the catchments, and for the investigation periods it is in the range of 91–98% for temperature, 71–93% for precipitation and 38–80% for discharge. Statistical methods to fill the missing values had to be applied using meteorological data of DHM stations in the vicinity of the catchments (for further details see Konz *et al*., 2006). Spatial data sets were derived from digital maps of the Survey Department, Nepal. The glacier covered area was taken from maps published in the glacier inventory of the International Center of Mountain Development (ICIMOD) (UNEP/ICIMOD, 2002).

RESULTS AND DISCUSSION

The model was initially applied to the Langtang Khola catchment (Table 2) for which glaciological data (glacier mass balances) of a glacier within the catchment are available from literature

Table 1 Catchment characteristics.

			Imja Khola	Modi Khola	Langtang Khola
Investigation period			1988–1995	1991–1994	1987–1998
Area	Total	(km²)	141.4	160.6	360.0
	Glacierized	(km²/%)	53.4/37.7	76.6/47.7	166.1/46.1
	Debris-covered glacier	(km²/%)	24.0/45.0[a]	6.96/9.1[a]	32.1/19.3[a]
Altitude	Range	(m a.s.l.)	4355–8501	3470–8091	3800–7234
	Average	(m a.s.l.)	5500	5327	5169
Exposition	North (315°–45°)	(%)	17.9	12.7	21.3
	South (135°–225°)	(%)	37.0	38.0	26.8
	East, west, horizontal [b]	(%)	45.1	49.3	51.9
	Mean slope	(°)	28.6	34.9	26.7
Land cover	Glacier	(km²/%)	53.4/37.7	76.6/47.7	166.1/46.1
	Barren land	(km²/%)	67.8/48.0	66.81/41.6	183.8/51.1
	Forest	(km²/%)	–	0.7/0.4	2.1/0.6
	Grass land	(km²/%)	17.6/12.5	15.0/9.3	3.4/0.9
	Others	(km²/%)	2.6/1.8	1.4/0.9	4.6/1.3

[a] in percent of glacier-covered area
[b] 45°–135° and 225°–315°

(Braun *et al.*, 1993; Fujita *et al*., 1998). These data were used for calibration and validation of the model beside discharge measurements. The model was calibrated using data from the period 1993–1998 and validated on an independent period, 1987–1993. The model obtained satisfying results for discharge and glacier mass balance simulations for the Langtang Khola catchment (Fig. 1) with objective evaluation criteria (Nash & Sutcliff, 1970) varying from 0.28 to 0.87 (Table 3) (Konz *et al*., 2006). The parameter values of the soil routine and runoff generation routine were derived from experiences from previous TAC^D-applications to other basins. In particular, the parameter values were defined such that our understanding of the dominant process behaviour is represented. We concentrated on ratios between parameters of the different HRUs

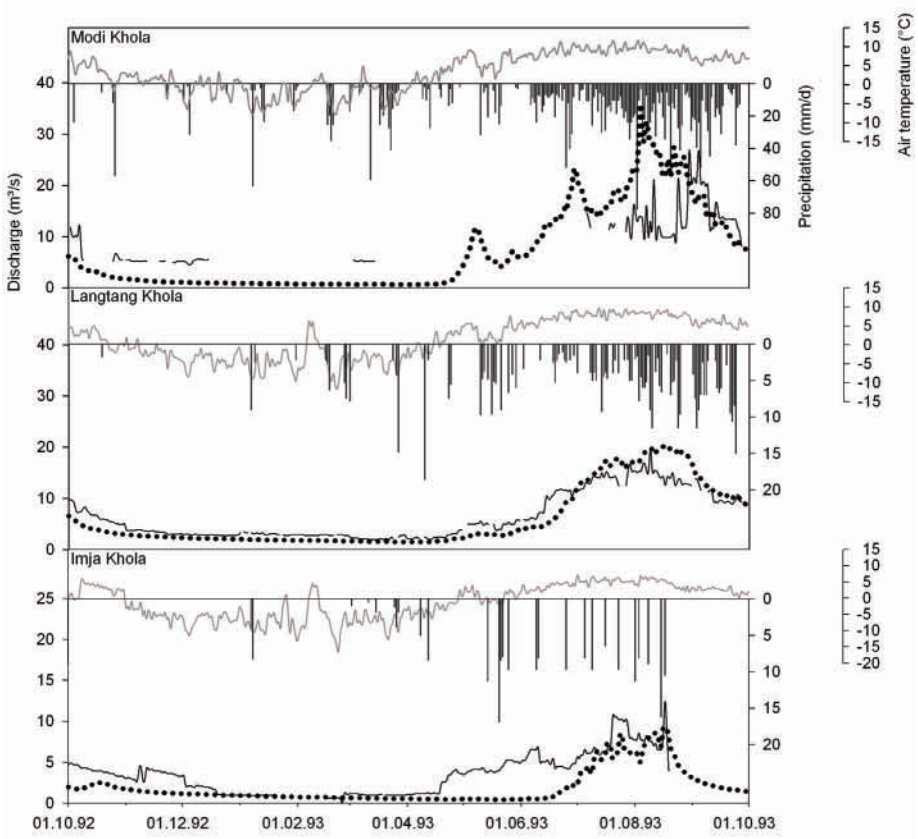


Fig. 1 Comparison of simulated (dotted) and measured discharge (solid) of the three catchments.

Table 2 Optimized parameter set of TAC^D for the investigated catchments. Bold, italic numbers are changed compared to the parameter set of the Langtang Khola catchment.

Parameter	Description	Determination	Langtang Khola	Modi Khola	Imja Khola	Unit
Precipitation correction and regionalization						
PCF	"Precipitation correction factor" for rain	Calibration	1.05	1.05	***1.15***	(–)
P_{Grad}	Vertical precipitation gradient	Calibration (externally set from values in literature)	0.04	0.04	0.04	(% 100 m^{-1} 100^{-1})
$P_{HorizGrad}$	Horizontal precipitation gradient	Calibration (set from values in literature)	–0.03	***0.0***	***0.0***	(% 1000 m^{-1} 100^{-1})
SFCF	"Snowfall correction factor"	Calibration	1.2	1.2	1.2	(–)
Temperature regionalization						
T_{Grad}	Vertical temperature gradient	Calibration (set from values in literature)	–0.5	–0.5	–0.5	(°C 100 m^{-1})
Potential evaporation calculation and regionalization						
ET_{max}	Maximum of potential evapotranspiration	Calibration (set from values in literature)	2.2	2.2	2.2	(mm day^{-1})
ETGrad	Vertical evapotranspiration gradient	Calibration (set from values in literature)	–0.01	–0.01	–0.01	(% 100 m^{-1} 100^{-1})
Snow and glacier routine						
TT	Threshold value of temperature for snowfall also general temperature correction	Calibration (set from values in literature)	–0.2	–0.2	***–0.5***	(°C)
CFMAX	Degree-day factor	Calibration	7.0	7.0	***9.0***	(mm °C^{-1} day^{-1})
CWH	Water holding capacity of snow	Literature (Bergström, 1992)	0.1	0.1	0.1	(–)
CFR	Coefficient of refreezing	Literature (Bergström, 1992)	0.05	0.05	0.05	(–)
R_{exp}	Correction factor for cells with maximum potential sunshine duration	Calibration	1.3	1.3	1.3	(–)
R_{ice}	Multiplicative factor to account for accelerated melt over ice cf. snow	Calibration	1.4	1.4	1.4	(–)
R_{debris}	Reduction factor of glacier melt over debris-covered parts of the glacier	Calibration (set from values in literature)	0.3	0.3	***0.6***	(–)
Soil routine						
LP	Reduction parameter of field capacity	Literature (Menzel, 1997)	0.6	0.6	0.6	(–)
Non-glacier area (nRGType 1)						
FC1	Maximum soil moisture storage (field capacity)	Calibration	20	20	20	(mm)
BETA1	Empirical parameter	Calibration	2.0	2.0	2.0	(–)
Glacier area (nRGType 2)						
FC2	Maximum soil moisture storage (field capacity)	Calibration	20	20	20	(mm)
BETA2	Empirical parameter	Calibration	1.5	1.5	1.5	(–)
Glacier area with inclination less 3° and debris cover (nRGType 3)						
FC3	Maximum soil moisture storage (field capacity)	Calibration	40	40	40	(mm)
BETA3	Empirical parameter	Calibration	1.5	1.5	1.5	(–)
Valley bottom with inclination less 8° (nRGType 4)						
FC4	Maximum soil moisture storage (field capacity)	Calibration	120	120	120	(mm)
BETA4	Empirical parameter	Calibration	2.5	2.5	2.5	(–)
Runoff generation routine						
Non-glacier area (nRGType 1)						
US_K1	Storage coefficient of upper storage	Calibration	0.13	0.13	0.13	(day^{-1})
LS_K1	Storage coefficient of lower storage	Calibration	0.005	0.005	0.005	(day^{-1})
US_P1	Percolation capacity	Calibration	1	1	1	(mm day^{-1})
US_H1	Limit of upper storage	Calibration	100	100	100	(mm)
Glacier area (nRGType 2)						
US_K2	Storage coefficient of upper storage	Calibration	0.1	0.1	0.1	(day^{-1})
LS_K2	Storage coefficient of lower storage	Calibration	0.02	0.02	0.02	(day^{-1})
US_P2	Percolation capacity	Calibration	3	3	3	(mm day^{-1})
US_H2	Limit of upper storage	Calibration	200	200	200	(mm)
Glacier area with inclination less 3° and debris cover (nRGType 3)						
GlacierLS_K	Storage coefficient of glacier storage	Calibration	0.01	0.01	0.01	(day^{-1})
GlacierLS_H	Limit of glacier storage	Calibration	3000	3000	3000	(mm)
Valley bottom with inclination less 8° (nRGType 4)						
ValleyLS_K	Storage coefficient of valley storage	Calibration	0.01	0.01	0.01	(day^{-1})
ValleyLS_H	Limit of valley storage	Calibration	1000	1000	1000	(mm)
Routing routine						
MaxBas	Empirical parameter	Set *a priori*	1	1	1	(–)

Table 3 Evaluation criteria of simulation results calculated using TAC^D for the investigated catchments (R_{eff}: Nash-Sutcliff coefficient, R^2: correlation coefficient, VE: volume error).

Hydrological year	R_{eff} (–)	*log* R_{eff} (–)	R^2 (–)	*VE* (mm year^{-1})
Langtang Khola				
1987–1998	0.20 – 0.87	0.05 – 0.84	0.72 – 0.91	–43 – 97
Modi Khola				
1991–1994	–1.41 – 0.37	–9.21 – 0.12	0.42 – 0.86	–68 – 289
Imja Khola				
1988–1995	0.03 – 0.79	–0.80 – 0.77	0.56 – 0.87	–69 – 323

which are considered to represent the different dynamics of the runoff generation processes. These parameters were not included in the calibration procedure (manual trial and error technique).

Intra-annual distribution of water with spatial distributed storage concepts as described above yielded satisfactory simulation results documented by the objective evaluation criteria if the available input data are of reliable quality (Table 3). This indicates that simple conceptual reservoir approaches to describe the hydrological processes of the Langtang Khola catchment can be considered as sufficient for runoff simulation. With the sequentially linked storages it is possible to simulate water storage mechanisms of glaciers as well as soft and hard rock with different hydraulic behaviour. The high potential of topographic information combined with land-cover data for the delineation of hydrological response units and for the regionalization of runoff generation processes and snow and ice melt, enables a robust runoff simulation in remote areas where additional information (e.g. nested catchments, tracer experiments, etc.) are not available.

In the second phase, the TAC^D model was applied to two catchments in the Khumbu and Annapurna region (Table 1). It is assumed that the hydrological conditions of the three catchments are relatively similar. Therefore, the optimized parameter set of the Langtang Khola catchment was taken for the simulation of the Modi Khola (Annapurna) and Imja Khola (Khumbu) catchments. No evidence was found in the literature for an unequal distribution of basin precipitation as is the case in the Langtang Khola catchment, where a mountain barrier running west–east at the southern side of the valley prevents moisture laden air from penetrating into the northern part of the valley (Konz *et al.*, 2006). Thus, the horizontal precipitation gradient ($P_{HorizGrad}$) was set *a priori* to zero in both catchments (Table 2). The parameters of the runoff generation routine were assumed to be constant for all catchments as the dominant hydrological processes appear similar in the three catchments. In the case of Modi Khola catchment, the data availability is very limited and the measurements are of questionable reliability. Therefore, no re-calibration of the model was conducted in this catchment.

Literature shows that glacier melt rates are higher in the Imja Khola catchment than in the Langtang Khola catchment (Kayastha *et al.*, 2000). This was considered by an increased degree-day factor (*CFMAX*, Table 2). Further parameters which were recalibrated for the application of TAC^D to the Imja Khola catchment are *PCF*, *TT and* R_{debris} (Table 2). Only five calibration runs were computed to adjust the parameter set of the Langtang Khola catchment to the situation of the Imja Khola catchment. Simulation without recalibration underestimated the discharge in all simulated monsoon periods. *CFMAX*, *TT* turned out to be sensitive for the simulation of the monsoon period, when melt water largely contributes to runoff generation.

The visual inspection of the hydrographs and the objective evaluation criteria show that discharge can be reproduced reasonable well if the input data and discharge measurement are of sufficient quality (Fig. 1, Table 3). However, significant deviations from measured discharge can be found in the Imja Khola catchment in the pre-monsoon season 1993 (Fig. 1). The unusually high measured discharge in the pre-monsoon season cannot be explained by the model and might well be an inconsistency (error) in the measurements. Snow and ice at the gauging station could cause too high water levels being recorded.

These results demonstrate that the model TAC^D can be applied satisfactory in highly glacierized catchments if one or more years of input and output measurements are available. The application of the model to the Modi Khola catchment is an example of the way in which a hydrological model can be used in areas with limited data. Regionalization of model parameters

was possible in the case of the parameters for the runoff generation routine and soil routine. Glacier mass balance data turned out to be appropriate data for the (re-) calibration of the parameters of the snow- and glacier routine. This enables water resources assessments in remote areas with limited data availability if spatial data (e.g. DEM, land cover data) are available.

CONCLUDING REMARKS AND OUTLOOK

The ability to regionalize the model structure and parameter set of the distributed catchment model TAC^D has been demonstrated based on the parameter set obtained for the relatively well investigated Langtang Khola catchment. As the application of TAC^D to the Imja Khola catchment showed, only the parameters of the snow and glacier routine had to be adjusted, while the parameters of the soil- and runoff generation routine remained unchanged to yield reasonable simulation results. The parameters of the snow and glacier routine could be determined through measured glacier mass balances. The mass balances are integral values of all the ablation and accumulation processes within a specified period, and are relatively simple and inexpensive to measure. Further research should evaluate the potential of targeted short term measurements (e.g. glacier mass balances or equilibrium line altitudes) to regionalize hydrological models.

Acknowledgements The authors thank the staff of SGHU for providing meteorological and hydrological data and ICIMOD for land cover data. Funding was provided by the German IHP/HWRP Secretariat and by the Bavarian Academy of Sciences, Commission of Glaciology. Special thanks to Lena Tallaksen for critical comments on the manuscript. The research work is a contribution to the FRIEND-HKH programme.

REFERENCES

Braun, L. N., Grabs, W. & Rana, B. (1993) Application of a conceptual precipitation runoff model in the Langtang Khola basin, Nepal Himalaya. In: *Snow and Glacier Hydrology* (ed. by G. Young), 221–237. IAHS Publ. 218. IAHS Press, Wallingford, UK.

Braun, L. N., Hottelet, Ch., Weber, M. & Grabs, W. (1998) Measurement and simulation of runoff from Nepalese head watersheds. In: *Hydrology, Water Resources and Ecology in Headwaters* (ed. by K. Kovar, U. Tappeiner, N. E. Peters & R. G. Craig), 9–18. IAHS Publ. 248. IAHS Press, Wallingford, UK.

Fujita, K., Takeuchi, N. & Seko, K. (1998) Glaciological observations of Yala Glacier in the Langtang Valley, Nepal Himalayas, 1994 and 1996. *Bull. Glacier Res.* **16**, 75–81.

Gottschalk, L., Beldring, S., Engeland, K., Tallaksen, L. M., Sælthun, N. R., Kolberg, S. & Motovilov, Y. (2001) Regional/macroscale hydrological modelling: a Scandinavian experience. *Hydrol. Sci. J.* **46**(6)**,** 963–982.

Grabs, W. & Pokhrel, A. P. (1993) Establishment of a measuring service for snow and glacier hydrology in Nepal – conceptual and operational aspects. In: *Snow and Glacier Hydrology* (ed. by G. Young), 3–16. IAHS Publ. 218. IAHS Press, Wallingford, UK.

Jansson, P., Hock, R. & Schneider, T. (2002) The concept of glacier storage: a review. *J. Hydrol.* **282**, 116–129.

Johst, M., Uhlenbrook, S., Tilch, N., Zillgens, B. & Kirnbauer, R. (2006) Process-oriented catchment modelling in an alpine catchment, Loehnersbach, Austria. *Nordic Hydrol.* (in review).

Kayastha, R. B., Takeuchi, Y., Nakawo, M. & Ageta, Y. (2000) Practical prediction of ice melting beneath various thickness of debris cover on Khumbu Glacier, Nepal, using a positive degree-day factor. In: *Debris-Covered Glaciers* (ed. by M. Nakawo, C. F. Raymond & A. Fountain), 71–81. IAHS Publ. 264. IAHS Press, Wallingford, UK.

Konz, M., Braun, L., Uhlenbrook, S. & Shrestha, A. (2006) Runoff from Nepalese head watersheds based on measurements and modelling. IHP/HWRP-Bericht, *Heft* **4**, ISSN 1614-1180.

Nash, J. E. & Sutcliffe, J. V. (1970) River flow forecasting through conceptual models, Part I – a discussion of principles. *J. Hydrol.* **10**, 282–290.

Ott, B. & Uhlenbrook, S. (2004) Quantifying the impact of land use changes at the event and seasonal time scale using a process-oriented catchment model. *Hydrol. Earth System Sci.* **8**(1), 62–78.

Uhlenbrook S., Roser, S. & Tilch N. (2004) Development of a distributed, but conceptual catchment model to represent hydrological processes adequately in the meso scale. *J. Hydrol.* **291**, 278–296.

UNEP/ICIMOD (2002) Inventory of glaciers, glacier lakes and glacier lake outburst floods monitoring and early warning systems in the Hindu Kush – Himalayan region [CD-ROM ISBN 92 9115 359 1].

Climate Variability and Change—Hydrological Impacts (Proceedings of the Fifth FRIEND World Conference held at Havana, Cuba, November 2006), IAHS Publ. 308, 2006.

Climate change impacts on glacial lakes and glacierized basins in Nepal and implications for water resources

SURESH RAJ CHALISE[1], **MADAN LALL SHRESTHA**[2], **OM RATNA BAJRACHARYA**[2] **& ARUN BHAKTA SHRESTHA**[2]

1 *Snow and Glacier Hydrology Group, HKH-FRIEND, GPO Box 4965, Kathmandu, Nepal*
srchalise@mcmail.com.np

2 *Department of Hydrology & Meteorology (DHM), Babar Mahal, GPO Box 406, Kathmandu, Nepal*

Abstract An increasing number of glacial lakes have been observed in recent years in Nepal and other Himalayan countries. Glacial lake outburst floods (GLOFs) causing destruction of life, agricultural land, hydropower installations, and other costly infrastructure have also occurred more frequently in recent years in Nepal, Tibet (China) and elsewhere in the Himalayas. Recent temperature and discharge data from the Tsho Rolpa glacial lake (4580 m a.s.l.) and two rivers from glacierized basins, Langtang (3900 m a.s.l) and Imja (4200 m a.s.l), were analysed. An increasing trend of warming and discharge were observed at high elevation. The potential impacts of climate change in Nepal Himalaya are likely to be seen in terms of increasing numbers of disastrous flood events, including GLOFs, and in the long-term reduced low flows. These will have implications for water resources development in Nepal and its neighbour, India.

Key words climate change; glaciers; glacial lake; glacial lake outburst flood (GLOF); low flow; water resources; Himalayas; India; Nepal; Tibet (China)

INTRODUCTION

Studies and observations made on a global scale have shown that although mountain glaciers have been retreating generally since the beginning of the last century, their retreat has accelerated since the 1980s (Dyurgerov & Meier, 1997; Haeberli & Hoelzle, 2001). The Himalayas, being the highest mountains of the world, have been profoundly impacted by climate warming, as shown by the rapid retreat of the Himalayan glaciers and appearance of glacial lakes in recent years (Hasnain, 1999; Fujita *et al.*, 2001a,b; ICIMOD/UNEP, 2001a,b; Chalise *et al.*, 2003, 2005; Rees & Collins, 2004; WWF, 2005).

The impact of climate warming on the glaciers and ice reserves of Nepal, China (Tibet) and other Himalayan countries will have serious implications for the freshwater reserve and consequently for low flows for Nepal and all other Himalayan countries. The total ice reserve of the Himalayas is approximately 3734.5 km^3 with 18 115 glaciers (Qin, 1999). According to Haeberli (1998), the wastage of the total Himalayan glacier ice reserve could contribute 16% of the total meltwater volume released from all the other glaciers and ice caps of the world excluding those of Antarctica and Greenland. Climate warming impacts in the Himalayas, therefore, have global implications .

CLIMATE WARMING IMPACTS ON GLACIAL LAKES OF NEPAL

Glacial lakes are found all over the Himalayas and the Tibetan Plateau. In general, comprehensive scientific data and information on the Himalayan glaciers and glacial lakes are not available. However, recent publications on glaciers and glacial lakes of Bhutan (ICIMOD/UNEP, 2001a), China/Tibet (LIGG/WECS/NEA, 1988; Qin, 1999) and Nepal (ICIMOD/UNEP, 2001b) indicate that glacial lakes are present in large numbers in these countries and some of them are growing dangerously.

The bursting of the Dig Tsho glacial lake in the Khumbu region of eastern Nepal on 4 August 1985 can be considered as the eye-opener and starting point for scientific investigation of glacial lake outburst floods (GLOF) and glacial lakes in Nepal and other countries of the Himalayas. The Dig Tsho GLOF lasted for only five hours but caused extensive damage for up to 40 km down-stream, destroying human life, settlement, bridges and the near-complete Namche hydropower plant 12 km downstream (Ives, 1986; Vuichard & Zimmerman, 1986, 1987; Yamada, 1998). As this disaster occurred in the Everest region, it drew wide national and international scientific and public interest (Galay, 1985; Ives, 1986; Vuichard & Zimmerman, 1986, 1987). Prior to this other

Copyright © 2006 IAHS Press

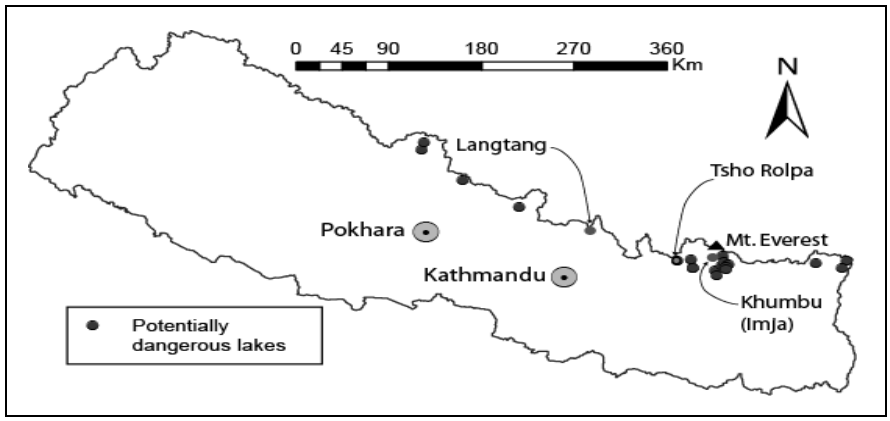


Fig. 1 Location map of high altitude stations (Langtang, Tsho Rolpa and Khumbu) and potentially dangerous glacial lakes in Nepal. Data source: ICIMOD/UNEP (2001b) and DHM.

GLOF events, including that in July 1981 in central Nepal on the Bhote Kosi and Sun Kosi rivers close to the China (Tibet) border were considered as catastrophic flash floods associated with extreme rainfall events during the monsoon. It was also apparent that GLOFs originating in Tibet (China) could cause damage across the border in neighbouring countries.

Almost all the glacier lakes in Nepal Himalaya are moraine-dammed (Yamada, 1998) and essentially unstable. According to a recent study there are 2323 glacial lakes in Nepal located at elevations of 3500 m a.s.l. and above, of which 20 are considered to be potentially dangerous (Fig. 1; ICIMOD/UNEP *et al.*, 2001b). Three of these potentially dangerous glacial lakes have past outburst history. Almost all of the potentially dangerous lakes are located east of Pokhara, in the central and eastern part of Nepal (Fig. 1). Similarly, of the 21 GLOF events reported so far all occurred east of Pokhara except one of unknown date which occurred in northwest Nepal (Mugu Karnali).

One of the reasons for this could be the higher monsoon precipitation in central and eastern Nepal compared to its western part. The other could be the impact of warming.

Most of the GLOF events occurred after the 1960s (ICIMOD/UNEP, 2001b). Shrestha *et al.*, (1999) analysed maximum temperature data for the period 1971–1994 and reported a warming trend in annual maximum temperatures from 0.06 to 0.12^{o}C year^{-1} after 1977 for the middle mountains and Himalayan regions of Nepal. Another study of average annual temperature for 15 stations above 1800 m in Nepal has reported an annual increase of over 0.1^{o}C year^{-1} for the period 1976–1996. (Rees & Collins, 2004) These values are more than double the +0.03^{o}C year^{-1} average global warming predicted by IPCC (IPCC, 2001a,b). Investigation of climate change scenarios carried out by Shrestha (1997) also indicates that the warming trend at higher elevations will be more than at lower elevations. Furthermore, the large glacial lakes in Nepal (e.g. Tsho Rolpa and Imja) did not exist prior to the late 1950s when they started forming and grew rapidly to their present size. The growth rate of Imja Lake is 0.016 km^2 year^{-1}and Tsho Rolpa grew from 0.23 km^2 in 1959 to 1.76 km^2 in 2002. All these indicate a higher rate of warming at higher elevations in eastern Nepal Himalaya since the 1960s.

The first ever attempt to mitigate GLOF from a potentially dangerous glacial lake in the Himalayas was made in Nepal in 1999 for the Tsho Rolpa glacial lake (4580 m a.s.l.), i.e. lowering the lake height by 3 m by constructing a gated canal. The project was completed in 2003 and installed an Early Warning System (EWS) and a 15 kW micro-hydro power plant at the project site (DHM, 1998; Shrestha *et al*., 2001, 2004; Chalise *et al.*, 2005).

In order to assess the impact of climate warming at higher elevations in the eastern part of Nepal, discharge data for Tsho Rolpa glacial lake for the periods 1993–1996 and 2000–2004 were analysed. The discharge from the natural outlet of Tsho Rolpa glacial lake was measured from June 1993 to May 1996 by the Glaciological Expedition in Nepal (GEN; Yamada, 1998). Since the completion of the construction of the open channel in June 2000 (Shrestha *et al*., 2001), DHM has been monitoring the lake discharge through the open channel (Fig. 2). There is no visible difference between the two data sets for the periods 1993–1996 data and 2000–2004. Monthly

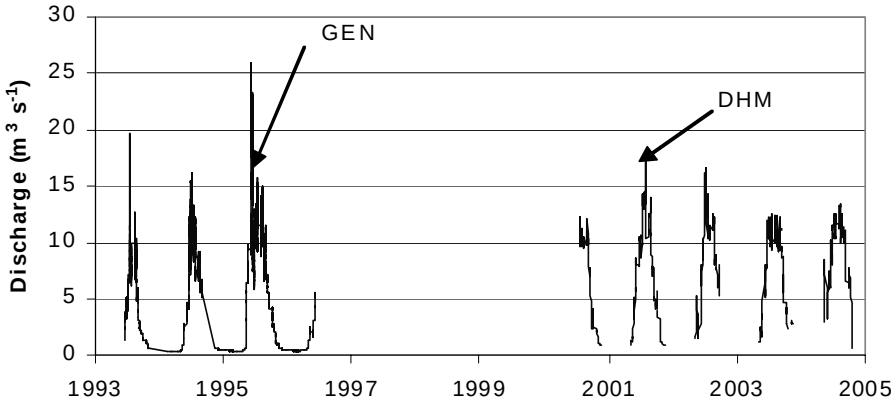


Fig. 2 Discharge from Tsho Rolpa Glacial Lake.

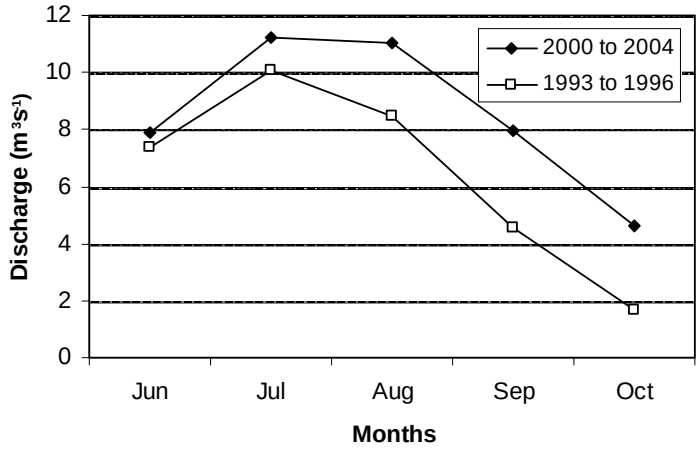


Fig. 3 Average monthly mean discharge at Tsho Rolpa.

mean discharges were computed for these two data sets covering the high flow period (June to October). It can be seen that the mean discharges of the latter period (2000–2004) is higher than that of the earlier period (1993–1996) for all months (Fig. 3). The difference in monthly mean discharge between these two periods is significant at $p > 95\%$. If this result is due to the intensification of melting in Trakarding and Trolambau glaciers (the parent glaciers of Tsho Rolpa) it can be anticipated that the lake level might start rising again and the risk of another GLOF will increase.

HYDROLOGICAL IMPACTS OF CLIMATE WARMING

In addition to the increased risk of the outburst of glacial lakes, climate change can have serious implications for the hydrological regime of the region as it is heavily dependent on the supply of water due to melting of snow and glaciers during the dry season (March–June). In order to assess the impact of atmospheric warming on dry season flows at higher elevations, temperature and discharge data from two high altitude hydrological and meteorological stations in Nepal, namely: Langtang (3900 m a.s.l.) and Khumbu (4200 m a.s.l.) were analysed. These stations were established in the late 1980s and have the longest climatological and hydrological records of the glacierized basins of Nepal. The Langtang station shows a distinct warming trend and the discharge from Langtang Khola shows a small but distinct increasing trend (Fig. 4). In contrast, neither temperature nor the discharge from Imja khola at Khumbu station show any trend.

The trends for Langtang might be an indication that climate warming has already started and is showing its impact on the river flows, although due to the short data period a definite conclusion cannot be made at this stage. A strong relationship exists between temperature and river discharge at both basins during the dry season, March–June (Fig. 5). This result supports the postulation that the hydrological regime of the Himalayan rivers will be affected by climate warming.

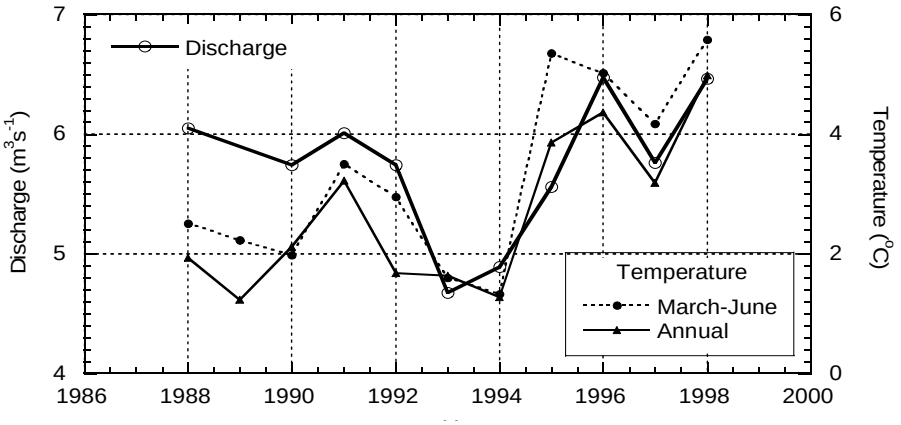


Fig. 4 Temperature and discharge at Langtang station.

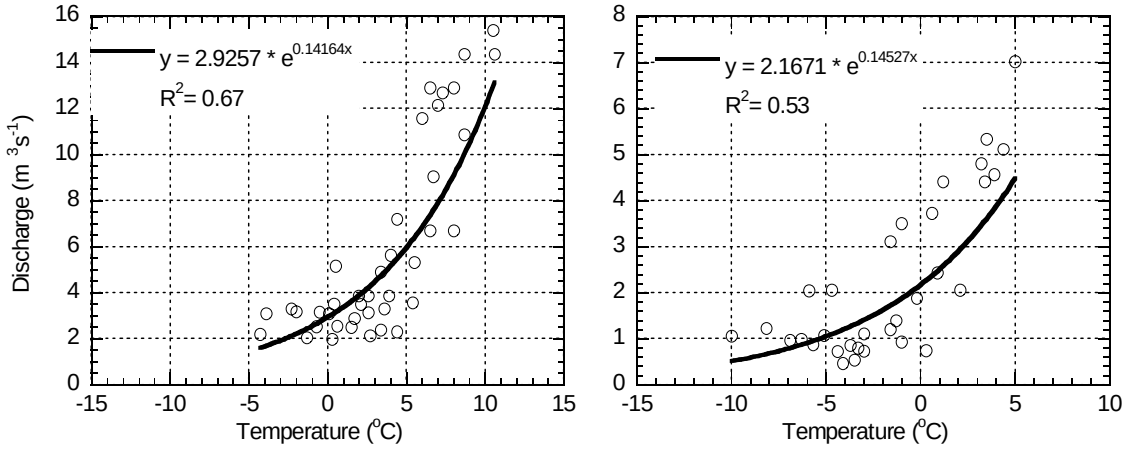


Fig. 5 Relationship between temperature and dry season discharge at Langtang (left) and Khumbu (Imja Khola, right)

IMPLICATIONS FOR WATER RESOURCES

Climate warming has two major implications for the water resources of Nepal, which show an increasing trend and impact at higher elevations. Firstly, the flash flood events, including GLOFs would increase due to increased melting of glacierized basins and glacial lakes. This will be further aggravated by the increase in summer precipitation including extreme precipitation events, due to global warming (Chalise, 1994; Shrestha, 1997; IPCC, 2001a,b). An increase in disastrous flash floods and GLOFs in the headwater regions would adversely affect the development of hydropower in Nepal. As a poor country with no other resources, Nepal hopes to develop its economy by exporting hydropower to its neighbours, particularly to India. With nearly 15% of its area (147 181 km^2) above 4500 m a.s.l. and under snow cover, Nepal is rich in water resources with a theoretical potential of 83 000 MW of which 42 000 MW is considered feasible and 22 000 MW exportable (NPC, 2003). The risk of major hydropower development in vulnerable, hazard prone areas could discourage large investments.

Secondly, the resource base, i.e. the ice reserve, is likely to shrink. This will seriously affect the dry season discharge in future. In general, the low flows in the Nepalese and other Himalayan rivers are at least 10–20 times smaller than the high flows. With a shrinking resource base the dry season flows are likely to decrease too. This will seriously affect not only the development of hydropower but also agricultural and industrial development, apart from causing acute shortage for human consumption.

The decrease in dry season flow in the Nepalese rivers is also going to affect the flow in the Ganga (Ganges) in India as all the Nepalese rivers drain into the Ganga. Although Nepal constitutes only 13% of Ganga basin by area, Nepalese rivers contribute 47% of the annual

discharge of 382 000 million m^3 of the Ganga at Farakka and their contribution is 75% for the three dry season months from March–May (Pun, 2004). A decrease in low flow in Nepalese rivers would also adversely affect the Ganga dependent areas in Bangladesh. The river linking project of India, which intends to link the Ganga and Brahmaputra rivers with the rivers in peninsular India (Prabhu, 2004) could also be affected.

CONCLUSION

Increasing deglaciation in Nepal and other Himalayan countries due to a warming climate will further intensify the "too much" (during the short wet period) and "too little" (during the long dry periods) situation in these countries. Identification of rapidly growing glacial lakes and increased understanding of their growth mechanism are important to develop strategies to cope with and mitigate the future disastrous GLOF events. It is urgent for these countries start sharing available relevant information and data, and work together to develop a comprehensive scientific database to develop national and regional strategies to cope with the potential impacts of climate warming on their snow and ice reserves. International scientific networks such as ICSIH/IAHS and the regional network of UNESCO's FRIEND project, viz. the Hindu Kush-Himalayan FRIEND, which are already contributing to improve scientific understanding of climate change impacts on the Himalayan cryosphere, should be encouraged to contribute to the national and regional research programmes.

Acknowledgements: The authors are thankful to Mr Kumar Rajbhandari of the Department of Hydrology and Meteorology (DHM) for his assistance in preparing the manuscript of this paper. Thanks are also due to staff members of Snow and Glacier Hydrology Section of DHM for their assistance in data processing.

REFERENCES

Chalise, S. R. (1994) Mountain environment and climate change in the Hindu Kush-Himalaya. In: *Mountain Environments in Changing Climate* (ed. by M. Beniston), 382–404. Routledge, London, UK.

Chalise, S. R., Kansakar, S. R., Rees, G., Croker, K. & Zaidman, M. (2003) Management of water resources and low flow estimation for the Himalayan basins of Nepal. *J. Hydrol* **282**, 24–35.

Chalise, S. R., Shrestha, M. L., Budhathoki, K. P. & Shrestha, M. S. (2005) Glacio-hydrological aspects of climate change in the Himalayas: mitigation of glacial lake outburst floods in Nepal. In: *Regional Hydrological Impacts of Climate Change – Impact Assessment and Decision Making* (ed. by T. Wagener, S. Franks, H. V. Gupta, E. Boegh, L. Bastidas, C. Nobre & C. D. O. Galvao), 309–316. IAHS Publ. 295. IAHS Press, Wallingford, UK.

DHM (1998) Tsho Rolpa GLOF risk reduction project, implementation report, Final Version. Department of Hydrology and Meteorology, Babar Mahal, Kathmandu, Nepal.

Dyugerov, M. B. & Meier, M. F. (1997) Mass balance of mountain and sub-polar glaciers: a new global assessment for 1961–1990. *Arctic and Alpine Research* **29**(4), 379–391.

Fujita, K., Kadota, T., Rana, B., Kayastha, R. B. & Ageta, Y. (2001a) Shrinkage of glacier AX 010 in Shorong region, Nepal Himalayas in the 1990s. *Bull. Glaciol. Res.* **18**, 51–54.

Fujita, K., Nakazawa, F. & Rana, B. (2001b) Glaciological observation on Rikha Samba glacier in Hidden Valley, Nepal Himalayas, 1998 and 1999. *Bull. Glaciol. Res.* **18**, 31–35.

Galay, V. J. (1985) Glacier Lake Outburst Flood on the Bohte/Dodh Kosi, August 4, 1985. WECS Internal Report. Water and Energy Commission Secretariat (WECS), Kathmandu, Nepal.

Haeberli, W. (1998) Historical evolution and operational aspects of worldwide glacier monitoring. In: *Into the Second Century of World-Wide Glacier Monitoring Prospects and Strategies.* (ed. by W. Haeberli, M. Hoelzie, & S. Suter), 35–51. UNESCO Studies and Reports in Hydrology no. 56. Paris, France.

Haeberli, W. & Hoeizle, M. (2001) The World Glacier Monitoring Service. (http://www.nerc-bas.ac.uk/public/icd/icsi/WGMS.html).

Hasnain, S. I. (1999) *Himalayan Glaciers Hydrology and Hydrochemistry.* Allied Publishers, New Delhi, India.

ICIMOD/UNEP (2001a) *Inventory of Glaciers, Glacial Lakes and Glacial Lake Outburst Floods-Monitoring and Early Warning Systems in the Hindu Kush-Himalayan Region-Bhutan* (ed. by P. K. Mool, S. R. Bajracharya & S. P. Joshi). International Centre for Integrated Mountain Development, Kathmandu, Nepal.

ICIMOD/UNEP (2001b*) Inventory of Glaciers, Glacial Lakes and Glacial Lake Outburst Floods-Monitoring and Early Warning Systems in the Hindu Kush-Himalayan Region-Nepal.* (ed. by P. K. Mool, S. R. Bajracharya & S. P. Joshi). International Centre for Integrated Mountain Development, Kathmandu, Nepal.

IPCC (2001a) Climate Change 2001: Impacts, Adaptation and Vulnerability. *Contribution of Working Group II to the Third Assessment Report of the Intergovernmental Panel on Climate Change* (ed. by J. J. McCarthy *et al.*). Cambridge University Press, UK.

IPCC (2001b) Climate Change 2001: The Scientific Basis. *Contribution of Working Group I to the Third Assessment Report of the Intergovernmental Panel on Climate Change* (ed. by J. T. Houghton *et al.*). Cambridge University Press, UK.

Ives, J. D. (1986) Glacial lake outburst floods and risk engineering in the Himalaya. *ICIMOD Occ. Paper 5.* ICIMOD, Kathmandu, Nepal

LIGG/WECS/NEA (1988) *Report on First Expedition to Glaciers and Glacial Lakes in the Pumqu (Arun) and Poiqu (Bhote-Sun Kosi) river basins, Xizang (Tibet), China, Sino-Nepalese Investigation of Glacier Lake Outburst Floods in the Himalaya.* Science Press, Beijing, China.

NPC (2003) *Tenth Five Year Plan of Nepal (2002–2007)*. National Planning Commission, Kathmandu, Nepal.

Prabhu, S. P. (2004) Garland of hope; river linking as a solution to water crisis. *Times of India* 14 August 2004. New Delhi, India.

Pun, S. B. (2004) Overview: Conflicts over the Ganga? In: *Disputes Over the Ganga. A look at potential water related conflicts in South Asia* (ed. by B. Subba & K. Pradhan), 2–12. Panos Institute South Asia, Kathmandu, Nepal.

Qin, D. (Chief Editor) *Map of Glacier Resources in the Himalayas* (I 999). Science Press, Beijing, China.

Rees, G. & Collins, D. N. (2004) *SAGARMATHA: Snow and Glacier Aspects of Water Resources Management in the Himalayas, Technical Report.* Centre for Ecology and Hydrology, Wallingford, UK.

Shrestha, M. L. (1997) Development of climate scenarios with reference to Nepal. In: *Proceedings of the Workshop on Climate Change in Nepal* (US Country Studies Program, Kathmandu, Nepal), 16–32.

Shrestha, A. B., Wake, C. P., Mayewski, P. A. & Dibb, J. E. (1999) Maximum temperature trends in the Himalayas and its vicinity: an analysis based on temperature records from Nepal for the period 1971–94. *J. Climate* **12**, 2775–2786.

Shrestha, A. B, Rana, B, Aryal, R & Pokhrel, A. P. (2001) Hazard assessment and remediation work at Tsho Rolpa glacier lake, Rolwaling Himal, Nepal. *J.Japanese Society of Civil Engineers* **86**, 72–75.

Shrestha, A. B., Budhathoki, K. P., Shrestha, R. K. & Adhikary, R. (2004) Bathymetric survey of Tsho Rolpa glacier lake, 2002. . *Hydrol. Met., Nepal* **1**(1) 13–15. Society of Hydrologist & Meteorologist, Kathmandu, Nepal.

Vuichard, D. & Zimmerman, M. (1986) The Langmoche flash flood, Khumbu Himal, Nepal. In: *Mountain Research and Development* **6**(1), 90–94.

Vuichard, D. & Zimmerman, M. (1987) The catastrophic drainage of a moraine-dammed lake, Khumbu Himal, Nepal: cause and consequence. In: *Mountain Research and Development* **7**(2), 91–110.

WWF (2005) An overview of glaciers, glacier retreat and its subsequent impacts in the Nepal, India and China, WWF Nepal Program, Kathmandu, Nepal.

Yamada, T. (1998) *Glacier Lake and its Outburst Flood in the Nepal Himalaya.* Monograph no. 1, Data Centre for Glacier Research, Japanese Society of Snow and Ice.

Climate Variability and Change—Hydrological Impacts (Proceedings of the Fifth FRIEND World Conference held at Havana, Cuba, November 2006), IAHS Publ. 308, 2006.

Variability of runoff from Alpine basins

DAVID N. COLLINS

Alpine Glacier Project, School of Environment & Life Sciences, University of Salford, Salford Crescent, Manchester M5 4WT, UK

d.n.collins@salford.ac.uk

Abstract Year-to-year variability of runoff from three moderately-glacierized (36–66% ice cover) and two (near-)ice-free (0–1.9%) headwater basins in the Alpine Aare and Rhône basins, Switzerland, was assessed for 50 years from 1956 to 2005. Variability, as coefficient of variation, was less in moderately-glacierized than in (near-) ice-free precipitation-influenced basins, but increased in basins with between 40 and 66% glacierization as energy-availability for snow/icemelt dominated. Mean summer air temperature increase of 1.13°C between 1956–1980 and 1981–2005, coupled with a 13% reduction in mean total annual precipitation, was associated with decreased runoff variability in basins having between 0 and 40% glacierization but with increased variability in more highly glacierized basins.

Key words coefficient of variation; runoff variability; glacierized basin; climatic variation

INTRODUCTION

Annual accumulation and melting of stable winter snowpack, together with summer glacier ice ablation, account for distinctive runoff characteristics in high mountain basins. In ice-free montane basins, maximum monthly discharge occurs in spring, annual runoff is less than annual total precipitation, and year-to-year variations in runoff follow those of precipitation. In glacierized basins, the greater the percentage ice cover, the later into summer is maximum monthly discharge delayed, the higher the annual runoff, which can be more than, equal to, or less than, annual precipitation, depending on changes in storage of water as glacier ice, and the more runoff variability is influenced by intra-annual changes in thermal energy available for melting. Runoff variability is negatively related to percentage basin ice-cover up to a point (e.g. Krimmel & Tangborn, 1974; Fleming & Clarke, 2005), but then as glacierization increases above about 20–25%, the relationship turns positive (Walser, 1960; Tvede, 1982). In basins with some but not extensive ice-cover, glaciers effectively moderate intra-annual variations in river flow, in cooler years by runoff arising from precipitation over the large ice-free area offsetting reduced glacier melt, and in warm dry summers through enhanced melt making up for reduced precipitation.

Thermal energy availability interacting with snowfall over the glacier ablation area strongly influences runoff variability in moderately-glacierized basins (Collins & Taylor, 1990), ice-free areas predominantly located at lower elevations producing limited runoff from less precipitation. In warm summers following dry winters, the transient snow line rises sooner and higher up-glacier, allowing more ice melt over a wider area than in years in which cool summers follow snowy winters. Runoff variability in long series will also be affected by changes in both overall glacier surface area, and area of ice exposed to melt as loss through marginal recession may be offset by general rising of the transient snow line (Collins, 1989a).

The aim of this paper is to describe the variability of runoff from moderately-glacierized Alpine basins during the 50-year period 1956–2005. Basins with glacierization in the range 35–70% were selected, and referenced against ice-free/near-ice-free basins. Overall glacier areas declined throughout the period, initially in spite of cool wet conditions which reduced runoff from more highly-glacierized basins. From the early 1980s, warmer summers and relatively dry winters, resulting from high pressure anomalies over Central Europe (Beniston & Jungo, 2002), generally enhanced runoff from moderately-glacierized basins into the early 1990s. The more extensively-glacierized the basin the more increased runoff was sustained into the 2000s (Collins, 2005). For basins in Switzerland with more than 10% glacierization, an upward trend in runoff was detected between the 1970s and 2000s (Birsan *et al*., 2005).

MEASUREMENTS

Five headwater basins in the Rhône and Aare catchments, Switzerland, basins for which runoff variability from the 1950s to the mid-1980s had previously been assessed (Collins, 1989a, Collins

Copyright © 2006 IAHS Press

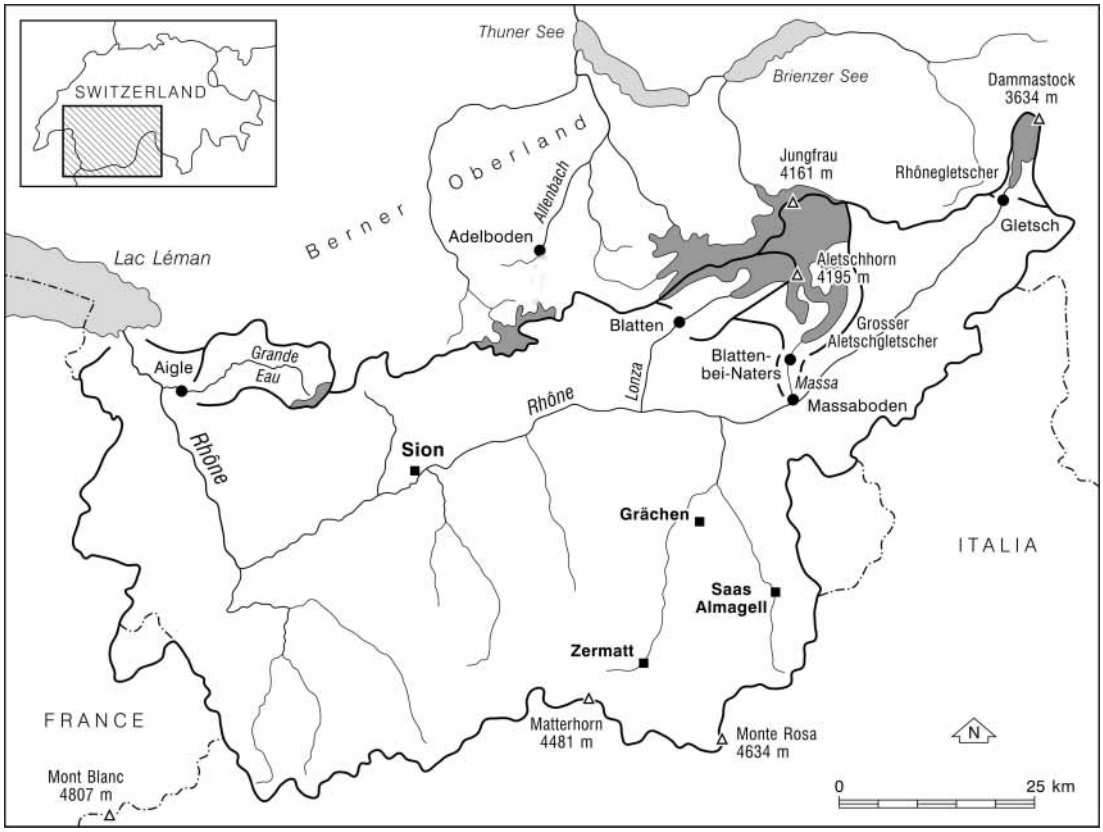


Fig. 1 Locations of the five study basins and meteorological stations from which records have been analysed in the upper Aare and upper Rhône basins, Switzerland.

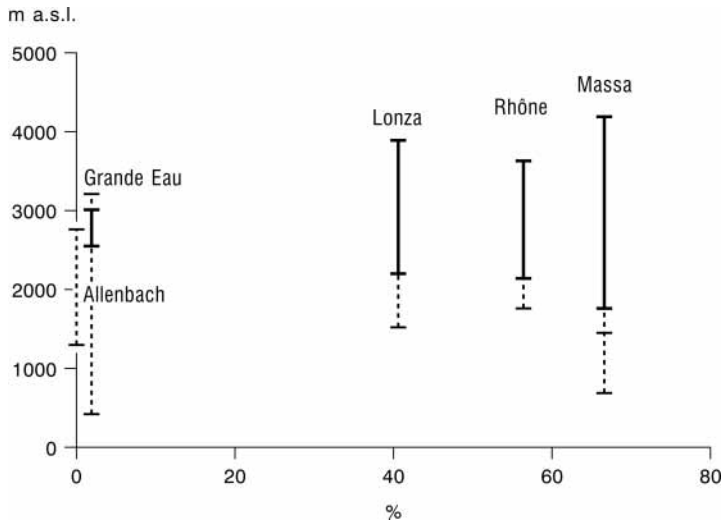


Fig 2 Elevations of gauging stations, lower and upper limits of glacierized areas (solid lines) and highest points in each study basin plotted against percentage basin glacierization.

& Taylor, 1990), were selected for the study (Fig. 1). All five basins are exposed to the same pattern of climatic influences. Basin characteristics are shown in Fig. 2 and Table 1. Runoff in the Grande Eau is slightly influenced by water storage. The Massa was gauged at Massaboden to 1964, before the station was moved upstream to Blatten-bei-Naters. Basin area was reduced by 3.47%, but discharge measurements in the Massa have not been adjusted. Otherwise, records are homogeneous and of natural flow regimes. Annual runoff ($Q_{1\text{-}12}$) is represented by total discharge in a calendar year, 1 January through 31 December.

Although Alpine precipitation is far from being uniformly distributed, total annual precipitation at Zermatt (1632 m a.s.l.) (Fig. 1) was taken as indicative of year-to-year variations

Table 1 Characteristics of basins: glacierized areas and runoff, 1956–2005.

River/Gauging station	Basin area (km²)	Basin glacierization (year)	(%)	Mean runoff (m)
Allenbach/Adelboden	28.8		0.0	1.312
Grande Eau/Aigle	132.0	1977	1.9	1.190
		2002	1.8	
Lonza/Blatten	77.8	1977	40.6	1.905
		2002	36.5	
Rhône/Gletsch	38.9	1977	56.4	2.218
		2002	52.2	
Massa/Massaboden	202.0	1957	64.1	2.112
Massa/Blatten-bei-Naters	195.0	1957	66.4	
		1977	66.6	
		2002	65.9	

over the study basins. Precipitation between November in year *n* and October in year *n* + 1 ($P_{11\text{-}10}$) reflects winter snow pack accumulation contributing to runoff on melting in spring, plus liquid precipitation contributing to summer flows. Mean summer air temperature between May and September ($T_{5\text{-}9}$) usefully indicates energy availability for melting. A part-synthetic record of $T_{5\text{-}9}$ for Sion (Couvent des Capucins) (542 m a.s.l.) has been derived from observations at Sion, Grächen and Saas Almagell, as described by Collins (1989a). Overall percentage glacier cover of a basin (Table 1) has been taken from the *Hydrologisches Jahrbuch der Schweiz* (e.g. Bundesamt für Wasser und Geologie, 2003).

BASIN CHARACTERISTICS AND RUNOFF

Whilst glacierized area in a basin increases with upper basin limit elevation (Table 1, Fig. 2), percentage glacierization is also influenced by the distance from glacier terminus to downstream gauging station location. Basins with gauging stations at low elevations also contain areas receiving lower precipitation contributing less runoff, which may explain why mean annual runoff in the Grande Eau and Massa was lower than in the Allenbach and Rhône respectively (Table 1). Area, hypsometry and elevation range of glaciers, all ice-cover properties influencing meltwater production, are not simply related to percentage glacierization.

For the (near-)ice-free basins, maximum monthly runoff occurred in May in both Grande Eau and Allenbach, with averages of 52.5 and 63.6%, respectively, of total annual runoff occurring during snowmelt in the four months April–July (Fig. 3). The smaller percentage for Grande Eau reflects more runoff in winter as a result of snowpack instability at lower elevations. With higher basin glacierization, maximum monthly runoff was delayed to July in Lonza and Rhône, and to August in the Massa, with averages of 85.1, 88.2 and 92.3%, respectively, of total annual runoff occurring in the five summer months May–September. Including October as a sixth summer month, these percentages of ablation season/total runoff become 90.7, 93.4 and 97.1, emphasizing glacial domination of runoff once ice covers a substantive portion of a basin.

In the 50-year period 1956–2005, glacier cover declined in all four basins with glaciers. In the Massa basin, Grosser Aletschgletscher was reduced in area by about 1 km^2 (0.8 %). From 1977, Rhônegletscher lost about 1.6 km^2 (7.3%), Langgletscher (in the Lonza basin) about 3.2 km^2 (10.1%) and Glacier de Pierredar (Grande Eau) 0.13 km^2 (10.6%), the percentage loss increasing with decreasing elevation. Such changes in glacier area will have influenced meltwater production and hence have tended to reduce annual runoff.

VARIABILITY OF RUNOFF

Coefficient of variation (CV), the ratio of standard deviation to mean, is usually used for comparisons of year-to-year variability of runoff between basins (e.g. Collins, 1989a). Annual runoff variability in the 50-year period was greatest in the Grande Eau (CV = 0.210), slightly higher than in the ice-free Allenbach (CV = 0.190) (Fig. 4). The CV of $P_{11\text{-}10}$ at Zermatt for the same period was

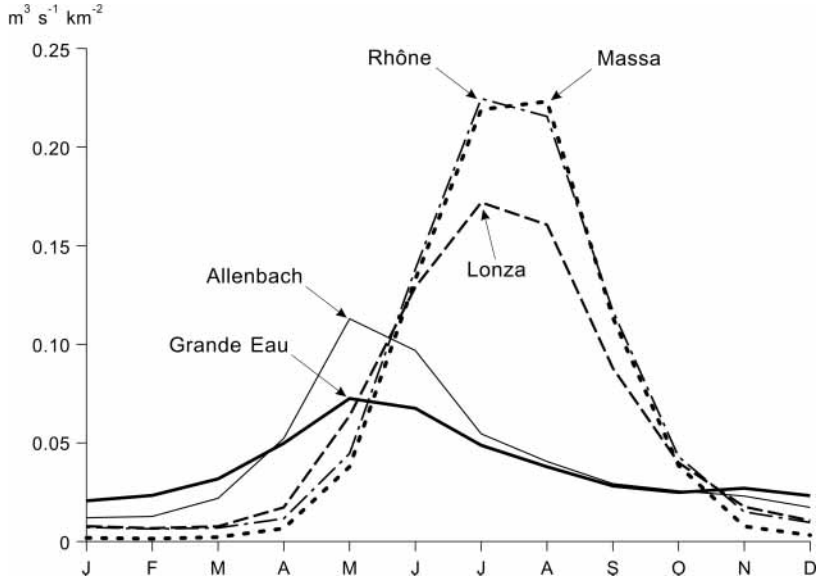


Fig. 3 Mean monthly specific discharge in the Allenbach, Grande Eau, Lonza, Rhône and Massa rivers for the period 1956–2005.

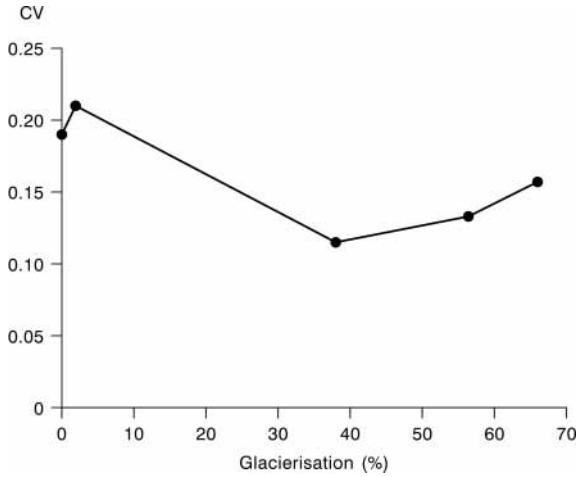


Fig. 4 Coefficient of variation (CV) of total annual runoff from the five study basins for the period 1956–2005 as a function of percentage basin glacierization.

close at 0.191. Variability of runoff was least in the Lonza (CV = 0.115) at a mean of 38.5% glacierization, but then increased with increasing glacierization to 0.157 in the Massa, at 66.3% ice cover the most highly glacierized basin although year-to-year variability of flow was still less than in the (near-)ice-free basins.

Monthly runoff totals were generally more variable from year to year than annual runoff, irrespective of basin glacierization (Fig. 5). Minimum variability of monthly flow occurred in July or August, months with the highest runoff, in the three moderately-glacierized basins. Months with considerable variability in flow were March, April, May, September, October and November, months marginal to the main ablation season. March, April and November are months in which absolute amounts of discharge are small, and hence variability of flow in those months contributed little to overall year-to-year variability of annual total runoff. Warmer springs, particularly those following drier winters, enhanced runoff totals in May and increased dispersion during the 50 years. Again in warmer years, the ablation season lengthened as energy availability extended into autumn. Variability of individual monthly runoff was in general greater in the (near-) ice-free than in the moderately-glacierized basins. Year-to-year variability in monthly runoff from the (near-) ice-free basins was also inversely related to volume of flow, lower in the spring months and higher in the autumn. November runoff was exceptionally variable, as in warmer years rain formed runoff rapidly, but in cooler years snow had already started to accumulate, delaying runoff until spring.

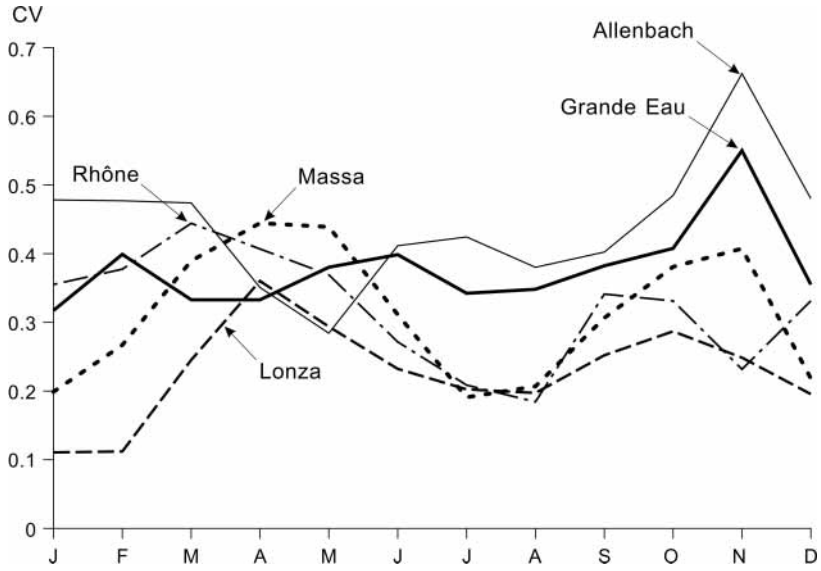


Fig. 5 Coefficients of variation (CV) of total monthly runoff for the Allenbach, Grande Eau, Lonza, Rhône and Massa rivers for the period 1956–2005.

CLIMATIC FLUCTUATION AND RUNOFF VARIABILITY

Division of the 50-year period into two equal-length sub-periods, 1956–1980 and 1981–2005, although arbitrary, allows consideration of the impact of climatic fluctuation on runoff variability. Summer 1982 was the first of many warm summers that occurred in the 1980s through 2000s. 1956–1980 was generally cool and wet, but in 1981–2005, $T_{5\text{-}9}$ at Sion was 1.13°C higher and mean precipitation at Zermatt was down by 13% (Table 2). Both mean annual runoff and year-to-year variability were lower in the (near-) ice-free basins in the second sub-period. In the glacierized basins, mean runoff increased into the warmer sub-period by between 8 and 16%, even though glacier areas had been reduced. Percentage increases in runoff above levels during the first sub-period were larger the higher the basin glacierization. Runoff variability in the warmer sub-period was lower in the Lonza but higher in both Rhône and Massa than in 1956–1980.

Table 2 Mean values (and coefficients of variation) of climate and runoff variables for the 25-year periods 1956–1980 and 1981–2005.

			1956–1980	1981–2005
Sion	$T_{5\text{-}9}$	°C	17.21	18.34
Zermatt	$P_{11\text{-}10}$	mm	740.1 (0.179)	646.0 (0.177)
Allenbach	$Q_{1\text{-}12}$	$\times 10^6$ m^3	37.96 (0.221)	37.62 (0.185)
Grande Eau	$Q_{1\text{-}12}$	$\times 10^6$ m^3	159.95 (0.223)	154.21 (0.190)
Lonza	$Q_{1\text{-}12}$	$\times 10^6$ m^3	142.15 (0.114)	154.06 (0.099)
Rhône	$Q_{1\text{-}12}$	$\times 10^6$ m^3	80.25 (0.095)	92.29 (0.125)
Massa	$Q_{1\text{-}12}$	$\times 10^6$ m^3	380.50 (0.129)	443.44 (0.142)

DISCUSSION

Throughout the 50-year period, precipitation appears generally to have been insufficient to offset ablation such that glaciers continued to lose mass and reduce in area, and precipitation declined during the warmer sub-period. By comparison with the ice-free Allenbach, minimal glacier cover had negligible impact on runoff variability in the Grande Eau. In the moderately-glacierized basins, for the 50-year period, runoff variability increased with increasing ice cover, but was lower for all three basins than for the (near-)ice-free basins, and also less than year-to-year variability of precipitation. As runoff in such moderately-glacierized basins is largely determined by energy availability, tempered to an extent by precipitation on the glacier, year-to-year variability of energy

availability must be less than that of precipitation. Coefficients of variation of summer energy availability (as positive degree days) at stations in the upper Rhône basin were 0.042 for 1935–1964 and 0.078 for 1968–1986 (Collins, 1989b).

Warm summers in the second sub-period produced exceptional annual total flows from the moderately-glacierized basins, widening the range of amounts of runoff by raising the upper margin. In basins in which the glacierized area extends to high elevation, the zone of snow and ice over which melting occurs can expand upwards in warmer summers, so increasing the area across which meltwater is produced. Expansion upwards of the melting zone and early rising of the transient snow line to high elevation contribute to enhanced runoff from such basins in warmer summers. Upward widening of the melting zone to higher elevation initially at least offsets ice area loss through glacier recession at lower elevations, a condition which can only continue until the upper limit of the glacierized area has been reached. Detailed analysis of runoff from these glacierized basins suggests that flow in both Lonza and Rhône had already started to decline before 2003, the year with the warmest summer in the 50-year period (Collins, 2005). As shown in Fig. 2, the position of a gauging station along the length of a river defines basin dimensions, and hence percentage glacierization. Percentage basin glacierization is thus an arbitrary characteristic, and, whilst continuing in widespread use as a framework for evaluation of water resources in glacierized basins (e.g. Fleming & Clarke, 2003; Kaser *et al*., 2003), it is not necessarily indicative of the hypsometry, planimetric dimensions or elevation range of the glacierized area, the characteristics which actually influence meltwater production and annual runoff from a glacierized basin.

CONCLUSION

In Alpine headwater basins of the Aare and Rhône, annual total runoff broadly increases as both basin elevation and basin glacierization increase. The month with the highest total flow is progressively delayed from May to August as basin glacierization increases. Year-to-year variability of annual runoff in ice-free and near-ice-free basins is about the same as that of annual total precipitation. In moderately-glacierized basins, runoff variability, whilst remaining considerably less than in ice-free basins, has been shown to increase as basin glacierization increases between about 38 and 66% ice-cover, influenced by year-to-year variability in thermal energy available for melting, which must be less than the variability of precipitation. In that range of ice-cover, variability of monthly total runoff is minimized in July and August, the months with the highest total discharge, and maximized in the months before and after the main ablation season. Availability of energy for producing runoff in May and September makes a considerable contribution to year-to-year variability of annual total runoff. In (near-)ice-free basins, exceptionally high monthly runoff variability occurs in November, a low flow month, in which runoff amount is influenced by whether thermal conditions lead to stable snow pack accumulation or rainfall-induced rapid runoff.

Between the 25-year sub-periods, 1956–1980 and 1981–2005, a 1.13°C rise in mean summer temperature, 13% reduction in mean total annual precipitation, and small reductions in glacierized areas, decreased runoff variability in basins with 0–40% glacierization, but resulted in increases in more highly glacierized basins. Mean annual flows from moderately-glacierized basins (40–66% glacierization) were enhanced in the second sub-period, as, in warmer summers, areas of snow and ice at higher elevations were exposed to melt. As percentage glacierization is arbitrarily defined by gauging station location, hypsometries and elevation ranges of glacierized areas may provide a more useful framework for assessing future reliability of water resources in glacierized mountain areas.

Acknowledgements The assistance of Bundesamt für Wasser und Geologie, and MeteoSchweiz, in making available discharge and meteorological records respectively, and of N. Scarle, in producing the diagrams, is gratefully acknowledged.

REFERENCES

Beniston, M. & Jungo, P. (2002) Shifts in the distributions of pressure temperature and moisture and changes in the typical weather patterns in the Alpine region in response to the behaviour of the North Atlantic Oscillation. *Theoretical and Appl. Climatol.* **71**, 29–42.

Birsan, M.-V., Molnar, P., Burlando, P. & Pfaundler, M. (2005) Stream flow trends in Switzerland. *J. Hydrol.* **314**, 312–329.

Bundesamt für Wasser und Geologie (2003) *Hydrologisches Jahrbuch der Schweiz 2002*. Bern, Switzerland.

Collins, D. N. (1989a) Hydrometeorological conditions, mass balance and runoff from Alpine glaciers. In: *Glacier Fluctuations and Climatic Change* (ed. by J. Oerlemans). Kluwer, Dordrecht, The Netherlands.

Collins, D. N. (1989b) Influence of glacierisation on the response of runoff from Alpine basins to climate variability. (Conference on Climate and Water). *Publications of the Academy of Finland* **9**/**89**(1), 319–328.

Collins, D. N. (2005) Climatic variation and runoff in mountain basins with differing proportions of glacier cover. In: *Proceedings Fifteenth Northern Research Basins Symposium*, 21–30.

Collins, D. N. & Taylor, D. P. (1990) Variability of runoff from partially-glacierised Alpine basins. In: *Hydrology in Mountainous Regions. 1 Hydrological Measurements, the Water Cycle* (ed. by H. Lang & A. Musy), 365–372. IAHS Publ. 193. IAHS Press, Wallingford, UK.

Fleming, S. W. & Clarke, G. K. C. (2003) Glacial control of water resource and related environmental responses to climatic warming: empirical analysis using historical streamflow data from north-western Canada. *Can. Water Resour. J.* **28**(1), 69–86.

Fleming, S. W. & Clarke, G. K. C. (2005) Attenuation of high-frequency interannual stream flow variability by watershed glacial cover. *J. Hydraul. Engng* **131**, 615–618.

Kaser, G., Juen, I., Georges, C., Gomez, J. & Tamayo, W. (2003) The impact of glaciers on the runoff and the reconstruction of mass balance history from hydrological data in the tropical Cordillera Blanca Peru. *J. Hydrol.* **282**, 130–144.

Krimmel, R. M. & Tangborn, W. V. (1974) South Cascade Glacier: the moderating influence of glaciers on runoff. In: *Proceedings of Western Snow Conference* 42, 9–13.

Tvede, A. M. (1982) Influence of glaciers on the variability of long runoff series. *Proceedings Fourth Northern Research Basins Symposium*, 179–189.

Walser, E. (1960) Die Abflussverhaeltnisse in der Schweiz waehrend der Jahre 1910 bis 1959. *Wasser- und Energiewirtschaft* **8/9/10**, 197–214.

Climate Variability and Change—Hydrological Impacts (Proceedings of the Fifth FRIEND World Conference held at Havana, Cuba, November 2006), IAHS Publ. 308, 2006.

An assessment of the potential impacts of climatic warming on glacier-fed river flow in the Himalaya

H. GWYN REES[1,2] **& DAVID N. COLLINS**[2]

1 *Centre for Ecology and Hydrology, Wallingford, Oxfordshire OX10 8BB, UK*
hgrees@ceh.ac.uk

2 *Alpine Glacier Project, University of Salford, Greater Manchester M5 4WT, UK*

Abstract A regional hydro-glaciological model has been developed to assess the potential impacts of climatic warming on glacier-fed river flows in the Indus and Ganges basins. The model, applied at a 20 km × 20 km grid resolution, considers glaciers contributing runoff to a cell as a single idealized glacier that is allowed to recede through time. Using 1961–1990 climate data as input, "baseline" flow estimates were derived for every stretch of river in either basin. A transient warming scenario of +0.06°C year^{-1} was then imposed for 100 years from an arbitrary start-date of 1991. Comparison of results at 10 sites in two representative areas suggest the impacts of such climatic warming are similar regionally, with estimates of future decadal mean flows continually increasing at 1–4% per decade, relative to baseline, at most sites considered. Flows peaked at only two of the sites several decades into the model run.

Key words regional hydro-glaciological model; climatic warming; river flow; Himalaya

INTRODUCTION

Mountain glaciers are considered sensitive indicators of climate change, and measurements taken over the last century reveal a "general shrinkage of mountain glaciers on a global scale" (Haeberli *et al.*, 1999). In the Himalayan region, there is particular concern about glacier recession because of the potential consequences downstream for the 500 million inhabitants of the Indus, Ganges and Brahmaputra basins, as river flows are first expected to increase but then decline. It has been said that Himalayan glaciers will vanish within 40 years, leading to drastic reductions in river flow and widespread water shortages (Pearce, 1999; WWF, 2005).

There have been few studies of the impact of climatic warming on glacier-fed river flows in the Himalaya (e.g. Singh & Kumar, 1997*a*; Singh & Bengtsson, 2005; Sharma *et al*., 2000). Most have involved the application of models in specific catchments where instantaneous step-changes in temperature were imposed for simulation periods of less than a decade, with glacier dimensions time-invariant. Climatic warming is, however, progressive and glacier volume and area change continually. The intensive data requirements of many of the models, together with their inability to consider transient conditions, preclude their application at a broad, regional-scale over longer timescales. A simple temperature-index-based hydro-glaciological model was therefore developed with a view to assessing, in a region where data measurements are sparse, how gradual changes in climate will affect glacier-fed river flows. The model, applied at a 20 km × 20 km grid-resolution, considers glaciers contributing to runoff in a cell as a single generic glacier whose dimensions are allowed to vary through time. Designed for glaciers in recession, the model generates estimates of long-term variation in river flows, as glacier thickness and area deplete.

The model was applied separately to the entire Indus and Ganges river basins, first with standard-period (1961–1990), or "baseline", climate data, and, then, with a transient climatic warming scenario of +0.06°C year^{-1} for a period of 100 years from an arbitrary start-date of 1991, with precipitation maintained at baseline levels. Estimates of future decadal mean flow were derived by routing the runoff generated in each 400 km^2 grid-cell through a digital elevation model (DEM). These were combined with similarly derived baseline flow estimates to provide estimates of future proportional changes in mean flow for every stretch of river in either basin. Results from 10 sites in two representative areas in the upper reaches of the two basins were analysed to show how the impacts of climatic warming on glacier-fed river flows might vary regionally.

THE HYDRO-GLACIOLOGICAL MODEL

The regional hydro-glaciological model developed in this study was a conceptual, physically-based semi-distributed model, in which the relevant river basin was subdivided into grid-cells at a

Copyright © 2006 IAHS Press

20 km × 20 km resolution. Runoff is calculated for each cell independently. The model comprises: a rainfall–runoff model, operating in the ice-free portion of the cell; a glacier-melt model for estimating melt from glaciers; and a snowpack module, to represent the accumulation and melting of snow.

Rainfall–runoff model

Each grid-cell was subdivided into 20 equal-height elevation bands, and the distribution of cell area between bands was allocated according to the Generalized Pareto Distribution, in which the shape and scale parameters were defined by the mean, minimum and maximum elevation of each 20-km cell, as described by the HYDRO1k DEM (USGS, 2001). The model runs at a daily time step, and requires, as input to each cell, daily values of precipitation, potential evaporation and temperature. These were derived by disaggregation of the 1961–1990 standard-period 0.5° global mean monthly climatology from Climatic Research Unit (CRU; New *et al.*, 2000). The input data were further adjusted for elevation within cells using lapse rates. Precipitation increased linearly (P_{lapse}) by 50 mm 100 m^{-1} $year^{-1}$ within a specified elevation range of 2500–5000 m ($zadj_{min}$, $zadj_{max}$) in the Indus, and by 90 mm 100 m^{-1} $year^{-1}$ from 1500–4000 m in the Ganges. Outside these ranges, precipitation remained constant. An air temperature lapse rate (T_{lapse}) of –6°C km^{-1} was applied in each band. Precipitation in a band was considered to fall as snow when the air temperature of the band ($T_{snow\text{-}rain}$) was ≤ +2°C. Daily runoff generated was aggregated at runtime to provide estimates of annual and seasonal runoff for each cell.

The rainfall–runoff calculations are based on the Probability Distribution Model (PDM) (Moore, 1985). Runoff from both rainfall and snowmelt in each band were routed through two parallel storage reservoirs, representing rapid runoff and baseflow. Daily runoff from a band was calculated as the sum of the water released from both stores each day, and cell runoff as the sum of the area-weighted runoff from all bands.

Snowpack module

Accumulation and melting of snow in an elevation band was represented in the snowpack module by a dry- and wet-store in series (Bell & Moore, 1999). New snowfall was added to the dry-store. Melt from the dry- enters the wet-store when daily air temperature for a band exceeds 0°C (T_{melt}), at a rate of 4 mm C^{-1} day^{-1}, the degree-day factor for snow (DDF_{snow}). Rain on snow contributes directly to the wet-store. Daily release from the wet-store is proportional to the water depth in the store.

Glacier-melt model

The model assumes that the meltwater contribution from a glacier can be adequately estimated by representing the glacier generically, as having an idealized shape and depth. In this study, glaciers contributing runoff to a 20-km cell (i.e. those with the terminus falling within a cell) were considered as a single "generic" glacier. The total surface area of contributing glaciers, obtained from the Digital Chart of the World (DCW) (ESRI, 1993), defines the initial surface area of the generic glacier (Fig. 1). Each generic glacier was given a simple shape and depth profile, described by 20 contiguous rectangular prisms, or "ice-bands". The horizontal elevations of the top surfaces of the ice bands were arranged at regular intervals between the minimum and maximum elevations of the generic glacier, which were determined as the minimum and maximum elevations, respectively, of all contributing glaciers. A wedge-shaped depth profile was assumed for the *thalweg* of each generic glacier, with a nominal minimum depth of 25 m set at both extremes and a maximum thickness halfway up the glacier. The maximum thickness varied according to the glacier's area, up to a maximum of 250 m (Liu & Ding, 1986). The area of each ice-band was defined according to a pre-defined shape profile that was considered typical of alpine valley glaciers.

Uniquely, the glacier-melt component allows the surface area of the generic glacier to reduce according to the prescribed geometry as the receding ice thins. The snowpack module was applied to ice-bands whenever daily precipitation fell as snow or if snow remained in a band. Ice-melt occurred in a band only when ice was exposed (i.e. when the snowpack dry- and wet-store were

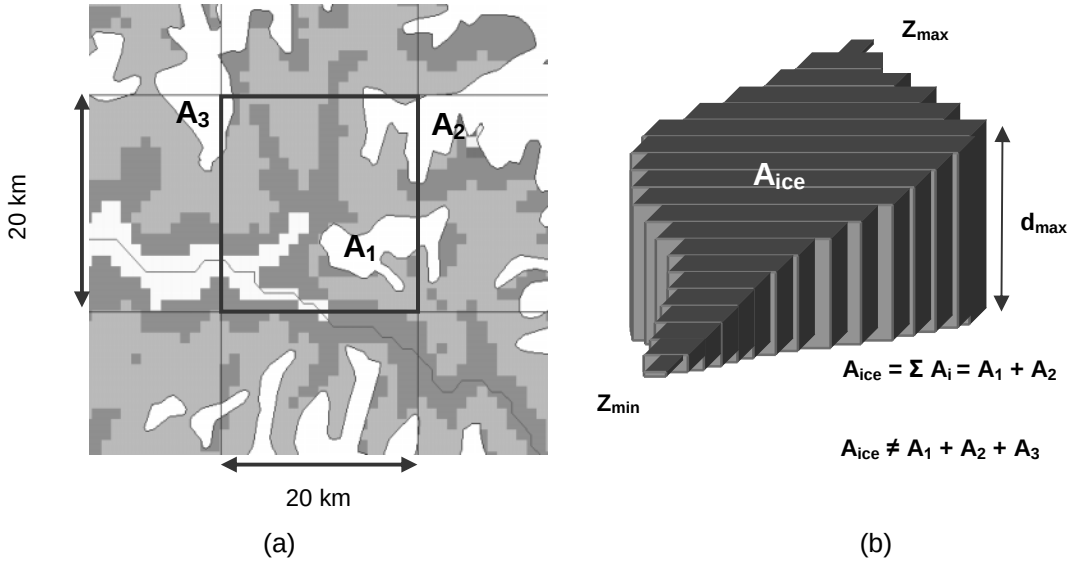


Fig.1 Defining a generic glacier: (a) identify contributing glaciers from DCW (polygons) and HYDRO1k (shaded); (b) conceptual representation of the glacier

both empty) and the air temperature at that elevation was >0°C. Ice-melt was calculated using a degree-day factor for ice (DDF_{ice}) of 12 mm °C^{-1} day^{-1}. Total discharge from the glacier was the sum of the runoff generated from all ice-bands. Once ice-depth depleted to zero the rainfall–runoff model was activated to calculate generate runoff in a band. At the end of each calendar year, accumulated snow was redistributed uniformly as ice over the remaining ice-bands.

MODEL APPLICATION

Baseline flows and model calibration

The model was applied in both basins at the daily time-step for a 10-year period using the CRU 1961–1990 climatology. The daily runoff output (mm) was aggregated at run-time to give estimates of standard-period average annual runoff for each cell. The runoff grids were then converted to river flows (m^3 s^{-1}) in GIS: the grids were first re-sampled to a 1-km resolution and overlaid onto the HYDRO1k flow-direction grid to derive a flow-accumulation grid; the accumulated average annual runoff of every 1-km cell was then converted to provide a grid of baseline mean flow in each basin.

Key model parameters were calibrated by an iterative process of comparing modelled baseline flows, derived from a variety of sensible parameter settings, with discharge measurements for 40 gauging stations in either basin (from Archer, 2003, and DHM, 1998). The aim of the calibration was not to achieve absolute accuracy for any particular catchment but simply to ensure that reasonably realistic estimates of flow were generated by the model. The final chosen parameter values, as stated in the previous section, were consistent with published data (e.g. Singh & Kumar, 1997*b*) and gave mean bias errors for modelled average annual runoff of +6% in the Upper Indus (no. 11, bias range: –47% to +93%, standard deviation: 38%) and –2% in the Upper Ganges (no. 29, bias range: –41% to +87%, standard deviation: 29%).

Climatic warming scenario

Next, the model was applied in both basins for 100 years from an arbitrary start-date of 1991 with a transient climatic warming scenario of +0.06°C year^{-1} applied, but maintaining standard period precipitation. This scenario is realistic against reported values of +0.06 to +0.12°C year^{-1} in Nepal (Shrestha *et al.*, 1999). Daily runoff outputs were aggregated at run-time to provide estimates of average decadal runoff for each 20-km cell in the respective basins. These too were converted to provide ten 1-km grids of decadal mean flow. A comparison of how flows vary from decade to decade, relative to baseline, could thus be made by overlaying the decadal flow grids onto the baseline flow grid. Resulting grids express future changes as a percentage (%) of baseline.

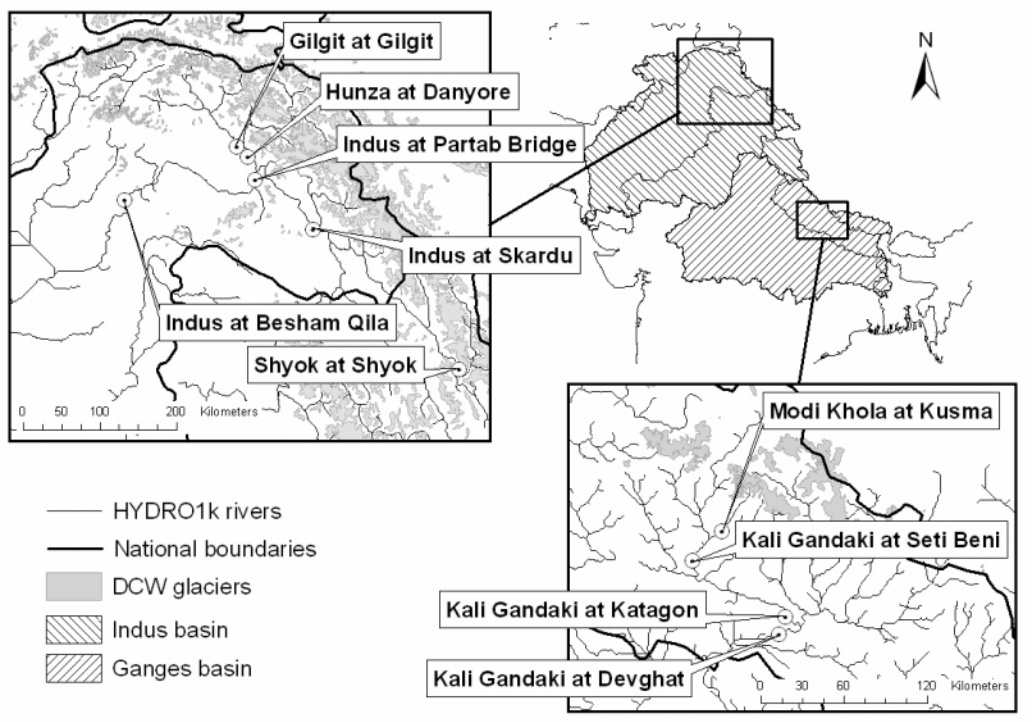


Fig. 2 Kali Gandaki and Upper Indus focal areas.

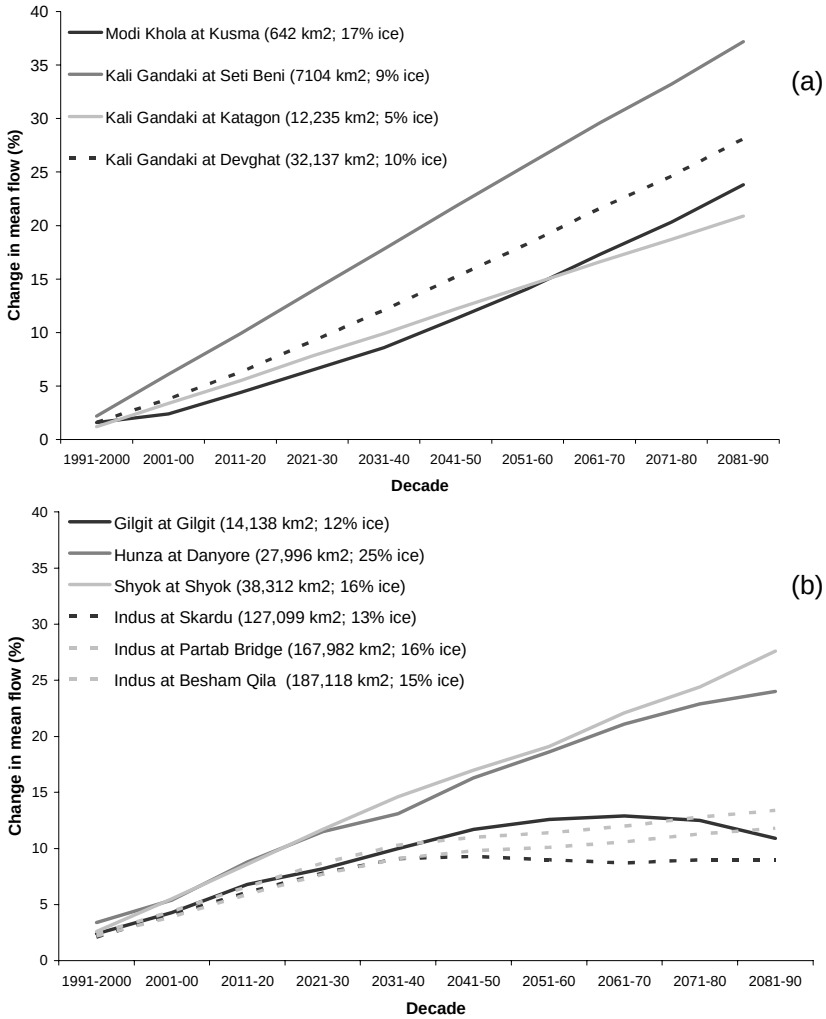


Fig. 3 Changes in decadal mean flows, relative to baseline, in the (a) Kali Gandaki and (b) Upper Indus basins.

RESULTS ANALYSIS

To assess the regional impact of glacier retreat on future river flows, changes in decadal mean flows were studied at 10 separate locations in two representative focal areas: the Upper Indus; and the Kali Gandaki River in the Upper Ganges in Nepal (Fig. 2). Under climatic warming, river flows in glacier-fed catchments are expected to show initial increases, as the area of exposed ice increases with rising temperature, followed, ultimately, by a reduction, once ice area begins to diminish. Model results from the two focal areas (Fig. 3) show decadal mean flows continually increasing at most sites at rates of around 1–4% per decade, relative to baseline, over the 100-year model run. Flows appear to peak at two of the sites in the Upper Indus only: for the Gilgit River at Gilgit, at about +13% of baseline in decade 2061–1970, and for the Indus River at Skardu, at +9.3% of baseline in decade 2041–1960. The results suggest that, under this particular warming scenario and for all but two of the selected catchments, headwater glaciers are exposed at a rate which exceeds that of ice area loss (due to recession) at their termini for the entire period, such behaviour being sustained by a sufficient volume of ice at high elevation. Different rates of flow increases reflect local variations in precipitation, the proportion of glacial ice within catchments, and the distribution of the ice with elevation. For the Indus at Skardu and the Gilgit at Gilgit, peak flows denote the moment the rate of ice loss from headwater glacier termini exceeds the rate at which ice is being exposed at higher elevations; flows reduce thereafter as ice area declines.

CONCLUSIONS

Developing an understanding of how glacier-fed rivers respond to climatic warming is difficult in the Himalaya because little is known of the hydrology and glaciology of the region and records of mountain climatic variables and runoff are sparse and short. To overcome this problem a simple temperature-index based macro-scale hydro-glaciological model was developed with parameter values consistent with the literature. Comparison between the observations and baseline model output show reasonably realistic estimates of mean flow being obtained, suggesting that the model provides an adequate basis for assessing the potential impacts of climatic warming. However, there is scope for improving the model, such as, through the use of more representative input data, better characterization of ice with elevation, and improved interpretation of glacier dynamics. Sensitivity analyses for the major parameters would also improve confidence in the forecasts, and may also have effect the timings and scales of river responses. Despite this, the results were plausible and indicated that the impacts of climatic warming on glacier-fed river flows are broadly similar across the region, with the feared widespread water shortages appearing unlikely for many decades.

Acknowledgements The study was funded by the UK Department for International Development and the Centre for Ecology and Hydrology (CEH). The authors are most grateful for the support provided by: Heather Musgrave and Alan Gustard, CEH; Adarsha Pokhrel and Arun Shrestha, Department of Hydrology and Meteorology, Kathmandu; and Rajesh Kumar and Syed Hasnain, Jawaharlal Nehru University, New Delhi.

REFERENCES

Archer, D. R. (2003) Contrasting hydrological regimes in the Indus Basin. *J. Hydrol.* **74,** 198–210.

Bell, V. A. & Moore, R. J. (1999) An elevation-dependant snowmelt model for upland Britain. *Hydrol. Processes* **13**, 1887–1903.

DHM (1998) *Hydrological records of Nepal – Streamflow Summary*. Department of Hydrology and Meteorology of Nepal, Kathmandu, Nepal.

ESRI (1993) *Digital Chart of the World for use with ARC/INFO: data dictionary*. ESRI, Redlands, California, USA.

Haeberli, W., Hoelzle, M. & Frauenfelder R. (1999) *Glacier mass balance bulletin. Bulletin no. 5 (1996–1997)*. IAHS-UNEP-UNESCO.

Liu C. & Ding L. (1986) The Newly Progress of Glacier Inventory in Tianshan Mountains. *J. Glaciol. Geocryol.* **8**(2), 168–169.

Moore, R. J. (1985) The probability-distributed principle and runoff production at point and basin scales. *Hydrol. Sci. J.* **30**, 273–297.

New, M. G., Hulme, M. & Jones, P. D. (2000) Representing twentieth-century space-time climate variability. Part II: Development of 1901–1996 monthly grids of terrestrial surface climate. *J. Climate* **13**, 2217–2238.

Pearce, F. (1999) Flooded out: retreating glaciers spell disaster for valley communities. *New Scientist* **162**(2189), 18.

Sharma, K. P., Vorosmarty, C. J. & Moore, B. (2000) Sensitivity of the Himalayan hydrology to land-use and climatic changes. *Climatic Change* **47**, 117–139.

Shrestha, A. B., Wake, C. P., Mayewski, P. A. & Dibb, J. E. (1999) Maximum temperature trends in the Himalaya and its vicinity: an analysis based on temperature records from Nepal for the period 1971–94. *J. Climate* **12**, 2775–2786.

Singh, P. & Bengtsson, L. (2005) Impact of warmer climate on melt and evaporation for the rainfed, snowfed and glacierfed basins in the Himalayan region. *J. Hydrol.* **300**, 140–154.

Singh, P. & Kumar, N. (1997*a*) Impact assessment of climate change on the hydrological response of a snow and glacier melt runoff dominated Himalayan river. *J. Hydrol.* **193**, 316–350.

Singh, P. & Kumar, N. (1997*b*) Effect of orography on precipitation in the western Himalayan region. *J. Hydrol.* **199**, 183–206.

USGS (2001) United States Geological Survey HYDRO1k Elevation Derivative Database (Asia).

WWF (2005) *An Overview of Glaciers, Glacier Retreat, and Subsequent Impacts in Nepal, India and China.* World Wildlife Fund, Nepal Program.

Climate Variability and Change—Hydrological Impacts (Proceedings of the Fifth FRIEND World Conference held at Havana, Cuba, November 2006), IAHS Publ. 308, 2006.

El glaciar 15 del Antisana: investigaciones glaciológicas y su relación con el recurso hídrico

BOLIVAR CACERES[1], BERNARD FRANCOU[2], VINCENT FAVIER[2], GUILLAUME BONTRON[2], PIERRE TACHKER[2], RODOLPHE BUCHER[2], JEAN DENIS TAUPIN[2], MATHIAS VUILLE[3], LUIS MAISINCHO[1], FANNY DELACHAUX[4], JEAN PHILIPPE CHAZARIN[4], ERIC CADIER[4] & MARCOS VILLACIS[4]

1 *INAMHI, Iñaquito, 700 y Corea, Quito, Ecuador*
bolivarc@inamhi.gov.ec

2 *IRD, CP 9214, La Paz, Bolivia*

3 *Climate System Research Center, Departament of Geosciences. University of Massachusetts, Amherst, Massachusetts, USA*

4 *IRD, Whymper 442 y Coruña , Quito, Ecuador*

Resumen Sobre el área de ablación de un glaciar del Antisana, el balance de masa ha sido medido a una escala mensual, proveyendo interesantes detalles acerca del patrón estacional que se encuentra en estos ambientes contrastados. Información no continua acerca de la recesión del hielo se la puede encontrar para las décadas anteriores. Los datos recogidos muestran una aceleración clara en el derretimiento de los glaciares desde comienzos de los ochenta:. La situación es particularmente dramática para los glaciares de pequeño tamaño (<1 km^2) los cuales podrían desaparecer en los próximos cinco años. Durante la década pasadas (noventa) las tasas de ablación fueron en promedio altas, llegando a ser más intensas durante la fase cálida de el ENSO (El Niño). Esta situación es analizada en relación con las peculiares condiciones climáticas que han prevalecido en los trópicos durante los últimos 25 años: un incremento en la temperatura sobre la mediana troposfera en alrededor de 1°C, relacionado a un largo período de incremento en la temperatura superficial del mar. Los glaciares tropicales se muestran como claros indicadores del calentamiento global y la variabilidad climática a una escala mundial y regional.

Palabras claves glaciares; balance; ablación; ENSO; clima

Glacier 15, Antisana, Ecuador: its glaciology and relations to water resources

Abstract Besides the Lewis glacier in Kenya, Glacier 15 of Antisana, Ecuador (5760–4830 m, 0.28 km^2) is the only one which provides regular information regarding glacier mass balance near to the Equator (Annual Report of the World Services for the Monitoring of Glaciers, WGMS 2005) to the scientific community. The surface of the glacier had been re-constructed using aerial-photogrammetry from 1956 to 1997. Since 1994, direct measurements have been taken over the terminal zone at the glacier tongue using topography. That process has shown the changes at the glacier limits and has determined the superficial speed at the terminal zone of the tongue (ablation zone). At the ablation zone (<5100 m) a wide net of stakes have been installed in order to measure the evolution of the glacier mass each month since 1995. In addition, holes to measure accumulation have been dug in the ablation zone at the end of the hydrological year (December–January) in order to calculate the net specific annual balance. Glacier 15 has lost an average of 600 mm of water a year since 1995 (11 years). The inter-annual variation is wide: very negative balances were observed in 1995 and 2002, two positive balances in 1999 and 2000, and negative balances for the remaining years. The dynamics of the glacier show a mass balance with very noticeable fluctuations. These variations are well synchronized with the glacier evolution. The variability of the ENSO (El Niño Southern Oscillation) has been an important factor in controlling the mass evolution of the Ecuadorian glaciers and the climate conditions. Those factors caused advances and retreats on the glaciers according to La Niña (cold event) or El Niño (warm event), respectively. This study has shown the relationship between glaciology and availability of hydrological sources.

Key words glacier; balance; abalation; ENSO; climate

INTRODUCCIÓN

El Balance de masa y las corrientes provenientes de los glaciares han tenido un monitoreo continuo desde 1995, sobre el glaciar 15 del Antisana (0°, Cordillera Oriental, Ecuador), debido a que se hace necesario tener un conocimiento sobre la disponibilidad del recurso hídrico en un futuro mediato, la ciudad de Quito que se encuentra en sus cercanías se abastece en gran medida de las aguas provenientes de los deshielos de los casquetes glaciares del Antisana y Cotopaxi.

Mediante este estudio se ha podido establecer que el área cubierta por los glaciares se ha reducido de manera apreciable en los últimos 49 años alcanzando un valor del 22% lo que afecta

Copyright © 2006 IAHS Press

de manera significativa el régimen hidrológico del río que sale del glaciar lo que afecta directamente a la disponibilidad futura de este recurso para uso del hombre (Cáceres *et al*., 2005).

METODOLOGÍA

Sobre el Glaciar 15 del Antisana se han utilizado tres métodos para realizar el estudio sobre su evolución:

(a) Restitución fotogramétrica de las fotografías existentes, las cuales corresponden a los años de 1956, 1965, 1993 y 1997 (IGM), las cuales proveen información clara sobre las fluctuaciones ocurridas en el glaciar durante los últimos 49 años (Cáceres, 2003).
(b) Medidas topográficas directas sobre el campo desde el año de 1996 sobre la zona de ablación.
(c) Una densa red de medida mediante la utilización de estacas sobre la zona de ablación (debajo de los 5100 m) la cual es visitada mensualmente, pozos de acumulación ubicados sobre esta zona (entre 5100 y 5760 m) con mediciones anuales y medidas de la cantidad de precipitación mensual mediante la utilización de pluviómetros totalizadores ubicados en la zona cercana al glaciar (Cáceres *et al*., 2005).

Para el cálculo del balance se utilizaron las siguientes relaciones:

$$B = -0.9(H_{m+1} - H_m) + 0.4(N_m - N_{m+1}) \quad (1)$$

$$B = -0.9(H_{m+1} - H_m) + 0.4(N_m + e_{m-1} - e_{m-2}) \quad (2)$$

Donde:

B = balance, equivalente en mm de agua de la cantidad de hielo/nieve perdida por el glaciar en el sitio de cada estaca.

H = emergencia de la baliza respecto a la superficie del hielo en cm.

N = espesor de la capa de nieve.

e = emergencia del extremo de la baliza respecto a la superficie superior en cm.

m = mes dado

$m \pm 1,2$ = mes anterior o posterior.

(1) ecuación para el caso de tener las medidas correctas.

(2) ecuación para el caso de tener errores sobre la medida del espesor del hielo.

RESULTADOS

Durante los últimos diez años, las longitudes de las dos lenguas en estudio han retrocedido 8 y 11 veces mas rápido que durante el período 1956–1993. El área de la cobertura de las dos lenguas se ha reducido tres veces mas rápido que durante el período 1956–1993. La longitudes y áreas se han reducido en un porcentaje de 12% y 7% respectivamente. Esta evolución se la puede relacionar con la ocurrencia de balances negativos como se evidencia en la Fig. 1.

Evolución del balance de masa sobre el Glaciar 15 del Antisana

El déficit sobre el Glaciar 15 del Antisana como promedio para estos once años de monitoreo alcanza el valor de –627 mm de equivalente agua repartidos sobre toda la superficie del glaciar (0.28 km^2) como promedio por año, ver Tabla 1 (Cáceres, 2005).

En la Fig. 2 se aprecia la relación que existe entre la ocurrencia del fenómeno ENSO el cual se lo caracterizo utilizando el índice MEI (Wolter *et.al*., 1993) y el balance de masa que se mide sobre la zona de ablación del glaciar (Cáceres, 2005). La sucesión de estos valores de balances negativos y positivos o menos deficitarios coincide con el aparecimiento de la fase cálida y fría de el ENSO.

Sobre el Glaciar 15 del Antisana se tiene una pérdida acumulada desde el año de 1995 con un valor de 35 903 mm en equivalente de agua (36 m) calculados en relación con la zona de ablación, considerando que el año hidrológico comienza en enero y termina en diciembre.

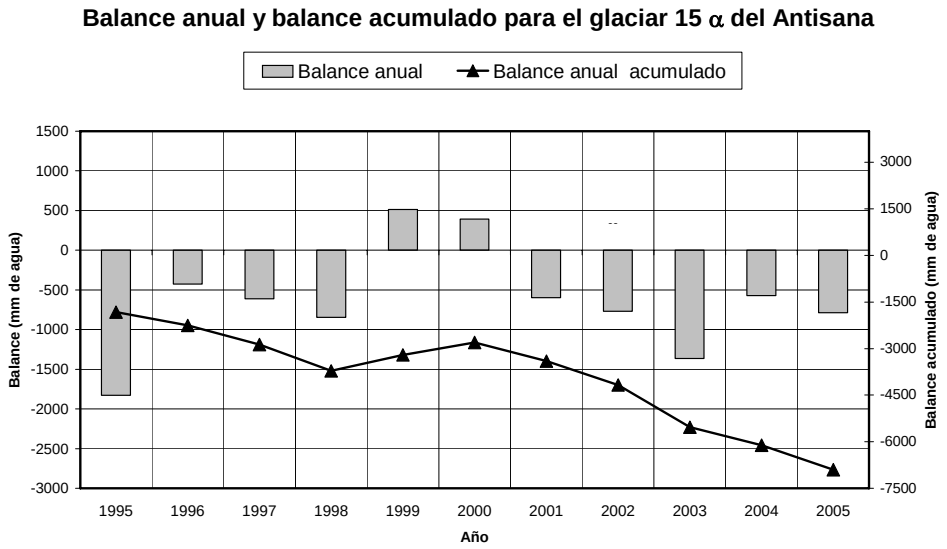


Fig. 1 Evolución del balance de masa sobre el Glaciar 15 a del Antisana.

Tabla 1 Recapitulación de los datos relacionados al balance neto específico para los once años de monitoreo del Glaciar 15 a.

Año (1)	B_n (2)	ΣB_n (3)	A (4)	B_{ter} (5)	B_{sum} (6)	ELA (7)	AAR (8)	Prec. (9)	Term. (10)	ΣTerm. (11)
1995	–1830	–1830	2580	–7624	+654	5245	45	750	–28.20	–28
1996	–428	–2258	1310	–4532	+826	5115	60	882	–40.62	–69
1997	–612	–2870	1597	–6949	+870	5110	62	985	–56.25	–125
1998	–845	–3715	1985	–6048	+675	5100	65	1140	–34.38	–159
1999	+515	–3200	700	–2214	+1080	4960	84	1215	+21.43	–138
2000	+393	–2807	632	–2045	+890	4980	80	1025	+17.80	–120
2001	–598	–3405	1348	–4830	+940	5085	60	750	–11.2	–131
2002	–769	–4174	1870	–4999	+900	5145	50	1101	–19	–150
2003	*–1362*	*–5536*	*2117*	*–6633*	*+810*	*5225*	*42*	*755*	*–55*	*–205*
2004	*–572*	*–6108*	*1352*	*–5420*	*+957*	*5145*	*56*	*780*	*–31*	*–236*
2005	*–789*	*–6897*	*1706*	*–6580*	*+878*	*5220*	*54*	*917*	*–28*	*–264*
Prom	**–627**	**–**	**1563**	**–5261**	**+862**	**5120**	**60**	**936**	**–24**	**–**

Leyenda (1) Año hidrológico (enero–diciembre), (2) Balance neto específico (mm de agua), (3) Balance neto acumulado (mm de agua), (4) Ablación específica: A = P – Bn (mm de agua), (5) Balance en la parte más baja (4833 m en mm de agua), (6) Balance en la parte más alta (5750 m en mm de agua), (7) Altitud de la línea de equilibrio (ELA), (8) Porcentaje de la área de acumulación (Accumulation Area Ratio (en %), (9) Precipitación en las cercanías del glaciar: P = [P2] (en mm de agua), (10) Retroceso del frente (en metros referidos a la marca precedente), (11) Retroceso acumulado del frente (en metros).

ANÁLISIS Y CONCLUSIONES

Los resultados mostrados confirman la dramática recesión reciente de los glaciares en los Andes tropicales y específicamente en el Ecuador. Durante la década pasada el promedio de déficit de balance para los glaciares Tropicales incluyendo el Antisana estuvo en el orden de 600 a 1400 mm equivalentes en agua de perdida por año. (Francou *et al*., 2000).

Para el Glaciar 15 del Antisana se ha observado para el período investigado de once años tres largos períodos de ablación, el primero durante el año de 1995, el segundo entre abril de 1997 y mayo de 1998 y un tercero que empieza en el 2001 y se mantiene hasta la actualidad. Entre estos dos se ubican dos períodos de ablación más moderada, uno en 1996 y otro que comienza en abril–mayo de 1998 y continuo hasta el mes de diciembre del 2001 (Cáceres, 2003). Por lo tanto se puede decir que la respuesta de los glaciares a las variaciones de temperatura al Este del Pacífico no experimenta un retraso significativo, se estableció un desfase de tres meses entre la ocurrencia de anomalías de temperatura a nivel del mar (SST) y la respuesta de los glaciares en el Ecuador, este hecho sugiere que existe una relación directa entre el fenómeno ENSO y la fusión de los glaciares ubicados sobre las cordilleras Occidental y Oriental de los Andes Ecuatorianos (Francou *et al.*, 2004).

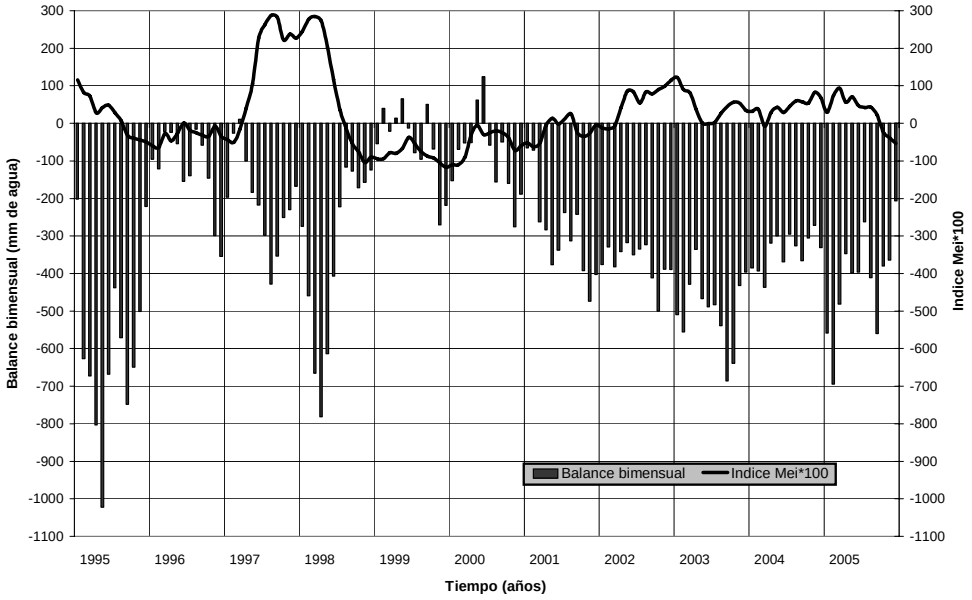


Fig. 2 Evolución bimensual del balance en la zona de ablación para el Glaciar 15 a del Antisana para el período 1995–2005 relacionada con la ocurrencia del fenómeno ENSO.

Los resultados obtenidos de la aplicación de los métodos topográficos y aero fotogramétricos son bastante consistentes con una precisión de 8 metros, los levantamientos obtenidos han sido mezclados para obtener el retroceso producido en le glaciar desde el año de 1956 (Cáceres, 2003).

Para los diez años, las lenguas alfa y beta han retrocedido de siete a ocho veces más rápido que durante el período comprendido entre 1956 y 1993, mientras que el área total del glaciar quince ha disminuido tres veces más rápido (Cáceres *et al.*, 2005).

El glaciar es un instrumento que nos permite estudiar la variabilidad del clima sobre una amplia región. Su estudio continuo contribuirá en el futuro para la elaboración de un modelo de la respuesta de los glaciares en el Ecuador frente a los cambios climáticos (Cáceres, 2003; Francou *et al*., 2004).

Para la cuenca hidrológica del glaciar Los Crespos cercano al glaciar 15 se pudo establecer que el escurrimiento proveniente de la fusión del glaciar corresponde al 26% del caudal total medido en un estación hidrológica cercana, el 74% restante corresponde al escurrimiento superficial de las precipitaciones, a los aportes de agua subterránea del acuífero y a las infiltraciones profundas que se producen bajo el lecho del glaciar, evidenciando la importancia del agua proveniente de la fusión del hielo, al momento se realizan estudios complementarios para definir de manera mas precisa estos valores y relacionarlos con la hidrología del páramo cuyo estudio recién se esta iniciando (Cáceres *et al*., 2005).

Agradecimientos Este programa de investigación se lo puede desarrollar gracias al aporte del IRD (Francia) y a la colaboración del INAMHI (Ecuador).

REFERENCIAS

Cáceres, B. (2003) Comportamiento de un Glaciar de la Cordillera Real del Ecuador en relación con los factores climáticos, cambios geométricos registrados sobre el glaciar en el período 1995–2001. Estudio realizado en el glaciar 15 Alfa (15a) del Antisana. Tesis de Grado, FIGEMPA- Universidad Central del Ecuador, Ecuador.

Cáceres, B., Maisincho, L., Taupin, J. D., Francou, B., Cadier, E., Delachaux, F., Bucher, R., Villacis, M., Paredes, D., Chazarin, J. P., Garcés, A. & Laval, R. (2005) Glaciares del Ecuador: Antisna y Carihuayrazo.Balance de masa, topografía, meteorología e hidrología. Informe IRD-INAMHI- EMAAPQ, Quito, Ecuador.

Cáceres, B. (2006) Cálculo de Balance de masa par el Glaciar 15 alfa del Antisana (en prensa).

Francou, B., Cáceres, B., Ramírez, E. & Mendoza, J. (2000) Glacier evolution in the tropical Andes during the last decades of the 20th century: Chacaltaya, Bolivia, and Antizana, Ecuador. *Ambio* **29**(7), 416–422.

Francou, B., Vuille, M., Favier, V. & Càceres, B. (2004) New evidence for an ENSO impact on low-latitude glaciers: Antizana 15, Andes of Ecuador, 0°28′S. *J. Geophys. Res.* **109**, D1806

Wolter, K. & Timlin, M. S. (1993) Monitoring ENSO in CADS with a seasonally adjusted principal component index. In: *Proc. 17th Climate Diagnostics Workshop* (Norman, Oklahoma), 52–57. NOAA/N MC/CAC, NSSL, Oklahoma Clim. Survey, CIMMS and School of Meteorology, University of Oklahoma, USA.

Climate Variability and Change—Hydrological Impacts (Proceedings of the Fifth FRIEND World Conference held at Havana, Cuba, November 2006), IAHS Publ. 308, 2006.

An historical analysis of drought in England and Wales

GWYNETH A. COLE & TERRY J. MARSH
Centre for Ecology and Hydrology, Wallingford, Oxfordshire OX10 8BB, UK
gco@ceh.ac.uk

Abstract This paper presents a chronology of drought in England and Wales from 1800 to the present day. It demonstrates how documented historical evidence of drought impact and synthetic flow series can be used to augment limited observed data and extend the period over which natural climate variability can be investigated. Rainfall deficiency analyses, seasonal partitioning of rainfall and an Aridity Index are presented to assess the relative severity of each event and examine long-term trends in drought frequency and magnitude. Over 30 important droughts were identified over the 200 year period, with a repeated tendency for dry years to cluster together to create multi-year droughts (e.g. 1798–1805, 1890–1909). Many predate observed hydrological data, leading to possible underestimation of drought risk. No compelling trends of increasing drought frequency or magnitude were found, although winter and summer rainfall showed marked spatial and temporal differences across England.

Key words drought; drought impact; historical analyses; BHS *Chronology*; deficiency; water resources; England and Wales

INTRODUCTION

A series of recent droughts in England and Wales has highlighted the UK's continuing vulnerability to this natural hazard and raises once again the issue of whether these events reflect climate change or natural climate variability. It is therefore vital that recent events are not viewed in isolation, but in the context of as long an historical record as possible. Droughts are multifaceted both in their meteorological character and range of impacts and there are many difficulties in quantifying a phenomenon which varies widely in its areal extent, duration and intensity (Tallaksen & van Lanen, 2004). This paper combines evidence from many sources, including the different, if overlapping, impacts associated with: meteorological drought – deficiency in rainfall; hydrological drought – accumulated deficiencies in runoff and aquifer recharge; and socio-economic drought – where the focus is on human impacts.

DATA SOURCES

In a global context the UK has a rich legacy of lengthy hydrometeorological records. However, raingauge coverage was poor prior to the 1850s and few river and groundwater level records exceed 100 years in length (Lees, 1987). In this historical review, observed hydrological data from the UK National River Flow Archive at CEH Wallingford, was augmented by extended synthetic runoff series, derived by the Climatic Research Unit (Jones *et al.*, 2003) from long-term rainfall and temperature series, and documentary evidence of drought impact. Observed data included long-term monthly catchment rainfall, river flow and groundwater level time series (from the British Geological Survey) and Chalk spring flows dating back to 1841 (Bayliss *et al.*, 2004). Documentary evidence of impact was obtained from the British Hydrological Society (BHS) *Chronology of British Hydrological Events* (http://www.dundee.ac.uk/geography/cbhe) and published drought review papers. The *Chronology*, launched in 1999, is an exceptionally valuable compilation of historical material (mostly pre-1935) drawn from wide-ranging sources. Although the extracts are often anecdotal and local in nature, they provide useful support when observed or synthetic data is limited.

IDENTIFYING DROUGHTS

Relatively simple indices based upon accumulated departures of monthly rainfall or runoff totals (e.g. Bryant *et al.*, 1994) have been shown to be useful in identifying drought events. This study used ranked rainfall and runoff deficiencies (departures from the long-term average) over a range of time scales as a primary identification tool (see Table 1). Short (4–6 month) intense rainfall deficiencies can threaten water supplies in areas dependent on surface water (e.g. northern England

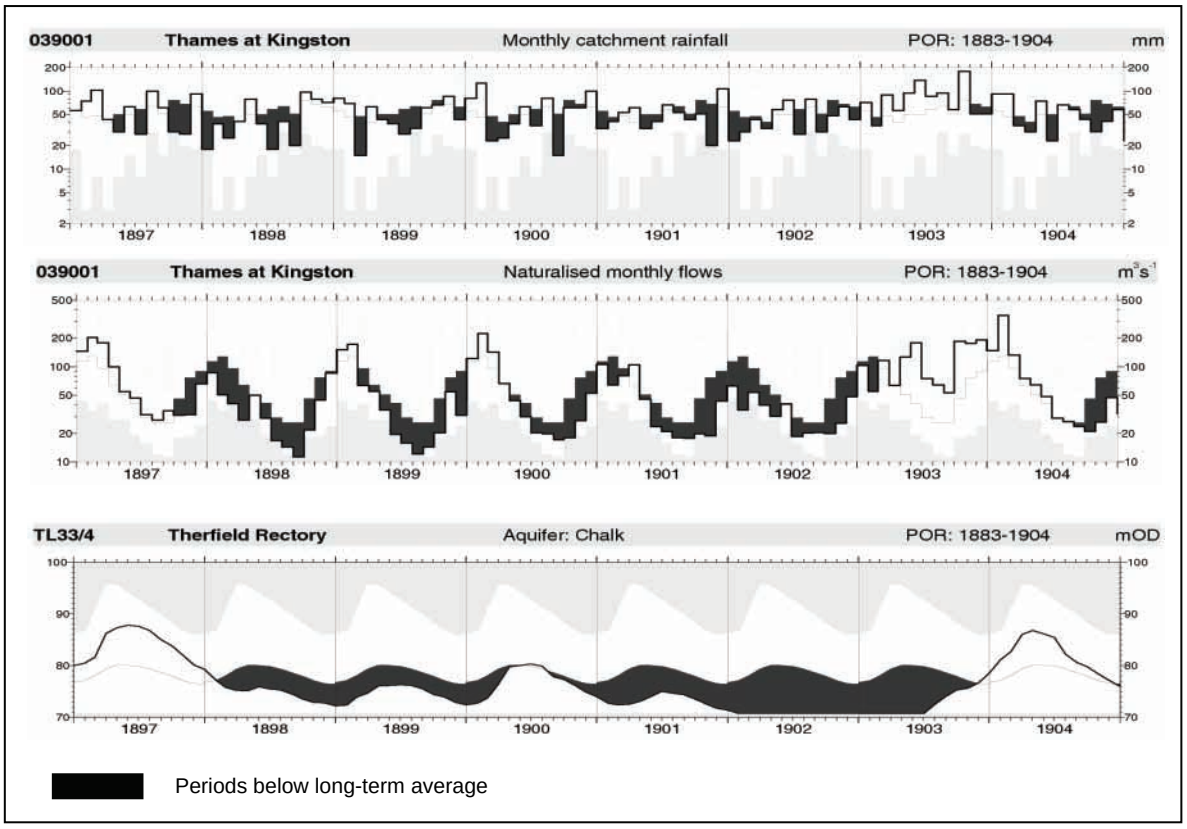
Copyright © 2006 IAHS Press

in 1984 and 1995), while for groundwater catchments, deficiencies over 18 months or longer pose the greatest threat (Marsh & Turton, 1996). Droughts identified as important at a national scale may not impact at the catchment scale if the most intense phase does not correspond to the critical period for water resources provision (Table 1). These indices were supported by visual appraisal of long hydrological time series – plotted with periods of rainfall or runoff deficiency highlighted.

Table 1 Ranked *n*-month rainfall deficiencies and runoff deficiencies to identify droughts[a].

Rank	Max. 6-month rainfall deficiencies for England & Wales	Max. 24-month rainfall deficiencies for England & Wales	Max. 6-month runoff deficiencies[b] – River Eden (surface water catchment)	Max. 18-month runoff deficiencies[b] – Great Ouse (groundwater catchment)
1	1921	1855	Sep 1995	Nov 1803
2	1976	1997	Sep 1826	Nov 1934
3	1995	1934	Sep 1984	Oct 1922
4	1887	1803	Oct 1989	Nov 1991
5	1929	1992	Sep 1996	Nov 1815
6	1870	1922	Oct 1919	Oct 1944
7	1990	1845	Sep 1806	Oct 1997
8	1854	1889	Nov 1915	Oct 1894
9	1826	1976	Sep 1870	Nov 1973
10	1938	1807	Oct 1887	Nov 1902

[a] The years and months featured relate to the end of each deficiency period.
[b] Based on synthetic naturalized flow series (from CRU) 1801–2002.



Extracts from the BHS *Chronology*

1902 Hascombe, Guildford: "All the wells in the neighbourhood were lower than in living memory and many were dry due to the succession of years of deficient rain."

1902 December Abingdon: "springs were exceptionally low at the end, and the outlook was serious."

Fig. 1 Example of data and information sources for the Thames Basin 1897–1904, an intense phase in the 1890–1910 drought: monthly catchment rainfall and naturalized monthly flows for the Thames at Kingston; groundwater levels for the Chalk aquifer at Therfield Rectory; extracts from the BHS *Chronology*.

Figure 1 presents an example of data and information sources which helped to characterize an intense phase of the 1890–1909 drought. The long-term Central England Temperature (CET) series proved useful for confirming documented assertions of outstandingly high temperatures.

MAJOR DROUGHTS IN ENGLAND AND WALES

Data from all sources was combined to identify drought episodes in England and Wales from 1800 to the present day. Major droughts are listed in Table 2 and other notable events in Table 3; some hydrological judgement was required particularly for event magnitudes close to the notable/major threshold. Nonetheless, it is considered a strength of this study that the classification combines a range of data and information sources, rather than relying on a single index to characterize each drought. As Tables 2 and 3 demonstrate, drought is a recurring feature of the UK climate, with 10 major and more than 20 notable droughts identified over the 200 year period. Of particular note is the repeated clustering of successive dry years in the late nineteenth century, which in an extreme case (1890–1909) was maintained for almost two decades, despite some very wet interludes. Many of these events have been identified by other authors (Jones *et al*., 1997; Jones & Lister, 1998), using different selection criteria.

Table 2 Major droughts in England and Wales

Year	Duration	Comments
1995–97	Spring 95 – Summer 97	Major drought. Third lowest 18-month rainfall total for England and Wales (1800–2002). Long duration drought with intense episodes (e.g. affecting eastern Britain in hot summer of 1995). Initial surface water stress, then very depressed groundwater levels and much diminished lowland stream network.
1990–92	Spring 90 – Summer 92	Major drought. Widespread and protracted rainfall deficiencies – reflected in exceptionally low groundwater levels (in summer 1992, overall groundwater resources for England and Wales probably at their lowest for at least 90 years). Intense phase in the summer of 1990 in southern and eastern England. Exceptionally low winter flows in 1991/92.
1976	May 75 – Aug 76	Major drought. Lowest 16-month rainfall in E&W series (from 1766). Extreme in summer 1976. Benchmark drought across much of England and Wales – particularly the lowlands; lowest flows on record for the majority of British rivers. Severe impact on surface water and groundwater resources.
1959	Feb–Nov	Major drought. Intense 3 season drought – most severe in eastern, central and north eastern England. Significant spatial variation in intensity. Modest groundwater impact.
1933/34	Autumn 32 – Autumn 34	Major drought. Intense across southern Britain. Severe surface water impacts in 1933 followed by severe groundwater impacts in 1934, when southern England heavily stressed (less severe in the more northerly, less responsive, Chalk outcrops).
1921–22	Autumn 1920 – Early 1922	Major drought. Second lowest 6-month and third lowest 12-month rainfall totals for E&W. Very severe across much of England and Wales (including Anglia and South East; parts of Kent reported <50% rainfall for the year); episodic in North West England.
1890–1909	Long drought	Major drought. Long duration (with some very wet interludes). Initiated by an extremely dry autumn and winter (driest Sept–April period on record). Exceptional cluster of relatively dry winters. Major and sustained groundwater impact, with significant water supply problems. Most severe phases: 1893, 1899, 1902, 1905. Merits separate investigation.
1887/88	Late winter 87 – Summer 88	Major drought. High ranking rainfall deficiencies across a range of timeframes. Very widespread (across most of British Isles). Extremely dry 5-month sequence in 1887. Primarily a surface water drought – severe in western Britain (including North West).
1854–1860	Long drought	Major long duration drought. Sequence of dry winters in both the lowlands (seven in succession at Oxford) and northern England. Major and sustained groundwater impact.
1798–1808	Long drought	Major long duration drought. Three separate (non-overlapping) periods feature among the dozen lowest 18-month rainfall totals for England and Wales. Limited direct hydrological evidence, further investigation required.

Table 3 Other notable droughts in nineteenth and twentieth centuries.

1800–1900	1814–15; 1826–7; 1844–45; 1863–5; 1867–8; 1869–71; 1873–5; 1884–5
1900–2000	1911; 1913; 1914–15; 1919; 1929; 1937–38; 1941; 1943–44; 1947-49; 1955–56; 1962–65; 1972–73; 1988–89

TRENDS IN DROUGHT FREQUENCY AND MAGNITUDE

The study also investigated if there had been any discernible change in drought frequency and magnitude over the last 200 years. An Aridity Index (Marsh, 2004) was used to compare summer drought severity. As the equation below shows, this combines rainfall anomalies (homogenized England and Wales Series from 1767) and temperature anomalies (Central England Temperature Series) for the summer half-year, April to September, standardized by their respective standard deviations. The *Av*. represents the full record average of rainfall and temperature respectively:

$$\textit{Aridity Index} = (\textit{Rainfall} - \textit{Av. Rainfall})/\textit{SD rainfall} + 0.5(\textit{Temp} - \textit{Av. Temp})/\textit{SD Temp}$$

As Fig. 2 demonstrates, the Aridity Index identifies the most familiar recent summer droughts (e.g. 1995, 1976 and 1959), but has less utility in identifying winter droughts or sustained periods of rainfall deficiency. Figure 2 shows a greater frequency of notably arid summer half-years in the recent past. This primarily reflects the exceptionally high summer temperatures over the last 30 years (Fig. 3), although the relatively low May–October rainfall over this period may also be influential (see Fig. 5).

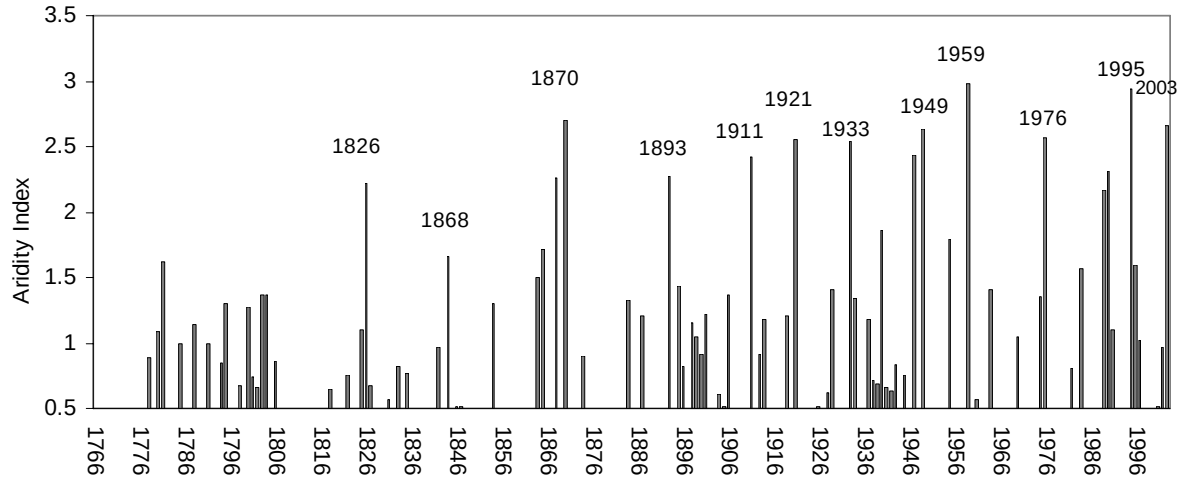


Fig. 2 Aridity Index for England and Wales (1776–2003).

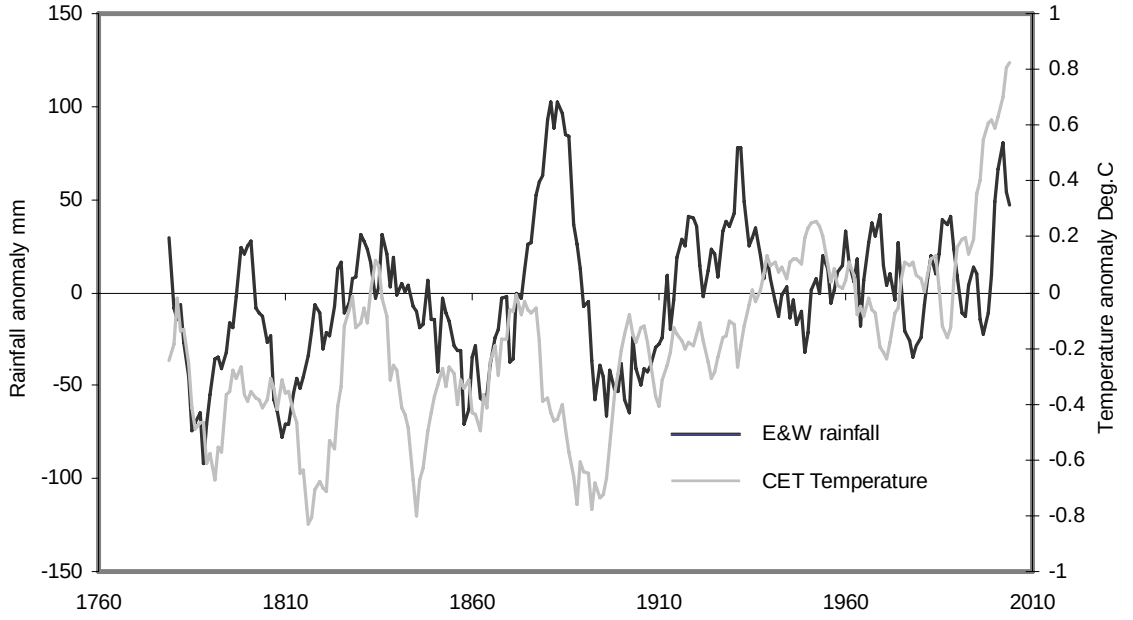


Fig. 3 Annual temperature (CET) and E &W rainfall anomalies (10-year moving average).

Figure 4 examines long-term 12-month rainfall deficiencies (based on any start month) for England and Wales. Exceptional rainfall events are distributed throughout the series. This is consistent with recent research (Hannaford & Marsh, 2006) which found no compelling trend in low flows in 45 natural benchmark catchments across the UK since 1963.

For water resources, the seasonal distribution of rainfall is particularly important, with the winter months critical for aquifer and reservoir recharge. Figure 5 compares long-term trends in summer (May–October) and winter (November–April) rainfall for the England and Wales rainfall series and five other rainfall series spatially distributed across England. These display substantial spatial and temporal variability in the seasonal distribution of rainfall. In high rainfall areas dominated by orographic influences, e.g. Central Lake District, the winter/summer partitioning of rainfall has remained relatively stable over time with winter rainfall consistently exceeding summer. The other four sites have low rainfall, more characteristic of lowland areas. Despite significant multi-year variability, these show a different seasonal distribution of rainfall in the nineteenth and twentieth centuries. In the nineteenth century, summer rainfall generally exceeded winter, while in the twentieth century the decline in summer rainfall has resulted in rainfall being roughly equal in the two seasons. Clusters of successive dry winters (and summers) are common throughout the record, often sustained for many years.

WATER RESOURCE IMPLICATIONS

The documentary and hydrometric evidence demonstrates that vulnerability to drought is not static, but changes with time. In the nineteenth century severe droughts often constituted a very real threat to lives and livelihoods; communities relied on a single or group of local sources for water and therefore had little scope for managing drought. Nowadays, we have complex and flexible multi-source supply systems and statutory drought plans. However, public and political perceptions of drought still tend to focus on intense summer droughts, such as 1976, 1995 and 2003. The 2003 drought, which extended across most of Europe, combined exceptional rainfall deficits with record-breaking high temperatures, with many severe and long-lasting impacts (UNEP, 2003). Unlike many European countries, the UK experienced no major restrictions on water use (Marsh, 2004), demonstrating the resilience of its water supply systems to short, intense droughts. However, the UK may be less resilient to a succession of dry winters, which, as the historical analysis and Fig. 6 show, have been relatively rare in the recent past (apart from 2005/06), but were substantially more common in the late nineteenth century. The 2005/06 drought in southern England is notable for the disproportionate contribution of the winter months to the overall rainfall deficiency.

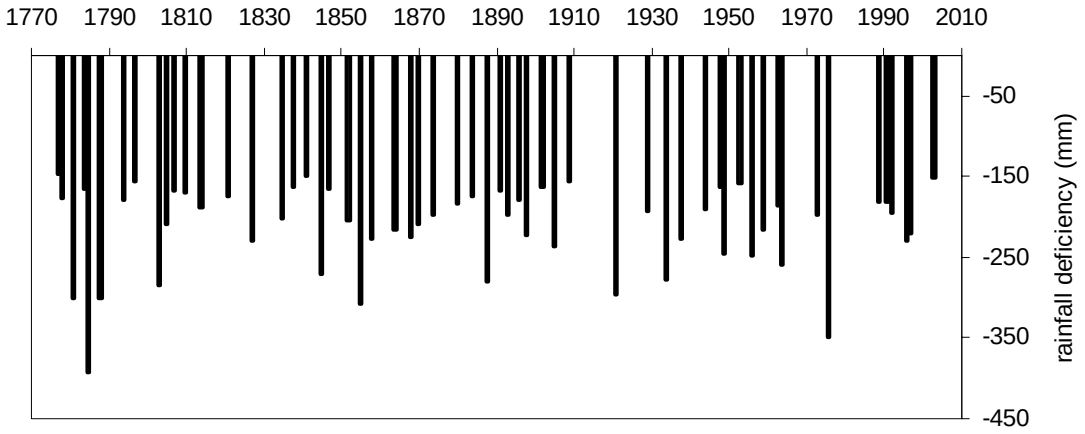


Fig. 4 Maximum non-overlapping 12-month rainfall deficiencies for England and Wales.

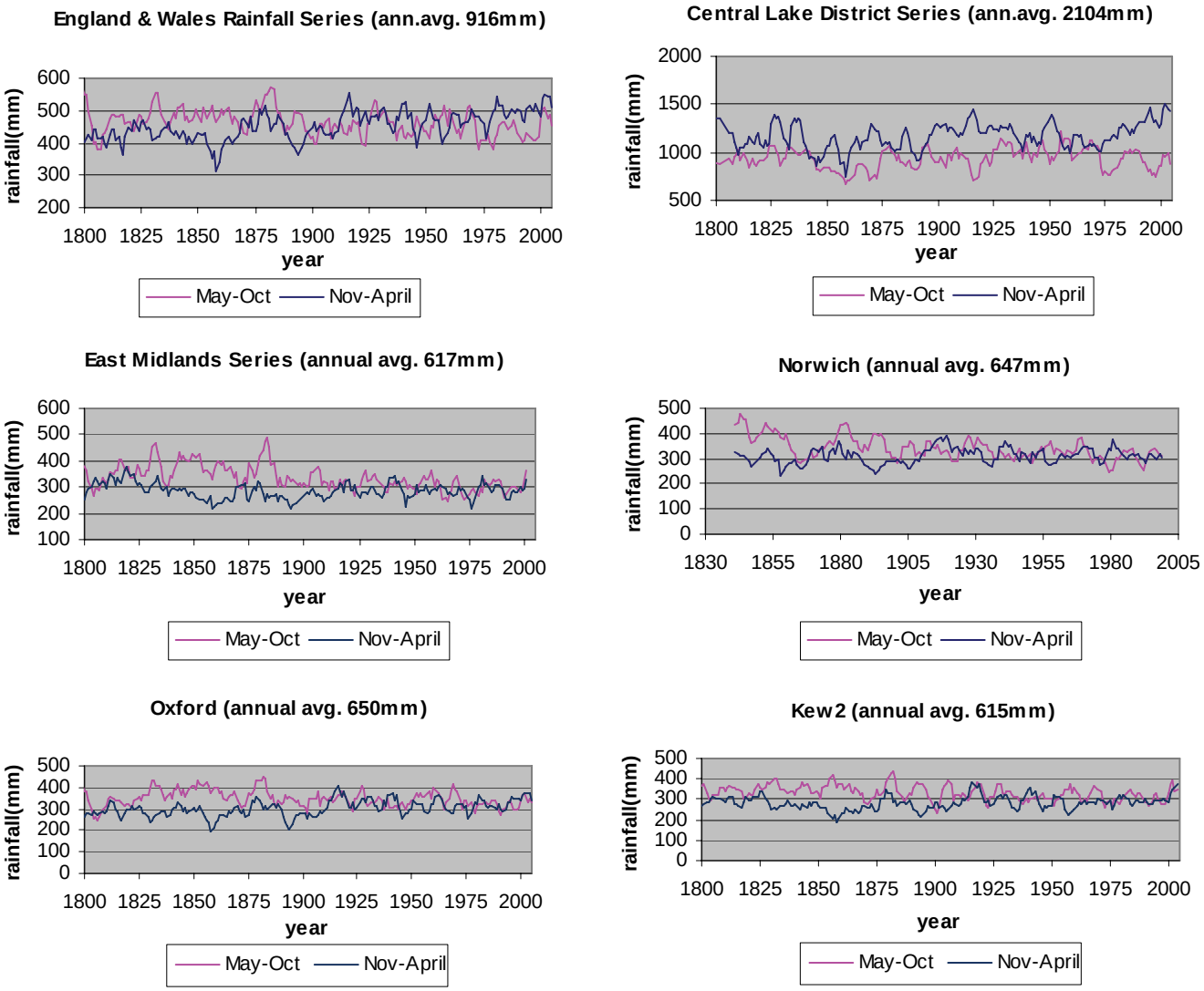


Fig. 5 Long-term summer and winter rainfall for the England and Wales rainfall series, and five raingauges distributed across England.

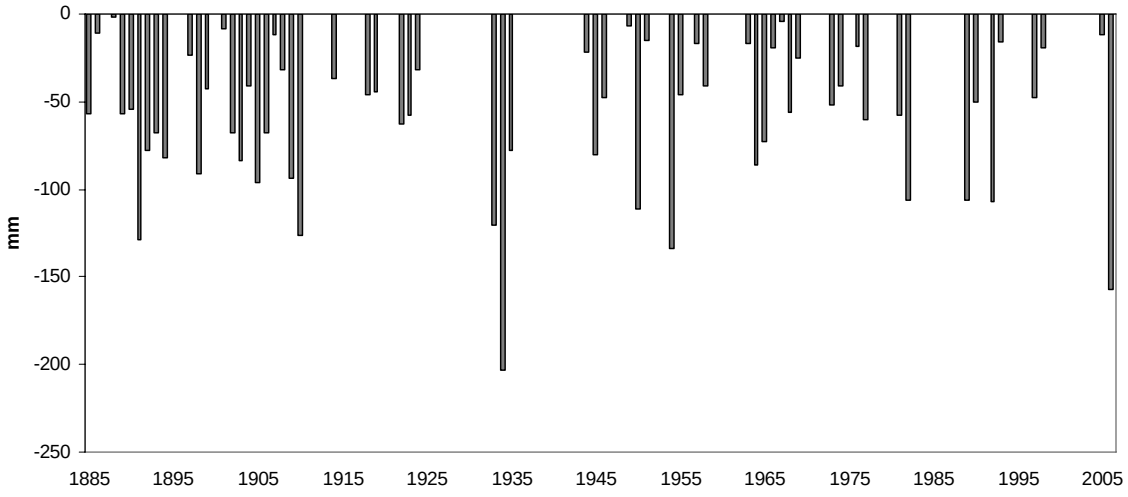


Fig. 6 Two-year November–January rainfall deficiencies in the Thames basin, 1885–2006.

Whilst most climate change scenarios indicate an increasing frequency of wet winters for the UK in a warmer world, the evidence presented here underlines the need for a fuller understanding of the mechanisms contributing to the substantial historical variability in rainfall patterns. A repeat of the protracted sequences of dry winters documented in Table 2 would represent a severe challenge to water management in the UK.

Acknowledgement This work was mainly funded by the UK Environment Agency, as part of a wider study of the impacts of climate change on severe droughts.

REFERENCES

Bayliss, A., Norris, J. & Marsh, T. (2004) The Wendover Springs record: an insight into the past and a benchmark for the future. *Weather* **59**(10), 267–271.

Bryant, S. J., Arnell, N. W. & Law, F. M. (1994) The 1988–92 Drought in its historical perspective. *J.IWEM* **8**(February 1994), 39–51.

Hannaford, J. & Marsh, T. (2006) An assessment of trends in UK runoff and low flows using a network of undisturbed catchments. *Int. J. Climatol*. **26**, 1237–1253.

Jones, P. D., Lister, D. H. & Kostopolou, E. (2003) Reconstructed river flow series from 1860s to present. *CRU, Environment Agency Science Research Report SC03/02*, 1–70.

Jones, P. D. & Lister, D. H. (1998) Riverflow reconstructions for 15 catchments over England and Wales and an assessment of hydrologic drought since 1865. *Int. J. Climatol.* **18**, 999–1013.

Jones, P., Conway, D. & Briffa, K. (1997) Precipitation variability and drought. In: *Climates of the British Isles: Present, Past and Future* (ed. by M. Hulme & E. Barrow), 197–219. Routledge, London, UK.

Lees, M. L (1987) Inland water surveying in the UK – a short history. In: *1985 Year Book: Hydrological Data UK*. Institute of Hydrology, Wallingford, UK.

Marsh, T. J. (2004) *The UK Drought of 2003 – An Overview*. Centre for Ecology and Hydrology, Wallingford, UK (extended version in *Weather* **59**(8), August 2004).

Marsh, T. J. & Turton, P. (1996) The 1995 drought – a water resources perspective. *Weather* **51**, 46–53.

Tallaksen, L. M. & van Lanen, H. A. J. (eds) (2004) *Hydrological Drought: Processes and Estimation Methods for Streamflow and Groundwater*. Elsevier, The Netherlands. ISBN 0-444-51688-3.

UNEP (2003). Impacts of summer 2003 heatwave in Europe. DEWA/Europe/GRID-Geneva http://www.grid.unep.ch/activities/earlywarning/preview/appl/climatic/images/heatwave_en.pdf.

The effect of record length on the analysis of river flow trends in Wales and central England

HARRY DIXON[1], DAMIAN M. LAWLER[1], ASAAD Y. SHAMSELDIN[2] & PAUL WEBSTER[3]

1 *School of Geography, Earth and Environmental Sciences, University of Birmingham, Edgbaston, Birmingham B15 2TT, UK*

hxd892@bham.ac.uk

2 *Department of Civil and Environmental Engineering, The University of Auckland, PB 92019, Auckland, New Zealand*

3 *Hydro-Logic Ltd, Old Grammar School, Church Street, Bromyard, Herefordshire HR7 4DP, UK*

Abstract The detection of trends in hydrological variables is directly affected by the length of time series available for analysis and is of key importance to the global FRIEND community. Long-term (≤50 years) seasonal gauging station records from Wales and the English Midlands are analysed for different time spans up to 2001 to demonstrate the effect of record length on linear trend analysis. Non-parametric Mann-Kendall trend methods are applied to time series of different flow quantiles, and for different seasons, thereby assessing trends across the streamflow spectrum. Key differences are quantified between trends of varying record lengths, but the dominant trend is for streamflow increases at high and low flows over time periods greater than 30 years. The implications for the FRIEND community are widespread and support the need to maintain gauging station networks and maximise instrumental records.

Key words high flows; hydrological data; Mann-Kendall; record length; seasonal river flow; streamflow; trend analysis; central England; Wales

INTRODUCTION

Defining temporal change in river discharge is a fundamental part of establishing hydrological variability, and crucially important for identifying climate–streamflow linkages, water resource planning, flood and drought management and for assessing geomorphological and hydro-ecological responses. Consequently, numerous studies of river flow time series have been carried out (e.g. Hisdal *et al.*, 2001; Burn & Hag Elnur, 2002; Robson, 2002; Lindstrom & Bergstrom, 2004), many using linear trend analysis (e.g. Lins & Slack, 1999; Zhang *et al.*, 2001).

Clearly, establishing the robustness of trend detection methods is vital to a sound definition of recent hydrological change. Ideally, long-term instrumental records are needed for secure establishment of trend, but few investigations have attempted to quantify the impact of different record lengths on hydrological trends. An exception is Hisdal *et al.*'s (2001) study of streamflow droughts across Europe that found substantial influences of study period on trend statistics. This paper, therefore, aims to highlight the effects of record length on river flow trends by analysing instrumental data at different decadal timescales drawn from Wales and central England, UK, over 35% of which are common to the FRIEND database. The paper focuses on seasonal breakdown analyses of the full discharge spectrum, from low to high flows. This is in contrast to many previous studies which tend to consider either floods or droughts for single sites or basins (but cf. Lins & Slack, 1999; Birsan *et al.*, 2005).

The work is part of a more comprehensive project on defining and explaining recent hydrological changes at larger spatial scales over the instrumental period in southern UK (Dixon *et al.*, 2005). The quantified impacts of record length on trend definitions will have significant implications for the analysis of spatial and temporal variability in hydrological systems which form the focus of much FRIEND community research.

STUDY AREA

This paper focuses upon the hydrologically dynamic, temperate Atlantic fringe of Wales and central England. For the purpose of this paper the area defined as Wales and the English Midlands covers a combined land area of around 46 800 km^2 of cool temperate basins at a range of scales (18–7500 km^2). The mountainous areas of Wales (maximum altitude 1085 m) and agricultural plains of the English Midlands fall within the study area. Urban coverage varies greatly and includes a number of major population centres, including Birmingham and Cardiff.

Copyright © 2006 IAHS Press

DATA SOURCES

Daily mean streamflow (DMF) records were selected for gauging stations from the National River Flow Archive (NRFA) at the Centre for Ecology and Hydrology (Wallingford) (http://www.nwl.ac.uk/ih/nrfa/). In most cases streamflow time series provided at Daily Mean (DMF) resolution were calculated from 15-minute recordings taken using a variety of gauging structures. A minimum record length of 25 years of continuous data was set, and where possible gauging stations were chosen that were free from large-scale local flow retention, notable gauging errors and changes in station location or gauging structure over the record length. The number of records included varies with the time series length under consideration, in that 56 stations were available for a 25 year period and eight stations for ≥50 years of record.

ANALYTICAL METHODS

Streamflow variables

As this paper is concerned with trends across the cumulative streamflow distributions, DMF records were used to calculate time series of flow quantiles at a seasonal resolution. The four standard UK Metl Office (http://www.met-office.gov.uk/) seasons were used: Dec/Jan/Feb; Mar/Apr/May; Jun/Jul/Aug; and Sep/Oct/Nov. This paper will mainly present regional trend patterns for the winter (Dec–Feb) streamflow spectrum.

The seasonal x-quantile $Q_x(i)$ of streamflow (q) was obtained for each year (i) as the value at which $\Pr(q \leq Q) = x$ (e.g. Birsan *et al.*, 2005). Trend tests were applied to time series of $Q_x(i)$, where $i = 1, \ldots, t$ years. In order to investigate the full discharge spectrum, trends were analysed for 11 quantiles of the streamflow distribution, from the minimum (Q_{Min}) to the maximum (Q_{Max}) (e.g. Lins & Slack, 1999). The following quantiles of flow (as opposed to exceedence probabilities) were calculated: 10th ($Q_{0.1}$) low flow, 20th ($Q_{0.2}$), 30th ($Q_{0.3}$), 40th ($Q_{0.4}$), 50th ($Q_{0.5}$), 60th ($Q_{0.6}$), 70th ($Q_{0.7}$), 80th ($Q_{0.8}$) and 90th ($Q_{0.9}$) high flow percentiles. Trends in the mean streamflow (Q_{Mean}) over each relevant period were also calculated.

Record length

There are a number of problems associated with the analysis of trends in relatively short time series. Analysis was conducted for four time spans: t = 25 years (1977–2001) for 56 stations; t = 30 years (1972–2001) for 44 stations; t = 40 years (1962–2001) for 24 stations; and t = 50 years (1952–2001) for eight stations.

Trend analysis

Monotonic trends were analysed using the nonparametric Mann-Kendall test (Helsel & Hirsch, 1992) for each of the quantiles of the cumulative streamflow distribution (e.g. Lins & Slack, 1999). The test examines a given time series for linear increases or decreases with time rather than detecting episodic or abrupt events. The method is a rank based test and particularly useful for hydrological data sets as it is robust against outliers (see Kundzewicz & Robson, 2004). Being distribution-free, it is suited to the analysis of streamflow time series which tend to be non-normally distributed (e.g. Lettenmaier *et al.*, 1994; Zhang *et al.*, 2001; Birsan *et al.*, 2005).

Because trends are calculated for time series with yearly intervals, it is assumed that the impacts of serial correlation are likely to be low (Lins & Slack, 1999). Birsan *et al.* (2005) for example, found low serial correlation coefficients in similar data sets and concluded that the potentially more conservative method of pre-whitening time series that displayed autocorrelation had little overall difference in such cases.

Test statistic significance levels were determined using the flexible and robust method of bootstrap resampling, which makes relatively few assumptions about the independence and distribution of the data set (e.g. Kundzewicz & Robson, 2004). One thousand resamples were conducted for each test using the more flexible bootstrap (with replacement) method. This paper focuses on the trend results found to be significant at or above the 10% level ($\alpha \leq 0.1$, two-tailed test).

The magnitude of trend (as change per year) has been calculated by applying Sen's (1968) nonparametric method to hydrological time series (e.g. Lettenmaier *et al.*, 1994; Burn & Hag Elnur, 2002; Kahya & Kalayci, 2004). In order to highlight any underlying longer-term variability in relation to different linear trends, example time series have been smoothed using the relatively robust locally-weighted regression smoothing method, LOESS (e.g. Robson, 2002).

RESULTS

Regional pattern

Figure 1 summarizes the effect of record length on statistically significant linear trends for all quantiles. It is important to note the different number of stations (n) available for analysis at the four different time periods. Figure 1 shows that, across all time periods and quantiles, the percentages of river flow records displaying statistically significant trends varies between 0 and 50%. Most significant changes are found at high and low flows. However, the impact of record length on trend patterns is immediately apparent. For example, the mixture of positive and negative trends present over the 25-year period (t = 25) is not found over the longer term. Winter maximum streamflow over the last 25 years (n = 56) show significant rising trends in 25% of time series and falling trends in around 18% (Fig. 1(a)). This streamflow decline, which represents 10 station records, is not found at $t \geq 30$ years. It is important to note that insufficient record lengths are not the cause of this isolated negative pattern as 9 out of the 10 stations in question are common to at least the t = 25 and t = 30 year analysis periods. At longer record lengths, the main pattern is an increasing trend for high and low flows.

The trend results of Fig. 1 are shown geographically in Fig. 2 for Q_{Max} flows, to allow identification of regional patterns. Analysis of the recent 25-year period (Fig. 2(a)) suggests a pattern of rising winter high flows in a band covering northern, central and southeast Wales, but falling high flows in lowland catchments to the east of the region. Although parts of the band of stations which display rising trends are still evident at $t \geq 30$ years, the pattern is patchy and many more stations display stationarity (Fig. 2(b) and (c)). The declining Q_{Max} flows in the Upper Trent

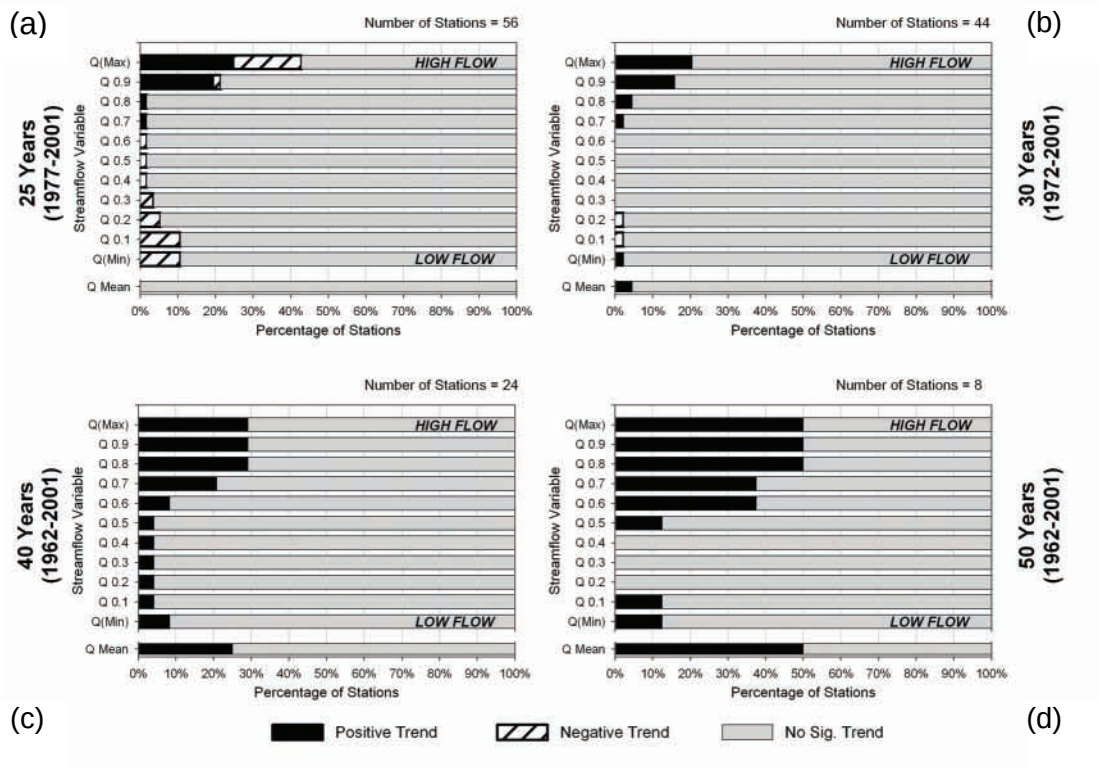


Fig. 1 Linear trends in winter (DJF) streamflow (significant at $\alpha \leq 0.1$) analysed for; (a) t = 25 years; (b) t = 30 years; (c) t = 40 years; (d) t = 50 years.

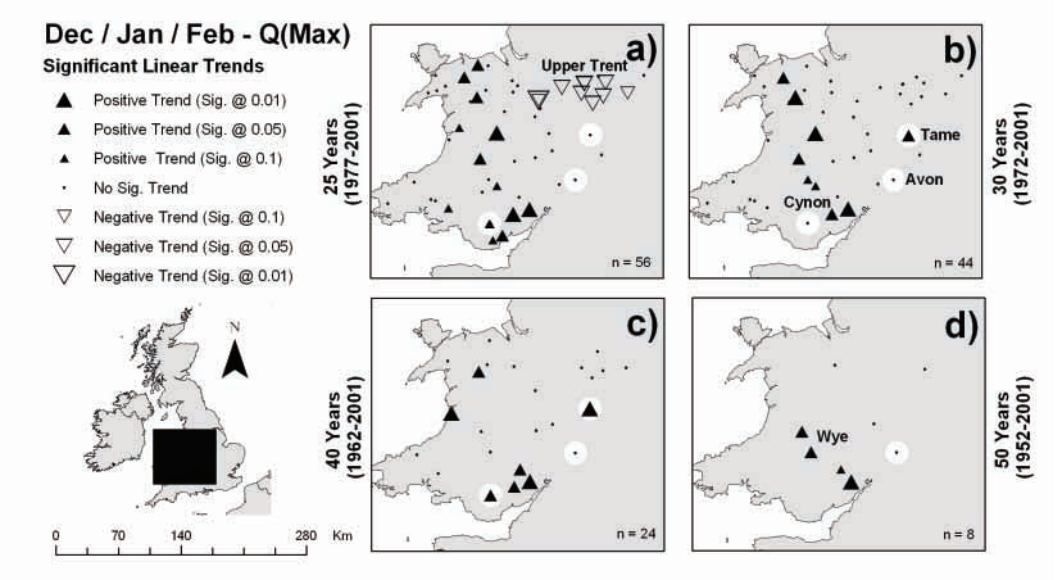


Fig. 2 Geographical variations in winter Q_{Max} streamflow trends (significant at $\alpha \leq 0.1$): (a) t = 25 years; (b) t = 30 years; (c) t = 40 years; (d) t = 50 years. Individual example gauging stations highlighted by white circles and labelled in 2(b).

show positive linear trends (Fig. 2(d)), the total number of records available is low (n = 8) and all of the statistically significant time series represent gaugings in the Wye catchment or tributaries.

Individual gauging station examples

The problems of varying analysis periods can be further demonstrated through the exploratory analysis of example time series for specific station quantiles for seasons (Figs 3, 4 and 5). The addition of LOESS smoothing and Sen's estimations of linear trend lines quantifies the record length issue. These example stations are located in Fig. 2(b).

For many time series the statistical significance of a trend can be directly affected by the analysis period chosen. Winter high flows on the River Tame (Fig. 2(b)), for example, display positive trends over 20, 30 and 40 years of the record (Fig. 3). However, the trend is only statistically significant (at α = 0.1) for t = 30 and 40, suggesting that significant increases in winter maximum flows have not been continued into the post-1990 period.

A similar pattern emerges for summer $Q_{0.3}$ flows on the River Avon at Evesham (Fig. 2(b)), 50 km to the south of the River Tame: in this case fluctuations in the length of period considered cause a reversal of trends (Fig. 4). Statistically significant *increasing* trends are present over both the 50- and 60-year periods up to 2001, while for a medium length of record (t = 40 and 30 years) the time series displays a high degree of *stationarity*. However, analysis for 25 years (1977–2001) results in statistically significant *negative* trends.

The final example shows winter low flows (Q_{Min}) of the Cynon at Abercynon in South Wales (Fig. 2(b)). Here the long-term (t = 39 year) trend is *stationary*, but an analysis confined to the most recent 25 or 30 years shows a clear, significant flow *decline* (Fig. 5). This demonstrates the importance of analysing the fullest possible record lengths when identifying historical trends or making future projections.

DISCUSSION AND CONCLUSIONS

The recent increase in research and media interest in long term climatic and hydrological change has lead to speculation about trends of a number of hydro-meteorological variables. The present study has examined the trends in streamflow data of 56 stations in Wales and the English Midlands: 21 stations are common to the FRIEND network.

The detection of trends in hydrological data is a complex issue. This study has shown that the results of trend analysis are dependent on the chosen period: in particular, it can have significant

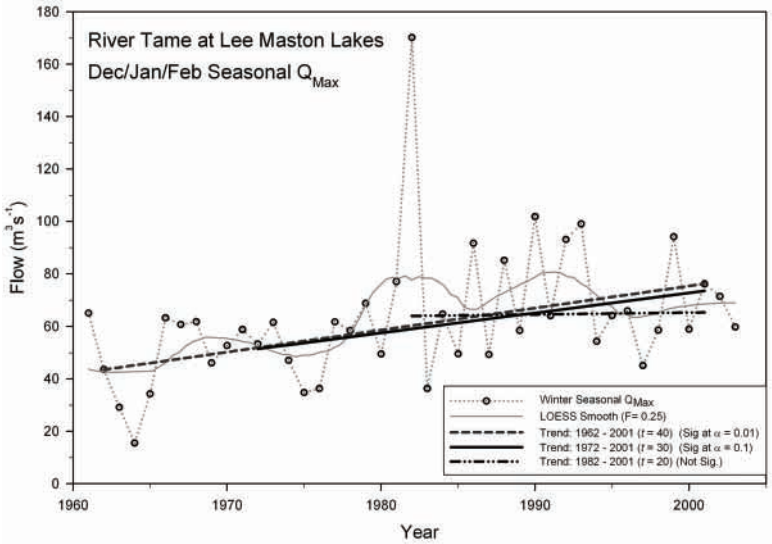


Fig. 3 Winter high flows (Q_{Max}) of the River Tame at Lee Marston Lakes. Mann-Kendall linear trends calculated over varying time periods.

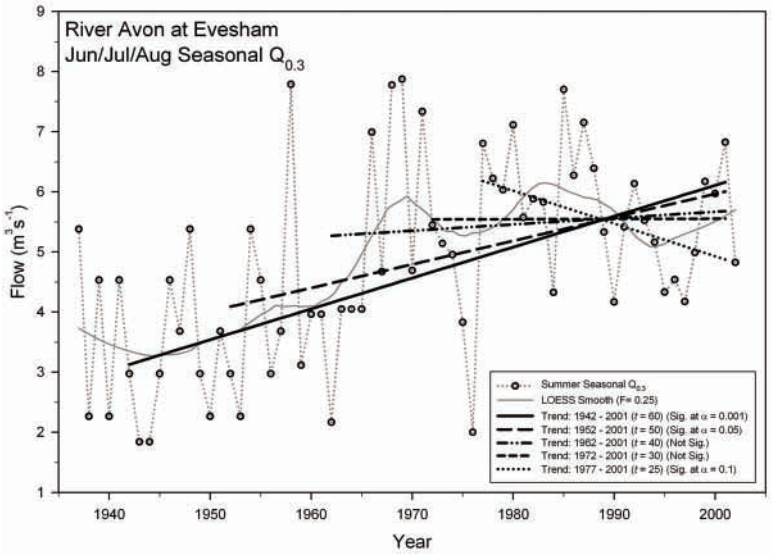


Fig. 4 Summer $Q_{0.3}$ flows of the Avon at Evesham. Mann-Kendall linear trends calculated over varying time periods.

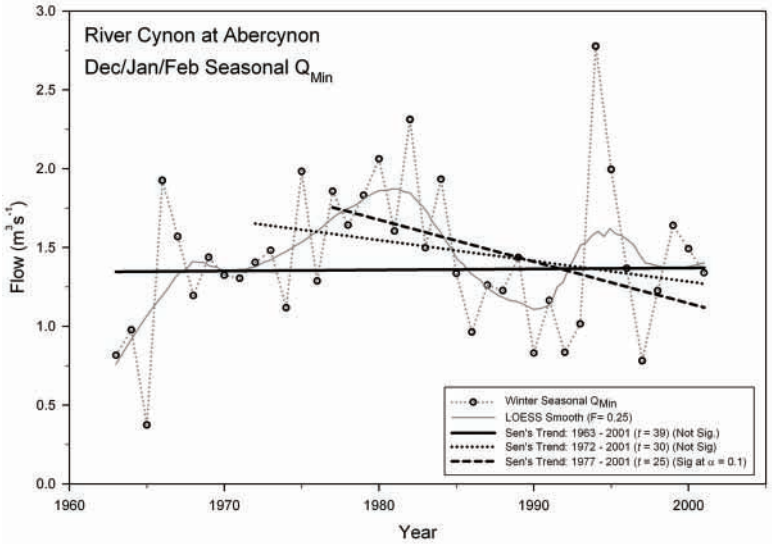


Fig. 5 Winter low flows (Q_{Min}) of the Cynon at Abercynon. Mann-Kendall linear trends calculated over varying time periods.

influence on both trend magnitude and the direction. The implications of analytical decisions on the interpretations of hydrological change are important and impact on planning and development in many fields including water resources, flood defence, hydro-ecology and climate-flow analysis. This study also confirms the importance of using the seasonal streamflow data in trend analysis, rather than simple annual means which can sometimes fail to reveal the full temporal complexity of flow trends.

Although, the trend analysis results here are found to vary across the flow quantiles used, the main feature is for streamflow increases at high and low flows for $t \geq 30$ years. The spatial pattern of trends is also affected by the chosen period of record. Some of the flow increases identified have recently been linked to increasing total rainfall receipts and the state of the North Atlantic Oscillation in the same area (Dixon *et al.*, 2005).

Future analysis will focus on any cyclic and step-change behaviour in the flow, rainfall and atmospheric circulation data, which has emerged for some stations (Dixon *et al.*, 2005). Other analysis could also incorporate a moving window method, using a shifting end date (e.g. Hisdal *et al.*, 2001; Lindstrom & Bergstrom, 2004).

The quantification presented here of the impact of record length in trend analysis demonstrates the need for careful analysis of hydrological time series and supports the use of the longest streamflow data sets available. The continued development of historical flow records, expansion of comprehensive river flow databases (such as the FRIEND European Water Archives: http://ewa.bafg.de/) and maintenance of high resolution river flow monitoring networks are central to further detection and understanding of hydrological change.

REFERENCES

Birsan, M.-V., Molnar, P., Burlando, P. & Pfaundler, M. (2005) Streamflow trends in Switzerland. *J. Hydrol.* **314**(1-4), 312–329.

Burn, D. H. & Hag Elnur, M. A. (2002) Detection of hydrologic trends and variability. *J. Hydrol.* **255**, 107–122.

Dixon, H., Lawler, D. M. & Shamseldin, A. Y. (2005) The application of time series analysis in the detection of hydrological change: The study of river flows in North Wales, UK. In: *Geophysical Research Abstracts*. European Geosciences Union General Assembly. Vienna, vol. 7. EGU05-A-08165

Helsel, D. R. & Hirsch, R. M. (1992) *Statistical Methods in Water Resources*. Studies in Environmental Science 49. Elsevier, Amsterdam, The Netherlands.

Hisdal, H., Stahl, K., Tallaksen, L. M. & Demuth, S. (2001) Have streamflow droughts in Europe become more severe or frequent? *Int. J. Climatol.* **21**(3), 317–333.

Kahya, E. & Kalayci, S. (2004) Trend analysis of streamflow in Turkey. *J. Hydrol.* **289**(1–4), 128–144.

Kundzewicz, Z. W. & Robson, A. J. (2004) Change detection in hydrological records—a review of the methodology. *Hydrol. Sci. J.* **49**(1), 7–19.

Lettenmaier, D. P., Wood, E. F. & Wallis, J. R. (1994) Hydro-climatological trends in the continental United States, 1948–88. *J. Climate* **7**, 586–607.

Lindstrom, G. & Bergstrom, S. (2004) Runoff trends in Sweden 1807-2002. *Hydrol. Sci. J.* **49**(1), 69–83.

Lins, H. F. & Slack, J. R. (1999) Streamflow trends in the United States. *Geophys. Res. Lett.* **26**(2), 227–230.

Robson, A. J. (2002) Evidence for trends in UK flooding. *Phil. Trans. Royal Society London* **360**(1796), 1327–1343.

Sen, P. K. (1968) Estimates of the regression coefficient based on Kendall's tau. *J. Am. Statist. Assoc.* **63**, 1379–1389.

Zhang, X., Harvey, K. D., Hogg, W. D. & Yuzyk, T. R. (2001) Trends in Canadian Streamflow. *Water Resour. Res.* **37**(4), 987–998.

Climate Variability and Change—Hydrological Impacts (Proceedings of the Fifth FRIEND World Conference held at Havana, Cuba, November 2006), IAHS Publ. 308, 2006.

High and low flow trends in a national network of undisturbed indicator catchments in the UK

JAMIE HANNAFORD & TERRY J. MARSH
Centre for Ecology and Hydrology, Wallingford, Oxfordshire OX10 8BB, UK
jaha@ceh.ac.uk

Abstract This paper presents the results of trend analyses applied to indicators of high and low flows in a network of undisturbed catchments in the UK, over the 1970–2004 period. Significant positive trends in high flows were identified across northern and western areas; these increases are associated with changing atmospheric circulation patterns associated with the North Atlantic Oscillation (NAO), and may reflect the impact of multi-decadal oscillations rather than climatic change. There was no compelling evidence for any pronounced decrease in low flows, despite the clustering of droughts in recent years. The recent trends are compared to several longer (>60 year) hydrometric records which show pronounced temporal fluctuations, but there is little evidence of long-term trend.

Key words flood(s); high flows; low flows; Mann-Kendall test; natural catchments; North Atlantic Oscillation; trends; UK

INTRODUCTION

It is widely speculated that greenhouse-gas induced global warming will lead to an increase in the severity of floods and droughts in many parts of the world. In the UK, scenario-based Regional Climate Model (RCM) forecasts envisage increases in extreme rainfall (Ekstrom *et al.*, 2005), and possible future impacts on flood frequency (Kay *et al.*, 2006). Similarly, Arnell (2003) presents simulations which project reductions in low flows, and Fowler & Kilsby (2004) report projected increases in drought severity. Hydrological monitoring programmes have an essential part to play in characterising historical variability in order to discern emerging trends in flow regimes—the identification of such trends is a necessary foundation for the development of appropriate water policy and management responses to climate-driven change.

A major obstacle in discerning climatic-driven changes in river flow patterns is the combined impact of anthropogenic disturbances, such as heavy abstraction rates and extensive impoundments. These and the varying hydrometric capabilities of gauging stations—particularly in the extreme flow ranges—may contribute to spurious trends. To overcome these obstacles, a "benchmark" network of 120 near-natural catchments, monitored by gauging stations with good hydrometric performance, has been identified in the UK (Bradford & Marsh, 2003).

This paper presents the results of trend tests applied to indicators of high and low flows for gauging stations in the benchmark network, over the 1970–2004 period. The results are evaluated in the context of possible climatic-driven changes. Finally, a selection of longer records is used to place recent trends in a fuller historical perspective.

DATA

The data used for this analysis are based on daily flow records from the benchmark catchments, derived from the National River Flow Archive at CEH Wallingford. Four variables were used:

(a) annual minimum 30-day flow ($m^3 s^{-1}$);
(b) annual maximum 30-day flow ($m^3 s^{-1}$);
(c) prevalence of low flows (number of days below the 90th percentile flow);
(d) prevalence of high flows (number of days above the 10th percentile flow).

The first two variables were chosen as indicators of low and high flow magnitude, the second two relate to low and high flow duration. For the low flow indicators, calendar years were used. For the high flow indicators, UK water years (1 October–30 September) were used; this limits dependence between high flow events, which frequently occur over the transition between calendar years.

Copyright © 2006 IAHS Press

The UK gauging station network expanded rapidly during the late 1960s—consequently, selection of an optimal study period is necessarily a compromise between geographical coverage and available record length. Trend tests were carried out for a 1970–2004 study period, for which 78 Catchments were available. Trend tests are sensitive to the analytical timeframe used (Kundzewicz & Robson, 2000); the implications of this are considered further under "long records".

METHODS

The Mann-Kendall (MK) test (Kendall, 1975) was used to test for trend. Permutation tests, as described by Kundzewicz & Robson (2000), were then used to asses the significance of trends.

Each time series was tested for autocorrelation, which can increase the probability of detecting trends when none are present (Yue *et al.*, 2002). There were relatively few catchments with significant autocorrelation in the indicators: for high flow prevalence, only three river flow series had significant lag-1 autocorrelation, but for low flows, 12 cases were significant. For these cases, a block resampling approach was used; essentially the permutation approach remains the same, but the data are permuted in two-year blocks to preserve the lag-1 autocorrelation (Kundzewicz & Robson, 2000).

A Trend Index (TI, Svensson *et al.*, 2005), was used to summarise results. The TI relates to the significance level, α, of the two-sided test as:

$$TI = 100 - \alpha, \text{ for positive trends, and} \quad (1)$$

$$TI = -(100 - \alpha), \text{ for negative trends} \quad (2)$$

Thus, a negative trend significant at the 10% level will have TI = –90.

RESULTS

High flow trends

The results for the high flow indicators are presented in Fig. 1. Significant positive trends in 30-day maxima and high flow prevalence were identified across northern and western areas—particularly in northern England and southern Scotland. The increases in high flow magnitude and duration are primarily in upland areas exposed to maritime climatic influences, contrasting with lowland areas in eastern England where there are few significant results. The increasing trend in long-duration high flow events in some northern and western areas has some parallels with observed increases in extended-duration rainfall (e.g. for 10-day maxima; Fowler & Kilsby, 2003) and annual runoff (Hannaford & Marsh, 2006).

The increase in high flows in western areas is consistent with changing atmospheric circulation patterns associated with the increasing North Atlantic Oscillation trend observed from the early 1960s until the late 1990s (Wilby *et al.*, 1997). The NAO Index (NAOI) has been shown to be correlated with winter rainfall (Wilby *et al.*, 1997) and runoff (Shorthouse & Arnell, 1999) in maritime areas of Great Britain. In the present study, winter (December–March, DJFM) q10 prevalence was correlated with winter (DJFM) NAOI. The winter season was chosen, as this is when the NAO influence on UK climate is most pronounced (Wilby *et al.*, 1997). The results (Fig. 2) suggest the NAO has an important influence on winter high flows in some maritime catchments. More vigorous westerly airflows in positive NAO years are associated with greater orographic rainfall in upland western areas. Sheltered eastern catchments have negative correlations with the NAO, in common with the analyses applied to runoff by Shorthouse & Arnell (1999). The results suggest the increasing trends in high flows identified in this study may be influenced by a shift towards a positive NAO since the early 1960s. However, many catchments correlated with the NAOI show no significant increasing flow trend (e.g. for northern Scotland, cf. Fig. 1(b) and Fig. 2). Clearly, further work is required to elucidate these relationships in more detail.

An increase in long duration high flow events and the prevalence of high flows could have significant impacts on future flood management. Some RCM analyses predict increases in extended duration rainfall events for northern and western areas (Ekstrom *et al.*, 2005). However, whilst the results of trend tests presented here have some parallels with such scenarios, the

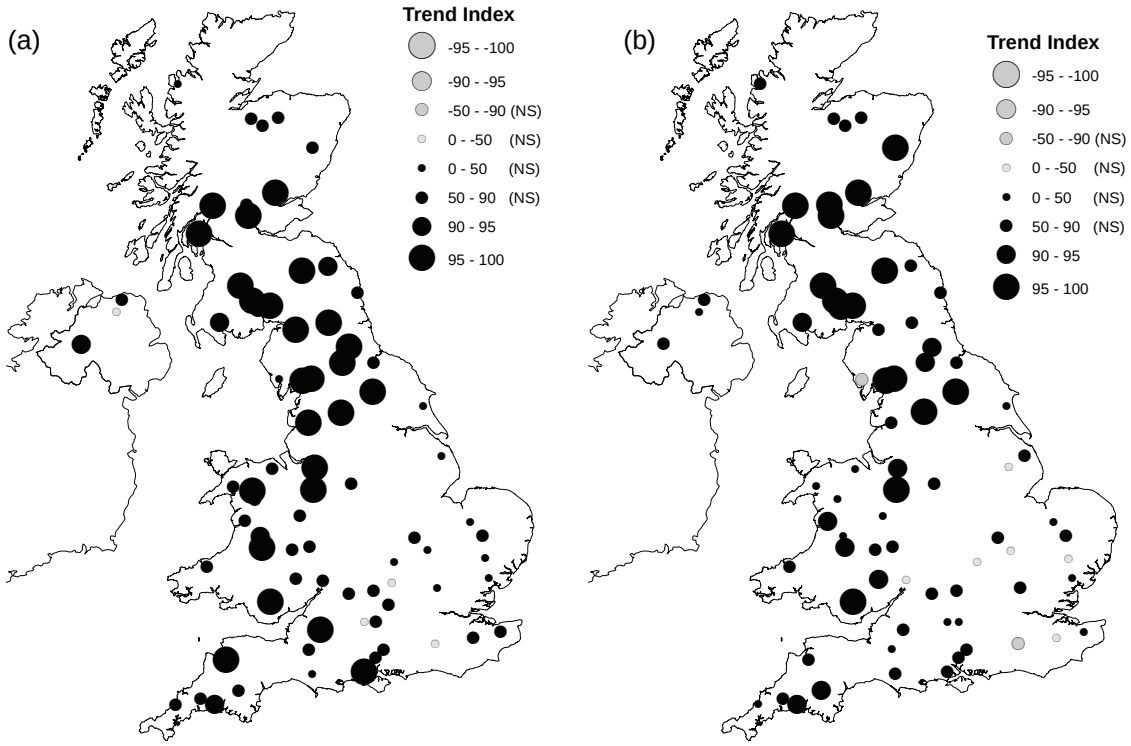


Fig. 1 Results of trend tests for high flow indicators: (a) 30-day maxima, (b) q10 prevalence. Trend Index shown according to legend.

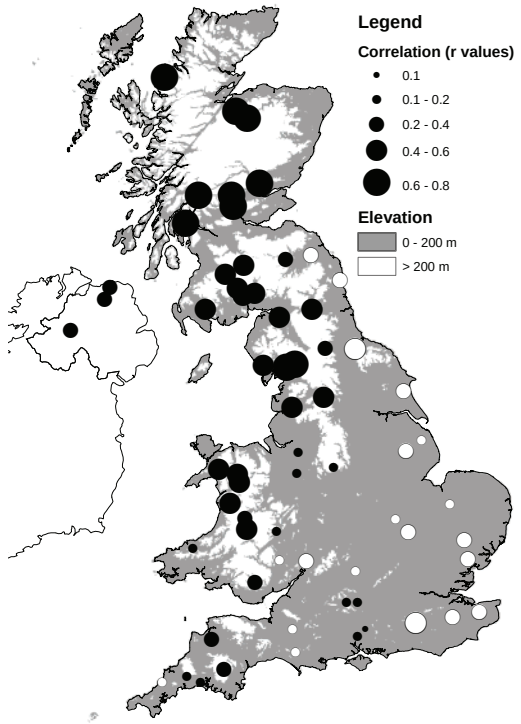


Fig. 2 Correlation between winter q10 prevalence and winter NAOI. Dark graduated circles show positive correlation, white shows negative. Elevation above 200 m is also highlighted.

association with the NAO means that recent trends may reflect multi-decadal oscillations rather than long-term climate change, although the NAO itself may be influenced by climate change (Gillet *et al.*, 2002).

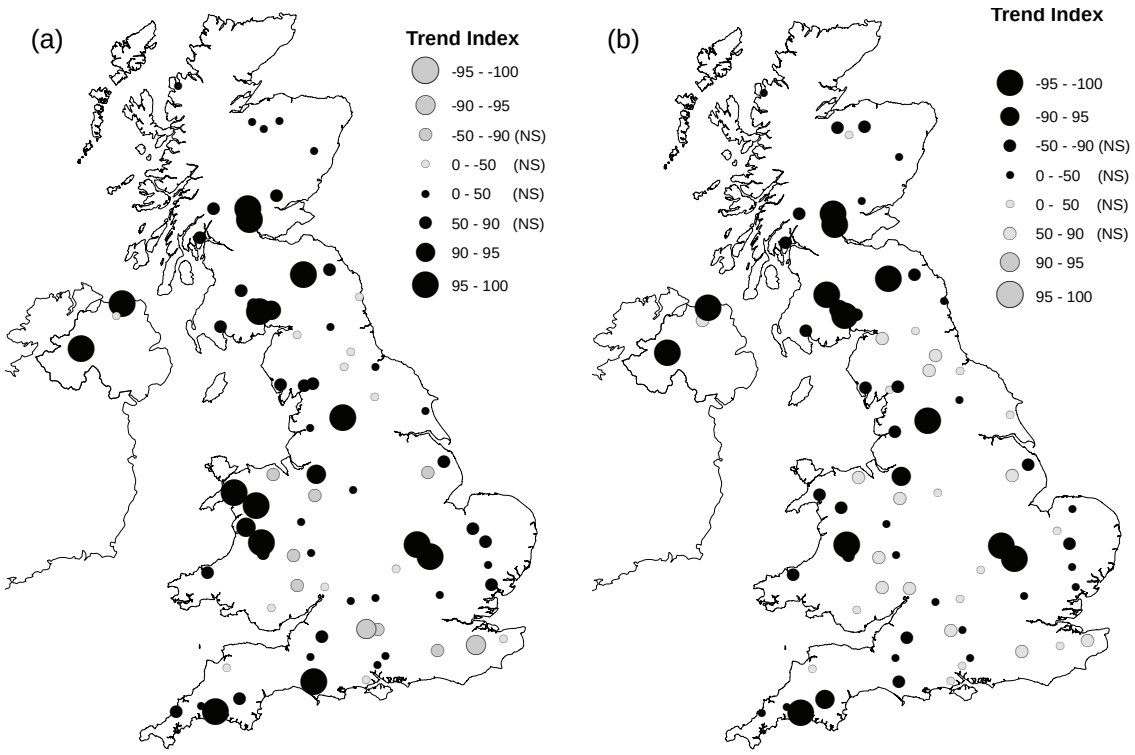


Fig. 3 Results of trend tests for low flow indicators: (a) 30-day minima, (b) q90 prevalence. Trend Index shown according to legend. Note that the prevalence results are reversed to allow comparison with the minima; a positive sign indicates a decrease in the time spent below q90, i.e. suggesting low flows are becoming less severe.

Low flow trends

The results from the low flow analyses are presented in Fig 3. Similarities with the high flow trends can be recognised (e.g. southwest Scotland) but generally the low flow trends display less spatial coherence.

There appears to be a tendency towards decreasing low flows in some southeastern catchments, but few of the trends are significant. This is particularly interesting, considering the clustering of recent drought periods which have impacted heavily in southeast England (e.g. 1988–1992, 1995, 2003). The lack of decreasing trends is not consistent with some scenario-based hydrological modelling forecasts (e.g. Arnell, 2003) which project significant decreases in Q95 flows by the 2020s, particularly for southeastern areas. This lack of congruency may reflect the uncertainties inherent in modeling, such as a possible countervailing effect of multi-decadal variability (Arnell, 2003), as well as the limitations associated with trend tests; e.g. the effect of high inter-annual variability and sensitivity to short record length (Kundewicz & Robson, 2000). With these caveats acknowledged, the observations presented in this study suggests there is little evidence for a pronounced shift towards lower flows or increased low flow duration over the last 35 years.

Long records

Limited record length is typically a major obstacle to interpreting the results of trend analysis, as there are often few homogeneous records on which to base long-term assessments of change. In this study three long hydrometric are used to examine recent trends in a fuller historical context. Figure 4 features high and low flow prevalence (long time series of minima and maxima were similar and are not presented). The Thames catchment is subject to major artificial influences, but naturalized data (Littlewood & Marsh, 1996) are presented here.

Over the longer timescales, a significant (at the 90% level) long-term trend in high flows was only observed for the Wye in Wales (1935–2004). For the Dee (Scotland), the long-term trend is non-significant, but the locally weighted regression (LOESS) smoothing suggests marked temporal

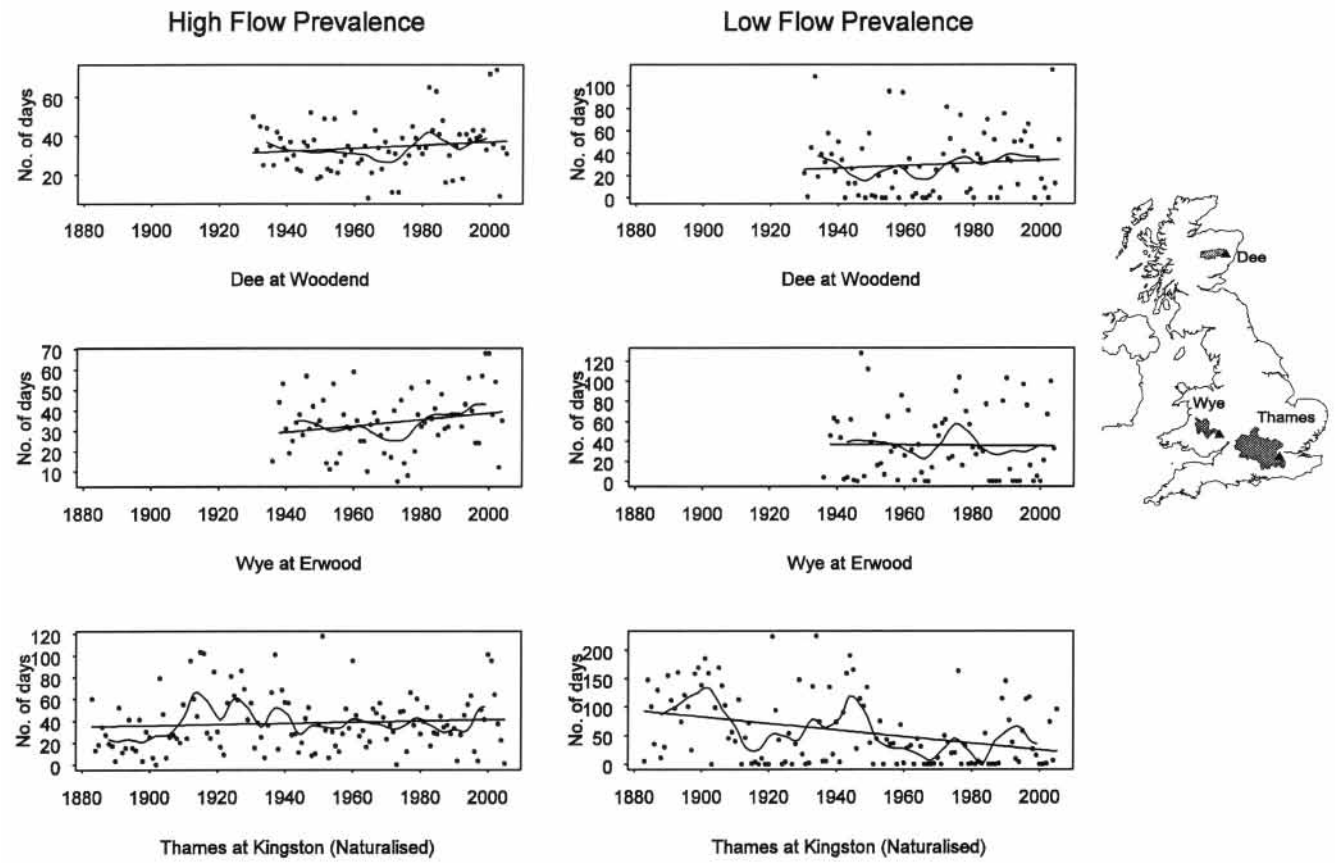


Fig. 4 Time series plots showing high flow (q10) and low flow (q90) prevalence trends for three long hydrometric records (LOESS smoothing curves are also shown), with a map showing the location of the three catchments.

fluctuations; a linear trend fitted from the early 1960s would yield a much steeper, significant positive trend.

For low flows, the Dee and the Wye show no evidence of significant long-term change. The negative low flow prevalence trend (reflecting a decrease in time spent at low flows) for the 121-year Thames record is partly influenced by a series of dry winters prior to 1910, but low flows during this period are known to be underestimated (Littlewood & Marsh, 1996). The long record does show clear evidence of clustering, which may lead to short-term trends implying decreasing low flows—there are a number of years with long periods of flows below q90 throughout the 1990s, in comparison with the 1980s where most years had no periods below q90.

Only three long records are presented in this short study—more work is required to appraise the quality of other long hydrometric records before a definitive characterization of long-term variability can be made.

CONCLUSIONS

This study has focused on a network of undisturbed catchments to discern natural variability from artificial impacts on flow regimes. This study has presented evidence for increasing high flows in maritime northern and western areas of the UK, complementing previous work on rainfall and runoff. Increasing high flow trends are consistent with some scenario-based climate model projections for the future although a predominantly positive NAOI over the latter half of the period suggests climatic variability is an important factor. There were few significant decreasing low flow trends in the benchmark catchments in lowland England, despite a clustering of droughts in the 1990s. The results presented here provide a baseline against which long-term historical variability and future change in river flow patterns can be quantified and interpreted.

Acknowledgements Grateful acknowledgement is made to the UK measuring authorities for the provision of flow data and assistance in the selection of the benchmark catchments.

REFERENCES

Arnell, N. W. (2003) Relative effects of multi-decadal climatic variability and changes in the mean and variability of climate due to global warming: future streamflows in Britain. *J. Hydrol.* **270**, 195–213.

Bradford, R. B. & Marsh, T. M. (2003) Defining a network of benchmark catchments for the UK. *Proceedings of the Institution of Civil Engineers, Water and Maritime Engineering* **156**, 109–116.

Ekstrom, M., Fowler, H. J., Kilsby, C. G. & Jones, P. D. (2005) New estimates of future changes in extreme rainfall across the UK using regional climate model integrations. 2. Future estimates and impact studies. *J. Hydrol.* **300**, 234–251.

Fowler, H. J. & Kilsby, C. G. (2003) A regional frequency analysis of United Kingdom extreme rainfall from 1961–2000. *Int. J. Climatol.* **23**, 1313–1334.

Fowler, H. J. & Kilsby, C. G. (2004) Future increases in UK water resource drought projected by a regional climate model. In: *Hydrology: Science and Practice for the 21st Century* ((ed. by B. Webb *et al.*) (Proc. British Hydrological Society International Conference). British Hydrological Society, London, UK.

Gillett, N. P., Graf, H. F. & Osborn, T. J. (2002) Climate change and the North Atlantic Oscillation. In: *The North Atlantic Oscillation –- Climatic Significance and Environmental Impact*. American Geophysical Union, Washington, USA.

Hannaford, J. & Marsh, T. J. (2006) An assessment of trends in runoff and low flows in a network of undisturbed catchments in the UK. *Int. J. Climatol.* **26**, 1237–1253.

Kay, A. L., Jones, R. G. & Reynard, N. S. (2006) RCM rainfall for UK flood frequency estimation. II. Climate change results. *J. Hydrol.* **318**, 163–172.

Kendall, M.G. (1975) *Rank Correlation Methods*. Charles Griffin, London, UK.

Kundzewicz, Z. W. & Robson, A. J. (2000) Detecting trend and other changes in hydrological data. World Meteorological Organisation, Geneva.

Littlewood, I. G. & Marsh, T. J. (1996) A reassessment of the monthly naturalized flow record for the River Thames at Kingston since 1883, and the implications for the relative severity of historic droughts. *Regulated Rivers: Research and Manage.* **12**, 13–26.

Shorthouse, C. A. & Arnell, N. W. (1999) The effects of climatic variability on spatial characteristics of European river flows. *Phys. Chem. Earth* **24**, 7–13.

Svensson, C., Kundzewicz, Z. W. & Maurer, T. (2005) Trend detection in river flow series: 2. Flood and low-flow index series. *Hydrol. Sci. J.* **50**, 811–824.

Wilby, R. L., O'Hare, G. & Barnsley, N (1997) The North Atlantic Oscillation and British Isles climate variability, 1865–1996. *Weather* **52**, 266–275.

Yue, S., P. Pilon, P., Phinney, B. & Cavadias, G (2002) The influence of autocorrelation on the ability to detect trend in hydrological series. *Hydrol. Processes* **16**, 1807–1829.

Climate Variability and Change—Hydrological Impacts (Proceedings of the Fifth FRIEND World Conference held at Havana, Cuba, November 2006), IAHS Publ. 308, 2006.

Past and future changes in flood and drought in the Nordic countries

HEGE HISDAL, LARS A. ROALD & STEIN BELDRING

Norwegian Water Resources and Energy Directorate (NVE), PO Box 5091 Majorstua, N-0301 Oslo, Norway
hege.hisdal@nve.no

Abstract Based on a data set of 46 daily streamflow records from the Nordic region for the period 1920–2002 the natural variability in trends and estimated return levels of flood and drought has been studied. In addition, for a subset of series, return level estimates based on historical records were compared to extreme estimates for a control period, 1961–1990, and a scenario period, 2071–2100. It was shown that detected trends and return levels strongly depend on the time period studied because the natural variability in the extremes is large. The scenarios indicated reduced annual floods in eastern Norway, increased annual floods in the western part and varying results for the basins in central and northern Norway. Droughts in general tended to become more severe in the scenarios. The expected changes in floods in the scenarios were only larger than the differences found due to natural variability for one AOGCM-Regional climate model combination.

Key words Scandinavia, flood, drought, trend, climate variability and change, scenarios

INTRODUCTION

The projected global temperature increase is expected to cause an intensification of the hydrologic cycle leading to changes in streamflow, including flood and drought. Major hydrological extremes in Europe are often interpreted as a result of human induced climate change. Recent Nordic examples are the flood in central Norway in January 2006 with estimated return levels of more than 200 years, and the drought in 2002/2003 covering the whole Nordic region, with estimated damage in Finland alone of more than 100 million € (Silander, 2004).

Climate change studies traditionally include identification of natural climate variability, attempts to detect a climate change signal in historical data and elaboration of possible scenarios for the future. It has previously (Hisdal *et al.*, 2006) been shown that in general for the Nordic countries, no clear spatiotemporal trend patterns can be found in flood peak, neither for the autumn nor the spring season. However, there is a clear tendency towards an earlier spring flood. There is also a tendency towards more severe summer droughts in southern and eastern Norway. In Roald *et al.* (2006) studies of the impacts of climate change on streamflow for catchments representing different runoff regimes in Norway were carried out based on the combined use of two global atmosphere–ocean general circulation models (AOGCMs), two regional climate models and a hydrological model. It is concluded that we can expect a reduction in the annual flood in basins with dominating snowmelt floods and an increase in basins with a dominating coastal climate. There will be more winter floods and the snowmelt flood will occur earlier.

This paper addresses: (a) the influence of time period on trends and estimated return levels of hydrological extremes, and (b) the comparison of historical extremes with extreme estimates based on a control period (1961–1990) and scenarios (2071–2100). In the next sections the data and methods are described, the results are presented and discussed and conclusions are given.

DATA AND METHODS

A total of 46 daily series from Denmark, Finland, Norway and Sweden covering the period 1920–2002 were collected (Fig. 1). This enables a regional study of changes in extremes. A quality control has ensured that the data, as far as possible, are uninfluenced by human activity in the basin.

All records were used in the study of how trends might vary depending on the time period and when evaluating the variability in estimated return levels. A selection of eight Norwegian records was studied when comparing historical and scenario extremes.

The annual maximum flood discharge was analysed. The streamflow was considered to be in a drought situation when the flow is below a specific threshold, the threshold level method

Copyright © 2006 IAHS Press

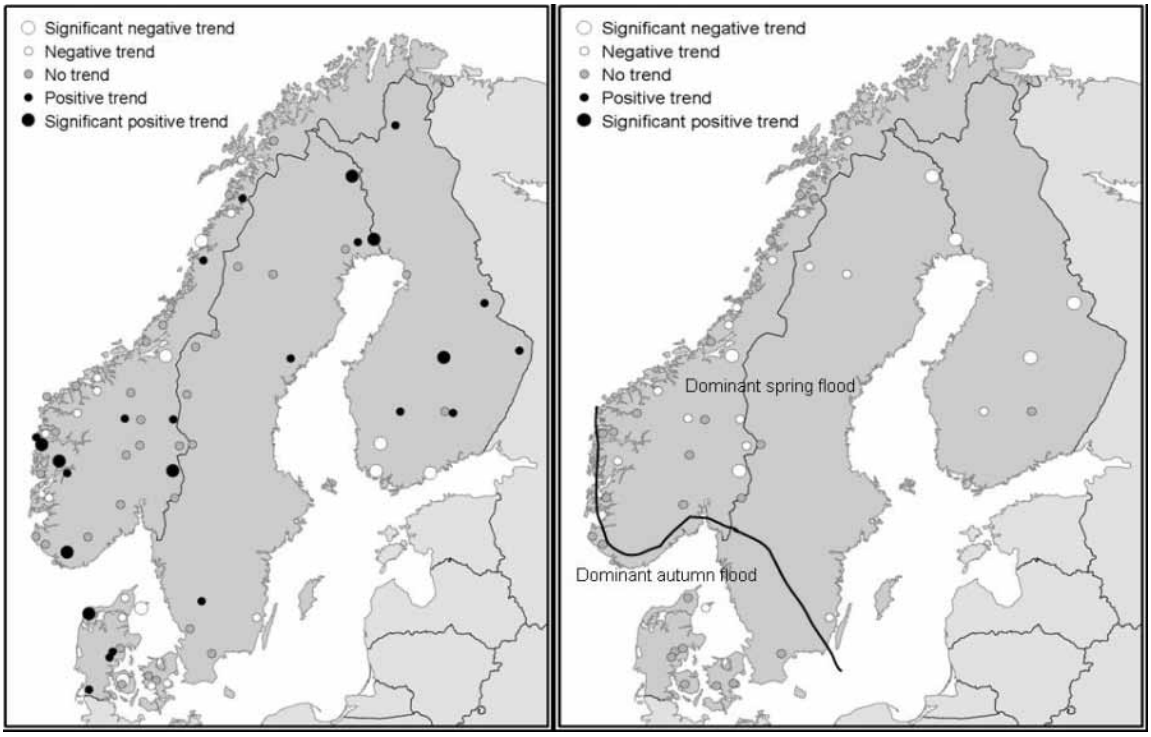


Fig. 1 Trend in annual maximum flood peak value (left) and timing (right) for the period 1920–2002.

(Hisdal *et al.*, 2004). The flow exceeded 70% of the time (70-percentile) was used as the threshold. This means that the drought duration and deficit volume can be identified. As these two drought characteristics are highly correlated, only the results for drought duration are presented here. To perform a consistent analysis of droughts it is necessary to distinguish between droughts caused by lack of precipitation and high evapotranspiration losses (summer droughts) and droughts caused by precipitation being stored as snow (winter droughts). Only summer drought was considered.

Trends in successive 30-year periods using the non-parametric Mann-Kendall test with a 5% significance level were estimated. It was then possible to study how potential trends change based on the time period studied.

According to extreme value theory, the block maxima of a sequence of identically, independently distributed (*iid*) random variables in the limit follows a Generalized Extreme Value (GEV) distribution (e.g. Coles, 2001). Assuming that annual maximum series of flood and drought are *iid*, the GEV distribution was fitted to the annual maximum flood peak and drought duration. The distribution parameters were estimated by Probability Weighted Moments (PWM). By estimating floods and droughts of specific return periods (5-, 10-, 20- and 50-year event) based on successive 30-year periods, the variability in floods and droughts was studied.

For a detailed description of the estimation of the streamflow scenarios see Roald *et al.* (2006). Results from two AOGCMs were used as boundary conditions for the regional climate model simulations: the ECHAM4/OPYC3 and the HadAm3H model. These models were run with assumptions according to the A2 and B2 greenhouse gas emission scenarios. The two regional models were the Regional Climate Development under Global Warming (RegClim) model and the Rossby Centre Regional Atmosphere–Ocean (RCAO) model. All of the hydrological simulations used the time slice approach whereby model simulations representing a slice of time (1961–1990) in present climate (control) and in a future (2071–2100) climate (scenarios) were performed. Daily precipitation and temperature from the regional climate models were further downscaled to meteorological stations using two different approaches. The RegClim approach was a statistical adjustment technique which preserves the frequency of precipitation and temperature as predicted by the climate models, aiming at reproducing observed monthly means and standard deviations for the control period (Engen-Skaugen *et al.*, 2005). Changes in meteorological variables between the control and the scenario simulations from the RCAO model were processed in a model interface before being transferred to an observed climate database, the delta change approach. The

downscaled regional climate model results were subsequently used for driving a spatially distributed version of the hydrological HBV-model (Beldring *et al.*, 2003), yielding an ensemble of streamflow simulations for present and future conditions.

RESULTS AND DISCUSSION

Trends and variability in floods and droughts

In Hisdal *et al.* (2006) it was concluded that no systematic pattern in autumn and spring flood peak values could be identified for the period 1920–2002. Trends in the *annual* flood peaks are shown in Fig. 1. As expected no regional pattern can be observed (Fig. 1, left). Seven of the 46 stations do have a significant trend at the 5% level, two towards more severe floods and five towards less severe floods. There is neither a tendency of positive trends (more severe floods) for stations with dominating autumn rain floods nor negative trends (less severe floods) for stations with dominating snowmelt floods during the spring. However, regarding the timing of the annual flood (Fig. 1, right) there are only trends towards an earlier timing, especially in regions with a dominating spring snowmelt flood. Regarding trends in drought duration for the period 1920–2002, around 60% of the stations (7 of 11) in Southeast Norway showed a tendency towards longer summer droughts. For this period the stations that tend to get shorter summer droughts were found in Denmark.

The dependency of the trend on the period analysed was found by calculating the trend for successive 30-year periods, starting in 1920–1949 and ending in 1973–2002. Figure 2 illustrates the changing Mann-Kendall test statistics for both flood and drought for the Knappom station in eastern Norway. For test statistics values larger than |1.96| (the 0.975 quantile of the standard normal distribution) a trend is significant with a 5% level of significance. It can be seen that significant negative and positive trends are found both for flood and drought depending on the underlying 30-year time period. The spatial pattern of the fluctuating Mann-Kendall test statistics varies. Regarding drought, all stations in Denmark have the same behaviour. There is some greater variability between the stations in Sweden and Finland whereas the spatial variability in Norway is largest with positive and negative trends for the same time period, reflecting the various climatic influences and hydrological regimes. As drought is a more persistent phenomenon than flood and also covers larger regions. The variability in trends between stations is therefore larger for floods than droughts.

Floods and droughts of various return periods (5, 10, 20 and 50 years) were also calculated for successive 30-year periods. For drought the 70 percentile for the period 1920–2002 was used to extract the drought events. The estimates may vary considerably depending on the underlying

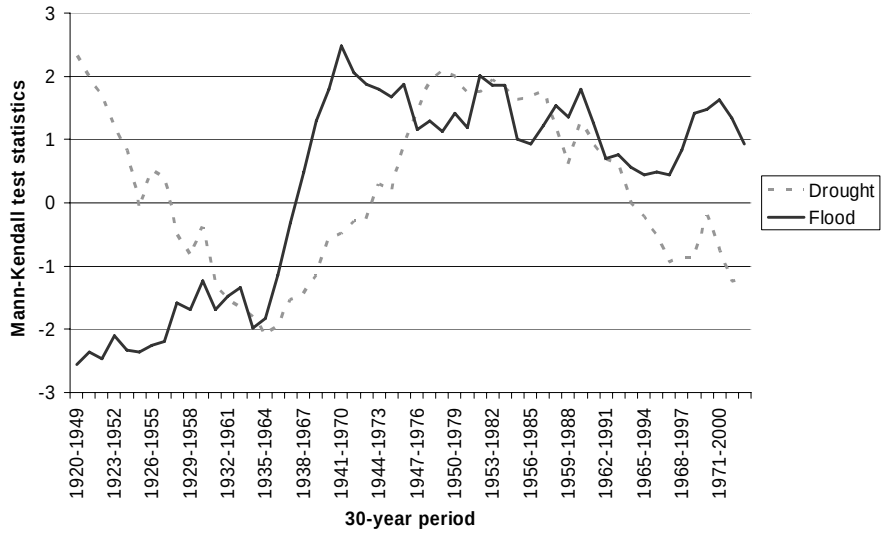


Fig. 2 Mann-Kendall trend test statistics for the annual maximum flood peak and drought duration for the Knappom basin calculated for consecutive 30-year periods.

30-year period, reflecting that the uncertainty in estimated return levels is large. The deviation (in percent) from the average estimated 50-year annual maximum flood and summer drought based on different 30-year periods of observation is illustrated in Fig. 3. For floods, on average the 50-year event estimates varied by 34% (min. deviation 13%, max. 80%). For drought the average deviation was 38% (min. deviation 15%, max. 79%). Normally, the percentage deviation was lower for the shorter return periods, but even for the mean annual flood and drought, the percentage deviation could be quite large.

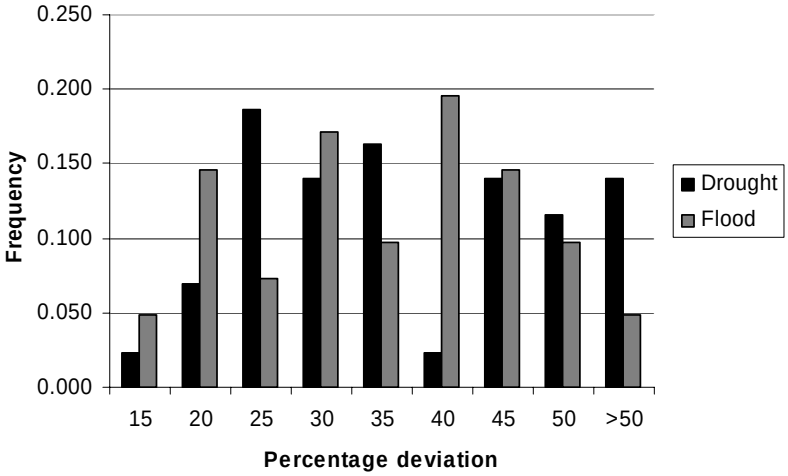


Fig. 3 The deviation (in percent) from the mean estimated 50-year event and the difference between the maximum and minimum estimated 50-year flood and drought.

Comparison to scenarios

The mean and standard deviation of the annual maximum floods based on observations (1961–1990), the control run (1961–1990) and the 2071–2100 scenarios were compared for eight stations in Norway (Table 1). For four of the stations seven scenarios exist; for the other four stations only three scenarios exist. When studying climate change effects on hydrological extremes it is important that the mean values and standard deviation observed in the historical data are reproduced in the control runs. It can be seen (Table 1) that the mean annual flood (MAF) is underestimated in all control runs. The largest underestimation is found for the Rossby control runs. These also underestimate the standard deviation. In the RegClim case the standard deviation is both over- and underestimated. The misfit observed for the MAF is mainly caused by the fact that the hydrological model in general simulates too small annual maximum discharge values. It might also be that the precipitation and temperature data are not representative. The unclear results regarding the standard deviation in the RegClim case could have been caused by the precipitation and temperature estimation procedures. The misfit between the moments in the observations and control runs complicates the interpretation of the expected changes in annual floods peaks and even more for floods of higher return periods.

Expected changes in the future were found by comparing the control-runs with the corresponding scenarios. The MAF was reduced by between 1% and 25% (seven scenarios) in the two inland and mountainous basins in eastern Norway with snowmelt dominated spring floods. All scenarios indicated an increase in MAF in basins in western Norway, where the floods are mostly caused by rainfall combined with some snowmelt. The RegClim and HadAm3H-Rossby scenarios indicate increases of up to 40%, and the ECHAM4-Rossby combination 51–99%. In central and northern Norway only Rossby scenarios exist and they diverged from slightly decreasing (2–9%) MAFs when based on the HadAm3H scenario to increases (35–69%) based on the ECHAM4 scenario. The order of magnitude of change for the 50-year flood was similar to annual flood changes. An exception was the ECHAM4-Rossby combination that increased the 50-year flood by more than

Table 1 MAF and standard deviation for the observed series, control runs and scenarios.

	Nybergs. E-Norway		Knappom E-Norway		Stordalsv. SW-Norw.		Bulken W-Norway		Viksvatn NW-Norw.		Høggås Central Norway		Øyungen Central Norway		Skarsvatn N-Norway	
	Mean (m^3s^{-1})	Std	Mean (m^3s^{-1})	Std	Mean (m^3s^{-1})	Std	Mean (m^3s^{-1})	Std	Mean (m^3s^{-1})	Std	Mean (m^3s^{-1})	Std	Mean (m^3s^{-1})	Std	mean (m^3s^{-1})	Std
Observed 1961–1990	326	121	181	58	76	21	346	83	181	32	148	36	117	42	47	16
RegClim Control, 61-90 HadAm3H	308	131	179	62	59	12			179	50						
RegClim HadAm3H-A2	279	113	140	53	67	18			211	50						
RegClim HadAm3H-B2	291	117	178	67	74	13			234	52						
RegClim Control, 61-90 ECHAM4	303	74	178	75	56	14			180	52						
RegClim ECHAM4-B2	231	97	135	57	76	14			232	49						
RCAO Control, 61-90	288	94	172	55	56	12	325	62	169	30	117	24	112	27	41	11
RCAO HadAm3H-A2	238	93	142	45	72	16	452	116	208	58	114	24	109	39	38	12
RCAO HadAm3H-B2	250	93	141	46	72	18	435	115	208	51	108	19	102	36	38	12
RCAO ECHAM4-A2	215	81	166	58	92	22	649	156	314	79	191	46	188	49	65	20
RCAO ECHAM4-B2	218	82	153	50	85	20	571	117	282	62	166	36	164	46	55	17

100% for the western coast basins. The topography of Norway causes strong dependency of the regional distribution of precipitation and floods on the atmospheric circulation. The two AOGMs produce differences in the projected pressure fields, which explain some of the differences in the regional distribution of the floods in the north.

Except for the ECHAM4-Rossby combination, the estimated human induced climate changes were less or equal to the differences found based on different historical 30-year periods. The exception was the western coast basins Bulken and Viksvatn that only had 18% difference in the different historical 30-year MAFs, but between 12% and 49% increases in the scenarios.

As drought duration was defined as the summer season maximum number of days below the 70 percentile, the mean drought duration and standard deviation remains unchanged. The change in drought duration therefore had to be evaluated by comparing the 70 percentile and the maximum drought duration in the control run and the scenarios. If the 70 percentile decreases in the scenario, the total number of days with low flow can be expected to increase. Coherent with the findings of Roald *et al.* (2006), where the scenarios indicate a reduction in summer flow in most of Norway, the 70 percentile generally decreased. The only significant increase was found for the two basins in central Norway with the ECHAM4-Rossby combination. Regarding the maximum drought duration, it increased for 56% of the scenarios and decreased for 36%. The increase was most pronounced for the two basins in eastern Norway (up to 17 days) and the decrease was largest for the northernmost basin (up to 25 days).

It is important to note that a preservation of the variability in the control period compared to the observations would probably either increase or decrease the variability in the scenarios. Large uncertainties are therefore related to the quantification of expected changes in floods and droughts.

The results show that the scenario summer drought duration is influenced by the increasing temperature that both increases evapotranspiration and causes an earlier snowmelt that again

increases the probability of having a long summer low flow period. Even if a temperature increase reduces the snow cover and to some extent the snowmelt floods, generally changes in floods are more influenced by changes in precipitation.

CONCLUSIONS

This study has focused on changes in floods and summer droughts in the Nordic region, both in historical data and scenarios. Past data are useful in clarifying the background of natural variability, and it was shown that the variability in estimated design events for flood and drought is large. In some cases this variability was even larger than the expected increase or decrease in flood peak or drought duration in the scenarios, reflecting the fact that the uncertainty in the design event estimates may outweigh the uncertainty in the estimated changes in hydrological extremes based on scenarios.

An improved estimation of the variability in the extremes is needed before we can conclude much about the expected quantitative changes in the extremes due to human induced climate change. However, it is possible to indicate a direction of change. In the eastern inland catchments in Norway the flood peaks can be expected to decrease. In the western part of the country the scenarios are uniform too, indicating increased flood peaks; when based on the ECHAM4-Rossby model, the increase is quite substantial. In central and northern Norway the picture is unclear with decreasing flood peaks based on the HadAm3H-Rossby model and increasing flood peaks based on the ECHAM4-Rossby model, reflecting differences in the pressure fields projected in the two AOGMs. Also, more severe droughts can be expected especially in southeast Norway. For the period 1920–2002, the trends in extremes show similar directions to the scenarios regarding the timing of the snowmelt flood and summer droughts in southeastern Norway, but not with respect to the flood peaks.

Acknowledgements This research is a part of the Nordic "Climate and Energy" project and the Norwegian "Climate Change and Energy Production Potential" project. The organizations that contributed data to the database are gratefully acknowledged. We thank T. Tonning, T. Fjeldstad, E. Klausen and T. Reitan all at NVE, for valuable support.

REFERENCES

Beldring, S., Engeland, K., Roald, L. A., Sælthun, N. R. & Voksø, A. (2003) Estimation of parameters in a distributed precipitation-runoff model for Norway. *Hydrol. Earth System Sci.* **7**, 304–316.

Coles, S. (2001) *An Introduction to Statistical Modeling of Extreme Values.* Springer Series in Statistics. Springer, London, UK.

Engen-Skaugen, T., Roald, L. A., Beldring, S., Førland, E. J., Tveito, O. E., Engeland, K. & Benestad, R. (2005) Climate change impacts on the water balance in Norway. *Met. No report, Climate, no. 1/2005*. Oslo, Norway.

Hisdal, H., Tallaksen, L. M., Clausen, B., Peters, E. & Gustard, A. (2004) Hydrological drought characteristics. In: *Hydrological Drought Processes and Estimation Methods for Streamflow and Groundwater* (ed. by L. M. Tallaksen & H. A. J. van Lanen), 139–198. Developments in Water Sciences 48. Elsevier Science Publisher, The Netherlands.

Hisdal, H., Holmqvist, E., Jónsdottir, J. F., Jónsson, P., Kuusisto, E., Lindström, G. & Roald, L. A. (2006) Has streamflow changed in the Nordic countries? *Climate Research* (submitted).

Roald, L. A., Beldring, S., Engen-Skaugen, T., Førland, E. J. & Benestad, R. (2006) Climate change impacts on streamflow in Norway. *NVE Consultancy report A 1/2006*. Oslo, Norway.

Silander, J. (2004) Economic impact of the drought in Finland during 2002-2003. In: *NHP Report No. 48, Proceedings of XXIII Nordic Hydrological Conference* (ed. by A. Järvet), 459–465.

Climate Variability and Change—Hydrological Impacts (Proceedings of the Fifth FRIEND World Conference held at Havana, Cuba, November 2006), IAHS Publ. 308, 2006.

Changes in runoff regimes in small catchments in Central Europe: Are there any?

LADISLAV HOLKO[1], ANDREAS HERRMANN[2] & ALENA KULASOVÁ[3]

1 *Institute of Hydrology, Slovak Academy of Sciences, Ondrašovecká 16, 031 05 Liptovský Mikuláš, Slovakia*
holko@uh.savba.sk

2 *Institute of Geoecology, Department of Hydrology and Landscape Ecology, Technical University Braunschweig, Langer Kamp 19c, D-38106 Braunschweig, Germany*

3 *Czech Hydrometeorological Institute, Na Šabatce 17, Praha 4, Czech Republic*

Abstract The objective of this paper is to explore what measured data in selected small, relatively undisturbed European catchments tell us about the frequency of floods over the past four decades. Daily discharge data from three mountain catchments in Germany, the Czech Republic and Slovakia from 1962 to 2001 was analysed. The analysis focused on trends in mean annual runoff, the seasonal distribution of runoff, maximum annual runoff, and the occurrence of high and low flows. The study did not confirm the hypothesis that the frequency of high flows is increasing. Distinct changes were only related to the seasonality of maximum annual runoff and the number of runoff events and dry periods in summer months.

Key words frequency of floods; trends in runoff regime; small catchments

INTRODUCTION

Severe floods that occurred recently in Africa, North America and Europe have brought much attention to this traditional hydrological issue and it is sometimes claimed that the frequency of floods is increasing. The primary objective of this paper was to test this hypothesis in small, relatively undisturbed European catchments.

The definition of a flood can be ambiguous. A researcher studying runoff generation could denote every runoff event as a flood. For a statistician, a flood could be represented by all peak discharges exceeding certain a threshold. Public understanding of floods is associated with high flows accompanied by property damage or even casualties. In addition to the ambiguity of their definition, hydrological extremes exhibit spatial variability as well.

Although it is commonly stated that the frequency of floods is increasing, an overview of written evidences about big floods in central Europe since the 11th century does not indicate their frequency is increasing. For example, Adamčák & Filip (1999) report that while the last large floods on the Danube occurred in 2002, there were major floods in 1012, 1210, 1501, 1526, 1572, 1594, 1598, 1670, 1682, 1721, 1787, 1809 , 1876 , 1897, 1899, 1954, 1965. Brázdil *et al.* (2005) presented historical data on floods in the Czech Republic from the period 1351–2000. They concluded that the highest number of floods occurred in the 19th and in the second part of the 16th centuries. The flood frequency in the 20th century was comparable with that of the 17th century. Floods in Germany were summarized by Glaser (2001) and Sturm *et al.* (2001). Although the variability of flood frequency was not always identical with that found in the Czech Republic, they also found a maximum in the 16th century.

Historical data from annals and other sources (water marks, personal correspondence, paintings, etc.) represent invaluable information that extends our climatological/hydrological records and enables study of the natural variability of extreme events over long time intervals. However, when testing the hypothesis on increased flood activity in the recent period, there is more precise *measured* runoff data available. It could be expected that if the frequency of high flows is increasing, it should be easily detected in measured data. The aim of this paper is to determine what measured data from small mountainous catchments indicate about the changes in the runoff regime in the last four decades.

METHOD AND DATA

Analyses of time series of hydrological data were performed on data collected since the middle of the 20th century. They resulted in a number of studies which can be roughly divided into three

Copyright © 2006 IAHS Press

groups (Pekárová, 2003) focused on:
– natural variability and periodicity of meteorological and hydrological data
– detection of the long-term trends in time series
– teleconnections of time series with general circulation of atmosphere and hydrosphere

The time series analyses are often done with annual or monthly data using sophisticated statistical methods. Here we have analysed series of daily runoff for the hydrological years 1962–2001 from three small mountain catchments in Central Europe using simpler techniques. These watersheds are located in Germany, the Czech Republic and Slovakia and occur along a gradient of increasing continental influence. The objective is the analysis and discussion of real data series, instead of exhaustive statistics, and focuses on changes in: annual runoff, the seasonal distribution of runoff, maximum annual runoff (R_{max}) and its seasonal occurrence, the number of runoff events, and the frequencies of high flows and droughts. The statistics of runoff events was based on the events that approximately reached or exceeded the mean daily runoff in a particular catchment. High flows events were defined as flows that occurred on 10% of the days (R_{10}). Droughts were defined by a fixed threshold representing flows which occur or are exceeded on 90% of days (R_{90}). Because we compared catchments with different climatic conditions and areas, the flows were expressed as mm of runoff, not as discharge. Therefore, we use R_{max}, R_{10} and R_{90} instead of more conventional Q_{max}, Q_{10} and Q_{90} notations.

According to the classification of Pardé (1933) the hydrological regime of all three catchments (Fig. 1, Table 1) can be characterized as mixed snowmelt–rainfall. The Lange Bramke catchment of the Harz Mountains in Germany, has an oceanic climate. It is made up by Lower Devonian rocks (quartzites, fine-grained quartzitic sandstones, sandy-silty slates) covered with autocthonous weathering and Pleistocene solifluvial materials. Hydrological research in the catchment started in 1949.

The Bílý potok catchment of the Jizera Mountains is situated in the wettest part of the Czech Republic. It is underlain by Proterozoic granitic rocks (granite-granodiorite). The bedrock is covered with shallow Quaternary deposits. Runoff measurements in the catchment started in 1956. The Bystrianka catchment of the Low Tatra Mountains in Slovakia, has a climate that represents a transition between oceanic and continental climates. The upper part of the catchment is underlain by gneiss. The lower part of the catchment is underlain by more variable Triassic rocks (limestone, sandstone, greywacke). Shallow Quaternary deposits overlay bedrock throughout the basin. Runoff measurements in the catchment started in 1923.



Fig. 1 Location of the study catchments; 1-Lange Bramke, 2-Bílý potok, 3-Bystrianka.

Table 1 Basic characteristics of studied catchments, where E, P, R and T are elevation, mean annual precipitation, runoff and air temperature, respectively.

	River basin	Area (km^2)	Forested area (%)	E (min–max, mean) (m a.s.l.)	P (mm)	R (mm)	T (ºC)
Lange Bramke	Weser	0.8	90	543–700, 661	1300	700	6.3
Bílý potok	Oder	26.1	80*	505–1124, 880	1517	1183	5
Bystrianka	Danube	34.4	70	650–2024, 1184	1370	890	3.4

*Before 1984, partially deforested in 1985–1987

RESULTS

Long-term runoff and its seasonality

The mean annual runoff in hydrological years 1962–2001 in the Lange Bramke, Bílý potok and Bystrianka catchments was 622 mm, 1145 mm and 836 mm, respectively. All data series exhibit a wetter period in the second half of the 1960s and a relatively dry period in the second half of the 1980s (Fig. 2). Data from Lange Bramke and Bystrianka show a slight decreasing trend caused by the difference between higher runoff in the 1960–1970s and lower runoff in the 1980–1990s. No trend is visible in the Bíly potok catchment where the second half of the 1990s was wetter.

The transition from the oceanic to continental climate of the catchments is reflected in the seasonal distribution of runoff (Fig. 2). Although the seasonal distribution of runoff varies in particular years, a year-by-year analysis does not indicate any distinct trend or changes. The differences in seasonal distribution of runoff among the catchments were the smallest in the year of 1970 when all the catchments had low runoff in November–March and a pronounced maximum in April or May.

High flows, number of runoff events, low flows

The analysis of the frequency of high flows was the main objective of this study. The time series of maximum daily runoff (R_{max}) do not indicate an increasing trend (Fig. 3). On the contrary, more recent values were smaller then the values observed in previous decades. The analysis of the frequency of higher values of R_{max} in the past decade does not indicate a dramatic increase compared to previous decades. Only in the Lange Bramke catchment it can be concluded that a higher R_{max} occurred in 5 of 8 years since 1994 (Fig. 3). Although R_{max} was higher in previous decades, such a frequency was not observed in the catchment before 1994.

R_{max} in the Lange Bramke catchment typically occurs in winter and spring (Fig. 3). Unlike in previous decades, R_{max} has only once occurred in October–December since 1992. In Bílý potok, R_{max} typically occurs in April, July and August. In Bystrianka, R_{max} usually occurs in April and May.

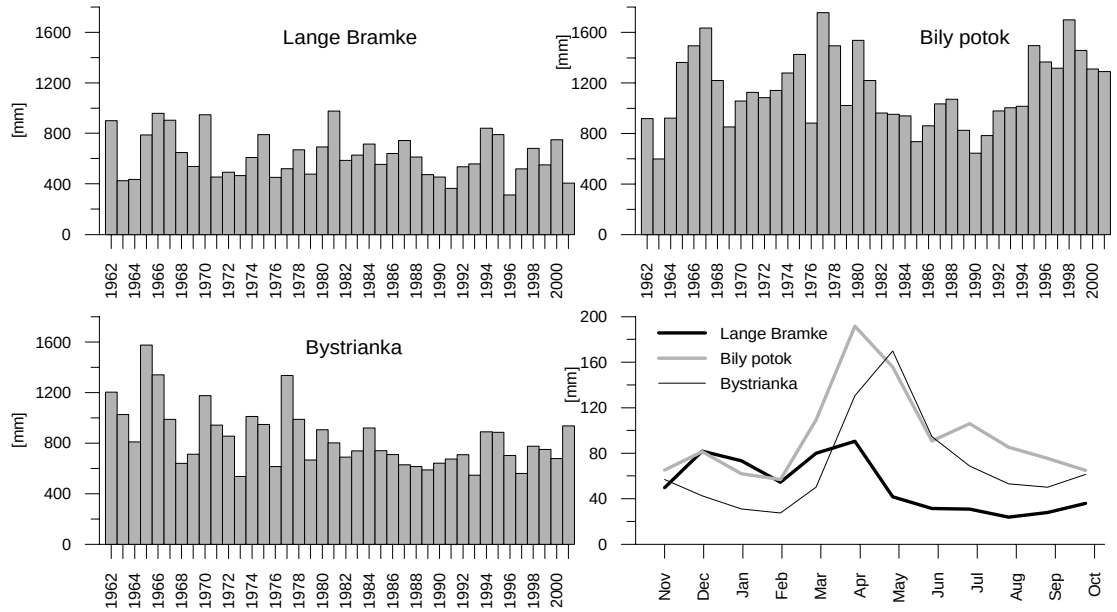


Fig. 2 Annual runoff in hydrological years 1962–2001(bar charts) and mean monthly runoff (line chart).

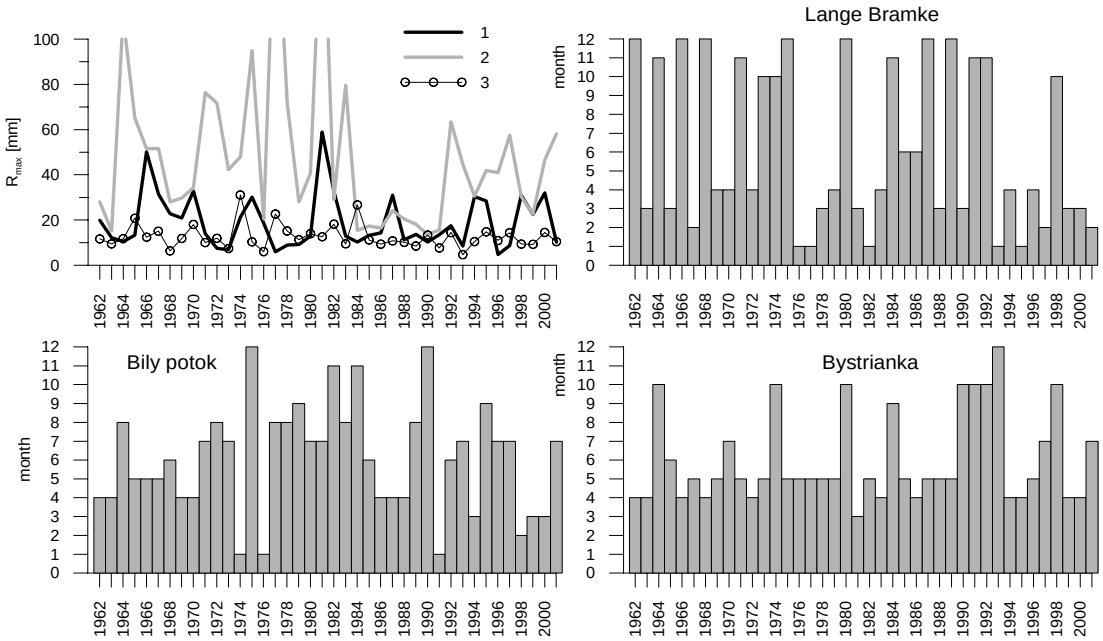


Fig. 3 Maximum daily runoff R_{max} (line chart) in the studied catchments (1-Lange Bramke, 2-Bílý potok, 3-Bystrianka) in hydrological years 1962–2001; maxima in the Bílý potok catchment in hydrological years 1964, 1977 and 1981 reached 109.8 mm.day^{-1}, 167 mm.day^{-1} and 170.6 mm.day^{-1}, respectively. The bar charts show the month of occurrence of R_{max} from January (1) to December (12).

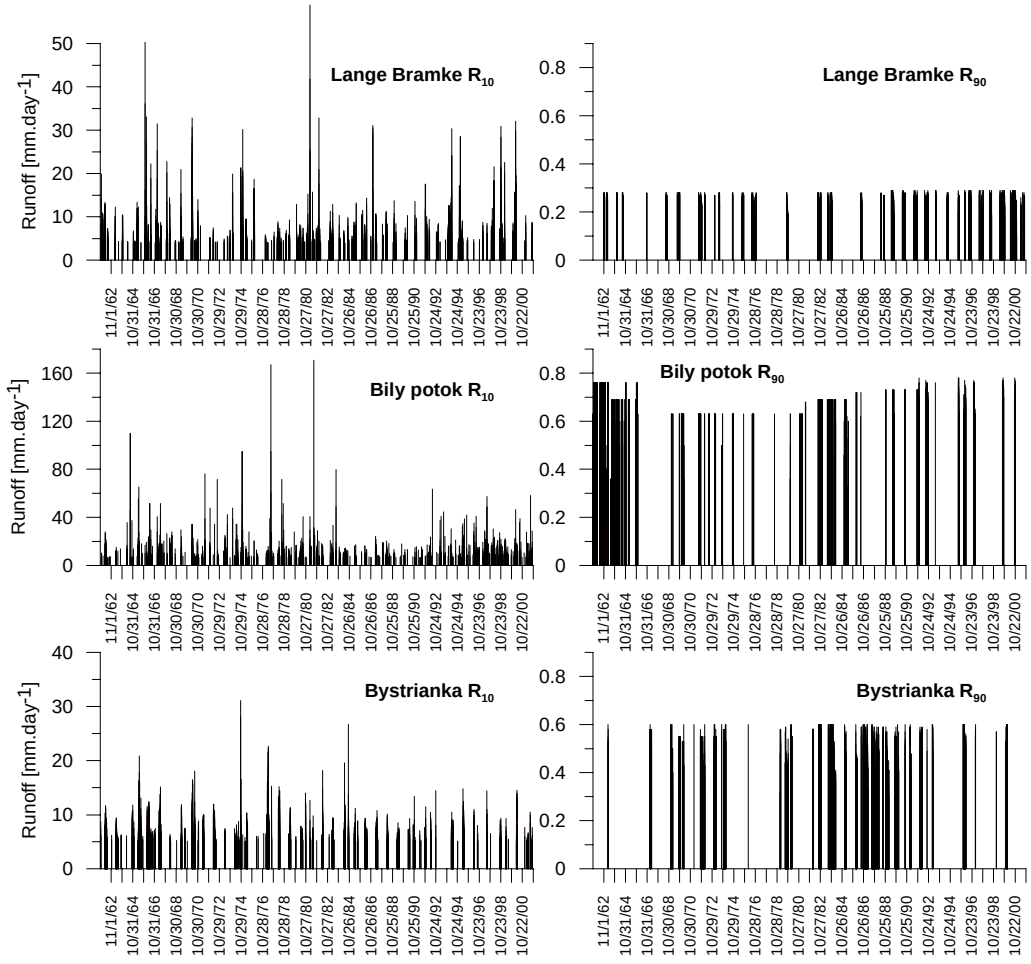


Fig. 4 Time series of high and low flows; R_{10} is the threshold that represents the highest 10% and R_{90} the lowest 10% of measured daily runoff, respectively.

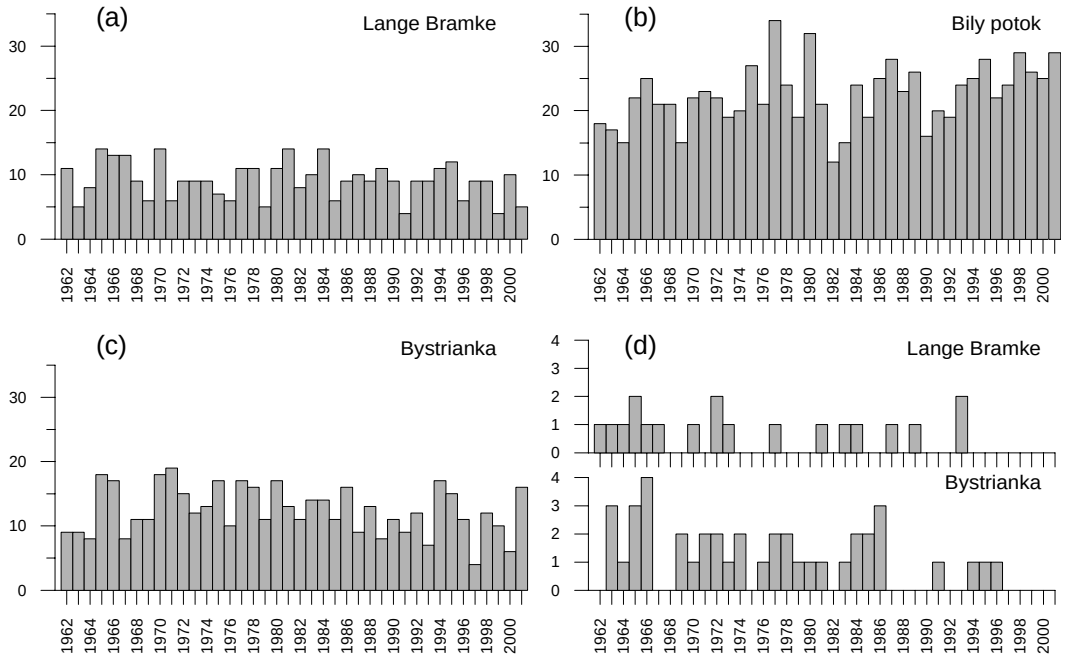


Fig. 5 Number of runoff events in hydrological years 1962–2001 (a)–(c); (d) shows the number of events in August.

Further analysis was devoted to the highest 10% of the daily flows (R_{10}). These flows are equal to runoff that is equal or higher than 3.87, 6.32 and 5.04 mm day^{-1} in Lange Bramke, Bílý potok and Bystrianka, respectively. The highest occurrence of R_{10} in the Lange Bramke catchment was observed at the beginning of 1980s (Fig. 4). Bílý potok is the only catchment in which the occurrence of R_{10} seems to increase since 1992, although the maxima are lower than in earlier decades (Fig. 4). R_{10} in the Bystrianka catchment decreased in the 1990s.

The final analysis focused on the number of runoff events and droughts in particular years (Figs 4 and 5). The frequency of dry periods increased recently in only the Lange Bramke catchment. In the other two catchments, it decreased. The number of runoff events, i.e. the events with the peak flows reaching or exceeding the mean runoff, in the Lange Bramke and Bystrianka catchments in 1992–2001 decreased slightly (Fig. 5). Analysis of seasonality has shown that since the 1980s the runoff events in the Lange Bramke catchment in May to August almost disappeared. The reduction in the number of events in August in the last years was also found in the Bystrianka catchment.

DISCUSSION

The main objective of our analysis was to evaluate the hypothesis that high flows in small undisturbed catchments occur more frequently in the present than in the recent past. This hypothesis was not confirmed in these three, undisturbed study basins. This suggests that the increase in damage caused by floods that was reported in the past few years was not caused by increased high flows in small undisturbed catchments and thus has other causes.

We realize that big floods are often connected with large river basins. Nevertheless, we believe that data from small catchments can be good indicators of changes and causes in the frequency of floods. There are several reasons for such an argument. The network of properly selected small catchments has been successfully, and repeatedly used to represent the regime of large river basins (Balek, 2006). Small catchments often have more consistent data than large river basins and the devastating floods often originate in small catchments (e.g. Balek, 2006).

CONCLUSIONS

The analysis of measured runoff data from three small, relatively undisturbed Central European catchments did not indicate an increasing frequency of high flows. On the contrary, the maxima

measured in the last two decades do not reach the values that occurred in the previous two decades.

The only obvious changes in daily runoff seem to be observed in the Lange Bramke catchment. This catchment has an oceanic climate and maximum annual runoff in the catchment in the last decade rarely occurred in October–December. At the same time, the number of runoff events in May to August was substantially reduced and dry periods have been rather frequent since the mid-1990s. A reduction of the number of events in August was also found in the Bystrianka catchment.

Statements on increasing frequency of floods should be supported by the analysis of measured data. Regionalization of high flow data from small catchments provided by international networks has the potential to address this issue and highlight the regions with changing hazards. This potential has not been fully used until now.

REFERENCES

Adamčák, M. & Filip, J. (1999) *Floods in Slovakia*. Bratislava (in Slovak).

Balek, J. (2006) Small basins as a continuous source of information. in Czech with an extended English abstract. *J. Hydrol. Hydromech.* **54**(2) (in press).

Brázdil, R., Dobrovolný, R., Elleder, L., Kakos, V., Kotyza, O., Macková, O. &Valášek, H. (2005) Study of historical floods in the Czech Republic as a contribution to the historical hydrology. In: *Czech Hydrologické dni 2005* (ed. by O. Majercakova, K., Nachazel & J. Szolgay) (September 2005, Bratislava, Slovakia), 321–329. ISBN 80-88907-53-5.

Glaser, R. (2001) *Klimageschichte Mitteleuropa. 1000 Jahre Wetter, Klima, Katastrohpen*. Primus Verlag, Darmstadt, Germany.

Pardé, M. (1933) Le régime des cours d'eau de l'Europe orientale (en collaboration avec St. Kolupaila). *Revue Geographie Alpine* **XXI**(4), 651–748.

Pekárová, P. (2003) *Dynamics of Runoff Variability in Slovak and World Rivers*. VEDA, Bratislava (in Slovak).

Sturm, K., Glaser, R., Jacobeit, J., Deutsch, M., Brázdil, R., Pfister, C., Luterbacher, J. & Wanner, H. (2001) Hochwasser in Mitteleuropa seit 1500 und ihre beziehung zur atmosphärischen Zirkulation. *Petermanns Geographische Mitteilungen* **145**(6), 14–23.

Climate Variability and Change—Hydrological Impacts (Proceedings of the Fifth FRIEND World Conference held at Havana, Cuba, November 2006), IAHS Publ. 308, 2006.

A national study on trends and variations of French floods and droughts

M. LANG[1], B. RENARD[1], E. SAUQUET[1], P. BOIS[2], A. DUPEYRAT[3], C. LAURENT[3], O. MESTRE[4], H. NIEL[5], L. NEPPEL[5] & J. GAILHARD[6]

1 *Cemagref, U.R Hydrologie-Hydraulique, 3 bis quai Chauveau, F-69336 Lyon cedex 03, France*
michel.lang@cemagref.fr

2 *LTHE, BP 53, F-38 041 Grenoble cedex 09, France*

3 *EDF /LNHE, 6 quai Watier, BP49, F-78401 Chatou cedex, France*

4 *Météo-France, Ecole Nationale de la Météorologie, 42, ave G. Coriolis, F-31057 Toulouse cedex, France*

5 *Maison des sciences de l'eau Laboratoire Hydrosciences, 300 ave Emile Jeanbrau, F-34095 Montpellier, France*

6 *EDF/DTG, 21 ave de l'Europe, F-38040 Grenoble cedex 9, France*

Abstract A French national project was set up in 2002 in order to study the variation of floods and droughts in France, based on a large set of discharge data series. Numerous approaches can be used to study trends and variations on hydrological data series, e.g. statistical tests, segmentation procedures, Bayesian approaches, and multivariate or regional models. A comparative analysis aimed at defining a general framework for the selection of a limited number of tests, based on the statistical properties of the hydrological data series (sample size, autocorrelation) and the prior knowledge of the type of distribution and the expected change. The first results on a set of about 200 French long data series do not show conclusive proof that climatic change has affected flood and drought regimes. A Bayesian model has finally been developed to incorporate hydrological nonstationarity into frequency analysis, using MCMC algorithms for the weighting of different time dependent models.

Key words floods; droughts; nonstationarity; climate change ; trends; France

INTRODUCTION

As stated by the last report of the International Panel for Climate Change (IPCC, 2001): "*The Earth's climate system has demonstrably changed on both global and regional scales since the pre-industrial era, with some of these changes attributable to human activities*"**.** Such an assessment, which was only a hypothesis one decade ago, is today considered as a fact. Several climate variables have changed due to the increase of the carbonic gas concentration in the atmosphere. The average earth temperature has increased by about 0.6°C (±0.2°C) since 1900, with an increase in the number of hot days and a decrease in the number of days of frost. Rainfall is supposed to have increased, at least in the northern hemisphere, despite strong regional differences (e.g. dryness in West Africa for the last 30 years). The spatial extent of snow and glaciers has also significantly decreased. Predictions of the Global Circulation Models (GCM) are qualitatively in agreement with a continuation of these trends. However, such predictions are affected by strong uncertainties. Firstly, the GCMs are sensitive to the various scenarios for carbonic gas concentration increase. Moreover, additional uncertainty has to be considered from physical processes at a small spatial scale, which are not precisely modelled. Lastly, predictions can differ significantly between GCMs. Therefore, the prediction of the temperature increase in 2100 is estimated between +1.4 and +5.8°C. The effects of the global warming on floods and drought regimes are even more difficult to assess as both evaporation and rainfall are supposed to increase. Furthermore, the impacts will be dependent on the flow regime (rainfall- or snow-related floods). A downscaling procedure is also needed to convert the large spatial and temporal scales of the GCMs to the hydrological scale of the rainfall–runoff models. Nevertheless, the studies from Kharin & Zwiers (2000) and Voss *et al.* (2002) show an increase in extreme precipitations in a future climate, together with an increase in extremely long dry spells, which might result in more severe hydrometrical extremes, both for floods and droughts. However, no significant and consistent change in runoff has been observed up to date at a global scale, even if some changes do exist at a regional scale (e.g. Hisdal *et al.*, 2001, for droughts).

After each catastrophic flood and drought, hydrologists are asked about the existence of trends due to human activities in basins or global warming. It is of primary importance to define the "natural" variation of the flow regime, in order to assess the internal and external long-lasting

Copyright © 2006 IAHS Press

actions. Moreover, the stationarity of the hydrological series is usually one of the main assumptions in flood or drought frequency analysis. This assumption should be relaxed when dealing with the effect of man's activity. A French national project, the National Research Programme on Hydrology (PNRH), on nonstationary flow series was set up in 2002 in order to study the variation of floods and droughts in France, based on a large set of discharge data series (Lang *et al.*, 2003). Three main objectives have been assigned to the PNRH project:

– to define a general framework for the selection of a limited number of tests for the detection of changes in hydrological series;
– to give an answer about the stationarity of floods and droughts in France;
– to develop a statistical tool which enables incorporating nonstationarity into frequency analysis.

GENERAL FRAMEWORK FOR THE DETECTION OF CHANGES

Methods

Various approaches can be used to evaluate the stationarity of a series (descriptive methods, segmentation procedures, Bayesian analyses, multivariate data analyses). The graphical approaches have been used in this project as a preliminary analysis. The segmentation procedure has not been used, mainly because the significance level is not easily computable for non-Gaussian extreme variables. We chose to focus on univariate statistical tests, in order to evaluate the significance of the possible changes, and to use a Bayesian approach for nonstationary frequency analysis.

Comparative analysis of statistical tests

Numerous studies have presented comparative analyses, but without a clear conclusion about the "best" procedure to apply for a specific problem. For example, Kundzewicz & Robson (2004) recommend the application of nonparametric tests because they are almost as powerful as parametric tests, with no distributional assumptions. In contrast, Zhang *et al.* (2004) favour the use of parametric tests adapted to extreme values, as the power is significantly improved.

Monte Carlo simulations have been developed within the PNRH project in order to define a general framework for the detection of changes on extreme hydrological values. The main criteria were the preservation of the significance level, the power (ability to detect a small change) and the robustness on departure from initial assumptions (e.g. distribution, independence). Parametric tests based on the likelihood ratio between two alternative hypotheses (LR tests) appear to be the most powerful, especially for extreme data, provided that the distributional assumptions (e.g. Generalized Extreme Value (GEV) or Generalized Pareto distributions) are fulfilled by the data. Such tests have only been scarcely used for climate change detection these last years (Coles, 2001; Zhang *et al.*, 2004; Parey *et al.*, 2006). Furthermore, a general framework for the selection of tests has been developed (Fig. 1 and Table 1), taking into account a possible autocorrelation, the distribution type, the type of change and the length of the data series.

Table 1 Applied trend tests for various hydrological variables.

Variable	Distribution	Autocorrelation, ρ	Applied trend-test
Annual maximum	GEV	No	LR
POT	Generalized Pareto	No	LR
Annual number of floods	Poisson	No	LR
Inter-arrival duration	Exponential	No	LR
VCN30	GEV	Has to be checked	MMK if ρ significant, LR otherwise
QCN30	GEV	Has to be checked	MMK if ρ significant, LR otherwise
Volume deficit	unknown	Has to be checked	MMK if ρ significant, MK otherwise
Drought duration	unknown	Has to be checked	MMK if ρ significant, MK otherwise

Abbreviations**:** LR: likelihood ratio; MMK: Modified Mann-Kendall; MK: Mann-Kendall.

Field significance of local tests

The significance level $(1 - \alpha)$ of a local test can be related to the risk α of being mistaken when rejecting the null hypothesis of no change. The question is to assess the regional significance level

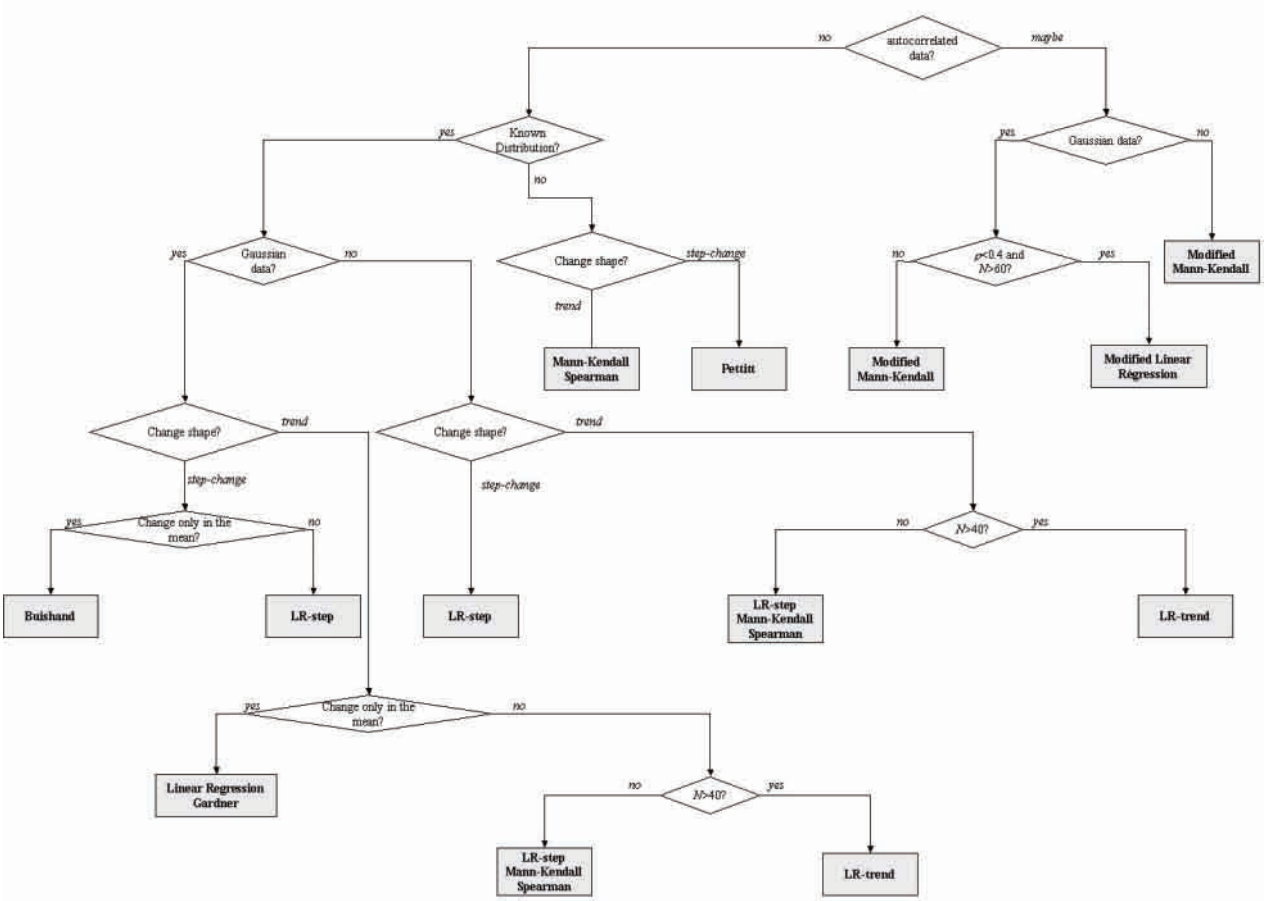


Fig. 1 Selection of a test for identifying change within a sample of hydrological extreme values.

$(1 - \alpha')$ when applying local tests on a data set of N stations. For example, a 5% test should, on average, be significant at 5 of 100 stations. But what would be the conclusion if the null hypothesis is rejected 6, 10 or 20 times? It is therefore necessary to develop a regional framework which enables the assessment of the minimum percentage of locally significant changes in order to ensure the field significance at risk α'. It should be pointed out that such an analysis is different from the detection of a regional change, as only the number of rejections is here considered, even if opposite diagnoses (increase/decrease) are possible at two similar stations.

Such regional significance has already been studied by Douglas *et al.* (2000) and Yue & Wang (2002) for instance, but is hardly used for the detection of environmental changes. Renard & Lang (2006) also proposed a Monte Carlo simulation based on a Gaussian copula which takes into account the spatial dependence between sites, to assess the field significance of changes. However, based on simulated spatial data, we found that the Bootstrap-based procedure of Douglas *et al.* (2000) was the most robust tool for this purpose.

Detection of a regional change

Climatic change is likely to have a regional impact which shows a spatial consistency on homogeneous hydroclimatological areas. It is therefore interesting to study the spatial consistency of observed changes. A first approach is to compute regional variables, such as the annual number of flood events within a region or the mean date of annual minima. A multivariate problem is therefore transformed into a univariate problem. A second approach consists in computing a statistic which is defined on the whole regional data set. As an example, Douglas *et al.* (2000) and Yue & Wang (2002) adapted the Mann-Kendall test to a regional data set, taking into account the mean correlation between sites. A third approach is currently under development by Renard (2006) and consists in estimating a regional distribution based on GEV margins, with local (e.g. position or scale) and regional (e.g. shape with a trend) parameters. A first application was presented by

Renard *et al.* (2006a) for a set of six French discharges stations. A major issue in regional trend estimation is related to the difficulty of describing spatial dependence for extreme values. Renard & Lang (2006) proposed an approximation based on a Gaussian copula for extreme rainfalls, but further developments are likely to improve such a description.

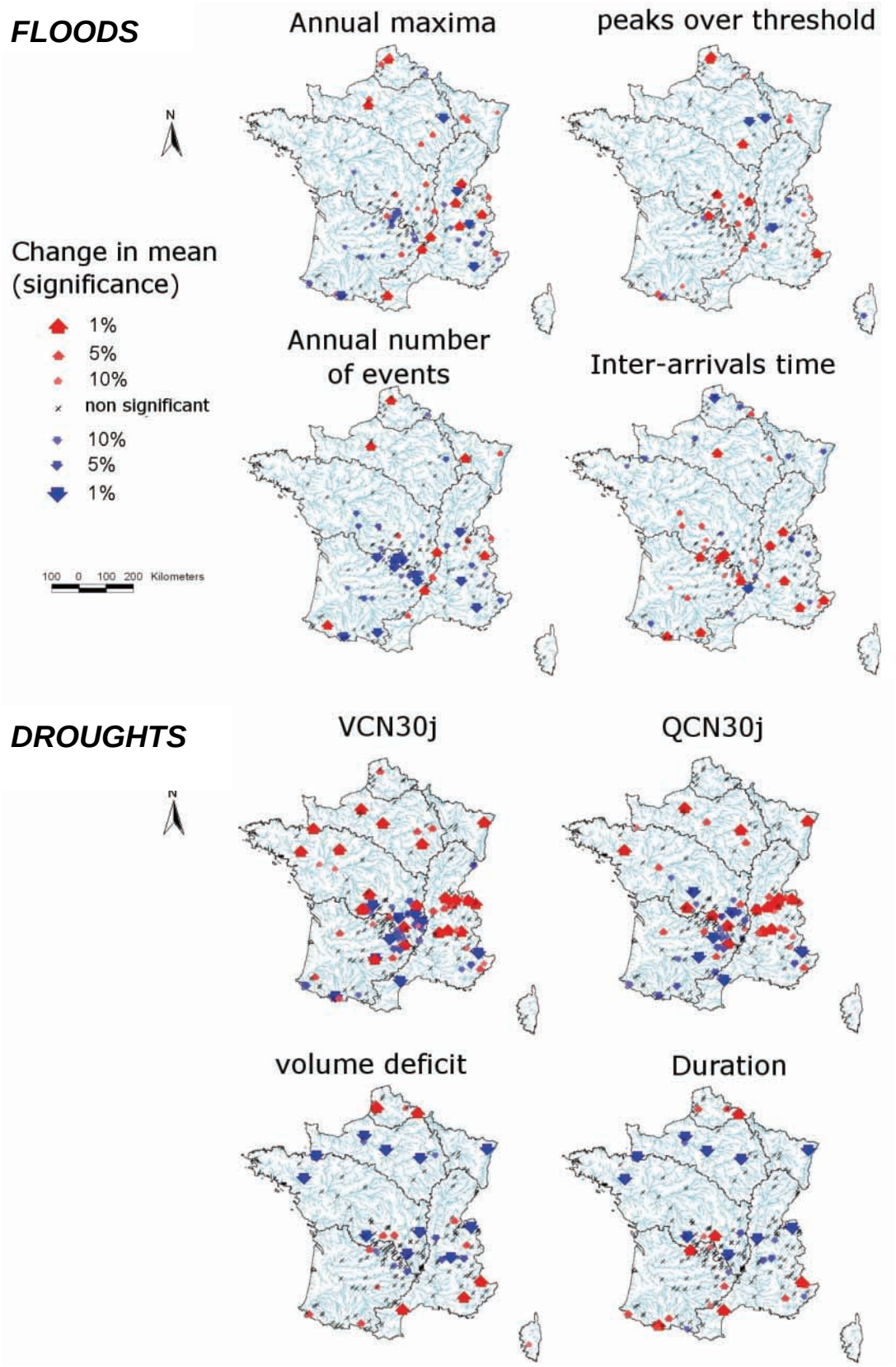


Fig. 2 Detection of changes on French extremes for floods and droughts.

Probabilistic approach in a nonstationary context

Renard *et al.* (2006b) have developed a Bayesian approach for incorporating possible non-stationarity in floods or droughts frequency analysis. The approach is based on the estimation of the posterior probability of several time-dependant models (stationary, shift, trend). Each model is therefore weighted with its relative probability and the final combination gives a distribution relative to a fixed date (today, in 10 years, in 50 years …), which incorporates nonstationarity as an additional uncertainty. Specific work has been undertaken by Renard *et al.* (2006a) in order to study the Monte Carlo Markov Chain (MCMC) procedures which are necessary for this Bayesian analysis.

RESULTS AND DISCUSSION

Following the general framework for trend detection (Fig. 1 and Table 1), Fig. 2 shows the detected changes on a set of 192 French hydrometric data series, with at least 40 years of record. No consistent trend emerged in the analysis of the flood magnitude (annual maximum (AM) or peak-over-threshold (POT) values), contrary to the significant increase in flood damages, which can be explained by the greater exposure to flooding. The number of flood events seems to decrease in a part of the data set, and therefore the duration between two successive events is increasing.

The procedure shows a different result for droughts, as the detected changes are more significant on the minimum discharges (annual minima of 30 days mean discharges *VCN30*, and annual minima of 30 days non-exceeded discharges *QCN30*). In contrast, the cumulated deficit of volume and the duration of droughts, computed from discharges not exceeding a low threshold, are less sensitive. Further investigations are necessary to explain such changes and to understand what is related to human influences (reservoir for drought compensation, pumped storage) and to climatic influences (dry periods).

CONCLUSIONS

The first and third objectives of the PNRH project have been achieved: a specific framework for the detection of trends and step changes has been developed for extreme value analysis (flood and drought) and a Bayesian model has allowed the incorporation of nonstationarity into frequency analysis. The second objective is currently under development (at the time of writing this paper) and will be realized at the end of 2006 (Renard *et al.*, 2006c,d). The first results on a set of 192 French long data series do not show conclusive proof that climatic change has affected flood and drought regimes. Complementary analysis is planned to consider the various explanations on the detected changes: data measurement errors, human activities on the catchment or climatic changes.

The various contributions of this project (MCMC software, methodological reports, results) are available on the following web site: http://www.lyon.cemagref.fr/hh/PNRH-NS/.

Acknowledgements This study has been funded by the PNRH programme. Benjamin Renard's work for his PhD has been sponsored by Cemagref and EdF. The authors wish to thank the French Ministry of Ecology and the various managers of hydrometric networks (Diren, EdF, Cnr) for allowing them to use and study the long discharge series.

REFERENCES

Coles, S. (2001) *An Introduction to Statistical Modeling of Extreme Values.* Springer-Verlag, Berlin, Germany.

Douglas, E. M., Vogel, R. M. & Kroll, C. N. (2000) Trends in floods and low flows in the United States: impact of spatial correlation. *J. Hydrol.* **240,** 90–105.

Hisdal, H., Stahl, K., Tallaksen, L. M. & Demuth, S. (2001) Have streamflow droughts in Europe become more severe or frequent? *Int. J. Climatology* **21,** 317–333.

IPCC (2001) *Climate Change 2001: Synthesis Report.* Edited by R. T. Watson and the Core Writing Team. Cambridge University Press, UK.

Kharin, V. V. & Zwiers, F. W. (2000) Changes in the extremes in an ensemble of transient climate simulations with a coupled atmosphere-ocean GCM. *J. Climate* **13,** 3760–3788.

Kundzewicz, Z. W. & Robson, A. J. (2004) Change detection in hydrological records - a review of the methodology. *Hydrol. Sci. J.* **49,** 7–19.

Lang, M., Bois, P., Mestre, O., Niel, H. & Sauquet, E. (2003) Détection de changements éventuels dans le régime des crues - Rapport de première année, projet PNRH. Cemagref, France.

Parey, S., Malek, F., Laurent, C. & Dacunha-Castelle, D. (2006) Trends and climate evolution: statistical approach for very high temperatures in France. *Climatic Change* (submitted).

Renard, B. (2006) Détection et prise en compte d'éventuels impacts du changement climatique sur les extrêmes hydrologiques en France. PhD Thesis. INPG, Cemagref, France.

Renard, B. & Lang, M. (2006) Use of a Gaussian copula for multivariate extreme value analysis: some case studies in hydrology. *Adv. Water Resour.* (submitted).

Renard, B., Garreta, V. & Lang, M. (2006a) An application of Bayesian analysis and MCMC methods to the estimation of a regional trend in annual maxima. *Water Resour. Res.* (submitted).

Renard, B., Lang, M. & Bois, P. (2006b) Statistical analysis of extreme events in a non-stationary context via a Bayesian framework: case study with peak-over-threshold data. *Stochastic Environmental Research and Risk Assessment* (in press).

Renard, B., Lang, M., Bois, P., Dupeyrat, A., Mestre, O., Niel, H., Prudhomme, C., Sauquet, E., Gailhard, J., Laurent, C. & Neppel, L. (2006c) Changes in extreme discharge in France. Part 1: At-site analysis. *J. Hydrol.* (submitted).

Renard, B., Lang, M., Bois, P., Gailhard, J., Neppel, L., Paquet E., Sauquet, E., Dupeyrat, A., Laurent, C., Mestre, O. & Niel, H. (2006d) Changes in extreme discharge in France. Part 2: Regional analysis. *J. Hydrol.* (submitted).

Voss, R., May, W. & Roeckner, E. (2002) Enhanced resolution modelling study on anthropogenic climate change: changes in extremes of the hydrological cycle. *Int. J. Climatology* **22,** 755–777.

Yue, S. & Wang, C. Y. (2002) Regional streamflow trend detection with consideration of both temporal and spatial correlation. *Int. J. Climatology* **22,** 933–946.

Zhang, X. B., Zwiers, F. W. & Li, G. L. (2004) Monte Carlo experiments on the detection of trends in extreme values. *J. Climate* **17,** 1945–1952.

Climate Variability and Change—Hydrological Impacts (Proceedings of the Fifth FRIEND World Conference held at Havana, Cuba, November 2006), IAHS Publ. 308, 2006.

Long-term trends and runoff fluctuations of European rivers

PAVLA PEKAROVA[1], PAVOL MIKLANEK[1] & JAN PEKAR[2]

1 *Institute of Hydrology, Slovak Academy of Sciences, Racianska 75, 831 02 Bratislava 3, Slovak Republic*
pekarova@uh.savba.sk

2 *Department of Applied Mathematics and Statistics, Faculty of Mathematics, Physics and Informatics, Comenius University, 842 48 Bratislava, Slovak Republic*

Abstract In this paper the occurrence of dry and wet periods for 18 major European rivers during the period 1850–1997 is analysed. Annual discharge series were standardized for three regions: West/Central Europe, East Europe and North Europe, and for the whole of Europe. The statistical analysis of these series did not confirm any long-term increase or decrease in discharge during the last 150 years. Dry cycles of about 13.5 years and 28–29 years were identified. In East Europe the occurrence of the wet and dry cycles are shifted compared to North and West/Central Europe by a few years. Similar periods have been reported in other world rivers (Amazon, Congo) as well as in the Southern Oscillation, North Atlantic Oscillation and Pacific Decadal Oscillation phenomena. The time shift of cycles in different regions is the regularity related to general oceanic and atmospheric circulation.

Key words long-term trends; discharge; Europe; natural fluctuation; wet and dry cycles

INTRODUCTION

Detection of changes in river discharge is the most important and (at the same time) the most complicated step within water resources prediction. Statistical analysis of periodicity or wet and dry cycles depends on the availability of long-term data series. Systematic measurements of runoff in the modern era started relatively late. The longest time series are available in Europe, but they do not exceed 200 years, e.g. the Göta River (1807), Rhine (1808), Neman (1812), Dnieper (1818), Weser (1821), Danube (1840), Wuoksi (1847), Elbe (1851), Neva (1859) and Loire (1863) (starting date given in brackets).

The aim of this paper is to perform a trend and runoff fluctuation analysis of discharge time series of selected main European rivers. The European runoff data series were obtained from the Global Runoff Data Center in Koblenz, Germany, and from a CD-ROM of World Freshwater Resources prepared by Shiklomanov (2000).

METHODS AND DATA

The basic methods for time series analyses of observed data are exploratory data analysis and statistical tests for step changes, periodicities (cycles) and trends. Generally, the most common assumptions in trend testing are normality (population is distributed normally) and statistical independence (randomness) of observations (Kundzewicz & Robson, 2004; Sheng & Pilon, 2004; Xiong & Guo, 2004; Callède *et al*., 2004; Radziejewski & Kundzewicz, 2004; Burn *et al*., 2004). Our main aim was to find whether, and if so when, long-term dry and wet periods occurred in the European runoff series and 18 annual runoff series have been analysed. In addition we analysed the time lag of cycles between different regions, and trend occurrence in the series.

In order to identify the cyclic component in European rivers we used the Hodrick-Prescott filter and combined periodogram (Pekarova & Pekar, 2004; Pekarova *et al*., 2003; Pekarova, 2003). The Hodrick-Prescott filter technique enables smoothing of the data series by increase of the α parameter value (the result for $\alpha \to \infty$ is the straight line). The combined periodogram method of Pekarova *et al.* (2003) consists in superposition of periodograms of different length of the same data series. Three statistical trend tests (tests of trend appearance, trend existence and for change in trend slope, according to Prochazka *et al.* (2001)) were used to identify a possible linear trend.

Missing data were completed by multiple regression of annual data (hydrological analogy) for the period 1850–1997 and standardized (value minus mean divided by standard deviation) average discharge time series were computed. The following number of discharge time series was used for the selected regions: eleven rivers in West/Central Europe, three rivers in East Europe and four in North Europe. Their locations are given in Fig. 1, and basic hydrological characteristics are presented in Table 1.

Copyright © 2006 IAHS Press



Fig. 1 Locations of the selected European rivers.

Table 1 Basic hydrological characteristics.

	River	Station	A	Since	To	Qa	qa	cs	cv	min	max	R
1	Thames	Kingston	10	1883	2000	78	7.9	0.12	0.29	30	132	2
2	Loire	Montjean	120	1863	1986	844	7.1	0.62	0.32	282	1967	27
3	Rhone	Mouth	99	1921	1986	2 052	20.7	–0.19	0.21	851	2932	65
4	Rhine	Koeln	144	1816	2000	2 087	14.5	–0.09	0.19	921	2996	66
5	Po	Pontelagoscuro	70	1918	1985	1 517	21.6	0.83	0.26	905	2617	48
6	Weser	Vlotho	18	1821	1999	172	9.8	0.11	0.26	62	284	5
7	Oder	Gozdowice	109	1900	2000	531	4.8	0.54	0.25	285	890	17
8	Vistula	Tczew	194	1900	1994	1 040	5.4	0.64	0.22	599	1780	33
9	Elbe	Decin	51	1851	2000	304	5.9	0.90	0.30	151	699	10
10	Danube	Orsova (1971:T. Severin)	576	1840	2000	5 583	9.7	0.44	0.17	3471	8265	176
11	Neman	Smalininkai	81	1812	1993	537	10.5	0.37	0.17	349	798	17
		West and Central Europe	1472			14 744	10.0					465
12	Dniepr	Locmanskaja Kamjanka	495	1818	1984	1627	3.3	0.77	0.33	673	3375	51
13	Don	Razdorskaya	378	1891	1990	778	2.1	0.87	0.40	286	1666	25
14	Volga	Mouth	1380	1882	1998	8 038	5.8	0.10	0.18	4541	12330	253
		East Europe	2253			10 443	4.6					329
15	Goeta	Vaenersborg	47	1807	2000	535	11.4	–0.003	0.19	225	855	17
16	Neva	Novosaratovka	281	1859	2000	2 499	8.9	0.24	0.16	1340	3670	79
17	N. Dvina	Ust-Pinega	348	1881	1998	3 332	9.6	0.35	0.19	1796	5245	105
18	Pechora	Mouth	320	1921	1987	4 352	14	–0.11	0.12	3154	5549	137
		North Europe	996			10 688	10.7					338

A – area (10^3 km^2), period of observation (Since – To), Qa – average annual discharge (m^{3}s^{-1}),
qa – mean annual specific yield (L s^{-1}km^2), cs – coefficient of asymmetry,
cv – coefficient of variation, min/max – minimal/maximal mean annual discharge (m^3 s^{-1}), R - annual runoff (10^6 m^{3}year^{-1}).

In recent years many scientists have studied relationships between the atmospheric phenomena of the Southern Oscillation (SO), Pacific Decadal Oscillation (PDO) and North Atlantic Oscillation (NAO), and certain hydroclimatic characteristics including runoff (Pekarova *et al*., 2003). In this study we tried to identify the relation between the occurrence of dry and wet periods in Europe, and the Amazon and Congo basins. By the way of cross-correlation we were looking for the connection between runoff from these regions and NAO, SO, and PDO phenomena.

LONG-TERM CYCLES OF EUROPEAN DISCHARGE SERIES

The 18 time series of annual average discharge show that the driest year during the period 1850–1997 was the year 1921. Extremely wet years were found in 1926 as well as 1941 (Fig. 2). A correlation matrix of the 18 discharge series is presented in Table 2. Negative correlations exist between discharge series of North and East European rivers and those of West/Central Europe. The time shift in the dry periods between the Danube (West/Central Europe) and Neva (North Europe) runoff is shown in Fig. 3. Dry periods have a time lag of about 12 years. Typically, the dry periods in the Danube basin were accompanied by wet periods in the Neva basin in the 20th Century. Such analysis supports the hypothesis, that the dry periods do not occur in European rivers simultaneously, but they are shifted a few years depending on the location of the basins.

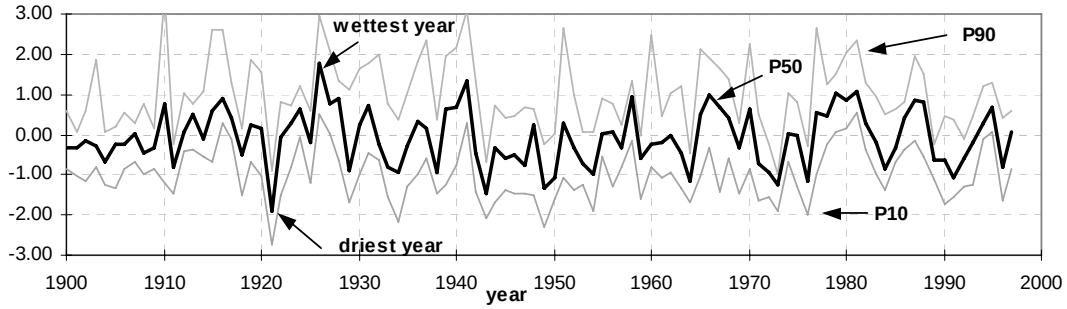


Fig. 2 Course of the 10, 50, and 90 percentiles (P10, P50 and P90) of the 18 standardized annual discharge time series of Europe for the 1900–1997 period. The driest year was 1921 and the wettest year, 1926.

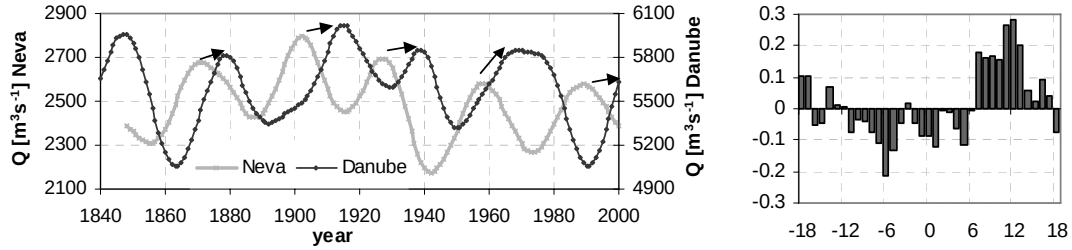


Fig. 3 Course of filtered annual discharge (m^3 s^{-1}) by Hodrick-Prescott filter HP for α = 400, Danube and Neva – left. Cross-correlation between Danube and Neva discharge (raw data) – right (time shift in years between the series is given on the x-axis).

Table 2 Correlation coefficients of annual discharge time series 1850–1997, main European rivers.

	Thames	Loire	Rhone	Rhine	Po	Weser	Oder	Vistula	Elbe	Danube	Goeta	Neman	Dnieper	Don	Volga	Neva	Dvina	Pechora
Thames	1.00																	
Loire	0.58	1.00																
Rhone	0.56	0.91	1.00															
Rhine	0.50	0.72	0.73	1.00														
Po	0.44	0.52	0.58	0.23	1.00													
Weser	0.37	0.40	0.40	0.77	0.05	1.00												
Oder	0.36	0.41	0.35	0.56	0.18	0.52	1.00											
Vistula	0.36	0.38	0.32	0.51	0.13	0.46	0.70	1.00										
Elbe	0.30	0.47	0.44	0.66	0.15	0.62	0.82	0.61	1.00									
Danube	0.34	0.47	0.46	0.61	0.17	0.46	0.52	0.67	0.69	1.00								
Goeta	0.35	0.30	0.28	0.33	0.15	0.28	0.12	0.02	0.07	*-0.02*	1.00							
Neman	0.30	0.31	0.34	0.36	0.08	0.36	0.31	0.52	0.25	0.29	0.19	1.00						
Dnieper	0.17	0.19	0.15	0.27	*-0.01*	0.34	0.27	0.45	0.25	0.34	*-0.02*	0.48	1.00					
Don	0.19	0.10	0.13	0.18	0.10	0.22	0.32	0.29	0.30	0.31	*-0.03*	0.27	0.64	1.00				
Volga	0.14	0.02	0.02	0.14	*-0.08*	0.27	0.14	0.19	0.12	0.05	0.03	0.36	0.39	0.49	1.00			
Neva	0.07	*-0.05*	*-0.02*	0.02	*-0.07*	0.11	*-0.20*	*-0.10*	*-0.13*	*-0.09*	0.28	0.27	0.07	*-0.01*	0.21	1.00		
N. Dvina	0.00	*-0.03*	*-0.06*	0.03	*-0.21*	0.10	*-0.06*	*-0.05*	*-0.04*	*-0.09*	0.03	0.22	0.12	0.17	0.58	0.38	1.00	
Pechora	*-0.01*	*0.03*	*-0.01*	0.03	*-0.13*	0.07	*-0.11*	*-0.08*	*-0.08*	*-0.17*	0.01	0.11	*-0.04*	*-0.04*	0.16	0.32	0.36	1.00

From the 18 discharge series we computed the mean runoff series (annual discharges were summed and then standardized) representing the runoff from the whole of Europe (called representative series). According to the test of normality it follows that the representative series for the whole of Europe are normally distributed. Using the Number of Runs test we can reject the hypothesis H_0 on the significance level 0.05, that is that the representative discharge series from the whole of Europe are independent. The test detected autocorrelations in the series.

In Fig. 4 calculated values of the combined periodogram and autocorrelogram with confidence intervals of the representative discharge series from the whole Europe (1850–1997) are presented. There is a statistically significant negative dependence of the discharge on the value before six years. As we can see from the combined periodogram (Pekarova *et al.*, 2003) in Fig. 4, the statistically significant period in the annual series is of 12.8 years. The other periods are 28.5, 16.4, 9, 4.2, 3.55, and 2.4 years. The non-integer results of the combined periodogram do not indicate a relation to phenomena having a 12 months periodicity (Pekarova & Pekar, 2004). The 28–29 year cycle of runoff variability can be clearly identified in the Neva River series that is naturally regulated by the Russian and Finnish lakes. Similarly, the period of 13 years was found by Kane (1997) in the precipitation series of Brazil where forecasts of droughts based on significant periodicities (13 and 26 years) gave reasonably good results.

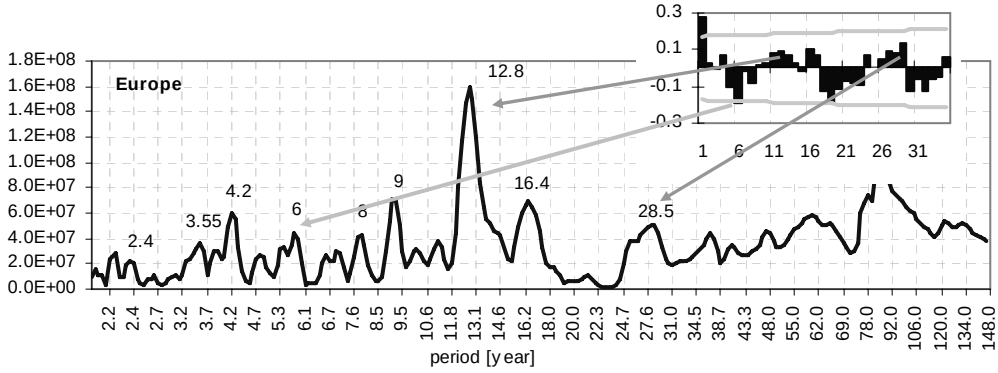


Fig. 4 Relationship between calculated values of combined periodogram (main figure) and auto-correlogram (upper right) for the representative discharge series of Europe.

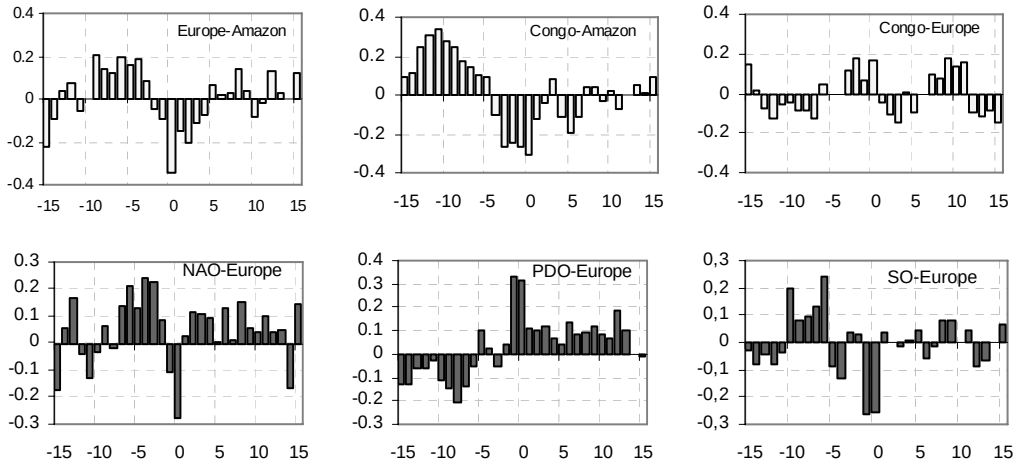


Fig. 5 Crosscorrelation between runoff (Europe, Amazon, Congo) and between runoff from Europe and NAO, PDO, and SO (time shift in years between the series is given on the x-axis).

By using cross-correlation we looked for connections between runoff from Europe and the Amazon and Congo basins, and NAO, SO, and PDO phenomena. The results of the cross-correlation analysis show a noticeable negative relationship between European runoff and the winter NAO index after Jones *et al.* (1997). Figure 5 shows that the cycle of the dry and wet period occurrence in the Amazon basin and Europe is inverse while the dry and wet periods in Europe

and in the Congo basin are generally synchronous though sometimes the peaks are shifted by 1–2 years. The analysis shows that the occurrence of dry and wet years is not fully random in individual regions but teleconnection exists between the continents. The detailed analysis of major world rivers shows that the dry and wet periods occur in different periods in different continents.

LONG-TERM TREND OF EUROPEAN DISCHARGE SERIES

For the general analysis of the long term trend of European runoff we used the representative runoff series of the whole Europe and the three regions. The filtered standardized discharge data by Hodrick – Prescott HP filter of the West and Central European time series is presented in Fig. 6(a), that of East Europe in Fig. 6(b), and that of North Europe in Fig. 6(c). Finally, the representative runoff time series for the whole of Europe is presented in Fig. 6(d) for the period 1850–1997. The representative series of Europe was tested for long-term trends.

If we want to identify any trend uninfluenced by the periodicity of the discharge time series (e.g. 13-, or 28–29 years, or any other), we must determine the trend during a closed multiple loop,

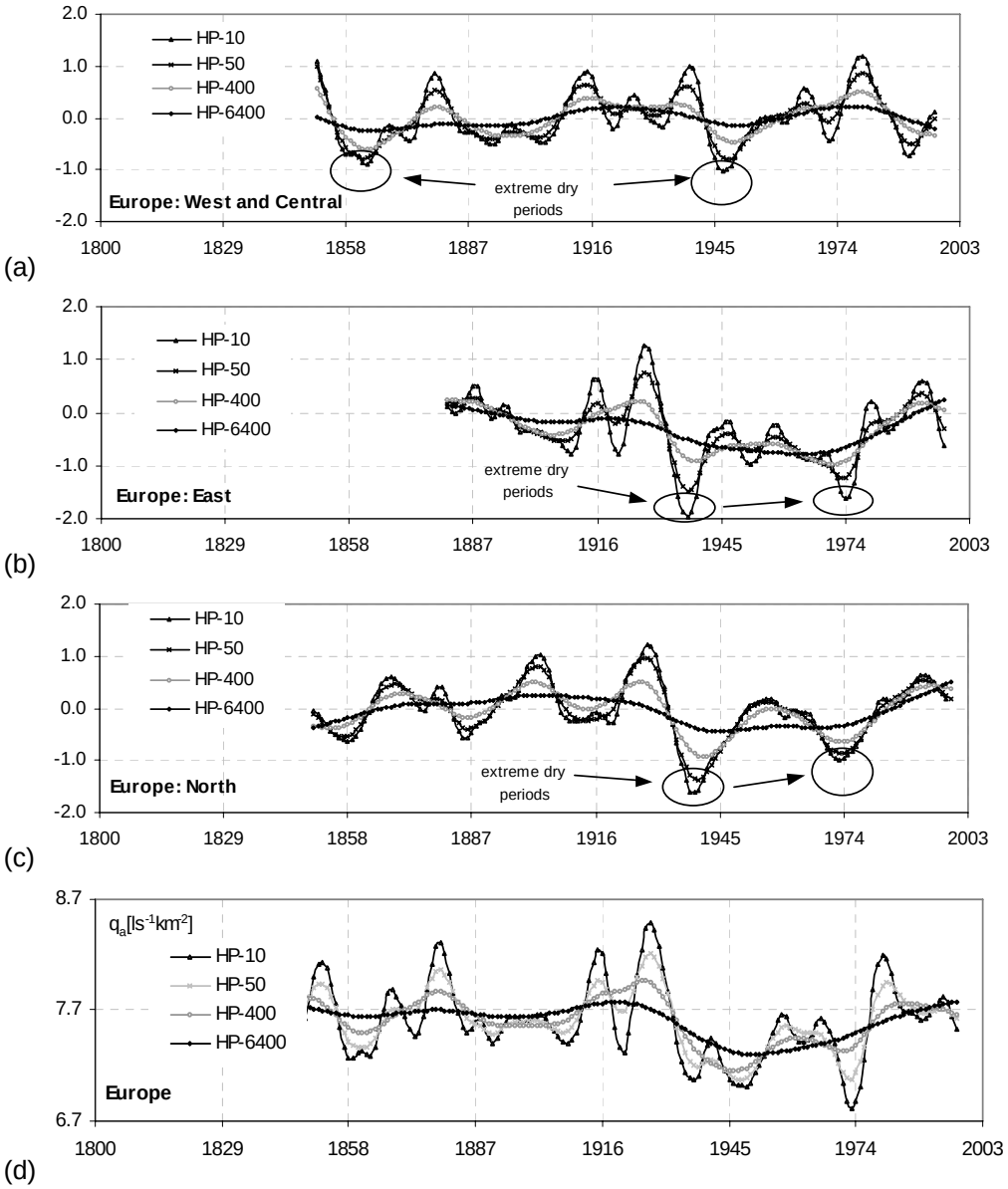


Fig. 6 Course of filtered standardized discharge during 1851–1997 for: (a) West/Central Europe; (b) East Europe; (c) North Europe; (d) Specific runoff from Europe, smoothed by Hodrick-Prescott filter HP for α = 10, 50, 400, 6400.

starting and terminating by either a minimum (e.g. 1858–1974 in Central Europe) or maximum (e.g. 1874–1988 in Central Europe). Trends determined for other periods are influenced by the periodicity of the series and depend on the position of the starting point on the raising or falling limb of the curve. In all trend tests, the H_0 hypothesis (the series fluctuates along its constant mean) was not rejected. The trend analysis does not show any significant linear trend in the long-term discharge series (1850–1997) in representative European discharge series.

From the analysis it follows that there is no statistically significant long-term continuous decrease or increase in the runoff. We can identify only dry and wet periods in river runoff series. In the case of cyclic series (and hydrological series are such) we cannot express the trend simply by the linear function and expect the continuation of the linear development in the future. If we want to apply the linear trend function, we must relate it to a specific period.

CONCLUSIONS

In this study, long-term trends and cyclicity in discharge time series of European rivers are identified. In Western Europe, extremely dry periods were those around the year 1860 and 87 years later around the year 1947. The runoff extremes (dry and wet periods) in West/Central Europe precede by 12 years the peaks in North Europe. The time lag increases with the distance between the basins. We can estimate the length of the cycles of dry periods as 12.8 and 28–29 years in both West/Central and North Europe regions. Generally, we can comment that the trend analysis did not show any significant trends in cumulative runoff series of the major European rivers in last 150 years.

Acknowledgement This work was supported by Science and Technology Assistance Agency (Slovakia) under contract no. APVT51-017804 and by the Science Granting Agency, contract no. VEGA-5056.

REFERENCES

Burn, D. H., Cunderlik, M. & Pietroniro, A. (2004) Hydrological trends and variability in the Liard River basin. *Hydrol. Sci. J.* **49**(1), 53–67.

Callède, J., Guyot, J. L., L'Hôte, Y., Niel, H. & De Oliveira, E. (2004) Evolution du débit de l'Amazone à Óbidos de 1903 à 1999. *Hydrol. Sci. J.* **49**(1), 85–97.

Jones, P. D., Jónsson, T. & Wheeler, D. (1997) Extension to the North Atlantic Oscillation using early instrumental pressure observations from Gibraltar and South-West Iceland. *Int. J. Climatol.* **17**, 1433–1450.

Kane, R. P. (1997) Prediction of droughts in North-East Brazil: role of ENSO and use of periodicities. *Int. J. Climatol.* **17**(6), 655–665.

Kundzewicz, Z. W. & Robson, A. J. (2004) Change detection in hydrological records – a review of the methodology. *Hydrol. Sci. J.* **49**(1), 7–19.

Pekarova, P. (2003) *Dynamika kolisania odtoku svetovych a slovenskych riek* (Dynamics of Runoff Fluctuation of the World and Slovak rivers). VEDA Publishing House, Bratislava, Slovak Republic.

Pekarova, P., Miklanek, P. & Pekar, J. (2003) Spatial and temporal runoff oscillation analysis of the main rivers of the world during the 19th–20th centuries. *J. Hydrol*. **274**, 62–79.

Pekarova, P. & Pekar, J. (2004) Teleconnections of AO, NAO, SO and QBO with interannual streamflow fluctuation in the Hron basin. *J. Hydrol. Hydromech.* **52**(4), 279–290.

Prochazka, M., Deyl, M. & Novicky, O. (2001) Technology for detecting trends and changes in time series of hydrological and meteorological variables – Change and Trend Problem Analysis (CTPA), User's Guide. CHMI, Prague, Czech Republic.

Radziejewski, M. & Kundzewicz, Z. W. (2004) Detectability of changes in hydrological records. *Hydrol. Sci. J.* **49**(1), 39–51.

Sheng, Y. & Pilon, P. (2004) A comparison of the power of the *t* test, Mann-Kendall and Bootstrap tests for trend detection. *Hydrol. Sci. J.* **49**(1), 21-37.

Shiklomanov, I. A. (2000) *World Freshwater Resources*. CD ROM, UNESCO, Paris, France.

Xiong, L. & Guo, S. (2004) Trend test and change-point detection for the annual discharge series of the Yangtze River at the Yichang hydrological station. *Hydrol. Sci. J.* **49**(1), 99–112.

Climate Variability and Change—Hydrological Impacts (Proceedings of the Fifth FRIEND World Conference held at Havana, Cuba, November 2006), IAHS Publ. 308, 2006.

Influence of the North Atlantic Oscillation on spatial and temporal patterns in Eurasian river flows

RAIMUND RÖDEL

Department of Geography and Geology, University of Greifswald, Jahnstraße 16, D-17489 Greifswald, Germany
roedel@uni-greifswald.de

Abstract Atmospheric circulation indices can be used to explain the variability of runoff at a continental scale. In Eurasia, besides well-known zonal anomalies of runoff that correlate with phases of the North Atlantic Oscillation (NAO), drifting fields of annual discharge anomalies exist. With the trend of the NAO these fields drift along a longitudinal direction from Western Russia to the Lena River basin in Siberia and back again. Similar observations can also be applied to changing river flow regimes. Drifting fields can be identified by a cluster approach. The centroids of the clusters can be linked to the driving processes of the NAO. Thus, the spatial drifting can be understood as an autoregressive process where the NAO-index determines the drifting direction. This paper describes the origin and causes of these fields which can explain important processes of climate variability in the Northern hemisphere.

Key words Eurasia; North Atlantic Oscillation; discharge anomalies; flow regimes; drifting fields; autoregressive process

INTRODUCTION

Large-scale changes of hydrological processes can be recorded as trends or anomalies in discharge time series. Usually the decadal and multi-decadal discharge variations in large-scale basins are examined by using time series of average annual values. Dettinger & Diaz (2000) introduce a global data set of interannual discharge variability and correlate these data with atmospheric circulation indices such as the El Nino/Southern Oscillation (ENSO) index and the North Atlantic Oscillation (NAO) index. South and North European river basins especially react sensitively to the phases of the NAO (Arnell, 1997; Popova & Shmakin, 2003).

Nevertheless in Eurasia only a quarter (24%) of gauging stations shows significant correlations between annual discharges (period 1950–1990) and the NAO-index (Hurrel, 1995). Thus Fig. 1 reflects only roughly the positive correlations with the NAO in Northern Europe while Southern Europe has negative correlations (for all gauging stations, Fig. 2). Arnell (1997) described such a pattern for the correlation of European winter discharges with the NAO-index.

Long-term correlations of river flows with climate indices presuppose that regions reacting to climatic fluctuations stay spatially stable. Under spatially non-persistent conditions the correlation between large-scale climate variability and river flows can be better explained by a time dependent spatial process.

DATA

In this paper long-term variability of annual discharges and seasonal figures with regard to climate variability of the northern hemisphere is described using 3241 Eurasian discharge time series provided by GRDC (Global Runoff Data Centre), NCAR ds552.1 and ds553.2 (Bodo, 2001) as well as from ArcticRiverNet. Nearly 70% of the time series used are longer than 30 years but 70% contain data before 1984, and 30% data before 1985. For detailed studies the climatological normal period, 1960–1990 was used. In, addition the dfjm NAO-index by Hurrel (1995) was used to describe the phases of the NAO.

METHODS

Anomalies in annual runoff

The first study was made by using annual deviations of the annual sums of the long-term discharge average for all gauging stations in Eurasia. By analysing maps of anomalies of annual discharges, clusters become visible which can be assumed to be a spatial response to the NAO. The driving processes are described in the Results section.

Copyright © 2006 IAHS Press

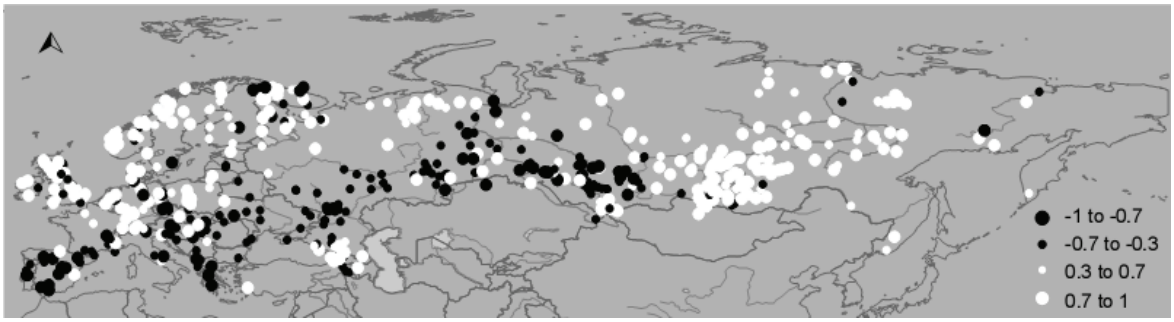


Fig. 1 Significant correlations (> |0.32|) of time series of Eurasian annual discharges with the NAO-index 1950–1990 (Hurrel, 1995).

Spatial clusters of positive and negative discharge anomalies were detected by hierarchical cluster analysis using latitude, longitude and discharge anomalies. For each year the standardized anomalies were classified using Squared Euclidian distance and Complete linkage. Subsequently, the spatial centroids of each cluster were determined by computing the weighted average of latitude and longitude. Anomalies of more than 0.5 were weighted with a factor 0.6, anomalies of more than 0.25 were weighted with a factor 0.3. All other anomalies of more than 0.1 were weighted with a factor 0.1. The computed longitudes of the centroids are visible in Figs 3 and 4.

Time dependent varying seasonal figures

In addition to the seasonally varying discharge curve, the discharge regime is overlaid by the long-term variability of the discharge regimes themselves. Thus, it is possible to detect climate fluctuations by using time series of discharge regimes. Under the influence of climatically varying boundary conditions, discharge regimes will react and show modifications. Besides a temporal variability of annual discharges, Burn & Soulis (1992) focused on seasonal discharge variability as well as on the appearance of extreme discharges and snowmelt induced floods. The latter reflect the climatic variability of hydrological processes clearest.

Elimination of impoundment effects

Many runoff time series are affected by impoundments. To assess the intensity of the impoundment impact on each gauging station their impoundment coefficients were computed. The impoundment coefficient can be calculated as the ratio of cumulated upstream dam capacity to annual discharge. Therefore all dams from the ICOLD database (ICOLD, 1998) in Europe and Russia were geo-referenced. The relevant upstream dams and their cumulated capacity were determined by using a digital elevation model and a digital river network (Rödel & Hoffmann, 2005).

Figure 2 shows the impoundment coefficients for Eurasia in 1990. For further analysis of temporal variability of flow regimes, 354 gauging stations classified as dam influenced (impoundment coefficients >0.001) were removed from the data set.

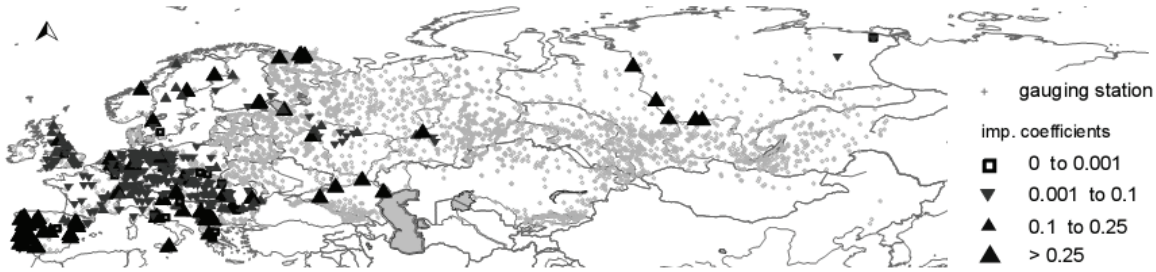


Fig. 2 Impoundment coefficients for Eurasia in 1990.

Balance point drift of discharge regimes

For analysing regime changes, annual flow regimes were determined as an order of discharge coefficients, q_i (equation (1)):

$$q_i = Q_i / Q_{Year} \text{ with } \sum_{i=1}^{n} q_i = 1 \qquad q_i \geq 0, \qquad i = 1,\ldots,12 \tag{1}$$

where Q_{Year} is the annual discharge and Q_i is the monthly discharge. When the monthly discharges are standardized in this way, the transitions between the regimes of successive years appear abrupt. Unless the discharge sums of two successive years are virtually the same, the last month of year one and the first month of year two will have different coefficients, even if discharge is the same in both months. To minimize this distortion, the one-year period that the description of the runoff regimes was based on, was delimited in a way resembling the method used for hydrological years. The beginning of the annual cycle was defined by that month *i* which had the lowest square deviation from its average discharge value over the whole time series:

$$\sum \left(Q_i - \overline{Q_i}\right)^2 \rightarrow Min! \tag{2}$$

Finally, changes in flow regimes were determined as an interannual shift of the balance point. The balance point is reached in that month *i* for which equation (3) is valid:

$$\sum_{1}^{i} q_i \geq 0.5 \tag{3}$$

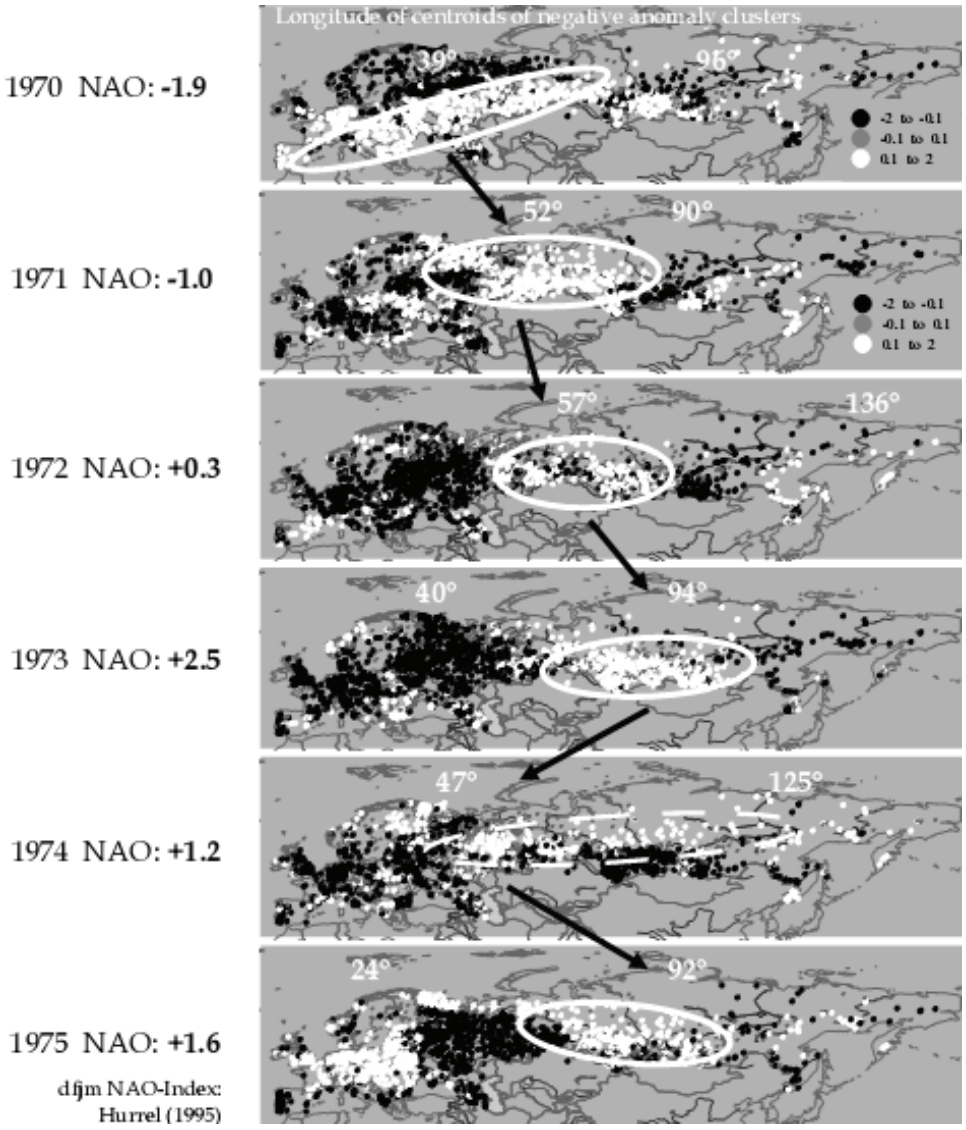


Fig. 3 Upward trend of the NAO; a field of positive anomalies (wetter than average) of the annual discharges drifts from Europe to Eastern Siberia. The longitudinal position of the clusters can be assumed as a process response to the NAO.

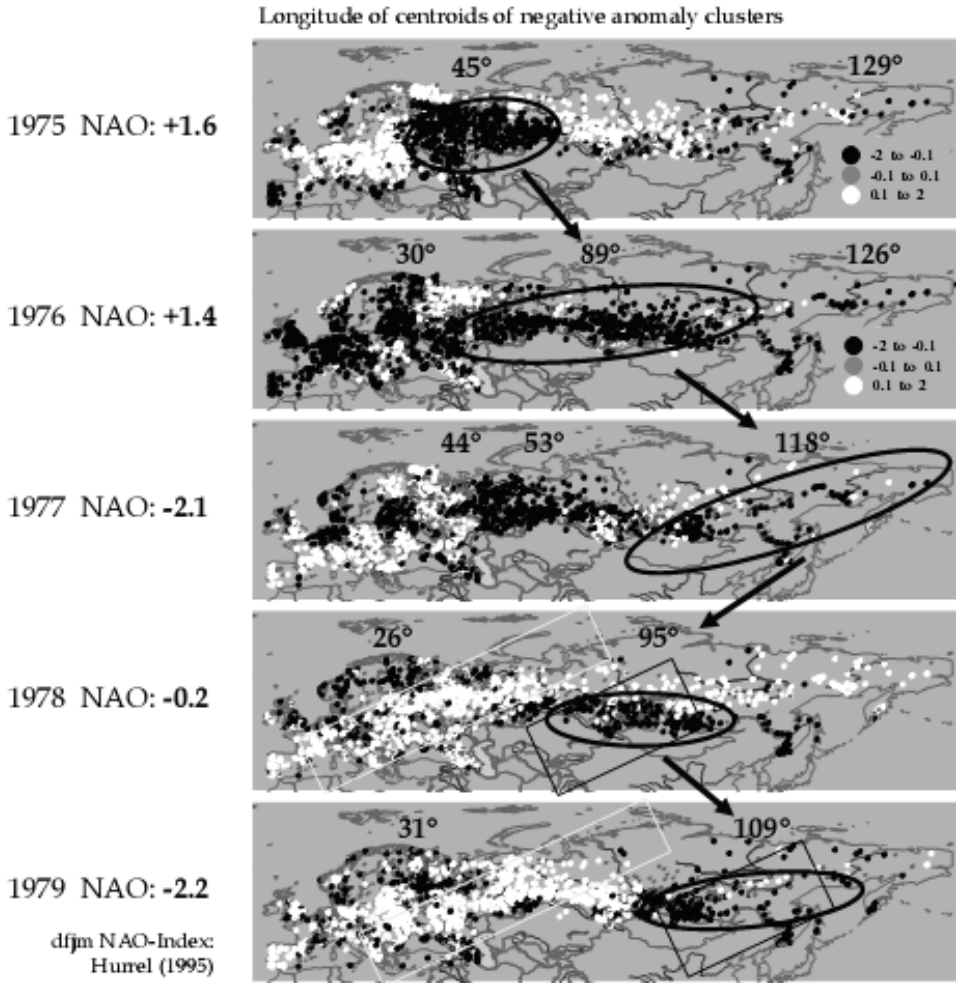


Fig. 4 Downward trend of the NAO; a field of negative anomalies (dryer than average) of the annual runoff drifts from western Siberia to eastern Siberia. The longitudinal position of the clusters can be assumed as process response to the NAO. Note the rectangles in the lower two pictures; these reflect the dipole-structure of the NAO reaction in river flows (Arnell, 1997), which is rotated and drifted eastward.

If the monthly discharge is constant (1/12 of the annual discharge), the balance point falls exactly in the sixth month of the cycle. To analyse the long-term variability of the balance point, the mode of balance points was calculated for each time series. Annual deviations from the mode were treated as positive or negative shifts of the balance point.

Negative balance point shifts co-occur with steep-shaped or earlier-than-usual runoff maximum peaks. Negative shifts are typical for years with an above-average temperature and an earlier-than-usual snowmelt in Northern Eurasia. Positive balance point shifts are typical for flat-shaped runoff maximum peaks that occur later in the year than usual. In Northern Eurasia, these shifts frequently occur in years in which the temperature is relatively low during the flood formation phase (snowmelt).

RESULTS

Large scale patterns in annual runoff

Figures 3 and 4 show deviations of long-term annual discharges during a downward trend and an upward trend of the NAO. Besides the dipole structure with higher runoff in Northern Europe and lower runoff in Southern Europe during a significantly positive NAO phase (Arnell, 1997), drifting fields of anomalies in annual runoff can be detected. These fields drift with the trend of the NAO along a longitudinal direction.

During a downward trend of the NAO, fields of reduced discharges (represented as negative anomalies of the long-term average of the annual discharges) drift eastward from Western Russia up to the Lena catchment area in Eastern Siberia (Fig. 4).

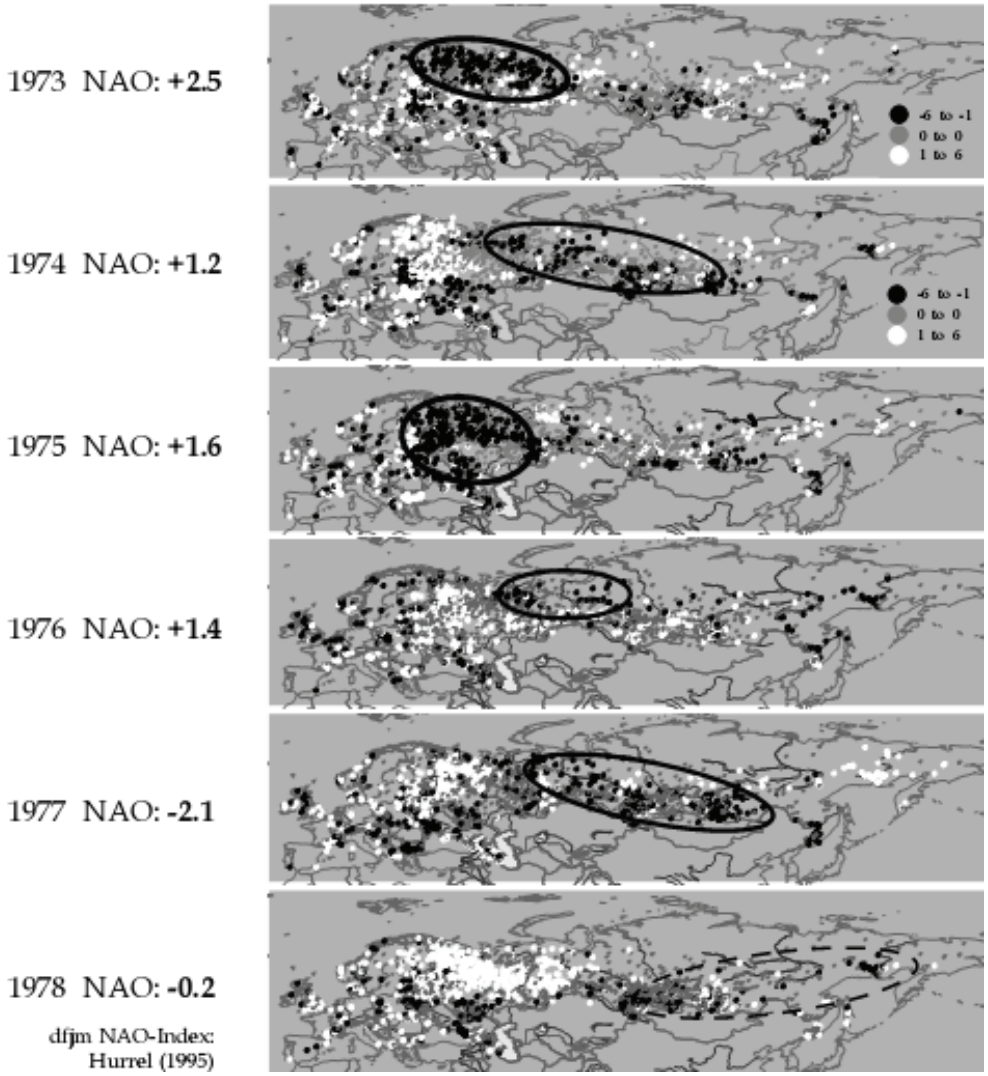


Fig. 5 Downward trend of the NAO; a field of negative shifted balance points in flow regimes (shown is shifting of balance points in each year in relation to the most frequent balance point) drifts from north-western Russia to Eastern Siberia. Strong runoff maxima which occur earlier than normal, drift to eastern Siberia.

If there is an upward trend of the NAO, a field of increased discharges drifts to the area of the Lena River basin. The westward drifting fields of higher runoff can be seen in context with an increased runoff in Northern Europe during a positive NAO phase (Arnell, 1997; Timmermann & Latif, 1998).

The NAO as the driver of large-scale pattern variations

The periodical increase of the discharges in Eastern Siberia seems to explain the dependence between the NAO variability and the variability of discharges. Mysak (1999) stated that fluctuations of annual discharge in large-scale basins are strongly correlated with decadal climate fluctuations and show response processes with them. He postulates that the long-term varying discharge volumes of the Mackenzie basin as a major reason for the formation of great ice and salt anomalies (GISA) in the North Atlantic. These anomalies influence the intensity of the oceanic circulation with a delay of 3–4 years and control the climate of the Northern hemisphere via the NAO and AO. Reduced salinity can be seen as control pulse for a weaker thermohaline circulation in the North Atlantic during negative NAO-index periods (Timmermann & Latif, 1998). Although focusing on increased discharges in the Mackenzie basin, Mysak (1999) also emphasizes that increased discharges from Siberian streams favour the setting up of ice cover in the Arctic Ocean.

Large scale spatial patterns for varying seasonal figures

Figure 5 shows that shifts in balance points of flow regimes can also be observed as drifting fields. During a downward trend of the NAO, a field of negative shifts of the balance point drifts eastward and reaches the Lena River basin.

The balance points of flow regimes were shifted into the preceding months during mild winters or flow regimes are characterized by steep-curved runoff maxima. If the pattern of a positive NAO (dipole of annual discharges in Europe) dissolves itself, the field of negative shifted balance points drifts eastward. This can be seen in relation to the more southern position of the higher discharges and negative shifted balance points in the case of the negative NAO-index. Assuming a southeastward direction of drifting, the fields can be thought of as moving on a southwest–northeast axis which generally drifts southward in correlation with the NAO-Index. During an upward trend of the NAO, the opposite situation can be observed. Fields of negative shifted balance points drift back westward from Eastern Siberia. At the same time increased annual discharges are visible in Northern Europe.

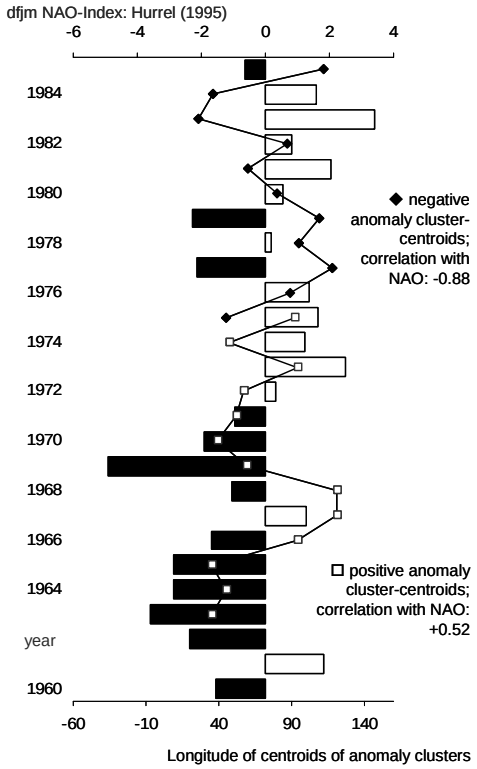


Fig. 6 Longitudinal drifting of large-scale patterns of discharge anomalies in Eurasia (lines) and the NAO-index (bars).

CONCLUSION

Assuming that the NAO is the driving process for drifting fields of discharge anomalies and that discharge represents the response of river flow to the NAO, the centroid longitudes of discharge anomaly clusters were identified (cf. Fig. 3 and 4). Fig. 6 shows the correlation between NAO and the centroid longitudes of anomaly clusters. This leads to an understanding of cluster shifting as an autoregressive process. Thus, the location of a cluster can be determined from its location at $t - 1$ and the drifting direction. The drifting direction itself can be obtained from the NAO-index. The results presented here lead to the hypothesis that discharge variability reflects large-scale hemispheric climate variability better than previously assumed (cf. Arnell, 1997; Dettinger & Diaz, 2000). Anomalies in annual discharges and shifts of the balance points of annual flow regimes point to those regions which are important for the processes of climate variability in the northern hemisphere. The NAO provides a basis for explaining large-scale anomalies of the annual discharges and of the river flow regimes in Eurasia.

Acknowledgements The author thanks the GRDC—Global Runoff Data Centre, Koblenz, Germany, for providing data for several gauging stations.

REFERENCES

Arnell, N. W. (1997) Spatial and temporal variability in European river flows and the North Atlantic Oscillation. In: *FRIEND ´97 – Regional Hydrology* (ed. by A. Gustard & S. Blazkova), 77–85. IAHS Publ. 264. IAHS Press, Wallingford, UK.

Bodo, B. A. (2001) *Monthly Discharge Data for World Rivers V1.3*, NCAR: http://dss.ucar.edu/ – date of access: 10.11.2005.

Burn, D. H. & Soulis, E. D. (1992) The use of hydrologic variables in detecting climate change: possibilities for single station and regional analysis. In: *Using Hydrometric Data to Detect and Monitor Climatic Change*. Proceedings of NHRI Symposium no. 8, April 1991, Saskatoon, Canada.

Dettinger, M. D. & Diaz, H. F. (2000) Global characteristics of stream flow seasonality and variability. *J. Hydromet.* **1**(4), 289–310.

GRDC – Global Runoff Data Centre, Koblenz, Germany.

Hurrel, J. W. (1995) Decadal trends in the North Atlantic Oscillation: regional temperatures and precipitation. *Science* **269**, 676–679. For actual data see: http://www.cgd.ucar.edu/cas/jhurrell/indices.html – date of access: 10.11.2005.

Mysak, L. A. (1999) Interdecadal variability of northern high latitudes. In: *Beyond El Niño. Decadal and Interdecadal Climate Variability* (ed. by A. Navarra), 1–23. Springer, Berlin, Heidelberg, Germany.

Popova, V. V. & Shmakin, A. B. (2003) Influence of the North Atlantic Oscillation on multiyear hydrological and thermal regime of Northern Eurasia. I. Statistical analysis of observational data. *Russian Meteorology and Hydrology* **5**, 47–56.

R-ArcticNET (v3.0) (2005) http://www.R-ArcticNET.sr.unh.edu—date of access: 10.11.2005.

Rödel, R & Hoffmann, T. (2005) Quantifying the efficiency of river regulation. *Adv. Geosci.* **5**, 75–82.

Timmermann, A. & Latif, M. (1998) Thermohaline circulation—a coupled node of the NAO. *J. Climate* **11**, 1906–1931.

Zhuravin, S. A. (2002) Change of hydrological regimes over the central part of European Russia resulting from climate variations. In: *FRIEND 2002 – Regional Hydrology* (ed. by H. A. J. van Lanen & S. Demuth), 441–447. IAHS Publ. 274. IAHS Press, Wallingford, UK.

Climate Variability and Change—Hydrological Impacts (Proceedings of the Fifth FRIEND World Conference held at Havana, Cuba, November 2006), IAHS Publ. 308, 2006.

Análisis del Comportamiento Hídrico en El Salvador: posibles causas e implicaciones

ADRIANA MARIA ERAZO CHICA, TOMAS RIVAS PACHECO & OSCAR HERNÁNDEZ

Servicio Nacional de Estudios Territoriales, Kilómetro 5½ calle a Nueva San Salvador, El Salvador
aerazo@snet.gob.sv

Resumen En el año 2002 se llevó a cabo en El Salvador una investigación con relación a la reducción de caudales en la época seca, que se ha producido a nivel general en el país. De acuerdo a los resultados obtenidos, se observa una tendencia de disminución de los caudales en el tiempo en forma generalizada, con mayor intensidad en las cuencas de los ríos Tamulasco, Sumpul, Quezalapa y Torola con valores que oscilan entre 35% a 80% por debajo de los caudales promedio de la década 1970–1980. En estas zonas críticas, se analizaron las variables de precipitación, evapotranspiración potencial, cambios en el uso del suelo y cambios en la demanda en el periodo de análisis. Los resultados indican que estos elementos han experimentado variaciones en mayor o menor medida y que al interactuar generan impactos potenciados que disminuyen las cantidades de aguas superficiales disponibles en los ríos.

Palabras claves El Salvador; reducción de caudales; cambios en uso del suelo; precipitación; evapotranspiración; impacto económico-social

Analysis of river flow trends in El Salvador: possible causes and consequences

Abstract During the year 2002, research was undertaken in El Salvador concerning the reduction of flows in the rivers during the dry season, a condition that was observed widely across the country. According to the results, a general trend of flow reduction can be observed with time; the zones with highest reduction of flows are the Tamulasco, Sumpul, Quezalapa and Torola river basins, with values in the range 35 to 80% below average flows for the 1970–1980 series. In these critical zones, variables such as precipitation, potential evapotranspiration, changes in land use and changes in demand were analysed. The results show that these parameters experienced some variations and when interacting together can generate potential impacts that diminish the quantity of water in rivers.

Key words El Salvador; reduction of flows; changes in land use; precipitation; evapotranspiration; economic-social impacts

INTRODUCCIÓN

Dada la preocupante disminución de los caudales en el periodo hidrológico 2001–2002 en El Salvador, se realizó el presente estudio, con el objeto de establecer una perspectiva de las condiciones hídricas en el país y una tendencia de su comportamiento desde la década de 1970 hasta el 2002. Para lo anterior, se realizó un análisis de la variación de los caudales en el tiempo, registrados en estaciones hidrométricas ubicadas a lo largo del territorio nacional. Tomando como base los resultados obtenidos en la investigación hidrológica, se procedió al análisis de los demás componentes del ciclo hidrológico, con el propósito de verificar en que medida inciden en el fenómeno observado. Como resultado de los análisis se presentan conclusiones y recomendaciones tendientes a optimizar el manejo y análisis de la información hidrológica del país y enfocar líneas de investigación que permitan establecer posibles causas que originen la variación de los caudales en el país.

DATOS

La información base para el estudio, corresponde a los caudales promedios mensuales registrados en 17 estaciones hidrométricas del país, en el periodo de 1970 a 2002. El análisis se enfocó en el estudio caudales de la época seca y la época lluviosa.

Para el análisis de la precipitación, se seleccionaron 26 estaciones meteorológicas con registro de precipitación mensual de alrededor de 30 años y para analizar la evapotranspiración potencial, se realizaron los cálculos utilizando como insumo, promedios mensuales de temperatura, humedad relativa y radiación solar, de 12 estaciones meteorológicas, aplicando la fórmula de Hargreaves.

Los cambios de uso del suelo fueron analizados a partir de información de los años 1973 (Perfil Ambiental de El Salvador), 1992 (Mapa de Cultivos de la FAO), 1997 (Uso de Suelo del MAG), 2000 (Mapa de Vegetación del MARN).

Copyright © 2006 IAHS Press

Los aspectos Geológicos e Hidrogeológicos se analizaron a partir del Mapa Geológico de la Misión Geológica Alemana.

El análisis de variación poblacional en las zonas críticas de reducción de caudales, se realizó con base a los datos poblacionales de censos nacionales realizados en los años 1971 y 1992 y cálculo de proyecciones para el año 2002.

METODOLOGIA

Inicialmente se analizó la calidad de la información de los caudales promedios mensuales de las 17 estaciones hidrométricas estudiadas, se revisaron y en algunos casos se descartaron los datos que presentaron una tendencia completamente diferente a los promedios mensuales de cada estación, considerándolos fuera de rango, los cuales pueden deberse a una mala digitalización o a errores en las lecturas en las curvas de descarga; igualmente se excluyeron del estudio, los eventos extremos como los huracanes, ya que estos eventos podrían afectar los promedios mensuales y no son representativos de los mismos. Con la información analizada, se trazaron gráficas que representan la variación temporal de dichos caudales. Es de anotar, que en El Salvador, la mayoría de los registros del periodo de 1980 a 1992, se perdieron debido al conflicto armado que sufrió el país, y para este análisis en particular no fueron completados para tener solo evidencia de los registrados. Se trazó un mapa que refleja los porcentajes de variación de caudales a nivel nacional, de los caudales de los años 2000 a 2002 con relación a los caudales de la década 1970 a 1980. Se identificaron las zonas que presentan mayor reducción de caudales en el periodo, y se analizaron las variables de precipitación, evapotranspiración, cambios de uso de suelo, aspectos geológicos e hidrogeológicos y variaciones poblacionales en dichas zonas.

Para la información de precipitación, se comprobó su confiabilidad por el método de doble masa. Se obtuvo información estadística anual y mensual para el análisis cualitativo y cuantitativo en términos absolutos y porcentuales para la elaboración cuadros resúmenes, mapas y gráficos de precipitación y evapotranspiración potencial.

Para el análisis de la información de los usos de suelo en los diferentes periodos, se compiló, depuró y homogenizó la información recolectada, con lo que se elaboraron cuadros y figuras para la interpretación del efecto del uso del suelo en la reducción de caudales.

En los aspectos Geológicos e Hidrogeológicos, se realizó un análisis de las litologías y características hidrogeológicas de las formaciones.

La variación poblacional se estudió con base en metodología de investigación bibliográfica y de campo, la cual consistió principalmente en la selección de los municipios dentro de cada cuenca a analizar que podrían presentar una influencia directa en la disminución de sus caudales; consulta de censos nacionales y cálculo de proyecciones para el año 2002; análisis de información y visitas de campo a algunas de las comunidades cercanas a los ríos en estudio. El impacto de reducción de caudales en la población fue evaluado a través de encuestas con la población en cuanto a la utilización de estas fuentes superficiales para su consumo.

RESULTADOS

Respecto a la década de los años 70, la disminución de los caudales de la época seca se observa con mayor intensidad en las cuencas del río Torola (Fig. 1), río Tamulasco (Fig. 2) y río Quezalapa, con valores que oscilan entre 35% a 80%. Las otras cuencas presentan igualmente reducción de caudales en menor proporción, alrededor del 20% a 30%, como el caso de las cuencas del río Sucio, río Paz (Fig. 3), río Suquiapa, río Grande de San Miguel. El río Acelhuate (Fig. 4) fue el único de los ríos analizados que presentó un incremento de los caudales respecto a los promedios mensuales en la estación, en un 35% en promedio, lo cual refleja los vertimientos que en él se producen y que se han incrementado con el aumento del área urbana. En la Fig. 5 se presenta el mapa de anomalías de caudal. Para la época de lluvias, los caudales no presentan una tendencia clara de variación en el tiempo.

Con relación a la precipitación, la mayoría de estaciones experimentan disminución de la cantidad promedio de precipitación en las últimas tres décadas. En las cuencas de los ríos Tamulasco, Sumpul,

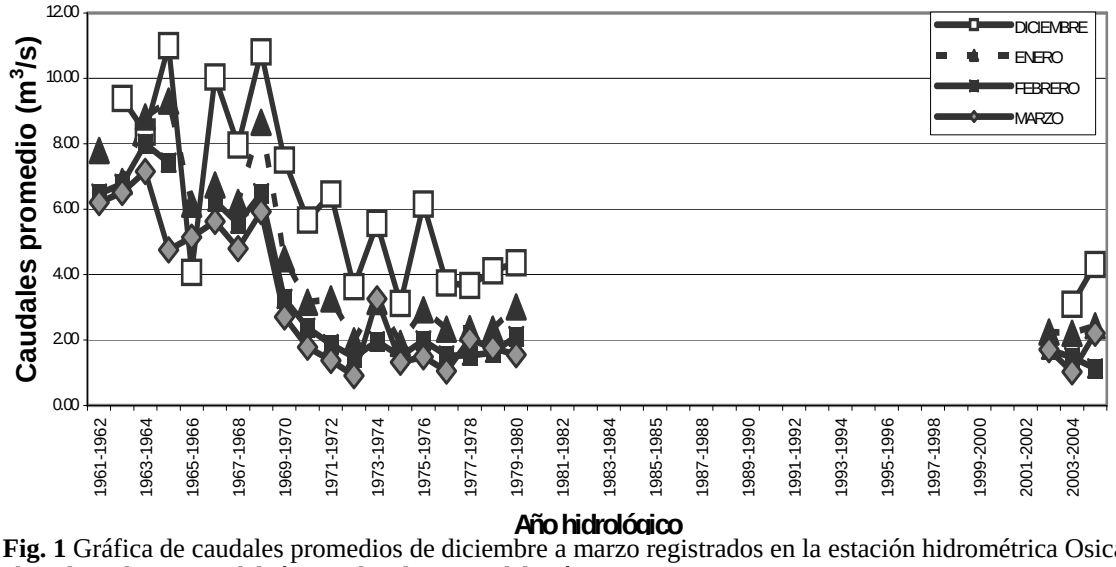


Fig. 1 Gráfica de caudales promedios de diciembre a marzo registrados en la estación hidrométrica Osicala ubicada en la cuenca del río Torola, al oriente del país.



Fig. 2 Gráfica de caudales promedios de diciembre a marzo registrados en la estación hidrométrica La Sierpe ubicada en la cuenca del río Tamulasco, al norte del país.

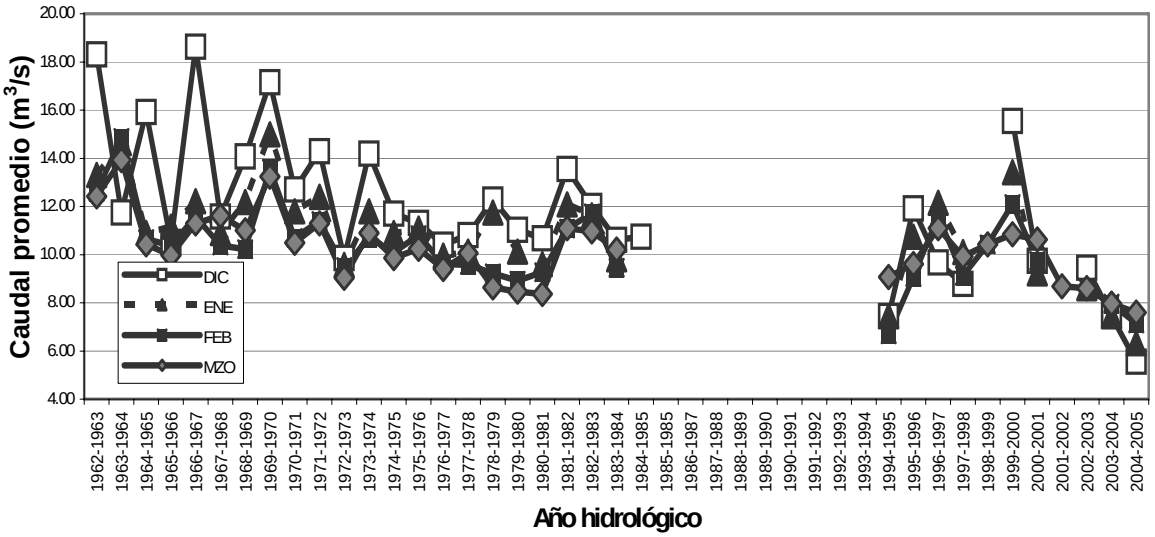


Fig. 3 Gráfica de caudales promedios de diciembre a abril registrados en la estación hidrométrica Hachadura ubicada en la cuenca del río Paz, al occidente del país.

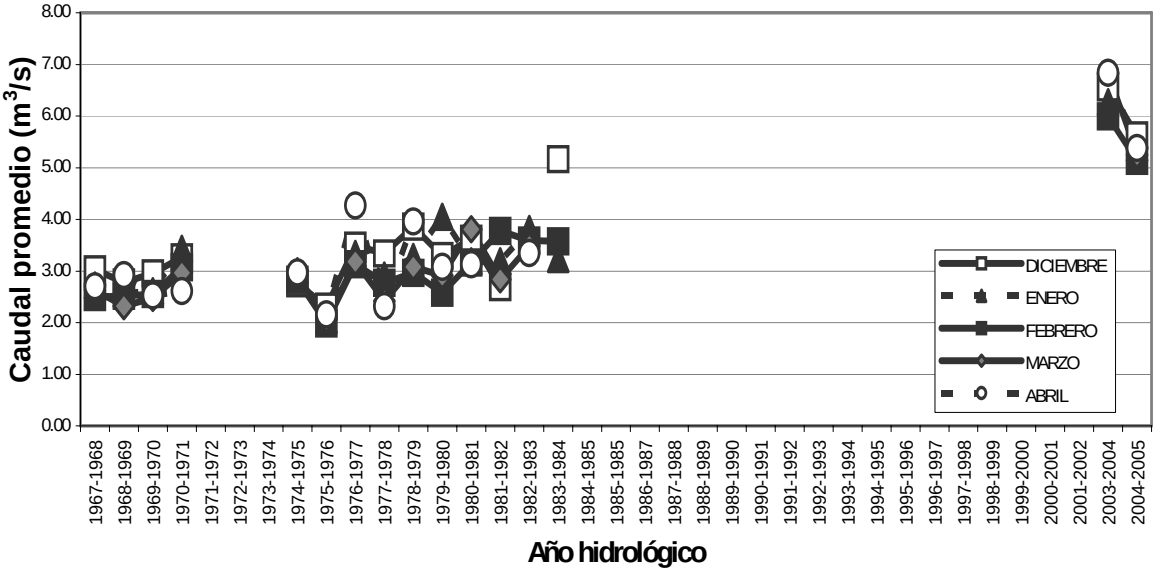


Fig. 4 Gráfica de caudales promedios de diciembre a abril registrados en la estación hidrométrica Guazapa ubicada en la cuenca del río Acelhuate.

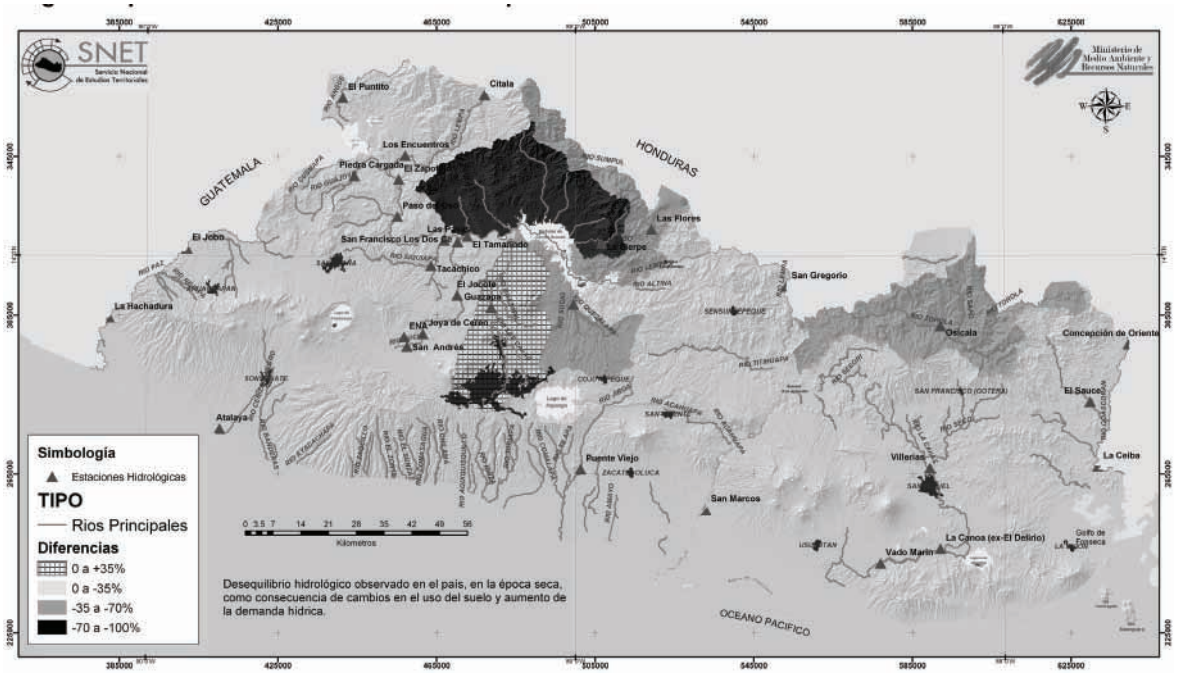


Fig. 5 Mapa que representa las anomalías de caudal promedio anual, en el periodo de 1970 a 2002.

Torola y Quezalapa, existe una disminución del 2 al 6% en cantidades de precipitación anual con respecto al registro histórico. En el resto del país, los cambios pueden considerarse como poco significativos, sin embargo, se han observado cambios en su patrón de distribución temporal con lluvias más intensas en periodos de tiempo más cortos.

La evapotranspiración potencial, también ha presentado cambios en el tiempo. Se observó que en la zona Occidental del país hubo un incremento, tanto en forma anual como mensual, con valores entre 4% y 5% por encima de los registrados en la década de 1970 a 1980; por el contrario en las zonas central y paracentral, hubo disminución de este parámetro en aproximadamente 3%.

Respecto a los cambios en el uso del suelo, en las tres zonas, hay una tendencia a la reducción del bosque latifoliado y de coníferas y un aumento de los granos básicos; para las cuencas de los ríos Tamulasco y Sumpul, se presenta una reducción del 32% en los bosques, de 1973 a 1992 y un incremento en los granos básicos de 38.5% en el periodo de 1973 a 1997. En la cuenca del río Quezalapa, los granos básicos aumentaron en un 30.63% de 1973 a 1997 y los bosques disminu-

yeron en 81.6% de 1973 a 1992; en la cuenca del río Torola se presenta disminución de 22.76% en bosques en el periodo 1973 a 1992 e incremento de granos básicos de 3.7% de 1973 a 1997.

El resultado del análisis de la variación poblacional muestra que en los municipios ubicados en las zonas consideradas como críticas, ha existido tanto aumento como disminución poblacional; sin embargo, en los casos donde se ha producido el aumento, no ha sido tan significativo con relación a la disminución de los caudales.

Con relación a los aspectos geológicos e hidrogeológicos en las áreas de estudio, responden a muchos miles de años de formación y no se observan cambios geológicos dramáticos regionales, que puedan causar una reducción drástica de los caudales de estiaje de los ríos.

Un aspecto relevante en algunas de las cuencas de la zona norte que se han visto afectadas, es el hecho de se han venido desarrollando sistemas de abastecimiento de agua potable, a partir de la captación de los manantiales, impidiendo que el agua los manantiales circule por las quebradas. Sin embargo, esta situación no se da en todas las cuencas que han sufrido reducción de caudales.

En cuanto al impacto económico–social, en las zonas de mayor reducción de caudal, se pudo establecer que los ríos investigados no son la fuente primaria para el desarrollo de las actividades diarias y productivas de los pobladores de las riberas, ya que éstos abastecen sus necesidades de agua de fuentes alternativas existentes en la zona, ya sea pozos o por medio de sistemas de abastecimiento que captan manantiales de la zona. La baja densidad poblacional de las zonas estudiadas hace que los requerimientos para otros usos tales como riego sea igualmente baja y de ahí que no se refleje en fuertes impactos, sin embargo se considera que los posibles impactos de estas reducciones podrían surgir en las grandes ciudades donde efectivamente existe una alta y diversa demanda del recurso hídrico.

Agradecimientos A Ivonne Jaimes, Celina Mena, Carolina Rivas, Walter Hernández, y demás profesionales y técnicos del Servicio Nacional de Estudios Territoriales, que colaboraron con el desarrollo de la investigación.

REFERENCIAS

Servicio Nacional de Estudios Territoriales (2002) *Bases de datos hidroclimatológicas.* El Salvador.

Climate Variability and Change—Hydrological Impacts (Proceedings of the Fifth FRIEND World Conference held at Havana, Cuba, November 2006), IAHS Publ. 308, 2006.

Methodologies for trend detection

ZBIGNIEW W. KUNDZEWICZ[1,2] **& MACIEJ RADZIEJEWSKI**[1,3]

1 *Research Centre for Agricultural and Forest Environment, Polish Academy of Sciences, Poznań, Poland*
zkundze@man.poznan.pl; zbyszek@pik-potsdam.de

2 *Potsdam Institute for Climate Impact Research, D-14412 Potsdam, Germany*

3 *Faculty of Mathematics and Computer Science, Adam Mickiewicz University, Poznań, Poland*

Abstract Methodologies for detection of change in river flow data are briefly reviewed. After discussion of the issue of data for change detection, the basics of statistical testing for trend detection are presented, including such concepts as the null hypothesis, the test statistic, the significance level and the trend index. Test assumptions are thoroughly discussed. A review of practical tests (parametric, distribution-free i.e. non-parametric, and resampling: permutation and bootstrap approaches) applicable for different properties of data, is presented. The case where the records are not independent and are not normally distributed is also included. A few special problems, such as extremes and spatial data (with correlation between gauges), and detectability of change are also discussed. Assessment of a few relevant recent publications is offered.

Key words change detection; resampling; river flow data; statistical testing; trend

INTRODUCTION

Detection of changes in long time series of river flow records is an important scientific issue and of considerable practical interest since rivers are the most easily available source of water upon which, worldwide, billions of people depend. Water resources systems have been designed and operated based on the assumption of stationary conditions, i.e. that the past is a key to the future. If this assumption is abandoned, i.e. if the process of river flow is subject to changes, then existing procedures for designing water supply, flood and drought control, environmental flows, hydropower, navigation, etc., have to be revised. In order to design reservoirs, dams, dykes, etc., scheduled to serve man for decades, one has to consider changes in the river flow process. Otherwise systems may turn out to be over- or under-designed, i.e. to not serve their purpose adequately, or to be overly costly. However, for a number of reasons discussed in the following, change detection in river flow data is not a trivial task. The search for weak changes in time series of hydrological data, which are subject to strong natural variability, requires use of both data and methodology of adequate quality.

There are many possible causes for change in time series of hydrological data. Some are directly man-caused (e.g. urbanization, deforestation) and others are of natural, e.g. climatic origin. Yet, even climate change-related signatures can be seen as a manifestation of an indirect human influence via the rising concentration of greenhouse gases in the atmosphere. Often it is not easy to detect a weak, if any, climate signature hidden amidst a strong natural variability of river flow. An essential problem also is: how to distinguish a greenhouse component and a land-use change signature.

The concept of change builds upon the assumption that some kind of constancy or repeatability is possible in the process and change is a negation of such constancy. For example, one may compare the river flow process in the past and the river flow process at present as described by the statistical properties of the process in two different time periods. One can state that the river flow has changed between these two periods if the distribution of the flow rate values in the two periods is no longer the same (nor sufficiently similar).

A trend is a continued change that occurs over time. One may either view it as a manifestation of a separate time-dependent deterministic component (this requires some previous knowledge of the underlying mechanism) or simply as a continuous tendency in the statistical properties of the process.

Usually trends of simple shape (linear, low-order polynomial, piecewise linear, exponential, etc.) are considered. Different trend shapes are possible, including steeper trends similar to abrupt step-like changes, so that there is a continuum of cases and, in practice, the terms “trend” and “change” are almost interchangeable. One can also speak of trends in a non-parametric, comparative sense; e.g. an increasing trend means that the values that occur later are usually higher

Copyright © 2006 IAHS Press

than those that occur earlier. Such a trend need not have a specific shape, but may still be called strong or weak, e.g. if the probability that a later value is higher than the earlier one is close to 1 or to 0.5, respectively.

There may be short-term or long-term trends in the past observation record. Neither implies that the observed change is going to last for long. However, the above assumptions make it reasonable to expect that a long-term trend will continue at least for a short period into the future.

The task of trend detection refers to a situation with no previous knowledge of a trend component. There are two different approaches to trend detection:

– Assume a specific model with a trend component and identify the possible trend by looking at the change in statistical properties;
– Study the change in statistical properties alone.

The model in the former bullet is usually linked to some possible cause of change, while the change in statistical properties may be interpreted as the effect. Even if only the latter changes are analysed, one usually has some cause in mind or looks for possible explanations of change. In this, attempting to carry out a trend or change detection helps identify the cause–effect relationships and lets one learn about the consequences of external factors or human actions. In turn, one gains some understanding of the system, either in the form of a simplified description (e.g. finding out that it is getting wetter), or a conceptual model of attribution (e.g. increased precipitation may be a climate change effect, like warming and changes in seasonal precipitation distribution). Finally one gets better knowledge of what is going to happen and better knowledge of what to do:

– What kind of future should one prepare for?
– What can one do now to influence the future evolution of the system in a requested way?

Unfortunately, in a complex system, such as the river flow process, it is not possible to identify and separate with certainty the effects of external or new factors, especially if they are gradual (such as climate changes or land-use changes) rather than abrupt, and the normal evolution of the system that would occur without such factors as well. This distinction is the main problem of change detection and is subject to much debate.

DATA FOR CHANGE DETECTION

Availability of a long time series of reliable data is essential for any attempt to detect a change in records of river flow, which is itself an integrative process controlled by several factors, such as precipitation (liquid and solid), evaporation, infiltration, snowmelt, catchment storage, and human impacts in the drainage basin and in the river itself. Hence, selection of which stations to use in a study is important. In order to study climate change signature, flow data should be taken from pristine (baseline) rivers, where human impacts are weak, should be of high quality and extend over a long period, preferably in excess of about 50 years (Kundzewicz & Robson, 2000), to distinguish climate change-induced trends from climate variability. Detailed suggestions on how to select a network of stations for climate change detection are given in Pilon *et al.* (2000).

Data should be quality-controlled before commencing an analysis of change. Furthermore, one should be open-minded at any stage of analysis for possible data quality problems, such as: typographical errors; instruments malfunctioning (zero-drift, bias); lack of homogeneity via changes in instruments and techniques of observations, changes in gauge location, in accuracy of data, and in data conversions, e.g. altered rating curves (stage–discharge relationships), censored data, etc.

Missing values and gaps in data are frequent complicating factors. It is not easy to issue a general guidance as to whether or not to fill them, and if so, in what way. This can be particularly critical when the gaps are non-random, e.g. following equipment damage by a flood event of exceptional magnitude. Such gaps would undermine studies of change detection in floods.

The form and frequency of the data for analysis depend on the main focus of the study (Kundzewicz & Robson, 2004). The form in which the data are collected is not always the most appropriate for the study in question (e.g. high flows and low flows being of interest to flood and drought studies, respectively). It can be worth simplifying the data by reducing the frequency (aggregating) or using summary measures, such as maxima or averages.

There are many different ways in which changes in hydrological series can take place. They may have different form, may occur in the mean values and/or in variability (variance, extremes, persistence and within-year distribution, e.g. changing river flow regimes). They may have different temporal scales. In addition, there may be complicating factors such as seasonality.

Trends are being sought in river flow data collected at a range of temporal intervals: hourly, daily, monthly, annually. Data records contain either instantaneous values (e.g. of flow, stage) or totals/means in a time interval (e.g. annual mean flow). The data may also pertain to different spatial scales, from a small creek to a continental-scale river. Abrupt changes can be expected as a result of reservoir construction, installing water diversions, etc. Changes of gauging structures and of rating curves can manifest themselves as step changes in a series of flow records. Yet, step-like changes may also result from gradual changes, since nonlinear system dynamics may feature cumulative effects and thresholds. Gradual hydrological changes may be attributed to gradual causative changes such as urbanization, deforestation, climate variability and change.

Different hydrological flow-rate related indices might be of interest in change detection studies (cf. Pilon *et al*., 2000), such as: instrumental records of water level/flow, seasonal mean flow, monthly mean flow, number of ice-cover days, extreme events and their characteristics (e.g. the frequency and severity of floods and droughts, number of incidences of independent flood events or the cumulative deficit below a prescribed threshold within a time interval, spring flood volume and the duration in days of the spring flood event). Timing of seasonal events is an important index of change. This refers to the start of snowmelt season, snowmelt flood-peak time, maximum-flow time, timing of river freeze-up, timing of ice break-up, etc.

ANATOMY OF STATISTICAL TESTING FOR CHANGE DETECTION

The definition of change is necessarily vague. In most phenomena that evolve in time, no two periods are identical as far as the process behaviour is concerned. Hence one can always find some changes in statistical properties, be it minor or large. Such changes, not related to external or new factors, but resulting inherently from the internal structure of a system, are termed natural variability. In other words, a change in the statistical properties estimated from samples does not necessarily imply a true change in the process; this behaviour may be natural for the process. In change detection one is interested in identification of changes in the process beyond the natural variability. Because of the strong natural variability of the river flow process, an observation that the mean values of river flow observed in two 30-year periods (standard climatic approach) are different would be trivial, unless one can support it by further analysis.

The distinction between genuine and apparent changes is the main problem of change detection and the existence of changes in a time series is often subject to much uncertainty. This may be contrasted with the situation in communication, where one can usually separate a signal from the noise beyond doubt and successfully discover the external factor: e.g. reliably state that someone has sent a message (with the signal-to-noise ratio being very high). In the latter case, one has a fair understanding of the essential parts of the system. In the case of a complex geophysical process (such as river flow), many observed changes may be attributed to its natural variability. Moreover, a change in such a complex system might be so complicated and so subtle itself, that it would be incomprehensible and it might not be possible to give a simplified description. If one does not understand the way in which the system is changing, one is not likely to detect it. Thus one has to look for changes that one can describe, keeping in mind that there might be other changes as well, that escape the analyst's attention.

The method of significance testing offers a way to distinguish "real changes" from chance occurrences resulting from natural variability. Instead of answering the question of the presence of changes, one states how unlikely a change larger than the observed one would be under natural variability alone. The starting point for a statistical test is to define the *null hypothesis* (H_0) of no change (only natural variability) and the *alternative hypothesis* of a specific kind of change (e.g. that the mean is either increasing or decreasing over time). The null hypothesis includes a complete statistical description of our understanding of the process in question. In other words, it defines a probability space that should reflect the present knowledge of the properties of the process. The alternative hypothesis should be plausible and supported by initial analysis of the

available data. The starting point for statistical testing is to assume that the null hypothesis is true, and then to check whether the observed data is consistent with this hypothesis. The null hypothesis is rejected if the data is not consistent with it. Otherwise, there is not sufficient evidence to reject the null hypothesis (even so this is not a proof that the null hypothesis holds, only that there is not enough reason to reject it).

In order to perform a statistical test for change one selects a *test statistic*, a numerical value calculated from the data series undergoing testing, which allows a comparison of the null and alternative hypotheses, by measuring, in quantitative terms, the change asserted by the alternative hypothesis. A good test statistic should highlight the difference between the two hypotheses. Given a dataset D the value $S(D)$ reflects the strength and possibly the direction of changes in D:

– In a two-sided (two-tailed) test, both large and low values of $S(D)$ suggest that changes are present in D. Usually the large values of $S(D)$ indicate increase and low ones indicate decrease of whatever $S(D)$ measures.
– In a one-sided (one-tailed) test, only large or only low values of $S(D)$ indicate changes. For simplicity it is assumed here that large values of $S(D)$ suggest changes and low values suggest lack of changes. No information on the direction of change is supplied.

A simple example of a test statistic is the linear regression gradient, which can be used to test for a trend in the mean. If there is no trend (the null hypothesis) then the regression gradient should have a value near to zero. If there is a large trend in the mean (the alternative hypothesis) then the value of the regression gradient may be very different from zero. In order to carry out a statistical test it is necessary to compare the observed test statistic with the expected distribution of the test statistic under the null hypothesis.

The *significance level* is the main parameter of significance testing. The *observed significance level* (*p*-value) is defined as the probability that a value of the test statistic as extreme as, or more extreme than the observed value, would occur assuming the null hypothesis (H_0) of no change (i.e. probability that a test detects trend when none is present). Given some $\alpha > 0$ one may state that the null hypothesis is rejected, and the alternative hypothesis supported, on a *significance level* α if the observed significance level is smaller than α. Specifically, for a two-sided test, the null hypothesis is rejected if:

$$2 \min (\mathrm{P}(S(D') \geq S(D)), \mathrm{P}(S(D') \leq S(D))) < \alpha$$

where D' denotes a random realization of the process to which the null hypothesis pertains. The factor 2 comes from probable changes in the other direction that can be compared to the observed change in the probabilistic sense (then “a change of similar magnitude” means “equally improbable”). If the probability density function of $S(D')$ is symmetric, the above may be simplified to:

$$\mathrm{P}(|S(D')| \geq |S(D)|) < \alpha$$

For a one-sided test with large values indicating change, the null hypothesis is rejected if:

$$\mathrm{P}(S(D') \geq S(D)) < \alpha$$

The significance level is selected arbitrarily (usually 5% or 1%) and guarantees that the probability of obtaining a false positive in the test is at most α on average, provided that the null hypothesis is stated correctly. The significance level expresses the probability of the error of the first kind (rejecting the hypothesis of absence of trends when it is true, i.e. detecting a trend that does not exist). Selecting the significance level is a trade-off and a matter of personal judgment. It should be small, so that errors of the first kind are reduced, but making it too close to zero would prevent the detection of even very strong changes (increase of errors of the second kind—accepting the hypothesis of absence of trend when it is false, i.e. failure to detect an existing trend). A possible interpretation of the significance level is as follows: changes significant on a level above 10% may provide very little evidence against the null hypothesis. Changes significant on a level between 5 and 10%, between 1 and 5% and below 1%, can be interpreted, respectively, as possible moderate, strong, and very strong evidence against H_0. Significance testing is a useful and consistent method of eliminating false positives. Nevertheless it must be emphasized that on any significance level $0 < \alpha < 1$ there may be:

– real changes not inducing significant test results; and
– significant test results not induced by real changes.

Statistical tests can support, but not prove, hypotheses. Whenever one has deeper understanding of the system in question, one should not restrict the study to significance testing alone.

It must be noted that in an analysis of 100 time series with no changes one would detect changes on the 5% significance level in 5 time series on average. It could as well be 4 or 7. Similarly, if one applies 10 different tests to these 100 time series, the number of falsely positive test results would become 50 on average. The number of positives in an analysis may be turned into a test statistic itself. Its distribution depends on the independence of the results, i.e. the independence of time series and tests used. At the very least one must keep in mind the average number of false positives possible and look for results supported by several tests rather than by one of several tests. One should always report on the entire scope of an analysis performed, data and methods applied, even if only a part of the study revealed interesting results. Selection of only a part of the study based on the results invalidates their significance.

A statistic combined with a specific null and alternative hypotheses forms a statistical test. For several traditional tests, regions of rejection and acceptance for desired significance levels can be looked up in reference tables or calculated from simple formulae, provided that the required test assumptions apply. In general, these regions can be found if the distribution of the test statistic under the null hypothesis (i.e. assuming the null hypothesis is true) is known or can be estimated.

Typical test assumptions include:

– *A specified form of distribution* (e.g. assuming that the data are normally distributed).
– *Constancy of the distribution* (i.e. all data points have an identical distribution) This assumption is violated if there are seasonal variations or any other cycles in the data, or if there is an alteration over time in the variance or any other feature of the data that is not allowed for in the test.
– *Independence* This assumption is violated if there is autocorrelation (also referred to as serial correlation or temporal correlation) or, in the case of a multi-site study, spatial correlation.

River flow data are often strongly non-normal, and this means that tests which assume an underlying normal distribution are not adequate. The data may also show autocorrelation and/or spatial correlation and, therefore, data values are not independent. They may also display seasonality, which violates assumptions of constancy of distribution. If the assumptions made in a test are not fulfilled by the data, then the test results can be meaningless, in the sense that the estimates of significance of the results via theoretical formulae would be grossly incorrect. In such a case the test can be treated as a mere method of exploratory data analysis rather than a rigorous examination tool.

A trend index (*TI*) can be defined as a measure related to the *observed significance level* (*p*-value) α, cf. Kundzewicz *et al*., 2005, Svensson *et al*., 2005. For two-tailed tests it ranges from –100% to +100%, with negative values indicating a negative trend and positive values a positive trend. The higher the absolute value of *TI*, the higher the trend significance.

$TI = (1 - \alpha) \times 100$ [%] for positive trends

$TI = -(1 - \alpha) \times 100$ [%] for negative trends

For one-tailed trends the value $TI = (1 - \alpha)$ is always in the range from 0 to +100%. This convenient measure puts test results on a common scale and lets one readily see if the result is significant on any desired level. For example a negative trend is significant at the 10% level if $TI < -90\%$.

A summary of the main stages of a statistical analysis of change follows:

– Decide what type of series/variable to test depending on the issues of interest.
– Decide what types of change are of interest (gradual trend or step-change).
– Check out data assumptions (e.g. use exploratory data analysis, or a formal test).
– Select a statistical test, i.e. a test statistic and a method for evaluating significance levels.
– Evaluate significance of the results (e.g. trend indices).
– Investigate and interpret results.

REVIEW OF TESTS

It is recommended to start change detection studies with the exploratory data analysis (EDA), which involves visual examination using graphs to explore, understand and present data. Looking at the data can change initial preconceptions, e.g. by altering the questions to ask, and unveiling important aspects that would otherwise have not been found. Visual analysis allows one to identify such features as data problems (outliers, missing values) or seasonality, to check out test assumptions such as independence, distribution assumptions, and also aids in understanding, interpreting and presenting the results of analysis. A well-conducted EDA is such a powerful tool that it can sometimes eliminate the need for a formal statistical analysis. Statistical tests become a way of confirming whether a pattern discovered via an EDA approach is significant (Kundzewicz & Robson, 2000, 2004).

Numerous tests for trend detection have been used in studies of long time series of river flow data and more information about tests can be found in (Kundzewicz & Robson, 2000). Therefore, the issue of the satisfactory choice of a test (or a series of tests) may come about. Tests differ by their skill, power, and underlying assumptions (thus, range of applicability) and computational efficiency. The skill, i.e. assessment of how well the test detects trends, embraces evaluation of the probability of errors of the first kind or of the second kind. A test which has low probability of error of the second kind is said to be powerful.

The process of testing for change in long time series of hydrological data starts from selecting a statistical test (more than one is good practice). This selection depends on the properties of the data. A short guideline for test selection can read as follows:

– *If data are normally distributed, independent and non-seasonal* (an unlikely scenario for river flow data), any general-use parametric or non-parametric test (e.g. slope-based tests, such as linear regression) should be suitable.
– *If data are independent and non-seasonal, but are non-normal*, any of the distribution-free tests are suitable. Distribution-free (non-parametric, e. g. rank-based) methods do not require any assumptions about the form of distribution that the data derive from e.g. non-normal distribution. However, tests that are based on the normality assumption can also be applied, either by usage of transformation to normal scores or ranks, or by using a relevant test statistic and evaluating significance using resampling techniques.
– *If data are not normal and are not independent* (i.e. they exhibit serial correlation, seasonality), one could use many standard tests, but it is necessary to evaluate significance levels using block permutation or block-bootstrap methods.

Parametric tests

Among parametric tests, which are based on assumptions of normal distribution and independence are tests for step change:

– *Student's t-test* (a standard parametric test for testing whether two samples have different means and a known change-point time is assumed);
– *The Worsley likelihood ratio test* (similar to Student's t-test but suitable for use when the change-point time is unknown);

and a test for gradual trend:

– *Linear regression* (one of the most common tests for trend—it uses the regression gradient as a test statistic and assumes that data are normally distributed).

Non-parametric (distribution-free) tests

Parametric tests are based on distributional and independence assumptions. However, the majority of hydrological series are non-normally distributed and it therefore makes sense to use distribution-free testing methods. Distribution-free methods are ones in which no assumptions about the underlying distribution of the data need to be made. However, the independence assumption still remains. It is assumed that sample elements are independent and identically distributed random (i.i.d.) variables.

Among commonly used distribution-free approaches are:

– *Rank-based tests* use the ranks of the data values (not the actual data values themselves). A data point has rank *r* if it is the *r*th smallest value in a data set. There are a number of widely used and useful rank-based tests (Kundzewicz & Robson, 2000). Rank-based tests have the advantage that they are robust and usually simple to use. They are usually less powerful than tests that are directly based on the data.
– *Tests using a normal scores transformation*. Many standard tests for change rely on assumptions of normality. When data are not normally distributed, as is often the case for river flow data, these tests can still be used if the data is first transformed. The normal-scores transformation results in a data set that has a normal distribution. It is similar to using the ranks of a data series, but instead of replacing a data value by its rank, *r*, it is replaced by the typical value that the *r*th largest value from a sample of normal data would have (the *r*th normal score). The advantages of using normal scores are that the original data need not follow a normal distribution, and the test is relatively robust to extreme values. Normal scores tests are likely to give slightly improved power for detection of change relative to equivalent rank-based tests.

Among non-parametric (distribution free) tests are such tests for step change as:

– *Median change point test* / *Pettit's test for change* (a powerful rank-based test for a change in the median of a series with the exact time of change unknown, considered to be robust to changes in distributional form);
– *Wilcoxon-Mann-Whitney test* / *Mann-Whitney U test* / *Mann test* / *Rank-sum test* (rank-based test that looks for differences between two independent sample groups, based on the Mann-Kendall test statistic);
– *Distribution-free CUSUM test* (rank-based test in which successive observations are compared with the median of the series with the maximum cumulative sum (CUSUM) of the signs of the difference from the median as the test statistic);
– *The Kruskal-Wallis test* (rank-based test for equality of sub-period means);
– *Cumulative deviations and other CUSUM tests* (e.g. rescaled cumulative sums of the deviations from the mean);

and tests for trend:

– *Spearman's rho* (rank-based test for correlation between time and the ranks series);
– *Kendall's tau* / *Mann-Kendall test* (another rank-based test, similar to Spearman's rho but using a different measure of correlation which has no parametric analogue. There is a seasonal Kendall test that allows for seasonality in the data, and a modified seasonal Kendall test that additionally allows for some autocorrelation in the data).

In general, the significance level can be found if the distribution of the test statistic under the null hypothesis (i.e. assuming the null hypothesis is true) is known or can be estimated. The above tests may be used in their original (standard or basic) form, providing test assumptions are met and significance levels can be looked up in reference tables or calculated from simple formulae. Alternatively, where test assumptions cannot be met, it is recommended that only the test statistic from each basic test is used, and that the significance level is evaluated using resampling. Resampling methods are robust, require minimal assumptions to be made and are very general.

All commonly used tests assume that, under the null hypothesis, the distribution of data values does not change with time. If this is not appropriate, then more sophisticated testing approaches will be necessary.

The skill of the many existing tests is usually good just for one particular type of change. Since one does not know the pattern of variability beforehand, using a number of tests is sensible. Therefore guidance as to the applicability of tests is important and an intercomparison of available tests is a much needed activity. Useful tests should be valid for realistic assumptions.

Resampling methods are a general and flexible approach, using the data to determine observed significance levels—which means that minimal assumptions about the data need to be made. Resampling methods are based on generating random reference data from the original observed

data, e.g. by changing the order of data points, and comparing test statistics calculated on these generated series with the test statistic for the original data series. Resampling methods can be applied to almost any test statistic and provide an alternative way of obtaining TI. Resampling tests are relatively powerful, e.g. for large samples, permutation tests can be shown to be as powerful as the most powerful parametric tests. Furthermore, resampling methods can be adapted to test data which are not independent.

Permutation tests are a very useful class of tests, based on changing the order (shuffling) of data points, calculating statistics, and comparing it with the observed test statistics. This helps identify evidence for the presence of a trend in the original series.

Consider a time series of data with a possible trend and regression gradient as an example of a possible *test statistic*. Suppose first that there is no underlying trend in the data. If that is true, then it should not matter if the data is re-ordered, as the regression gradient should not change very much. Each time the data is shuffled as part of the permutation test, the selected test statistic (here: regression gradient) is recalculated. At the end of all the shuffling, there is a distribution of possible values of the test statistic under permutation, the *permutation distribution*, which depends on the data and must be recalculated for each data set. The rationale behind this approach is that under the null hypothesis of absence of change in the data, each ordering of the data set is similarly likely. Hence, the null distribution of the test statistic can be estimated from the permutation approach. If there is no trend in the observed series, then one would expect that the observed test statistic (regression gradient) for the original data is not very different to any of the generated test statistic values, i.e. it is somewhere in the middle of the permutation distribution. So to test for trend, the observed test statistic (regression gradient) is compared with the permutation distribution. If the gradient is larger (or smaller) than almost all the values in the permutation distribution (the allowed fraction of exceptions given by the significance level), one concludes that a trend is present. Conversely, if the original gradient is somewhere in the middle of the permutation distribution, one concludes that there is no evidence of trend (Kundzewicz & Robson, 2000, 2004).

Bootstrapping approaches are similar to permutation techniques. The main difference is that instead of reordering the data, the new data series are generated by sampling with replacement. For example, for a series of N values, a bootstrap sample would take N values at random from the original series: the resulting series might perhaps include two occurrences of the original first value, but none at all of the last value.

For both permutation and bootstrap methods, the generated series has the same distribution as the empirical (i.e. observed) distribution of the data. The bootstrap is generally but not always, less powerful than a permutation test. However, bootstrap methods are often to be preferred where a test is looking for change in variance. Further, bootstrap methods are also applied outside of the area of change detection, e.g., for estimating the confidence intervals of the mean and median. Permutation tests cannot be applied with these and other statistics that do not change when the data are permutated. The tests given here can be used with either method. In general, bootstrap methods are more flexible than permutation methods and can be used in a wider range of circumstances.

Summary of methods for resampling

The basic method for carrying out a permutation or bootstrap test, once the test statistic has been selected, is as follows:

– calculate the test statistic for the observed data;
– resample the data series many times (e.g. 1000) to generate new data series;
– recalculate the test statistic for each of these series;
– estimate the significance level.

To estimate the observed significance level, the data are resampled a large number of times, N. For each of these generated series, the test statistic, S, is calculated to give N artificial values of S. These are then ordered as:

$$S_1 \leq S_2 \leq ... \leq S_N$$

If the original test statistic is S_0 and:

$$S_k \le S_0 \le S_{k+1}$$

then the probability of the test statistic being less than or equal to S_0 under the null hypothesis is approximately:

$$p = k/N$$

Assuming that large values of S indicate departure from the null hypothesis and a two-sided test, i.e. a test in which the direction of change is assumed unknown, the significance level for this test is then:

$$2 \min(p, 1 - p) \times 100\%$$

while the trend index reads:

$$TI = (2p - 1) \times 100\%$$

Further details on the application of resampling methods can be found in Kundzewicz & Robson (2000, 2004).

Block resampling: resampling when data are not independent

As noted by Yue *et al*. (2003), the existence of spatial correlation which is not accounted for, can complicate the identification of changes—a positive serial correlation may inflate the results of change detection.

The basic resampling methods, as described above, avoid any distributional assumptions, but they still assume that data values are independent of one another. Frequently measured hydrological data (e.g. daily data) are typically not independent: they show serial dependency (autocorrelation). In block resampling, the data is permutated or bootstrapped in blocks (e.g. all values within a year are kept together). With this approach, the dependency structure within each block is built into the test and independence assumptions are thus no longer violated (see Kundzewicz & Robson, 2000). Seasonality can be taken into account by using annual, or multiples of annual, blocks of data for the bootstrapping.

SPECIAL PROBLEMS

Extremes

Testing for trend or other non-stationarity in extremes (uncommon, infrequent events) is particularly difficult (cf. Robson & Chiew, 2000). Indeed, the consequence of the tautology: extreme (rare) events are rare, is that even in a very long series of record there may only be a few really extreme values leading to catastrophic damages.

Because extremes are rare, it is necessary to construct a data series that emphasizes extremes. One option is an annual maxima series, obtained by taking the largest value in each year or season of interest. However, the information on some extremes may be insufficiently reflected in such a series (e.g. if two extreme events occur within a year). The series may contain values that are not extreme (e.g. if no extreme event occurs within a year).

A peak-over-threshold (POT) series (also called a partial duration series, PDS) consists of independent daily mean river flows that exceed a certain threshold (this threshold is the same throughout the time series). This approach has advantages over annual maxima series in that all major events are included (not just one largest in a year) and all data points in the POT series are indeed extreme events. Furthermore, POT series can be used to examine whether there is a change in either the magnitude or frequency (counts) of extreme events. To obtain a POT series, it is necessary to identify a suitable threshold and to determine whether events are independent. There should not be multiple peaks corresponding to the same event. Judging independence can be complex. The threshold should be such that the average number of events per year is within adequate bounds, e.g. on average, one or three POT events are selected per year. The former case provides information about changes in large floods, while the latter also gives knowledge about changes in moderate events. Testing more than one series gives a better picture of what is occurring.

Testing for trends in droughts is more difficult because it is often the duration of the drought that is critical. Furthermore, severe droughts may span a number of years, i.e. longer data sets are required

for change detection. Detection of effects due to climate change is likely to require much longer data sets than detection of effects with a clear anthropogenic cause (cf. Robson & Chiew, 2000).

If a data series is strongly seasonal or if changes relating to a particular season are important, then it may be appropriate to consider a seasonal extreme series, e.g. for summer.

Whenever a change is detected, it is important to seek attribution, e.g. by examining other related hydrological series. For example, if trend is seen in river flow data for a catchment that has experienced land-use change, examining a rainfall series can provide information about whether climatic conditions have been steady across the period of record.

Recent detection studies of changes in floods and droughts do not support the hypothesis of ubiquitous change in severity and frequency of extremes. Using 600 daily streamflow records in Europe, Hisdal *et al.* (2001) conclude that it is not possible to establish that drought conditions in general have become more severe or frequent. Using 195 long series of daily mean flow records to analyse annual maximum flows, Kundzewicz *et al.* (2005) did not detect ubiquitous growth of high flows. A similar result was obtained by Svensson *et al.* (2005), who examined a subset of these data using a POT approach.

Spatial analysis

Univariate analyses of long time series of flows at single sites can be extended into an approach where all the available data for the area under study are used. Regional studies of long time series of river flows may allow important corollaries to be drawn as to the observed changes in a number of neighbouring gauges, thus being a property of the area.

The assessment of regional trends in hydrological conditions can be approached from two distinct perspectives (Lins, 2000), one inherently univariate (testing for changes in series at individual sites and then performing regionalization) and one multivariate (for pre-defined, homogeneous, regions). The former approach involves applying a test for trend to the hydrological time series collected at a number of individual sites and then grouping or *regionalizing* sites having similar test results. The latter (multivariate) approach differs in that *regions* are first identified from the hydrological time series collected at multiple sites, and a new derived time series for each region is then tested for trends. The former is more applicable if the analyst wants to preserve much of the temporal information at a single site, while also identifying adjacent sites exhibiting similar behaviour. The latter is more useful in applications where the goal is to emphasize the temporal behaviour of coherent regional patterns of variability; as in a hydro-climatic analysis. Because of land-use changes, reservoir construction, and other local effects, homogeneous spatial patterns seldom emerge from regional studies of changes in flow.

The majority of studies of change detection in river flow records assume that the data at different gauges are spatially independent. However, some recent studies account spatial dependence through the application of "field" significance, which accounts the observed regional cross-correlation of river flows and allows determination of the percentage of sites that are expected to show a trend by chance. The presence of spatial correlation affects the ability of a test to assess the field significance of trends over the network. Consideration of inter-site spatial correlations (overlap in information) dramatically reduces the effective size of the sample available for trend assessments. The effect of cross-correlation in the records under study is to increase the expected number of significant trends occurring by chance. If spatial dependence (regional cross-correlation) is ignored, then significant trends are typically found in a great many more cases than with cross-correlation considered (cf. Douglas *et al.*, 2000; Burn & Hag Elnur, 2002). Using a field significance rather than significance for the individual sites is recommended for regional studies when large amounts of spatially-distributed records are available.

Naturally trendy?

Cohn & Lins (2005) demonstrated that the choice of the null hypothesis (i.e. adequate test assumptions) is critical for the results of significance testing. Significance depends on subjective assumptions about the underlying process. In fact, it can be argued that for any time series of observations with a trend one could find a null hypothesis that would render the trend insignificant. Any observed changes could thus be attributed to natural variability. It is obvious

that the null hypothesis should not include a trend component, so that it differs from the alternative hypothesis. Similarly, if the null hypothesis includes nonstationary processes with high persistence it may be barely distinguishable from the alternative hypothesis when the evidence is limited to a single time series. Therefore, it is important to support the selection of the null hypothesis, ideally by evidence from a period before the supposed trend. One must also consider and study the possibility that a test may confuse a trend with higher-than-real natural variability and persistence leading to lower detection power. It is still sensible to perform studies of changes where one expects under-detection, because conservative, lower-bound estimates of the intensity of changes may be obtained in this way and more light is shed on the degree of inherent uncertainty of the results.

A much greater danger than under-detection seems to be over-detection, due to choosing a null hypothesis that does not encompass the natural variability of the process in an appropriate way. This was discussed in detail in the section on test assumptions. Statistical tests that rely on the assumption of i.i.d. (independent, identically distributed observations) are sometimes applied without question to annual time series of river flows, because of the lack of time, the lack of a better tool, and the lack of appropriate data. While the i.i.d. assumption may be valid in some cases, the studies based on it should at least be accompanied by tests for serial dependence in the data. It would also be worthwhile to always supply a corresponding conservative result obtained using tests with more general assumptions.

In some cases it is known that the process has changed, but one may wish to know how it has changed (e.g. increased concentrations of greenhouse gases have affected the climatic system and therefore have some influence on the global temperature). The question is: what is this effect and how can it be detected? In this setting, significance testing still has a merit, namely, one can hope to say something sensible about the amount of change if the change is larger than the natural variability of the process. If the change is not significant, it means that the uncertainty about the magnitude of change is at least comparable to the observed change itself.

Unfortunately, in hydro-climatic studies the options are much more limited than, say, in public opinion sampling or medical tests, where insignificant results may usually be made more precise by a repeated test or a wider survey. Increasing the length of a time series sufficiently may not be possible if precise observations were not performed in an earlier period. The only solution then is to gather as much data as possible to confirm or disprove the existence of changes, and to give a full account of the uncertainty of the result when reporting on it.

CONCLUDING REMARKS

Change detection in hydroclimatic variables is a challenging task, because it is hard to define what change is, and one does not have a complete understanding of the statistical properties of the processes involved. Change is often bad news. The increasing number of extremes is of the worst kind and also the particularly difficult one to detect. Significance testing offers a way to distinguish “real changes” from “chance occurrences”. Although for hydroclimatic variables one can never distinguish with certainty, at least “significant changes” are well defined, based on an arbitrary selection of a significance level and probability space (null hypothesis). The results of testing depend critically both on the selection of the test object and the testing method (the test and the null hypothesis).

A few general guidelines on change detection in river flow records are in order. It is necessary to make assumptions in a change detection procedure, and one must be aware of them. Any statistical description of a process is only an idealized view of reality, and even in this idealized view there is room for surprises. One needs to make assumptions in order to apply methodological tools, keeping in mind that the results depend on the assumptions taken. It is important to remember that inappropriate test assumptions are dangerous. If the assumptions made in a statistical test are not fulfilled by the data then the test results can be meaningless. Statistical tests results express probability and not certainty, hence they provide evidence rather than proof. There is always a chance that the null hypothesis was true when a test result suggests it should be rejected, and if the null hypothesis is accepted, then this result says only that the available

evidence does not contradict the null hypothesis. Application of different methodologies to the same original data set may result in different trend estimates, hence use of several tests is recommended.

Acknowledgements This paper draws from the work accomplished within the framework of the World Climate Programme – Water Project. Financial support provided to the authors within the projects "Extreme meteorological and hydrological events in Poland" (the Ministry of Education and Science of the Republic of Poland) and ENSEMBLES (EU Sixth Framework Programme) is gratefully acknowledged. The second author was supported by the Foundation for Polish Science.

REFERENCES

Burn, D. H. & Hag Elnur, M. A. (2002) Detection of hydrologic trends and variability. *J. Hydrol.* **255**, 107–122.

Cohn, T. A. & Lins, H. F. (2005) Nature's style: naturally trendy. *Geophys. Res. Lett.* **32**, L23402, doi:10.1029/2005GL024476.

Douglas, E. M., Vogel, R. M. & Kroll, C. N. (2000) Trends in floods and low flows in the United States: impact of spatial correlation. *J. Hydrol.* **240**, 90–105.

Hisdal, H., Stahl, K., Tallaksen, L. M. & Demuth, S. (2001) Have streamflow droughts in Europe become more severe or frequent? *Int. J. Climatol*. **21**, 317–333.

Kundzewicz, Z. W. & Robson, A. (ed.) (2000) *Detecting Trend and Other Changes in Hydrological Data*. World Climate Programme – Water, World Climate Programme Data and Monitoring, WCDMP-45, WMO/TD – No. 1013. World Meteorological Organization, Geneva, Switzerland.

Kundzewicz, Z. W. & Robson, A. (2004) Change detection in river flow records – review of methodology. *Hydrol. Sci. J.* **49**(1), 7–19.

Kundzewicz, Z. W., Graczyk, D., Maurer, T., Pińskwar, I., Radziejewski, M., Svensson, C. & Szwed, M. (2005) Trend detection in river flow series: 1. Annual maximum flow. *Hydrol. Sci. J.* **50**(5), 797–810.

Lins, H. F. (2000) Spatial/regional trends. In: *Detecting Trend and Other Changes in Hydrological Data* (ed. by Z. W. Kundzewicz & A. Robson), chapter 9. World Climate Programme – Water, World Climate Programme Data and Monitoring, WCDMP-45, WMO/TD – no. 1013. World Meteorological Organization, Geneva, Switzerland.

Pilon, P. Kundzewicz, Z. W. & Parker, D. (2000) Hydrological data for change detection. In: *Detecting Trend and Other Changes in Hydrological Data* (ed. by Z. W. Kundzewicz & A. Robson), chapter 3. World Climate Programme – Water, World Climate Programme Data and Monitoring, WCDMP-45, WMO/TD – no. 1013. World Meteorological Organization, Geneva, Switzerland.

Robson, A. & Chiew, F (2000) Detecting changes in extremes. In: *Detecting Trend and Other Changes in Hydrological Data* (ed. by Z. W. Kundzewicz & A. Robson), chapter 7. World Climate Programme – Water, World Climate Programme Data and Monitoring, WCDMP-45, WMO/TD – no. 1013. World Meteorological Organization, Geneva, Switzerland.

Svensson, C., Kundzewicz, Z. W. & Maurer, T. (2005) Trend detection in river flow series: 2. Flood and low-flow index series. *Hydrol. Sci. J.* **50**(5), 811–824.

von Storch, H. (1995) Misuses of statistical analysis in climate research. In: *Analysis of Climate Variability Applications of Statistical Techniques* (ed. by H. von Storch & A. Navarra), 11–26. Springer Verlag, Berlin, Germany. http://w3g.gkss.de/staff/storch/pdf/misuses.pdf.

Yue, S., Pilon, P. & Phinney, B. (2003) Canadian streamflow trend detection: impacts of serial and cross-correlation. *Hydrol. Sci. J.* **48**(1), 51–64.

5 Ecosystems

In-stream ecology	*553–572*
Flood plains	*573–585*
Water quality	*586–611*
Sediments	*612–616*
Groundwater	*617–640*
Water balance, soils, land cover	*641–684*
Human influences	*685–702*

Climate Variability and Change—Hydrological Impacts (Proceedings of the Fifth FRIEND World Conference held at Havana, Cuba, November 2006), IAHS Publ. 308, 2006.

Water demand in the Zhalong Wetland ecosystem

WANG JIAN-QUN[1], HAN LI[1] & MA TIE-MIN[2]

1 *State Key Laboratory of Hydrology-Water Resources and Hydraulic Engineering, Hohai University, Nanjing 210098, China*
wangjq@hhu.edu.cn

2 *Hydrology Bureau of Soliao Water Resources Committee, Changchun, 130000, China*

Abstract Methods for calculating the eco-environmental water demand in the Zhalong Wetland are presented. The eco-environmental water demand for the main types of land use including the lakes and reservoirs, the shallow water areas and the reed marshes in the Zhalong wetland are calculated and the total appropriate and minimum water demand quantities assessed. Results show that the eco-environmental water demand for the whole Zhalong Wetland varied between 522×10^6 m^3 and 592×10^6 m^3 during the period from 1986 to 2002. The appropriate quantity for the eco-environmental water demand is calculated as 555×10^6 m^3; the minimum eco-environmental water demand, with an assurance probability of 75% or 95%, is 288 or 354×10^6 m^3, respectively.

Keywords wetland; eco-environmental water requirement; water resources; ecological security; sustainable development; China

INTRODUCTION

The wetland is a special natural synthesis formed by the interaction between water and land. It is one of the most productive ecosystems and one of the most important environments for humans. Water resources are the main aim of wetland protection and the study of the rules of water demand in the wetland ecosystem plays an important role in its protection, and is therefore of great importance. Cui & Yang (2002) explain the concepts of eco-environmental water requirement; Cui & Yang (2003) give a classification of the eco-environmental water requirements of wetlands. Examples of water demand quantification for wetlands in China include a superficial lake in Nansihu (Zhang, 2004), bayou, estuaries, break river, coastal swamps, lakes and reservoirs, pool and canal habitats in the TianJin wetland (Wang *et al.*, 2004) and swamps in the Honghe National Nature Reserve (Luan *et al.*, 2004). In this literature, the changing seasonal and annual variability of the eco-environmental water requirement are not studied in detail. There are many factors that influence the eco-environmental water requirement but the detailed mechanism, particularly the instability and resilience of the ecosystem, are not fully understood. It is therefore important to analyse and understand the spatial and temporal variability of the eco-environmental water demand in wetlands.

The Zhalong Wetland is located in lower reaches of the Wuyuer River running through the SongNen Plain, to the southeast of Qiqihaer city, Heilongjiang province of P.R.China (Fig. 1). Its geographical coordinate is 46°48'–47°31.5'N, 123°51.5'–124°37.5'E. As the biggest natural reserve for cranes in China, it was listed as one of the world's most important wetlands in 1992. Recent population increases and associated economic development, combined with severe droughts, have led to a decrease in wetland area and a reduction in the crane population. This is destroying the biodiversity and threatening the survival of the Zhalong Wetland. The Zhalong Wetland ecosystem needs to be rescued quickly. In order to protect the wetland, the water conservancy department launched a new water project, transferring 1150×10^6 m^3 of water from the Nenjiang River into the Zhalong Wetland from 2001 to 2005. Water resources were the priority of the project, which created an opportunity to alleviate the shortage of water resources and reasonably redistribute eco-environmental water in the Zhalong Wetland. An urgent problem is how to efficiently allocate the water resources from the Nenjiang River, and how to supply the appropriate quantity of the eco-environmental water demand, while meeting the water demands of agriculture, industry and daily life.

Copyright © 2006 IAHS Press



Fig. 1 Geographical location of the Zhalong Wetland in P.R.China.

METHODS FOR QUANTIFYING THE ECO-ENVIRONMENTAL WATER DEMAND IN THE ZHALONG WETLAND

Eco-environmental water demand types

Reduced flows entering the wetland, degeneration of vegetation, the weakening of the protecting riverhead's function, the salinization of the soil, water pollution and reduced biological diversity are the main environmental problems in the Zhalong Wetland. With economic development it should be possible to alleviate and eventually eliminate the problem without harm to the sustainable development of the economy. This is the aim of eco-environmental protection.

The main land uses in Zhalong are agricultural land, residential land, lakes and reservoirs, grassland, salina land, reed marshes and shallow water areas. Because the wetland is flat, using water to dilute and leach the super-abundant salinity in the soil will result in more serious harm to the wetland; pollution in the salina land is reduced only by new production and irrigation technologies. The quantity of water required to dilute and leach out soil salinity is not needed when calculating the eco-environmental water demand. The grassland that covers the majority of the lower catchment of the Wuyuer River (including the natural reserve) mostly depends on rainfall, and the development of irrigation over such a large area is not possible. The only method to alleviate the degeneration of the grassland is to reduce the pressure due to farming, using natural techniques. For the lake wetland ecosystem, in addition to maintaining the water demand for the growth and propagation of the aquatic plant and animal life, the water is needed to maintain aquatic habitats which offer the necessary growing, spawning and living areas through the winter for many species. The drop in lake water levels is detrimental to the eco-environment, and would lead, if completely dried out, to the disappearance of the whole lake ecosystem. It is thus important that the water level necessary for the Zhalong Wetland to survive is maintained and that evapotranspiration demands are included when quantifying the lake eco-environmental water demand. The natural vegetation around the wetland, including marshy bulrush, bosky, grassland and meadows, is principally irrigated from surface water and groundwater sources. It acts as a natural eco-barrier and plays an important habitat role for plants and animals. The water necessary for the natural vegetation around the wetland to survive is included when quantifying the eco-environmental water demand. There are more than 460 plant species in the Zhalong Wetland amongst which key species should be selected when calculating plant water demand. The basic character of the plants in Zhalong Wetland is described as a swamp mainly of brushwood type, consisting principally of reed, including small grass species, bulrush species and calamus species. Thus, the eco-environmental water demand should be calculated according to the water demand of the reed.

In the Zhalong Wetland, the eco-environmental water demand should be calculated considering the individual demands of lakes, plants, soil and wild life habitats in the key areas of lakes, swamps and reed (including reed and soil).

Method to calculate appropriate and minimum eco-environmental water demand

The appropriate quantity of the eco-environment water demand in a wetland is the quantity necessary to maintain and gradually improve the eco-environment of the wetland. It can be estimated from the average of the past water demands. The area of the lakes and reservoirs, shallow water areas and reed marshes in Zhalong Wetland have all gradually changed. This means that the quantity of the eco-environment water demand, calculated according to the land types and the past average rainfall over many years, has also changed. The methodology for calculating appropriate water demand is as follows: first, determine the appropriate area of the main land use types including lakes and reservoirs, shallow water areas and reed marshes, then calculate the quantity of the eco-environment water demand for each of these main land-use types based on the past average rainfall. The sum of the quantity of the eco-environment water demand for the appropriate area of these main land-use types is the appropriate quantity of the eco-environment water demand in the Zhalong Wetland.

The minimum quantity of the eco-environmental water demand is the smallest quantity necessary to maintain the ecosystem without it shrinking, degenerating, or disappearing. The central part of the Zhalong Nature Reserve is the core area that must be protected for endangered wildlife (animals and plants) to survive. The ecological water consumption of the core area is therefore the minimum eco-environmental water demand of the Zhalong wetland. It is essential to prevent the eco-function of the core area from degenerating. The appropriate quantity of the eco-environment water demand of a given area is the historical average quantity that has been necessary to maintain the eco-environment of this area, while the minimum quantity of the eco-environmental water demand of this area should consider the concept of the assurance probability. The minimum quantity of the eco-environmental water demand of the Zhalong Wetland is defined as the quantity of the eco-environmental water demand of the core area, which has a certain assurance probability, calculated on the basis of the design rainfall process.

CALCULATION OF THE ECO-ENVIRONMENTAL WATER DEMAND IN THE ZHALONG WETLAND

Land-use types and areas

Variations in land use extent in Zhalong Wetland over the years were assessed from 12 Landsat TM satellite images from 1986 to 2002. In 2002, swamp was the main land-use type, covering an area of 605.51 km^2, representing 83.67% of the core area (Table 1); swamp and grassland were the main land types of the sloping buffer (glacis) area with 530.06 km^2 (81.65% of the glacis area). Swamp, grassland and farmland were the main land types of the periphery area, where residential land was also found.

The sequence of monthly eco-environment water requirement

Based on average monthly rainfall and evaporation between 1986 and 2002, and using experimental evapotranspiration measurements in the reed, the monthly eco-environmental water demand for lakes and reservoirs, shallow water areas and reed marshes (including reed and soil) areas were calculated. Results showed an eco-environmental water demand in the whole Zhalong Wetland varying between 522 × 10^6 m^3 and 592 × 10^6 m^3 from 1986 to 2002 (Table 2).

Table 1 Land-use types and areas in the functional area of the ZaLong nature reserve in 2002 (km^2).

Land-use type	Core area	Buffer	Periphery	Total
Fields	18.81	56.77	174.9	250.48
Residential land	1.23	2.66	16.72	20.61
Lakes and reservoirs	18.51	31.74	36.73	86.98
Reed marshes	461.77	324.81	203.00	989.58
Shallow water areas	143.74	83.21	101.60	328.55
Grassland	66.80	122.04	126.85	315.39
Salina land	13.16	27.96	67.29	108.41
Total	723.71	649.19	727.09	2100.00

Table 2 Sequence of monthly and annual eco-environment water demand quantities in the Zhalong nature reserve in different periods ($\times 10^6$ m^3).

Time	Jan	Feb	Mar	Apr	May	June	Jul	Aug	Sep	Oct	Nov	Dec	Annual
1986-11	2.95	9.49	35.23	106.82	130.84	89.86	24.57	57.25	69.85	38.34	14.08	2.26	[illegible]
1988-9	1.94	6.24	23.13	88.31	115.88	86.58	43.47	68.14	68.32	27.92	9.24	1.48	[illegible]
1989-8	1.26	4.05	15.00	82.09	116.09	93.82	65.55	85.94	74.98	21.85	5.99	0.97	[illegible]
1998-5	2.26	7.29	27.05	90.63	114.66	82.07	31.84	58.44	64.28	30.74	10.81	1.73	[illegible]
1998-10	1.97	6.34	23.52	91.73	121.02	90.96	47.12	72.55	71.86	28.67	9.39	1.51	[illegible]
1999-10	1.80	5.82	21.59	87.59	116.68	88.64	48.35	72.30	70.14	26.83	8.63	1.39	[illegible]
2000-9	0.76	2.45	9.08	77.35	115.91	98.80	81.33	98.56	79.59	17.40	3.63	0.58	[illegible]
2001-4	0.51	1.64	6.07	74.63	115.31	100.86	88.90	104.47	81.55	15.08	2.42	0.39	[illegible]
2001-10	0.60	1.93	7.15	75.08	114.68	99.33	85.41	101.49	80.21	15.83	2.85	0.46	[illegible]
2002-4	0.63	2.02	7.53	73.98	112.38	96.88	82.29	98.32	78.17	15.90	3.00	0.48	[illegible]
2002-7	1.38	4.44	16.49	82.49	114.83	91.37	60.42	81.45	72.85	22.83	6.58	1.06	[illegible]
2002-10	1.29	4.15	15.39	81.61	114.82	92.32	63.37	83.82	73.72	22.01	6.15	0.99	[illegible]

Table 3 Appropriate and minimal monthly and annual eco-environment water demand quantities in the Zhalong nature reserve ($\times 10^6$ m^3).

Water demand quantity	Jan	Feb	Mar	Apr	May	June	Jul	Aug	Sep	Oct	Nov	Dec	All year
Appropriate	1.35	4.35	16.14	81.97	114.46	91.32	60.99	81.81	72.84	22.55	6.45	1.04	[illegible]
Minimal (the assurance probability is 75%)	0.54	1.77	6.55	40.44	58.28	47.93	35.56	45.27	38.41	10.23	2.61	0.42	[illegible]
Minimal (the assurance probability is 95%)	0.67	2.17	8.05	49.71	71.63	58.91	43.72	55.64	47.21	12.57	3.21	0.51	[illegible]

Appropriate eco-environment water requirement

Following suggestions from the Zhalong Nature Reserve Authority and the results of Table 1, the appropriate areas of the lakes and reservoirs, the shallow water areas and the reed marshes of the Zhalong Wetland were confirmed as 93 km^2, 343 km^2 and 965 km^2, respectively. The appropriate eco-environment water demand based on these areas is 555×10^6 m^3 (Table 3). Maintaining such a water supply for the wetland would prevent the lake from shrinking, prevent degeneration of the vegetation, and protect endangered animals and plant species.

Minimum eco-environment water requirement

In 2002 the areas of the lakes and reservoirs, the shallow water areas and the reed marshes in the core of the Zhalong Wetland were respectively 18.51 km^2, 143.74 km^2, 461.77 km^2 (Table 1). The eco-environment water demands for these areas are calculated based on the design rainfall process. The minimum quantity of the eco-environmental water demand with as assurance probability of 75% and 95% are 288 and 354×10^6 m^3 respectively (Table 3). Our research results showed that the average area needed by a couple of cranes is 2 km^2, the area of the reed marshes in the core of the Zhalong Wetland is 461.77 km^2 and can assure 461 cranes survival. This shows that the minimum eco-environment water requirement of the core of the Zhalong Wetland is sufficient for the protection of the endangered species in the Zhalong Wetland (there are 346 cranes in the Zhalong Wetland).

CONCLUSION AND SUGGESTIONS

Methods to calculate the appropriate and minimum eco-environmental water demand in the Zhalong Wetland have been suggested. However, due to the complexity of the wetland protection, we believe the following issues require more research:

1. How to satisfy the eco-environment water demand in the Zhalong Wetland from the perspective of whole catchment? Improving uniform water resources management, optimizing

the collocation of water resources, adjusting the industry structure in the upper stream, and implementation of agricultural practices that encourage water saving, should be the main approaches.

2. Conduct a feasibility study which uses flood water from the Nenjiang River to meet the eco-environmental water demand of the Zhalong Wetland.
3. Study of the harmony between human and wetlands.

REFERENCES

Cui Baoshan & Yang Zhifeng (2002) Water consumption for eco-environmental aspect on wetland. *J. Environ. Sci.* **22**(2), 219–224.

Cui Baoshan & Yang Zhifeng (2003) Classification and case study on eco-environmental water requirement of wetlands. *Resources Science* **25**(1), 21–28

Luan Zhaoqing, Deng Wei & Zhu Baoguang (2004) Estimation of eco-environmental water consumption for Hong River National Nature Reserve Wetlands. *J. Arid Land Resour. Environ.* **18**(1), 59–63.

Wang Dongsheng, Zhu Yao, Tan Hongwu & Li Guibao (2004) Eco-environmental water demand in the Tianjin Wetland. *Science Technique Engng* **4**(2), 127–130.

Zhang Xuliang (2004) Study on eco-environmental water requirement of Nansi Lake. *J. Qiqihaer University* **20**(2), 69–72.

Climate Variability and Change—Hydrological Impacts (Proceedings of the Fifth FRIEND World Conference held at Havana, Cuba, November 2006), IAHS Publ. 308, 2006.

Estimation of minimum acceptable (compensatory) flow for the rivers of Costa Rica

SADĹ LAPORTE, ALEXIA PACHECO & CARLOS R. RODRIGUEZ

C.S. Estudios Básicos de Ingeniería. Instituto Costarricense de Electricidad, PO Box 10032-1000, San José, Costa Rica
slaporte@ice.go.cr

Abstract A project for establishing minimum acceptable flow (MAF) is presented. The approach synthesizes knowledge about the natural river flow variability in space and time under low flow conditions in terms of probabilities and relates these to ecological demands, as well the demands of selected instream water uses. A hydraulic model linking discharges to the extent of usable area for biological indicator species and for socio-economic uses allows development of different hydropower regulation schemes in search for the optimal one. Testing different water regulation scenarios and their impact on natural runoff conditions, as well as ecological conditions and selected water uses offers a basis for sustainable solutions, preserving biodiversity and striving at equity in water use. The approach can be applied in any river basin of the humid tropics adjusting the chosen biological and socio-economic indicators to the characteristics of a particular basin.

Key words low flow; compensatory runoff; sustainability; humid tropics

INTRODUCTION

Availability of water is a natural constraint for all living organisms. However, in connection to human activities, water also becomes an invaluable natural resource of increasing importance and which is exploited more and more intensively. One severe negative impact on water resources is when too little water left in the river as a result of water use/withdrawals. This is not only a serious menace to the aquatic/riparian biota and basin environment as a whole, but is also a threat to many instream flow activities such as water supply, recreation, etc., and a factor that tends to aggravate eventual pollution problems. A sustainable development of water resources implies a policy balancing the interests of anthropogenic water uses and the requirements of the biotic environment. In response to this a new project has been started at the Instituto Costarricense de Electricidad (ICE) in Costa Rica with the aim of developing a methodology for determination of the compensatory[1] runoff based on the estimation of the minimum acceptable flow (MAF). The main aim is to optimize the use of water resources under low flow conditions, corresponding to the lowest boundary set up by the environment and various instream water uses; sustainability, balance and precaution being in focus. The demand for sustainability includes consideration of such aspects as biodiversity, equity, gender and poverty. This methodology will offer a reliable tool for water resources management and planning at the national level. The project, which will be finalized in 2007, consists of five interrelated parts (Fig. 1), and has six aims:

(1) Assessment of the natural low flow conditions for rivers in Costa Rica and their variability in space and time.
(2) Establishment of criteria (indicators) coupled to the maintenance of natural amenities, and identification of the minimum acceptable flow that satisfies the indicator species selected.
(3) Identification of the MAF requirements from the defined water uses.
(4) Combination of the information in 1-3 to determine MAF for two case studies.
(5) Establishment of a tool for testing different hydropower regulation scenarios under low flow conditions with respect to MAF in terms of usable parts of the river.
(6) Development of necessary software and databases.

As obvious from the aim formulation, the project is interdisciplinary, which is reflected in the project staff consisting of hydrologists, hydropower engineers, biologists and socio-economists. The project is carried out in co-operation with a multidisciplinary team of Swedish and Norwegian scientists. Below different parts of the project are presented in more detail.

[1] "Compensatory runoff" is a term commonly used in Costa Rica referring to the river runoff that can sustain the natural biological functioning of a river after hydropower regulation.

Copyright © 2006 IAHS Press

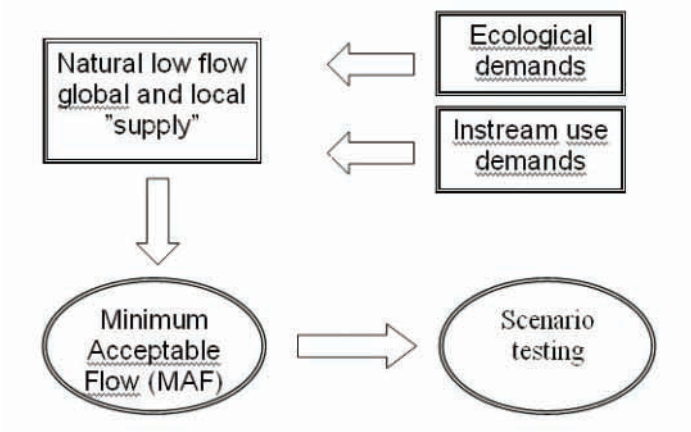


Fig. 1 Project blocks. "global" and "local" supply refers to the national and basin levels, respectively.

ASSESSMENT OF THE NATURAL LOW FLOW CONDITIONS

The first step when developing operational schemes for hydropower is correct description of the state of the runoff system in a historical perspective. Running water (lotic) ecosystems are extremely dynamic and reflect the natural variability of the water flow and the subsequent shifts in fluvial morphology. Before analysing the environmental impact of hydropower regulation schemes it is necessary to get a good idea of the regional runoff in terms of its temporal and spatial variation. This is usually done considering the **average** behaviour of runoff (assuming its stationarity), often described on the basis of a limited number of point observations and with no seasonal relevance. At the same time it is **extreme floods and droughts** that in combination with inappropriate water management may cause an irreversible deterioration of the water resources. The task is especially difficult if the observation records are short and scarce, since the credibility of the conclusions drawn on their basis must then be questioned. Regional approaches for the analyses of extreme low flow and dry spells (as well as floods) are generally preferred to an at-site analysis as it offers a more reliable ground for planning because the probability of observing an extreme event in a region is always bigger than the probability of observing such an event at one single station. A regional approach developed by Gottschalk *et al.* (2006b,c) and Sauquet *et al.* (2006) has been adopted in this study. This approach combines the theory of extreme events with an interpolation method considering basin support (i.e. development with area and time). It makes use of observed precipitation and runoff for the whole of Costa Rica, analysing dry spells jointly with the recession curves. Regionalization of flow duration curves (Krasovskaia *et al.*, 2006), water balance elements (Gomez *et al.*, 2006), low flow characteristics (Pacheco *et al.*, 2006), and runoff moments has been accomplished. Regional curves and digital maps allow determining the above variables for any river basin in Costa Rica (see example in Fig.2).

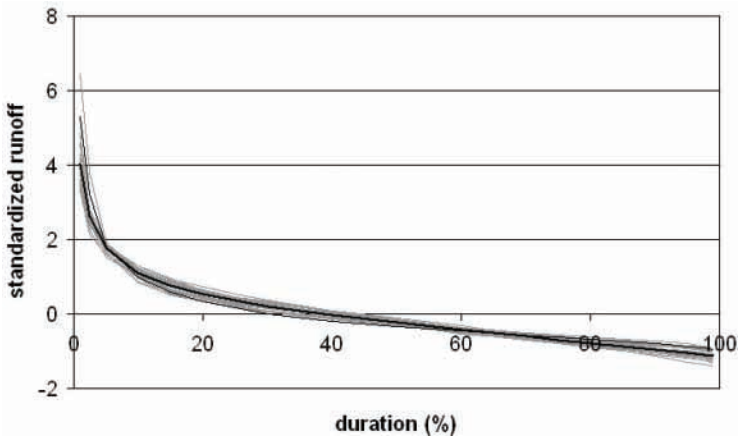


Fig. 2 Regional flow duration curve for basins of the Caribbean slope. Flow duration curves for individual basins are given as a background (from Krasovskaia *et al.*, 2006).

IDENTI FYING INDICATORS SPECIES AND THEIR DEMANDS TO MAF

Sustainability, balance and precaution represent the principle demands with respect to use of instream water, reflected in the directives for water resources development and management in many countries (e.g. Petts, 1996). Aquatic and riparian wildlife communities are dependent on instream flow that satisfies some basic ecological needs. During the last decade the environment has been recognised more and more as a legitimate user of water and some countries have even gone further claiming that "water belongs to the environment" (Dunbar *et al*., 1998).

This part of the project aims to identify biological demands to minimum flow with respect to useful biological indicators. Indicators are organisms or phenomena that have proven to be particularly sensitive to disturbance and which, in addition, are regarded as essential to sustain biodiversity. The maintenance of the natural biodiversity at some state is necessary for preventing the extermination of species. Some fish appear to be particularly useful as indicators, since they, by virtue of their food choice, integrate conditions on several trophic levels. In this study an Expert Panel approach (EPA) was utilized to identify first a ranked list of the indicator species to be used (Table 1) and then their habitat demands (Chavez *et al*., 2006). This approach proved to be very useful for humid tropical conditions with difficult access to the rivers. The expert opinions about the habitat demands of the indicator species were summarized using fuzzy logic into rules for tests of different scenarios (Gottschalk *et al*., 2006a). In parallel, direct fish sampling was carried out in two study areas noting at the same time habitat conditions in terms of stream velocities, depth and substrate. The data were stored in a database attributing the information to pre-defined river stretches. This information was needed for the validation carried out for case studies.

Table 1 List of the selected indicator species.

Group	Family, genus or species	Common name
Mammalia	*Noctilio* sp	Bats
	Lutra longicaudus	River Otter
	Procyon sp	Racoon
Aves	Ardeidae	Egrets and herons
	Alcedinidae	Kingfisher
	Phalacrocoracidae	Cormorant
Amphibia	*Bufo* sp	Toads
	Smilisca sordida	Tree frog
	Centrolenidae	glass frogs
Reptilia	*Rhinochlemmys*	Fresh water turtle
	Basiliscus sp	Jesus Christ lizard
	Leptophis sp	snake
Osteichthyes	*Joturus pichardi*	Hog mullet
	Sicydium altum	Gobiid
	Parachromis dovii	Rainbow bass
	Agonostomus monticola	Mountain mullet
	Brycon sp	Tetra
	Poecilia gilli	Molly

IDENTIFYING THE DEMANDS TO MAF FROM WATER USES

Within the framework of the project, specific demands for MAF from different water uses (e.g. domestic, fishing, agriculture, tourism, etc.) in two study areas were quantified. The data were collected with the help of personal interviews with stake-holders, questionnaires and studies of concessions for water use. The data were stored in a database attributing information to each river stretch (Table 2). Together with purely quantitative estimates of requirements to MAF from the stake-holders, qualitative information related to gender, family size and composition, main income source and economic activity were also collected during personal interviews. This qualitative information provides an important background for testing regulation schemes with special foci on sustainability, equity, poverty and gender.

Table 2 An example of data collected on water uses.

GENERAL LOCATION			
Basin	Savegre	Sector	3 Silencio – Río Blanco
Place	Santo Domingo		
Informant	Alfredo Grajal Gambo. From small store 100 m to south. White house at right		
ACTIVITY DESCRIPTION			
Use	Watering		
Name	Alfredo's Farmer		
Code	02-01-1	Site type	Point
Period of use	Season	Dry	
	Months	January to April	
	Days	Every day	
	Comments	5 hours by day. 3 hours in the morning (6–9) and 2 in the afternoon (3–5).	
Activity description	Crops: Melon and water melon Extension: 1–2 ha year^{-1} Consume 6–8 L s^{-1} when uses water in short distances (less than 100 m) and 3–4 L s^{-1} otherwise. He rents the equipments for watering.		
Estimated water discharge	Average: 5 L s^{-1} = 18 m^3 h^{-1} × 5 h day^{-1} = 90 m^3 day^{-1} × 30 days = 2700 m^3 month^{-1} × 4 months = 10 800 m^3 total during period of use		
Coordinates (CRTM)	498 049.93 1 044 153.00		
Photography			
Point description	From small store in Santa Domingo, 200 m on the way to bridge. First gate on left hand side, crossing the small river		

DETERMINATION OF MAF FOR CASE STUDY AREAS

The approach for establishing MAF synthesizes the knowledge about the natural river flow variability in space and time under low flow conditions in terms of probabilities and relates these to ecological demands outlined on the basis of the selected indicator species, as well the demands from the selected instream water uses. A simple hydraulic model links discharges to the extent of usable area for indicator species and water uses in terms of depths and velocities (Gottschalk *et al.*, 2006a). It allows testing of different hydropower regulation scenarios and their impact to find the optimal one. The modelled results are validated on field data for fish presence in different sectors of the river. Figure 3 shows a validation case for the Savegre River.

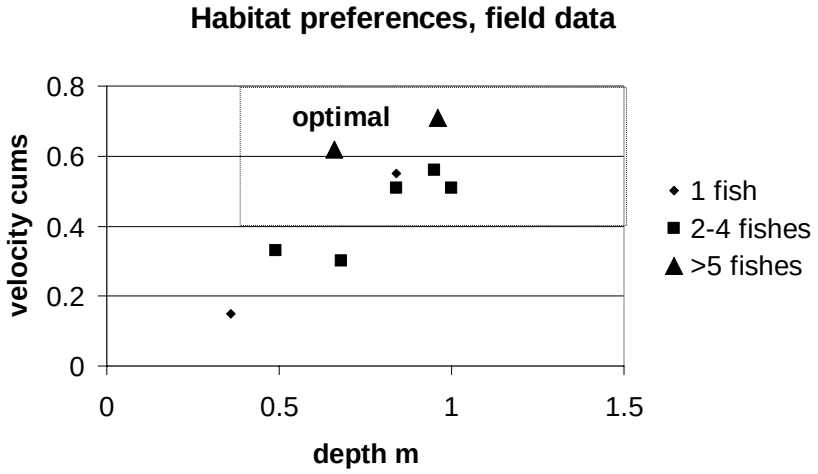


Fig. 3 Habitat preferences in terms of depth & velocity with optimal conditions shaded, field validation (from Gottschalk *et al.*, 2006a).

CONCLUSIONS

The approach described is now being introduced at Instituto Costarricense de Electricidad (ICE) and the project will be finished in spring 2007. When installed, the approach will make it possible to test different hydropower regulation scenarios for compensatory runoff in search of the optimal one. Consideration of environmental as well as socio-economic demands in such scenarios facilitates identification of the solutions that are sustainable, i.e. safeguarding biodiversity as well as equity of water use. Databases with biological and socio-economic data from the field, as well as information on identified biological and socio-economic indicators and their demands, offer well-structured reference materials for other environmental and socio-economic studies in the country and in the humid tropics. The approach can be applied in any river basin adjusting the chosen biological and socio-economic indicators to the characteristics of a particular basin.

Acknowledgements The project is being carried out with a financial support from the Swedish International Development Agency (SIDA) which help is gratefully acknowledged. Acknowledgements are also due to the University of Oslo, Norway, for granting a possibility to participate in the project to their scientists and supporting knowledge transference.

REFERENCES

Chavez, A., Krasovskaia, I. & Gottschalk, L. (2006) Environmental demands for sustainable regulation schemes in humid tropics. In: *Climate Variability and Change—Hydrological Impacts* (Proc. Fifth FRIEND World Conference held at Havana, Cuba, November 2006). IAHS Publ. 308. IAHS press, Wallingford, UK (this volume).

Dunbar, M. J., Gustard, A., Acreman, M. C. & Elliott, C. R. N. (1998) Overseas approaches to setting River Flow Objectives. Environment Agency and Institute of Hydrology, R&D *Technical Report W6-161*.

Gómez, F., Krasovskaia, I., Gottschalk, L. & Leblois, E. (2006) Interpolation of water balance components for Costa Rica. In: *Climate Variability and Change—Hydrological Impacts* (Proc. Fifth FRIEND World Conference held at Havana, Cuba, November 2006). IAHS Publ. 308. IAHS Press, Wallingford, UK (this volume).

Gottschalk, L., Gómez, F., Krasovskaia, I. & Chaves, A. (2006a) Estimation of the "minimum acceptable flow" for rivers of Costa Rica. Nordic Hydrological Conference NHK-2006, Denmark (accepted).

Gottschalk, L., Krasovskaia, I., Leblois, E. & Sauquet, E. (2006b) Mapping runoff characteristics in a river basin. In: *Climate Variability and Change—Hydrological Impacts* (Proc. Fifth FRIEND World Conference held at Havana, Cuba, November 2006). IAHS Publ. 308. IAHS Press, Wallingford, UK (this volume).

Gottschalk, L., Krasovskaia, I., Leblois, E. & Sauquet, E. (2006c) Mapping of mean and variance of runoff in a river basin. *HESS Discuss.* **3**, 1–35. http://www.hydrol-earth-syst-sci-discuss.net/3/1/2006/.

Krasovskaia, I., Gottschalk, L, Leblois, E. & Pacheco, A. (2006) Regionalization of flow duration curves. In: *Climate Variability and Change—Hydrological Impacts* (Proc. Fifth FRIEND World Conference held at Havana, Cuba, November 2006). IAHS Publ. 308. IAHS Press, Wallingford, UK (this volume).

Pacheco, A., Gottschalk, L. & Krasovskaia, I. (2006) Regionalization of low flow in Costa Rica. In: *Climate Variability and Change—Hydrological Impacts* (Proc. Fifth FRIEND World Conference held at Havana, Cuba, November 2006). IAHS Publ. 308. IAHS Press, Wallingford, UK (this volume).

Petts, G. E. (1996) Water allocation to protect river ecosystems. *Regulated Rivers: Research & Management* **12,** 353–365.

Sauquet, E., Gottschalk, L., Krasovskaia, I., Leblois, E. (2006) Predicting river flow statistics at ungauged locations—a hydrostochastic approach. In: *Large Sample Basin Experiments for Hydrological Model Parametization: Results of the Model Parameter Experiment–MOPEX* (Proceedings of the Paris (2004) and Foz de Iguaçu (2005) workshops). IAHS Publ. 307. IAHS Press, Wallingford, UK (in press).

Climate Variability and Change—Hydrological Impacts (Proceedings of the Fifth FRIEND World Conference held at Havana, Cuba, November 2006), IAHS Publ. 308, 2006.

Hidrología de laguna albúfera Reserva El Yali, humedal RAMSAR, Chile

PABLO GALDAMES, CHI SUN & ALEJANDRO DUSSAILLANT J.

Departamento de Ingeniería Hidráulica y Ambiental, Pontificia Universidad Católica de Chile, Vicuña Mackenna 4860, Santiago, Chile.

pgaldame@ing.puc.cl

Resumen La laguna albúfera El Yali es un humedal de gran importancia en la zona central de Chile, especialmente debido a su relación con la avifauna tanto nativa como foránea que llega aquí periódicamente, siendo hábitat para cerca de un 25% de la biodiversidad de aves en Chile. Este estudio pretende identificar y cuantificar las principales variables del ciclo hidrológico de la laguna e caracterizar las principales variables físico-químicas de las aguas superficiales y subterráneas, en pos de estimar un balance hidrológico del humedal que permita en el futuro evaluar la vulnerabilidad de este cuerpo de agua. Los datos aún no permiten identificar el ciclo hidrológico de la laguna, pero serán presentados los registros recabados, incluyendo el comportamiento de la napa en los lados costero e interior de la laguna. Se ha detectado una importante concentración de fosfatos provenientes del acuífero, cuya magnitud (sobre los 2 mg $(PO)_4^{3-}$ L^{-1}) triplica la existente en el cuerpo de agua (alrededor de 1 mg $(PO)_4^{3-}$ L^{-1}).

Palabras clave humedal; eutroficacion; laguna costera; balance hídrico; nutrientes

Hydrology of the El Yali coastal marsh reserve, a RAMSAR site in Chile

Abstract The El Yali tidal salt marsh is a very important wetland in the central zone of Chile, especially due to its relation with the native bird fauna; it is the habitat for about 25% of the bird biodiversity in Chile. This study is trying to identify and quantify the main variables in the hydrological cycle of the lagoon and to characterize the main physiochemical variables for the surface water and groundwater. This will be the base information from which to estimate a hydrological budget for the wetland that allows evaluation of the vulnerability of this water body in the future. The data collected does not allow us to quantify the hydrological cycle for the lagoon as yet, but cumulative data are presented, including the groundwater signals on the oceanic and interior sides of the lagoon. An important concentration of phosphates coming from the aquifer has been detected, with a magnitude greater than 2 mg $(PO)_4^{3-}$ L^{-1}, which triples that existing in the water body (around 1 mg $(PO)_4^{3-}$ L^{-1}).

Key words wetland; eutrophication; coastal lagoon; hydrologic budget; nutrients

INTRODUCCIÓN

El Yali comprende más de 10 cuerpos y cursos de agua, y es el único humedal mediterráneo del neotrópico que esta adherido a la Convención Ramsar (Möder *et al*., 2002). Constituye un área de concentración y descanso de varias especies migratorias tanto a nivel altitudinal, latitudinal como inter-hemisferios. Este complejo posee un alto dinamismo estacional (invierno–verano) y cíclico, esto último asociado al fenómeno ENSO (Möder *et al*., 2002). Parte del Complejo de Humedales El Yali es un área silvestre protegida administrada por la Corporación Nacional Forestal (CONAF), el servicio forestal chileno, y tiene una superficie de 520 ha, denominada "Reserva Nacional El Yali", que se encuentra en la Comuna de Santo Domingo, en la V Región de Chile, 33°44′ a 33°47′S y 71°39′ a 71°46′N (Dussaillant, 2005).

El clima de la zona es mediterráneo, atenuado por la influencia marina, presentando una marcada estacionalidad en relación a las precipitaciones, con otoño e inviernos lluviosos y veranos secos. Como típica cuenca costera de la zona, la cuenca del humedal tiene régimen puramente pluvial. Tanto el estero El Yali como sus afluentes permanecen largos períodos de tiempo secos, presentando escurrimiento superficial solamente después de precipitaciones intensas (DGA, 2000).

En general el sector ha sido de particular interés (y por tanto protegido) básicamente debido a la abundancia de avifauna, unas 115 especies, lo que representa aproximadamente el 25% de la diversidad autóctona de avifauna chilena (Leiva *et al*., 1995). El sector es fuente de un estudio ecológico en proceso sobre la respuesta de las comunidades vegetacionales a gradientes de variables fisicoquímicas y en particular de nutrientes (Fariña *et al.*, 2004).

En base a visitas en terreno, recopilación de antecedentes y datos, así como análisis, se estima que el balance hidrológico de la laguna es función de los siguientes elementos: precipitación (invernal), estero Yali, drenaje de las aguas lluvia por acequias desde pendiente arriba, conexión

Copyright © 2006 IAHS Press

esporádica superficial con el océano (inundaciones mareales y tormentas de invierno), intrusión subsuperficial de agua desde (y hacia) océano, flujo de agua dulce subterránea desde pendiente arriba y evapotranspiración.

La dinámica hidrológica de la laguna albúfera es de singular importancia, pues afecta al menos los siguientes: altura de agua en la laguna y su efecto en la distribución y abundancia de plantas; elementos abióticos: temperatura, pH, potencial redox, solutos (sales, nutrientes)—también con efecto en zonación y abundancia de especies vegetales (y animales). A su vez, la dinámica hidrológica puede ser afectada potencialmente por las siguientes perturbaciones naturales y antrópicas: extracción de agua subterránea por crecimiento del turismo y cultivos (palta) en el balance de agua de la laguna; cambio climático y El Niño (precipitaciones, tormentas costeras); erosión y depositación de sedimento; contaminación de aguas entrantes a la laguna (Dussaillant, 2005).

Hasta la fecha se desconoce el balance hídrico correspondiente a las entradas y salidas de agua que presenta la laguna albúfera de la Reserva El Yali, por lo que este estudio tiene por objetivos identificar y cuantificar los principales flujos de agua de la laguna albúfera, establecer la calidad de las aguas entrantes y salientes del sistema, realizar un balance de masa de variables fisicoquímicas (oxígeno disuelto, pH, nitrógeno, fósforo, salinidad) y determinar las variaciones estacionales de cantidad y calidad de las aguas, así como los procesos clave que afectan éstos.

METODOLOGÍA

La laguna tiene una forma alargada, dispuesta en forma paralela a la playa, conectada en un extremo con el Estero Yali, y eventualmente conectada en forma superficial con el mar. Una imagen satelital de la laguna se muestra en la Fig. 1. Dada su configuración, se destacan dos zonas con características diferentes: pendiente arriba de la laguna, donde el flujo se relaciona con el acuífero de la cuenca que, en teoría, estaría descargando hacia esta zona, y en el sector entre la laguna y el mar hay influencia de este último tanto en la magnitud de los flujos como en la calidad de éstos.

Debido a la fuerte dependencia del nivel de la laguna—y presumiblemente, la napa adyacente—con el nivel de la marea, los monitoreos se están realizando para los eventos de luna llena de cada mes, ya que para entonces las mareas son más vivas, registrando mayores amplitudes en la oscilación diaria, por lo que la hipótesis es que en estas ocasiones se debiera producir un mayor movimiento del agua y las sustancias presentes en ella se estarían transportando en mayor volumen.

Medición de la cantidad de agua

Para la medición de la cantidad de las aguas que ingresan al sistema por vía subterránea se utilizará la ecuación de Darcy para suelos saturados: $Q = S \cdot Ks \cdot \Delta H$, con Q el caudal circulante, S, la sección de flujo, Ks, conductividad hidráulica saturada y ΔH, el gradiente de energía entre dos puntos de medición de la napa. La conductividad hidráulica saturada se ha obtenido con pruebas de laboratorio, pero se espera realizar mediciones en terreno para corroborar los valores obtenidos. En cuanto a la obtención del gradiente de energía, se ha instalado una red de piezómetros dispuestos a ambos lados de la laguna: hacia la zona de pendiente arriba para conocer la conexión con el acuífero de la cuenca, y en dirección al mar para estimar flujos hacia y desde el mar. Los piezómetros están instalados algunos centímetros bajo el nivel de la napa, de manera de obtener información sobre la posición de la superficie libre para todo momento y acceder así a información sobre la dependencia de estos niveles con las fluctuaciones de las mareas.

La medición de la cantidad de agua que ingresa al sistema vía superficial se realizará mediante la instalación de una estación de aforo en el estero Yali, y de aforadores en acequias existentes en la zona de pendiente arriba del sistema. Además, se instalarán piezómetros en los costados de las acequias para determinar si existe influencia de la napa en el flujo y calidad de agua que circula por ellas

Medición de la calidad de agua

Además de la determinación de la cantidad de agua que está entrando o saliendo, se quiere conocer el gradiente de concentración de sales y nutrientes presentes (específicamente se están analizando concentraciones de nitratos y fosfatos disueltos), para obtener información acerca de la dependencia

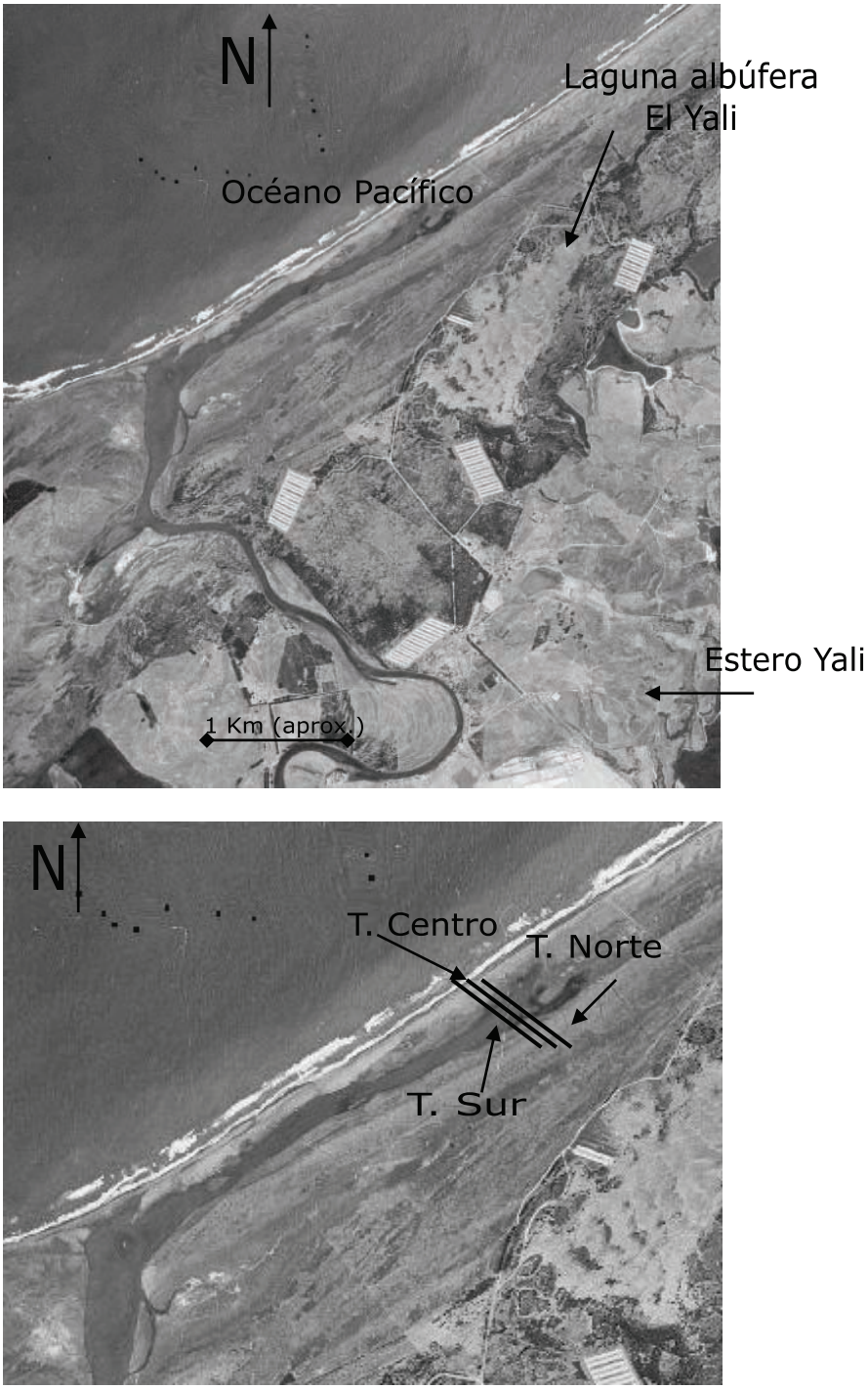


Fig. 1 Imagen satelital de laguna albúfera El Yali con ubicación general (arriba) y de transectos de piezómetros (abajo).

con el mar y tener indicios sobre la vulnerabilidad de este humedal a la posibilidad de sufrir eutroficación natural o antropogénica. Además, se registran los valores medidos de oxígeno disuelto y acidez (pH) para tener más información de las condiciones ambientales existentes. Esta información está siendo recolectada desde los piezómetros instalados en terreno, la laguna albúfera, el mar, el estero y las acequias.

RESULTADOS PARCIALES

Con los datos que se obtengan en el desarrollo del estudio se tendrá información desconocida hasta el momento sobre la magnitud de los principales ingresos y egresos de agua a la laguna albúfera, y

de la vulnerabilidad de este sistema lacustre frente a posibles contaminantes que pudieran ingresar desde la parte alta de la cuenca o desde el mar. Se conocerá la dependencia de la fluctuación del nivel de agua de la laguna con la variación de las mareas tanto a nivel diario como estacional, así como las principales características físico-químicas de las aguas del humedal y las zonas aledañas.

Actualmente los datos con los que se cuenta no permiten llegar a conclusiones definitivas, pero se puede indicar que en todo el sector adyacente a la albúfera hay un buen drenaje, ya que son suelos gruesos que contienen grava y arena fina cuya conductividad hidráulica saturada varía entre los 2.5 a 4.5 m d^{-1} en el lado oriente de la laguna para los ensayos realizados, mientras que en el lado poniente (Fig. 1) el rango es entre 0.5 a 0.6 m d^{-1}. En base a información hidrogeológica que sostiene que en la zona en que acuífero llega al mar, éste tiene una profundidad promedio de 100m (MOP, 2005), y con niveles registrados en pozos de observación durante el verano, se estima que durante esta época es el mar quien recarga al acuífero con caudales entre los 1.8 y 2.2 $m^3 d^{-1}$ por metro de ancho de la zona de flujo, dependiendo de la fase de la Luna. En invierno, se produce una conexión directa por vía superficial entre el mar y la laguna, induciendo una oscilación diaria del nivel de la laguna alrededor de un orden de magnitud mayor a lo registrado en verano; este efecto se encuentra aún en estudio hasta el momento de la publicación de este artículo.

En lo referente a la calidad de las aguas, se puede apreciar que las aguas provenientes desde el acuífero superior son claramente aguas dulces, presentando salinidades promedio inferiores a 3‰, mientras que la laguna presenta valores de salinidad promedio de 35‰ en la zona oriente y 45‰ en la zona poniente, cercana al mar, existiendo así un gradiente de salinidad al interior del cuerpo de agua (Fig. 2). Además, en la zona subterránea entre la laguna y el mar, se detectó que la salinidad del agua disminuye conforme se aleja de ambos cuerpos de agua alcanzando un promedio mínimo cercano a 10‰, aproximadamente a 27 m de la orilla poniente de la laguna, por lo que se estaría en presencia de una doble cuña salina producida por la presencia de cuerpos de agua salobre a ambos lados de la napa en este sector de estudio, como se puede apreciar en la Fig. 2, de un transecto representativo de la zona.

En cuanto a la acidez de las aguas, en la napa se registran todos los valores en niveles neutros, alcanzando en los pozos estudiados un promedio mínimo de 6.53 y máximo de 7.76, mientras que en la laguna misma los promedios son de 8.60 y 8.62 para la orilla oriente y poniente, respectivamente, a la vez que el mar se sitúa en 8.06.

El oxígeno disuelto no parece seguir un patrón espacial definido. Los valores en la napa se sitúan entre los 2 y 4 mg L^{-1}, mientras que las aguas superficiales de la laguna (máximo medido de 12 mg L^{-1}) y el mar son del orden de 6 a 9 mg L^{-1}.

De los nutrientes evaluados en las muestras, el nitrato se presenta en forma relativamente constante tanto en los piezómetros como en los cuerpos superficiales de agua, tomando valores inferiores a 1.0 mg $N\text{-}NO_3^-$ L^{-1} en gran parte de las muestras evaluadas (Fig. 2). Por otro lado, el fosfato presenta un comportamiento bastante diferente al del nitrato, ya que los promedios de las concentraciones registradas parecen manifestar una clara tendencia a ir descendiendo a medida que el agua se va acercando al mar (Fig. 2). Los puntos más orientales de medición están prácticamente todos sobre los 2.0 mg $(PO)_4^{3-}$ L^{-1} (salvo el pozo margen oriental, situación que aún se encuentra en estudio) manifestando un punto con un peak de 25.6 mg $(PO)_4^{3-}$ L^{-1}, con un promedio alrededor de 0.97 mg $(PO)_4^{3-}$ L^{-1} en la laguna y valores de la napa poniente que decrecen hasta llegar a los 0.21 mg $(PO)_4^{3-}$ L^{-1} en el mar. Para el caso de las aguas que fluyen por las acequias, las muestras presentan una concentración más alta de nitrato comparado con el agua subterránea y la laguna, y varía dependiendo del punto de muestreo. Una posible explicación a esta variación es la presencia, en forma ocasional durante el día, de ganado bovino en el humedal que ocupan las acequias como fuentes de agua. Los resultados de los análisis en tres puntos de muestreos, de este a oeste, arrojaron valores promedios de 1.09, 1.97 y 2.00 mg $N\text{-}NO_3^-$ L^{-1}, con un máximo de 4.6 mg $N\text{-}NO_3^-$ L^{-1}, medido en la acequia central. El fosfato también presenta una variación espacial y con concentraciones tan altas, salvo en un punto de muestreo, como los medidos en el agua subterránea. El promedio de las concentraciones es de 2.73, 4.19 y 2.03 mg $(PO)_4^{3-}$ L^{-1}, con un máximo de 9.28, registrado en la acequia sur de muestreo.

TRABAJO FUTURO

Dado que el proyecto se encuentra aún en una fase inicial, el trabajo que se vislumbra a futuro pretende completar las mediciones de la conductividad saturada de campo con las cuales se podría mejorar la estimación de la recarga de agua dulce desde el acuífero al humedal (o recarga al acuífero desde el humedal si la información recolectada del nivel de la napa y salinidad así lo indicasen), además, se analizará el efecto de las mareas -y consecuente nivel de la laguna- con el sentido del flujo vertical del fondo de la laguna mediante la implementación de un sistema de *seepage meters.*

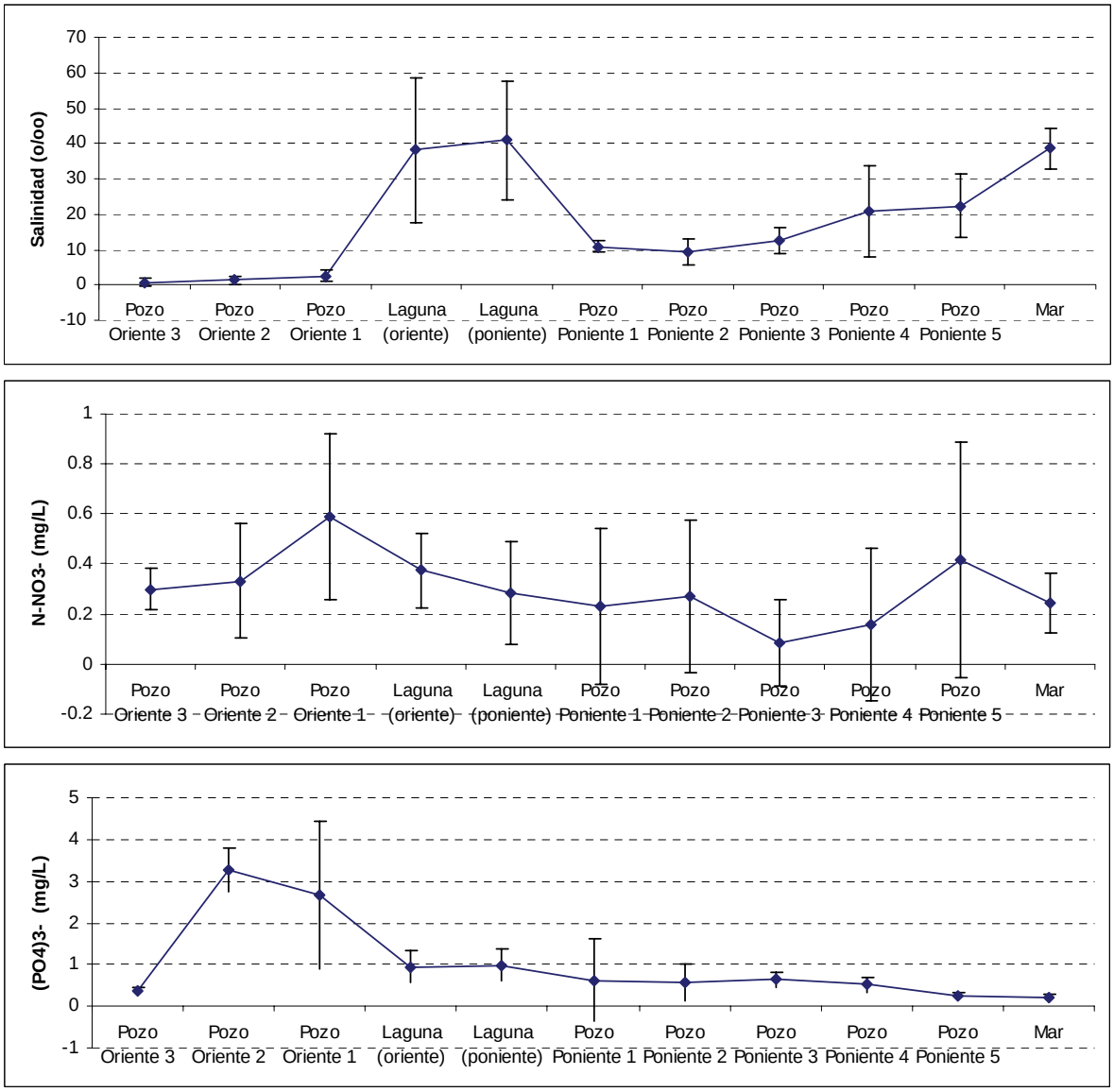


Fig. 2 Calidad de agua subterránea en un transecto de piezómetros representativo: salinidad (arriba), nitrato (medio), fosfato (abajo). Promedios ± desviación estándar.

Además, se mantendrán las mediciones periódicas de los niveles de la laguna y de piezómetros de la napa (transductores con data logger), y análisis químico de las muestras obtenidas para completar la base de datos y poder tener una certeza estadística del comportamiento de los parámetros estudiados. Adicionalmente, se estudia la aplicación de un modelo de simulación del agua subterránea.

Agradecimientos Los autores agradecen el permiso y apoyo en terreno de la Corporación Nacional Forestal (CONAF-Chile) V Región, así como la colaboración con el grupo de ecología de ecosistemas del Dr. José Miguel Fariña del CASEB PUC.

REFERENCIAS

DGA (Dirección General de Aguas, Ministerio de Obras Públicas) (2000) Evaluación de los Recursos Hídricos Subterráneos Cuenca Estero Yali: Informe Final.

Dussaillant, A. (2005) Propuesta de investigación aplicada RAMSAR. Hidrología y efectos ecológicos en laguna albúfera Reserva Nacional El Yali, V Región, Chile.

Fariña, J. M., Bertness, M. D. & Silliman, B. (2004) Informe de Resultados Primer Año. Efectos de la competencia, estrés ambiental y herbivoría en los patrones de zonación del ensamble de plantas presentes en el humedal costero de El Yali, V Región, Chile.

Leiva, I., Meza, J. & Möder, L. (1995) Fundamentos para la creación de la Reserva Nacional El Yali. CONAF.

Ministerio de Obras Públilcas (MOP) (2005) Area de restricción sector hidrogeológico de aprovechamiento común de Yali bajo El Prado.

Möder L., Gallardo H., Vilina Y. (2002) Ficha informativa de los humedales Ramsar. Humedal El Yali.

Climate Variability and Change—Hydrological Impacts (Proceedings of the Fifth FRIEND World Conference held at Havana, Cuba, November 2006), IAHS Publ. 308, 2006.

Environmental demands for sustainable regulation schemes in the humid tropics

ANNY CHAVES[1], IRINA KRASOVSKAIA[2] & LARS GOTTSCHALK[2]

1 *Centro de Gestión Ambiental, Instituto Costarricense de Electricidad, PO Box 10032-1000 San José, Costa Rica*
achaves@ice.go.cr

2 *Department of Geosciences, University of Oslo, PO Box 1022 Blindern, N-0315 Oslo, Norway*

Abstract Water is one of the most important natural resources in many countries of the humid tropics. It supports many socio-economic activities and provides a renewable energy source for economic development. Sustainability of water projects includes maintenance of biodiversity. Consideration of environmental demands in the basins is an essential component in regulation schemes. This study utilized an Expert Panel Approach to select indicator species for a sustainable runoff in a tropical environment of Costa Rica and to identify their environmental demands. A ranked list of indicator species, chosen based on their sensitivity to changes in river flow caused by regulation, was suggested by experts on tropical flora and fauna at the first expert panel. The second expert panel defined environmental demands of the proposed indicator species in terms of water depth, stream velocity and substrate type. The information obtained provides the necessary background for evaluation of the impact of different regulation schemes on the aquatic environment.

Key words indicator species; habitat preference; Expert Panel Approach; environmental demands; sustainable runoff

INTRODUCTION

Water is one of the most important natural resources in many countries situated in the humid tropics. It supports many socio-economic activities and its development provides a renewable energy source for economic growth. The sustainability of such development also includes the maintenance of biodiversity. Consideration of environmental and social demands in the basins is an essential part in regulation schemes. Using bio-indicators as an early warning of degradation in an ecosystem can help sustain water resources. Indicators are groups or types of biological resources that can be used to assess environmental conditions. There has been a rapid increase in the number of studies devoted to developing biological criteria for sustainability during recent years (e.g. Hirvonen, 1992; Nip *et al.*, 1992; Lovejoy, 1994). Biological indicator species are species that are particularly sensitive to disturbances and are essential for the maintenance of biodiversity. Their decline may indicate a disturbance that alters the ecosystem. Which species are selected depends on the questions being posed and especially whether one aspect of an ecosystem is monitored for a specific purpose. Using biological indicator species is particularly useful when the extremely rich biodiversity of a system (e.g. the Costa Rican humid tropics environment) makes it difficult to assess the whole bio-community.

Selection of indicator species can be approached in different ways. They can be chosen based on literature surveys for analogue environments or based on the experience of long-term monitoring of habitats. Judging from the scientific literature, Costa Rica is rather well known in terms of its aquatic and riparian biological communities (e.g. Wootton & Oemke, 1992; Ramirez & Pringle, 1998). Literature references offer useful data sources but this information was not sufficient for the choice of indicator species as it has been collected for different purposes. This study is part of the project "Estimation of minimum acceptable (compensatory) flow for the rivers of Costa Rica" (Laporte *et al.*, 2006) with the aim to develop sustainable water regulation schemes for low flow conditions in tropical environments. Information from the literature has been used in this study as a complement to other sources.

The time schedule of the project excluded long-term monitoring possibilities. That is why an Expert Panel Approach (EPA) has been used here to identify the indicator species for the particular aim of the project and to describe their habitat demands. The EPA approach is a well-established scientific tool used in many disciplines and also in hydrology and ecology (e.g. Marcot *et al.*, 1997; Kumar *et al.*, 2002). This paper presents the procedures for selecting indicator species for the humid tropics and identification of their habitat demands for developing criteria for sustainable water regulation schemes under low flow conditions. Field sampling in two case-study basins will be used for validation purposes.

Copyright © 2006 IAHS Press

INDICATOR SPECIES FOR INSTREAM FLOW

Certain fish, terrestrial vertebrates that are dependent on an aquatic system and macro-invertebrates can be used as indicators of ecological runoff conditions in a river. Among those, migrating species have a capacity to reflect conditions in larger areas than those that permanently stay in a limited area and thus reflect the conditions only there. This is why fish are often used when defining the biological integrity of streams and rivers, i.e. the overall functioning of lotic ecosystems (Angermeier & Karr, 1986; Davis & Simon, 1995). The species chosen should provide standards of consistency and precision about changes in a community and they should be reliable enough so that changes and trends are detected unambiguously (Watson *et al.*, 1995). Selection of biological indicators must also be guided by the uses to which the indicators will be put. A number of general attributes have been suggested for indicator species (Hutcheson *et al.*, 1999), such as:

(a) being sensitive to change over a short time-frame within the period of measurement;
(b) being widespread through the study area;
(c) being widespread through time and not just ephemeral;
(d) having occurrence related to dynamic processes or functions;
(e) being clearly measurable, e.g. in size, abundance, growth, structure or frequency;
(f) being cross-referable to other indicators, while having independent attributes.

The use of EPA may offer a good solution considering the difficulty of the selection task. The EPA has been used in this study for this purpose. A group of 15 experts in tropical flora and fauna with a background in both academia and operative services were invited to the EP. As a first step, the experts worked individually to select and recommend the indicator species with a view to the aim of the project. The selection of indicator species was based on their tolerance and sensitivity to changes in river flow as a result of regulation. Tolerance and sensitivity to the following effects was considered: interruption of migration possibilities; impact on physiological processes; decrease of the wetted perimeter; collapse of the associated wet areas; and change of trophic conditions. The tolerance and sensitivity were graded from one to ten, the latter describing the highest grade of sensitivity. As complementary criteria, species abundance and habitat abundance were ranked to ensure that it is possible to easily find the indicator species. In the second phase of the panel an open discussion of the suggestions from individual experts took place to reach a consensus. Three species in each group (*Mammalia*, *Aves*, *Amphibia*, *Reptilia*, *Osteichthyes*) that obtained the highest summary grade were then selected as indicator species. As the fish group was chosen as a focus in the investigation, six indicator species were suggested for this group. Table 1 shows the list of indicator species suggested in this study.

Table 1 List of the selected indicator species.

Group	Family, genus or species	Common name
Mammalia	*Noctilio* sp	Bats
	Lutra longicaudus	River Otter
	Procyon sp	Racoon
Aves	Ardeidae	Egrets and herons
	Alcedinidae	Kingfisher
	Phalacrocoracidae	Cormorant
Amphibia	*Bufo* sp	Toads
	Smilisca sordida	Tree frog
	Centrolenidae	Glass frogs
Reptilia	*Rhinochlemmys*	Fresh water turtle
	Basiliscus sp	Jesus Christ lizard
	Leptophis sp	snake
Osteichthyes	*Joturus pichardi*	Hog mullet
	Sicydium altum	Gobiid
	Parachromis dovii	Rainbow bass
	Agonostomus monticola	Mountain mullet
	Brycon sp	Tetra
	Poecilia gilli	Molly

HABITAT PREFERENCES FOR INDICATOR SPECIES

Identification of the habitat preferences of the indicator species is of a great importance while developing criteria for sustainable flow regulation. Similar to the selection of indicator species, such information can be obtained from the literature, from long-term habitat monitoring or by means of Expert Panels. No long-term monitoring was feasible in the time frame of the project but a two-year long field measurement programme has been started in two case-study areas in order to provide validation data for habitat demands. Previous studies described in the scientific literature were used in this study for terrestrial vertebrates and macro-invertebrates. For the fish that were the focus of the study, the EP approach has been chosen. This allows use of the knowledge accumulated by experienced specialists during many years of work in the field that often has not been documented in publications. For validation based on field data, one fish species, the Mountain Mullet (*Agonostomus monticola)*, common in Costa Rica and also in other parts of the world, has been chosen. Other species were also considered for validation purposes: Hog Mullet (*Joturus pichardi)* that was highly ranked by the first EP. However, this species is found primarily in the basins of the Caribbean slopes of Costa Rica and its population has decreased during recent years.

The second Expert Panel allowed definition of the environmental demands of the proposed indicator species in terms of water depth, stream velocity and substrate type, ranking these as optimal, normal or inadequate. The choice of these habitat descriptors was made with respect to the practical possibilities of acquiring such data, as the basins concerned for regulation in humid tropics as a rule are situated in mountainous areas that are difficult to access. Possible velocities in the rivers of Costa Rica during the limiting dry season were classed in advance as: very slow; slow; moderate; fast and very fast, offering a linguistic "transference" table to the experts. The linguistic classification proved to be much easier for the experts compared to quantitative velocity classes. Six classes of substrate were distinguished: clay; silt; sand; gravels; stones; and blocks. To facilitate the answers for depths and velocities, graphical illustrations were provided. The experts compiled habitat characteristics for each of the chosen indicator species attributing a corresponding category, i.e. optimal, normal or inadequate. Intervals of values were allowed. Table 2 presents the questionnaire suggested to the experts during the second EP and their answers on the example of Mountain Mullet (*Agonostomus monticola)*. All qualitative and quantitative data have been stored in a database as reference material for other environmental studies in Costa Rica.

The information was assembled and discussed at a plenary meeting where the final scheme for characterizing habitat demands for the chosen indicator species was compiled. Using this information fuzzy rules have been developed for further use in combination with a simple hydraulic model to test different regulation scenarios in terms of usable habitat areas in a river (Gottschalk *et al.*, 2006).

Table 2 Questionnaire for the experts at the second EP; example for *Agonostomus monticola*.

Question		Answer		
1.	*What are the general habitat preferences for the species?*	Current from moderate to rapids, with good source of food (aquatic insects). Altitude from the sea level to 800 m.		
2.	*What range do you consider as inadequate, regular and optimum for the following habitat characteristics: substrate, velocity and depth?*	Inadequate	Regular	Optimum
		Velocity:		
		Very slow	Moderate to very strong	Strong
		Depth:		
		<0.25	0.25–0.35; 2.00–3.00	>0.35 – <2.00
		Substrate:		
		Clay and loam	Sand and gravel	Rocks and boulders
3.	*To which factors are species highly sensible according to your opinion?*	Slow currents, excess of sediments, and substrate for insects. Clean waters well oxygenated.		
4.	Comments	Evidence of migratory behavior, the continuity of flow and absence of any kind of barrier are very important for the species.		

Field investigation

As noted earlier, field investigations have been started in two study areas to collect data for validation of habitat demands established with the help of the EPs for two example species: *Agonostomus monticola* and *Joturus pichardi*. The presence of these species was evaluated visually by means of snorkeling in each river section in the two basins of study, at the same time measuring flow velocity and depth and classifying substrate. Information about the characteristics of the ecosystem is also registered. This sampling will be on-going during two years to yield field data about habitat preferences.

CONCLUSIONS

EPA is an effective and low-cost tool for selecting indicator species and establishing their habitat demands in the humid tropics, especially when financial resources are limited and difficult access to rivers limits extensive field investigations. A useful list of indicator species for studies related to minimum acceptable river flow in the humid tropics has been successfully established using EPA. The EPA also identified habitat demands for the selected indicator species. Simple and readily available habitat characteristics related to river flow would allow direct tests of sensitivity of habitats to different flow regulation schemes. The choice of habitat characteristics can be easily adjusted to the needs and practical possibilities of each particular study, while the list of indicator species can be used as a reference for other projects in the humid tropics. Supported by field validation the method provides reliable and indispensable information for testing different scenarios of river flow regulation in search of environmentally sustainable schemes. A similar approach has also been developed for evaluation of the effects of regulation for socio-economic activities in a basin.

REFERENCES

Angermeier, P. L. & Karr, J. R. (1986) Applying an index of biotic integrity based on stream fish communities: considerations in sampling and interpretation. *North American J. Fisheries Management* **6**, 418–429.

Davis, W. S. & Simon, T. P. (eds) (1995) *Biological Assessment and Criteria: Tools for Water Resource Planning and Decision Making.* Lewis, Boca Raton, USA.

Dunbar, M. J., Gustard, A., Acreman, M. C. & Elliott, C. R. N. (1998) Overseas approaches to setting River Flow Objectives. Environment Agency and Institute of Hydrology, R&D Tech. Rep. W6-161.

Gottschalk, L., Gómez, F., Krasovskaia, I. & Chaves, A. (2006) Estimation of the "minimum acceptable flow" (MAF) for rivers in Costa Rica. Nordic Hydrologic Conference, NHK-2006, Denmark (submitted).

Hirvonen, H. (1992) The development of regional scale ecological indicators: a Canadian approach. In: *Proc. Int. Symp. on Ecological Indicators* (ed. by D. H. McKenzie, D. E. Hyatt & V. J. McDonald). Elsevier Science Publishers Ltd, London, UK & New York, USA.

Hutcheson, J., Walsh, P. & Given, D. (1999) Potential value of indicator species for conservation and management of New Zealand terrestrial communities. *Science for Conservation 109*, Department of Conservation, Wellington, New Zealand

Kumar, A., Burton, I. & Etkin, D. (2001) Managing Flood Hazard and Risk: Report of an Independent Expert Panel. Ottawa, Ont.: Office of Critical Infrastructure Protection and Emergency Preparedness. HV 609 K843 2001.

Laporte, S., Pacheco, A. & Rodriquez, C. R. (2006) Estimation of minimum acceptable (compensatory) flow for the rivers of Costa Rica. In: *Climate Variability and Change—Hydrological Impacts* (Proc Fifth FRIEND World Conference held at Havana, Cuba, November 2006). IAHS Publ. 308. IAHS Press, Wallingford, UK (this volume).

Lovejoy, T. E. (1994) The quantification of biodiversity: An esoteric quest or a vital component of sustainable development? *Phil. Trans. Royal Soc. London, B - Biological Sci.* **345**(1311), 81–87.

Marcot, B. G., Castellano, M. A., Christy, J. A., Croft, L. K, Lehmkuhl, J. F., Naney, R. H., Rosentreter, R. E., Sandquist, R. E. & Zieroth, E. (1997) Terrestrial ecology assessment. In: *An Assessment of Ecosystem Components in the Interior Columbia Basin and Portions of the Klamath and Great Basins* (ed. by T. M. Quigley & S. J. Arbelbide), vol. 3, 1497–1713. USDA Forest Service General Tech. Rep. PNW-GTR-405. USDA Forest Service Pacific Northwest Research Station, Portland, Oregon, USA.

Nip, M. I., Latour, J. B., Klijn, F., Koster, P. K., Groen, C. L. G., Udo de Haes, H. A. & De Kruijf, H. A. M. (1992) Environmental quality assessment of ecodistricts: a comprehensive method for environmental policy. In*: Proc. Int. Symp. on Ecological Indicators* (ed. by D. H. McKenzie, D. E. Hyatt & V. J. McDonald). Elsevier Science Publishers Ltd. London, UK & New York, USA.

Ramirez, A. & Pringle, C. M. (1998) Structure and production of a benthic insect assemblage in a neotropical stream. *J. North American Benthological Society* **17**(4), 443–463.

Watson, R. T., Heywood, V. H., Baaste, I., Dias, B., Gamez, R., Janetos, T., Reid, W. & Ruark, G. (1995) *Global Biodiversity Assessment. Summary for Policy Makers.* UN Environment Programme, Cambridge University Press, Cambridge, UK.

Wootton, J. T. & Oemke, M. P. (1992) Latitudinal differences in fish community trophic structure, and the role of fish herbivory in a Costa Rican stream. *Environmental Biology of Fishes* **35**(3), 311–320.

Climate Variability and Change—Hydrological Impacts (Proceedings of the Fifth FRIEND World Conference held at Havana, Cuba, November 2006), IAHS Publ. 308, 2006.

Interaction between surface and groundwater in the flooding of riparian wetlands: Biebrza wetlands case study

TOMASZ OKRUSZKO, JAROSŁAW CHORMAŃSKI & DOROTA ŚWIĄTEK

Department of Hydraulic Engineering and Environmental Restoration, Warsaw Agricultural University, Nowoursynowska 159, 02-776 Warsaw, Poland

t.okruszko@levis.sggw.pl

Abstract The Biebrza Wetlands is located in a marginal-ice valley in north-eastern Poland and covers some 195 000 hectares in area. The most characteristic feature of the Biebrza River is flooding, which appears there almost every year. In the period 1999–2002, investigation of the flooding phenomena was carried out in order to understand the main processes involved in the inundation of the river valley and to combine them with characteristic vegetation patterns. The investigation used Landsat images, a hydrodynamic 1-D model of river and flood plain flow, and chemical analysis of flood waters. It was shown that river water is responsible for inundation of part of the valley only. Other parts of the valley were inundated by groundwater seepage or *in situ* snow melt. These observations agree with qualitative descriptions of water sources for the particular plant communities.

Key words Biebrza wetlands; flooding; RS; hydrological models

INTRODUCTION

The Biebrza wetlands occupy 195 000 ha of a marginal-ice valley in north-eastern Poland. It forms one of the last extensive, fairly undisturbed river-margin peatlands in Europe and contains endangered plant and animal species in a large variety of fully developed ecosystems.

The Biebrza valley is also a large reservoir for surface and shallow groundwater. Water which flows into Biebrza valley is accumulated here due to the small longitudinal slopes of the basins as well as the fact that valley is closed downstream by the moraine formation. As the flooding phenomena is vital for protection of wetland ecosystems, changes in inundation extent as well as the role of different sources of water were investigated.

DATA

Hydrological and topographical data

Hydrological data were obtained form the Polish Weather Service which has operated three gauges controlling the flows in the Lower Basin since 1951. Floods during the investigation years (1999–2002) were close to the 50-years maximum average except for the flood of 2001. In this year, the maximum flood water level reached bank full only.

Two types of data were analysed to describe the topography of the Lower Biebrza basin: (a) 13 river and valley cross-sections, which were gathered during the measurement campaigns; and (b) a Digital Elevation Model (DEM) representing the topography of the valley (Fig. 1).

The river bed elevations were measured by manual sounding. Near the river, valley cross-sections were measured on both sides of the river channel by coupling the traditional levelling survey with Differential GPS (DGPS) techniques. The cross-sections were then extended to the edge of the valley by capturing elevation every 100 m from the DEM (Chormański *et al*., 2002).

Remote sensing

One satellite images from each year of a flood event were analysed. The floods in 1999 and 2001 were registered on Landsat TM images, while sensors of Landsat ETM+ captured the floods in 2000 and 2002. The Lower Basin area was located on Landsat images 187/23 in 1999, 2001 and 2002, and on image 188/24 in 2000. These images captured peak flows.

Hydro-chemical survey

Surface water samples were collected in several transects during peak flows in 2001 and 2002 at a depth of less than 5 cm below the water surface. The EC (adjusted to 25°C) values of all samples

Copyright © 2006 IAHS Press

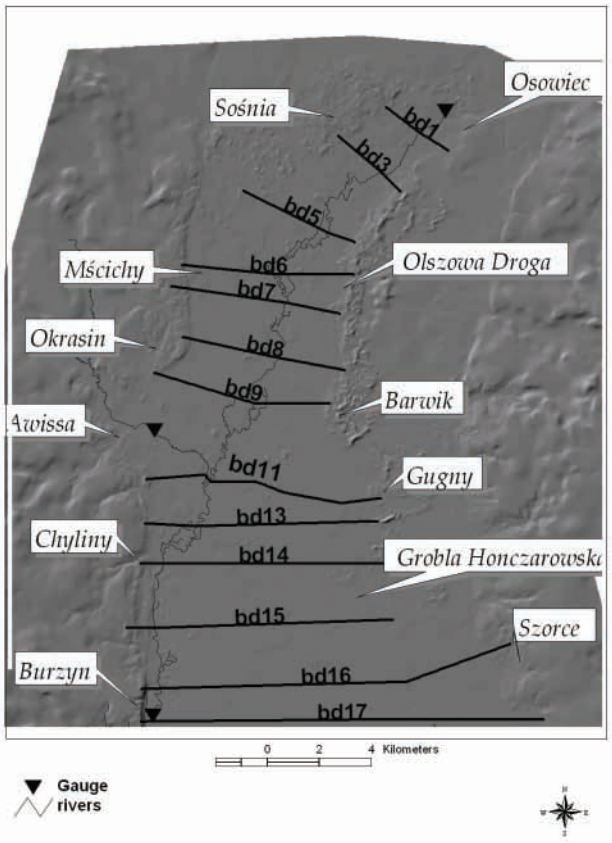


Fig. 1 Digital Elevation Model of the Lower Biebrza Basin and cross sections location.

were measured in the field. Within eight hours after sampling the acidity (pH) and alkalinity of the water samples were measured. The other analyses were performed using Inductively Coupled Plasma Atomic Emission Spectrometry techniques and colorimetrically on a continuous flow autoanalyser at the laboratory of the University of Utrecht. The concentrations of the followed ions were analysed: Ca^{2+}, Mg^{2+}, Na^{+}, K^{+}, $Fe^{2+/3+}$, Al^{3+}, Mn, Si, SO_4^{2-}, Cl^{-}, NH_4^{+}, PO_4^{3-}.Cd, Cu, Pb, Zn. In total 233 samples were collected in 2001 and 563 in 2002. For all the samples, the ionic balance was calculated according to the Stuyfzand (1989) method. This kind of reliability test allows decision making about including the particular samples in the next analysis. Samples with an ionic balance deviating more than 10% from electro neutrality (30 samples of 2001 and 14 samples of 2002) were eliminated from statistical analysis (Chormański, 2003).

METHODS

Remote sensing

The ratio TM7/TM4, Normalized Difference Vegetation Index (NDVI) and PC1 were used for pre-processing of the Landsat satellite images. The results of these three transformations were stored in new bands, and then, were used for class determination and the development of training regions. In all, 14 generalized classes, containing different cover types, were developed. The homogenous training regions were based on field observation and GPS measurements as well as analysing the land-use map. Next, a supervised classification using the maximum likelihood method was performed. Using the flood of 2002 and 796 points with known cover type, a high classification accuracy of 88% was obtained. Finally, the classified images were reclassified into two classes “inundated” and “dry”. The inundated class included deep water, shallow water, inundated tall sedges and reeds, flooded alder forest, flooded meadow, alder birch forest, reeds and shrubs, sedges, shrubs and sedges, and moss-sedge communities. The dry class included coniferous forest, leafy forest, grasslands, and bare soil. This procedure was applied for determination of the total inundation area of the floods in 1999–2002.

Statistical analysis of the hydro-chemical patterns

Samples obtained from hydro-chemical transects were statistically analysed using a PCA procedure following Verhoeven *et al*. (1996) and Bridgham (1998). The variables that were not normally distributed were standardized by log-transformation to approximate the normal distribution. They were then standardized to have a zero mean and unit variance.

The results of the statistical analysis were imported to the ArcView GIS system and linked with geographical sample location measured by GPS to create a map of the spatial distribution of the first three components. To get a better impression of the variation in ionic composition of the flood water, an iterative process was used to find the cluster centre of the scores of the three components. The *K*-means cluster analysis method was performed establishing six clusters, which finally were interpreted as three different water sources: river, groundwater and snowmelt.

Table 1 shows values of water properties calculated as the mean and standard deviation for each group. Cluster 4 is predominant in the river water and is characterized by: high EC, Cl, K and Ca values, the highest pH and SO_4 values and low values of Si, Zn, PO_4, Mn. The spatial location of samples classified as cluster 4 is close to the Biebrza River. The second cluster, which characterized the river water, is cluster 5. This group is only represented by one sample collected from the Wissa River, which flows through urban areas. Clusters 3 and 6 are similar and both have low mineral richness related to low HCO_3 content and Ca concentrations that are associated with low pH. These clusters can be interpreted as rain/snowmelt dominated water types. However, cluster 3 has properties, like very high concentrations of K, PO_4 and Cl, that are similar to other types of water such as river or groundwater and suggests that the cluster represents a mixed type of water. In cluster 1 and 2, groundwater predominates. Such properties like very high HCO_3 contents and Ca concentration, and pH smaller than in river water are characteristic of groundwater flux. The increase of Cl, Na, K in cluster 2 could be an indicator of human related pollution influences.

Table 1 Chemical properties presented as average values and standard deviation calculated for each water cluster determined for water samples collected during flood event in year 2002.

Variable	Cluster 1		Cluster 2		Cluster 3		Cluster 4		Cluster 5	cluster 6	
	Average	Std.	Average	Std.	Average	Std.	Average	Std.		average	Std.
EC	405.80	104.01	426.93	107.74	262.86	73.35	390.25	41.72	570.00	246.87	55.61
pH	7.09	0.29	7.20	0.49	6.95	0.30	7.90	0.37	7.80	7.09	0.30
$HC0_3$	261.45	76.08	234.14	56.21	127.34	35.01	197.55	23.63	317.20	157.19	34.74
Al^{3+}	0.00	0.01	0.01	0.01	0.02	0.06	0.00	0.01	0.00	0.00	0.01
Ca^{2+}	75.60	20.69	74.52	21.06	42.42	13.15	65.08	6.95	96.77	39.99	12.40
Cd	0.01	0.00	0.01	0.00	0.00	0.00	0.01	0.00	0.01	0.00	0.00
Cu	0.02	0.04	0.01	0.01	0.01	0.00	0.01	0.00	0.01	0.01	0.00
$Fe^{2+/3+}$	0.96	1.51	0.36	0.51	0.48	1.82	0.08	0.04	0.31	0.21	0.32
K^+	0.52	0.42	2.33	1.80	2.65	3.63	2.33	0.75	79.37	0.67	0.54
Mg^{2+}	13.49	3.77	14.37	3.69	7.46	1.98	11.07	1.28	15.67	7.54	2.01
Mn	0.17	0.20	0.20	0.66	0.06	0.20	0.00	0.01	0.06	0.02	0.06
Na^+	4.88	1.14	6.08	2.11	5.23	1.29	5.95	0.70	7.79	4.65	1.31
Pb	0.04	0.00	0.04	0.01	0.04	0.02	0.04	0.00	0.04	0.04	0.00
PO_4^{3-}	0.24	0.31	0.33	0.42	0.45	1.19	0.09	0.06	0.25	0.12	0.07
Si	7.40	1.80	6.66	2.39	3.94	1.75	1.25	1.28	6.33	4.24	1.91
SO_4^{2-}	4.64	3.12	25.13	20.06	22.24	16.88	33.23	7.25	42.42	6.72	6.33
Zn	0.05	0.05	0.08	0.13	0.04	0.03	0.03	0.02	0.03	0.03	0.02
NH_4^+	0.13	0.00	0.14	0.06	0.19	0.25	0.13	0.02	0.13	0.26	1.43
Cl^-	6.47	2.97	12.37	4.39	9.72	3.98	9.84	1.81	80.82	6.09	1.69
No. of samples	25		75		80		251		1	117	

Numerical model of Lower Biebrza River Flow

In order to simulate flood flow in the Lower Biebrza basin a one-dimensional unsteady model flow was applied. This model solves an unsteady one-dimensional open channel flow, based on the St Venant equations (Liggett & Cunge, 1975). The Lower Biebrza River is represented as a 1-D

single channel starting from the Osowiec gauge (BD1) and terminating at Burzyn gauge, BD17 (Fig. 1). The Wissa River is treated as a point of lateral inflow located 8 km upstream of Burzyn and is described by the flow hydrograph at the Czachy gauge (Q_C). A flow hydrograph forms the upstream boundary condition and the rating curve is used as a downstream boundary condition at Burzyn gauge. The uniform lateral inflow is imposed along the river section according to the large lateral inflow from subcatchment during the flood event. The field monitoring in the Lower Biebrza Basin shows that during flood periods, the river valley consists of areas which mainly act as storage for flood water and areas that are effective in water transport. The 1-D model is capable of describing flood conditions using the appropriate geometry of cross-sections, which are limited to the flow-active zones. In developing the model, the location of each cross-section was identified according to the water source distribution determined by chemical transects and topography according to the DEM.

The calculated and observed discharge hydrographs at cross-section BD17 were compared in the model validation process using RMSE computation (Table 2). However, the good congruence of the model results with discharge rates at the downstream boundary condition does not necessarily mean that the developed model correctly reproduces water levels upstream from the Burzyn gauge.

Table 2 The RMSE calculated for different flood events.

Year	Peak flow ($m^3 s^{-1}$)	RMSE ($m^3 s^{-1}$)
1999	184	10.4
2000	80,3	3.24
2002	168	6.98

RESULTS

Flood extent and source of water

The total inundation maps prepared by the remote sensing technique for 2001 and 2002 floods were analysed to determine the different water sources. On the basis of statistical analysis and classification of water samples, three types of water were determined and attached to every sampling point. The zones representing different types of water were drawn (Fig. 2(b)). The area flooded by river water (active part of the valley) usually covered less than a half of the total inundation area (Table 3).

Table 3 Inundation area and volume of water stored in active and non-active part of the valley.

Year of event	Total inundation area (km^2)	Area of the active part of the valley (km^2)	Area of the non-active part of valley (km^2)	Volume of the non-active part of valley (m^3)	Volume of the active part of valley (m^3)	Calculated maximum daily outflow volume at Burzyn gauge (m^3)
1999	180.7	72.0	108.7	32 610 000	43 410 000	16 830 000
2000	192.7	68.3	124.4	24 884 000	27 140 000	6 580 000
2001	113.5	56.1	57.4	8 610 000	–	–
2002	188.8	77.5	111.3	33 390 000	44 520 000	14 730 000

Hydraulic model result vs Remote Sensing (RS) method and vegetation zones

Water stages calculated by hydrodynamic modelling at cross-sections were mapped across the entire flood plain using the DEM in ArcView GIS. Comparison of the inundated area generated by the hydraulic model and obtained by the remote sensing method (Fig. 2 (b)) show large differences in the downstream part of the valley. However they are in good agreement with the border between the active and non-active zones. The volume of water stored in both zones (Table 3) is similar, varying from 24×10^6 m^3 to 44×10^6 m^3 for the floods that were investigated. Comparing those volumes with volume of daily discharges during the peak flow shows that the storage capacity of each zone is equal to between two to five days of flow.

There is a very good match between the flooding area coming from the river during average flood conditions and the vegetation zones of reeds, tall sedges and sedges (Fig. 3). Those types of vegetations are normally associated with fluvial types of hydrological feeding. The groundwater

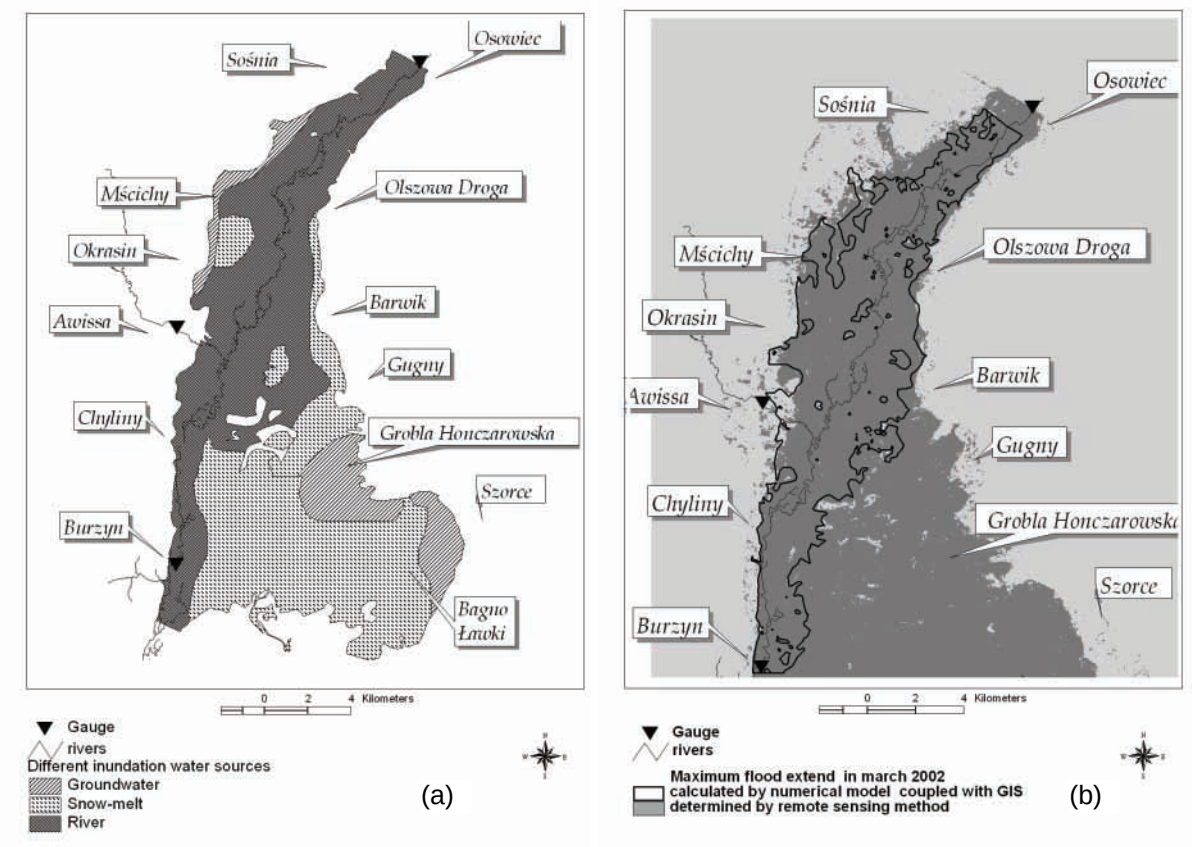


Fig. 2 (a) Inundation of river valley with water of different sources in 2002. (b) Comparison of the inundated area extent obtained by the remote sensing method and hydraulic model in 2002.

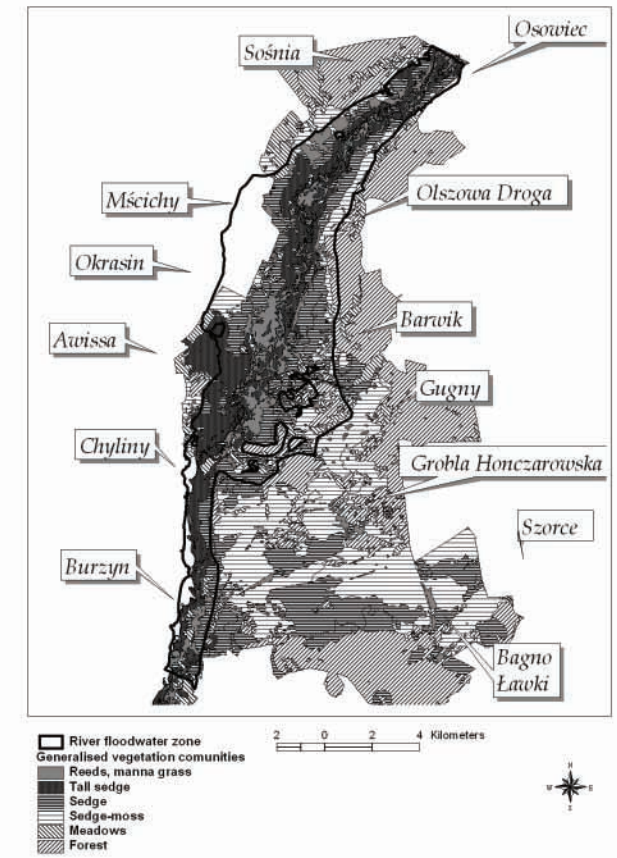


Fig. 3 Comparison of average river flood with major plant vegetation zones of Biebrza wetlands.

fed ecosystem of sedge-moss vegetation is also clearly visible outside the active zone. The lack of detailed observation of flood events of bigger magnitude (floods of 2003 and 2004 were also close to average) made investigation of the interplay between indicated water sources during such events impossible.

CONCLUSIONS

As results of our study we came to the following conclusions:

1. Inundation of the Biebrza Wetlands results from the interaction of water coming from three different sources: flooded river water, exfiltrated groundwater as well as water coming from *in situ* snow melt. The most accurate information on the sources of water was obtained from chemical transects.
2. There is a good match between the flood extent obtained as a result of this hydrological study and generalized vegetation map. It indicates that natural vegetation can be a good indicator for estimation of average flood extend.
3. A one dimensional hydrodynamic model can be effectively use in this type of river valleys when the water conveying parts of the valley are identified. The location of the water conveying parts of the valley depend on the magnitude of the flood event, and can be detected during the flood event using surveys of water chemistry or velocity. However, identifying the conveying parts of the valley for historical floods using gauge records only is difficult.
4. The exclusion of water storage areas from the inundation model leads to significant errors in the estimation of flood extend. In the case of flood event of average magnitude more then 60 % of the inundated area in the Biebrza comes from sources other then water river sources. This error has limited impact on accuracy of storage efficiency of the river valley, as it is only a few days storage of the peak flows. However, it is a major factor constituting the wetlands habitat in a river valley of this type.
5. In the case of ecological studies aiming on conservation/restoration of habitat conditions of riparian wetlands, there is a need for coupling regional ground water models with the hydrodynamical models for predicting the flood extend.

REFERENCES

Bridgham S. D., Updegraff K. & Pastor, J. (1998) Carbon, nitrogen and phosphorus mineralization in northern wetlands. *Ecology* **79**, 1545–1561.

Chormański, J., Okruszko, T., Wassen, M. J. & Skąpski, J. (2002) Surface water system analysis. Flood extent measurements and topography of the valley. In: *Hydrological System Analysis in the Valley of Biebrza River* (ed. by W. Mioduszewski & E. P. Querner). 39–57. IMUZ Press, Falenty, Poland.

Chormański J. (2003) Methodology for the flood extent determination in the Lower Biebrza Basin. PhD Thesis. Warsaw Agricultural University, Poland.

Liggett, J. A. & Cunge, J. A. (1975) *Numerical Methods of Solution of the Unsteady Flow Equations*, vol. 1, Chapter 4. Water Resources Publications, Fort. Collins, Colorado, USA.

Lilesand, T. M & R. W. Kiefer (2000) *Remote Sensing and Image Interpretation.* John Wiley, New York, USA.

Profeti, G. & Macintosh, H. (1997) Flood management through Landsat TM and ERS SAR data: a case study. *Hydrol. Processes* **11**, 1397–1408.

Townsend, P. A. & Walsh, S. J. (1998) Modeling floodplain inundation using integrated GIS with radar and optical remote sensing. *Geomorphology* **21**, 295–312.

Stuyfzand, P. J. (1989) A new chemical classification of water types. In: *Regional Characterization of Water Quality.* (ed. by S. Ragme), 89–98. IAHS Publ 182. IAHS Press, Wallingford, UK.

Verhoeven, J. T. A., Keuter, A., van Logtestijn, R., van Kerkhoven, M. B. & Wassen, M. J. (1996) Control of local nutrient dynamics in mires by regional and climatic factors: a comparison of Dutch and Polish sites. *J. Ecol.* **84**, 647–656.

Climate Variability and Change—Hydrological Impacts (Proceedings of the Fifth FRIEND World Conference held at Havana, Cuba, November 2006), IAHS Publ. 308, 2006.

Modelling of inundation patterns on the Pilica River flood plain, Poland

MUSTAFA ALTINAKAR[1], EDYTA KIEDRZYŃSKA[2,3] & ARTUR MAGNUSZEWSKI[4]

1 *The National Center for Computational Hydroscience and Engineering. The University of Mississippi, Oxford, Mississippi 38677, USA*
asmagnus@uw.edu.pl

2 *University of Lodz, Department of Applied Ecology, Banacha Str. 12/16, 90-237 Lodz, Poland*

3 *European Regional Centre for Ecohydrology under the auspices of UNESCO, 3 Tylna Str., 90-364 Lodz, Poland*

4 *Warsaw University, Faculty of Geography and Regional Studies, Krakowskie Przedmiescie 30, 00-927 Warszawa, Poland*

Abstract Eutrophication of inland waters can be significantly prevented by enhancing the natural self-purification ability of rivers through deposition of their sediment load on the flood plain. One of the efficient ways to achieve natural sedimentation on the flood plain is through modification of natural vegetation cover by introducing willow plantations. Planning and implementation of such plantations require a sound understanding of the flow and sediment transport dynamics. In the present study, CCHE2D, a two-dimensional numerical hydrodynamic model developed at the National Center for Computational Hydroscience and Engineering (NCCHE) of the University of Mississippi, was used to investigate the flow pattern and sedimentation processes on a flood plain of the Pilica River, with and without plantations.

Key words Pilica River; flood plain sedimentation; river hydraulic modelling

INTRODUCTION

Suspended sediments transported by rivers are one of the main sources of phosphorus that controls the eutrophication process of inland and offshore waters. Several researchers have shown that, based on a sound understanding of natural ecosystems, the ecohydrology and biotechnologies can be used to prevent or reduce eutrophication of inland reservoirs and lakes (Zalewski, 2000; Zalewski, 2002; Wagner-Łotkowska *et al*., 2004; Kiedrzyńska *et al*., 2006). River self-purification by deposition of the sediment load in the channel and on the flood plains is one of the available mechanisms.

The water quality problems of the Pilica River are also related to the high concentrations of total phosphorous, which usually varies between 100 to 300 μg dm^{-3}, but can reach 699 μg dm^{-3} during high flows (Wagner-Łotkowska *et al.*, 2004). The Sulejów Reservoir, located downstream from the study area, is the main drinking water source for the Łódź conglomeration (over 1 million inhabitants) and also serves as a recreational area. The eutrophication of the reservoir during summer months (Tarczyńska *et al*., 2001) leads to high phytoplankton biomass productivity with cyanobacteria domination. This is a very important problem for the entire region.

River flood plains play a crucial role in the exchange of water masses and matter between the river and terrestrial ecosystems and in the functioning of the river ecosystem (Junk *et al*., 1989). Sedimentation processes in river flood plains have been extensively discussed by several researchers (Nanson & Croke, 2002; Howard 1992; Tockner *et al*., 2000; Amoros & Bornette, 2002). Introduction of, for example, willow plantations to change the hydraulic resistance of the flood plain can be efficiently used to control the deposition rate of sediments on the flood plain and thus to enhance the retention of nutrients. However, many of the studies reviewed by Nanson & Croke (2002) have shown that the modification of the river flood plain vegetation cover may have broader consequences. It must, therefore, be studied carefully.

In the Pilica River case this problem is studied by predicting flow and velocity field patterns, as well as the sediment fluxes, with the help of a two-dimensional (2-D) numerical hydrodynamics and sediment transport model, called CCHE2D. Developed at the National Center for Computational Hydroscience and Engineering (NCCHE) of the University of Mississippi, CCHE2D is a depth integrated 2-D model for simulating free surface flows and sediment transport. It is based on depth-averaged Navier-Stokes equations, and is capable of bed load and/or suspended sediment transport simulations. The turbulent shear stresses are approximated using Boussineq's approximation and the turbulent eddy viscosity, with the use of three different closure schemes. The set of equations is solved implicitly using a control volume approach and efficient element method. The sediment flow

Copyright © 2006 IAHS Press

is calculated assuming non-uniform material in a non-equilibrium transport model. The equations for suspended, bed load or total load are solved using the efficient element method or an exponential difference scheme. The model has been extensively verified and validated. It has been successfully applied to modelling complex flows in natural channels and is proven to constitute an efficient tool for hydraulic research and engineering projects (Jia *et al*., 2002). It can be efficiently used for simulating shallow water flow conditions on flood plains.

According to Lewin (2001) there is a relatively good understanding of fluvial processes at the discrete spatial scales of bed forms, channel processes and relief formation, but there is no single theory linking these various spatial scales. Sedimentation processes are acting across the scales, and they are controlled by factors such as the sediment-transport rate, channel relocation, reaction and relaxation time. An across-scales description of the fluvial processes is possible with the use of 2-D hydrodynamic models, which allow simulation of local flow parameters, as well as the general picture of the flow pattern and internal circulation. The complicated nature of flood plain flows during inundation by low probability floods is one of the principal rationales behind the use of numerical models, in spite of their limitations as discussed by Cao & Carling (2002).

DATA

Study site description

Located in central Poland, the Pilica River (Fig. 1) is a right-side tributary of the Vistula River. It has a length of 342 km and catchment area of 9258 km^2. It is mainly an agricultural catchment; forests comprise 30.7%, and other non agricultural land cover occupy 5.1%. Pilica River has a network of hydrological gauges operated by the Institute of Meteorology and Water Management (IMGW). Closest to the study site are the Sulejów gauge, located downstream (catchment area, A = 3909 km^2, river length, L = 161.3 km), and the Przedbórz gauge located upstream (A = 2536 km^2, L = 201.1 km). The study site is an experimental flood plain (26.6 ha) of the Pilica River valley located 4.5 km southwest of Sulejów town (Fig. 1).

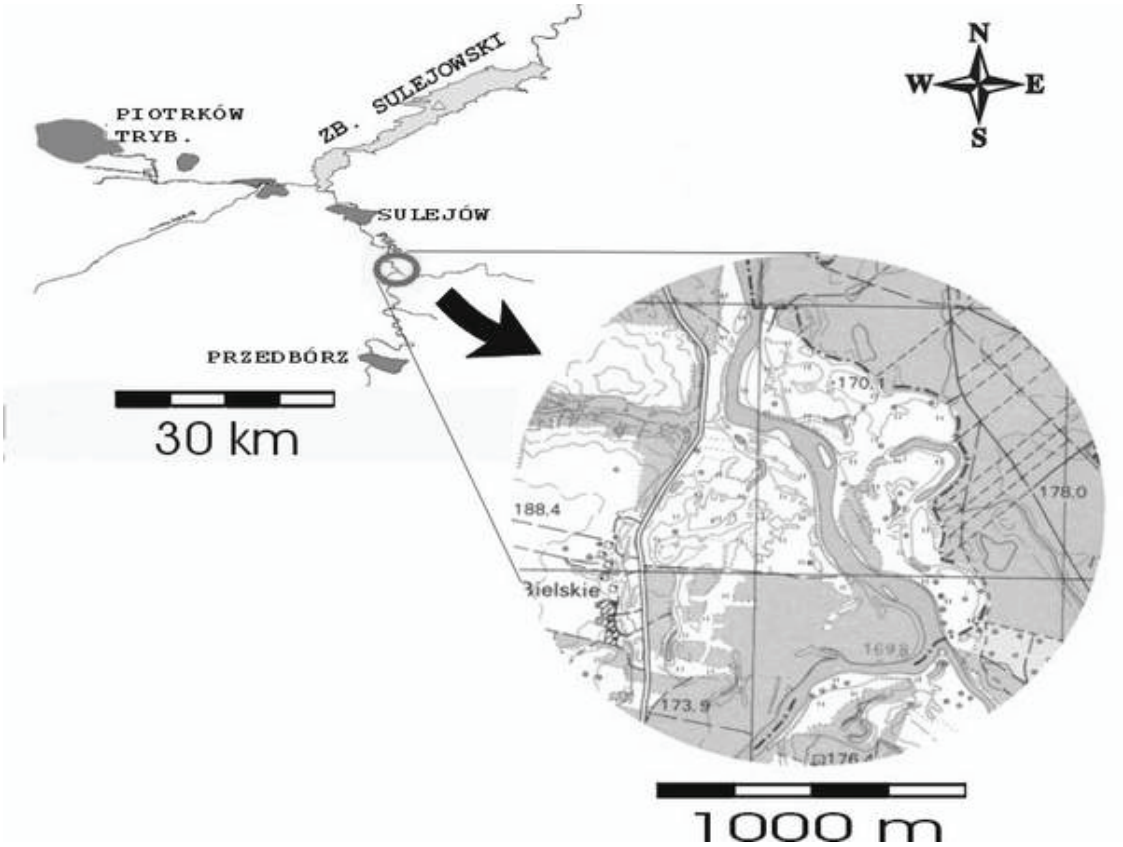


Fig. 1 Location of the study site on the Pilica River flood plain.

Suspended sediments concentrations were measured by IMGW at the Przedbórz gauge during the period 1957–1988. Concentration extremes vary from a minimum of 1 g m^{-3} to a maximum of 150 g m^{-3}. Average annual suspended sediment transport is 9500 t (data from the period 1957–1990), which corresponds to a denudation rate of 3.7 t km^{-2} (Brański & Banasik, 1996).

Nanson & Croke (1992) proposed classification of the flood plains formed in non-cohesive sediments into three classes: high, medium and low energy. According to this classification, the Pilica River flood plain at the study site belongs to the medium energy class, and is formed by a meandering channel. The Pilica River channel is not trained and has a free meandering pattern with natural sedimentation and erosion processes. The main channel near the study site is 20–60 m wide, with a large meander loop. Local depressions related to flood plain formation by meandering processes are visible in the flood plain relief.

The type of vegetation on the flood plain depends on the groundwater level and hydraulic conditions during flooding. Grasslands of the hay meadow type occupy the largest percentage of the flood plain surface. Sedge rushes grow on the plain to a lesser extent; the predominant species is the sharpened sedge, *Carex gracilis L.*, which occurs in small mid-meadow hollows, and to a lesser degree *Carex vesicaria L*. Rushes with common reeds (*Phragmites australis, Cav.*) Trin. Ex Stend. (common reeds), belonging to the habitat of rushes proper, grow in the old river bed of the Pilica River, in which water is retained throughout the year. For this reason also, the river valley and the researched flood plain have little agricultural value.

Data for the model

The CCHE2D hydraulic model requires the following input data to characterize the study site:

– elevation points which characterize the channel and flood plain form,
– Manning roughness coefficients representing various vegetation covers,
– boundary conditions of discharge at the inlet to the studied river reach,
– sediment properties and transport intensity.

A set of elevation points obtained from digitizing the contour lines on a topographic map supplemented by 815 levelling measurements were used to compute a Digital Elevation Model (DEM) using the inverse distance algorithm.

Using the field data from a botanical inventory and aerial photographs, a land-use map was produced containing five classes. The following Manning roughness coefficients were assigned to various parts of the flood plain: sand channel of Pilica, 0.025; oxbow channel, 0.070; grass, 0.035; reed; 0.050; willow, 0.150; forest, 0.100.

Hydrological data from the Sulejów gauge measured by IMGW was used for statistical analysis of water-stage frequency. GIS examination of the DEM gave the picture of flood plain inundation which starts at stage H = 210 cm (Q = 50 m^3 s^{-1}) reaching a maximum discharge at H = 300 cm (Q = 166 m^3 s^{-1}). Average duration of flood plain inundation in days was calculated by comparing the DEM with water levels and is represented graphically in Fig. 2.

The numerical grid of the model was generated using the Mesh Generator software developed at the NCCHE. A set of *x,y,z* coordinates were used as input to calculate the geometry of the river channel and flood plain for the CCHE2D model.

METHOD

The underlying concept of the project is the enhancement of sedimentation on the Pilica River flood plain by introducing plantations of willow trees to alter the vegetation cover. The four experimental plantations were introduced in the part of the flood plain under investigation (Fig. 2). The two largest are plantation No. 1 (900 m^2) and plantation No. 3 (1225 m^2). In the first approach the effect of the introduction of the plantations was studied by comparing the numerical results of natural conditions (Scenario 0), with those with the plantations (Scenario 1). The velocity fields were calculated for both scenarios assuming steady-flow conditions at water stages H = 210–300 cm with 10 cm intervals. Simulation time was 1000 s with the time step 1 s. The computed depth-averaged velocities in both scenarios were compared at two monitoring points located at the centres

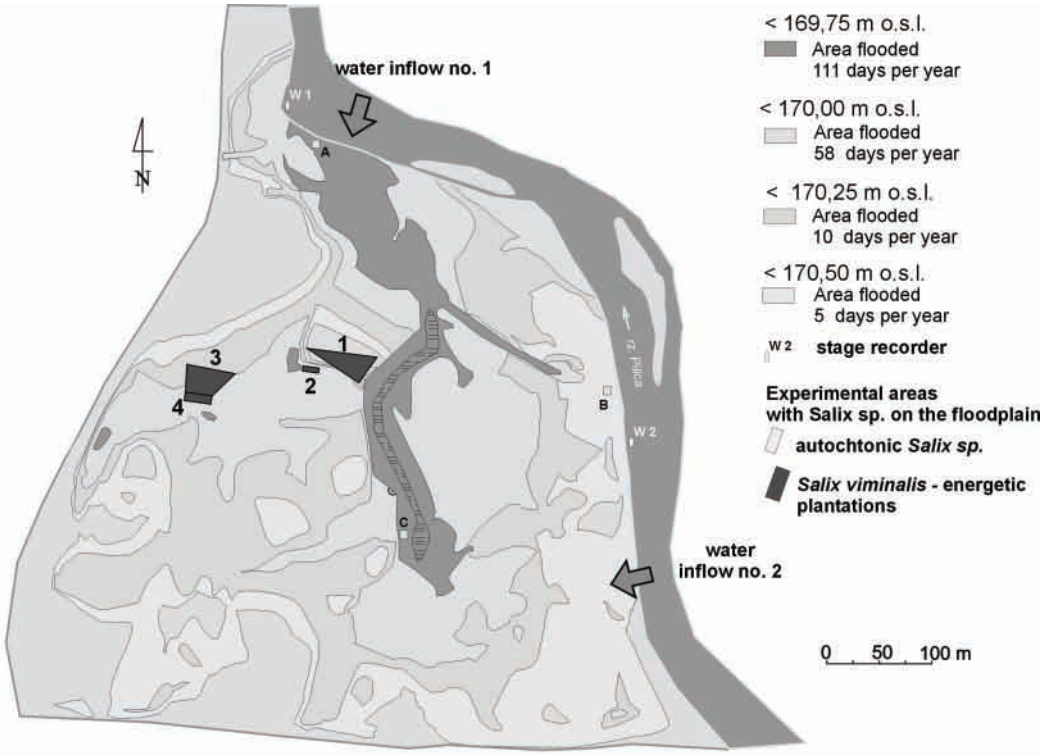


Fig. 2 Location of willows plantation and floodplain inundation duration in days.

of the largest plantations. Monitoring point MP1 is located at the centre of plantation No. 1, and monitoring point MP2 at the centre of plantation No. 3.

The relationship between suspended-sediment concentration and discharge was analysed using water stages from the Sulejów gauge and suspended-sediment concentrations from the Przedbórz gauge based on the observations recorded between 1984 and 1988. The relationship for the entire data set is very complex. The sediment supply is controlled by the snowmelt in the spring and vegetation cover in the summer. The best relationship between suspended sediment-concentration and discharge has been obtained for the period of late autumn, when sediment supply from the catchment to the river channel is not constrained. Generally, it is difficult to assign a single suspended-sediment concentration value to a given water stage or discharge.

In the period 1996–2003 suspended sediment-concentration measurements of the Pilica River at Sulejów profile were also made by the Department of Applied Ecology of Łódź University (Wagner-Łotkowska *et al.*, 2002). Detailed analysis of daily values of suspended sediment concentrations and discharges show a hysteresis effect, with the highest concentrations recorded earlier than peak flow. For example, during the small magnitude flood of 16–30 March 1996, which occurred after a longer period of low flows, the maximum suspended sediment concentration of 22 g m^{-3} was observed four days before the peak flow. The second flood wave 06–15 April 1996, with a similar peak discharge, caused sediment concentrations of only 4–9 g m^{-3}. This sequence of flows can cause a flushing effect on the sediments accumulated at the channel bottom. During moderate magnitude peak flows, we can expect the highest suspended sediment concentrations to be in the range of 20 g m^{-3}.

Samples of the suspended sediments from the Pilica River were collected using the PIHM bottle sampler, and processed by laser particle-size measurement. It was decided that in the numerical model a single diameter of suspended sediment, $d_{50} = 2.00 \times 10^{-5}$ m, will be used as the representative size.

The properties of the material deposited on the flood plain have been estimated from the samples collected in the field covering various sedimentation environments, such as the river channel, banks and oxbow lake deposits. The sample were analysed using a sieve-analysis method. River channel deposits are coarse, $d_{50} = 2.05–3.68 \times 10^{-4}$ m, and well graded. Bank deposits have a

median diameter of d_{50} = 1.37–1.97 $\times 10^{-4}$ m and also show rather good grading. Sediments in the wetlands on the floodplain have median grain diameter, d_{50} = 1.08–1.76 $\times$ 10^{-4} m are poorly graded, with a high proportion of fine fractions (more details are given in Magnuszewski *et al.*, 2005).

The sedimentological properties of the Pilica River bed load and suspended sediments at the study site are distinctly different. Bed load material is transported in the river channel where the water energy is adequate. The analysis of soil samples indicates that the material deposited on the flood plain has a smaller diameter than river channel sediments. The suspended sediment transport and deposition play a more significant role in forming the flood plain surface than the bed load transport of coarse sediments. Therefore, it was decided that the simulation of the sedimentation processes at the Pilica River flood plain study site will be done taking into account only suspended sediment transport.

RESULTS

Influence of willow plantations on water and sediments fluxes

The results of the calculations are given in Table 1. Plantation No. 1 is situated on a higher terrace, and is inundated only at stages H = 280 cm (Q = 133 m^3 s^{-1}) and higher. This elevation is flooded only during major floods. Plantation No. 3 is located at an elevation which flooded on average 10 days per year. Comparisons of the numerical simulation results for two scenarios, natural conditions (Scenario 0) and land cover altered by willow plantations (Scenario 1) shows that changing the roughness of even a relatively small area considerably reduces the velocity field. Willow plantations are found to be particularly useful in creating dense and compact vegetation cover with high Manning coefficients values.

Table 1 Results of the velocity calculations at the monitoring points according to scenario 0 – natural conditions, and scenario 1 – implementation of the plantation scheme; *H* is water stage, *Q* is discharge, and v_h is average velocity.

H (cm)	*Q* (m^3 s^{-1})	MP1: Scenario 0 v_h (m s^{-1})	Scenario 1 v_h (m s^{-1})	MP2: Scenario 0 v_h (m s^{-1})	Scenario 1 v_h (m s^{-1})
210	50.0	0	0	0	0
220	59.0	0	0	0	0
230	68.0	0	0	0.00308	0.00135
240	79.0	0	0	0.00173	0.00215
250	90.0	0	0	0.00521	0.00496
260	102	0	0	0.0121	0.00910
270	117	0	0	0.0181	0.0152
280	133	0.247	0.0670	0.0397	0.0256
290	149	0.291	0.0667	0.0577	0.0255
300	166	0.328	0.0852	0.0687	0.0384

The influence of willow plantations on the sediment trapping ability of the floodplain was analysed for flood simulation with H = 300 cm, using the same monitoring points located at the centre of larger plantations, No. 1 and 3. Suspended sediment concentration corresponding to Q = 166 m^3 s^{-1} has been calculated as C_s = 0.035 kg m^{-3}. For this run, the simulation duration for the suspended sediments transport was increased to 10 000 s. The results obtained (Table 2) give an idea of the spatial distribution of suspended sediment transport (Fig. 3), and provide a good indication of the potential sedimentation zones at the study site. Both willow plantations, No. 1 and No. 3, are located at the edge of high sediment transport and sedimentation areas. This location is a compromise between moderate sedimentation potential, proper moisture conditions at the willows root zone, and the availability of space for performing the experiments (land ownership).

The sediment-transport pattern calculated by the CCHE2D model has shown that suspended-sediment concentration decreases with distance from the main channel, but exhibits a plume-like behaviour along major flow paths. This is in accordance with the findings of Nicholas (2003), who suggests that suspended-sediment transport on the natural flood plains is dominated by advection.

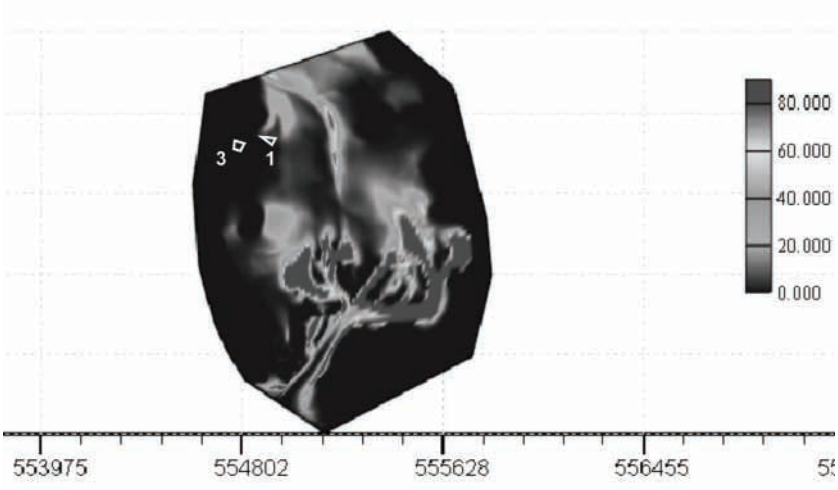


Fig. 3 Results of the suspended sediment transport simulation with willow plantations No. 1 and No. 3. Water stage H = 300 cm, Q = 166 m^3 s^{-1}, Cs = 0.035 kg m^{-3}, simulation time 10 000 s, time step 0.1 s.

Table 2 Results of the simulations at H = 300 cm flood with the suspended sediments transport for two selected monitoring points according to Scenario 0 – natural conditions, and Scenario 1 – implementation of the plantation scheme.

Hydraulic parameters from NCCHE2D model simulations at flood stage H = 300 cm	MP1 at plantation No. 1 z = 170.4 m a.s.l.		MP2 at plantation No. 3 z = 169.9 m a.s.l.	
	Scenario 0	Scenario 1	Scenario 0	Scenario 1
Sediment transport (kg s^{-1} m^{-1})	7.83	2.52	0.000255	0.000559
Elevation change (m)	–0.076	0.095	–0.00001	0.00001
Average velocity (m s^{-1})	0.236	0.185	0.0578	0.0472
Bed shear (N m^{-2})	1.24	0.835	0.0541	0.0376
Water column depth (m)	0.358	0.272	0.916	0.810
Specific discharge (m^2 s^{-1})	0.0846	0.0505	0.0530	0.0382

CONCLUSIONS

(a) Hydrodynamic model CCHE2D has been used successfully to simulate the water flow of the Pilica River for the case of flood plain inundation. The sediment-transport module of the model proved to be a very useful tool for studying fluvial processes, and self-purification of natural river channels.

(b) The location of willow plantations should be selected by considering various factors such as the risk of extreme flooding and the related bed deformations, damage due to high water velocities, and also the ice flow in spring time.

(c) Sequences of calculations at different water stages have shown the complex pattern of flood plain inundation and location of topographic lowering where water from the river channel cross the banks.

Acknowledgements This work is a result of research sponsored by the US State Department Agency for International Development (US–AID) under Agreement no. EE-G-00-02-00015-00 and The University of Mississippi, which was technically supported by National Center for Computational Hydroscience and Engineering (NCHE). The research was supported also by the Polish Ministry of Education and Science, project: 2 PO4F 053 28.

REFERENCES

Amoros, C. & Bornette, G. (2002) Connectivity and biocomplexity in water bodies of riverine floodplains. *Freshwater Biology* **47**, 517–539.

Cao, Z. & Carling, P. A. (2002) A critical reflection on computational fluid dynamics applications to fluvial sedimentary systems. In: *The Structure, Function and Management Implications of Fluvial Sedimentary Systems* (ed. by F. J. Dyer, M. C. Thoms & J. M. Olley), 463–470. IAHS Publ. 276. IAHS Press, Wallingford, UK.

Howard, A. D. (1992) Modelling channel migration and floodplain sedimentation in meandering streams. In: *Lowland Floodplains River: Geomorphological Perspectives* (ed. by P. A. Carling & G. E. Petts), 1–41. John Wiley & Sons, Chichester, UK.

Jia, Y., Wang S. S. & Xu, Y. (2002) Validation and application of a 2D model to channels with complex geometry. *Int. J. Computational Engineering Science* **1,** 57–71.

Junk, W. J., Bayley, P. B. & Sparks, R. E. (1989) The flood pulse concept in river-floodplain systems. In: *Proceedings of the International Large River Symposium* (ed. by D. P. Dodge), 110–127. *Spec. Publ. Can. Fish. Aquat. Sci.* **106**.

Kiedrzyńska, E., Wagner-Łotkowska, I. & Zalewski, M. (2006) Quantification of phosphorus retention efficiency by floodplain vegetation and management strategy for an eutrophic reservoir restoration. *Wetlands* (in press).

Lewin, J. (2001) Alluvial systematics. In: *River Basin Sediment Systems: Archives of Environmental Change* (ed. by D. Maddy, M. G. Macklin & J. C. Woodward), 19–41. Balkema Publishers, Lisse, The Netherlands.

Nanson, G. C., & Croke, J. (1992) A genetic classification of floodplains. *Geomorphology* **4**, 459–486.

Nanson, G. C. & Croke, J. (2002) Emerging issues in floodplain research. In: *The Structure, Function and Management Implications of Fluvial Sedimentary Systems* (ed. by F. J. Dyer, M. C. Thoms & J. M., Olley), 271–278. IAHS Publ. 276. IAHS Press, Wallingford, UK.

Nicholas, A. P. (2003) Modelling and monitoring flow and suspended sediment transport in lowland flood plain environment. In: *Erosion and Sediment Transport Measurement in Rivers: Technological and Methodological Advances* (ed. by J. Bogen, T. Fergus & D. Walling), 45–54. IAHS Publ. 283. IAHS Press, Wallingford, UK.

Magnuszewski, A., Kiedrzyńska, E., Wagner-Łotkowska, I. & Zalewski, M. (2005) Immobilizing of sediments in a lowland river floodplain. In: *Computational Modeling for the Development of Sustainable Water Resources Systems in Poland*. (ed. by M. S. Altinakar, W. Czernuszenko, P. Rowiński & S. Y. Wang), 239–260. Publs. Inst. Geophys. Polish Acad. Sci. E-5 (387).

Skibiński, J. (1976) A trial quantitative estimation of bed-load discharge in the rivers of central Poland, Zeszyty Naukowe SGGW AR w Warszawie, Rozprawy Naukowe 74 (in Polish).

Tarczyńska, M., Z. Romanowska-Duda, T. Jurczak & M. Zalewski (2001) Toxic cyanobacterial blooms in a drinking water reservoir-causes, consequences and management strategy. *Water Science and Technology: Water Supply* **1**(2), 237–246.

Tockner, K., Malard, F. & Ward, J. V. (2000) An extension of the flood pulse concept. *Hydrol. Processes* **14**, 2861–2883.

Wagner-Łotkowska, I., Bednarek, A. & Zalewski, M. (2002) Management of flows in large rivers for water quality improvement. In: *UNEP – IETC Guidelines for the Integrated Management of the Watershed – Phytotechnology and Ecohydrology*. (ed. by M. Zalewski), 127–135. IETC Technical Publication Series 5.

Wagner-Łotkowska, I., Kiedrzyńska, E. & Sumorok, B. (2004) Floodplains and natural wetlands: reduction of nutrient transport. In: *Integrated Watershed Management – Ecohydrology et Phytotechnology – Manual* (ed by M. Zalewski & I. Wagner-Łotkowska), 163–168. UNESCO Regional Bureau for Science in Europe, Venice, Italy.

Zalewski, M. (2000) Ecohydrology – the scientific background to use ecosystem properties as management tools toward sustainability of water resources. *Ecol. Engng J. Ecohydrology* **16**, 1–8.

Zalewski, M. (2002) Ecohydrology – the use of ecological and hydrological processes for sustainable management of water resources. *Hydrol. Sci. J.* **47**(5), 825–834.

Climate Variability and Change—Hydrological Impacts (Proceedings of the Fifth FRIEND World Conference held at Havana, Cuba, November 2006), IAHS Publ. 308, 2006.

A global assessment of chemical effluent dilution capacities from a macro-scale hydrological model

VIRGINIE D. J. KELLER[1], MICK J. WHELAN[2] & H. GWYN REES[1]

1 *Centre for Ecology and Hydrology, Wallingford, Oxfordshire OX10 8BB, UK*
vke@ceh.ac.uk

2 *Safety and Environmental Assurance Centre, Unilever Colworth, Colworth Park, Bedfordshire MK44 1LQ, UK*

Abstract Environmental risk assessments for "down-the-drain" chemicals (e.g. pharmaceuticals and household product ingredients) are generally based on a comparison between predicted environmental concentration (*PEC*) and predicted no effect concentrations (*PNEC*) for a generic environment with a fixed dilution factor. For PEC calculations spatial and temporal variability is often not explicitly taken into account. In the absence of detailed local-scale information for specific point-sources, spatially-explicit approximations can be made, based on the ratio of available surface water and domestic water consumption. In this paper, a new methodology is proposed for predicting surface water dilution at a global scale. The approach employs 0.5° resolution geographical data on national boundaries, population density, runoff (from water balance model calculations) and domestic water consumption to produce dilution factor maps for the global land surface. The proposed methodology has great potential for improving screening-level chemical risk assessments.

Key words chemicals; dilution; environmental risk assessment; GIS; global-scale; population; runoff

INTRODUCTION

Environmental risk assessments for chemicals usually make comparisons between Predicted Environmental Concentrations (PECs) and Predicted No Effect Concentrations (PNECs). For many so-called "down-the-drain" chemicals (such as pharmaceuticals and the ingredients used in household cleaning products), the principal disposal route after use is via the wastewater stream. Screening-level exposure assessments (i.e. PEC calculations) for these substances are usually based on a simple ratio of per capita chemical consumption and per-capita domestic water use. This is then adjusted for removal during sewage treatment, if applicable, and for dilution in the receiving aquatic environment using a generic dilution factor (e.g. EC, 2003). This approach is simple but it is also reasonably robust scientifically and is appropriate for comparative screening-level risk assessments. However, it does not take into account spatial and temporal variability in dilution which changes with the relative magnitude of point-source loads and river discharge at the point of emission. This information may be required when trying to compare risks in different geographical areas with different hydrological regimes and population densities. In the absence of detailed local-scale information for specific point-sources, tolerable spatially-explicit approximations can be made, based on the ratio of available surface water and domestic water consumption, for discrete areas. Reasonable estimates of mean monthly and mean annual runoff can be obtained from long-term meteorological data using simple water balance models. Domestic water consumption can be estimated from country- or region-specific data for per-capita domestic water use and population density. These calculations allow the spatial variability of dilution and its seasonality to be examined at different spatial scales (catchment, regional, national and continental) anywhere in the world.

This paper presents a new methodology which has been developed to estimate the spatial variability of dilution factors using global-scale data. These predictions will inevitably be crude estimates of local conditions which will vary on a case by case basis but may provide a reasonable initial estimate which can be refined locally if required (e.g. using more sophisticated exposure assessment tools such as GREAT-ER (Feijtel *et al.*, 1997). The approach can be used to compare screening-level *PEC*s on a regional, country-specific or catchment basis and help to identify geographical areas with relatively high risk ("hot spots"), thereby guiding targeted risk mitigation measures at various scales. It can also be used to help generate statistical distributions of *PEC* required in probabilistic risk assessments.

Copyright © 2006 IAHS Press

APPROACH

The methodology was specifically derived for estimating concentrations of "down-the-drain" chemicals in fresh surface waters.

Concept

PEC for raw waste water (PEC_{SEWAGE}) can be estimated from:

$$PEC_{SEWAGE} = \frac{U}{W} \tag{1}$$

where U is the daily per capita consumption of chemical (mg cap^{-1} day^{-1}) and W is the daily per capita water use (L cap^{-1} day^{-1}). U is calculated from the annual mass of chemical used nationally, T (t year^{-1}) using:

$$U = \frac{T \cdot 10^9}{365 \cdot P_{COUNTRY}} \tag{2}$$

where $P_{COUNTRY}$ is the population of the country concerned. The surface water PEC (PEC_{AQ}), immediately after mixing, but before any decrease in chemical concentration has occurred as a consequence of degradation and dilution, can be estimated from:

$$PEC_{AQ} = \frac{(1-F) \cdot PEC_{SEWAGE}}{DF} \tag{3}$$

where F is the fraction of chemical removed in wastewater treatment, derived from monitoring data or from standard laboratory biodegradation and partitioning studies. *DF* is the dilution factor which is defined as:

$$DF = \frac{(Q+q)}{q} \tag{4}$$

where Q is the discharge (m^3 s^{-1}) of the receiving water and q is the point-source discharge (m^3 s^{-1}). Unfortunately, in many parts of the world, the data required to estimate *DF* at a local (catchment or river reach) scale is not readily available. However, a proxy for *DF* can be derived from public-domain gridded runoff R (mm year^{-1}) and population density ρ (cap m^{-2}) data sets which are available at a global scale. Using gridded data and adopting dimensional units, *DF*, for any grid cell at a specified resolution can be defined as:

$$DF = \frac{Q_i + q_i}{q_i} = \frac{\sum_{j=1}^{i} (R_j \cdot A_j) + W_i \cdot A_i \cdot \rho_i}{W_i \cdot A_i \cdot \rho_i} \tag{5}$$

where W is the domestic water use per capita (L^3 cap^{-1} T^{-1}), A is the cell area (L^2), i is an index for any cell in the grid and j is an index for all cells contributing flows to cell i (i.e. defined by cell-to-cell flow routing from the topographic divide).

Runoff data

Long-term average (usually 1960–1990) annual runoff can be predicted using macroscale hydrological models (e.g. Arnell, 1999). Such models, which commonly have a resolution of 0.5º latitude by 0.5º longitude, have been used to define land-surface parameterization schemes in general circulation models (e.g. Nijssen *et al.*, 1997) and for estimating water resource availability at global, continental or regional scales (e.g. Alcamo *et al.*, 2003; Abdulla & Lettenmaier, 1997).

In this paper, the composite runoff fields produced by Fekete *et al.* (1999) were used. These runoff estimates were generated by combining a simple water balance model with observed river discharge data. The water balance model uses the data set of Legates & Willmott (1990) for global precipitation, soil type data from the FAO/UNESCO soil data bank (FAO/UNESCO, 1986), topographic data from the ETOPO5 global elevation data set (Edwards, 1989) and a contemporary

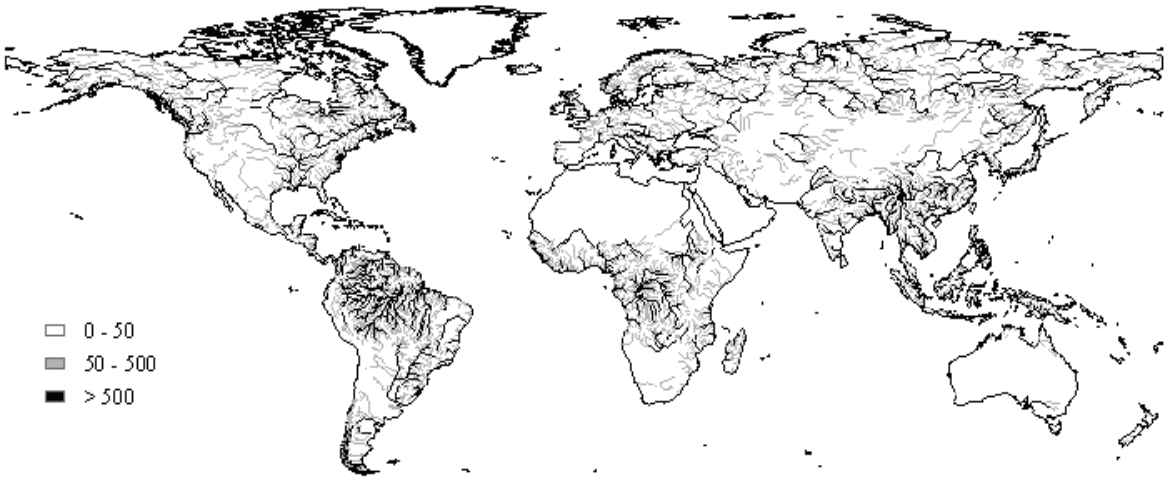


Fig. 1 Predicted river discharge ($m^3 s^{-1}$) from the annual composite runoff fields (CRF) data (Fekete *et al.*, 1999).

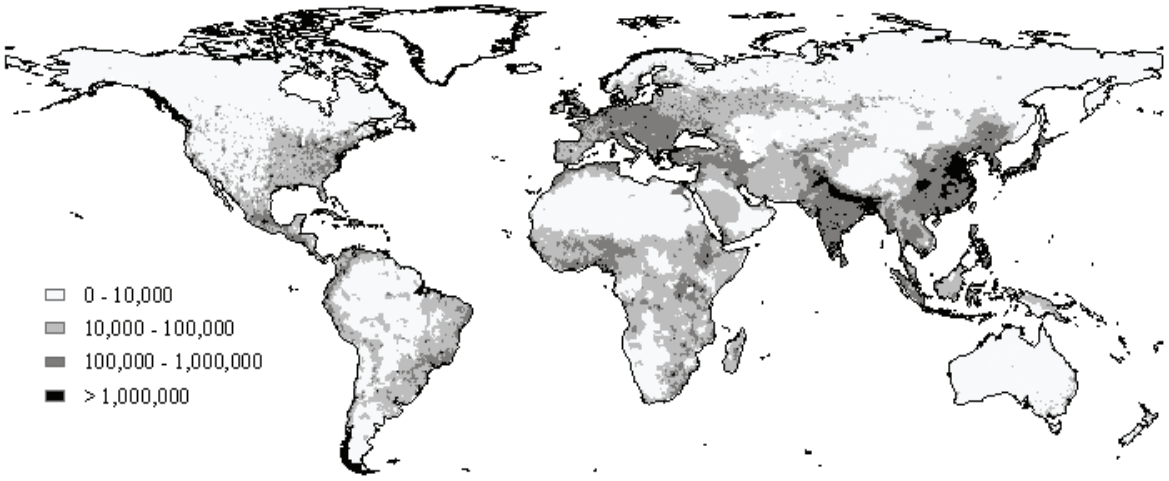


Fig. 2 Global population per grid cell derived from the Gridded Population of the World (GPW) v.2 data set for 1995 (SEDAC, 2000), degraded to 0.5° × 0.5° resolution.

land cover classification derived from the Terrestrial Ecosystem Model (Melillo *et al.*, 1993) and Olson's land use classification (Olson, 1992).

The topographically-derived flow direction grid provided by Fekete *et al.* (1999) was used for accumulating runoff in the grid, thereby estimating cell-specific discharge Q_i (Fig. 1).

Population data

The GPW v.2 data set for 1995 (Gridded Population of the World – GPW, SEDAC, 2000) was used to estimate the distribution of global population density. This data set has been adjusted to correspond with national-level population estimates issued by the United Nations. The resolution of the original data was 2.5 arc minutes which was aggregated to a 0.5° ×0.5° (latitude, longitude) resolution corresponding to the runoff grids (Fig. 2).

Domestic water use

Per-capita domestic water use (*W*) varies widely from country to country and even within countries as a consequence of water availability, infrastructure, wealth and habits. Individual values of *W* were generated for each 0.5° × 0.5° grid cell using mean values for each country. National statistics were extracted from several public domain data sources (Gleick, 1996; OECD, 2002; WRI, 2003, FAO, 2000). Where discrepancy existed between data sources, the lowest value was selected to provide a more conservative value for *DF*.

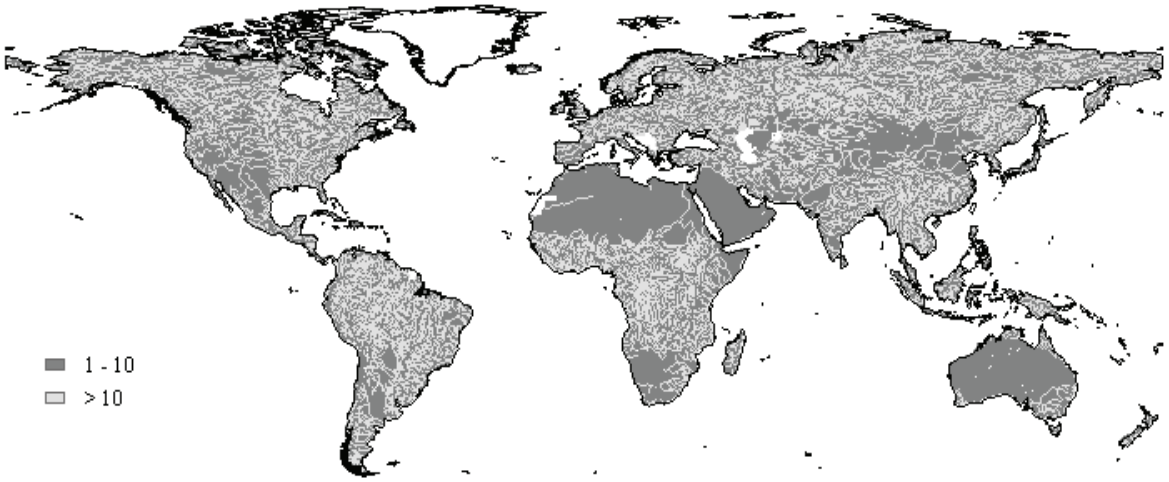


Fig. 3 Predicted values of global dilution factor (*DF*) at 0.5° × 0.5° resolution.

RESULTS AND DISCUSSION

The spatial distribution of *DF* values calculated using equation (5) is shown in Fig. 3.

Large areas with low *DF* values are visible in the western half of North America, the Pampas of Argentina, North Africa and the Middle East, parts of central Asia, Australia and southern Africa. Values of *DF* in the equatorial belt and in most of northern Europe, Canada and Siberia are generally high. Within the methodology described here, *DF* can be influenced by two main factors: (a) surface water discharge, and (b) population density and domestic water use. Low values can be due to either arid conditions or very high population density (or both). It should be noted that low values of *DF* do not necessarily represent areas of high risk in receiving environments resulting from chemical emissions. For example, in the case of some very arid regions (e.g. the Sahara desert), both runoff and population density may be very low resulting in low values of *DF*. However, the impact of emissions on surface waters in these systems may not be significant because of negligible wastewater flow.

There are a number of ways in which the cell-based estimates of *DF* can be used. Often, environmental management (and associated risk assessments) is conducted on a national basis. For screening-level PEC assessments, a single statistic of *DF* (e.g. the mean or a percentile value) for an individual country may be required. However, the use of mean values on their own may be misleading, particularly for large countries with a high degree of spatial variability in population density and climate. The use of mapped values such as those presented here, which could include the influence of flow seasonality, provide a better picture of the geographical distribution of *DF*. This information would be required in probabilistic approaches to risk assessment (e.g. Feijtel *et al.*, 1999).

The following factors are not explicitly considered in the methodology presented here but are likely to be important in determining actual PECs locally: wastewater treatment provision (and consequent chemical removal); in-sewer and in-stream losses (e.g. adsorption to sediment and volatilization); and the possibility that certain products are used more intensively on certain days. Where suitable data are available these factors might be considered in more detailed (and more realistic) risk assessments.

Further work is required to develop the proposed methodology. This includes more rigorous testing of the hydrological predictions with respect to gauged flows from around the world, including the effects of flow seasonality and the mitigating role of groundwater discharge. It is possible that the suitability of the hydrological model employed will vary from region to region. In some cases it may be necessary to apply different models to different regions of the world with the distribution of runoff globally derived from a composite of outputs from several models.

CONCLUSIONS

This paper describes a methodology which, for the first time, allows consistent, hydrologically-based environmental risk assessments for "down-the-drain" chemicals discharged to freshwaters to be performed in any country in the world. The methodology represents an intermediate level model between generic multi-media models (e.g. EC, 2003) and detailed spatially referenced catchment-scale models, such as GREAT-ER (Feijtel *et al.*, 1997). Such an intermediate-level assessment can help to identify particular regions where chemical concentrations in surface waters may be a cause for concern and, thus, provide a means of targeting more detailed local-scale risk assessments and risk management measures where necessary.

Acknowledgements We would like to thank the providers of all the data utilised in this paper, without whom this analysis would not have been possible. We also thank Dr Henry King of Unilever for helpful comments on the manuscript.

REFERENCES

Abdulla, F. A. & Lettenmaier, D. P. (1997) Application of regional parameter estimation schemes to simulate the water balance of a large continental river. *J. Hydrol.* **197**(1–4), 258–285.

Alcamo, J., Doll, P., Henrichs, T., Kaspar, F., Lehner, B., Rosch, T. & Siebert, S. (2003) Global estimates of water withdrawals and availability under current and future "business-as-usual" conditions. *Hydrol. Sci J.* **48**(3), 339–348.

Arnell, N. W. (1999) A simple water balance model for the simulation of streamflow over a large geographic domain. *J. Hydrol.* **217**(3–4), 314–335.

Edwards, M. (1989) Global Gridded Elevation and Bathymetry (ETOPO5), Digital Raster Data on a 5-minute Geographic Grid.: NOAA National Geophysical Data Center, Boulder, Colorado, USA.

European Commission (EC) (2003) Technical guidance document on Risk Assessment in Support of Commission Directive 93/67/EEC on Risk Assessment for New Notified Substances, Commission regulation (EC) no. 1488/94 on Risk Assessment for Existing Substances, and Directive 98/8/EC of the European Parliament and of the Council Concerning the Placing of Biocidal Products on the Market. Part II. Office for Official Publications of the European Communities.

FAO/UNESCO (1986) Gridded FAO/UNESCO Soil Units. UNEP/GRID, FAO Soil Map of the World in Digital Form, Digital raster data on 2 minute Geographic (lat × lon) 5400 × 10800 grid. UNEP/GRID, Carouge, Switzerland.

Feijtel, T., Boeije, G., Matthies, M., Young, A., Morris, G., Gandolfi, C., Hansen, B., Fox, K., Holt, M. & Koch, V. (1997) Development of a Geography-referenced Regional Exposure Assessment Tool for European Rivers – GREAT-ER contribution to GREAT-ER #1. *Chemosphere* **34**(11), 2351–2373.

Feijtel, T. C. J., Struijs, J. & Matthijs, E. (1999) Exposure modeling of detergent surfactants - Prediction of 90th-percentile concentrations in the Netherlands. *Environ. Toxicol. Chem.* **18**(11), 2645–2652.

Fekete, B. M., Vorosmarty, C. J. & Grabs, W. (1999) Global, Composite Runoff Fields on Observed River Discharge and Simulated Water Balances. GRDC Report no. 22. Global Runoff Data Centre, Koblenz, Germany.

Food and Agriculture Organisation of the United Nations (FAO) (2000) AQUASTAT database. http://www.fao.org/ag/agl/aglw/aquastat/dbase/index2.jsp, FAO's Land and Water Development division website.

Gleick, P. H. (1996) Basic water requirements for human activities: Meeting basic needs. *Water International* **21**(2), 83–92.

Legates, D. R. & Willmott, C. J. (1990) Mean Seasonal and Spatial Variability in Gauge-Corrected, Global Precipitation. *Int. J. Climatol.* **10**(2), 111–127.

Melillo, J. M., McGuire, A. D., Kicklighter, D. W., Moore, B., Vorosmarty, C. J. & Schloss, A. L. (1993) Global Climate-Change and terrestrial net primary production. *Nature* **363**(6426), 234–240.

Nijssen, B., Lettenmaier, D. P., Liang, X., Wetzel, S. W. & Wood, E. F. (1997) Streamflow simulation for continental-scale river basins. *Water Resour. Res.* **33**(4), 711–724.

Olson, J. S. I. (1992) World Ecosystems (WE1.4). Digital Raster Data on a 10-minute Cartesian Orthonormal Geodetic 1080 × 2160 grid. n: Global Ecosystems Database, version 2.0. National Geophysical Data Center, Boulder, Colorado, USA.

Organisation for Economic Co-operation and Development (OECD) (2002) OECD Environmental Data—Compendium 2002. http://www.oecd.org/dataoecd/8/19/2958157.pdf, OECD website.

SEDAC (Socioeconomic Data and Applications Center) (2000) Gridded population of the world (v2). http://sedac.ciesin.columbia.edu/plue/gpw/index.html?main.html&2, Center for International Earth Science Information Network (CIESIN) website.

World Resources Institute (WRI) (2003) Water Resources and Freshwater Ecosystems – Freshwater Resources 2003. http://earthtrends.wri.org/datatables/index.cfm?theme=2, WRI EarthTrends Environmental Information Portal.

Climate Variability and Change—Hydrological Impacts (Proceedings of the Fifth FRIEND World Conference held at Havana, Cuba, November 2006), IAHS Publ. 308, 2006.

Wet and dry deposition of atmospheric nitrogen in three hydrographic basins in Cuba

OSVALDO CUESTA-SANTOS, ARNALDO COLLAZO, MARIA GONZALEZ & ANTONIO WALLO

Atmospheric Environment Research Center, Meteorological Institute of Cuba, Aptdo 17032, Havana 17, PC 11700, Cuba
osvaldo.cuesta@insmet.cu

Abstract Acid deposition remains an important environmental issue in Europe and North America. Furthermore, it is emerging in new geographical areas, including parts of South/Central America. In these areas, emissions of nitrogen oxides are increasing rapidly as industrialization proceeds and the use of fossil fuels increases. In Cuba, main atmospheric nitrogen deposition compounds varies approximately from 19.3 to 71.2 kg-N ha^{-1} $year^{-1}$ in rural areas. The oxidized nitrogen forms being provided 34% as average and wet deposition depends on the Cuba tropical rain climate features. The NH_3 and ammonium are the most important elements in Cuban tropical conditions. This paper is showing more relevant results about main compounds of atmospheric nitrogen in Cuba and its potential impact on environment.

Key words acid deposition; nitrogen compounds; wet deposition; oxidized nitrogen

INTRODUCTION

Human efforts to produce food and energy are changing the nitrogen (N) cycle of the Earth. Many of these changes are highly beneficial for humans, while others are detrimental to people and the environment. These changes transcend scientific disciplines, geographical boundaries, and political structures. They challenge the creative minds of natural and social scientists, economists, engineers, business leaders, and decision makers (Cowling, 2001).

Nowadays, most anthropogenic activities endanger the functioning and structure of natural and semi-natural ecosystems due to the effects on the endemic species of animals and plants. One of the major dangers is the increase of atmospheric pollution by nitrogen compounds during recent decades. The most important messages for environmentalists and policy makers are:

(a) Increase circulation of nitrogen in the atmosphere and biosphere is occurring in all parts of the globe.
(b) Nitrogen has a range of well-understood beneficial and detrimental consequences for humans and environment.
(c) Scientists and decision makers needs to work together to develop integrated approaches to solve nitrogen related problems.

Knowledge of the atmospheric component of the nitrogen cycle is of great importance because of the different compounds involved, their chemistry and the atmospheric pollution they cause. These pollutants have the capacity to affect human health, different aquatic and terrestrial ecosystems, and climate.

In many areas, soil acidification due to nitrification of ammonium deposited from the atmosphere is comparable to that from the deposition of nitric acid (Rodhe, 1995). Currently ammonia (NH_3) emissions are of the same magnitude as that of nitrogen oxides (NO_x) and sulphur dioxide (SO_2) emissions and are potentially even more acidifying.

The nitrogen compounds are nitrogen oxides (nitrogen dioxide and nitric oxide), ammonia (NH_3), nitrate (NO^-_3) and ammonium (NH^+_4) in aerosols and rainfall. In this paper, the deposition of atmospheric nitrogen compounds at three hydrographic basins in Cuba, is discussed for the period 1985 to 2005. The most relevant results regarding the main compounds of atmospheric nitrogen in Cuba and its potential impact on environment, are presented.

MATERIALS AND METHODS

In preparing this paper, data from the air pollution control station network of the Meteorological Institute of the Cuban Ministry of Science, Technology and Environment were used (Fig. 1). The

Copyright © 2006 IAHS Press

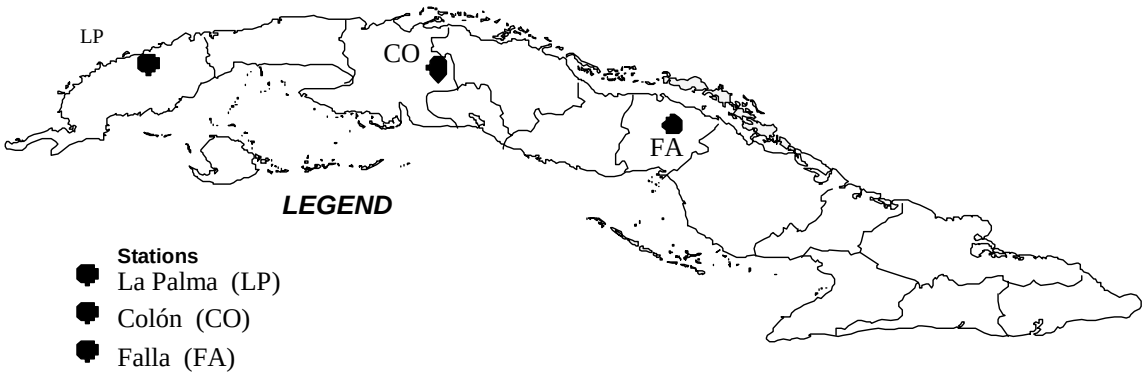


Fig. 1 Monitoring stations for nitrogen compounds.

work of this network is conducted using methodologies recommended by the World Meteorological Organization for monitoring and chemically analysis of the above-mentioned compounds at the regional level. The stations are situated in three important hydrographic basins.

For calculation of wet and dry deposition of atmospheric nitrogen, the concentrations expressed in μg m^{-3} for NO_2, NO, NH_3, NO_3^- and NH_4^+ were converted into nitrogen (N). Concentrations in rainfall are expressed as mg L^{-1}. Samples were collected and analysed using World Meteorological Organization approved methods for rainfall, aerosols and gases; all methods were quantitatively determined colorimetrically. Nitrates react in the acidified sample with 2,4 xylenol, which is then extracted with synthetic toluene and finally re-extracted from the synthetic toluene with sodium hydroxide solution. Ammonium ion concentration is reacted with hypochlorous acid, phenol and a manganese sulphate solution. The blue indophenol formed is quantitatively determined colorimetrically. Ammonia (NH_3) in air is collected by passing it through dilute sulphuric acid and determined using a minor modification of the indophenol technique (WMO, 2004).

For the dry deposition flux, because of the known deficiencies of existing monitoring methods, the quantities were recalculated using the deposition velocity (Cuesta *et al.*, 1998) and the concentrations obtained from monitoring. For wet deposition fluxes, the mean heavy concentrations for each year (starting from a summary of monthly samples) and the rainfall quantities were used for both concentrations. Deposition fluxes are expressed in kg-N ha^{-1} $year^{-1}$. The values of deposition velocity were obtained after analysis of data reported by different authors and selection of those which are most adapted to the climatic conditions of Cuba (Whelpdale & Kaisser, 1995; Cuesta *et al.*, 2001); they are shown in Table 1.

All statistical analyses were performed in SPSS Plus. In addition, trends in the concentration data 1985–2005 were analysed. This allows the behaviour of both the natural and anthropogenic sources of the above-mentioned compounds to be understood.

Table 1 Selected values of the deposition velocity in cm s^{-1} for the gases and aerosols in dependency of land use and climatic conditions.

Stations	NO_2	NO	NH_3	NO_3^-	NH_4^+
La Palma	0.2	0.15	0.5	0.5	0.5
Colon	0.2	0.15	0.3	0.2	0.2
Falla	0.2	0.15	0.3	0.2	0.2

RESULTS AND DISCUSSION

The total deposition values (dry and wet) for the main nitrogen compounds at the three stations are shown in Fig. 2. La Palma's station presents the highest deposition values for ammonia indicating a bigger deposition velocity for this compound. Colon's station presents the highest values of ammonium in the rainfall. The strength of the sources of N compounds, and the high rainfall at these stations are due to its geographical location in the middle of the country, and in addition it is a farming and livestock zone. Farming is recognized as major source of atmospheric ammonia (NH_3) in Europe and contributes about half of the global NH_3 emissions (Sommer & Hutchings, 1995).

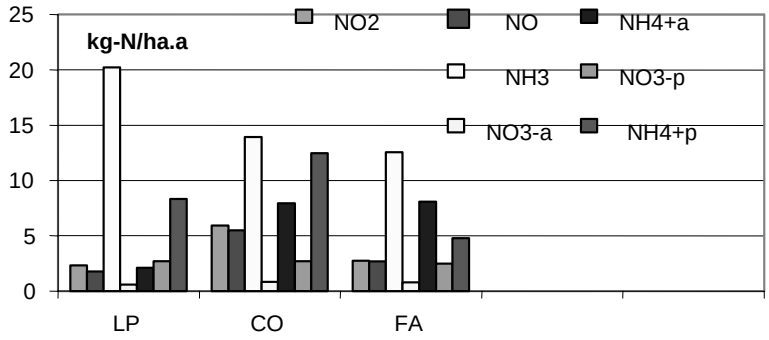


Fig. 2 Annual mean of nitrogen deposition by compound and station (1985–2005). LP is La Palma; Co is Colon; FA is Falla; p is precipitation, a is aerosol.

In general these annual values are similar to those reported in most of Europe and North America (Driscoll, 2001), except in the large urban and industrialized centres, where the deposition in Europe is significantly higher. The annual values at the three stations vary from a minimum of 19.3 kg-N ha^{-1} $year^{-1}$ recorded at Falla station in 1998, where it is due to the low values of NH_3, to a maximum of 71.2 kg-N ha^{-1} $year^{-1}$ in 2001 at La Palma station, where the ammonia deposition was considerably higher. As can be appreciated, in the tropical Cuban conditions, the natural and anthropogenic emissions of ammonia are very important in the biogeochemical cycle of nitrogen.

Wet deposition of inorganic nitrogen from nitrate in the USA during 2000 varied from 1 to 20 kg-N ha^{-1} $year^{-1}$ or more. On the other hand, wet deposition of ammonium ranged from 1 to 4.5 kg-N ha^{-1} $year^{-1}$. The wet deposition of nitrate in Cuba is similar to that in the south of the USA, but wet deposition of ammonium is moderately higher in Cuba than in the USA (NADP, 2001).

In Cuba, the data from these stations show that wet deposition of nitrogen represents more than 20% of the total deposition. Although as a general rule the dry deposition is greater, at Colon and La Palma stations, where rainfall is high, wet deposition has even greater influence.

The values obtained for Cuba refer to the main kinds of oxidized nitrogen species; they represent 34% on average. However, Colon and La Palma stations receive the lowest amount of oxidized nitrogen because of the great importance of natural reduced nitrogen sources. Ammonia (NH_3) and ammonium are the most important nitrogen species in the tropical conditions in Cuba.

These values reflect a very large amount of ammonia deposition, so it is considered that over short timescales the ammonia neutralizes the atmosphere's acidity and associated damage. On the another hand, it can produce soil and underground waters acidification over longer time periods.

Responses of terrestrial ecosystems to anthropogenic nitrogen inputs are likely to vary geographically. However, not all ecosystems respond to N deposition similarly; their response depends on factors such the successional state, ecosystem type, N demand or retention capacity, land-use history, soils, topography, climate, and the rate, timing, and type of nitrogen deposition (Matson *et al.*, 2002).

La Palma station is representative of the forest ecosystem of western Cuba and at this moment this station receives the 20% from acid deposits. The soil of this region is classified with very high acidity (pH 4.1–4.5), and will be very sensitive to acid deposition; this can produce harmful ecological risks in soil productivity, affecting trees growing in forest areas, as well as the productivity of some other crops. Forest areas are able to receive from five to six times more dry deposition (gas and aerosol) due to the greater deposition flux that they generate, and so make this region ecologically more sensitive. The response and reaction of forest ecosystems to chemical changes in the environment are complex.

Through studies of the behaviour of diverse nitrogen species at the La Palma station, it is possible to see (Fig. 3) that the NH_3 and ammonium (rainfall and aerosol) contributions are greater than 70% of the total nitrogen deposition. These values reflect the very large proportion due to the ammonia deposition, and it is considered that the ammonia neutralizes, in the short term, the atmosphere's acidity, and also it avoids the damages. On the other hand, it can produce soil erosion and underground waters acidification in the longer term (Galloway, 1995).

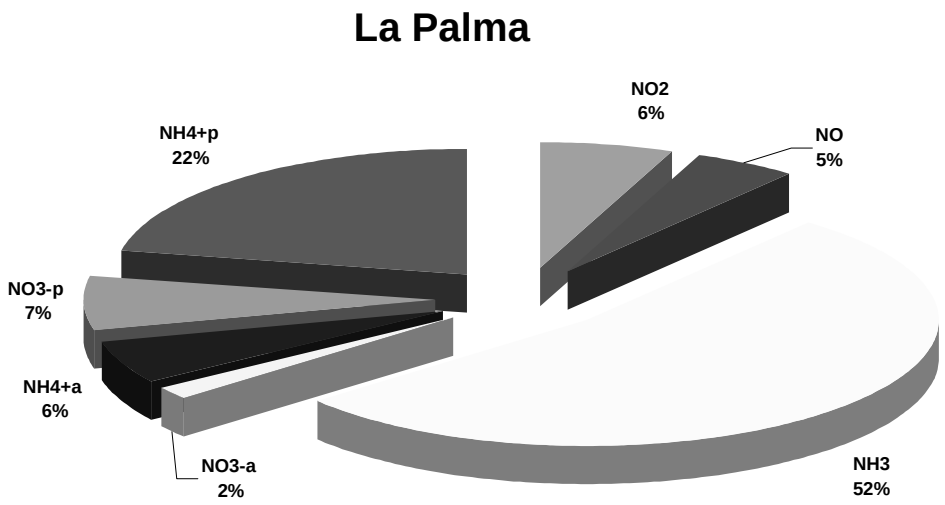


Fig. 3 Breakdown of nitrogen deposition by compound for La Palma station.

Another of the potential effects that can provoke deposition of oxidized nitrogen compounds is acidification of surface freshwater streams and lakes; this causes reduction of the bicarbonate ion and the increase of nitrate concentrations, which produces and increase concentrations of some metals in freshwater bodies. Metals such as aluminium, cadmium, zinc, lead and mercury are very toxic and can be ingested by different types of aquatic life, and through alimentary chains, even arrive in man's food.

Some nitrogen compound concentrations (see Table 2) showed a significant trend in the period from 1985 to 2005.

La Palma, Colon and Falla rural stations present a significant trend for NO_2 and NH_3 concentration increase (Fig. 4). These rural stations seem to be influenced by the biomass burning for

Table 2 Direction of the trend for nitrogen atmospheric compounds.

Stations	NO_2	NO	NH_3	$NO_3^+{}_{(a)}$	$NH_4^+{}_{(a)}$	$NO_3^+{}_{(p)}$	$NH_4^+{}_{(p)}$
La Palma	+	+	+	–	+	–	+
Colón	+	+	+	–	–	–	–
Falla	+	+	+	–	–	–	–

Note: (–) direction to decrease, (+) to increase, (a) aerosol, (p) precipitation.

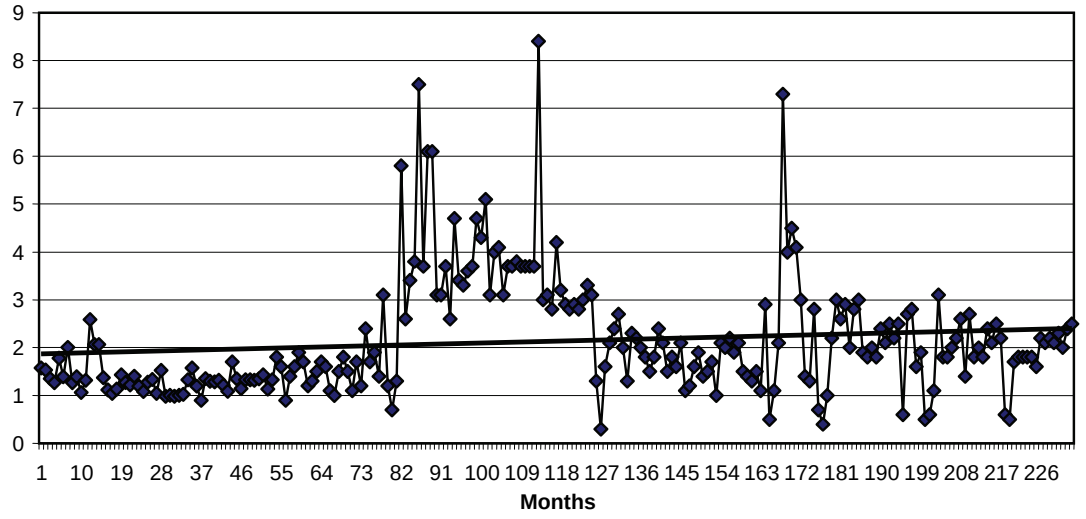


Fig. 4 The NO_2 concentrations trend in Colon station. Units of vertical axis are mg-N m^{-3}.

energy purposes and it is possible that the change in land use and application of fertilizers also influences this increase. In addition, the trend of an increase of ammonium aerosols is very important and its increase has been significant at rural La Palma station, mainly caused by the use of ammonia as a fertilizer in these regions. The increase of ammonium in rainfall is only present at La Palma station.

The potentially harmful effects due to acid deposition influence the aquatic and terrestrial ecosystems, and also cause corrosion of materials and human health problems, so a system of integrated monitoring must be imposed to assess and to be able to mitigate its effects.

CONCLUSIONS

In Cuba, the total deposition for main nitrogen compounds varies from 19.3 to 71.2 kg-N ha^{-1} $year^{-1}$. Dry deposition of nitrogen represents somewhat more than 70% of total nitrogen deposition. NH_3 is very important in dry deposition. The relative weights of dry and wet deposition depend on the characteristics of Cuba's rainy tropical climate. Oxidized forms of nitrogen contribute to approximately 34% of the total.

The Colón and La Palma stations receive the lowest amount of oxidized nitrogen because of greater strength of natural reduced nitrogen sources. NH_3 and ammonium are the most important nitrogen compounds in the tropical conditions in Cuba.

It is necessary to maintain systematic monitoring at the rural La Palma, Colón and Falla stations because trends for increasing concentrations of oxidized nitrogen compounds could potentially cause future damage to the agriculture and forest of these regions.

Acknowledgements We wish to thank to the Cuban Environmental Agency for the financial support for the accomplishment of this work.

REFERENCES

Cowling, E. (2001) Optimizing nitrogen management in food and energy production and environmental protection: Summary statement from the second international nitrogen conference. In: *Optimizing Nitrogen Management in Food and Energy Production and Environment Protection* (Proc. Second International Nitrogen Conference on Science and Policy). The Scientific World 1(S2), 1–9.

Cuesta, O., Ortiz, P. & Gonzalez M. (1998) Deposition and atmospheric nitrogen concentrations trend in Cuba. *Water, Air and Soil Pollution* **114**, 163–167.

Cuesta-Santos, O., Collazo, A., Wallo, A., Labrador, R, González, M. & Ortiz, P. (2001) Deposition of atmospheric nitrogen compounds in humid tropical Cuba. In: *Optimizing Nitrogen Management in Food and Energy Production and Environment Protection* (Proc. Second International Nitrogen Conference on Science and Policy). The Scientific World 1(S2), 238–244.

Driscoll, C. (2001) Acid deposition in the Northeastern United Stated: sources and inputs, ecosystem effects, and management strategies. *BioScience* **51**(3).

Galloway, J. (1995) Acid deposition: perspectives in time and space. *Water, Air and Soil Pollution* **1**, 15–24.

Matson, P., Lohse, K. A. & Hall, S. J. (2002) The globalization of nitrogen deposition: consequences for terrestrial ecosystems. *AMBIO* **31**(2), 113–119.

NADP (2001) National Atmospheric Deposition Program. 2000 Annual Summary. http://nadp.sws.uiuc.edu.

Rodhe, H. (1995) Acid Reign'95? Conference summary statement. *Water, Air and Soil Pollution* **85**(1), 1–14.

Sommer, S. G. & Hutchings, N. (1995) Techniques and strategies for the reduction of ammonia emission from agriculture. *Water, Air and Soil Pollution* **85**(1), 237–248.

Whelpdale, D. M., & Kaisser, M. S. (1995) *Global Acid Deposition Assessment*. GAW no. 106, WMO-TD 777. Geneva, Switzerland.

World Meteorological Organization (2004) *Manual for GAW Precipitation Chemistry Programme*. WMO-TD 1251. Geneva, Switzerland.

Climate Variability and Change—Hydrological Impacts (Proceedings of the Fifth FRIEND World Conference held at Havana, Cuba, November 2006), IAHS Publ. 308, 2006.

Application of hydrogeochemical modelling to the characterization and water quality control of coastal karst aquifers

J. R. FAGUNDO CASTILLO[1], P. GONZÁLEZ HERNÁNDEZ[1], J. FAGUNDO SIERRA[1], M. SUÁREZ MUÑOZ[1], C. MELIÁN RODRÍGUEZ[1] & E. ALVAREZ VARELA[2]

1 *National Center of Natural and Traditional Medicine (CENAMENT), Ave 243 ·#19815. Fontanar. Ciudad de la Habana, Código Postal 19250, Cuba*
juanrfag@infomed.sld.cu

2 *National Center for Scientific Research (CNIC), Ave 25 esq. 158. Playa. Ciudad de la Habana, Código Postal 6412, Cuba*

Abstract A set of computer systems (HIDROGEOQUIM, SAMA, GEOQUIM, BATOMET, SACAN, SIMUCIN, MODELAGUA and TEMADAT) for hydrochemical data processing with the aim of characterizing and controlling water quality, and simulating the water–rock interaction process, are detailed. Examples of their application to karst costal aquifers are discussed.

Key words hydrogeochemical models; water quality; karst costal aquifers

INTRODUCTION

To enable determination of the quality of the water resources, as well as the changes to them as a result of human activity, there are, in many countries, large networks of systematic sampling stations at which the local hydrometeorological conditions and some water quality indicators are continually monitored. The mathematical processing of these data by means of statistical and hydrogeochemical models can offer rich information about the regularities among the different variables and the environmental characteristics of the aquifers. These models apply the physical-chemical principles (thermodynamics and kinetics) to the interpretation of these hydrogeochemical systems. With this purpose, two approaches are used: (a) the inverse model (mass-balance), that uses the chemical composition data of the water and the rock with the objective of quantitatively identifying the geochemical reactions that give rise to the composition of waters; and (b) the direct model that, on the basis of some well-known initial conditions of the water–rock system, predicts the characteristics of the resulting solution through hypothetical chemical reactions (Gimeno & Peña, 1994; Plummer *et al*., 1991).

Since the 1990s, at the Cuban National Center for Scientific Research and at the National Center of Thermalism (now in the National Center of Natural and Traditional Medicine), a set of software based on statistical and hydrogeochemical (thermodynamic, kinetic, pattern recognition, mass balance and mixing water) models was developed with the aim to characterize and monitor the water quality of the karst aquifers and mineral water springs (Fagundo *et al*., 2004). The more recent version of the computer programs were designed in DELPHI3 language for WINDOWS. In this paper some of these informatics systems are described and examples of their applications for characterizing and controlling the water quality of the coastal karst aquifer in western Cuba, are discussed.

METHOD

The hydrogeochemical data were processed using the following computer programs: HIDROGEOQUIM (System for Hydrogeochemical Data Processing), SAMA (System for water quality monitoring), GEOQUIM (System for statistical data processing), BATOMET (System for monitoring the water quality of coastal aquifers), SACAN (System for water chemical composition characterization, based on a pattern recognition model), SIMUciN (System to process hydrochemical data from the water–rock interaction in a kinetics experiment), MODELAGUA (System for modelling the natural water chemical composition), and TEMADAT (database system).

Copyright © 2006 IAHS Press

RESULTS

The SAPHIQ system (Alvarez & Fagundo, 1991), and more recently, HIDROGEOQUIM (Fagundo *et al*., 2005), allow the hidrochemical characterization of the aquifers, to study the temporal variation of water quality and to determine the state of the water in its equilibrium with respect to the aquifer constituent minerals. These systems have been applied for the characterization of underground waters of the karst coastal aquifer in the Matanzas (Ferrera *et al*., 1999), Havana (Fagundo *et al*., 2002) and Pinar del Río (Fagundo & Arellano, 1991) provinces; gypsum aquifers of Punta Alegre (Fagundo *et al*., 1994) and saline waters at Cauto basin (Fagundo *et al*., 1995), some of them with high salinity. Also, these software systems were used to study the human effects (overexploitation of the aquifers for public and agricultural supply) on the karst coastal aquifers (Fagundo & González, 1999). Figure 1 shows a chronological series of electric conductivity (EC) and some parameters calculated by HIDROGEOQUIM.

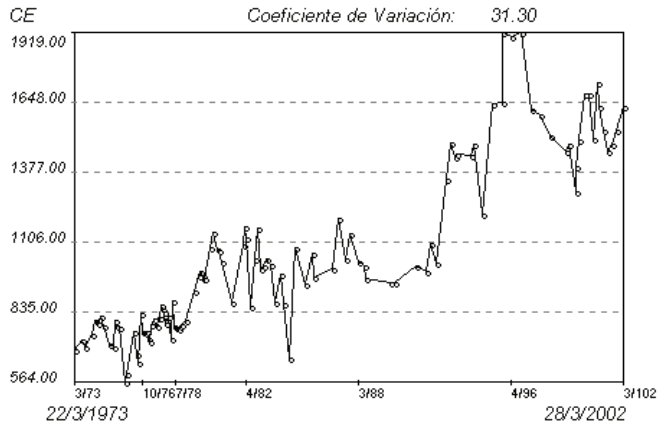


Fig. 1 Variation at time of the electric conductivity (HYDROGEOQUIM).

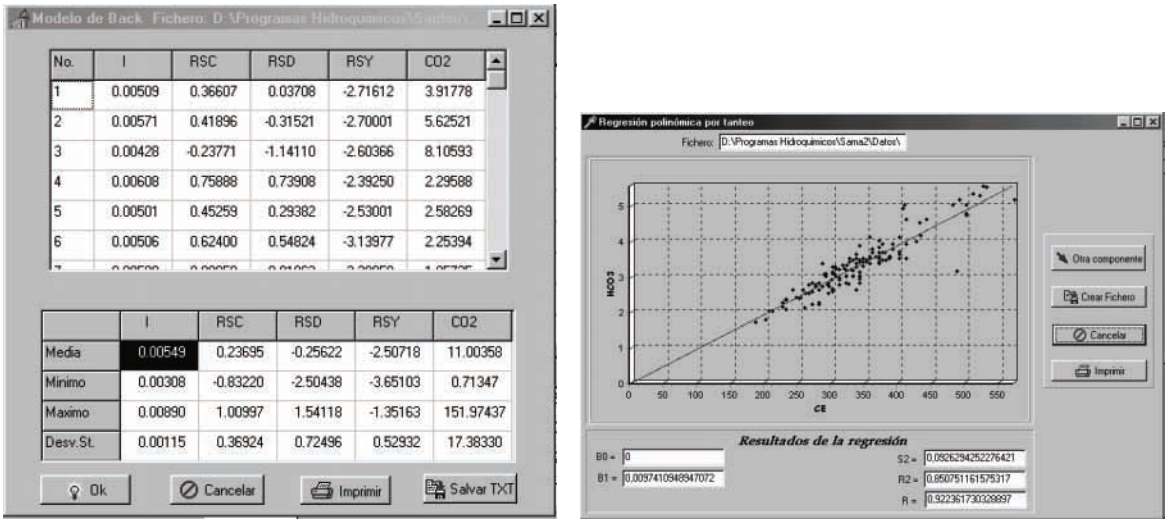


Fig. 2 (a) HYDROGEOQUIM output: ionic strength (I), calcite saturation ratio (RSC), dolomite saturation ratio (RSD), gypsum saturation ratio (RSY) and CO_2 content. (b) Plot by SAMA of the relationship between HCO_3^{2-} content and electric conductivity.

The SAMA system (Alvarez *et al*., 1990), designed to determine mathematical correlations among ionic concentration and EC, and later, to estimate the chemical composition using the above equations and measures of the EC, has been largely used for water quality monitoring for the basins and control network of the Cuban National Institute of Water Research (INRH). Some examples of the application of this software are discussed in Fagundo & Rodríguez (1992) and Fagundo *et al*. (1993, 1994, 1995). Figure 2(a) and (b) show two output windows with results of this system.

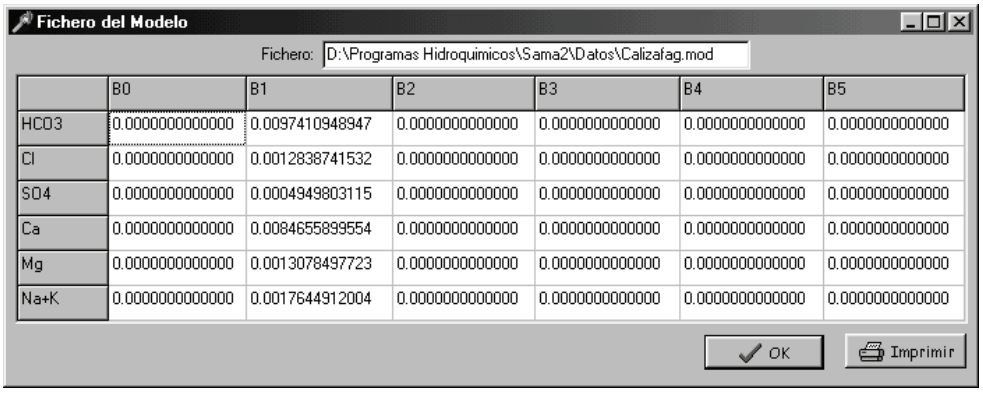


Fig. 3 Relationships between ionic contents and electric conductivity (SAMA).

The GEOQUIM system (Alvarez *et al*., 1993), was designed for the statistical processing of hydrochemical data, and was applied along with SAMA to determine the mathematical correlation equations established among chemical composition and electric conductivity of the water quality control net of INRH in the Pinar del Río region. BATOMET (Vinardell *et al*., 1995), based on a pattern recognition model, sorts the data according to its Cl^-/HCO_3^- ion ratio and later determines the mathematical correlations among chemical composition and EC of each sorted group, estimating the chemical composition of the water using mathematical equations (Fig. 3) and the measured EC (Fig. 3). This system has been applied for monitoring the water quality of the systematic observation well network of INRH in South Pinar del Río basin (Fagundo & Rodríguez, 1991); South Havana basin (Fagundo *et al*., 2002); as well as Zapata swamp, in Matanzas province (Fagundo *et al*., 1993). The karst waters of these coastal aquifers are stratified as a consequence of the mixing of the freshwaters with the seawaters. BATOMET, which joins SAPHIQ and SAMA, was also applied to evaluate the salinity and to control the water quality in the Cauto river basin (Fagundo *et al*., 1995), where the water composition changes drastically in short time intervals.

SACAN, has been used more in the context of mineral waters than in coastal aquifer waters (Tillán *el al*., 1996) due the minor component data available.

SIMUCIN was applied to study the laboratory chemical simulation processes established between the waters and aquifer materials of the karst aquifers (Alvarez *et al*., 1996), including experiments in mixing conditions with seawaters.

MODELAGUA (Fagundo-Sierra *et al*., 2001) was created to determine the geochemical processes that originate the chemical composition of natural waters, by means of mass-balance models and mixture analysis, also allowing the plot of Stiff graphics and the determination of

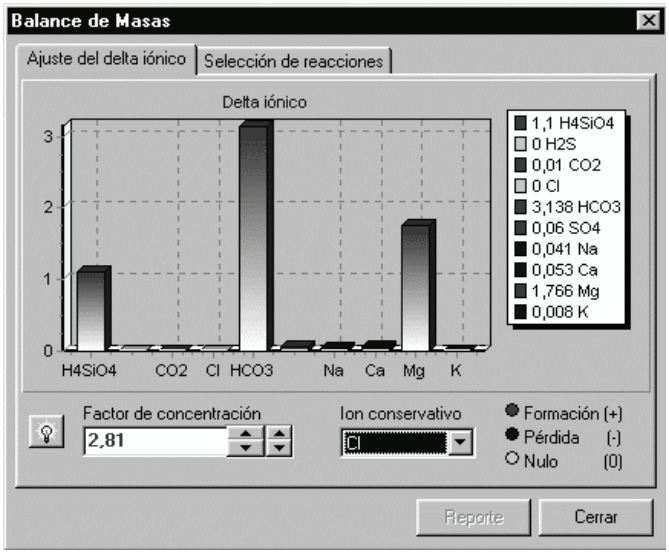


Fig. 4 Computation of ionic delta (Δi) by MODELAGUA.

hydrogeochemical patterns for the classification of different water types. By means of the algorithm of this computer program, the percent of freshwater–seawater mixing and the ionic delta (ΔSO_4^{2-}, ΔNa^+, ΔCa^{2+} and ΔMg^{2+} where Δ represents the mass transferred in the geochemical process) at the karst coastal aquifer of Zapata Swamp (Ferrera *el al*., 1999) and Güira-Quivicán Hydrogeologic Sector (Fagundo *et al*., 2002) were determined. The main hydrogeochemical processes, which explain the chemical composition of these waters, are: calcite and dolomite dissolution, calcite precipitation, dolomitization, sulfate anaerobic reduction and direct and inverse ionic interchange. At the karst coastal aquifer adjacent to a swamp, the variation of the Δ ion magnitude is more intense and also, is in these sites where there are disposed biodegradable organic wastes.

TEMADAT (Fagundo-Sierra *et al.*, 2002) is a database system used to store and manage the hydrochemical data.

CONCLUSION

The informatic systems, implemented by the authors, have been applied to study different underground basins of western Cuba, allowing hydrochemical characterization of the aquifer, analysis of the temporal variation of water quality, to determination of the state of the water and its equilibrium with respect to the aquifer constituent minerals, calculation of the degree of freshwater–seawater mixing as a consequence of marine intrusion, determination of the origin of the water's chemical composition and the geochemical processes which explain this composition, evaluation of water quality and design of water monitoring and automatic control systems. The results of these investigations have been published in different papers, and presented at scientific congresses as part of some Master and Doctoral theses.

REFERENCES

Alvarez, E., Vinardell, I., Fagundo, J. R., Reguera, E. & Cardoso, M. E. (1990) Control de la calidad de las aguas mediante un sistema automatizado. *Estudios Geológicos* (Madrid) **46**(5–6), 409–414.

Alvarez, E. & Facundo, J. R. (1991) SAPHIQ, un sistema para el procesamiento automatizado de datos hidroquímicos. *Revista CENIC Ciencias Químicas* **22**(1), 59–65.

Alvarez, E., Vinardell, I., Fagundo, J. R. & Rodríguez, J. E. (1993) Sistemas para el procesamiento de datos hidroquímicos: SAPHIQ, GEOQUIM, SAMA y BATOMET. *Libro de Comunicaciones*, 189–194. *Ed. Univ. Jaume I*, Castellón, Spain.

Alvarez, E., Fagundo, J. R., González, P., Ferrera, V. & Benítez, G. (1996) Aplicación de métodos de simulación química y matemática al estudio de la disolución de carbonatos en diferentes condiciones experimentales. In: *Contribuciones a la hidrogeología y medio ambiente en Cuba* (ed. by J. R. Fagundo Castillo, D. Pérez Franco, A. Alvarez Nodarse, J. M. García & I. Morell), 91–103. Universidad de Castellón, Spain.

Fagundo, J. R. & Arellano, D. M. (1991) Hydrogeochemical impacts of coastal karstified aquifer overdrawals. *Studia Carsologica* (Brno) **5**, 37–47.

Fagundo J. R. & Rodríguez, J. E. (1992) Hydrogeochemical pattern and mathematical correlations in karst at the examples of Cuba. *Quaderni del Dipartimento di Geografia* **13**, 361–369.

Fagundo, J. R., Rodríguez, J., Benítez, G., Morera, W., Fernández, C. & Vega, J. (1993) Caracterización Hidroquímica y control de la calidad de las aguas del carso de la cuenca Zapata. *Libro de Comunicaciones*, 73–81. Ed. Univ. Jaume I, Castellón, Spain.

Fagundo, J. R., Rodríguez, J. E., de la Torre, J., Arencibia, J. A. & Forti, P. (1994) Hydrologic and hydrochemical characterization of the Punta Alegre Gypsum Karst Massif, Cuba. *Newsletter of Geology, Climate and Karst Formation, Guilin* (China), 95–106.

Fagundo J. R., Ferrera, V., Alvarez, E., Vinardell, I., Torres, A. & Alvarez, J. (1995) Control automatizado de la calidad de las aguas mediante patrones hidrogeoquímicos y mediciones de conductividad eléctrica en el ejemplo de la cuenca del Cauto. In: *Proc. del II Congreso AIDIS de Norteamérica y el Caribe y IV Congreso de la Asociación de Ingeniería Sanitaria y Ambiental* (Santiago de Cuba 1995), vol. I, 106–114.

Fagundo, J. R & Gonzalez, P. (1999) Agricultural use and water quality at karstic west Cuban Southern Plain. In: *Karst and Agriculture in the World*. *Int. J. Speleology* (ISSN 0392-6672) **28**B(1/4), 175–185.

Fagundo, J. R., González, P., Jiménez, S., Suárez, M., Fagundo-Sierra, J., González, A., Romero, E. & Orihuela, D. (2002) Procesos geoquímicos naturales e inducidos por el hombre en acuíferos kársticos costeros. Caso de estudio: Sector hidrogeologico Güira Quivicán (Cuenca Sur de La Habana). *Revista Latinoamericana de Hidrogeología* **2**, 71–79.

Fagundo J. R., González, P., Alvarez, E., Tillán, G., Vinardell, I., Fagundo-Sierra, J., Suárez, M. & Melián, C. (2004) Sistema informático para la caracterización y monitoreo de la calidad de las aguas superficiales y subterráneas. *Memorias de EXPOAGUA*. Ed. INRH, CIH, Cuba.

Fagundo J. R., González, P., Suárez Muñoz, M., Fagundo-Sierra, J., Melián, C. & E. Alvarez (2005) HIDROGEOQUIM. *Contribución a la Educación y Protección Ambiental* ISCTN, vol. 6 (XI Taller), 58–67. ISBN 959-7136-35-X.

Fagundo-Sierra, J. Fagundo, J. R. González, P.& Suárez, M. (2001) Modelación de las aguas naturales. En: *Contribución a la Educación y la Protección Ambiental*. ISCTN. vol. 2 (VII Taller), 8 pp. ISBN 959-7136-09-0.

Fagundo-Sierra, J. R., Fagundo, J., González, P., Suárez, M. & Melián,. C. (2002) Sistema de base de datos de aguas minerales y mineromedicinales: TERMADAT. En: *Contribución a la Educación y la Protección Ambiental*. ISCTN, vol. 3 (VIII Taller), 6 pp. ISBN 959-7136-13-9

Ferrera, V., Fagundo, J. R, González, P., Morrell, I., Pulido-Boch, A., López-Chicano, M. & López-Vera, F. (1999). Caracterización Hidrogeoquímica de los acuíferos kársticos de la Cuenca y Zapata, Matanzas, Cuba. *Voluntad Hidráulica*, **91**, 21–27.

Gimeno, M. J. & Peña, J. (1994) Basics principles of direct and inverse geochemical models. *Geological Study* **50**(1/5), 359–367.

Plummer L. N., Prestemon E. C. & Parkhurst D. L. (1991) An interactive code (NETPATH) for modeling net geochemical reaction along a flow path. *US Geological Survey Water-Resources Investigations Report 94-4169.*

Tillán, G., Vinardell, I., Fagundo, J. R., Ferrera, V., González, P. & Sánchez,. L. (1996) SACAN: Sistema Automatizado para la Caracterización de Aguas Minerales. En: *Contribuciones a la hidrogeología y medio ambiente en Cuba* (ed. by J. R. Fagundo Castillo, D. Pérez Franco, A. Alvarez Nodarse, J. M. García & I. Morell), 113–121. Universidad de Castellón, Spain.

Vinardell I., Alvarez, E. & Fagundo, J. R. (1995) Sistema automatizado para el control de las aguas cársicas afectadas por la intrusión marina mediante reconocimiento de patrones, BATOMET. En: *El Karst y los acuíferos Kársticos, ejemplos y métodos de estudio*. Ed. by J. Fagundo, A. Pulido Bosch, J. Rodríguez & I. Morell), 251–256. ISBN 84-605-1917-1 Publicado por la Facultad de Ciencias. Univ. Granada.

Climate Variability and Change—Hydrological Impacts (Proceedings of the Fifth FRIEND World Conference held at Havana, Cuba, November 2006), IAHS Publ. 308, 2006.

Studying waste load dispersion in Songkhla Lake using a simulation model

WINAI SAE-CHEW
Civil Engineering Department, Faculty of Engineering, Prince of Songkhla University, Hatyai, Songkhla 90112, Thailand
winai.c@psu.ac.th

Abstract Songkhla Lake is a large lagoon-like estuarine lake in southern Thailand which has been increasingly polluted in recent years by industrial and urban wastewater draining into the lake through various canals. This study was undertaken to construct a model of the dispersion of the pollution in the lake around the mouths of these canals in order to aid in the planning of effective pollution abatement measures. Results show pollutants dispersing up to 2 km in the sea during high tide, while at low tide, pollutants stay longer in the lake before being discharged into the Gulf of Thailand.

Key words waste load dispersion; Songkhla Lake Thailand; simulation model

INTRODUCTION

Songkhla Lake Basin is a significant natural resource in Thailand (Fig. 1). During the last several decades of population increase, which has required more land for farming and urban-industrial development, there has been a significant decline in the amount and quality of natural water resources in this area – as, indeed, across the entire country. In Songkhla Lake, this has led to shallowing of the lake due to the higher annual sediment loads; increased intrusion of saline water to the inner, normally mostly freshwater, part of the lake; a shortage of freshwater in the dry season (March–May) in some areas; and a reduction of some species of aquatic life. These problems must be addressed if Thailand is not to permanently lose this valuable natural water resource.

OBJECTIVES OF THE STUDY

To properly design mitigation measures for Songkhla Lake, it is necessary to understand the pollution impacts and their extent. This study was designed to construct a dispersion model to understand how the pollution in the wastewater in Songkhla Lake circulates, where it is dispersed to and how long it is retained in the lake, which will then lead to realistic ideas about how to solve the pollution of the lake.

MATERIALS AND METHODS

Data were mainly obtained from sites nearby the U-Tapao Canal, which has a major influence on the lower Songkhla Lake as it drains from Hat Yai city, the largest city in southern Thailand (Fig. 1, Table 1). Physical characteristics of the lake such as the tidal movement, wave movement, wind speed and inflow discharge from the surrounding land were studied along with major waste load parameters such as the Biochemical Oxygen Demand (BOD), Dissolved Oxygen (DO), salinity, coliform bacteria and suspended sediment, all required to construct an accurate simulation of the concentration of the waste load in the lake.

PHYSICAL DESCRIPTION OF THE STUDY AREA

Songkhla Lake basin

Songkhla Lake basin is situated on the east coast of southern Thailand. It has a total area of 9807 km^2, of which 1046.04 km^2 is water and 8761 km^2 land (Fig. 1) (Sae-chew *et al.*, 1995). The climate is equatorial monsoon with a humid, hot rainy season. The mean temperature is 26.9ºC, the annual average precipitation 1800 mm and average evaporation 139 mm. The lake is surrounded by coastal plain, becoming rolling hills and finally mountains to the west and south. The plain and

Copyright © 2006 IAHS Press

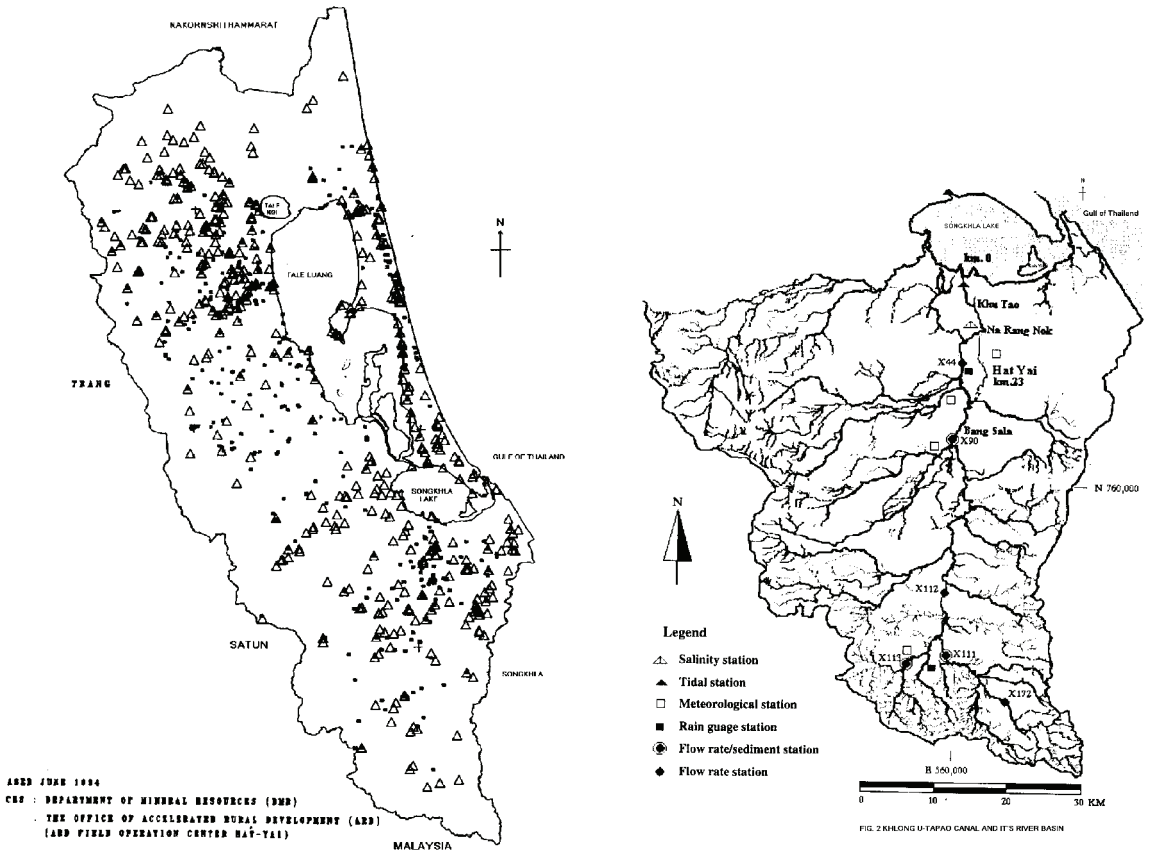


Fig. 1 Songkhla Lake and the river basin.

Table 1 Sediment station and mean annual sediment load.

River and station	Location	Drainage area (km^2)	Mean annual suspended sediments (tons) (year of record)
Khlong U-Tapao, Ban Bangsala	Hatyai, X90	1562	5458 (1978–1985)
Khlong Sadao, Ban Phrai	Sadao, X11	256	7218 (1979–1985)
Khlong Lam, Ban Thungprap	Sadao, X113	129	5689 (1979–1985)
Khlong Wat, Tonngachang	Hatyai ,NEA	14	2158 (1980–1984)

coastal areas are primarily used for agriculture and habitation, and the lake and surrounding ocean have always been a bountiful fishery.

The major canals draining into Songkhla Lake

U-Tapao Canal The U-Tapao Canal has a catchment area of 2305 km^2. The soil of the catchment is generally sandy and most of the area is covered with rubber plantations. The topography varies from a mild mountainous plateau on the west to the flat fluvial coastal landscape bordering Songkhla Lake on the east. The U-Tapao River basin gives a water yield to the catchment of 791.94×10^6 m^3 (1967–1986) and the U-Tapao canal has a discharge of 7.80 m^3 s^{-1} in the dry season (March–May) and 88.60 m^3 s^{-1} in the wet season (September–November). The width of the water surface varies 40–80 m and the depth of the canal 3.0–8.0 m. The distance from the upper regions to the mouth of the canal is about 70 km, with varying channel slopes.

Khlong Pavong There is a considerable fishery industry in this area, but most people are poor, with the overall result that a lot of municipal and industrial wastewater is released into the lake with insufficient water treatment via this canal which enters to the south of Koh Yo Island.

Khlong Sam Rong Around 6000 people live along this canal (Brans *et al.*, 1995) and contribute a significant amount of polluted water to the lake, which is also thought to have contributed to the demise of fish farming in the area neighbouring the lake in 1989 (R&D, 1989).

The process of waste load dispersion in Songkhla lake

The waste load dispersion process depends on the influences of tidal fluctuation, wind speed and direction, the density of the suspended load, the temperature difference of the water, turbulence of the flow, etc. Some additional parameters such as streamflow and flocculation were also considered in this study.

EQUATIONS OF THE MATHEMATICAL MODEL

A two-dimensional hydrodynamics simulation model (Swanson, 1986) was constructed by considering the equations of shallow water waves and the approximation method of Boussinesq. Curvilinear coordinate applications were adapted into the continuity and momentum equations. The conceptual calculation by the numerical solution method was applied by using a staggered grid (Lax-Wendroff explicit finite difference scheme), semi-different approximation and convective-diffusion of mass.

Continuity equation

$$\frac{\partial \zeta}{\partial \tau}+\frac{1}{r\cos\theta\partial\phi}\frac{\partial UH}{\partial \phi}+\frac{1}{r}\frac{\partial VH}{\partial \theta}-\frac{VH\tan\theta}{r}=0$$

Momentum equation of ϕ

$$\frac{\partial UH}{\partial \tau}+\frac{1}{r\cos\theta\partial\phi}\frac{\partial UUH}{\partial \phi}+\frac{1}{r}\frac{\partial UVH}{\partial \theta}-\frac{UVH\tan\theta}{r}=-\frac{1}{\rho_o r\cos\theta}\varphi\phi+\frac{\tau_b\phi}{\rho_o}$$

$$\varphi_\phi=\int_{-h}^{\zeta}\frac{\partial pdr}{\partial\phi}=\rho_o gH\frac{\partial(h+\zeta)}{\partial\phi}+\frac{gH^2}{2}\frac{\partial\rho'}{\partial\phi}$$

$$\tau_{b\phi}=\rho c_f U\ (U^2+V^2)$$

Momentum equation of θ

$$\frac{\partial VH}{\partial \tau}+\frac{1}{r\cos\theta\partial\phi}\frac{\partial UVH}{\partial \phi}+\frac{1}{r}\frac{\partial VVH}{\partial \theta}+\frac{U^2-V^2}{r}H\tan\theta=-\frac{1}{\rho_o r}\varphi\theta+\frac{\tau_b\theta}{\rho_o}$$

$$\varphi_\theta=\int_{-h}^{\zeta}\frac{\partial pdr}{\partial\theta}=\rho_o gH\frac{\partial(-h+\zeta)}{\partial\theta}+\frac{gH^2}{2}\frac{\partial\rho'}{\partial\theta}$$

$$\tau_b\theta=\rho c_f\, v\ \ (U^2+V^2)$$

with U, V = depth-averaged velocities in ϕ- and θ- directions, respectively; ζ = water surface elevation; $\tau_{b\phi}$, $\tau_{b\theta}$ = bottom shear stress in ϕ- and θ- directions, respectively; H = depth (mean sea level, m.s.l.); and C_f = bottom friction coefficient.

2-D vertically averaged model of waste load

$$\frac{\partial c}{\partial t}+\frac{1}{r}\frac{U\partial c}{\partial\theta}+\frac{1}{r}\frac{V\partial c}{\partial\phi}=\frac{D_H}{r^2\cos^2\theta}(c_{\theta\theta}-c_{\theta\phi}+c_{\phi\phi})-D_H\tan\theta\frac{\partial c}{\partial\theta}\quad+s$$

$$S=-K_1 c$$

with c = concentration of mass; D_H = diffusion coefficient in ϕ- and θ- directions; S = source term; K_1 = decay rate = 0.3–04 day^{-1}

RUNNING THE HYDRODYNAMIC MODEL

With a Songkhla Lake grid area designated for the model, a suitable grid width (500–1000 m) and grid number (18 × 20) with a time step of six hours for an explicit finite difference scheme were selected. The actual mean depth of the lake in selected areas was input (maximum mean depth is about 9 m at the outflow of the lake into the Gulf of Thailand and at the middle of the lake about



Fig. 2 Water depth contours in Songkhla Lake.

1.5 m; Fig. 2), followed by the tidal fluctuation. The initial condition of the current velocity in the lake was assumed to be zero. The dry season discharges of the canals around the lake were input. The model was run in one-hour increments for 16 days to simulate flows to be compared with measured field data. The coefficient of roughness was adjusted to achieve the best fit, by iteration of the whole calibration process, until a suitable level of agreement was achieved.

RUNNING THE WASTE LOAD TRANSPORT MODEL

The waste load transport model was tested in association with the calibrated hydrodynamic model to simulate the waste load dispersion pattern. First the fluctuation data (i.e. tide level) was entered, and the initial condition of the current in the lake was set as stationary with a velocity of zero. The initial lake water concentration conditions were also set to be zero in order to consider only the concentration from the canal itself. One by one the concentration of the wastewater discharges from each canal that flows into the lake was entered in order to visualize the individual impact from each flow. Using a time step of one hour the model was tested for a 16-day period to observe for critical events.

RESULTS OF THE MODEL TESTS

The model shows that the concentration of the waste dispersion varies in accordance with the current of the flow in the lake. The field data collected during the dry season (Fig. 3) showed that the salinity varied between 25 and 31 part per thousand (ppt) at Koh Yo Island, lessening to 12–29 ppt at the junction of the lake and the Gulf of Thailand. A salinity layer separation appeared at a level of more than 3 m depth, causing partial mixture of the water. The water temperature averaged 28ºC. The temperature difference between the surface and the bottom of the lake was approximately 1ºC. The concentration of the suspended load was between 6 and 25 mg L^{-1}. The bed load sediment varied from mud in most areas to sandy deposits nearer the outlets of the lake. The BOD5 (untreated) was 2–7 mg L^{-1}. Coliform bacteria counts were between 2 and 31 Most Probable Number (MPN)/100 ml in the lake, but increased in the canals to over 2400 MPN/100 ml. The tidal difference was about 40 cm with a phase difference of 3.5 hours. Maximum tidal current was about 0.67 m s^{-1} in the north, reducing to 0.43 m s^{-1} in the southern part of the lake close to the junction with the U-Tapao canal. The roughness coefficient of the lake was about 0.0015 and the current velocity simulation was accurate within a maximum velocity of 0.77 m s^{-1} and minimum velocity of 0.08 m s^{-1}. The collision of water masses in the lake due to phase and elevation differences induced complicated vortexes at the middle and the east side of the lake, but in the west part of the lake the currents were much smoother. The waste load released from the Khlong U-Tapao canal tended to disperse radially up to 2 km from the mouth of the canal, where there was still a concentration of 10 mg L^{-1} (Fig. 4). The model showed that if there is a consecutive and continuous release of wastewater for more than 2–3 days the east side of the lake will be the first

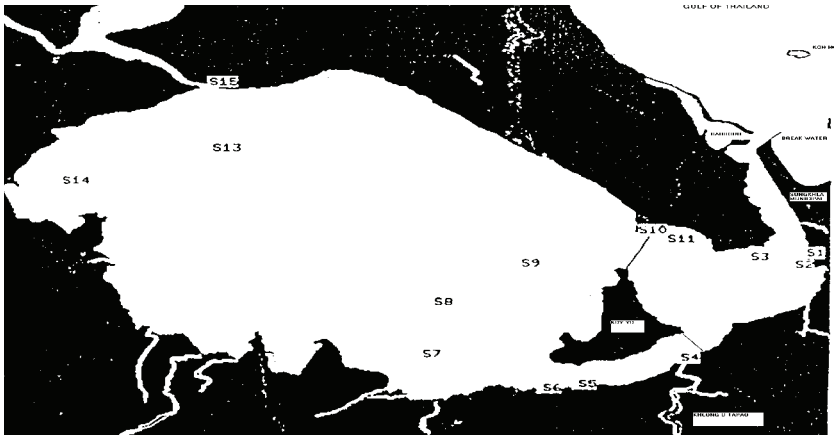


Fig. 3 Location of data collection points.

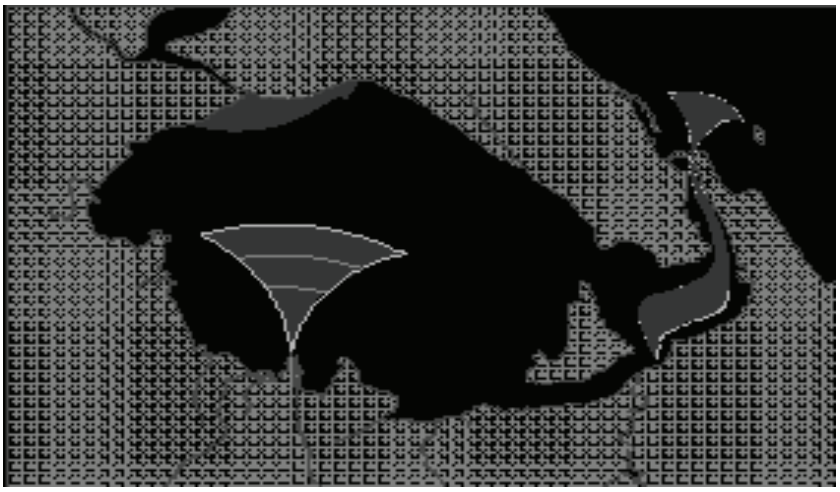


Fig. 4 Pattern of dispersed waste load in Songkhla Lake from U-Tapao Canal (lake is in black, land in grey and waste dispersion pattern in lighter grey).

place to be impacted seriously with a concentration of up to 50 mg L^{-1}, though minimal impact on the settled areas and fish farming areas of Koh Yo Island. However this area was seriously impacted from the waste dispersion of the Pavong Canal, which reaches out as far as 3 km from the mouth of the canal. The waste from Sam Rong Canal dispersed at the northern part of Koh Yo Island rapidly (Fig. 4), but still tended to accumulate within the lake as there was not enough time for it to be carried out to sea when there was a low tide.

CONCLUSION

The computer simulation model that was constructed to examine the dispersal of pollutants from the canals flowing in to Songkhla Lake accurately shows the dispersion patterns, and with it we can, in the future, predict the effect of decreased or increased pollutant loads from these sources, thus assisting in the development of suitable environmental regulations to reduce the pollution to acceptable levels in order to maintain the integrity of this valuable resource for Thailand.

REFERENCES

Brans, R. P. & Ruyg, B. S. (1995) *Improvement of the Klong Sam Rong*. TU Division of Hydraulics, Faculty of Civil Engineering, TU Delft, The Netherlands.

Research and Development (1989) Environmental Impact Assessment of Songkhala Lake Basin. Final report, Prince of Songkhala University, Thailand.

Sae-chew, Winai & Pornpinatepong, Somboon. (1995) Feasibility study of sedimentation in Khlong U-Tapao canal by a simulation model (presented at Int. Symp. on Floods and Droughts, Nanjing, China, October 1999; available from this author).

Swanson, J. C. (1986) A three-dimensional numerical model system of coastal circulation and water quality. PhD Dissertation, Department of Ocean Engineering, Univ. of Rhode Island, USA.

Climate Variability and Change—Hydrological Impacts (Proceedings of the Fifth FRIEND World Conference held at Havana, Cuba, November 2006), IAHS Publ. 308, 2006.

Risques d'eutrophisation et de comblement des retenues d'eau au Burkina Faso

AMADOU HAMA MAIGA, YACOUBA KONATE, KOKOU DENYIGBA, HAROUNA KARAMBIRI & JOSEPH WETHE

Groupe EIER-ETSHER, Ecole Inter-Etats d'Ingénieurs de l'Equipement Rural (EIER), BP 7023, Ouagadougou, Burkina Faso

amadou.hama.maiga@eieretsher.org

Résumé Le Groupe EIER-ETSHER a entrepris d'évaluer les risques d'eutrophisation et de comblement des plans d'eau en menant une étude sur une dizaine de retenues d'eau choisies dans les trois principales zones climatiques du Burkina Faso à savoir: la zone soudanienne de savane, caractérisée par une végétation boisée; la zone soudano sahélienne de savane à graminées; et la zone sahélienne de steppe arbustive. Sur la base de mesures d'indicateurs de niveau d'eutrophie et de mesures bathymétriques, les résultats de l'étude révèlent que: (a) le comblement par transport de solides représente la menace prépondérante pour les plans d'eau en zone sahélienne; ce risque est plutôt faible en zones soudanienne et soudano sahélienne; et (b) le risque d'eutrophisation de grande envergure s'avère faible pour les plans d'eau en zone soudanienne et soudano sahélienne. Ce risque semble inexistant en zone sahélienne à cause des suspensions solides dans l'eau qui réduisent la pénétration de la lumière solaire et, par conséquent, limitent le développement d'activité photosynthétique.

Mots clefs eutrophisation; comblement; transport solides; barrages; petites retenues d'eau; Burkina Faso

Risk of eutrophication and filling-up of small reservoirs in Burkina Faso

Abstract In order to evaluate the risks of eutrophication and re-filling of small reservoirs, a monitoring study was undertaken on ten water reserves chosen in the three main climatic zones of Burkina Faso: the soudanian zone, characterized by a vegetation of wooded savannah; the soudano-sahelian zone, characterized by mixed vegetation from savannah to graminaceous annual shrubs; and the sahelian zone, characterized by an open-field vegetation of thorny shrubby steppe. The level of eutrophication was measured on the basis of a series of referenced indicators and the re-filling level was evaluated by bathymetric measurements. The provisional results show that: (a) re-filling by transport of solids represents the dominant threat for the surface water reserves in the sahelian zone; this risk is rather weak with regard to water reserves in the soudanian and soudano-sahelian zones; and (b) the risk of large-scale eutrophication seems weak for the water reserves in the soudanian and the soudano-sahelian zones in Burkina Faso, and it is rather non-existent in the sahelian zone, where solid suspensions in water reduce light penetrations and, consequently, limit photosynthesis and algal development.

Key words eutrophication; re-filling; solids transport; dams; small reserves of water; Burkina Faso

INTRODUCTION

Dans la plupart des pays d'Afrique subsaharien et particulièrement au Burkina Faso, la pression démographique a entraîné une forte augmentation des surfaces cultivées au détriment du couvert végétal. La dégradation des sols résultant de l'intensification des activités anthropiques sur les bassins versants des retenues d'eau a pour effet d'accélérer dans certaines régions du Burkina Faso leur comblement progressif par érosion et sédimentation, réduisant ainsi la capacité de stockage et les activités socio-économiques qui se sont développées autour des plans d'eau. L'ampleur de ces phénomènes dépend de l'état de surface et de la nature du couvert végétal (Leprun, 1999).

Au Burkina Faso, on estime qu'entre les années 1950 et 1990, 40% du couvert boisé naturel a été détruit (Parkan 1986). Selon Marchal (1983) les pertes en terre par érosion peuvent atteindre 1.86 t ha^{-1} an^{-1} en zone sahélienne sous couvert herbacé et arbustif dégradé, et 3 t ha^{-1} an^{-1} sur des glacis avec des sols argileux cultivés. Yacouba *et al*. (2002) rapportent des pertes en terre moyenne de 5.35 t ha^{-1} an^{-1} sur les glacis dénudés de la zone soudano-sahélienne et sahélienne du Burkina Faso. Les travaux de Lhote (2000) et ceux de Maiga & Denyigba (2002), ont déjà permis d'esquisser sur une échelle spatiale globale, les risques éventuels d'eutrophisation et de comblement selon les grandes zones climatiques, de la Côte d'Ivoire vers le Burkina Faso. La présente étude tente d'évaluer l'importance de la dégradation et du comblement des retenues d'eau par eutrophisation ou transport de solides et les risques liés à ces phénomènes selon les zones climatiques du Burkina Faso.

Copyright © 2006 IAHS Press

PRESENTATION DE LA ZONE D'ETUDE

L'étude est menée sur un échantillon de 10 retenues d'eau choisies pour obtenir une bonne représentativité des zones climatiques du pays. (Tableau 1 et Fig. 1), à savoir:

– la zone soudanienne au sud-ouest du pays avec une pluviométrie moyenne annuelle comprise entre 900 et 1200 mm concentrée sur environ 6 mois de l'année (mai–octobre) et une végétation constituée majoritairement de savane boisée ;
– la zone soudano-sahélienne au centre du pays avec une pluviométrie moyenne annuelle est comprise entre 600 et 900 mm sur une période de 4–5 mois par an, avec une végétation de savane à graminées arbustives et arborées et des sols sous fortes pressions d'activités agricoles et pastorales;
– la zone sahélienne dans le nord du pays, la plus aride avec une pluviométrie annuelle moyenne de 600 mm, s'étalant sur 3 mois environ et caractérisée par des averses brèves et de fortes intensités. Les ruissellements qui en découlent constituent un facteur important d'érosion des sols abritant une végétation de type steppe arbustive épineuse clairsemée.

Tableau 1 Les 10 retenues d'eau étudiées au Burkina Faso.

Retenues	Longitude	Latitude	Année de construction	Capacité (10^6 m^3)	Superficie bassin (km^2)	Domaine climatique
Douna	05°05′45″O	10°40′48″N	1987	37.5	680	Soudanien
Toussiana	04°37′11″O	10°52′06″N	1982	6.1	130	
Moussodougou	04°56′50″O	10°46′47″N	1991	38	560	
Kanazoé	02°04′50″O	13°01′05″N	1994	75	–	Soudano-Sahélien
Yitenga	00°23′00″O	12°11′26″N	1987	3.35	100	
Dakiri	00°16′35″O	13°18′03″N	1960	10.5	2300	
Titao	02°03′50″O	13°46′31″N	1951	3.7	400	Sahélien
Thiou	02°39′29″O	13°49′13″N	1981	4.3	328	
Djibo	01°36′57″O	14°06′53″N	1970	2.2	610	
Yalgo	00°16′46″O	13°34′46″N	1954	10	8175	



Fig. 1 Carte du Burkina Faso: localisation des retenues d'eau étudiées.

MATERIEL ET METHODE

L'étude est faite sur la base des indicateurs et de la méthode de classement des lacs selon l'OCDE (1982). Il s'agit notamment de la chlorophylle *a*, l'oxygène dissous, la transparence, la concentration en azote et en phosphore.

La transparence a été mesurée au disque de Secchi. Nous avons associés à cet indicateur la mesure de la turbidité réalisée à l'aide d'un spectrophotomètre d'absorption moléculaire de type DR 2000 sur l'échelle de Formazine, et celle des matières en suspension (MES).

L'oxygène dissous, la température, le pH et la conductivité électrique ont été mesurés *in situ* à l'aide d'un multimètre (Multiline P4) muni de sonde spécifique pour chaque paramètre.

La chlorophylle *a* a été mesurée en laboratoire par spectrométrie d'absorption moléculaire après filtration et extraction à l'acétone 90%. Après centrifugation, la densité optique de l'extrait d'acétone a été mesurée aux longueurs d'onde de 665 nm et 750 nm, selon la méthode de Lorenzen.

Le phosphore et l'azote ont été mesurés à l'aide d'un spectrophotomètre d'absorption moléculaire de type DR2000.

Le niveau de comblement des retenues d'eau a été évalué pour les retenues d'eau pour lesquelles les profondeurs initiales sont connues, par calcul différentiel des tirants d'eau entre la mise en eau et la période de la campagne d'échantillonnage et pour les autres, à partir du jaugeage de l'épaisseur de la densité des boues au moyen d'une barre rigide.

RESULTATS ET DISCUSSION

Le comblement des plans d'eau

Le comblement d'un plan d'eau peut être dû à des processus endogènes (la production primaire à l'intérieur de la retenue) et exogènes (les apports du bassin versant). Les mesures de tirants d'eau révèlent une tendance au comblement croissant des retenues d'eau du sud vers le nord, c'est-à-dire de la zone soudanienne vers la zone sahélienne. L'ampleur du phénomène n'a pu être encore quantifiée en raison de l'insuffisance des données disponibles sur les tirants d'eau à la mise en eau de certains barrages. Il apparaît tout de même une corrélation assez forte entre le niveau de comblement et la vulnérabilité des sols à l'érosion, elle même corrélée avec la zone climatique.

A titre indicatif, la capacité de la retenue d'eau de Yitenga (en zone soudano sahélienne) est passée de 3.1×10^6 m^3 à la mise en eau en 1987 à 2×10^6 m^3 en 2001, soit un rythme de comblement de 2.5% par an. Des études antérieures menées au Burkina suggèrent un niveau d'envasement des barrages, rapporté à la superficie du bassin versant variant annuellement de 4–8.4 t ha^{-1} dans les zones soudano sahélienne et sahélienne. Les matières en suspension représentent la forme dominante (plus de 90%) des produits de comblement (Karambiri & Ribolzi, 2003). En zone soudanienne, la végétation sur des sols peu favorables à l'érosion, s'avère être un facteur déterminant dans la limitation des apports de matériaux terreux vers les plans d'eau.

Turbidité, transparence et matières en suspension

Les valeurs obtenues pour la transparence sont inférieures à 1.5 m pour toutes les retenues d'eau (Tableau 2 et Fig. 2). Sur la base de ce paramètre, toutes les 10 retenues d'eau seront classées dans la catégorie des lacs eutrophes selon OCDE (1982).

Les résultats des mesures suggèrent un lien de causalité assez fort entre la transparence, la turbidité et les matières en suspension. La tendance est à la diminution de la transparence de la zone soudanienne vers la zone sahélienne, et conséquemment, une augmentation de la turbidité des eaux (Fig. 3), et plus modestement une augmentation des MES dans le même ordre (Fig. 4).

De même, la mesure de la conductivité suggère une minéralisation relativement faible en zone soudanienne et de plus en plus élevée à mesure que l'on va vers le sahélien (Fig. 5).

Si les faibles valeurs de transparence observées en zone soudanienne sont probablement dues aux micro algues (représentant la fraction organique des matières en suspension), les valeurs élevées de la turbidité mesurées en zones soudano sahélienne et sahélienne prouvent que ce sont plutôt les fines particules colloïdales (matière minérale) qui sont responsables des faibles valeurs de transparence. Ces valeurs ne traduisent donc pas une eutrophie des retenues d'eau puisque

Tableau 2 Transparence, turbidité et matières en suspension mesurées dans les 10 retenues d'eau en mars 2004.

Retenues d'eau	Douna	Toussiana	Moussodougou	Kanazoé	Yitenga	Dakiri	Titao	Thiou	Djibo	Yalgo
Transparence (m)	0.75	0.75	0.75	0.55	0.15	0.25	0.3	0.1	0.2	0.12
Turbidité (FTU):										
Surface	8	13	5	17.3	98	62	40	212	67	143
Fond		10		17	96	53	30			169
Conductivité ($\mu s\ cm^{-1}$)	28	19	40	82	201	95.5	105.5	80	109	123
MES ($mg\ L^{-1}$):										
Surface	7	6	60	10	33.5	12	10	70	40	33.5
Fond		10		10	29.5	20	10			34.5

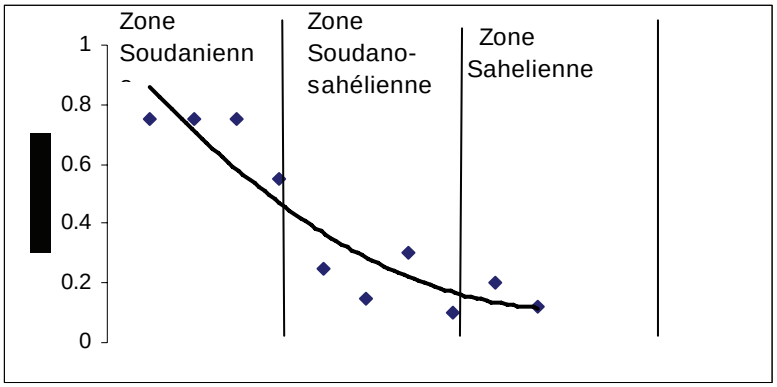


Fig. 2 Tendance évolutive de la transparence en fonction des zones climatiques.

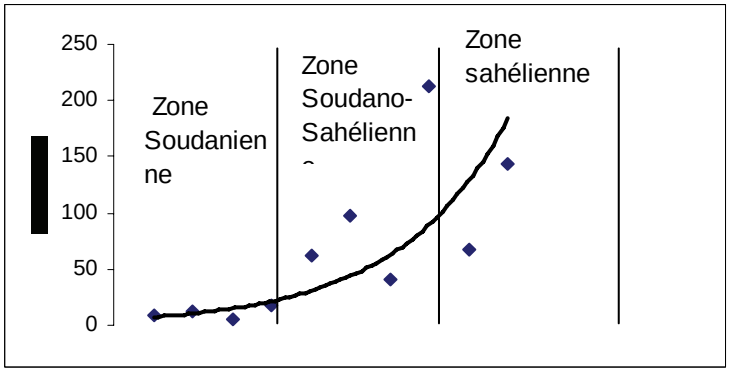


Fig. 3 Tendance évolutive de la turbidité en fonction des zones climatiques.

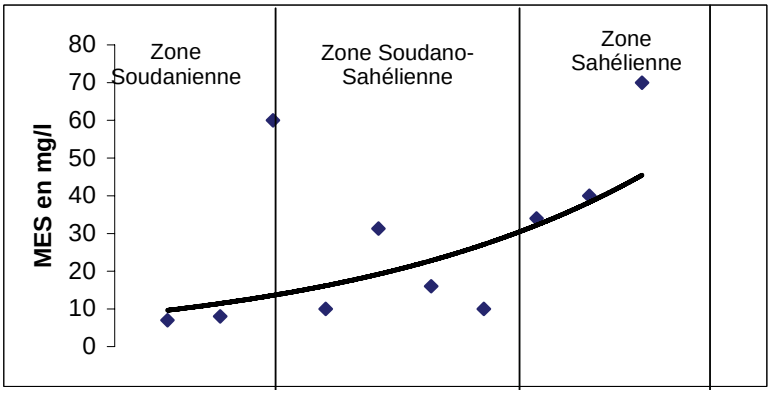


Fig. 4 Tendance évolutive des MES en fonction des zones climatiques.

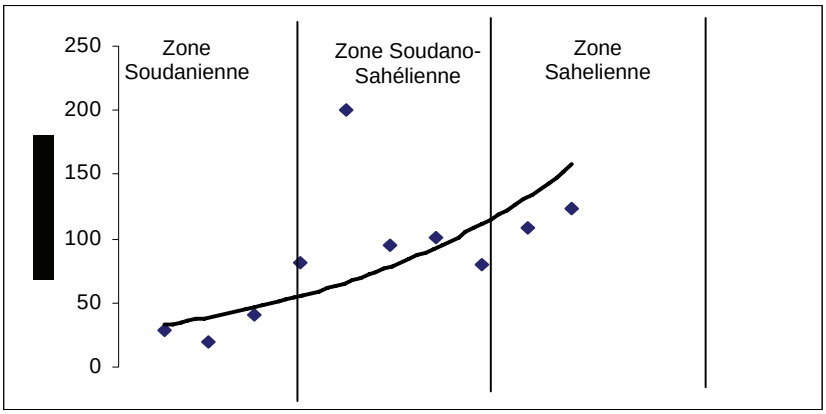


Fig. 5 Tendance évolutive de la conductivité en fonction des zones climatiques.

aucun signe d'eutrophisation par prolifération algale ni de macrophytes n'est perceptible. Du reste, les autres paramètres d'évaluation ne confirment pas une situation d'eutrophie de ces plans d'eau.

Ces résultats nous conduisent à déclarer que la transparence n'est pas vraiment un indicateur pertinent pour caractériser le niveau d'eutrophie des plans d'eau dans les zones où le transport de solides est prépondérant.

La Chlorophylle *a*

La mesure de la chlorophylle *a* a pour but d'évaluer l'activité de la photosynthèse dans les plans d'eau. Dans les retenues d'eau de la zone soudanienne, la production primaire est peu perceptible. Dans le cas particulier de la retenue d'eau de Moussodougou, on a observé un faible développement des micros algues sur les berges comme (les *Ceratophyllum* sp, *Oryza* sp, *Azolla* sp). L'analyse de chlorophylle *a* faite dans des études antérieures révèle des valeurs relativement faibles de l'ordre de 73 μg L^{-1} à Toussiana (zone soudanienne), et très faible (0.01 μg L^{-1}) à Yalgo en zone sahélienne (Maiga & Denyigba, 2001). L'absence quasi-totale d'activité photosynthétique dans les retenues d'eau en zone sahélienne est donc due en partie à la charge trop élevée en particules en suspension qui réduit la pénétration de la lumière. En effet, selon plusieurs auteurs, même lorsque des facteurs limitant de la productivité primaire (azote, phosphore) sont satisfaits, la production primaire reste limitée lorsque l'intensité lumineuse est faible (Lhote, 2000).

L'oxygène dissous

Les 10 retenues d'eau sont en sursaturation d'oxygène avec des concentrations supérieures à 8 mg L^{-1} (Tableau 3). Les mesures effectuées en profils verticaux n'ont pas révélé de stratification significative. Les retenues d'eau étant de faibles profondeurs (entre 0,73 m pour la retenue d'eau de Djibo et 5.6 m pour la retenue d'eau de Douna), leur brassage par effet de vent a pu homogénéiser leur milieu et empêcher leur stratification. En se référant à l'échelle de classification de l'OCDE (1982), qui qualifie d'eutrophe un plan d'eau ayant moins de 5 mg L^{-1} d'oxygène dissous, elles seront classées toutes dans la catégorie des plans d'eau oligotrophes.

Tableau 3 Oxygène dissous mesuré dans les 10 retenues d'eau en mars 2004.

O_2 dissous	Douna	Toussiana	Mousso-dougou	Kanazoé	Yitenga	Dakiri	Titao	Thiou	Djibo	Yalgo
Surface (mg L^{-1})	11.3	10.5	11.3	10.3	7.75	8.29	13	11.3	9.4	10.6
Fond (mg L^{-1})	11	11	11	10.3	7.54	8.4	12			10.39

Phosphore et azote

Le phosphore mesuré ($P\text{-}PO_4^{3-}$) est relativement faible et ne présente pas de grandes disparités entre les retenues d'eau, ni une tendance particulière par rapport à une zone climatique (Tableau 4). Les teneurs ne paraissent pas être de nature à limiter le développement algal et

Tableau 4 Phosphore et azote mesurés dans les 10 retenues d'eau en mars 2004.

Indicateurs	Douna	Toussiana	Mousso-dougou	Kanazoé	Yitenga	Dakiri	Titao	Thiou	Djibo	Yalgo
$P\text{-}PO_4^{3-}$ (mg L^{-1}):										
Surface	0.05	0.01	0.18	0.29	0.29	0.16	0.11	0.2	0.3	0.16
Fond	NM	0.04	NM	0.34	0.18	0.16	0.12	NM	NM	0.22
$N\text{-}NO_3^-$ (mg L^{-1}):										
Surface	0	0	2.2	2.2	0.44	0	1.22	NM	2.2	1.32
Fond	NM	0	NM	1.32	0.44	0	1.46	NM	NM	0.88
$N\text{-}NH_4^+$ (mg L^{-1}):										
Surface	0.06	0.01	0.13	0.41	0.23	0.27	0.7	0.19	1.35	0.11
Fond	NM	0.04	NM	0.38	0.24	0.21	0.9	NM	NM	0.28

NM = non mesuré.

végétatif, car il suffit de quelques μg L^{-1} de phosphore pour assurer une intense activité photosynthétique.

Les teneurs en azote ($N\text{-}NH_4^+$ et $N\text{-}NO_3^-$) ne sont pas particulièrement élevées non plus, mais elles sont suffisantes pour ne pas être limitatives dans les activités de photosynthèse.

Il semble que contrairement au milieu tempéré où le phosphore est fréquemment limitant, une tendance claire ne puisse pas être dégagée à la réponse trophique des retenues d'eau des milieux tropicaux Lhote (2000). En zone sahélienne les plans d'eau semblent tolérer des teneurs en phosphore et en azote plus élevées que les eaux de la zone guinéenne et pré guinéenne (en Côte d'Ivoire par exemple). L'hypothèse d'une apparition tardive et difficile de l'eutrophisation en zone sahélienne semble être vraisemblable avec des teneurs relativement élevées en phosphore et en azote.

CONCLUSION

Le risque de comblement des retenues d'eau au Burkina Faso est réel à des degrés variables selon les zones climatiques. Le comblement par transport de solides représente la menace première surtout dans les zones sahéliennes, marquées par une érosion intense, conséquence de la dégradation des terres et de celle du couvert végétal des bassins versants. Le risque de comblement est plutôt faible pour les retenues d'eau des zones soudaniennes dont les bassins versants comportent un couvert végétal de protection anti-érosive et dont les sols sont de nature à résister à cette érosion.

Le risque d'une eutrophisation de grande envergure est plutôt faible pour les plans d'eau en zone soudanienne. Ce risque semble inexistant en zone sahélienne car la forte turbidité des eaux paraît être un facteur limitant les activités de photosynthèse.

REFERENCES

Karambiri, H. & Ribolzi, O. (2003) Caractérisation des évènements averses-crues et de l'érosion hydrique à l'échelle d'un petit bassin versant pastoral sahélien (nord du Burkina Faso). *Rev. Sud Sciences et Technologies* **11**, 35–45.

Leprun, J. C. (1999) The influences of ecological factors on tiger bush and dotted bush patterns along a gradient from Mali to northern Burkina Faso. *Catena* **37**, 25–44.

Lhote, A. (2000) Critères d'évaluation de la qualité de l'eau d'un système lacustre tropical. Approche statistiques. Thèse de doctorat. Université de Poitiers, Poitiers, France.

Maiga, A. H. & Denyigba, K. (2002) Le comblement précoce des petites retenues d'eau par eutrophisation et par transport de solides: une menace réelle de disparition des plans d'eau en Afirque de l'Ouest. In: 2ème Journée scientifique du Groupe EIER-ETSHER, 91–96. EIER-ETSHER, Ouagadougou, Burkina Faso.

Maiga, A. H. & Denyigba, K. (2001) Eutrophication of small dams in West Africa. The case of Lobo dam (Côte d'Ivoire). In: *Fourth Inter-regional Conference on Environnment and Water* (Fortalega, Brasil, August 2001). Assoc. Bras. Irrig. Dren, Brasil.

Marchal, J. Y. (1983) Yatenga. Nord Haute Volta. La dynamique d'un espace rural soudano-sahélien. *Trav. Doc. ORSTOM* **167**, 872. ORSTOM, Paris, France.

OCDE (Organisation de Coopération et de Développement Economique de l'Europe) (1982) Eutrophisation des eaux: methodes de surveillance, d'évaluation et de lutte. Document OCDE. Paris, 1–65.

Parkan, J. (1986) Bilan et évolution des disponibilités en bois-Alternatives de productions forestières et d'actions sur la consommation, 1986–1995. *Rapport de synthèse FO: DP/UPV/78/004.* FAO, Rome.

Yacouba, H., Da D. E. C., Yonkeu S., Zombré P. & Soulé M. (2002) Caractérisation du ruissellement et de l'érosion hydrique dans le bassin supérieur du Nakambé (Burkina Faso). *Envirowater 2002* (5 ème Conférence Inter-régionale sur l'Environnement et l'Eau) Ouagadougou, 5-8 novembre 2002 Burkina Faso. (ed. A. H. Maïga, L. S. Pereira & A. Musy), 318–325. SOGIF.

Climate Variability and Change—Hydrological Impacts (Proceedings of the Fifth FRIEND World Conference held at Havana, Cuba, November 2006), IAHS Publ. 308, 2006.

Characteristics of sediment and nutrient flows in the lower reach of the Yellow River

JIANYAO CHEN[1], DONG KE[1], XINFENG ZHAO[1], YOSHIHIRO FUKUSHIMA[2] & MAKOTO TANIGUCHI[2]

1 *School of Geography Sciences and Planning, Zhongshan(Sun Yat-sen) University, Guangzhou 510275, China* chenjianyao@hotmail.com or chenjyao@mail.sysu.edu.cn

2 *Research Institute for Humanity and Nature, Motoya, Kamigamo, Kita-ku, Kyoto, Japan*

Abstract Water shortage and flooding risk are two major concerns in the lower reach of the Yellow River, and both are closely related to the transport of sediment and nutrients. Temporal and spatial change of sediment and nutrient flow in the lower reach are discussed with regard to the possible impacts of the Xiaolangdi Reservoir, which was completed in 2001. A negative sediment flux –1179 kg s^{-1} was found in the lower reach, indicating an erosive state since 2002. Average sediment load measured at Lijin was 16 kg m^{-3} and the highest in the lower reach. Ammonium (NH_4^+) and dissolved oxygen at Huayuankou were found to be temperature dependent, while electrical conductivity (EC) is closely related to discharge. Low EC was observed in the rainy season, while high EC occurs in March and April, due mainly to low discharge and water draining from irrigated upstream areas.

Key words sediment load; water quality; lower reach; Yellow River; nutrient flux

INTRODUCTION

The lower reach of the Yellow River is defined as the range between Huayuankou and Lijin and has a length of approximately 660 km (Fig. 1). The large amount of nutrients and sediment transported through this reach to the delta and the ocean is significant to global water and biogeochemical cycles, especially in the western Pacific. Nevertheless, dyke breaches and major shifts of the reach's course have occurred 26 times in the last 3000 years (Yu, 2002). Today, the 1.7 million people who live inside the dykes are vulnerable to a flooding disaster. Overall, about 87 million people would be affected by a dyke failure. At the same time, water shortages in the Yellow River basin results in reduced flow in the main channel (i.e. the drying up problem) and increased deposition of sediment which elevates the main channel and increases the risk of flooding. It was reported that the river bed at Lijin was raised by about 2.26 m from the 1950s to 1990s (Ye *et al*., 1997). Drying up has not taken place since 1998 due to artificial control of outflow from the dams in the middle and upper reaches.

The objectives of the study are to identify temporal changes of sediment and water quality in the reach by analysing relationships among discharge, sediment and water quality, and estimating the amount of sediment and mass transported to the delta and the ocean.

METHODS

A network monitoring precipitation, discharge, groundwater table depth, sediment load, and water quality has been operating in the lower reach since the 1950s. The main gauging stations in this network are located at Huayuankou, Gaocun, Sunkou, Aishan, Luokou and Lijin (Fig. 1). An automatic monitoring station (AMS) for water quality that measures water temperature (T), dissolved oxygen (DO), electrical conductivity (EC), pH, NH_4^+, and turbidity, has been operating at the Huayuankou station since June 2002. The data set of the AMS for the period of June 2002 to the end of 2005, together with monthly and/or daily discharge and sediment data, was collected and analysed for this study. Sediment load was measured only in the rainy season, i.e. from July to the end of October.

RESULT AND DISCUSSIONS

Sediment

The Yellow River is world famous for its high sediment load. While average loads are about 35 kg m^{-3}, they can be more than 1000 kg m^{-3} in some tributaries (SG, 1984). The annual average

Copyright © 2006 IAHS Press

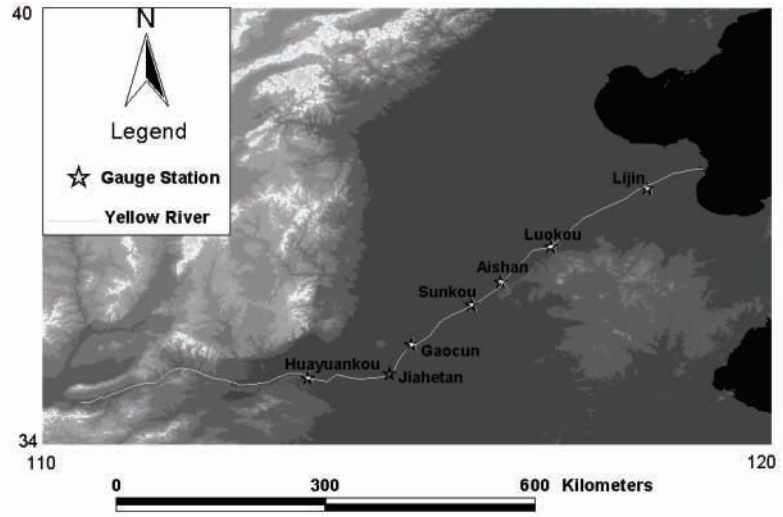


Fig. 1 Location map of the lower reach (defined as from Huayuankou to Lijin) of the Yellow River.

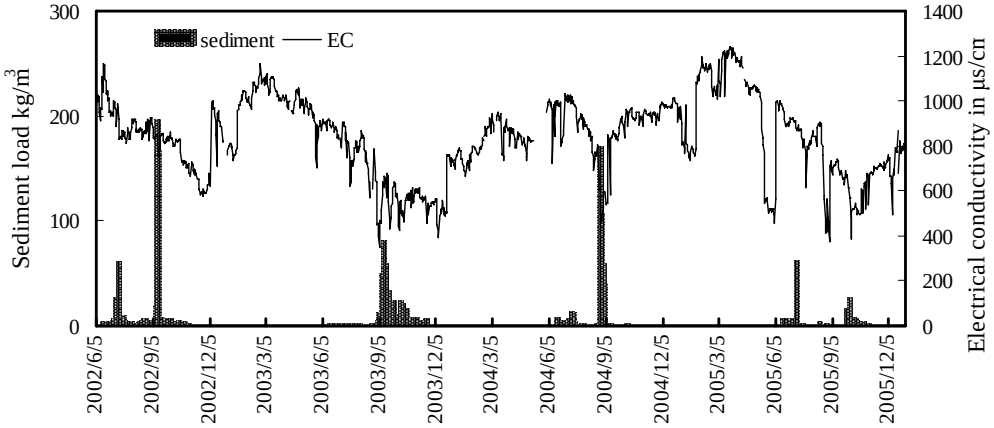


Fig. 2 Change of sediment load and EC at Huayuankou Station from June 2002 to December 2005. Sediment is measured only during the rainy season when sediment load is high.

sediment load transported in the lower reach until 1979 is estimated to be 1.6×10^9 tons. Since then it has been sharply reduced by water shortage and low flows in the basin. While the sources, causes and transport characteristics of sediment in the middle and upper reaches are well documented in the Chinese literature, they are less well reported for the lower reach (Ran *et al*., 2000; Liu & Chen, 2001). Total sediment flow at Huayuankou in 2002, 2003, 2004, and 2005 was calculated as the product of flow rate and sediment concentration and was found to be 8.9×10^7 tons over 139 days, 1.72×10^8 tons over 91 days, 1.43×10^8 tons over 39 days and 4.9×10^7 tons over 29 days respectively (Fig. 2). The highest sediment load typically occurred in September and most likely corresponds to high sediment flows in the upper stream, which typically start in July and August.

Average sediment load during the period from June 2002 to Dec. 2005 was 9.8, 11.9, 10.8, 11.0, 11.7, 10.8, and 16.0 kg m^{-3} at Huayuankou, Jiahetan, Gaosun, Sunkou, Aishan, Luokou and Lijin stations respectively. The declining flow rate due to water diversion in the lower reach contributes to the downstream increase of sediment load.

The difference in sediment flux (DSF) along the reach between Huayuankou and Lijin, is calculated from the average discharge and the average sediment loads as:

DSF = (Lijin discharge)(Lijin sediment load) – (Huayuankou discharge) (Huayuankou sediment load)
= (553.9 $m^3 s^{-1} \times 16.0$ kg m^{-3})– (784 $m^3 s^{-1} \times 9.8$ kg m^{-3}) = 1179 kg s^{-1}

The simple calculation indicates that net erosion could occur in the lower reach. The erosive capacity is then estimated to be 3.72×10^7 tons year^{-1}. This phenomenon is best explained by the construction of the Xiaolangdi Reservoir, which was completed in 2001. This reservoir has a total water capacity of 1.265×10^{10} m^3 and a design capacity of 1.0×10^{10} tons for sediment deposition (YRCC, 2002). Actually, erosion of the riverbed in the lower reach occurred during the period October 1960 to October 1964, immediately after the construction of the Sanmenxia Reservoir which started operation in September 1960 with a total capacity of 9.64×10^9 m^3. The total sediment deposition inside this reservoir was estimated to be 4.2×10^9 tons in October 1964, with an annual average of about 1.0×10^9 tons (SG, 1984), causing the erosion downstream mentioned previously. Sanmenxia Reservoir was thus reformed due to the serious deposition problem. On the other hand, reservoir operations for flushing deposition at Xiaolangdi in June/July could contribute to the change of sediment flow downstream. The sediment load was interpolated based on its relationship with turbidity, and the annual average load in 2002, 2003, 2004, and 2005 is calculated to be 5.5, 4.0, 3.3, and 2.4 kg m^{-3} respectively, indicating a declining trend (Fig. 3). As a result, it is reasonably inferred that the construction of Xiaolangdi causes erosion and a decrease of silt content in the lower reach.

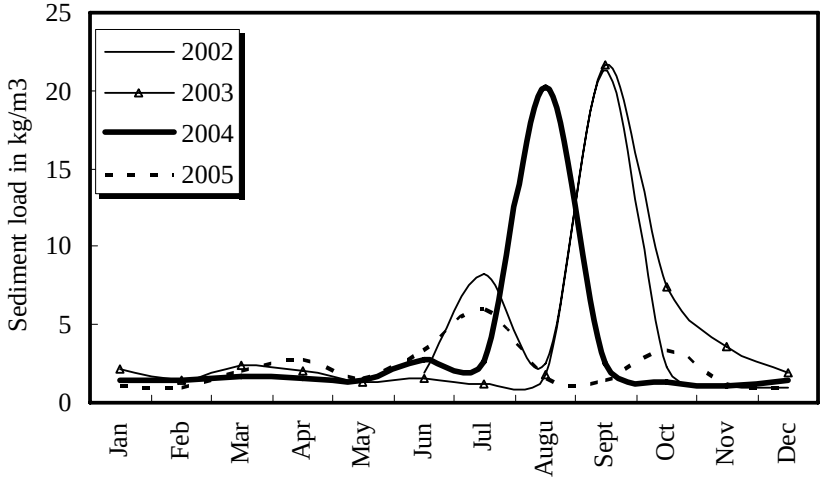


Fig. 3 Average monthly sediment load at Huayuankou station from June 2002 to the end of 2005.

Mass flow at Huayuankou station

Monitoring from the AMS indicated that EC reaches its lowest level as discharge increases in the rainy season (Fig. 2). The highest levels occur during the dry season of March and April when water is diverted for irrigation in the middle and upper reaches of the river and in the North China Plain (CDCID, 2002). The seasonal pattern of water quality is opposite to that of discharge and sediment. Return flow to the main channel, either from the drainage canal of irrigation field or from groundwater discharge upstream, contributes to a high EC and pH in the river water of the lower reach. Irrigation was found to be the main reason for the increase of major ions in the river water in the last 50 years (Chen *et al*., 2003).

Monthly EC data collected at Huayuankou confirms the temporal pattern collected, i.e. high EC values in March and April, low values in the rainy season till October, and medium values in the winter (Fig. 4). In contrast, high monthly NH_4^+ occurs from January to April when the water temperature is low (Fig. 5). Since 2003 the time of peak NH_4^+ values has shifted by one month. Annual average EC, water temperature, NH_4^+, and discharge in 2002, 2003, 2004 and 2005 are given in Table 1. The NH_4^+ content is inversely related to T (Fig. 5). Both DO and NH_4^+ are temperature dependent and have similar temporal patterns (Fig. 6). EC and pH at Huayuankou are poorly correlated with T.

An empirical relationship between EC (in ms m^{-1}) and total anions, TAN (meq L^{-1}), was found within the study area (Chen *et al*, 2002): $TAN = 0.1241 \times EC - 0.706$, with $R^2 = 0.9895$. This relationship was used to calculate TAN at Huayuankou. Mass flow (meq s^{-1}) was then estimated as

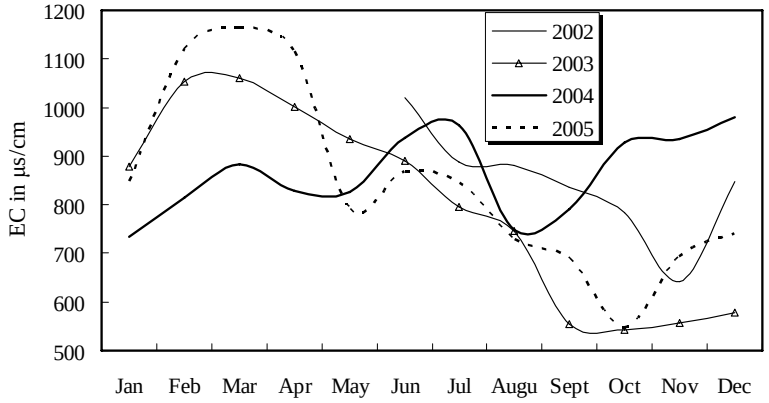


Fig. 4 Average monthly EC at Huayuankou station from June 2002 to the end of 2005.

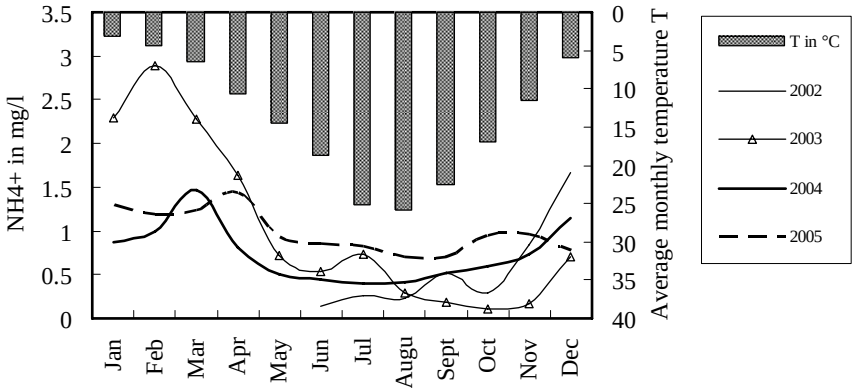


Fig. 5 Average monthly NH4+ from June 2002 to the end of 2005 and water temperature at Huayuankou.

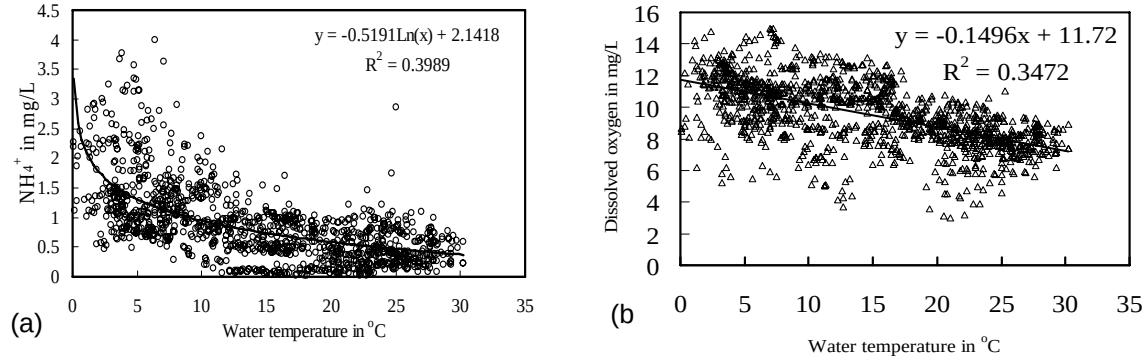


Fig. 6 Relationships of NH_4^+ and DO with water temperature at Huayuankou station, y refers to NH_4^+ and DO in (a) and (b) respectively, while *x* refers to water temperature.

Table 1 Annual average water temperature, EC, NH_4^+ and discharge at Huayuankou.

Year	T (°C)			EC (µs cm^{-1})			NH_4^+ (mg L^{-1})			Discharge (m^3 s^{-1})		
	Sample size	Mean	Std	Sample size	Mean	Std	Sample size	Mean	Std	Sample size	Mean	Std
2002*	204	18.3	7.8	205	842.6	124	204	0.56	0.58	210	654	546
2003	364	14.1	7.9	360	798.8	205.8	355	1.04	0.96	365	862	789
2004	342	13.7	7.6	342	864.8	108.1	317	0.74	0.37	366	756	563
2005	362	13.7	8.3	362	845.8	218	361	0.99	0.28	365	806	652

*No data available from January to May in 2002. Std refers to standard deviation of the means.

the product of TAN and discharge. Using this technique for 2002, 2003, 2004, 2005 the mass flow was found to be 4.34×10^{16} meq (during the period of 5 June–31 December), 7.46×10^{16} meq, 8.12×10^{16} meq, and 8.73×10^{16} meq for each year, respectively. Since chloride accounts for about 22% of TAN, annual Cl^- flux transported to the ocean can also be estimated.

The impacts of Xianlangdi Reservoir on water quality are an interesting issue. Though it is difficult to give a conclusive remark regarding the impacts of the reservoir on EC and water temperature, mass flux defined as the product of TAN and discharge shows a trend of increase. The hydrological regime has been modified by the construction of the Xiaolangdi Reservoir, and the possible upsurge of nutrient release in the reservoir due to fragmentation and flow regulation could contribute to the potential change of EC and the increase of mass flux in the lower reach, similar to that reported in the other rivers of the world (Nilsson *et al*., 2005).

Acknowledgements This study is supported by National Natural Science Foundation of China (no. 40571027), "985 Project" of GIS and remote sensing for geosciences from Ministry of Education of P.R. China, and Monbusho of Japan for Revolution Research Project.

REFERENCES

CDCID (China Development Center for Irrigation and Drainage, eds) (2002) *Strategic Study on Water-Saving Reconstruction for Large Irrigation Projects in the Yellow River Basin*, 82–85. The Yellow River Conservancy Publishing House, Zhengzhou, China.

Chen, J. S., He, D. W. & Cui, S. B. (2003) The response of river water quality and quantity to the development of irrigated agriculture in the last four decades in the Yellow River Basin, China. *Water Resour. Res.* **39**(3), 1047, doi:10.1029/2001WR001234.

Chen, J. Y., Tang, C. Y/, Sakura, Y., Kondoh, A. & Shen, Y. J. (2002) Groundwater flow and geochemistry in the lower reaches of the Yellow River: a case study in Shandong Province, China. *Hydrogeol J.* **10**, 587–599.

Liu, C. M. & Chen, X. G. (2001) *Evolving Law and Maintaining Mechanism of Renewable Capacity of Water Resources in the Yellow River Basin*. The Yellow River Conservancy Publishing House, Zhengzhou, China.

Nilsson, C., Reidy, C. A., Dynesius, M. & Revenga, C.(2005) Fragmentation and flow regulations of the world's large river system. *Science* **308**, 405–408.

Ran, D. C., Liu, L. W., Zhao, L. Y., Bai, Z. G., Liu, B. & Wang, H. (2000) *Soil Conservation and Change of Water and Sediment in the Middle Reach of the Yellow River from Hekou Town to Longmen*. The Yellow River Conservancy Publishing House, Zhengzhou, China.

Study group (SG), for governing the Yellow River, Yellow River Conservancy Commission (1984) *Governance and Development of the Yellow River*, 39–45. Shanghai Education Press, China.

YRCC (Yellow River Conservancy Committee, eds) (2002) *Primary Control and Development Plan of the Yellow River*. The Yellow River Conservancy Publishing House, Zhengzhou, China.

Ye, Q. C., You, L. Y., Xu, J. X., Gong, G. Y. & Chen, Z. Q. (1997) *Development Trend and Environmental Impacts of Suspended Sediment in the Lower Reach of the Yellow River*, 73–76. The Yellow River Conservancy Publishing House, Zhengzhou, China.

Yu, L. S. (2002) The Huanghe (Yellow) River: a review of its development, characteristics, and future management issues. *Continental Shelf Research* **22**, 389–403.

Climate Variability and Change—Hydrological Impacts (Proceedings of the Fifth FRIEND World Conference held at Havana, Cuba, November 2006), IAHS Publ. 308, 2006.

Factors affecting the groundwater regime in the High Tatra Mountains

MIRIAM FENDEKOVA[1] **& MARIAN FENDEK**[2]

1 *Department of Hydrogeology, Faculty of Natural Sciences, Comenius University in Bratislava, Mlynska dolina, Pav. G, 842 15 Bratislava, Slovak Republic*
fendekova@fns.uniba.sk

2 *Geological Survey of the Slovak Republic, Mlynska dolina 1, 817 04 Bratislava, Slovak Republic*

Abstract The groundwater regime of the Quaternary sediments of the High Tatra Mountains was studied in order to estimate factors affecting the regime, to assess the present status of groundwater resources and to outline their future development regarding the envisaged climate change. Data from 24 wells and three springs of the state monitoring network and temporary monitoring wells, as well as data on precipitation, air temperature and streamflow discharge, were analysed. Four types of groundwater level regime were distinguished based on the results of correlation matrix, factor and cluster analyses. The climatic and hydrological factors were identified as the principal influencing factors. The altitude is also of utmost importance controlling, through the air temperature, the length of the freezing period during which the water is stored in the drainage basin in the form of snow. The decrease in groundwater resources was documented by comparison of the present research results with results from the 1980s.

Key words Slovakia; High Tatra Mountains; groundwater regime; influencing factors; factor and cluster analyses

INTRODUCTION

The groundwater regime develops as a result of the influence of the regime-affecting factors within a certain area. The identification of those factors, together with the analysis of developments in their temporal trends is fundamental for assessment of the present state and the future development of the groundwater regime itself.

The groundwater regime of the Quaternary sediments of the High Tatra Mountains and their foreland was studied within the research project "Crystalline of the part of the High Tatra Mts and the Quaternary of their foreland – Hydrogeological District QG-139" financed by the Ministry of the Environment of the Slovak Republic (Fendek *et al.*, 2003). An estimation of usable groundwater resources in the area was the main goal of the investigation.

NATURAL CONDITIONS

The area of interest, the High Tatra Mountains, is located in the northern part of the Slovak Republic where it forms a natural border between Slovakia and Poland.

Hydrogeological District QG-139 has very variable geomorphic and climatic conditions influenced mainly by the very different geological setting and altitude differences between the mountainous part and the River Poprad valley bordering the district from the south. The highest point of the area – Gerlachovsky peak reaches 2655 m a.m.s.l.; the lowest point is Kezmarok precipitation gauging station at only 626 m a.m.s.l.

The Slovak Republic is situated in the mild climate zone where the effects of ocean and continental climate meet together and mix. The area of interest, however, belongs to the cold climate district, where the annual air temperature varies between –3.9ºC on the mountain ridge (Lomnicky Peak) and 5.8ºC in the river valley (Poprad city). The precipitation comes mainly from the west and northwest with the average annual amounts of 600–700 mm in the river valley and more than 2000 mm on the mountain peaks (*Landscape Atlas of the Slovak Republic*, 2002).

From the hydrological point of view, the area studied belongs to the River Poprad drainage basin with the main stream flowing into the Baltic Sea. The River Poprad headwaters come mainly from the High Tatra Mts; the main stream has a lot of short left-side tributaries and only a few tributaries from the other side of the valley bordered by the Low Tatra Mts. The discharge regime is natural, with the low flow period during the winter months. The discharges increase gradually from March and peak in the period from May to June depending on the altitude. Summer–autumn decreases in the discharge reach their minima in the winter low flow period (January and February).

Copyright © 2006 IAHS Press

The area studied is built of the crystalline complexes of the High Tatra Mts in its mountainous part, and of Palaeogene flysch sediments and Quaternary sediments in the foreland. All these complexes have very different hydrogeological properties which influence the groundwater flow and accumulation in the rock environment. The crystalline complexes, composed mainly of granitoids, typically have shallow groundwater flow and fissure springs with quite low yields, mainly less than 1 L s^{-1} (Hanzel *et al.*, 1984). The Palaeogene flysch sediments consist of three different sequences: basal Borove Sequence (conglomerates), Huty Sequence (claystone) and the uppermost Zuberec Sequence consisting of typical flysch sediments, i.e. an alternation of sandstone and claystone layers. The hydrogeological importance of the Palaeogene complexes is not very high. The Huty Sequence is an aquitard and the water retaining properties of the Zuberec Sequence are higher only in the case of tectonic failures. The main aquifers in the area are made of different types of the Quaternary sediments, which are mainly of glacial, glacial-fluvial and fluvial origin. Different types of slope sediments are present as well.

INPUT DATA AND METHODS

The groundwater regime was evaluated using data from 21 groundwater level monitoring wells and three monitored springs. Being factors that possibly influence the regime, the data from four discharge gauging stations, nine precipitation gauging stations and six stations measuring air temperature, were involved, too. The stations represent different altitudes in the drainage basin.

The assessed time series were not shorter than 10 years (1992–2001); the longest time series (more than 40 years) were available for some types of groundwater level monitoring (1962–2001). The data analysis consisted of a basic statistical characterization, data set normality and homogeneity assessment, time series analysis and analysis of inter-relationships among variables and classification of the groundwater regime using factor and cluster analyses.

RESULTS

The climatic characteristics, average annual precipitation amounts and average annual air temperatures calculated for the period 1991–2001, were compared with the long-term averages for the period 1951–1980. The comparison of these two periods has shown that the average annual air temperatures increased within the range from +1.1ºC (ΔT) in the river valley to +0.6ºC (ΔT) on the mountain peaks (see Table 1). However, the average annual precipitation amounts varied around the long-term average with the exception of the highest altitude, where they reached 129% (ΔP) of the long-term average (Table 1). There were obtained different results for the station P 12020 at Strbske Pleso. The deviations from the coincident developments at the other stations are explained by the misplacement of the gauging station in 1992. The change in its placement resulted in systematically lower values of measured air temperatures of 1.2 to 2.0ºC and lower precipitation amounts due to precipitation shadow (Fasko, personal communication).

The statistical evaluation of river discharges has shown a rather low variability expressed by the coefficient of variation (C_v) with values less than 25% (1977–2001). The same result was obtained for variability of groundwater levels in almost all monitoring objects. The values of C_v varied between 6 and 24%; but in two cases they reached 41% (W 8906) and 87% (W 999). The coefficient of variation for spring yields ranged from 22 to 67%.

Table 1 Differences in long-term average temperatures and precipitation amounts between periods 1951–1980 and 1991–2001 in selected gauging stations.

Number and name of the gauging station	Gauging station altitude (m a.m.s.l.)	T (ºC)	ΔT (ºC)	P (mm)	ΔP (%)
12100 Lomnicky stit	2653	–3.4	+0.5	1979	129
12120 Skalnate Pleso	1778	2.2	+0.6	1420	109
12020 Strbske Pleso*	1354	3.1	–0.4	737	77
12140 Tatranska Lomnica	827	–	–	809	102
12040 Poprad	694	6.3	+1.1	600	101
12180 Kezmarok	626	–	–	615	105

* Location of the gauging station changed in 1992.

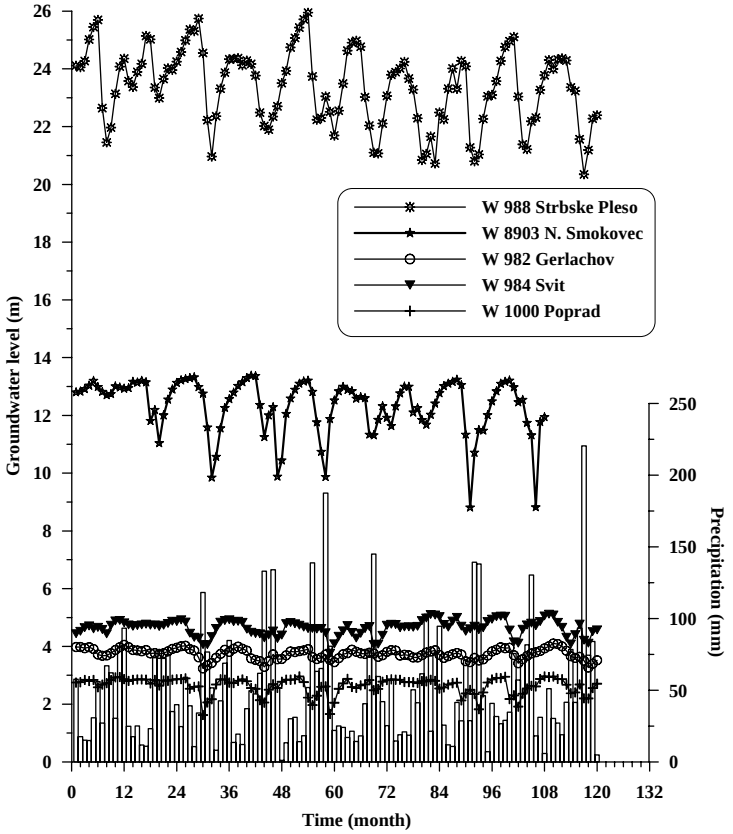


Fig. 1 Time series of mean monthly groundwater levels in selected wells with monthly precipitation from Poprad gauging station (western part of the area).

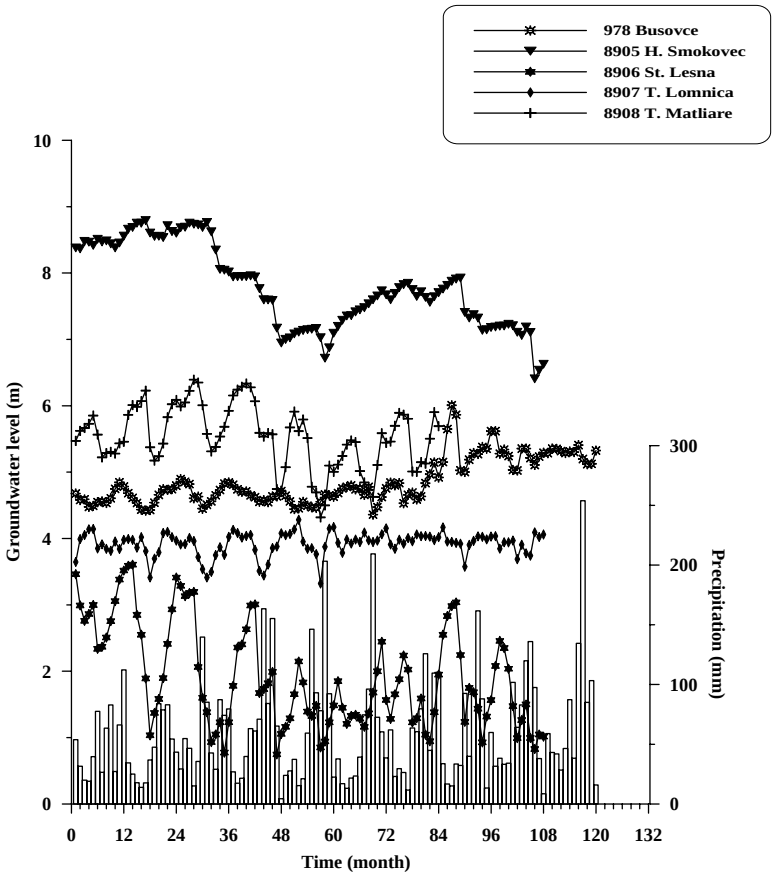


Fig. 2 Time series of mean monthly groundwater levels in selected wells with monthly precipitation from Poprad gauging station (central and eastern part of the area).

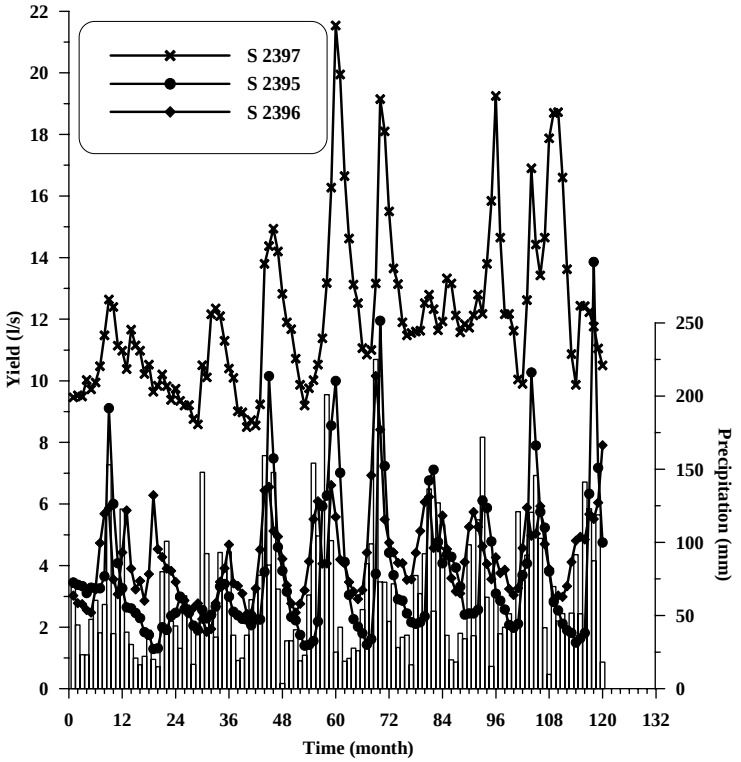


Fig. 3 Time series of mean monthly spring yields with monthly precipitation from Stara Lesna gauging station.

The time series analysis of groundwater levels (1992–2001 period) has shown a quite stable course without distinct trends except for three wells. An increasing trend was confirmed for wells W 988 Strbske Pleso and 8903 Stary Smokovec in the western and central part of the study area (Fig. 1); a decreasing trend was quite distinct in the well W 978 Busovce in the eastern part (Fig. 2). The time series analysis of spring yields confirmed an increasing trend of yields for spring No. 2397, which also manifests an increase in maximum extreme values for the last six years (Fig. 3). There is a visible matching of the course of spring yields and monthly precipitation (vertical bars) with the lag of zero or one month in Fig. 3.

The analyses of the altitude data, climatic, hydrological and hydrogeological settings at the monitoring locations enabled assessment of the temporal differences and causal factors of the groundwater regime formation. Based on the results of correlation matrix, factor analysis (Table 2) and cluster analysis (Fig. 4), four groups of groundwater level regimes were distinguished. The groups were characterized by describing regime temporal and causal factors, where the precipitation, air temperature (controlling the length of the freezing period of the top-most soil layer and starting time of snow melt) and surface stream discharges were identified as the main affecting factors. The altitude is also very important, influencing through the air temperature the length of period during which the precipitation is stored in the area in the form of snow. Therefore, the time of the groundwater level increase is closely connected with the change in altitude.

The first type of groundwater regime is represented by wells W 983 Batizovce, 984 Svit, 998 Poprad-Spisska Sobota, 999 and 1000 Poprad, located in the western part of the area in the alluvial sediments of the Poprad River, as well as W 993 Kezmarok in the eastern part (Fig. 4, Type 1). They can be characterized by increase of the groundwater level in the period from April till August with maxima in May due to high discharges of the surface streams and response to the frequent storms typical of the summer season. The subsequent decline of the groundwater levels continues reaching the minima period during the autumn and winter months. High correlation coefficients in the correlation matrix were obtained for the relation of groundwater levels with stream discharges and precipitation amounts. The seasonal fluctuation of the groundwater levels is quite distinct.

The second type of the groundwater regime is represented by wells W 979 Spisska Bela and 1375 Velka Lomnica (the eastern part of the area). The seasonal component of the groundwater level

Table 2 Factor loadings after VARIMAX rotation.

Type, no. and location	F1	F2	F3	F4	F5	F6
S 2395 Tatr. Polianka	–0.045	**–0.859**	0.179	–0.173	0.023	0.296
S 2396 Tatr. Lomnica	0.185	**–0.569**	–0.062	–0.494	0.122	0.116
S 2397 Tatr. Matliare	–0.061	–0.372	**0.526**	**–0.528**	–0.185	–0.155
W 978 Busovce	0.151	–0.092	–0.012	–0.128	**0.906**	0.026
W 979 Spisska Bela	**0.743**	0.166	–0.219	0.460	–0.162	0.086
W 993 Kezmarok	**0.846**	0.103	–0.166	0.133	0.106	0.116
W 1373 St. Smokovec	0.348	**0.862**	–0.112	0.083	0.003	0.186
W 1375 V. Lomnica	**0.659**	0.158	–0.188	0.272	**–0.558**	0.098
W 8904 St. Smokovec	0.376	**0.699**	–0.474	0.069	0.075	0.202
W 8905 H. Smokovec	0.087	0.337	–0.007	**0.819**	–0.259	–0.013
W 8906 St. Lesna	0.445	**0.525**	–0.084	**0.474**	–0.081	0.324
W 8907 T. Lomnica	0.432	–0.155	–0.452	–0.117	0.284	0.171
W 988 Strbske Pleso	–0.044	**0.643**	–0.495	0.188	–0.100	**0.408**
W 8901 N. Polianka	0.043	**0.901**	–0.083	0.210	–0.186	0.131
W 8903 N. Smokovec	0.281	**0.749**	–0.426	0.148	0.048	0.147
W 982 Gerlachov	**0.606**	0.541	–0.140	–0.124	0.021	**0.415**
W 983 Batizovce	**0.879**	–0.138	–0.080	0.095	–0.103	–0.130
W 984 Svit	**0.795**	0.246	–0.084	0.070	0.298	0.018
W 998 Spiska Sobota	**0.832**	0.181	–0.211	–0.052	0.036	0.266
W 999 Poprad	**0.739**	0.054	–0.385	–0.255	0.319	–0.022
W 1000 Poprad	**0.818**	0.261	–0.314	–0.180	–0.052	0.106
P 12090 St. Lesna	–0.183	–0.173	**0.903**	–0.001	0.037	0.049
P 12040 Poprad	–0.185	–0.128	**0.899**	0.067	0.061	0.031
D 7990 Poprad-S.Pleso	–0.185	–0.191	**0.699**	–0.072	–0.064	**–0.592**
D 8000 Poprad-Svit	–0.287	–0.161	**0.689**	–0.039	–0.019	**–0.582**
D 8060 Velicky brook	–0.387	–0.245	**0.769**	–0.222	0.006	–0.253
D 8070 Slavkovsky br.	**–0.584**	–0.380	**0.616**	–0.147	0.006	0.029

S spring, W well, P precipitation gauging station, D streamflow discharge

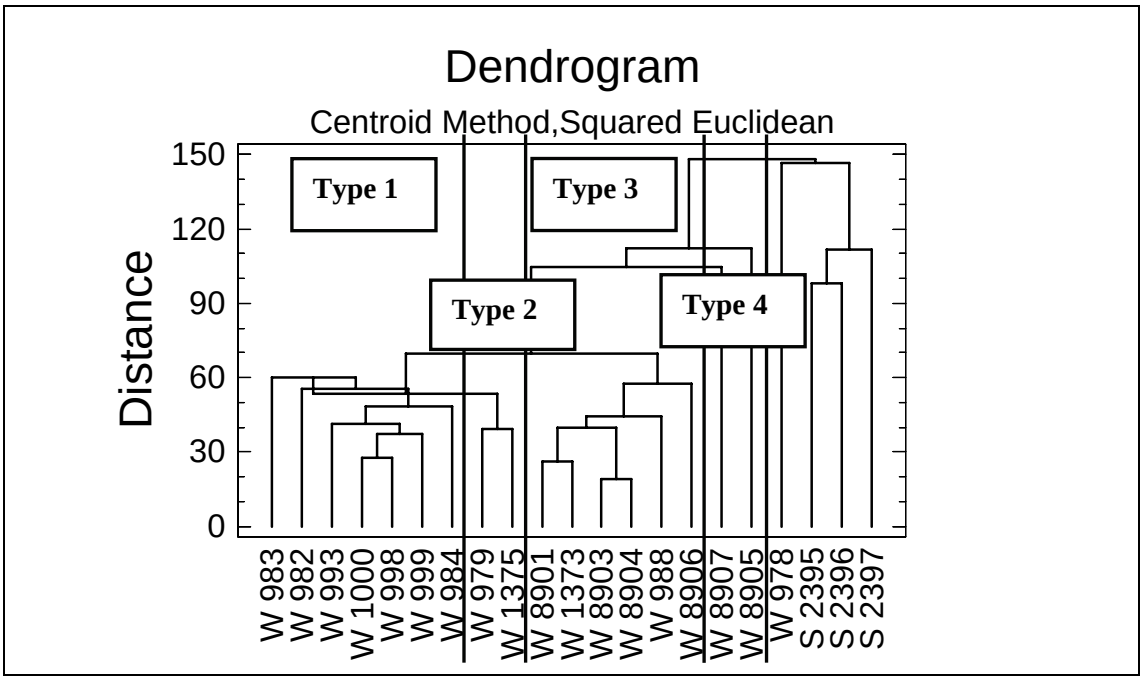


Fig. 4 Dendrogram of clusters for main objects of interest (S: spring, W: well, P: precipitation, D: discharge).

fluctuation is distinct; the time components are similar to those in the first group (Fig. 4, Type 2). The difference is in the shifting of the groundwater level increase to earlier in the spring months March–April, because of the wells location downstream of the Poprad River and the earlier snowmelt time.

The third type of the groundwater regime is represented by the group of wells W 988 Strbske Pleso, 8901 Nova Polianka, 8903 Novy Smokovec, 8904 Stary Smokovec and 1373 Stary Smokovec (Fig. 4, Type 3). These wells are located at relatively high altitudes. The groundwater level increase maximum is shifted to June–July because of later snowmelt and thawing of the ground in the mountainous part of the area. The lowest levels are typical for the winter and the early spring periods. A similar groundwater regime is typical for well W 8908 Tatranske Matliare, the only difference is in a slightly earlier starting time of the groundwater level increase, i.e. February. Well W 8906 Stara Lesna stands on the border between type 3 and type 4 of the groundwater regime.

The fourth type of groundwater regime is represented by wells 8905 Horny Smokovec and 8907 Tatranska Lomnica (Fig. 4, Type 4). They are located at middle altitudes and their regime is the most complicated. The groundwater levels show two maxima, the first one in the early spring March–April period and the second one, the less distinct, in June. They react to increased streamflow discharges and later also to snow melting in the mountainous part of the area. According to the seasonal component of the time series, well W 992 Strane pod Tatrami belongs to this group, too.

It was not possible to place unambiguously the two wells into any of the above groundwater regime types. At well 978 Busovce (Fig. 4) human interference is probable. At well 982 Gerlachov the interference of the groundwater regime affecting factors is more complicated as was shown by the results of factor (loadings in F1 and F6) and cluster analyses (Type 1). The springs created a separate cluster, however, the position of S 2397 is a bit different from S 2395 and S 2396, as was confirmed by the results of the factor analysis. It may be caused by the location of the spring at the lowest altitude of the assessed springs.

The research results have confirmed that there is a decrease in groundwater amounts in the area, which is in agreement with the prediction by Majercakova *et al.* (1997). However, the change is caused by the more extreme behaviour of precipitation influencing the surface and groundwater runoff distribution in the specific conditions of crystalline complexes.

REFERENCES

Fendek, M., Kordik, J., Fendekova, M., Bajtos, P., Svasta, J., Kohut, M., Maglay, J., Bottlik, F. & Benkova, K. (2003) *Krystalinikum casti Vysokych Tatier a kvarter ich predpolia, Hydrogeologicky rajon QG-139* (Crystalline of the part of High Tatra Mountains and Quaternary of their foreland, Hydrogeological District QG-139). Final report, Geological Survey of the Slovak Republic, Bratislava, Slovakia.

Hanzel, V., Gazda, S. & Vaskovsky, I. (1984) Hydrogeologia juznej casti Vysokych Tatier a ich predpolia (Hydrogeology of the southern part of the High Tatra Mountains and their foreland) (in Slovak with English summary). *Zapadne Karpaty, Ser. Hydrogeologia a Inzinierska geologia.* Geologicky Ustav D. Stura, Bratislava, Slovakia.

Ministry of the Environment of the Slovak Republic (2002) *Landscape Atlas of the Slovak Republic* (first edn), Bratislava, Slovakia.

Majercakova, O., Fendeková**,** M. & Leskova, D. (1997) The variability of hydrological series due to extreme climatic conditions and the possible change of the hydrological characteristics with respect to potential climate change. In: *Regional Hydrology: Concepts and Models for Sustainable Water Resources Management* (ed. by A. Gustard *et al.*), 59–65. IAHS Publ. 246. IAHS Press, Wallingford, UK.

Climate Variability and Change—Hydrological Impacts (Proceedings of the Fifth FRIEND World Conference held at Havana, Cuba, November 2006), IAHS Publ. 308, 2006.

A new, physically-based, numerical runoff generation model system for study of surface–shallow groundwater relationships and system reactions to environmental changes

ANDREAS HERRMANN, MATTHIAS SCHÖNIGER & SYBILLE SCHUMANN

Institute of Geoecology, Department of Hydrology and Landscape Ecology, Technical University Braunschweig, Langer Kamp 19c, D-38106 Braunschweig, Germany

a.herrmann@tu-bs.de

Abstract A new concept is presented for modelling streamflow generation on a small basin scale. It is based on process knowledge realised using the Integrated Catchment Approach (ICA), and the FEFLOW software package for numerical groundwater flow simulation. The study relates to the Lange Bramke research basin in the Harz Mountains, Germany. First simulations for steady-state confirm the drain line function of the major cross-faults. A main future perspective concerns the coupling of FEFLOW with MIKE11 for calculation of groundwater exfiltration rates into defined individual channel sections.

Key words Harz Mountains, Germany; numerical groundwater modelling; runoff generation; fissured rock aquifer; hydraulic conductivity

INTRODUCTION

During storms, groundwater can be a dominant component of runoff in many regions under different climatic conditions. This has been shown by environmental tracer studies (Herrmann, 1997). It means that groundwater recharge is appropriately high in such cases. An open question is how possible changes of hydrological boundary conditions due to global warming will influence the physical processes that govern the event-based turn-over of water and matter in environmental systems (Herrmann, 2004). Furthermore, dynamic hydrological systems have often been modelled with unrealistic process simplification, i.e. with a number of numerical methods that are not physically-based, but solve a set of ordinary differential equations.

At the small basin scale, runoff formation is a primary ecohydrological process. The study of runoff formation has a long tradition as shown in the compilation of benchmark papers by IAHS (2006), but the use of integrated hydrological system approaches still plays a marginal role. Hence, a new tool for the study of runoff generation was developed that considers the holistic ecohydrological Integrated Catchment Approach (ICA; Herrmann *et al.*, 2001), which is based on combined field experiments and numerical modelling, and which has meanwhile become good practice. The tool allows for integrated water management systems for drinking water reservoirs and environmental protection at least in mountainous Central European hard rock regions of Palaeozoic age. The approach fits the IAHS PUB (Predictions in Ungauged Basins) activities and perspectives.

RUNOFF FORMATION STUDY CONCEPT

The concept of the runoff generation study (Fig. 1) consists of combining experimental and modelling components, and establishing classical water balances on different time scales with the highest resolution for single runoff events. Hydrological and hydraulic input data are determined as required for calibration and validation of the numerical model. The relevant water fluxes for the study system are also calculated. Their successful quantification (expressed as basin averages in Herrmann *et al.*, 1989) together with the appropriate hydraulic parameter values like mean transit times for the three subsurface storages, mark the starting point for this concept. Another precondition was the progress in numerical modelling at small space and time scales in the 1990s.

The new model is based on the following physical process pattern: streamflow generation is activated by a rainfall or meltwater input pulse that mobilizes water and solutes in subsurface storages. Once the infiltration process begins, water and solutes can be exported, and the recharge process is initiated.

The new approach aims to quantify near surface water gains and subsurface soil and groundwater losses on a small basin scale by analysing simple cases in the Lange Bramke basin

Copyright © 2006 IAHS Press

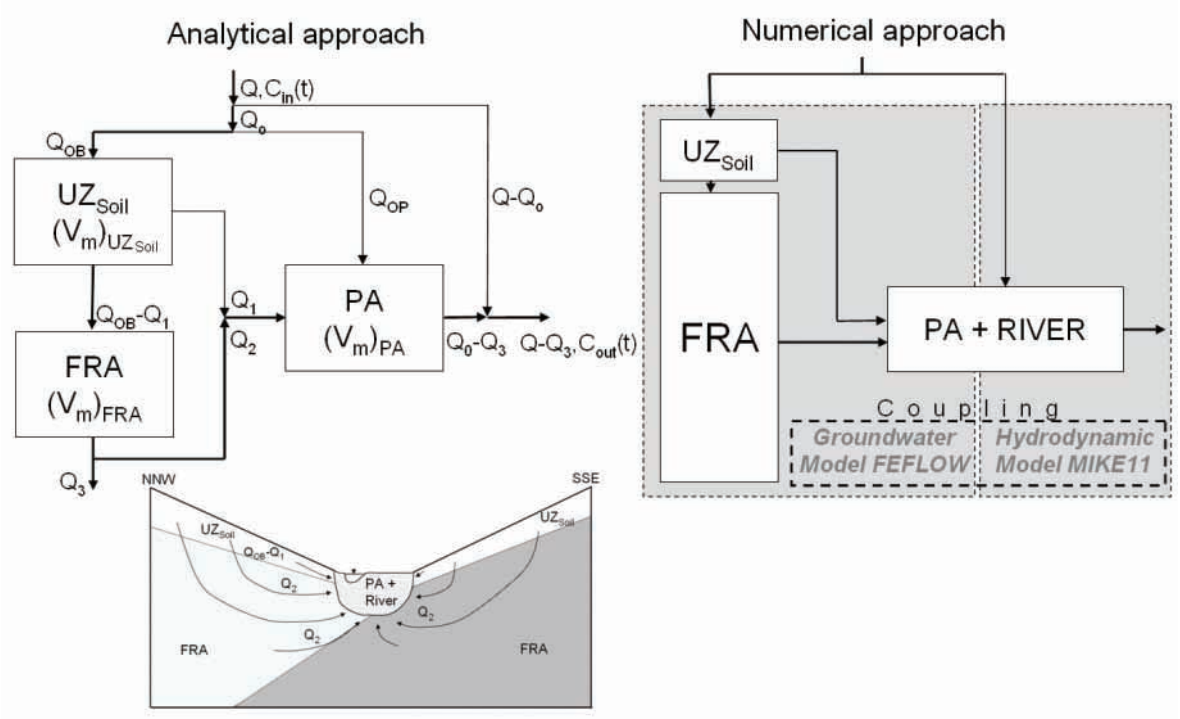


Fig. 1 The runoff formation concept with analytical solution of relevant water fluxes and subsurface storages (left) and numerical approach with spatial discretization (right).

where overland flow is negligible and the unsaturated zone (UZ: soil and upper weathered and fractured/fissured bedrock) is non-layered. In this case the interflow is close to zero. The channel flow originates predominantly from groundwater in the saturated zone (SZ: fractured/fissured bedrock). It is assumed, that UZ and SZ have shortened preferential flow paths. This enables fast percolation of infiltrating water and hence groundwater recharge throughout the year. Information on the origin, age and pathways of the water fluxes that cause channel inflow and generate flood hydrographs are required at a sufficient resolution in space and time.

EXPERIMENTS AND MODELLING

Isotope and experimental hydrological data as well as hydraulic data were collected in the Lange Bramke research basin, area 0.76 km^2 and altitude 540–700 m a.m.s.l., that is located in the Harz Mountains, Germany. It has been monitored since 1948. The basin is 90%forested by Norwegian spruce, resulting in negligible surface runoff. The wet valley floor, fire breaks aligned perpendicular to slopes, and forestry roads represent open areas. The basin has a fissured Lower Devonian rock aquifer (FRA) of sandstones, quartzite, slates and has a minor porous aquifer (PA) in the valley bottom. Experiments with artificial tracers showed that UZ and SZ are connected through preferential flow paths which indicate that SZ is just a transient storage with respect to runoff generation, and that major cross faults function as natural drain lines that favour quick and efficient groundwater exfiltration (Maloszewski *et al.*, 1999).

Topography and basic instrumentation in the Lange Bramke are shown in Fig. 2, and the geology in Fig. 5. In this context, 4″ and 2″ (1″ = 2.54 cm) piezometers were installed in FRA, and 1″ in PA. The deepest piezometers are HKLU (55 m) and HKLT (25 m). Six piezometric triple-sets of 5 m, 10 m and 15 m depth (HKLA,B,C to HKLR,S,T) were installed for hydraulic and artificial tracer experiments. HKLQ and HKLW are 15 m deep. In contrast, 1″ groundwater pipes in the shallow PA of the valley filling are only up to 4 m deep. HKLQ, U and W are recorded with automatic pressure transducers.

In the conceptual hydraulic basin model (Fig. 1) UZ is treated as a transient zone, which can be described by a specific transfer function. The SZ resembles a fissured rock aquifer (FRA) model system which is characterized within the GIS based FE FEFLOW programme package

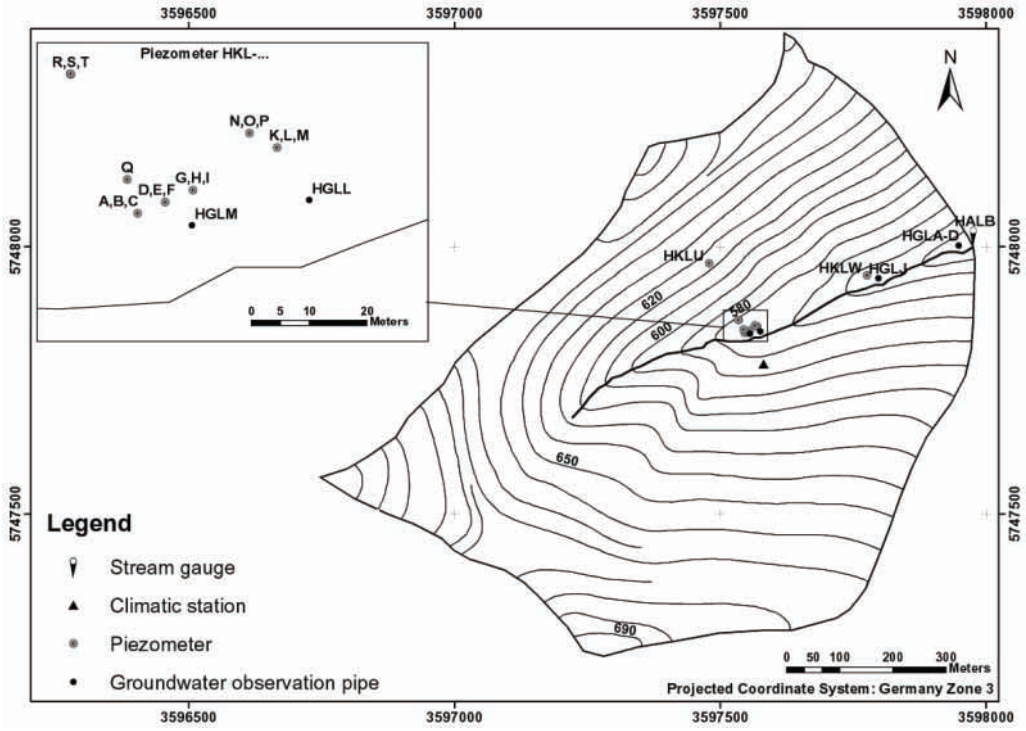


Fig. 2 Topography and instrumentation of the Lange Bramke research basin, Harz Mountains, Germany.

(Diersch, 2005), that allows simulation of the groundwater flow and transport. To quantify and verify the simulated groundwater exfiltration volumes along the main flow channel, FEFLOW will be coupled with the surface water software MIKE11 channel and wave propagation model in the near future by means of a special interface manager.

RESULTS

The results here concentrate on the runoff relationships with the fissured rock groundwater that is known to be the main streamflow generating component of the system. Discharge and water tables of the confined to semi-confined FRA react similarly in the long-term and for single events, but they vary in individual detail depending on the given inputs (Fig. 3). Accordingly, FRA can be considered and modelled as one hydraulic system. The closely corresponding groundwater table relationships for the fissured aquifer verified by the piezometers recordings shown in Fig. 4(a) strengthen this finding, whereas Fig. 4(b) proves the intercalated hydraulic position of PA as a transfer storage with a mean transit time of three months as compared to >3 years for FRA (Herrmann *et al.*, 1989). The groundwater–discharge relationships have frequently been found to be hysteretic, i.e. higher discharges are observed at given groundwater tables for the rising than for the falling limbs of the same hydrograph (Herrmann, 2004).

As a consequence of these findings, runoff generation must be attributed to the dominant groundwater contributions of different ages that follow diverse pathways. The related processes correspond to three distinct development stages of streamflow generation as formerly proposed by Herrmann (1994): (1) infiltration causes saturation of the top soils that results in compression of the capillary fringe; (2) the rise of groundwater tables, i.e. of groundwater potential; and (3) increase of groundwater exfiltration into channels through pressure transmission and combined groundwater ridging and macropore flow (see Buttle, 1998). Many event analyses confirm these stages which were hence introduced into the conceptual model system in Fig. 1. Furthermore, isotope findings show that annual groundwater recharge is about three times the amount determined by traditional methods (Herrmann *et al.*, 1989).

Good hydrological system knowledge and data availability allowed the application of FEFLOW to a small basin with a dominating fissured rock aquifer for the first time. The progressive 1-D to 3-D mesh generator enabled the fracture system to be simulated as shown in

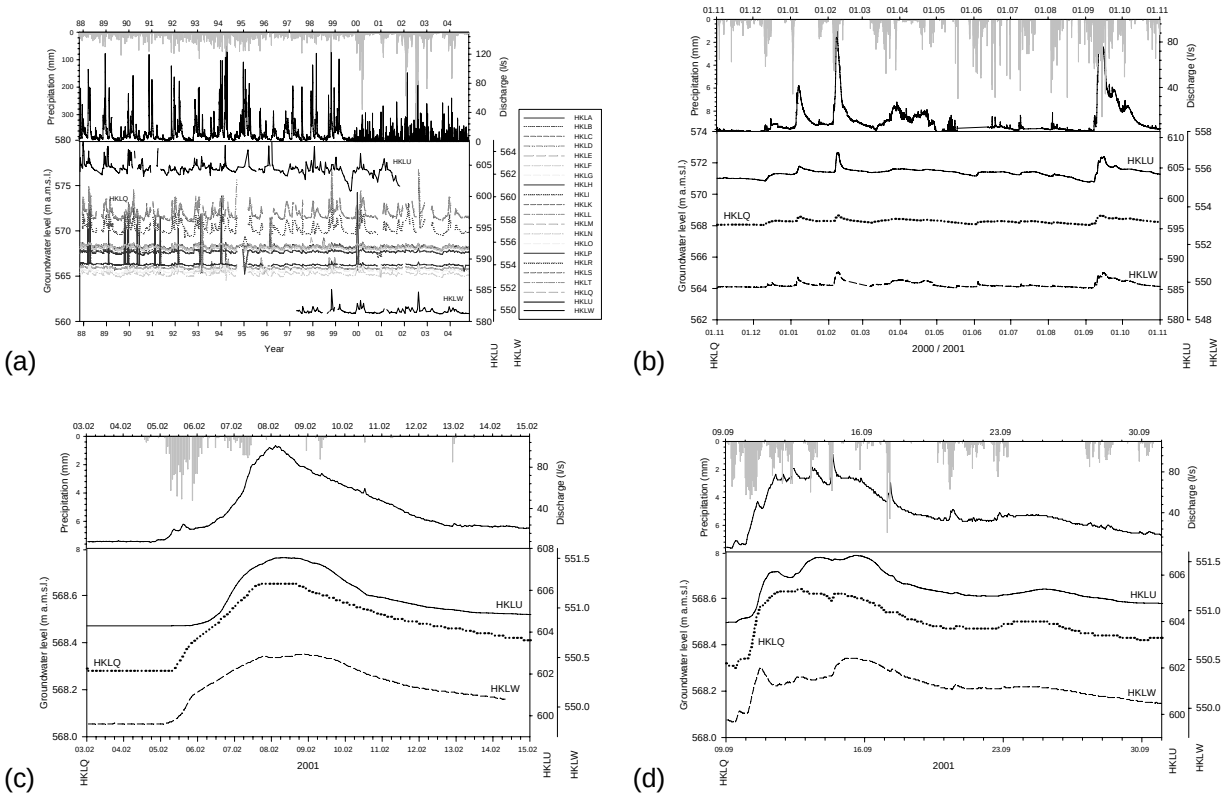


Fig. 3 Lange Bramke basin: precipitation, discharge and fissured rock groundwater tables measured manually and automatically (HKLQ, -U, -W) (a) for 1987–2005; (b) for 2001 (only HKLQ, -U, -W); and for single precipitation-runoff events in 2001 with rain on snow (c) and rain (d).

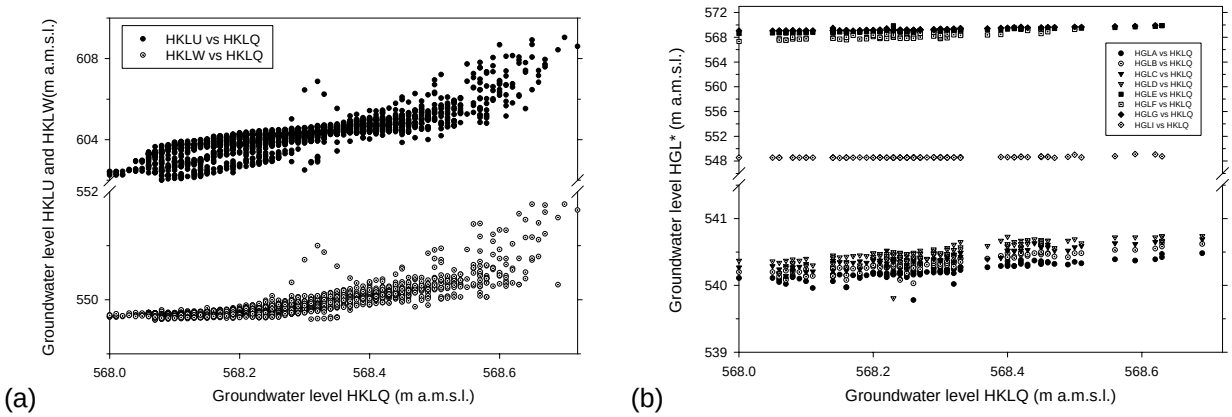


Fig. 4 Groundwater table relationships in respect to HKLQ for FRA piezometers HKLU and HKLW in 2000–2005 (a); and between FRA HKLQ and PA (HGL*, manual measurements) piezometers (b).

Fig. 5 as a block of fractured rock with discrete, oriented fractures and a fault network. The parameters of the 2-D fracture elements derived from analytical solutions for tracer experiments in Maloszewski *et al.* (1999) for preliminary steady-state flow simulations, i.e. with all boundaries and material data including conductivity as time-constant were: cross-section area 1.0 m^2 (est.), conductivity 1.00E-04 ms, compressibility 1.00E-04 m^{-1}, in-transfer rate/out-transfer rate 8.57 day^{-1} (est.). The "cubic" Darcy Law was used which governs flow and pressure gradient relationships in the case of flow in individuals fractures, which is assumed as flow between two parallel and smooth plates. The vertical fractures are represented as discrete quadrilateral 2-D feature elements which are integrated in a FE mesh of over 50 000 six-node triangular prisms.

The simulated distribution of the hydraulic head is shown, together with the corresponding equipotential lines in Fig. 6. One should note the deep 45 m circulation of groundwater in the

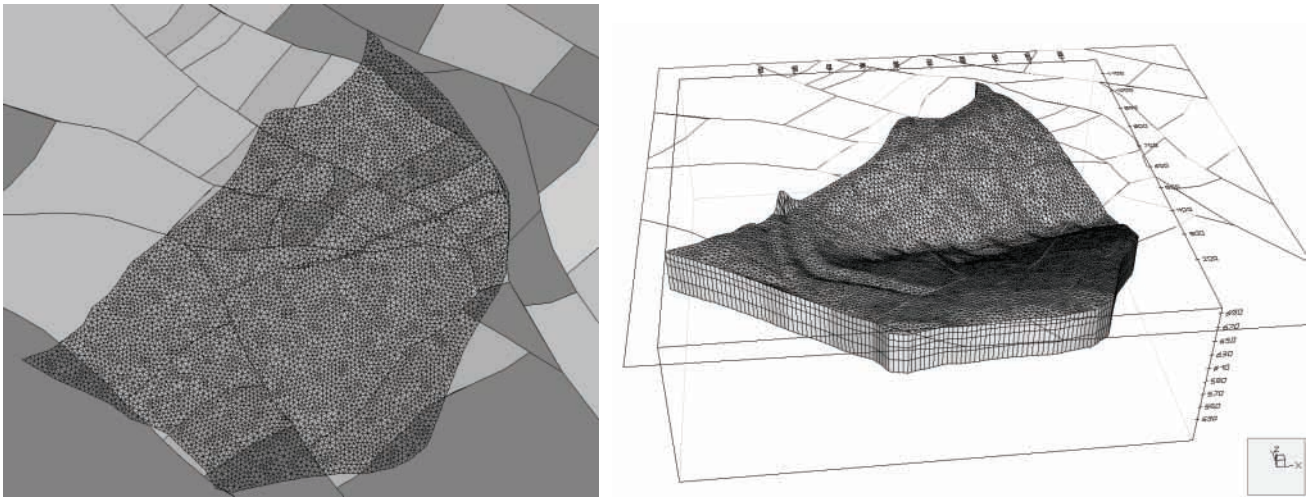


Fig. 5 Finite element mesh with mesh refinement of faults and geological background map (left) in 3-D with four layers and top slice reflecting the DTM (right).

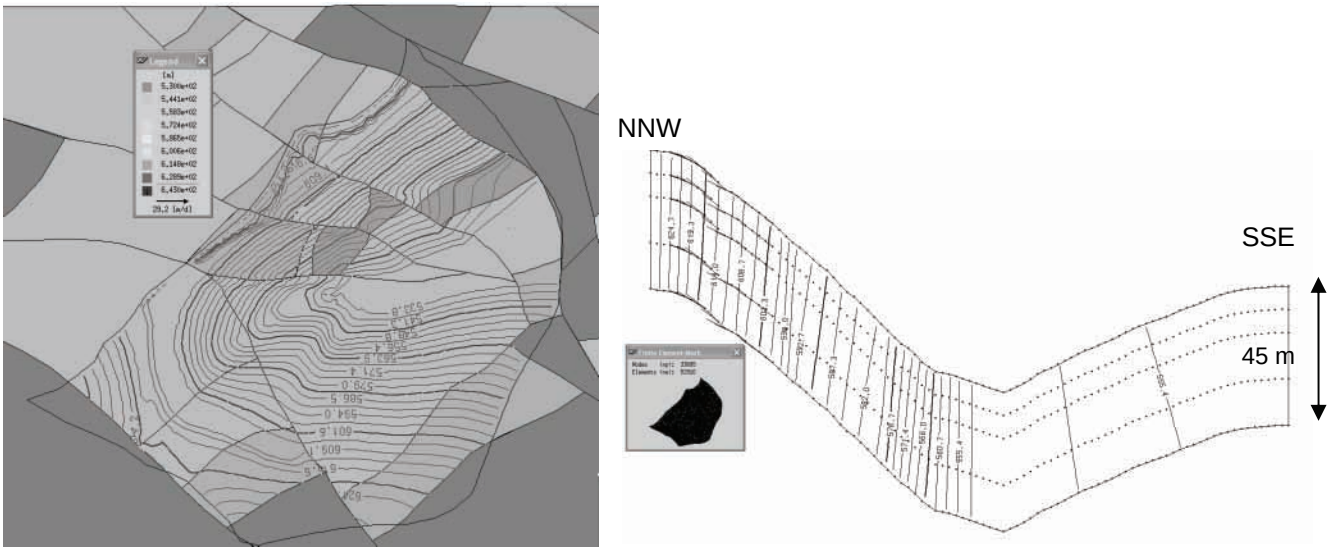


Fig. 6 Steady-state hydraulic head of FRA from FEFLOW (left) and equipotential lines (right).

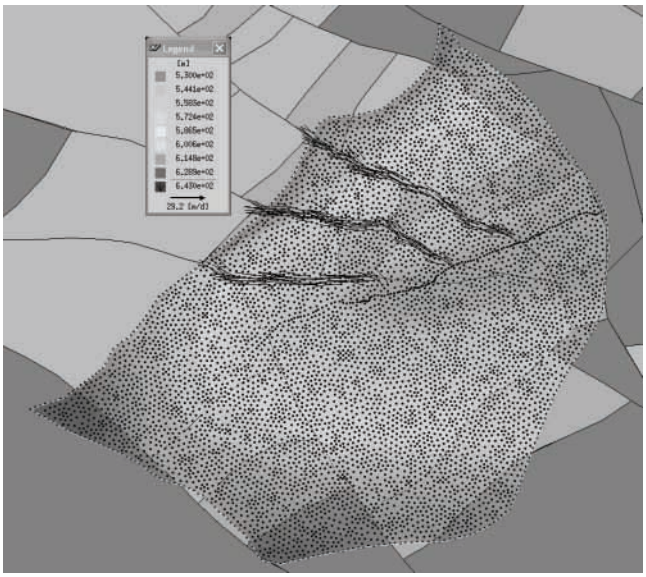


Fig. 7 Continuous flow velocities and velocity vectors (cf. legend) in FRA as calculated from FEFLOW and concentrating on the left slope area.

faults. This was confirmed 15 years ago by electromagnetic VLF-R measurements on water-bearing cross-fault structures (Herrmann *et al*., 1989). The head isolines allows for the estimation of the (regional) meso-scale groundwater flow pattern.

The flow velocity fields in Fig. 7 indicate the importance of the major cross-faults for basin turnover of fissured rock groundwater. The high fracture flow velocities of up to 30 m day^{-1} contrast with the extended low ones for matrix flow in the less disturbed bedrock. Hydraulic conductivities of the regular rock mass (two orthogonal families of small-sized quasi-parallel fractures) from *in situ* pump and slug tests range between 2.20E-06 to 3.5E-05 m s^{-1}, and in highly fractured zones near the top of the non-weathered bedrock and close to faults, are on the order of 8.20E-05 m s^{-1}. A previous multi-tracer experiment in the centre one of the three major cross-faults (cf. Fig. 7) helped to determine the average flow velocity to be 12 m h^{-1} which corresponds to turbulent flow (Maloszewski *et al.*, 1999) and agrees with the present modelling findings.

The results portray the functioning of major cross-faults as main groundwater drain lines. However, analysis shows that the exfiltration amounts from these faults are too little for the formation of single flood hydrographs. Hence, additional exfiltration volumes need to be included in the process, i.e. that which originates from the matrix flux of the less conductive bedrock. Therefore special emphasis must be paid to the transfer role of PA, i.e. on the coupling of the groundwater system and the main channel. This will be realised with the help of MIKE11 and the construction of 3rd Cauchy-type boundary conditions to assess the groundwater inflow rates separately from each channel section.

CONCLUSIONS

The initial numerical modelling results show that fissured rock groundwater flow as a main streamflow generating component in the Lange Bramke basin is a reasonable hypothesis. An advantage of the physically-based numerical systems approach is that it allows for a regionalization of the runoff formation process with scarce data in the near future. This meets the requirements for Predictions in Ungauged Basins (PUB). However, further tracer experiments are needed to improve model calibration, and a stochastic fracture network model will be developed for the transfer and regionalization of results.

The more precise information on the variability of water availability in space and time during single precipitation–runoff events is of great interest to water management authorities and for environmental scientists. The modelling tools are found to be able to simulate a change in the physical process pattern. If these process changes are caused by climate change then the ecohydrological impact can be predicted by this model. Therefore the results may be used in planning strategies for appropriate counter measures to cope with climate change.

REFERENCES

Buttle, J. M. (1998) Fundamentals of small catchment hydrology. In: *Isotope Tracers in Catchment Hydrology* (ed. by C. Kendall & J. J. McDonnell), 1–49. Elsevier, The Netherlands.

Diersch, H.-J. G. (2005) *User's Manual Feflow 5.2*. WASY GmbH, Institute for Water Resources Planning and Systems Research, Berlin, Germany.

Herrmann, A. (1994) Ecohydrological research on a small basin scale: scientific approach of the runoff formation key process. *Beiträge zur Hydrologie der Schweiz* **35**, 83–95.

Herrmann, A. (1997) Global review of isotope hydrological investigations. In: *Third FRIEND Report 1994–1997* (ed. by G. Oberlin), 307–316. Cemagref Editions, Antony, France.

Herrmann, A. (2004) Runoff formation in mountainous environments and possible effects of global warming. In: *Studies in Mountain Hydrology* (ed. by A. Hermann & U. Schroeder), 1–12. IHP/HWRP Berichte 2, Koblenz, Germany.

Herrmann, A., Schöniger, M. & Schumann, S. (2001) Integrated approach of investigating and modelling runoff formation considering information from environmental and artificial tracers. *Freiburger Schriften zur Hydrologie* **13**, 90–97.

Herrmann, A., Koll, J., Leibundgut, Ch., Maloszewski, P., Rau, R., Rauert, W., Schöniger, M. & Stichler, W. (1989) Wasserumsatz in einem kleinen Einzugsgebiet im paläozoischen Mittelgebirge (Lange Bramke/Oberharz). Eine hydrologische Systemanalyse mittels Umweltisotopen als Tracer (Turnover of water in a small basin in Paleozoic highlands – Lange Bramke/Upper Harz Mts. A hydrological system analysis using environmental isotopes as tracers). *Landschaftsökologie und Umweltforschung* **17**, Braunschweig, Germany.

IAHS (2006) *Streamflow Generation Processes* (Selection, Introduction and Commentary by Keith J. Beven). *Benchmark Papers in Hydrology*, IAHS Press, Wallingford, UK.

Maloszewski, P., Herrmann A. & Zuber, A. (1999) Interpretation of tracer tests performed in fractured rock of the Lange Bramke basin, Germany. *Hydrogeol. J.* **7**, 209–218.

Climate Variability and Change—Hydrological Impacts (Proceedings of the Fifth FRIEND World Conference held at Havana, Cuba, November 2006), IAHS Publ. 308, 2006.

Isotopic evidence of the overexploitation of karst aquifers

L. F. MOLERIO LEÓN
CESIGMA, S.A., PO Box 6219, CP 10600, Habana 6, Ciudad de La Habana, Cuba
leslie@cesigma.com.cu

Abstract Tritium behaviour has been successfully used as evidence to forecast aquifer overexploitation before it becomes a management problem and creates a water use conflict. The most important evidence is the onset of serial but not consecutive recharge events, the variation in ^{3}H activity at the same measuring points during the year and, especially, the presence of groundwater with no ^{3}H activity, or at least none related with known or measured ^{3}H inputs.

Key words karst; overexploitation; tritium; aquifer; Cuba; tracer; isotopes; safe yield; recharge

INTRODUCTION

The most common, simple and intuitive definition of overexploitation of an aquifer is a continuous disequilibrium between the groundwater abstraction and groundwater replenishment. It is supposed that when more water than that entering the aquifer is extracted, the available resources become systematically exhausted or its quality deteriorates, but the concept is incomplete because it is known that overexploitation can occur, even when recharge is greater than abstraction, due to bad management practices. A more general agreement states that overexploitation of groundwater takes place when a limit in volume, yield or water quality is surpassed. Therefore beyond those limits, some side effects—usually ambiguously defined as *undesirable effects*—due to over-exploitation appear, e.g. systematic groundwater level decline that in turn causes the exhaustion of springs and the abandonment of water wells, loss of water quality and, in turn, contamination of the productive aquifer, and subsidence.

For water supply purposes, this limit is often called the "safe yield" or "groundwater resource". Conventionally, overexploitation should take place when this boundary is exceeded, but experience show that sometimes water is abstracted beyond this limit and no undesirable side effects become apparent. Therefore the concept of overexploitation, which is important to know given the kind of problem managers are dealing with, falls into a category of ambiguous definitions: (a) the limit established by the "safe yield" and the safe yield itself; (b) the limit established by the management practices; and (c) the limit established by the water quality that is particularly required.

Therefore, a scarcity in water quantity and a loss of water quality commonly come together as a consequence of aquifer overexploitation. Because of the socio-economic impact caused by the high costs of aquifer remediation (increasing groundwater reserves and improving water quality) Young (1992) defined aquifer overexploitation as a failure to achieve maximum economic returns to the resource. Overexploitation can also allow a loss of groundwater quality when waters of undesired chemical composition are drained into a productive formation. Sea water intrusion is the most common but not the only source of water quality deterioration due to overexploitation. Acid mine drainage, oily waters or even untreated domestic waste waters could enter the aquifer when flow lines are altered by pumping. Another important side effect of aquifer overexploitation is subsidence.

But, as Adams & MacDonald (1995) have pointed out, "*certain aquifers are more susceptible to overexploitation than others—equally certain managing practices are conducive to over-exploitation*". Karst aquifers, particularly those of the Humid Tropics, fall into this category because of the particular way in which groundwater flow is organized within them.

In a regional karst aquifer system, groundwaters converging from different local and sub-regional flow systems do not necessarily contribute continuously to groundwater resources (Fig. 1). This singularity means that different parts of the aquifer behave differently in time and space. In fact, according to the degree of karst development, its distribution within the aquifer, its relation to local erosion base levels and the way they modulate the recharge inputs, karst aquifers show very complex hydrodynamic responses. Under certain boundary conditions some of the local flow

Copyright © 2006 IAHS Press

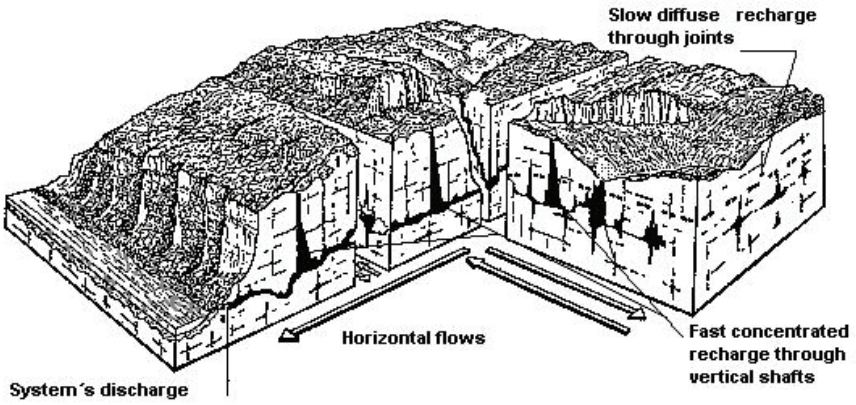


Fig. 1 Recharge patterns of a karst aquifer (modified after Mangin).

systems and even its associated epikarst could seasonally or inter-annually become saturated by water or be completely dry. This changing behaviour is not necessarily reflected in the yield of springs or in the water level decline. The generally big fluctuations recorded in groundwater levels —sometimes associated with the effect of hurricanes or heavy rains—of large, regional karst flow systems masks the actual behaviour of the aquifer. Some cave levels or local flow systems become hydrologically active for several months or years leading to an erroneous assessment of groundwater reserves and, therefore, to the establishment of an abstraction plan based on an erroneous safe yield estimation that eventually could lead to overexploitation.

On the other hand, groundwater abstraction can isolate local flow systems interrupting their contribution to major systems and reducing the reserve therein. Sometimes an active epikarst can be completely drained producing a local and sometimes abrupt lack of water supply. River runoff can be shortened and even interrupted if fed by karst springs (concentrated or diffuse) that become dry when their own local flow systems are drained. The inverse is also true and some episodic rivers flow only when their local flow systems become hydrological active.

It is very common that evidence of overexploitation appears suddenly. That is why Adams & McDonald (1995) remarked that "*overexploitation is normally diagnosed a posteriori because hydrogeological assessment can often only be achieved when an aquifer has been stressed*". But, in fact, different types of evidence that appear during the overexploitation process are commonly not well interpreted because they are not integrated with groundwater monitoring and used for adequate prevention. Induced local pollution, isolated episodes of local subsidence, fluctuations in the yield of springs, or in the particular case of karst aquifers, desiccation of water filled caves, changes in the hydrological behaviour of the epikarst, variations in the drainage stratification (or in the hydrology of cave levels) among others, appear during the whole historic process of over-exploitation and can be used as evidence of it.

It would be highly profitable if overexploitation could be detected before its undesirable side effects (groundwater level decline, recharge of poor quality waters and subsidence) become apparent. Considering that time is already involved in the concept of safe yield and that side effects become apparent according to the degree of mixing of waters from different sources, which is also a time dependent variable, a good approximation for the identification of overexploitation hazard has been obtained by the author using radioisotope techniques involving tritium and radon-222 modelling in Cuban karst aquifers. This paper focuses on the constraint that time, and more precisely, groundwater residence time, introduces in safe yield and how, in the case of karst aquifers, aquifer exploitation management practices should take it into account.

SAFE YIELD AND AQUIFER OVEREXPLOITATION

The safe yield of an aquifer is defined as the quantity of water that can be extracted annually from an aquifer without producing undesirable effects (Todd, 1970). As Todd points out, this intuitive definition is more complex than it seems at first sight, since "*there can be more than an undesired*

result effect … the safe may be limited to an amount less than the net amount of water supplied to the basin and that the safe yield can vary as the conditions governing it vary" (Todd, 1970, p.201). The concept is completed when he points out that "*the safe yield cannot exceed the long time mean annual water supply to the basin…Extractions exceeding this supply must come from storage within the aquifer*". And continues "*… in any one year the draft can exceed the recharge without causing permanent depletion. But on a long-term basis, when series of wet and dry years would tend to average out, the draft becomes an overdraft if the mean supply is exceeded*" (Todd, 1970, p.201).

THE CONCEPT OF RESIDENCE TIME (TW)

The residence time of waters (that is used as a synonym for turnover time, transit time, mean residence time of waters, age of the waters, kinematic age, hydraulic age, among others) is the relationship between the mobile water volume (V_m) and the volumetric flow rate (Q) in the system: $t_w = V_m/Q$. For vertical flow in the recharge area, especially in the unsaturated area, Q is equal to the infiltration rate or the recharge (I): $t_w = V_m/I$. If the system can approach a pattern of one-dimensional flow, this definition yields (Maloszewski & Zuber, 2004) $t_w = x/v_w$, where x is the length for which t_w is determined, and v_w it is the mean velocity of water that equals the relationship between the flow velocity (v_f) and the effective porosity (n_e). As tritium is a tracer, it is convenient to introduce the concept of mean tracer age (t_t) that can be defined as $t_t = \frac{\int_0^\infty t' C_I(t') dt'}{\int_0^\infty C_I(t') dt'}$, where C_I is the concentration of tracer observed at the measuring site (the outlet of the system) as a result of an instantaneous injection at the system's entrance.

Mean tracer age is only similar to the half-life of waters if immobile, static areas do not exist (stagnant zones) in the aquifer and the tracer is injected and measured in the flux. When the radioisotope age of an atmospheric radioisotope does not have sources or sinks other than radioactive disintegration, it can be identified by the age of the water (Maloszewski, 1992; Maloszewski *et al*., 1983, 2004). In this way, the radioisotope age (t_a) is defined exclusively for the radioactive disintegration as $C(t_a)/C(0) = \exp(-\lambda t_a)$, where $C(t_a)$ and $C(0)$ are the current and initial radioisotope concentrations, respectively, and λ, the disintegration constant. Regrettably, as Maloszewski & Zuber (2004) pointed out, few radioisotope tracers are available for dating groundwater when in motion and immobile. Obviously, as these authors point out, the ages of immobile systems or of systems that can be partially immobile for certain periods of time cannot be interpreted, directly, in terms of the hydraulic parameters.

THE SINGULARITY OF KARST AQUIFERS

The typical heterogeneity of the system of collectors and conducts of groundwaters and the differences in the natural recharge patterns in karst systems (Fig. 1) is the main cause of the differentiated space and time distribution of the replenishment of groundwater resources. In fact, two extreme recharge patterns are recognized in karst systems: a rapid, fast concentrated recharge along vertical shafts and open cracks in bare karst areas; and a slow, diffuse, recharge through joints and soil cover in buried karst systems. This means that different recharge rates exist for the same recharge event. Even more, different arrival times to the outlet are then recognized depending on the degree of water mixing. In turn, this allows for different isotopic behaviour. This difference is the reason why, in particular flow domains, water with different age coexists.

The sustained extraction of groundwaters belonging to the current hydrological cycle causes, inexorably, the exhaustion of the available resources and this relationship could be rigorously determined with the use of the proper isotopic tracers. In general, the variable "residence time" is not taken into account in the water balance and in the assessment of groundwater resources. But

the abstraction of "old" ground waters or the exploitation of water of very slow replenishment leads to the, sometimes very fast, exhaustion of the resources, particularly in karst aquifers. Remediation works like artificial recharge, protection against the contamination of the water supply wells and springs or the deep injection of waste liquids, are other aspects in which the residence time is fundamental and yet, regrettably, it is not usually considered in either. As a basic principle it is strongly recommended that waters not participating in the current hydrological cycle should not be exploited in any way, to guarantee its replenishment. However, the term "current hydrological cycle" is ambiguous by nature and has to be more precisely defined. Anyway, isotopic techniques provide appropriate resources to determine the residence time of groundwater. Quantifying this variable provides criteria for adopting appropriate management practices without damaging the aquifer by the exhaustion of its resources or the artificial recharge of contaminated waters (Maloszewski & Zuber, 1990, 1992, 2004).

RESULTS AND DISCUSSION

The sustained application of environmental stable (^{18}O, ^{2}H) and radioactive (^{3}H, ^{222}Rn) isotope techniques has allowed the identification of the recharge patterns in some karst aquifers of Western Cuba (Arellano *et al*., 1992; Molerio, 1994, 2004, 2005; Molerio *et al*., 1993, 2000, 2002a,b). Until now the most profitable approach has been based on that of Maloszewski (Herrman *et al*., 1990; Maloszewski, 1992; Maloszewski & Zuber, 1990, 1992, 2004; Maloszewski *et al.*, 1983, 2004), but the Exponential Model for Input Function (Clark & Fritz, 1997) was also successfully applied. Research carried out by the author and his colleagues following that approach (Molerio, 1994, 2004, 2005; Molerio & Pin, 2002; Molerio *et al*., 1993, 2002a,b) in two important karst aquifers showed that the corresponding tritium based isotopic balance for the different flow systems indicated the overexploitation of the groundwater. As a consequence, those results provided the appropriate managerial tools to redistribute the groundwater exploitation abstraction well system and for the design of proper locations for artificial recharge wells and to improve the protection against the contamination. The most important results obtained were the following:

(a) The isotopic balance of the groundwater showed that in the discharge area and in some points of the aquifer, waters with different residence times converge, indicating a stratification of the aquifer system associated with the development of different cave levels.

(b) During the dry season, certain boreholes and the system's outlet convey waters with no tritium activity. It is highly probable that these waters are not linked with the natural replenishment associated with the current hydrological cycle or at least that which took place in the last fifty years. Modelling shows the best fit for waters of 100 years residence time (Fig. 2). During the dry season the exploitation of the volumes that might eventually be recharged associated with the "cold front" rains does not reach the aquifer, limiting or impeding its natural regulation and, in turn, contributing to the exhaustion of the aquifer because of the systematic lack of replenishment.

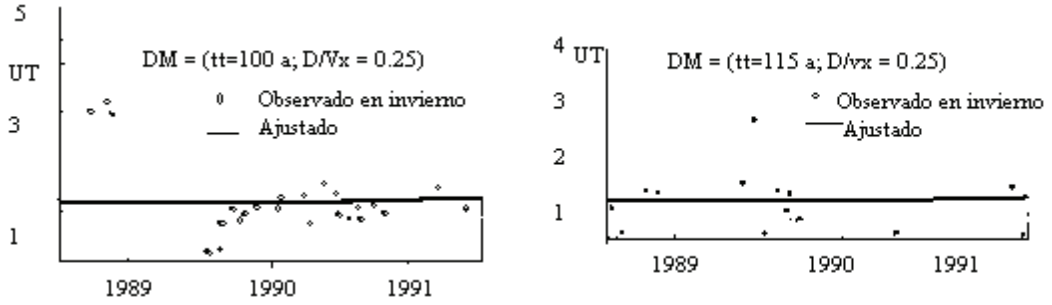


Fig. 2 Best fits for the tracer transit time.

(c) In some cases, the difference between transit times varies from three months in the upper part of the flow system to 100 years in the lowest levels. The exploitation of these waters during the dry season represents a constant reduction of water resources.
(d) Because of the nature of the integration of the cave system, a good mixing of waters exists. The fact that successive recharge events are not consecutively identified is good evidence of this; i.e. recharge waters arrive at the outlet and at other sampling points in a differentiated way, some earlier than others, but without following a strict chronological order, in what seems to be a typical feature of the Cuban karst systems.
(e) Most recharge events that can be identified with a well-known tritium input in the rainwater basically take place during the rainy period (May–October). This fact confirms that these karst system receive some fresh recharge annually but not across the whole extent of the aquifer.
(f) The isotopic results show that, at least for a part of the year, losses by evaporation take place in several parts of the aquifer, mainly close to the outlet or in karst depressions where groundwater outcrops. Therefore, some of these karst features behave as points of groundwater loss, and not recharge, as anticipated intuitively.

FINAL REMARKS

Isotope techniques, mainly those based on the ^{3}H balance, are valuable tools for detecting over-exploitation of karst aquifers. Because ^{3}H is part of the water molecule and hence travels with it, its use as a tracer reduces the uncertainty in the determination of water residence time. The strong seasonal effect on recharge in the Humid Tropics is a useful tool for the application of isotope techniques in water balance studies. Evidence derived from the seasonal behaviour of isotopes like ^{3}H are enough to detect overexploitation trends before they become apparent. Among these types of evidence the most important are the onset of serial but not consecutive recharge events, the variations in ^{3}H activity at the same measuring points during the year and, especially, the presence of groundwater with no tritium activity or at least not related with known or measured ^{3}H inputs.

Acknowledgements Tritium modelling was first applied in Cuba in a karst polje in the framework of the IAEA's ARCAL XIII Project in the early 1990s under the advice of Dr Piotr Maloszewski (GSF-Institute of Hydrology, Munich, Germany) whose contribution together with that of L. Araguas (IAEA), C. O. Rodríguez (Colombia National University) and my Cuban colleagues M. Guerra (Institute of Geophysics) and K. del Rosario (National Institute of Water Resources) is acknowledged. Ana, my wife, shared much of this field work in recent years.

REFERENCES

Adams, B & MacDonald, A. (1995) Overexploitation of aquifers. Final Report**.** *Tech. Rep. WC/95/3.* British Geol. Surv. Keyworth, Nottingham, UK.

Arellano Acosta, M., Molerio León, L. F. & Surí Hijos, A. (1992) Efecto de altitud del ^{18}O en la zona de articulación de llanura criptocársica con carso de Montaña? *GTICEK. Taller Internac. sobre Cuencas Experimentales en el Karst, Matanzas*, 29–42. Publ. Universitat Jaume I de Castelló.

Clark, I. D. & Fritz, P. (1997) *Environmental Isotopes in Hydrogeology*. Lewis Publ., Boca Raton, New York, USA.

Herrman, A., Finke, B., Schöniger, M., Maloszewski, P. & Stichler, W. (1990) The environmental tracer approach as a tool for hydrological evaluation and regionalization of catchment systems**.** In: *Regionalization in Hydrology* (ed. by M. A. Beran, M. Brilly, A. Becker & O. Bonacci), 45–58. IAHS Publ. 191. IAHS Press, Wallingford, UK.

Maloszewski, P. (1992) Mathematical modelling of tracer transport in different aquifers: results from ATH test fields. In: *Proc. 6th Int. Symp. Water Tracing* (Karlsruhe, Germany), 25–30. Balkema, Rotterdam, The Netherlands.

Maloszewski, P. & Zuber, A. (1990) Mathematical modelling of tracer behaviour in short term experiments in fissured rocks. *Water Resour. Res.* **26**(7), 1517–1528.

Maloszewski, P. & Zuber, A. (1992) On the calibration and validation of mathematical models for the interpretation of tracer analysis in groundwater. *Adv. Water Resour.* **15**, 47–62.

Maloszewski, P. & Zuber, A. (2004) Manual of lumped parameter models used for the interpretation of environmental tracer data in groundwaters**.** Unpublished Report. GSF-Institute of Hydrology, Nehuerberg, Germany.

Maloszewski, P., Rauert, W., Stichler, W. & Herrmann, A. (1983) Application of flow models in an alpine catchment area using tritium and deuterium data. *J. Hydrol.* **66**, 319–330.

Maloszewski, P., Stichler, W. & Zuber, A. (2004) Interpretation of environmental tracers in groundwater systems with stagnant water zones. *Isotopes in Environmental and Health Studies* **40**(1), 21–33.

Molerio León, L. F. (1994) Isotopic and geochemical regionalization of a tropical karst aquifer**.** In**:** *Int. Symp. Isotopes in Water Resources Management* (IAEA, Vienna, Austria), Paper IAEA-SM-336/88P.

Molerio León, L. F. (2004) Cave levels, safe yield and turnover time in karst aquifers. *Int. Symp. Isotope Hydrology and Integrated Water Resources Management* (IAEA, Vienna, Austria). Paper IAEA-CN-104/p-76.

Molerio León, L. F. (2005) Balance isotópico de tritio y rendimiento seguro de acuíferos cársicos**.** RH-035. *Convención Internacional de Medio Ambiente*. La Habana, Cuba.

Molerio León, L. F. & Pin González, M. (2002) Diseño de la Red de Monitoreo de Tritio en las aguas subterráneas de la cuenca de Vento, Habana, Cuba. Unpublished Report.

Molerio León, L. F., Maloszewski; P., Guerra Oliva, M. G., Regalado, O. A., Arellano Acosta, D. M., March Delgado, C. & del Rosario, K. (1993) Dinámica del Flujo Regional en el Sistema Cársico Jaruco-Aguacate, Cuba. In: *Estudios de Hidrología Isotópica en América Latina 1994*, 139–174**.** IAEA TECDOC-835, Vienna, Austria.

Molerio León, L. F., del Rosario, K., Torres Rodríguez, J. C., Rocamora Alvarez, E. & Guerra Oliva, M. G. (2002a) Factores de control de la composición química e isotópica de las aguas subterráneas en la región Varadero-Cárdenas, Matanzas, Cuba**.** *Ing. Hidr. y Ambiental, La Habana* **XXIII**(2), 36–46.

Molerio León, L. F., Maloszewski, P., Guerra Oliva, M. G., Arellano, D. M. & del Rosario, K. (2002b) Hidrodinámica isotópica de los sistemas acuíferos Jaruco y Aguacate, Cuba. *Ing. Hidr. y Ambiental, La Habana* **XXIII**(2), 3–9.

Todd, D. K. (1970) *Ground Water Hydrology*. Edic. Revolucionaria, La Habana, Cuba.

Climate Variability and Change—Hydrological Impacts (Proceedings of the Fifth FRIEND World Conference held at Havana, Cuba, November 2006), IAHS Publ. 308, 2006.

Contaminación del acuífero yucateco por lixiviado de residuos municipales

ROGER GONZÁLEZ HERRERA[1] **& RAMIRO RODRÍGUEZ CASTILLO**[2]

1 *Universidad Autónoma de Yucatán, Facultad de Ingeniería, Apartado Postal 150, Administración de Correos Urbana 10, Cordemex 97111 Mérida, Yucatán, México*
gherrera@uady.mx

2 *Universidad Nacional Autónoma de México, Instituto de Geofísica 1, Departamento de Recursos Naturales, Ciudad Universitaria, Circuito Investigación, México, 04510 D.F.*

Resumen Mérida, Yucatán, es el principal centro poblacional del sureste mexicano. Las características del subsuelo originan que el manejo y disposición de los desechos representen un potencial de contaminación del acuífero, principal fuente de abastecimiento para la población. El mayor componente de la basura son los residuos alimenticios y un alto contenido de materia orgánica que incrementan su porcentaje biodegradable. El clima cálido prevaleciente en la región y la humedad aumentan la velocidad de putrefacción de los desechos, haciendo que antes de 24 horas de generados se encuentren en la etapa acidogénica, que son substratos adecuados para la proliferación de agentes transmisores de enfermedades. Los resultados indican que el agua subterránea subyacente al basurero es la más contaminada. Las concentraciones de los parámetros estudiados se incrementaron considerablemente en la época de lluvias, debido a la generación de lixiviados, que adquieren sales disueltas de los desechos, que al infiltrarse llegan al acuífero.

Palabras claves acuífero cárstico; contaminación de aguas subterráneas; lixiviado; basureros; Yucatán

Contamination of the Yucatan aquifer by leachate from municipal waste

Abstract Merida, Yucatan is the main urban centre of southeast Mexico. The ground characteristics and the waste management and disposal practices there result in a potential for contamination of the aquifer that is the main source for water supply purposes. The waste is composed primarily of food residues and a high content of organic matter which increase its biodegradable proportion. The hot climate prevailing in the area, and the humidity, increase the rate of putrefaction of wastes in such a way that within 24 hours of disposal they undergo an acidogenic phase, becoming adequate substrates for vectors that transmit diseases. Results indicate that groundwater underlying the waste disposal site is the most contaminated. The concentrations of studied contaminants increased considerably during the rain season because of leachate generation, dissolving salts from wastes and infiltrating down to the aquifer.

Key words karstic aquifer; groundwater contamination; waste disposal site; leachate; Yucatan

INTRODUCCION

La ciudad de Mérida se encuentra enclavada en una plataforma calcárea con una superficie cárstica que presenta hoyos, hendiduras, agujeros y cavidades y una casi total ausencia de suelo. Como los suelos son muy delgados y a veces inexistentes, la característica cárstica regional impide la formación de cauces, permitiendo que la lluvia encuentre fácilmente conductos para su infiltración directa al subsuelo cuyo nivel freático se encuentra a 5 m de profundidad aproximadamente.

Hasta abril de 1998, la disposición final de residuos recolectados en la ciudad de Mérida, Yucatán, México, se realizó en el tiradero municipal (Fig. 1). En este sitio se conformaron los residuos sólidos implementando el método de área. Los desechos se depositaron en el área sin impermeabilización en el fondo y sin colectores de lixiviado y muchas veces sin cubierta superficial por largo tiempo. Después de cinco años de actividad, el sitio se encuentra actualmente cerrado pero aún no se elabora un plan para su remediación y clausura definitiva, el cual está contemplado en el Plan de Desarrollo Municipal 2004–2007 (Ayuntamiento de Mérida, 2004).

Se sabe que la basura sufre un proceso de descomposición y fermentación después de depositarla en un sitio de disposición final. Sin embargo, es muy difícil predecir tal descomposición debido a la heterogeneidad del material y al poco conocimiento que existe sobre los mecanismos de descomposición que operan en la basura. Estudios realizados en México (Esquinca *et al*., 1997; Gaxiola, 1997; CNA, 1997; SEDESOL, 1994) indican que la materia orgánica domina en porcentaje en la composición de los desechos.

Como consecuencia de la descomposición de los desechos sólidos se producen líquidos percolados o lixiviados y gases que después de atravesar las celdas de basura pasan a los suelos afectándolos de manera nociva (Trejo, 1996). Esta es una de las razones por lo que en la actualidad dichos lixiviados son objeto de estudio.

Copyright © 2006 IAHS Press

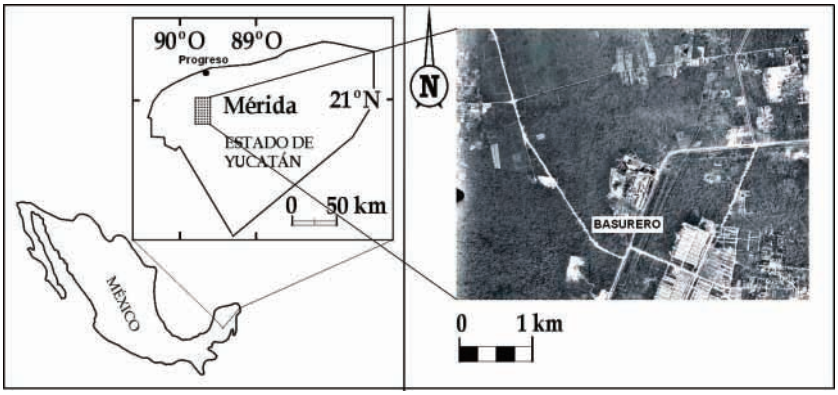


Fig. 1 Ubicación del basurero municipal de Mérida, Yucatán.

METODOLOGIA

En el afán de obtener muestras representativas del lixiviado que percola del basurero se implementó un dispositivo que permitiera la interceptación del mismo, para su posterior análisis (González & Kú, 2002). Con la recolecta semanal de muestras de lixiviado se realizaron las pruebas físicas, químicas y sanitarias del mismo.

Se implementó una red de monitoreo de agua subterránea tomando en consideración lo siguiente: (a) el desplazamiento de los contaminantes tiene la misma dirección hacia la cual fluye el agua subterránea local; (b) la ubicación de pozos alrededor del tiradero municipal, el cual se considera como la fuente de contaminación del sistema, permitió detectar la pluma de contaminación y su desarrollo con el tiempo; (c) los pozos de monitoreo dentro del tiradero municipal dieron la pauta en cuanto a la calidad del agua subterránea en la porción acuífera por debajo del mismo. Esto tuvo como finalidad definir los parámetros que caracterizan a la contaminación. La toma de muestras de agua subterránea fue a nivel freático, trimestralmente, durante los meses de enero, abril, julio y octubre. La periodicidad de los muestreos se determinó considerando, dentro del ciclo hidrológico, las épocas de sequía y lluvias en la zona, y en base a la experiencia de estudios previos sobre calidad del agua subterránea en el Estado de Yucatán (Frías & Gómez, 1985).

En el campo se realizaron determinaciones de temperatura, pH, conductividad eléctrica, oxígeno disuelto y Eh, introduciendo una sonda multiparamétrica; asimismo, se determinó la alcalinidad inmediatamente antes de colectar las muestras en el pozo en cuestión. Se preservaron las muestras para la determinación posterior de iones principales, parámetros sanitarios y metales, en el laboratorio.

Entre los parámetros físicos medidos en el laboratorio, se tomaron en cuenta la temperatura, salinidad, conductividad y también se midió el pH. Los elementos químicos que se analizaron en el laboratorio son los que por su concentración juegan un papel importante en la caracterización de la calidad del agua subterránea de la región. Se determinaron los iones calcio (Ca^{++}), magnesio (Mg^{++}), sodio (Na^{+}), potasio (K^{+}), cloruros (Cl^{-}), carbonatos ($CO_3^{=}$), bicarbonatos (HCO_3^{-}), sulfatos ($SO_4^{=}$) y nitratos (NO_3^{-}). También se determinaron los compuestos químicos como la alcalinidad total, la dureza carbonatada de calcio y magnesio y la dureza total. Al igual que para el lixiviado, las técnicas de análisis empleadas son las publicadas en el Standard Methods for the Examination of Water and Wastewater (APHA *et al*., 1992).

RESULTADOS

Al comparar los valores de los parámetros analizados con resultados de lixiviado de rellenos sanitarios reportados en la literatura, estos caen dentro del rango de las características químicas del lixiviado de un relleno sanitario de mayor antigüedad (Robinson, 1986) poniendo de manifiesto una mayor rapidez de descomposición de basura y generación de lixiviado en la zona. Se obtuvieron los siguientes valores promedios; pH entre 7 y 8, temperatura 30ºC y la conductividad eléctrica (CE) entre 10 000 a 25 000 µmhos cm^{-1}.

En los pozos que circundan al basurero municipal se encontraron aguas que corresponden al tipo bicarbonatada cálcica el cual predomina en la región (Coronado *et al*., 1997; Frías & Pacheco, 1997). Por el contrario, el agua que se encuentra en los pozos ubicados en y muy próximos al basurero es, en general, del tipo mixta con tendencia a clorurada sódica. Esto confirma una vez más lo establecido por Canul (1996) quien reportó que dichos puntos de muestreo son los más afectados por la contaminación que producen los lixiviados del basurero provenientes de los desechos de origen doméstico ya que se encuentran en sitios en donde éstos les llegan de manera importante (ver Fig. 2). En estos pozos se observaron las máximas concentraciones de cloruros, el cual es un ión aportado principalmente por los desechos de tipo doméstico. Las concentraciones de cloruros excedieron el límite máximo permisible para uso y consumo humano, de 250 mg L^{-1} (DOF, 1995); las más altas sobrepasan por un amplío margen el rango establecido para aguas naturales, hasta un máximo de más de 4500 mg L^{-1}.

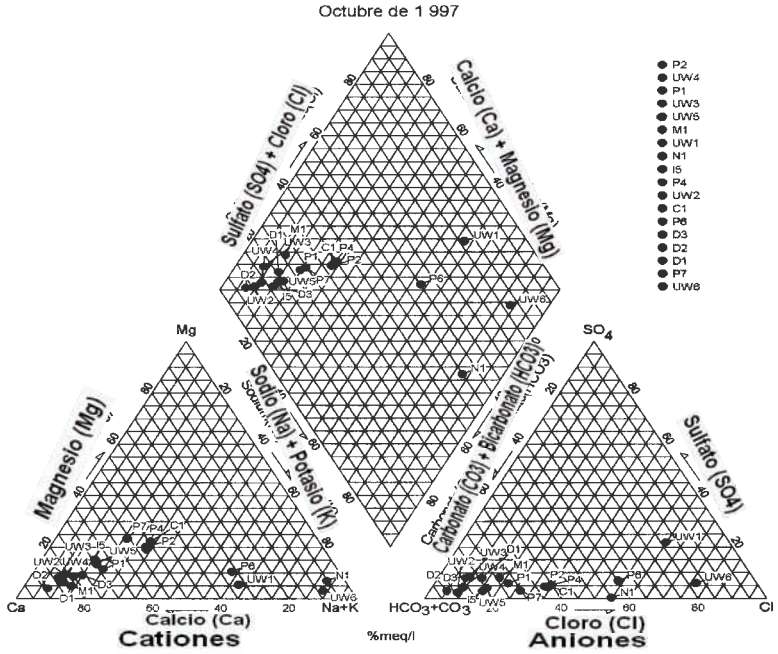


Fig. 2 Clasificación del agua subterránea en la zona de estudio, según el diagrama de Piper.

El agua contaminada se dispersa en el agua subterránea produciendo un efecto de mezcla que ocasiona una dilución de los contaminantes y por consiguiente una disminución en las concentraciones a medida que aumenta la distancia de los pozos de muestreo con respecto al basurero (Fig. 3). La Fig. 4 muestra que el incremento de la relación Cl^-/HCO_3^- es proporcional a la conductividad eléctrica demostrando la mineralización del agua al convertirse al tipo clorurada con el tiempo; esto es, el agua subterránea está afectada por el lixiviado que se produce en el basurero. La tendencia, en incremento, de la curva indica el avance de la contaminación en dirección N–NW que concuerda con el movimiento natural del flujo del agua subterránea en la zona.

En el caso del basurero el diagrama de Wilcox (Fig. 5) indica que el agua de los pozos que circundan al mismo es del tipo C_3S_1; es decir, tiene un alto contenido salino y un bajo contenido en sodio. En tanto que los pozos del interior son del tipo C_4S_2; o sea, tienen una cantidad de sales disueltas muy alta y un alto contenido de sodio.

CONCLUSIONES

El clima cálido que prevalece en la zona incrementa la velocidad de putrefacción de los desechos generando lixiviados los cuales rápidamente entran a la etapa acidogénica. El lixiviado producido se encuentra en el rango de la composición de líquidos lixiviados de basuras domésticas en otras partes del mundo, con características químicas del lixiviado de un relleno sanitario de mayor antigüedad.

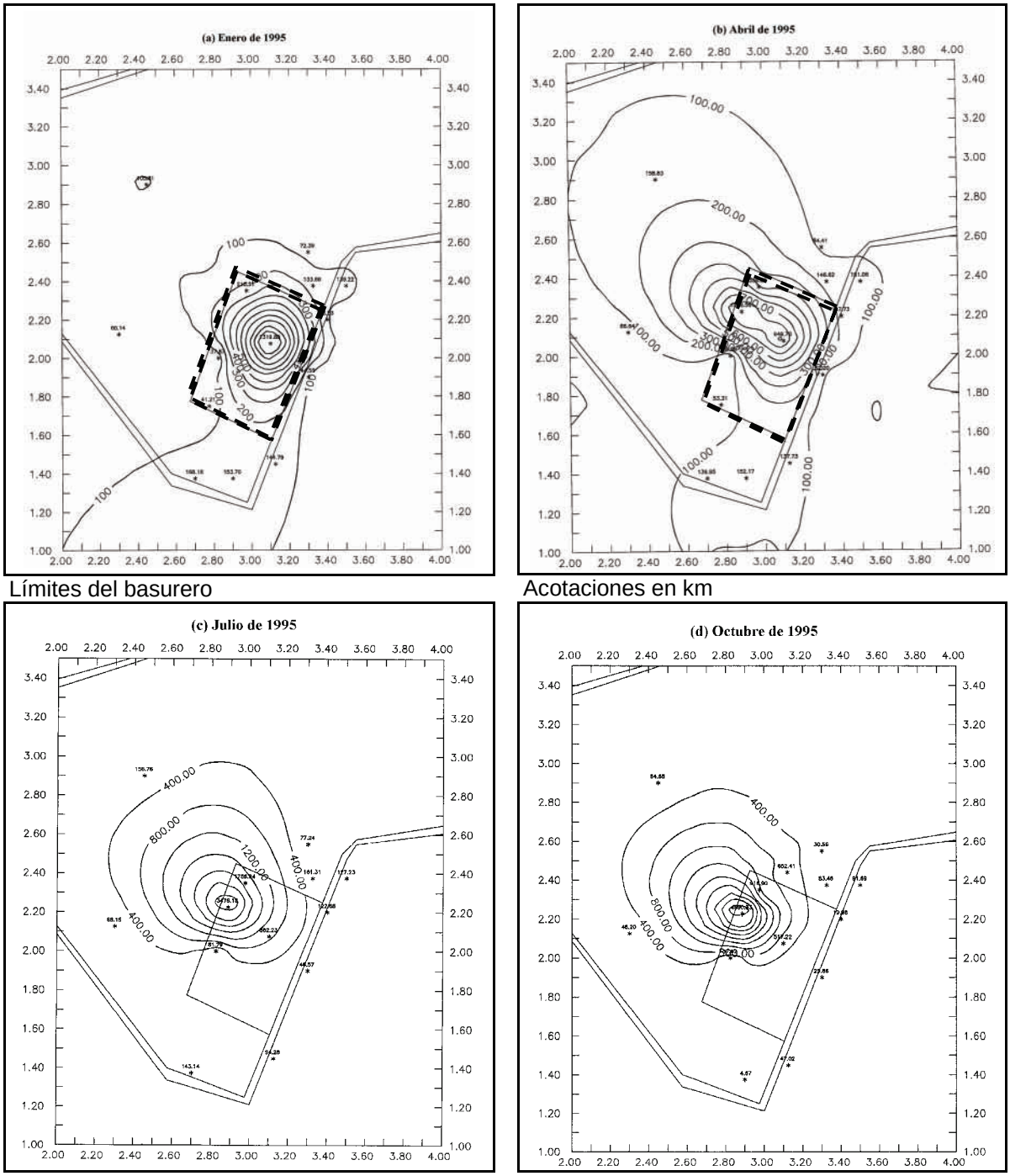


Fig. 3 Mapa de isoconcentraciones de cloruros en el agua subterránea a nivel freático (mg L^{-1}).

Los pozos de monitoreo más próximos al basurero fueron los que presentaron las máximas concentraciones para todos los parámetros analizados. El elevado contenido de cloruros encontrado en éstos, pone de manifiesto que son los más afectados por la contaminación por desechos de tipo doméstico.

La mayoría de los pozos excedió los límites establecidos para considerar que el agua es de buena calidad; por lo que esta no puede ser empleada como agua de consumo, especialmente la de los pozos más próximos al tiradero.

La disminución de las concentraciones de los parámetros estudiados pudo ser causada por un proceso de dilución de las mismas ya que el agua contaminada se mueve siguiendo el flujo de agua subterránea y al entrar en contacto con la que proviene de la precipitación pluvial se mezclan

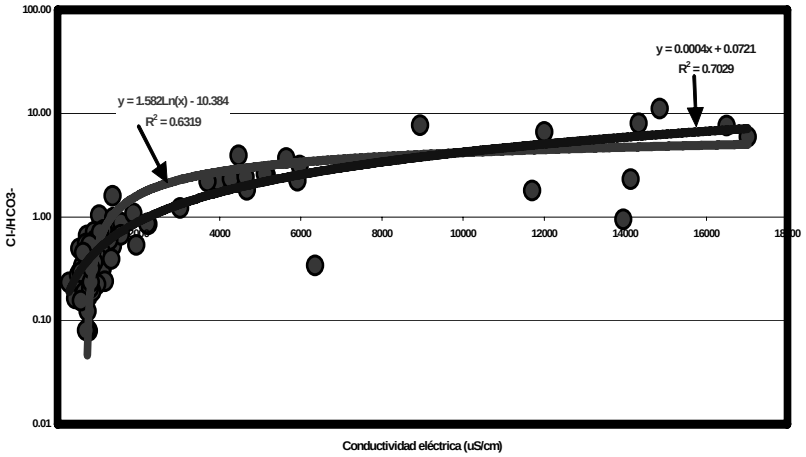


Fig. 4 Relación del índice Cl^-/HCO_3^- con la conductividad eléctrica del agua subterránea del área de estudio.

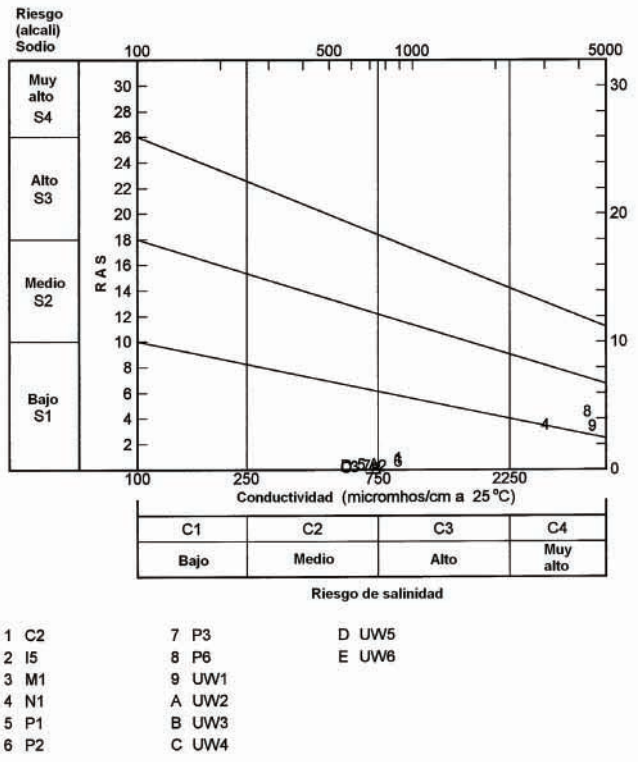


Fig. 5 Clasificación del agua subterránea, en la zona de estudio, para riego.

produciéndose este proceso hidroquímico. La pluma de contaminación se movió durante casi todo el ciclo anual en dirección N–NW.

El tipo de agua de los pozos que circundan al basurero municipal de la ciudad de Mérida pertenece al tipo bicarbonatada cálcica que es el tipo de agua que predomina en la región, en tanto que la de los pozos que están dentro y muy próximos a él, pertenecen al tipo mixto con tendencia al tipo clorurada sódica.

Las conductividades eléctricas permiten concluir que el acuífero contiene una gran cantidad de iones en disolución; este parámetro es proporcional a la relación Cl^-/HCO_3^-. La tendencia, en incremento, indica el avance de la contaminación en dirección natural del flujo de agua subterránea en la zona.

El agua que subyace al basurero municipal no puede ser empleada como agua de riego a menos que se seleccionen plantas que sean tolerantes a un alto contenido de sales disueltas. Se podría utilizar para regar cualquier tipo de suelo, incluyendo al del propio basurero; sin embargo, no es recomendable hacerlo ya que las concentraciones de sodio se incrementan en la época de recarga.

De llegar a concretarse la clausura definitiva del actual basurero municipal, no se puede garantizar que las concentraciones de sodio tenderán a disminuir, puesto que los contaminantes seguirán infiltrándose al medio subterráneo por tiempo indefinido ocurriendo el fenómeno citado en la época de lluvias.

Agradecimientos Los autores agradecen el apoyo brindado para la realización de los proyectos 1864-T9212 y 32489-T por el CONACYT y el YUC-2002-C01-8724 por los Fondos Mixtos del CONACYT y el Gobierno del Estado de Yucatán.

REFERENCIAS

APHA *et al.* (1992) *Standard Methods for the Examination of Water and Wastewater* (18th edn) (ed. by A. E. Greenberg, L. S. Clesceri & A.D. Eaton). APHA, AWWA & WEF (American Public Health Association, American Water Works Association and Water Environment Federation), USA.

Ayuntamiento de Mérida (2004) *Plan de Desarrollo Municipal 2004 – 2007*. Mérida, Yucatán, México.

Canul, J. L. (1996) *Hidrogeoquímica del Basurero Municipal de Mérida y su Zona Circundante*. Tesis de Licenciatura en Química Industrial. Facultad de Ingeniería Química. Universidad Autónoma de Yucatán. Mérida, Yucatán, México.

CNA (Comisión Nacional del Agua) (1997) *Diagnóstico de la Región XII. Península de Yucatán*. Comisión Nacional del Agua. Subdirección General de programación. Gerencia de Planeación Hidráulica. Gerencia Regional de la Península de Yucatán. Subgerencia de Programación. México, D.F.

Coronado, V. M., Pacheco, J. G. & Cabrera, S. A. (1997) Calidad del agua subterránea al norte de Mérida, Yucatán. *Ingeniería. Revista Académica de la Facultad de Ingeniería. Universidad Autónoma de Yucatán* **1**(1), 69–79.

DOF (*Diario Oficial de la Federación*) (1995) NOM-127-SSA1-1994. Salud ambiental, agua para uso y consumo humano. Límites permisibles de calidad y tratamientos a que debe someterse el agua para su potabilización. 30 de noviembre de 1995.

Esquinca, C. F., Escobar, J. L., Hernández, L. A., Sánchez, L. G., & Suárez, H. D. (1997) Estudio de la caracterización y generación de residuos sólidos municipales en 5 localidades de la costa del estado de Chiapas. En: *Memorias Técnicas. XI Congreso Nacional de Ingeniería Sanitaria y Ciencias Ambientales* (Zacatecas, Zac., México. Del 4 al 7 de noviembre de 1997), tomo II, 436–446.

Frías, J. & Gómez, J. A. (1985) *Diseño de una Red de Monitoreo para el Control de la Calidad del Agua*. Tesis de Licenciatura en Química Industrial. Facultad de Ingeniería Química. Universidad Autónoma de Yucatán. Mérida, Yucatán, México.

Frías, J. & Pacheco, J. G. (1997) Evolución y fenómenos modificadores de la calidad del agua subterránea en el estado de Yucatán. *Ingeniería. Revista Académica de la Facultad de Ingeniería. Universidad Autónoma de Yucatán* **1**(1), 45–55.

Gaxiola, C. E. (1997) El sistema de Manejo de desechos sólidos municipales en Culiacán Sinaloa. En: *Memorias Técnicas. XI Congreso Nacional de Ingeniería Sanitaria y Ciencias Ambientales* (Zacatecas, Zac., México. Del 4 al 7 de noviembre de 1997), tomo II, 448–496.

González, R. A. & Kú, L. H. (2002) Muestrador de lixiviados para SDFDS que no cuentan con sistemas de recolección. XVIII Congreso Interamericano de Ingeniería Sanitaria y Ambiental. "Gestión Inteligente de los Recursos Naturales" Desarrollo y Salud! Cancún, Quintana Roo, México. Octubre 27 a Noviembre 1º. Anales del Congeso. En CD.

Robinson, W. (1986) *The Solid Waste Handbook: A Practical Guide*. John Wiley and Sons Inc., New York, USA.

SEDESOL (Secretaría de Desarrollo Social) (1994) Dirección General de Infraestructura y Equipamiento. Subsecretaría de Desarrollo Urbano. México, D.F.

Trejo, R. (1996) *Procesamiento de la Basura - México*. Editorial Trillas. México, D.F.

Climate Variability and Change—Hydrological Impacts (Proceedings of the Fifth FRIEND World Conference held at Havana, Cuba, November 2006), IAHS Publ. 308, 2006.

Interpolation of water balance components for Costa Rica

FEDERICO GÓMEZ[1], IRINA KRASOVSKAIA[2], LARS GOTTSCHALK[3] & ETIENNE LEBLOIS[3]

1 *Centro Nacional de Planificación Eléctrica, Instituto Costarricense de Electricidad, Sabana Norte, San José 10032-1000, Costa Rica*
fgomezd@ice.go.cr

2 *Department of Geosciences, University of Oslo, PO Box 1022 Blindern, N-0315 Oslo, Norway.*

3 *Cemagref, 3 bis quai Chauveau, CP220, F-69336 Lyon cedex, France*

Abstract Patterns of spatial variation of precipitation and runoff have been studied at the annual time scale for Costa Rica. Stochastic interpolation using data from the meteorological and hydrological networks were used to produce digital precipitation maps, as well as runoff maps. In the latter case the basin area has been taken into account. The maps were produced by integrating along the rivers to achieve basin-average values. Linking these estimated basin values for the two studied variables assists in developing the water balance constraints. It proved to be an excellent diagnostic tool for data in an exploratory phase of studying patterns of variability. The development of the maps assisted in gaining insight into the basic processes such as systematic underestimation of precipitation in areas with cloud forest due to "horizontal precipitation", local patches of very high precipitation or of rain shadow as well as basins with leakage to deep groundwater.

Key words stochastic interpolation; water balance; Costa Rica

INTRODUCTION

Map representation of spatial and temporal variability of water balance components has many areas of application. Mean annual runoff (MAR) is the basic variable for the majority of hydrological studies (Gottschalk & Krasovskaia, 1998) and it has been chosen as a starting element for estimation of all other runoff characteristics (e.g. Krasovskaia *et al*., 2006; Pacheco *et al*., 2006) in the frame of a larger study of minimum acceptable flow (Laporte *et al.*, 2006). Mean annual runoff is a robust characteristic that can be estimated with relatively high accuracy. At the annual scale the small time scale dynamic processes are smoothed. At this level, both input data and interpolated output can be controlled as the water balance should be closed. Indeed, the interpolated (and observed) runoff values should not exceed the precipitation values for the same basin.

The study presents the interpolation of precipitation and runoff for the basins of Costa Rica. Special attention is given to the accuracy of the results for the available data using the interpolated basin precipitation to diagnose discrepancies in runoff and precipitation data.

DATA USED

Annual precipitation for 178 stations and annual runoff for 66 runoff stations for the period 1979–2000 have been used in the study. There are gaps in the data series and only years with at least 80% of data were considered. The number of series used varied between the years; on average 87% of precipitation and 79% runoff series were used each year. Hydrological years (from May to April) were used for both precipitation and runoff. The location of stations is shown in Fig. 1.

There are many places with no stations at all (e.g. southwestern Pacific) or very few stations (e.g. northwestern Pacific, northeastern and southeastern Caribbean). As the interpolation schemes are based on the observed data, in the regions without observations the error in the interpolated values might be large. In regions close to the high mountain chain dividing Costa Rica into Caribbean and Pacific parts which have different environmental and climatic conditions, the interpolation results need to be treated with caution due to the very steep gradients.

A digital elevation model (DEM) with a resolution 500 × 500 m represents the second important data source used in interpolation routines. For comparisons and as a support for identification of the drainage net, the digitized river net of Costa Rica was used. Manually produced maps of mean annual precipitation for the period 1970–1989 (isohyets); mean annual discharges (isolines); specific runoff (isolines) and potential evapotranspiration (isolines) for the same period were used for comparisons.

Copyright © 2006 IAHS Press

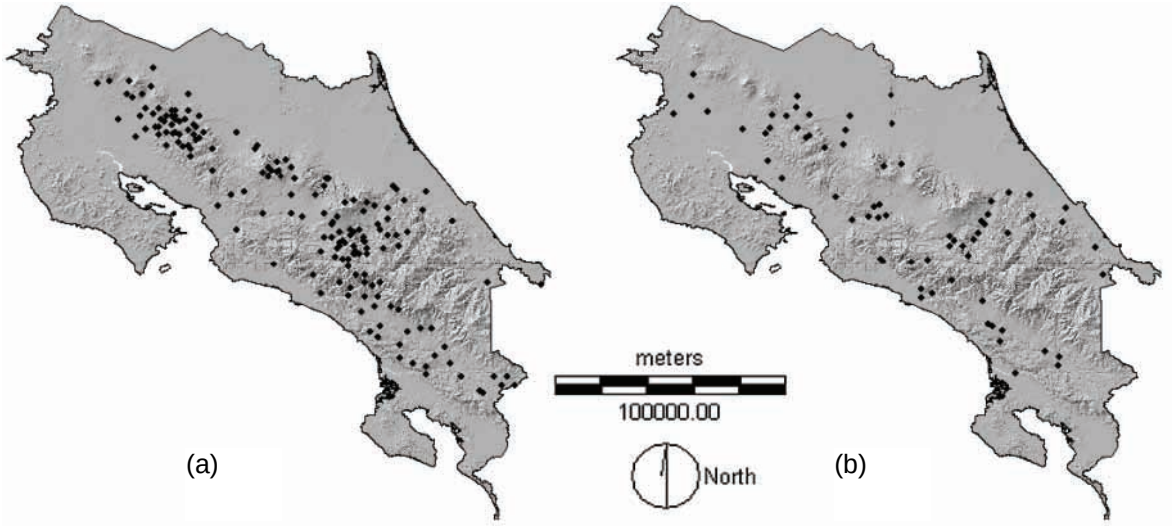


Fig. 1 Location of precipitation (a) and hydrological (b) stations.

Preparing geographical information: identification of the drainage net

The HydroDem software (Leblois & Sauquet, 2000) has been used for the identification of the drainage net using the DEM for Costa Rica. This software is specially developed for hydrological purposes and its main advantage is that it allows building of a hierarchically consistent drainage pattern. It also allows determination of a drainage basin for each identified segment of a drainage net so preserving hierarchical consistency in all algorithms. The digitized map of the river network of Costa Rica has been used for comparisons and as a reference in cases where manual corrections were needed. The automatically obtained drainage net showed good agreement with the digitized one except for the plain regions (northern Caribbean region), for which the resolution of the DEM was too coarse. The accuracy of identification of the drainage patterns was tested using the routines within HydroDem based on comparing estimated basin areas to the actual ones. The drainage pattern obtained served as the basis for all interpolation routines for both basin precipitation and different runoff characteristics.

Interpolation of precipitation

In meteorology automatic methods for interpolation of random fields are referred to as “objective methods” (Gandin, 1963). These methods are referred to very little in hydrological literature. On the other hand, kriging methods (Krige, 1951; Matheron, 1973) developed in geology, have been used frequently in hydrology. Kriging or Gandin interpolation is of wide use for interpolation and integration of precipitation fields (Rodriguez-Iturbe & Mejia, 1974; Creutin & Obled, 1982).

In this study, Gandin interpolation is applied for mapping precipitation for each individual year of the 22 years of observations. Climatic anisotropic semivariograms (Lebel & Labord, 1988) have been constructed for each year. An exponential semivariogram with a constant range of 12 km was fitted to the empirical semivariograms. An example is shown in Fig. 2(a). The analysis accounted for anisotropy by considering angles with the following directions: 36º (perpendicular to the main mountain system of the country); 126º (parallel to the mountains) and omnidirectional. The variation of the sill parameter (variance in space) during the period of observations seems to be independent of ENSO during 1979–2000. On average the difference in the standard deviation in space between the individual years was about 1400 mm.

Precipitation maps for the whole of Costa Rica for each year in the period 1979–2000 were obtained by applying Gandin interpolation based on the theoretical climatic semivariograms keeping the range constant and allowing the sill to vary between years. An example of such a map is shown in Fig. 2(b). These maps give precipitation as point values. They have been averaged along rivers to obtain the basin mean annual precipitation. The algorithm for obtaining basin values from point values within HydroDem is based on conventional downstreaming procedures (for details see Leblois & Sauquet, 2000).

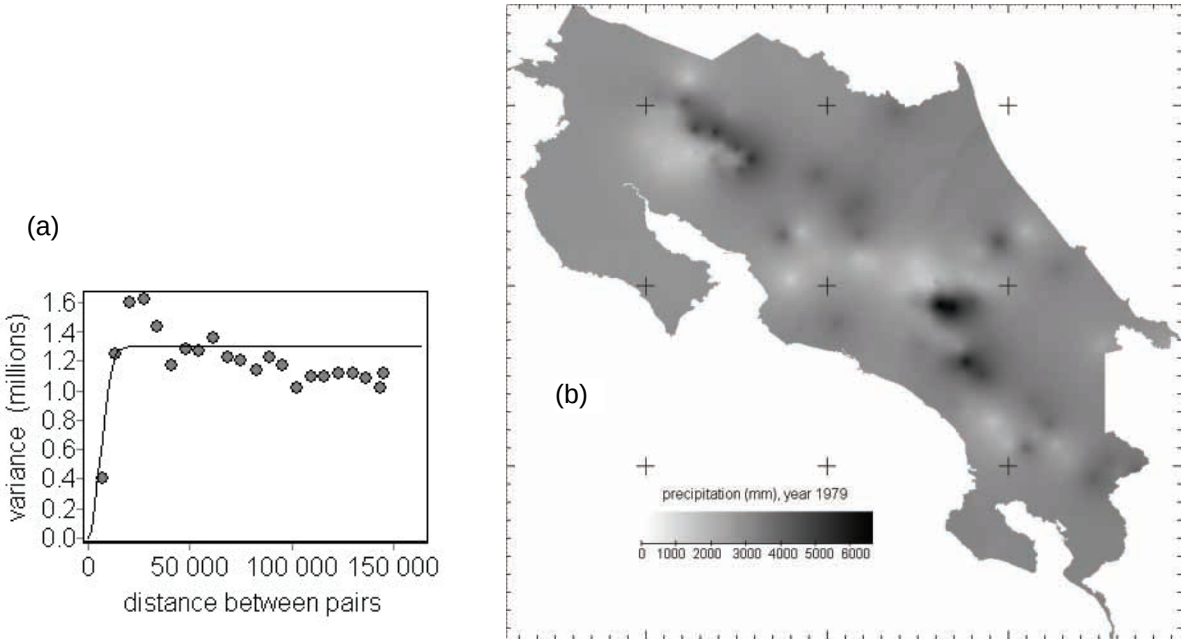


Fig. 2 (a) Empirical and theoretical (exponential) semivariograms of annual precipitation for 1979. (b) Map of annual average rainfall for 1979.

Interpolation of annual average basin runoff

Various methods have been used in hydrology for mapping annual runoff. Empirical relationships between streamflow and land use, geomorphology and climate have been frequently used for this purpose (e.g. Solomon *et al.*, 1968; Liebscher, 1972; Gustard *et al.*, 1989). The main disadvantage of this empirical approach is that the empirical relationships are valid only for the region for which they have been developed and thus are not transferable. An alternative is given by objective methods based on stochastic interpolation widely used to map point processes. There have been some attempts to apply such methods using simplified assumptions and directly interpolating runoff as a point process (Villeneuve *et al*., 1979; Hisdal & Tveito, 1993). If this approach is used properly, only data from small drainage basins can be applied so that a "point" covariance model can be constructed. A more general approach is to use Gandin interpolation with local support (Gottschalk, 1993). The support is related to the basin area. Distances between stations are in this case replaced by the average distances between basins, here referred to as Ghosh distances (Ghosh, 1951). The suggestion by Gottschalk has been followed here. The interpolation is performed in two steps. First a "point" map is produced, then secondly it is averaged to give basin runoff along rivers. Figure 3 shows an example of an integrated map along rivers for the whole period of observations.

DIAGNOSTIC TESTS OF DATA USING MEAN ANNUAL BASIN PRECIPITATION AND RUNOFF

The final precipitation as well as runoff maps for each individual year were basin averaged maps along rivers in accordance with the example in Fig. 3. Subtracting the runoff map from the corresponding precipitation map for an individual year, or as an average for the whole period, should thus result in an estimate of the actual evapotranspiration for that period. Preliminary existing estimates give the range 500–1000 mm for this variable (E. R. Chacon, personal communication). Figure 4 shows one example when the average precipitation for each basin was plotted against the registered average runoff for one year (1980). Three lines are plotted as support: one to one; 500 mm deviation and 1000 mm deviation. The discharge outliers in the graph are not confirmed by local rain estimates. On the other hand some stations show very low runoff compared to the estimated basin precipitation. In most cases with discrepancies the deviations are systematic for all years of observations. Figure 5 offers an example of a station with a systematic higher runoff than precipitation (marked with a circle in Fig. 4). The very high deviation in 1988 might have been caused by hurricane "Juana". Most of the larger deviations of this kind apply to

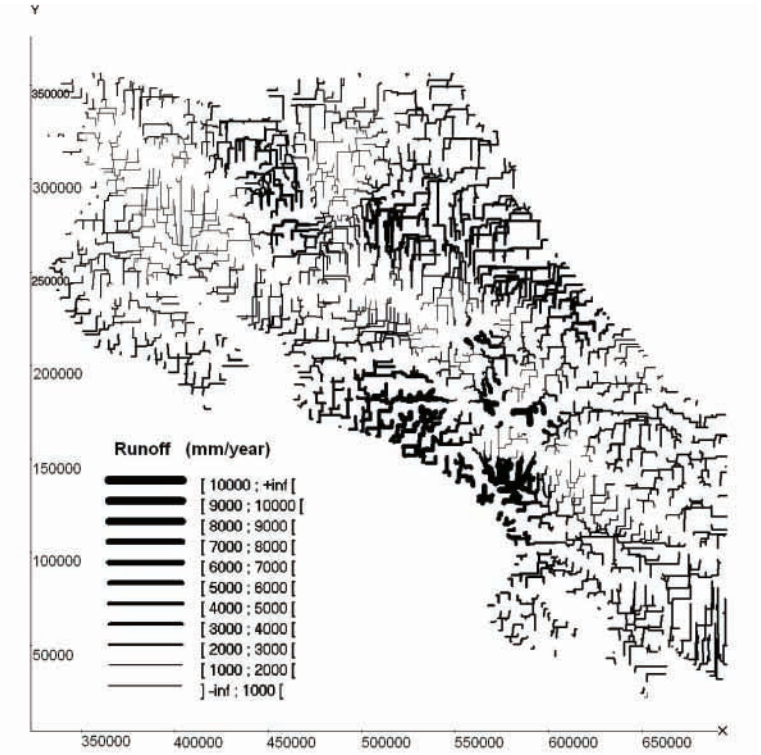


Fig. 3 Map of long-term runoff for Costa Rica averaged along rivers for basins bigger than 50 km^2.

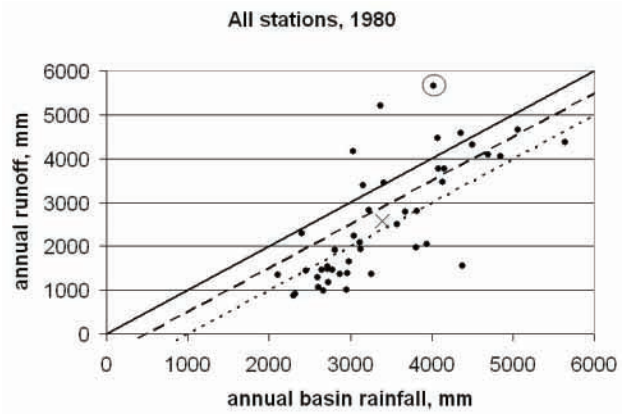


Fig. 4 Average annual basin precipitation plotted against registered average annual basin runoff for 1980. The asterisk shows the average annual precipitation and runoff for all stations for a respective year. Three lines are plotted as support: one to one; 500 mm deviation (coarse dashed) and 1000 mm deviation (dashed). The station with a systematic error is circled.

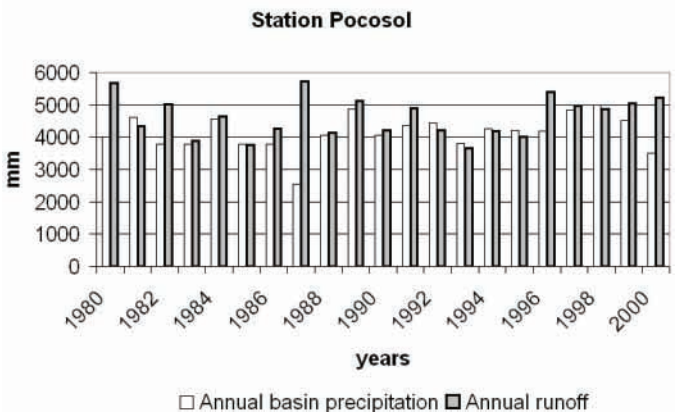


Fig. 5 Average annual basin precipitation plotted against registered average annual basin runoff for a station with systematically higher runoff than precipitation (Pocosol).

small basins in mountainous areas with strong gradients in precipitation and a lack of gauges at higher altitudes. The immediate explanations for the inconsistencies might be errors in the recorded data, poor rating curves, as well as errors induced by the interpolation methods. However, several other factors might explain the inconsistencies in the water balance, which at present are not investigated well enough:

(a) underestimation of precipitation in areas with cloud forest due to "horizontal precipitation",
(b) local patches of very high precipitation or of rain shadow not reflected by the observation network,
(c) basins with leakage to deep groundwater in volcanic/karstic areas.

CONCLUSIONS

The results of a first attempt of interpolation of water balance elements in Costa Rica using objective methods are presented. Unlike many other studies on interpolation of water balance components, these were estimated not only as point values but also as integrated values for the basins. This allowed identification of inconsistencies in data. Comparisons of the maps produced with the previous manually produced versions (E. R. Chacon, personal communication) demonstrated a good agreement except for the regions with scarce or no data. In such regions manual maps reflect implicitly the subjective experience of the meteorologist/hydrologist, which is not readily transferable. An attempt was made to coarsely close the balance using manually produced evaporation maps, and was successful in some parts and less successful in others. Such a comparison gives insight to the order of magnitude of possible errors in interpolation. The analysis also points to processes that at present are not well understood like "horizontal precipitation", local variability in precipitation and groundwater leakage. The maps obtained are now in the process of revision to incorporate changes due to the discrepancies revealed. The final version of the mean annual runoff map will be used as the basis for interpolation/regionalization of other hydrological characteristics for the basins of Costa Rica.

REFERENCES

Creutin, J. D. & Obled, C. (1982) Objective analysis and mapping techniques for rainfall fields: an objective comparison. *Water Resour. Res.* **18**, 413–439.

Gandin, L. S. (1963) *Objektivnyi analyz meteorologicheskikh polei* (Objective analysis of meteorological fields) Gidrometeoizdat, Leningrad (in Russian).

Gosh, B. (1951) Random distances within a rectangle and between two rectangles. *Bull. Calcutta Math. Soc.* **43**.

Gottschalk, L. (1993) Interpolation of runoff applying objective methods. *Stochastic Hydrol. Hydraul.* **7**, 269–281.

Gottschalk, L. & Krasovskaia, I. (1998) Grid estimates of runoff data. *WMO /TD no. 870*.

Gustard, A., Roald, L. A., Demuth, S., Lumadjeng, H. S. & Gross, R. (1989) *Flow Regimes from Experimental and Network Data (FRIEND)*. Institute of Hydrology, Wallingford, UK.

Hisdal, H. & Tveito, O. E. (1993) Generation of runoff series at ungauged locations using empirical orthogonal functions in combination with kriging. *Stochastic Hydrol. Hydraul.* **6**, 255–269.

Krasovskaia, I., Gottschalk, L, Leblois, E. & Pacheco, A. (2006) Regionalization of flow duration curves. In: *Climate Variability and Change—Hydrological Impacts* (Proceedings of the Fifth FRIEND World Conference held at Havana, Cuba, November 2006). IAHS Publ. 308 (this volume). IAHS Press, Wallingford, UK.

Krige, D. G. (1951) A statistical approach to some basic mine evaluation problems on the Witwaterstrand. *J. Chem. Metall. Min. Soc. S. Africa* **52**, 119–139.

Laporte, S., Pacheco, A. & Rodriquez, C. R. (2006) Estimation of minimum acceptable (compensatory) flow for the rivers of Costa Rica. In: *Climate Variability and Change—Hydrological Impacts* (Proceedings of the Fifth FRIEND World Conference held at Havana, Cuba, November 2006). IAHS Publ. 308 (this volume). IAHS Press, Wallingford, UK.

Lebel, Th. & Laborde, J. P. (1988) A geostatistical approach for areal rainfall statistics assessment. *Stochastic Hydrol. Hydraul.* **2**, 245–261.

Leblois, E. & Sauquet, E. (2000) Grid elevation models in hydrology. Part 1: Principles and a literature review; Part 2: HydroDem, User's Manual. Technical Notes, Cemagref, Lyon, France.

Liebscher, H. (1972) A method for runoff-mapping from precipitation and air temperature data. In: *World Water Balance* (Proc. Reading Symposium, July 1970), vol. 1, 115–121. IAHS Publication 92. IAHS-UNESCO-WMO.

Matheron, G. (1973) The intrinsic random functions and their applications. *Adv. Appl. Prob.* **5**, 439–468.

Pacheco, A., Gottschalk, L. & Krasovskaia, I. (2006) Regionalization of low flow in Costa Rica. In: *Climate Variability and Change—Hydrological Impacts* (Proceedings of the Fifth FRIEND World Conference held at Havana, Cuba, November 2006). IAHS Publ. 308 (this volume). IAHS Press, Wallingford, UK.

Rodriguez-Iturbe, I. & Mejia, J. M. (1974) On transformation of point rainfall to areal rainfall. *Water Resour. Res.* **10**(4), 729–735.

Solomon, S. I., Denouvilliez, J. P., Chart, E. J., Wooley, J. A. & Cadou, C. (1968) The use of a square grid system for computer estimation of precipitation, temperature and runoff. *Water Resour. Res.* **4**(5), 919–929.

Villeneuve, J. P., Morin, G., Bobee, B., Deblanc, D. & Delhomme, J. P. (1979) Kriging in the design of streamflow sampling networks. *Water Resour. Res.* **15**(6), 1833–1840.

Climate Variability and Change—Hydrological Impacts (Proceedings of the Fifth FRIEND World Conference held at Havana, Cuba, November 2006), IAHS Publ. 308, 2006.

Physical insights into soil water storage in the soil–plant–atmosphere system

URSZULA SOMOROWSKA

Faculty of Geography and Regional Studies, Department of Hydrology, Warsaw University, Krakowskie Przedmiescie 30, 00-927 Warsaw, Poland

usomorow@uw.edu.pl

Abstract This paper provides insights into preferential states of soil water storage that are active in the soil–plant–atmosphere system. Considerations are based on *in situ* soil moisture data and the NOAA-NCEP/NCAR re-analysis data. The major findings are: (1) re-analysis data generally reproduce the dynamics of the soil moisture detected by *in situ* observations, (2) analysis of the propagation of preferential wetness states has lead to the separation of wet and dry conditions, and (3) the applied theoretical framework sufficiently links chosen parameters of soil and climate to the relative frequency of wetness states and provides a tool for the simulation of the probability of wetness states.

Key words soil water storage; data sets; preferential states; frequency; central Poland

INTRODUCTION

The moisture content of the upper soil layers plays an important role in the soil–vegetation–atmosphere system and is integral to most of the processes present at the land–atmosphere interface. Moreover, soil moisture essentially controls relationships between precipitation, infiltration, evapotranspiration and groundwater recharge (Harter & Hopmans, 2005). Although the importance of the vadose zone in the hydrological cycle has been recognized for a long time, the dynamics of soil water is rarely controlled through regular *in situ* monitoring. Therefore the *in situ* data collected from reference sites are still an integral part of the regional monitoring and research strategies, because they provide reliable, direct estimates for the verification of conceptual models and theories. Soil moisture parameters can also be retrieved from the re-analysis of remote sensing data. One of the most widely known soil moisture re-analysis data sets is available from the National Center for Environmental Prediction/National Center for Atmospheric Research (NCEP/NCAR) that operate in the USA within NOAA (National Oceanic & Atmospheric Administration) (Kistler *et al*., 2001).

The aim of this study is to provide insights into soil water storage by comparing *in situ* measurements with the re-analysis data sets. In particular, the study investigates the existence of wet and dry modes of soil water storage, as hypothesized by D'Odorico & Porporato (2004). The specific objectives of this study were: (1) to investigate the possibility of using soil moisture re-analysis data to support *in situ* observations; (2) to document and define the propagation of preferential wetness states on seasonal and inter-annual time scales; and (3) to display the interactions between effective soil water storage and essential climate traits. Following the approach proposed by Porporato *et al*. (2004), the probability density function of effective relative soil moisture was simulated as an analytical solution of a simplified stochastic model of soil water balance. This approach links the plant-available soil water storage with rainfall and evapotranspiration parameters. An example of wetness conditions detected and modelled in the small basin of the Lasica Channel in central Poland, in moderate climate (52°13′N–52°26′N and 20°15′E–20°57′E) is presented.

DATA

A data set of soil moisture inferred from the *in situ* measurements was used for this study (Somorowska, 2005). It covers a 10-year period (1995–2004) of measurements conducted at 14 experimental sites in the Lasica basin. In addition, soil moisture data from two soil layers (0–10 cm and 10–200 cm) were inferred from surface variables of the NOAA-NCEP/NCAR re-analysis project. The extracted data was from the grid point 52.38°N, 20.625°E, which completely covers the area of the analysed basin. They were retrieved in the netCDF-format and processed using the NetCDF Toolbox of Matlab.

Copyright © 2006 IAHS Press

Data from the MARS-STAT Data Base Project (Monitoring Agricultural Statistics with Remote Sensing Project) were also used (Goot, 1997). Thus the data retrieved consisted of daily precipitation as well as Penman potential evaporation and transpiration at a horizontal resolution of 1°. The area of the analysed basin corresponded to their internal grid number 62074.

METHODS OF ANALYSIS

Comparison of soil moisture *in situ* data with re-analysis

Using 10 years of *in situ* soil moisture data from 1995 to 2004, a comparison of soil moisture observations with re-analysis data was conducted. The values of effective relative soil moisture are compared. The effective relative soil moisture is defined in this study as $x = (s - s_w)/(s_{fc} - s_w)$, where s is relative soil moisture, s_{fc} is relative soil moisture at field capacity, s_w is relative soil moisture at the wilting point. Relative soil moisture s can be expressed as $s = \theta_v/n$, where: θ_v is fractional volumetric soil moisture, n is porosity. Thus, the effective relative soil moisture is a dimensionless parameter that can be alternatively expressed as $x = (\theta_v - \theta_{min})/(\theta_{max} - \theta_{min})$, where θ_{min} is minimum measured volumetric soil moisture relative to the wilting point and θ_{max} is maximum measured volumetric soil moisture relative to field capacity. Effective relative soil moisture derived from *in situ* data is denoted as $x_{insitu.}$ For the re-analysis data it is denoted as x_{noaa}. Since the land surface scheme in the re-analysis data has two soil layers (0–10 and 10–200 cm), both of them were retrieved, processed and presented as time series of the effective relative soil moisture. As the *in situ* soil moisture data set (1995–2004) consisted of discrete measurements, a continuous record of soil moisture was reconstructed with two-week time steps using groundwater monitoring conducted in years 1999–2004, and relations established between soil moisture and groundwater level. The set of soil moisture scaled to the effective relative soil moisture (x_{insitu}) comprises 157 values calculated at two week intervals for years 1999–2004 with a two-week interval. These values were related to the scaled re-analysis soil moisture (x_{noaa}) using regression in form of exponential function: $x_{noaa} = a \cdot \exp(b \cdot x_{insitu})$. The value of x_{insitu} was calculated for three types of soil profiles representing different soil texture, as well as for an average value derived as their mean. Both values of x_{insitu} and x_{noaa} represent effective relative soil moisture averaged over the depth, giving an insight into average wetness conditions present in the soil layer.

Propagation of wetness states

Histograms of the relative frequency of effective relative soil moisture were constructed for separate months from March to October using the daily re-analysis data from 1995 to 2004. In this way the preferential wetness states were displayed in each month, presenting a switch from wet to dry states. Additionally, the relative frequency histogram was constructed jointly for months March–October for years 1995–2004, providing an insight into preferential wetness states within vegetation period. This histogram was then applied as a background to the values of probability distribution simulated by the analytical function.

Simulating probability density function of effective relative soil moisture

Identified input values to the model simulating the probability density function of the soil moisture comprise the parameters of rainfall frequency λ (0.325 day^{-1}), mean rainfall depth α (0.48 cm), and maximum evapotranspiration ET_{max} (0.49 cm day^{-1}). All of these parameters were estimated from the MARS-STAT data base. Maximum soil water storage w_0 available to plants in the top soil layer of 0–30 cm was estimated from *in situ* data (w_0 = 6 cm). Following Porporato *et al*. (2004), the master equation of the probability density function of the soil moisture $p(x)$ can be obtained from a simple stochastic model for soil moisture dynamics. The applied equation is: $p(x) = (N/\eta)x^{(\lambda/\eta)-1}\exp(-\gamma x)$ for $0 < x \leq 1$, with normalization constant N assumed as $N = (\eta\gamma^{\lambda/\eta})/[\Gamma(\lambda/\eta) - \Gamma(\lambda/\eta,\gamma)]$, where Γ is the gamma function, γ is defined as $\gamma = w_0/\alpha$ (–/–), and η is defined as $\eta = ET_{max}/w_0$ (–/–).

RESULTS

In the course of the effective relative soil moisture, the seasonal and inter-annual fluctuations are present (Fig. 1). The comparison of the soil moisture *in situ* data with the re-analysis is presented in

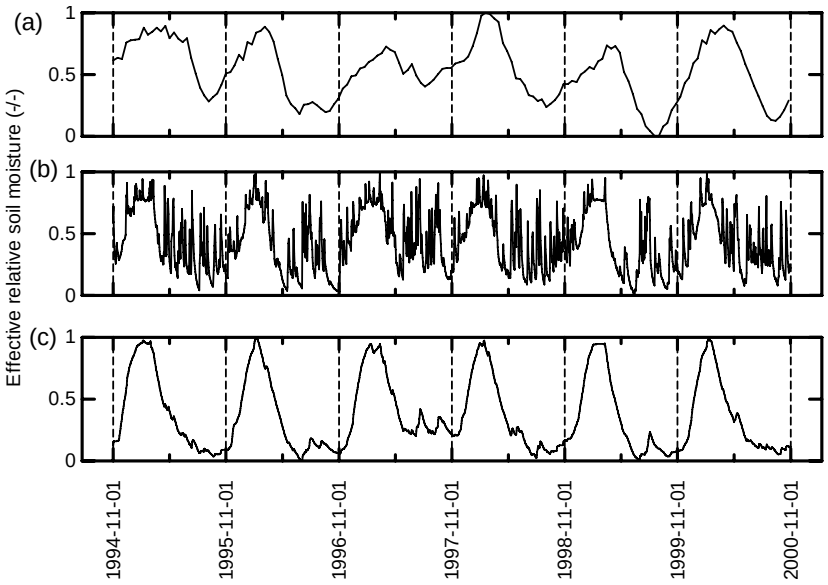


Fig. 1 Variation of the effective relative soil moisture in years 1999–2004: (a) derived from the *in situ* data as an average in three different types of soil profiles; (b) retrieved from re-analysis, averaged over the depth of 0–10 cm; and (c) retrieved from re-analysis, averaged over the depth of 10–200 cm.

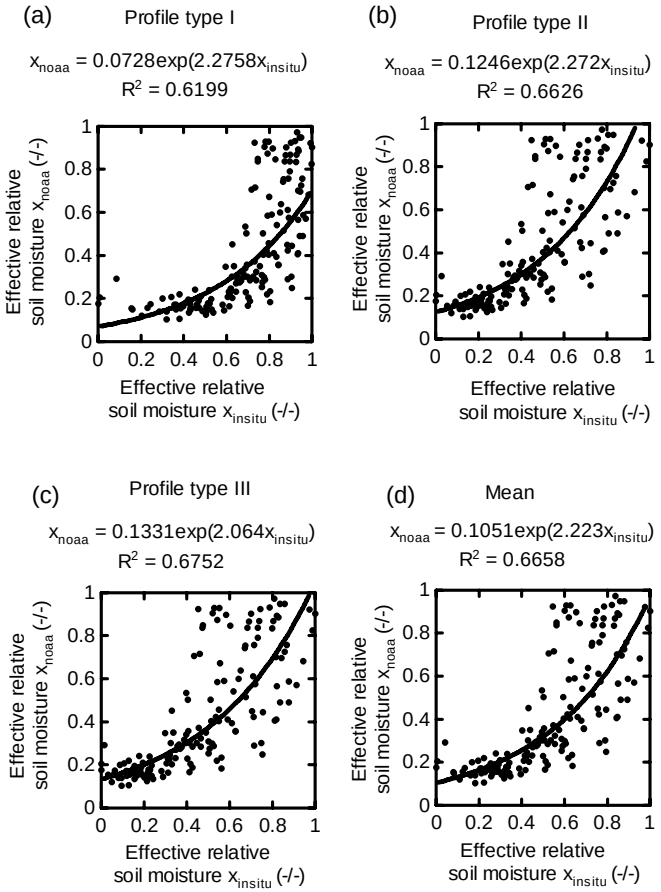


Fig. 2 Relationship between values of the effective relative soil moisture retrieved from re-analysis as dependent on the *in situ* data: (a) profile type I, (b) profile type II, (c) profile type III, (d) mean value.

Fig. 2. The effective relative soil moisture was derived for three different types of soil moisture profiles and for their mean. The value of the coefficient of determination R^2 shows that most of the variance between the considered variables is explained by the regression. However, its value is the smallest for the profile type I, which is highly influenced by very shallow groundwater level and high retention capacity in the upper soil layers. The model has higher R^2 values and a better overall fit for type II and III profiles which are generally of drier regime. Assuming that most of the variance is explained by the regression, it is concluded that the re-analysis data generally reproduce the dynamics of the soil moisture detected in the *in situ* observations.

The dominant states of wetness conditions on a monthly basis are presented in Fig. 3. In March the dominant state detected has an effective relative soil moisture between 0.7 and 0.8, 0.4 and 0.5 in April, and in 0.2–0.3 in May–October. Thus there is a gradual propagation of wet state conditions in March to dry state conditions between May and October. The dominant state detected for the whole season March–October is within the range of 0.2–0.3 (Fig. 4(a)). The simulated relative frequency of effective relative soil moisture presented in Fig. 4(b) generally reproduces the values estimated in the histogram. Comparison of empirical and simulated values is presented in Fig. 4(c). The simulated frequencies generally fit the empirical values (Fig. 5).

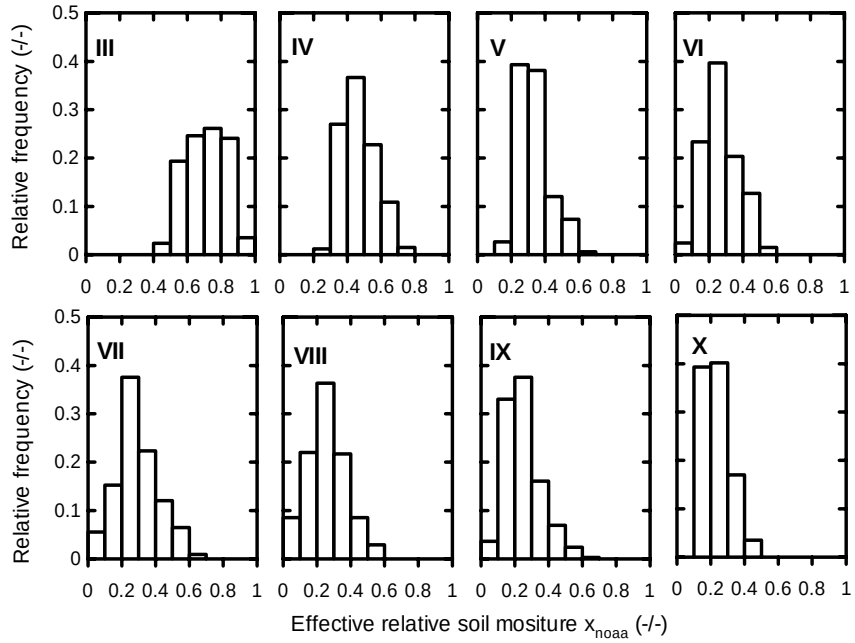


Fig. 3 Frequency histograms of the effective relative soil moisture in particular months of the March–October season in years 1995–2004, based on the re-analysis data.

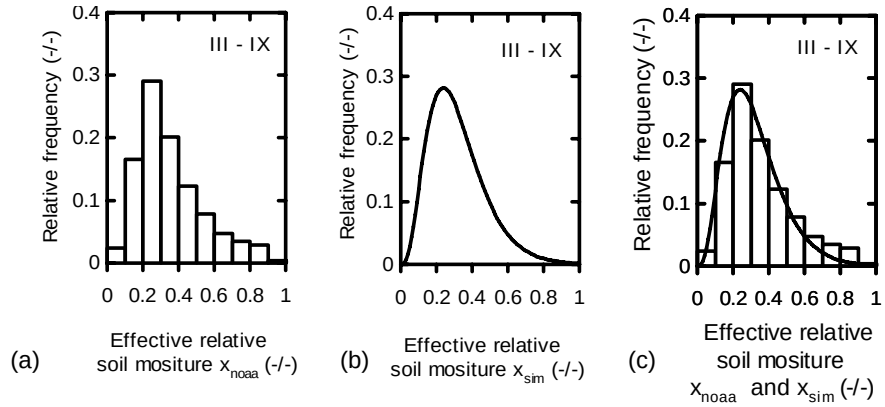


Fig. 4 Simulation of the relative frequency of the effective relative soil moisture in months March–October in years 1995–2004: (a) empirical relative frequency, (b) relative frequency based on probability density function according to Rodriguez-Iturbe & Porporato (2004), (c) comparison of the empirical and simulated values of relative frequencies.

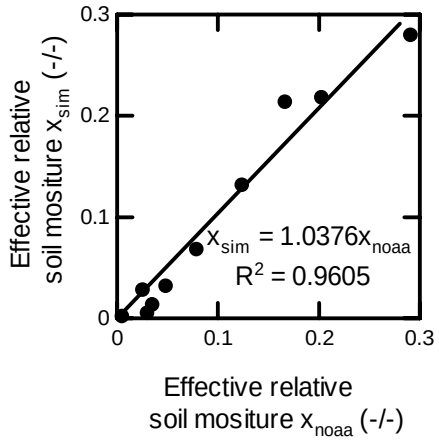


Fig. 5 Values of the simulated relative frequencies as related to the empirical relative frequencies retrieved from re-analysis.

Thus it can be concluded that the applied theoretical framework sufficiently links the chosen parameters of soil and climate and provides a tool for simulations in modified climate conditions. Re-analysis data can be applied in support of *in situ* data however further investigations on discrepancies are required.

Acknowledgements The soil moisture research has been supported by the Department of Environmental Sciences and Policy of the Central European University, Budapest by Grant no. 92-14. Additional support has been received from the Committee for Scientific Research, Ministry of Science, Poland as the Investment Grant no. 4441/IA/115/2003. NCEP/NCAR re-analysis data were obtained from the NOAA-CIRES Climate Diagnostics Center, Boulder, Colorado, USA, from their web site at http://www.cdc.noaa.gov/. MARS-STAT data were obtained from the Joint Research Centre, Institute for the Protection and Security of the Citizen, Agriculture & Fisheries Unit, Ispra, Italy, from their web site at http://agrifish.jrc.it/marsstat/datadistribution/.

REFERENCES

D'Odorico, P. & Porporato, A. (2004) Preferential states in soil moisture and climate dynamics. *Proc. Nat. Acad. Sci. USA.* **101**(24), 8848–8851.

Goot, E., van der (1997) Technical description of interpolation and processing of meteorological data in CGMS. Joint Research Centre of the European Commission, Ispra, Italy.

Harter, T. & Hopmans, J. W. (2005) Role of vadose-zone flow processes in regional scale hydrology: review, opportunities and challenges. In: *Unsaturated-Zone Modeling: Progress, Challenges and Applications* (ed. by R. A. Feddes, G. H. de Rooij, & J. C. van Dam), 179–208. (Papers for the FRONTIS Workshop, 3–5 October 2004, Wageningen, The Netherlands).

Kistler, R., Kalnay, E., Collins, W., Saha, S., White, G., Woollen, J., Chelliah, M., Ebisuzaki, W., Kanamitsu, M., Kousky, V., van den Dool, H., Jenne, R. & Fiorino, M. (2001) The NCEP-NCAR 50-year reanalysis: Monthly means CD ROM and documentation. *Bull. Amer. Meteorol. Soc.* **82**, 247–267.

Porporato, A., Daly, E. & Rodríguez-Iturbe I. (2004) Soil water balance and ecosystem response to climate change. *Am. Naturalist* **164**(5), 625–632.

Somorowska, U. (2005) Temporal patterns of subsurface water storage inferred from the TDR measurements. In: *Progress in Surface and Subsurface Water Studies at Plot and Small Basin Scale* (ed. by F. Maraga & M. Arattano). (Proc. 10th ERB Conf., October 2004, Turin, Italy). IHP-VI, Technical Documents in Hydrology no.77, 27–34. UNESCO, Paris, France.

Climate Variability and Change—Hydrological Impacts (Proceedings of the Fifth FRIEND World Conference held at Havana, Cuba, November 2006), IAHS Publ. 308, 2006.

Determination of the soil hydrophysical characteristics and vegetation parameters of a river basin in a permafrost region

YEUGENIY GUSEV & OLGA NASONOVA

Institute of Water Problems, Russian Academy of Sciences, Gubkina St. 3, Moscow 119991, Russia
gusev@aqua.laser.ru

Abstract This paper describes two techniques for estimating the soil hydrophysical and vegetation parameters required for runoff modelling using the land surface model SWAP (Soil Water–Atmosphere–Plants): (1) *a priori* parameter estimation on the basis of information on spatial distribution of different soil and vegetation types within a basin, and (2) optimization of the most influencing parameters by means of model calibration to measured daily streamflow. The estimated sets of parameters were applied for runoff simulations using the SWAP model and the data measured during a 10-year period (1969–1978) at the Kolyma water balance station located within the permafrost zone of the Kontaktovyi Creek basin, in the upper course of the Kolyma River, Russia. The values of runoff from several watersheds and sub-basins (area: from 0.27 to 21.2 km^2) of the Kontaktovyi Creek basin were simulated using *a priori* estimated and calibrated parameters and were compared with each other and with observations. For daily streamflow, application of calibrated parameters, instead of *a priori* estimated, resulted in an increase of the efficiency of simulations, on average from 0.38 to 0.55, and the coefficient of correlation from 0.66 to 0.77. The bias was reduced from 14 to 17%.

Key words *a priori* parameter estimation; land surface modelling; parameter calibration; permafrost zone; river runoff

INTRODUCTION

Recent investigations aimed at physically-based modelling of a complex and multifactor Soil–Vegetation/snow cover–Atmosphere System (SVAS), has resulted in Land Surface Models (LSMs) that treat the processes of heat and water exchange within SVAS from simple parameterization schemes. These models, which were originally intended for setting boundary conditions in atmospheric general circulation models, can be applied, not only in climate modelling in the context of coupled land-atmosphere models, but also for hydrological and environmental studies of broad interest. Currently the implementation of LSMs is moving towards high latitudes and highlands, which are characterized by a long and severe cold season and are among the landscapes most sensitive to natural and anthropogenic effects. Because many of these regions are within the permafrost zone, the modelling community is faced with the need to simulate heat and water exchange between the land surface and the atmosphere under permafrost conditions. Unfortunately, permafrost regions are also among the almost inaccessible and insufficiently known areas and do not have the data on soil and vegetation parameters required for LSM simulations. In this connection, the goals of the present work are to develop techniques for estimation (both *a priori* and by means of model calibration) of the land surface parameters of such basins located within the permafrost zone and to apply the obtained parameters for model simulations.

MODEL

The SWAP model (Gusev & Nasonova, 1998), used in this study, is a physically based land-surface model describing heat and water exchange between the land surface and the atmosphere throughout a year at local to global scales. The model is oriented towards the use of atmospheric forcing data from the lowest atmospheric layers of the GCMs (Global Circulation Models) or from any reference height. Initially, SWAP's parameterizations were designed only for non-frozen and seasonally frozen soils (Gusev & Nasonova, 1998, 2002, 2003). Recently the model was modified for permafrost conditions (Gusev & Nasonova, 2004, 2006).

Copyright © 2006 IAHS Press

HYDROLOGICAL OBJECT

The hydrological object under study is the Kontaktovyi Creek basin (area: 21.2 km^2), a highland area located in the upper course of the Kolyma River (61°53′N, 147°43′E) in the permafrost zone of far-eastern Russia. This is an experimental basin of the Kolyma water balance station (KWBS). The absolute elevations within the basin vary from 830 to 1700 m a.m.s.l. The climate of the region is subarctic continental. Between 1969 and 1978 the average mean annual air temperature was negative (–11°C). Mean daily temperature varied from –52 to 23°C. Annual precipitation varied within a basin from 300 to 460 mm. The depth of seasonal soil thawing ranged from 0.3–0.4 to 1.5–2 m, depending on slope exposition, lithological composition of ground, vegetation and air temperature.

For the simulation of streamflow, the Kontaktovyi Creek basin was divided into five sub-basins (Fig. 1(a),(b), Table 1). Because the slopes of the southern and northern expositions of the first, second and fifth sub-basins had different natural conditions, they were modelled separately. More detailed division of the basin seems to be unreasonable because of the lack of reliable data. Three types of land surface were distinguished within each calculational element: sparse larch forest growing below 1000 m, low creeping cedar, and bare areas represented by talus. Model simulations were performed for each of these land surface types and streamflow for each sub-basin was calculated as the weighted average value after accounting for the spatial coverage of each land surface type.

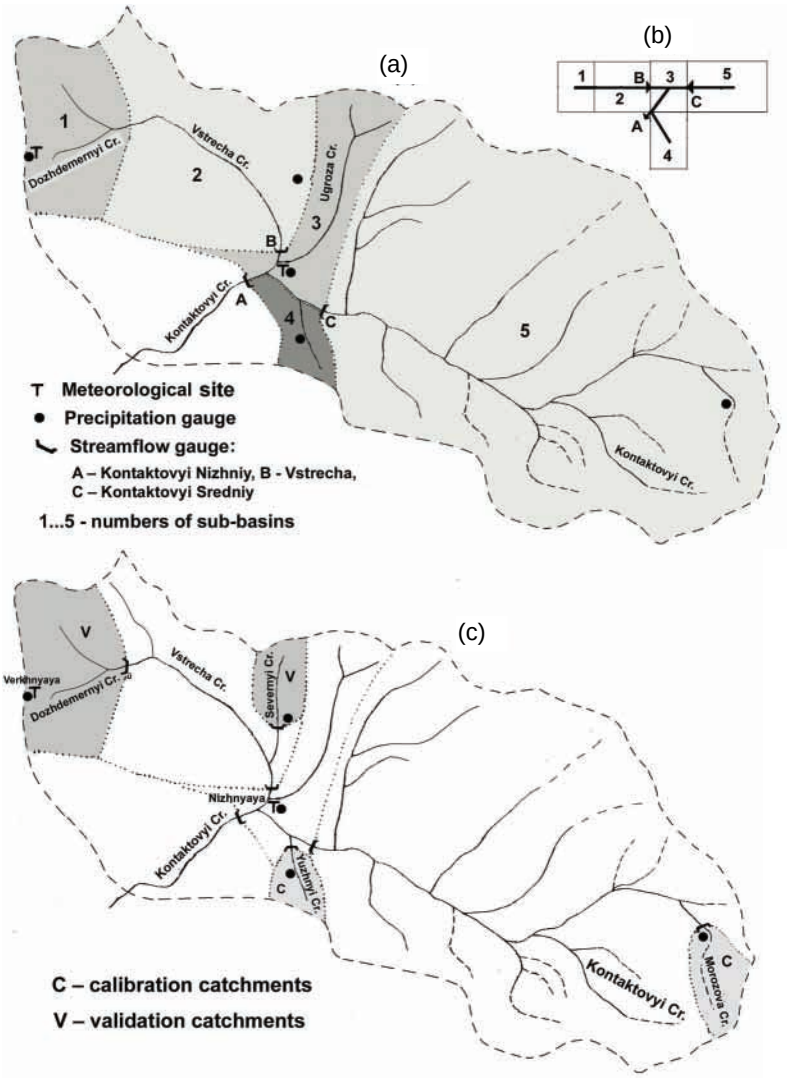


Fig. 1 Schematic representation of the Kontaktovyi Creek basin divided into five sub-basins and streamflow evaluation sites (A, B, C) (a); schematized routing directions (b); location of the four calibration and validation catchments (c).

Table 1 Characteristics of experimental catchments and calculational sub-basins within the Kontaktovyi basin.

Catchment or calculational sub-basin*	Area (km^2)	Mean altitude (m, a.m.s.l.)	The land surface type (%)		
			Talus	Short vegetation	Larch forest
Small catchments for parameters calibration and validation					
Morozova Creek	0.63	1370	100	0	0
Yuzhnyi Creek	0.27	985	25	60	15
Severnyi Creek	0.38	1020	30	45	25
Dozhdemernyi Creek	1.43	1180	68	0	32
Calculational sub-basins of the Kontaktovyi Creek basin					
1a	0.72	1180	68	0	32
1b	0.72	1180	68	0	32
2a	1.96	1050	16	33	51
2b	1.96	1000	16	33	51
3	1.18	920	20	10	70
4	0.47	960	16	38	46
5a	9.94	1150	49	22	29
5b	4.26	1000	49	22	29

*, numbers of sub-basins correspond to those given in Fig. 1; a and b near numbers are related, respectively, to the slopes of southern and northern exposition.

Two small catchments (Morozova Creek and Yuzhnyi Creek) were chosen for parameter calibration. Two other catchments (Severnyi Creek and Dozhdemernyi Creek) were used for validation (Fig. 1(c)). The main characteristics of the catchments are presented in Table 1.

DATA

The model requires the following forcing data: air temperature and humidity, atmospheric precipitation, wind speed, air pressure and incoming short- and longwave radiation. All the forcing data, with the exception of radiation, were measured at the Nizhnyaya (1969–1978) and Verkhnyaya (1969–1972) meteorological sites located at 850 and 1220 m a.m.s.l., respectively (Fig. 1); their daily values are given in Kolymskoye UGKS (1977). Meteorological measurements (with the exception of precipitation) from the Nizhnyaya site were adjusted to the mean elevation of each calculational element using additional data from the Verkhnyaya site and accounting for the difference in the elevation of these two sites. Precipitation gauges were also located within each small experimental catchment (Fig. 1(c)) where measurements were performed daily during the warm season (May–September). During the cold season, precipitation measurements were carried out only at the Yuzhnyi and Severnyi Creek catchments once in a 10-day period. For model simulations, daily precipitation was restored for each catchment and then uniformly adjusted to 3-hr time steps. Incoming short- and longwave radiation values for each calculational element were calculated on the basis of meteorological data (with accounting for cloudiness), latitude, solar declination, view factor, average slope in meridional and latitudinal directions, and mean monthly values of atmospheric transmissivity.

Application of the SWAP model requires soil and vegetation parameters. Soil hydrophysical parameters include field capacity W_{fc}, wilting point W_{wp}, soil porosity W_{sat}, and relations of soil hydraulic conductivity k and soil matric potential ϕ with soil moisture W, i.e. $k(W)$ and $\phi(W)$. In SWAP, Clapp and Hornberger (1978) parameterizations for $k(W)$ and $\phi(W)$ are used. These parameterizations require information on soil matric potential at saturation ϕ_0, B-parameter, W_{sat}, and soil hydraulic conductivity at saturation k_0. Besides that, snow-free albedo of bare soil α_{soil} and soil depth h_{soil} are also required. As to vegetation parameters, the SWAP model needs root depth h_{root}, leaf and stem area indexes (LAI and SAI, respectively), roughness length of vegetation, zero plane displacement height, snow-free albedo of vegetation, albedo of vegetation with intercepted snow on crowns, effective linear leaf size, interception capacity of vegetation for liquid and solid precipitation. Since these parameters were not available for the selected basins, we had to estimate them by ourselves by means of techniques described in the next section.

PARAMETER ESTIMATION

A priori estimation

A priori estimation of soil and vegetation parameters was based on qualitative description of the soil and vegetation types and their spatial distribution within the Kontaktovyi Creek basin. Two soil classes (following the USDA soil texture classification) were found within the basin: sandy loam in the bottom and middle parts of the basin, and sand in its upper parts. These classes were used as predictors to determine $k(W)$ and $\phi(W)$ (including W_{sat} and k_0) in accordance with van Genuchten (1980) and the Rosetta code (Schaap *et al*., 1998). The values of ϕ_0 and B were then obtained on the basis of interpolation of the estimated $\phi(W)$ by the Clapp and Hornberger equation within the range –33 to –1500 kPa. The values of W_{wp} and W_{fc} were determined as soil moisture at ϕ = –1500 kPa and at ϕ = –33 kPa, respectively. In such a manner, the hydrophysical parameters were estimated for the two soil classes. For each catchment and sub-basin, soil parameters were calculated as weighted average values accounting for the spatial coverage of each soil class. For k_0, logarithms of k_0 were averaged. For vegetation parameters, we assigned their typical values for each vegetation type (on the basis of literature data and our experience) and then calculated their weighted average values for each catchment and sub-basin.

Calibration

To improve runoff simulations based on *a priori* parameters, six parameters (W_{fc}, W_{wp}, W_{sat}, k_0, h_{soil}, h_{root}), were optimized by minimization of the root-mean-square-deviation (*RMSD*) between the simulated and measured (during 1969–1978) daily total runoff from the two calibration catchments (Morozova Creek and Yuzhnyi Creek). Four parameters (W_{fc}, W_{wp}, W_{sat}, k_0) were optimized for two soil layers (SWAP uses two soil layers: root zone and the layer between the lower boundary of the root zone and the upper boundary of impermeable layer). Each parameter was calibrated for three land surface types. In all, 30 parameters were optimized. The model calibration was performed by means of automatic procedure for optimization based on a stochastic or Monte-Carlo technique.

RESULTS

First of all, the obtained set of optimized parameters was validated by comparison of simulated and measured runoff from the two validation catchments (Severnyi Creek and Dozhdemernyi Creek). The results of calibration and validation were close to each other, so the optimized parameters could be applied for the other sub-basins of the Kontaktovyi Creek basin. Simulations of river runoff from the Kontaktovyi Creek basin were performed for a 10-year period (1969–1978) with the two sets of parameters (*a priori* estimated and calibrated). All the results of streamflow simulations (including the calibration and validation cases) on a daily and annual basis are summarized in Table 2, which contains mean observed $\bar{x}_{obs}$ and simulated $\bar{x}_{cal}$ values, bias, *RMSD*, the Nash-Sutcliffe efficiency of simulation (*Eff*), and the coefficient of correlation (r).

Comparison of streamflow simulation with the two sets of parameters for all sub-basins and small catchments has shown that the main differences are related to runoff hydrograph (whereas for annual values of runoff, the statistics obtained are very close). Thus, for daily streamflow, application of calibrated parameters instead of *a priori* estimated resulted in increase of *Eff*, on the average, from 0.38 to 0.55, r – from 0.66 to 0.77. In both cases, the bias was negative (i.e. runoff was underestimated) and its decrease, on the average, was small (3%). Only in one case (for the Dozhdemernyi Creek catchment) the bias decreased greatly (from 43 to 17%). The results mean that *a priori* estimated parameters are quite adequate and optimization of the more important of them improves the simulated streamflow with respect to timing rather than volume.

In general, the agreement between streamflow simulations and observations is not quite satisfactory, even in the case of application of the calibrated parameters. Underestimation of streamflow, by 14% in the case of calibrated parameters, can be mainly connected with poor precipitation measurements. First, measured precipitation is usually underestimated due to wind, especially during the cold season which lasts up to 7 months in this region. According to the climatic data, such underestimation may reach as much as 14–25% in the given region, which is

Table 2 Statistical characteristics of comparison of simulated and observed daily (numerator) and annual (denominator) streamflow.

Catchments	Number of years	$\bar{x}_{obs}$ (mm)	$\bar{x}_{cal}$ (mm)	Bias (%)	*RMSD* (mm)	*Eff*	*r*
Calibrated parameters							
Morozova Creek	8	1.20/440	1.04/380	–13.5	2.46/69.1	0.45/0.53	0.74/0.95
Yuzhnyi Creek	10	0.52/189	0.46/167	–11.8	1.04/35.5	0.58/0.76	0.77/0.92
Severnyi Creek	10	0.60/219	0.48/175	–20.1	1.14/51.2	0.47/0.44	0.72/0.93
Dozhdemernyi Creek	3	0.44/161	0.36/133	–17.2	0.94/ –	0.61/ –	0.79/ –
Vstrecha Creek, B	10	0.58/212	0.46/168	–20.4	1.02/50.7	0.57/0.60	0.76/0.97
Kontaktovyi Creek, C	10	0.76/277	0.74/268	–3.0	1.28/45.8	0.53/0.56	0.78/0.84
Kontaktovyi Creek, A	7	0.73/266	0.64/235	–11.4	1.10/48.7	0.64/0.63	0.81/0.88
Mean		0.69/252	0.60/218	–14.1	1.28/50.2	0.55/0.59	0.77/0.92
A priori estimated parameters							
Morozova Creek	8	1.20/440	1.03/376	–14.5	2.69/72.6	0.34/0.48	0.65/0.95
Yuzhnyi Creek	10	0.52/189	0.48/174	–7.9	1.36/43.9	0.29/0.63	0.61/0.82
Severnyi Creek	10	0.60/219	0.50/181	–17.2	1.33/46.5	0.29/0.54	0.62/0.92
Dozhdemernyi Creek	3	0.44/161	0.25/91	–43.2	1.23/ –	0.33/ –	0.59/ –
Vstrecha Creek, B	10	0.58/212	0.45/166	–21.5	1.17/53.9	0.42/0.55	0.66/0.96
Kontaktovyi Creek, C	10	0.76/277	0.74/268	–3.0	1.37/47.0	0.46/0.54	0.72/0.82
Kontaktovyi Creek, A	7	0.73/266	0.64/232	–12.5	1.23/51.3	0.55/0.59	0.75/0.86
Mean		0.69/252	0.58/213	–17.1	1.48/52.5	0.38/0.56	0.66/0.89

$\bar{x}_{obs}$ and $\bar{x}_{cal}$ are mean observed and simulated values, respectively; *RMSD* is the root-mean-square deviation; *Eff* is the Nash-Sutcliffe efficiency of simulation and *r* is the coefficient of correlation.

comparable with our results. Second, as mentioned above, most of the basin precipitation values during the cold season were estimated. Third, adjustment of daily precipitation to 3-hour time steps also contributes to underestimation of streamflow during the warm season when showers occur. Besides that, inaccuracy of the estimated incoming radiation may also influence the results. Nevertheless, after taking into account such uncertainties in the forcing data, the results obtained can be considered as satisfactory and the technique of *a priori* parameter estimation is suitable for application for ungauged basins located in the permafrost zone.

Acknowledgements This work was supported by the Russian Foundation for Basic Research (Grant 05-05-64161).

REFERENCES

Clapp, R. B. & Hornberger, G. M. (1978) Empirical equations for some soil hydraulic properties. *Water Resour. Res.* **14**, 601–604.

Gusev, Ye. M. & Nasonova, O. N. (1998) The land surface parameterization scheme SWAP: description and partial validation. *Global Plan. Change*. **19**(1–4), 63–86.

Gusev, Ye. M. & Nasonova, O. N. (2002) The simulation of heat and water exchange at the land-atmosphere interface for the boreal grassland by the land-surface model SWAP. *Hydrol. Processes* **16**(10), 1893–1919.

Gusev, Ye. M. & Nasonova, O. N. (2003) Modelling heat and water exchange in the boreal spruce forest by the land-surface model SWAP. *J. Hydrol*. **280**(1–4), 162–191.

Gusev, E. M. & Nasonova, O. N. (2004) Simulation of heat and water exchange at the land–atmosphere interface on a local scale for permafrost territories. *Eurasian Soil Sci.* **37**(9), 1077–1092.

Gusev, E. M., Nasonova O. N. & Dzhogan, L. Ya. (2006) The simulation of runoff from small catchments in the permafrost zone by the SWAP model. *Water Resour*. **33**(2), 115–126.

Kolymskoye UGKS (1977) *Materials of observations of the Kolyma water balance station*, vol. 18. Kolymskoye UGKS, Magadan, Russia.

Nash, J. E. & Sutcliffe, J. V. (1970) River flow forecasting through conceptual models: 1 A discussion of principles. *J. Hydrol*. **10**(3), 282–290.

Schaap, M. G., Leij, F. J. & van Genuchten, M. Th. (1998) Neural network analysis for hierarchical prediction of soil water retention and saturated hydraulic conductivity. *Soil Sci. Soc. Am. J*. **62**, 847–855.

van Genuchten, M. Th. (1980) A closed-form equation for predicting the hydraulic conductivity of unsaturated soils. *Soil Sci. Soc. Am. J*. **44**, 892–898.

Climate Variability and Change—Hydrological Impacts (Proceedings of the Fifth FRIEND World Conference held at Havana, Cuba, November 2006), IAHS Publ. 308, 2006.

Minor changes of water conservation capacity in 50 years of forest growth: analysis with data from the Ananomiya Experimental Forest, Japan

MICHIO HASHINO[1] **& HUAXIA YAO**[2]

1 *Department of Civil Engineering, The University of Tokushima, 2-1 Minami-josanjima, Tokushima 770-8506, Japan*

2 *Environmental Protection Branch, Department of Environment, Province of Saskatchewan, Box 3003, Prince Albert, Saskatchewan S6V 6G1, Canada*

hyao@serm.gov.sk.ca

Abstract Forest planting and growth over 50 years have not produced significant water conservation in an experimental watershed in Japan. Comparisons of hydrological responses between two periods (1930–1937, and 1983–1990) showed that the afforested watershed had increased annual evapotranspiration by 12% and water storage of soil by 15%, and reduced flood flows by about 20%. However, annual runoff from the watershed was reduced by 8.5% and low flows became even smaller, which was unfavourable for both water conservation and water supply. The minor increase in soil storage capacity produced a very limited water conservation effect and so flood reduction. In contrast, the increased evaporative consumption made annual runoff and low flows smaller.

Key words forest growth; water conservation; flood; low flow; water supply; soil storage; rainfall; evapotranspiration; Japan

INTRODUCTION

The hydrological impacts of afforestation and forest growth have been researched by a vast body of scientists in the past 100 years. A summary and review (Bosch & Hewlett, 1982) of 94 catchment experiments showed that increases in forest cover have resulted in reductions of water yield, and decreases in cover have resulted in increases of water yield. Schulze & George (1987) reviewed the effects of afforestation on water yield in South Africa, and applied a process model to simulate the effects. Results from South African experiments identified decreases in water yield because of increases in evapotranspiration by the forest. The effects of afforestation in Scotland on water resources (Johnson, 1995) showed that both mean flow and annual minimum flow were reduced and the flow duration curves were shifted downwards.

Recently, Farley *et al*. (2005) completed a global synthesis on the effects of afforestation on water yield by analysing 26 catchment data sets selected from many countries. They identified the differences caused by the original land use (grassland or shrubland), climate region (wetter or drier), and plantation species (Eucalyptus or pine). Most of the data were from paired catchment studies in which the streamflow of grassland or shrubland catchments was compared with that of nearby afforested catchments. They did not include data from non-paired or single catchment studies where streamflow data before and after afforestation were available at the same catchment. Their data sets also excluded other countries such as Japan and China. Paired catchments are good for avoiding climate effects on streamflows, but include possible effects of different geology and topography. Single catchments include climate effects, but exclude basin property effects and therefore would be valuable additions to a global synthesis analysis.

Lane *et al*. (2003) proposed a technique of separating the climate and vegetation impacts on the annual flow regime following afforestation, and applied it to ten catchments in Australia, New Zealand and South Africa. They characterized flow changes due to forest plantations without using the paired-catchment method, and both annual water yield and low flows (including zero flow days) were the focus. However, there were very few data from the single catchments.

The vast literature on forest hydrology has given a strong impression that a plantation forest's contribution to the basin's water conservation capacity is limited in its amount and direction. Minor or minimal change in the capacity could be created when a watershed is converted to a forested condition within a short time such as 10–50 years, especially when the watershed was originally sparsely vegetated. Furthermore, when a forest reduces flood flows, it does not increase low flows at a later time or in the same year, but decreases low flows and annual water yield. Additional examples of single catchment studies with long duration data sets are needed to enrich

Copyright © 2006 IAHS Press

the general impression. Therefore, this paper presents a single-catchment study using 60 years of data from the Ananomiya Experimental Forest, The University of Tokyo, in the Aichi Prefecture of Japan. The reasons for flow decreases—evaporative increase and minimal change in soil water storage—are analysed.

DATA

The Ananomiya watershed (Fig. 1(a)) is located at latitude 35°15′N and longitude 137°06′E, with an area of 13.9 ha and altitude of 140–218 m a.m.s.l. The original vegetation in the 1920s was sparse shrubs and pine trees, and the initial planting of pine trees for soil erosion prevention started in 1925. The plantations were further extended during the 1930s to 1960s. The forested area reached 6.3 ha or 45% coverage in the 1930s and increased to 13.5 ha or 97% coverage in the 1980s (Fig. 1(b)). Daily meteorological and hydrological data were collected during the 60-year period, 1930–1990.

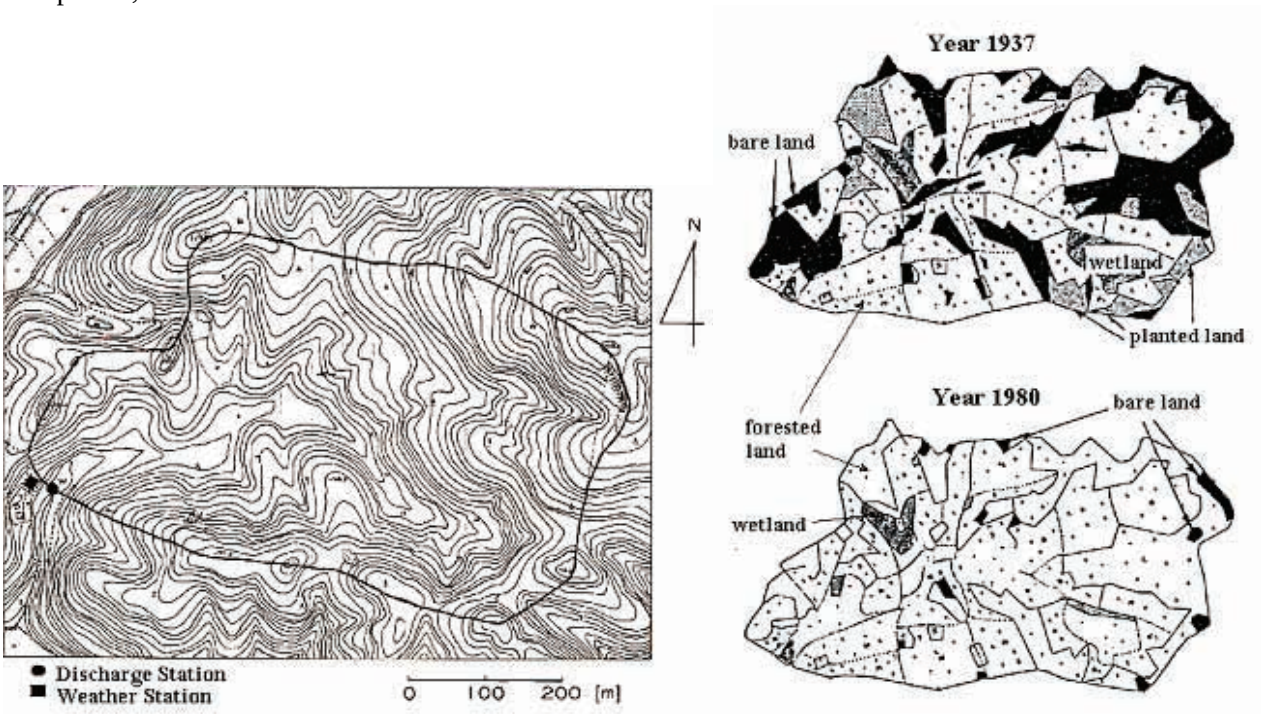


Fig. 1 (a) Ananomiya watershed and observation stations. (b) Forested and bare lands in 1930s and 1980s.

METHOD

Two representative periods were selected for comparison analysis: the eight years 1930–1937 when forest coverage was 45%, and another eight years, 1983–1990, when the forest coverage was 97%. A favourable situation for comparison of runoff or evaporation is given by the similarity of the precipitation and temperature regimes (mean annual precipitation 1580 mm and mean temperature 15°C) for both periods. The number of days having more than 50 mm rainfall are also the same at 8 days per year on average, and the days having 100 mm storm rain are similar at 1 day per year, during both eight-year periods. Comparisons of storm events, annual runoff and soil storage between the two periods were conducted.

Differences in hydrological responses to storm rainfall events or annual precipitation are revealed by the comparisons. If discharges in dry seasons became less and annual water yield became less because of forest growth, the water conservation represented by reduced flood flows would be weakened. Forest could not both reduce floods and increase low flows.

Water conservation capacity is strongly related to the water storage capacity of soils. A conceptual largest soil storage (LSS) for the watershed is defined as the largest volume of water stored in the soil for a month. It is neither the saturated water storage nor the maximum storage in

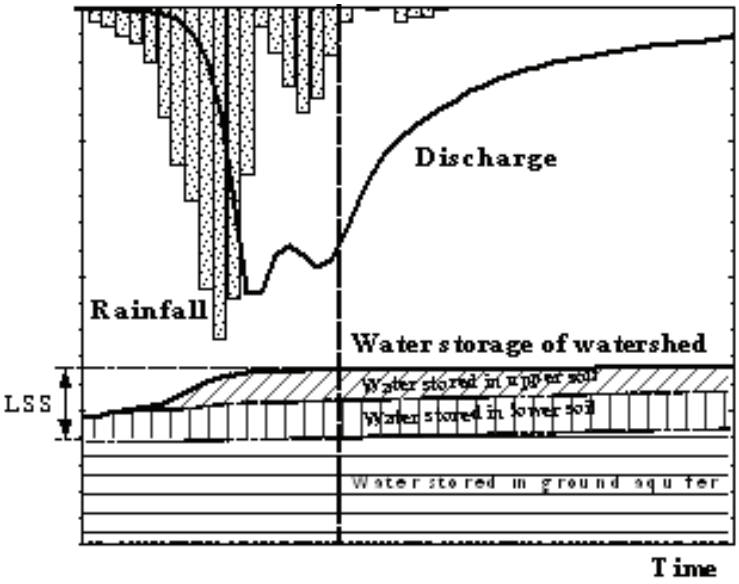


Fig. 2 Illustration of water storage of soil, and the largest soil storage (LSS).

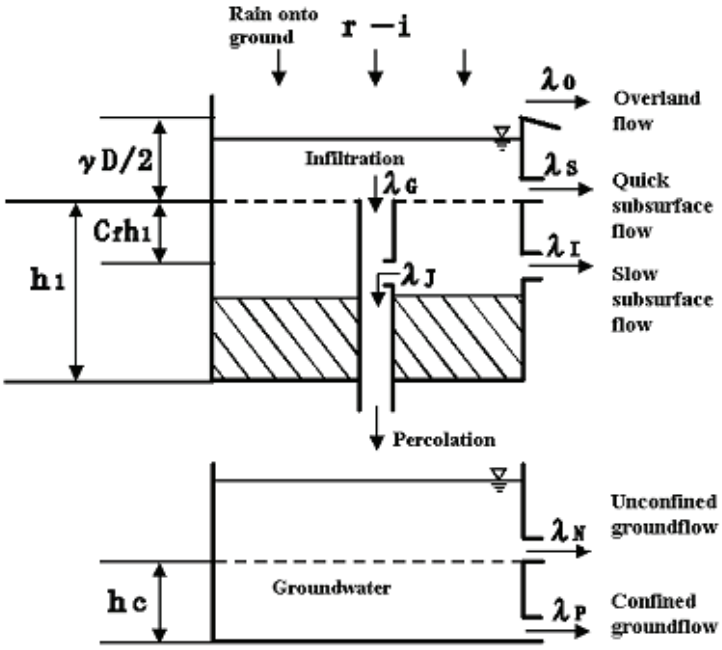


Fig. 3 Tank model of water movement and storage in soil and groundwater aquifer.

a year, but rather the relatively largest value in any month. Therefore LSS changes from month to month, and from year to year. A typical LSS is illustrated in Fig. 2.

The daily soil water storage and the LSS of each month are not measured but calculated using a lumped two-layer Tank model (Hashino *et al*., 2004). The model structure (not including the canopy and its interception) is shown in Fig. 3 and its parameters are calibrated separately for the eight years in the 1930s and the eight years in the 1980s. The soil water storage of each day and largest soil storage of each month are estimated by the model. The LSS, as representative of soil storage capacity, will indicate how large the difference of storage capacity is for the two periods.

In the model, after calculations of rainfall interception by the forest canopy and associated interception evaporation, the rain falling onto the ground surface (the rainfall rate *r* above canopy minus interception rate *i*) infiltrates into a soil layer (or tank), and then percolates to a groundwater aquifer tank. When rainfall infiltration reaches the saturation level of the soil tank, surface storage and overland flow will occur. Otherwise runoff from the soil (quick and slow subsurface flows),

the upper and lower groundwater aquifers constitute the total runoff from the watershed. Parameter h_1 is the soil saturation content, C_f is related to the initial water storage in the soil tank, *hc* is the initial water sorted in aquifer tank and λ_O is related to the overland flow coefficient. λ_G, λ_J are infiltration coefficients, λ_S, λ_I, λ_N, and λ_P are the outflow coefficients respectively for quick and slow subsurface flows, unconfined groundwater flow, and confined groundwater flow, while γD is a parameter related to quick subsurface flow. The parameters are calibrated using a Simplex method (Nocedal & Wright, 1999).

RESULTS

Runoff responses of storm events

Twelve storm events that have more than 100 mm rainfall volume were chosen from the period 1930–1937, and eight storm events were chosen from the period 1983–1990. Runoff responses of storm events differed between the two periods, with the ratios of runoff volume to rainfall for the 1980s being, on average, 20% less than that for the 1930s among the chosen events, as shown in Fig. 4. This indicates the extent to which flood volumes were decreased by forest plantation and tree growth. Possible reasons for a reduction in flood response include increased evaporation and transpiration due to increased leaf area and rooting depth, different rainfall characteristics such as duration and intensity, and increased soil water storage.

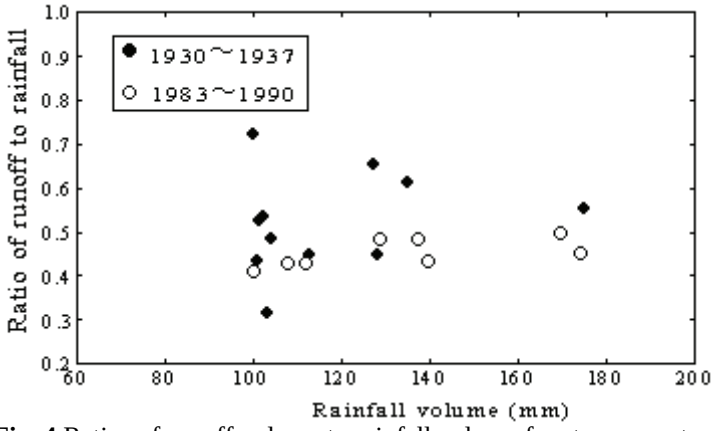


Fig. 4 Ratios of runoff volume to rainfall volume for storm events over 100 mm.

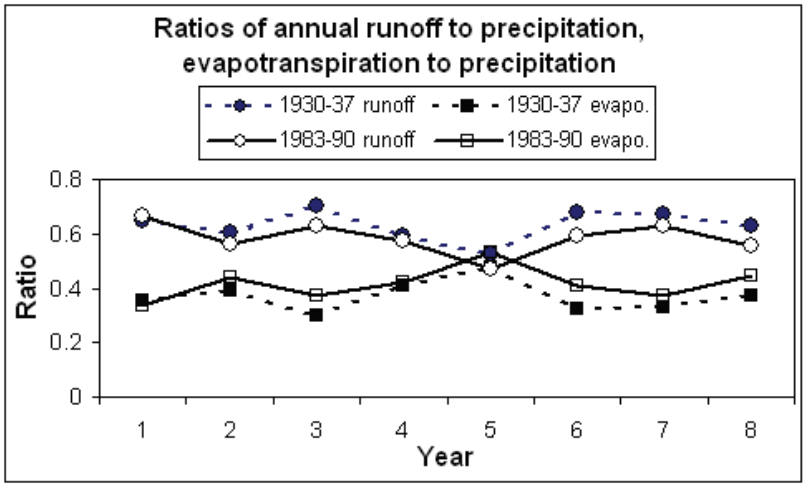


Fig. 5 Difference of annual runoff or annual evapotranspiration between two periods.

Annual runoffs and low flows

Annual runoff volumes during the 1980s are less than those of the 1930s. In contrast, annual evapotranspiration during the 1980s was definitely higher (Fig. 5). The 8-year-mean runoff of

1983–1990 was 928 mm, 8.5% less than the mean of 1014 mm for 1930–1937. The 8-year-mean evapotranspiration of 1983–1990 was 649 mm, 12% more than the mean of 578 mm for 1930–1937. Increased trees and leaves have increased consumptive evaporation or transpiration not only during the flood seasons, but also during dry seasons, causing the reduction of annual runoff. Forest plantation and growth did improve flood control as discussed above, but did not improve water resource supply in the dry seasons.

The ten smallest daily flows in a year were used as representative of the low flows of the watershed. The ten smallest flows were chosen from each year of the two periods, and a period-averaged value was obtained for each of the ten smallest. For example, the average first smallest flow in 1930–1937 was 0.6 mm day^{-1}, the averaged tenth smallest flow in 1930–1937 was 1.5 mm day^{-1}. As shown in Fig. 6, all the smallest flows in the period 1983–1990 were less than those in 1930–1937, clearly indicating a reduction in low flows following plantation growth.

Changes of LSS

The Tank model was calibrated for the periods 1930-37 and 1983-90. Two examples of simulated and observed flows are shown in Fig. 7, for year 1937 and 1990, respectively. The model gave reasonably good estimations of daily flows.

The values of largest soil storage (LSS) for each of the two periods were estimated using the calibrated model, and are shown in Fig. 8. The horizontal axis represented the accumulated rainfall of those rain events that appeared before a LSS was formulated in the soil (also see Fig. 2). In total, 65 LSSs for period 1930–1937, and 53 LSSs for period 1983–1990 were included in Fig. 8, and they did not show a significant difference between the two periods. The average LSS for the two periods was 27.3 mm and 27.8 mm.

It was noted that the soil water would be saturated when accumulated rainfall was around 150 mm or more. If only taking into consideration the LSSs when the accumulated rainfall was more than 150 mm, the 8-year-averaged LSS for 1930–1937 was 48.6 mm, while the averaged LSS for 1983–1990 was 56.0 mm. Therefore, the soil water storage capacity might have been increased by 7.4 mm (or 15%) which could not account for the reduction in flood flow that was mentioned previously.

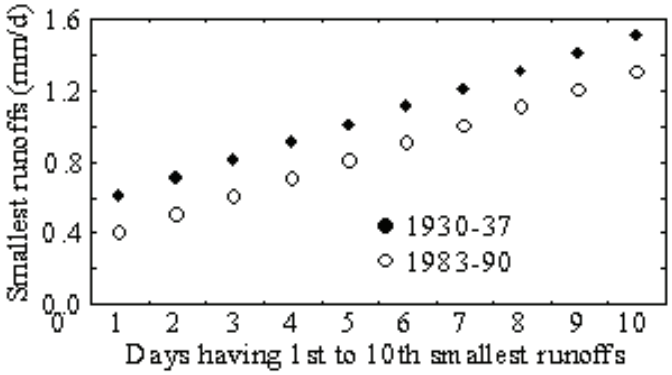


Fig. 6 Difference of smallest daily runoffs between two periods.

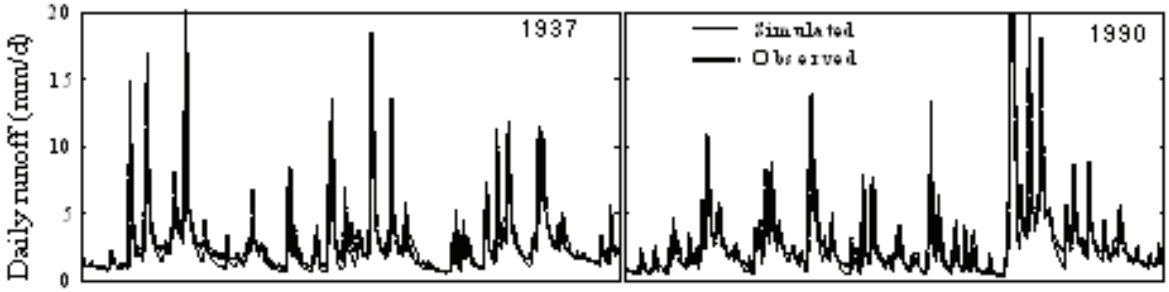


Fig. 7 Examples of simulated runoffs *vs.* observed runoffs.

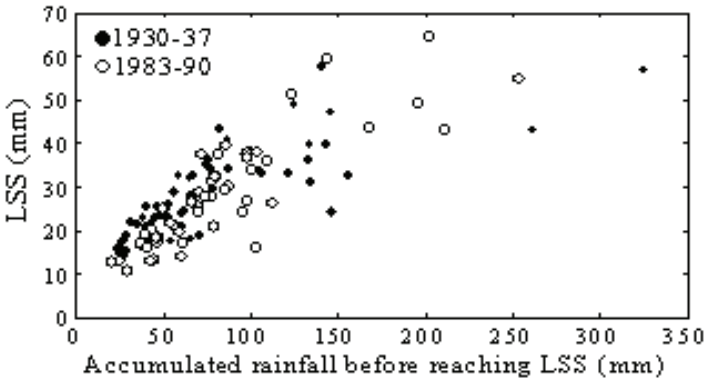


Fig. 8 Estimated LSS of two periods.

In conclusion, tree planting and growth at Ananomiya watershed have increased evapotranspiration and therefore decreased runoff, both for flood and dry seasons. The foliar change in the short time of 50 years did not appear to produce significant increases in soil storage capacity. The forested watershed was not acting as a reservoir that reduces flood flows and increases low flows. This is a further contribution to the body of science on the impacts of afforestation.

Acknowledgements The authors are grateful to Dr Denis Hughes for providing suggestions and comments that improved the manuscript.

REFERENCES

Bosch, J. M. & Hewlett, J. D. (1982) A review of catchment experiments to determine the effect of vegetation changes on water yield and evapotranspiration. *J. Hydrol.* **55**, 3–23.

Farley, K. A., Jobbagy, E. G. & Jackson, R. B. (2005) Effects of afforestation on water yield: global synthesis with implications for policy. *Global Change Biology* **11**, 1565–1576.

Hashino, M., Tamura, T., Tabuchi, M. & Fujikawa, Y. (2004) Separation of interception evaporation, transpiration and non-overland flow in a forest watershed. *J. Hydraul. Engng, JSCE* **48**, 31–36 (in Japanese with English summary).

Johnson, R. C. (1995) Effects of upland afforestation on water resources, the Balquhidder Experiment 1981–1991. *Institute of Hydrology Report no. 116*. Wallingford, UK.

Lane, P., Best, A., Hickel, K. & Zhang, L. (2003) The effects of afforestation on flow duration curves. *Technical Report 03/13, Cooperative Research Centre for Catchment Hydrology*. Monash University, Australia.

Nocedal, J. & Wright, S. J. (1999) *Numerical Optimization.* Springer-Verlag, New York, USA.

Schulze, R. E. & George, W. J. (1987) Simulation of effects of forest growth on water yield with a dynamic process-based user model. In: *Forest Hydrology and Watershed Management* (ed. by R. H. Swanson, P. Y. Bernier & P. D. Woodard), 575–584. IAHS Publ. 167. IAHS Press, Wallingford, UK.

Climate Variability and Change—Hydrological Impacts (Proceedings of the Fifth FRIEND World Conference held at Havana, Cuba, November 2006), IAHS Publ. 308, 2006.

Respuesta de los caudales máximos al manejo de bosques de plantaciones en cuencas experimentales en el sur de Chile

ANDRÉS IROUMÉ[1], CLAUDIA CASTILLO[2], HELEN PRIMROSE[3], ANTON HUBER[4] & JAMES BATHURST[5]

1 *Universidad Austral de Chile, Facultad de Ciencias Forestales, Instituto de Manejo Forestal, Casilla 567, Valdivia, Chile* airoume@uach.cl

2 *Universidad Austral de Chile, Escuela de Ingeniería Forestal, Casilla Postal 567, Valdivia, Chile*

3 *University of Newcastle upon Tyne, School of Civil Engineering and Geosciences, Newcastle upon Tyne NE1 7RU, UK*

4 *Universidad Austral de Chile, Facultad de Ciencias, Instituto de Geociencias, Casilla 567, Valdivia, Chile*

5 *University of Newcastle upon Tyne, Institute for Research on Environment and Sustainability, Devonshire Building 3.16, Newcastle upon Tyne NE1 7RU, UK*

Resumen Se discuten resultados sobre cambios hidrológicos generados por intervenciones en bosques de plantaciones en el sur de Chile, con especial énfasis en los caudales máximos. En una de las áreas de estudio (cuenca La Reina, 34,4 ha) se comparan los caudales máximos del periodo de pre-cosecha (1997 a 1999) con los del periodo de post-cosecha (desde 2000). Los caudales máximos aumentaron un 66% en los eventos 'menores' y un 42% en los eventos 'mayores', luego de la cosecha a tala rasa de la plantación de *Pinus radiata*. Los análisis mostraron que los caudales máximos de cada año del periodo post-cosecha seguían siendo significativamente mayores que los registrados antes de la cosecha del bosque. Estos resultados, junto a los obtenidos en las otras áreas de estudio, pretenden contribuir a la gestión integrada de bosques y aguas y al desarrollo sustentable de la actividad forestal en bosques de plantaciones en Chile.

Palabras claves caudales máximos; plantaciones forestales; cuencas experimentales; Chile

Peak flow changes in a managed-forest experimental basin in southern Chile

Abstract Results on hydrological changes following forest operations in southern Chile are discussed. In one of the study areas (La Reina catchment, 34.4 ha) peak flows from the pre-harvesting period (1997–1999) are compared with those from the post-harvesting period (since 2000). Peak flows increased by 66% in the "small" rainfall events and 42% during "large" events after clearcutting the *Pinus radiate* plantation. The analysis showed that peak flows in each year of the post-harvest period were still significantly higher than those registered before clearcutting. These results, together with those obtained in the other study areas, are intended to contribute to the integrated forest and water resources management and to the sustainability of the forest plantation development in Chile.

Keywords peak flows; forest plantations; experimental catchments; Chile

INTRODUCCION

Diversos estudios han estado analizado críticamente una serie de "mitos" asociados a la hidrología forestal, en particular algunos no suficientemente respaldados por evidencia científica respecto a los impactos de los bosques en los caudales extremos, al rol de la cubierta forestal en la generación de precipitaciones y en el mejoramiento de la calidad del agua (McCulloch & Robinson, 1993; Calder, 1999; FAO & CIFOR, 2005).

Respecto al efecto de los bosques en los caudales medios anuales y en los períodos de estío hay una mayor concordancia: estos caudales son menores en cuencas forestadas al comparar con una condición de menor coberturas arbórea, y esto parece ser cierto en un amplio rango de condiciones climáticas (Bosch & Hewlett, 1982; Kirby *et al.*, 1991; Whitehead & Robinson, 1993; Calder, 1993; Robinson *et al.*, 2003; Iroumé *et al.*, 2005). Aún cuando persisten dudas sobre el efecto de diversas practicas de manejo forestal (incluyendo los métodos de cosecha y madereo) y el impacto en la hidrología local durante el periodo de post-cosecha, tanto la cantidad de investigaciones como las conclusiones resultantes son suficientemente comprehensivas (Robinson *et al.*, 2003).

En contraste, las investigaciones respecto a los efectos de los bosques y su manejo en los caudales máximos (e.g. Jones & Grant, 1996; Thomas & Megahan, 1998), son menos concluyentes. Gran parte de la controversia vinculada a los cambios en los caudales máximos asociados a las intervenciones forestales se genera, entre otros, por la incertidumbre respecto al efecto del tamaño de las cuencas, a la respuesta de las mismas frente a tormentas de distintas magnitudes y a la duración del efecto luego de la remoción de la plantación hasta que los caudales alcanzan los niveles de la condición de pre-cosecha.

Copyright © 2006 IAHS Press

En relación con la magnitud de las tormentas, mientras muchos estudios concuerdan que "en promedio" los caudales máximos generalmente aumentan luego que el bosque es intervenido, se han presentado conclusiones a veces contradictorias al comparar la influencia de la cubierta en los caudales máximos generados por tormentas menores con los de tormentas extremas. Respecto a esto ultimo, Smith (1987) encontró que la cosecha de un bosque afecta crecidas de periodos de retorno de hasta 100 años mientras que Thomas & Megahan (1998) no detectaron ningún cambio para crecidas con periodos de retorno mayores a 2 años.

Sobre la duración del efecto, Bari *et al.* (1996) reportan que sólo se aprecia los primeros años luego de la cosecha pero Ruprecht & Stoneman (1993) han encontrado que puede durar hasta 12–15 años.

Este trabajo aborda el análisis de caudales máximos generados por tormentas de lluvia de diferente magnitud, tanto para los periodos de pre y post-cosecha en una misma cuenca como entre cuencas vecinas con plantaciones de diferente estado de desarrollo, todas ellas localizadas en el sur de Chile.

Este estudio se enmarca en el proyecto EPIC FORCE (Evidence-Based Policy for Integrated Control of Forested River Catchments in Extreme Rainfall and Snowmelt), investigación financiada como parte del "Sixth Framework Programme-Specific Measures in Support of International Cooperation (INCO) in Developing Countries, 2004" de la Comunidad Europea. Reconociendo la existencia de limitaciones en América Latina en la aplicación de políticas integradas para el manejo de bosques y agua, EPIC FORCE pretende mejorar la comprensión de la dinámica de la intervención de bosques durante eventos extremos de precipitación, e incorporar mayor base científica en las decisiones de gestión para facilitar el aprovechamiento sustentable de los recursos hídricos y forestales.

MATERIAL Y MÉTODOS

El área de estudio corresponde a tres cuencas experimentales, denominadas La Reina, Los Ulmos1 y Los Ulmos2, ubicadas en la Décima Región, Chile. La localización y algunos antecedentes geográficos de las cuencas se muestran en la tabla 1. La descripción del clima y suelos se encuentra en Iroumé *et al*. (2005) e Iroumé *et al*. (2006).

En la cuenca La Reina (34.4 ha) se comparan los caudales máximos del periodo de pre-cosecha (años 1997 a 1999, plantación de *Pinus radiata* establecida el año 1977 cosechada a tala rasa a fines de 1999–principios de 2000) con los del periodo de post-cosecha (desde el año 2000, plantación de *Eucalyptus nitens* establecida el año 2000). En el sector Los Ulmos se compara durante el periodo 2000–2005 el efecto en los caudales máximos de bosques de plantaciones de similares características pero de diferente edad, en las cuencas Los Ulmos1 (10.8 ha, plantación de *Eucalyptus nitens* del año 1997) y Los Ulmos2 (16.1 ha, plantación de *Eucalyptus nitens* del año 2000).

En la investigación, las tormentas de lluvia se clasificaron según el volumen de las precipitaciones en eventos "pequeños" (5–10 mm), "medios" (10–50 mm) y "grandes" (mayores a 50 mm). Se definieron tormentas individuales aquellos periodos con precipitación antecedidos y seguidos por 5 horas sin lluvias. No se consideraron en los análisis las tormentas con volúmenes de precipitación inferiores a 5 mm dado su errático comportamiento en la generación de caudales de crecida (en estas tormentas de muy bajo volumen, las condiciones previas de contenido de humedad del suelo y de las copas son relevantes en la respuesta hidrológica a una lluvia).

Tabla 1 Localización y antecedentes geográficos de las cuencas.

Cuenca	Localización	Superficie (ha)	Densidad de drenaje (m ha^{-1})	Pendiente media (%)	Rango de altitud (m s.n.m.)
La Reina	40°20′25″S 73°27′59″W	34.4	78.8	23.7	35–225
Los Ulmos1	40°02′50″S 73°06′86″W	10.8	165.1	12.0	175–230
Los Ulmos2	40°02′40″S 73°05′44″W	16.1	58.9	23.7	155–210

La magnitud de las diferencias en caudal máximo, entre distintos períodos, para la cuenca La Reina y entre cuencas, para Los Ulmos 1 y Los Ulmos 2, se calculó mediante la relación de medias expresada en porcentaje. La significancia de éstas se determinó con la prueba no paramétrica U de Mann Whitney, para un 99% de confiabilidad.

RESULTADOS

Los resultados presentados en la tabla 2, muestran que en la cuenca La Reina, para las tres categorías de tamaño de eventos de precipitación, los caudales de post-cosecha son mayores que los de pre-cosecha (diferencias estadísticamente significativas), lo que indica que la remoción de la cubierta vegetal tiene un efecto significativo en los caudales, incluso en los eventos extremos. Sin embargo, el aumento en los caudales del período de post-cosecha en los eventos grandes es menor que los de la categoría pequeños. Esto parece confirmar que el efecto de las operaciones forestales es de mayor importancia en eventos de periodos de retorno menores.

Considerando el primer y último de los años después de la cosecha de la plantación en la cuenca La Reina (años 2000 y 2005, respectivamente), el cálculo del porcentaje de aumento en las medianas de los valores de caudales máximos de cada categoría de eventos produce los siguientes resultados:

– Eventos pequeños: pre-cosecha al año 2000, aumento es 67%, y pre-cosecha al año 2005, aumento es 87%.
– Eventos medios: pre-cosecha al año 2000, aumento es 38%**,** y pre-cosecha al año 2005, aumento es 65%.
– Eventos grandes: Pre-cosecha al año 2000, aumento es 32%**,** y pre-cosecha al año 2005, aumento es 52%.

Estos resultados, junto a la información presentada en la tabla 2, muestran que a pesar del desarrollo de la nueva plantación establecida el año 2000, los caudales al quinto año de la intervención son aún significativamente mayores a los del periodo de pre-cosecha. Para observar estos resultados en forma gráfica y poder visualizar alguna tendencia, los valores de las medianas de los caudales máximos de cada periodo y tamaño de evento se presentan en la figura 1.

Tabla 2 Mediana de los caudales máximos por tamaño de evento, para el periodo de pre-cosecha y cada año del periodo de post-cosecha, cuenca La Reina.

	Año	Tamaño del evento Pequeño	Medio	Grande
Mediana de los caudales máximos, condición de pre-cosecha (L s^{-1})	Todos	4.6	18.5	69.2
Mediana de los caudales máximos, condición de post-cosecha (L s^{-1})	2000	13.8	29.8	101.3
	2001	11.7	29.5	180.2
	2002	14.2	46.6	100.6
	2003	13.1	41.2	154.9
	2005	35.4	53.1	144.6

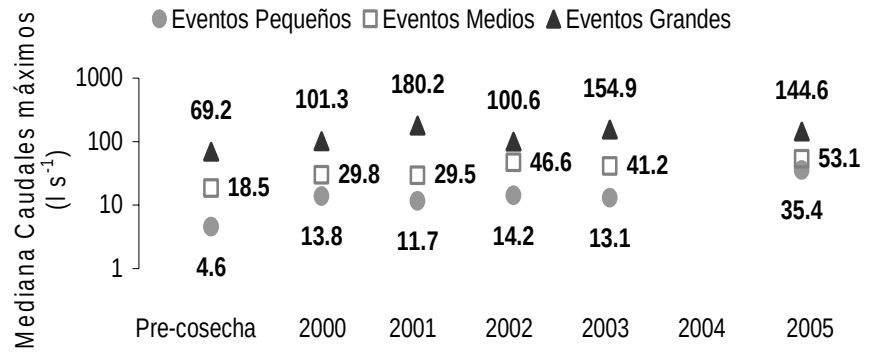


Fig. 1 Tendencias en los valores de la mediana de los caudales máximos para el periodo de pre-cosecha y cada uno de los años del periodo de post-cosecha, cuenca La Reina.

De la tabla 2 y la Fig. 1 se puede observar que los cambios en los valores de los caudales durante los primeros años luego de la remoción de la plantación no muestran un aumento importante inicial seguido de una gradual disminución tendiendo hacia los niveles de caudales de la condición de pre-cosecha. No hay un patrón consistente para ninguna de las categorías de tamaño de eventos, y tampoco es posible notar, por ejemplo, un año particular del periodo de post-cosecha donde todas las medianas de caudales máximos hayan alcanzado un "máximo".

En la figura 2 se muestra gráficamente la comparación de la mediana de los caudales máximos (L s ha^{-1}) registrados en las cuencas Los Ulmos1 y Los Ulmos2.

Para las tormentas "pequeñas", los caudales máximos en Los Ulmos 2 (con una plantación con 4 años de mayor desarrollo que la de Los Ulmos1) son mayores que los registrados en Los Ulmos1 (Fig. 2(a)). Estas diferencias son significativas sólo entre los años 2000 y 2003. Para los años 2004 y 2005 los caudales no muestran diferencias importantes, lo que se explicaría por el nivel de desarrollo del bosque en Los Ulmos1 que empieza a ser similar en términos de cobertura al de Los Ulmos2.

Para las tormentas de la categoría "grandes", no se presenta ninguna tendencia clara (Fig. 2(b)). En este tipo de tormentas extremas, es posible que la diferencia entre las coberturas tenga un menor efecto en los procesos de generación de caudales, y variables como densidad de la red de drenaje o pendiente de las cuencas tengan un rol más preponderante.

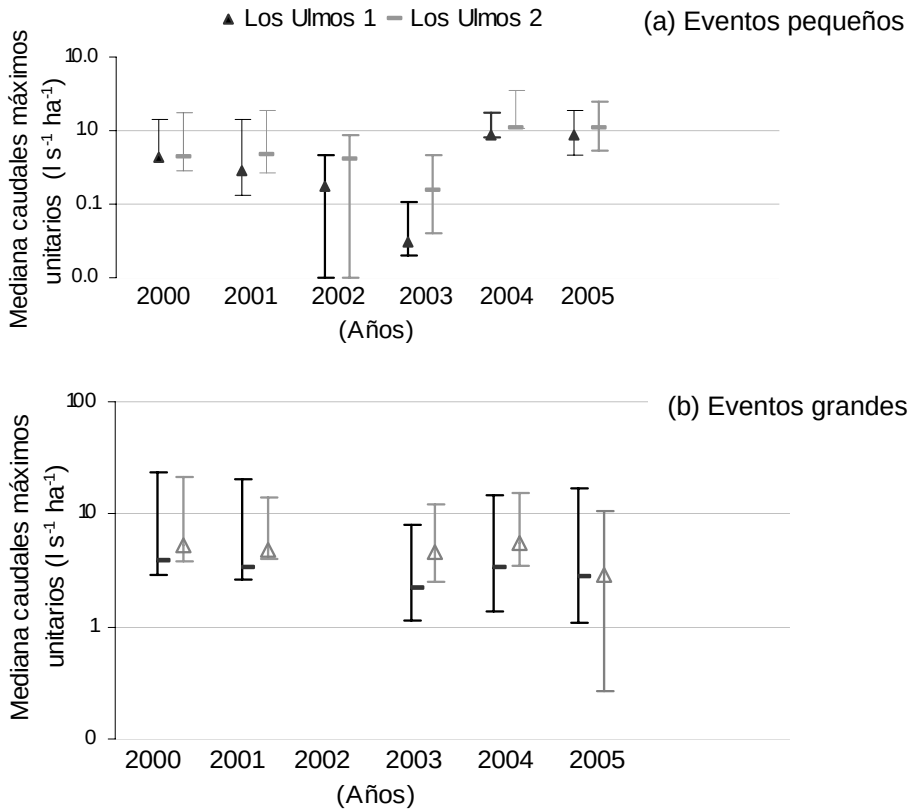


Fig. 2 Comparación de la mediana de los caudales máximos de las cuencas Los Ulmos 1 y Los Ulmos 2, para tormentas pequeñas (arriba) y tormentas grandes (abajo).

CONCLUSIONES

La cosecha a tala rasa del bosque de la cuenca La Reina generó aumentos en los caudales del período de post-cosecha, al compararlos con los registrados en el de pre-cosecha. Las mayores diferencias ocurren para las tormentas menores, y los caudales máximos luego de la remoción de la plantación no muestran una tendencia como pudiera haberse esperado de un aumento importante inicial seguido de una gradual disminución tendiendo hacia los niveles de caudales de la condición de pre-cosecha.

Tal como se aprecia de los análisis en las cuencas Los Ulmos, el efecto de 4 años de mayor desarrollo del bosque en Los Ulmos2 en comparación con el Los Ulmos1 sólo se nota al comparar los caudales generados por tormentas menores.

Los mayores impactos ocurren ante cambios importantes en la cobertura forestal.

Agradecimientos Este trabajo se desarrolló en el marco del Proyecto EPIC FORCE, contrato INCO-CT2004-510739.

REFERENCIAS

Bari, M. A., Smith, N., Ruprecht, J. K. & Boyd, B. W. (1996) Changes in streamflow components following logging and regeneration in the southern forest of Western Australia. *Hydrol. Processes* **10**, 447–461.

Bosch, J. M. & Hewlett, J. D. (1982) A review of catchment experiments to determine the effect of vegetation changes on water yield and evapotranspiration. *J. Hydrol.* **55**, 3–23.

Calder, I. R. (1993) The Balquhidder Catchment water balance and process experiment results in context—what do they reveal? *J. Hydrol.* **145**, 467–477.

Calder, I. R. (1999) *The Blue Revolution.* Earthscan, London, UK.

FAO & CIFOR (2005) *Forests and Floods, Drowning in Fiction or Thriving on Facts?* RAP Publication 2005/03, Forest Perspectives 2.

Iroumé, A., Huber, A. & Schulz, K. (2005) Summer flows in experimental catchments with different forest covers, Chile. *J. Hydrol*. **300**, 300–313.

Iroumé, A., Mayen, O. & Huber, A. (2005) Runoff and peak flow responses to timber harvest and forest age in Southern Chile. *Hydrol. Processes* **20**, 37–50.

Jones, J. A. & Grant, G. E. (1996) Peak flow response to clearcutting and roads in small and large basins, western Cascades, Oregon. *Water Resour. Res.* **32**, 959–974.

Kirby, C., Newson, M. D. & Gilman, K. (1991) *Plynlimon Research: The First Two Decades*. Institute of Hydrology Report no. 109, Wallingford, UK.

McCulloch, J. S. G. & Robinson, M. (1993) History of forest hydrology. *J. Hydrol.* **150**, 189–216.

Robinson, M., Cognard-Plancq, A.-L., Cosandey, C., David, J., Durand, P., Führer, H.-W., Hall, R., Hendriques, M. O., Marc, V., McCarthy, R., McDonnell, M., Martin, C., Nisbet, T., O'Dea, P., Rodgers, M. & Zollner, A. (2003) Studies of the impact of forests on peak flows and baseflows: a European perspective. *Forest Ecol. Manage.* **186**, 85–97.

Ruprecht, J. K. & Stoneman, G. L. (1993) Water yield issues in the jarrah forest of south-western Australia. *J. Hydrol.* **150**, 369–391.

Smith, P. J. T. (1987) Variation of water yield from catchments under grass and exotic forest, east Otago. *J. Hydrol. NZ* **26**, 175–184.

Thomas, R. B. & Megahan, W. F. (1998) Peak flow response to clear-cutting and roads in small and large basins, western Cascades, Oregon: a second opinion. *Water Resour. Res.* **34**, 3393–3403.

Whitehead, P. G. & Robinson, M. (1993) Experimental basin studies-an international and historical perspective of forest impacts. *J. Hydrol.* **145**, 217–230.

Climate Variability and Change—Hydrological Impacts (Proceedings of the Fifth FRIEND World Conference held at Havana, Cuba, November 2006), IAHS Publ. 308, 2006.

UNESCO Working Group on the impacts of climate variability and land-cover change on flooding and low flows as a function of scale

GÜNTER BLÖSCHL[1], SANDRA ARDOIN-BARDIN[2], MIKE BONELL[3], MANFRED DORNINGER[4], DAVID GOODRICH[5], DIETER GUTKNECHT[1], DAVID MATAMOROS[6], BRUNO MERZ[7], PAUL SHAND[8] & JAN SZOLGAY[9]

1 *Institute of Hydraulic and Water Resources Engineering, Vienna University of Technology, Karlsplatz 13, A-1040 Vienna, Austria*
bloeschl@hydro.tuwien.ac.at

2 *UMR HydroSciences Montpellier, France*

3 *UNESCO Division of Water Sciences, Paris, France*

4 *University of Vienna, Austria*

5 *USDA-ARS-SWRC, Tucson, Arizona, USA*

6 *Escuela Superior Politecnica del Litoral (ESPOL), Campus Gustavo Galindo, Guayaquil, Ecuador*

7 *GeoForschungsZentrum Potsdam, Germany*

8 *British Geological Survey, Wallingford, UK*

9 *Slovak University of Technology, Bratislava, Slovakia*

Abstract In the context of the IHP-VI Project 2.1 (Extreme events), and the cross-cutting activities of the FRIEND and HELP programmes, the UNESCO Division of Water Sciences has initiated a working group on identifying the relative role of climatic variability and land-cover change on floods and low flows as a function of spatial scale. The mandate of the working group is to summarize the state of the art of the subject, develop the key science questions, plan a five year research strategy for testing in HELP basins and other research experimental basins, and plan a series of workshops. This paper summarizes the findings of the first working group meeting held in Vienna during November, 2005.

Key words floods; low flows; land use; climate change; scale; scaling

INTRODUCTION

Land use, land cover and climate are linked in complex ways. While land-use change often drives environmental changes, a changing climate can in turn affect land use. Because of these links, changes of both systems are important contributors to the magnitude of change and variability of different hydrological processes, in particular to floods and droughts. In addition, such interlinked changes are likely to affect ecosystems and society.

Determining the effects of land-use change on floods and droughts depends on an understanding of land-use practices, current land-use management as affected by society, economic development, technology, and other factors. HELP basins with diverse land-use practices under a variety of climatic conditions in different parts of the world, highlight differences in regional and national vulnerability and resilience, constitute a variety of natural and socio-economic environments and form a focus for the study of scientific questions connected to these changes.

To address such overarching questions, there is a need for a focused, integrated research agenda. This should include observations, experimental research, process studies, modeling and prediction at different scales. The challenge of collaboration is vital, HELP basins can play a catalytic role among scientists and other research programmes to gain understanding of the direct impacts of land-use change on climate, as well as the combined effects of land use and climate change on floods and droughts.

The HELP (Hydrology for the Environment, Life and Policy) programme has been created to cut across all themes of the International Hydrological Programme (IHP) of UNESCO. Specifically, the aim of the HELP programme is to deliver social, economic and environmental benefit to stakeholders through sustainable and appropriate use of water by directing hydrological science towards improved integrated catchment management basins (http://www.unesco.org/water/ihp/help). In the context of the IHP-VI Project 2.1 (Extreme events), and the cross-cutting activities of the FRIEND and HELP programmes, the UNESCO Division of Water Sciences has initiated this working group on identifying the relative role of climatic variability and land cover change on

Copyright © 2006 IAHS Press

floods and low flows as a function of spatial scale. The mandate of the working group, over a period of five years, is to

- summarize the state of the art of the subject, in particular, to identify at what scales each of the controls become important;
- develop the key science questions;
- plan a five year research strategy for testing in HELP basins and other experimental research basins;
- plan a series of workshops and potential publications from the workshops;
- consider possible locations of the workshops, one per year; and
- any other follow-up activities that the group may identify.

The research strategy should integrate modelling requirements with field experimental hydrology. These activities will provide a road map of how to address these issues and act as a catalyst for motivating communication and targeted research. This paper summarizes the findings of the working group meeting held in Vienna, 28–30 November 2005.

Hydrology is a context dependent discipline, i.e. it matters *where*/*when*/*how* processes occur. For example, land cover effects in the tropics are fundamentally different from those in humid climates. In different hydrological settings the impacts will become important at different scales. With these specifications, the science question to be addressed by the present working group was thus identified as: What are the relative roles of climatic variability and land-cover change on floods and low flows as a function of scale in different environments?

PROCESSES

Land cover is typically a local phenomenon, so its impact is likely to strongly decrease with catchment size. The position of the disturbance in the landscape will modulate the scale effects. In contrast, climate impacts may occur at larger scales so one would expect them to be apparent in both small and large catchments and be consistent in a region. River training impacts are likely to increase with catchment size as there is a general tendency for larger settlements and hence large-scale flood protection works on larger streams. The schematic of Fig. 1 visualizes hypothesized relative roles of climate and land-use changes. Note that the relative roles of these (crossover point on the figure) is likely to vary from catchment to catchment. These are general considerations and the impacts and their scales may differ widely between different hydrological settings. For the particular case of catchments in the Sahel, analyses by Mahé *et al.* (2005a) suggest that environmental change effects in runoff stem, in equal parts, from climate oscillation and land-cover changes. However, very little is known about the scales of impact of the various controls that can be generalised to different environments.

From a methodological perspective, the concept of change is central to the mission of the working group. Questions such as: “how do the various Earth science disciplines consider change, what are suitable methods of change analysis/detection, what feedbacks of land cover/climate impacts on water resources exist”, will stand at the forefront of the research agenda and stimulate exchange between various disciplines.

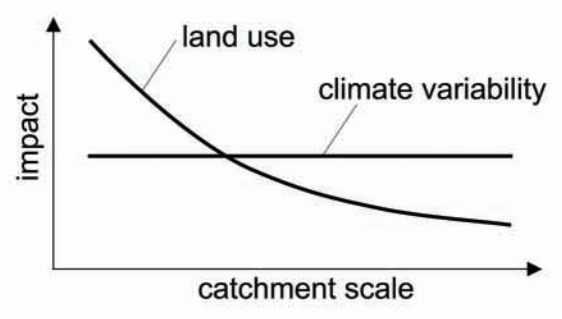


Fig. 1 Hypothesized impact of land use and climate variability on hydrological response as a function of scale.

The type of change may be closely related to the degree of nonlinearity of the system as well as any feedback effects present in the system. Climate regimes may change over a spectrum of time scales and may involve changes in the El Niño/ENSO cycles. Land cover and climate variability effects on floods and low flows are strongly controlled by the flow paths in catchment systems that differ in their time scales and the degree of connectivity. As to flow paths, there are two key issues. The first is: How do land use change and climate variability modify flow pathways and storage? The second, related, issue is: What are the changes in soil structure due to vegetation changes? Different mosaics of land-cover types exist and will impact in a complex way on low flows and floods. In assessing the effects of changes in the inputs to the system output and/or the system characteristics, the way the components interact are important, i.e. feedbacks may either exaggerate a disturbance or stabilize the system.

However, as data never exhaustively represent the hydrological environment, heterogeneity and scale effects enter the scene in impact analyses. A key issue is how to combine measurements and models across a range of scales (Blöschl, 2006). In the context of the implications of the current science question, an important issue is how changes in the hydraulic characteristics of soil, due to vegetation changes, transfer to larger scales and what is the interplay of groundwater dynamics and stream flow dynamics in response to changed land cover and climate variations. This is related to the feedback issues mentioned above. Of general interest is: how one can upscale local information on soils, vegetation, groundwater and surface water–groundwater interactions to the scale of HELP basins (10 000 km^2)?

Methodological perspectives of change and feedbacks, drawing from different Earth science disciplines are also of interest in this respect. Issues to be addressed include: how do floods and low flows change with time and what are the feedback mechanisms controlling them, what are the positive and negative feedback loops, how does the water balance affect runoff components (interactions between long and short time scales), what are the changes in the coupling between groundwater and surface water linked with land cover change.

MANAGEMENT ISSUES

The HELP programme has a management focus. Issues of climate and land cover impact on hydrological response are management relevant in a range of climates, particularly, if financial and sustainability impacts are involved such as in the salinity problems in parts of Australia. Often, incentives are necessary for land managers and end-users to cooperate. For example, the land care programme on salinity in Australia was successful as farmers were loosing money or land unless they cooperated. With nitrate issues in the UK, for example, a lower level of cooperation was observed as there is less obvious economic incentive. Other economic incentives for land managers may be to keep jobs in the region. In many countries, there is a tendency for water management to be short-term profit driven or driven by emergency requirements, e.g. drought in poorer countries. From a land development perspective, a key issue is how far one can develop a catchment before significantly impacting on the sustainability of water resources. Assessment tools include measurements and scenario analyses of the impact of alternative management strategies (Kepner *et al*., 2004). Scenarios can include quantified recharge and surface water–groundwater exchanges.

The management focus of HELP provides a special challenging framework for science questions concerning climate variability and land cover changes, flow path changes in response to such forcing, and the effects of these on low flows and floods. Issues to be addressed could consider how one can best use climate model results in view of the scale gap, how does uncertainty propagate from climate to hydrological models, if circulation patterns change—does this decrease/increase floods, how do land-use change and climate variability modify flow pathways and storage, what are the changes in soil structure due to vegetation changes?

More generally, the methods and tools depend on the goals. Management issues associated with soils include the resilience of soil systems, e.g. whether land will be degraded to a point where it will not recover. Management issues associated with vegetation include reforestation strategies, e.g. how best to restore a tropical forest. One possibility, for water quality issues, would be to let forests follow the riparian zone but this may involve time scales of 100 years and more. Modelling may be a platform for combining various sources of information and a vehicle for

transferring information to managers and for consensus building among stakeholders. What may help are standardized sets of climate/surface manipulation to be tested in multiple places in a stakeholder relevant way. Clearly, for science–management interaction to become productive, the problem to be solved needs to be a management focused problem on the ground rather than getting a published paper. To truly integrate science with decision making, a primary goal of HELP, it is essential for scientists to work more closely with decision makers and land and water mangers on an on-going basis. In this way, the scientific challenges to ultimately address the management problems can be identified. Research can then be formulated to directly aid in solving the management problems while producing peer-reviewed publications. This process requires a great deal of time and will likely impact the number of publications per unit time of a researcher. The reward is recognition that research results will have a near-term impact on resource and management decisions *versus* the typical slow diffusion of research out of the scientific journals. These journals are rarely read by resource managers and elected decision makers.

DATA SPARSE REGIONS, GENERALIZATION AND POTENTIAL OF TYPOLOGIES

As mentioned above, hydrology is a data limited discipline so, in a sense, all catchments of the world are data sparse. However, in developing countries data density is particularly low. Alternatives to expensive instrumentation are therefore needed. There exist a number of low cost options for measuring hydrological response at various scales. One example at the small catchment scale is simple tubes used as overland flow indicators (Vertessy *et al*., 2000). At larger scales, low cost monitoring strategies may involve enlistment of volunteers, such as in a successful programme with primary school teachers in Ecuador and the GLOBE programme. Optimizing measurement strategies is another corner stone in addressing the data scarcity issue. Hydrological observatories based on this philosophy have been established, or will soon be established, in a number of countries including the UK and the USA (e.g. by the CUAHSI initiative). Some data types are relatively easy to obtain, so another variant of optimizing the measurement strategy is a prudent choice of the variables to be sampled. If data are scarce, surrogate measures or indices are often extremely useful. Indices are usually designed to represent the main drivers or effects in a particular context with a minimum of information required. Such indices can be based on similarity measures across a landscape focusing on what makes patches of the landscape similar to other patches in terms of hydrological response, what makes aquifers similar to others or, more generally, what makes two catchments similar. Examples of indices include terrain indices to tag processes as a function of landscape position and flash flood guidance indices to tag rainfall intensities needed to produce a flood of a given magnitude (Georgakakos, 2006). Indices can be developed through both the upward and downward approaches. In a downward approach one usually classifies the objects of interest into types or classes to obtain a typology. A typology may help in generalizing findings from experimental catchments and is one method of dealing with the context dependence of hydrology and with data scarcity. A catalogue of catchment types, in terms of flow paths, runoff mechanisms and hydrological regimes would be of great value (Woods, 2002) as would be a worldwide catalogue of aquifer facies geometry and properties (de Marsily *et al.*, 2005).

Data issues and the development of simple indices that could assist in identifying the potential response of low flows and floods to change are therefore of high relevance. The typology approach could be considered instrumental in identifying such indices in diverse hydrological environments. Issues to be addressed include questions as to how climate/rainfall, catchments, aquifers, soils and vegetation can be classified (with a view on floods and low flows) with the help of experimental basins, what processes switch between regimes (in time, spatially), how to give guidance on the necessary regulations given a monitoring network, what variables should be strategically collected that would more directly address impact on hydrological response?

RELATIONSHIP TO HELP INITIATIVE AND OTHER PROGRAMMES

There are a number of avenues for relating the agenda of this working group to HELP and other programmes. First, important links should be established on a personal basis. As noted above, establishing good scientist to manager/decision-maker relationships takes time. Trust must be

established and maintained. As a next step, some of the methods developed and/or summarized during the workshops could be applied to a selection of HELP basins. For example, the typologies could be tested in a number of HELP basins as a demonstration exercise keeping data poor areas in mind. In a similar vein, some of the water managers of HELP basins could be involved in the workshops to be held. If this is to occur, the typical scientific workshop format must be modified and tailored to decision-makers. These include representatives of departments of water affairs or EPAs. In particular, the typologies would be of interest from a management perspective because of the potential of simple indices. Winning the acceptance of funding authorities can be greatly assisted by managers' testimonies of the usefulness of tools that have been developed in co-operative research efforts. Some of the HELP sub-basins are research catchments and would hence be a logical starting point for testing novel concepts. Another avenue of interaction with the HELP initiative is to disseminate the proceedings of the workshops to coordinators of HELP basins with a summary to water managers of the respective basins. Another potential contact point is the international flood initiative. This is an interagency initiative that involves UNESCO. The Predictions in Ungauged Basins (PUB) initiative of IAHS has a focus on reducing uncertainty, in particular in ungauged basins (Sivapalan *et al.*, 2003). There are a number of growth areas where synergies between PUB and this working group could be exploited. Commonalities are issues of data scarce areas and modelling issues. What sets this group apart from PUB is a focus on change, climate issues and scales including a broader interdisciplinary perspective of management.

SUMMARY

The purpose of each workshop is to summarize the state of the art, to contribute to the planning of research strategies for testing in HELP basins and to further the understanding of land use and climate impact on hydrological extremes. The workshops will be designed to provide a road map of how to address impact issues and to act as a catalyst for motivating communication and targeted research. Some of the topics identified at the working group meeting are closely related to each other and should therefore be dealt with at the same workshop. Issues of change and feedbacks are intimately linked as the type of feedback often controls system dynamics, including their resilience. This could be the topic of a first workshop. Data issues and ways of identifying simple indices of change, e.g. through hydrological typologies, could be the topic of a second workshop. The focus of the third workshop could be on understanding both atmospheric processes and catchment flow processes in the context of impact analyses. The third workshop could hence deal with the effect of climate variability and land-use changes on flow paths in catchments and on their consequences for hydrological extremes. The final workshop could integrate the findings of the previous workshops with a scale focus. Management aspects should be integrated in all workshops.

Acknowledgements The first author would like to thank Mike Bonell for his enthusiasm, energy and advice in establishing and running this working group.

REFERENCES

Blöschl, G. (2006) Hydrologic synthesis: across processes, places, and scales. *Water Resour. Res.* **42**, W03S02, doi: 10.1029/2005WR004319.

de Marsily, Gh., Delay, F., Goncalves, J., Renard, Ph., Teles, V. & Violette, S. (2005) Dealing with spatial heterogeneity. *Hydrogeol. J.* **13**, 161–183.

Georgakakos, K. P. (2006) Analytical results for operational flash flood guidance. *J. Hydrol.* **317**, 81–103.

Kepner, W. G. Semmens, D. J., Bassett, S. D., Mouat, D. A. & Goodrich, D. C. (2004) Scenario analysis for the San Pedro River, analyzing hydrological consequences of a future environment. *J. Environ. Monitor. Assess*. **94**, 115–127.

Mahé, G., Olivry, J. C. & Servat, E. (2005) Sensibilité des cours d'eau ouest-africains aux changements climatiques et environnementaux: extrêmes et paradoxes. In: *Regional Hydrological Impacts of Climate Change—Hydroclimatic Variability* (ed. by S. W. Franks *et al.*), 169–177. IAHS Publ. 296. IAHS Press, Wallingford, UK.

Sivapalan, M., Takeuchi, K., Franks, S. W., Gupta, V. K., Karambiri, H., Lakshmi, V., Liang, X., McDonnell, J. J., Mendiondo, E. M., O'Connell, P. E., Oki, T., Pomeroy, J. W., Schertzer, D., Uhlenbrook, S. & Zehe, E. (2003) IAHS decade on Predictions in Ungauged Basins (PUB), 2003–2012: shaping an exciting future for the hydrological sciences. *Hydrol. Sci. J.* **48**, 857–880.

Vertessy, R. A., Elsenbeer, H., Bessard, Y. & Lack, A. (2000) Storm runoff generation in a small tropical rainforest catchment with spatially variable soil hydraulic properties. In: *Spatial Patterns in Catchment Hydrology: Observations and Modelling.* (ed. by R. Grayson & G. Blöschl), 247–271. Cambridge University Press, Cambridge, UK.

Woods, R. (2002) Seeing catchments with new eyes. *Hydrol. Processes* **16**, 1111–1113.

Climate Variability and Change—Hydrological Impacts (Proceedings of the Fifth FRIEND World Conference held at Havana, Cuba, November 2006), IAHS Publ. 308, 2006.

Overview of land cover change in tropical regions

RUDI DRIGO
Forestry Specialist (currently collaborating with the Forest Products Division of FAO)
Loc. Collina 5, 53036 Poggibonsi, Siena, Italy
rudi.drigo@tin.it; rudi.drigo@fao.org

Abstract The change of tropical forests, reported by the FAO's 2005 Forest Resources Assessment, showed a moderate negative trend: for the period 2000–2005 the net annual change was estimated at –11.8 million ha, while the rate for the previous decade was –11.65. Tropical Asia showed the highest rate and most negative trend, passing from –0.8 to –0.96 percent per year. The remote sensing survey done for previous FRA editions covering the period 1980–2000 revealed distinct change processes in the three tropical regions. Survey results indicated that socio-economic and cultural aspects that characterize and differentiate the geographic regions determine the nature of the change processes and underlying cause–effect mechanisms, while the ecological setting determines the intensity of change and reveals its environmental implications. A comparison of deforestation processes of the two decades indicated an on-going process of radicalization of the dynamics determined by an increasing frequency of high-gradient changes (e.g. total clearing rather than fragmentation and degradation) and by a shift of deforestation fronts towards wetter zones, with a consequent higher per-hectare carbon emission associated with deforested areas.

Key words deforestation; global forest assessments; land cover change processes; tropical forest

GLOBAL FOREST INFORMATION SOURCES

During the last 60 years systematic country by country information on forest area and change have been produced exclusively by the FAO, whose reports, in spite of some criticism (e.g. Stokstadt, 2001), have been the main reference for discussion and analysis at the regional and global level. The FAO's assessment techniques have changed considerably over the time, from the initial "questionnaire" approach that was used until the 1970s, to the review, country-by-country, of original inventory date complemented by experts' judgment (FRA of 1980), to sub-national forest area time series integrated by modelling techniques (FRA of 1990), to the return to national-level statistics complemented by experts' opinions and in-depth studies (FRA of 2000). In addition, a pan-tropical remote sensing survey was implemented during the FRAs of 1990 and 2000 with the aim of producing consistent data on forest cover change, and trends, at the regional and pan-tropical level (FAO, 1996, 2003). The last assessment, the FRA of 2005, whose results have recently been released, based its updated country data on a pre-determined set of tables to be filled in by country correspondents formally appointed by the respective governments; in practice an advanced questionnaire approach based on a set of clear definitions and standard formats. The final country statistics were the result of an iterated dialogue between FRA staff and the national correspondents, especially in cases of incomplete or inconsistent data. This process was led by the countries that remain sole owners of the data finally published, with FRA playing essentially the role of facilitator and coordinator. Unfortunately, in this last assessment the remote sensing survey was discontinued and therefore there are no updates on the analysis of tropical change processes beyond the periods 1980–1990 and 1990–2000.

The TREES project of the European Joint Research Centre (JRC) carried out a survey of forest cover in humid tropical regions (Achard *et al.*, 2002) based on an analysis of time series of high-resolution satellite imagery at statistically chosen locations covering the period 1990–1997. The study did not produce country statistics and the comparison at regional scales with FAO data was constrained by the TREES' survey limitation to dense forest formations in humid tropical regions. In spite of these limitations, a combined analysis of FAO and TREES remote sensing surveys revealed a substantial agreement on forest change rates in Africa and Asia, while in the case of Latin America the TREES study gave a much lower rate due, most probably, to the exclusion of seasonally deciduous forests from the analysis (Drigo, in Bonell & Bruijnzeel, 2005).

Other sources of data relevant to the analysis of land cover at the global level are grouped under the Global Observation of Forest and Land Cover Dynamics (GOFC-GOLD) initiative, which is a panel of the Global Terrestrial Observing System (GTOS). The potential of this coordinated effort to assist in the production of globally consistent and reliable information of

Copyright © 2006 IAHS Press

forest cover and change is great. Specifically, in the context of forest hydrology, spatially-discrete data showing variation of canopy density is far more useful than crude forest–non forest maps and statistics (Held & Rodriguez, in Bonell & Bruijnzeel, 2005). Interesting products in this respect are the global tree cover percent data and the forthcoming change maps based on MODIS satellite data at 500 m resolution (Hansen *et al*., 2003). To date, however, there are no statistics resulting from these programmes that may be considered as an alternative to those produced by the FAO.

In the following sections, FRA 2005 and the pan-tropical remote sensing survey of FRA 1990 and 2000 were used as main sources of information on tropical forests changes.

SUMMARY OF FRA 2005 COUNTRY STATISTICS

The net annual change of tropical forest area, defined as total man-made and natural afforestation minus total deforestation, was estimated at –11.8 million ha for the period 2000–2005, while the rate for the previous decade was –11.65 million ha (Table 1). This represented a non-negligible increase in net annual change rate from –0.59% to –0.63% of the forest areas. This negative trend was observed in all tropical regions, with Asia showing the most negative trend, passing from –0.8 to –0.96% per year. The situation when looking at natural forest only appears even worse. All change rates are higher and Asia deforestation rate rises to 1.11% per year (Table 1, lower section). Still, these values hide the true magnitude of ongoing deforestation, i.e. areas of forest cleared and the land converted to other uses, because they include natural afforestation, i.e. through natural expansion of forests, e.g. on abandoned agricultural land that are not separately reported by the countries (FAO, 2005). A very tentative, and certainly conservative, estimation of the true annual deforestation (determined considering only the countries with negative change and deducting plantation areas) may be in the order of 13.5 million ha at the global level, with some 12.4 million ha in tropical countries alone.

While writing, the media report the terrible disaster of the Philippines, where over a thousand lives from two villages in southern Leyte (the sad count still going on) were taken by a mudflow caused by heavy rains and high deforestation and triggered by a relatively weak earthquake. I checked the table: the current Philippines deforestation rate is 2.1%, the highest in Asia and was 2.8% in the previous decade. A predictable disaster?

Figure 1 provides a global geographic overview of FRA 2005 deforestation statistics from which the dominant role of the tropical countries appears very clearly both in terms of deforestation rates and negative trends.

REGIONAL CHARACTER OF PROCESSES GOVERNING LAND COVER CHANGE

Insight on the processes of change by broad geographic regions and ecological zones was produced by the remote sensing survey carried out by the FRAs of 1990 and 2000 over the entire

Table 1 Tropical forest areas and change rates as assessed by the Forest Resources Assessment 2005 of FAO.

Tropical sub-regions	Area			Annual change rate			
	1990 1000 ha	2000 1000 ha	2005 1000 ha	1990–2000 1000 ha year^{-1}	2000–2005 1000 ha year^{-1}	1990–2000 %	2000–2005 %
	Total forest (natural and plantations)						
Tropical Africa	682 698	638 179	617 679	–4 452	–4 100	–0.65	–0.64
Tropical America	941 393	896 866	873 515	–4 453	–4 670	–0.47	–0.52
Tropical Asia	323 156	297 380	283 126	–2 578	–2 851	–0.80	–0.96
Tropical Oceania	36 891	35 164	34 268	–173	–179	–0.47	–0.51
Tropical World	1 984 138	1 867 589	1 808 588	–11 655	–11 800	–0.59	–0.63
	Natural forest *						
Tropical Africa	673 569	628 847	608 154	–4 472	–4 139	–0.66	–0.66
Tropical America	934 177	888 730	865 033	–4 545	–4 739	–0.49	–0.53
Tropical Asia	310 391	282 179	266 492	–2 821	–3 137	–0.91	–1.11
Tropical Oceania	36 696	34 928	34 021	–177	–181	–0.48	–0.52
Tropical World	1,954 833	1 834 684	1 773 700	–12 015	–12 197	–0.61	–0.66

* Natural forest values were not reported by FRA 2005 but were calculated by the author by deducting from the total forest the areas of plantations. Since for several countries plantation statistics were missing or incomplete, the calculated values should be considered as indicative only. This means that natural forest areas are probably smaller and that their changes are probably higher. Source: Elaboration of FAO, 2005.

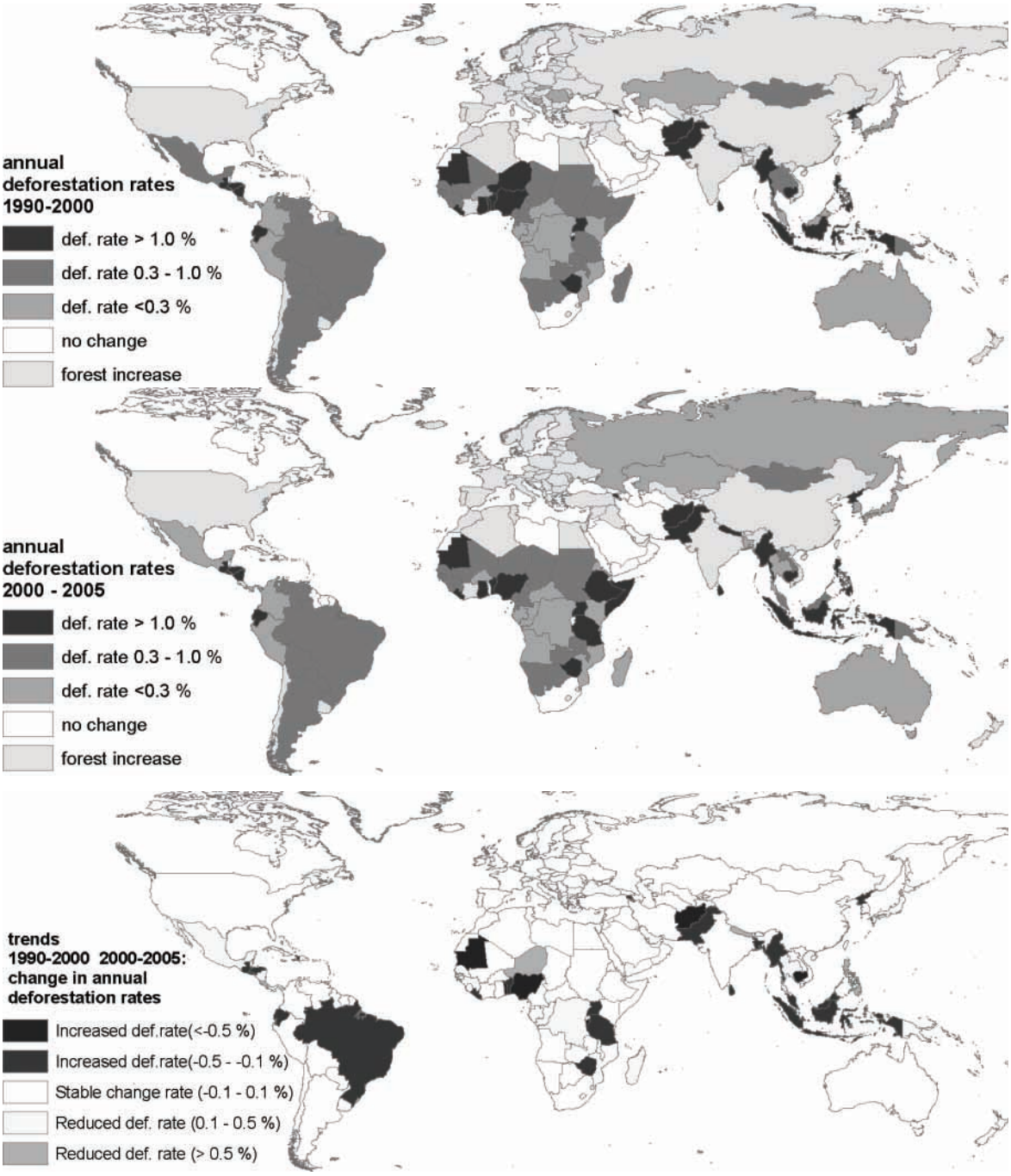


Fig. 1 Global maps of annual deforestation rates for the periods 1990–2000 and 2000–2005 and trends.

tropical belt. The country data discussed above and the remote sensing survey are independent and complementary and the latter is here presented in order to analyse the typology rather than the quantity of change. The survey was based on a 10% sample, consisting of 117 randomly selected sampling units, each unit covering approximately 3.2 million ha (FAO, 1996, 2003). At each sample location, satellite images of the best quality and appropriate season, separated by an approximate 10-year interval, tentatively 1980, 1990 and 2000, were analysed following the interdependent interpretation method (FAO, 1991, 1996; Drigo, 1996) to assess class-to-class transitions within the two periods and the main trends.

The regional processes of change may be best visualized through the flux diagrams (Fig. 2). In these diagrams the changes (*x*-axis, divided into positive and negative changes) are associated to an indicative biomass density gradient (*y*-axis, with the land cover classes used in the study ordered by their estimated biomass per hectare) that allows visualization and better understanding of the change processes, and even assessment of their environmental impact through the release or seques-

tration of woody biomass related carbon. The left side of the graph shows the positive class transitions (the arrow pointing upward indicates an increment in biomass), while the right-hand side of the graph shows the negative class transitions (the arrow pointing downward indicates a loss of biomass).

Each transition is defined by the % of total change observed in the region (*x*-axis) and by the biomass value determined as the difference between the biomass values of the class of destination and the class of origin (*y*-axis) (FAO, 1996). Each flux diagram represents a kind of signature of the dynamic processes taking place. From the diagrams in Fig. 2, which show the changes for the period 1990–2000, we can rapidly visualize the considerable differences in the processes of changes among the three regions, which can be summarized as follows:

Africa

In Africa, the processes of change show phases of progressive degradation, rather than outright deforestation, caused mainly by high rural and urban population pressure (Fig. 2, top). The typology of change appeared as characterized by a variety of relatively small changes, both in terms of area and biomass, caused mainly by rural population demands for land (subsistence farming, pastures) and wood (mainly woodfuels and, to a lower extent, timber and construction material). The dominant transitions are:

– **closed forest → short fallow**, which is the effect of small-scale subsistence farming whereby the fertility of the soil is regenerated during fallow periods of a few years;
– the sequence **closed forest → open forest → fragmented forest → other land cover** clearly represents the various stages of forest depletion, and is an effect of rural and urban population needs for land and energy. Most probably, commercial logging triggered many of these processes, at least in the more productive forest zones.

Key factors behind the pressure on forests in Africa are (FAO, 2001a): rapid population growth, particularly that of the urban population; poverty, slow economic development, inadequate economy; wars and conflicts; insecurity of land tenure; desertification/climate change (Drigo, in Bonell & Bruijnzeel, 2005). Among the direct causes of deforestation the following can be identified (FAO, 2001a): poor farming practices; conversion to cash crop estates; shrimp farming in mangrove areas; increased clearing and tree cutting for fuelwood and charcoal; poor logging practices and overexploitation; commercial logging as a direct cause of degradation and indirect cause of full deforestation; mining; desertification in Sahelian countries.

Woodfuels (wood-based fuels such as fuelwood and charcoal) play an important but largely undisclosed role in the cause–effect mechanisms associated with deforestation and forest degradation in tropical regions and particularly in Africa (Drigo, 2001, Drigo, in Bonell & Bruijnzeel, 2005). An element of special concern that should be studied with priority is the fast rising demand for charcoal linked to the rapid increase in urbanization.

Latin America

A totally different typology of change dominates in Latin America. Here the single transition **closed forest → other land cover**, which represents deforestation with the highest possible biomass loss resulting mainly from the direct conversion of the original forest to cattle ranching and permanent agriculture, was by far the most important change (Fig. 2, middle). The estimated biomass loss associated with these transitions certainly is the highest anywhere in the tropics.

The second most frequent transition, **shrubs → other land cover**, represents the large areas of Brazilian *caatinga* (steppe typical of the northeast regions of Brazil) and *cerrado* formations (tree and shrub savanna of south-west and central Brazil) that were being converted to cattle ranching.

Most of these changes were the effect of policies and incentives to cattle ranching and other centrally planned operations on a comparatively large scale (large land ownership, energy schemes, resettlement and forest exploitation/conversion programmes), usually availing of consistent financial investment and heavy mechanization (Serrao, in Bonell & Bruijnzeel, 2005).

The transition **closed forest → short fallow** as well as a number of other, less frequent changes in land cover, represent the effect of high rural population pressure and small-scale farming, such as in the Amazon and Yucatan, and is often associated with resettlement programmes. This type of changes appeared less frequent than in the previous decade due to several factors such as, for

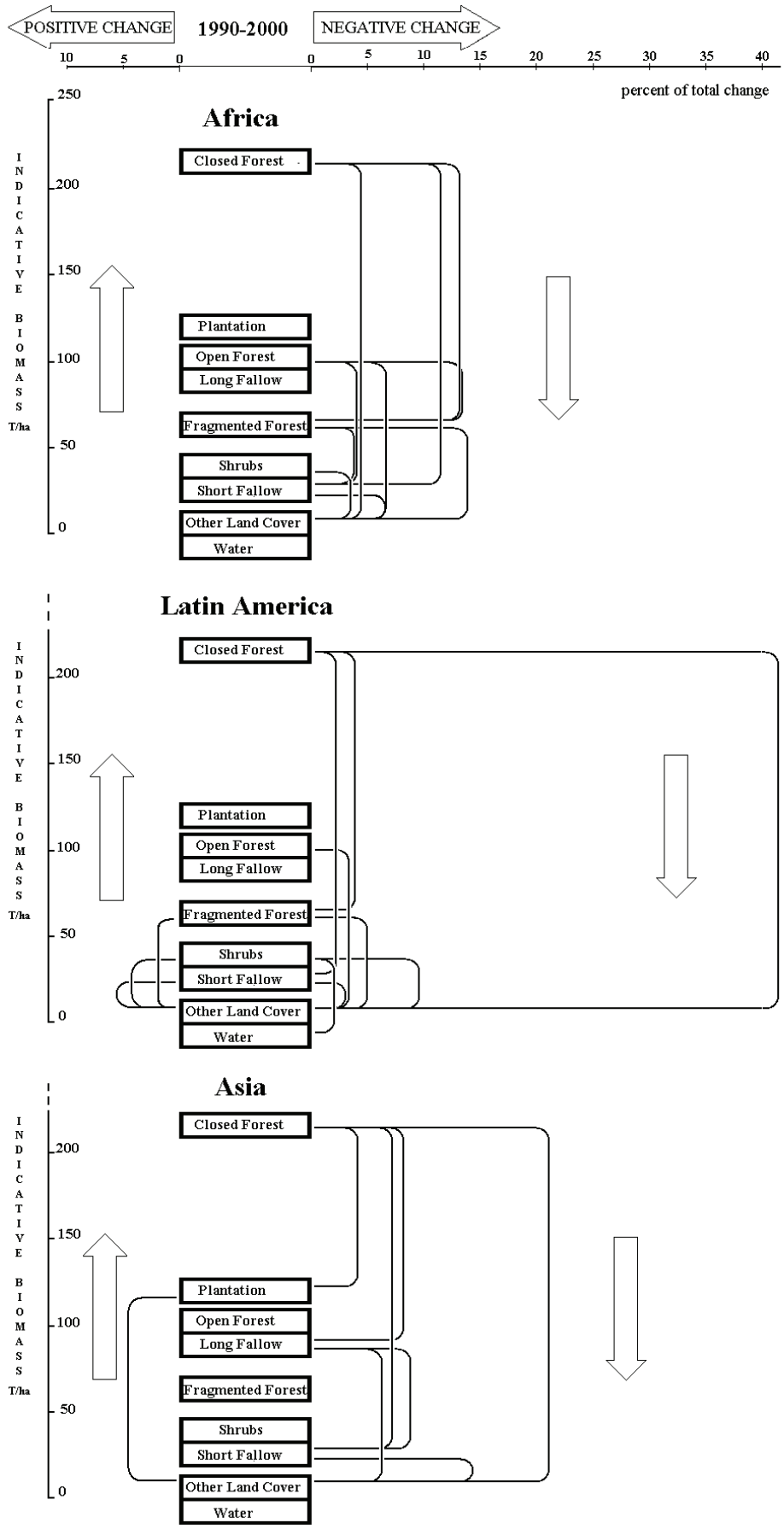


Fig. 2 Woody biomass flux diagrams for tropical Africa, Latin America and Asia for the period 1990–2000 (elaboration of FAO, 2003; transitions below 2% are not shown).

instance, changes in Brazilian policies regarding resettlement programmes (Serrao, in Bonell & Bruijnzeel, 2005). Nowadays it seems that the overwhelming majority of cleared forest is converted for cattle ranching rather than agriculture (Fujisaka *et al*., 1996).

Asia

Tropical Asia presented the highest rates of deforestation and forest degradation among the three regions, as confirmed also by FRA 2005 statistics (Table 1). These rapid changes were the effect of both high rural population pressure and centrally planned conversion programmes, as can be deduced from Fig. 2 (bottom). Deforestation was represented by the conversion of forests to **other land cover** and to **short fallow shifting cultivation**. The former is largely the effect of centrally planned conversion programmes, mostly in the form of large resettlement schemes involving forest exploitation/conversion (particularly in Indonesia and Malaysia) and intensification of permanent agriculture on traditional shifting cultivation areas (South and Southeast continental Asia). The second major conversion reflects the effect of high rural population pressure, and is represented by the expansion of subsistence farming into forest areas along logging roads and from existing croplands. The process of forest **degradation** is represented mainly by the expansion of traditional shifting cultivation (long fallow shifting cultivation), that encroached on previously dense or undisturbed forest. An equal amount of the **long fallow** forest class was converted to **short fallow** and, a little less, to **other land cover**, reflecting a sequence of progressive forest depletion as a direct effect of the growing population and related needs for farm land. Shifting cultivation is by definition a cyclic form of land use. Traditionally, new areas under shifting cultivation were balanced by areas where cultivation was abandoned to revert to (secondary) forest conditions. Since a long time, this balance has been lost, thereby converting the cycle into a sequence of progressive degradation. The difference between the forest area going into long fallow and the area of long fallow reverting to forest shows how unbalanced, and hence unsustainable, this originally sound practice has become (cf. Malmer *et al*., in Bonell & Bruijnzeel, 2005).

The area covered by plantations in Asia, both forestry and agricultural plantations, increased significantly, partly at the expense of closed forest and partly in previous denuded lands (other land cover).

The comparison with the changes of the previous decade gave the impression of a certain radicalization that favored land use changes associated with high-gradient transitions (i.e., clear-felling). Another difference is that in the previous period the quasi-totality of the new plantation area was established on previous dense forest areas. This represents an important element counterbalancing, to a small extent at least, the negative general trend.

SUMMARY OF REGIONAL PERSPECTIVE

Comparing the three regional situations, the dominance of the changes in Latin America becomes even more pronounced, as these combine the largest area of change (Table 1) with the highest biomass loss. In fact, the biomass gradient of Latin America's most frequent class transition (**closed forest → other land cover**), represents the maximum biomass loss observed anywhere (cf. Fig. 2).

The effects of **centrally planned operations** are evident in Latin America and in Asia but to a much lesser degree in Africa. Typical land uses related to these processes are: cattle ranching in the Brazilian Amazon, large resettlement and plantation programmes in Southeast Asia and, to a lesser degree, in West Africa. Comparing the 1980s and 1990s there are strong indications that, except for Africa, these relatively high-investment and high-gradient transitions are taking the lead in recent years, thereby contributing to the radicalization of land use change (Drigo, in Bonell & Bruijnzeel, 2005).

The other important component of the process, **rural population pressure**, is characterized by combinations of low-gradient transitions associated with subsistence and small-scale farming, such as long and short fallow shifting cultivation, processes of forest fragmentation and degradation, etc. This component remains dominant in Africa but it seems to be losing terrain in Asia and Latin America.

ECO-REGIONAL DISTRIBUTION OF FOREST CHANGE

Another interesting perspective is offered by the analysis of land cover change by broad ecological zones (FAO, 1996, 2003). Main results indicated that in all regions the forest resources of the

moist tropical zone (rainfall 1000–2000 mm) suffered the highest pressure, both in the form of full deforestation and forest degradation, with a rate of change which appeared to be (at least) twice of that observed for the wet (rainfall >2000 mm) and dry (rainfall 200–1000 mm) zones (FAO, 1996). More specifically, a comparison of the different ecological zoning adopted by FRA 1990 and FRA 2000 allowed the deduction that the most active fronts of deforestation during 1980–1990 was within the wetter Moist sub zone characterized by a short dry season, and that these hot fronts are getting more intense and that they are fast moving towards the wetter cores of the remaining forest areas (Drigo, in Bonell & Bruijnzeel, 2005). This impression is confirmed by the acceleration of the deforestation rate in the Rain Forest zone, where the corresponding annual rate of change went up from –0.50 to –0.61%, which is one of the statistically most significant trends observed (FAO, 2003). This acceleration is accompanied by the indication of a possible deceleration of the deforestation rate in the Moist Deciduous Forest. Arguably, this shift of the deforestation front towards the wetter zones is the most significant trend observed in this study.

GENERAL TRENDS OF PROCESSES OF CHANGE

A comparison of deforestation processes of the two decades of the FRA survey indicated that the conversion to subsistence farming associated with re-settlement programs and traditional practices, which represented a large share of the total change in the pre-1990 period, was reduced considerably during the 1990–2000 decade. This reduction, combined with the increased frequency of the transition from **closed forest** to other **land cover**, which appeared significant at least in the Tropical Rain Forest Zone, gives strong indications of an on-going process of radicalization of the dynamics whereby the expansion of large-scale cattle ranching and permanent agriculture becomes more and more the dominant land use change associated with deforestation (Drigo, in Bonell & Bruijnzeel, 2005). This transition towards high-gradient changes, associated with the "wet" shift of the deforestation front and the consequent higher biomass densities of the forest formations being cleared and degraded, implies a significant trend towards a higher per-hectare carbon emission associated with deforested areas. These elements further strengthen the impression of a radicalization of the processes of tropical deforestation. In fact, from the carbon budget viewpoint, the increased biomass density of the forests currently under pressure will probably offset the beneficial effect of the slight reduction in the net forest area change announced by FRA 2005 at global level (FAO, 2005).

The analysis of change processes is far more informative than country time series of forest areas. It is highly recommended that FAO in its future assessments, or other programmes, continue global/regional/ecological level analyses taking advantage of the experience already accreted on monitoring methodologies and of the progress in satellite data availability.

REFERENCES

Achard, F., Eva, H., Stibig, H. J. Mayaoux, P., Gallego, J., Richards, T. & Malingreau, J.-P. (2002) Determination of deforestation rates of the world's Humid Tropical Forests. *Science* **297**, 999.

Bonell M. & Bruijnzeel, L. A. (eds) (2005) *Forests, Water and People in the Humid Tropics. Past, Present and Future Hydrological Research for Integrated Land and Water Management.* Cambridge University Press, Cambridge, UK.

Drigo, R. (1996) Survey of pan-tropical forest resources based on multi-date high resolution satellite data. In: *Proc. EUROSTAT Esquilino Seminar* (November 1995), 111–141.

Drigo, R. (2001) Wood energy information in Africa. Working Document FOPW/01/4, FAO Project GCP/RAF/354/EC.

FAO (1981) Tropical Forest Resources Assessment project (in the framework of GEMS). Asia; Latin America; Africa. Rome.

FAO (1991) Monitoring Methodology. Forest Resources Assessment 1990 Project Paper by R. Drigo.

FAO (1993) Forest Resources Assessment 1990. Tropical Countries. *FAO Forestry Paper 112.*

FAO (1996) Survey of tropical forest cover and study of change processes. *FAO Forestry Paper 130*.

FAO (2001) Global Forest Resources Assessment 2000. Main report. *FAO Forestry Paper 140.*

FAO (2003) Pan-tropical survey of forest cover changes 1980–2000. *FRA Working Paper 49*.

FAO (2005) Global Forest Resources Assessment 2005. *FAO Forestry Paper 147*. http://www.fao.org/docrep/008/a0400e/a0400e00.HTM.

Fujisaka, S., Bell, W., Thomas, N., Hurtado, L. & Crawford, E. (1996) Slash-and-burn agriculture, conversion to pasture and deforestation in two Brazilian Amazon colonies. *Agric. Ecosystems & Environ.* **59**, 115–130.

GOFC-GOLD (2006) Global Observation of Forest and Land Cover Dynamics http://www.fao.org/gtos/gofc-gold/index.html.

Hansen, M., DeFries, R., Townshend, J. R., Carroll, M., Dimiceli, C. & Sohlberg, R. (2003) 500m MODIS Vegetation Continuous Fields. The Global Land Cover Facility. College Park, Maryland, USA.

Stokstad, E. (2001 UN Report suggests slowed forest losses (A review of:) *Science* **291**, 2294.

Climate Variability and Change—Hydrological Impacts (Proceedings of the Fifth FRIEND World Conference held at Havana, Cuba, November 2006), IAHS Publ. 308, 2006.

The impacts of land-use/land-cover change and climate variability on the hydrology of the Sahel

GIL MAHE

HydroSciences Montpellier Laboratory (UMR CNRS, IRD, UM1, UM2), Case MSE, University Montpellier 2, F-34 095 Montpellier cedex 5, France

gil.mahe@msem.univ-montp2.fr

Abstract The joint effect of climate change and of human activities on land cover is responsible for an increase of the runoff coefficients of the West African Sahelian rivers since the 1970s, as revealed by the analysis of runoff time series of rivers from Mauritania, Burkina-Faso and Niger. The runoff coefficients have increased in regions with less than 750 mm of annual rainfall, under Sahelian and sub-desertic climates, leading to increased flood peaks, occurring earlier in the season. Studies have shown a rapid change in land-use/land-cover (LUCC) since the 1970s over Sahelian river basins in Burkina-Faso and Niger. It is likely that the aridification of the environment—triggered by climatic change, especially rainfall shortage—is, to an important extent, enhanced by increasing agricultural activities. The relationships between hydrology and LUCC are studied using hydrological modelling. Rainfall/runoff modelling is improved when taking into account the spatio-temporal evolution of the LUCC through a time varying water holding capacity (WHC). The WHC, considered as the soil water reservoir in hydrological models, decreases as the natural vegetation is replaced by cultures or bare soil, leading to increased surface runoff. Long-term observations on "reference river basins" should be set from now on, to collect comparative information for the future.

Key words climate variability; hydrology; land use/land cover change; West African Sahel

INTRODUCTION

Since 1970, West Africa has experienced one of the most abrupt and long-lasting changes of climate ever in the world since the beginning of the records (1900) (Paturel *et al.*, 1997; Mahe *et al.*, 2001; Hulme *et al.*, 2001). This period of rainfall diminution is still ongoing (Lhote *et al.*, 2001, 2003; Dai *et al.*, 2004), although less strong since the mid 1990s than during the 1980s. As for 35 years annual rainfall has remained below the 1900–1970 average in this region, this might well be an impact of the global climate change induced by the increasing of the greenhouse gases concentration in the atmosphere. What the causes and the mechanisms of this lasting drought are is a matter for other studies. From a hydrological point of view, the relevant question for West Africa is: How has climate change (and especially rainfall) affected the rainfall–runoff relationships and the river regimes?

For almost all the rivers of West Africa, runoff has decreased post-1970. But the changes in the rainfall–runoff relationships are far from proportional (Mahe *et al.*, 2000), and even show paradoxical situations. The first hydrological paradox in West Africa is that in most cases the runoff diminution rate largely exceeds that of the rainfall, which is explained mainly by the long-lasting deepening of the water table, and hence a lower contribution from the baseflow to the river regime post-1970 (Mahe *et al.*, 1999, 2000). In more arid regions, as in the Sahel, only surface runoff drives the hydrological regime (Casenave & Valentin, 1989, 1992). Only a few long-time runoff series for this region have been recently studied, from which has been described the second "paradox": the increase of runoff coefficients of the Sahelian rivers since 1970. Pouyaud (1987) had already observed such an increase but only for very small catchments. Recent studies show that these hydrological changes also modified hydrological regimes of large Sahelian river basins (Amani & Nguetora, 2002; Mahe *et al.*, 2003, 2005a).

In this paper we present a synthesis of studies about land-use/cover change (LUCC) and climate variability on the hydrology of the Sahel. Some previously unreleased material about rainfall–runoff changes in the Sahelian part of Mauritania is also presented, which confirms the first observations from the central Sahel catchments.

CLIMATE VARIABILITY IN WEST AFRICA

Climate is mostly related to rainfall and temperature. Rainfall changes over West Africa have been comprehensively described for the last 30 years, after the 1970s drought. Temperature changes over West Africa have been studied less. We present some results about PE variations since the 1950s.

Copyright © 2006 IAHS Press

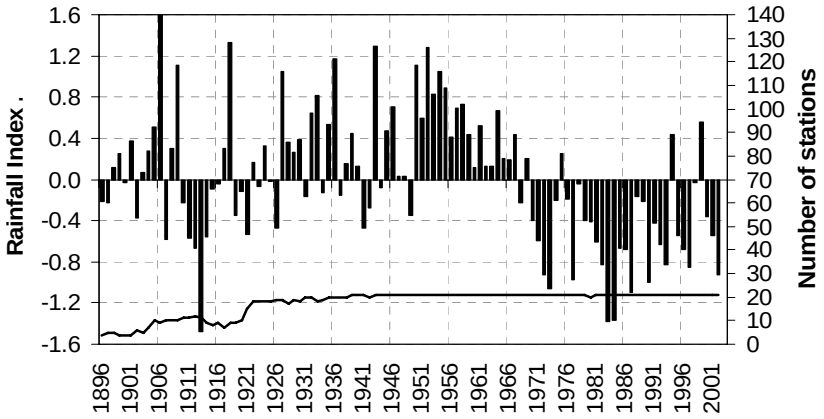


Fig. 1 Sahelian rainfall index (after L'Hote *et al.*, 2002).

The rainfall variability over West Africa and particularly over the Sahel is naturally high. The rainfall shortage during the 1980s, relative to the 1950s, is about 10–15% over tropical humid Africa, and about 15–20% over the Sahel. Since the mid 1990s the rainfall average over the region slightly increased to reach the level of 1970s rainfall (Fig. 1).

In a preliminary work, Ould (2001) studied monthly and annual PE for big river catchments in West Africa, calculated from CRU data (University of East Anglia, UK) (New *et al.*, 2000). PE is related to temperature changes, but also to cloud cover, air humidity and wind changes. This study shows a significant and systematic increase by about 1–1.5% of the annual PE (Penman-Monteith and Thom and Oliver formulas, Ardoin-Bardin *et al.*, 2005) over great rivers like the Niger and Volta. Discontinuities within monthly time series of catchments' PE have been detected by statistical tests (Pettitt and Hubert tests, Lubes-Niel *et al.*, 1998; Paturel *et al.*, 1998); they all show an increase of PE since mainly the late 1970s or the early 1980s, and mainly for the months of January, April, August and September. This is mainly due to the increase of temperature, which is slight over Africa, only 0.5°C, but significant since the late 1970s (Hulme *et al.*, 2001). The predicted increase of temperature and PE over the 21st century should affect West Africa river regimes by reducing surface runoff for most of the rivers in tropical and equatorial humid West Africa (Mahe *et al.*, 2005b), but up to now it has not been possible to predict anything for Sahelian rivers as the performances of the hydrological models are not good enough.

RELATIONSHIPS BETWEEN CLIMATE VARIABILITY/CHANGE, LUCC AND HYDROLOGY OF THE SAHEL

Recent changes in Sahelian hydrology: the counter-intuitive Sahelian paradox

The Sahel can be defined by several characteristics. The most commonly used is the annual rainfall amount. Between May and October, with a rainfall maximum usually in August, annual rainfalls reach between 250 and 750 mm from the north to the south. In this area, runoff coefficients are very low (a few %), as almost all rainfall is evaporated. Groundwater does not contribute to the surface runoff, and the surface runoff produced at each point of a basin is transferred downstream with nearly no losses. The equilibrium between soil and vegetation is very fragile, and changes in rainfall and/or changes in human activities have rapid consequences on the environment.

Rainfall and runoff for hundreds of river basins have been studied in West Africa (Mahe *et al.*, 2005b). For nearly all basins we observe a runoff reduction, except for Sahelian rivers. Figures 2 and 3 show the runoff coefficient increase relative to the rainfall variability both in the Central Sahel (Burkina-Faso and Niger, Fig. 2) and in the Western Sahel (Mauritania, Fig. 3). It is also surprising to report that this runoff increase occurs when in the same period: rainfall is decreasing, yet human consumption and dam storage capacity are increasing.

The aridification process and its impact on hydrological regimes

Natural causes Over the past 35 years, by natural equilibrium, vegetation and soil have adapted to the new climatic conditions, leading to more "arid" conditions in the Sahel. But it is

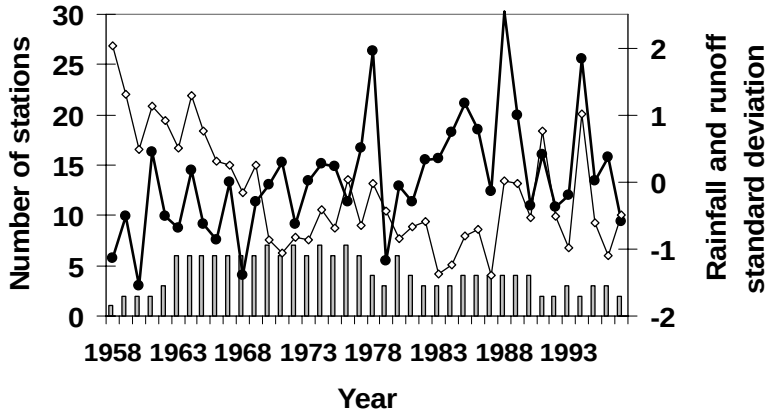


Fig. 2 Standard deviation for rainfall (white dots) and runoff coefficient (black dots) variability for Sahelian river basins of Burkina-Faso and Niger (bars: number of basins per year, maximum = 7).

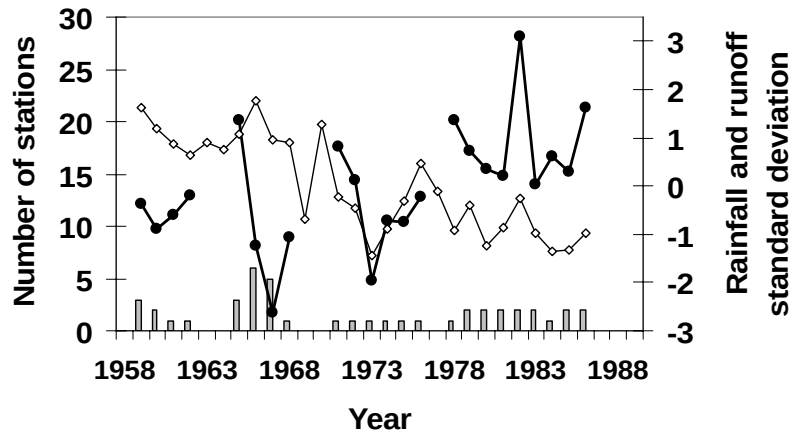


Fig. 3 Standard deviation for rainfall (white dots) and runoff coefficients (black dots) variability for Sahelian river basins of Mauritania (bars: number of basins per year, maximum = 8).

very difficult to separate natural causes from human causes, as there is no "witness" basin, protected from human impacts, which could be used for reference hydrological studies. Nevertheless, the Dargol River basin, at the boundary between Burkina-Faso and Niger, only poorly inhabited, could serve as a reference for comparison with highly anthropogenized basins like the Nakambe River. The increase of the runoff coefficient for the Dargol River at the Tera station is only 37% against 108% for the Nakambe (Mahe *et al.*, 2003).

Human impact on the Sahelian environment, is increasing the speed of the land cover change. Humans need to "deforest" to increase agricultural production. In Sahel this means that grasses, bushes and rare small trees are removed and burned. This has several impacts on the soil-vegetation relationships. It causes a reduction of the net biomass production going back to the soil after the rainy season. After several years, this leads to a soil–vegetation equilibrium which corresponds to that of a drier area. The second point is that the soil top layer becomes very sensitive to rainfall: nutrients are washed out very rapidly and an impermeable crust appears which is responsible for an increase of the surface runoff and a reduction of the water holding capacity.

Impact on the hydrological regimes Surface runoff has been measured over several small Sahelian catchments covering different kinds of environments, by agronomists, soil scientists and hydrologists. One can recall that the annual average runoff coefficient over a natural vegetation area is about 13%, over a cultivated area about 20% (average between several kinds of species and agricultural techniques), and over a bare soil 50%. These values are increased by 5% in the northern Sahel (Yacouba *et al.*, 2003). It is most likely that annual surface runoff might increase for any size of river basin, from small ones (Pouyaud, 1987) to very larges ones (Mahe *et al.*, 2005a). Increases of runoff coefficients and even of annual discharges have been observed for a lot of Sahelian basins from Mauritania to Burkina-Faso and Niger since the 1970s. In Mauritania

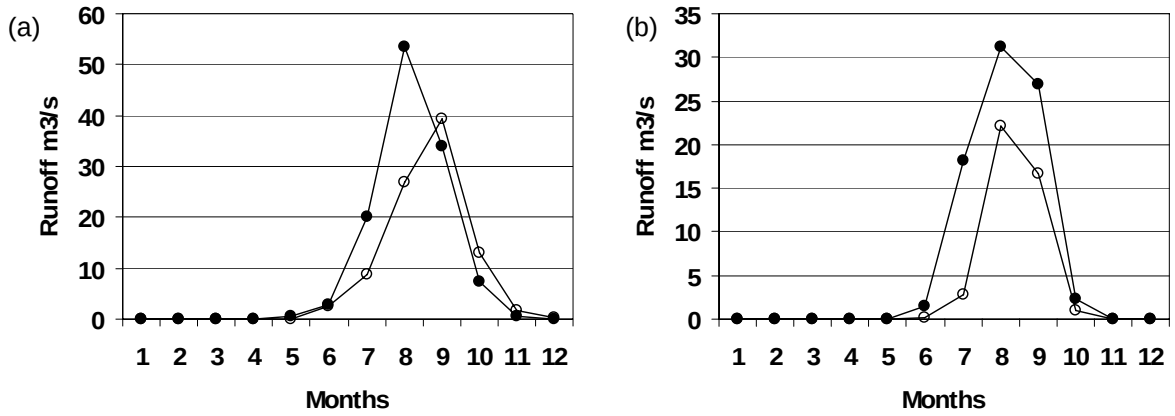


Fig. 4 (a) Runoff up to 1972 (white dots) and after 1972 (black dots), for central Sahel countries (Burkina-Faso and Niger). (b) Runoff up to 1972 (white dots) and after 1972 (black dots), for western Sahel (Mauritania).

runoff is higher for all months since 1972. In the Central Sahel, runoff is higher in July and August after 1972, but not in September. This increase is most likely due to the increasing land degradation. Flood peaks are also observed one month earlier (August instead of September) after 1970 than before, in the Central Sahel (Fig. 4(a) and (b)). Unfortunately we have no examples to show from countries like Senegal, Mali or Chad. But we assume that these hydrological changes should be of the same kind for all Sahelian rivers.

RIVER MODELLING FOR SAHELIAN RIVERS

Conceptual river modelling

Conceptual river models are commonly used for large river basins, where data are not easily available, and most often available only at the monthly time step, especially for transboundary basins. The knowledge developed around this kind of models is very useful from the perspective of the PUB decade of IAHS (Predictions in Ungauged Basins). GR2M and Water Balance Model (WBM) (Conway, 1997; Ambroise, 1999; Mahe *et al.*, 2005a) are two conceptual models with two parameters and one reservoir, the depth of which corresponds to the water holding capacity (WHC), i.e. the maximum water stored in the upper layer of the soil to the average root depth. For our studies in West Africa, the WHC has been derived from the FAO soil map of the world (FAO, 2001), and gave better results than WHC from Dunne & Willmott (1996). Ardoin *et al.* (2005) have tested the three FAO values: minimum, maximum and average, with conceptual hydrological modelling of 50 rivers in West Africa and found the best results with the FAO maximum WHC (FAO max).

Most of the hydrological models use a fixed WHC. It has been shown that in the Sahel the impermeabilization of the soil top layer leads to a proportional loss of WHC (Fournier *et al.*, 2000). River modelling in the Sahel is then very difficult after 1970, as when introducing less rainfall the models are not able to reproduce a runoff increase.

Time varying WHC data files

For Sahelian basins we developed a method for taking into account LUCC in river modelling. The idea is to create a time varying WHC data file, rather than to use a fixed value over time for WHC. WHC is then no more a constant value but varies according to environmental changes. Satellite imagery, and for years prior to 1970 aerial photography, are used to map the land-use/land cover at different periods of time. In our case study on the Nakambe River in Burkina-Faso, we set the first map for 1965. We assume that FAO WHC corresponds to a situation of land-use/land-cover prior to 1970, so that the WHC max values are considered as the initial values for the model, in 1965. Following the LUCC visible on the other maps of 1975, 1985 and 1995, we modified the WHC value. In our case study, the reduction of the area of natural vegetation leads to a decrease of the WHC (Table 1).

In the last step we created the WHC “pseudo” annual series, by increasing WHC each year by one tenth of the WHC difference between two maps. When using time varying WHC data rather

than fixed WHC, the performances of the conceptual models are significantly increased (Table 2).

We are currently working on using a population model, based on the national population data, for distributing the values between the maps, more accurately. We assume that the population increase is correlated to the LUCC to some extent, and in addition with a "climatic" index. This approach will be tested in a near future over the Nakambe basin (Diello *et al.*, 2005).

Table 1 Nakambe river, Burkina-Faso, (20 800 km^2), changes in LUCC and impact on the WHC. Initial values are taken from the FAO (1981).

Year	Natural vegetation	Cultivated area	Bare soil	WHC reduction
Initial values	100%	0%	0%	0%
1965	43%	53%	4%	0%
1975	34%	58%	8%	23%
1985	15%	75%	10%	57%
1995	13%	76%	11%	62%

Table 2 Results of the river flow modelling, Nash performance criteria, for calibration and validation, for fixed and time-varying WHC data. D&W refers to Dunne and Willmott (1996), and FAO to FAO (1981).

Precipitation file	Source file WHC	Fixed WHC Calibration %	Time varying WHC Calibration %	Fixed WHC Validation %	Time varying WHC Validation %
CRU	FAO	50.6	67.3	37.0	63.2
CRU	FAO	64.5	72.2	47.7	58.3
IRD	D&W	52.3	72.5	36.8	63.7
IRD	D&W	67.7	72.2	48.9	58.2

CONCLUSION

The hydrological regime of the Sahelian rivers has changed since the 1970s, following the beginning of the lasting drought which is still ongoing over West Africa. For river basins north of the 750-mm annual isohyet, runoff coefficients have increased and flood peaks occur one month sooner, in August, according to runoff data available for Sahelian basins in Mauritania, Burkina-Faso and Niger. This is correlated with land-use/land-cover change, which leads to the impermeabilization of the soil top layer, and thus to the reduction of the WHC. This hypothesis is tested significantly by using conceptual hydrological models which use WHC as the soil water reservoir. WHC is modified according to the LUCC as seen from the analysis of satellite or aerial imagery. Other observations in the Sahelian area confirm this hypothesis. For example, in the country near the city of Niamey in Niger, the level of the water table has been rising for the last 50 years (Leduc *et al.*, 2001). This water table is too deep and cannot participate in increasing the baseflow of Sahelian rivers. The local geography is unusual, with small endorheic ponds being increasingly refilled by surface runoff increases from year to year.

The hydrological regime of the Niger River itself has changed at Niamey (400 000 km^2) due to this Sahelian runoff increase. Over the period 1923–1979 the flood peak coming from the Guinean and Malian upper basin (300 000 km^2) had always been the highest one. Since 1980, a higher flood peak coming from the local Sahelian tributaries (100 000 km^2) has been observed several times (Mahe *et al.*, 2003).

All studies have also noted the increasing agricultural activity, correlated with deforestation and alteration of local soil properties, specifically infiltration. It is nevertheless very difficult to separate the human induced and climate induced variability in the observed hydrological changes of Sahelian basins (Hulme, 2001; IPCC, 2003). There is a need to create a set of "reference basins" which could serve as witnesses of the natural climate/vegetation equilibrium, in regard to the ever-growing human induced changes of the environment.

Acknowledgements We acknowledge the National Hydrological and Meteorological Services of Mauritania, Burkina-Faso and Niger, for providing data, and thank IRD and the FRIEND-AOC program (UNESCO PHI) for funding and support.

REFERENCES

Amani, A. & Nguetora, M. (2002) Evidence d'une modification du régime hydrologique du fleuve Niger à Niamey. In: *FRIEND 2002 – Bridging the Gap between Research and Practice* (ed. by H. A. J. van Laanen & S. Demuth), 449–456. IAHS Publ. 274. IAHS Press, Wallingford, UK

Ambroise, B. (1999) Genèse des débits dans les petits basins versants ruraux en milieu tempéré. 2. Modélisation systémique et dynamique. *Rev. Sci. Eau* **12**(1), 123–153.

Ardoin-Bardin, S., Dezetter, A.., Servat, E., Mahé, G., Paturel, J. E., Dieulin, C. & Casenave, L. (2005) Évaluation des impacts du changement climatique sur les ressources en eau d'Afrique de l'Ouest et Centrale. In: *Regional Hydrological Impacts of Climatic Change—Hydroclimatic Variability* (ed. by S.W. Franks *et a*l.), 194–202. IAHS Publ. 296. IAHS Press, Wallingford, UK

Casenave, A. & Valentin, C. (1989) *Les etats de surface de la zone sahelienne.* IRD-Orstom, Coll. Didactiques, Paris. France.

Casenave, A. & Valentin, C. (1992) A runoff capability classification system based on surface features criteria in semi-arid areas of West Africa. *J. Hydrol.* **130**, 231–249.

Conway, D. (1997) A water balance model of the Upper Blue Nile in Ethiopia. *Hydrol. Sci. J.* **42**, 841–859.

Dai, A. G., Lamb. P. J., Trenberth, K. E., Hulme, M., Jones, P. & Xie, P. (2004) The recent Sahel drought is real. *Int. J. Climatol.* **24** (11), 1323–1331.

Diello, P., Mahe, G., Paturel, J. E., Karambiri, H. & Servat, E. (2005) Diminution des pluies et augmentation des écoulements au Sahel : relation entre hydrologie, dégradation du sol et dynamique de la population. *FRIEND International Seminar*, Montpellier, November 2005.

Dunne, K. A. & Willmott, C. J. (1996) Global distribution of plant extractable water capacity of soil. *Int. J. Climatol.* **16**, 841–859.

FAO (1981) *Digital Soil Map of the World*. UNESCO, Rome, Italy.

Fournier, J., Serpantie, G., Delhoume, J. P. & Gathelier, R. (2000) Rôle des jachères sur les écoulements de surface et l'érosion en zone soudanienne du Burkina: application à la gestion des terres cultivées. *Sud Sciences Technologies* **5**, 4–14, EIER/ETSHER.

Hulme, M. (2001) Climatic perspectives on Sahelian desiccation: 1973–1998. *Global Environmental Change – Human and Policy Dimensions* **11** (1), 19–29.

Hulme, M., Doherty, R., Ngara, T., New, M. & Lister, D. (2001) African climate change: 1900–2100. *Climate Research* **17**(2), 145–168.

IPCC (2003) Intergovernmetnal Panel on Climate Change, Third assessment report. WMO, UNEP.

L'Hote, Y., Mahe, G., Some, B. & Triboulet, J. P. (2002) Analysis of a Sahelian annual rainfall index updated from 1896 to 2000; the drought still goes on. *Hydrol. Sci. J.* **47**(4), 563–572.

L'Hote, Y., Mahe, G. & Some, B. (2003) The 1990s rainfall in the Sahel: the third driest decade since the beginning of the century. Reply to discussion. *Hydrol. Sci. J.* **48**(3), 493–496.

Leduc, C., Favreau, J. & Schroeter, P. (2001) Long-term rise in a Sahelian water-table: the Continental Terminal in South-West Niger. *J. Hydrol*. **243**, 43–54.

Lubes-Niel, H., Masson, J. M., Paturel J. E., & Servat, E., (1998) Variabilité climatique et statistiques. Etude par simulation de la puissance et de la robustesse de quelques tests utilisés pour vérifier l'homogénéité de chroniques. *Revue Sci. de l'Eau* **11**(3).

Mahe, G. & Olivry, J. C. (1999) Assessment of freshwater yields to the ocean along the intertropical Atlantic coast of Africa. *Comptes Rendus de l'Academie des Sciences*, Series IIa **328**, 621–626.

Mahe, G., Olivry, J. C., Dessouassi, R., Orange, D., Bamba, F. & Servat, E. (2000) Relations eaux de surface – eaux souterraines d'une rivière tropicale au Mali. *Comptes Rrendus de l'Academie des Sciences, Serie IIa* **330**, 689–692.

Mahe, G., L'Hote, Y., Olivry, J. C. & Wotling, G. (2001) Trends and discontinuities in regional rainfall of west and central Africa, 1951–1989. *Hydrol. Sci. J.* **46**(2), 211–226.

Mahe, G., Leduc, C., Amani, A., Paturel, J. E., Girard, S., Servat, E. & Dezetter A. (2003) Augmentation récente du ruissellement de surface en région soudano-sahélienne et impact sur les ressources en eau. In: *Hydrology in the Mediterranean and Semiarid Regions* (ed. by E. Servat, Wajdi Najem, Christian Leduc & Ahmed Shakeel), 215–222. IAHS Publ. 278. IAHS Press, Wallingford, UK.

Mahe, G., Paturel, J. E., Servat, E., Conway, D. & Dezetter A. (2005a) Impact of land use change on soil water holding capacity and river modelling of the Nakambe River in Burkina-Faso. *J. Hydrol.* **300**(1–4), 33–43.

Mahé, G., Rescan, M., Dezetter, A., Ardoin, S. & Dieulin, C. (2005b) Water resources prediction in West and Central Africa for the 21st century. Poster. Abstracts book. *First International AMMA conference*, Dakar, Senegal.

New, M. G., Hulme, M. & Jones P. D. (2000) Representing 20th century space–time climate variability. II: Development of 1901–1996 monthly terrestrial climate fields. *J. Climate* **13**, 2217–2238.

Ould, M. (2001) *Détermination de ruptures statistiques dans les séries chronologiques des paramètres météorologiques – application aux bassins des Voltas et du Niger*. Mémoire d'ingénieur, groupe EIER-ETSHER, Ouagadougou, Burkina-Faso.

Paturel, J. E., Servat, E., Kouame, B., Lubes, H., Ouedraogo, M. & Masson, J. M. (1997) Climatic variability in humid Africa along the Gulf of Guinea. Part two: An integrated regional approach. *J. Hydrol.* **191**, 16–36.

Paturel, J. E., Servat, E., Delattre, M. O. & Lubès-Niel, H. (1998) Analyse de séries pluviométriques de longue durée en Afrique de l'Ouest et Centrale non sahélienne dans un contexte de variabilité climatique. *Hydrol. Sci. J.* **43**(6), 937–946.

Pouyaud, B. (1987) Variabilité spatiale et temporelle des bilans hydriques de quelques bassins versants d'Afrique de l'ouest en liaison avec les changements climatiques. In: *The Influence of Climate Change and Climate Variability on the Hydrologic Regime and Water Resources* (ed. by S. I. Solomon *et al.*), 447–461. IAHS Publ. 168. IAHS Press, Wallingford, UK.

Yacouba, H., Da Dapola, E., Yonkeu, S., Zombre, P., Soule, M. & Bagayoko, F. (2002) Etude du processus de dégradation du bassin supérieur du Nakambé (Burkina-Faso), écoulement de surface et pertes de terres liées l'eau. Deuxièmes Journées Sci. EIER/ETSHER, CD-Rom, Ouagadougou, Burkina-Faso.

Climate Variability and Change—Hydrological Impacts (Proceedings of the Fifth FRIEND World Conference held at Havana, Cuba, November 2006), IAHS Publ. 308, 2006.

Impact des modifications d'habitats (déforestation, aménagements hydro-agricoles, extension des cultures) sur la santé des populations rurales: cas de l'ulcère de Buruli en Côte d'Ivoire

TELESPHORE BROU[1,2], HELENE BROUTIN[2], MIREILLE DOSSO[3] & JEAN-FRANCOIS GUEGAN[2]

1 *Université d'Artois, 9 rue du Temple, BP 665, Arras cedex France*
broutelesphore@yahoo.fr

2 *UMR 2724 IRD-CNRS, Génétique & Evolution des Maladies Infectieuses, Equipe "Evolution des Systèmes Symbiotiques", Centre IRD de Montpellier, BP 64501, F-34394 Montpellier cedex 5, France*

3 *Institut Pasteur de Côte d'Ivoire, 01 BP 409 Abidjan 01, Côte d'Ivoire*

Résumé Cet article montre la relation qui existe entre la prévalence de l'ulcère de Buruli et plusieurs variables du milieu physique en Cote d'Ivoire. L'étude repose sur trois années de données épidémiologiques sur la maladie (1995–1997), collectées dans les centres de santé de base du pays par l'Institut Follereau. Le contexte écologique le plus favorable au développement de cette maladie est incontestablement la proximité des barrages à vocation agricole, particulièrement dans la partie centrale du pays.

Mots clef Cote d'ivoire; ulcère du Buruli; facteurs environnementaux

Environment change (deforestation, agricultural-water management, increased cultivation) impact on rural population health: Buruli ulcer prevalence in Ivory Coast

Abstract This paper details relationships between Buruli ulcer prevalence and some natural conditions in Ivory Coast. Three years of epidemiologic data (1995–1997) has been used in the analysis. These data were collected by the Ivory Coast's Raoul Follereau Institute. The results of the analysis show that the best relationship occurs between the proximity of agricultural dams and diseases cases. This link is particularly strong in the centre of the country.

Key words Ivory Cost; Buruli ulcers; environmental factors

INTRODUCTION

La Côte d'Ivoire a connu des évolutions rapides de ses états de surface liées à une stratégie de développement presque essentiellement basée sur l'agriculture (comme la plupart des pays tropicaux d'Afrique). Ces évolutions des états de surface résultent du remplacement de la végétation naturelle (forêt dense, forêt claire) par des espèces cultivées. Entre 1960 et 2000, la forêt dense humide ivoirienne est ainsi passée de 12 millions à 4 millions d'hectares (Brou, 2005). Les changements des états de surface s'opèrent du fait de nombreux aménagements hydro-agricoles (petits barrages) réalisés en vue d'étendre la production de certaines cultures hygrophiles comme la riziculture, ou pour le développement de la pisciculture. La production de riz irriguée se fait à partir de barrages hydro-agricoles et de bas-fonds humides aménagés. La gestion de ces bas-fonds humides représente aujourd'hui un enjeu important pour la production rizicole du pays, puisque que l'agriculture ivoirienne est encore basée sur les systèmes agraires pluviaux et donc toujours tributaire des aléas climatiques, rendant la production incertaine. C'est pourquoi, à partir des années 60, les pouvoirs publics se sont intéressés aux aménagements hydro-agricoles en créant des périmètres irrigués.

Plusieurs travaux scientifiques ont montré les conséquences des modifications des écosystèmes naturels sur l'altération des interactions entre les populations humaines et leur environnement augmentant les risques de transmission de maladies infectieuses (Aron & Patz 2001). Les statistiques sont plus effrayantes en ce qui concerne l'Afrique; on estime qu'un enfant sur cinq sur le continent ne vivra pas jusqu'à son cinquième anniversaire principalement à cause des maladies liées à l'environnement (OMS, 2003).

L'Ulcère de Buruli, dont l'agent étiologique est *Mycobacterium ulcerans*, représente l'infection causée par des Mycobactéries la plus fréquente rencontrée chez l'homme immunocompétent après la lèpre (*M. leprae*) et la tuberculose (*M. tuberculosis*). Cependant, dans certains pays africains, l'Ulcère de Buruli devient majoritaire depuis ces dix dernières années.

Copyright © 2006 IAHS Press

Cette infection humaine semble récente et donc encore très mal connue - d'où son appellation de "maladie mystérieuse" ou "nouvelle lèpre". Observée pour la première fois en Ouganda (région de Buruli, d'où le nom) en 1872, puis en Australie en 1948, le nombre de cas connaît une augmentation spectaculaire dans le monde depuis les années 1980. Cette augmentation est particulièrement impressionnante en Afrique de l'Ouest. Sur le plan épidémiologique, bien que sa localisation dans les écosystèmes et ses modalités de transmission à l'homme ne soient pas encore parfaitement caractérisées, les conditions environnementales et ses modifications, et en particulier de la flore et de la faune aquatiques, semblent jouer un rôle important dans l'écologie de *M. ulcerans* (Marsollier *et al.*, 2003). Le pathogène se transmettrait par effraction de la peau, mais on ignore encore si une transmission directe à travers une peau humaine intacte est possible, ou si la morsure-piqûre d'un insecte-vecteur est absolument nécessaire. En Afrique, *M. ulcerans* a été retrouvé dans les glandes salivaires de punaises d'eau de la famille des *Naucoridae,* et il a été montré expérimentalement que les punaises d'eau pouvaient transmettre le pathogène à la souris lors de piqûres (Marsollier *et al.*, 2003). En dépit de ces incertitudes sur les liens environnement-santé, tous les auteurs s'accordent à souligner l'existence d'un contexte écologique stéréotypé: présence de marécages, lacs et cours d'eau s'écoulant lentement. Certains insistent même sur l'importance de la composition chimique des sols (siliceux, pH acide) et les modifications de l'environnement (inondations, etc.) comme facteurs favorables au développement de *M. ulcerans* et à son transfert vers les populations humaines. Dans ce contexte, l'objectif de cette étude est de caractériser les causes environnementales prédisposant à l'apparition de cas d'Ulcère de Buruli en Côte d'Ivoire à travers la mise en évidence des relations spatio-temporelles entre les données de cas morbides et les données environnementales considérées être *a priori* des facteurs qui causent et contrôlent le développement de cette maladie dans les populations humaines.

DONNEES ET METHODES

Les données épidémiologiques

Les données d'Ulcère de Buruli ont été collectées par l'institut Raoul Follereau de Côte d'Ivoire sur une période de 3 ans : 1995, 1996 et 1997. Elles indiquent pour chaque "centre de santé de base" du pays et pour chacune des trois années, le nombre de fréquentation des malades atteints de l'Ulcère de Buruli. Situé à l'échelon du village ou d'agglomérations de petites tailles (i.e. inférieure à 5000 habitants), le "centre de santé de base" est le maillon élémentaire du système sanitaire ivoirien. Il a pour principale mission d'assurer les soins de santé primaire des populations rurales. Les données comportent également les cas de maladies recensés dans les centres hospitaliers des agglomérations de grandes tailles (i.e. plus de 5000 habitants). Même si les centres de santé de base sont limités dans leurs activités médicales, la couverture sanitaire est relativement forte en Côte d'Ivoire. On compte en moyenne un centre chaque 20 kilomètres avec les situations suivantes (Ministère de la Solidarité, de la Sécurité Sociale et des Handicapés, 2004): 54% de la population vivent dans une localité disposant d'une formation sanitaire; 14% sont à une distance de moins de 5 km; 15% entre 5 et 10 km; 8% entre 10 et 15 km; 5% entre 15 et 20 km; 4% à plus de 20 km.

Pour rendre les données épidémiologiques des centres de santé comparables entre elles et afin de contrôler l'effet de la taille de population, nous avons exprimé ces valeurs de cas en pourcentage par rapport à la population villageoise (pour 100 000 habitants), traduisant ainsi le niveau de prévalence (ou incidence) de cas dans chacun de ces villages.

Les données environnementales

Ces données concernent les états de surface et se répartissent en deux types. Il s'agit, d'une part, des données sur les grandes formations végétales et leurs évolutions. Ces informations sont basées sur la carte de végétation de Guillaumet (1971) et sur la carte des réserves forestières du BNETD (1999). La Côte d'Ivoire est caractérisée par des situations contrastées en matière d'écosystème naturel. Les zones de forêt dense humide (fdh) et de mosaïque f.d.h./savane "pré-forestière" s'étendent sur la partie méridionale du pays, au sud d'une ligne suivant grossièrement le 8ème parallèle, le Nord étant occupé par des forêts denses sèches, des forêts claires et des formations savanicoles soudaniennes. Le déterminisme de ce partage entre types de végétation est essentielle-

ment climatique, avec des corrections liées aux réserves en eau des sols. Sur le plan climatique, le passage des milieux de forêts denses humides aux savanes herbeuses correspond à une transition entre des climats équatoriaux à quatre saisons et des climats tropicaux à deux saisons. Des évolutions récentes (entre 1960 et 1990) ont aboutit à la mise en place de nouveaux paysages (forêt secondaire, forêt dégradée, jachère, culture, etc.). Ces évolutions se poursuivent encore aujourd'hui (Brou, 2005). Seuls quelques blocs relictuels, protégés par l'Etat restent peu ou pas encore soumis à l'agriculture: les forêts classées et les parcs nationaux (cf. Fig. 2). Les données sur les états de surface concernent, d'autre part, les aménagements hydro-agricoles. Il s'agit des petits barrages et des cultures qui en dépendent (rizicultures irriguées, piscicultures). La Côte d'Ivoire compte plus de 500 petits barrages, construits pour la plupart entre 1970 et 1990 afin d'assurer la maîtrise de l'eau, notamment dans les régions du centre et du nord, à pluviométrie déficitaire. La vocation de ces barrages est, plus clairement, de permettre d'une part, le développement de la riziculture irriguée à deux cycles de production et/ou des cultures de contre-saison, et d'autre part, l'approvisionnement en eau des troupeaux régionaux qui pâtissent de rudes conditions d'abreuvement en saison sèche.

Méthodes d'analyses

L'étude est fondée sur des méthodes géostatistiques. Ces méthodes permettent de mettre en relation des données environnementales (végétation, sols, altitude, pente, etc.) et socio-économiques (agglomérations, données épidémiologiques, densité de populations, voies de communication, activités agricoles, etc.). Pour rendre superposable l'ensemble des données analysées, celles-ci ont été reéchantillonnées sur des mailles régulières de 10 km × 10 km (Fig. 1). Cette distance correspond au rayon d'influence moyen d'un dispensaire en Côte d'Ivoire. L'utilisation du Système d'Information Géographique, idéal pour traiter un ensemble d'objets géographiques et les relations qu'ils entretiennent les uns avec les autres, facilite le croisement d'informations géographiques transversales. Les données de diverses sources (physique, économique, sociale, épidémiologique, politique, culturelle, etc.) sont en effet facilement mises en relation, dans un SIG, rendant ainsi aisées les requêtes et l'analyse multivariée. Les problèmes d'échelles étant résolus dans le SIG, l'approche multicouche est privilégiée dans ce travail, permettant ainsi à partir du croisement des différentes informations disponibles, de mettre en évidence les relations spatiales avec les cas de maladies et les phénomènes environnementaux étudiés. Il s'agira donc dans ce travail d'établir des zones d'influence autour de chacun des paramètres environnementaux pris en compte dans l'étude. Le croisement de la couche « classe de distance » avec celle de l'Ulcère de Buruli est susceptible de mettre en évidence le rayon d'influence de chaque paramètre environnemental sur la maladie. Il est alors possible d'établir des cartes de risque lié à la proximité d'un paramètre environnemental.

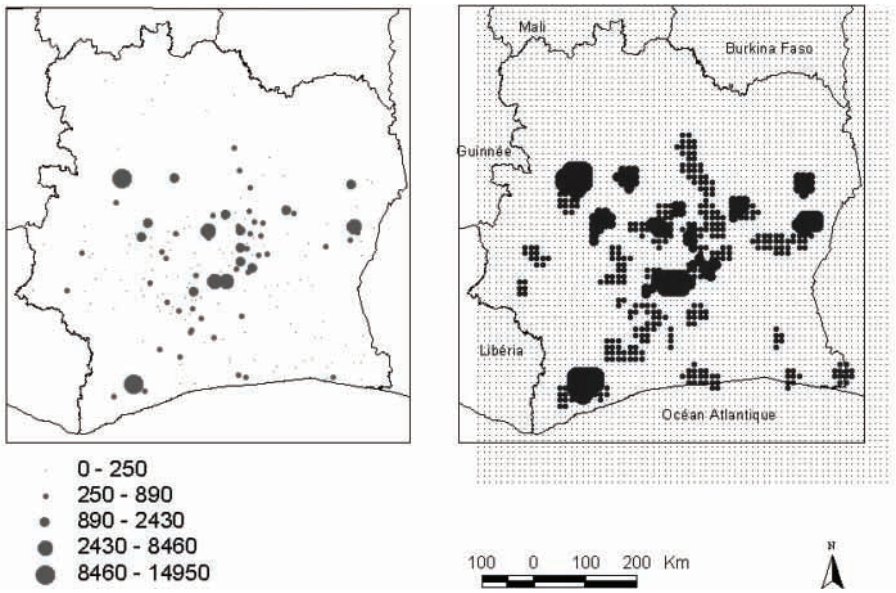


Fig. 1 Données brutes (à gauche) et données sur une maille de 10 km x 10 km (à droite).

RESULTATS

Ulcère de Buruli et végétation naturelle

La moitié sud du pays, région de forêt et de contact forêt/savane, semble fournir les meilleures conditions écologiques au développement de l'Ulcère du Buruli (Fig. 2).

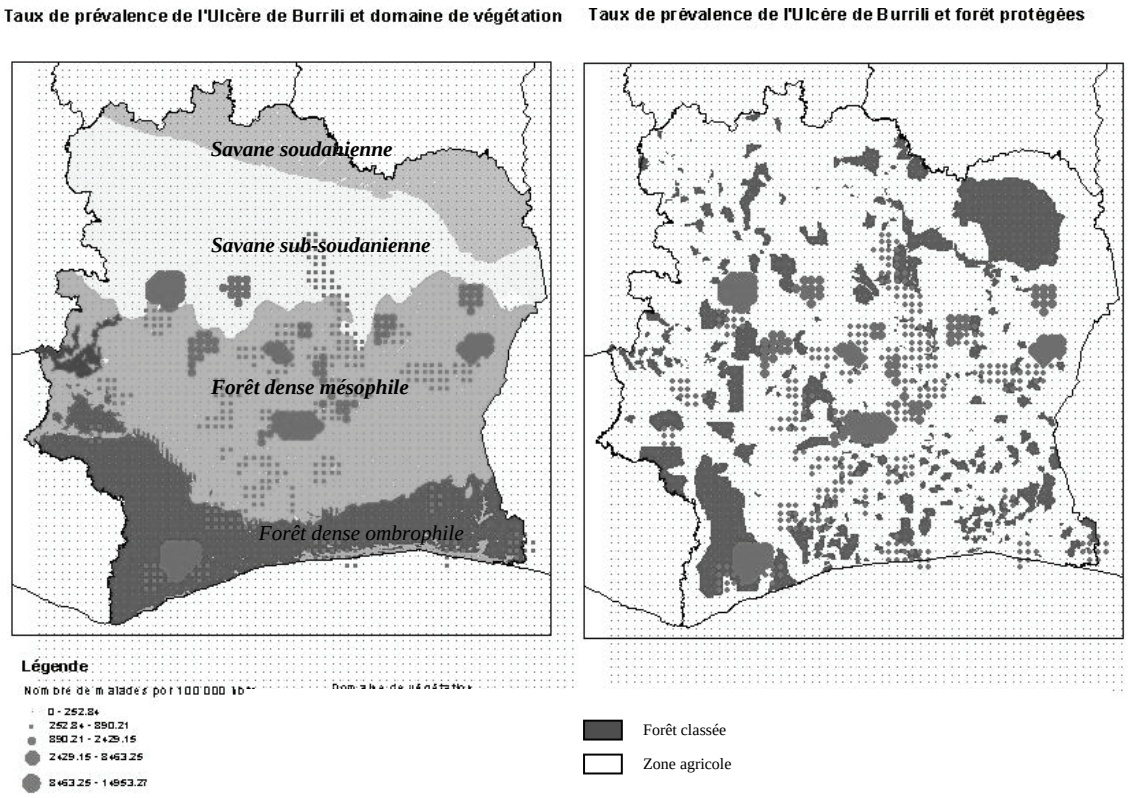


Fig. 2 Végétation naturelle et Ulcère de Buruli.

En effet, contrairement aux régions de savane où les taux sont très faibles, voir nuls, de très forts taux de prévalence sont notés au sud du pays. C'est surtout dans la partie mésophile de la zone forestière, notamment dans la zone pré-forestière de contact forêt/savane ("V baoulé") que les taux sont les plus élevés. La Fig. 2 permet également de mettre en évidence la proximité des grands foyers de maladie avec les îlots forestiers. Les périphéries immédiates de ces derniers massifs forestiers constituent des secteurs d'intenses activités agricoles, du fait des meilleures conditions écologiques offertes par l'écosystème forestier. Bien que considérés comme le domaine permanent de l'Etat, ces îlots forestiers abritent souvent de nombreux clandestins: près de 20% de la production cacaoyère est issue de ces forêts dites classées.

Ulcère de Buruli et aménagements hydro-agricoles

La mise en relation des niveaux de prévalence avec les aménagements hydro agricoles révèle une forte prévalence à proximité des barrages. La Fig. 3 met clairement en évidence la relation existante entre la densité des barrages et les grands foyers de la maladie. C'est surtout dans la région des lacs (dans le centre) que cette relation est la plus forte. Dans cette région, le nombre de barrages est le plus important de l'ensemble de la moitié sud du pays. Corrélativement à la densité des barrages, les régions rizicoles enregistrent un fort taux de prévalence comme l'indique la situation de la région des lacs. Cette région fournit près de 40% de la production nationale grâce aux barrages de dérivation (CCT, 1999).

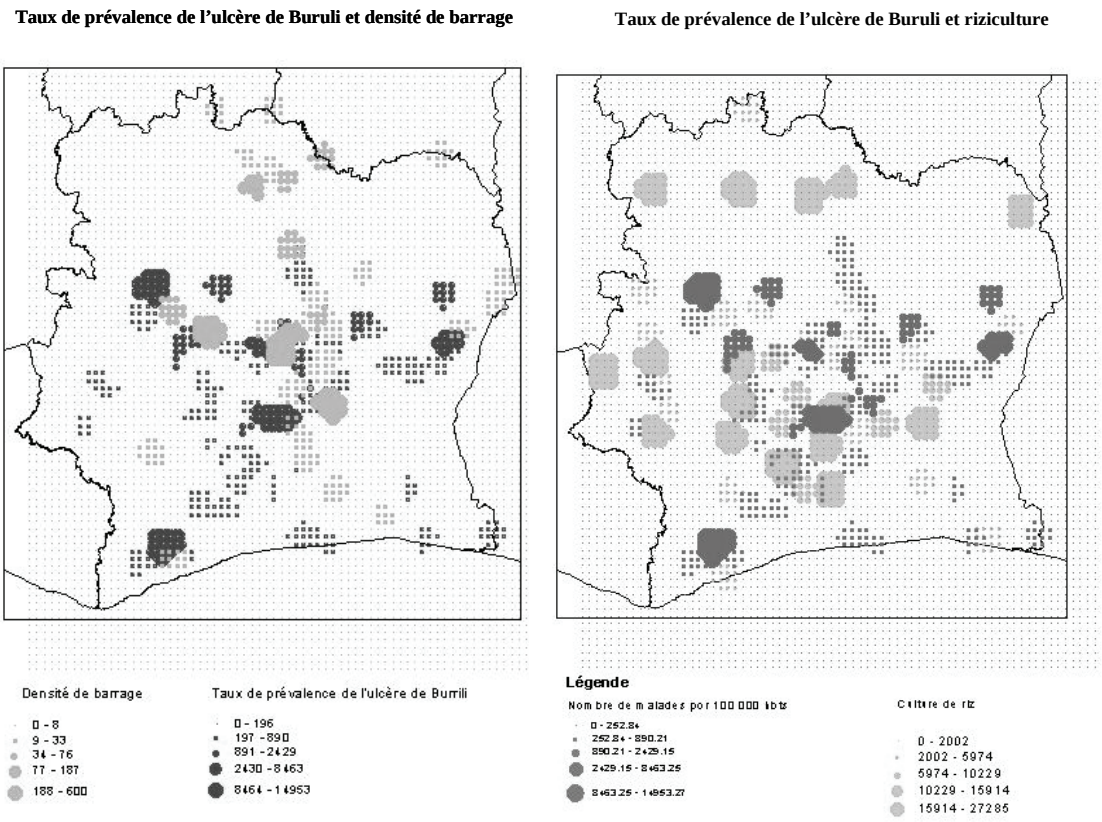


Fig. 3 Aménagements hydro-agricoles et taux de prévalence de l'Ulcère de Buruli.

Sur le reste du pays, l'augmentation de la densité des barrages et des milieux rizicoles n'est pas forcement suivie d'une augmentation du taux de prévalence. Il s'agit du nord du pays qui bénéficie, comme le centre, d'un important réseau d'aménagements hydro-agricoles. Le faible taux de prévalence enregistré dans cette région confirme l'existence d'une limite latitudinale liée possiblement à la variation nord-sud des conditions bioclimatiques. En effet, contrairement à la moitié sud, la longueur de la saison sèche dans le nord (plus de 4 mois) fait que très peu de barrages et de cours d'eau restent permanents tout au long de l'année. Inversement, la faible densité de barrages dans la zone de forêt dense ombrophile est compensée par la présence de nombreux bas-fonds à humidités permanentes. Tout ce contexte pourrait permettre d'expliquer l'existence d'un grand foyer de malades dans le sud-ouest à proximité de la forêt hygrophile de Taï (Figs 2 et 3).

Relations entre la distance par rapport aux paramètres environnementaux et le taux de prévalence de l'Ulcère de Buruli

La Fig. 4 ci-dessous met en évidence une augmentation du taux de prévalence de l'ulcère de Buruli par rapport aux barrages et aux îlots forestiers. Mais, c'est autour des barrages que les taux sont les plus forts. Les valeurs peuvent atteindre 40 malades pour 100 000 habitants à proximité des ouvrages hydro-agricoles dans la zone forestière, alors qu'elles n'atteignent pas les 25 malades pour 100 000 habitants à proximité des massifs forestiers. Ce taux est très fort dans la vallée du Bandama (région des lacs). Dans cette région, en effet, le taux de prévalence est d'environ 100 malades pour 100 000 habitants à moins de 5 km des barrages. On note une régression rapide de ce chiffre en s'éloignant des barrages. Une chute brutale est, en effet, enregistrée entre 5 et 10 km, passant de 100 à 40 malades, puis au-delà des 20 km, le nombre de malades atteint à peine les 20 pour 100 000 habitants. A l'ouest du pays en revanche, autour du barrage de Buyo, le taux de prévalence reste faible avec seulement 40 malades pour 100 000 habitants dans les 5 premiers km. La pente de la variation de la maladie par rapport à la distance reste également peu prononcée par rapport à ce qui est observé dans le centre du pays.

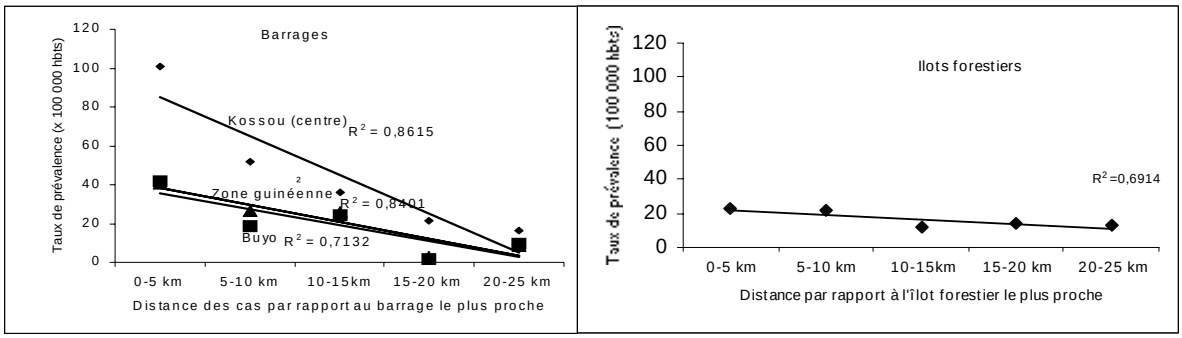


Fig. 4 Variation du taux de prévalence en fonction des paramètres environnementaux.

CONCLUSION

Les résultats préliminaires de cette étude mettent donc bien en évidence des relations spatiales importantes entre l'Ulcère de Buruli et certaines données environnementales comme les zones humides. Cette relation se manifeste par un fort taux de prévalence dans le centre du pays dans la région des Lacs (Yamoussokro), région qui présente les plus fortes densités de barrages hydro-agricoles. Ce travail se poursuit vers une recherche des indicateurs environnementaux pertinents permettant de comprendre le fonctionnement des foyers d'Ulcère de Buruli en Côte d'Ivoire. Il mériterait d'être ensuite complété avec des études sur des données épidémiologiques plus longues et plus détaillées. L'Ulcère de Buruli devient, en effet, une maladie prioritaire en Côte d'Ivoire car elle constitue un réel problème de santé publique. Cette maladie est tout autant inquiétante par son ampleur aujourd'hui que la lèpre et la tuberculose en Côte d'Ivoire, et aussi dans tout le sous-continent ouest-africain. Cette recherche sera à mettre en regard de celle menée sur d'autres terrains notamment au Ghana et au Bénin où la maladie prend également de l'importance, mais aussi en Guyane française où les recherches sur les relations Ulcère de Buruli-environnement sont bien avancées grâce à l'existence d'un observatoire.

REFERENCES

Aron, J. L. & Patz, J. A. (2001) *Ecosystem Change and Public Health*. The Johns Hopkins University Press, Baltimore, USA.

BNETD (Bureau National d'Etude Technique et de Développement) (1999) Bilan de la politique forestière en Côte d'Ivoire et proposition d'orientations, de principes et de règles de fonctionnement du secteur. Rapport de projet, BNETD, Abidjan.

Brou, Y. T, Oswald, Y., Bigot, S. & Servat, E. (2005) Risques de déforestation dans le domaine Permanent de l'État en Côte d'Ivoire: quel avenir pour ses derniers massifs forestiers? *TELA2004004* **5**(1–3), 17–33.

CCT (Centre de cartographie et de télédétection) (1998): Projet sectoriel forestier–Bilan forêt, carte 1/20 000, Abidjan.

Guillaumet, J. L. (1971) La végétation. In: *Atlas de la Côte d'Ivoire*, A6a–A6b. ORSTOM / IGT, Paris, France.

Marsollier, L., Aubry, J., Saint-Andre, J. P., Robert, R., Legras, P., Manceau A. L., Bourdon S., Audrain, C. & Carbonnelle, B. (2003) Ecology and transmission of Mycobacterium ulcerans. *Pathol. Biol.* (Paris) **51**, 490–495.

Ministère de la Solidarité, de la République de Côte d'Ivoire, Sécurité Sociale et des Handicapés (2004) Colloque sur la couverture du risque maladie en Afrique francophone (WBI–IMA Paris, 26–30 avril 2004).

Organisation Mondiale de la Santé (2003) Rapport sur la santé dans le monde- Façonner l'avenir.

Climate Variability and Change—Hydrological Impacts (Proceedings of the Fifth FRIEND World Conference held at Havana, Cuba, November 2006), IAHS Publ. 308, 2006.

Methodologie et application d'une demarche de modelisation hydrologique prenant en compte l'evolution des etats de surface en milieu sahelien d'Afrique de l'ouest

PIERRE DIELLO[1], JEAN-EMMANUEL PATUREL[1], GIL MAHE[1], BRUNO BARBIER[2], HAROUNA KARAMBIRI[3], ERIC SERVAT[1]

1 *UMR HydroSciences – MSE, Place Eugène Bataillon, F-34095 Montpellier cedex 5, France*
eric.servat@msem.univ-montp2.fr
2 *CIRAD, Avenue du Président Kennedy, 01 BP 596 Ouagadougou 01 Burkina Faso*
3 *EIER-ETSHER, 03 BP 7023, Ouagadougou 03, Burkina Faso*

Resume Les études menées depuis une vingtaine d'années montrent que l'effet conjoint du changement climatique et des activités humaines sur les états de surface est à l'origine d'une variabilité hydrologique paradoxale observée depuis les années 1970 sur les bassins versants sahéliens. En effet, en dépit d'une diminution marquée de la pluviométrie de cette région, les coefficients d'écoulement ont très fortement augmenté, entraînant des écoulements plus importants qu'auparavant. Ces modifications de la relation Pluie–Débit nécessitent de nouvelles approches permettant de prendre en compte conjointement la variabilité climatique et la dimension anthropique dans la modélisation hydrologique de ces bassins. Une méthodologie est présentée et des résultats préliminaires sont discutés.

Mots clef activites anthropiques; Burkina Faso; états de surface; fonction logistique; modélisation démographique; modélisation hydrologique; Sahel**;** variabilité climatique; variabilité hydrologique

A hydrological modelling approach that allows for evolution of the land surface in African Sahel basins

Abstract The hydrological studies undertaken during the last twenty years have shown that the hydrological variability observed since the year 1970 on the Sahelian river basins is due to the combined effect on land-cover of climate changes and human activities. Runoff coefficients have increased, inducing more important flows than in the earlier years despite a reduction in rainfall. These modifications to the rainfall–runoff relationship require new approaches that make it possible to take into account both the climatic variability and the human dimension in hydrological modelling of these basins. A method is presented and preliminary results are analysed and discussed.

Key words human activities; Burkina Faso; Sahel; land cover; logistic function; demographic modelling; hydrological modelling, climatic variability; hydrological variability

INTRODUCTION

Les études hydrologiques menées depuis une vingtaine d'années en Afrique de l'Ouest ont montré que les coefficients d'écoulement ont fortement augmenté sur certains hydrosystèmes du Sahel, en dépit d'une diminution marquée de la pluviométrie régionale. Ces nouvelles conditions de ruissellement apparaissent plus favorables dans les zones caractérisées par une diminution du couvert végétal, une extension des surfaces cultivées et des surfaces dégradées (Pouyaud, 1987; Albergel & Valentin, 1991; Mahe *et al.*, 2003; Seguis *et al.*, 2003). Dans ces régions, les états de surface représentent les facteurs prépondérants des phénomènes d'infiltration et de ruissellement. Une voie vers l'amélioration de notre aptitude à simuler par modèle le fonctionnement hydrologique de ces hydrosystèmes est donc de pouvoir prendre en compte la dynamique du milieu dans les modèles. De nombreux modèles de simulation hydrologique existent, mais peu d'entre elles prennent en compte la dynamique d'évolution du milieu. Les modèles conceptuels à réservoirs tels que GR2M, WBM, et, Yates (Makhlouf, 1994; Yates, 1997; Conway & Jones, 1999), ne font pas exception, même s'ils intègrent comme paramètre ou variable d'entrée une donnée caractérisant la hauteur maximale d'un réservoir "sol". C'est cette dernière donnée qui nous intéresse plus particulièrement car des indicateurs de pression anthropique et/ou climatique peuvent servir de base à la transcription de la dynamique du milieu sur ce paramètre ou cette variable.

MODELES HYDROLOGIQUES ET ETATS DE SURFACE

Le milieu naturel peut être considéré comme une juxtaposition d'états de surface associés ou interdépendants. On entend par état de surface, tout ensemble homogène, constitué du couvert

Copyright © 2006 IAHS Press

végétal, du type de sol et de l'organisation pédologique superficielle (croûte). Il est acquis qu'en milieu sahélien, la répartition des pluies entre infiltration et écoulement est sous le contrôle quasi exclusif de cette donnée (Casenave & Valentin, 1992). Le modèle conceptuel GR2M, que nous utiliserons dans le cadre de ce travail, comporte un réservoir "sol" qui se caractérise par une hauteur maximale. Cette hauteur peut être assimilée à la capacité de rétention en eau du sol (WHC: Water Holding Capacity), caractéristique des états de surface. Les données de WHC que nous utilisons sont extraites de la *Digital Soil Map of the World* (FAO-UNESCO, 1974–1981). Des unités de sols sont définies en fonction de la profondeur des horizons et de la texture des constituants, et on y associe des classes de WHC. Les données WHC sont fixées pour chaque unité de terrain et pour toute la durée des simulations. Ces valeurs n'intègrent pas la dynamique d'évolution globale du climat et de l'environnement et ne sont pas évolutives dans le temps. Or, une bonne transcription de la dynamique des états de surface, et donc de la WHC, permettrait d'améliorer les résultats de simulation des modèles hydrologiques.

MODES DE TRANSFORMATION DU MILIEU ET INDICATEURS DE PRESSION ANTHROPIQUE ET/OU CLIMATIQUE

Assurer une certaine "sécurité alimentaire" dans un contexte de baisse globale de la pluviométrie, de manque de terres arables, et de pauvreté sévère, est une question de survie pour les populations sahéliennes d'Afrique de l'Ouest. Ce contexte, que l'on pourrait qualifier de "climato-socio-économique", a engendré de profondes mutations dans les pratiques culturales et agropastorales des populations concernées. De nos jours, les terres encore arables sont, pour la plupart, exploitées sans interruption (pas de jachère). Les terres, qui, jadis, étaient considérées comme marginales, sont colonisées en faisant appel à de nouvelles pratiques de conservation et de restauration des sols (zaï, demi-lune, cordons pierreux, …). Les derniers espaces encore en végétation sont défrichés et transformés en champs. Les politiques gouvernementales ont également favorisé la construction de nombreuses retenues d'eau à caractère agro-pastoral dans le but de mobiliser et rendre disponible un maximum d'eau pour les populations et le bétail (le cas du Burkina Faso est très révélateur de cette politique).

L'analyse de ces pratiques dans le contexte hydroclimatique actuel permet, globalement, de dégager quatre modes de transformation possible du milieu:

- *La dégradation des sols:* dessèchement du couvert végétal avec encroûtement et dénudation des sols sous l'effet conjugué des actions de l'homme et du climat.
- *La mise en culture:* défrichage de la végétation et transformation en champs*;*
- *La mise en jachère:* ne pas ensemencer un champ au cours d'une ou de plusieurs saisons successives afin de permettre au sol de se régénérer.
- *La restauration des sols:* récupération des terres dégradées à l'aide de pratiques telles que le zaï, les demi-lunes ou le reboisement.
- De ces pratiques, nous déduisons trois types d'état de surface: les sols en végétation naturelle (jachères y compris), les sols cultivés, les sols nus (dégradés et encroûtés) auxquels nous ajoutons les plans d'eau (barrages et autres retenues d'eau). Les proportions de ces états de surface pour une unité de surface donnée (par exemple un demi-degré carré, # 2500 km²) et leurs évolutions dans le temps seront prises comme indicateurs de pression anthropique et/ou climatique.

CARACTERISATION DE L'EVOLUTION DES INDICATEURS

Le traitement des images satellites combinées avec les données des statistiques agricoles permet de dresser, à des dates bien précises, des cartes d'occupation du sol. L'intervalle de temps entre deux images satellites successives n'étant pas forcément annuel, il faut pouvoir modéliser l'évolution des indicateurs entre deux dates.

Hypothèse simple d'une évolution linéaire des indicateurs: On considère que les proportions de chaque type d'état de surface évoluent linéairement entre deux périodes. Si $S_{T\,initial}(ES_i)$ est la

surface occupée par l'état de surface ES_i à la date $T_{initial}$, et $S_{T\,final}(ES_i)$ la surface occupée par ce même état de surface à la date T_{final}, on peut écrire, si n est le nombre d'années entre $T_{initial}$ et T_{final}, que:

$$\begin{cases} S_{T\,initial+j}(ES_i) = S_{T\,initial}(ES_i) + jr \\ r = \dfrac{S_{T\,final} - S_{T\,initial}}{n} \\ j \in [1, n] \end{cases} \quad (1)$$

L'équation 1 permet ainsi de calculer les données annuelles des proportions de chaque type d'état de surface.

Un modèle d'évolution "réaliste": On peut concevoir que pour un bassin versant donné, la surface S_{cult}, occupée par les cultures ne peut dépassée une certaine valeur maximale $S\max_{cult}$ (on ne peut mettre en culture plus de terres qu'il n'y en a!). De même, la surface S_{Vg} occupée par la végétation naturelle de descendra pas en dessous d'un certain seuil (on ne va tout de même pas tout défricher! il y a toujours des aires protégées: forets classées et autres…). Pour ces deux indicateurs, la variation de superficie entre deux dates, peut être considérée comme proportionnelle à la différence $S_{seuil} - S$ où S_{seuil} est un maximum ou un minimum et $\boldsymbol{S}$ la valeur actuelle de l'indicateur. La différence $S_{seuil} - S$ s'interprète comme la "place libre" dans le milieu que chaque type d'état de surface pourrait occuper au cours de son évolution dans le temps. On peut donc écrire que:

$$\frac{1}{S}\frac{\mathrm{d}S}{\mathrm{d}t} = k(S_{seuil} - S) \quad (1)$$

En normalisant par $x = \dfrac{S}{S_{seuil}}$ et en posant $r = kS_{seuil}$, on obtient une équation différentielle de la forme $\dfrac{\mathrm{d}x}{\mathrm{d}t} = f(x)$ où $f(x)$ est connu sous le nom de fonction logistique et définie comme suit: $f : x \mapsto rx(1-x)$. La solution de l'équation différentielle $\dfrac{\mathrm{d}x}{\mathrm{d}t} = f(x)$ est de la forme:

$$x(t) = \frac{K}{1 + e^{-r(t-t_0)}} \quad (2)$$

Ce type de fonction que l'on retrouve en dynamique de la population (Delmas, 2004) correspond au mécanisme naturel de croissance ou de décroissance d'une variable, freinée par le niveau de sa valeur (x) et par la résultante d'autres paramètres que l'on considère comme constantes. Dans notre cas, ces paramètres peuvent être déterminés à l'aide de séries annuelles de statistiques agricoles et de données de population. L'utilisation des données de population se justifie par le fait que l'accroissement de la population est un facteur induisant des variations de surface cultivées et de surfaces en végétation naturelle.

La surface totale du bassin étant la somme des superficies des quatre indicateurs, on déduit par différence l'évolution des surfaces nues, connaissant celle des surfaces cultivées, des surfaces en végétation naturelle et des plans d'eau.

MODULATION DE LA WHC EN FONCTION DE L'EVOLUTION DES ETATS DE SURFACE

On fait l'hypothèse que: *toute variation de coefficient de ruissellement dans un sens, due au passage de l'un quelconque des quatre types d'états de surface à un autre, se traduit par une même variation, en sens contraire, de la capacité de rétention en eau.* La Fig. 1 montre les différentes façons de moduler la WHC pour le cas d'une modification de la végétation naturelle en sols cultivés, sols nus et plans d'eau.

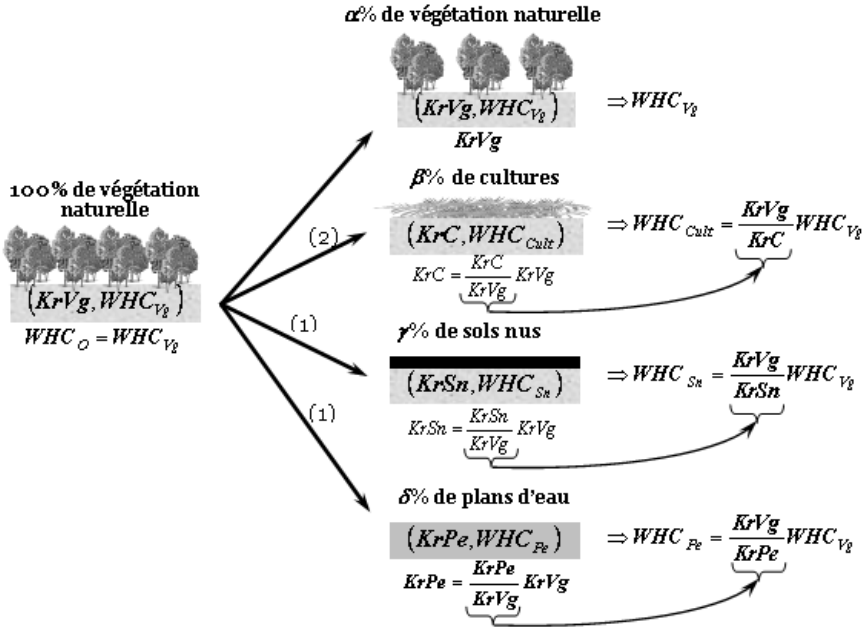


Fig. 1 Modulation de la WHC pour le cas d'une évolution d'un état de végétation naturelle vers un état anthropisé constitué des 4 types d'états de surface. [(1): Mise en culture; (2): Dégradation anthropique et/ou climatique].

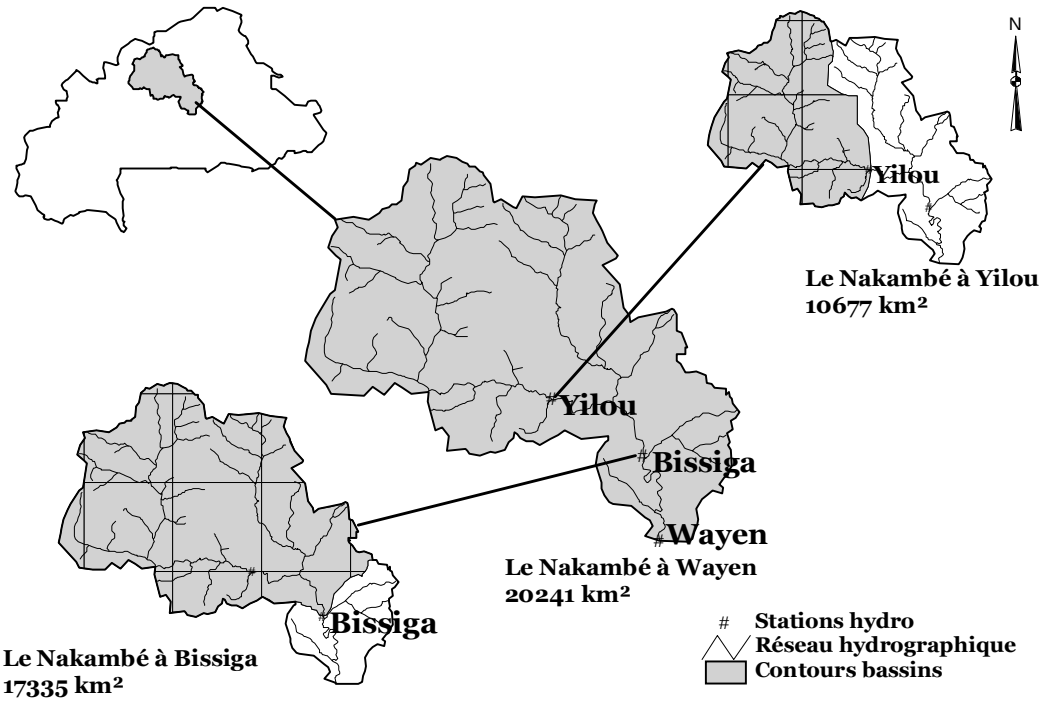


Fig. 2 Bassins tests du fleuve Nakambé au Burkina Faso.

Si la WHC de la surface $S_{Vg}(T_0)$ était WHC_{Vg} à la date T_0, elle sera, à la date T :

$$WHC = \alpha\%WHC_{Vg} + \beta\%WHC_{Cult} + \gamma\%WHC_{Sn} + \delta\%WHC_{Pe} \quad (3)$$

Où les proportions α, β, γ, et δ sont déterminées dans chaque cas à l'aide des modèles dévolution des états de surface.

Soit, en fonction de WHC_{Vg} :

$$WHC = \left[\alpha\% + \beta\% \frac{KrVg}{KrC} + \gamma\% \frac{KrVg}{KrSn} + \delta\% \frac{KrVg}{KrPe} \right] WHC_{Vg} \quad (4)$$

On peut mener le même raisonnement pour les autres types d'états de surface et aboutir aux mêmes types d'équations.

PREMIERS RESULTATS D'APPLICATION

Les résultats que nous présentons ici concernent trois bassins versants emboîtés du fleuve Nakambé (Volta Blanche) au Burkina Faso (Fig. 2).

Les données de télédétection utilisées pour cette application sont des images LANDSAT acquises en 1975, 1986 et 2002. Les résultats des différents traitements permettent de déduire les proportions de chaque classe d'états de surface en 1975, 1986 et 2002. Un exemple de traitement est présenté à la Fig. 3.

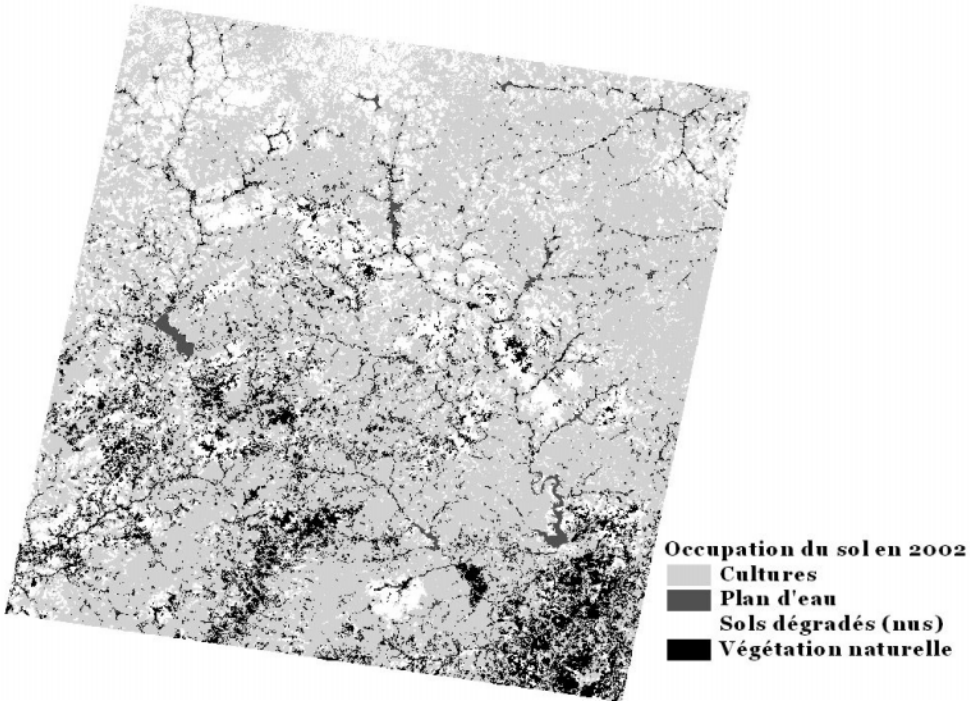


Fig. 3 Résultat de Classification d'image—Occupation du sol en 2002.

Les paramètres de la fonction logistique ont été déterminés à partir des données de recensements généraux de la population (RGP) et des séries de statistiques agricoles au Burkina Faso. La Fig. 4 donne l'allure générale des courbes d'évolution des surfaces cultivées et des surfaces en végétation naturelle.

Les données de pluie et d'ETP Penman utilisées dans ce travail proviennent d'une part de l'Unité de Recherche en Climatologie de l'Université d'East Anglia (CRU), et, d'autre part, de la base de données SIEREM (Système d'Information Environnementale sur les ressources en Eau et leur Modélisation) de l'UMR HydroSciences Montpellier. Ces sont des données mensuelles spatialisées au demi-degré carré.

Les résultats des simulations (Tableau 1) montrent que, comparé au cas où la WHC reste constante dans le temps, les performances du modèle sont quasiment identiques. En effet, sur l'ensemble des trois bassins testés, les gains de performances en calage sont faibles: +3 points pour Bissiga, +0.7 points pour Yilou et +2.2 points pour Wayen. En dehors de la station de Wayen (+ 5.7 et +9.6 points selon la source de données pluie), aucune amélioration en validation n'est observée sur les autres bassins.

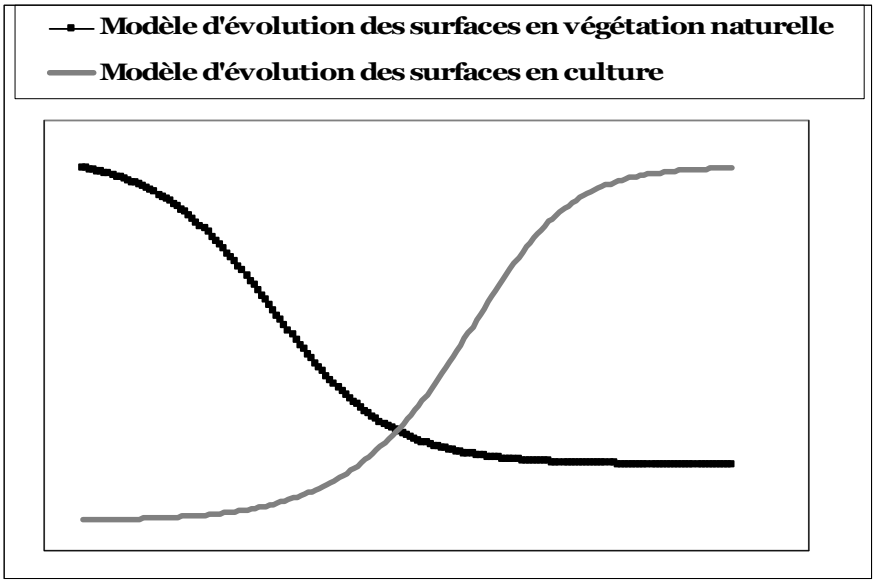


Fig. 4 Modélisation de la dynamique des surfaces cultivées et des surfaces en végétation naturelle à l'aide à partir d'une fonction logistique.

Tableau 1 Résultats préliminaires pour trois bassins versants du Nakambé au Burkina Faso.

Bassins testés		WHC Fixe		WHC évolutif	
		Pluie IRD ETP Penman	Pluie CRU ETP Penman	Pluie IRD ETP Penman	Pluie CRU ETP Penman
Bissiga	Calage 1976–1988	NASH= 54.5	NASH= 48.6	NASH= 57.2	NASH= 51.6
	Validation 1989–1995	NASH= 63.3	NASH= 60.5	NASH= 44.7	NASH= 41
Yilou	Calage 1973–1979	NASH= 75.4	NASH= 75.6	NASH= 76.1	NASH= 75.8
	Validation 1980–1982	NASH= 85.5	NASH= 83.7	NASH= 83.8	NASH= 82.7
Wayen	Calage 1975–1985	NASH=61.1	NASH=57.7	NASH= 63.3	NASH= 59.9
	Validation 1986–1995	NASH= 49.6	NASH= 40	NASH= 55.3	NASH= 49.6

CONCLUSIONS ET PERSPECTIVES

Ces résultats ne concernent que trois bassins et ne permettent pas d'évaluer la méthodologie qui a été exposée dans ce travail. En dehors des problèmes sur la fiabilité des données, de la non unicité des solutions liée au processus d'optimisation des paramètres, de l'influence de la longueur des périodes de calage et de validation, on peut se poser la question de la sensibilité des modèles à la variable (ou au paramètre) WHC. Des réflexions sont en cours dans le cadre d'une thèse. Toutefois, il semble nécessaire qu'à l'avenir les modèles puissent prendre en compte dans leur conceptualisation une évolution de l'environnement.

REFERENCES

Albergel J. & Valentin C. (1991) "Sahélisation" d'un petit bassin versant: Boulsa-Koghnere au centre du Burkina Faso. In: Dégradation des Paysages en Afrique de l'Ouest (ed. by J. F. Richard), 119–133. (Dakar, 21–26 novembre 1988). Presse Universitaire de Dakar, Dakar, Senegal.

Casenave A. & Valentin C. (1992) A runoff capability classification system based on surface features criteria in semi-arid areas of west Africa. *J. Hydrol.* **130**(1–4), 231–249.

Conway, D. & Jones P. D. (1999) Assessing the impac of future climatic change on the water ressource and the hydrology of the Rio dela Planta basin, Argentina. Climatic Research Unit. University of East Anglia, UK.

Delmas, B. (2004) Dossier "démographie mathématique": Pierre-François Verhulst et la loi logistique de la population. *Math. Social Sci.* **167**, 51–81.

Mahe, G., Leduc, C., Amani, A., Paturel, J. E., Girard, S., Servat, E. & Dezetter, A. (2003) Augmentation récente du ruissellement de surface en zone soudano-sahélienne et impacts sur les ressources en eau. In: *Hydrology in the Mediterranean and Semiarid Regions* (ed. by E. Servat, W. Jajem, C. Leduc & A. Shakeel), 215–222 (Montpellier, France). IAHS Pub. 278. IAHS Press, Wallingford, UK.

Makhlouf, Z. (1994) Compléments sur le modèle pluie-débit GR4J et essai d'estimation de ses paramètres. Thèse de doctorat Thesis, Université Paris-Sud, Paris, France.

Penman, H. L. (1956) Evaporation: an introduction survey. *J. Agric. Sci.* **1**, 9–29.

Pouyaud, B. (1987) Variabilité spatiale et temporelle des bilans hydriques de quelques bassins versants d'Afrique de l'Ouest en liaison avec les changements climatiques, ORSTOM, Montpellier (France).

Seguis, L., Cappelaere, B., Peugeot, C., Leduc, C. & Milesi, G. (2003) Influence de la sécheresse et du défrichement sur les écoulements d'un petit bassin versant sahélien. In: *Hydrology in the Mediterranean and Semiarid Regions* (ed. by E. Servat, W. Jajem, C. Leduc & A. Shakeel), 429–434. IAHS Publ. 278. IAHS Press, Wallingford, UK.

Yates, D. N. (1997) Approaches to continental scale runoff for integrated assessments models. *J. Hydrol.* **201**, 289–310.

Climate Variability and Change—Hydrological Impacts (Proceedings of the Fifth FRIEND World Conference held at Havana, Cuba, November 2006), IAHS Publ. 308, 2006.

Efecto de las plantaciones de *Pinus radiata* sobre el recurso agua en Chile

ANTON HUBER[1] **& ANDRÉS IROUMÉ**[2]

1 *Instituto de Geociencias, Facultad de Ciencias Universidad Austral de Chile, Independencia 567, Valdivia, Chile*
ahuber@uach.cl

2 *Instituto de Manejo, Facultad de Ciencias Forestales, Universidad Austral de Chile, Independencia 567, Valdivia, Chile*

Resumen Se determinó el efecto que tienen las plantaciones de *Pinus radiata* (D. Don) sobre el recurso hídrico para algunas regiones de Chile con diferentes características edafoclimáticas. Para ello se determinaron los distintos componentes del balance hídrico de plantaciones de *Pinus radiata* entre 12 y 17 años y una densidad entre los 700 y 800 árboles ha^{-1}. Los resultados fueron comparados con los de cubiertas herbáceas o arbustivas habituales adyacentes a las plantaciones. Las pérdidas relativas de agua por intercepción del dosel con respecto a las precipitaciones aumentaron de sur a norte (15–40%). La misma distribución tuvo la evapotranspiración neta (32–55%). La percolación fue mínima en el norte y mayor en el sur (5–53%). Las plantaciones de *Pinus radiata* registraron una mayor pérdida de agua por intercepción, un superior consumo por evapotranspiración y una menor percolación en comparación con las demás cubiertas vegetales.

Palabras claves efecto plantaciones; *Pinus radiata*; recurso agua; Chile

The effect of *Pinus radiata* plantations on water resources in Chile

Abstract The effect of *Pinus radiata* (D. Don) plantations on water resources at some Chilean sites having different edapho-climatic characteristics was determined. The different components of the water balance were measured at each site where the *Pinus radiata* plantations were 12 to 17 years old and between 700 and 830 trees ha^{-1} dense. The results were compared with those obtained from areas covered with perennial grasses and shrubs at the same sites. Annual interception losses (as a percentage of incoming precipitation) increased from south to north (from 15 to 40%). The same occurred with annual net evapotranspiration, which was 32% of incoming precipitation for the southernmost site and 55% for the one located in the lower latitude. Annual percolation registered its minimum value in the northern site (5% of incoming precipitation) and its maxima in the southern one (53%). Compared with the shrub or grass covers, sites under *Pinus radiata* plantations registered higher water consumption by evapotranspiration and reduced percolation.

Key words interception; evaporation; forest hydrology; percolation; water balance; water resources, Chile

INTRODUCCIÓN

El reemplazo de cubiertas herbáceas o arbustivas por plantaciones forestales produce modificaciones en el balance hídrico, porque se aumentan las pérdidas de agua por intercepción del dosel (Calder, 1998; Xiao *et al*., 2000; Huber & Iroumé, 2001; Iroumé & Huber, 2002), incrementa la evapotranspiración y reduce la percolación (Duncan, 1995; Calder *et al*., 1997; Oyarzún & Huber, 1999; Putuhena & Cordery, 2000; Bronstert *et al*., 2002; Huber & Trecaman, 2003).

La cantidad de agua consumida por las plantaciones está influida principalmente por las características de la cubierta forestal, condiciones climáticas y la capacidad de retención de agua útil de los suelos (Iroumé & Huber, 2000; Putuhena & Cordery, 2000; Sun *et al*., 2002; Huber & Trecaman, 2002; Huber & Trecaman, 2003)

Las plantaciones forestales en Chile se ubican preferentemente en ambas vertientes de la Cordillera de la Costa y en la Depresión Intermedia del país, entre los 30 y 41° latitud sur. Esta zona posee condiciones edafoclimáticas muy diversas, que tienen incidencia en el desarrollo de las plantaciones forestales y en el balance hídrico.

El objetivo del presente estudio es determinar el efecto que tienen las plantaciones de *Pinus radiata* sobre el recurso hídrico en de Chile. Para ello se establecerán las pérdidas de agua por intercepción del dosel y la cantidad de agua involucrada en la evapotranspiración y percolación de plantaciones de *Pinus radiata* de aproximadamente 15 años y una densidad cercana de 750 árboles/ha. Los resultados serán comparados con los de cubiertas herbáceas o arbustivas habituales colindantes a las mismas plantaciones.

Copyright © 2006 IAHS Press

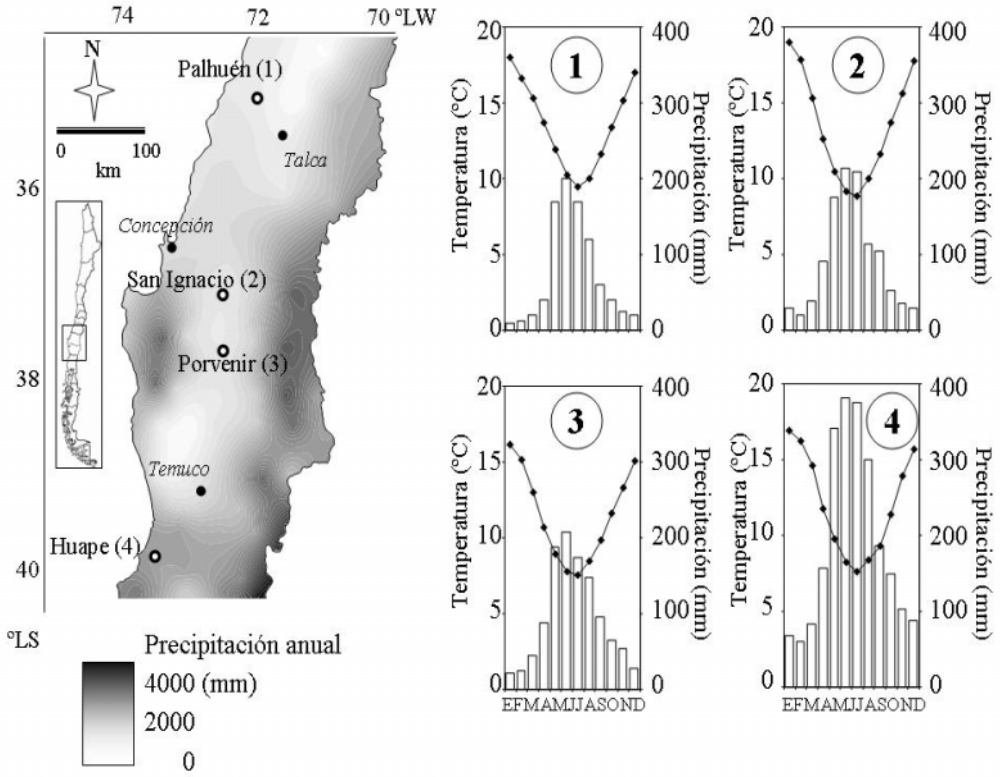


Fig. 1 Ubicación y características termopluviométricas de cada una de las localidades.

Tabla 1 Temperatura (Tº) y precipitación promedio anual (Pp), tipo de suelo con su correspondiente capacidad de retención de agua útil (CRA) y características de las cubiertas vegetales colindantes a cada una de las plantaciones de *Pinus radiata* según localidad.

Localidad	Pp anual (mm)	T° media (°C)	Suelo Tipo	CRA (%)	Vegetación
Palhuén	1000	15	Alfisoles	11	*Avena barbata*, *Nesella chilensis* y *Agrostis capillaris*
San Ignacio	1100	14	Etisoles	5	*Avena barbata* y *Nessella chilensis*
Porvenir	1200	11	Alfisoles	28	*Agrostis capillaris* y *Holcus lanatus*
Huape	2100	12	Ultisoles	26	*Agrostis capilaris*, *Holcus lanatus*, *Taraxacum officinalis*, *Aristotelia chilensis* y *Rubus constrictus*

MATERIAL Y MÉTODOS

La ubicación de las plantaciones de *Pinus radiata* consideradas en el estudio y las características edafoclimáticas de las mismas se presentan en la Fig. 1 y Tabla 1.

Las precipitaciones disminuyen de sur a norte, y la distribución oeste-este está influida por la topografía. Las mayores precipitaciones se registran al lado barlovento (oeste) de la Cordillera de la Costa y de la Cordillera de los Andes, mientras que las menores en la Depresión Intermedia, al lado sotavento de la Cordillera de la Costa.

Para hacer posible la comparación de los resultados entre las distintas localidades, se utilizaron sólo plantaciones de *Pinus radiata* con edades cercanas a los 15 años y una densidad próxima a los 750 árboles/ha.

La evapotranspiración neta (*EvTrn* = agua extraída exclusivamente del suelo (1)) y la total (*EvTrt* = evapotranspiración neta más las pérdidas de agua por intercepción (2)) se determinaron con la metodología del balance hídrico, basada en la ecuación de continuidad de Feller (1981).

$$EvTrn = Pp - (Ic - \Delta W + A + Per) \quad (1)$$

$$Evtrt = Pp - (A - \Delta W + Per) \quad (2)$$

donde *EvTrn* es la evapotranspiración neta (mm), *EvTrt* la evapotranspiración total (mm), *Pp* la precipitación incidente (mm), *Ic* las pérdidas de agua por intercepción del dosel (mm), ΔW variación del contenido de agua del suelo (mm), *A* la escorrentía superficial (mm) y *Per* la percolación (mm). Los distintos componentes del balance hídrico fueron determinados según la metodología propuesta por Huber (Huber & Trecaman, 2003).

RESULTADOS Y DISCUSIÓN

El balance hídrico de las plantaciones de *Pinus radiata* y de las demás cubiertas vegetales para las distintas localidades se presenta en la Fig. 2.

El porcentaje de agua interceptado por el dosel con respecto a las precipitaciones aumentó de sur a norte y varió entre un 15 y 40%. La distribución latitudinal de estos valores son atribuibles al régimen anual y a las características de las precipitaciones como también a las condiciones climatológicas que regulan la evaporación (Crockford & Richardson, 2000). Por consiguiente, la forestación reduce la fracción de las precipitaciones que alcanza el suelo. Especial importancia tiene este efecto en las zonas menos lluviosas. A su vez, Calder (1998) y Crockford & Richardson (2000) señalan que las características del dosel aumentan su influencia sobre el monto de agua que es interceptada cuando las precipitaciones disminuyen.

Las pérdidas de agua por intercepción de las cubiertas herbáceas y arbustivas en es estudio fueron despreciadas debido a su baja densidad y reducido desarrollo (Martínez & Navarro, 1996; Schlosser *et al*., 1997).

La evapotranspiración neta de las distintas plantaciones osciló entre los 694 y 401 mm año^{-1} y no tuvo un ordenamiento latitudinal. Distinta fue la distribución espacial cuando se utilizaron los valores relativos con respecto a la precipitación anual. En este caso aumentaron de sur a norte (32% Huape y 55% Palhuén). La excepción se registró en los arenales (38%), debido a la baja capacidad de retención de agua útil que tienen estos suelos. Las lluvias saturan rápidamente estas superficies dando paso a la percolación. En consecuencia, la evapotranspiración neta estuvo influida por la distribución anual de las precipitaciones y la capacidad de retención de agua de los suelos.

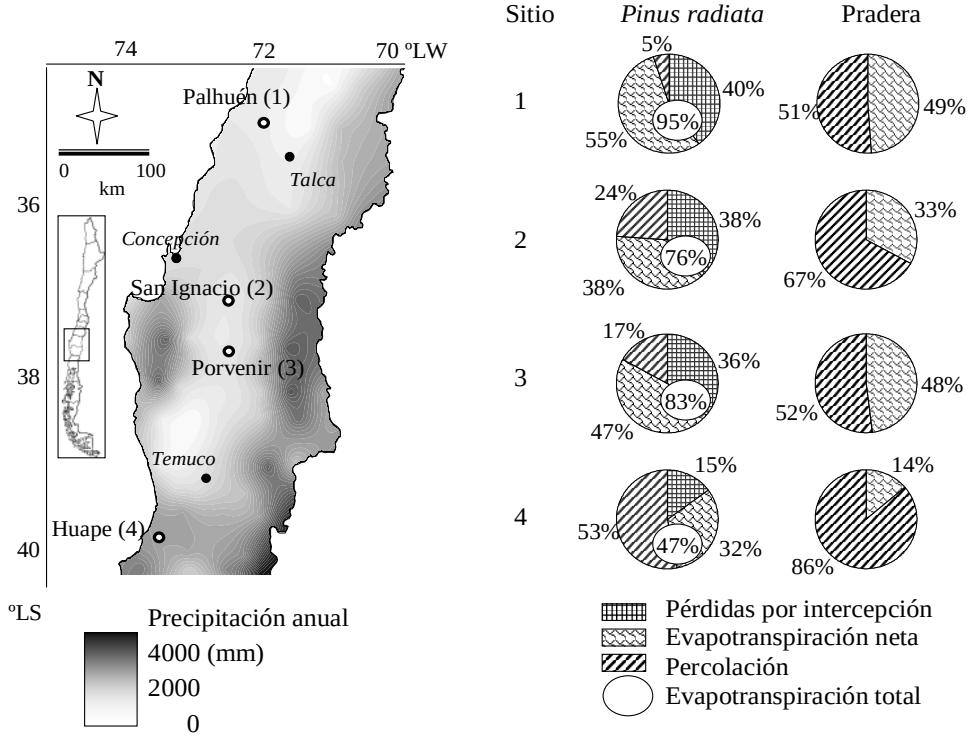


Fig. 2 Componentes del balance hídrico de cada una de las plantaciones de *Pinus radiata* y la de sus correspondientes cubiertas herbáceas/arbustivas colindantes.

Cuando a los valores de la evapotranspiración neta se le adicionaron las correspondientes pérdidas de agua por intercepción, la evapotranspiración total anual aumentó al 47% en Huape y 95% en Palhuén.

En Palhuén, en un año con un régimen pluviométrico similar al promedio, la sumatoria de las pérdidas de agua por intercepción con la evapotranspiración neta es similar a la precipitación anual; en consecuencia, durante estos períodos no se produce percolación.

Debido al incremento relativo que tuvo la evapotranspiración en el balance hídrico de sur a norte, la percolación registró una distribución latitudinal inversa (Fig. 2).

En la zona de los arenales, debido a la baja capacidad de retención de agua de sus suelos, la percolación se registró por más tiempo y fue más intensa que en zonas cercanas con precipitaciones similares pero con suelos arcillosos. En consecuencia, las plantaciones en los arenales tuvieron un menor impacto sobre el recurso agua que las establecidas en suelos arcillosos.

La evapotranspiración neta determinada para las demás cubiertas vegetales también se presentadas en la Fig. 2. Su distribución latitudinal fue semejante a la de las plantaciones forestales y sus montos bastante similares a éstas. La excepción se registró en Huape donde el régimen anual de precipitaciones permite que casi siempre haya suficiente cantidad de agua en el suelo para satisfacer los requerimientos de los árboles. Bajo estas condiciones, la plantación forestal pudo mostrar su mayor potencial de transpiración, la que a su vez fue aumentada por la presencia de una cubierta arbustiva-herbácea permanente.

En las localidades ubicadas más hacia el norte, donde las precipitaciones son menores, la evapotranspiración neta de las plantaciones y de las demás cubiertas vegetales fueron bastante similares. Ello se explica parcialmente por la menor cantidad de precipitaciones que alcanzó el suelo de las plantaciones debido a las mayores pérdidas por intercepción. Por consiguiente, las cubiertas herbáceas dispusieron de una superior cantidad de agua para la evapotranspiración. Esta disimilitud es más trascendente para los períodos con menores precipitaciones. Además, como estos suelos posen de una rala cubierta vegetal y de poco desarrollo, los dejan más expuestos a las condiciones medioambientales que favorecen la evaporación. Estos resultados concuerdan con los de Huber & Trecaman (2001) y Sternberg *et al*. (2001), quienes indican que al final del período estival los primeros 50 cm de un suelo con una cubierta herbácea rala registró un menor contenido de agua que otro forestado con *Pinus radiata.*

La percolación disminuyó de sur a norte (Fig. 2) porque ella está determinada principalmente por el diferencial entre las precipitaciones y evapotranspiración.

La plantación en Palhuén registró la menor percolación, fue equivalente al 5% de la precipitación anual (Fig. 2). Para la misma localidad, en el matorral de espino, este valor alcanzó el 53%, valor ampliamente superior al de la plantación. Por consiguiente, en esta zona el cambio de uso del suelo afecta considerablemente la recarga del agua subterránea.

CONCLUSIONES

Existen diferencias importantes entre los valores de los componentes del balance hídrico de las cubiertas herbáceas o arbustivas ralas y las plantaciones de *Pinus radiata.* El mayor efecto de las plantaciones sobre el recurso agua en las zonas menos lluviosas se debe principalmente a la superior importancia que adquiere la intercepción del dosel.

El superior impacto que tienen las plantaciones de *Pinus radiata* sobre el recurso agua en Chile se produce principalmente en las zonas con menores precipitaciones.

Agradecimientos Este trabajo forma parte del Proyecto FONDECYT 1010713 y contó con el apoyo de la Forestal Mininco S.A., Forestal Celco S.A., Forestal Copihue S.A. y el Centro Forestal de la Facultad de Ciencias Forestales de la Universidad Austral de Chile.

REFERENCIAS

Bronstert, A., Niehoff, D. & Bürger, G. (2002) Effects of climate and land-use change on storm runoff generation: present knowledge and modeling capabilities. *Hydrol. Processes* **16**, 509–529.

Calder, I. R. (1998) Water use by forest, limits and control. *Tree Physiology* **18**, 625–631.

Calder, I. R., Rosier, P., Prasanna, K. & Parameswarappa, S. (1997) Eucalyptus water use greater than rainfall input—a possible explanation from southern India. *Hydrol. Earth System Sci.* **1**(2), 249–256.

Carrasco, P., Millán, J. & Peña, L. (1993) Suelos de la cuenca del río Biobío. Características y problemas de uso. Gestión de recursos hídricos de la cuenca del río Biobío y del área marina costera adyacente. *Serie análisis territorial.* Editorial Universidad de Concepción, Chile.

Crockford, R. H. & Richardson, D. P. (2000) Partitioning of rainfall into throughfall, stemflow and interception: effect of forest type, ground cover and climate. *Hydrol. Processes* **14**, 2903–2920.

Duncan, M. J. (1995) Hydrological impacts of converting pasture and gorse to pine plantation, and forest harvesting, Nelson, *New Zealand. J. Hydrol. NZ* **34**(1), 15–41.

Feller, M. (1981) Water balance in *Eucalyptus regnans*, *E. oblicua*, and *Pinus radiata* forest in Victoria. *Australian Forestry* **44**(3), 153–161.

Huber, A. (1970) *Diez años de observaciones climatológicas en la Estación Teja-Valdivia (Chile) 1960–1969*. Instituto de Geología y Geografía, Universidad Austral de Chile.

Huber, A. & Iroumé, A. (2001) Variability of annual rainfall partitioning for different sites and forest covers in Chile. *J. Hydrol.* **248**, 78–92.

Huber, A. & Trecaman, R. (2000) El efecto de las características de una plantación de Pinus radiata en la distribución espacial del contenido de agua edáfica. *Bosque* **21**(1), 37–44.

Huber, A. & Trecaman, R. (2002) Efecto de la variabilidad interanual de las precipitaciones sobre el desarrollo de las plantaciones de Pinus radiata (D.Don) en la zona de los arenales VIII Región, Chile. *Bosque* **23**(2), 43–49.

Huber, A. & Trecaman, R. (2003) Modificaciones del recurso hídrico por plantaciones de *Pinus radiata* (D.Don) en dos tipos de suelo de la cuenca del río Biobío. *Revista Geográfica de Chile Terra Australis* **48**, 15–24.

Iroumé, A. & Huber, A. (2002) Comparison of interception losses in a broadleaved native forest and *Pseudotsuga menziesii* (Douglas fir) plantation in the Andes Mountains of southern Chile. *Hydrol. Processes* **16**, 2347–2361.

Martínez, A. & Navarro J. (1996) Hidrología forestal, El Ciclo Hidrológico. *Secretariado de publicaciones. Universidad de Valladolid. España*.

Oyarzún, C. & Huber, A. (1999) Balance hídrico en plantaciones jóvenes de *Eucalyptus globulus* y *Pinus radiata* en el sur de Chile. *Terra* **17,** 35–44.

Peña, L., Carrasco, O., Figueroa, M., Oyarzún, C. & Lo Cascio, B. (1993) Pérdidas por erosión hídrica en suelos agrícolas y forestales de la cuenca del río Biobío. pp 47 -59. In: Elementos cognoscitivos sobre el recurso suelo y consideraciones generales sobre ordenamiento agroforestal. Gestión de recursos hídricos de la cuenca del río Biobío y del área marina costera adyacente. *Serie propuestas de ordenamiento* (4). Editorial Universidad de Concepción, Chile.

Putuhena, W.M. & Cordery, I. (2000) Some hydrological effects of changing forest cover from eucalypts to *Pinus radiata*. *Agric. Forest Met.* **100**, 59–72.

Sternberg, M., Danin, A. & Noy-Meir, I. (2001) Effects of clearing and herbicide treatments on coniferous seedling establishment and growth in newly planted Mediterranean forests. *Forest Ecol.Manage.* **148,** 179–184.

Sun, G., McNulty, S. G., Amayta, D. M., Skaggas, R. W., Swift Jr., L. W., Shepard, J. P. & Riekerk, H. (2002) A comparison of the watershed hydrological of coastal forested wetlands and the mountainous uplands in the Southern US. *J. Hydrol.* **263**, 92–104.

Xiao, Q., McPherson, E. G., Ustin, S. L., Grismer, M. E. & Simpson, J. R. (2000) Winter rainfall interception by two mature open-grown trees in Davis, California. *Hydrol. Process* **14,** 763–784.

Key word index

a priori parameter estimation, 651
abalation, 479
acid deposition, 591
advection, 413
agricultural drought, 315, 332
agroclimatic
  mapping, 332
  zoning, 315
air-masses, 344
alert system, 175
Amazon, 44
Amazon
  basin, 424
  River, 220
ANN, 10
Annapurna, 454
antecedent influencing factor (AIF), 275
aquifer, 413, 629
Argentina, 175
Athens, Greece, 31
atmospheric circulation, 338
Australia, 10
autoregressive process, 526

balance, 479
basin, 186
basin
  management, 186
Bayesian inference, 226
BHS *Chronology*, 483
Biebrza wetlands, 573
BILAN model, 418
Bivariate Generalized Pareto Distribution, 139
borehole, 394
Brazil, 220
Bua River, 239
Burkina Faso, 606, 691
Buruli ulcers, 685

capacity building, 3
Caribbean, 304
catastrophic flood, 175
catchment grouping, 117
central England, 490
central Poland, 646
change detection, 538
changes in land use, 533
chemicals, 586
Chile, 662, 698
China, 553
classification, 344
climate, 344, 447, 479
climate
  change, 256, 389, 401, 407, 418, 442, 460, 514, 667
  change impacts, 375, 382
  scenarios, 407
  variability, 679
  variability and change, 502
climate–river flow linkages, 350
climatic
  scenarios, 436
  variability, 319, 394, 691
  variation, 466
  warming, 473
  water balance, 139
climatological radar, 214
cluster analyses, 617
coastal lagoon, 86, 563
coefficient of variation, 466
cold climate, 169
communication, 196
compensatory runoff, 558
complexity, 10
composite analysis, 350
conceptual model, 37, 145
contamination, 413
contingency table, 369
continuous simulation, 134
Costa Rica, 105, 111, 641
cross validation, 117
Cuba, 315, 332, 629

daily rain, 310
dams, 606
data collection, 51
data sets, 646
database, 31
day with rain, 300
DBM modelling, 356, 362
DBMS, 19
debris flows, 232
decadal rainfall analysis, 294
deficiency, 483
deficit volume, 418
deforestation, 186, 672
demographic modelling, 691
developing countries, 75
dew point, 287
dilution, 586
discharge, 220, 394, 424, 520
discharge
  anomalies, 526
  deficit, 401

non-homogeneity, 10
nonstationarity, 514
North Atlantic Oscillation, 350, 496, 526
northern North Atlantic, 350
northwest Bangladesh, 99
numerical
  groundwater modelling, 623
  modelling, 325
nutrient flux, 612
nutrients, 86, 563
Nysa Klodzka River, Poland, 139

Óbidos, 220
observatory, 44
Okavango basin, 382
ORE HYBAM, 44
overexploitation, 629
oxidized nitrogen, 591

Pang catchment, UK, 128
parameter
  calibration, 651
  estimation, 250
PDHI, 169
PDSI, 169
peak
  flows, 662
  runoff, 186
percolation, 698
permafrost zone, 651
Peru, 220, 424
Pilica River, 579
Poland, 139
population, 586
precipitable water, 287
precipitation, 26, 256, 533
precipitation
  spatial variability, 281
prediction, 3
prediction
  at ungauged sites, 117
  in ungauged basins, 163
preferential states, 646
principal components analyses, 319
probabilities, 332
probability, frequency, 265
probable maximum precipitation, 287
process-oriented runoff simulation, 454
propagation, 122
proxy, 91
PUB, 3, 37, 117, 250
public awareness, 31
Puerto Rico, 81
pumping strategy, 26

rain probability, 369
rainfall, 128, 180, 424, 656
rainfall
  anomalies estimation, 294
  data, 75
  forecasting, 201
  prediction, 310
  scenarios, 430
  trends, 37
rainfall–runoff, 325
rainfall–runoff models, 134, 214, 239
RCM, 375
real time, 196, 207
recession, 145
recharge, 629
record length, 490
reduction of flows, 533
re-filling, 606
regimes, 344
regional
  climate, 325
  climate models, 389, 401
  drought characteristics, 128
  forecasting, 169
  frequency analysis, 226
  hydro-glaciological model, 473
  regression, 117
regionalization, 56, 105, 111, 117, 134,163, 344, 454
reliability, 407
relief, 62
representative catchment, 56
resampling, 538
reservoir storage capacity, 418
resilience, 10
return period, 186
return period
  for rainfall intensities, 270
risk value, 207
risk, 186
river basin, 180, 394
river flow, 158, 344, 473
river flow
  data, 538
river hydraulic modelling, 579
river runoff, 651
RS, 573
runoff, 586
runoff
  generation, 623
  variability, 466

SADC-HYCOS, 51
safe yield, 629
Sahel, 430, 691
Salado River, 175
Santa Fe, 175
satellite data, 75
scaling, 667
Scandinavia, 502
Scandinavian pattern, 350
scenarios, 180, 502
SDSM, 375

seasonal
  forecasting, 158
  river flow, 490
seasonality, 117
sediment load, 612
sediments, 44
semiarid, 122
Senegal River, 319
simulation model, 601
Slovakia, 617
small catchments, 508
small reserves of water, 606
snow, satellite images, 244
soil
  classes, 68
  storage, 656
  water storage, 646
solids transport, 606
Songkhla Lake, Thailand, 601
Southeast Asia, 356, 362
Southern Africa, 51, 75
spatial
  aspects, 128
  information, 56
  interpolation, 81
SPI, 169
statistical
  models, 158
  prediction, 344
  testing, 538
  tests, 319
stochastic, 265
stochastic
  interpolation, 641
  model, 99
storage basin, 26
stratification, 413
stream network, 81
streamflow, 169, 256, 490
streamgauge network, 175
subsurface, 122
surface water, 81, 180
sustainability, 558
sustainable
  development, 553
  runoff, 569
synoptic patterns, 310
system type of model, 239

TACD model, 454
telemetric transmission, 196
telemetry, 31
temporal cycles, 356, 362
terciles, 369
The Netherlands, 26
threshold
  approach, 122
  level method, 169, 338
thunderstorms, 300
Tibet (China), 460
tracer, 629
trend analysis, 490
trends, 332, 496, 502, 514, 538
trends
  in runoff regime, 508
tritium, 629
tropical forests, 672

UK, 128, 158, 483, 496
uncertainty, 281, 375, 401
ungauged basin, 37
urbanization, 394

variability, 10
vertical pressure gradient, 304
Vistula River, 191
vulnerability, 265

Wales, 490
warning systems, 207
Warsaw, Poland, 191
waste
  disposal site, 635
  load dispersion, 601
water
  balance, 641, 698
  conservation, 656
  demand, 389
  Framework Directive, 418
  holding capacity, 68
  management, 91
  quality, 394, 596, 612
  reservoir, 407
  resources modelling, 389
  resources, 10, 19, 75, 134, 294, 382, 418, 436, 460, 483, 553, 698
  scarcity, 389
  stress, 91
  supply, 407, 656
  system control, 26
weather forecast, 26
web interface, 19
West Africa, 250
West African Sahel, 679
West and Central Africa, 19, 68, 436
Western Europe, 344
wet and dry cycles, 520
wet deposition, 591
wetland, 86, 553, 563

Yellow River, 612
Yucatan, 635

resource estimation models in southern Africa *Denis A. Hughes*

Application of digital terrain analysis to estimate hydrological variables in the Luquillo Mountains of Puerto Rico *Andrew S. Pike* 81

Submodelo de erosión en laderas para modelo precipitación–escorrentía en SIG / A hillslope erosion submodel for use with rainfall–runoff models in GIS *Alejandro Dussaillant J.* 86

A European case-based reasoning tool to inter-compare hydrological information on water stress among drainage sub-basins *Jasper Griffioen, Sophie Vermooten, Neno Kukuric & Slavek Vasak* 91

3 HYDROLOGICAL EXTREMES

Low flow prediction and forecasting

Stochastic model of flow duration curves for selected rivers in Bangladesh *M. F. Bari & Kh. Md. Shafiul Islam* 99

Regionalization of flow duration curves *Irina Krasovskaia, Lars Gottschalk, Etienne Leblois & Alexia Pacheco* 105

Regionalization of low flow in Costa Rica *Alexia Pacheco, Lars Gottschalk & Irina Krasovskaia* 111

Low flow estimation in Austria *Gregor Laaha & Günter Blöschl* 117

Drought propagation through the hydrological cycle *Henny A. J. Van Lanen* 122

Propagation of drought in a groundwater fed catchment, the Pang in the UK *Lena M. Tallaksen, Hege Hisdal & Henny A. J. Van Lanen* 128

Predicting low flows in ungauged basins: a hydrological response unit approach to continuous simulation *Andrew R. Young, Virginie Keller & Jim Griffiths* 134

Temporal and spatial variability of drought in mountain catchments of the Nysa Klodzka basin *Tamara Tokarczyk & Wojciech Jakubowski* 139

Le dispositif PRESAGES: un ensemble d'outils pour la prévision des étiages / PRESAGES: A collection of tools for predicting low flows *Claire Lang, Emmanuel Gille, Didier François & Jean-Claude Auer* 145

Multi-model technique for low flow forecasting *Mary-Jeanne Adler & Valentina Ungureanu* 151

Seasonal forecasting of river flows: a review of the state-of-the-art *Jennifer Easey, Christel Prudhomme & David M. Hannah* 158

Predicting low flows in ungauged catchments *Kolbjørn Engeland, Hege Hisdal & Stein Beldring* 163

Drought indices suitable to study the linkages to large-scale climate drivers in regions with seasonal frost influence *Anne K. Fleig, Lena M. Tallaksen & Hege Hisdal* 169

Flood prediction and forecasting

Sistema de alerta hidrológico de la cuenca del Río Salado, provincia de Santa Fe, Argentina: avances en su implementación / The Salado River basin (Santa Fe, Argentina) flood warning system: advances in its implementation *Gustavo Ferreira* 175



International Association of Hydrological Sciences

Association Internationale des Sciences Hydrologiques

IAHS AISH

www.iahs.info

IAHS Publication 308 ISBN 1-901502-78-7 ISSN 0144-7815